

**SORPTION AND TRANSPORT PROCESSES IN RELATION TO SOIL
STRUCTURE, WATER RETENTION, SOLUTE MOBILITY AND WATER UPTAKE
BY PLANT ROOTS**

by

L. A. G. AYLMOORE B.Sc., Ph.D. (The University of Adelaide)

Selected Research Publications

Submitted to The University of Adelaide

for the

DEGREE OF DOCTOR OF SCIENCE

VOLUME 2 Nos. 51 - 105

April, 2002

SUMMARY

The research described in this submission has provided a number of major advances in knowledge and practical outcomes including in particular:

1. The detailed description of the microporous structure of clay mineral systems by gas and vapour sorption leading to the recognition of quasi-crystals and clay domains as the assemblages of primary particles which constitute the operational elements in determining soil physical behaviour.
2. An enhanced understanding of electro-kinetic phenomena and the effects of ions on water structure and movement near the charged surfaces of clay particles.
3. A comprehensive analysis and theoretical description of the mechanisms involved in solute transport in soils including in particular, the effects of competitive adsorption between species and time dependency of sorption.
4. The detailed elucidation of the factors determining the persistence and mobility of pesticides in the soil profile and their potential for groundwater pollution leading to the development of a practical management model.
5. The adaption of computer assisted tomography applied to the attenuation of X- and gamma radiation (CAT Scanning), to the non-destructive *in situ* measurement of soil water content and structural changes and in particular to water uptake by plant roots. Coupled with the innovative use of ion specific microelectrodes, these studies provided the first detailed measurements of the temporal and spatial distribution of soil water and solute contents close to single plant roots.
6. The development of the Modulus of Rupture – Exchangeable Sodium Percentage (MOR – ESP) approach as a practical method for evaluating the structural status of soils and the influence of management practices. The method allows separate quantitative assessment of the roles of dispersive and non-dispersive mechanisms in contributing to structural instability in hard setting soils.

NOTE: The extended summary is presented at the front of Volume I together with the complete list of publications cited.

The effects of flow rate on the adsorption of pesticides in soils.

***Proc. Inter. Conf. on the Vulnerability of Soil and Groundwater to Pollutants*, Noordwijk, Wageningen, The Netherlands, Ed. W. van Duyvenbooden, 835-844 (1987).**

Singh, R., Adeney, J.A., Gerritse, R.G. and Aylmore, L.A.G.,

THE EFFECT OF FLOW RATE ON THE ADSORPTION
OF PESTICIDES IN SOILS

R. Singh¹, J.A. Adeney², R.G. Gerritse², and L.A.G. Aylmore¹

¹Soil Science and Plant Nutrition, School of Agriculture,
University of Western Australia, Nedlands, W.A. 6009, Australia.

²CSIRO Division of Groundwater Research,
Private Bag, P.O., Wembley, W.A. 6014, Australia.

ABSTRACT

Adsorption kinetics of diquat, linuron, phenamiphos and simazine were studied using a flow technique in columns of a sand and a sandy loam soil from Western Australia. A decrease in the rate of adsorption with time to a constant value was observed for all pesticides. This constant rate of adsorption could be fitted to a first order kinetic equation. The batch method and the flow technique gave comparable adsorption results for similar equilibration times. Extrapolation of the results from the column experiments show that considerable deviation from equilibrium in the adsorption of pesticides can occur under field conditions.

1. INTRODUCTION

Adsorption and degradation are the major processes affecting pesticide transfer through soils. Both the extent and the rate of adsorption at the solid-liquid interface determine the susceptibility of a particular pesticide to leaching. Little information on kinetics of adsorption of pesticides in soils is available from the literature (Yaron et al. 1985).

The batch slurry method, which is commonly used to study adsorption kinetics, has many limitations. The solution concentration of pesticide decreases with time and alterations in the surface chemistry of soil particles can occur with vigorous mixing (Barrow and Shaw 1979). It is also difficult to distinguish between adsorption and degradation when using the batch method. Because of these factors, data cannot be reliably applied at the field scale. Flow techniques in columns of soil provide a better representation of field conditions (Murall and Aylmore 1983). Mechanical agitation is absent and degradation can be measured by comparing column input and output.

This paper reports on studies of the adsorption kinetics of diquat, linuron, phenamiphos and simazine. The adsorption data obtained by a flow technique were fitted to a first order rate equation in two soils of different texture. Equilibrium adsorption isotherms obtained by the flow technique and batch method were compared. The effect of the rates of adsorption on distribution of pesticides under flow velocities encountered in the field situation is discussed.

2. MATERIALS AND METHODS

2.1 Soils and Pesticides

A sandy soil of the Bassendean association of the Swan Coastal Plain near Perth (Western Australia) and a sandy loam soil of the Gascoyne association near Carnarvon (Western Australia) were used in this study. The characteristics of Bassendean sand are given by McArthur and Bettenay (1974) and of Gascoyne sandy loam by Bettenay et al. (1971). Relevant properties of the Bassendean sand and Gascoyne sandy loam are respectively, clay (%) 6.3, 16.8; silt (%) 0.7, 11.8; organic carbon (%) 0.63, 0.84; and pH (1:5, 0.01 M CaCl₂) 5.4 and 7.1.

Horticultural crops are grown on both soils. The groundwater below Bassendean sands is used for domestic and irrigation purposes. On the Gascoyne soils, the groundwater is used for irrigation but drinking water is supplied mainly from the Gascoyne River.

Four pesticides were used in this study, three herbicides: diquat, linuron, simazine, and a nematicide, phenamiphos. Analytical grade samples (+99%) of pesticides were obtained from ICI Australia Ltd. (diquat); Hoechst Australia Ltd. (linuron); Bayer Australia Ltd. (phenamiphos) and Ciba-Geigy Australia Ltd. (simazine).

Diquat, linuron, phenamiphos and simazine are some of the commonly used pesticides in Western Australia. The amounts generally used per application are: diquat (3 l/ha), linuron (4 kg/ha), simazine (4 kg/ha) and phenamiphos (20 l/ha).

2.2 Equilibrium adsorption study

Batch distribution isotherms for the four pesticides in the two soils were determined at $20 \pm 2^\circ\text{C}$. Five grams of air-dried soil were equilibrated in polypropylene centrifuge tubes with 10 ml of pesticide solution in 0.01 M CaCl_2 . Pesticide concentrations ranged from 150 to 6000 $\mu\text{mole/litre}$ (diquat) and from 50 to 6000 $\mu\text{mole/litre}$ (other pesticides). The tubes were shaken (end over end) for 16 h (diquat) or 24 h (other pesticides). Soil adsorption was found to be almost complete after this time. Pesticides were not noticeably adsorbed to the walls of the centrifuge tubes. After shaking the suspension was centrifuged at 12000 rpm for 15 minutes. The supernatant was pipetted off and analysed. The adsorbed amount was calculated from the initial and final concentrations of pesticides in solution.

2.3 Pesticide analysis

Simazine and linuron were analysed directly in the soil solution phase by liquid chromatography (Vickery et al. 1980) using a Spherisorb 10 μm ODS column, 30 cm x 1.6 mm ID (Phase Separation Ltd.) and a mobile phase of methanol and water (65:35 v/v). The pesticides were detected at 220 nm with a variable wavelength UV detector (ETP-Kortec). Detection limit for simazine was 0.1 $\mu\text{g/ml}$ and for linuron 0.5 $\mu\text{g/ml}$. Diquat was measured colorimetrically at 376 nm after reacting the soil solution phase with sodium dithionite (Lott et al. 1978). Detection limit was 0.1 $\mu\text{g/ml}$.

Phenamiphos was analysed by capillary gas chromatography (Hewlett-Packard) using a HP-5 column (25 m x 0.31 mm ID) and He as carrier gas at 44 cm/sec. Operating conditions were, injection port temperature was 250°C, initial column temperature 175°C programmed to 250°C at 25°C/min. Detection was with a single ion monitoring mass spectrometer (Hewlett-Packard 5970) at $m/e = 303$. Detection limit for phenamiphos was 0.05 µg/ml. Phenamiphos was analysed after extracting the soil solution phase with 15% methylene chloride in hexane. The average recovery was 97%.

2.4 Soil column studies

Air-dried soil was vibrated into columns. A HPLC pump (ETP-Kortec) supplied a solution of 0.01 M CaCl₂ to the columns. Saturated flow rates were varied from 0.01 ml/min to 2.0 ml/min. Samples were injected in a volume of 300 µl with a six port stainless steel valve (Rheodyne). Details of experimental conditions for soil columns are given in Table 1. To avoid slaking of the Gascoyne sandy loam, a mixture of soil and diatomaceous earth (2.4:1) was used. Pesticide adsorption by diatomaceous earth was negligible. Breakthrough curves (BTCs) were monitored with a UV detector and chart recorder or alternatively off line from analysis of automatically collected fractions.

Dynamic distribution isotherms of pesticides were measured from BTCs at various rates of flow in small columns of soil under saturated conditions. The isotherms were obtained by applying the peak maxima method (Huber and Gerritse 1971). This method is based on the transport equation for non-linear distribution of a solute:

$$(\delta\langle C \rangle / \delta t) + ((1-\theta)/\theta)(\delta\langle S \rangle / \delta t) = -(\delta\langle V \rangle / \delta z) + D(\delta^2\langle C \rangle / \delta z^2) \dots (1)$$

where z = length co-ordinate

t = time

S = adsorbed concentration

C = solution concentration

V = pore water velocity

- $\langle \rangle$ = average over corresponding cross-sectional area
 θ = fraction of cross-sectional area occupied by solution
 $1-\theta$ = fraction of cross-sectional area occupied by solid phase
 D = longitudinal dispersion coefficient

Assuming the dispersion coefficient to be effectively zero, an expression describing the residence time (t_c) of the maximum solution concentration in the BTC from a column of soil can be derived.

$$(t_c - t_0)/t_0 = ((1-\theta)/\theta)(d\langle S \rangle/d\langle C \rangle) \dots\dots\dots(2)$$

where t_0 = retention time of non-retained solute (C_1 -)

The adsorbed concentration (S) can be calculated by applying Equation 2 to the locus of concentration maxima of the BTCs and integrating. The adsorption rate coefficients were calculated from the change in the amount of adsorbed pesticide with residence time (t_c in Equation 2).

Table 1. Soil column characteristics and experimental conditions

Properties	Bassendean sand		Gascoyne sandy loam	
	Diquat	Other Pesticides	Diquat	Other Pesticides
Length (cm)	4.9	15	4.9	13
Internal diam.(cm)	0.44	1.0	0.44	1.0
Soil wt. (g)	1.2	18.6	1.1	6.0+2.8*
Bulk density (g/cm ³)	1.54	1.6	1.48	0.9
Porosity (cm ³ /cm ³)	0.46	0.44	0.60	0.73
Pore volume (ml)	0.36	5.4	0.45	7.5
Pesticide injected	(μ g) 10-80	1-20	30-150	1-20
Range of pore water velocities (m/day)	20-500	1-40	10-300	2-30

*Diatomaceous earth (BDH, particle range 5-10 μ m)

3. RESULTS AND DISCUSSION

Results of applying the flow technique to the breakthrough of simazine from a column of Bassendean sand are shown in Figure 1a and 1b. Recoveries calculated from the BTCs were always better than 90%, showing that pesticide degradation during the column experiments was not significant. A comparison of adsorption isotherms measured by batch and by the flow technique is shown in Figure 1b for simazine and in Table 2 for all pesticides. Results from the flow technique and batch method are similar.

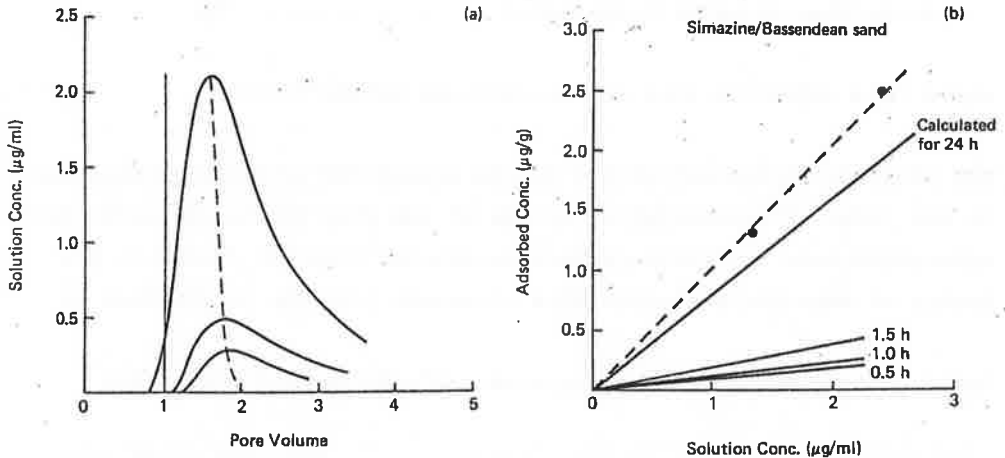


Figure 1a. Dynamic adsorption isotherm obtained by peak maxima method. Pore water velocity 2.2 m/day. Amount of simazine injected, 3-12 µg. Chloride ———: Pesticide - - - - -

Figure 1b. Dynamic adsorption isotherms of simazine obtained by flow technique and comparison with batch values. Observed batch values after 24 h ----•; adsorption isotherms by flow technique at various residence times (t_c) ———.

Data from the column experiments were fitted to a first order kinetic equation derived for constant solution concentration of the pesticide:

$$\ln(1 - S_t/S_\infty) = -bt$$

where S_t = amount adsorbed at time t

S_∞ = amount adsorbed at $t = \infty$ obtained from batch experiment

b = adsorption rate coefficient

Table 2. Distribution constants (K_∞) of pesticides by batch and flow technique measured after 24 h *

Pesticide	Bassendean sand		Gascoyne sandy loam	
	(ml/g)		(ml/g)	
	Flow	Batch	Flow	Batch
Diquat	234	260	755	800
Linuron	5.6	7.0	5.8	9.0
Phenamiphos	4.3	4.5	4.0	4.0
Simazine	1.0	1.6	2.4	2.5

* Diquat - 16 h

The first order plots of four pesticides in the two soils are shown in Figure 2. A decrease in the rate of adsorption with time to a relatively constant value is observed for all pesticides in both soils. Similar results have been reported by Graham-Bryce (1972). The limiting values of the rate coefficients as calculated from Figure 2 are shown in Table 3.

Table 3. Limiting values of rate coefficients of pesticides

Pesticide	Bassendean sand	Gascoyne sandy loam
	(day ⁻¹)	(day ⁻¹)
Diquat	3.2	3.6
Linuron	1.3	0.8
Phenamiphos	1.9	2.6
Simazine	1.2	2.7

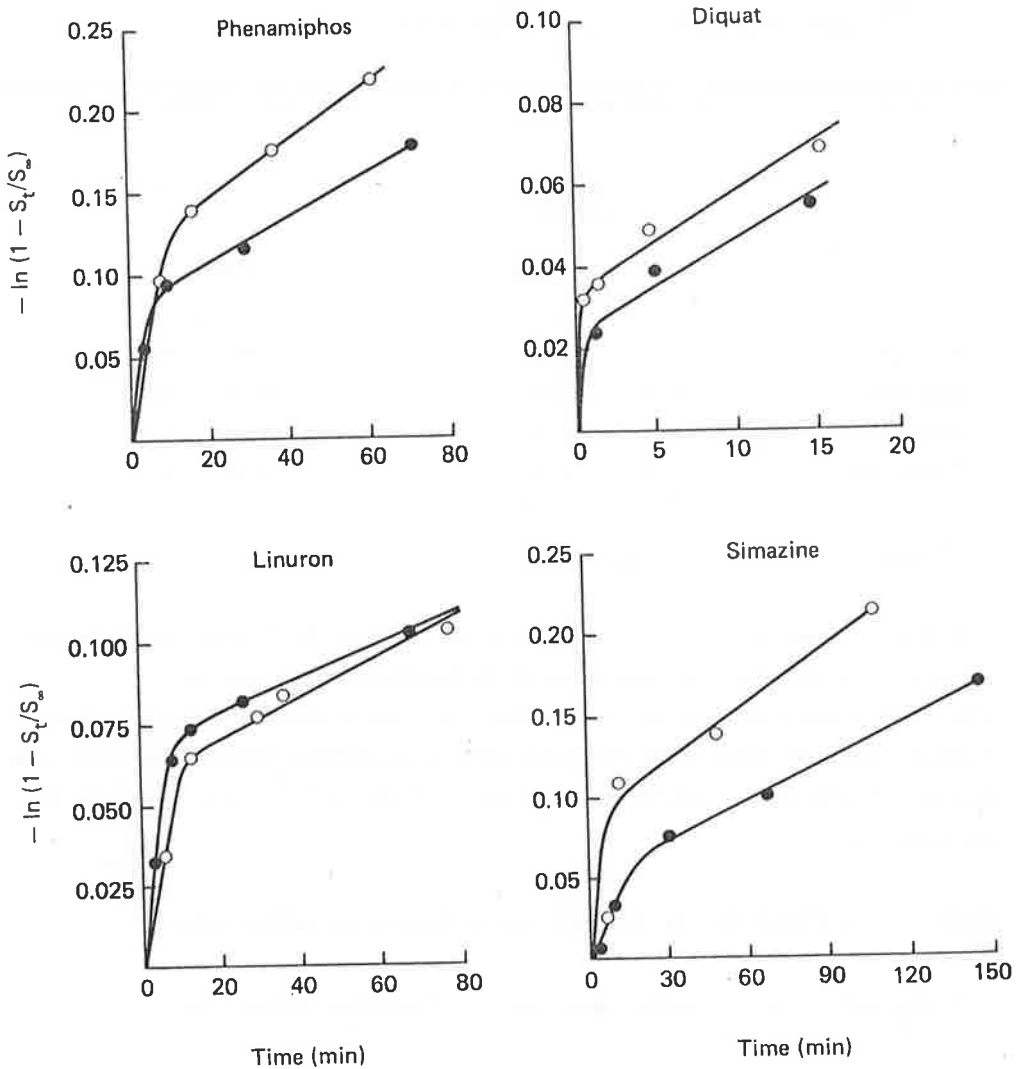


Figure 2. First order plots of diquat, linuron, phenamiphos and simazine. in two soils. Bassendean sand ---●; Gascoyne sandy loam---○.

The effect of pore water velocity on the distribution of the various pesticides in the soils used in this study are shown in Figure 3a and 3b. In the calculations dispersion length (Disp) is taken as the smallest soil unit within which complete mixing of solute occurs.

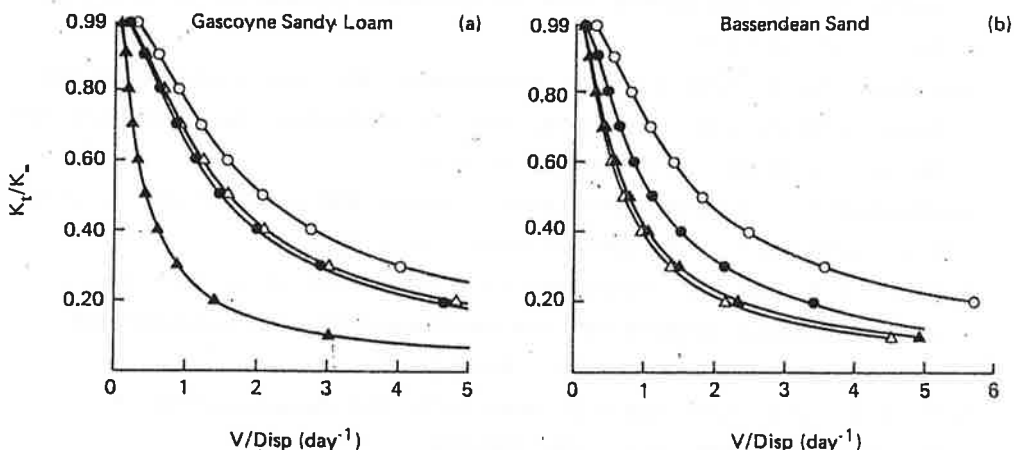


Figure 3. Effect of pore water velocity (V) on distribution (K_t/K_∞) of pesticides in soil. The pore water velocity is expressed relative to dispersivity ($V/Disp$) and the distribution relative to the equilibrium value approached at $t = \infty$ ($V \rightarrow 0$). Diquat -- \circ ; Simazine-- Δ ; Phenamiphos-- \bullet ; and Linuron-- \blacktriangle

The time necessary to attain complete longitudinal mixing at a pore water velocity V is then $Disp/V$. The value of the dispersion length in the literature for sand/sandy loam varies from 0.2 mm to 7.9 cm (Rose 1977). In surface soils of Western Australia used in the study, the value of $V/Disp$ can range from 0.1 to 10.0 day^{-1} showing that significant departure from equilibrium distribution is possible during pesticide transfer.

REFERENCES

- Barrow, N.J. and T.C. Shaw 1979. Effects of solution: soil ratio and vigour of shaking on the rate of phosphate adsorption by soil. *Soil Sci.*, 119: 167-177.
- Bettenay, E., J. Keay and H.M. Churchward 1971. Soils adjoining the Gascoyne River near Carnarvon, Western Australia. *Soil and Land Use Series 51, CSIRO, Melbourne, Australia.*
- Graham-Bryce, I.J. 1972. Herbicide movement and availability in soils. *Proc. 11th Brit. Weed Control Conf.*, 3: 1193-1195.
- Huber, J.F.K. and R.G. Gerritse 1971. Evaluation of dynamic gas chromatographic methods for the determination of adsorption and solution isotherms. *J. Chrom.*, 58: 137-158.
- Lott, P.F., J.W. Lott and D.J. Doms 1978. The determination of paraquat. *J. Chrom. Sci.*, 16: 390-395.
- McArthur, W.M. and E. Bettenay 1974. Development and distribution of soils of the Swan Coastal Plain, Western Australia. *Soil Publ. 16 CSIRO, Melbourne, Australia.*
- Murali, V. and L.A.G. Aylmore 1983. Competitive adsorption during solute transport in soils: 3. A review of experimental evidence of competitive adsorption and an evaluation of simple competition models. *Soil Sci.*, 136: 279-290.
- Rose, D.A. 1977. Hydrodynamic dispersion in porous materials. *Soil Sci.*, 123: 277-283.
- Vickery, T.M., D.L. Karlesky and G.L. Blackmer 1980. Colorimetry and high performance liquid chromatography of atrazine residues in soil: comparison of methods. *J. Assoc. Off. Anal. Chem.*, 63: 507-510.
- Yaron, B., Z. Gerstl and W.F. Spencer 1985. Behaviour of herbicides in irrigated soils. In: *Advances in Soil Science*, B.A. Stewart (ed) Springer-Verlag, New York, Vol.3 pp. 121-211.

**Application of computer assisted tomography (CAT) scanning
in the study of soil-plant-water systems**

**IASTED Inter. Symp. on Signal Processing and its Applications,
507-512.**

Law, K.T., Hainsworth, J.M., Aylmore, L.A.G. and Attikouzel, Y

APPLICATION OF COMPUTER ASSISTED TOMOGRAPHY (CAT) SCANNING
IN THE STUDIES OF SOIL-PLANT WATER RELATIONS

K. T. Law^{*}, J.M. Hainsworth^{**}, L. A. G. Aylmore^{**} and Y. Attikiouzel^{*}

Joint contribution from:

^{*}Department of Electrical & Electronic Engineering
and

^{**}Soil Science and Plant Nutrition, School of Agriculture
University of Western Australia

ABSTRACT

Until recently, no experimental technique has been capable of measuring spatial distribution of soil water content in a continuous and non destructive manner. Previous techniques have been either destructive and hence lacked continuity, perturbed the sensitive balance of the specimen under examination, were too slow in their response time or simply lacked the dimensional resolution for meaningful definitions of the soil water content distributions. The ideal technique for measuring soil water content should clearly be both non destructive and have sufficient sensitivity to follow the water content variations of less than 0.2% over the distances of a few millimetres.

Until 1970, a similar problem existed in diagnostic radiology in seeking to obtain non destructive representations of the human brain. This problem has been overcome with the aid of Computer Assisted Tomography (CAT) scanning using X-rays, and a commercially available CAT scanner has been used to measure spatial distributions of soil water content. However, the cost of these commercial X-ray CAT scanners is prohibitive, and they are unlikely to be generally available for studies of soil water content distributions. As gamma radiation has been frequently used for measurement of bulk soil water content, there appears no reason why the CAT technique could not be applied to gamma ray attenuation measurements of soil water content.

This paper describes the design and implementation of a prototype gamma CAT scanner, named Mini CAT, and gives an overview of the hardware and software of the Mini CAT system. In particular, the various image reconstruction algorithms and their performances are compared. A comparison of the results obtained using the Mini CAT system and a commercially available X-ray CAT scanner showed that the accuracy of the Mini CAT system was comparable to that

of the X-ray system, and was capable of distinguishing differences in soil water content of 0.009g/cm^3 over distances of 2mm. Applications of the Mini CAT system to studies of soil-plant water relations, soil wetting agents and soil structure showed that the applications of CAT to gamma ray attenuation will become a major tool in soil physics, allowing detailed examination of soil physical properties on a micro scale never achieved before.

Introduction

An appreciation of the physical, chemical and biological factors determining the supply, availability, status and movement of water in plant ecosystem, is essential to the understanding of the mechanism and dynamics of water in soils and their biological implications. The importance of this field of study cannot be over emphasized in semi-arid environments. In these environments, the availability of scarce water resources for agriculture necessitates its most efficient utilization. Limits of plant growth and production are most commonly set by limitations on our knowledge of such factors.

Until recently, the main obstacle to such studies was the lack of experimental technique capable of measuring the spatial distribution of soil water content in a continuous and non-destructive manner or with sufficient resolution for meaningful definition of water content distributions [1]. Until 1970, similar problems existed in diagnostic radiology in seeking to obtain non-destructive three dimensional representation of the human brain. This problem was essentially overcome by Hounsfield [2], who developed the technique known as Computer Assisted Tomography (CAT). Since that time, many CAT scanners have been constructed for both medical and industrial applications. Most commercially available CAT scanners use the measurement of linear attenuation coefficients of X-rays in a slice to reconstruct the image. X-ray CAT scanners are capable of detecting differences in attenuation as low as 0.1% over distances of a few millimetres.

Recently, Hainsworth and Aylmore [3] used an X-ray CAT scanner to determine the spatial changes in soil water content and reported its potential

for soil water studies. However, the cost of commercially available scanners precludes their use by soil and plant scientists.

As the change in the attenuation of gamma radiation has been frequently used to determine the soil water content [4], it should be equally possible to apply the CAT technique using a considerably cheaper gamma system to determine the spatial variation of soil water content.

This paper gives an overview of the various CAT techniques and also describes a prototype system named "MINICAT" that was constructed to investigate the possibility of applying the CAT techniques to soil water studies.

Theory Of CAT

The object under CAT examination may be modelled by an $(M \times M)$ matrix consisting of uniform pixels. The purpose of CAT is to determine the density, $\mu(x,y)$ of each pixel.

The principal idea of tomography is the intersection of an image plane with rays not from above but from the side! An X-ray or gamma pencil beam with incident intensity I_0 is confined to the wanted slice and the intensity of the transmitted ray, I , is measured by a detector at the other side of the slice (see Figure 1). Both the source and detector translate linearly along the image plane so that the beam is shifted parallel in steps of distance Δr . At each step the attenuation or the "raysum" is calculated,

$$p(r,\varnothing) = -\ln(I/I_0) \quad (1)$$

For a specified r and \varnothing shown in Figure 1, p is called the "raysum". A set of linear raysums at a specified angle \varnothing is known as a projection or profile.

After one linear scan is completed, the direction of the beam, \varnothing , is changed by an angle

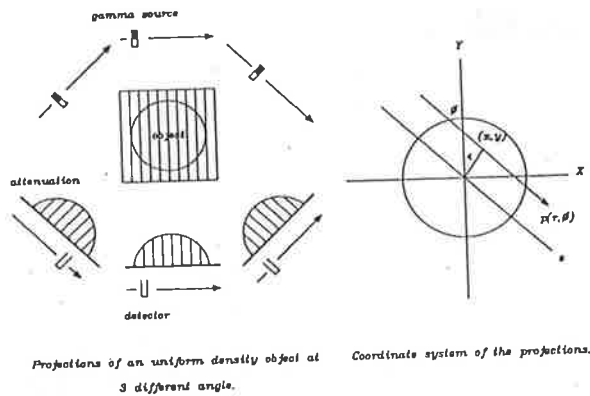


Figure 1

$\Delta\theta$. Successive scans are made in M different direction within the half circle.

$$\Delta\theta = \pi/M \quad (2)$$

Using the model of an $(M \times M)$ matrix of pixel with density, $\mu(x,y)$, the raysum can be represented by the line integral along the ray (Figure 1)

$$p(r,\theta) = \int_{r,\theta} \mu(x,y) ds \quad (3)$$

Image Reconstruction Algorithms

There are a large number of techniques for image reconstruction from projections. However, they can be classified broadly into three methods:

i) Direct Back Projection

This method was used by Oldendorf [4] and others [5-6]. The back projected pixel value is obtained by superimposing projections together and is given by:

$$\mu(x,y) = \sum_{i=1}^M p(r_i, \theta_i) \Delta\theta \quad (4)$$

with $r_i = x \cos \theta_i + y \sin \theta_i$ being the distance of the ray from the center ray, and θ_i the projection angle of the i th projection.

However, images reconstructed using direct back projection may have "star-artifacts" due to the point spreading function resulting from objects of high density (Figure 2). The star artifact causes the density function to vary from the true density function by an intolerable margin, hence this method is rarely used nowadays.

ii) Iterative Reconstruction

There are three well known iterative reconstruction techniques

- a) Algebraic Reconstruction (ART) [2]
- b) Iterative Least Square Techniques (ILST) [7]
- c) Simultaneous Iterative Reconstruction (SIRT) [8]

The ART technique is the most efficient of these methods but it is also the most susceptible to noise [9]. Also, iterative methods are considerably slower than other methods, hence are not popular.

iii) Analytical Reconstruction

The star-artifact of an image reconstructed by the direct back projection method may be described by a convolution of the correct image function $\mu(x,y)$ with another function which represent the background blurring star-function S .

$$\mu(x,y) (X) S = \mu_b(x,y) \quad (5)$$

where $\mu_b(x,y)$ is image function obtained by Direct Back Projection.

Equation (5) suggest that the star-artifact can be eliminated if a correction filtering is applied to the projections before the Back Projection process. The correction filtering process required is effectively the convolution of the inverse Fourier Transform of the star-function, S , with the image obtained from Direct Back Projection, $\mu_b(x,y)$.

The process of obtaining the filter function which removes the star artifact is strictly an analytical approach, hence the name Analytical Reconstruction.

In Analytical Reconstruction, the projected profiles $p(r,\theta)$ are filtered before they are Back Projected i.e. the reconstructed density function $\mu(x,y)$ is analogous to equation (3) except that p is replace by the filtered version p^* ,

$$\mu(x,y) = \sum_{i=1}^M p^*(r_i, \theta_i) \Delta\theta \quad (6)$$

A number of filtering techniques have been developed. Derivation of the formulae for the different filters can be found in Brooks and Di Chiro [10]. Of all the filtering techniques, currently in use, the Bracewell's Convolution Filtering is the most popular filtering method. The formula for Bracewell's Filtering [11] is

$$p^*(r_k, \theta) = \frac{p(r_k, \theta)}{4W} - \frac{1}{\pi^2 W} \sum_{j=1, \text{odd}}^L \frac{p(r_j, \theta)}{(k^2 - j)^2} \quad (7)$$

where W is the distance between two pixels and L is the number of linear raysums in a projection.

An approximation is necessary because for a given projection angle, the filtered profile p^* is only calculated at discrete points r_k , with $1 \leq k \leq L$, so that the values are not available at arbitrary values of r as required by equation (7). Linear interpolation between the two nearest values of p^* has to be performed i.e.

$$p^*(X) = p^*(IX) + [p^*(IX+1) - p^*(IX)] * (X - IX) \quad (8)$$

where $IX < X < (IX+1)$ and IX and (IX+1) are the closest integer to X.

Of all the image reconstruction algorithms, Filtered Back Projection using Bracewell's Convolution Filter is the most commonly used technique in CAT scanners and was also chosen as the reconstruction method used for the MINICAT system.

Computation Of Water Content

The result of a CAT scan and the image reconstruction is in the form of an (M x M) matrix of numbers which represent the linear attenuation coefficients, $\mu(x,y)$, of a specified location described by the cartesian coordinates (x,y).

For the case of wet soil the attenuation μ can be expanded into

$$\mu_{wet} = \mu_s \rho_s + \mu_w \theta_v \quad (9)$$

where μ_s , μ_w are the mass attenuation coefficients of soil and water respectively; ρ_s and θ_v are the soil bulk density and water content respectively.

When the soil is dry, $\theta_v = 0$ and

$$\mu_{dry} = \mu_s \rho_s \quad (10)$$

Thus the water content can be determined by subtracting equation (10) from equation (9). Therefore, the spatial distribution of water content in a column of soil can be determined from the results of two CAT scans, one of the dry soil and the other of wet soil.

The Prototype Scanner - MINICAT

A prototype CAT system named MINICAT was constructed to explore the potential of CAT in soil science research. Gamma radiation was chosen as the source of radiation in preference to the much more expensive and hard to maintain X-ray system. Figure 3 shows the schematic representation of the MINICAT system.

The main body of the scanner consists of two parts :

- a) the Gamma Platform - which provides the vertical scanning motion and
- b) the Catscan Platform - which provides the linear translation and rotational motion required in a CAT scan procedure.

The gamma source is mounted in a lead container mounted directly opposite the detector on the Gamma Platform. The Catscan Platform is placed at a fixed level in the middle of the Gamma Platform such that the Gamma Platform can move independently of the Catscan Platform, therefore providing the vertical scanning motion. Three stepper motors were used together with worm drive shafts to provide the scanning motion required.

As shown in Figure 3 an enhanced XT compatible personal computer (PC-EXT) was used for performing the task of controlling the scanning motion, acquiring the data from the radiation measurement system, processing the data and finally presenting the results in graphics form and producing hardcopies of the results.

Raysums Acquisition

Caesium 137 (Cs137) and Americium (Am-241) are the main gamma sources used in the MINICAT system. A plastic scintillation detector is used to measure the radiation intensity. The signal from the plastic scintillation detector is amplified through a photo-multiplier tube under extra high tension (EHT) voltage and then further amplified by a fast amplifier. The output is then passed through a window discriminator to select only pulses of a specific range of energy for recording. This discrimination is essential, as the energy distribution function of the gamma rays is not an impulse function. If this filtering is not done then the measured attenuation will not have a linear relationship with the thickness of object under examination. This is because lower energy radiation is absorbed in preference to higher energy pulses giving rise to the phenomenon known as *beam hardening*. The window discriminator helps to minimise the effect of beam hardening in the measurement of raysum.

The output of the discriminator is connected to a scaler to record the number of pulses which is the measure of beam intensity. The scaler is interfaced to the computer, PC-EXT, through the CAT Controller Card (Figure 3) allowing full control from the computer.

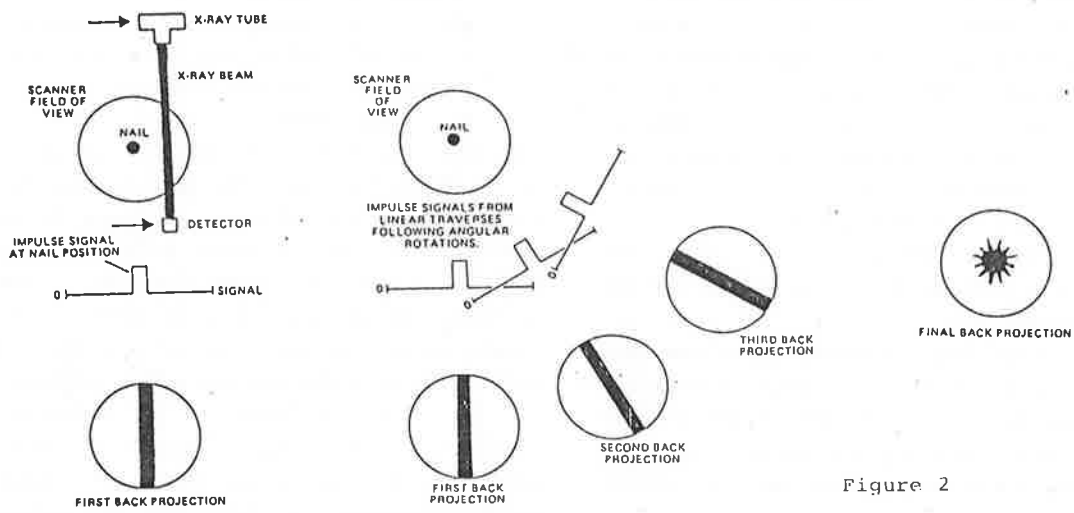


Figure 2

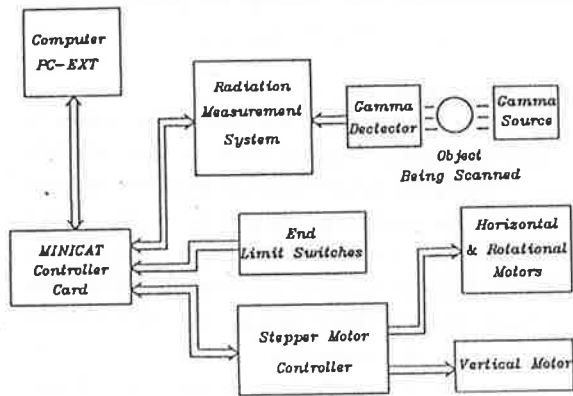


Figure 3 Block Diagram of MINICAT System

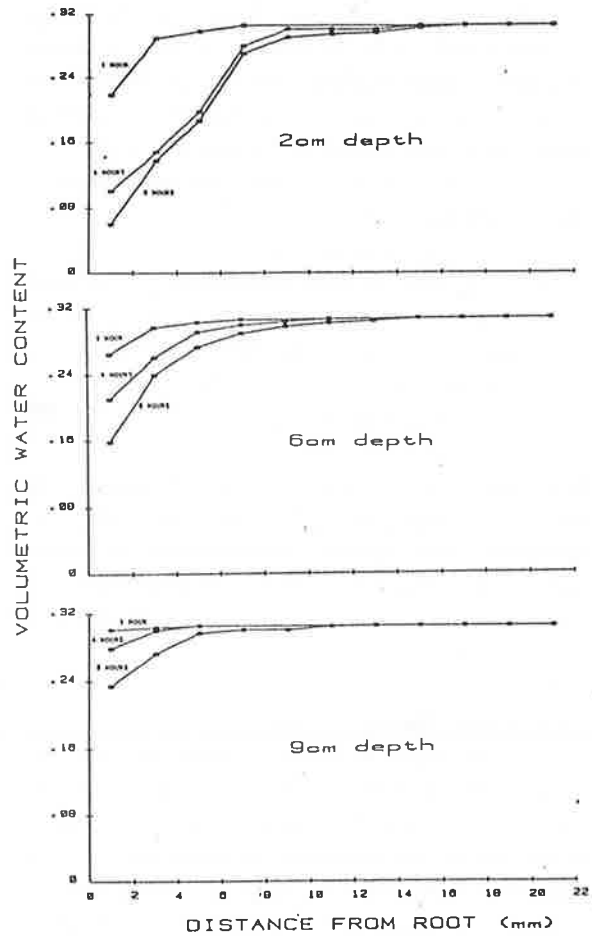


Figure 4

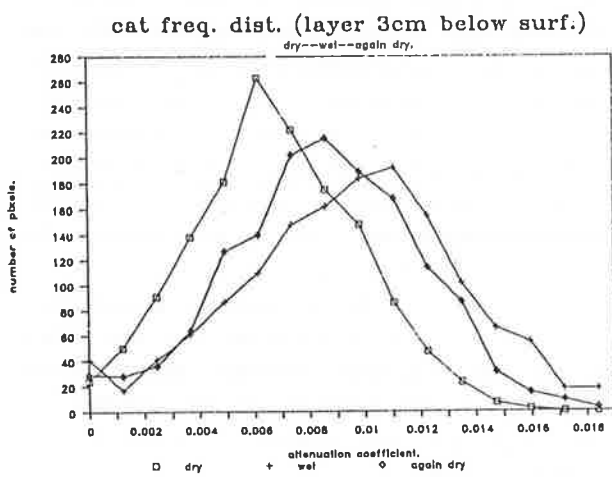


Figure 5

Facilities and Capabilities of MINICAT system

The MINICAT system has been designed to run under two modes:

- 1) Menu-driven mode - which is a user-friendly approach, allowing user interactive control and
- 2) Program mode - a language interpreter known as Language For Advance Gamma Attenuation Scan (LAGAS) which has also been developed to make the MINICAT system, a fully programmable and flexible system.

With the configuration of MINICAT, the system is currently capable of performing five different tasks:

- a) Vertical Up-down Scan. This scan has two uses: one is for determining the bulk density of soil and the other is to determine the velocity of a water front passing down a soil column i.e. chasing the water front,
- b) Stationary Time Scan - which can be used for determining the rate of water uptake by plant roots at a specific location,
- c) CAT scan,
- d) Successive CAT scan - which allows multiple CAT scans to be performed at different levels of the column, thus enabling a three dimensional water distribution in the column of soil to be determined and
- e) any combination of (a)-(d).

Applications of MINICAT

Application of CAT requires that the attenuation of gamma ray source remains linear with distance. With suitable setting of the discriminator this was achieved with the Cs-137-plastic scintillation detector. Subsequently, the MINICAT system has been used in three major studies of soil and soil plant water phenomenon.

Using the MINICAT system a soil water dispersion index (SOWADIN) has been developed to measure the effectiveness of soil wetting agents applied to non wetting soils. In this case the MINICAT system is used to determine the number and size of wet areas within a soil column several hours after water has been applied to it.

A major limitation in understanding the mechanisms of soil water extraction by plant roots

was the inability to directly measure the change in soil water content with distance away from the root in a non-destructive manner. Figure 4 shows the drawdowns in soil water content along a single plant root and how they change with time obtained by the MINICAT system, and represent the most detailed observations of water extraction by a plant root yet made.

Changes in soil structure are important in determining the availability of soil water to plants, for example, collapses in the structure, result in the destruction of soil macro pores which is important in the infiltration of water into soil. The MINICAT system has been used to monitor the changes in soil structure with subsequent wetting to and drying cycles. Figure 5 shows a greater number pixels having a higher attenuation coefficient after one wetting drying cycle indicating that the soil structure is deteriorating.

Conclusion

The application of CAT technique to soil and soil water studies has made available invaluable data, not possible in the past. For example, its ability to elucidate the mechanisms involved in the uptake of water by plant roots, and in particular to resolve the major controversies surrounding the physics of the process [12].

REFERENCES

1. So, H.B., Aylmore, L.A.G., and Quirk, J.P. (1976): Measurement of Water Fluxes In A Single Root System. I. The Tensiometer-potometer System, *Plant Soil*, 45, 577-94.
2. Hounsfield, G.N.A.(1972), *Method of and Apparatus for Examination of body by radiation such as X-ray and Gamma Radiation*, British Pattern Np. 12883915, London.
3. Hainsworth, J.M. and Aylmore, L.A.G.(1983), The Use of Computer Assisted Tomography to Determine Spatial Distribution of Soil Water Content, *Aust. J. Soil Res.*, 21, 435-43
4. Oldendorf, W.H.(1961), Isolated Flying Spot Detection of Radiodensity Discontinuities Displaying The Internal Structural Pattern of A Complex Object, *IRE Trans. Bio.-Med. Elec., DME*, 8, 68-72.

5. Kuhl, D.E. and Edwards R.Q.(1963), Image Separation Radio-isotope Scanning, *Radiology*, 80, 653-661.
6. Kuhl, D.E, Hale, J. and Eaton W.L.(1966), Transmission Scanning: A Useful Adjunct of Conventional Emission Scanning for Accurately Keying Isotope Deposition to Radiographic Anatomy, *Radiology*, 87, 278-284.
7. Coitin, M.(1972), Three Dimensional Density Reconstruction From A Series of Two Dimensional Projections, *Nucl. Instr. and Meth.*, 101, 509.
8. Gilbert, P.F.C.(1972), Iterative Method For The Reconstruction Of Three Dimensional Objects from Projections, *J. Theor. Biol.*, 36, 105-117.
9. Herman, G.T., Gabor, T. and Rowland, S.W.(1973), Three Methods For Reconstructing Objects From X-rays: a comparative study, *Computer Graphics and Image Processing*, 2, 151-178.
10. Brooks, R.A. and Di Chiro, G.(1976), Principles of Computer Assisted Tomography (CAT) in Radiographic and Radioisotopic Imaging, *Phys. Med. Biol.*, 21, 5, 689-732.
11. Bracewell, R.N. and Riddle, A.C.(1967), Inversion of Fan-beam Scans in Radio Astronomy, *Astrophysics J.*, 150, 427.
12. Molz, F.J.(1976), Models of Water Transport in the Soil Plant System, *A Review Water Resources Res.*, 17, 1245-1260.

**The quantitative characterisation of soil physical status and potential behaviour
- A fundamental approach**

**Natl. Symp. on the Effects of Management Practices on Soil Physical Properties
Toowoomba, Qlds., Sept., 1987: 200-203. (Invited Paper)**

L.A.G. Aylmore and H.R. Cochrane

THE QUANTITATIVE CHARACTERISATION OF SOIL PHYSICAL STATUS
AND POTENTIAL BEHAVIOUR - A FUNDAMENTAL APPROACH

L. A. G. Aylmore and H. R. Cochrane

Soil Science and Plant Nutrition, University of Western Australia, Perth.

The major impediment to progress in understanding the physical behaviour of agricultural soils and in using that knowledge to formulate appropriate management strategies for any given soil, lies in the failure to develop a systematic, coherent and comprehensive methodology for quantitatively characterising and classifying the physical status and potential behaviour of soils. Such a system requires the use of parameters which while relating directly to plant requirements, hydrology, soil susceptibility to degradation, erosion etc. on the one hand, are adequately defined in terms of their dependence on the basic properties of the soil constituents on the other.

Traditional procedures for characterising soil structure and classifying soils, owe their origins to a more descriptive than quantitative era and area of investigation. In the main existing parameters (for example soil texture, water stable aggregation) are technically inconvenient, numerically cumbersome, poorly defined in fundamental terms or poorly definitive in terms of any practical classification of soil physical behaviour. In particular there is little uniformity or agreement in practice as to the most appropriate parameters to use in characterising the structural properties of a soil. Soil structure assessment frequently involves considerations not only of the physical configuration of the soil matrix at any time but of its susceptibility to disruption by wetting and mechanical forces.

In sandy soils of low colloid content, physical assessment procedures are not generally concerned with the degree of development of secondary structural units or the stability of the soil matrix. The major management induced problem is the development of tillage or traffic induced compaction pans. For soils susceptible to this form of structural degradation, measurements of penetration resistance provide the most effective and sensitive method of assessment. In most other soils however the presence of various amounts of colloidal constituents dominates and complicates the physical behaviour. In these circumstances the stability of the soil matrix and changes in structural configuration produced by processes of wetting and drying, become major considerations.

On wetting a soil matrix the two major mechanisms which act to disrupt the matrix structure are (1) non-dispersive failure associated with mechanisms such as the explosive compression of entrapped air in pores and (2) differential swelling and dispersion associated with diffuse double layer development on the clay surfaces (dispersive failure). On drying, the matrix formed depends on the extent of this previous disruption but also on other rheological properties of the colloidal constituents. Thus the most appropriate method for assessment for soils of sandy loam and heavier texture will depend upon the relative importance of these factors.

In the absence of any modifying factors eg. bonding or cementing agents, swelling and dispersion of colloidal systems such as the clay minerals, are reasonably well defined and can be related directly to the specific surface area, surface density of charge, nature of the exchangeable cation and electrolyte concentration (Verwey and Overbeek 1947; Aylmore and Quirk 1962). Consequently for such soils where colloidal properties dominate, there have been a number of attempts with varying success in recent years to develop assessment criteria based on the susceptibility of the clay and silt fractions to dispersion (Quirk and Schofield 1955; Emerson 1967; Rengasamy et al. 1984). Such criteria are likely to be most successful when applied to soils containing higher clay contents or more active clay minerals such as the smectites since for these materials swelling and dispersion will largely determine the matrix configuration.

For soils of low to moderate colloid contents, there is evidence that swelling and dispersion while still operative, have less influence on the net physical properties than more mechanical factors such as particle to particle interaction, packing facility etc.. For such soils measurements of dispersible clay do not necessarily provide a reliable guide to physical properties or potential physical behaviour and alternative assessment methods are required.

For soils from the WA wheatbelt in the sandy loam to clay loam textural classes and where kaolinite is the dominant clay mineral, measurements of modulus of rupture-exchangeable sodium percentage relationships (MOR-ESP) have proved a reliable guide to field behaviour for example gypsum responsiveness (Aylmore and Sills 1982; Aylmore and Cochrane 1986). This is because the development of dry strength in soils subjected to this testing procedure is dependent on the same mechanisms and forces within the soil as are responsible for the strength characteristics of soils in the field. Non-dispersive failure and other rheological properties of the colloidal constituents appear to be the controlling factors. Because they are determined by similar features of the soil matrix, hydraulic conductivity, gaseous transfer and to some extent water retention, correlate closely with this measurement of friability or strength.

Incorporation of the effects of exchangeable sodium percentage on the MOR into the testing procedure (Figure 1), appears to provide a valuable distinction between the consequences of mechanical disruption of the matrix structure by explosive compression of entrapped air (described as incipient failure by Quirk and Panabokke (1962) and the effects of swelling and dispersion.

The Baseline MOR or soil strength when ESP is zero, by and large represents the reaction of the matrix to the incipient (non-dispersive) failure process. Dispersion and swelling are at a minimum or non-existent under these conditions of testing (calcium saturated) and the Baseline MOR is essentially insensitive to changes in electrolyte concentration.

The Sodium Sensitivity or slope of the MOR-ESP relationship, on the other hand depicts clearly the rapid increase in dispersion and swelling forces associated with increasing sodium on the exchange complex. When not controlled by other bonding materials this dispersive failure is very sensitive to electrolyte concentration.

Figure One

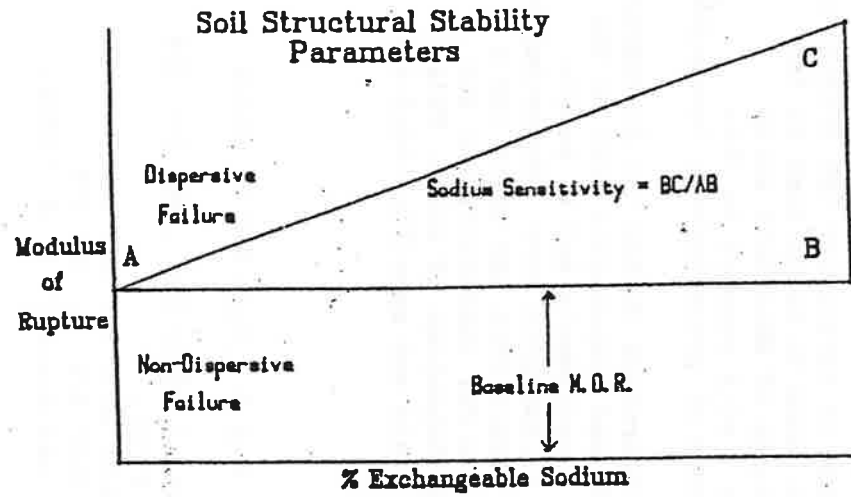


Figure Two

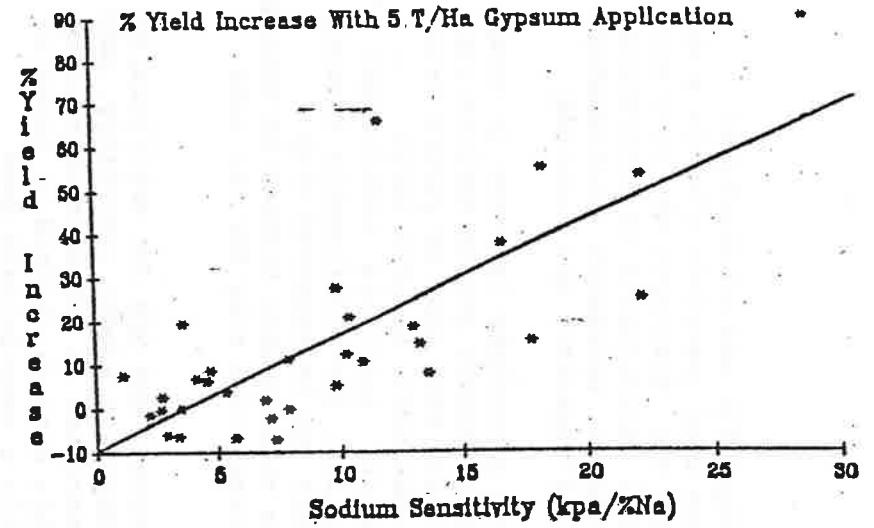


Figure Three

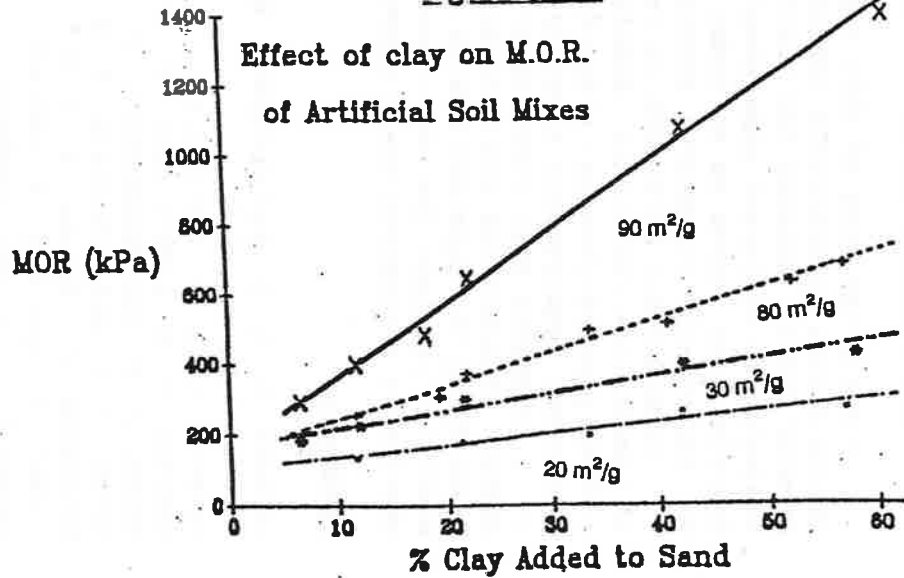
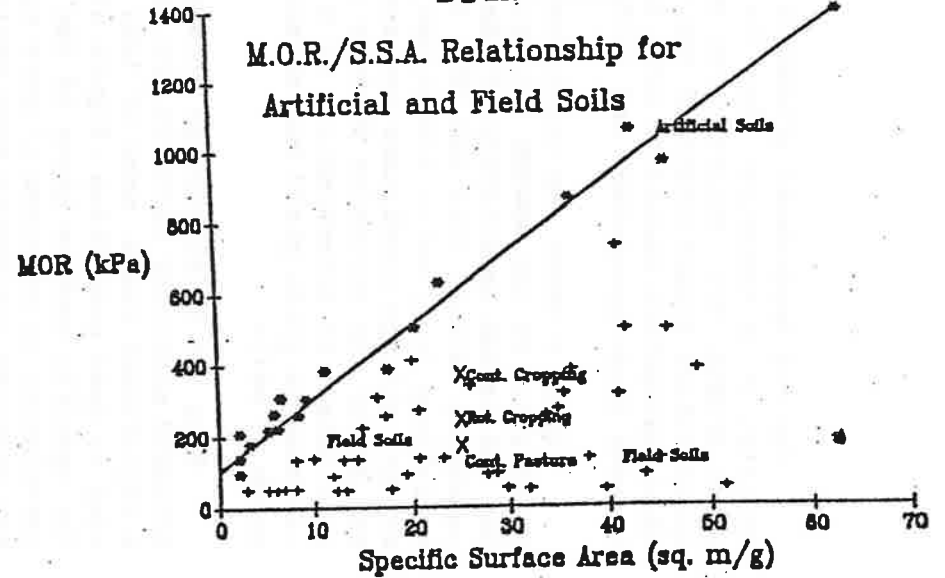


Figure Four



For any assessment procedure to be meaningful and of practical utility, it is essential that the parameters used correlate closely with plant growth, soil conservation determinants etc. Similarly the role and quantitative significance of the various soil constituents in determining these parameters should be well defined, that is, benchmark relationships between these parameters and surface physical chemistry are required.

Figure 2 shows the relationship between percentage increase in wheat grain yield in the season following a 5 tonne/hectare gypsum application and the sodium sensitivity of the surface soils from some 32 gypsum trials conducted between 1982 and 1985 in the WA wheatbelt. Despite large variations in climatic conditions, crop density, cultivars, nutritional status, tillage conditions and weed competition, the relationship accounts for 60% of the variation between trials. This can be compared with a coefficient of determination of 0.10 in the relationship between percentage increase in grain yield and mechanically dispersible clay for the same group of soils.

When the relationships between clay content and MOR for artificially prepared sand-clay mixtures are examined there are almost invariably, over a significant range, more or less linear increases in MOR with increasing clay to sand proportion (Figure 3). When this data is plotted in terms of the specific surface areas of the whole soils a surprisingly good correlation is obtained (Figure 4) for the limited number of materials so far examined (including both kaolinite and illite clays). This benchmark relationship obtained on reconstructed soils, can be viewed as indicative of the properties of the completely degraded soils devoid of any secondary structural organisation or stability.

Clearly the form of this relationship and in particular the effects of cation status, electrolyte concentration etc. need to be defined in far greater detail. However the positions of a range of wheatbelt soils subjected to different management procedures, with respect to this degraded line, serve as an index to their state of grace between favourable and unfavorable structural conditions.

Considerably more work is required to rigorously define the dependence of penetration resistance, modulus of rupture and dispersible clay on the surface physico-chemical properties of soil constituents and to relate management requirements directly to them as illustrated here. Nevertheless it is suggested that these three parameters should form the basis for a modern, standardised and more scientific system for characterising and classifying the physical status and potential behaviour of soils. This would not preclude the use of more detailed field and specific localised assessment procedures where appropriate.

REFERENCES

- Aylmore, L. A. G. and Cochrane, H. R. (1986) N.Z.S.S.S./A.S.S.S. Joint Conf. Rotarura, N.Z.
- Aylmore, L. A. G. and Sills I. D. (1982) *Aust. J. Soil Res.*, 20: 213-224.
- Emerson, W. W. (1967) *Aust. J. Soil Res.* 7: 47-57.
- Quirk, J. P. and Panabokke C. R. (1962) *J. Soil Sci.* 13: 60-70.
- Quirk, J. P. and Schofield, R. K. (1955) *J. Soil Sci.* 6: 163-178.
- Rengasamy, P., Greene, R. J. B., Ford, G. W. and Mikanni, G. H. (1984) *Aust. J. Soil Res.* 3: 493-497.
- Verwey E. J. W. and Overbeek, J. Th.G. (1948) *Theory of the stability of the lyophobic colloids*, Elsevier Publ. Co. Inc., London.

An Electrophoretic Mobility Study of Uric Acid with Special Reference
to Kidney Stone Formation

J. H. ADAIR,* L. A. G. AYLMOORE,* J. G. BROCKIS,† AND R. C. BOWYER‡

**Soil Science and Plant Nutrition, †Department of Surgery, and ‡Department of Clinical Biochemistry, University of Western Australia, Nedlands, Western Australia 6009*

An Electrophoretic Mobility Study of Uric Acid with Special Reference to Kidney Stone Formation

J. H. ADAIR,* L. A. G. AYLMOORE,* J. G. BROCKIS,† AND R. C. BOWYER‡

*Soil Science and Plant Nutrition, †Department of Surgery, and ‡Department of Clinical Biochemistry, University of Western Australia, Nedlands, Western Australia 6009

Received May 6, 1986; accepted July 27, 1987

Particle electrophoretic mobility measurements were used to determine ζ potentials of uric acid as a function of concentration for various ionic species found in human urine. Uric acid ζ potentials are qualitatively described as a function of solution pH in a synthetic urine. A theoretical model is proposed to describe the mechanism of uric acid surface-charge formation in terms of the monoprotic surface group model of T. W. Healy and L. R. White [*Adv. Colloid Interface Sci.* **9**, 393 (1978)]. © 1988 Academic Press, Inc.

INTRODUCTION

Uric acid is a common constituent of human kidney stones (Fig. 1) (1). Coagulation of particles in urine has often been proposed as part of the mechanism of stone formation (2–4). The role of ionic crystal growth inhibitors or promoters present in urine is also thought to be mediated by chemical adsorption of these species at crystal surfaces (5). Adsorption at crystal surfaces may also play a role in nucleation of insoluble salts of ionic species by epitaxy (6). This study was designed to determine the electrophoretic mobility (EM) of uric acid as a function of concentration for various ionic salts commonly found in human urine. The magnitude of the ζ potentials related to the EM indicates the likelihood of coagulation in a particle suspension (7). Changes in the sign of ζ potentials as a function of salt concentration are also useful in evaluating chemical adsorption of ionic species at particle surfaces (8). Thus, the influence of solution pH and common electrolytes contained in urine (such as sodium, ammonium, calcium, and magnesium chlorides) on uric acid electrophoretic mobilities was determined. The influence of pH in a complex, “synthetic” urine was also evaluated.

Another objective of this work was to develop a theoretical model to explain the variation in the ζ potential of uric acid as a function of salt concentration. Human urine has such a high ionic strength (9) that routine ζ potential determinations in it are difficult. If a suitable model were found, “theoretical” ζ potentials could be calculated for uric acid in urine. Such a model could provide guidance as to whether or not coagulation is an important mechanism in uric acid kidney stone disease. In addition, a theoretical model would help us to understand the mechanism of charge formation at uric acid surfaces. The model would indicate the most pertinent ionic equilibrium conditions in developing ζ potentials of uric acid in urine and urine-like solutions.

THEORETICAL BACKGROUND

The role of interfacial phenomena in controlling the properties of suspensions (such as rheological behavior) is well established. Increasingly sophisticated models have been developed to describe the interactions between particle surfaces and surrounding solution. The models have several common features. All models are based on formation of charge

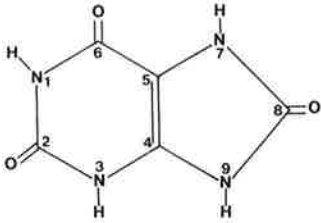


FIG. 1. Structural diagram of uric acid.

at the particle surface via one or more distinct mechanisms. The surface charge is balanced by one or more layers of counterions such that no net charge surrounds the particles. At least one counterion layer in each model is based on the analytical expression developed by Gouy (10) and Chapman (11) wherein ions are attracted solely by electrostatic forces. The Gouy–Chapman layer in most models extends at some intermediate distance into the bulk solution at infinite distance from the particle surface. The region from the particle surface to the intermediate distance at which the Gouy–Chapman layer begins provides most of the differences among models describing the solid–solution interface.

A hierarchy of increasing complexity analytically describes the nature of the interactions at solid–solution interfaces. The complexity of the model depends on the complexity of the solid and solution phases and the nature of their interactions. Accordingly, there are models as simple as the monoprotic surface group (MSG) model of Healy and White (12) and as complex as those required for oxide–water interactions where multiple counterion layers and model parameters are necessary to accurately fit analytical calculations to experimental data (13–17). The MSG model consists of (a) a mass-action equation describing the relationship among the neutral and negatively charged sites and protons at the solid surface, (b) an expression for the formation of surface charge via the loss of protons at the solid surface, and (c) the balance of the surface charge via a Gouy–Chapman counterion layer. Reactions of soluble species from the solid that lead to ionic equilibria in the bulk solution are

reconciled with surface reactions that lead to electrostatic equilibrium at the solid–solution interface.

Solid–solution systems displaying only negative or zero surface charge or potential are consistent with the MSG model. The loss of a surface proton leads to the formation of a negative surface site. If the proton is present, there is no charge and the site is neutral. There is no charging mechanism within the boundary conditions of the model discussed above for the formation of positive surface charge. The best known example of a material that displays behavior fitting that predicted by the MSG model is polystyrene (12).

An uncertainty in the MSG model is the distance from the solid surface at which to compare calculated potentials in the Gouy–Chapman layer to experimentally determined ζ potentials. ζ potentials calculated, for example, using measured electrophoretic mobilities are assumed to occur at the shear plane between moving solution and solution adhering to the particle surface. The distance from the particle surface at which the shear plane occurs is not clear. Therefore, the distance used to compare calculated potentials in the Gouy–Chapman layer to ζ potentials is rather arbitrary.

Uric acid is a naturally occurring material with many of the features common to solids in aqueous suspension whose solid–solution interfaces are most consistent with the MSG model. It is composed of adjacent pyridine and purine rings and has two dissociable protons (18, 19). The first proton dissociation constant believed to be that at Site 9 is equal to 5.46. The second dissociation constant is at 10.30. The solubility of uric acid over the pH range 2 to 5 is about $2.6 \times 10^{-3} M$. The material has a slight increase in solubility up to pH 6 (solubility equals $1 \times 10^{-3} M$). Above pH 6, the solubility increases exponentially. The increase in solubility, although slight over the pH range investigated (pH 2 to 6.5), prohibited potentiometric titrations to determine surface charge because of changes in surface area. Urate ions will precipitate with most cations

of interest including ammonium, sodium, potassium, and calcium at pH values greater than pH 7. It is believed that the stability of cation-urate complexes is low below pH 7, but only the stability constant for the sodium-urate complex (K_{sp} equal to 8.50×10^{-3}) has been determined (19). Thus, uric acid loses only one proton to any appreciable degree, does not appear to form any significant cation complexes in solution, and has low but increasing solubility over the pH range of interest, pH 2 to 6.5.

MATERIALS AND METHODS

Preparation of Uric Acid Suspensions

Commercial uric acid was purified as described by Porter (22) with the following modification. The uric acid-anhydrous sulfuric acid solution was dripped into 3°C deionized water instead of the reverse. This procedure yielded uric acid crystals with a regular flat-plate morphology instead of the poorly formed and less easily characterized dendritic shape usually encountered. Based on scanning electron microscopy examinations the plate-like particles were 2 to 20 μm across a face and 0.5 to 1.0 μm thick, giving an average particle size of about 5 μm . Recrystallization was repeated until the UV extinction at 292 nm was constant. Final extinction was $1.2174 \pm 0.0276 \times 10^4$. X-ray diffraction confirmed the powder as anhydrous uric acid. X-ray fluorescence spectroscopy of the powder gave 0.06 wt% sulfur and 0.004 wt% iron. The powder's specific surface area determined by BET analysis was $1.528 \text{ m}^2 \text{ g}^{-1}$.

To minimize bacterial degradation of uric acid, techniques used by previous investigators were employed (20–23). All suspensions were prepared using deionized water and reagent-grade chemicals. Spectroscopic analysis of the water gave no indication of the ion-exchange resins used to purify it.

Stock uric acid suspensions were prepared by adding 1.5 g powder per liter of autoclaved water. Electrolyte dilutions were added to

stock suspensions to yield 100-ml suspensions with the desired salt concentrations. Solution pH was adjusted by adding HCl or NaOH. After addition of the electrolyte, the density of the uric acid in suspension was no less than 1.48 g powder per liter, because small volumes of the stock 1 M electrolyte solutions were used to prepare the 100-ml aliquots. Electrophoretic mobilities measured for similar suspensions equilibrated from 24 to 96 h were not significantly different. Therefore, following pasteurization and sonication, suspensions were equilibrated at 38°C for 48 h prior to particle electrophoretic mobility measurements.

It is the usual practice to have an indifferent electrolyte present of sufficient concentration in suspensions to minimize changes in the ionic strength with, for example, acid or base additions. For the uric acid system there is no obvious indifferent ion that can be used to control ionic strength without possible reaction. Urate ions in solution will precipitate with most of the cations commonly used as part of an indifferent ion system. Sparingly soluble urate salts have been reported to form with ammonium, potassium, sodium, and calcium (1, 18–20, 22, 23). Therefore, the EM data are presented as a function of the added salt concentration, with the pH at which the measurement was made indicated. The ionic strengths of the suspensions were calculated using a computer program (see the description of EQUIL below) based on the acid or base additions, measured pH values, and any electrolyte additions for the theoretical calculations. This approach has been used in other surface chemical investigations where ambiguities in the complex ionic equilibria may arise with the use of electrolyte to control ionic strength (26).

A synthetic urine was prepared using a previously reported formula (9). Ionic concentrations in the synthetic urine were 4.55×10^{-2} M (ammonium), 6×10^{-4} M (calcium), 4×10^{-4} M (oxalate), and 1×10^{-4} M (pyrophosphate). Dry uric acid (0.1 g in 25 ml) was added to prepare suspensions. Suspension pH was adjusted by adding HCl or NaOH.

Electrophoretic Mobility Determinations

A particle electrophoresis apparatus Mark II (Rank Brothers, United Kingdom) was used to determine electrophoretic mobilities of uric acid particles in suspensions. Standard techniques discussed elsewhere (8, 24) were used to make the measurements. All electrophoretic mobility measurements were made using the flat cell. Electrophoretic mobilities at each electrolyte concentration were determined at least in triplicate for a minimum of 20 particles each time to obtain mean values and 95% confidence intervals using Student's *t* test.

Calculation of Ionic Strength and Equilibria

A FORTRAN version of a computer program (EQUIL) was used to calculate the ionic equilibria in uric acid suspensions (25). The calculations in EQUIL use Davies' modification to Debye-Huckel theory to calculate ionic strength and ionic equilibria. The solubility product and stability constants used in the modification are given in Table I. The pH values of uric acid suspensions required for EQUIL calculations were measured with a Beckman Model 4500 digital pH meter with a combined glass electrode calibrated with standard buffer solutions (Beckman Instruments Inc., Irvine, CA). Calculated and measured total urate concentrations determined as described by Porter (22) and Finlayson and Smith (19) were in good agreement. Stability constants for urate complexes with NH_4^+ , K^+ ,

Ca^{2+} , and Mg^{2+} are not known. Measured total urate concentrations in suspensions containing these ions indicated that cation-urate complex formation was negligible for the range of concentrations and solution pH values investigated.

RESULTS AND DISCUSSION

Experimental Findings

The EM or uric acid is most strongly influenced by solution pH. Urinary ionic species introduced as cation chloride or sodium anion salts to suspensions decrease the magnitude of EM as a function of their ionic strength when solution pH values are constant. More significantly, increased cation concentrations, including hydronium ion at low pH, do not reverse EM from negative to positive values over the range of pH values investigated, 2.0 to 6.5.

The magnitude of EM values increases with decreasing solution pH, but the polarity of EM values does not change at lower pH values. The EM magnitudes approach values near zero as a function of decreasing pH over the pH range investigated, 2.0 to 6.5.

EM as a function of solution pH in uric acid suspensions is summarized in Fig. 2. EM values decrease to a minimum of about $-6.5 \mu\text{m s}^{-1}/\text{V cm}^{-1}$ as pH values increase to about pH 5.6, then increase slightly as pH increases. The pH range studied was limited to pH 6.35 maximum because uric acid becomes much more soluble as pH exceeds this value. As solution pH decreases, ζ potentials increase until at pH 3.0 or below they are less than $1.0 \mu\text{m s}^{-1}/\text{V cm}^{-1}$. All EMs are negative from pH 2.2 to 6.35.

EM as a function of the concentration of chloride salts of Na^+ , K^+ , NH_4^+ , Ca^{2+} , and Mg^{2+} is summarized in Figs. 3 and 4. Since the EM of uric acid varies as a function of solution pH, two pH ranges are reported: pH 4.3 to 4.6 (Fig. 3) and pH 5.6 to 5.8 (Fig. 4). The pH range of each salt concentration series is given in each figure. EM magnitudes decrease as a function of salt concentration for both pH ranges. Generally, the rate of decrease

TABLE I

Uric Acid Solubility Product and Stability Constants Used to Modify Equilibrium

Solubility product (37°C)			
Phase	Equilibrium ^a	K_{so}	Reference
H_4U	$[\text{H}^+][\text{H}_3\text{U}^-]F_1^2$	9.86×10^{-10}	(18)
Stability constants			
Reaction	$K^\circ(37^\circ\text{C})$ liters mol^{-1}	Reference	
$\text{H}^+ + \text{H}_2\text{U}^{2-} = \text{H}_3\text{U}^-$	1.99×10^{10}	(19)	
$\text{Na}^+ + \text{H}_3\text{U}^- = \text{NaH}_3\text{U}$	8.50×10^{-3}	(19)	

^a F_1 is the activity coefficient of ± 1 valent species.

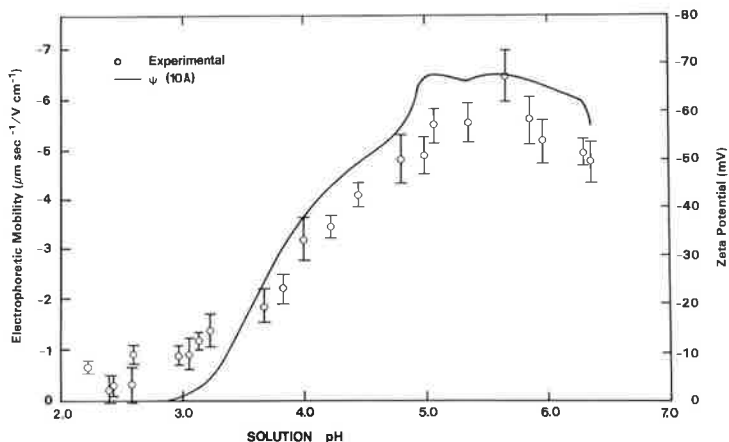


FIG. 2. EM and ζ potential of uric acid as a function of solution pH. Data points indicate experimental values. Solid line gives theoretical electric potentials 10 Å from the surface.

is greater for suspensions containing the divalent species, Ca^{2+} and Mg^{2+} . EM magnitudes in low-pH suspensions (Fig. 3) are lower than those in the higher pH range (Fig. 4). This finding is consistent with the high EM values determined at high pH values. However, the

rates of decrease for individual salts in both pH ranges are about the same.

EM as a function of sodium salts of various anions is summarized in Figs. 5–8. The effects of SO_4^{2-} and H_2PO_4^- are given in Fig. 5. As with the cation chloride salts, EM magnitudes

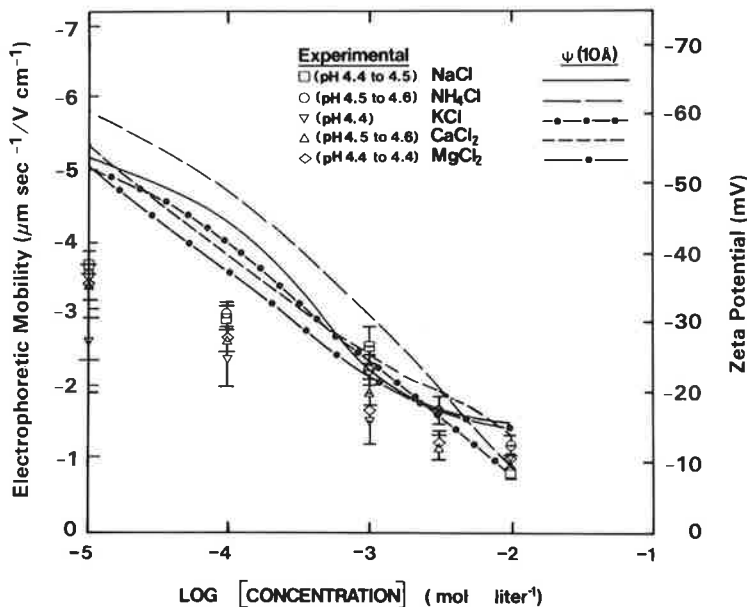


FIG. 3. EM and ζ potential of uric acid as a function of the concentration of various cation salts of chloride for solution pH 4.3 to 4.6. pH ranges for individual salts are indicated in the figure. Data points are experimental values. Lines indicate $\psi(10 \text{ \AA})$.

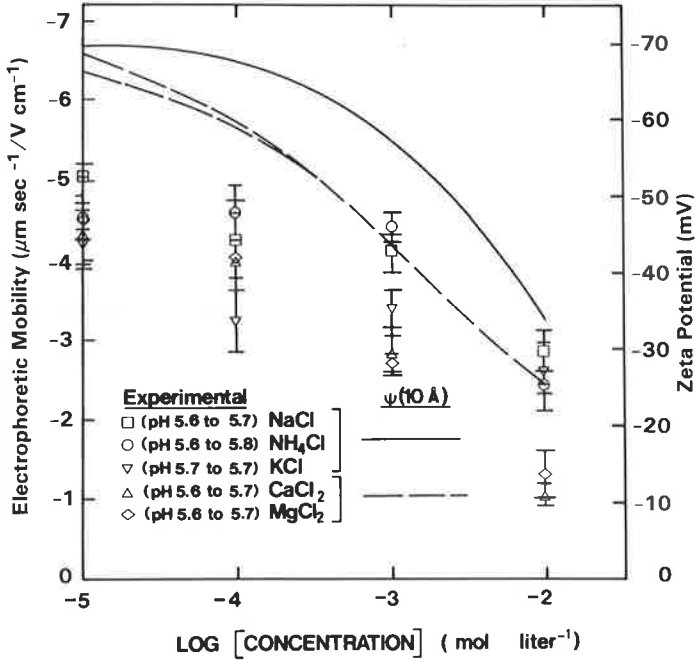


FIG. 4. EM and ζ potential of uric acid as a function of the concentration of various cation salts of chloride for solution pH 5.6 to 5.8. pH ranges for individual salts are indicated in the figure. Data points are experimental values. Lines indicate $\psi(10 \text{ \AA})$.

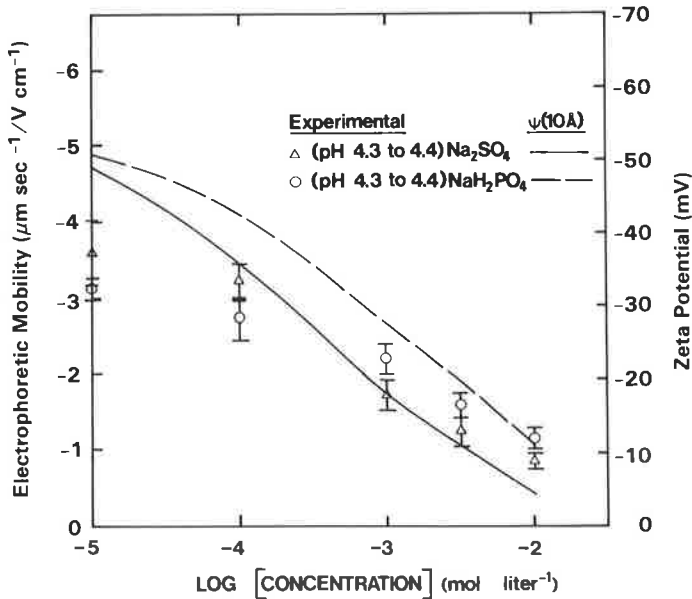


FIG. 5. EM and ζ potential of uric acid as a function of Na_2SO_4 and NaH_2PO_4 concentrations. pH ranges are indicated in the figure. Data points give experimental values. Lines give $\psi(10 \text{ \AA})$.

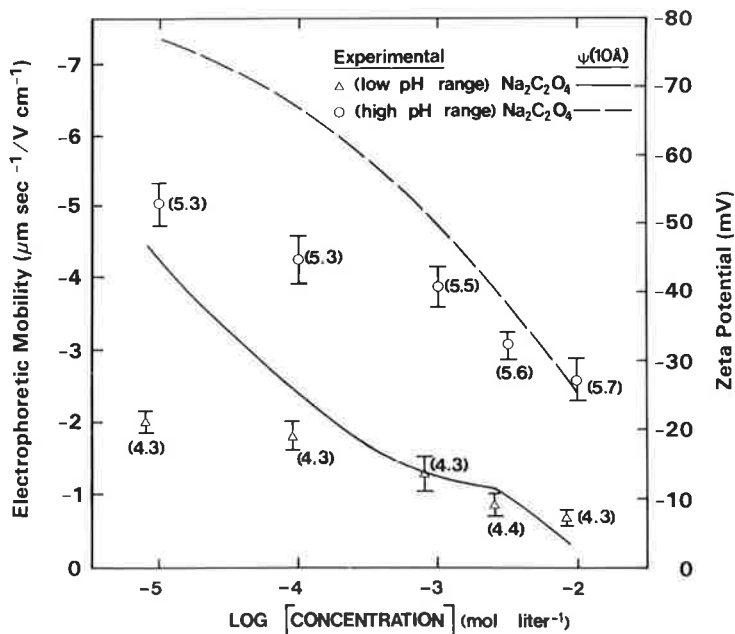


FIG. 6. EM and ζ potential of uric acid as a function of sodium oxalate concentration. Two pH ranges are given: (low) pH 4.3 to 4.4 and (high) pH 5.3 to 5.7. Data points give experimental values. Lines give $\psi(10 \text{ \AA})$.

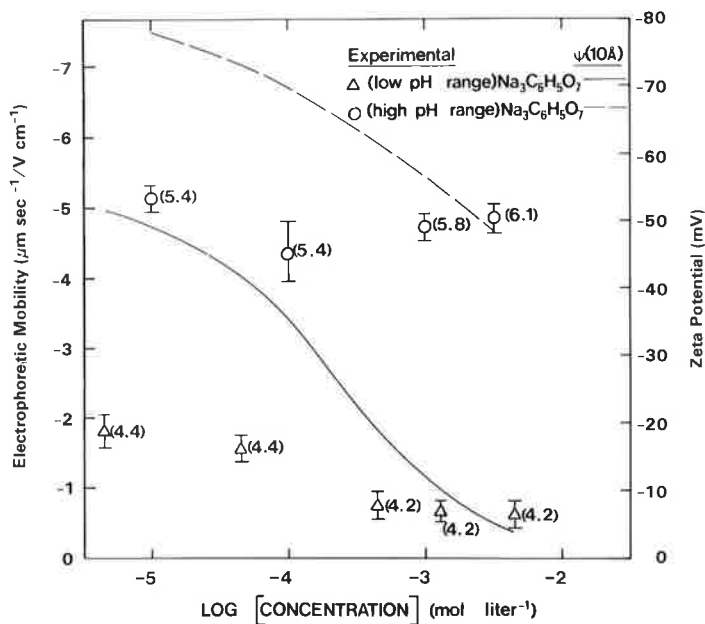


FIG. 7. EM and ζ potential of uric acid as a function of sodium citrate concentration. Two pH ranges are given: (low) pH 4.2 to 4.4 and (high) pH 5.4 to 6.1. Data points are experimental values. Lines give $\psi(10 \text{ \AA})$.

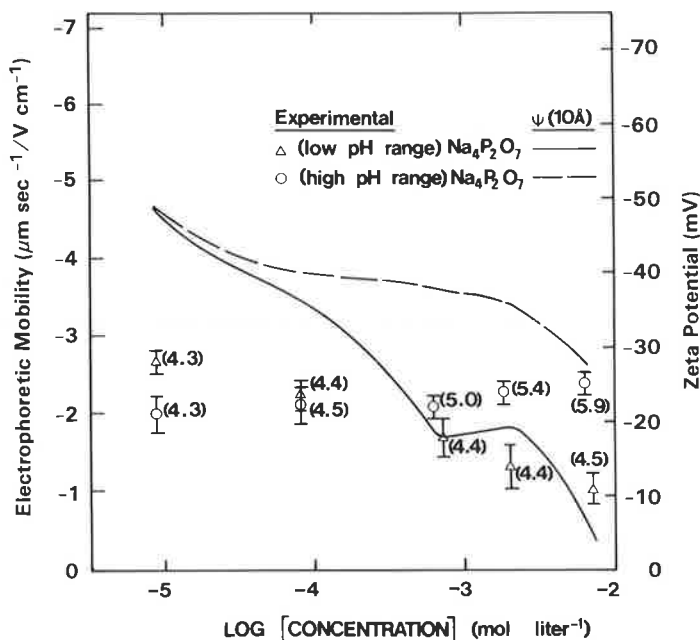


FIG. 8. EM and ζ potential of uric acid as a function of sodium pyrophosphate concentration. Two pH ranges are given: (low) 4.3 to 4.5 and (high) 5.0 to 5.9. Data points are experimental values. Lines give $\psi(10 \text{ \AA})$.

decrease as functions of Na_2SO_4 and NaH_2PO_4 concentration for the pH range investigated, 4.3 to 4.4. The influence of sodium oxalate on EM is given in Fig. 6. In both ranges reported, pH 4.3 to 4.4 and pH 5.3 to 5.7, EM magnitudes decrease with increasing NaC_2O_4 concentration. In the low pH range, most of the oxalate was present as HC_2O_4^- . In the higher pH range at least 90% of the oxalate was $\text{C}_2\text{O}_4^{2-}$, with most of the remainder HC_2O_4^- . Figure 6 shows the influence of sodium citrate concentration on uric acid EM values. The ζ potential values as a function of citrate have complex behavior. For example, at the higher pH range values, the zeta potential values appear to reach a plateau as citrate concentration increases. However, this is a result of the slight increase from pH 5.4 to 6.1 which produces a higher negative potential on the uric acid particles (compare Fig. 6 with Fig. 7). In the low pH range, 4.2 to 4.4, EM magnitudes decrease as a function of $\text{Na}_3\text{C}_6\text{H}_5\text{O}_7$ concentration. In this pH

range the citrate present was about 30% $\text{H}_2\text{C}_6\text{H}_5\text{O}_7^-$ and 70% $\text{HC}_6\text{H}_5\text{O}_7^{2-}$. In the higher pH range, 5.4 to 6.1, ζ potentials as a function of $\text{Na}_3\text{C}_6\text{H}_5\text{O}_7$ are relatively constant. Most of the citrate in this pH range was present as $\text{HC}_6\text{H}_5\text{O}_7^{2-}$ or $\text{C}_6\text{H}_5\text{O}_7^{3-}$.

Figure 8 summarizes the influence of sodium pyrophosphate concentration on uric acid EM values. In the lower pH range, EM generally decreases as a function of concentration. In this range most of the pyrophosphate was present as $\text{H}_2\text{P}_2\text{O}_7^{2-}$. It was difficult to prepare suspensions at a relatively constant solution pH because of the mutual buffering capacity of uric acid pyrophosphate. This produced apparent inflections and other complicated behavior in the ζ potential values as a function of increasing pyrophosphate concentration. Problems were encountered in controlling the pH of the suspensions containing pyrophosphate at the higher pH range while still maintaining sterile conditions. The need for sterile conditions prohibited introduction

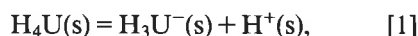
of the pH electrode directly into the suspensions while adjusting the pH. To overcome this problem, $\text{Na}_4\text{P}_2\text{O}_7$ solutions were adjusted to pH 6.0 and filtered through 0.22- μm filters to remove bacteria prior to their addition to suspensions. The lower concentration dilutions of $\text{Na}_4\text{P}_2\text{O}_7$, 10^{-3} and 10^{-2} M, were subsequently buffered by the uric acid. As a result, the higher pH range (4.3–5.9) is much broader than that reported for the other sodium anion suspensions. Over the higher pH range, EM is relatively constant but this effect is due to the increase in pH and, hence, EM magnitude offset by the increase in ionic strength. Most of the pyrophosphate was present as $\text{HP}_2\text{O}_7^{3-}$ in this pH range.

The EM values in the synthetic urine are slightly negative or in some cases essentially zero. EM values as a function of solution pH for uric acid in synthetic urine are summarized in Table II. As expected in these high-ionic-strength solutions, 0.28 to 0.31 M, the electrophoretic mobility determination was difficult. This, coupled with the observation that EM magnitudes decrease with increasing ionic strength and the large particle size of about 5 μm and enhanced coagulation under these conditions, made quantitative determinations difficult. Therefore, we have reported the EM values for most of the pH values qualitatively. At pH values from 4.38 to 5.38, either the mobility was slightly negative or no movement was detected in the applied field of 10 V. At pH 5.62 and 5.86 we were able to track about

10 particles in each suspension to determine EM values. These values were $-0.5 \pm 0.4 \mu\text{m s}^{-1}/\text{V cm}^{-1}$. However, it was obvious that most of the particles in these suspensions exhibited no discernable movement. At pH 6.30, slight negative movement was detected.

Use of the Monoprotic Surface Group Model to Describe the Uric Acid–Water Interface

The monoprotic acid group model of Healy and White (12) is suitable for explaining, at least qualitatively, uric acid ζ potential behavior. Several different models were evaluated to explain the experimental data. Only the MSG model was consistent with the experimentally observed zero or negative EM. For example, the Nernst–Gouy–Stern model (26) predicted positive EM values within the range of experimental concentrations for uric acid, even when adsorption potentials in the Stern equation were assumed to be zero. The experimental results in Fig. 2 indicate that surface charges on uric acid arise from the loss of a proton from surface uric acid molecules. This process results in negatively charged urate ions on the surface and is consistent with the chemistry of uric acid. The surface dissociation reaction is expressed by



where $\text{H}_4\text{U}(\text{s})$, $\text{H}_3\text{U}^-(\text{s})$, and $\text{H}^+(\text{s})$ are uric acid, urate, and hydronium ion, respectively, at the surface. The mass-action equation is given by

$$K_a = \frac{\text{H}_3\text{U}^-(\text{s})a_{\text{H}}(\text{s})}{\text{H}_4\text{U}(\text{s})} \quad [2]$$

where K_a is the acid dissociation constant, taken to be that of the bulk solution equal to 3.404×10^{-6} M for uric acid in water. The term $a_{\text{H}}(\text{s})$ is the surface activity function for $\text{H}^+(\text{s})$ given by (12)

$$a_{\text{H}}(\text{s}) = a_{\text{H}} \exp\left(\frac{-e\psi_0}{KT}\right). \quad [3]$$

Using Eq. [2], Healy and White (12) have shown that for a surface composed of monoprotic acid groups, surface charge is given by

TABLE II

ζ Potential as a Function of Solution pH for Uric Acid in Synthetic Urine

Solution pH	ζ potential (mV)	$\psi(10 \text{ \AA})$
4.38	No movement detected	-2.74×10^{-3}
4.82	No movement detected	-8.62×10^{-3}
5.29	Slightly negative	-4.64×10^{-3}
5.38	Slightly negative	-5.01×10^{-3}
5.62	-5.30 ± 4.0	-6.78×10^{-3}
5.86	-5.50 ± 3.0	-7.70×10^{-3}
6.30	Slightly negative	-2.80×10^{-3}

$$\sigma_0 = \frac{-eK_a N_s}{K_a + a_H \exp(-e\psi_0/KT)} \quad [4]$$

The terms e , k , and T have the usual meanings. N_s is the maximum number of surface sites. For uric acid, crystallographic data (27) indicate that N_s equals 8.52×10^{13} sites cm^{-2} . The term a_H is $\text{H}^+(\text{aq})$ activity and ψ_0 is the surface potential. The details of Eq. [4] are discussed by Healy and White (12). Since all ionic species investigated (except H^+) acted indifferently, the Gouy–Chapman equation is used to express the charge in the layer of counter ions arising from the surface charge. The Stern equation (28) is not used because the ζ potential data give no evidence of chemical adsorption. The generalized formula for the Gouy–Chapman equation, taking into account all major ionic species, is given by (29)

$$\sigma_{\text{GC}} = \left(\frac{DD_0 kT}{2\pi} \right)^{1/2} \times \sum_i n_i \left[\exp - \left(\frac{z_i e \psi_0}{kT} \right) - 1 \right]^{1/2}, \quad [5]$$

where σ_{GC} is charge in the counterion layer, D is relative dielectric constant of the aqueous phase, and D_0 is the absolute permittivity in a vacuum. The terms n_i and z_i are the concentration and valence of the i th species in the bulk solution.

The equation needed to express the maintenance of charge neutrality is

$$\sigma_0 + \sigma_{\text{GC}} = 0. \quad [6]$$

Finally, to compare ζ potentials a finite distance from the solid surface at the shear plane, electric potential at 10 \AA from the surface, $\psi(10 \text{ \AA})$, is calculated by integrating the Poisson–Boltzmann equation (7). This equation is given by

$$\frac{d\psi(x)}{dx} = \left(\frac{8\pi kT}{DD_0} \right)^{1/2} \sum_i n_i \left[\exp \left(- \frac{e\psi(x)}{kT} \right) - 1 \right]^{1/2}. \quad [7]$$

Equations [4], [5], and [6] were solved simultaneously in a subroutine of EQUIL.

EQUIL ionic equilibrium calculations were used for values of n_i in Eq. [5]. Values of ψ_0 were used to calculate the $\psi(10 \text{ \AA})$ values (lines in Figs. 2–8) against ζ potentials (data points in Figs. 2–8).

ζ potentials were calculated from experimentally determined EM values using the Smoluchowski equation (26). The restrictions to this equation have been reviewed elsewhere (24, 26, 30, 31). In general, the large particle size and relatively high ionic strengths under most of the measurement conditions validate the use of this relationship. The Smoluchowski equation is given by

$$\xi = \frac{4\pi\eta}{\epsilon} \text{EM}, \quad [8]$$

where ξ is ζ potential, η is solution viscosity, and ϵ is permeability.

A comparison of ζ potentials versus $\psi(10 \text{ \AA})$ as a function of solution pH is given in Fig. 2. It was necessary to balance the total charge in solution using Na^+ or Cl^- in EQUIL calculations because of H^+ adsorption at lower pH or desorption at higher pH. At pH values below about pH 3.0, theoretical values were essentially zero. ζ potentials in this pH range were about 5 to 10 mV more negative than $\psi(10 \text{ \AA})$ values. At pH values above pH 4.0 and into the pH range 5.0 to 6.35, $\psi(10 \text{ \AA})$ values are about 10 mV more negative than ζ potentials. In general, $\psi(10 \text{ \AA})$ values are substantially more negative at low salt concentrations than ζ potentials. However, for the low pH range good agreement is reached at concentrations exceeding $10^{-3} M$. In the high pH range, about 10 mV separates theoretical and experimental values above $10^{-3} M$ salt concentrations.

ζ potentials and $\psi(10 \text{ \AA})$ values agree for uric acid suspensions containing $10^{-3} M$ or greater of a given electrolyte. The influence of cation chloride salt concentrations is shown in Figs. 3 and 4 for the low and high pH ranges, respectively. There is somewhat better agreement between theoretical and experimental values at the low pH range than the high pH range. There are about 10-mV differences be-

tween experimental ζ potentials and theoretical $\psi(10 \text{ \AA})$ values at the high pH range. These differences are also observed at the high and low pH ranges in the electrolytes composed of sodium anion salts.

In Figs. 5–8, ζ potentials and $\psi(10 \text{ \AA})$ values are summarized as functions of sodium anion salt concentrations. For Na_2SO_4 and Na_2HPO_4 in Fig. 5, there is good agreement between theory and experiment below $10^{-3} M$. For $\text{Na}_2\text{C}_3\text{O}_4$, $\text{Na}_3\text{C}_6\text{H}_5\text{O}_7$, and $\text{Na}_4\text{P}_2\text{O}_7$ in the low pH ranges in Figs. 6, 7, and 8, respectively, once again there is good agreement below $10^{-3} M$ salt concentrations. However, ζ potentials and $\psi(10 \text{ \AA})$ values do not compare as favorably in the high pH range for these salts. The ζ potentials are usually about 10 mV less negative below 10^{-3} and up to 30 mV less negative at lower concentrations.

Table II gives ζ potentials and $\psi(10 \text{ \AA})$ values for uric acid in synthetic urine at various pH values. The $\psi(10 \text{ \AA})$ values are very small. The very low ζ potential magnitudes that we were able to estimate in these suspensions tend to confirm our belief that chemical adsorption of positive species is negligible in this system. Cations probably do not adsorb to urate surface sites because urate does not readily complex with cations in solution, despite the fact that insoluble urate salts may form with all of the salts investigated (18–19, 21). Stability constants for NH_4^+ , K^+ , Ca^{2+} , and Mg^{2+} urate complexes are not available. However, the low stability constant for $\text{NaH}_3\text{U}(\text{aq})$, 8.50×10^{-3} liter mol^{-1} at 37°C (19), supports this argument.

The best theoretical fit to the experimental data for the cation chloride electrolyte solutions, even in the high pH suspensions where considerable negative charge is available for adsorption of cations, is when these species are treated as indifferent ions such that no specific adsorption of these species is assumed in the calculation of theoretical values.

The MSG model explains most of the experimental observations for the ζ potential behavior for the uric acid–water system. No reversal to positive ζ potential values is predicted

for the range of solution conditions investigated. The magnitude of ζ potentials is accurately predicted to decrease with decrease with solution pH.

Comparison of experimental and theoretical values for ζ potentials as a function of added electrolytes is more ambiguous. At low concentrations of the electrolytes there is poor agreement, with predicted magnitudes exceeding experimental ones by as much as 20 mV, and the deviation between the values decreasing with increasing electrolyte concentration (and ionic strength) such that above $10^{-3} M$ there is reasonably good agreement for all electrolytes.

The failure of experimental values to agree with theoretical ones for electrolyte concentrations below $10^{-3} M$ may be due to several phenomena that compromise either the assumptions on which the MSG model is based or the experimental ζ potential determinations. The following may act singly or may combine to lead to the deviations: maximum number of surface sites used for the theoretical calculations, particle shape, retardation and relaxation, location of the shear plane for ζ potential calculations, and surface conduction (8, 24, 30–38). It is not clear at the present time which one(s) may have the most important influence, but the latter two possibilities cannot easily be eliminated.

Phenomena influencing EM measurements such as retardation and relaxation effects are expected to have only a small effect because of the large particle size of uric acid (i.e., about $5 \mu\text{m}$) and the relatively high ionic strength in all suspensions evaluated. Particle shape anisotropy is also expected to exert only a relatively small influence on ζ potential values for the same reasons (31).

Recent scanning tunnelling microscopy and high-resolution transmission electron microscopy indicate that the maximum number of surface sites can be significantly less than that calculated from crystallographic data (36–38). The net effect in reduction of the number of maximum surface sites will be to decrease the magnitudes of surface charge and ζ potential

in direct proportion to the actual number of sites (Eq. [4]). A reduction in the number of surface sites will not explain the decrease in the difference between theoretical and experimental ζ potential values as the electrolyte concentration is increased.

Another possibility that would lead to differences between experimental and theoretical values is the location of the shear plane. The selection of 10 Å as the distance from the uric acid surface at which the shear plane is located is arbitrary. Experimental and theoretical ζ potential values at the lower electrolyte concentrations would be much closer if, say, 20 Å was selected as the shear plane. This would imply that the shear plane distance is a function of ionic strength. This could be the case, for example, if hydration is a possibility at the uric acid-water interface.

Surface conduction on the solid phase can lower the measured EM values and reduce the magnitude of experimental ζ potentials, but is difficult to evaluate (30). The relatively delocalized electrons in the pi cloud associated with the double-ring structure of uric acid (27) would lend themselves to conduction. Thus, surface conduction and the distance for the shear plane from the surface may explain the discrepancy between experimental and theoretical ζ potentials for uric acid suspensions at low ionic strengths.

CONCLUSIONS

ζ potentials of uric acid become more negative as a function of solution pH. With decreasing solution pH, ζ potentials approach zero. Even at pH values below pH 3.0, ζ potentials remain negative, although small in magnitude.

Cation chloride salts and sodium anion salts act as indifferent electrolytes with respect to uric acid ζ potentials. Increasing the concentration of these salts at constant pH reduces the magnitude of negative ζ potentials, but results in no change in sign.

Qualitatively, the ζ potentials in these suspensions were very close to zero, but still neg-

ative, or displayed no detectable movement in the applied electric field.

A theoretical model based on the monoprotic surface group model was proposed to explain uric acid ζ potential behavior. The monoprotic surface group model is consistent with general trends in the experimental data. Relatively poor agreement was found between experimental and theoretical values for suspensions with ionic strengths below 10^{-3} M. At physiological ionic strengths, reasonably good agreement was found between experimental ζ potentials and electric potentials 10 Å from the surface calculated using the proposed model.

REFERENCES

1. Lonsdale, K., *Science* **152**, 1511 (1966).
2. Robertson, W. G., and Peacock, M., *Clin. Sci.* **43**, 499 (1972).
3. Fleisch, H., *Kidney Int.* **13**, 361 (1978).
4. Felix, R., Monod, A., Broge, L., Hensen, N. M., and Fleisch, H., *Urol. Res.* **5**, 21 (1977).
5. Walton, A. G., "The Formation and Properties of Precipitates," reprint ed., pp. 166-174. Robert E. Kreiger, Huntington, NY, 1967.
6. Koutsoukos, P. G., Lam-Erwin, C. Y., and Nancollas, G. H., *Invest. Urol.* **18**(2), 178 (1980).
7. Verwey, E. J. W., and Overbeek, J. Th. G., "Theory of the Stability of Lyophobic Colloids." Elsevier, New York/Amsterdam, 1948.
8. Hunter, R. J., "Zeta Potential in Colloid Science: Principles and Applications." Academic Press, New York, 1981.
9. Burns, J. R., and Finlayson, B., *Invest. Urol.* **18**(2), 167 (1980).
10. Gouy, G., *J. Phys.* **9**(4), 457 (1910).
11. Chapman, D. L., *Phil. Mag.* **25**(6), 475 (1913).
12. Healy, T. W., and White, L. R., *Adv. Colloid Interface Sci.* **9**, 393 (1978).
13. Lyklema, J., *J. Electroanal. Chem. Interfacial Electrochem.* **18**, 341 (1968).
14. Bowden, J. W., Posner, A. M., and Quirk, J. P., *Aust. J. Soil Res.* **15**(2), 121 (1977).
15. Westall, J., and Hohl, H., *Adv. Colloid Interface Sci.* **12**, 265 (1980).
16. Yates, D. E., Levine, S., and Healy, T. W., *J. Chem. Soc. Trans. Faraday Soc.* **1** **70**(10), 1807 (1974).
17. Onoda, G. Y., Jr. and Casey, J. A., in "Ultrastructure Processing of Ceramics, Glasses, and Composites" (L. L. Hench and D. R. Ulrich, Eds.). Wiley, New York, 1984.
18. Hammarsten, G., *Carlsberg Lab.* **19**(7), 1 (1932).

19. Finlayson, B., and Smith, A., *J. Chem. Eng. Data* **19**(1), 94 (1974).
20. Allen, D. J., *Arthritis Rheum.* **18**(6), 1123 (1965).
21. Lam, C. Y., Nancollas, G. H., and Ko, S. J., *Invest. Urol.* **15**(6), 473 (1978).
22. Porter, P., *Res. Vet. Sci.* **4**, 580 (1963).
23. Porter, P., *Res. Vet. Sci.* **4**, 592 (1963).
24. James, A. M., in "Surface and Colloid Science" (R. J. Good and R. R. Stromberg, Eds.), Vol. 11. Plenum, New York, 1979.
25. Werness, P. G., Brown, C. M., Smith, L. H., and Finlayson, B., *J. Urol.* **134**, 1242 (1985).
26. Curreri, P., Onoda, G. Y., Jr., and Finlayson, B., *J. Colloid Interface Sci.* **69**, 170 (1979).
27. Ringertz, H., *Acta Crystallogr.* **20**, 397 (1966).
28. Stern, O., *Z. Elektrochem.* **30**, 508 (1924).
29. Grahame, D. C., *Chem. Rev.* **41**, 441 (1947).
30. Henry, D. C., *Trans. Faraday Soc.* **44**, 1021 (1948).
31. deKeizer, A., Vander Drift, W. P. J. T., and Overbeek, J. Th. G., *Biophys. Chem.* **3**, 107 (1975).
32. Israelachvili, J. N., "Intermolecular and Surface Forces with Applications to Colloidal and Biological Systems," pp. 201-207, 267-268. Academic Press, New York, 1985.
33. Yousef, A., and McCoy, B. J., *J. Colloid Interface Sci.* **94**, 497 (1983).
34. Drost-Hansen, W., *J. Colloid Interface Sci.* **58**, 251 (1977).
35. Lyklema, J., *J. Colloid Interface Sci.* **58**, 251 (1977).
36. Robinson, A. L., *Science* **230**, 304 (1986).
37. Robinson, A. L., *Science*, **232**, 451 (1986).
38. Tromp, R. M., Hamers, R. J., and Demuth, J. E., *Science* **234**, 304 (1986).

Application of Computer Assisted Tomography (CAT) to Gamma Attenuation Measurement of Soil Water Content

J. M. Hainsworth and L. A. G. Aylmore

Soil Science and Plant Nutrition, School of Agriculture,
University of Western Australia, Nedlands, W.A. 6009.

Abstract

This paper demonstrates the successful application of computer assisted tomography (CAT) to γ -ray attenuation measurements and the modification of a conventional gamma scanning system to enable changes in the spatial distribution of soil water content to be accurately monitored in soil columns. The relatively inexpensive gamma system has been shown to provide a resolution comparable to that obtainable with commercially available but extremely expensive X-ray CAT scanning systems. However, longer counting times are required with gamma radiation, thus limiting the usefulness of the technique for some soil water studies. A comparison of the efficiency of several source-detection combinations illustrates their relative advantages and disadvantages.

Introduction

Until recently, no experimental technique has been capable of measuring spatial distributions of soil water content in a continuous and non-destructive manner and with sufficient resolution to enable detailed studies of water movement in proximity to plant roots. Previous techniques for the direct measurement of soil water content distributions were either destructive and hence lacked continuity, or perturbed the sensitive balance being examined, or were too slow in their response time, or simply lacked the dimensional resolution for meaningful definitions of water content distributions (So *et al.* 1976).

Application of the technique known as computer assisted tomography to the attenuation of X-rays (CAT scanning) (Hounsfield 1972) has essentially overcome similar problems which existed in diagnostic radiology, and recently X-ray CAT scanners have been used successfully to measure spatial changes in soil bulk density (Petrovic *et al.* 1982) and soil water content (Hainsworth and Aylmore 1983, 1986). In particular Hainsworth and Aylmore (1983) demonstrated that a commercially available EMI scanner could determine soil water content distributions with a sensitivity of $\pm 0.006 \text{ g cm}^{-3}$ within pixel regions of 1.5 by 1.5 mm. This application has provided an exciting new tool for soil-plant water studies (Hainsworth and Aylmore 1986).

Unfortunately, commercially available X-ray CAT scanners developed for medical purposes are extremely expensive, inconvenient in design and unlikely to be generally available for studies of many other systems (e.g. soil and plant systems). On the other hand, relatively inexpensive γ -ray attenuation systems have frequently been used to



Fig. 1. Gamma scanning system with associated scalar and microcomputer control unit.

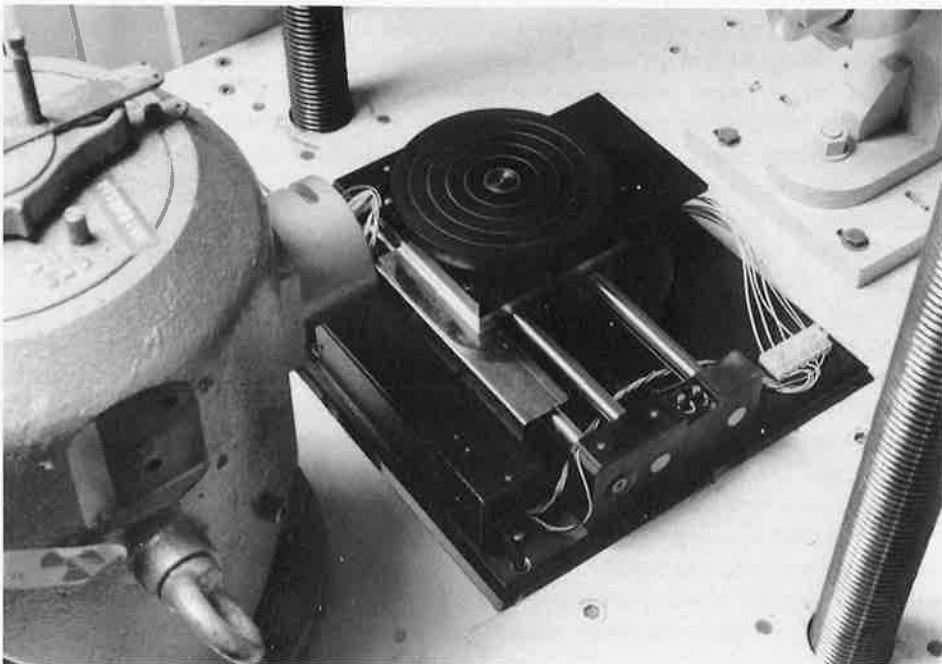


Fig. 2. Close-up of CAT scan platform.

determine bulk soil water contents (Gurr 1962; Groenvelt *et al.* 1969; Ryhiner and Pankow 1969). The present paper demonstrates the application of CAT to gamma scanning attenuation measurements and the modification of a conventional gamma scanning system in order to examine spatial changes in soil water content.

Materials and Methods

A modified conventional gamma scanner was used in these experiments (see Fig. 1). This scanner utilizes a 2 mm wide by 5 mm long collimated beam from a gamma radiation source and a similarly collimated detector. Three radiation source-detector combinations were evaluated. The combinations tested were (i) 240 mCi americium-241 source-NaI crystal detector, (ii) 1 Ci ytterbium-169 source-NaI crystal detector and (iii) 500 mCi caesium-137 source-plastic scintillant detector. The source and detector are mounted on a platform which can be moved a vertical distance of 1.5 m, with an incremental control of 0.01 mm, by two 4 cm diameter worm drives situated on either side of the platform and driven by a HY-200-3424 stepper motor. In between the source and detector is a 12 cm platform constructed to enable soil columns to be rotated and moved horizontally across the beam of radiation between source and detector (see Fig. 2). The platform is moved horizontally by means of a 1 cm diameter worm drive powered by an RS-332-947 stepper motor. Maximum horizontal movement is 25 cm which allows a 12 cm diameter soil column to be scanned. At the end of each horizontal scan the platform is rotated 5°-10° by an RS-332-953 stepper motor and then moved horizontally in the reverse direction. This procedure is continued until the object had been rotated through 180°. At 2 mm intervals along the horizontal scan, the amount of transmitted radiation is measured and stored directly in a 640K RAM microcomputer which also controls the movements of the scanning platform.

Table 1. Comparison of features of potential gamma CAT scanning sources with an EMI X-ray source used in a commercial CAT scanner

Source	Activity	Energy (keV)	Detector	Pixel width (mm)	Pixel ht (mm)	Att. coeff. water for			Scan time ^A (min)
						5 cm diam.	7 cm column	12 cm (cm ⁻¹)	
Am-241	240 mCi	60	NaI	2	5	0.189	0.189	0.190	~90
Yb-169	1000 mCi	63	NaI	2	5	0.184	0.184	0.184	~15
Cs-137	500 mCi	661	Pl. sc.	2	2	0.073	0.074	0.074	~15
X-ray	120 keV	~59	NaI	1.5	10	—	—	0.191	1

^A For 7 cm diameter object.

Processing of the raw data is carried out by a modified algorithm of Brooks and Di Chiro (1975) and results in a 50 by 50 matrix of 2 mm square pixels containing the spatial distribution of the linear attenuation coefficient of the 5 mm thick slice of the column under examination. The water content of each pixel was then determined by the method of Hainsworth and Aylmore (1983). As the formula of Hainsworth and Aylmore (1983) requires the mass attenuation of water to be known, this was calculated by scanning 5, 7 and 12 cm diameter acrylic cylinders filled with water placed equidistant from source and detector and by using the formula of Bridge (1971). A further constraint that the attenuation of the beam of radiation remains linear with distance (Phanton 1981) was checked by placing 25 acrylic slides, each 2 mm thick, between source and detector, and progressively removing two slides, one from the detector side and one from the source side, and measuring the transmitted intensity of radiation until only one slide remained.

A preliminary check of the CAT scanning system was carried out by using a column consisting of three concentric rings 7 cm, 5 cm and 1.5 cm in diameter; the outer ring was filled with water, the middle ring with kerosene and the inner ring was left empty. As the attenuation coefficients of water, kerosene and air were known, this experiment allowed the accuracy of the CAT scanning system to be measured. Once the preliminary check had been completed, the concentric ring column was uniformly packed with dry soil and then scanned. After the scanning of the dry soil was completed, the soil in the outer ring was watered to 0.325 g cm⁻³, the soil in the middle

ring to 0.150 g cm^{-3} , the inner ring was left dry, and the system was rescanned. The water content of each pixel was then determined and compared with values obtained by taking a series of 1 g samples from each ring.

Results and Discussion

The values for the mass attenuation coefficient of water for each source are presented in Table 1. The values obtained for the Am-241 and Cs-137 sources are comparable with the values published by Groenvelt *et al.* (1969) and Bridge (1971) for a similarly collimated source and detector. The value obtained for the Yb-169 source is comparable with that of the Am-241 source as these two sources have similar energy levels. Furthermore, the attenuation coefficients for water for these two sources are comparable with the value calculated for a 120 keV X-ray tube in an EMI CAT scanner by McCullough (1975) (see Table 1). Thus the Am-241 and Yb-169 sources should have the same sensitivity to spatial changes in soil water content as commercially available CAT scanners. Hainsworth and Aylmore (1983) reported the sensitivity to changes in soil water content of a commercially produced CAT scanner operating at 120 keV to be of the order of 0.006 g cm^{-3} .

The attenuation of radiation from all three sources remained perfectly linear with increase in distance. This is confirmed by the fact that the attenuation coefficient for water remained approximately constant for a given source for the three sized cylinders used. However, in the case of Am-241 and Yb-169, a 1 cm layer of polyalkathene beads had to be placed in front of the source collimator. Without the polyalkathene beads the attenuation of the beam was not linear with distance. This was undoubtedly due to beam hardening (Brooks and Di Chiro 1976) which results in a proportionally higher number of low-energy photons being absorbed with increase in distance.

Table 2. Comparison between the measured and calculated linear attenuation coefficient μ

μ was measured by scanning a 7 cm diameter column containing either water or kerosene or air; μ was calculated from a CAT scan of a concentric ring column containing water, kerosene and air

	μ (Am-241) (cm^{-1})	μ (Yb-169) (cm^{-1})	μ (Cs-137) (cm^{-1})
Measured μ			
Water	0.189 ± 0.007	0.184 ± 0.008	0.074 ± 0.002
Kerosene	0.138 ± 0.004	0.137 ± 0.005	0.057 ± 0.002
Air	0.000 ± 0.001	0.000 ± 0.001	0.000 ± 0.001
Calculated μ			
Water	0.201 ± 0.011	0.199 ± 0.012	0.079 ± 0.006
Kerosene	0.130 ± 0.010	0.130 ± 0.009	0.055 ± 0.009
Air	0.000 ± 0.005	0.000 ± 0.006	0.000 ± 0.004

The preliminary CAT scan of the three concentric rings clearly shows that the gamma system is capable of resolving spatial changes in density (see Table 2). Whilst the calculated linear attenuation coefficients in the pixels containing water were slightly higher than the value measured for water alone, and those containing kerosene slightly lower than the value measured for kerosene alone, there was no significant difference between measured and calculated attenuation coefficients for all three sources. The

standard deviations in the calculated attenuation coefficients were also comparable with the errors in measuring the attenuation coefficient of water alone and were similar in magnitude to the value of 0.004 cm^{-1} cited as the standard deviation for commercial CAT scanners by Brooks and Di Chiro (1976). Clearly there is no reason why it should not be possible to use the system to examine spatial distributions of soil water content.

Table 3. Comparison between calculated water content θ_v for the three gamma sources and θ_v determined gravimetrically

Standard deviations cited refer to the actual variation in water content measured within each ring and not those associated with errors in determination

Ring	θ_v (Am-241) (g cm^{-3})	θ_v (Yb-169) (g cm^{-3})	θ_v (Cs-137) (g cm^{-3})	θ_v (grav.) (g cm^{-3})
Outer	0.350 ± 0.040	0.347 ± 0.041	0.349 ± 0.040	0.325 ± 0.045
Middle	0.142 ± 0.040	0.145 ± 0.042	0.144 ± 0.047	0.150 ± 0.020
Inner	0.000 ± 0.060	0.000 ± 0.050	0.001 ± 0.061	0.001 ± 0.001

The results of the CAT scans on the soil-water system for the three sources are presented in Table 3. A three-dimensional representation of the Am-241 scan is essentially identical with that obtained with a commercial X-ray scanner and is presented by Hainsworth and Aylmore (1983). The standard deviations cited in Table 3 refer to actual variations in soil water content within each ring and not to those associated with errors of determination. These results clearly show that the system can be used to examine spatial distributions in soil water content. The calculated water content values are comparable with the measured values but are higher than the measured values in the outer ring and lower than those in the middle ring. As this situation occurred in the previous example, it is likely that this error arises from spatial limiting of the Fourier transform used in the reconstruction of the image. Hainsworth and Aylmore (1983) found a similar artifact with a commercially available X-ray CAT scanner.

Whilst all three sources could be used to determine spatial distributions of soil water content, both the time required to successfully complete a scan and the spatial resolution varied as a result of differences in transmission intensities and hence in count rates. For example, a CAT scan of a 7 cm diameter object with the Am-241 source took approximately 90 min to complete. This scan time is not sufficiently rapid to follow the rapid changes in soil water content which may be associated with, for example, water extraction by plant roots or water infiltration into the soil surface. This problem can be overcome by use of the 1 Ci Yb-169 source which has a similar attenuation coefficient for water and hence a similar sensitivity to changes in soil water content, but has approximately 10 times the photon output allowing scan times to be reduced to approximately 15 min. However, a major disadvantage of the Yb-169 source is its relatively short half-life of 31 days, resulting in a working life of approximately 2 months. In these experiments, the Cs-137 source-plastic scintillant detector combination showed the greatest potential for γ -ray CAT scanning, having a scan time of 15 min for the 7 cm diameter column plus an added advantage of a reduction in pixel height from 5 to 2 mm. However, the low attenuation coefficient for water when Cs-137 is used implies that it may not be as sensitive as Yb-169 to

small changes in water content. This problem may be overcome by slightly increasing the scan time and pixel size.

Despite the above differences in source suitability, these experiments demonstrate that conventional gamma scanners can be successfully converted to carry out the CAT scanning procedure. There seems to be no reason why gamma CAT scanning with some refinements should not become a major research tool in soil water studies and a variety of other investigations where two- or three-dimensional images of objects need to be obtained in a non-destructive or repetitious manner.

Acknowledgments

This research was funded by grants from the Australian Research Grants Scheme and the Australian Water Resources Council; support is gratefully acknowledged.

References

- Bridge, B. J. (1971). The effect of ground surface conditions on water movement and storage in cracking clay soils. Ph.D. Thesis, University of Sydney.
- Brooks, R. A., and Di Chiro, G. (1975). Theory of image reconstruction in computed tomography. *Radiology* 117, 561.
- Brooks, R. A., and Di Chiro, G. (1976). Principles of computer assisted tomography (CAT) in radiographic and radioisotope imaging. *Phys. Med. Biol.* 21, 689.
- Groenvelt, P. H., de Swart, J. G., and Cirler, J. (1969). Water content measurement with 60 keV gamma ray attenuation. *Bull. Int. Assoc. Sci. Hydrol.* 14, 67.
- Gurr, C. G. (1962). Use of gamma rays in measuring water content and permeability in unsaturated columns of soil. *Soil Sci.* 94, 224-9.
- Hainsworth, J. M., and Aylmore, L. A. G. (1983). The use of computer assisted tomography to determine spatial distribution of soil water content. *Aust. J. Soil Res.* 21, 435.
- Hainsworth, J. M., and Aylmore, L. A. G. (1986). Water extraction by single plant roots. *Soil Sci. Soc. Am. J.* 50, 841-8.
- Hounsfield, G. N. (1972). A method of and apparatus for examination of a body by radiation such as X or gamma radiation. Brit. Pat. No. 1283915.
- McCullough, E. C. (1975). Photon attenuation in computed tomography. *Med. Phys.* 2, 307.
- Petrovic, A. M., Siebert, J. E., and Lieke, P. E. (1982). Soil bulk density analysis in three dimensions by computed tomographic scanning. *Soil Sci. Soc. Am. J.* 46, 445.
- Phanton, D. M. (1981). Mathematical reconstruction techniques in computer axial tomography. *Math. Sci.* 6, 87-102.
- Ryhiner, A. H., and Pankow, J. (1969). Soil moisture measurement by the gamma transmission method. *J. Hydrol.* 9, 194-205.
- So, H. B., Aylmore, L. A. G., and Quirk, J. P. (1976). Measurement of water fluxes in a single root system 1: The tensiometer-potometer system. *Plant Soil* 45, 577.

Studies of Soil-Plant Water Systems using CAT Scanning

Application of the technique known as Computer Assisted Tomography (CAT scanning) to X-ray and gamma-ray attenuation measurements provides an exciting new method for soil and plant scientists to study soil water availability for plant growth.

New Era

In semi-arid environments the availability of scarce water resources for agriculture makes it imperative that its most efficient utilisation by plants is achieved. Unfortunately, progress in understanding the factors which control soil water availability for plant growth has been severely hindered by the lack of suitable experimental techniques for the accurate determination of detailed soil water content distributions in proximity to plant roots. Previous techniques have either been destructive and hence lacked continuity, perturbed the sensitive balance being examined, were too slow in their response time or simply lacked the dimensional resolution necessary for meaningful definition of soil-water content distributions.

Recent work in the Soil Science and Plant Nutrition laboratories at The University of Western Australia involving the adaption of the technique known as CAT scanning using X- and gamma-ray attenuation has provided an extremely exciting and powerful method for the detailed investigation and elucidation of the physics of water uptake by plant roots and of the ways in which plant-root systems respond to differing soil physical conditions and environmental stress. The X-ray technique was originally developed in the early 1970s to overcome similar problems which existed in diagnostic radiology in obtaining non-destructive representations of the human brain. For this work G.N. Hounsfield was awarded the Nobel Prize in 1979.

In CAT scanning a slice of the object under examination is modelled as an $n \times n$ matrix of small squares called pixels (Fig. 1). The purpose of the CAT technique is to determine the linear attenuation coefficient and hence the density of each pixel. This is achieved by scanning across the object linearly at $1-10^\circ$ intervals for 180° using a collimated radiation source and detector. The linear profiles at various angles are

back-projected and filtered. The summation of these back projections proves an accurate measurement of the attenuation in each pixel.

CAT scanning has been shown to resolve spatial changes in soil-water content repetitively and non-destructively. The zone of

soil-water content resulting from infiltration of water into soil from a porous 1 mm diameter alundum tube (artificial root) increases with time and is readily defined scanned by CAT (Fig. 2). X-ray CAT scanning is capable of resolving water content differences of 0.006 g/cm^3 over a distance of 1.5 mm. Examination of

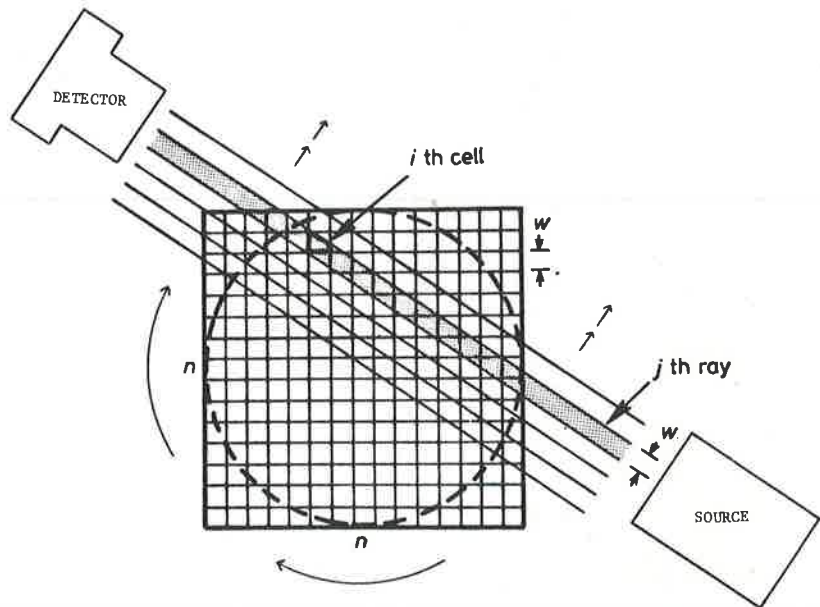


Figure 1. Schematic illustration of CAT scanning procedure.

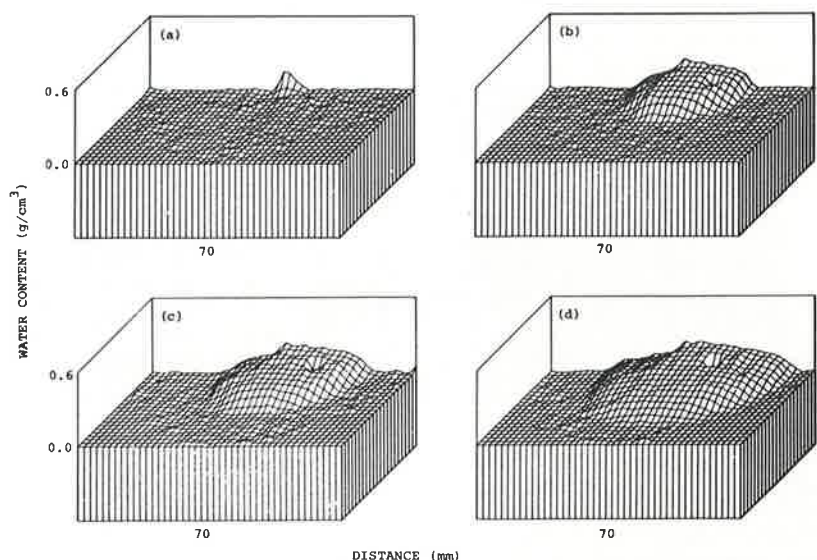


Figure 2. Half-slice three dimensional plots showing changes in soil-water content with time due to the infiltration of water into a soil column from an artificial root (alundum tube). Representations at (a) 1 min, (b) 10 min, (c) 15 min and (d) 20 min infiltration are illustrated.

the reverse phenomenon of water uptake by plant roots is equally amenable to this technique, which has also been used to examine water extraction by single plant roots.

Commercially available X-ray CAT scanners are extremely expensive (about \$2 million), are unlikely to be generally available for studies of soil-plant water relationship and are not conveniently designed for such studies. In recent decades, however, gamma-ray attenuation has frequently been used to determine bulk soil-water content and such systems are relatively inexpensive (about \$30,000) to design and construct. At the University of Western Australia's Soil Science and Plant Nutrition laboratories, a conventional gamma scanner has been modified to enable the system to carry out CAT scanning. The modified scanner utilises a 2 mm wide by 5 mm long collimated ^{137}Cs gamma radiation source and a similarly collimated detector. The source and detector are mounted on a platform which can be moved a vertical distance of 1.5 m with an incremental control of 0.01 mm. In between the source and detector a 13 cm platform was constructed to enable soil columns to be rotated and moved across the beam of radiation between source and detector. Maximum horizontal movement is 12.5 cm

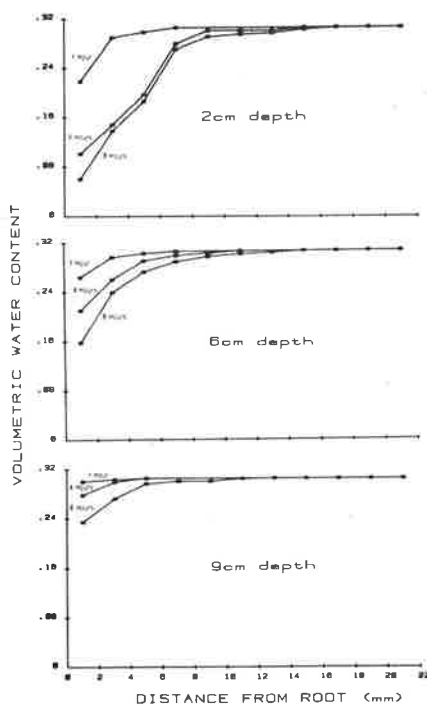
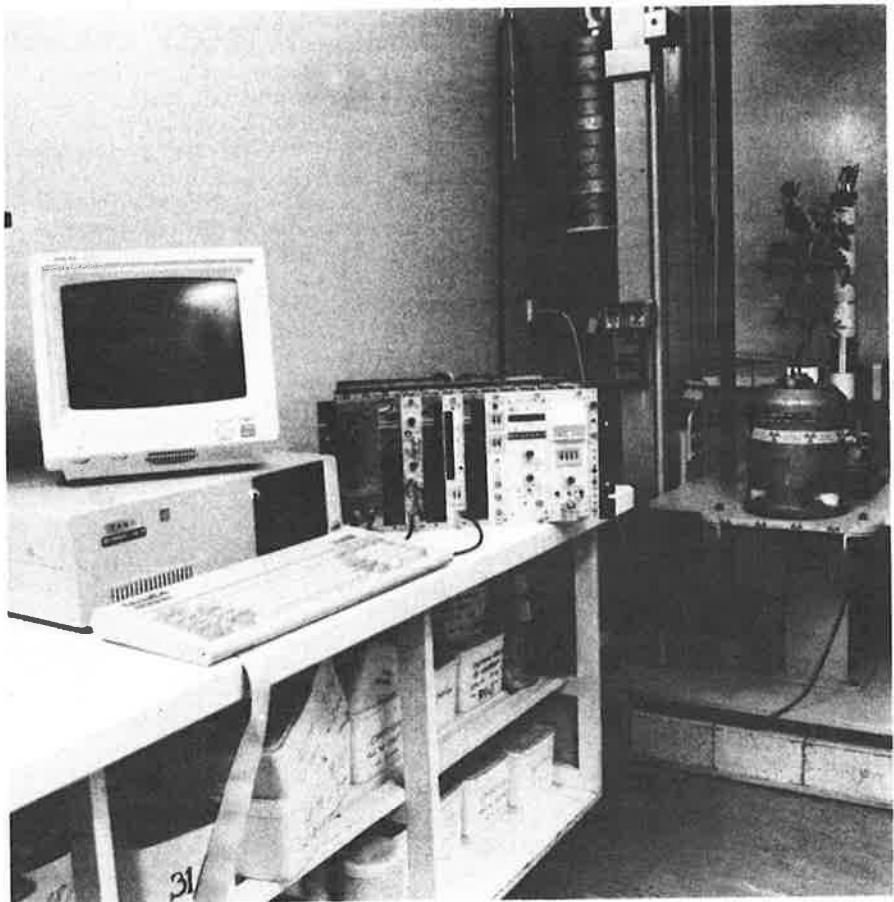


Figure 3. Change in drawdowns of soil water content in proximity to a radish root at various depths after one, four and eight hours transpiration obtained by application of CAT to gamma ray attenuation.

which allows a 12 cm diameter soil column to be CAT scanned. At the end of each horizontal scan the platform is rotated 1-5° and then moved horizontally in the reverse direction until the soil column has been rotated 180°. An enhanced XT compatible personal computer (PC-EXT) is used to control the scanning motion, to acquire and process the data from the radiation measurement system and finally to present the results in graphics and hardcopy forms.

Promising results have been achieved using the modified conventional gamma scanner in showing the changes in drawdown with time associated with water extraction by a single radish root (Fig. 3). These results, which illustrate the way in which water extraction varies along the root, provide the most detailed observations of this type yet available, particularly by a non-destructive technique. Comparison of the data with existing theoretical models demonstrates that the assumption in these models that a root acts as a uniform absorbing cylinder is clearly erroneous and that significant improvements in the

physical concepts on which these are based are still required.

CAT scanning clearly has considerable potential to elucidate the mechanisms involved in the uptake of water by plant roots and, in particular, to resolve the major controversies surrounding the physics of the process. This novel approach, which allows scientists to effectively 'see' inside soil columns without disturbing the processes occurring, has many other possible applications. At the University of Western Australia, Professor Aylmore and his post-graduate students are applying it not only to studies of soil-water extraction by a range of plant species under different environmental conditions and in a range of soil types at different water contents, but also to examine the effectiveness of soil wetting agents in dispersing infiltration, changes in soil structural status with wetting and the effects of soil physical conditions on the activity of soil fauna (worms, dung beetles, etc.).

L.A.G. Aylmore
J.M. Hainsworth
Soil Science and Plant Nutrition
The University of Western Australia
Nedlands, WA 6009

Hardpan development in loamy sand and its effect on crop growth

**Proc. 11th ISTRO (Inter. Soil and Till. Res. Organ.) Conf., Edinburgh, Scotland, July,
1988, V.1 233-238**

Daniel, H., Jarvis, R. and Aylmore, L.A.G.

HARDPAN DEVELOPMENT IN LOAMY SAND AND ITS EFFECTS UPON SOIL CONDITIONS AND CROP GROWTH

H. DANIEL¹, R.J. JARVIS² and L. A.G. AYLMORE¹

¹*Soil Science and Plant Nutrition, School of Agriculture, University of Western Australia, Nedlands, W.A. 6009 (Australia)*

²*Western Australian Department of Agriculture, South Perth, W.A. 6151 (Australia)*

ABSTRACT

During 1984 and 1985, the effects of seven compaction treatments ranging from zero traffic to ten tractor passes across the full width of experimental plots on the structure of a previously ripped loamy sand profile and on subsequent wheat yields have been studied. Increased traffic resulted in increased soil strength and compaction, with cone resistance at 19-cm depth ranging from 2.2 to 4.1-MPa in the winter. Under conditions of high moisture stress when the reformed hardpan was most effective in reducing root penetration and hence the availability of both water and nutrients for later growth, wheat yields were reduced (up to 34%) and were generally less than for the original unripped soil.

INTRODUCTION

In recent years there has been a trend towards the use of heavier tractors, tillage and harvesting equipment on Australian farms. Söhne (1953) showed that increased weight increases the severity and depth in the soil profile to which compaction occurs. Many recent experiments in both Europe (Canarache et al., 1984; Blackwell et al., 1986; Campbell et al., 1986; Soane et al., 1986) and North America (Fausey and Dylla, 1984; Voorhees et al., 1985; Chaplin et al., 1986) have examined the effects of traffic on soil compaction in those regions.

Light soils in Western Australia tend to develop a hardpan soon after being taken into cultivation. These soils show a marked reduction in root growth in the compacted zone (Hamblin and Tennant, 1979) and have in many cases been shown to respond to deep tillage with substantial increases in yield (Jarvis et al., 1985).

The present study examines the effects of deep ripping followed by wheel traffic on soil physical properties and crop yield, associated with subsequent hardpan redevelopment on a loamy sand soil.

MATERIALS AND METHODS

Site, climatic and soil conditions

The experiment was conducted at the Wongan Hills Research Station of the Western Australian Department of Agriculture, where the average annual rainfall is 345-mm and the average annual Class A pan evaporation is 2521-mm (Luke et al., 1987).

The soil has been classified as a Typic Xeropsamment (Soil Survey Staff, 1975) and was a well drained, deep, loamy sand, which is common in much of the north and central Western Australian wheatbelt. The soil site was last cropped in 1980 and had been under pasture between 1981 and 1983. A distinct hardpan had developed at 15 to 20-cm depth. Some physical properties of the soil are presented in Table I.

TABLE I

Soil physical properties

Depth (cm)	Particle size distribution (% w/w)			Water content at field capacity (% w/w)	pH (water)	Organic matter content (% w/w)
	2000-60	60-2	<2 μ m			
0-10	82	14	4	15	6.1	0.9
10-20	76	16	8	12	5.6	0.5
20-30	72	17	11	14	5.7	0.2

Treatments and measurements

In November 1983 experimental plots measuring 40 x 2.5-m with a 2.5-m buffer between each plot were arranged in three replicate blocks. For each replicate seven plots were deep ripped (R) to 30-cm using an Agrowplow, achieving rips on 16-cm spacing, and two plots were retained as controls (UR) in which the original hardpan remained intact. The traffic treatments chosen were zero (0P), one (1P), three (3P), five (5P), ten (10P) passes and five passes on 1/2 wheel overlap (5P1/2) of an unladen tractor applied uniformly across the full plot width. A 5.2-t tractor (Table II) was used

TABLE II

Tractor tyre data

	Tyre size	Inflation pressure (kPa)
Front	900-16	193
Rear	23.1-26	110

to apply the five recompaction treatments to the ripped plots in early May 1984. Zero traffic was applied to the remaining two ripped and two unripped plots per replicate. Before sowing a crop of winter wheat using a 12-run-combine, all plots except one each of the R/0P and UR/0P plots were scarified (SC) with a 3-m-scarifier and harrows to 10-cm depth. The trial was cropped again in 1985 with the SC treatment applied as described above after the stubble had been burned.

Penetration resistances were measured to 0.47-m depth using a Bush recording penetrometer (Anderson et al., 1980). Transects of 10 penetrometer probings were taken in randomly chosen areas of each plot at 0.2-m lateral spacing. At the same time the gravimetric soil water content was measured using ring samples from a location near the penetrometer probings to 0.35-m depth at 0.05-m depth intervals per plot. Similarly, for determination of bulk density and saturated hydraulic conductivity, K_{sat} (Hartge, 1971), soil cores with a diameter of 73-mm and a height of 100-mm were sampled from two positions per plot (UR/0P, R/0P and 3P treatments only) to 0.40-m depth at 0.05-m vertical intervals. Soil strength and water content measurements were repeated throughout the growing season at monthly intervals. The soil cores for bulk density and K_{sat} were taken immediately after application of the recompaction treatments.

A modified combine harvester with a 1.78-m cut width was used to harvest 10 rows of wheat from the middle of each plot for the grain yield determinations.

RESULTS AND DISCUSSION

Soil conditions

The deep ripping operation disrupted the hardpan at 15 to 20-cm depth. Subsequent wheel traffic recompacted the loosened soil according to the number of wheel passes, with penetration resistance at 19-cm depth for the R/0P and 10P treatments being 12% and 67% respectively of the UR/0P treatment (Fig. 1a). There were no significant differences in penetration resistance between the 10P and 5P1/2 treatments.

TABLE III

Hydraulic conductivity on 17 May 1984

Depth (cm)	Saturated hydraulic conductivity, K_{sat} (m/d)			
	UR/0P	R/0P	3P	Std. error
0-20	7.8 ^a	34.4	7.9 ^a	2.00
20-40	16.6 ^a	23.6	13.8 ^a	1.98

^a Different from R/0P at 1% level.

The average soil water content on 17 May 1984 ranged from 9% (w/w) at 5-cm depth to 8% (w/w) at 35-cm depth with differences between treatments being very small and not significant. K_{sat} was significantly higher after ripping but after recompaction with three tractor passes, K_{sat} showed no significant differences when compared with the undisturbed hardpan (Table III).

Although remains of the original hardpan were still evident, deep ripping reduced soil bulk density to a depth of 30-cm (Fig. 1c). The 3P treatment recompacted the soil bulk densities to similar values to those found for the undisturbed UR/OP treatment. However, recompaction to the same bulk densities does not necessarily produce as high penetration resistances as were found in the original hardpan. For example even though bulk densities for 3P and UR/OP were similar, penetration resistance values were lower for the 3P treatment (Fig. 1d). These results suggest that chemical bonding contributes significantly to the hardpan strength and that the passage of time enhances the cohesive bonds between particles.

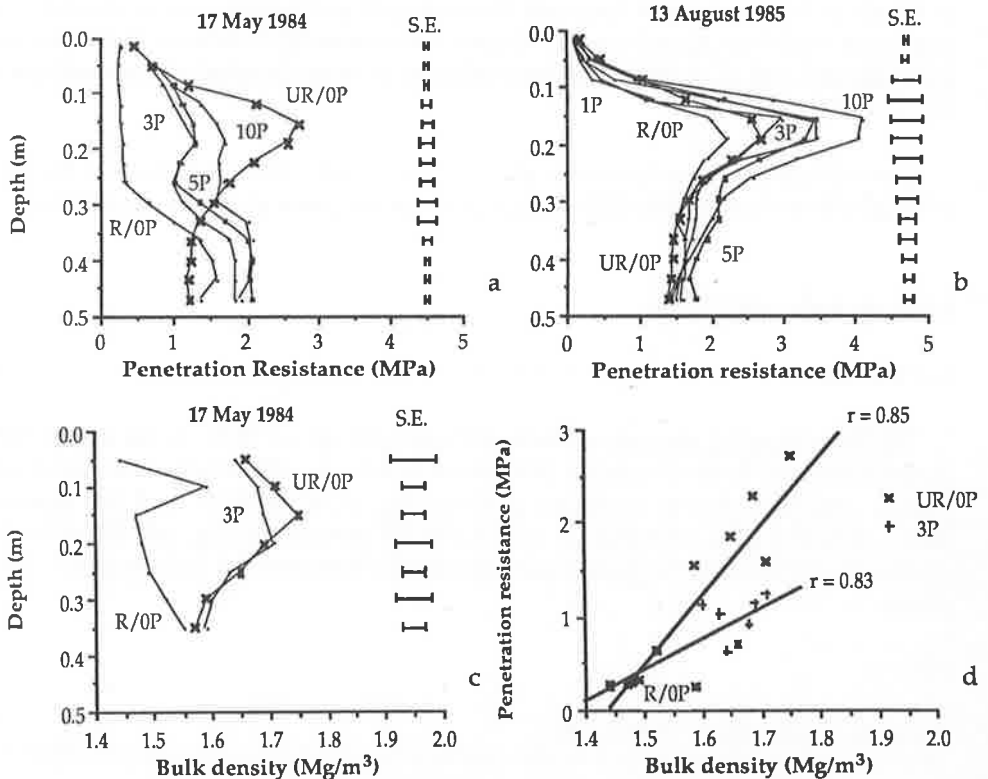


Fig. 1. Effects of deep ripping and subsequent recompaction on (a) and (b) penetration resistance at different dates and (c) bulk density. (d) Correlations between bulk density and penetration resistance on 17 May 1984 for zero traffic (OP) data (unripped and ripped), and for combined ripped (OP) and recompaction (3P) data.

Typical penetration resistances after crop emergence are shown in Figure 1b. The hardpan reformed at 15 to 20-cm depth with penetration resistance at 19-cm depth for the R/OP and 10P treatments being 83% and 150% respectively of that of the UR/OP treatment.

The average soil water content on 13 August 1985 increased from 5.5% (w/w) at 5-cm depth to 7% (w/w) at 35-cm depth with differences between treatments being very small and usually not significant.

In 1984 topsoil penetration resistances of the recompaction treatments were generally lower or similar to that for the undisturbed hardpan while in 1985 all recompaction treatments had equal or higher penetration resistances than UR/OP. During the course of the experiment, the UR/OP plots showed evidence of structural improvement probably partly due to termite activity which was observed during sampling, particularly on the undisturbed plots. Topsoil bulk densities measured specifically at some plot areas with termite activity, were significantly lower than for the UR/OP treatment on average and similar to those after deep ripping.

Crop growth

In the first year following ripping (1984), grain yields were essentially independent of traffic treatments and were generally similar or larger for the ripped treatments than for the unripped UR/OP treatment (Fig. 2a). Yields in 1985 decreased significantly with increasing number of tractor passes. Of the ripped treatments only R/OP had a larger yield than UR/OP, with the 5P1/2 treatment producing the lowest yield (1.66-t/ha).

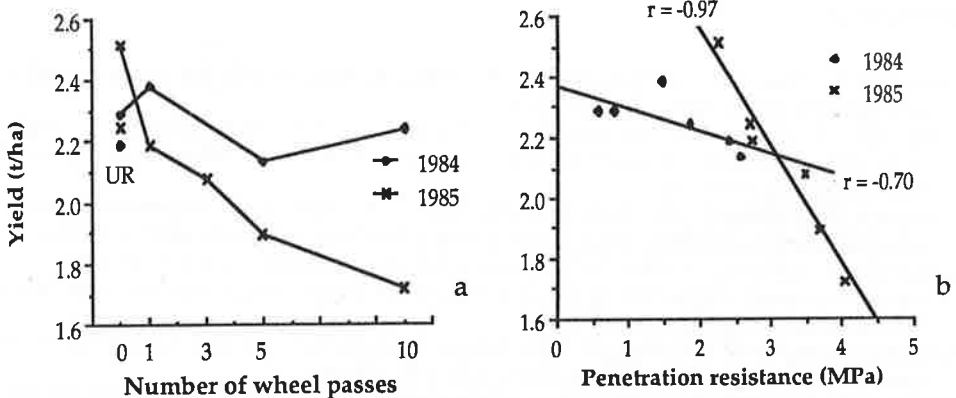


Fig. 2. (a) Variation of grain yield with number of tractor passes (the two single points show yield for the UR/OP treatment). (b) Correlation of grain yield with penetration resistance (13 August '84/'85 data) at 19-cm depth.

Figure 2b shows that yields in 1985 were correlated with penetration resistance at 19-cm depth ($r = 0.97^{**}$), but not in 1984 ($r = 0.70$). This difference undoubtedly resulted from the variation in rainfall between the two years. In 1984 precipitation between 1 April and 31 May was 178-mm, with rainfall recorded on 21 days in May. The same period in 1985 had 65-mm of rain, with only 6 days in May with rainfall, of which 63% fell in one day. Although 1985 had sufficient rainfall later in the season, only the crop of the R/OP treatment seemed to have benefited and produced a significantly higher yield than in 1984.

Since the greatest constraint for root growth and plant establishment is the high soil strength of the hardpan layer, the effect of increasing traffic on yield is greater in

years of moderate to high moisture stress. During the early stages of plant development under these conditions, root penetration through the compact hardpan is more severely restricted and the plant will subsequently be less efficient in utilizing subsoil nutrients and water.

CONCLUSIONS

- (1) Disruption of a hardpan by deep ripping markedly decreased penetration resistance and bulk density. Deep ripping remained beneficial for following crops only if recompaction was avoided, e.g. by minimum tilling.
- (2) Recompaction of the ripped soil by subsequent traffic together with age hardening, resulted in soil strengths exceeding that of the unripped soil.
- (3) Under conditions of high moisture stress during the early stages of plant development excessive soil strength of the hardpan reformed by traffic, depressed grain yields even more than did the original hardpan.

REFERENCES

- Anderson, G., Pidgeon, J.D., Spencer, H.B. and Parks, R., 1980. A new hand-held recording penetrometer for soil studies. *J. Soil Sci.*, 31: 279-296.
- Blackwell, P.S., Graham, J.P., Armstrong, J.V., Ward, M.A., Howse, K.R., Dawson, C.J. and Butler, A.R., 1986. Compaction of a silt loam soil by agricultural vehicles. I. Effects upon soil conditions. *Soil Tillage Res.*, 7: 97-116.
- Campbell, D.J., Dickson, J.W., Ball, B.C. and Hunter, R., 1986. Controlled seedbed traffic after ploughing or direct drilling under winter barley in Scotland, 1980-1984. *Soil Tillage Res.*, 8: 3-28.
- Canarache, A., Colibas, I., Colibas, M., Horobeau, I., Patru, V., Simota, H. and Trandafirescu, T., 1984. Effect of induced compaction by wheel traffic on soil physical properties and yield of maize in Romania. *Soil Tillage Res.*, 4: 199-213.
- Chaplin, J., Lueders, M. and Rugg, D., 1986. A study of compaction and crop yields in loamy sand soil after seven years of reduced tillage. *Trans. ASAE* 29: 389-392.
- Fausey, N.R. and Dylla, A.S., 1984. Effects of wheel traffic along one side of corn and soybean rows. *Soil Tillage Res.*, 4: 147-154.
- Hamblin, A.P. and Tennant, D., 1979. Interactions between soil type and tillage level in a dryland situation. *Aus. J. Soil Res.*, 17: 177-189.
- Hartge, K.H., 1971. *Die physikalische Untersuchung von Böden*. Ferdinand Enke Verlag, Stuttgart, 168 pp.
- Jarvis, R.J., Hamblin, A.P. and Delroy, N.D., 1985. Continuous cereal cropping with alternative tillage systems in Western Australia. *Western Australian Dept. Agric. Techn. Bull.*, 71, 37 pp.
- Luke, G.J., Burke, K.L. and O'Brien, T.M., 1987. Evaporation data for Western Australia. *Western Australian Dept. Agric., Techn. Report*, 65, Div. Resource Management, 29 pp.
- Soane, G.C., Godwin, R.J. and Spoor, G., 1986. Influence of deep loosening techniques and subsequent wheel traffic on soil structure. *Soil Tillage Res.*, 8: 231-237.
- Söhne, W., 1953. Druckverteilung im Boden und Bodenverformung unter Schlepperreifen. *Grundl. Landtechnik*, 5: 49-63.
- Soil Survey Staff, 1975. *Soil Taxonomy. A basic system of soil classification for making and interpreting soil surveys*. Agric. Handbook No. 436. USDA. U.S. Government Printing Office, Washington, D.C., 754 pp.
- Voorhees, W.B., Evans, S.D. and Warnes, D.D., 1985. Effect of preplant wheel traffic on soil compaction, water use, and growth of spring wheat. *Soil Sci. Soc. Am. J.*, 49: 215-220.

Physico-chemical interaction and mobility of pesticides in soils.

Singh, Rai, Gerritse, R.G. and Aylmore, L.A.G.

National Workshop on Persistence of Herbicide Residues in Wheat Cropping Systems in
Australia , Melbourne, Oct., 1988. 32-47.

PHYSICO-CHEMICAL INTERACTIONS AND MOBILITY OF PESTICIDES IN SOILS

Rai Singh¹, R.G. Gerritse² and L.A.G. Aylmore¹

1 Soil Science and Plant Nutrition
School of Agriculture
The University of Western Australia
Nedlands W.A. 6009

2 Division of Water Resources
CSIRO
Wembley W.A. 6014

ABSTRACT

The effect of soil conditions such as pH, salinity, organic matter content, presence of organic co-solvent and competitive adsorption by other inorganic salts (e.g. gypsum) on the adsorption-desorption behaviour of a number of commonly used pesticides in soils varying in texture from sand to clay have been examined. Pesticides examined include paraquat, diquat, simazine, linuron and fenamiphos.

The extent and mechanism of retention of the pesticides in soil is directly related to their chemical nature (i.e. whether ionic or non-ionic, basic or acidic). In general, pesticide adsorption followed the order paraquat > diquat > linuron > fenamiphos > simazine in all soils. The amount adsorbed increased with increasing organic matter and clay content of the soil. The amount adsorbed was more affected by organic matter content than clay content in all cases except for paraquat and diquat where clay content was more important.

The adsorption of simazine and to lesser extent of fenamiphos and linuron decreased with increase in pH while the adsorption on diquat was essentially unaffected by the change in soil pH. Increasing background salt concentration markedly decreased the adsorption of diquat and paraquat, but only slightly altered the adsorption of other pesticides.

While pesticides such as diquat and paraquat are generally considered to be essentially irreversibly retained by soil, it is significant that in the present work some 60% of adsorbed diquat could be released to solution from a sandy soil by extraction with 0.05 M CaCl₂.

Presence of organic co-solvent in soil solution affected the adsorption of linuron and simazine. The adsorption was found to decrease exponentially with increasing methanol concentration in background solution, thus suggesting that under waste disposal sites where the soil solution most likely contains organic co-solvents, the mobility of pesticides can be much higher than that expected from adsorption from aqueous solutions.

The ground water pollution potential of these pesticides was evaluated from the adsorption and their biochemical decay data using a recent model. Except simazine, all other herbicides fall under low risk categories. However, simazine comes under a high risk category under conditions favouring potentially high pollution.

INTRODUCTION

Adsorption and degradation of pesticides in soils are the major processes which affect their movement through the soil profile and determine their potential to reach non-target organisms. Since most weed roots are close to the soil surface, the movement of herbicides in soil can result in loss of their efficiency, phytotoxic effect on crop plant roots or contamination of ground and surface water bodies depending on the extent of their adsorption and persistence in soil.

The soil environment is a dynamic one sustaining numerous physical, chemical and biological reactions. Soil properties constantly undergo changes imposed by the cultivation and subsequent management practices to maintain or improve soil fertility. Soil properties such as organic matter content, pH and concentration and composition of salts in the soil solution can change as a result of liming, gypsum application, fertilization, irrigation, different crop species, etc. For example, Isensee and Walsh (1971) reported a change of 1.3 units in pH around (i.e. within 3.8 cm) a band of urea applied at 22.4 kg N/ha and changes in Ca^{2+} concentration up to 1200 ppm (equivalent to 0.03 M) around KCl or ammonium nitrate fertilizer bands (Isensee and Walsh, 1972). Gypsum application can also result in fairly high electrolyte concentrations in the soil solution and the solubility of gypsum (0.03 M) can increase 2 to 3 fold in the presence of NaCl (Williams, 1988). There is evidence that soil acidification is occurring progressively in Western Australian soils. A slow and, at least in the short term, irreversible decline in organic matter is occurring in many Australian soils (Gerritse and George, 1988).

These changes in soil properties can have an important bearing on the efficiency and safe usage of pesticides. Some herbicides are phytotoxic even at very low levels and may become mobile under favourable soil conditions. Also some pesticides, due to their persistent nature (e.g. paraquat), tend to accumulate in the system and changes in soil properties at some later stage, with subsequent release, may produce harmful effects.

This paper reports on the adsorption-desorption characteristics of some commonly used pesticides representing different chemical classes, in Western Australian soils exhibiting a range of physico-chemical properties. In addition the effects of pH, organic matter, clay content, type and content of salts in soil solution on the adsorption-desorption behaviour of the pesticides has been examined and their pollution potential has been evaluated.

MATERIALS AND METHODS

Soils and Pesticides

Four Western Australian soils which differ appreciably in their physico-chemical properties were used. These were Bassendean sand (1.2% o.m. and clay, pH 5.0); Cobiac loamy sand (0.6% o.m., 13.7% clay and pH 5.1); Gascoyne sandy loam (1.7% o.m., 15.3% clay and pH 6.9) and Wellesley clay (4.6% o.m., 64% clay and pH 5.9). The pH was measured in 1:5 0.01 M CaCl_2 . More detailed soil properties are given elsewhere (Singh *et al.* 1988).

Five pesticides, including the herbicides diquat, linuron, paraquat and simazine and a nematicide, fenamiphos, were used in the study. Diquat and paraquat are knockdown herbicides and are undoubtedly the most commonly used pesticides in Western Australia. Linuron, fenamiphos and simazine pesticides are applied directly to the soil. Detailed properties of these pesticides have been given by Hartley and Kidd (1987).

Adsorption-Desorption Studies

The equilibrium distribution at 25 °C of the pesticides, was studied using a batch technique. Five grams of air-dried soil with 10 ml of 0.005 M CaCl₂ solution containing a range of pesticide concentrations, was equilibrated on a shaker for 24 hours. After centrifugation, the soil solution was decanted and the pesticide concentration in the soil solution was measured by HPLC. The methods for the analysis of the pesticides have been described elsewhere (Singh *et al.* 1988). Adsorption was calculated from differences in solution concentration before and after equilibration. To obtain the desorption isotherms, the soil solution containing pesticide was replaced by pesticide-free solution (0.05 M CaCl₂) after the adsorption equilibration, the soil suspensions were then shaken for 24 hours, centrifuged for 15 mins and the supernatant analysed for desorbed pesticide concentration. This procedure was repeated a number of times to obtain successive desorption points.

To study the effect of pH on adsorption, the pH of soil solution was pre-adjusted with HCl or NaOH before use. The effect of salinity was studied using various concentrations of CaCl₂.

RESULTS AND DISCUSSION

The adsorption of the pesticides followed the order: paraquat > diquat > linuron > fenamiphos > simazine in all the soils studied. Adsorption isotherms for the various pesticides on Bassendean sand are compared in Figure 1. The extent of adsorption depends on the nature of the pesticide. Paraquat and diquat, being divalent cations, are readily adsorbed to negatively-charged clay and organic matter particles and hence are the most strongly adsorbed. In contrast, fenamiphos and linuron are non-ionic pesticides, while simazine is ionizable to a cation to an extent dependent on the pH of soil.

The equilibrium adsorption coefficients [based on the Freundlich equation: $S=KC^n$; where S is the adsorbed concentration (ug/g), C is the solution concentration (ug/ml), and K and n are coefficients] for the various pesticides and soils are given in Table 1. It should be noted that the adsorption isotherms of diquat and paraquat more closely fitted the Langmuir isotherm, but the Freundlich parameters are used here for the purpose of comparison. The adsorption of diquat and paraquat increased with increasing clay content of the soils, while that of the other pesticides increased with organic matter content. The exception was the Gascoyne soil which showed less adsorption than Bassendean sand despite its high o.m. and clay contents, and this can be explained in terms of the effects of soil pH.

The effects of removal of organic matter by hydrogen peroxide treatment on adsorption has as yet only been studied for linuron and diquat. The Freundlich equation K value of linuron for the clay soil decreased from 29 to 9 ug¹⁻ⁿ mlⁿ g⁻¹, while the soil adsorption capacity for diquat decreased from 27000 to 19000 ug/g.

Adsorption isotherms for fenamiphos, linuron and simazine at different pH of the soil solution are shown in Figure 2. The adsorption of these pesticides decreased with increasing pH of the soil solution. This effect was more pronounced in case of simazine than for linuron and fenamiphos. This occurs because simazine is a weakly basic herbicide and has a pKa of 1.4 (the pH value at which half the simazine is in the cation form and the rest in molecular form). As the pH increases, the proportion of simazine cations in solution decreases and hence the adsorption decreases. Fenamiphos and linuron are adsorbed by other mechanisms such as Hydrogen bonding and this is also affected by pH to some extent. Because of its comparatively higher pH, the Gascoyne soil showed less adsorption of these pesticides (Table 1). The adsorption of paraquat and diquat was unaffected by change in pH.

The adsorption of the cationic herbicides, diquat and paraquat, decreased markedly with increase in salt concentration in soil solution (Figure 3). However, the adsorption of other pesticides was only slightly affected. An increase in background salt concentration from 0.005 to 0.05M CaCl₂ resulted in a decrease by a factor of 2 and 5, respectively, in the Freundlich K value for paraquat and diquat in Bassendean sand. Also the total capacity of the soil to adsorb diquat (calculated from Langmuir isotherm) was reduced by some 20% in sand, 30% in loamy sand, 30% in sandy loam and 20% in clay soil due to the increase in salt concentration.

Figure 4 shows the adsorption of paraquat and of diquat corresponding to various concentrations of Ca²⁺ and Na⁺ in the soil solution. Both Ca²⁺ and Na⁺ compete for the adsorption sites with paraquat and diquat. Ca²⁺ was found to be more effective than Na⁺ for both pesticides, however Na⁺ was more effective in reducing the adsorption of diquat than of paraquat.

Desorption was similarly found to be affected by the presence of salts. Figure 5 shows increasing desorption of paraquat and diquat with increasing salt concentration in the extracting solution. The percentage extraction increased from 7.5 to 35 for paraquat and from 13 to 46 for diquat in Bassendean soil as the salt solution concentration increased from 0.005 to 0.05 M. Total diquat in five successive extractions with 0.05 M CaCl₂ for other soils were 62, 18 and 7% in Cobiac loamy sand, Gascoyne sandy loam and Wellesley clay soils, respectively.

The increased extraction with any given salinity was greater in the sandy than in the clay soil. Diquat and paraquat have generally been considered to be essentially irreversibly adsorbed, and for their extraction such harsh treatment as boiling with 18 N sulfuric acid is usually needed. However, it is significant that in the present study, up to 62% of diquat could be extracted from a loamy sand soil. It is shown in Figure 6 that a sudden increase in salinity (e.g. due to irrigation with salty water as practised in vegetable growing areas, Farmnote No. 93/82) can result in a very high increase in the concentration in solution of the diquat. Due to the very persistent nature of paraquat and diquat (10% loss per year of paraquat, Hance *et al.* 1980) their build-up is possible following repeated applications, and subsequent change in landuse or management practices could result in harmful effects. This may have implications for herbicide recommendations such as spray seed (mixture of paraquat and diquat) for puccinellia saltland grass establishment in saltlands (Farmnote No 17/80).

The Freundlich adsorption coefficient of simazine herbicide in the presence of different concentrations of methanol in equilibrating solution in clay soil are given in Figure 7. It is evident from the figure that the adsorption of the herbicides decreased exponentially with the increase in methanol concentration in soil solution. The Freundlich adsorption coefficients corresponding to different fractions of methanol in soil solution for simazine and linuron along with retardation factors for their mobility in soil are given in Table 2.

Retardation factor (R) may be viewed as an index of herbicide mobility in soil relative to free water tracer such as chloride or bromide and can be calculated from adsorption coefficient (K) according to the relationship:

$$R = 1 + D_b K/\theta$$

where D_b is bulk density of soil (g/cm^3) and θ is volumetric moisture content (cm^3/cm^3). When a herbicide does not show any adsorption, the retardation factor is one - i.e. the herbicide will move with leaching soil solution.

The retardation factors for simazine and linuron decreased sharply with increase in methanol concentration in soil solution (Table 2). This has implications for waste disposal sites where the soil solution may not be purely of an aqueous solution and may contain significant amounts of organic co-solvents. The mobility of pesticides under such situations could be much higher than that expected from the adsorption data from aqueous solutions.

The potential risk of ground water contamination associated with the use of these pesticides was evaluated from the data on sorption and persistence according to the model of Jury *et al.* (1987).

The model assumes that during leaching through soil at a uniform flow rate the pesticides undergo a linear reversible, equilibrium adsorption and first-order biochemical decay. The model takes into account the decrease in the microbial activity with the depth in soil profile, but assumes uniform organic matter content throughout the soil profile. Jury *et al.* (1987) evaluated potential risk of about 50 pesticides under two pollution potential scenarios (a high and a low pollution situation). The main soil parameters used were organic matter content of 0.5% and a drainage rate of 1 m/yr for situations favouring potentially high pollution, while for low pollution risk the respective conditions were 3.0% and 0.5 m/yr. For other details the reader is referred to the paper by Jury *et al.* (1987).

The low and high risk regions for the two potential pollution situations are shown in Figure 8, separated by continuous lines. The positions of different herbicides have been shown on the basis of their sorption data in these soils and their biochemical half lives from the literature (Jury *et al.*, 1987).

The sorption in terms of K_{oc} (i.e. $K \times 100/\text{organic carbon in } \%$) and the half lives values for the pesticides plotted in Figure 8 show that all other pesticides fall under a low risk region except simazine. Simazine, however, falls in high risk region under situations of high pollution potential for the four soils studied. In the case of diquat, half life was assumed to be 200 days in the absence of data from the literature. The figure also shows that despite high adsorption of a pesticide, it can still come under a high risk region due to its long half life.

These laboratory studies show that change in soil conditions associated with management practices such as liming, gypsum application, fertilization, irrigation with saline water etc. can significantly influence the retention and release of pesticides in soils. The adsorption is directly related to the movement of pesticides. Such effects can be important from the point of view of mobility of these pesticides in soils. Also the disposal of herbicides and other wastes together can have serious implications in terms of pesticide mobility and contamination of ground water. Clearly, more detailed studies of the adsorption-desorption behaviour of pesticides under a wider range of soil conditions is urgently required and this behaviour should be seriously considered prior to the introduction of particular management practices in conjunction with pesticide usage as well as pesticide waste disposal.

REFERENCES

- Farmnote No. 93/82. Irrigation of vegetables with salty water. W.A. Dept. Agriculture, Agdex 250/563.
- Farmnote No. 17/80. Sprayseed for puccinellia establishment. W.A. Dept. Agriculture, Agdex 343/21.
- Gerritse, R.G. and George, R. (1988). The role of soil organic matter in the geochemical cycling of chloride and bromide. *J. Hydrol.* (in press)
- Hance, R.J., Byast, T.H. and Smith P.D. (1980). Apparent decomposition of paraquat in soil. *Soil Biol. Biochem.* **12**: 447-448.
- Hartley, D. and Kidd, H. (1987). (eds.) The Agrochemicals Handbook. The Royal Soc. Chem. The University of Nottingham, England.
- Isensee, A.R. and Walsh, L.M. (1971). Influence of banded fertilizer on the chemical environment surrounding the band. I. Effect on pH and solution nitrogen. *J. Sci. Fd Agric.* **22**: 105-109.
- Isensee, A.R. and Walsh, L.M. (1972). Influence of banded fertilizer on the chemical environment surrounding the band. II. Effect on soil solution cations, cation-anion balance and solution phosphorus. *J. Sci. Fd. Agric.* **23**: 509-516.
- Jury, W.A., Focht, D.D. and Farmer, W.J. (1987). Evaluation of pesticide groundwater pollution potential from standard indices of soil-chemical adsorption and biodegradation. *J. Environ. Qual.* **16**: 422-428.
- Singh, R., Gerritse, R.G. and Aylmore, L.A.G. (1988). Adsorption desorption of selected pesticides in Western Australian soils. (in preparation).
- Williams, B.G. (1988). Management of saline and alkaline soils in Australia. CSIRO Division of Water Resources Tech. Memo. No. 88/4. p 7.

Table 1. Freundlich coefficients (K in $\mu\text{g}^{1-n} \text{m}^n \text{g}^{-1}$) for adsorption of pesticides.

	sand	loamy sand	sandy loam	clay
		Diquat		
K	103	140	2500	12300
n	0.3	0.2	0.3	0.4
		Fenamiphos		
K	5.0	0.7	2.0	19.4
n	0.7	0.9	0.8	1.0
		Linuron		
K	7.0	3.0	4.0	29.2
n	0.8	0.7	0.7	0.8
		Simazine		
K	1.2	0.5	0.9	13.3
n	0.9	0.9	1.0	0.8

Table 2. Freundlich adsorption coefficient (K in $\mu\text{g}^{1-n} \text{m}^n \text{g}^{-1}$) of linuron and simazine in clay soil at different concentrations of methanol in solution.

Methanol fraction	Log K	n	Retardation factor
		Linuron	
0.10	1.186	1.00	41.92
0.20	0.976	0.95	26.23
0.40	0.468	0.77	8.83
0.50	0.259	0.64	5.84
		Simazine	
0.10	0.834	0.74	19.2
0.20	0.706	0.66	14.55
0.40	0.2788	0.59	6.06
0.60	-0.1537	0.61	2.87

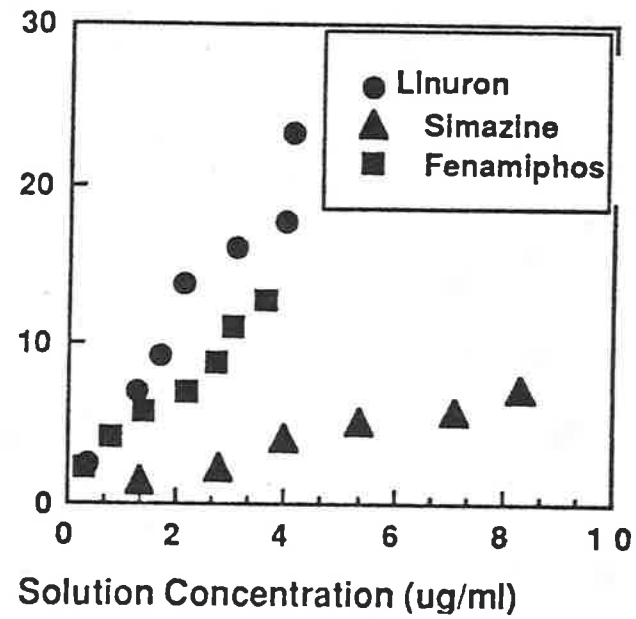
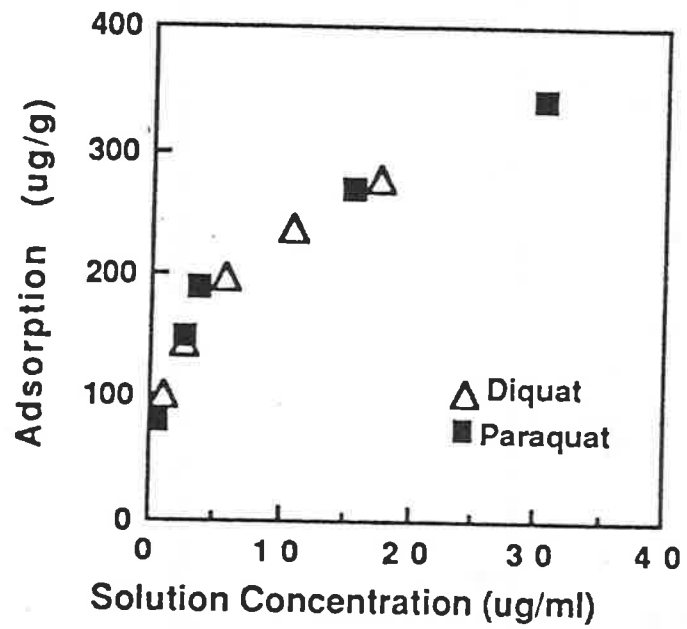


Fig 1. Comparison of adsorption of five pesticides in Bassendean sand.

Adsorption ($\mu\text{g/g}$)

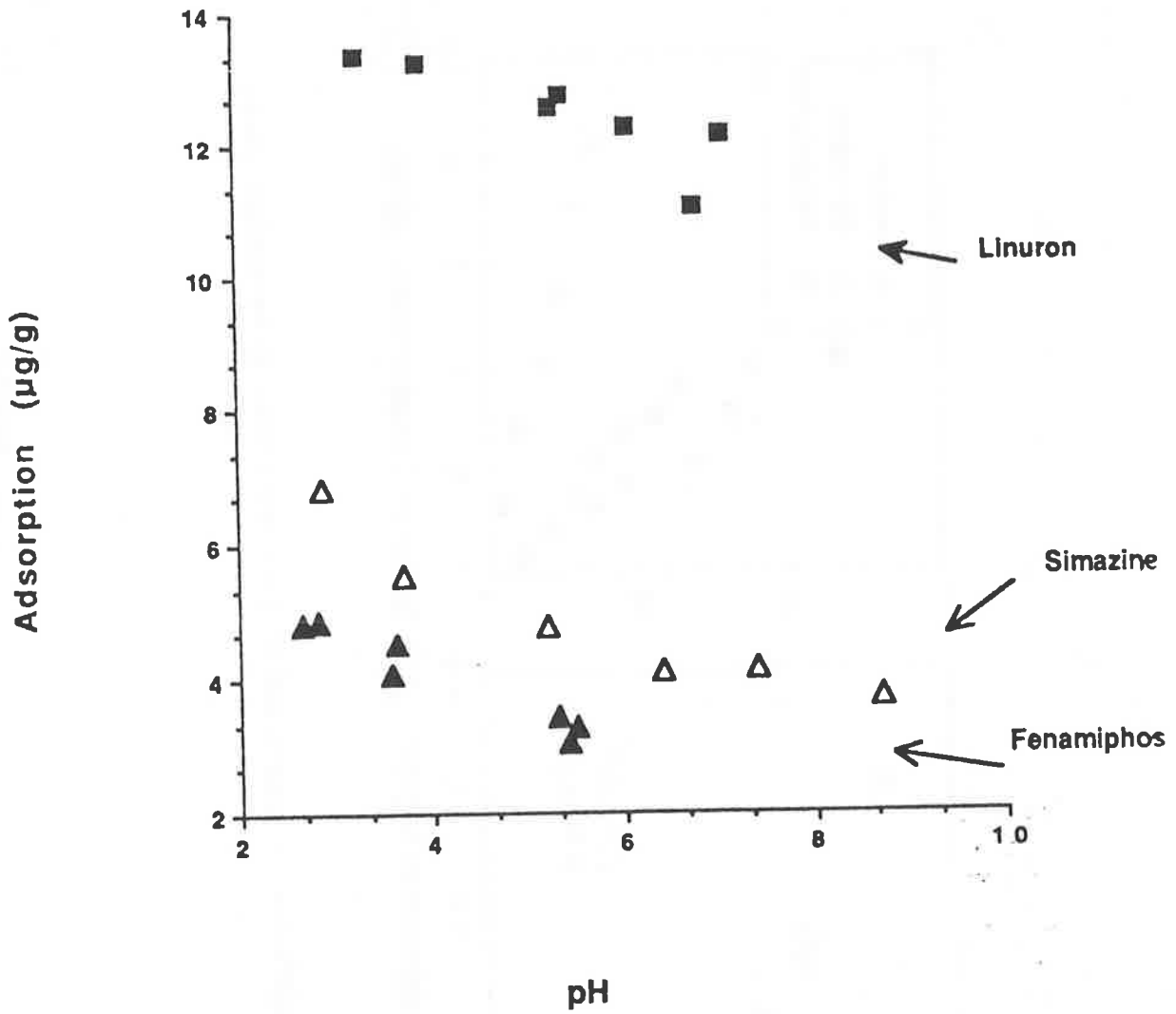


Fig 2. Effect of pH on adsorption of pesticides.

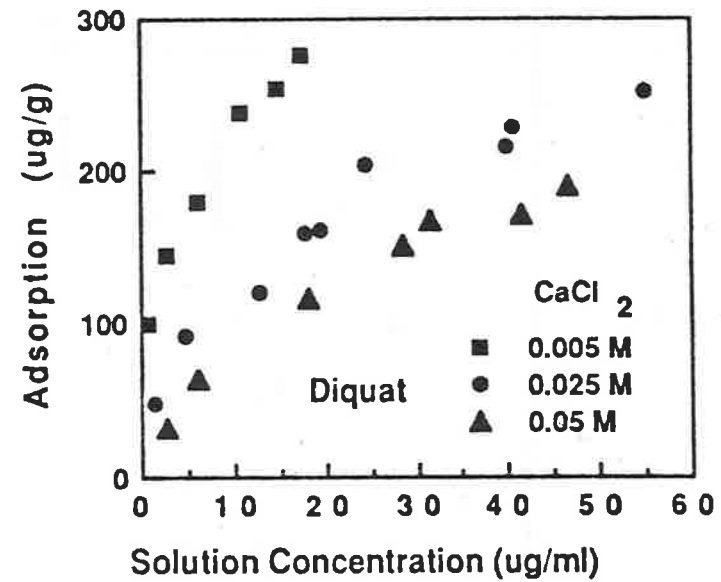
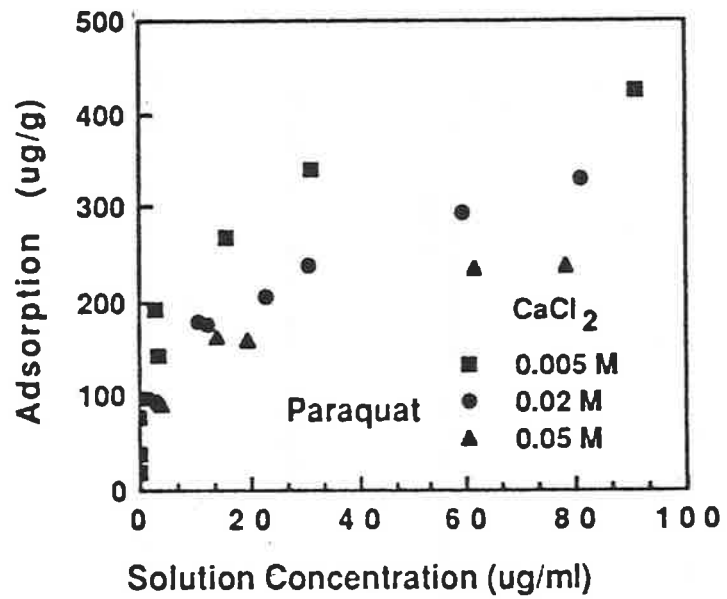


Fig 3. Effect of solution salt concentration on adsorption.

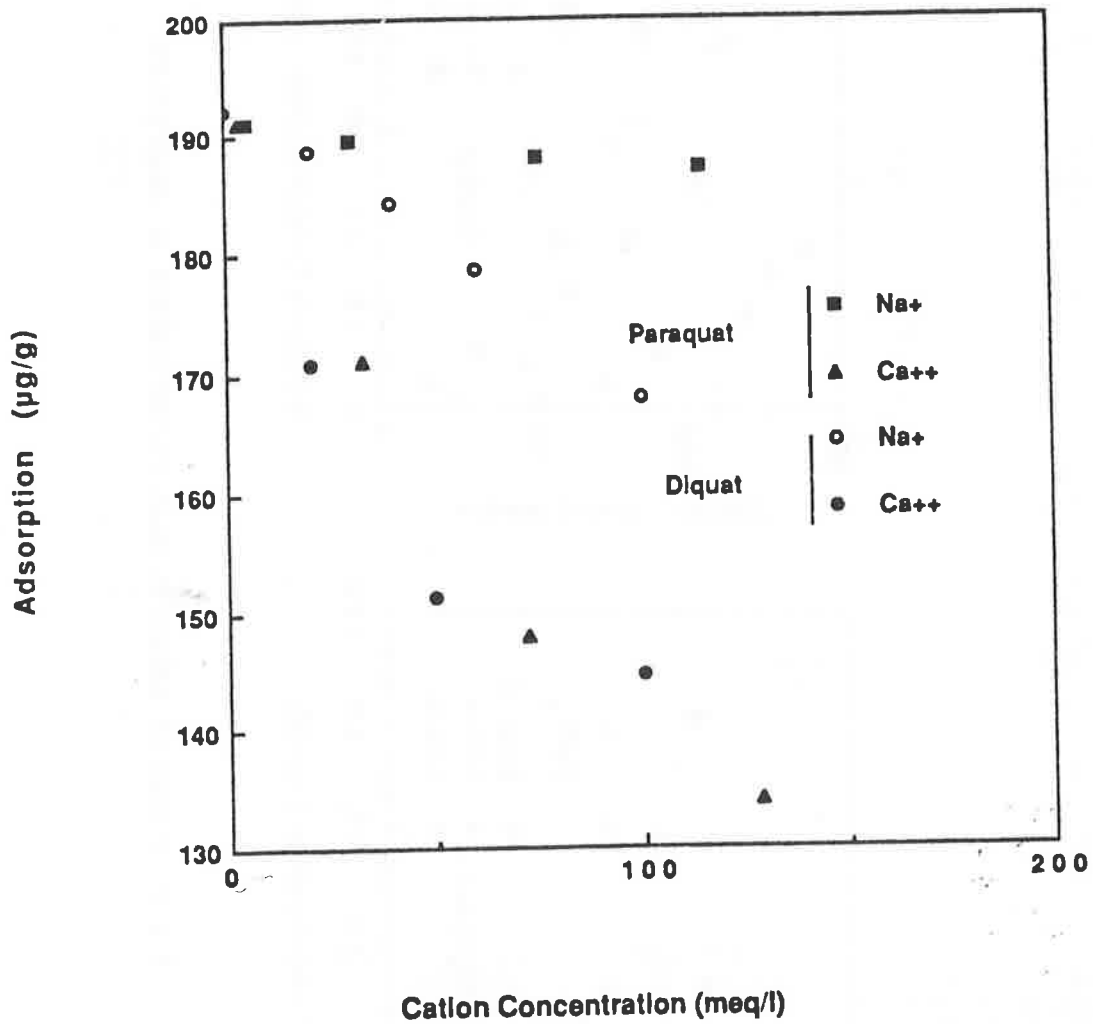


Fig 4. Effect of type of inorganic salts on adsorption.

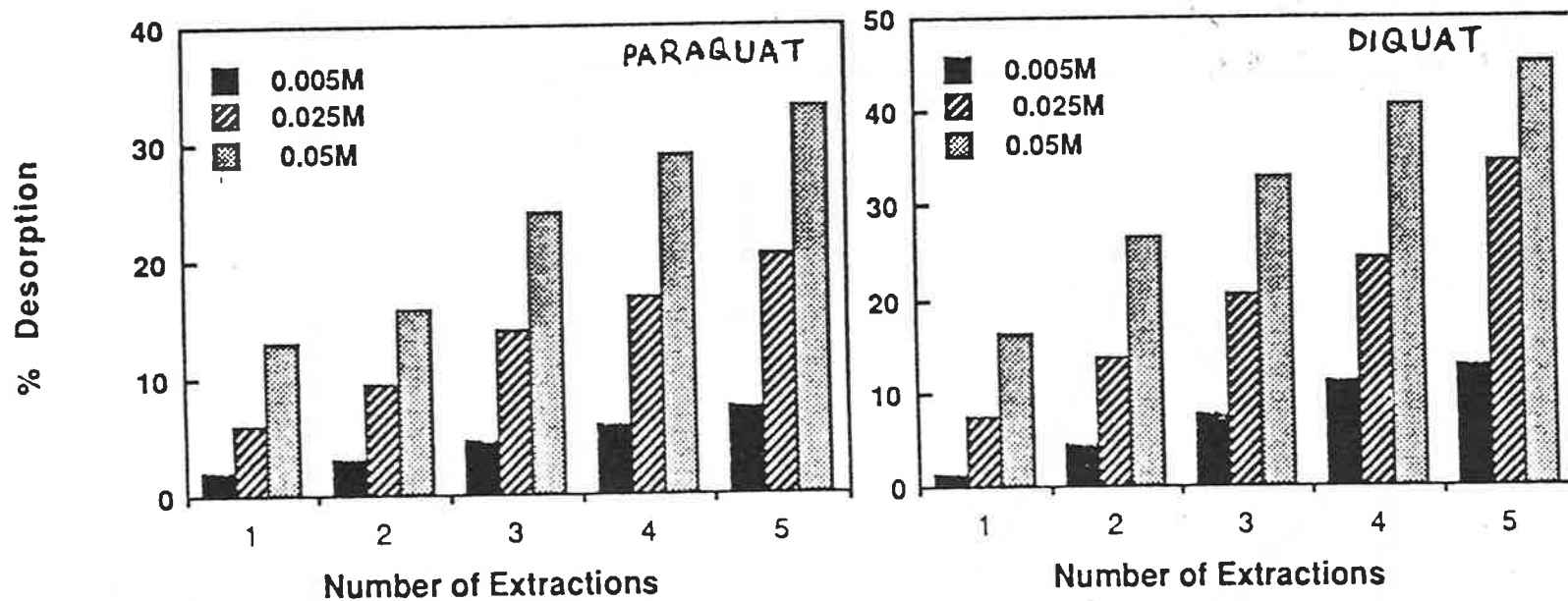


Fig 5. Effect of solution salt concentration on desorption.

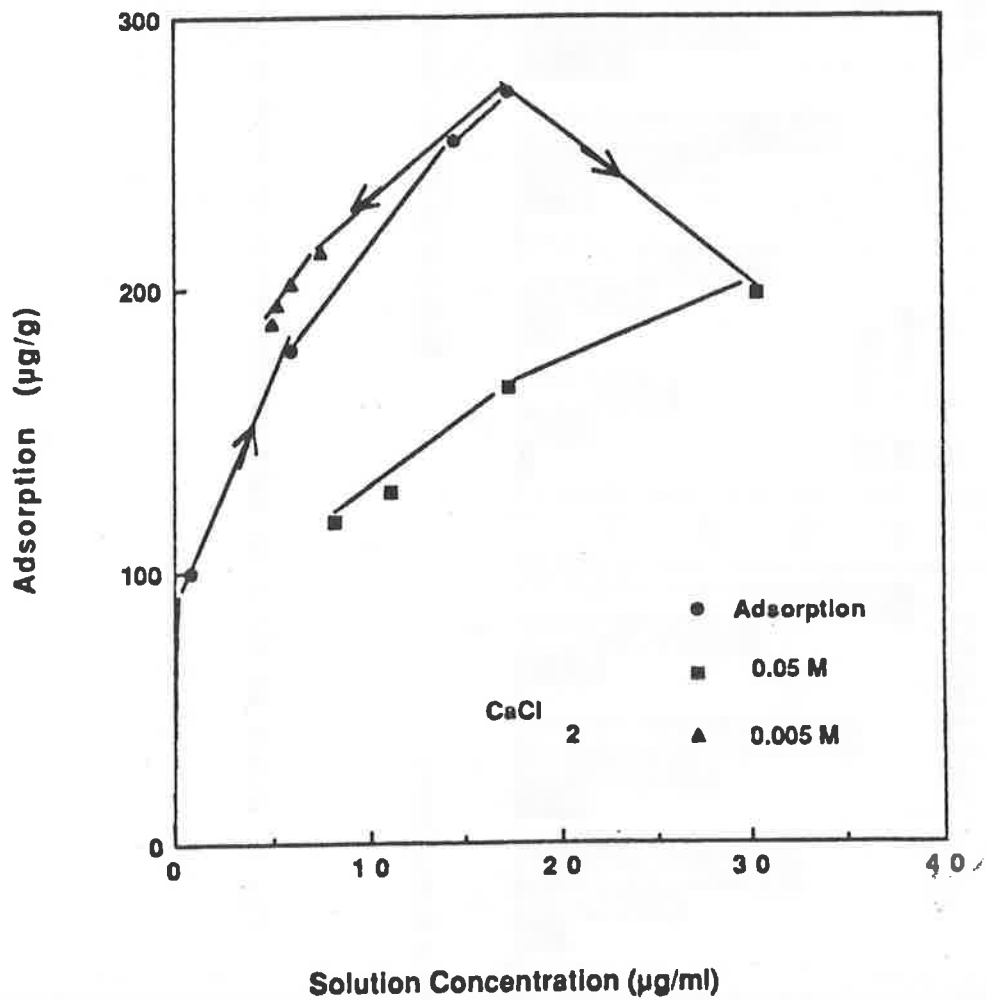


Fig 6. Desorption isotherms of diquat at two salt concentrations.

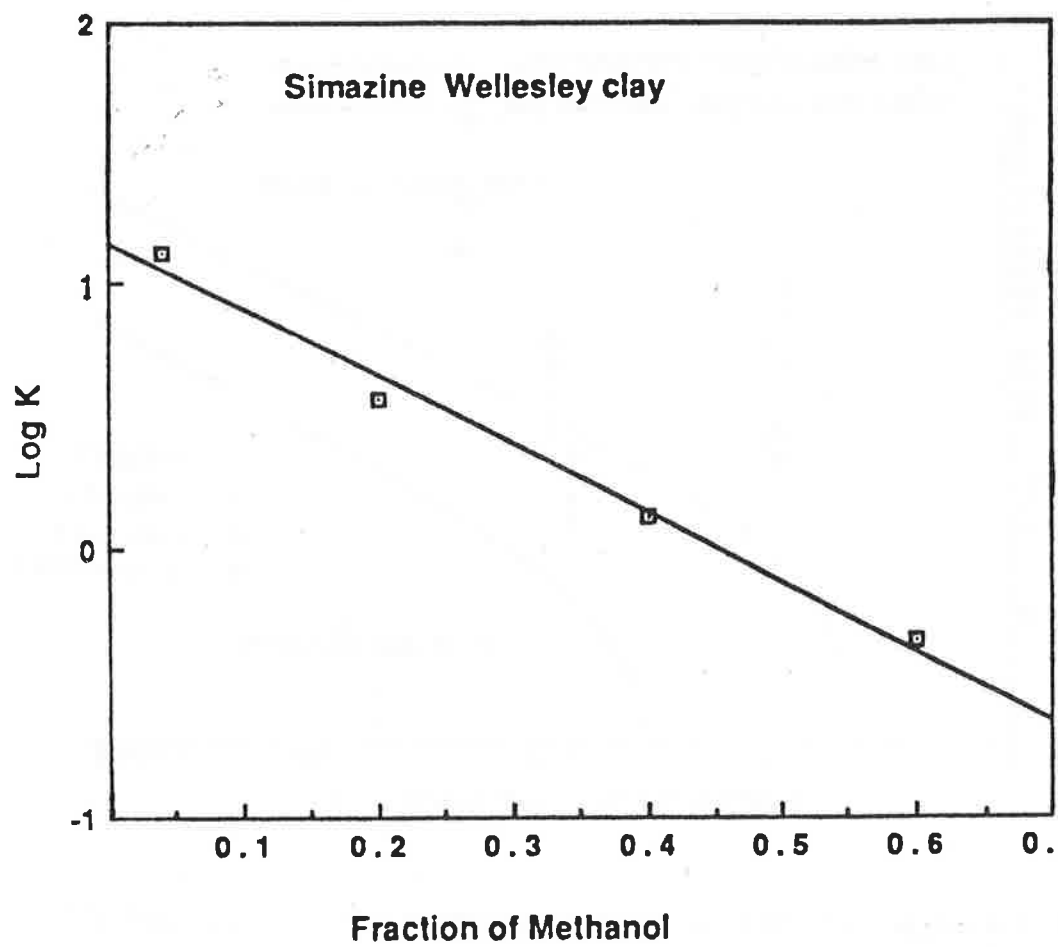


Fig 7. Effect of methanol concentration in soil solution on Freundlich adsorption coefficient (K) of simazine.

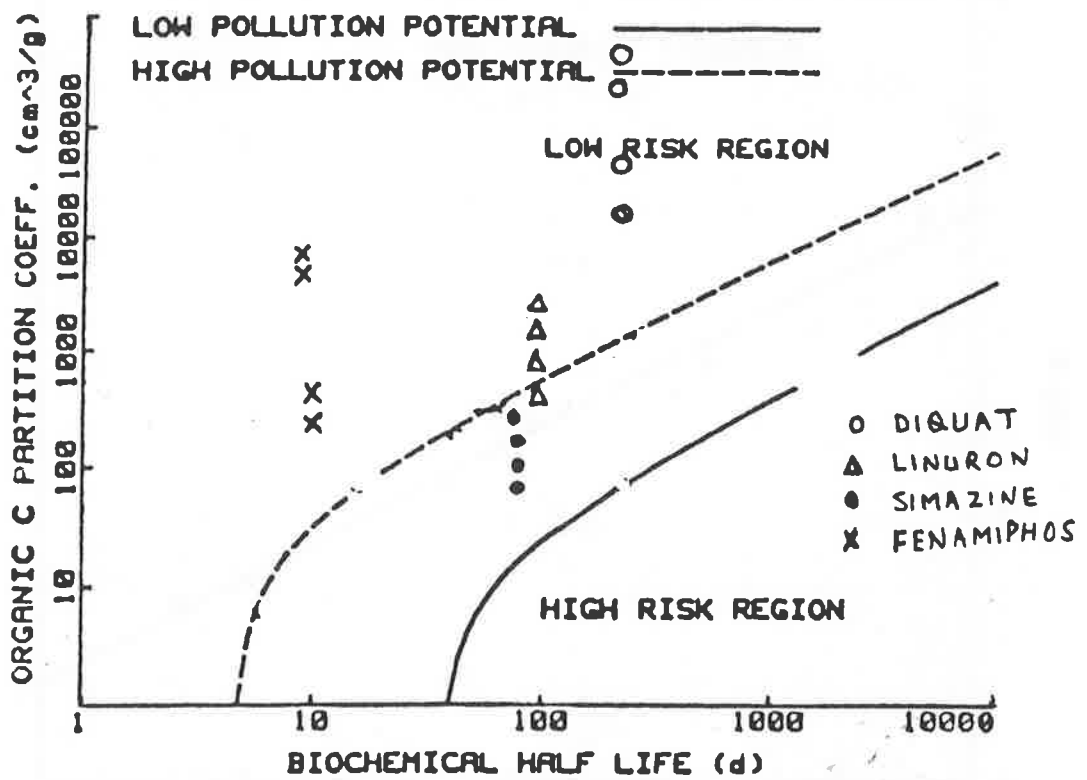


Fig 8. Pollution potential of pesticides under low and high pollution situations.

Non-uniform soil water extraction by plant roots

J.M. HAINSWORTH and L.A.G. AYLMORE

Soil Science and Plant Nutrition, School of Agriculture, The University of Western Australia, Nedlands, W.A. 6009, Australia

Received 25 May 1987. Revised August 1988

Key words: CAT scanning, drawdown, plant roots, resistance, water uptake

Abstract

Using the technique of Computer Assisted Tomography applied to gamma ray attenuation measurement of soil water content, it has been shown that the assumption of uniform absorption of soil water along a plant root is clearly erroneous and that drawdown distance is a function of time. The results suggest that the plant sequentially removes water from the top to the bottom of the root as soil hydraulic resistance becomes a major limiting factor in the upper layers, even at the high soil water potential (-0.30 MPa) used.

Introduction

Soil water extraction by single plant roots is often described using the framework of Gardner (1960) and Cowan (1965). The conceptual basis of these two models of water extraction is the assumption that water flows radially through the soil to the plant root which acts as a uniform absorbing cylinder, and that water is supplied uniformly to the root from a soil cylinder, the outer radius of which is determined by root density, and the inner radius by the outer edge of the root. Whilst such models have increased our understanding of water extraction by plant roots several of the above assumptions appear to be unrealistic.

The presence of an axial root resistance along a root suggests that water extraction would be greatest at the top of the root. The results of Hainsworth and Aylmore (1986) showed that this appeared to be the case for 9–10 days old radish roots. In the case of older roots Caldwell (1976) has suggested that the more suberised parts of the root would be less active in extracting soil water. In either case it would appear that the assumption of the root acting as a uniform absorbing cylinder is likely to be erroneous. The results of Caldwell (1976) and Hainsworth and Aylmore (1986) sug-

gest that a consequence of non uniform absorption of soil water would be that soil resistance to water flow could become limiting at points along the roots. The work of Hainsworth and Aylmore (1986) also indicates that the drawdown distance over which water is supplied to the plant root may be a function of the rate of water extraction which suggests that the outer radius of the supply zone is not entirely dependant on root density.

Until recently a major problem in validating the assumptions used in single root models of water extraction has been the lack of a suitable technique to examine the changes in soil water drawdowns along a plant root, with time, in a non destructive manner. Previous evidence of non-uniform absorption of water by roots has depended largely on measurements conducted in culture solutions (Shone and Flood, 1980; Sanderson, 1983) or on indirect measurements (So *et al.*, 1978). However, Hainsworth and Aylmore (1983; 1986) have shown that this problem can be overcome by application of Computer Assisted Tomography (CAT) to radiation scanning techniques. In the course of more detailed studies of soil-plant water balances, a point of particular interest with respect to the assumptions outlined above was observed and is reported here.

Materials and methods

A conventional gamma scanner modified to enable the CAT scanning procedure to be undertaken (Hainsworth and Aylmore, 1988) was used in these experiments. The scanner utilises a 500 milli Ci Cs-137 source and a Plastic Scintillant detector and takes approximately 2 minutes to measure the water content distribution in a 5 mm slice of a 42 mm diameter soil column. The water content distribution of the slice is then mapped into a 21 by 21 matrix of 2 mm square pixels.

A 4.2 cm diameter, 12 cm tall acrylic cylinder was uniformly packed with a soil mix containing 15% Clackline kaolinite and 85% Bassendean sand from Western Australia and scanned at 2, 6 and 9 cm depth from the top of column. The column was then watered to 0.31 g/cm and a pre-germinated radish seedling planted in the centre of the column. After 9 days the column was re-watered to 0.30 g cm⁻¹ (-0.30 MPa) and the column placed in darkness for 24 hours to allow the water content to equilibrate. The column was then placed in a growth cabinet mounted on the CAT scanning platform and the lights turned on. The column was re-scanned at 2, 6 and 9 cm depth at 1, 4 and 8 hours after transpiration had commenced. During the experiment conditions in the growth cabinet remained approximately constant with a temperature of 19.9 degrees and relative humidity of 21%.

At the conclusion of the experiment the soil column was carefully excavated and root morphology examined. There was no evidence of laterals or root hair development on the single tap root. Soil water drawdowns were plotted by averaging the water content values of the pixels equidistant from the plant root. Water extraction from the slices was calculated by summing the water loss from each pixel.

Results and discussion

The results obtained are presented in Figs. 1a-c which show the changes in soil water drawdown along the root with time. During the eight hours water extraction was greatest in the top layer and least in the bottom layer. However, the results

presented in Figs. 1a-c and Table 1 show that the patterns of extraction changed with time.

In the first hour of transpiration, the rate of water extraction was greatest in the topmost layer. Presumably this occurred in response to the combination of an axial resistance along the root (Oosterhuis, 1981) and the tapering radish root having a greater surface area for water uptake at the top of the root (see Table 1). The result of increased uptake in the topmost layer was a larger gradient in soil water content from bulk soil to plant root (see Fig. 1a). The consequence of this increased gradient was that the rate of extraction from this slice increased from 0.035 g h⁻¹ cm⁻¹ to 0.071 g h⁻¹ cm⁻¹ during the following 3 hours. Clearly, during this

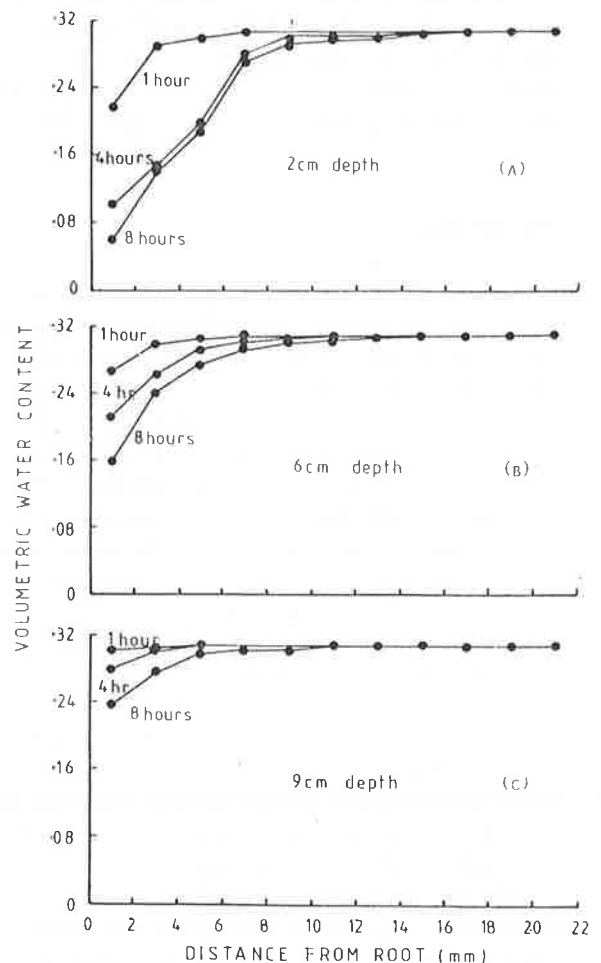


Fig. 1. Change to drawdowns of soil water content in proximity to a radish root at 2, 6 and 9 cm depth after one, four and eight hours transpiration.

Table 1. Cummulative extraction, incremental extraction and rate of extraction for the three different depths

Depth from surface (cm)	Root radius (mm)	Time (h)	Cummulative extraction (g)	Incremental extraction (g)	Rate of extraction (g h^{-1})
2	0.26	1	0.035	0.035	0.035
		4	0.251	0.216	0.072
		8	0.320	0.069	0.017
6	0.19	1	0.017	0.017	0.017
		4	0.070	0.053	0.018
		8	0.136	0.066	0.016
9	0.09	1	0.003	0.003	0.003
		4	0.010	0.007	0.002
		8	0.060	0.050	0.012

time, the hydraulic conductivity of the soil was not limiting and the increased gradient resulted in a greater flux to the root. However, in the next 4 hours extraction rate decreased to $0.021 \text{ g g}^{-1} \text{ cm}^{-1}$. The increased extraction from this layer during the previous 3 hours resulted in a large drop in water content at the root surface (see Fig. 1a) and presumably the soil water potential at the root surface had become limiting in this slice at 4 hours. However, the fact that soil water content and hence water potential at the root surface had continued to decrease in the following 4 hours suggests that the plant may have lowered its root water potential. Unfortunately it was not possible to monitor leaf water potentials in this experiment.

It is interesting to note that at 4 and 8 hours from commencement of transpiration the shape of the drawdowns in the topmost layer have a sigmoidal nature similar to that found by Hainsworth and Aylmore (1986). Whilst Hainsworth and Aylmore (1986) suggested that this may be the result of soil compaction around the root as the root grows through the soil this explanation appears to be unsatisfactory as the stepped drawdowns were not evident in the same layer earlier (see Fig. 1a) or in lower layers (see Figs. 1b-c). Presumably the stepped nature of the drawdowns at 4 and 8 hours in the topmost layer resulted from increased extraction in close proximity to the plant root caused by a decrease in root water potential. Such a result is of interest as it indicates that the soil resistance to water flow from bulk soil to the soil immediately surrounding the root is a major limiting factor in determining soil water availability, even at high soil water potentials. The reduction in soil water extraction from this layer during hour 4 to 8 suggests that there is an adequate supply of soil water at some

point lower on the root.

In contrast to the top layer, extraction from the middle layer remained constant with time (see Table 1). The results in Fig. 1b show that at hour 4 the magnitude of the gradient in soil water content was approximately that in the top layer at hour 1. Whilst in the top layer this gradient led to an increase in extraction from the layer, in the case of the middle layer it did not. The difference in response may arise as a result of a larger, intervening, root resistance at this depth. As a reduction of root water potential has not yet overcome root resistance, it must be presumed that there was an adequate supply of water from the layers above. Such results suggest that the plant modifies its potential in order to sequentially remove soil water from the top to the bottom of the root and may explain why the drawdowns at 9 cm depth were considerably smaller than in the layers above (see Fig. 1c).

The results presented clearly show that the distance to the outer boundary of the drawdown increased with time in all three layers reaching 17, 15 and 15 mm at 2, 6 and 9 cm depth respectively at hour 8. Whilst such results are not entirely consistent with the finding of Hainsworth and Aylmore (1986) that drawdown distance was a function of extraction rate, the results show that drawdown distance is a function of time and not dependant on root density alone. Thus the assumptions that a root acts as a uniform absorbing cylinder, and that water is supplied uniformly to the root from a soil cylinder the outer radius of which is determined by root density, are clearly erroneous in this case. Further examination of non-uniform absorption of soil water is required to enhance our understanding of water extraction by plant roots.

References

- Caldwell M M 1976 *In Water and Plant Life*. Eds O L Lange, L Kapper, and E D Schulze. Springer-Verlag Berlin.
- Cowan I R 1965 *J. Appl. Ecol.* 2, 221-239.
- Gardner W R 1960 *Soil Sci.* 89, 63-73.
- Hainsworth J M and Aylmore L A G 1983 *Aust. J. Soil Res.* 21, 435-443.
- Hainsworth J M and Aylmore L A G 1986 *Soil Sci. Soc. Am. J.* 50, 841-848.
- Hainsworth J M and Aylmore L A G 1988 *Aust. J. Soil Res.* 26, 105-110.
- Oosterhuis D M 1981 Ph.D. Thesis, Utah State University, Logan U.S.A.
- Sanderson J 1983 *J. Exptl. Botany* 34, 240-253.
- Shone M G T and Flood A V 1980 *J. Exptl Botany* 31, 1147-1159.
- So H B *et al.* 1978 *Plant and Soil*.49, 461-475.

Development of a Soil Water Dispersion Index (SOWADIN) for Testing the Effectiveness of Soil-wetting Agents

Y. Sawada, L. A. G. Aylmore and J. M. Hainsworth

Soil Science and Plant Nutrition, School of Agriculture,
The University of Western Australia, Nedlands, W.A. 6009.

Abstract

Computer-assisted tomography (CAT) applied to gamma-ray attenuation measurements has been used to develop an index termed the soil water dispersion index (SOWADIN), which describes quantitatively the amount and distribution of water in soil columns. The index, which is determined by classifying pixels in a scanned slice into three categories according to their attenuation coefficients, contains two numerical values. The first value corresponds to the water content of the scanned slice and the second value is a measure of the dispersion of the water throughout the slice. Artificially wetted zones were created in soil columns to give one-third of the scanned layer wetted with various patterns of wetted-area distribution. The SOWADIN values obtained accurately reflected the differences in water distribution associated with the different patterns. Application of SOWADIN to columns of a water-repellent sand before and after treatment with a soil-wetting agent clearly illustrates both the increase in water content and improvement in water distribution in the soil column following treatment.

Introduction

The problem of soil water-repellency has been recognized in various parts of the world including Australia (DeBano 1981) and has caused serious land-use problems on turfs (Wilkinson and Miller 1978), in agriculture (Bond 1964, 1965), burned watersheds (Valores *et al.* 1974) and home gardens (McGhie 1979). It is generally accepted that the water repellency of soils develops as a result of surface coatings of hydrophobic organic compounds on the soil particles (Roberts and Carbon 1972; Savage 1974; Miller and Wilkinson 1977).

Soil-wetting agents have been developed as a possible means for overcoming the problems caused by water-repellent soils (Letey *et al.* 1975; McGhie and Tipping 1983, 1984). In the past, studies of the effectiveness of soil-wetting agents applied to water-repellent soils have focussed on water infiltration (Letey *et al.* 1961, 1962; Mustafa and Letey 1971; McGhie and Tipping 1983; Carnell 1984) and the behaviour of the wetting agents in soils (Krammes and DeBano 1967; Valores and Letey 1968; Miller and Letey 1975; Valores *et al.* 1976). Whilst these aspects are undoubtedly important, it is clear that a true test of the effectiveness of a soil-wetting agent must include an assessment of the uniformity of distribution of the water in the soil, as well as the increase in water content. Bond (1964) and Gilmour (1968) noted that water tends to drain downward through narrow channels in water-repellent soils. Poor water dispersion would thus be an important factor limiting the establishment and

growth of plants on such soils. Provided that the wetting agent has a strong affinity with both the hydrophobic soil particles and water molecules, rapid water infiltration would be produced by strong adsorption of the wetting agent at the soil surface. On the other hand, good water dispersion throughout the profile would require uniformity of penetration of the wetting agent in the profile. The ideal wetting agent should possess these capacities, be effective at a minimum application rate and cost, and should also last for a substantial period.

The lack of definitive studies on the effect of wetting agents on water dispersion in water-repellent soils in the past arose largely because there was no practical technique which would allow the spatial distribution of water in soil to be measured in sufficient detail. However, the recent application of computer-assisted tomography by using X-ray and gamma-ray attenuation (Hainsworth and Aylmore 1983, 1986, 1988) has provided a method for the accurate and detailed determination of water content distributions.

This paper describes the development of an index termed the soil water dispersion index (SOWADIN) by using gamma CAT scanning as a quantitative evaluation of the effectiveness of soil wetting agents, not only in enhancing infiltration, but also in achieving a more uniform distribution of water throughout the soil.

Theory

In computer-assisted tomography (Brooks and DiChiro 1976), a slice of the object under examination is divided into a $M \times M$ matrix consisting of small squares called pixels (Hounsfield 1972). The CAT scan produces an array of numbers representing the values of the linear attenuation coefficient, μ , for each pixel. For wet soil, the value of μ is given by

$$\mu = \mu_s \rho_s + \mu_w \theta_v, \quad (1)$$

where μ_s and μ_w are the mass attenuation coefficients of soil and water and ρ_s and θ_v are the soil bulk density and volumetric water content respectively. In gamma-ray CAT studies, the result of the image reconstruction is expressed by the modified Hounsfield unit which is defined by the following equation:

$$H_m = \mu / \mu_w. \quad (2)$$

By using equation (1), H_m can be written as

$$H_m = (\mu_s \rho_s / \mu_w) + \theta_v. \quad (3)$$

Since the value of $(\mu_s \rho_s / \mu_w)$ is constant for a given soil,

$$H_m = K + \theta_v, \quad (4)$$

where K is a constant.

The purposes of the SOWADIN index are (i) to determine the area in a slice of a soil column at a given depth which has been effectively wet after surface-watering, and (ii) to evaluate quantitatively the distribution of wet areas in the slice at that depth. The approach used has its origin by analogy with the concept of hydrodynamic dispersion which was used to describe miscible displacement of soil solutions (Nielsen and Biggar 1962, 1963; Biggar and Nielsen 1962, 1963). Taylor and Ashcroft (1972) defined the term 'dispersion' as a process by which individual elements of the moving fluid are continually changing direction as a result of the complexity of the pore system, and the process causes individual fluid elements to be mixed with each other and to be 'dispersed' throughout the medium.

To assess the wettability and the wet-area distribution of a slice of a soil column by scanning, it is necessary to define what constitutes a 'wet area'. Each pixel in the slice of the object under examination by the gamma-ray CAT scanning carries a value of attenuation coefficient (H_m) according to its water content. Thus, a certain value of H_m or water content can be defined, which enables individual pixels to be classified as either 'WET' or 'DRY'. As the gamma-ray CAT can resolve spatial changes in water content of the order of 0.006 g cm^{-3} , and bearing in mind that a position of the slice once wet should facilitate further water uptake, it seems reasonable to designate pixels having water contents greater than 0.006 g cm^{-3} as WET pixels. Hence, this 'cut-off' water content, $\theta_x (= 0.006 \text{ g cm}^{-3})$, was used for the calculation of SOWADIN; thus, if

$$\theta_v \text{ of a pixel} \leq \theta_x (= 0.006 \text{ g cm}^{-3}) \Rightarrow \text{DRY},$$

$$\theta_v \text{ of a pixel} > \theta_x (= 0.006 \text{ g cm}^{-3}) \Rightarrow \text{WET}.$$

By classifying every pixel inside a scanned slice as either WET or DRY on this basis, the percentage of the wet surface area of the slice wet can be calculated as

$$\text{Surface area wet (SAW)} = 100(\text{WP/TP}), \quad (5)$$

where WP is the number of the WET pixels and TP is the total number of the pixels in the slice. The SAW value is 100 if the slice is completely wet, while in the case of absolute water-repellency of the soil, the value would be zero.

One problem in the use of the SAW value alone is that it fails to describe how the WET pixels are distributed within the slice when the SAW value is $0 < X < 100$. With a given number of WET pixels in a slice, the WET pixels may be clustered together forming several 'wet patches', they may be evenly scattered in the slice, or they can be present in any one of a variety of intermediate distributions.

The uniform wetting of soil soon after rainfall or irrigation is most important in achieving maximum germination rate and establishment of plants in the field. This means, in terms of the CAT scan study, that WET pixels should be present throughout the scanned layer. Water-repellent soils are likely to have a poor dispersion of WET pixels. To be effective, the application of a wetting agent should improve both the number and degree of dispersion of the WET

pixels in the scanned layer. Moreover, it seems likely that in unsaturated soil the DRY pixels directly next to WET pixels are more likely to become new WET pixels if further watering occurs. Hence, even when the SAW value is low, it is important that the WET pixels should be scattered throughout the soil. Conversely, the larger the area of dry patches, the more difficult it would be to wet the soil layer thoroughly.

The most useful index is therefore one which allows comparison of the distribution of the WET pixels in the scanned soil layer. In CAT matrices with a given number of WET pixels, the number of the DRY pixels, each of which is directly adjacent to at least one WET pixel vertically or horizontally, varies depending upon the way the WET pixels are distributed. Similarly, the number of the DRY pixels, each of which is surrounded by DRY pixels vertically and horizontally, also changes with the distribution of the WET pixels. The pixels diagonally adjacent to a DRY pixel were not considered, since the diagonal link between pixels is not as close as the vertical and horizontal links between the pixels, and a DRY pixel is likely to be under less influence from WET pixels in the diagonal directions.

DRY pixels can thus be divided into two groups. A DRY pixel which is adjacent to at least one WET pixel(s) in either the vertical or horizontal direction is classified as a 'Wettable-DRY' pixel (W-DRY pixel). A DRY pixel which is surrounded by other DRY pixels, vertically and horizontally, is classified as an 'Isolated-DRY' pixel (I-DRY pixel). Fig. 1 illustrates the relationship between WET, DRY, I-DRY and W-DRY pixels.

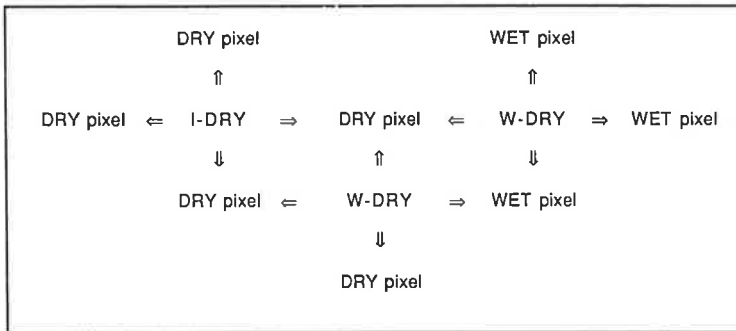


Fig. 1. Relationship between WET, DRY, Isolated-DRY (I-DRY) and Wettable-DRY (W-DRY) pixels. A DRY pixel surrounded by other DRY pixels vertically and horizontally in the CAT matrix, is classified as Isolated-DRY (I-DRY). If adjacent to at least one WET pixel it is classified as Wettable-DRY (W-DRY).

The comparison of the distribution of water in a scanned layer of the soil can then be made by either of the following equations:

$$WD = 100 \left(\frac{TP - \sum(I-DRY)}{TP} \right), \quad (6)$$

$$WD = 100 \left(\frac{WP + \sum(W-DRY)}{TP} \right), \quad (7)$$

where WD is the water distribution and TP and WP are defined in equation (5). Other more detailed methods of analysing the distribution of properties in space are available [e.g. clumping or cluster statistics (Ripley 1981)]. However, the previous relatively simple procedure adequately characterizes both the degree of dispersion of soil water content and the relative susceptibility of the soil to wetting.

Both SAW and WD are important in characterizing water-repellent soils. The higher the SAW value, the less water-repellent the soil and the better the soil for most land uses. On the other hand, the WD value, particularly at lower SAW values, is important in assessing the difficulty in uniformly wetting the soil. At a low SAW value, a small difference between WD and SAW for a scanned layer means that the wet areas are present in patches. When WD is much higher than SAW, water is well dispersed in the layer and further watering should ensure the complete wetting of the soil without much difficulty. The SOWADIN index is therefore defined as

$$\text{SOWADIN} = \text{WD}/\text{SAW}. \quad (8)$$

It should be emphasized that SOWADIN is not the quotient (WD/SAW), but consists of two independent values, rather analogous to the medical presentation of blood pressures as a ratio of systolic to diastolic pressures.

Experimental

The gamma-ray CAT scanner, developed in the Soil Science and Plant Nutrition laboratories of the University of Western Australia (Hainsworth and Aylmore 1988), utilizes a collimated ^{137}Cs (600 keV) 500 mCi source and a sodium iodide (NaI) or plastic scintillant detector, enabling a 5 mm thick slice of the object to be examined. Thirty-nine measurements are taken for each linear scan and 30 linear scans through 180° are completed. From these measurements, linear attenuation coefficients, expressed in modified Hounsfield units, are mapped into a 39×39 pixel array by using the filtered back-projection. The horizontal size of each pixel is approx. 2 by 2 mm. The distribution of water content in the pixels can be determined from these attenuation coefficients.

The soil used in these experiments was a water-repellent sand collected from Boyanup, Western Australia. Large plant debris and stones were removed by using a 5 mm sieve.

SOWADIN of Different Wetting Patterns

Five PVC columns (7 cm diameter \times 20 cm height), with sealed bottoms and containing various thin-walled plastic centrifuge tubes approx. 14 mm in diameter and plastic straws approx. 4.8 mm in diameter, were prepared. The sieved soil was randomly distributed in the columns to provide approximately 396 cm^3 of soil per column and five different wetting patterns were created inside the columns as shown in Fig. 2. The soil in column A was divided by a plastic sheet. The portions inside the smaller segment in column A and inside the tubes in columns B, C, D and E were completely wetted with 0.5% soil-wetting agent solution prior to CAT scanning. It was not possible for the solution to diffuse from the wetted portions inside the segment or tubes. The wetting agent used was 'Wetta Soil', a nonionic commercial product, which was generously supplied by Wetta Chem Products Co. Scans were conducted at approx. 2 cm below the soil surface.

The expected SOWADIN values were determined by using the photographs of the wetting patterns (Fig. 2), dividing the inside of each column into 2 by 2 mm squares (i.e. pixels), and classifying individual squares either as WET, W-DRY, or I-DRY, with the assumption that, if greater than half of the area inside the square is occupied by the wet portion, the square should be classified as WET.

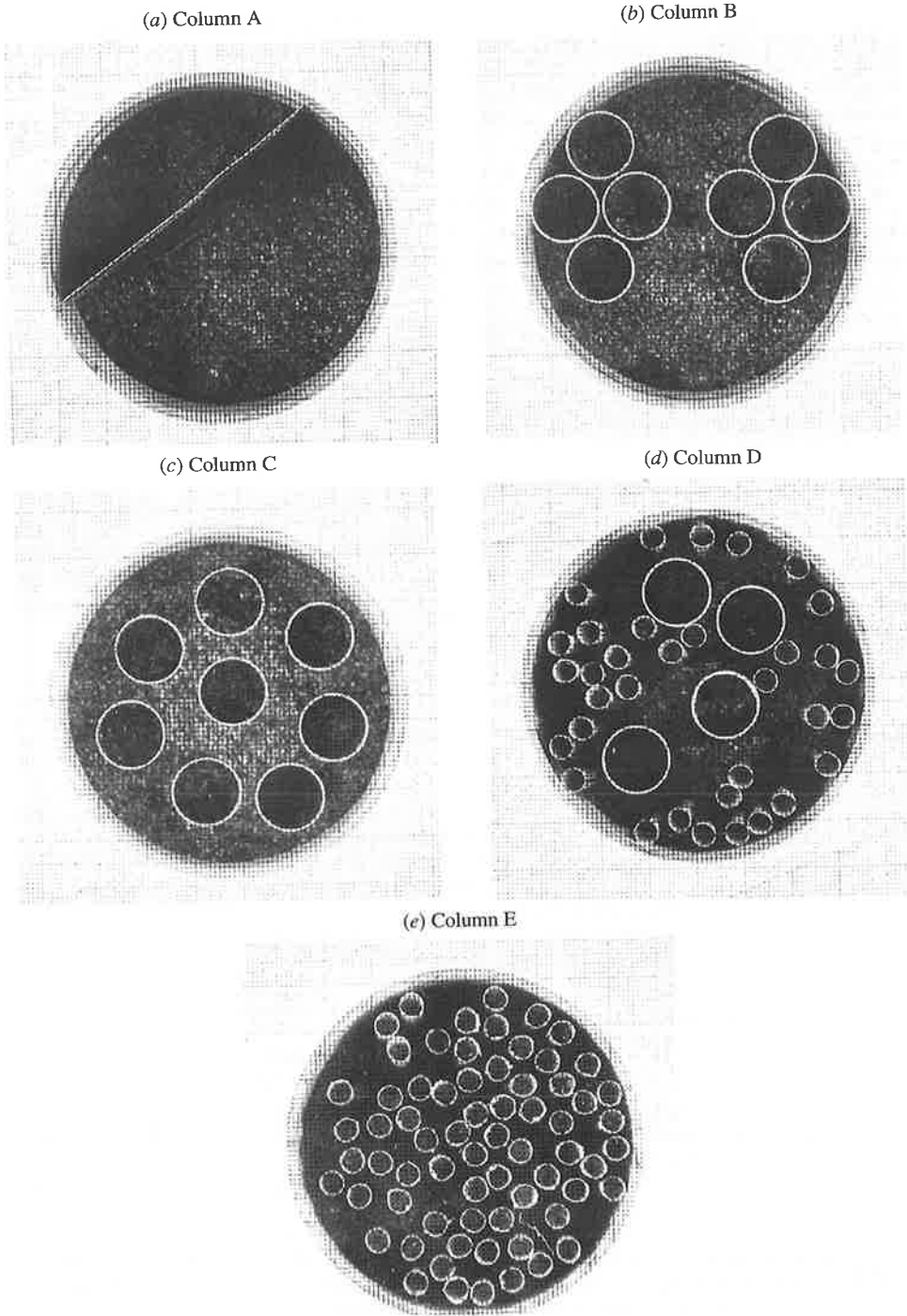


Fig. 2. Surface images of the artificially created wetting patterns in Boyanup soil columns used for comparison of expected SOWADIN values, with values obtained from CAT scan data.

SOWADIN of Soil with/without Wetting Agent

Two columns were prepared to examine the SOWADIN, one column with the surface application of a wetting agent solution and the other without. The sieved Boyanup soil was packed in the columns (7 cm diam., 20 cm height), each containing approximately 396 cm³ of soil. The inside of the walls of both columns had previously been greased with Castrol LM grease to minimize the tendency of water to drain rapidly along the space between sand particles and the wall of the column. The application rate of the wetting agent was 0.02 ml of water per column, which is equivalent to the recommended application rate (i.e. 5 ml l⁻¹ water m⁻²). The soil surface of the other column received 4 ml of deionized water only. After the treatments, the columns were air-dried in a glasshouse for 10 days, and each column was scanned (dry scan) prior to the surface application of 38.5 ml of water per column and again at 60 min after wetting (wet scan). The amount of the applied water was equivalent to 10 mm rainfall per column.

Table 1. Classification of pixels in the scanned layer of the columns with various wetting patterns

Column	WET	W-DRY	I-DRY	Total
(A)	317	31	676	1024
(B)	345	153	526	1024
(C)	338	195	492	1024
(D)	349	342	333	1024
(E)	358	461	205	1024

Table 2. SOWADIN of the soil layers with various wetting patterns

Column	SOWADIN (by CAT)	SOWADIN (expected)
(A)	34/31	32/30
(B)	49/34	47/33
(C)	52/33	50/32
(D)	67/34	63/32
(E)	80/35	76/33

Results and Discussion

The wetted areas created inside the test columns were set in such patterns that the surface area wet (SAW) for each column should give a value corresponding to one-third of the total surface of the scanned layer. The SAW values determined from the CAT scan and equation (5) for the columns were 31, 34, 33, 34 and 35, for columns A, B, C, D, and E, respectively.

The artificially created wetting patterns shown in Fig. 2 are unlikely to be completely realistic for water-repellent soils, even for those in which water tends to drain through preferred channels. However, these patterns represent useful examples for measuring the range of the moisture distribution in the soil that may be encountered. The wetting pattern in column E can be considered the most favourable for plant establishment and growth, followed by column D, and then C and B. The pattern in column A can be regarded as the other extreme to column E. Table 1 shows the numbers of the W-DRY and I-DRY pixels in the scanned layers of the test columns.

When the WET pixels are found in one part of the layer, as in column A, the DRY pixels consist predominantly of I-DRY pixels. On the other hand, if

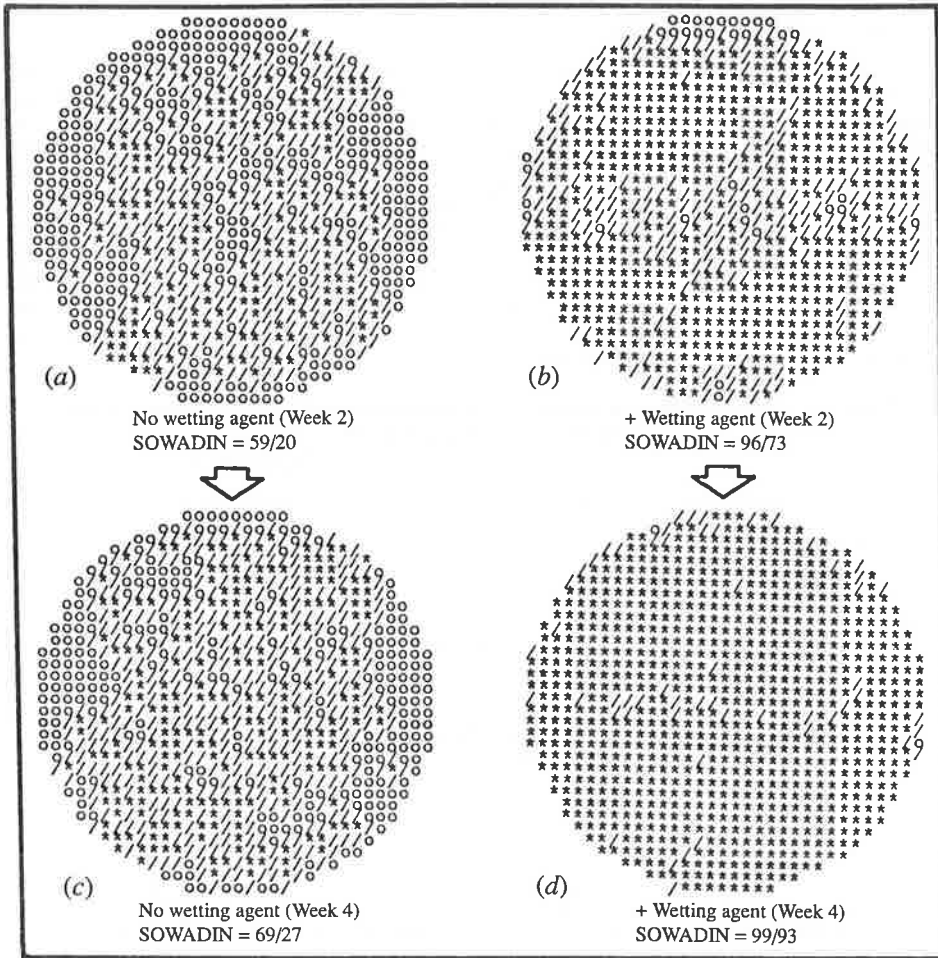


Fig. 3. Changes in the distribution of WET (*), W-DRY (/) and I-DRY (O) pixels and SOWADIN values of Boyanup soil, for (a, c) soils without wetting agent, and (b, d) soils with wetting agent.

the WET pixels are more widely scattered in the layer, as in columns D and E, there are more W-DRY pixels in the scanned layer. The calculated values of WD of the test columns by using equation (6) or (7) are 34, 49, 52, 67 and 80, for columns A, B, C, D and E, respectively. It is clear that the value of WD increases with the more scattered distribution of WET pixels. A poor dispersion of the WET pixels is indicated by the low WD value for column A, while a high WD values is obtained from the soil layer having widely scattered WET pixels (e.g. column E). Table 2 shows the SOWADIN values of the test columns obtained by measurement with the CAT scanning system, compared with the SOWADIN values prepared. This clearly shows that application of the soil water dispersion index to the data obtained from computer-assisted tomography gives excellent agreement with the actual distributions.

The applicability of SOWADIN was further tested by scanning an untreated soil column and one treated with the wetting agent. The SOWADIN value of

the treated soil two weeks after treatment (Fig. 3*b*) was 96/73, whereas that of the untreated column (Fig. 3*a*) was 59/20. A follow-up wetting some two weeks later produced SOWADIN values of 99/93 and 69/27 for the treated and untreated columns respectively (Figs 3*d* and 3*c*). This indicates that the wetting-agent treatment more than doubled the wettability of the soil, and secondly that the moisture in that scanned layer was much better distributed than that in the column without the treatment. The SOWADIN of the untreated soil is similar to that of the test column C, and the low WD value (59) indicates that the water was present in patches.

This approach has proven very effective in examining the water repellency of 'undisturbed' soil cores sampled from various locations (e.g. golf courses, bowling greens, playing fields, as well as agricultural areas) and in studies of the effectiveness and longevity of commercially available soil-wetting agents on different soil types (Sawada 1988).

Acknowledgment

The authors are grateful to Dr D. A. McGhie of the Western Australian Department of Agriculture for helpful discussions on this work.

References

- Biggar, J. W., and Nielsen, D. R. (1962). Miscible displacement: II. Behaviour of tracers. *Soil Sci. Soc. Am. Proc.* **26**, 125.
- Biggar, J. W., and Nielsen, D. R. (1963). Miscible displacement: V. Exchange processes. *Soil Sci. Soc. Am. Proc.* **27**, 623.
- Bond, R. D. (1964). The influence of the microflora on the physical properties of soils. II. Field studies on water repellent sands. *Aust. J. Soil Res.* **2**, 123.
- Bond, R. D. (1965). Water-repellent sands. *Rural Res. CSIRO* **51**, 30.
- Bond, R. D., and Harris, J. R. (1964). The influence of the microflora on physical properties of soils. I. Effects associated with filamentous algae and fungi. *Aust. J. Soil Res.* **2**, 111.
- Brooks, R. A., and Di Chiro, G. (1976). Principles of computer-assisted tomography (CAT) in radiographic and radioisotopic imaging. *Phys. Med. Biol.* **21**, 689.
- Carnell, W. J. (1984). Investigation of soil wetting agents. Rep. No. 28, Government Chemical Laboratories, W.A.
- DeBano, L. F. (1981). Water repellent soils: a state-of-the-art. Gen. Tech. Rep. PSW-46. Pacific Southwest Forest and Range Experiment Station, U.S.D.A., U.S.A.
- Gilmour, D. A. (1968). Water repellence of soils related to surface dryness. *Aust. For.* **32**, 143.
- Hainsworth, J. M., and Aylmore, L. A. G. (1983). The use of computer-assisted tomography to determine spatial distribution of soil water content. *Aust. J. Soil Res.* **21**, 435.
- Hainsworth, J. M., and Aylmore, L. A. G. (1986). Water extraction by single plant roots. *Soil Sci. Soc. Am. J.* **50**, 841.
- Hainsworth, J. M., and Aylmore, L. A. G. (1988). Application of computer assisted tomography (CAT) to gamma attenuation measurement of soil water content. *Aust. J. Soil Res.* **26**, 105.
- Hounsfield, G. N. (1972). A method of and apparatus for examination of a body by radiation such as X- or gamma-radiation. Brit. Pat. No. 1283915.
- Krammes, J. S., and DeBano, L. F. (1967). Leachability of a wetting agent treatment for water-resistant soils. *Soil Sci. Soc. Am. Proc.* **31**, 709.
- Letey, J., Osborn, J., and Pelishek, R. E. (1962). Measurement of liquid-solid contact angles in soil and sand. *Soil Sci.* **93**, 149.
- Letey, J., Pelishek, R. E., and Osborn, J. (1961). Wetting agents—can increase water infiltration or retard it, depending on soil conditions and water contact angle. *Calif. Agric.* **15**, 8.

- McGhie, D. A. (1979). Water repellent soils in the home garden. Farmnote No. 79/79, W.A. Dept of Agric.
- McGhie, D. A., and Tipping, P. I. (1983). Beating the non-wetting soil problem. *J. Agric. West. Aust.* 4th Ser., 84.
- McGhie, D. A., and Tipping, P. I. (1984). Soil wetting agents for improving crop and pasture establishment, and for improving the efficiency of carbon water use. Aust. Soil Sci. Soc. Conf., Brisbane, May 1984.
- Miller, W. W., and Letey, J. (1975). Distribution of nonionic surfactant in soil columns following application and leaching. *Soil Sci. Soc. Am. Proc.* **39**, 17.
- Miller, R. H., and Wilkinson, J. F. (1977). Nature of the organic coating on sand grains of nonwetttable golf greens. *Soil Sci. Soc. Am. J.* **41**, 1203.
- Mustafa, M. A., and Letey, J. (1969). The effect of two nonionic surfactants on aggregate stability of soils. *Soil Sci.* **107**, 343.
- Nielsen, D. R., and Biggar, J. W. (1962). Miscible displacement. III. Theoretical considerations. *Soil Sci. Soc. Am. Proc.* **26**, 216.
- Nielsen, D. R., and Biggar, J. W. (1963). Miscible displacement. IV. Mixing in glass beads. *Soil Sci. Soc. Am. Proc.* **27**, 10.
- Ripley, B. D. (1981). 'Spatial Statistics.' (John Wiley: New York.)
- Roberts, F. J., and Carbon, B. A. (1972). Water repellence in sandy soils of south-western Australia. II. Some chemical characteristics of the hydrophobic skins. *Aust. J. Soil Res.* **10**, 35.
- Savage, S. M. (1974). Mechanism of fire-induced water repellency in soil. *Soil Sci. Soc. Am. Proc.* **38**, 652.
- Sawada, Y. (1988). Studies of the effectiveness of soil-wetting agents on water repellent soils in Western Australia by application of computer-assisted tomography (CAT) to gamma ray attenuation. M.Sc. Thesis, The University of Western Australia.
- Taylor, S. A., and Ashcroft, G. L. (1972). Simultaneous movement of water and other materials or energy in soil. In 'Physical Edaphology—the Physics of Irrigated and Non-irrigated Soils'. p. 221. (W. H. Freeman: New York.)
- Valores, N., and Letey, J. (1968). Quantitative analysis for nonionic surfactants in soil leachates. *Soil Sci. Soc. Am. Proc.* **32**, 737.
- Valores, N., Letey, J., Martin, J. P., and Osborn, J. (1976). Degradation of a nonionic surfactant in soils and peat. *Soil Sci. Soc. Am. J.* **40**, 60.
- Valores, N., Osborn, J. F., and Letey, J. (1974). Wetting agents for erosion control on burned watersheds. *Calif. Agric.* **28**, 12.
- Wilkinson, J. F., and Miller, R. H. (1978). Investigation and treatment of localized dry spots on sand golf greens. *Agron. J.* **70**, 299.

Evaluation of Soil Structure by using Computer Assisted Tomography

V. K. Phogat and L. A. G. Aylmore

Soil Science and Plant Nutrition, School of Agriculture,
The University of Western Australia, Nedlands, W.A. 6009.

Abstract

Computer assisted tomography applied to gamma ray attenuation (CAT scanning) has been evaluated as a method for directly measuring the spatial distribution of soil macroporosity and for monitoring changes which occur during wetting and drying processes, in a non-destructive manner.

Total porosity calculated from the bulk density of soil and glass tube samples varying in bulk density from 0.759 to 1.602 g cm⁻³ correlated well with total porosity calculated from CAT scan data. The system was able to detect changes in bulk density for a loam soil of the order of 16 mg cm⁻³, and objects of 2.0 by 2.0 mm dimensions could be pictorially resolved in the scanning plane. Statistically, the system resolves pixels differing by at least 6.14% in attenuation coefficient value from surrounding pixels.

Average macroporosity and the spatial and frequency distribution of macroporosity for soil samples were determined by assigning the value of zero macroporosity to pixels having gamma attenuation coefficients corresponding to the bulk density of a soil aggregate, 100% macroporosity to pixels with zero attenuation coefficients and proportional values to pixels with intermediate coefficients. The CAT scanning of soil samples before and after a wetting and drying cycle illustrated the greater reduction in macroporosity for soil wetted under flooding compared with that wetted under capillary action.

The CAT scanning clearly has considerable potential for studying the spatial distribution of soil macrostructure and for monitoring the changes in macroporosity which occur during wetting and drying processes in soil columns.

Introduction

Soil structure and its stability govern the rainfall acceptance at the soil surface and hence the relative amounts and rates of surface runoff and subsurface flow. It largely determines the pore size distribution which is responsible for the temporal and spatial distribution of soil water. Within a well structured soil matrix there are both textural pores inside aggregates and macropores between the aggregates themselves. Usually macropores are most abundant in the soil immediately after cultivation if this is carried out at the appropriate soil moisture content. Their continued existence in the soil, however, depends on the stability of the aggregates. In unstable soils, the macropores become smaller both in total volume and in size as the soil slakes and/or disperses on wetting, and the advantages associated with their presence are lost. Hence, most interest centres not so much on the total pore volume as on the total macropore volume and its spatial distribution in the

soil. This is because of the strong influence of these pores on infiltration, aeration and root development.

Until recently, there has been no experimental technique which was capable of directly and repetitively measuring the spatial distribution of this macroporosity in a non-destructive manner and, in particular, of monitoring changes accompanying wetting and drying processes. However, application of the technique known as computer assisted tomography (CAT) (Hounsfield 1972) to X- and gamma-ray attenuation has provided an exciting new method for non-destructive three-dimensional imaging within a solid matrix. Hainsworth and Aylmore (1983, 1986, 1988) have, for example, used both X- and gamma-ray CAT scanning to measure the spatial variation in soil water content distributions in proximity to plant roots.

There seems little reason why it should not be equally possible to apply this technique to assess soil structure in terms of the spatial distribution and total volume of macropores. The present research was carried out to investigate the sensitivity, linearity, spatial resolution and suitability of the CAT application to gamma ray attenuation as a method for assessing the structural status of a soil and for monitoring changes associated with wetting and drying processes.

Materials and Methods

Instrumentation

A prototype CAT scanning system constructed in the Soil Science and Plant Nutrition Laboratories of the University of Western Australia (Hainsworth and Aylmore 1988) was used for these studies. This scanner utilizes a gamma source (500 millicuries of caesium-137) which is monitored by a plastic scintillant or NaI crystal detector. The beam is collimated to give a slice thickness of 2 mm and a pixel (picture element) size of 2 by 2 mm. As the source and detector are fixed, the object is moved across the beam and scanned at 2 mm intervals. Successive linear scans are made after rotating the object progressively in 5° increments through 180°. The minimum number of rotations required for accurate image reconstruction is given by $\frac{1}{4}\pi M$, where M is the number of points in the linear scan (Panton 1981). The linear scans are back-projected by using filtered back-projection (Herman 1980) for a given number of rotations. Once the back projections have been completed, the two-dimensional mapping of gamma attenuation coefficient values into an $M \times M$ element array is carried out.

System Response

To determine the variation in count rates due to random emission/transmission of gamma photons and to reduce this to an acceptable level of precision with minimum scan time, an acrylic cylinder (48 mm i.d. by 40 mm depth) was filled with distilled water to provide a uniform field and was scanned by using scalar counting times of 50, 100, 200, 500, 750, 1000, 2000, 3500 and 5000 ms. Average gamma attenuation coefficients and coefficients of variation were calculated for the different scalar counting times.

Linearity response of the system with increasing density was studied by scanning similar acrylic cylinders containing bundles of glass tubes of outer diameters of 8, 6, 5, 4, 3 and 2 mm. Different combinations of these different sized tubes were made by placing smaller diameter tubes inside the larger diameter tubes to attain overall bulk densities in the range 0.759–1.602 g cm⁻³. Each cylinder was scanned at three successive layers of 2 mm thickness each and the results were averaged.

The total porosities of these cylinders were determined from the density of glass and the sizes and number of tubes in the cylinder. Total porosities were also determined from

attenuation measurements by using the equation

$$P_t = 100\{(\mu_x - \mu_a)/\mu_x\}, \quad (1)$$

where P_t is the percent total porosity, μ_x (cm^{-1}) is the linear attenuation coefficient for the glass (density 2.37 g cm^{-3}), and μ_a is the average linear attenuation coefficient over the entire sample cross section (cm^{-1}).

The application of equation (1) depends on a linear relationship between P_t and μ_a and also on the value determined for μ_x corresponding to the density of the material used. The value of μ_x was calculated from the equation for linear regression of the gamma attenuation coefficient with bulk density of the columns containing glass tubes. The value of P_t for any system containing this material can then be determined from equation (1).

The ability of the scanner to resolve voids of different size and spacing in a scanned slice was examined by scanning an acrylic cylinder (90 mm o.d. by 40 mm depth) in which holes of radius 6, 5, 4, 3, 2, 1, 0.5 and 0.25 mm had been drilled in duplicate, in a known pattern.

Soil Studies

Surface (0–7 cm) soil samples were collected from Kulin, Western Australia, and separated into their natural aggregate sizes. Known bulk densities in the range $1.141\text{--}1.516 \text{ g cm}^{-3}$ were achieved by packing acrylic columns (84 mm i.d. by 40 mm in height) by using single sized aggregates and mixtures of aggregate sizes. One column was filled with finely ground (<0.5 mm) soil and a soil clod was prepared by applying water and pressure to produce a massive uniform structure. Three successive slices were scanned in each column by raising the source and detector by 2 mm increments. Average gamma attenuation coefficients over the sample cross sections were obtained for each column. All samples were oven dried at 60°C for at least 24 h before scanning.

The total porosity of each soil sample was calculated from the attenuation measurements as for the glass tubes. The linear attenuation coefficient value (μ_x) for soil at a density of 2.684 g cm^{-3} , equal to the particle density, was calculated by extrapolating the linear regression line of soil bulk density and gamma attenuation coefficient to this value.

Prior to the determination of the macroporosities of these soil samples, the value of the gamma attenuation coefficient (μ_x), corresponding to the bulk density of the soil aggregates (1.76 g cm^{-3}), was determined from the relationship between bulk density and gamma attenuation coefficient for these soil samples. The macroporosities of these samples were then determined by using equation (1).

To assess the stability of the soil aggregates, aggregates of 2.8–4.0 mm size were packed in two 48 mm i.d. columns. One column was wet under capillary action, while the second column was wet by flooding. Both columns were subsequently dried. These columns were scanned twice, firstly with the initially dry aggregates and secondly, following the wetting and drying cycle. The changes in the distribution of macroporosity were examined for the two methods of wetting.

Results and Discussion

Examples of the two-dimensional pixel matrix patterns obtained by using the gamma CAT scanning system are presented in Fig. 1. These illustrate the ability of the system to provide a clear picture of the distribution and density of material within the scanned region and to resolve voids of different size by using the present pixel dimensions (2 by 2 mm) and divisions of the attenuation coefficient. Features of these images will be discussed in the following sections.

Precision Requirements

Gamma attenuation is the ratio of transmitted to incident radiation, and scalar counting time is used to count the number of photons. Since gamma

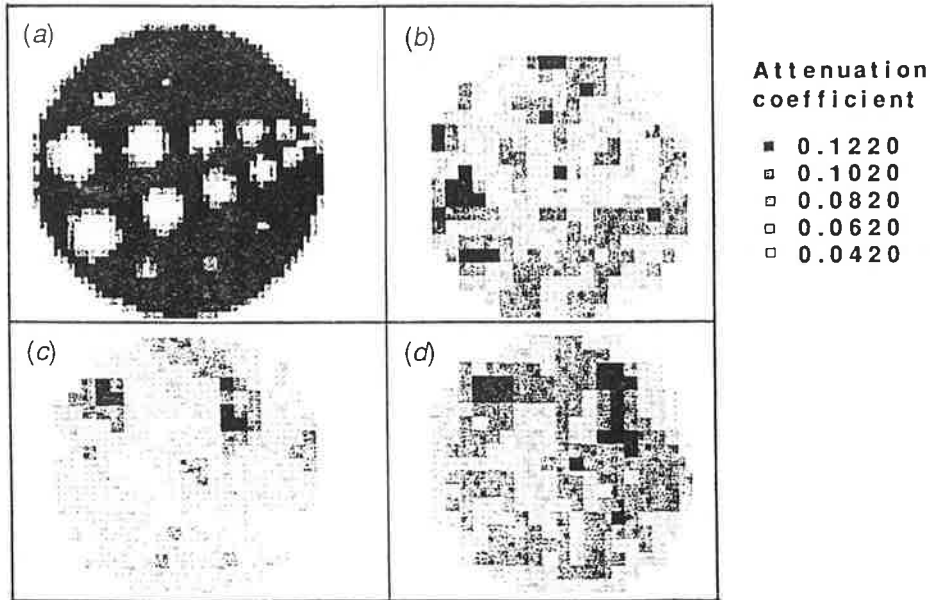


Fig. 1. CAT images of an acrylic cylinder containing various sizes of air-filled holes (a) and soil columns containing aggregates of sizes 4.7–8.0 mm (b), and 2.8–4.0 mm before (c) and after (d) flood wetting—pixel size 2 by 2 mm).

radiation is a random process, measurements with sufficiently long counting times are required to reduce the error in counting to any desired level of precision. Generally a compromise is required between acceptable precision and the time required for a scan.

Measurements of the coefficient of variation in pixel attenuation for different scalar counting times, in scanning a 50 mm diameter column containing water, indicated a rapid reduction in the coefficient of variation on increasing scalar counting time up to 750 ms, but little further reduction occurred for larger counting periods. A scalar counting time of 1 s gave an acceptable level of precision (<5%) and the 15 min required to complete a CAT scan is acceptable in practice. The mean attenuation values remain essentially constant over the range of counting time examined. Hence, a scalar counting time of 1 s was used in obtaining the results reported in this investigation.

The ability of the system to distinguish two objects from one another that differ greatly in density is analogous to differentiation between a soil aggregate and an air-filled pore. In the first instance, the contrast between air and acrylic was used and the CAT image obtained is shown in Fig. 1a. The smallest hole visible, by using the present pixel dimensions (2 by 2 mm) and divisions of attenuation coefficient, was 1 mm in radius as seen in the top centre of Fig. 1a, although holes of this dimension were not visible as separate entities when the distance between the holes was less than the size of a pixel. This is largely a consequence of the attenuation ranges used for pictorial

representation and detailed examination of actual attenuation coefficients for individual pixels can be considerably more informative.

In practice, the spatial resolution and resulting image of voids of pixel dimensions depends on the juxtaposition of CAT pixels and any given void. For example, if a pixel of 2 by 2 mm falls exactly over a cylindrical void of radius 1 mm, then 80% of the pixel volume will be occupied by air whereas, in the least favourable case, the same void may fall at a point where four pixels intersect and will provide only 20% air space in each of the four pixels. The resulting image of the same void will be different in each case.

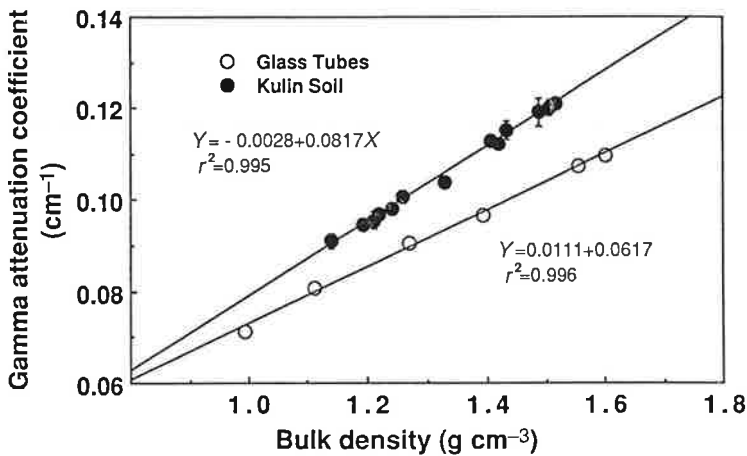


Fig. 2. Average gamma attenuation coefficient against bulk density of Kulin soil and glass tube samples. Vertical bars represent standard deviations.

Linearity of Response

Fig. 2 demonstrates that the CAT scanner responded linearly with increase in the average bulk density of the columns containing glass tubes. Similarly, scanning of Kulin soil samples provided an essentially linear change in gamma attenuation coefficient with increase in bulk density of the soil. A larger standard deviation in some of the soil samples indicates a greater variation in bulk density and reflects the greater heterogeneity on a 2 mm slice scale in larger aggregate systems than in finer aggregate materials or the glass samples.

The standard deviations of attenuation coefficients for the Kulin soil samples (Fig. 2) were used to examine the density resolving power of the system. The standard deviation of these soil samples ranged from 0.0003 to 0.0031 gamma attenuation coefficient, with most being about 0.0013. In contrast, scanning of a uniform field of deionized water yielded a value of standard deviation of 0.0002. Thus, the variation in the density of these soil samples substantially exceeded the variation inherent in the CAT technique itself. A change in soil density of 16 mg cm⁻³ caused a change of 0.0013 in gamma attenuation coefficient and this was considered the lower limit of density resolution with this scanner and Kulin soil.

The slope of the linear regression lines for columns containing glass tubes and those containing Kulin soil varied slightly and is akin to similar results obtained by Petrovic *et al.* 1982. This probably occurs as a result of the differences in atomic composition of the two materials. Linear attenuation coefficients are a function of the effective atomic number of the absorbing material when density and photon energy are held constant (Ter-Pogossian *et al.* 1977).

Table 1. Mean and standard deviation of gamma attenuation coefficient of pixels in scans for Kulin soil samples and for deionized water

Aggregate size (mm)	Bulk density ^A (g cm ⁻³)	Attenuation coefficient (cm ⁻¹)	
		Mean	s.d. of pixels
<i>Kulin soil</i>			
0.5-1.0	1.329	0.1040	0.0059
1.0-2.0	1.260	0.1007	0.0075
2.0-2.8	1.141	0.0911	0.0086
2.8-4.0	1.193	0.0947	0.0102
4.0-4.7	1.210	0.0956	0.0104
4.7-6.3	1.241	0.0980	0.0122
6.3-8.0	1.219	0.0971	0.0138
<0.5	1.419	0.1123	0.0058
<1.0	1.407	0.1128	0.0080
<2.0	1.505	0.1200	0.0081
<2.8	1.488	0.1191	0.0082
<4.0	1.516	0.1210	0.0095
<4.7	1.484	0.1190	0.0098
<6.3	1.432	0.1152	0.0111
<i>Deionized water</i>			
	1.000	0.0863	0.0053

^A Obtained from single size aggregates and their mixtures.

The spatial distribution of bulk density or porosity in a soil slice is determined by the distribution of pixels having different attenuation coefficients over the entire cross section of the slice. The mean and standard deviation of gamma attenuation coefficient values of pixels in scans for Kulin soil samples, at various bulk densities obtained from single size aggregates and their mixtures, and for deionized water are shown in Table 1. These data indicate that, statistically, the system can resolve pixels that have a difference of at least 6.14% in attenuation coefficient value from the surrounding pixels, as the mean and standard deviation values of the scan for a uniform field of water were 0.0863 and 0.0053, respectively.

Evaluation of Soil Structure

Variations in the standard deviation of pixel attenuation coefficients for a scanned layer reflect changes in the uniformity of the layer arising from changes in the spatial distribution of pore volume and soil matrix (soil aggregate). This effect can be used to assess the structural status of the soil.

In evaluating soil structure, interest centres on the quantity, size distribution and stability of the soil aggregates, as these parameters are important in

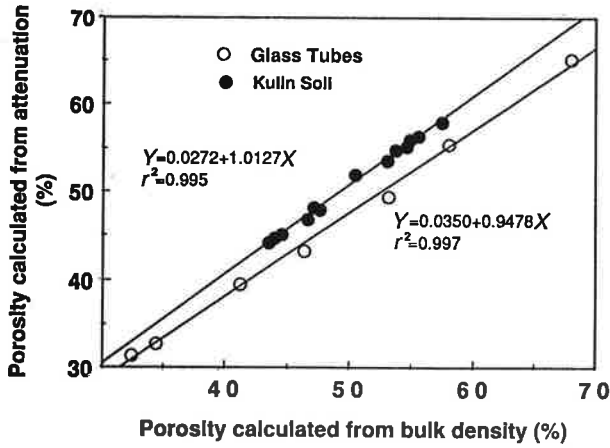


Fig. 3. Total porosity calculated from bulk density against total porosity calculated from CAT attenuation measurements for Kulin soil and glass tube samples.

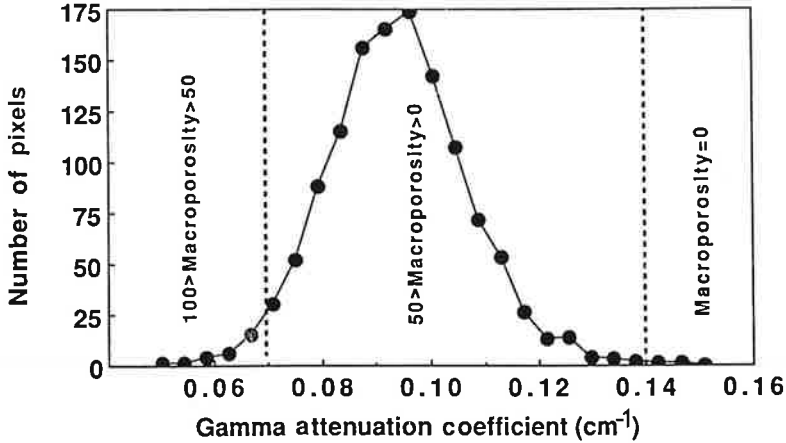


Fig. 4. Frequency distribution for pixel macroporosity, as indicated by the gamma attenuation coefficient, for soil containing 6.3–8.0 mm aggregates.

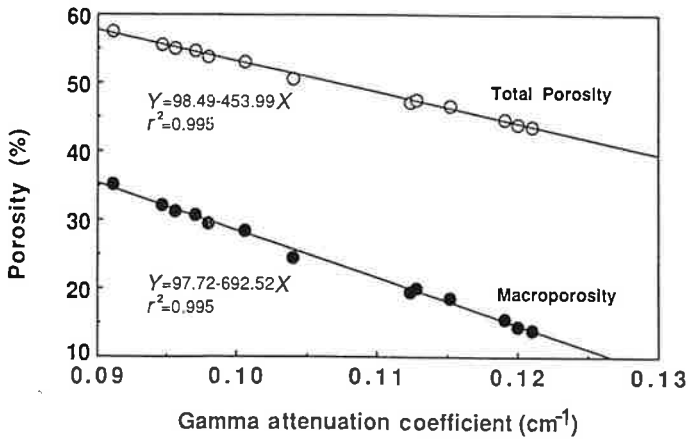


Fig. 5. Total and macroporosities against average gamma attenuation coefficient for different soil samples.

determining the amount and distribution of the pore spaces associated with the aggregates. Similarly, changes in soil macroporosity and its spatial distribution under various treatments provide information concerning the susceptibility of the soil structure to disruption by water.

Initially, the ability of the scanner to determine the total porosity of the slice scanned was confirmed by a comparison of mathematically calculated porosities for columns containing glass tubes with the porosities measured from attenuation (Fig. 3). Similarly, a good correlation between total porosities calculated from bulk densities and from gamma attenuation measurements was obtained for the Kulin soil (Fig. 3). These results clearly illustrate the ability of the CAT scanner to measure accurately total porosity in a scanned slice, as the values of intercepts and slopes were 0.03 and 0.95 for glass tubes and 0.03 and 1.01 for soil samples, respectively. The systematic, slight underestimation of porosity for the glass media probably arises because the packing of the glass tubes against the column wall creates slightly larger pore spaces than tube to tube contact.

As shown in Fig. 4, the spatial distribution of macroporosity for each soil sample was determined by assigning the value of zero macroporosity to the pixels with gamma attenuation coefficients of 0.1410 cm^{-1} or more (the value corresponding to the bulk density for a soil aggregate) and 100% macroporosity to pixels with essentially zero attenuation coefficient. Proportional values were ascribed to pixels with intermediate coefficients. The positions of the two vertical dotted lines on the x -axis show the attenuation coefficient values corresponding to zero and 50% macroporosity. The frequency distribution of the attenuation coefficient shown in Fig. 4 was obtained from scan data of a column containing 6.3–8.0 mm size aggregates (the CAT image of this is shown in Fig. 1*b*).

The relationships between total and macroporosities for the different soil samples and average attenuation coefficient are shown in Fig. 5. The slope of the line for macroporosity is greater than that for total porosity, which suggests that a slight change in macroporosity will cause a greater change in attenuation coefficient value. Thus, the change in macroporosity may be a more sensitive determinant of the susceptibility of the soil aggregates to disruption on wetting.

The spatial distribution of macroporosities for representative soil samples scanned are shown in Fig. 6. There are three significant features to these distributions:

- (i) the height of the distribution at any point indicates the relative frequency of pixels having that particular macroporosity;
- (ii) the position of the peak of the distribution curve corresponds to the most common macroporosity;
- (iii) the shape of the distribution curve indicates the distribution of pixels of particular porosities in a scanned slice.

A decrease in the peak height of the distribution curve is associated with greater spreading of macroporosity about the mean value and this is related to the heterogeneity of the slice arising from the distribution of pore spaces and the soil aggregate matrix [cf. curve A (<0.5 mm) and curve E (6.3–8.0 mm)]. A

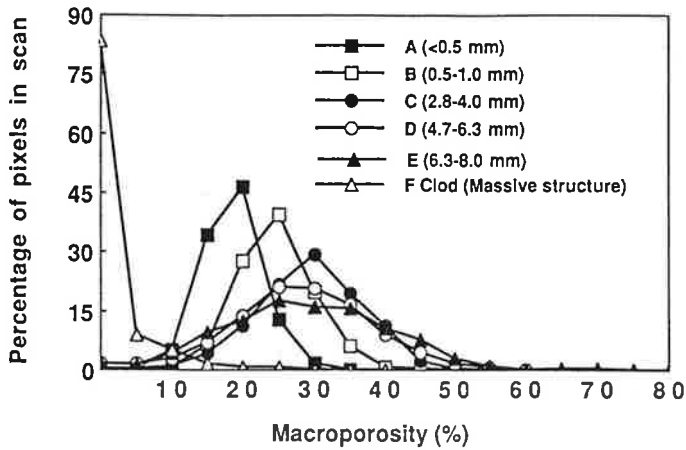


Fig. 6. Macroporosity distribution for scans of different size aggregates.

greater peak height for the distribution curve represents increased uniformity of distribution of density over the entire cross section of the slice scanned.

A shift in position of the peak of the distribution curve to the left indicates a loss of macroporosity in the sample (curves C, B and A). Following compaction or severe slaking of the soil aggregates, the macroporosity in the soil is invariably reduced, which is clearly illustrated by the distribution curve for the artificially prepared soil clod (curve F). In this clod, approximately 83% of the pixels in the slice scanned exhibited a massive structure with no macroporosity. As shown by curves D and E, soil samples having approximately the same average macroporosities, but with different spatial distribution of porosities in the slice, can be readily differentiated from the shapes of the two distribution curves and from a comparison of mean and standard deviation values (Table 1).

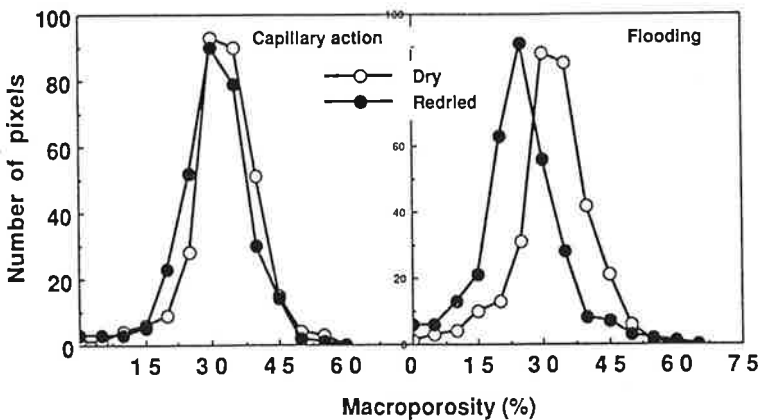


Fig. 7. Change in macroporosity distribution on wetting (capillary action and flooding) and subsequent drying.

Changes in the mean and spatial distribution of macroporosity for Kulin soil samples after wetting the aggregate under either capillary action or by flood wetting and subsequent drying are shown in Fig. 7. The CAT images of

scans for the initially dry and redried aggregates after flood wetting are shown in Figs 1c and 1d, respectively. These two methods of wetting the aggregates simulate important field phenomena; for example, surface soil subjected to flood irrigation or a heavy rainstorm is physically similar to flood wetting. Aggregates at lower depth in the profile will be more slowly wetted. On the other hand, sprinkler irrigation and light rainfall on the surface soil are physically similar to wetting the soil under capillary action. The shift of the macroporosity distribution curve (Fig. 7) towards the left (lower macroporosity end) in both the cases, indicates an instability in the system upon wetting. Comparison of the magnitude of the shift of the macroporosity distribution curve under flooding and capillary action clearly shows that the Kulin soil aggregates are less stable if wetted quickly (flooding), but retain their structure to a greater extent when wetted under capillary action. Similarly, Collis-George and Figueroa (1984) have used high energy moisture characteristics of soil to assess soil stability, in particular, by comparing relative structure to rapid or slow wetting.

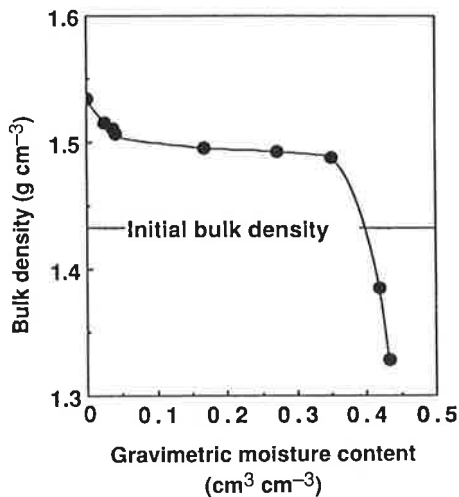


Fig. 8. Change in bulk density of Kulin soil as water content is decreased following saturation.

Fig. 8 shows the change in bulk density of the Kulin soil as the soil water content is decreased following saturation. This was obtained by subtracting the attenuation due to the relevant water content from the total gamma attenuation observed. This gives the attenuation due to the soil alone and hence the bulk density at various water contents. The initial saturation reduces the soil bulk density, undoubtedly as a result of swelling. As the water content is subsequently decreased, the bulk density increases to exceed the initial bulk density of the dry soil. This can be attributed to slaking and/or shrinkage of the soil matrix. Changes in the proportion and spatial distribution of macroporosity during the wetting and drying cycle would require an independent measure of attenuation for swollen aggregates, and this can only be obtained by a dual source procedure.

It seems clear that the CAT system is a potentially valuable tool for assessing the structural stability of soil under different treatments. The present system of using a single radiation source and 2 by 2 mm pixel size, is clearly capable

of describing the macro-structural status of a dry soil and of providing details of spatial changes in macroporosity following wetting and drying processes. Reductions in pixel size and 2D spline interpolation will undoubtedly provide more detailed resolution of macrostructure. Current work is directed to the application of CAT techniques to dual source scanning to enable the changes in attenuation arising both from changes in bulk density and changes in water content to be monitored concomitantly and continuously. Development of this facility should provide an exciting new approach to the study of structural changes occurring in surface soils during water entry and redistribution.

Acknowledgment

V. K. Phogat is grateful to AIDAB for the award of an Australian Commonwealth Fellowship, while on study leave from Haryana Agricultural University, India.

References

- Collis-George, N., and Figueroa, B. S. (1984). The use of high energy moisture characteristics to assess soil stability. *Aust. J. Soil Res.* **22**, 349-56.
- Hainsworth, J. M., and Aylmore, L. A. G. (1983). The use of computer-assisted tomography to determine spatial distribution of soil water content. *Aust. J. Soil Res.* **21**, 435-43.
- Hainsworth, J. M., and Aylmore, L. A. G. (1986). Water extraction by single plant roots. *Soil Sci. Soc. Am. J.* **50**, 841-8.
- Hainsworth, J. M., and Aylmore, L. A. G. (1988). Application of computer assisted tomography (CAT) to gamma attenuation measurement of soil water content. *Aust. J. Soil Res.* **26**, 105-10.
- Herman, G. T. (1980). 'Image Reconstruction from Projections.' (Academic Press: New York.)
- Hounsfield, G. N. (1972). A method of and apparatus for examination of a body by radiation such as X- or gamma-radiation. Brit. Pat. No. 1 283 915, London.
- Panton, D. M. (1981). Mathematical reconstruction techniques in computer axial tomography. *Math. Sci.* **6**, 87-102.
- Petrovic, A. M., Siebert, J. E., and Rieke, P. E. (1982). Soil bulk density analysis in three dimensions by computer tomographic scanning. *Soil Sci. Soc. Am. J.* **46**, 445-50.
- Ter-Pogossian, M., Phelps, M., and Brownell, G. L. (1977). 'Reconstruction Tomography in Diagnostic Radiology and Nuclear Medicine.' (University Park Press: Baltimore.)

Manuscript received 11 July 1988, accepted 9 November 1988

Adsorption-Desorption Behaviour of Selected Pesticides in some Western Australian Soils

R. Singh,^A R. G. Gerritse^B and L. A. G. Aylmore^A

^A Soil Science and Plant Nutrition, School of Agriculture, The University of Western Australia, Nedlands, W.A. 6009.

^B Division of Water Resources, CSIRO, P.O. Bag, Wembley, W.A. 6014.

Abstract

The adsorption-desorption behaviour of four pesticides, in four Western Australian soils differing in their physico-chemical properties, has been studied using a batch technique. Sorption data for Fenamiphos, Linuron and Simazine could be fitted to a Freundlich-type equation, while that for Diquat more closely fitted the Langmuir equation. The value of the exponent in the fitted Freundlich isotherms varied from 0.70 to 1.00 for the various pesticide and soil combinations.

Adsorption was found to be better correlated with organic matter than other soil properties, and decreased with increasing pH for all pesticides except Diquat. This study supports the observation of B. T. Bowman that the Freundlich equation in mole fraction form is more useful for comparing relative adsorption.

Comparison of the present adsorption data with previous studies showed that the organic matter in these soils behaved differently in terms of pesticide adsorption. In particular, the octanol-water partition approach, for predicting the adsorption of non-ionic organic compounds, gave unsatisfactory predictions of Linuron and Fenamiphos adsorption in these soils.

Desorption by a consecutive method showed hysteresis with all pesticide-soil combinations examined. The magnitude of the hysteresis was unaffected by changes in the soil : solution ratio. Using a dilution method, experimental procedures such as centrifugation and shaking have been shown to only slightly affect desorption hysteresis. The suggestion that hysteresis results from organic matter effectively 'locking in' the adsorbed pesticides is supported. The presence of methanol in the desorption solution results in swelling of organic polymers and facilitates the release of the adsorbed pesticides. Consequently, hysteresis was found to be essentially absent from the Linuron isotherm on removal of organic matter from the soil.

Introduction

Adsorption of pesticides by soil is one of the major processes influencing their accessibility to target organisms and their potential to reach non-target organisms. Adsorption may result in decreased biological activity, in enhanced rates of degradation and in retardation in movement with leaching solutions (Weed and Weber 1974).

Numerous studies on pesticide adsorption have been reported, including both inorganic and organic surface interactions (reviewed by Bailey and White 1970; Weber 1972; Weed and Weber 1974). However, it is well established that organic matter is the major constituent determining the extent of adsorption in soils, particularly of non-ionic pesticides (Hamaker and Thompson 1972). In

recent years, sorption of non-ionic organic compounds has been found to be well correlated with the octanol-water partition coefficient of the pesticide, and accurate estimations of soil water distribution coefficients from octanol-water partition coefficients have been claimed to be universally applicable (Chiou *et al.* 1979; Briggs 1981*a*). Briggs (1981*b*) demonstrated the applicability of this approach for non-ionic pesticides in Australian soils.

In practice, the physical and chemical nature of organic matter varies appreciably from soil to soil (Weed and Weber 1974) and Australian soils differ in many respects from other soils throughout the world (Sanchez and Isbell 1979; Hubble *et al.* 1983). Although relatively little information is available on the behaviour of pesticides in Australian soils, Jackson (1983) has concluded that pesticides often behave differently in Australian soils.

Numerous workers (e.g. Swanson and Dutt 1973; van Genuchten *et al.* 1974; Rao and Davidson 1980; Di Toro and Horzempa 1982) have reported irreversibility and the presence of hysteresis in the adsorption-desorption reactions of pesticides in soils. The reversibility of the adsorption reaction plays a significant role in determining the mobility of any pesticide in the soil profile. That is, whether the solid phase provides a permanent sink or merely a temporary reservoir, releasing the chemical back into solution in response to a decrease in solution concentration. However, the origins of this irreversibility remain an issue of some contention in the literature, in some cases being attributed to 'lock in' or 'cage' effects, where the sorbate is sterically hindered from desorption (Johnson and Starr 1972; Ogner and Schnitzer 1971) and in others to artifacts arising from experimental procedures, failure to attain equilibrium during desorption, or chemical or microbial transformations (Rao and Davidson 1980; Bowman and Sans 1985).

This paper reports on the adsorption-desorption characteristics of selected pesticides from different chemical classes in four Western Australian soils. The ability to predict the adsorption of non-ionic pesticides from their octanol-water partition coefficients has been examined. In addition, the degree of irreversibility in the adsorption reactions and, in particular, the influence of factors such as shaking and centrifugation, soil:solution ratio, the presence of organic solvent and the removal of organic matter on desorption hysteresis have been investigated.

Materials and Methods

Soils

A sandy soil from the Bassendean Association of the Swan Coastal Plain, a sandy loam soil from the Gascoyne Association, a clay soil (Wellesley series) from the Serpentine River Association and a loamy sand soil with high sesquioxide content of the Cobiac Valley Series were used in this study. The characteristics of Bassendean sand, Wellesley clay and Gascoyne sandy loam have been described by McArthur and Bettenay (1960) and Bettenay *et al.* (1971). The characteristics of Cobiac soil have been described by Churchward and Batini (1975).

The soils were air-dried and passed through a 2 mm sieve. Particle size distributions were determined by the pipette method (Loveday 1974) and organic carbon contents by the Walkley-Black method. The cation exchange capacity (CEC) was measured by Sr^+ saturation and total free Fe and Al oxides were determined according to the procedure of Mehra and Jackson (1960). Clay minerals present were identified by X-ray diffraction and specific surface areas were measured by application of the BET theory to N_2 adsorption at 78 K. Some physico-chemical properties of the soils are given in Table 1.

Table 1. Some physico-chemical properties of the soils

Property	Bassendean sand	Gascoyne sandy loam	Cobiac loamy sand	Wellesley clay
Northcote class.	Uc 1	Um 5.2	Uc 1.2	Ug 5.1
OM ^A (%)	1.2	1.7	0.6	4.6
Silt (%)	1.5	8.3	2.5	14.2
Clay (%)	1.25	15.3	13.6	63.7
pH (1 : 5, 0.01 M CaCl ₂)	5.0	6.9	5.1	5.9
CEC (cmol(+) Kg ⁻¹)	2.42	24.79	3.5	42.96
Surface area (m ² g ⁻¹)	0.36	22.48	13.39	73.05
Fe ³⁺ (%)	0.08	1.80	1.15	0.43
Al ³⁺ (%)	0.02	0.07	0.36	0.07
Exchang. cations (mmol kg ⁻¹)				
Ca ^{+0.5}	11.8	6.5	2.2	6.5
Mg ^{+0.5}	1.2	3.1	5.1	95.1
Na ⁺	1.8	7.16	2.4	17.2
K ⁺	0.7	1.05	0.6	2.1
Water retention (g g ⁻¹)				
10 kPa	0.03	0.30	0.10	0.59
30 kPa	0.02	0.13	0.06	0.44
Clay minerals ^B	K, I	K, I	K, Go, Gi	S, K

^A Organic matter, OM.

^B Clay minerals: K, kaolinite; I, illite; Go, goethite; Gi, gibbsite; S, smectite.

Pesticides

The distributions in the soils of four commonly used pesticides comprising three herbicides and one nematicide were studied (Hartley and Kidd 1987). The herbicides were Diquat (1,1'-ethylene-2,2'-dipyridilium dibromide), mol. wt 344.06, aqueous solubility 7×10^5 mg l⁻¹ at 20°C; Linuron [3-(3,4-dichlorophenyl)-1-methoxy-1-methylurea], mol. wt 249.1, aqueous solubility 81; and Simazine [2-chloro-4,6-bis(ethylamino)-1,3,5-triazine], mol. wt 201.7, aqueous solubility 3.5. The nematicide was Fenamiphos (ethyl-4-methylthio-*m*-tolyl isopropylphosphoramidate), mol. wt 303.4, aqueous solubility 700. Analytical grade samples (99%+ purity) of the pesticides were obtained from ICI Australia Ltd. (Diquat); Hoechst Australia Ltd (Linuron); Bayer Australia Ltd (Fenamiphos) and Ciba-Geigy Australia Ltd (Simazine).

Diquat is a knockdown herbicide and is generally considered to be irreversibly adsorbed by soil. Linuron and Simazine are soil-applied herbicides, while Fenamiphos is used for nematode control in horticultural soils. These pesticides are applied in W.A. in amounts of active ingredient per application ranging from 0.1–0.8 kg ha⁻¹ (Diquat), 1–3 kg ha⁻¹ (Linuron), 1–4 kg ha⁻¹ (Simazine) and 5–10 kg ha⁻¹ (Fenamiphos), at frequencies ranging from 1–3 times per year.

Pesticide Analyses

Pesticide concentrations were determined by high performance liquid chromatography (HPLC). Simazine and Linuron were separated in a Spherisorb 10 μm ODS column, 30 cm x 1.6 mm internal diameter (Phase Separation Ltd) and a mobile phase of methanol and water (65 : 35 v/v) (Vickery *et al.* 1980). Diquat was also analysed by reversed phase ion pair liquid chromatography on an ODS column using a mobile phase of methanol in water (25 : 75) containing sodium heptane sulfonate, cetrimide, phosphoric acid and diethylamine (Gill *et al.* 1983). Fenamiphos was analysed using a normal phase silica gel column (Spherisorb 5 μm) with a mobile phase of acetonitrile : water (20 : 80), pH 2.2 (Singh 1989). The pesticides were detected at 220 nm (Linuron, Simazine), 200 nm (Fenamiphos) and 350 nm (Diquat) with a variable wavelength u.v. detector (K35 ETP-Kortec, N.S.W.).

Adsorption Studies

Batch distribution isotherms for the pesticides in soils were determined at $20 \pm 2^\circ\text{C}$. In general, 5 g of air-dried soil was equilibrated in polypropylene centrifuge tubes with 10 ml of pesticide solution in 0.01 N CaCl_2 . However, for Diquat adsorption, the amount of soil used varied with the soil to allow for the larger differences in sorption encountered: 0.1 g (Wellesley clay), 0.2 g (Gascoyne sandy loam), 2.5 g (Cobiac soil) and 5 g (Bassendean sand) in 5 ml solution. Pesticide concentrations for different pesticides before equilibration ranged from 4 to 40 μM (Linuron), 2 to 25 μM (Fenamiphos), 20 to 100 μM (Simazine) and 20 to 3000 μM (Diquat). The tubes were shaken (end-over-end) for 16 h (Diquat) or 24 h (other pesticides). Generally, 95% of the adsorption was found to occur in the first 3–4 h.

After equilibration, the suspension was centrifuged at 12000 r.p.m. for 15 min. The supernatant was pipetted off and analysed immediately or stored at 4°C in a refrigerator for later analysis. The amount adsorbed by a soil was calculated from the difference between the initial and final concentrations of pesticide in solution. Pesticide adsorption onto the walls of the centrifuge tubes was checked by taking blanks and was found to be negligible. The effect of varying pH was examined by the addition of HCl or NaOH and equilibrating overnight.

The adsorption of Simazine directly from aqueous solution is difficult to study because of its low solubility (3.5 mg l^{-1}). Consequently, Simazine standard solutions prepared in methanol were used in this adsorption study. The concentration of methanol in the soil solution varied from 1 to 2.5% for all soils except Wellesley clay (1–5%), depending on the concentration of Simazine required. Previous studies (Singh *et al.* 1989) have demonstrated that the use of methanol as a co-solvent at concentrations up to 5%, to facilitate measurements of the adsorption of sparingly soluble pesticides, has no significant effect on the adsorption measured.

Desorption Studies

(1) Consecutive desorption

In the first instance, desorption of the pesticides was studied using the traditional consecutive desorption method involving a number of steps of shaking, centrifugation and resuspension. On completion of the initial adsorption, the suspension was centrifuged and the soil solution was carefully removed. The solution still remaining in the soil was noted. A known amount of pesticide-free solution in 0.01 N CaCl_2 was then added to the soil and the contents were again shaken for 24 h. After centrifugation, the soil solution was removed for analysis and the soil was suspended in herbicide-free solution. This procedure was repeated to generate a desorption isotherm.

(2) Dilution desorption

To eliminate any contributions of repeated shaking and centrifugation to adsorption-desorption hysteresis, desorption of Simazine from both sand and clay soils was studied using a dilution method (Bowman and Sans 1985). In this procedure, a number of samples were taken through the same adsorption step, i.e. subjected to the same concentration of pesticide solution. After equilibration, three samples were used for measuring the solution concentration and to calculate the average adsorption. The contents of the remaining samples were then diluted to different levels with pesticide-free solution. After shaking for 24 h, the soil suspension was centrifuged (12000 r.p.m. for 15 min) and pesticide concentrations in solution were determined. Each level of dilution thus provides one point on the desorption isotherm.

Adsorption Equations

The fit of the data to the Langmuir and Freundlich equations was tested. The linear form of the Langmuir equation is

$$C/S = C/X_m + 1/bX_m \quad (1)$$

where S is the amount of pesticide adsorbed by soil ($\mu\text{mol kg}^{-1}$), C is the equilibrium pesticide concentration in solution (μM), X_m is the adsorption maximum ($\mu\text{mol kg}^{-1}$) and b is a constant related to the energy of adsorption.

The linear form of the Freundlich equation is

$$\log S = \log K + n \log C, \quad (2)$$

where K ($\mu \text{mol}^{1-n} \text{kg}^{-1} \text{L}^n$) and n ($\text{L} \mu\text{mol}^{-1}$) are empirical constants.

Unfortunately, the Freundlich adsorption coefficient (K) for pesticides in soils has been expressed in the literature in a variety of units by different workers (Bowman 1981). In equation (2), the units of K depend upon the value of the slope (n), and these cannot be directly converted to another set of units by using a simple conversion factor unless $n=1$. Simple conversion leads to errors, depending on the deviation of n from unity and the magnitude of K itself (Bowman 1981). These anomalies frequently result in difficulties in making comparisons between the relative amounts of adsorptions measured.

An alternative approach is to express the adsorption data in the mole fraction form of the Freundlich equation, whence the modified equation becomes

$$S = K_{mf} Z^n. \quad (3)$$

The log transformation is then

$$\log S = \log K_{mf} + n \log Z, \quad (4)$$

where S is the amount of pesticides adsorbed by the soil (mol g^{-1}), K_{mf} is a coefficient without any physical significance, being no longer a measure of adsorption because it is evaluated at $\log Z=0$ ($Z=1$), i.e. when no solvent is present, and Z is the mole fraction of pesticide in the equilibrium solution (molar pesticide concentration/molar pesticide plus molar water concentrations). Relative adsorptions can then be evaluated from this equation at appropriate $\log Z$ values.

Results and Discussion

Adsorption Isotherms

All adsorption data, except that for Diquat, fitted well to a Freundlich-type equation (equation 2). The adsorption isotherms obtained for Fenamiphos, Linuron and Simazine for the different soils plotted in this form are shown in Fig. 1. Adsorption parameters from the Langmuir isotherm for Diquat and the Freundlich adsorption isotherms (for the other pesticides) in the different soils are given in Table 2.

In studies of pesticide transport, the Freundlich coefficient (n) has, for convenience, frequently been assumed by many workers to be equal to 1. In the present work, it was generally found to be less than unity for the three pesticides, ranging from 0.71 to 1.00 for Fenamiphos, 0.70 to 0.86 for Linuron and 0.70 to 1.00 for Simazine in the various soils. Similar deviations from linearity have also been noted by other workers (Hamaker and Thompson 1972; Calvet 1980). Osgerby (1970) observed that such low values of n are frequently associated with high soil organic matter content, but no such trend was observed in the present work.

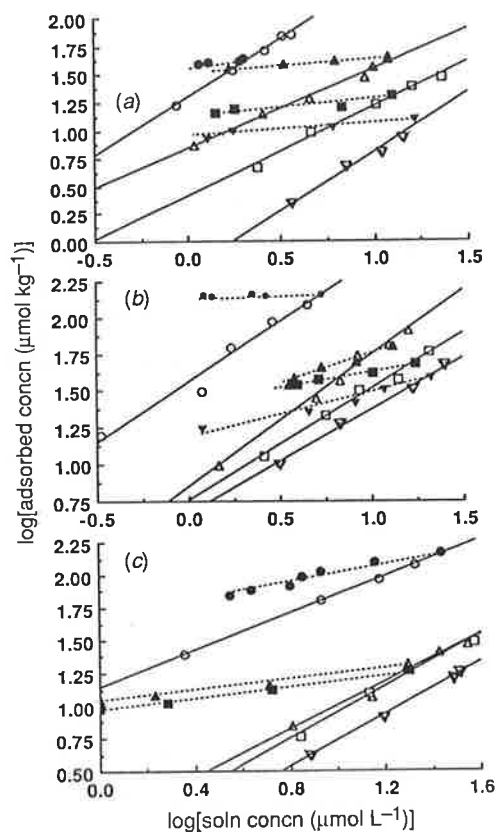


Fig. 1. Freundlich adsorption-desorption isotherms for (a) Fenamiphos, (b) Linuron and (c) Simazine in four soils. Symbols represent Wellesley clay (○), Bassendean sand (△), Gascoyne sandy loam (□) and Cobiac loamy sand (▽). Adsorption is represented by open symbols and desorption by closed symbols.

Table 2. Freundlich adsorption coefficients K and n and Langmuir adsorption coefficients K_m of pesticides in soils

Pesticide	Coefficient ^A	Bassendean sand	Gascoyne sandy loam	Cobiac loamy sand	Wellesley clay
Diquat	K_m	1765	39067	4905	146430
	b	0.05	0.03	0.01	0.19
	K_{mCEC}	0.15	0.31	0.28	0.68
Linuron	K	7.06	5.77	4.68	38.17
	n	0.85	0.76	0.70	0.81
	K_{OM}	676	390	780	830
Fenamiphos	K	6.86	2.58	0.56	19.66
	n	0.71	0.80	1.00	1.00
	K_{OM}	572	152	93	421
Simazine	K	1.23	0.93	0.53	13.87
	n	0.90	0.97	1.00	0.70
	K_{OM}	103	55	88	302

^A Units of the coefficients are: K ($\mu\text{mol}^{1-n} \text{kg}^{-1} \text{L}^{1-n}$), n ($\text{L} \mu\text{mol}^{-1}$), K_m ($\mu\text{mol} \text{kg}^{-1}$).

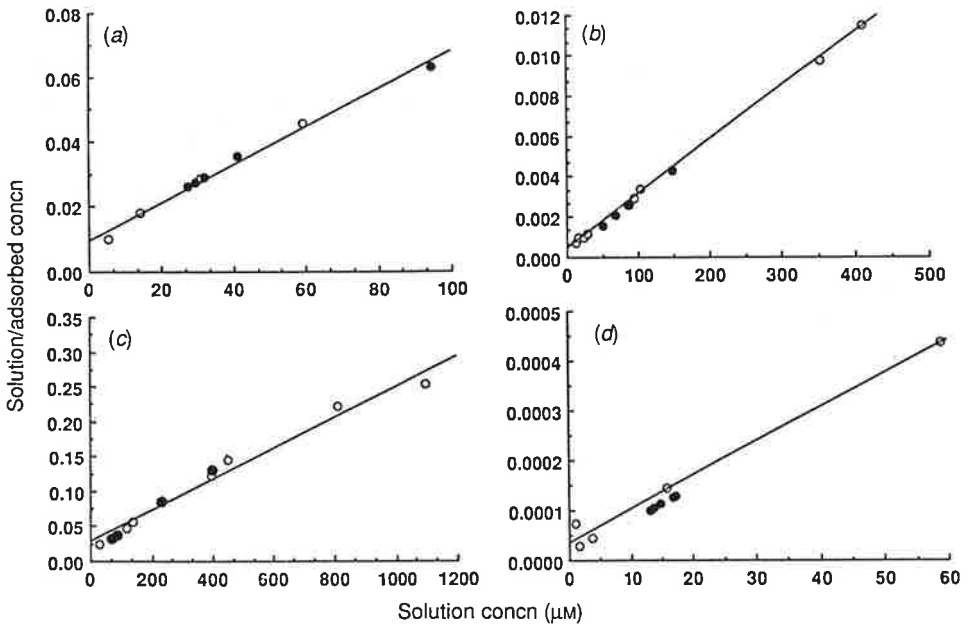


Fig. 2. Langmuir adsorption-desorption isotherms for Diquat in (a) Bassendean sand, (b) Gascoyne sandy loam, (c) Cobiac sandy loam and (d) Wellesley clay soil. Open symbols represent adsorption points and closed symbols represent desorption.

Adsorption isotherms for Diquat on the four soils (linear plots of the data are shown in Fig. 2) conform well to a Langmuir-type equation (L-type according to the classification of Giles *et al.* 1974). Similar isotherms have been observed for Diquat sorption on soil organic colloids and on some mineral soils (Weber 1972; Gamar and Mustafa 1975).

Effect of Soil Properties on Pesticide Adsorption

Much of the previously published work on Diquat and Paraquat adsorption has been carried out on ideal materials such as pure clay minerals, ion exchange resins, charcoal, etc. Adsorption studies for Diquat on soils are still meagre compared with those for Paraquat. However, the adsorption behaviour of Diquat and Paraquat is generally considered to be similar. In the present case, the values of the adsorption maxima (K_m) for Diquat were measured with clay content in the soil. The ratio of the adsorption maxima to CEC of the soils ranged from 0.15 in the sand to 0.68 in the clay soil. Other workers have reported values for Diquat ranging from 0.4 to 0.7 in soils of high clay content (>40%) from the arid region of Africa (Gamar and Mustafa 1975) and approaching the value of 1 for pure montmorillonite and kaolinite (Weed and Weber 1969). Values ranging from 0.1 to 0.3 for Paraquat in soils have also been observed (Tucker *et al.* 1967). Khan (1973) reported that humic and fulvic acids retain considerably less Paraquat and Diquat than that which corresponds to their cation exchange capacities. Thus, the low values of the ratio, particularly in these soils with low clay contents, suggest that organic matter may provide a significant contribution to the adsorption of Diquat.

Other factors may, however, also contribute to the low values of the ratio observed here. For example, the determination of CEC using Sr^+ saturation at pH may not accurately represent the situation at the lower pH used during adsorption measurements (except in the case of the Gascoyne soil). Furthermore, Diquat, because of its larger size, may be sterically hindered from filling positions to which Sr^+ has access. Khan (1973), for example, has observed the phenomena of steric hindrance to the adsorption of Diquat in organic matter.

With the exception of the adsorption of Simazine and Fenamiphos on the Gascoyne sandy loam, the values of the Freundlich adsorption coefficients (K) for Simazine, Fenamiphos and Linuron generally followed the order of the organic matter contents in the soils (Table 2). The soils in order of decreasing adsorption were Wellesley clay > Bassendean sand > Gascoyne sandy loam > Cobiac loamy sand.

Simple linear regressions of K with various soil properties indicate that adsorption is strongly correlated with the organic matter content ($r^2 = 0.94-0.97$) and clay content ($r^2 = 0.83-0.96$). Soil organic matter content has similarly been found to correlate well with adsorption of non-ionic chemicals in European and North American soils (Hamaker and Thompson 1972). Grover (1974) also found a good correlation between K and organic matter content of soil for a number of phenylurea herbicides in Canadian soils. A high correlation does not, however, always give a valid picture of adsorption, as such properties are frequently interrelated (Burchill *et al.* 1981).

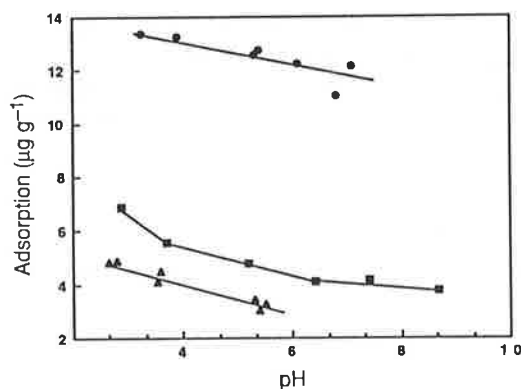


Fig. 3. Effect of pH on adsorption of Linuron (●), Simazine (■) and Fenamiphos (▲) in Bassendean sand.

Adsorption isotherms for Fenamiphos, Linuron and Simazine on Bassendean sand at different pH values of the soil solution are shown in Fig. 3. The adsorption of these pesticides decreases with increasing pH of the soil solution. This effect appears slightly more pronounced in the case of Simazine than for Linuron and Fenamiphos. This occurs because Simazine is a weakly basic herbicide and has a pK_a of approximately 1.4 (the pH value at which half the Simazine is in the cation form and the rest is in molecular form). As the pH increases, the proportion of Simazine cations in solution decreases and hence the adsorption decreases. Fenamiphos and Linuron are adsorbed by other mechanisms, such as hydrogen bonding, and this is also affected by pH to some extent. The adsorption of Diquat was unaffected by change in pH.

In general, because of the interaction with other soil properties, there was only poor correlation ($r^2 < 0.38$ for all soils and pesticides) overall between adsorption and pH for the soils examined.

Table 3. Adsorption of Fenamiphos, Linuron and Simazine using the modified Freundlich equation at two mole fractions of pesticides in solution

Soil	Fenamiphos		Linuron		Simazine	
	-6.6	$10^5 \times \text{adsorption (mol kg}^{-1}) \text{ at log } Z \text{ values of: } -7.2$	-6.6	-7.2	-6.2	-6.8
B. sand	3.236	1.244	7.224	2.137	3.020	0.912
G. sandy loam	6.607	2.454	4.168	1.479	3.019	0.758
C. loamy	0.832	0.223	2.951	1.148	1.820	0.478
W. clay	3.467 ^A	6.092	—	10.96	16.59	6.31

^A At $\log Z = -7.5$.

Comparison of adsorptions between different soils on the basis of K values from the nonlinear Freundlich equation is of limited value. The K values are obtained by extrapolating to $\log C = 0$, and hence, independently of n values (equation 2), do not give a clear picture of adsorption over the experimental concentration range. It has been suggested (Bowman 1981) that the Freundlich adsorption isotherm modified to the mole fraction form is more suitable for comparison between different studies. Hence, the adsorption values expressed in the mole fraction format corresponding to two different solution concentrations (mole fraction of pesticide in solution) provide an indication of the adsorption over the full experimental range of solution concentration. These values for Fenamiphos, Linuron and Simazine are given in Table 3.

Comparison of the Freundlich K values from Table 2 would suggest that Gascoyne soil has a lower adsorption affinity than Bassendean sand for Simazine ($K = 0.93$ compared with 1.2). However, comparison of the adsorption of Simazine between these soils on the basis of the corresponding modified Freundlich parameters (Table 3) demonstrates that Gascoyne sandy loam and Bassendean sand in fact achieve similar adsorption affinities at higher concentrations. This is also apparent from the linear plots in Fig. 1. Thus, the observation by Bowman (1981), that use of the modified Freundlich equation is a better method for comparison of adsorption between different soils, appears valid.

Surprisingly, Gascoyne sandy loam soil, despite its higher organic matter and clay content, showed less adsorption than Bassendean sand. This difference can be attributed largely to the higher pH of this soil, since the adsorption of both Simazine and Fenamiphos was observed to decrease with increasing pH of the soils (see Fig. 3). Cobiac soil, despite its high clay and sesquioxide contents, exhibited the lowest adsorption for all the pesticides except Diquat. Thus, a comparison in adsorption between Bassendean and Cobiac soil indicates that the poorly crystalline sesquioxides are not as important adsorbents as organic matter for these pesticides.

Prediction of Adsorption from Octanol-Water Partition Coefficients

Many workers have reported that adsorption of non-ionic compounds (such as Linuron and Fenamiphos) by different soils can be well correlated with their

partition between octanol and water (Karickhoff *et al.* 1979; Briggs 1981*a*). The prediction of adsorption from the octanol-water partition coefficient is based on the similar role of soil organic matter to that of the organic solvent (octanol) in partitioning a neutral organic compound between soil organic matter and water (Briggs 1981*a*). For Australian soils, it has been reported that, in the adsorption of non-ionic pesticides, the organic matter (OM) of these soils behaves similarly to that of British and American soils, and the following relation has been obtained (Briggs 1981*b*)

$$\text{Log}K_{\text{OM}} = 0.52 \text{log}K_{\text{OW}} + 0.69, \quad (5)$$

where $K_{\text{OM}} = (100K/\text{OM}\%)$ and K_{OW} is the octanol-water partition coefficient for the pesticide.

If the organic matter in different soils behaves similarly, then the adsorption of a given pesticide per unit weight of organic matter (K_{OM}) for different soils should be similar. The values of K_{OM} for the three pesticides given in Table 2 varied from one soil to another for any given pesticide. However, the variation was much lower than in the case of the K values. The values for Fenamiphos and Simazine were more variable than those for Linuron, presumably because of the role of pH in the adsorption of the two pesticides.

The K_{OM} values for Linuron for the soils used in the present study and for other soils reported in the literature have been plotted against organic matter content of the soils in Fig. 4. Comparison of these K_{OM} values shows that they differ significantly between soils from the same region as well as between soils from different regions. Values observed ranged from 295 to 932 $\mu\text{g}^{1-n} \text{mL}^n \text{g}^{-1}$ in five Canadian soils (Grover 1974) and from 269 to 1217 in six British soils (Hance 1965). Briggs (1981*b*) reported K_{OM} values for 17 Australian soils ranging from 57 to 205 $\text{mL} \text{g}^{-1}$. However, these values were obtained by assuming linear adsorption isotherms and using only one solution concentration. The range of K_{OM} values found in the present study for Linuron (using similar units but with nonlinear isotherms) was from 239 to 635 $\mu\text{g}^{1-n} \text{mL}^n \text{g}^{-1}$. This discrepancy may be partly attributable to the assumption of linearity of the adsorption isotherm made by Briggs (1981*b*) and his extrapolation from one solution concentration to obtain K values, since the assumption of linearity would, if anything, overestimate the correct values.

Similarly for Fenamiphos, the range observed with soils studied was higher (104–496 $\mu\text{g}^{1-n} \text{mL}^n \text{g}^{-1}$) than that reported for some soils of the South Western United States (73–121 $\mu\text{g}^{1-n} \text{mL}^n \text{g}^{-1}$) (Bilkert and Rao 1985) and for a silty clay loam (215 $\mu\text{g}^{1-n} \text{mL}^n \text{g}^{-1}$) (Lee *et al.* 1986). The higher range of values for K_{OM} observed for Linuron and Fenamiphos suggests that significant differences occur in the nature of the organic matter in soils. Similar variations in K_{OM} values up to 10 orders of magnitude, have been reported in the literature for the adsorption of other organic adsorbents in soils (Mingelgrin and Gerstl 1983).

The K_{OM} values for Linuron and Fenamiphos, predicted by using the relation given by Briggs (1981*b*) for Australian soils (equation 5), are also shown in Fig. 4. The values of $\text{log} K_{\text{OW}}$ used for prediction were 2.76 and 3.18 for Linuron and Fenamiphos respectively (Briggs 1981*a*). It is evident from Fig. 4

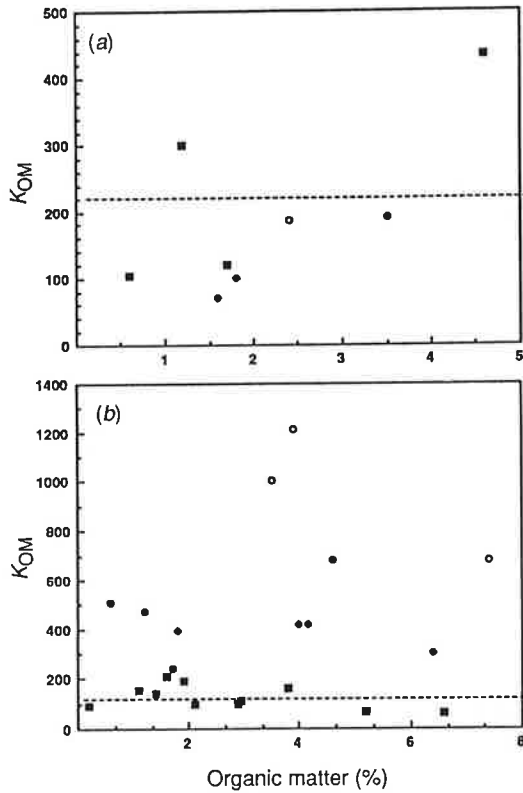


Fig. 4. Adsorption ($K_{OM} = K/OM\%$) of (a) Fenamiphos and (b) Linuron against soil organic matter content. In (a) the symbols represent data from present study, ■; Bilkert and Rao (1985), ◆; Lee *et al.* (1986), ○; and Briggs (1981*b*), ●. In (b) the symbols represent data from present study, ●; Grover (1974), ◆; Hance (1965), ○; and Briggs (1981*b*), ■. The dotted line represents the value of K_{OM} predicted from the octanol-water partition coefficients for the pesticides.

that the predicted values do not agree with the values observed by different workers. Even the data obtained by Briggs (1981*b*) shows considerable scatter.

Clearly, the prediction of adsorption by using octanol partition coefficients is of little practical value in transport studies, since a small difference in the distribution coefficient may greatly affect the mobility of pesticides in soils (Mingelgrin and Gerstl 1983).

Desorption Isotherms

Once again, the desorption data for all pesticides except Diquat followed the Freundlich equation. Fig. 1 shows both the adsorption and desorption data for these pesticides obtained by the consecutive method as fitted to equation (1). Swanson and Dutt (1973) similarly reported that desorption data for Atrazine followed the Freundlich equation and this equation was also found to best describe Picloram desorption (van Genuchten *et al.* 1974). Since both adsorption and desorption data are well described by the Freundlich equation, the data in this form can readily be incorporated in pesticide transport models.

Desorption data obtained with the consecutive method invariably exhibited hysteresis with all pesticide-soil combinations. This is illustrated by the different slopes for the desorption and adsorption isotherms (Fig. 1).

Desorption of Diquat followed the Langmuir equation for all soils. As in the case of the other pesticides, hysteresis was also evident for Diquat, particularly in the Wellesley clay soil (Fig. 2).

Usually in the analysis of bipyridylum groups of herbicides, such as Paraquat and Diquat, extraction requires boiling of the soil with 18 M H_2SO_4 . However, it is interesting to note that in the present study significant amounts of Diquat could be desorbed for different soils without such treatment. Five successive desorptions with 0.01 M $CaCl_2$ solution resulted in Diquat desorption for the different soils ranging from 3 to 34% of the amount adsorbed. Up to 62% of adsorbed Diquat could be desorbed using 0.1 M $CaCl_2$. However, the clay soil showed relatively less desorption than the sand. Kaolinite is the dominant clay mineral in these soils. However, the clay soil, in addition to its higher clay content, had some smectite clay minerals present. Diquat is less strongly bound to kaolinite than to montmorillonite and up to 80% of adsorbed Diquat can be desorbed back from kaolinite (Weber and Weed 1968).

Effect of Soil : Solution Ratio on Desorption

In using the dilution method for studying desorption it is assumed that the partition coefficient is independent of the adsorbent concentration. However, there is some conflict in the literature over the validity of this assumption. In contrast to earlier reports (Di Toro *et al.* 1982; O'Connor and Connolly 1980), Karickhoff *et al.* (1979) and, recently, Bowman and Sans (1985) found the partition coefficient to be independent of adsorbent concentration.

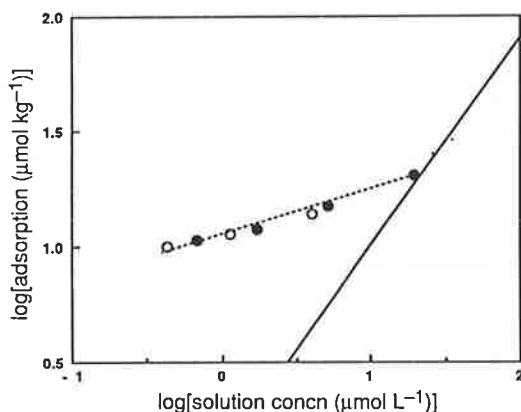


Fig. 5. Effect of soil : solution ratio during desorption on hysteresis for Simazine in Bassendean soil. Symbols represent soil : solution ratios of 1 : 2 (●) and 1 : 3 (○).

The desorption isotherms for Simazine at two soil : solution ratios are shown in Fig. 5. Changes in soil : solution ratio had a negligible effect on desorption hysteresis, suggesting that the changes in adsorbent concentration,

which may occur at the bottom of centrifuge tubes during centrifugation, have little effect on the hysteresis. This also demonstrated that the dilution method can successfully be used for desorption studies.

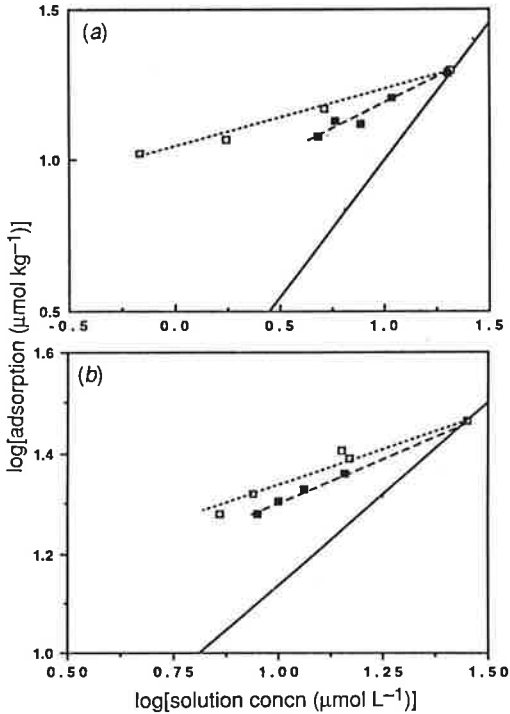


Fig. 6. Effect of method employed for desorption on hysteresis for Simazine in (a) Bassendean sand and (b) Wellesley clay soil: consecutive method (□); dilution method (■).

Effects of Shaking and Centrifugation on Desorption

Examples of the isotherms for Simazine obtained by both the dilution method and the consecutive method are shown for two soils in Fig. 6. Although the dilution method involves one step of centrifugation and shaking, Bowman and Sans (1985) have shown that the partition is not affected by this single step of centrifugation. A decrease in the magnitude of hysteresis is observed with the dilution method but significant hysteresis is still present. This result is in contrast to the observation by Bowman and Sans (1985) that the dilution method considerably reduced the level of hysteresis for two organophosphorus pesticides. On the other hand, Horzempa and Di Toro (1983), in studying the desorption of polychlorinated biphenyls (PCBs) from sediments by using a dilution method, found an increase in hysteresis compared with the consecutive method. They suggested that the effect of centrifugation is more significant for ionic water-soluble molecules than for neutral non-ionic species. Simazine is an ionizable compound, but centrifugation had little effect on desorption hysteresis. Since the dilution method is a relatively more rapid method for studying desorption than the consecutive method, the possibility of degradation of pesticides during desorption studies is reduced. Hence, the differences observed in desorption hysteresis by Bowman and Sans (1985) may be partly due to degradation effects. The organophosphorus compounds studied by

Bowman and Sans (1985) are more readily degradable than Simazine and this may explain the differences observed in the results of the two studies. This aspect needs further investigation before definitive conclusions can be drawn.

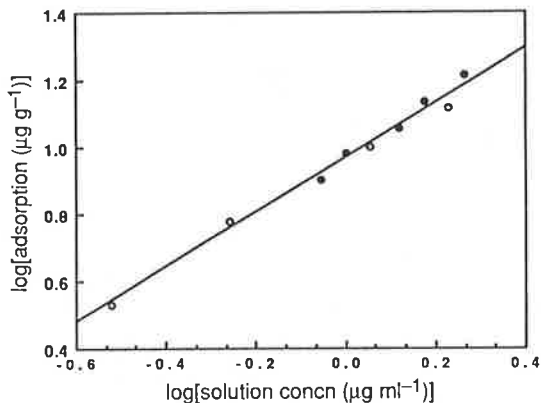


Fig. 7. Adsorption and desorption points for Linuron in Wellesley clay soil after removal of organic matter. Open symbols represent adsorption and closed symbols desorption.

Effect of Removal of Organic Matter

The desorption of Linuron was studied after removal of organic matter by hydrogen peroxide treatment (Kunze 1965) from Wellesley clay soil. The adsorption-desorption isotherms for the pesticide are shown in Fig. 7. No hysteresis was found in the absence of organic matter. These observations provide evidence that the organic matter fraction of the soil is responsible for the presence of hysteresis. Other workers have similarly concluded that desorption hysteresis is associated with the organic matter present. For example, Peck *et al.* (1980) found that the hysteresis became more pronounced as the organic matter contents of sediments increased.

The report that complete desorption of lipophilic organic compounds from sediments could be achieved with certain organic solvents (Freeman and Cheung 1981) is also of particular interest. Singh *et al.* (1989) demonstrated that at concentrations above 10%, the presence of the organic co-solvent markedly affected adsorption for both Linuron and Simazine on Wellesley clay soil and, in particular, produced a decrease in hysteresis with increasing methanol content in the solution. Hysteresis was almost absent when the methanol content was 50% in the mixed solution.

Organic solvents in mixed solvent systems may cause swelling or shrinkage of an organic carbon matrix which can influence the rate of desorption of an adsorbed species (Freeman and Cheung 1981). It has been suggested that isotherm nonsingularity can occur as a result of resistant or irreversible components (Di Toro and Horzempa 1982), some 'lock in' mechanism (Johnson and Starr 1972), or cage effects (Ogner and Schnitzer 1971). The almost complete desorption of Linuron and Simazine with 50% methanol can be explained on the basis of the observations and model of sorption on sediments given by Freeman and Cheung (1981). This model assumes that adsorption

is due to organic polymers associated with the complex of clay sediments. The gel-type swelling of polymers occurs due to liquid-polymer interactions. Although the organic co-solvent (methanol) used by Singh *et al.* (1989) did not result in maximum swelling of organic matter and maximum desorption rate according to the model, considerably more swelling than in water is to be expected. The decrease in the magnitude of desorption hysteresis with increasing methanol concentration observed by Singh *et al.* (1989) is thus consistent with the model and suggests that soil organic matter plays a significant role in producing desorption hysteresis.

Acknowledgments

This research was aided by a joint CSIRO-University of Western Australia Research Grant. R.S., currently on leave from Haryana Agricultural University, Hisar (India), is grateful for the award of a Commonwealth Fellowship from the Australian International Development Assistance Bureau.

References

- Bailey, G. W., and White, J. L. (1970). Factors influencing the adsorption, desorption and movement of pesticides in soils. *Residue Rev.* **32**, 29-92.
- Bettenay, E., Keay, J., and Churchward, H. M. (1971). Soils adjoining the Gascoyne River near Carnarvon, Western Australia. CSIRO Aust. Soil Land Use Ser. No. 51.
- Bilkert, J. N., and Rao, P.S.C. (1985). Sorption and leaching of three non-fumigant nematicides in soils. *J. Environ. Sci. Health*, **B 20**, 1-26.
- Bowman, B. T. (1981). Anomalies in the log Freundlich equation resulting in deviations in adsorption *K* values of pesticides and other organic compounds when the system of units is changed. *J. Environ. Sci. Health*, **16**, 112-23.
- Bowman, B. T., and Sans, W. W. (1985). Partitioning behaviour of insecticides in soil-water systems II. Desorption hysteresis effects. *J. Environ. Qual.* **14**, 270-3.
- Briggs, G. C. (1981a). Theoretical and experimental relationships between soil adsorption, octanol-water partition coefficients, water solubilities, bioconcentration factors and the parachor. *J. Agric. Food Chem.* **29**, 1050-9.
- Briggs, G. G. (1981b). Adsorption of pesticides by some Australian soils. *Aust. J. Soil Res.* **19**, 61-8.
- Burchill, S., Hayes, M.H.B., and Greenland, D. J. (1981). Adsorption. In 'The Chemistry of Soil Processes'. (Eds D. J. Greenland and M. H. B. Hayes.) pp. 221-400. (John Wiley: New York.)
- Calvet, R. (1980). Adsorption. In 'Interaction between Herbicides and the Soil'. (Ed. R. J. Hance.) pp 1-30. (Academic Press: London.)
- Chiou, C. T., Peters, L. J., and Freed, V. H. (1979). A physical concept of soil-water equilibria for nonionic organic compounds. *Science* **206**, 831-2.
- Churchward, H. M., and Batini, F. E. (1975). Soil pattern and resources utilization in the Wungong Brook catchment, Western Australia. CSIRO Aust. Land Resour. Mang. Ser. No. 1.
- Di Toro, D. M., and Horzempa, L. M. (1982). Reversible and resistant components of PCB adsorption-desorption: isotherms. *Environ. Sci. Technol.* **16**, 594-602.
- Di Toro, D. M., Horzempa, L. M., and Casey, M. C. (1982). Adsorption and desorption of hexachlorobiphenyl. Manhattan College Tech. Rep. Bronx, NY pp 1-217.
- Freeman, D. H., and Cheung, L. S. (1981). A gel permeation model for organic desorption from pond sediment. *Science* **214**, 790-2.
- Gamar, Y., and Mustafa, M. A. (1975). Adsorption and desorption of Diquat and Paraquat on arid zone soils. *Soil Sci.* **119**, 290-5.
- van Genuchten, M.Th., Davidson, J. M., and Wierenga, P. J. (1974). An evaluation of kinetic and equilibrium equation for the prediction of pesticide movement through porous media. *Soil Sci. Soc. Am. Proc.* **38**, 29-36

- Giles, C. H., Smith, D., and Huitson, A. (1974). A general treatment and classification of the solution adsorption isotherm. I. Theoretical. *J. Colloid Interface Sci.* **47**, 755-65.
- Gill, R., Qua, S. C., and Moffat, A. C. (1983). High-performance liquid chromatography of Paraquat and Diquat in urine with rapid sample preparation involving ion-pair extraction on disposable cartridges of octa-decyl silica. *J. Chromatogr.* **255**, 483-90.
- Grover, R. (1974). Adsorption and desorption of urea herbicides on soils. *Can. J. Soil Sci.* **55**, 127-35.
- Hamaker, J. W., and Thompson, J. M. (1972). Adsorption. In 'Organic Chemicals in the Soil Environment'. Vol. 1. (Eds C.A.I. Goring and J. W. Hamaker.) pp. 49-143. (Marcel Dekker: New York.)
- Hance, R. J. (1965). The adsorption of urea and some of its derivatives by a variety of soils. *Weed Res.* **5**, 98-107.
- Hartley, D., and Kidd, H. (1987). 'The Agrochemical Handbook.' (The Royal Society of Chemistry: University of Nottingham, England.)
- Horzempa, L. M., and Di Toro, D. M. (1983). The extent of reversibility of polychlorinated biphenyl adsorption. *Water Res.* **17**, 851-9.
- Hubble, G. D., Isbell, R. F., and Northcote, K. (1983). Features of Australian soils. In 'Soils: An Australian Viewpoint'. pp. 17-47. (CSIRO Aust.: Melbourne/Academic Press: London.)
- Jackson, R. B. (1983). Pesticides residue in soils. In 'Soils: An Australian Viewpoint'. pp. 825-42. (CSIRO Aust.: Melbourne/Academic Press: London.)
- Johnson, R. E., and Starr, R. I. (1972). Ultrarapid extraction of insecticides from soil using a new ultrasonic technique. *J. Agric. Food Chem.* **20**, 48-51.
- Karickhoff, S. W., Brown, O. S., and Scott, T. A. (1979). Sorption of hydrophobic pollutants on natural sediments. *Water Res.* **13**, 241-8.
- Khan, S. U. (1973). Interaction of humic substances with bipyridylum herbicides. *Can. J. Soil Sci.* **53**, 199-204.
- Kunze, G. W. (1965). Pretreatment for mineralogical analysis. In 'Methods of Soil Analysis: Part I'. pp. 568-77. (Am. Soc. Agron. Madison, Wisc.)
- Lee, C. C., Green, R. E., and Apt, W. J. (1986). Transformation and adsorption of Fenamiphos, f. sulfoxide and f. sulfone in Molokai soil and simulated movement with irrigation. *J. Contm Hydrol.* **1**, 211-25.
- Loveday, J. (1974). Methods for analysis of irrigated soils. *Commonw. Bur. Soils Tech. Commun.* No. 54.
- McArthur, W. M., and Bettenay, E. (1960). Development and distribution of soils of the Swan coastal plain, W.A. CSIRO Aust. Soil Publ. No. 16.
- Mehra, O. P., and Jackson, M. L. (1960). Iron oxide removal for soils and clays by dithionite-citrate system buffered with sodium bicarbonate. *Clays Clay Miner.* **7**, 317-27.
- Mingelgein, U., and Gerstl, Z. (1983). Re-evaluation of partitioning as a mechanism of nonionic chemicals adsorption in soils. *J. Environ. Anal.* **12**, 1-11.
- O'Connor, D. J., and Connolly, J. P. (1980). The effect of concentration of adsorbing solids on the partition coefficient. *Water Res.* **14**, 1517-23.
- Ogner, G., and Schnitzer, M. (1971). Chemistry of fulvic acid, a soil humic fraction, and its relation to lignin. *Can. J. Chem.* **49**, 1053-63.
- Osgerby, J. M. (1970). Sorption of pesticides by soils. In 'Sorption and Transport Processes in Soils'. Monogr. No. 37. pp. 63-78. (Soc. Chem. Ind.: London.)
- Peck, D. E., Corwin, D. L., and Farmer, W. J. (1980). Adsorption-desorption of diuron by freshwater sediments. *J. Environ. Qual.* **9**, 101-6.
- Rao, P. S. C., and Davidson, J. M. (1980). Estimation of pesticide retention and transformation parameters required in nonpoint source pollution model. In 'Environment Impact of Nonpoint Source Pollution'. (Eds., M. R. Overcash and J. M. Davidson.) pp. 23-67. (Ann Arbor Science Publishers: Ann Arbor, M. I.)
- Sanchez, P. A., and Isbell, R. F. (1979). A comparison of the soils of tropical Latin America and tropical Australia. In 'Pasture Production in Acid Soils of the Tropics'. (Eds P. A. Sanchez and L. E. Tergas.) Proc. Seminar held at CIAT California, Columbia. pp. 22-52.
- Singh, Rai (1989). Simultaneous determination of Fenamiphos, its sulfoxide and sulfone in water by high performance liquid chromatography. *Analyst*, **114**, 425-7.
- Singh, Rai, Gerritse, R. G., and Aylmore, L. A. G. (1989). Effects of organic co-solvent on adsorption and desorption of Linuron and Simazine in soil. *Aust. J. Soil Res.* (in press).

- Swanson, R. A., and Dutt, G. R. (1973). Chemical and physical processes that affect atrazine and distribution in soils. *Soil Sci. Soc. Am. Proc.* **37**, 872-6.
- Tucker, B. V., Pack, D. E., and Ospenson, J. N. (1967). Adsorption of bipyridylum herbicides in soil. *J. Agric. Food Chem.* **15**, 1005-8.
- Vickery, T. M., Karleskey, D. L., and Blackmer, G. L. (1980). Colorimetry and high performance liquid chromatography of atrazine residues in soil: comparison of methods. *J. Assoc. Off. Anal. Chem.* **63**, 507-10.
- Weber, J. B. (1972). Interactions of organic pesticides with particulate matter in aquatic and soil systems. In 'Fate of Organic Pesticides in Aquatic Environment'. (Ed. R. F. Gould.) *Am. Chem. Soc.* **111**, 55-120.
- Weber, J. B., and Weed, S. B. (1968). Adsorption-desorption of Diquat, Paraquat and Prometone in montmorillonitic and kaolinitic clay minerals. *Soil Sci. Soc. Am. Proc.* **32**, 485-7.
- Weed, S. B., and Weber, J. B. (1969). The effect of cation exchange capacity on the retention of Diquat and Paraquat by three layer type clay minerals: 1. Adsorption and release. *Soil Sci. Soc. Am. Proc.* **33**, 379-82.
- Weed, S. B., and Weber, J. B. (1974). Pesticide-Organic matter interactions. In 'Pesticides in Soil and Water'. (Ed. W. D. Guenzi.) pp. 39-66. (Soil Sci. Soc. Am.: Madison, Wisc.)

Manuscript received 31 January 1989, accepted 13 September 1989

**Evaluation of potential for groundwater pollution by some pesticides in a deep sand of
Western Australia**

Proc. Natl. Workshop on Herbicide Persistence, Melbourne, Nov. 1989, 47-58.

Singh, R., Aylmore, L.A.G. and Gerritse, R.G.

Evaluation of Potential for Groundwater Pollution by Four Pesticides in a Deep Sand of Western Australia

Rai Singh, L.A.G. Aylmore and R.G. Gerritse*

Soil Science and Plant Nutrition,
The University of Western Australia, Nedlands, W.A. 6009

* Division of Water Resources, CSIRO,
Private Mail Bag, P.O., Wembley, W.A. 6014

Abstract

Pollution potentials of diquat, linuron and simazine herbicides and fenamiphos nematicide have been evaluated from their sorption and degradation behavior in a Bassendean sand. A mathematical screening model available in the literature was used. The original model assumes a decreasing rate of pesticide degradation but a constant organic matter content with depth in the soil profile. Calculations based on this model showed that for a recharge rate of 0.5 m/yr, about 0.02 percent of applied diquat and simazine; and less than 2×10^{-12} percent of applied linuron and fenamiphos, reach groundwater. However, when decreasing organic matter content with depth in the soil profile (as observed for three profiles of Bassendean sands) was incorporated in the model, the calculations indicated that upto 40 % of diquat, 18 % of simazine and approximately 1 % of both fenamiphos and linuron applied, could potentially reach groundwater. The time needed for a pesticide to reach the water table varied with its sorption to soil.

Introduction

Evaluation of the potential of pesticides to reach groundwaters needs to take into account both the extent of their retention and the rate of degradation as a consequence of biochemical activity. Retention can be estimated from thin layer soil chromatography (Helling, 1971); octanol/water partition coefficients (Lambert, 1967); partition coefficients for soil organic matter (Rao and Davidson, 1980) etc. Jury et al (1983) developed a screening model for estimating the pollution potential of a number of pesticides (Jury et al 1987) based on the mobility and the persistence of pesticides in soils. Similarly, Rao et al (1985) used an index based on the residence time and half life of the pesticides in the vadose zone.

In view of the significance of groundwater as a supply for domestic and other purposes in the Perth region and the increasing use of a wide range of pesticides, it is essential that realistic estimates of pollution potentials of pesticides be obtained. In this paper, the amounts of pesticides reaching groundwater through Bassendean sand profiles common in the Swan Coastal Plain have been calculated as a function of depth to water table and organic matter distribution in the soil profile using the model of Jury *et al* (1983)

Theory

The model developed by Jury *et al* (1983) assumes a steady water flow, equilibrium adsorption and a depth dependent rate of biodegradation. It takes into account the decrease in microbial population with depth in a soil profile, but assumes a uniform organic carbon content throughout the soil profile. In practice, the subsurface layers of soil profiles almost invariably have significantly lower organic carbon contents than the surface layers.

A chemical is assumed to undergo linear, reversible, equilibrium adsorption and first order biochemical decay, while being leached at a uniform average drainage rate J_w ($m d^{-1}$). The soil profile is divided into three zones:

- (1) a surface zone (from surface to a depth L) with a constant microbial population density and hence a constant rate of degradation of a chemical;
- (2) a lower vadose zone (from depth L to H) with an exponentially declining microbial population density and wherein the degradation constant is proportional to microbial population; and
- (3) a deep zone (depth below H) with a residual value of both microbial population density and the degradation constant.

The adsorption of a chemical by a soil is given by its organic carbon distribution coefficient K_{oc} ($Kg m^{-3}$) and degradation by biochemical half-life τ (d). It is assumed that the soil has constant values of volumetric water content (θ), soil bulk density B_d ($Kg m^{-3}$) and fraction of organic carbon (foc).

The chemical is assumed to be applied at the surface ($z=0$) in a single application of mass M_0 per unit area at $t=0$.

For simplicity, diffusion and dispersion are neglected and thus piston flow is assumed. Though, this can lead to an underestimation of the time needed for a chemical to reach groundwater and an overestimation of the concentration reaching groundwater. Under these conditions, the resultant mass balance equation can be written as

$$\partial C_t / \partial t + J_w (\partial C / \partial z) + \mu(z) C_t = 0 \quad \dots (1)$$

The total solute concentration C_t (g m^{-3}) is given by

$$C_t = B_d S + \theta C \quad \dots (2)$$

where, S (g kg^{-1}) is adsorbed concentration, C (g m^{-3}) is solution concentration, and $\mu(z)$ (d^{-1}) is the biochemical degradation rate constant. The equilibrium adsorption is represented by a linear adsorption relation

$$S = K_d C = f_{oc} K_{oc} C \quad \dots (3)$$

where K_d ($\text{m}^3 \text{kg}^{-1}$) is the distribution coefficient

Combining Eq. (2) and (3) gives

$$C_t = (B_d f_{oc} K_{oc} + \theta) C = R_L C \quad \dots (4)$$

where R_L is ratio of total to solution concentration.

Combining Eq.(1) with Eq.(4) gives

$$\partial C_t / \partial t + V_E (\partial C_t / \partial z) + \mu(z) C_t = 0 \quad \dots (5)$$

where the effective solute velocity $V_E = J_w / R_L$.

Assuming the soil to be initially free of solute i.e. $C_t(0, z) = 0$ and considering a single flux of mass M_0 applied to the soil at $t=0$, the amount of mass reaching a depth z is given by (Jury et al 1983).

$$M(z) = M_0 \exp [(-1/V_E) \int_0^z \mu(z) dz] \quad \dots (6)$$

The degradation rate coefficient μ is assumed proportional to the microbial population density $E(z)$ of the different zones.

In the surface zone $0 < z < L$;

$$E = E_0 \quad \dots (7)$$

$$\mu = \mu_0 = 0.693/\tau \quad \dots (8)$$

In the transition zone $L < z < H$

$$E = E_0 \exp [-\Omega(z-L)] \quad \dots (9)$$

$$\mu = \mu_0 E/E_0 \quad \dots (10)$$

where Ω (m^{-1}) is the depth constant.

In the residual zone $z > H$

$$E = E_0 \exp [-\Omega(H-L)] = E_r \quad \dots (11)$$

$$\mu = \mu_0 E_r/E_0 = \mu_r \quad \dots (12)$$

With the depth dependence of degradation described in Eqs. (7) to (11); the fraction of mass applied at the surface that has not degraded ($M(z)/M_0$) is given by

1. Surface zone

$$M(z)/M_0 = \exp [-\mu_0 z/V_E] \quad \dots (13)$$

2. Transition zone

$$M(z)/M_0 = \exp [\{-\mu_0/(\Omega V_E)\} (1 - \exp \{-\Omega(z-L)\})] \quad \dots (14)$$

For $\Omega(z-L) \gg 1$, $M(z)/M_0$ approaches the constant value M_r in the transition zone given by

$$M(z)/M_0 = M_r = \exp [-(\mu_0/V_E) (L + (1/\Omega))] \quad \dots (15)$$

3. Residual zone

The mass will continue to degrade at a rate described by Eq. (12). Thus for time greater than the residence time ($t_H = H/V_E$) required to reach $z = H$, the mass fraction $M(t)/M_0$ will follow the equation:

$$M(t)/M_0 = M_r \exp (-\mu_r t) \quad \dots (16)$$

The model described above was also modified to take into account the decreasing organic carbon content generally

observed in soil profiles. For example, organic carbon data from three soil profiles of a Bassendean sand indicated an exponential decrease in organic carbon contents down to 0.5 m depth of soil. The surface organic carbon contents varied from 1 to 7 %. The ratio of organic carbon at a given depth (foc_z) to the organic carbon in the surface layer (foc_0) is plotted against depth in Figure 1. A best fit line for the three soil profiles was obtained with :

$$foc_z/foc_0 = foc_0 \exp (-5.0 z) \quad \dots(17)$$

where z is depth of soil in meters.

At soil depths greater than 0.5 m the organic carbon contents were almost constant. Hence, based on organic carbon contents, the soil profile could be divided into two zones.

A surface zone ($0 > z > L$) where

$$foc = foc_0 \exp (-5.0 z) \text{ and} \quad \dots(18)$$

a subsurface zone ($z > L$) where

$$foc = foc_0 \exp (-5.0 L) \quad \dots(19)$$

The solute flow velocity V_E , is determined by the organic carbon contents of the soil profiles (given by Eq. (18) and Eq. (19)). For the two zones these are given by:

$$V_E = Jw/[{\exp (-5.0 z)} foc_0 Koc Bd + \theta] \quad \dots(20)$$

for the surface zone ($0 > z > L$) and

$$V_E = Jw/[{\exp (-5.0 L)} foc_0 Koc Bd + \theta] \quad \dots(21)$$

for both the transition and deep zones ($z < L$)

The fraction of mass applied at the surface that has not degraded is obtained by incorporating the appropriate expression for V_E (Eq. 20 and 21) in Eq. (13) to (16).

Model parameters

Calculations were made for the four pesticides in Bassendean sand. The adsorption parameters, Koc , for the pesticides, were obtained from batch adsorption experiments, and are given in Table 2. Biochemical half-lives were taken from the literature, although actual half-lives for these pesticides may be different in Bassendean sand. Other required soil and environmental parameters e.g., Jw ; Bd ; foc ;

and θ were measured in the laboratory. Moisture content at saturation of a Bassendean sand was $0.3 \text{ m}^3/\text{m}^3$, and decreased rapidly to 0.05 at a water potential of 10 KPA. An average of $0.2 \text{ m}^3/\text{m}^3$ was chosen for the calculations. Considering an annual rainfall between 700-800 mm, an average θ of $0.2 \text{ m}^3/\text{m}^3$ and a recharge rate equivalent to 19 % of annual rainfall (reported by Ventriss, 1988 for part of Swan coastal plain); a $J_w = 0.5 \text{ m/yr}$ was assumed to be appropriate for the calculations. The microbial population density was assumed to decrease with a depth factor $\Omega = 3 \text{ m}^{-1}$ as reported by Focht and Joseph (1973). Values of parameters used in the calculations are summarized in Table 1.

Table 1 Parameters used in the calculations

Bd	1500	kg/m^3
θ	0.2	m^3/m^3
foc	0.006	kg/kg
L	0.5	m
H	3.0	m
J_w	0.5	m/yr
Ω	3	m^{-1}

Results and Discussion

The distributions of simazine in the profile of a Bassendean sand, obtained for different rates of degradation and conditions given in Table 1, are shown in Fig. 2. The concentration of simazine decreased exponentially in the zone of constant degradation and approached a residual value in the transition zone. The marked effect of bio-chemical half life on the pesticide distribution is apparent.

Residual concentrations of pesticides reaching a three meter depth of Bassendean sand, under various degradation rates along with times taken to reach the depth for the four pesticides are given in Table 2. In Fig. 3, the concentration distributions for the four pesticides are shown. Simazine, because of its lower adsorption and slower degradation rate, shows much higher concentrations in solution at all soil depths. The fraction of applied concentration of fenamiphos and linuron fell to very low values (less than 10^{-12} percent of applied mass) at depths below the surface zone ($>0.5 \text{ m}$). Although diquat, is adsorbed by soil in much greater amounts

than the other pesticides (Table 2), concentrations similar to those for simazine, were observed at all depths. This is because of the very slow rate of degradation used for diquat. In the absence of reports on degradation for diquat (Corwin and Farmer, 1985), a half life of 20 years, as reported for paraquat (ICI, 1984), was used in the calculations.

Fenamiphos, despite higher application rates, shows very low concentrations at a depth of 3 m, because of its faster degradation rate. Fenamiphos is oxidized very quickly (half-life = 10 d; Jury *et al* 1987) to its sulfoxide and sulfone, which also have pesticidal properties. For degradation of fenamiphos and its two metabolites as total residue, a range of half lives (from 38-67 d) have been found (Bilkert and Rao, 1986). Applying these values shows that a significant fraction of fenamiphos residues can leach to depths greater than 1 m, particularly when the organic carbon content in the soil profile decreases rapidly.

A comparison of the calculated distributions of pesticides in the soil profile for constant and variable organic carbon contents (Table 2) shows that with decreasing organic carbon contents in the soil profile, much higher residual concentrations (e.g. 40 % c.f. 0.017 % for diquat and 18% c.f. 0.021 % for simazine) reach to groundwater. The time needed for a pesticides to reach groundwater is significantly reduced (e.g. 9 yrs c.f. 2 yrs for simazine and 45 yrs c.f. 7 yrs for linuron, Table 2).

These calculations show that while the time taken for a pesticide to reach groundwater depends on the extent of its adsorption to soil, the actual concentrations reaching groundwaters are determined by both adsorption and degradation. The distribution of organic matter in a soil profile must be taken into account while evaluating the pollution potential of a pesticide. Assumption of a constant organic matter throughout the profile, as in the model of Jury *et al* (1983), can significantly underestimate the concentrations of pesticides reaching groundwaters.

Table 2 Residual concentrations of pesticides reaching a depth of 3 meters in Bassendean sand under 0.5 m/yr recharge rate.

Koc Kg m ⁻³	Half- life d	Fraction of applied mass	Time (t _H) yrs	Applied mass a.i. Kg/ha**	conc [@] at 3 m depth mg/l
Simazine					
0.037	32(1)	2.4x10 ⁻⁹	9	1.0	1.2x10 ⁻⁷
0.037	75(2)	2.1x10 ⁻⁴	9	1.0	1.0x10 ⁻²
0.037	75* (2)	1.8x10 ⁻¹	2	1.0	9.0
Fenamiphos					
0.137	10(2)	6.2x10 ⁻⁹³	30	10.0	3.1x10 ⁻⁹¹
0.137	38(3)	5.4x10 ⁻²⁵	30	10.0	2.7x10 ⁻²³
0.137	67(3)	1.7x10 ⁻¹⁴	30	10.0	8.5x10 ⁻¹²
0.137	67* (3)	7.2x10 ⁻³	7	10.0	3.6x10 ⁻¹
Linuron					
0.21	75(2)	2.9x10 ⁻¹⁹	45	2.25	1.4x10 ⁻¹⁷
0.21	75* (2)	1.1x10 ⁻²	7	2.25	5.5x10 ⁻¹
Diquat					
4.25	7300(4)	1.7x10 ⁻⁴	450	1.0	0.8x10 ⁻²
4.25	7300*(4)	4.0x10 ⁻¹	166	1.0	2.0x10 ¹

Figures in parenthesis refer to the source of data

(1) Piper (1989; unpublished)

(2) Jury *et al.* (1987)

(3) Bilkert and Rao (1986)

(4) ICI, 1984

* Calculated with decreasing organic carbon content

** Based on recommended rates of application in Western Australia

@ In 1 cm soil layer with θ of 0.2 cm³/cm³.

References

- Bilkert, J.N. and Rao, P.S.C. (1985). Sorption and leaching of three non fumigant nematicides in soils. *J. Environ. Sci. Health*. B20 : 1 - 26.
- Corwin, D.L. and Farmer, W.J. (1985). A mathematical model of diffusion under saturated conditions to assess the pollution potential of herbicides to aquatic systems. *Hilgardia* 53: 1-35.
- Focht, D.D. and Joseph, H. (1973). An improved method for the enumeration of denitrifying bacteria. *Soil Sci. Soc. Am. Proc.* 37:698-699.
- Helling, C.S. (1971). Pesticide mobility in soils. III Influence of soil properties. *Soil Sci. Soc. Am. J.* 35: 743-748.
- ICI (1984). Paraquat: its fate and effects in the soil. ICI Agrochemical Monograph, pp 6.
- Jury, W.A., Focht, D.D., and W.J. Farmer (1987). Evaluation of pesticide groundwater pollution potential from standard indices of soil-chemical adsorption and biodegradation.
- Jury, W.A., Spencer, W.F. and W.J. Farmer (1983). Behavior assessment model for trace organics in soil. I. Model description. *J. Environ. Qual.* 12: 558-564.
- Lambert, S.M. (1967). Functional relationship between sorption in soil and chemical structure. *J. Agric. Food Chem.* 15: 572-576
- Rao, P.S.C. and Davidson, J.M. (1980). Estimation of pesticide retention and transformation parameters required in non point source pollution model. p 23-67 In Overcash and J.M. Davidson (ed.). Environmental impact of nonpoint source pollution. *Ann Arbor Science Publ.*, Ann Arbor, MI.
- Rao, P.S.C., Hornsby, A.G. and Jessup, R.E. (1985). Indices for ranking the potential for pesticide contamination of groundwater. *Proc. Soil Crop Sci. Soc. Fla.* 44: 1-8.
- Ventriss, H.B. (1988). Groundwater management - The players and the processes. Proc. Swan Coastal Plain Groundwater Management Conf. Oct, 1988 (In press).

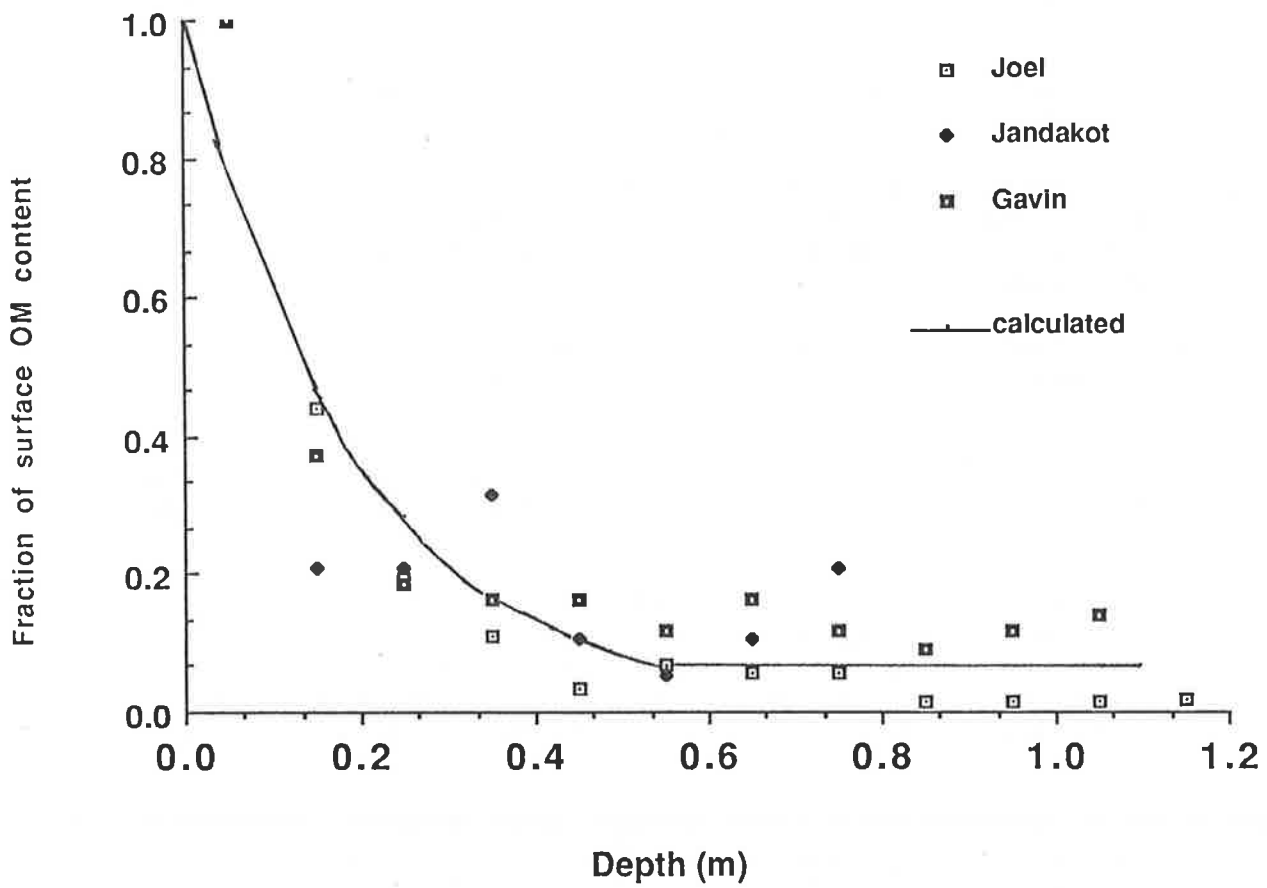


Fig. 1. Organic matter distributions in three soil profiles.

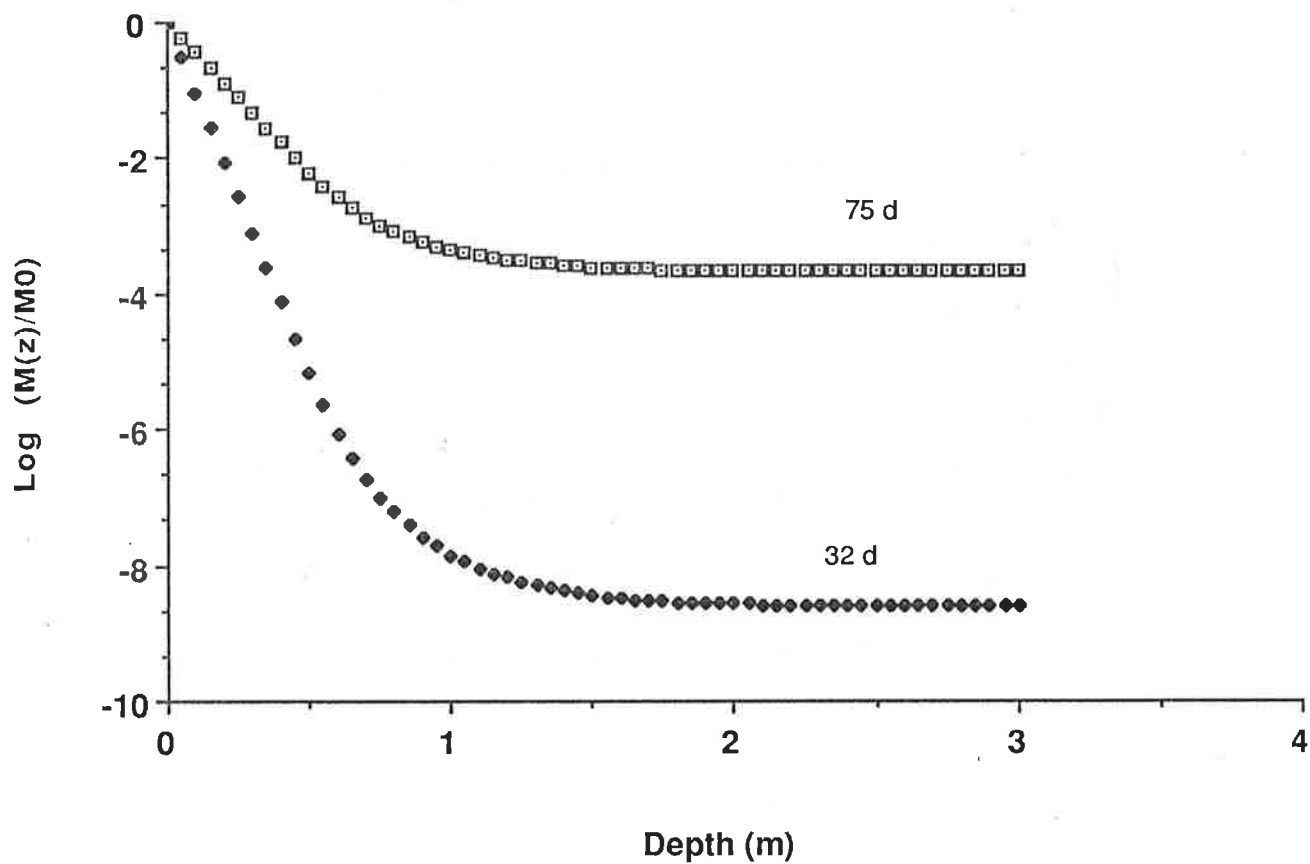


Fig. 2. Calculated distributions of simazine concentrations
obtained with two rates of degradation.

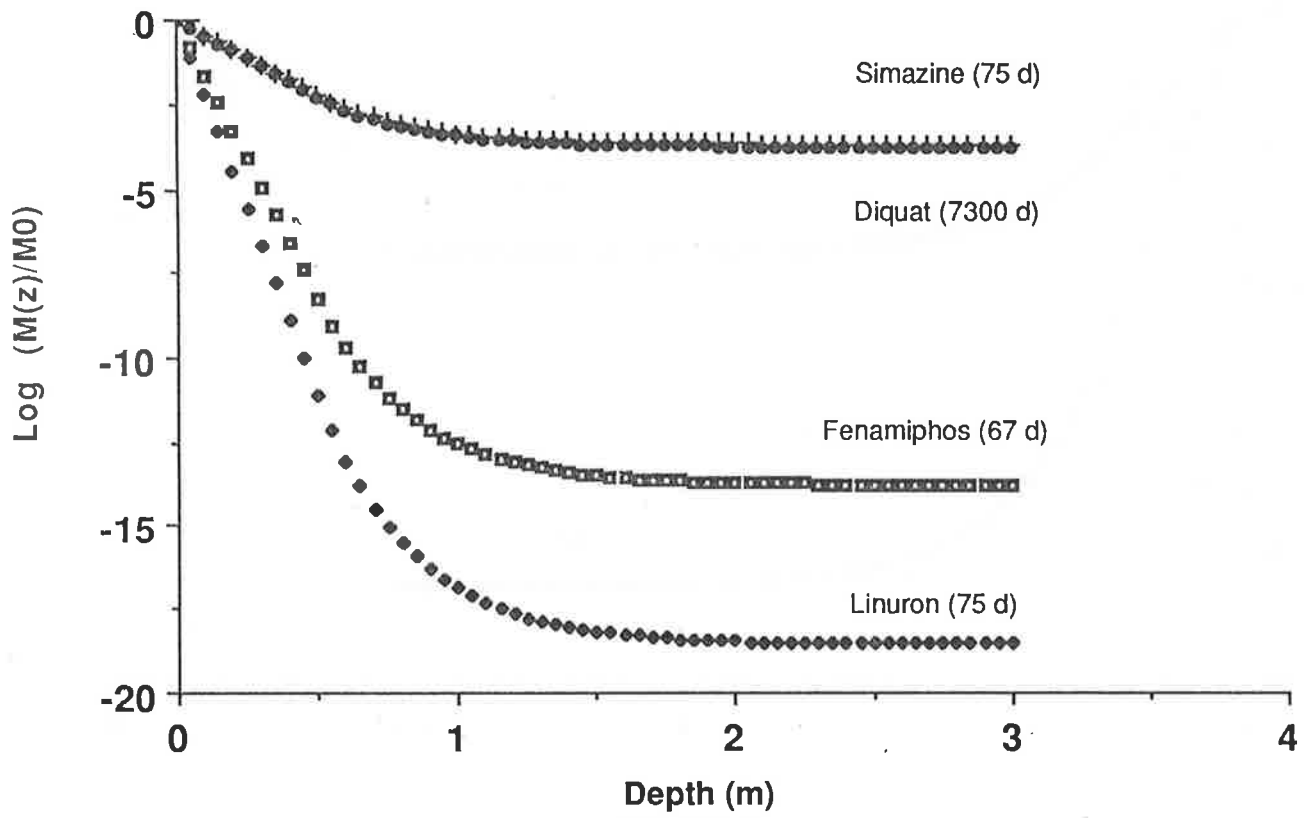


Fig. 3. Calculated distributions of concentrations of the pesticides. Figures in parenthesis are half - lives.

SIMULATING CATION TRANSPORT DURING UNSTEADY, UNSATURATED WATER FLOW IN SANDY SOIL¹

R. S. MANSELL,² S. A. BLOOM,² AND L. A. G. AYLMORE³

A finite-difference numerical model is presented for the transport of multiple-species cations coupled with ion exchange during unsteady, unsaturated water flow in soil. The model requires consecutive solutions of the continuity equation for water flow to obtain distributions of soil water content $\theta(z, t)$ and a convective-dispersive transport equation for each major cation species i to obtain corresponding aqueous-phase concentrations $C_i(z, t)$.

Experimental data from the literature were used to validate water flow and common-anion transport for conditions of unsteady flow in unsaturated soil. Simulated transport of two divalent cation species during unsteady, unsaturated flow in sandy soil demonstrated the importance of exchange selectivity by soil sites in the leaching of native ion species by invading species. Transport involving three cations was simulated during a sequence of infiltration of electrolyte solution, redistribution of soil water, and irrigation with ground water for a sandy soil.

Current mathematical formulations of the transport model limit simulations to conditions where soil solution normality is not allowed to approach very small values.

Transport of chemicals during conditions of unsteady water flow in water-unsaturated soils has important implications for managing soils in ways that minimize ground water contamination. Such conditions occur commonly in agriculture when rainfall or irrigation induces water infiltration into soil that has received applications of agrichemicals such as nutrients and herbicides.

Transport of Conservative Solutes in Soil During Unsteady, Unsaturated Water Flow: Review

Quantitative description of chemical transport through the vadose zone during unsteady

¹ Published as Univ. of Florida Journal Series No. R-00571.

² Soil Science Dept., G159 McCarty Hall, Univ. of Florida, Gainesville, 32611.

³ Soil Science and Plant Nutrition Dept., Univ. of Western Australia, Nedlands, 6009.

Received 8 Mar. 1989; revised 12 Mar. 1990.

flow is well known (Bresler 1973; Nielsen et al. 1986) to require quantitative description of water flow as a first approximation. A number of complex, interactive, physical, chemical, and microbiological mechanisms affect (Nielsen et al. 1986) both chemical transport and water flow in the vadose zone. Chemical transport in the vadose zone is often a controlling determinant of groundwater quality since recharge occurs as a consequence of net water flow through unsaturated soil.

For transport of nonreactive solutes during unsteady, unsaturated water flow through soil with uniform initial water content θ_n , results from mathematical models (Warrick et al. 1971; Smiles et al. 1981; Wilson and Gelhar 1981; Smiles and Gardiner 1982; Bond and Smiles 1983; Watson and Jones 1984), and experimental data (Smiles and Philip 1978; Bond et al. 1984; Bond 1986) have shown that the solute front tends to lag behind the advancing wetting front during unsteady, unsaturated flow.

The hydrodynamic dispersion coefficient for a conservative solute has been shown to increase (Watson and Jones 1982; Bond 1986) with pore velocity of the water during transient flow, with the most pronounced velocity-dependence taking place during infiltration at high rates.

When water is ponded at the soil surface (Warrick et al. 1971), the ratio of the asymptotic rates for solute- and water-front advance is simply $\Gamma = [\theta_s - \theta_n]/[\theta_s] \leq 1$, where θ_n is the initial soil water content and θ_s is the saturated water content at the soil surface. This ratio Γ decreases with increasing θ_n , because solute movement represents actual displacement of soil solution through available pore space (Wilson and Gelhar 1981), whereas changes in the water content behave simply, as the result of propagation of a disturbance in water content or pressure.

If the soil pores are completely accessible (solution is thus mobile) to invading solution, then complete pistonlike displacement (Smiles and Philip 1978; Grismer 1986) may be assumed; however, incomplete displacement has been reported (Laryea et al. 1982; Smiles and Gardiner 1982) for aggregated soils. Immobility of water in soil micropores (de Smedt et al. 1986), anion exclusion (Bresler 1973), and preferential flow

in macropores (Nielsen et al. 1986) all may contribute to incomplete displacement. Complete displacement in relatively wet soil has been reported (Grismer 1986) to require a larger liquid flux at the soil surface during infiltration than for a soil that is initially drier. Leaching of soluble salts from field soils is known (Nielsen and Biggar 1967) to occur more efficiently under conditions of low-intensity rainfall or irrigation in comparison to ponded infiltration. Intermediate low-intensity rainfall with intervening periods of redistribution is also more efficient (Nielsen and Biggar 1967) than continuous rainfall.

A nonuniform distribution of initial soil water content $\theta_n(z)$ during either steady or transient infiltration has been shown (Wilson and Gelhar 1981) to either stretch or contract an applied solute pulse as it propagates through the soil.

Bond (1986 and 1987) demonstrated that asymmetry of solute pulses may occur during unsteady flow in unsaturated soil due to differences in hydrodynamic dispersion coefficients at the two edges of the moving pulse. Such pulses become more symmetric as time increases. If the pulse is small and the initial water content is relatively large, then the transition from asymmetry to symmetry occurs rapidly.

Using numerical analysis of transient water flow in field soils, Russo et al. (1989) showed that the transport of conservative solutes could be retarded relative to that predicted by assuming a homogeneous and nonhysteretic soil water system. Failure to account for vertical heterogeneity in soil hydraulic properties may tend to retard solute transport near the soil surface because highly resistive zones in the profile may limit the flow and cause an irregular water content distribution. Failure to account for soil water hysteresis was also shown to retard solute transport through the surface zone due to underestimation of actual water content.

Transport of Inorganic Cations in Soil During Unsteady, Unsaturated Water Flow: Review

For nonconservative solutes which react chemically and/or microbiologically with components in the porous soil matrix, rates of solute transport during unsteady flow in unsaturated soil may be many orders of magnitude smaller than the rate of water movement. Reactions such as cation exchange (Cho 1985; Mansell et al. 1986; Schulin et al. 1986; Mansell et al. 1988), sorption-desorption of anions (Mansell and Se-

lim 1981), and sorption-desorption of herbicides (Elzeftawy et al. 1976; Selim et al. 1976; Jyothi⁴) may result in pronounced retardation of advancing solute fronts in unsaturated as well as saturated soils.

Although considerable literature is devoted to cation transport during steady flow in saturated soils (Lai et al. 1978; Valocchi et al. 1981; Cho 1985; Mansell et al. 1988), limited experimental research has been reported for transport of cations during unsteady flow in unsaturated soil. In the cation transport model for steady, saturated flow presented by Valocchi et al. (1981), constant cation exchange capacity imposed electroneutrality requiring that exchange sites be occupied by ions, and invariant selectivity coefficients for binary ion exchange provided the basis for describing competition among ion species. Using a similar approach, Cho (1985) investigated the displacing of solutions containing one ion (displacing or invading species) through soil initially saturated with another ion (native species). A large selectivity coefficient which favored the displacing ion resulted in efficient removal of the native ion from the soil. Under those conditions the advancing front for the invading ion was sharp with smaller rates of advance, compared to a diffuse front with a larger rate of advance when the selectivity was small. Cho (1985) also noted that large ratios of cation exchange capacity to solution normality tended to provide greater retardation of the advancing front for ion A. During heterovalent exchange, larger magnitudes of that ratio generally favored adsorption of divalent over monovalent ions. This trend was reversed for smaller ratios.

For steady, saturated flow in columns of sandy soil with low cation exchange capacity, Starr and Parlange (1979) reported that displacing initial soil solution with a high normality solution containing a preferred invading ion resulted in near quantitative replacement of exchangeable native ions within <2 pore volumes of effluent. Simple mass action resulted in displacement of the native ions as a "snow plow effect."

Laryea et al. (1982) reported spatial distributions of water content and ion concentrations as a result of horizontal infiltration of a 1 M solution of KCl into an initially air-dry, Ca-

⁴ V. Jyothi, 1971, Miscible displacement of 2,4-D Herbicide during constant liquid flow velocity into initially dry soils. Ph.D. diss., Univ. of Florida, Gainesville.

saturated, silty clay loam soil. The anion front was observed to lag slightly behind the water front due to the presence of initial soil water with low molarity. However, ion exchange resulted in a much larger lag of the potassium front behind the chloride front.

Bond and Phillips (1990) reported an approximate analytical solution for describing binary cation transport in soil during unsteady, unsaturated water flow conditions. Their solution was based upon a moving coordinate system or set of characteristics (Wilson and Gelhar 1981). Constant cation exchange capacity and local chemical equilibrium were assumed. They showed that water content and pore water velocity could be treated as constant over the region of dispersion of cations during unsteady water flow in unsaturated soil. Under conditions where initial and displacing solution normalities (C_T) differed and the bulk of the exchange reaction occurred well behind the anion front, exchange was assumed to have occurred in a region of constant normality. Effects of dispersion and the shape of the exchange isotherm were treated separately and then combined.

Nonequilibrium Behavior of Cation Transport in Soils: Review

In a recent review of cation transport coupled with ion exchange, Selim et al. (1989) indicated that experimentally-observed nonequilibrium behavior of cation exchange during water flow in some aggregated soils is attributable to physical as well as chemical processes. Two-site models with sites characterized by instantaneous and diffusion-controlled mass transfer (kinetic) between solid and solution phases have been used (Parker and Jardine 1986) to simulate cation transport coupled with ion exchange. Two-region models with diffusion-controlled mass transfer between exchange sites located within mobile (large pores between aggregates) and immobile (small pores within aggregates) flow regions have also been used (Schulin et al. 1986; Selim et al. 1987) to simulate cation transport coupled with ion exchange. Both the two-site and the two-region models provide an apparent kinetic behavior to cation exchange during transport with water through the soil.

Mansell et al. (1988) modified a transport model reported by Valocchi et al. (1981) to include mobile/immobile flow zones (two-region model approach) in the soil. Exchange selectivity coefficients were allowed to vary locally in

the soil as the composition of the solution changed over time and space. Solution normality was held time-invariant. The presence of an immobile solution zone led to breakthrough curves (BTC) in effluent from soil columns that were characteristically early and sharp, but that included tailing. Diffusive transfer of ions between the two flow regions imposed an effective time-dependency on ion exchange during flow even though local chemical equilibrium was maintained throughout. Allowing binary selectivity coefficients to vary with solution composition permitted more realistic description of BTC shape, tailing, and retardation. The model was observed to successfully simulate the transport of Na^+ and Mg^{2+} during steady flow through a loam soil that was initially saturated with Ca^{2+} .

OBJECTIVES

Objectives for our paper were: 1) to present a numerical mathematical model for describing the simultaneous transport of multiple species of cations during the case of unsteady water flow in unsaturated soil, 2) to use data from the literature to validate use of the model to describe water flow and transport of a conservative solute during infiltration, 3) to use model sensitivity analysis to demonstrate the importance of the exchange selectivity coefficient in describing binary, homovalent ion transport during infiltration in sandy soils, and 4) to demonstrate utility of the model by simulating the transport of three ion species during transient water flow (salt solution infiltration, redistribution, and irrigation) in a soil profile.

MATHEMATICAL MODEL

Mathematical description of cation transport in soil during unsteady, unsaturated water flow requires sequential solutions of highly-nonlinear differential equations (Bresler 1973; Nielsen et al. 1986) for water flow and for solute transport. Nonhysteretic, one-dimensional water flow is commonly described by the continuity equation

$$\partial\theta/\partial t = -\partial q/\partial z \quad [1]$$

where t is time (s), z is distance (m), θ is volumetric water content ($\text{m}^3 \text{m}^{-3}$), and q (m s^{-1}) is the Darcy water flux. For vertical flow which is gravity-enhanced, z can be designated as depth and flux can be written as

$$q = -\kappa(h) [\partial h/\partial z - 1] \quad [2]$$

where $\kappa(h)$ is hydraulic conductivity (m s^{-1}) and h is water pressure head (m of water). For hori-

zontal flow, z is lateral distance and the gravitational term (i.e., -1) is omitted from equation [2]. Equations [1] and [2] can be combined to yield the Richards' equation in terms of pressure head

$$\Psi(h) \partial h / \partial t = \partial[\kappa(h) \partial h / \partial z] / \partial z - \partial \kappa(h) / \partial z \quad [3]$$

where $\Psi(h) = \partial \theta / \partial h$ is the water capacity or slope of the soil water-retention curve $\theta(h)$.

For infiltration of water into very dry soil, the presence of very steep gradients of h is well known to cause special difficulties with numerical simulations of equation [3]. Recently Hills et al. (1989) reported efficient algorithms for predicting water flow in relatively dry, layered soils using two-step Crank-Nicholson versions of θ - and h -based forms of Richards' equation.

Equation [3] can be solved numerically if specific input information is provided (Nielsen et al. 1986) for unsaturated hydraulic conductivity $\kappa(h)$ and soil-water retention $\theta(h)$ functions. For water content near saturation, a small finite value ($7 \times 10^{-7} \text{ m}^{-1}$) was used for Ψ in equation [3]. Both $\kappa(h)$ and $\theta(h)$ functions are generally highly nonlinear for most soils. A commonly-used alternative to the time-consuming direct measurement of $\kappa(h)$ is to utilize an analytical model (van Genuchten 1980) to calculate this function. Experimental data for θ versus h was least-square fitted with the van Genuchten equation for effective water saturation, resulting in the empirical constants α and η . Optimized values for α , η , and κ_s (an experimentally-determined value for the hydraulic conductivity at field water saturation) for a specific soil are then used to calculate hydraulic conductivity $\kappa(\Phi)$ as a function of effective saturation. The van Genuchten (1980) method for predicting unsaturated hydraulic conductivity has been shown (Nielsen et al. 1986) to work well for coarse- and medium-textured soils. Less accurate predictions have been obtained for fine-textured soils.

A constant-flux boundary condition is assumed for the upper soil surface ($z = 0$)

$$q_0 = \Omega \quad \text{for } t > 0, \quad [4]$$

and the semi-infinite soil profile is assumed to have uniform hydraulic and chemical properties. If the intensity (flux) of applied water Ω is less than the saturated hydraulic conductivity κ_s , unsaturated flow is assured and the water content at the soil surface θ_u (Hanks and Ashcroft 1980) tends to increase with Ω , because θ_u corresponds to κ_u when $\Omega = \kappa_u$. For a finite profile

of length L , a no-flow condition is imposed at $z = L$ by setting $\partial h / \partial z = 1$ until the pressure head at L reaches zero. Outflow flux at $z = L$ then occurs according to

$$q(L, t) = -\kappa_s[\partial h / \partial z - 1] \quad [5]$$

Initially, a uniform water content θ_n and pressure head h_i are assumed for the soil profile.

A chromatographic modeling approach (Rubin and James 1973; Valocchi et al. 1981; Mansell et al. 1988) has been used previously to describe the simultaneous transport of multiple cation species in soil during steady, saturated water flow. This approach is adopted here to describe cation transport during unsteady, unsaturated water flow. A coupled system of N nonlinear partial-differential equations are required to describe convective-dispersive transport for N cation species in water-unsaturated soil during unsteady liquid flow

$$\partial(\theta C_i + \rho S_i) / \partial t = -\partial F_i / \partial z \quad [6]$$

$$i = 1, 2, 3, \dots, N$$

where C_i is the concentration ($\text{mol}_e \text{ m}^{-3}$) of species i in the solution phase, S_i is the concentration ($\text{mol}_e \text{ Mg}^{-1}$) of species i in the exchange phase, F_i is the flux ($\text{mol}_e \text{ s}^{-1} \text{ m}^{-2}$) of species i and is defined as

$$F_i = -\theta D_i \{ \partial C_i / \partial z \} + q C_i \quad [7]$$

and D_i is the hydrodynamic dispersion coefficient ($\text{m}^2 \text{ s}^{-1}$) for species i . D_i is taken here as equal to D for all species and is assumed to be dependent upon pore-water velocity $v = q/\theta$ (m s^{-1}) according (Watson and Jones 1982) to

$$D = D_0 + \beta |v| \quad [8]$$

where D_0 is the diffusion coefficient ($\text{m}^2 \text{ s}^{-1}$) and β is the dispersivity (m). During unsteady liquid flow, the parameters $\theta(z, t)$ and $q(z, t)$ in equations [6], [7], and [8] vary with time and space.

Using the approach of Valocchi et al. (1981) and equation [1], equations [6] and [7] can be combined to give

$$\begin{aligned} [\theta R_i] \partial C_i / \partial t &= \partial[\theta D \{ \partial C_i / \partial z \}] / \partial z - q \partial C_i / \partial z \\ &+ [\rho / g_i] \sum_{j \neq i} h_{ij} \partial C_j / \partial t \quad [9] \end{aligned}$$

$$i = 1, 2, 3, \dots, N$$

where the coupling functions g_i , h_{ij} , and h_{ji} and the retardation function R_i are defined (Rubin

and James 1973; Valocchi⁵) as

$$g_i = 1 + [1/r_i S_i] \sum_{j \neq i} r_j S_j \quad [10]$$

$$h_{ii} = [1/r_i C_i] \sum_{j \neq i} r_j S_j \quad [11]$$

$$h_{ij} = S_j/C_j \quad [12]$$

and

$$R_i = 1 + [\rho/\theta] [h_{ii}/g_i] \quad [13]$$

The parameters r_i and r_j represent the valences for ion species i and j , respectively. This approach (Valocchi et al. 1981) assumes a constant cation exchange capacity S_T (mol_e Mg⁻¹) where $S_T = \sum_{i=1} S_i$ but does not require constant solution normality $C_T = \sum_{i=1} C_i$. The coupling functions g_i ,

h_{ii} , and h_{ij} were calculated (Valocchi⁵) using a general binary ion exchange isotherm

$$S_T^{r_i r_j} K_{ij} C_i^{r_j} S_j^{r_i} = S_i^{r_j} C_j^{r_i} \quad [14]$$

where K_{ij} is a binary ion-exchange selectivity coefficient given by

$$K_{ij} = C_T^{r_i r_j} K_{ij}^* \quad [15]$$

The dimensionless form for K_{ij} is defined as

$$K_{ij}^* = \left[\frac{S_i^*}{C_i^*} \right]^{r_j} \left[\frac{S_j^*}{C_j^*} \right]^{-r_i} \quad [16]$$

C_T is the total solution normality (mol_e m⁻³), C_i^* is the equivalent fraction of species i in the solution phase, and S_i^* is the equivalent fraction of species i in the exchange phase. Adopting the approach of Valocchi et al. (1981), activity coefficients for ion concentrations in the solution phase were assigned a value of unity, so concentrations rather than activities were actually used throughout the model. Valocchi et al. (1981) showed earlier that the use of concentrations provided adequate simulations for cation transport in an aquifer. Because of the assumption of local chemical equilibrium in the model described by equations [9] through [16], zero values for solution normality C_T must be approximated locally in the soil by small finite values during model simulations. For a constant value for C_T , selectivity coefficients K_{ij} may be held constant or may be allowed to vary (Mansell et al. 1988) with the ionic composition of the soil solution according to experimental exchange

isotherms for each binary combination of all major cation species in the system. The model allows the use of variable C_T , but K_{ij} is also known to vary with C_T during heterovalent exchange. In general, ion exchangers prefer counter ions of higher valence (Helfferich 1962), and preference increases with dilution of the solution. For example, increasing C_T during heterovalent exchange in soil tends to enhance (Lai et al. 1978) the adsorption of a monovalent ion. Thus, variable C_T implies the need for variable K_{ij} in the model. Although the use of binary exchange coefficients to describe competitive exchange among three or more ion species violates principles of chemical thermodynamics, the mathematical complexity of the model is greatly simplified by the use of binary K_{ij} values as long as the correspondence of simulated to observed data remains good (Mansell et al. 1988).

If a single common anion species occurs in the soil/water system, equation [1] can be summed across all cation species i to provide a transport equation for solution normality

$$\partial C_T / \partial t = \partial [\theta D \{ \partial C_T / \partial z \}] / \partial z - q \partial C_T / \partial z \quad [17]$$

This equation is only needed when solution normality $C_T(z, t)$ is designated as a variable in space and time.

A constant concentration boundary condition for each ion species i in solution is maintained at the soil surface ($z = 0$)

$$C_i(0, t) = C_{i0} \quad \text{for } t > 0 \quad [18]$$

A soil profile of semi-infinite length is assumed here. For a profile of finite length L , the boundary condition at $z = L$ when water outflow occurs is given by

$$\partial C_i / \partial z = 0 \quad [19]$$

A Crank-Nicholson finite-differencing technique (Selim et al. 1976) was used to solve equation [3] in order to obtain soil water-pressure head $h(z, t)$ during unsteady liquid flow. Pressure head values were then used in equation [2] to calculate water flux $q(z, t)$ values for input to the cation transport equation [9]. Each of the terms in equation (3) was expressed in finite-difference form for depth $z = k\Delta z$ and time $t = [n + 1/2]\Delta t$, where Δz is the spacing between nodes, Δt is the time step, k is an index for incremental depth, and n is an index for incrementing time during simulations.

⁵ A. J. Valocchi, 1981, Transport of ion-exchanging solutes during groundwater recharge. Ph.D. diss., Stanford Univ., Palo Alto, California.

A Crank-Nicholson finite-differencing technique was also used to solve equation [9] for cation concentrations $C_i(z, t)$ in the soil solution during unsteady flow. Values of Δz and Δt for numerical simulations were chosen to provide rapid convergence, minimum mass-balance errors, and good computational efficiency. Overall mass-balance error as well as mass-balance errors for each ion species were automatically monitored by the computer program. A uniform node spacing using $\Delta z = 0.25$ cm and a variable time step Δt were used in all simulations for cation transport and for water flow. The time step was automatically started using 0.1 s and increased stepwise to a maximum value of 50 s as the simulation progressed. The maximum Δt value was used thereafter. Values for $C_i(z, t)$ were then used in equation [15] to determine corresponding values for concentrations $S_i(z, t)$ of each ion species in the exchange phase.

SIMULATED TERNARY-CATION TRANSPORT DURING STEADY, SATURATED WATER FLOW IN SOIL

The current published literature contains only a limited number of fully-documented experimental investigations that can be used to evaluate a cation-transport model for multiple ion species under conditions of either steady, saturated flow or unsteady, unsaturated flow. Experimental results from Lai et al. (1978) were used earlier (Mansell et al. 1988) to demonstrate the capability of a model similar to the one presented here for describing cation transport involving three ion species— Na^+ , Mg^{2+} , and Ca^{2+} —during steady flow in a fine-textured soil. Lai et al. (1978) displaced pulses of solution containing Na^+ and Mg^{2+} through 25-cm long columns of water-saturated Yolo loam soil which were initially saturated with Ca^{2+} . Breakthrough curves were reported for Na^+ and Mg^{2+} concentrations in effluent from soil columns which were maintained with different values for input-pulse size \bar{Y} and for C_T .

SIMULATED SALT TRANSPORT IN SANDY SOIL DURING UNSTEADY, UNSATURATED WATER FLOW

Using experimental data from Smiles et al. (1981) for constant-flux horizontal infiltration into columns of Bungendore fine sand with an initial water content of $0.10 \text{ m}^3 \text{ m}^{-3}$, Watson and Jones (1982) concluded that the hydrodynamic dispersion coefficient D can be considered

to depend upon pore water velocity v during unsteady, unsaturated water flow, particularly for larger values of v . Earlier, Smiles et al. (1981) had concluded that the dispersion coefficient was insensitive to the pore water velocity v and could be taken as a function of water content θ only. Watson and Jones (1982) showed that an experimental range of influent fluxes from 3.28×10^{-7} to $105 \times 10^{-7} \text{ m s}^{-1}$ provided a small but finite dispersivity value β of $1 \times 10^{-4} \text{ m}$ for equation [8]. They stated that the data were not inconsistent with the concept of velocity-dependent dispersion. Chloride concentrations of the applied aqueous solutions (C_{T_0}) and initial soil solution (C_{T_n}) were 100 and $1000 \text{ mol} \cdot \text{m}^{-3}$, respectively.

The closed-form analytical model of van Genuchten (1980) was used here to obtain smooth functions of soil water content $\theta(h)$, hydraulic conductivity $\kappa(h)$, and water capacity $\Psi(h)$ for Bungendore fine sand [Fig. 1]. Experimental data from Smiles et al. (1981) for soil water retention were least-square fitted using the van Genuchten (1980) method to obtain optimum values [Table 1] for the parameters θ_r , η , and α . These values as well as reported values for θ_s and κ_s [Table 1] were used to calculate $\kappa(h)$ and $\Psi(h)$ input functions for water-flow simulations. Over the pressure head range from 0 to -70 cm, water content decreased only from 0.34 to $0.08 \text{ m}^3 \text{ m}^{-3}$, but a several-fold decrease in hydraulic conductivity was observed. Water capacity was zero near water saturation and developed a maximum value at $h = 40$ cm and $\theta = 0.22 \text{ m}^3 \text{ m}^{-3}$. These soil-water characteristics were considered typical for a coarse-textured soil. A single case for unsteady, unsaturated flow where the applied liquid flux was $8.75 \times 10^{-7} \text{ m s}^{-1}$ and infiltration was terminated after 70,500 s was selected from Watson and Jones (1982) to validate our numerical model for water flow and conservative solute transport. Excellent agreement (Fig. 2) was observed between simulated and experimental distributions for water content θ and reduced concentration $[C - C_{T_n}]/[C_{T_0} - C_{T_n}]$. The relatively slow influent flux, combined with the relatively high initial water content for the column of Bungendore fine sand, resulted in a diffuse wetting front. In contrast, a very sharp concentration front for Cl^- occurred at a given horizontal distance ($x \cong 30$ cm) located behind the water front ($x \cong 65$ cm). The spatial separation of the chloride and water fronts was attributed to displacement of the initial soil solution as the invading solution advanced (Wilson

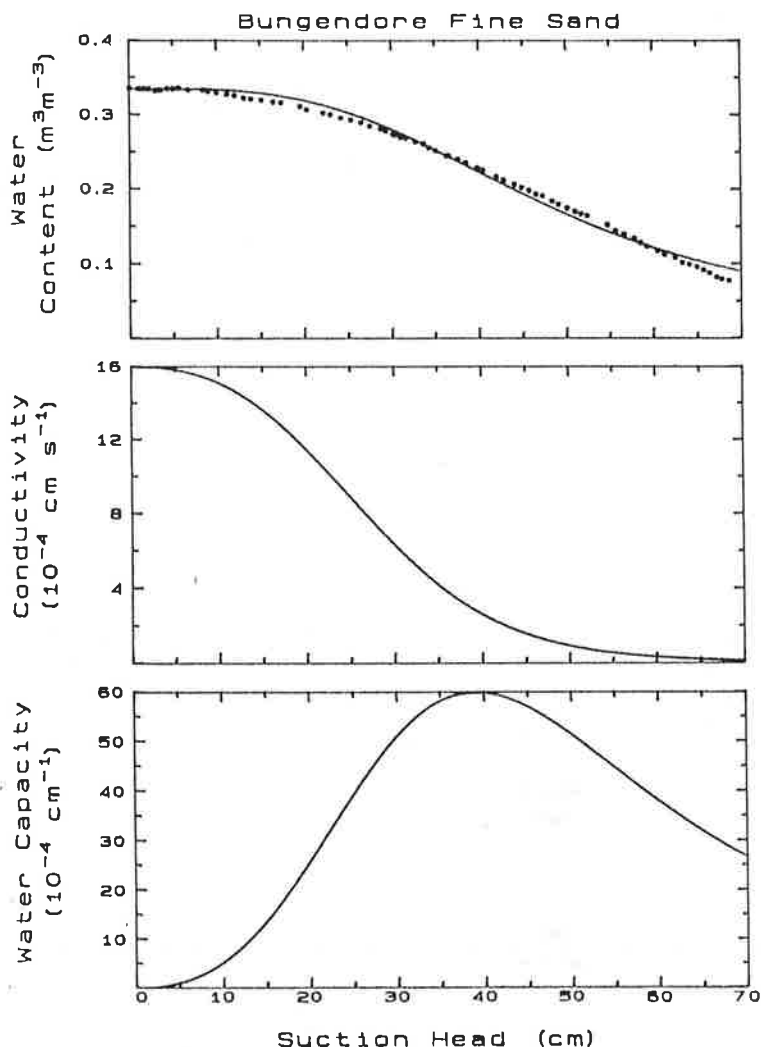


FIG. 1. Functional relationships of volumetric water content, hydraulic conductivity, and water retention capacity to water suction head are given for Bungendore fine sand (Watson and Jones 1982). Experimental data for water content versus suction head are given as discrete points.

TABLE 1

Soil-water and hydrodynamic-dispersion characteristic parameters used for Bungendore fine sand. Parameters η , α and θ_r were obtained by least-square fitting the analytical model of Van Genuchten (1980) to the experimental soil water retention data (Watson and Jones 1982)

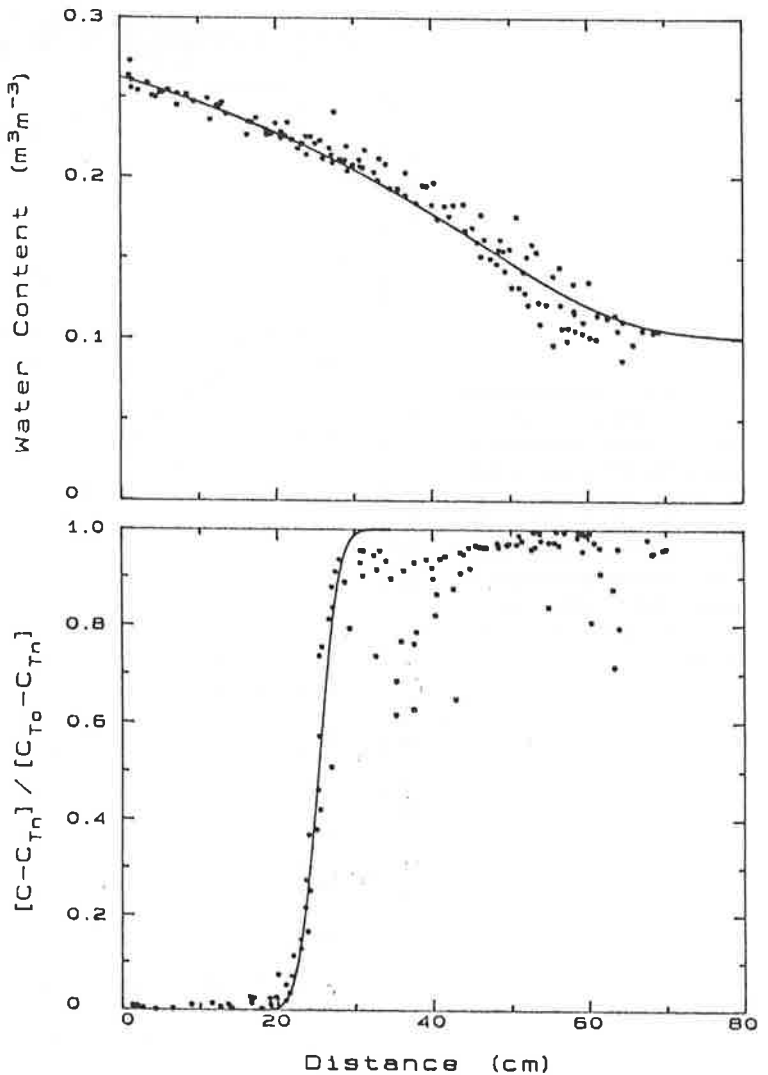
Parameter	Units	Magnitude
ρ	Mg m^{-3}	1.84
θ_s	$\text{m}^3 \text{m}^{-3}$	0.347
κ_s	m s^{-1}	148×10^{-7}
θ_r	$\text{m}^3 \text{m}^{-3}$	0
η	dimensionless	3.3428
α	dimensionless	2.469×10^{-2}
D_0	$\text{m}^2 \text{s}^{-1}$	4.3×10^{-10}
β	m	1.0×10^{-3}

and Gelhar 1981) into the soil. Mass-balance errors obtained for water and Cl^- during the simulation were only -0.252 and -0.096% , respectively.

INFLUENCE OF EXCHANGE SELECTIVITY COEFFICIENT UPON SIMULATED BINARY-CATION TRANSPORT DURING TRANSIENT WATER FLOW IN SANDY SOIL

Employing soil-water parameters for Bungendore fine sand, the numerical model was used to demonstrate sensitivity of the exchange selectivity coefficient K_{ij} to simulated transport of two divalent cation species, I^{2+} (invader) and II^{2+} (native), during constant-flux ($q_0 = 8.75 \times 10^{-7}$

FIG. 2. Simulated (solid lines) and experimental (discrete points from Watson and Jones 1982) distributions of water content and relative chloride concentration with horizontal distance for a column of Bungendore fine sand after constant-flux infiltration.

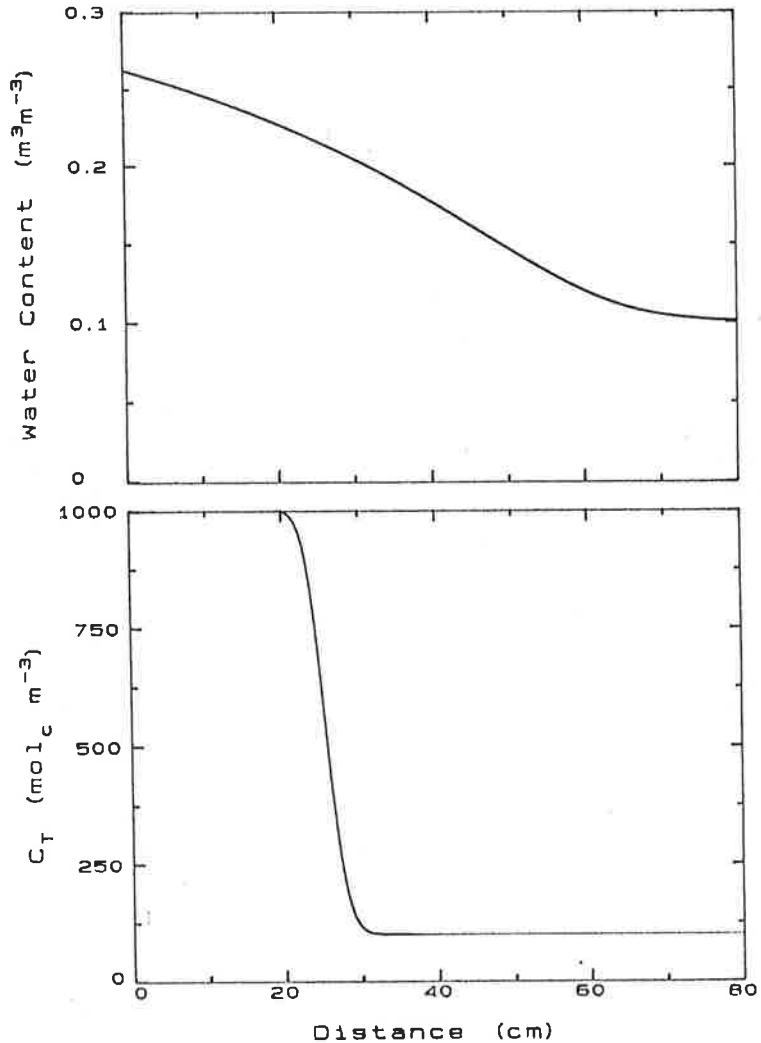


m s^{-1}) infiltration of electrolyte solutions having normality $C_{T0} = 1000 \text{ mol}_c \text{ m}^{-3}$ as $\{\text{I}\}\text{Cl}_2$. Initial water content θ_n and normality C_{Tn} in the soil were $0.10 \text{ m}^3 \text{ m}^{-3}$ and $100 \text{ mol}_c \text{ m}^{-3}$ as $\{\text{II}\}\text{Cl}_2$, respectively. Infiltration was terminated after 70,500 s. A value of $100 \text{ mol}_c \text{ Mg}^{-1}$ was arbitrarily chosen for S_T in these simulations. Other parameters used for the simulations are shown in Table [1]. Fixed values for K_{ij} were used, and changes in these values with respect to changes in C_T were ignored. Simulations were performed using values of 0.01, 0.10, 1.00, and 10 for K_{ij} ($i = \text{species I}$ and $j = \text{species II}$) where the magnitude indicates the relative preference of soil exchange sites for species I over species II.

Simulated distributions for water content θ and solution normality C_T (i.e., Cl^-) are presented in Fig. [3]. Distributions of invading C_1

(species I^{2+}) and native C_2 (species II^{2+}) ions in the solution phase are given in Fig. [4]. As expected, the sharp solution normality front ($x \cong 25 \text{ cm}$) which lagged behind the water front ($x \cong 65 \text{ cm}$) was independent of K_{ij} , but an increase in the selectivity coefficient from 0.01 to 10 resulted in a transition from diffuse to sharp fronts for the invading ion species as well as increased thickness of a zone of maximum concentration of invader near the infiltration surface. Cho (1985) reported similar trends for cation transport during steady flow through water-saturated soil. An increase in K_{ij} consequently resulted in an increase in the completeness and efficiency of displacement of the native cation through the soil. As expected, the C_T front was composed predominantly of the native ion species for all selectivities used and, as the pref-

FIG. 3. Simulated distributions of water content and chloride concentration in the soil solution are given for distance in fine sand after constant-flux horizontal infiltration.



erence of exchange sites for the invading species increased, the composition of the C_T front became increasingly dominated by the native species. Ion exchange occurred in a zone of constant solution normality (C_{T_0}) as suggested by Bond and Phillips (1990). Between the anion and water fronts, solution normality was similar to that of the initial solution (C_{T_0}), such that only native ions occurred in the solution phase. Because of model specification of binary exchange with constant S_T for the soil, spatial distributions of exchange-phase concentrations S_1 and S_2 (Fig. 5) corresponding to different values of K_{12} were mirror-images of each other. In contrast, spatial distributions of solution-phase concentrations C_1 and C_2 were not mirror-images since C_T was not constant ($C_{T_0} \neq C_{T_0}$).

With increasing K_{12} , the fronts for S_1^* and S_2^* became steeper.

SIMULATED TERNARY-CATION TRANSPORT DURING INFILTRATION OF SALT SOLUTION, REDISTRIBUTION, AND IRRIGATION

Again using soil-water parameters for Bunge-dore fine sand, the model was used to simulate the transport of invading divalent I^{2+} (Mg^{2+}) and monovalent III^+ (Na^+) species in a vertical profile of soil having native divalent species II^{2+} (Ca^{2+}), during unsteady, unsaturated flow for constant-flux infiltration of a high-normality electrolyte solution for 1800 s, followed by redistribution until 12,600 s and subsequent constant-intensity sprinkler irrigation with ground

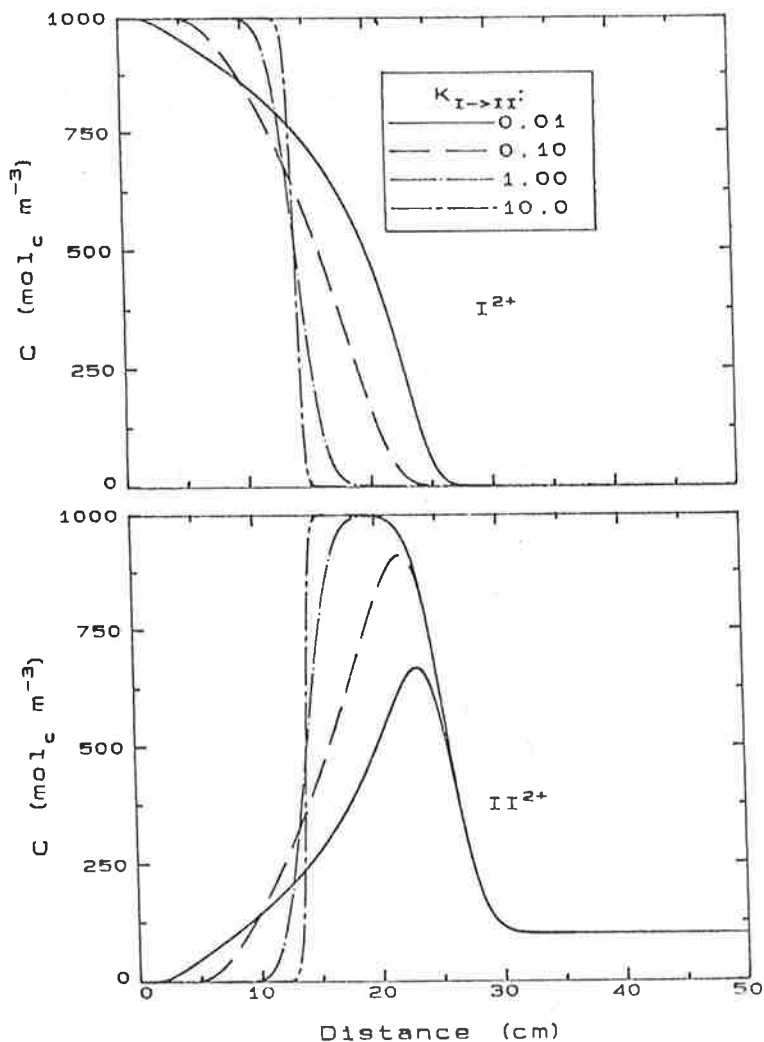


FIG. 4. Distributions of aqueous-phase concentrations of divalent invader (I^{2+}) and native (II^{2+}) species are given for distance in fine sand after constant-flux horizontal infiltration with exchange selectivity coefficients $K_{I/II}$ of 0.01, 0.10, 1.00, and 10.00.

water until 30,600 s. A liquid flux value of $2.78 \times 10^{-6} \text{ m s}^{-1}$ was used both for infiltration of the salt solution and for irrigation. Normalities of the applied salt solution (C_{T_0}), ground water (C_{T_n}), and the initial soil solution (C_{T_i}) were 10,000, 1000, and 1000 $\text{mol}_e \text{ m}^{-3}$, respectively. The applied solution contained 7,500 $\text{mol}_e \text{ m}^{-3}$ NaCl and 2,500 $\text{mol}_e \text{ m}^{-3}$ MgCl_2 . Groundwater used for irrigation was assumed to contain 1000 $\text{mol}_e \text{ m}^{-3}$ CaCl_2 . The large normality of the salt solution was chosen to represent accidental spillage of concentrated fertilizer solution. The initial soil water content θ_n was $0.03 \text{ m}^3 \text{ m}^{-3}$ and the cation exchange capacity S_T was 100 $\text{mol}_e \text{ Mg}^{-1}$. The exchange selectivity coefficients K_{12} , K_{13} , and K_{23} (Mansell et al. 1988) were 0.845, 3.346, and 3.640 $\text{mol}_e \text{ m}^{-3}$, respectively, where subscripts 1, 2, and 3 represent ion species Mg^{2+}

(I^{2+}), Ca^{2+} (II^{2+}), and Na^{2+} (III^+), respectively. Values for K_{ij} were assumed here to be invariant with changes in C_T (Mansell et al. 1988). Thus, soil exchange sites exhibited highest and lowest relative preferences for the native divalent species Ca^{2+} (II^{2+}) and the invading monovalent species Na^+ (III^+), respectively.

After the addition of 5 mm of infiltrated salt solution, the simulated distributions of θ and C_T (Fig. 6) penetrated the soil profile to a depth of only 5 cm during the 1,800 s period. During the postinfiltration or redistribution period from 1,800 to 12,600 s, the water and salt fronts penetrated to 15 cm. Subsequently, 50 mm of irrigation water moved these fronts to 33 cm depth. Low initial θ_n in the soil profile resulted in only minimal separation of the mobile salt (or Cl^-) and water fronts with depth and time.

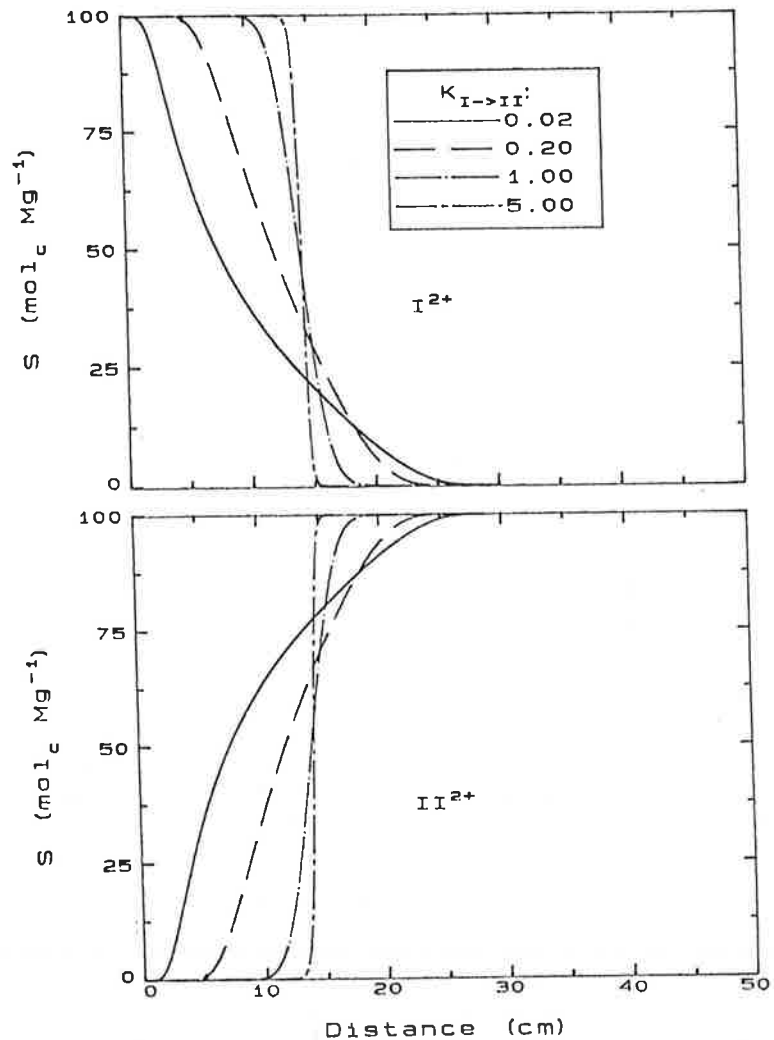


FIG. 5. Corresponding distributions of exchange-phase concentration of divalent species I^{2+} and II^{2+} are given for distance in fine sand after simulated constant-flux horizontal infiltration of salt solution.

Infiltrated electrolyte solution resulted in a moving chloride pulse (Fig. 6) in the upper portion of the soil. This mobile Cl^- pulse resulted from the summed effects of mobile concentration pulses (Fig. 7) for both the initial invading (Na^+ and Mg^{2+}) and native (Ca^{2+}) ion species. Later, during irrigation with groundwater, invading Ca^{2+} ions also contributed to the total solution concentration in the upper portion of the soil profile. Because the native Ca^{2+} species was preferred over both initial invader species and because of the high concentration of the monovalent Na^+ invader species in the infiltrated electrolyte solution, maximum concentrations for Mg^{2+} and Na^+ species in the downward-moving salt pulse decreased readily with depth and time. In contrast, maximum concentrations for the native Ca^{2+} species increased initially

during infiltration of salt solution, resulting in a pulse that tended to move with the chloride front as the wetting front moved into the drier soil. The Ca^{2+} pulse was attributed to ions originally present in the exchange phase of the soil which underwent exchange with the invading species. Distributions of solution (Fig. 7) and exchange-pulse (Fig. 8) concentrations for Ca^{2+} after 1800 and 12,600 s indicate that only the upper 1 to 2 cm of soil were completely leached of the native cation during infiltration of the salt solution and subsequent redistribution. During the period of irrigation, invading Ca^{2+} ions in the infiltrating ground water solution increased both solution and exchange phase concentrations near the soil surface, resulting in separate pulses of invading and native Ca^{2+} cations moving through the soil.

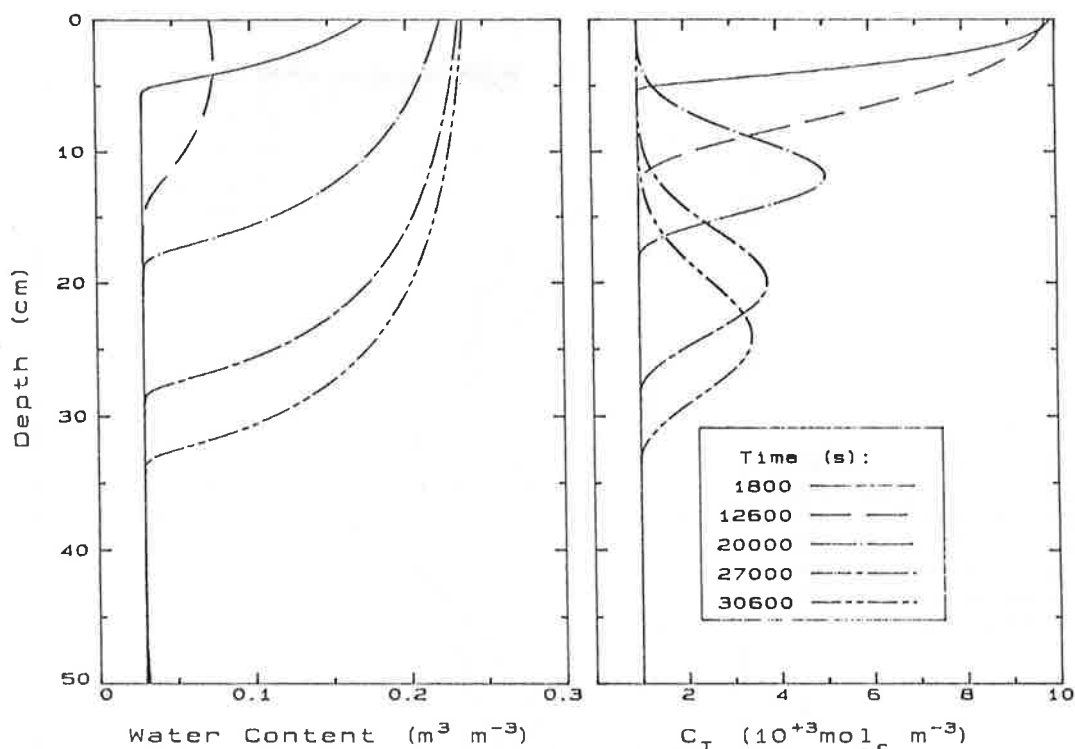


FIG. 6. Simulated distributions of water content and chloride concentration in the soil solution are given for vertical distance in fine sand for three selected times during a period of infiltration of salt solution, soil-water redistribution, and irrigation with groundwater.

Mass-balance errors for water and all cations were -0.73 and -0.72% , respectively, during mass-transport simulation for the period of infiltration, redistribution and irrigation. Individual mass-balance errors were -1.32 , -0.52 , and -1.38% , respectively, for Mg^{2+} , Ca^{2+} , and Na^+ species. These small errors indicate that the program was operating effectively.

In general, adequate simulations of the transport of multiple cations using differential equations [6, 9] and the Crank-Nicholson numerical method may require very small time (Δt) and space (Δz) steps if the term $\rho\Delta S_i/\Delta t$ specifying the rate of exchange for a given species becomes very large. Values for this exchange-rate term can be large due to large exchange selectivity coefficients, nonlinear exchange isotherms, large pore water velocity v , highly competitive invading ion species relative to native species, large imposed changes in concentration of invading ions such as step-function increases in concentration, the magnitude of Δt chosen, and the magnitude of Δz . Extreme (both large and small) values for the exchange-rate term may occur as a result of extreme values in the variable

slope (i.e., $\partial S_i^*/\partial C_i^*$) for highly nonlinear exchange isotherms that are greatly magnified by heterovalent exchange. During constant-flux infiltration into soil with low θ_m values for v tend to be larger in the vicinity of the advancing wetting front, thus magnifying any influence of extreme values for the exchange-rate term that might exist. When simulations involved infiltration of an aqueous solution containing an invading ion into a soil saturated with a native ion, much smaller time steps were required to prevent unacceptable mass-balance errors for individual ion species when invading species were highly competitive (very large K_{ij}) relative to native species than when the invading species were less competitive. Mass-balance errors for individual species were observed to provide a more sensitive indication of problems with large $\rho\Delta S_i/\Delta t$ than did the overall mass-balance error for those simulations.

For soil-water conditions where C_T is a variable and $\theta C_T/\rho S_T$ is much less than unity, the current mathematical formulation as given by equations [6-9] has inherent limitations due to oscillations caused by random computer round-

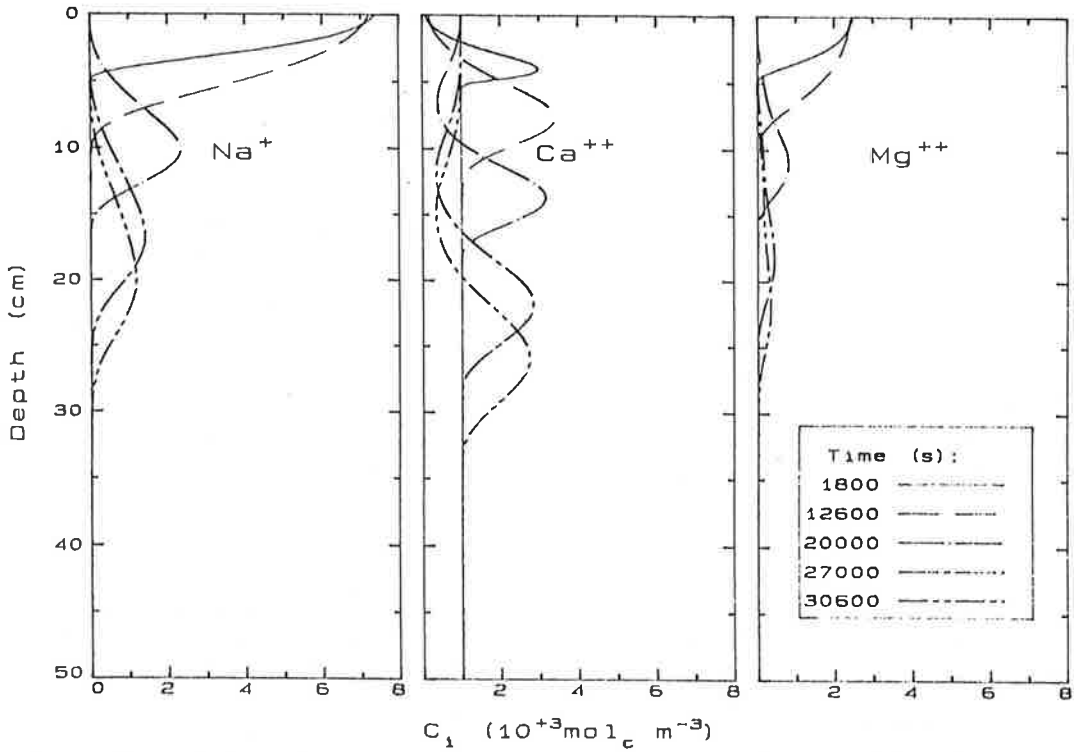


FIG. 7. Simulated distributions of solution-phase concentrations for ion species I^{2+} (Mg^{2+}), II^{2+} (Ca^{2+}), and III^+ (Na^+) are given for vertical distance in fine sand for three selected times during a period of transient, unsaturated flow.

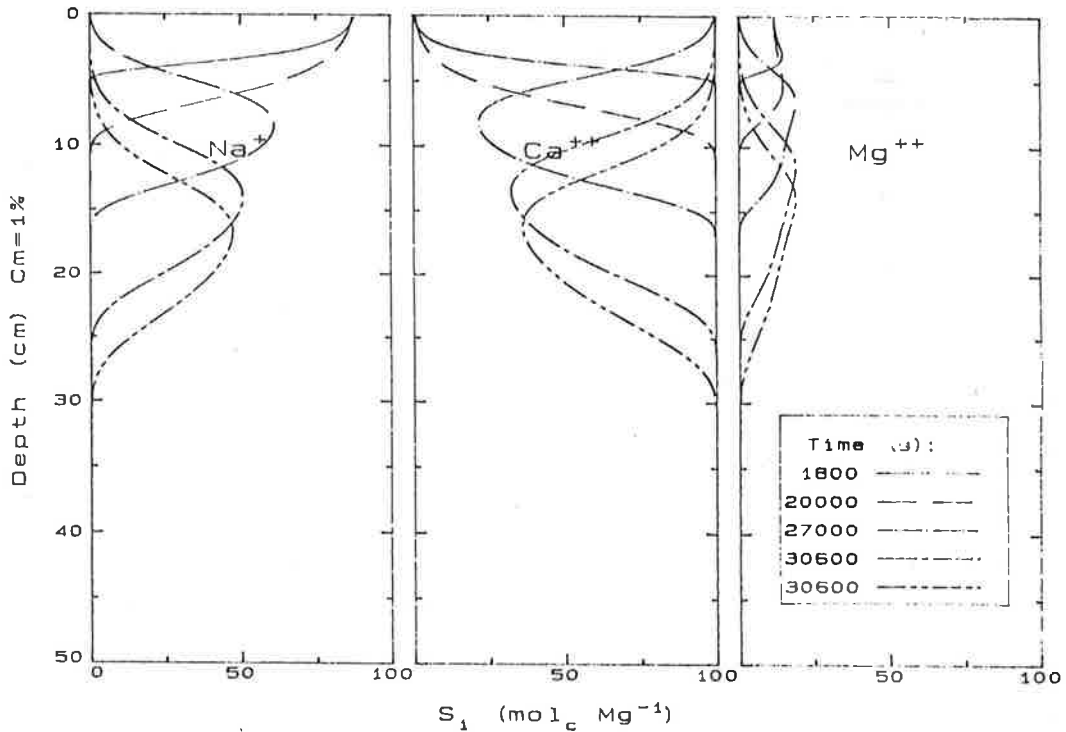


FIG. 8. Simulated distributions of exchange phase concentrations of ion species I^{2+} (Mg^{2+}), II^{2+} (Ca^{2+}), and III^+ (Na^+) are given for vertical distance in fine sand for three selected times during a period of transient, unsaturated flow.

ing errors. When the total amount of an ion for a given ion species in the solution phase will not support ion exchange for that species, the transport model will generate erroneous results with spurious mass-balance errors for individual ion species. Since C_T for natural rainfall is characteristically low, a need exists to permit model simulation of cation transport in surface soils when $\theta C_T / \rho S_T$ is very small.

CONCLUSIONS

A finite-difference numerical model was presented for multiple-species cation transport and water flow during unsteady liquid flow in unsaturated soil. The approach used requires consecutive solutions of the Richards' equation to obtain water pressure head $h(z, t)$ and a chromatographic solute equation for each major cation species i to obtain aqueous-phase concentrations for each species $C_i(z, t)$. Using an assumption of local chemical equilibrium, binary-exchange isotherms were used to obtain exchange-phase concentrations $S_i(z, t)$ which correspond to $C_i(z, t)$. Pressure-head results were used to calculate water content $\theta(z, t)$ and water flux $q(z, t)$ variables as required inputs for solving the transport equations. All of the chromatographic transport equations are coupled through competitive ion exchange for soil exchange sites.

Experimental data were used to validate the cation-transport portion of the model for conditions of steady liquid flow in saturated soil and to validate water flow and salt transport for conditions of unsteady flow in unsaturated flow. Simulations of cation transport during unsteady, unsaturated flow in sandy soil demonstrated the importance of exchange selectivity for soil sites in the leaching of native ion species by invading species.

Although the present mathematical formulation for cation transport in soil operates well for conditions involving transient, unsaturated water flow and variable solution normality, simulations involving very low values for C_T tend to generate incorrect results.

ACKNOWLEDGMENTS

This paper was initiated while the first author was a Visiting Research Fellow at the University of Western Australia in Perth in 1987.

REFERENCES

- Bond, W. J. 1986. Velocity-dependent hydrodynamic dispersion during unsteady, unsaturated soil water flow: Experiments. *Water Resour. Res.* 22:1881-1889.
- Bond, W. J. 1987. Solute transport during unsteady, unsaturated soil water flow: The pulse input. *Aust. J. Soil Res.* 25:223-241.
- Bond, W. J., and I. R. Phillips. 1990. Cation transport during unsteady, unsaturated soil water flow: A simple approximate solution. *Water Resour. Res.* (in press).
- Bond, W. J., and D. E. Smiles. 1983. Influence of velocity on hydrodynamic dispersion during unsteady soil water flow. *Soil Sci. Soc. Am. J.* 47:438-441.
- Bond, W. J., B. N. Gardiner, and D. E. Smiles. 1984. Movement of CaCl_2 solutions in an unsaturated clay soil: The effect of solution concentration. *Aust. J. Soil Res.* 22:43-58.
- Bresler, E. 1973. Simultaneous transport of solutes and water under transient unsaturated flow conditions. *Water Resour. Res.* 9:975-986.
- Cho, C. H. 1985. Ionic transport in soil with ion-exchange reaction. *Soil Sci. Soc. Am. J.* 49:1379-1386.
- de Smedt, F., F. Wauters, and J. Sevilla. 1986. Study of tracer movement through unsaturated sand. *Geoderma* 38:223-236.
- Elzeftawy, A., R. S. Mansell, and H. M. Selim. 1976. Distributions of water and herbicide in Lakeland sand during initial stages of infiltration. *Soil Sci.* 122:297-307.
- Grismer, M. E. 1986. Nondestructive observations of solution displacement in soils. *Soil Sci.* 141:185-189.
- Hanks, R. J., and G. L. Ashcroft. 1980. *Applied Soil Physics*. Springer-Verlag, New York, pp. 81-82.
- Helfferich, F. 1962. *Ion Exchange*. McGraw Hill, New York, pp. 156-158.
- Hills, R. G., I. Porro, D. B. Hudson, and P. J. Wierenga. 1989. Modeling one-dimensional infiltration into very dry soils. 1. Model development and evaluation. *Water Resour. Res.* 25:1259-1269.
- Lai, S.-H., J. J. Jurinak, and R. J. Wagenet. 1978. Multicomponent cation absorption during convective-dispersive flow through soils: Experimental study. *Soil Sci. Soc. Am. J.* 42:240-243.
- Laryea, K. B., D. E. Elrick, and M. J. L. Robin. 1982. Hydrodynamic dispersion involving cationic adsorption during unsaturated transient water flow in soil. *Soil Sci. Soc. Am. J.* 46:667-671.
- Mansell, R. S., and H. M. Selim. 1981. Mathematical models for predicting reactions and transport of phosphorus applied to soils. In *Modeling wastewater renovation*. I. K. Iskandar (ed.). John Wiley and Sons, New York, pp. 600-646.
- Mansell, R. S., S. A. Bloom, H. M. Selim, and R. D. Rhue. 1986. Multispecies cation leaching during continuous displacement of electrolyte solutions through soil columns. *Geoderma* 38:61-75.
- Mansell, R. S., S. A. Bloom, H. M. Selim, and R. D. Rhue. 1988. Simulated transport of multiple cations in soil using variable selectivity coefficients. *Soil Sci. Soc. Am. J.* 52:1533-1540.
- Nielsen, D. R., and J. W. Biggar. 1967. Miscible displacement and leaching phenomena. In *Irrigation of agricultural lands*. Monograph no. 11. R. M. Hagan, H. R. Haise, and T. C. Edminister (eds.). American Society of Agronomy, Madison, Wis., pp. 254-274.

- Nielsen, D. R., M. Th. van Genuchten, and J. W. Biggar. 1986. Water flow and solute transport processes in the unsaturated zone. *Water Resour. Res.* 22:89S-108S.
- Parker, J. C., and P. M. Jardine. 1986. Effect of heterogeneous adsorption behavior on ion transport. *Water Resour. Res.* 22:1334-1340.
- Rubin, J., and R. V. James. 1973. Dispersion-affected transport of reacting solutes in saturated porous media: Galerkin Method applied to equilibrium-controlled exchange in unidirectional steady water flow. *Water Resour. Res.* 9:1332-1356.
- Russo, D., W. A. Jury, and G. L. Butters. 1989. Numerical analysis of solute transport during transient irrigation. 1. The effect of hysteresis and profile heterogeneity. *Water Resour. Res.* 25:2109-2118.
- Schulin, R., H. Fluhler, R. S. Mansell, and H. M. Selim. 1986. Miscible displacement of ions in aggregated soils. *Geoderma* 38:311-322.
- Selim, H. M., R. S. Mansell, and A. Elzeftawy. 1976. Distributions of 2,4-D and water in soil during infiltration and redistribution. *Soil Sci.* 121:176-183.
- Selim, H. M., R. Schulin, and H. Fluhler. 1987. Transport and ion exchange of calcium and magnesium in an aggregated soil. *Soil Sci. Soc. Am. J.* 51:876-884.
- Selim, H. M., R. S. Mansell, L. A. Gaston, H. Fluhler, and R. Schulin. 1989. Prediction of cation transport in soils using cation exchange reactions. Proceedings of International Workshop entitled "Field Scale Water and Solute Flux in Soil" held in Monte Verita, Switzerland.
- Smiles, D. E., and B. N. Gardiner. 1982. Hydrodynamic dispersion during unsteady, unsaturated water flow in a clay soil. *Soil Sci. Soc. Am. J.* 46:9-14.
- Smiles, D. E., and J. R. Philip. 1978. Solute transport during absorption of water by soil: Laboratory studies and their practical implications. *Soil Sci. Soc. Am. J.* 42:537-544.
- Smiles, D. E., K. M. Perroux, S. J. Zegelin, and P. A. C. Raats. 1981. Hydrodynamic dispersion during constant rate absorption of water by soil. *Soil Sci. Soc. Am. J.* 45:453-458.
- Starr, J. L., and J. Y. Parlange. 1979. Dispersion in soil columns: The snow plow effect. *Soil Sci. Soc. Am. J.* 43:448-450.
- Valocchi, A. J., R. L. Street, and P. V. Roberts. 1981. Transport of ion-exchanging solutes in groundwater: Chromatographic theory and field simulation. *Water Resour. Res.* 17:1518-1527.
- van Genuchten, M. Th. 1980. A closed-form equation for predicting the hydraulic conductivity of unsaturated soils. *Soil Sci. Soc. Am. J.* 44:892-898.
- Warrick, A. W., J. W. Biggar, and D. R. Nielsen. 1971. Simultaneous solute and water transfer for an unsaturated soil. *Water Resour. Res.* 7:1216-1225.
- Watson, K. K., and M. J. Jones. 1982. Hydrodynamic dispersion during absorption in a fine sand. 2. The constant flux case. *Water Resour. Res.* 18:1435-1443.
- Watson, K. K., and M. J. Jones. 1984. Algebraic equations for solute movement during absorption. *Water Resour. Res.* 20:1131-1136.
- Wilson, J. L., and L. W. Gelhar. 1981. Analysis of longitudinal dispersion during absorption in a fine sand: 1. The constant concentration case. *Water Resour. Res.* 18:91-100.

Water and solute movement to plant roots

**Proc. 14th Cong. Inter. Soil Sci. Soc., Kyoto, Japan, Aug. 1990,
V 2, 124-129.**

Aylmore, L.A.G. and Hamza, M.

WATER AND SOLUTE MOVEMENT TO PLANT ROOTS

L.A.G. Aylmore and M. Hamza

Soil Science and Plant Nutrition, School of Agriculture,
The University of Western Australia,
Nedlands, Western Australia, 6009.

INTRODUCTION

Much of the controversy surrounding both water and solute uptake by plant roots has arisen from the lack of suitable methods for measuring the values of water and solute potentials in the soil surrounding plant roots and simultaneous rates of water and solute uptake by the plant. Such measurements should be continuous and non-destructive to produce meaningful data associated with the time-space relationships for water and solute uptake by plant roots. Unfortunately previous methods for measuring soil water content and salinity continuously and in a non-destructive manner, although able to achieve this in bulk soil, have been unable to provide detailed measurements of water content or salinity with sufficient resolution to enable studies to be carried out in close proximity to the root surface. In the present work, a combination of Computer Assisted Tomography (CAT) and Sodium-Liquid Ion exchanger (Na^+ -LIX) microelectrode techniques has been used to examine, repetitively and in a non-destructive fashion, the dynamics of the simultaneous processes of water uptake and solute (NaCl) accumulation in proximity to lupin and radish roots.

METHODS

Application of CAT to gamma and X-ray attenuation measurements (Hainsworth and Aylmore, 1986, 1988) was used to determine the spatial distribution of soil water content and hence water uptake by individual root layers of eighteen day old plants subjected to two levels of transpirational demand (with and without a fan) and five Na^+ concentration levels (zero, 25, 50, 75, and 100 mol/m^3) at initial soil water contents of $0.3 \text{ cm}^3/\text{cm}^3$. These were monitored at three root depths of 3, 6 and 9 cm and at zero, 2, 4, 6 and 8 hour intervals from the commencement of transpiration. Na^+ -LIX microelectrodes were used, in situ, to determine Na^+ concentrations at the root surface with time of transpiration. For this purpose soil pots were specifically designed and constructed to allow accurate positioning of the microelectrode tips at the root surface (Hamza and Aylmore, 1990).

RESULTS AND DISCUSSION

Water Extraction Along The Root

The water extraction rates (Q) from individual layers increased with time of transpiration for both plants and for all layers, with the most rapid increase occurring during the first two hours of the transpiration followed by a more gradual increase in Q in an essentially linear fashion over the remaining 6 hours (eg. Figure 1 for top layer of lupins). The divergence of the graphs illustrates that the transpiration rate was progressively decreased with increasing solute concentration in the treatments and this decrease became relatively larger with time of transpiration.

The lupin and radish roots showed markedly different patterns of water extraction along their length. The almost equal diameters and consequently equal root surface areas for all lupin root layers resulted in an essentially uniform absorption along their length. In contrast, the tapering radish roots extracted generally about 50 and 70% more water

from their top layers as compared with the middle and bottom layers respectively. Figure 2 shows a comparison of the water drawdowns from the top, middle and bottom layers of radish single roots after 2 hours of low/high transpiration demand for the no-solute treatments. The main water drawdowns, where the roots extract most of the water, occurred within regions one to five mm from the root surface. However as the Na^+ concentration in the treatments increased from zero to 100 mol/m^3 , the differences in the water extraction rates between the top layers and middle and bottom layers, decreased by approximately 10%. The water content at any point in the drawdown area decreased as transpiration progressed but the distance to the outer boundary of the drawdowns varied little over the period of observation indicating that the roots took up more water from the region close to them rather than from the bulk soil.

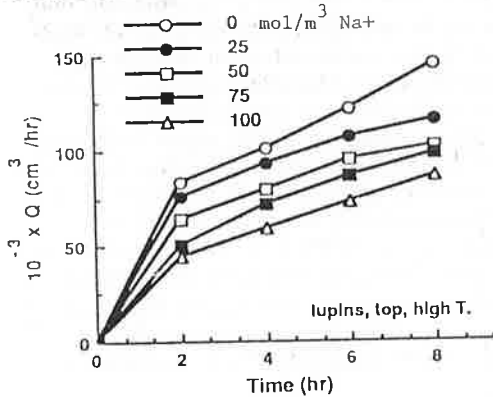


Fig. 1. Water extraction rate (Q) versus time for lupins.

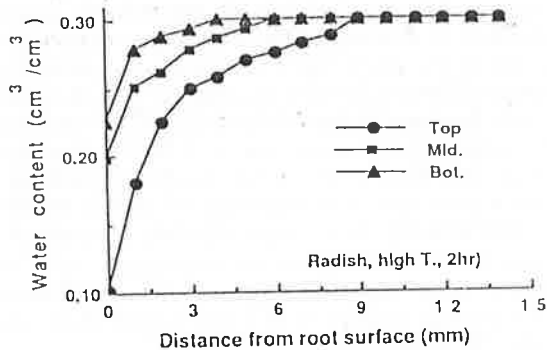


Fig. 2. Water drawdowns from top, middle and bottom layers of radish roots.

The essentially constant drawdown distances with time over the period of measurement conflict with Gardner's (1960) suggestion that the drawdown distance is a function of time. The latter may only be true for a short time and depend on the bulk soil water content. On the other hand the smaller drawdown distances which occurred under the low transpiration demand and also the smaller drawdown distances for the radishes in contrast to the lupins, are consistent with Gardner's suggestion that the drawdown distance is a function of soil water diffusivity. Since water diffusivity is a function of water content in the soil and hydraulic conductivity decreases by several orders of magnitude as the soil dries (Passioura, 1980), then in both cases more water is available in the soil leading to a higher soil diffusivity and thus to smaller drawdown distances. This indicates that the drawdown distance is controlled not only by soil water diffusivity but also by the water extraction rate (Hainsworth and Aylmore, 1986). For the radish plants both the degree of water drawdown and the drawdown distances, showed a noticeable decrease along the tapering radish root (Figure 2). The drawdown distances for the bottom layers were almost half those of the top layers. Since more water is available at the bottom layers the soil would have a higher water diffusivity leading to the observed shorter drawdown distances.

All layers of the roots for both plants showed similar patterns as far as the reduction in Q with increasing solute treatment is concerned. Despite substantial decreases in the leaf water potentials with increasing solute concentration (see Figure 5), the water extraction rates from the individual layers were reduced progressively as the Na^+ concentration in the treatments increased from zero to 100 mol/m^3 by values ranging from 9 to 48% respectively after 8 hours. As the total root-soil interface potential decreased the leaf water potentials for both plants decreased continuously with time of transpiration and decreased rapidly with increasing soil solute concentration. The more rapid accumulation of solute at the root surface at higher concentrations was evident from the greater decrease in leaf water potential with increase in soil solute concentration.

Solute Accumulation at the Root Surfaces

Figure 3 shows the effect of electrolyte concentration on the drawdowns for the top layers of the radish roots. The accumulation of Na^+ at both the lupin and radish root surfaces increased gradually with time of transpiration in a near linear fashion (see Figure 4 for radish) and was only slightly higher under the higher transpiration demand. For both lupin and radish plants the concentrations of Na^+ increased slightly more rapidly with increasing Na^+ concentration in the treatments. At the end of the transpiration period (8 hours) the lupin roots had accumulated slightly more Na^+ at their surfaces than had the radishes. It is significant that these increases were not exponential as would be expected with non-absorption by the roots (Passioura, 1980) and this is presumably due to back diffusion from the epidermis or hypodermis to the bulk soil, at the relatively high water contents and potentials used (Munns and Passioura, 1984). The minimum matric water potential at the root surface reached after 8 hours was -140 kPa.

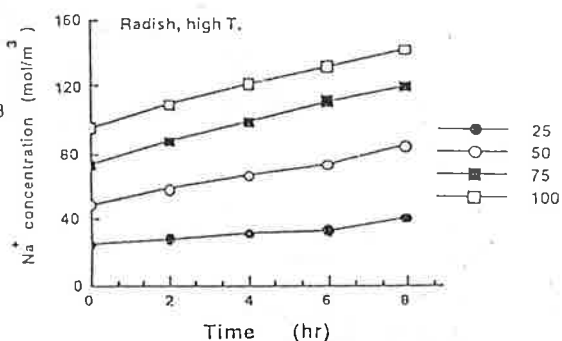
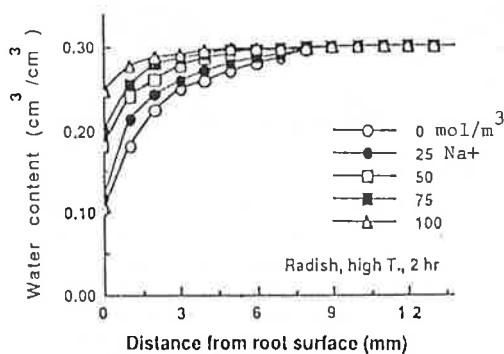


Fig. 3. Drawdowns near top layers of radish single roots at different Na^+ concs.

Fig. 4. Na^+ conc. at radish root surfaces versus time for different treatments.

The leaf water potentials, Ψ_l , and the total water potentials at the root surfaces, Ψ_t , decreased with increasing time of transpiration and the relationships between Ψ_l and the osmotic potential at the root surface, $\Psi\pi$, were essentially linear (Figure 5) indicating that the decrease in the total water potential at the root surface is transmitted across the root to the leaves. Furthermore the relationships between Ψ_l and Q were linear for both plants and under both transpirational demands indicating a constant plant resistance. Radish leaf water potential values were higher than those for the lupins under the low transpiration demand (including the values at zero time of transpiration) but they were, in general, lower under the the high transpiration demand except for that at zero time of transpiration. Furthermore Figure 5 shows that at any given transpirational interval the

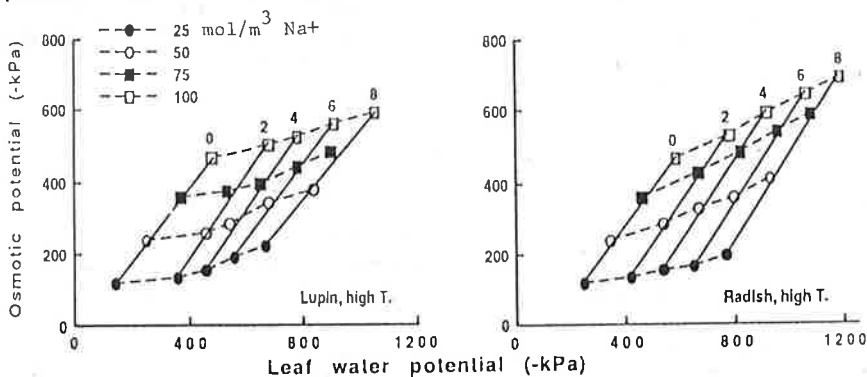


Fig. 5. Osmotic potential at root surface versus leaf water potential.

relationship between Ψ_l and Ψ_π at the root surface was essentially linear with the decrease in Ψ_l approximately matching that corresponding to the decrease associated with increasing solute concentration in the irrigation solutions. The main decrease in Ψ_l with time is undoubtedly associated with the plant requirement to increase the water flux.

The osmotic potentials at the root surface, Ψ_π , were greater than the matric potentials at the root surface, Ψ_m , for both plants and for both transpiration demands by 3.5 to 10 times (Figure 6). Assuming both potentials are additive then it is clear that Ψ_π had a greater influence than Ψ_m on transpiration.

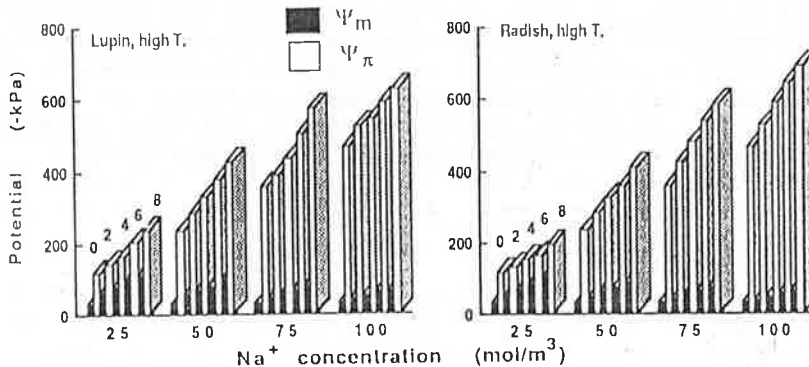


Fig. 6. Relative magnitudes of osmotic and matric potentials at root surfaces.

A linear relationships between the transpiration rate, Q , and the difference in hydrostatic pressure between the root surface and the leaves, ΔP , was observed for both the lupins and the radishes subjected to both transpiration demands (Figure 7). ΔP was calculated as the difference between Ψ_m at the root surface and the water potential at the leaves, Ψ_l , for the transpiring plants. Strictly speaking ΔP calculated in this fashion includes changes in the osmotic component of the leaf cell walls. However other considerations demonstrated that this component is essentially constant (Munns and Passioura, 1984). Also the relationships between Q and the total water potential difference between the root surface and the leaves, $\Delta\Psi$ were in general linear. Contrary to the theoretical predictions of Dalton et al. (1975) and Fiscus (1975), that interaction occurs between the flows of solute and water producing non-linearities between water uptake and driving force, the linear relation observed here between the driving force and Q imply that both plant roots acted as near-perfect osmometers.

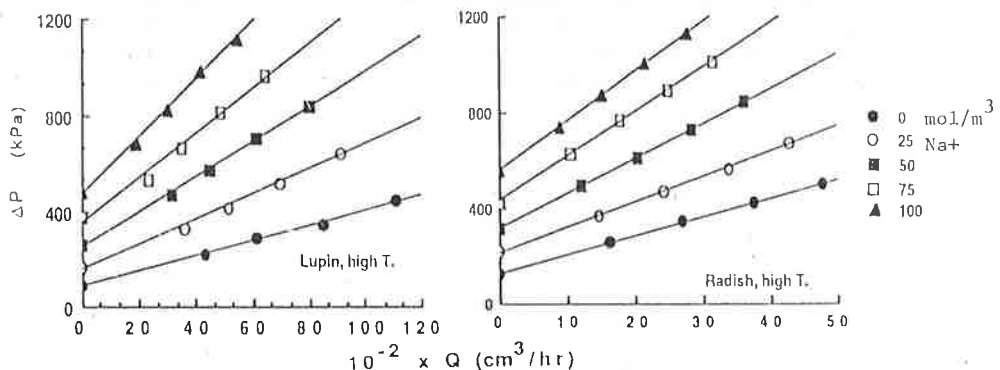


Fig. 7. Hydrostatic pressure differences between root surfaces and leaves, versus transpiration rate.

The numerical values of ΔP were invariably much greater than the numerical values of the osmotic potential at the root surface which implies that the restriction on the flow of water imposed by the osmotic pressure at the root surface is far exceeded by the hydrostatic pressure difference between the root surface and the leaves. The continuous

increase in Q with the time of transpiration is likely to be due to such high ΔP values as well as to the ready supply of water at the high initial water content in the soil.

For both plants $\Delta\Psi$ increased with increasing transpiration rate for all lupin and radish treatments and for both transpiration demands. However this increase was higher under the high transpiration demand. Water potential gradients between the root surface and the leaves were invariably observed at zero time of transpiration and these gradients ranged from 10 to 87 kPa for lupins and from 83 to 127 kPa for radishes depending on the soil solute concentration. ΔP_o values for the no flow condition undoubtedly reflect the potential gradient involved in plant growth. As the salt concentration in the treatments increases and osmotic potential at the root surface decreases, the ΔP_o necessary to maintain growth in the plant system increases accordingly. The values of ΔP_o derived from the leaf water potential and CAT matric potential at the root surface for the no flow situation (zero time of transpiration) agreed fairly closely with the values of the osmotic potential obtained by the Na^+ -LIX microelectrode for the lupin plants but they were higher by 80-100 kPa for the radish plants. The fact that both lupin and radish plants behaved as near-perfect osmometers is indicated by the very close values between the increase in ΔP_o with the associated decrease in $\Psi\pi$ with increasing solute concentration in the treatments.

Plant resistances increased with increasing solute concentration in the treatments (Table 1). Hounsfield units (H) (Hounsfield, 1972), which usually increase with increasing density of the media, increased from the stele toward the root surface suggesting higher radial relative to axial resistances. Radish plant resistances were invariably higher than those for the lupin plants by about 1.5 to 2.5 times presumably due to the smaller root surface area in contact with the soil water as compared with lupin plants. Also, since the radish root diameter is much smaller than that of lupin root, the axial resistance in the radish root could be expected to be higher. Lupin plant resistances, R_p , were 3 to 15 times higher than the corresponding soil resistances, R_s (46 to 151 kPa hr cm^{-3}), and radish plant resistances 4 to 12 times higher than R_s (51 to 210 kPa hr cm^{-3}). These values emphasise the importance of the plant resistance over that of soil at high soil water potentials. The soil resistance increased with time of transpiration because the soil around the root became drier while the plant resistance was essentially constant with time of transpiration. Consequently the differences between the plant and soil resistances decreased with time of transpiration.

TABLE 1. Plant hydraulic resistance (kPa hr cm^{-3}) for the lupin and radish plants obtained from the slopes of $\Delta\Psi(Q)$ curves.

Treatments Na+mol/m ³	Low Transpiration		High Transpiration	
	lupin	radish	lupin	radish
0	471	728	323	785
25	562	808	386	884
50	682	958	488	992
75	769	1048	578	1110
100	1105	1206	882	1235

CONCLUSIONS

The present studies carried out at relatively high initial water contents (i.e. high soil water potential) have demonstrated clearly the interrelations between the important parameters within the soil-plant system. However major questions remain to be answered as to how the relations between parameters measured here such as leaf water potential and plant and soil resistances, change as the soil water diffusivity becomes a more

limiting factor in the transpiration process. In drier conditions back diffusion would be reduced and the effect of solute accumulation at the root surface would be enhanced. More information is also needed on the role which water potential gradient along the roots plays in the redistribution of water and solutes and how this changes with overall soil water potential. A particularly interesting and important extension of the present studies would be the use of the microelectrode techniques developed here to study simultaneous (and preferably in conjunction with the CAT technique) the ionic concentrations both within the root xylem and outside the root and the changes which occur as the soil solution concentration increases.

The development of these innovative experimental techniques using computer assisted tomography and ion specific microelectrodes, provides a major advance for soil-plant-water studies and undoubtedly has the potential to elucidate the major controversies surrounding the physics of water and solute uptake by plants.

REFERENCES

- Dalton, F.N., Raats, P.A.C. and Gardner, W.R. Simultaneous uptake of water and solute by plant roots. *Agron. J.* 67: 334-339; 1975.
- Fiscus, E.L. The interaction between osmotic and pressure-induced water flow in plant roots. *Plant Physiol.* 55: 917-922; 1975.
- Gardner, W.R. Dynamic aspects of water availability to plants. *Soil Science* 89: 63-73; 1960.
- Hainsworth, J.M. and Aylmore, L.A.G. Water extraction by single plant roots. *Soil Sci. Soc. Amer. J.* 50: 841-848; 1986.
- Hainsworth, J.M. and Aylmore, L.A.G. Application of computer assisted tomography to gamma attenuation measurement of soil water content. *Aust. J. Soil Res.* 26: 105-110; 1988.
- Hainsworth, J.M. and Aylmore, L.A.G. Non-uniform water extraction by a single plant root. *Plant and Soil* 113: 121-124; 1989.
- Hamza M. and Aylmore, L.A.G. The use of liquid ion exchanger microelectrodes to study soil solute concentrations in proximity to plant roots. *Soil Sci. Soc. Amer.* (in press); 1990.
- Hillel, D., Van Beck, C.G.E.M. and Talpaz, H. A microscopic-scale model of soil water uptake and salt movement to plant roots. *Soil Science*, 120: 385-399; 1975.
- Hounsfield, G.N. A method of and apparatus for examination of a body by radiation such as X- or gamma radiation. *Brit. pat. No.1283915*; 1972.
- Munns, R. and Passioura, J.B. Hydraulic resistance of plants III. Effect of NaCl in barley and lupins. *Aust. J. Plant Physiol.* 11: 351-359; 1984.
- Passioura, J.B. The transport of water from soil to shoot in wheat seedlings. *J. Exp. Botany* 31: 333-345; 1980.

SUMMARY

A combination of computer assisted tomography (CAT) and sodium liquid ion exchanger (Na^+ -LIX) microelectrode techniques has been used to examine, repetitively and in a non-destructive fashion, the dynamics of the simultaneous processes of water uptake and solute (NaCl) accumulation in proximity to lupin and radish roots. Water uptake along the roots was found to be a function of the diameter and hence the surface area per unit length of the roots. The accumulation of Na^+ at the roots increased in a near linear fashion rather than exponentially as would be expected with non-absorption by the roots and this is attributed to back diffusion at the relatively high water potentials applicable (>-140 kPa). The linear relationships between the driving forces and transpiration rate implies that both plant roots acted as near perfect osmometers. Plant resistances increased with increasing solute concentration and were an order of magnitude higher than soil resistances.

Adsorption-desorption behaviour of pesticides in soil and implications for groundwater pollution

Inter. Conf. Water 89, Bangkok, Thailand, EQM; (1989), 4-9.

Aylmore, L.A.G. , Singh, Rai and Gerritse, R.G.

L.A.G. Aylmore, Rai Singh and R.G. Gerritse*

Soil Science and Plant Nutrition, School of Agriculture,
The University of Western Australia, Nedlands, W.A. 6009

*CSIRO, Division of Water Resources, Wembley, W.A. 6014

Abstract

The adsorption-desorption behaviour and hence susceptibility to leaching to groundwater, of five commonly used pesticides in soils varying in texture from sand to clay have been examined. The influence of soil conditions such as pH, salinity, organic matter content and in particular the influence of methanol as an organic cosolvent are illustrated. Pesticides investigated were Paraquat, Diquat, Simazine, Linuron and Fenamiphos.

The extent and mechanism of retention of the pesticides in soil was directly related to their chemical nature (i.e. whether ionic or non-ionic, basic or acidic) and in general pesticide adsorption followed the order Paraquat > Diquat >>> Linuron > Fenamiphos > Simazine in all soils. The amounts adsorbed were more directly related to organic matter contents than clay contents in all cases except for Paraquat and Diquat where clay content was more important. The sorption of all pesticides from aqueous solution exhibited hysteresis, i.e. only partial reversibility of the adsorption reaction.

The adsorption of Simazine and to a lesser extent of Fenamiphos and Linuron, decreased with increase in pH while the adsorptions of Diquat and Paraquat were essentially unaffected by a change in pH. Increasing background salt concentration markedly decreased the adsorption of Diquat and Paraquat but only slightly altered the adsorption of the other pesticides. The adsorption of all pesticides was markedly affected by the presence of methanol, decreasing exponentially with increasing methanol content in solution. Furthermore, with increasing methanol concentrations in the soil solution, a decrease in hysteresis occurred.

Decreasing adsorption as a result of increasing pH, increasing salt concentration or increased release of adsorbed pesticides in the presence of an organic cosolvent, would significantly enhance their mobility. Application of a mathematical screening model to this data illustrates the considerable potential of these pesticides for groundwater pollution in a sandy soil.

KEY WORDS: Pesticides; Adsorption-Desorption; Groundwater Pollution; Organic Cosolvent; Pesticide Mobility; Diquat; Fenamiphos; Linuron; Simazine; Paraquat.

Address for Correspondence:
Soil Science and Plant Nutrition,
The University of Western Australia,
Nedlands, Western Australia, 6009.
Phone No. (61) (9) 380 2484

Introduction

Herbicide and pesticide usage is increasing rapidly throughout the world and there is increasing concern at the extent to which these chemicals may contaminate surface and groundwaters and ultimately water for human consumption. The mobility of these materials through the soil profile is markedly dependent on the extent to which they interact with soil components. In addition to the physico-chemical properties of the soil components, adsorption-desorption behaviour can be greatly influenced by a number of other factors including soil pH, competitive adsorption of other species, ionic concentration etc. In particular, recent concern has centered on the effects on the behaviour of organic compounds in soils of the presence of organic cosolvents. This concern arises from the possibility of organic cosolvents occurring in conjunction with pesticides and other organic compounds in soil solutions at waste disposal sites, at land treatment sites for concentrated wastes and in cases of accidental spills.

In this paper the sorption and desorption behaviour of a number of commonly used pesticides representing different chemical classes, in soils differing in their physical and chemical properties have been examined and in particular the influence of methanol as an organic cosolvent.

Materials and Methods

Soils and Pesticides

Four Western Australian soils which differ appreciably in their physico-chemical properties were used in this study. These were Bassendean sand (1.2% organic matter and clay, pH 5.0); Gascoyne sandy loam (1.7% organic matter, 15.3% clay and pH 6.9); Cobiac loamy sand (0.6% organic matter, 13.7% clay and pH 5.1) and Wellesley clay (4.6% organic matter, 64% clay and pH 5.9). The pH was measured keeping the soil to solution ratio at 1:5 in 0.005 M CaCl₂. The characteristics of Bassendean sand, Gascoyne sandy loam and Wellesley clay have been described by McArthur and Bettenay (1960) and Bettenay *et al.* (1971). The characteristics of the Cobiac sandy loam which has a high sesquioxide content have been described by Churchward and Batini (1975).

Five pesticides, including the herbicides Diquat, Linuron, Paraquat and Simazine and a nematicide,

Fenamiphos, were used. Diquat and Paraquat are knockdown herbicides and are undoubtedly amongst the most commonly used pesticides. Linuron, Fenamiphos and Simazine pesticides were applied directly to the soil. Detailed properties of these pesticides have been given by Hartley and Kidd (1987).

Adsorption Studies

Batch distribution isotherms for the pesticides in soils were determined at $25 \pm 2^\circ\text{C}$. Five grams of air-dried soils were equilibrated in polypropylene centrifuge tubes with 10 ml of pesticide solution in 0.01 N CaCl_2 . Pesticide concentrations for different pesticides before equilibration ranged from 4 to 40 $\mu\text{mol/l}$ (Linuron); 2 to 25 $\mu\text{mol/l}$ (Fenamiphos); 20 to 100 $\mu\text{mol/l}$ (Simazine) and to 3000 $\mu\text{mol/l}$ (Diquat). The tubes were shaken (end over end) 24 h. Generally some 95% of the adsorption was found to occur in the first three to four hours.

After equilibration the suspension was centrifuged at 12000 rpm for 15 minutes. The supernatant was pipetted off and analysed immediately or stored at 4°C in a refrigerator for later analysis. The amount adsorbed by a soil was calculated from the difference between the initial and final concentrations of pesticide in solution. Pesticide adsorption on to the walls of the centrifuge tubes was checked by taking blanks and was found to be negligible.

Desorption Studies

Desorption of the pesticides was studied using the traditional consecutive desorption method involving a number of steps of shaking, centrifugation and resuspension. On completion of the initial adsorption the suspension was centrifuged and the soil solution carefully removed. The solution still remaining in the soil was noted. A known amount of pesticide free solution in 0.005M CaCl_2 was then added to the soil and

the contents were again shaken for 24 hours. After centrifugation, the soil solution was removed for analysis and the soil was resuspended in herbicide free solution. This procedure was repeated to generate a desorption isotherm.

To study the effect of pH on sorption, the pH of the soil solution was pre-adjusted with HCl or NaOH and equilibrated overnight before use in the sorption study. The effect of solution salt concentration on sorption was studied by providing different concentrations of CaCl_2 in background solutions. The influence of methanol as a cosolvent on sorption and desorption was examined by including various proportions of methanol in the equilibrating solution.

Results and Discussion

Effect of Nature of Pesticides

Adsorption isotherms for five pesticides in Bassendean sand are compared in Figure 1. The sorption data for Simazine, Fenamiphos and Linuron were fitted to a Freundlich equation, $S = KC^n$, where S is the adsorbed concentration ($\mu\text{g/g}$), C is the solution concentration ($\mu\text{g/ml}$) and K and n are coefficients. Diquat and Paraquat more closely followed a Langmuir equation. The adsorption of the pesticides followed the order: Paraquat > Diquat >>> Linuron > Fenamiphos > Simazine. Paraquat and Diquat being divalent cations, are readily adsorbed by negatively charged clay and organic matter particles and hence are the most strongly adsorbed. In contrast, Linuron and Fenamiphos are non-ionic in nature. Although Simazine is ionizable to a cation to an extent dependent on the pH of soil, it is the least strongly adsorbed under the present conditions.

Effect of Soil Type

Freundlich plots of adsorption isotherms for Linuron in the four soils are shown in Figure 2. With

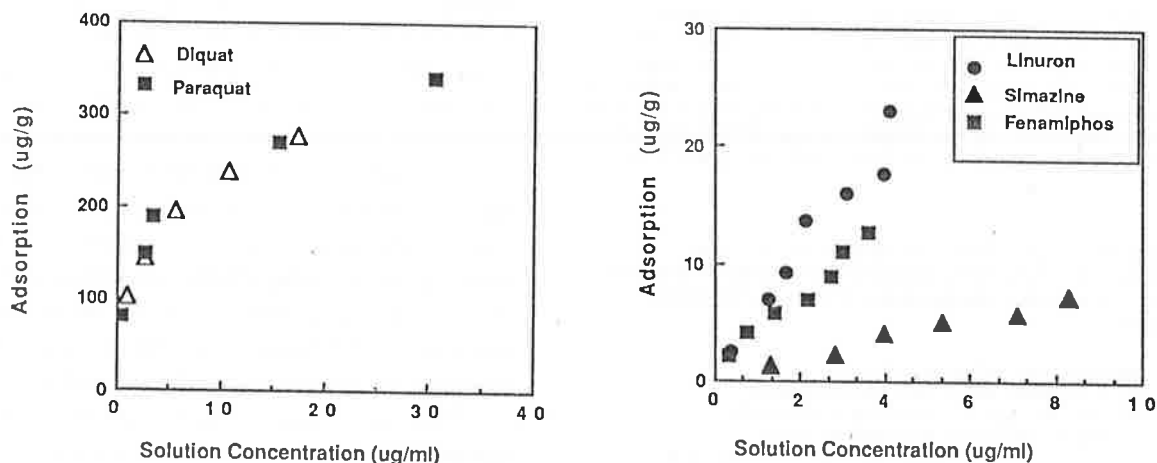


Fig. 1. Adsorption isotherms of five pesticides in Bassendean sand.

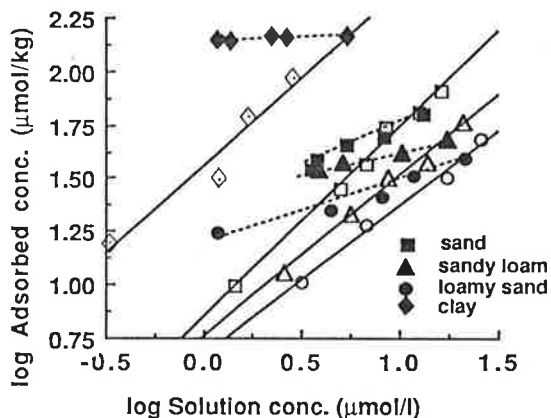


Fig. 2. Freundlich isotherms for Linuron in four soils.

the exception of the Gascoyne sandy loam the values of the Freundlich adsorption coefficients (K) followed the organic matter contents of the soils rather than clay contents. Gascoyne soil, despite its higher organic matter content, showed less adsorption than Bassendean sand and this difference can be largely attributed to the differences in the pH of the soils as illustrated later. Simple linear regression of K with various soil properties indicated that adsorption is strongly correlated with organic matter ($R^2 = 0.94-0.99$). Soil organic matter has similarly been found to correlate well with adsorption of non-ionic pesticides in other soils of the world (Hamaker and Thompson, 1972).

Effect of pH

Adsorption of Simazine, Linuron and Fenamiphos pesticides decreased with increasing pH of the soil solution as illustrated for Bassendean sand in Figure 3(a). This effect was more pronounced in the case of Simazine than for Linuron and Fenamiphos.

The effect of pH on Simazine adsorption in three different soils is shown in Figure 3(b). A marked

decrease in Simazine adsorption with increasing soil pH was apparent in all three soils. At pH < 4.0, Wellesley clay soil could adsorb almost all of the added Simazine (97 - 99%) compared to 62% at pH 8.8. In Bassendean sand an increase in pH from 3.5 to 6.5 decreased the adsorption of added Simazine from 42% to 23%. In Gascoyne sandy loam soil the adsorption at pH 4.9 and 7.3 was found to be 46% and 13% respectively. This shows that the adsorption of Simazine in an alkaline soil can be significantly less than that in a soil with pH in the acid range.

Simazine is a weakly basic herbicide which at lower pH can become a cation by accepting a proton. Simazine has a dissociation constant (pKa) of 1.65 (Weber, 1972). As the pH approaches the pKa value the proportion of Simazine cations in solution increases and hence the adsorption increases with decreasing pH.

The pH dependent negative charge on soil surfaces decreases with a decrease in pH and hence should be unfavourable towards Simazine adsorption. Nevertheless, the magnitude of negative charges at a given pH would still be much higher than required to adsorb small amounts of Simazine. In acid soils management practices such as liming, fertilization and gypsum application can bring about changes in pH such that it can alter the behaviour of pesticides such as Simazine. Although Fenamiphos and Linuron are non-ionic, the slight decrease in adsorption with increasing pH may be due to its influence on other mechanisms of adsorption such as hydrogen bonding. The adsorption of Diquat and Paraquat was unaffected by a change in pH (Figure 3(a)).

Effect of Salt Concentration

Adsorption

Adsorption of the cationic Diquat and Paraquat on Bassendean sand decreased markedly with increase in salt concentration in soil solution (e.g. Figure 4 for Diquat). However, the adsorption of other pesticides

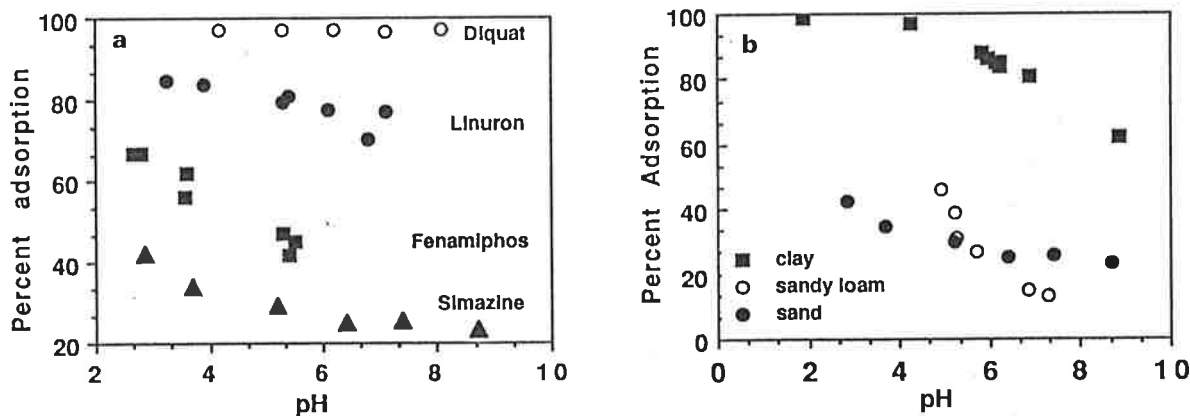


Fig. 3. Effect of pH (a) on pesticide sorption in sand, and (b) on Simazine adsorption in three soils.

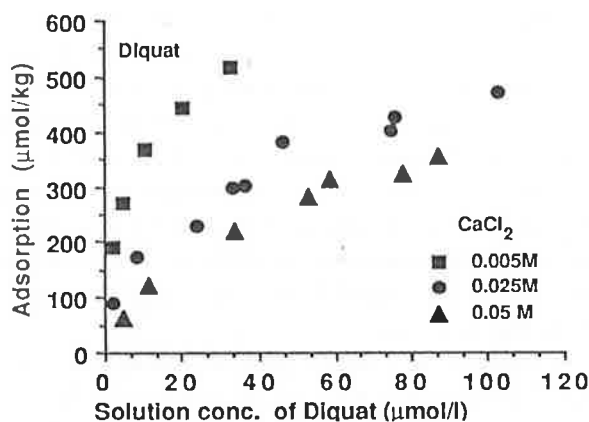


Fig. 4. Effect of salt concentration on Diquat sorption was only slightly affected. Diquat adsorption capacities (calculated from the Langmuir isotherms) were reduced by some 20% to 30% in different soils with an increase in CaCl_2 concentration from 0.005 M to 0.05 M. This is because of competition between inorganic and organic cations for exchange sites (Best *et al.*, 1972; Burns *et al.*, 1973).

Adsorption of Simazine and Linuron increased slightly, while the adsorption of Fenamiphos was found to decrease slightly with the increase in CaCl_2 concentration in the soil solution. An increase in solution salt concentration has been reported to increase the adsorption of triazines (Hurle and Freed, 1972); Picloram (Farmer and Aochi, 1974) and Prometryne (Abernathy and Davidson, 1971). Fusi and Corsi (1968) reported that Atriazine adsorption is slightly affected by increasing the salt concentration. In contrast, Nearpass (1969) noted a marked decrease in the adsorption of Amitrole (a cationizable herbicide), with an increase in NaCl concentration in soil solution. Thus, the presence of inorganic salts only significantly affects the adsorption of cationic pesticides.

Desorption

Desorption was also affected by changes in salt concentration. Figure 5 shows increasing Diquat desorption with increasing salt concentration of the extracting solution. Diquat desorption increased from 13% to 45% in Bassendean soil as the CaCl_2 concentration increased from 0.005 to 0.5 M. Total Diquat desorbed after five successive extractions with 0.05M CaCl_2 was 62, 18 and 7% in Cobiac loamy sand, Gascoyne sandy loam and Wellesley clay soils, respectively. The extraction of Diquat (and similarly Paraquat) at all CaCl_2 levels, was greater in the sandy than in the clay soil. The lower amounts of Diquat desorbed in the clay soil was because of the presence

of the smectite group of clay minerals. Weber and Weed (1968) reported that four successive equilibrations with 1M BaCl_2 could remove 80% of Diquat from kaolinite clay mineral but only 5% from montmorillonite.

Diquat and Paraquat have generally been considered to be essentially irreversibly adsorbed and for their extraction harsh treatment such as boiling with 18N sulfuric acid is usually required. However, it is significant that in the present study, up to 62% of Diquat could be extracted with 0.05 M CaCl_2 from a loamy sand soil. It is shown in Figure 5 that a sudden increase in salt concentration, for example due to irrigation with salty water, can result in a marked increase in Diquat concentration in solution.

Paraquat and Diquat are very persistent in soils. Fryer *et al.* (1975) concluded that Paraquat may not breakdown at all in soil and if the microbial breakdown occurs then it is at an extremely slow rate. An eleven year study showed only a 10% loss per year of Paraquat (Hance *et al.*, 1980). After seven years of repeated applications in red earth soil in N.S.W., Australia, from 50 to 78% of applied Paraquat could be recovered (Osborne and Donohoe, 1977). Since a buildup of these pesticides in soil is possible following repeated applications, a change in landuse or management practices on a soil with a history of usage of the pesticides could induce their release from the adsorption complex and result in harmful effects.

Effects of Methanol as Organic Cosolvent Adsorption

Adsorption isotherms of Simazine and Linuron for the clay soil from various mixtures of methanol and water, are given in Figure 6. Adsorption for both herbicides followed a Freundlich adsorption isotherm. The Freundlich parameters, given in Table 1, show a decreasing adsorption of Simazine and Linuron with increasing concentrations of methanol in the soil

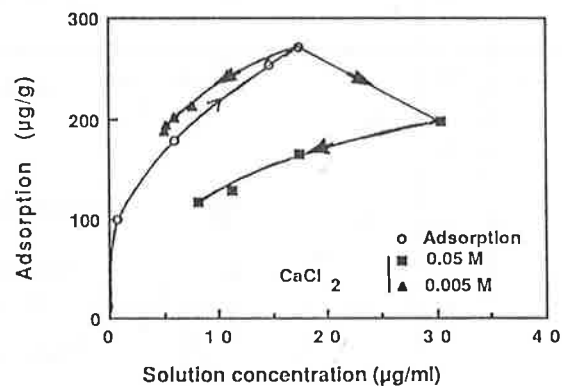


Fig. 5. Diquat desorption at two salt levels.

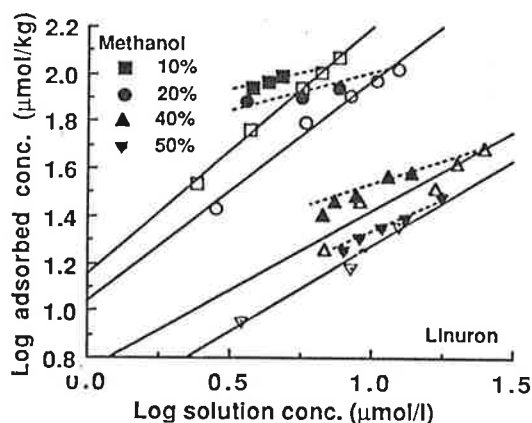
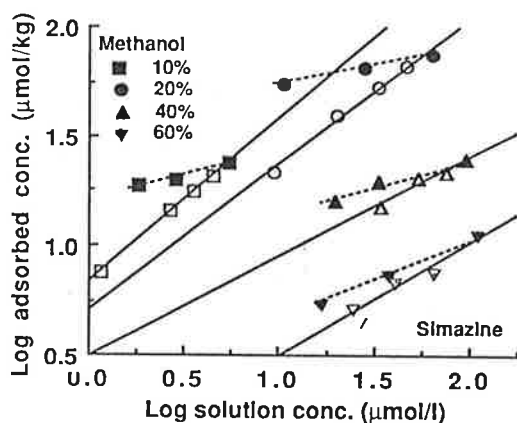


Fig. 6. Effect of methanol on adsorption-desorption of pesticides in clay soil.

solution. The Freundlich exponent (n) generally decreased with an increase in the proportion of methanol in solution, in contrast to the report by Zachara *et al.* (1988).

Adsorption of both herbicides, decreased in a log linear fashion with increasing methanol concentration in solution. This is consistent with the solvophobic theory (Rao *et al.*, 1985). Similar effects of organic solvents on adsorption of hydrophobic organic compounds, (Rao *et al.*, 1985) and ionizable organic compounds (Fu and Luthey, 1986b; Miller *et al.*, 1988; Zachara *et al.*, 1988) including pesticides, have been reported. The decrease in adsorption in the presence of methanol has been ascribed in the main part to the increased solubility in mixed solvent systems (Rao *et al.*, 1985; Fu and Luthey, 1986a,b). Competitive adsorption of methanol may also contribute to the decrease but it has been suggested (Mingelgrin and Gerstl, 1983) that at low concentrations, no competition for adsorption sites occurs because of the presence of adequate soil adsorption sites to adsorb both solutes.

Table 1. Adsorption parameters in presence of different concentrations of methanol in soil solution.

Methanol fraction	K ($\mu\text{mol}^{1-n} \text{kg}^{-1}$)	n ($1/\mu\text{mol}^{-1}$)	Retardation factor (Eq. 1)
Simazine			
0.00	9.50	0.96	20.90
0.10	6.82	0.74	12.07
0.20	5.08	0.66	8.34
0.40	3.08	0.46	4.09
0.60	0.97	0.51	2.08
Linuron			
0.00	38.17	0.81	68.46
0.10	16.25	0.97	33.43
0.20	10.84	0.93	23.00
0.40	05.49	0.67	09.09
0.50	02.97	0.73	05.73

Calculations based on the solvophobic theory indicate that in the present study, most of the decrease in adsorption can be accounted for by the solubility effect of methanol.

The effect of organic cosolvents on adsorption is a complex process, which may involve various other factors including their effects on electrical double layer, solvation of organic molecules and reduction in activity of water of hydration of soil particles (Zachara *et al.*, 1988) depending on circumstances.

Desorption

Figure 6 shows that adsorption-desorption isotherms for both Simazine and Linuron from various methanol/water mixtures exhibit varying degrees of hysteresis. The magnitude of the hysteresis decreased as the fraction of methanol in the desorption solution increased. One simple reason for this could be that the absolute amount of adsorption is reduced in the presence of the organic cosolvent and hence the hysteresis observed will also be reduced. However, other factors could contribute to a more reversible adsorption-desorption mechanism in the presence of an organic cosolvent. Freeman and Cheung (1981) have, for example, discussed the swelling effect of organic solvents on soil organic matter, consisting of highly branched polymer chains forming a three dimensional network. The absorption of liquid can cause the network to swell and form a gel to a degree depending upon the 'network compatibility' with the liquid. The increasing concentration of methanol in the solvent mixture presumably results in increasing swelling of soil organic matter and hence greater accessibility for a solute to get into and out of the organic polymers. In the present study, the decreasing hysteresis with increasing methanol concentration is consistent with these observations as this presumably coincides with increasing swelling of the organic matter.

In addition to its direct effect on adsorption, increased reversibility of the adsorption process (i.e. less hysteresis) in the presence of organic solvents will increase the mobility of a pesticide in the soil profile. The kinetics of the adsorption-desorption process is also likely to be influenced by the presence of organic cosolvents. Any effects of organic solvents on the soil solution transmission properties of the porous media (Brown and Anderson, 1983) may further influence the mobility of pesticides in solution.

The mobility of Simazine and Linuron can be estimated in terms of the retardation factor (R) calculated according to the relation (Rao and Jessup, 1983)

$$R = (1 + (Bd/\theta)n K C^{n-1}) \dots (1)$$

where Bd is bulk density of soil (g/cm^3), θ is water filled porosity (cm^3/cm^3), K is the Freundlich adsorption coefficient, n is the Freundlich exponent and C is solution concentration. Since the adsorption isotherm is non-linear, the retardation factor will also be a function of solution concentration of the herbicides.

The values of R for Simazine and Linuron (calculated at herbicide concentrations of $1 \mu g/ml$) corresponding to various concentrations of methanol are given in Table 1. There is a marked decrease in R values with increasing fraction of organic cosolvent. At 10% methanol content the R values for both the herbicides decreased to almost half the value in aqueous solution. The presence of methanol at a level of 50% and 60% of solvent mixture, decreased the retardation factor of Simazine and Linuron by a factor of 10 and 12, respectively. These studies show that both the adsorption and the desorption behaviour of pesticides are significantly affected by the presence of organic solvents.

Using the previous adsorption data in a mathematical screening model available in the literature (Jury *et al.*, 1983), and assuming constant organic matter content with depth in the soil profile, it can be shown that at a recharge rate of 0.5 m/year, about 0.02% of applied Diquat and Simazine, and less than 2×10^{-12} % of applied Linuron and Fenamiphos, are likely to reach groundwater at 3 meters depth. However, where decreasing organic matter content with depth in the soil profile, as is most commonly observed, is incorporated in the model the calculations indicate that up to 4% of Diquat, 18% of Simazine and approximately 1% of both Fenamiphos and Linuron applied could potentially reach groundwater.

- Abernathy, J.R. and Davidson, J.M. (1971). *Weed Sci.* 19: 517-521.
- Best, J.A., Weber, J.B. and Weed, S.B. (1972). *Soil Sci.* 114: 444-450.
- Bettenay, E., Keay, J. and Churchward, H.M. (1971). *Soil and Land Use Series 51*: CSIRO, Aust.
- Brown, K.W. and Anderson, D.C. (1983). EPA-600/S2-83-016, NTIS, Springfield, VA.
- Burns, I.G., Hayes, M.H.B. and Stacey, M. (1973). *Pestic. Sci.* 4: 629-641.
- Churchward, H.M. and Batini, F.E. (1975). *Land Resources Management Series No. 1*, CSIRO.
- Farmer, W.J. and Aochi, Y. (1974). *Soil Sci. Soc. Am. Proc.* 38: 418-423.
- Freeman, D.H. and Cheung, L.S. (1981). *Science* 214: 790-792.
- Fryer, J.D., Hance, R.J. and Ludwig, J.W. (1975). *Weed Res.* 15: 189-194.
- Fu, J.K. and Luthey, R.G. (1986a). *J. Environ. Eng.* 112: 328-345.
- Fu, J.K. and Luthey, R.G. (1986b). *J. Environ. Eng.* 112: 346-366.
- Fusi, P. and Corsi, R. (1968). *Agrochimica* 12: 109-119.
- Hamaker, J.W. and Thompson, J.M. (1972). In: C.A.I. Goring and J.W. Hamaker (Eds.): *Organic chemicals in the soil environment*. Dekker, New York, pp. 49-144.
- Hance, R.J., Byast, T.H. and Smith, P.D. (1980). *Soil Biol. Biochem.* 12: 447-448.
- Hartley, D. and Kidd, H. (1987). (Eds.). *The Agrochemicals Handbook*. The Royal Soc. Chem. The University of Nottingham, England.
- Hurle, K. and Freed, V.H. (1972). *Weed Res.* 12: 1-10.
- Jury, W.A., Spencer, W.F. and Farmer, W.J. (1983). *J. Environ. Qual.* 12: 558-564.
- McArthur, W.M. and Bettenay, E. (1960). *Development and distribution of soils of the Swan Coastal Plain*, W.A. CSIRO Soil Publ. 16: Aust.
- Miller, N.A., Wolf, D.C. and Scott, H.D. (1988). *Water, Air Soil Pollution* 39: 101-112.
- Mingelgrin, U. and Gerstl, Z. (1983). *J. Environ. Qual.* 12: 1-11.
- Nearpass, D.C. (1969). *Soil Sci. Soc. Am. Proc.* 33: 524-528.
- Osborne, C.J. and Donohoe, T.M. (1977). *J. Aust. Inst. Ag. Sci.* 43: 169-170.
- Rao, P.S.C., Hornsby, A.G., Kilcrease, D.P. and Nkedi-Kizza, P. (1985). *J. Environ. Qual.* 14: 376-383.
- Rao, P.S.C., Jessup, R.E. (1983). In: D.W. Nelson, K.K. Tanji and D.E. Elrick (Eds.) *Chemical mobility and reactivity in soil systems*. Am. Soc. of Agron. and Soil Sci. Soc. Spec. Publ. No. 11, Am. Soc. of Agron., Madison, Wis. pp. 183-201.
- Weber, J.B. (1972). In: R.F. Gould (Ed.) *Fate of organic pesticides in aquatic environment*. *American Chemical Soc.* 111: 55-120.
- Weber, J.B. and Weed, S.B. (1968). *Soil Sci. Soc. Amer. Proc.* 32: 485-487.
- Zachara, J.M., Ainsworth, C.C., Schmidt, R.L. and Resch, C.T. (1988). *J. Contam. Hydrol.* 2: 343-364.

Acknowledgements

These studies are being supported by a grant from the Australian Water Research Advisory Council. Rai Singh is grateful to the Australian International Development Assistance Bureau for providing a Commonwealth Fellowship.

Effect of Organic Cosolvent on Adsorption and Desorption of Linuron and Simazine in Soil

Rai Singh Kookana,^A R. G. Gerritse^B and L. A. G. Aylmore^A

^A Soil Science and Plant Nutrition, School of Agriculture, The University of Western Australia, Nedlands, W. A. 6009.

^B Division of Water Resources, CSIRO, Private Bag, P.O. Wembley, W.A. 6014.

Abstract

The adsorption and desorption of two herbicides, Linuron and Simazine, on a clay soil have been studied in mixtures of methanol and water. Adsorption of the herbicides decreased with increasing methanol content of the solution. An inverse log-linear relationship between the Freundlich adsorption coefficients for the two herbicides and the concentration of methanol was found. Adsorption of the herbicides in the presence of methanol followed the solvophobic theory, which describes the adsorption of hydrophobic organic compounds in soils. Values of the Freundlich adsorption coefficient for aqueous solutions, of the two herbicides extrapolated from adsorption data for the methanol/water mixtures, showed close agreement with those obtained experimentally. Hence, adsorption in aqueous solutions for pesticides of low aqueous solubility can readily be predicted on this basis.

Hysteresis, observed after desorption in CaCl₂ solution, decreased with increasing methanol contents for both herbicides. The decrease in hysteresis was ascribed to the swelling of the organic matter and the accompanying increased accessibility to solutes. The study showed that the presence of an organic solvent significantly affected not only the adsorption but also the desorption of herbicides in soils.

Introduction

Recently, interest has been shown by various workers in the behaviour of organic compounds in soils in the presence of organic cosolvents (Woodburn *et al.* 1986; Miller *et al.* 1988; Zachara *et al.* 1988). This interest arises from the possibility of organic solvents occurring in soil solutions at waste disposal sites, at land treatment sites for concentrated wastes containing solvents and in cases of accidental spills. Most of these studies have dealt only with the adsorption aspects of the hydrophobic organic compounds in soil. Adsorption of herbicides in the presence of organic cosolvents has received some attention (e.g. Nkedi-Kizza *et al.* 1985), but the desorption behaviour of pesticides in the presence of organic cosolvents has apparently received little attention. In addition, it is a common practice among workers to use pesticide stock solutions prepared in organic solvents for adsorption studies (Calvet 1980), particularly for pesticides having low aqueous solubility (Dunigan and McIntosh 1971). The applicability of adsorption data obtained in this way to aqueous situations needs to be examined. An alternative to the use of organic solvents for such pesticides, however, can be the prediction of the adsorption for

aqueous solutions, from the adsorption data obtained with mixtures of water and organic solvent using the solvophobic theory (Rao *et al.* 1985).

This paper reports the effects of methanol at various concentrations on both the adsorption and desorption of Linuron and Simazine herbicides in a clay soil.

Materials and Methods

Soil and Pesticides

A Wellesley clay soil (organic matter, 4.6%; clay, 60%; pH, 5.6) of the Serpentine river association was used in the study. The soil contains some smectite minerals and showed considerable swelling on wetting. General soil characteristics have been given by McArthur and Bettenay (1960) and physico-chemical properties of the soil have been reported by Singh *et al.* (1990).

Simazine (2-chloro-4,6-bis(ethylamino)-1,3,5-triazine) and Linuron (3-(3,4-dichlorophenyl)-1-methoxy-1-methylurea) are soil-applied herbicides and are commonly used in Australia. Application rates for Simazine and Linuron range from 1–4 kg active ingredient per hectare per application with the number of applications ranging from 1–3 per year. The aqueous solubility of Simazine is 3.5 mg L⁻¹ and of Linuron, 81 mg L⁻¹ (Hartley and Kidd 1987). Analytical grade samples (99%+ purity) of Simazine and Linuron were supplied by Ciba-Geigy Australia Ltd. and Hoechst Australia Ltd., respectively.

Adsorption and Desorption

Batch distribution isotherms of the pesticides in soils were determined at 20±2°C. Air-dried soil (5 g) was equilibrated in polypropylene centrifuge tubes with 10 mL of pesticide solutions of various concentrations in solvent mixtures of 0.01 M CaCl₂ and various proportions of methanol. The tubes were shaken (end-over-end) for 24 h and the suspensions were then centrifuged at 12 000 r.p.m. for 15 min. The supernatant was pipetted off and analysed immediately or stored at 4°C. The amount adsorbed by the soil was calculated from the initial and final concentrations of pesticides in solution.

Desorption of the pesticides involved a number of steps of shaking, centrifugation and resuspension. After the adsorption was complete, the soil solution was carefully removed. A known amount of pesticide-free solution in 0.01 M CaCl₂ containing the relevant proportion of methanol was added to the soil, and the mixture was shaken for 24 h. After centrifugation, the soil solution was removed for analysis and the soil was resuspended in herbicide-free solution. This procedure was repeated to generate a desorption isotherm.

Both Simazine and Linuron were analysed by high performance liquid chromatography (HPLC). The herbicides were separated in a Spherisorb 10 µm ODS column [(30 cm×1.6 mm i.d. (Phase Separation Ltd Clywd, U.K.))] with a mobile phase of methanol and water (65:35 v/v). The herbicides were monitored with a variable wavelength u.v. detector (Vickery *et al.* 1980). Pesticide adsorption onto the walls of the centrifuge tubes was checked by taking blank readings and was found to be negligible.

Adsorption data were fitted to the Freundlich equation

$$S = KC^n, \quad (1)$$

where S is the adsorbed concentration (µmol kg⁻¹), C is the solution concentration (µmol L⁻¹), K is the adsorption coefficient (µmol¹⁻ⁿ Lⁿ kg⁻¹) and n is the exponent (L µmol⁻¹).

Because of its high aqueous solubility, Linuron presents no difficulty for accurate measurement of solution concentrations. Unlike many other pesticides (e.g. Trifluralin), the aqueous solubility of Simazine, although relatively small, is, because of the availability of sensitive analytical methods (Vickery *et al.* 1980), high enough for the adsorption to be studied directly from aqueous solutions. Thus, the adsorption of both the herbicides could be determined directly from water and also estimated indirectly by extrapolating the adsorption data obtained in the presence of methanol in solution to zero methanol content. For this, the solvophobic theory for the adsorption of some hydrophobic organic compounds

from binary solvent mixtures given by Rao *et al.* (1985) was used. The use of Simazine provides a reasonable test of the success of this procedure for herbicides of low aqueous solubilities.

The theory is based on the reciprocal relationship between mole-fraction solubility and the activity coefficient of the compound. This relation can be put in the form of the organic carbon (OC) normalized adsorption coefficient ($K_{OC} = K/\%OC$) as being proportional to the ratio of the compound's activity coefficient in the aqueous phase to that in the organic carbon phase (Karickhoff 1984). For mixed solvent systems, the following relation between the sorption coefficient and the fraction of the organic cosolvent is obtained (Rao *et al.* 1985):

$$\ln(K_m/K_w) = -\alpha\beta(f_c), \quad (2)$$

where K is the sorption coefficient, subscripts w and m denote water and mixed solvents respectively, f_c is the fraction of organic cosolvent, α is a constant and β is a parameter dependent only on adsorbate and solvent properties and not on adsorbent characteristics.

Adsorption for both herbicides was studied from mixtures of methanol/water and water alone. Adsorption in water was also measured indirectly by extrapolating the data obtained at different concentrations of methanol, to zero methanol content, as suggested by Nkedi-Kizza *et al.* (1985). Sorption data from each solvent mixture were fitted to the Freundlich equation (1). The sorption coefficient (K_m) was plotted against f_c and the value of K_w was estimated by extrapolating to $f_c = 0$ (equation 2). The results were compared with experimental data obtained from aqueous solution.

Results and Discussion

Adsorption in the Presence of Methanol

Adsorption isotherms of Simazine and Linuron for the clay soil in various mixtures of methanol and water are given in Fig. 1. Adsorption data for both herbicides followed a Freundlich adsorption isotherm and these parameters are given in Table 1. The adsorption coefficient (K) of Simazine and Linuron decreased with increasing concentrations of methanol in the soil solution. The exponent (n) also generally decreased with an increase in the proportion of methanol in solution. This contrasts with the increase in the exponential term with increasing fraction of organic cosolvent for Quinoline observed by Zachara *et al.* (1988).

Adsorption of both Simazine and Linuron decreased log-linearly with increasing methanol concentration in solution (Fig. 2). This relationship is to be expected according to the solvophobic theory (equation 2) given by Rao *et al.* (1985). Similar effects of organic solvents in decreasing the adsorption of hydrophobic organic compounds (Rao *et al.* 1985) and ionizable organic compounds (Fu and Luthey 1986*b*; Miller *et al.* 1988; Zachara *et al.* 1988) including some pesticides have been reported. The decrease in sorption in the presence of methanol has been ascribed, in the main part, to the increased solubility of these compounds in mixed solvent systems (Rao *et al.* 1985; Fu and Luthey 1986*a*, 1986*b*). Competitive adsorption of methanol may also contribute to the decrease in herbicide adsorption, but it has been suggested (Mingelgrin and Gerstl 1983) that at low concentrations no competition for adsorption sites occurs because of the presence of adequate soil adsorption sites to adsorb both solutes.

Fu and Luthey (1986*a*) have shown a general semilogarithmic increase in the solubility of aromatic compounds with increasing fraction of organic cosolvents and this was accompanied by a semilogarithmic decrease in their sorption

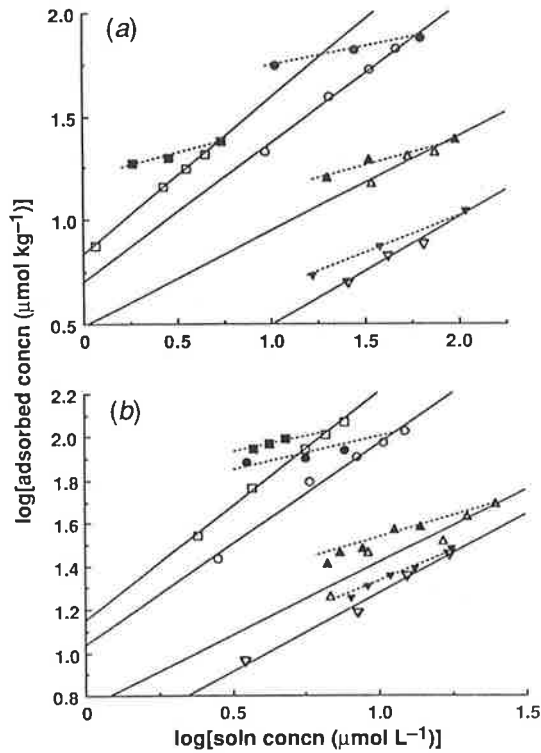


Fig. 1. Freundlich adsorption-desorption isotherms in various water/methanol mixtures for (a) Simazine (\square , \circ , \triangle , ∇ for 10, 20, 40 and 60% methanol respectively), and (b) Linuron (\square , \circ , \triangle , ∇ for 10, 20, 40 and 50% methanol respectively). Closed symbols represent desorption.

Table 1. Adsorption parameters in the presence of different concentrations of methanol in soil solution

Methanol fraction	K ($\mu\text{mol}^{1-n} \text{L}^n \text{kg}^{-1}$)	n ($\text{L} \mu\text{mol}^{-1}$)	Retardation factor ^A
<i>Simazine</i>			
0	9.50	0.96	20.90
0.10	6.82	0.74	12.07
0.20	5.08	0.66	8.34
0.40	3.08	0.46	4.09
0.60	0.97	0.51	2.08
<i>Linuron</i>			
0	38.17	0.81	68.46
0.10	16.25	0.97	33.43
0.20	10.84	0.93	23.00
0.40	5.49	0.67	9.09
0.50	2.97	0.73	5.73

^A Equation (3).

to soil (Fu and Luthey 1986b). However, the decrease in adsorption which they observed was not as significant as the increase in the solubility. The decrease in the sorption partition coefficient was about half of that expected from the increase in solubility. This was indicated by a value of 0.5 for the ratio of $\alpha\beta$ [slope in equation (2)] to the value of γ (a parameter obtained by regression of log mole fraction solubility to the fraction of methanol in solution). However, this ratio for Simazine in the present study was found to be 0.9, which is consistent with the value for the data of Rao *et al.* (1985) as calculated by Fu and Luthey (1986b). This suggests that, in the present study, most of the decrease in adsorption was accounted for by the solubility effect of methanol. However, the effect of organic cosolvents on sorption is undoubtedly a complex process which may involve various other factors including their effects on the electrical double layer, solvation of organic molecules and reduction in activity of water of hydration of the soil particles (Zachara *et al.* 1988) depending on circumstances.

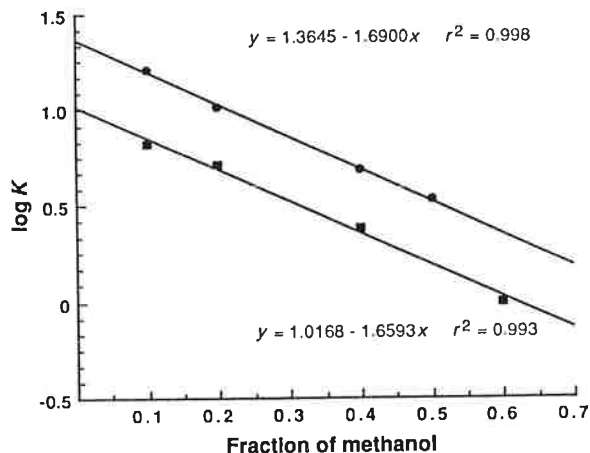


Fig. 2. Log-linear relations between the Freundlich adsorption coefficient (K) and fraction of methanol for Simazine (■) and Linuron (●).

Simazine is a weakly basic organic compound and is ionizable to a cation to a degree dependent on the pH of the system. The relationship observed in Fig. 2 indicates that the adsorption behaviour of Simazine from solvent mixtures is similar to that of non-ionizable hydrophobic organic compounds (HOC). The solvophobic theory considers that the mechanism of partitioning between water and the soil organic carbon phase is the dominant process for sorption of these compounds (Chiou *et al.* 1983). The present data and that reported by Zachara *et al.* (1988) suggest that, for ionizable compounds also, the effect of cosolvents on the adsorption is predominantly a consequence of their effect on the solubility of compounds, as is the case with HOC. The possible increase in surface acidity of the adsorbent due to the organic solvent (Zachara *et al.* 1988), thereby increasing protonation of the ionizable compound, should result in an increased adsorption of Simazine. However, any such effect is clearly outweighed by the solubility effect.

Prediction of Simazine Adsorption from Aqueous Solution using Organic Cosolvent Data

Nkedi-Kizza *et al.* (1985) suggested that, for hydrophobic organic solutes having low aqueous solubility, the adsorption coefficient can be estimated from sorption data determined from mixed solvent systems, provided that the data follow the solvophobic theory. In the present case, the adsorption of Simazine from aqueous solutions can be extrapolated by using the relationship given in Fig. 2. From the exponential relationship, the predicted K_w value for Simazine was found to be $10.4 \mu\text{mol kg}^{-1}$ as compared with the experimental value of $9.5 \mu\text{mol kg}^{-1}$, providing reasonable agreement between predicted and observed values. This suggests that, for pesticides of such low aqueous solubility that the study of adsorption from aqueous solutions is difficult, the adsorption can still be predicted reasonably accurately using the solvophobic theory. However, its applicability will of course depend upon factors such as the adsorption behaviour of the particular pesticides, their solubility in the organic cosolvent used, etc. Furthermore, for pesticides showing very low adsorption to soil, the prediction would be difficult as the adsorption could conceivably be further decreased in the presence of an organic solvent. In general, however, nonionic pesticides of low aqueous solubility show relatively higher adsorption as the two factors are inversely related (Leenheer and Ahlrichs 1971). It must be noted that only the Freundlich adsorption coefficient (K), and not the exponent (n), can be predicted.

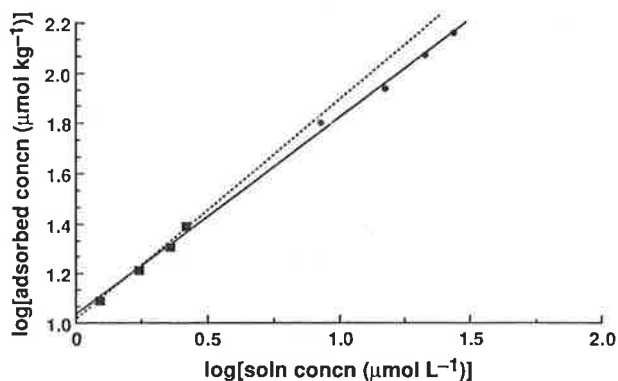


Fig. 3. Freundlich adsorption isotherms for Simazine obtained from pure aqueous solution (■) and from stock solutions in methanol (●). The solid line is fitted to all data. The dashed line is fitted to data from aqueous solution.

A comparison between the adsorption data obtained for Simazine by using pure aqueous solutions and those obtained by using aqueous dilutions of stock solutions prepared in pure methanol to provide methanol concentrations ranging from 1% to 5% is shown in Fig. 3. Data points from both methods can be fitted to the same Freundlich isotherm within an r^2 value of 0.99. This indicates that the use of an organic cosolvent at low concentrations to facilitate adsorption studies of sparingly soluble pesticides can be acceptable. However, even at these low concentrations, there is an indication that the presence of the methanol is producing a slight but progressive decrease in Simazine adsorption with increasing concentration of methanol above about 2%.

Organic solvents are commonly used for adsorption studies (Dunigan and McIntosh 1971) because they allow higher solution concentrations to be used and hence more accurate measurement. For instance, a review of some adsorption studies on Simazine by Hamaker and Thompson (1972) reported the use of a range of solution concentrations of Simazine from 0.1 to 3.9 ppm with corresponding adsorbed concentrations varying from 0.2 to 19 ppm. Such high soil concentrations cannot be achieved by the use of aqueous solutions of Simazine. The results presented in this paper indicate that published adsorption data obtained using organic cosolvents may not accurately reflect those which would occur from aqueous situations, to an extent depending on the concentrations of organic solvents in solution.

Desorption in the Presence of Methanol

Fig. 1 shows that adsorption-desorption isotherms for both Simazine and Linuron from various methanol/water mixtures exhibit varying degrees of hysteresis. The magnitude of the hysteresis decreased as the fraction of methanol in the desorption solution increased.

The absolute amount of adsorption which occurs is reduced in the presence of the organic cosolvent and hence the hysteresis observed will also be reduced. However, other factors may contribute to a more reversible adsorption-desorption mechanism in the presence of an organic cosolvent. Freeman and Cheung (1981) have, for example, discussed the swelling effects of organic solvents on soil organic matter. Organic matter frequently consists of highly branched polymer chains forming a three-dimensional network, which allows the internal absorption of liquids. The absorption of liquid can cause the network to swell and form a gel to a degree depending upon the 'network compatibility' with the liquid. Increased swelling of organic matter in the presence of organic cosolvents would thus result in greater accessibility for the solute to get into and out of the humin-kerogen polymer network. Maximum swelling would be expected to occur when the solubility parameter d (Hildebrand and Scott 1950) of the liquid approaches that for the organic matter gel, i.e. $d = 10.3$ (if the organic matter in soil behaves similarly to *n*-octanol) (Briggs 1981). The value of d for methanol is approximately 14.5 as compared with 23.5 for water (Freeman and Cheung 1981) and, hence, the increasing concentration of methanol in the solvent mixture would be expected to result in increased swelling of soil organic matter. The decreasing hysteresis in the present study with increasing methanol concentration is consistent with these observations as this presumably coincides with increasing swelling of the organic matter.

Effect of Methanol on Mobility

In addition to their direct effect on adsorption, increased reversibility of the adsorption process (i.e. less hysteresis) in the presence of organic solvents will increase the mobility of a pesticide in the soil profile. Any effects of organic solvents on the soil solution transmission properties of the porous media (Brown and Anderson 1983) may also influence the mobility of pesticides in solution.

The mobility of Simazine and Linuron in soils can be estimated in terms of the retardation factor (R) calculated according to the relation (Rao and Jessup 1983)

$$R = 1 + (D_b/\theta_s)^n KC^{n-1}, \quad (3)$$

where D_b is the bulk density of soil (g cm^{-3}); θ_s is the water-filled porosity ($\text{cm}^3 \text{cm}^{-3}$), K and n are the Freundlich adsorption coefficient and exponent, respectively, and C is the solution concentration. Since the adsorption isotherm is nonlinear, the retardation factor will also be a function of solution concentration of the herbicides.

The values of R for Simazine and Linuron (calculated at herbicide concentrations of $1 \mu\text{g mL}^{-1}$), corresponding to various concentrations of methanol, are given in Table 1. There is a marked decrease in the R values with increasing fraction of organic cosolvent in the mixture. At 10% methanol content, the R values for both the herbicides decreased to almost half the value in aqueous solution. The presence of methanol at a level of 50% and 60% of solvent mixture decreased the retardation factor of Simazine and Linuron by factors of 10 and 12, respectively.

Conclusions

This study clearly shows that the adsorption and desorption behaviour of pesticides are both significantly affected by the presence of organic solvents. These observations have implications with respect to the transport of pesticides and other organic solutes in any situation where organic solvents may be involved, e.g. at waste disposal and land treatment sites.

Acknowledgment

R.S.K. is grateful to the Australian International Development Assistance Bureau for the award of a Commonwealth Postgraduate Fellowship while on study leave from Haryana Agricultural University, Hisar, India.

References

- Briggs, G. G. (1981). Theoretical and experimental relationships between soil adsorption, octanol-water partition coefficients, water solubilities, bioconcentration factors and the paracher. *J. Agric. Food Chem.* **29**, 1050-9.
- Brown, K. W., and Anderson, D. C. (1983). Effects of organic solvents on the permeability of clay soils. EPA-600/S2-83-016, NTIS, Springfield, VA.
- Calvet, R. (1980). Adsorption-desorption phenomena. In 'Interactions between Herbicides and the Soil'. (Ed. R. J. Hance.) pp. 1-30. (Academic Press: London.)
- Chiou, C. T., Porter, P. E., and Schmedding, D. W. (1983). Partition equilibria of nonionic organic compounds between soil organic matter and water. *Environ. Sci. Technol.* **17**, 227-31.
- Dunigan, E. P., and McIntosh, T. H. (1971). Atrazine-soil organic matter interaction. *Weed Sci.* **19**, 279-82.
- Freeman, D. H., and Cheung, L. S. (1981). A gel partition model for organic desorption from pond sediment. *Science* **214**, 790-2.
- Fu, J. K., and Luthey, R. G. (1986a). Aromatic compound solubility in solvent/water mixtures. *J. Environ. Eng.* **112**, 328-45.
- Fu, J. K., and Luthey, R. G. (1986b). Effect of organic solvent on sorption of aromatic solutes onto soils. *J. Environ. Eng.* **112**, 346-66.

- Hamaker, J. W., and Thompson, J. M. (1972). Adsorption. In 'Organic Chemicals in the Soil Environment'. (Eds C. A. I. Goring and J. W. Hamaker.) pp. 49-144. (Dekker: New York.)
- Hartley, D., and Kidd, H. (1987). 'The Agrochemicals Handbook.' (The Royal Society of Chemistry: London.)
- Hildebrand, J. H., and Scott, R. L. (1950). 'The Solubility of Nonelectrolytes.' 3rd Edn. (Reinhold: New York.)
- Karickhoff, S. W. (1984). Organic pollutant sorption in aquatic systems. *Am. Soc. Civ. Eng. J. Hydraul. Eng.* **110**, 707-35.
- Leenheer, J. A., and Ahlrichs, J. L. (1971). A kinetic and equilibrium study of the adsorption of carbaryl and parathion upon soil organic matter surfaces. *Soil Sci. Soc. Am. Proc.* **35**, 700-4.
- McArthur, W. M., and Bettenay, E. (1960). Development and distribution of soils of the Swan coastal plain, W.A. CSIRO Aust. Soil Publ. No. 16.
- Miller, N. A., Wolf, D. C., and Scott, H. D. (1988). Influence of methanol and hexane on soil adsorption of Simazine. *Water, Air, Soil Pollut.* **39**, 101-12.
- Mingelgrin, U., and Gerstl, Z. (1983). Re-evaluation of partitioning as a mechanism of nonionic chemical adsorption in soils. *J. Environ. Qual.* **12**, 1-11.
- Nkedi-Kizza, P., Rao, P. S. C., and Hornsby, A. G. (1985). Influence of organic cosolvents on sorption of hydrophobic chemicals by soil. *Environ. Sci. Technol.* **19**, 975-9.
- Rao, P. S. C., Hornsby, A. G., Kilcrease, D. P., and Nkedi-Kizza, P. (1985). Sorption and transport of hydrophobic organic chemicals in aqueous and mixed solvent systems: Model development and preliminary evaluation. *J. Environ. Qual.* **14**, 376-83.
- Rao, P. S. C., and Jessup, R. E. (1983). Sorption and movement of pesticides and other toxic organic substances in soils. In 'Chemical Mobility and Reactivity in Soil Systems'. (Eds D. W. Nelson, K. K. Tanji and D. E. Elrick.) Am. Soc. Agron. and Soil Sci. Soc. Am. Spec. Publ. No. 11. pp. 183-201. (Am. Soc. Agron.: Madison, Wis.)
- Singh, R., Gerritse, R. G., and Aylmore, L. A. G. (1990). Adsorption-desorption of selected pesticides in Western Australian soils. *Aust. J. Soil Res.* **28**, 227-43.
- Vickery, T. M., Karleskey, D. L., and Blackmer, G. L. (1980). Colorimetry and high performance liquid chromatography of atrazine residues in soil: comparison of methods. *J. Assoc. Off. Anal. Chem.* **63**, 501-10.
- Woodburn, K. B., Rao, P. S. C., Fukui, M., and Nkedi-Kizza, P. (1986). Solvophobic approach for predicting sorption of hydrophobic organic chemicals on synthetic sorbents and soils. *J. Contam. Hydrol.* **1**, 227-41.
- Zachara, J. M., Ainsworth, C. C., Schmidt, R. L., and Resch, C. T. (1988). Influence of cosolvents on Quinoline sorption by subsurface materials and clays. *J. Contam. Hydrol.* **2**, 343-64.

Assessing management-induced changes in the structural stability of hardsetting soils

H.R. Cochrane and L.A.G. Aylmore

*Soil Science and Plant Nutrition, The University of Western Australia, Nedlands, W.A. 6009
(Australia)*

(Accepted for publication 9 August 1990)

ABSTRACT

Cochrane, H.R. and Aylmore, L.A.G., 1991. Assessing management-induced changes in the structural stability of hardsetting soils. *Soil Tillage Res.*, 20: 123–132.

A method which permits separate quantitative assessment of the role of both dispersive and non-dispersive mechanisms contributing to structural instability in hardsetting soils is described. The technique has been used to assess the impact of various tillage intensity, rotational, stubble management and gypsum amendment practices on the structural stability of some hardsetting soils from Western Australia.

In soils subjected to a full structural analysis, dispersive failure was found to be the dominant mechanism contributing to structural instability. On average, dispersive failure accounted for 66% and slaking 20%, of total instability as measured by the modulus of rupture-based techniques employed. Minimising slaking, by reducing the rate of soil wetting, greatly reduced the expression of dispersive behaviour in all soils. This implies that management practices which confer on the soil a resistance to slaking can be effective remedial measures on soils which are predominantly susceptible to dispersive failure. Dispersive failure was found to be the major determinant of crop response to gypsum.

INTRODUCTION

Soil structural instability restricts the productive capacity of a significant area of the sandy loam to clay loam textured topsoils of the Western Australian wheatbelt. Both the timeliness of cultural operations and crop growth can be hindered by low permeability when the soil is wet and by high strength when the soil is dry. Typically these soils are unstable when wet. The disruption of structure which occurs on wetting results from two mechanisms: (1) dispersion – caused by double layer swelling forces and characterised by the detachment of clay-sized particles; (2) slaking – where larger compound particles of soil are broken down by rapid wetting but clay dispersion does not necessarily occur. While there is evidence that many of these soils were structurally fragile prior to clearing, inappropriate agricultural management has

been a major contributor to the poor structural status of the soils (Stoneman, 1962).

Numerous methods have been proposed for assessing the dispersive and slaking behaviour of soils. The most widely adopted quantitative tests measure clay dispersion in soil/water suspension and water-stable aggregation by wet sieving, with many variants being suggested for each method (Williams et al., 1966; Rengasamy et al., 1984).

These techniques have proven to be inadequate for assessing the hardsetting behaviour of soils of the Western Australian wheatbelt for a number of reasons: the disruptive forces applied during the measurement are generally arbitrary and differ in their mode of action to the forces experienced by the soil in situ. Dispersible clay measurements can give a misleading assessment of structural stability when used for comparisons between different soil types because the same quantity of clay dispersed from different soils can have very different expressions in terms of structural effect. Water-stable aggregation is not a sensitive method for those soils in which only a small portion of the soil volume exists as macroaggregates as is the case for much of the hardsetting soil in the Western Australian wheatbelt. Equally important, however, is the fact that dispersion and slaking have generally been measured on different scales. Although Rengasamy et al. (1987) have proposed a classification scheme which combines results from both the above tests to give an index of structural stability, the basis used for combining the two scales of measurement comprising the index is somewhat arbitrary.

The objective of the work reported here was to develop a method which could be used to characterise quantitatively the structural status of hardsetting soils and to discriminate between the mechanisms contributing to their instability. The method of analysing structural stability that we describe is based on the modulus of rupture (M.O.R.) procedure in which disruption to soil structure is caused by a single wetting and drying cycle. Thus, the soil is being subjected to a process and a level of disruptive energy input similar to that which it experiences in the field situation. We have found M.O.R. to be a reliable indicator of soil physical behaviour for the hardsetting soils of the Western Australian wheatbelt, being strongly correlated with seedling emergence and early growth performance of plants grown under controlled conditions (Aylmore and Cochrane, 1986). The method developed has been used to assess the influence of some common management practices on the structural stability of a typical hardsetting soil type from the eastern wheatbelt and to assess the response to gypsum application on a range of trials located throughout the Western Australian wheatbelt.

MATERIALS AND METHODS

Merredin trials

Surface soils were collected in the winter of 1986 from five trials on the Merredin Research Station (31°31'S, 118°12'E) 250 km east of Perth, Western Australia. The soil is a Brown solonetzic soil of the Merredin series (Bet-tany and Hingston, 1961), with an average pH of 6.7 (1:5 in water), sodium accounted for 3.5% of the exchangeable bases (range 1.3–7.8%), average organic carbon was 1.01% (range 0.66–1.31%) and soil texture ranged from loam to light clay. Separate samples were taken from the top 2 cm and top 7 cm of two replicates of each treatment selected for analysis. Details of the treatment comparisons made on each trial are contained in Table 1. Trial codes are those allocated by the West Australian Department of Agriculture which was responsible for initiating and maintaining the trials.

Gypsum trials

Surface soils (0–7 cm) were collected in the autumn/early winter of the first year of each of 34 trials set up to determine the efficacy of gypsum application in ameliorating poor soil physical conditions. Trial design was not uniform, wheat cultivars, fertilizer and seeding rates being chosen on the basis of local recommendations. All trials, however, incorporated a 5 t ha⁻¹ gypsum treatment and responses to gypsum are reported at this application rate, although this is not necessarily the optimum rate tested in each trial. Trial locations varied from Kalannie (32°22'S, 117°07'E) in the northwest to Salmon Gums (32°59'S, 121°38'E) in the southeast and were initiated between 1982 and 1985. As management practices in subsequent years differed for each trial, only responses obtained in the first year of each trial are reported.

TABLE 1
Soil management practices

Trial code	Duration (years)	Treatments sampled
M13	10	Tillage intensity (continuous cropping)
M13	4	Broadcast gypsum application
M56	10	Tillage intensity (rotational cropping)
M29	20	Wheat cropping; Medic pasture continuous and in rotation
M1	2	Stubble addition; Stubble burning
M34	4	Stubble retention; burning × tillage intensity

Testing procedure

Soils were collected moist using thin-walled, 70-mm-diameter brass cores to minimise structural disruption at sampling. Soil was air-dried over a 2 week period, gently crushed and sieved to pass a 2-mm aperture and thoroughly mixed. Soils from replicate plots of one treatment were combined in equal weights to form a composite sample for that treatment prior to analysis. Exchangeable sodium, calcium, magnesium and potassium, and organic carbon were measured on each composite sample using the methods described by Aylmore and Sills (1982). Particle size analysis was determined on a sample composed of equal weights of soil from all plots sampled on each trial, again using the methods described by Aylmore and Sills (1982). Structural analysis was carried out using methods based on the modulus of rupture (M.O.R.) technique described by Richards (1953), with the exception that where soil blocks cracked in the mould, determinations of soil strength were carried out on briquette fragments using a shorter briquette support.

In the modulus of rupture procedure, initially air-dry soil is taken through a single wetting/drying cycle and the resulting disruption to structure is measured as the strength of the soil block formed. Table 2 describes the variations from the standard modulus of rupture procedure required to give a full structural analysis. For example, modulus of rupture of the previously calcium-saturated soil wet rapidly, assesses the total non-dispersive component of structural instability and the difference between this value and that obtained when calcium-saturated soil is wet slowly prior to saturation wetting assesses the slaking component.

Calcium saturation was achieved by the following procedure. Approximately 160 g air-dry soil was placed in a 50-mm-diameter perspex permeameter and slowly wet to saturation with a calcium chloride solution having an

TABLE 2

M.O.R. determinations required for structural analysis

Wetting conditions	Exchangeable cation status	Soil structural parameter derived by:	
		Measurement	Subtraction
Rapid	Natural	Total instability	Dispersive
Slow	Natural	Total instability (slaking eliminated)	
Rapid	Ca-saturated	Non-dispersive	Slaking
Slow	Ca-saturated	Residual	

Dispersion
(no slaking)

ionic strength of 93 mmol dm^{-3} . The soil was then leached with 1 l of this solution followed by 1 l of calcium chloride having an ionic strength of 23 mmol dm^{-3} . Excess solution was removed by suction applied to the base of the permeameter and the soil dried at 45°C prior to gentle crushing and sieving to pass a 2-mm aperture. Leaching was generally done over a 9 h period; however, some of the less permeable soils required up to 36 h for the passage of the solutions, in these cases the flow rates for all soils from that trial were reduced to that of the least permeable sample and all soils remained saturated for the same length of time. The leached soils were found to have, on average, exchangeable sodium and calcium levels of 0.6 and 96%, respectively, of the exchangeable bases.

The slow wetting procedure involves wetting the soil under tension prior to saturation wetting. Soil briquettes were prepared in standard size brass moulds which had a thin nylon mesh ($25 \mu\text{m}$ aperture nylal cloth) base. The soil-filled moulds were placed on sintered glass plates overlain by thick blotting paper to improve soil/plate contact. The sintered glass plates supplied water at a suction of 20 cm water. For selected samples the rate of wetting was measured by recording the rate of movement of the water meniscus in a calibrated capillary tube connected to the plates. Soils normally wet to an equilibrium moisture content in 20–40 min. All soils tested in this series of experiments were left to wet up under suction for 60 min as this was the time required for the least permeable soils to wet up completely. The procedure is completed by saturation wetting for 1 h and drying at 45°C as for the normal wetting procedure.

RESULTS AND DISCUSSION

Measuring the components of structural instability

Each component in the structural analysis described above is expressed as a modulus of rupture value whether measured directly, as in the assessment of total instability, or derived by subtraction of one modulus of rupture value from another, as in assessment of dispersive failure. In unmodified soils, slaking and dispersion are to some extent interdependent mechanisms of structural failure; truly quantitative separation of the role of these mechanisms therefore requires adherence to a standard procedure. Assessment of total instability with slaking minimised by subjecting unmodified soil to the slow wetting procedure (see Table 2), frequently is not possible in highly dispersive soils as the longer total duration of wetting involved increases the expression of dispersive failure to a value in excess of that determined for total structural instability. Substituting prewetting under vacuum for prewetting under the tension can be used to overcome this problem.

Merredin trials

Figure 1a presents the components of structural instability for soils collected from the 10th year of the long-term continuous tillage trial M13. Both tillage intensity and gypsum have a highly significant effect on soil structural stability ($P < 0.001$), the largest differences being in the dispersive failure mechanism. Reducing tillage intensity significantly reduced slaking failure ($P < 0.05$), whereas gypsum application resulted in a small but non-significant increase in slaking failure on each tillage treatment.

Figure 1b demonstrates the effect on dispersive failure of minimising the slaking component of structural instability for the same set of soils. Slaking is minimised by wetting the unmodified soil under suction prior to saturation wetting. Dispersive failure is reduced by a factor varying from 55 to 100% of the level found in the same soils subjected to the full disruptive effect of rapid wetting.

This analysis indicates that adoption of management practices that confer on the soil a resistance to slaking, can be as effective a remedial measure as direct manipulation of dispersive failure through gypsum application. The results of the structural analysis on this trial are the most unequivocal of all the trials examined and corroborate the evidence for structural change associated with management at this site reported by Jarvis et al. (1986).

Figure 2a and b shows the structural analysis for soils collected from the adjacent long-term rotational tillage trial M56, where the same tillage treatments are applied in yearly rotation with a pasture phase. In contrast to the continuous cropping situation, there is no stabilisation of structure associated with the zero tillage (T.D.D.) treatment.

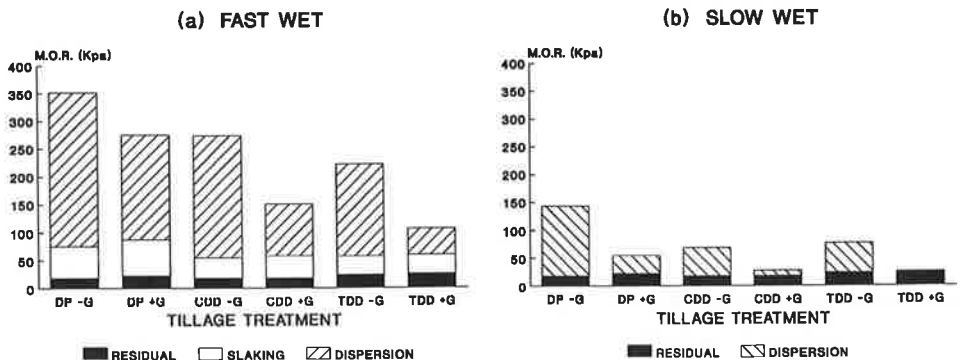


Fig. 1. Components of structural instability for soils from the 10th year of continuous cropping trial M13 (0–7 cm): (a) fast wetting; (b) slow wetting to minimise slaking. Tillage treatments in order of decreasing tillage intensity are: DP, scarified twice, sown using a combine drill; CDD, direct drilled using a combine drill; TDD, direct drilled using a triple disk drill; +G, gypsum broadcast at 4.7 t ha^{-1} just prior to the 7th season of cropping.

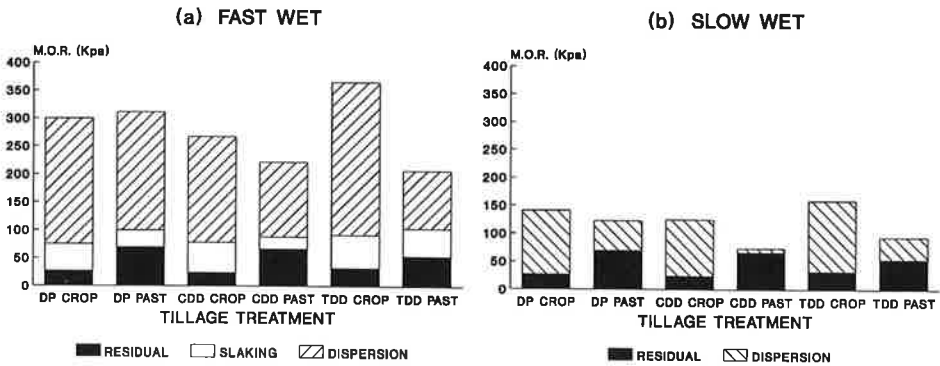


Fig. 2. Components of structural instability for soils from the 10th year of rotational cropping trial M56 (0–7 cm): (a) fast wetting; (b) slow wetting to minimise slaking. Tillage treatments in order of decreasing tillage intensity are: DP, Scarified twice, sown using a combine drill; CDD, Direct drilled using a combine drill; TDD, Direct drilled using a triple disk drill.

The most feasible explanation for this apparently anomalous behaviour between the two trials lies in the interaction between tillage intensity and grazing management. Treading by sheep, particularly when the pasture phase of the rotational trial is grazed wet during winter, constitutes the major difference between the two trials in terms of structurally disruptive forces applied to the soil. The structural status of soils sampled in winter from rotational trials is determined partly by the management practices in the current season and partly by management in previous seasons. We cannot quantitatively determine the influence of grazing management on structural stability from this sampling but our data indicate that although soils from the surface 2 cm, which would be more exposed to structural damage by treading animals, are always more stable than their 0–7 cm counterparts, the difference between them is least in the winter-grazed soils.

The most noteworthy findings from the structural analysis of all the management comparisons made are summarised in Table 3. Residual failure was initially conceived as being determined by inherent soil physico-chemical properties not directly affected by normal management practice. Results from four of the trials appear to validate this view; differences between treatments being small relative to slaking and dispersion effects. The long-term rotational trial M56, however, shows a highly significant effect of current year pasture on the residual component at both sampling depths across all tillage treatments. Whether this is a management-induced change, an inherent difference in soils between the two paddocks forming the trial area or the result of a short-lived soil component affecting the effectiveness of the reduced rate of wetting procedure is as yet unclear.

The effect of a particular management practice will depend on the length of time it has been applied and the manner in which it is applied. For example,

TABLE 3

Summary of treatment effects on soil structural stability

Treatment A	Total	Dispersive	Slaking	Residual	Treatment B	Trial
Pasture	<	<	<	=	Crop (continuous)	M29
Pasture	<	<	=	=	Crop (rotation)	M29
Pasture	<	<	<	>	Crop (rotation)	M56
Gypsum	<	<	=	=	Nil gypsum	M13
Min. till	<	<	<	=	Con. till	M13
Min. till	<	×	×	=	Con. till (in pasture)	M56
Min. till	×	×	>	=	Con. till (in crop)	M56
Min. till	<	<	=	=	Con. till (stubble retained)	M34
Min. till	>	>	>	=	Con. till (stubble burned)	M34
Stubble added	<	<	<	=	Stubble retained	M1
Stubble burned	>	>	=	=	Stubble retained	M1
Stubble burned	=	=	<	=	Stubble retained (min. till)	M34
Stubble burned	>	>	=	=	Stubble retained (ploughed)	M34

>, Treatment A had a higher M.O.R. than Treatment B; <, Treatment A had a lower M.O.R. than Treatment B; =, Treatment A did not differ significantly from Treatment B; ×, Treatment effects were not consistent.

poor pasture will have less potential for structural enhancement than high yielding pasture and may explain why the pasture phase of the rotation has effectively reduced soil susceptibility to slaking in trial M56 but not in trial M29. The influence of stubble burning compared with stubble retention in increasing susceptibility to dispersion under conventional cultivation in trials M1 and M34 indicates a trend towards declining structural stability which was not detectable by field observations at the time of sampling.

Gypsum trials

Figure 3 shows the relationship between the percentage increase in wheat grain yield in the season following a 5 t ha⁻¹ gypsum application and the dispersive failure component in topsoils from the 34 gypsum trial sites. Despite large variations in climatic conditions, wheat cultivar sown, seeding rate, tillage technique, and weed population, the linear least squares regression relationship shown accounts for 71% of the variation in response to gypsum between trials. The poor response to gypsum on those trials initiated in 1985, a year of low but well distributed rainfall, demonstrates that seasonal factors may restrict the expression of potential dispersive behaviour just as dispersion is restricted when slaking is minimised.

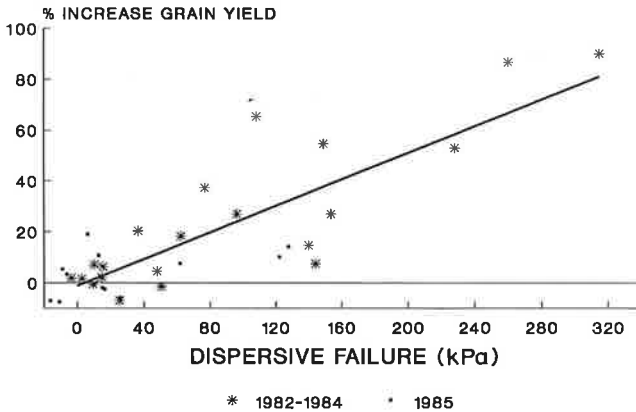


Fig. 3. Percentage increase in grain yield following a 5 t ha^{-1} gypsum application versus dispersive failure at 34 trial sites.

CONCLUSIONS

The method of structural analysis outlined above can be used to assess the susceptibility of hardsetting soils to structural disruption and to measure the impact of soil management practice on the major components of structural instability. In particular, dispersive failure assessed by this method is a good indicator of the potential for soil and crop response to gypsum application over a wide range of soil types. The technique provides a basis for tailoring management practice to the structural characteristics of individual soils – a prerequisite to developing land management systems which will enhance the long-term productivity of these structurally fragile soils.

ACKNOWLEDGEMENTS

We are grateful to R.J. Jarvis and I.C. Rowland of the West Australian Department of Agriculture for permission to sample their trials and to the Wheat Industry Research Committee of Western Australia for financial support.

REFERENCES

- Aylmore, L.A.G. and Sills, I.D., 1982. Characterization of soil structure and stability using modulus of rupture – exchangeable sodium percentage relationships. *Aust. J. Soil Res.*, 62: 213–224.
- Aylmore, L.A.G. and Cochrane, H.R., 1986. Predicting structural amelioration and crop response on hardsetting soils. *Proc. N.Z. Soc. Soil Sci.–Aust. Soc. Soil Sci. Inc. Rotorua*, November 1986, pp. 49–54.
- Bettany, E. and Hingston, F.J., 1961. The soils and land use of the Merredin area, Western Australia. CSIRO Australia Div. Soils, Soils Land Use Ser. No. 41.
- Jarvis, R.J., Hamblin, A.P. and Delroy, N.D., 1986. Continuous cereal cropping with alternative tillage systems in Western Australia. *W.A. Dept. Agric. Tech. Bull.* 71.

- Rengasamy, P., Greene, R.S.B., Ford, G.W. and Mehanni, A.H., 1984. Identification of dispersive behaviour and the management of red-brown earths. *Aust. J. Soil Res.*, 22: 413-431.
- Rengasamy, P., Ford, G.W. and Greene, R.S.B., 1987. Classification of aggregate stability. In: K.J. Coughlan and P.N. Truong (Editors), *Effects of Management Practices on Soil Physical Properties*. QDPI Conference and Workshop Series QC87006, Toowoomba, September 1987, pp. 97-101.
- Richards, L.A., 1953. Modulus of rupture as an index of crusting of soil. *Soil Sci. Soc. Am. Proc.*, 17: 321-323.
- Stoneman, T.C., 1962. Loss of soil structure in wheatbelt soils. *J. Dept. Agric. West. Aust.*, 3: 493-497.
- Williams, B.G., Greenland, D.J., Lindstrom, G.R. and Quirk, J.P., 1966. Techniques for the determination of the stability of soil aggregates. *Soil Sci.*, 101: 157-163.

**Liquid Ion Exchanger Microelectrodes Used to Study Soil Solute
Concentrations near Plant Roots**

M. Hamza and L. A. G. Aylmore

Liquid Ion Exchanger Microelectrodes Used to Study Soil Solute Concentrations near Plant Roots

M. Hamza and L. A. G. Aylmore*

ABSTRACT

A technique for using Na⁺ liquid ion exchanger (Na⁺-LIX) microelectrodes to accurately measure, repetitively, and in a nondestructive fashion, Na⁺ concentrations in the soil solution at single points is described. The method has been used to examine solute (NaCl) accumulation in proximity to single roots of lupine (*Lupinus angustifolius* L.) and radish (*Raphanus sativus* L.) plants subjected to two levels of transpirational demand and five soil solute concentrations. The results obtained indicate that, at soil water contents corresponding to matric water potentials > -140 kPa, back diffusion of solute significantly counteracts the tendency for solute accumulation at root surfaces during transpiration.

MUCH OF THE CONTROVERSY surrounding both water and solute uptake by plant roots has arisen from the lack of suitable methods for measuring the values of water and solute potentials in the soil surrounding plant roots with sufficient resolution and in a continuous and nondestructive manner. The limitations on water content and potential determination have been largely removed by the recent innovative application of computerized axial tomography (CAT) to x- and gamma-ray attenuation measurements (Hainsworth and Aylmore, 1983, 1986, 1988, 1989). Methods for measuring soil solute concentration, however, generally remain limited to macroscopic determination by conductivity terminals or to destructive sampling and soil solution extraction techniques (Rhoades and van Schifgaarde, 1976; Richards, 1966; Oster and Ingvalson, 1967).

Although ion-sensitive microelectrodes are widely used in biology to measure intercellular ion concentrations, they have previously received very limited use in soil-plant ecology for measuring ionic concentrations at or near the root surface (Xuan, 1982; Talibudeen and Page, 1983). Microelectrodes are sensitive enough to monitor even a slight change in ion concentration and clearly should be capable of precise, continuous, and in situ measurement of ionic concentrations at the root surface and in other situations in the soil where single-point determinations are required. The major difficulty to be overcome in this respect lies in the fragility of the glass tip of the microelectrode, which is only a few micrometers in diameter, and in locating the microelectrode tip at the desired point in the soil. This study developed a method by which Na⁺-liquid ion exchanger microelectrodes have been used to study on a microscale, the accu-

mulation of solute in proximity to the roots of lupine and radish plants.

MATERIALS AND METHODS

Ion-Sensitive Microelectrode Techniques

The first full-sized ion-sensitive electrodes to be widely used in the laboratory were pH-sensitive glass electrodes (Caldwell, 1954). With subsequent developments, it is now possible to make microelectrodes that are sensitive to H⁺, Na⁺, K⁺, Cl⁻, and some other ions, and that are capable of giving continuous readings during periods of many hours. The development of liquid ion-sensitive membranes, or LIX, in the late '60s (Ross, 1969) and their commercial availability led to the development of a simple method that allows such materials to be held in the tips of glass microelectrodes (Walker, 1971). The major drawback associated with the most readily available LIX solutions is their poor specificity, permitting interference by other ions. For example, the selectivity of LIX for Na⁺ over K⁺ is not competitive with NAS II-18 Na-sensitive glass that has a selectivity for Na⁺ over K⁺ in microelectrodes of well over 100:1 (Dick and McLaughlin, 1969; Hinke, 1969). Nevertheless, a rather better Na⁺/K⁺ selectivity (15:1) has been obtained with a monensin-based Na⁺-LIX by Kraig and Nicholson (1976). Unfortunately, monensin is very difficult to crystallize in the right form, making the microelectrode Na⁺ sensitive for only a day or so.

In practice, the difficulties experienced in making sharp microelectrodes with NAS II-18 Na⁺-sensitive glass, make Na⁺-LIX a somewhat more attractive way to measure Na⁺ concentrations at the root surface, especially when the soil solution has very small or zero K⁺ concentration, compared with Na⁺ concentration.

Preparation of Liquid-Membrane Microelectrodes

A batch of 2.0-mm o.d., 1.6-mm i.d. borosilicate glass tubing was cleaned in hot ethanol vapor and dried (Thomas, 1978). Micropipettes with 10- μ m tips (larger than generally used for conventional microelectrodes) were then made, using a microelectrode puller, by applying a weak extension force. Once a microelectrode had been constructed, it was kept in a dessicator with dried silica gel in the bottom to avoid absorption of excess water by the glass surface. Since LIX is composed of an organic electrolyte or neutral ligand dissolved in a water-immiscible solvent (Thomas, 1978), the tip of the microelectrode, which possesses the hydrophilic nature of a glass surface, allows water to rapidly displace any water-immiscible liquid from the tip of an untreated glass micropipette. For this reason, the tips were dipped in a fresh 2.5% (v/v) solution of tri-*n*-butylchlorosilane in dry 1-chloronaphthalene for 10 s. The micropipettes were then placed with their tips upwards in a drilled metal block and baked in an oven at 120 °C for 1 h. Typically, silane (an organic Si compound) reacts with the hydroxyl groups on the glass surface and H is replaced by a Si atom with two or three

Soil Science and Plant Nutrition, School of Agriculture, the University of Western Australia, Nedlands, W.A., 6009. Received 28 June 1989. *Corresponding author.

organic radicals attached to it. Thus, the glass surface becomes covered with organic groups and is made very hydrophobic. After cooling, the batch was stored in a dry desiccator with silica gel in the bottom.

Filling the Microelectrode with Sodium-Liquid Ion Exchanger

A small volume of Na⁺-LIX (Na⁺ cocktail of composition: 10.0% (w/w) Na ionophorel [ETH 227], 89.5% (w/w) 2-nitrophenyl octyl ether and 0.5% (w/w) Na tetraphenylborate) was injected into the top of the microelectrode shank using a syringe with a fine plastic tubing. The microelectrode was then placed under a low-power microscope. To ensure complete filling of the tip with LIX all trapped air must be expelled. This can be achieved by pushing a cat (*Felis catus*) or rabbit (*Oryctolagus cuniculus*) whisker through the LIX until it reaches through the shank and then withdrawing it a few micrometers. The LIX should then run down the end of the whisker and start filling the tip. Sometimes a meniscus may form near the end of the whisker, trapping a volume of air between it and the micropipette tip. This can generally be removed by moving the whisker up and down until the LIX runs down or by pushing the trapped air out. Alternatively the microelectrode tip can be broken, provided the filled tip has an acceptable diameter. When the shank has been filled with LIX, the microelectrode shaft is filled with 0.1 M NaCl solution. Finally an Ag/AgCl wire is inserted in the 0.1 M NaCl solution and left for a few hours to stabilize before connecting it to an electrometer (Model 610, Keithley Instruments, Cleveland, OH).

The characteristics of the electrode prepared in this fashion as provided by the manufacturers of the neutral ionophores (Fluka Chemical Corporation, NY) are as follows:

Selectivity Factors. The $\log K_{NaM}^{Pot}$ (M refers to the opposing cation; Pot identifies these as potentiometric selective factors) as obtained by the separate solution method (0.1 M solutions of the chloride salts) (Steiner et al., 1979): $\log K_{NaLi}^{Pot} = 0.4$; $\log K_{NaK}^{Pot} = -1.7$; $\log K_{NaCa}^{Pot} = 0.2$; $\log K_{NaMg}^{Pot} = -2.4$; $\log K_{NaAcetylcholine}^{Pot} = -1.8$.

Electrode Function, Detection Limit. Slope of linear regression: 53.0 ± 2.5 mV (20 °C, 10^{-1} - 10^{-3} M NaCl). Detection limit (NaCl, ionic background of 200 mM K⁺, 2.0 mM MgCl₂, 0.01 mM Ca²⁺): $\log a_{Na}$ (activity) ≈ -2.5 .

Electrical Resistance. Tip diameter ≈ 2 μ m: $\approx 10^{10}$ Ω .

Response Time. 90% response time: ≤ 5 s.

The potential is read with respect to a reference wire (Ag/AgCl) 0.5 mm in diameter inserted to a depth of ≈ 3 cm in the soil at a distance of 6 cm from the microelectrode/root surface contact point. Across the concentration range used, the potential difference between the sensing electrode and the reference electrode prior to the commencement of transpiration (i.e., zero transpiration) was both constant and very small ($< 5 \pm 1$ mV during 24 h). Changes in soil water content in the vicinity of the microelectrode, through the range involved in the present measurements, produced essentially no change in this small baseline potential. Furthermore, concomitant CAT-scanning measurements of the drawdowns in soil water content demonstrated that the water content in the bulk soil in the vicinity of the reference wire was constant throughout the experiments. As indicated above, the response of the microelectrode to change in soil solute concentration is essentially instantaneous (Thomas, 1978). A schematic diagram of the system for measuring the Na⁺ concentration at the root-soil interface using the Na⁺-LIX microelectrode is shown in Fig. 1b.

Construction of Microelectrode Pots

To obtain good contact between the microelectrode tip and the root surfaces, polyvinyl chloride pots (Fig. 1a) were

specifically designed to allow accurate positioning of the microelectrode tip to the root surface. The sloping bottom of the pot was made of transparent acrylic plate and a hole to allow access to the root surface was located on one side of the pot just above the inside edge of this plate, 5 cm below the pot top and 3 cm away from the pot leg. Accurate positioning of the microelectrode was achieved by inserting a plastic tube with diameter such that the tube could move relatively freely into the hole. The plastic tube was positioned 1 cm away from the point where the root first intercepted the acrylic plate. To ensure root/tube contact, a 0.1-mm-diam. hole was made from the surface of the soil to the perspex bottom to encourage the root subsequently planted to follow and to intercept the perspex bottom at the required position. Invariably, once the root intercepted the surface of the perspex bottom, it grew along the surface of the acrylic plate toward the plastic tube. If the root did not make immediate contact with the tube end, this could be delicately repositioned by pushing it the fractions of millimeters required. Usually, a careful positioning of the plastic tube relative to the hole made for the root prior to planting yielded a good contact between the plastic tube and the root surface (Fig. 2).

The inside end of the plastic tube was covered with a layer of Whatman no. 1 filter paper to prevent soil particles from

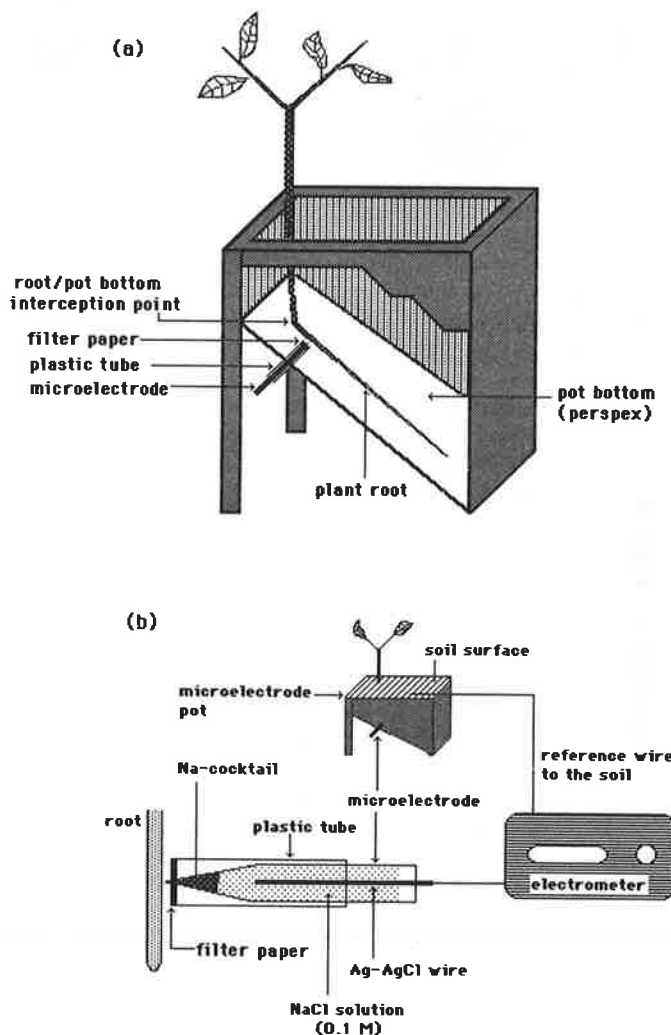


Fig. 1. Schematic diagrams showing (a) microelectrode pot, and (b) arrangement for measuring Na⁺ concentration at root-soil interface using Na⁺-liquid ion exchanger microelectrode.

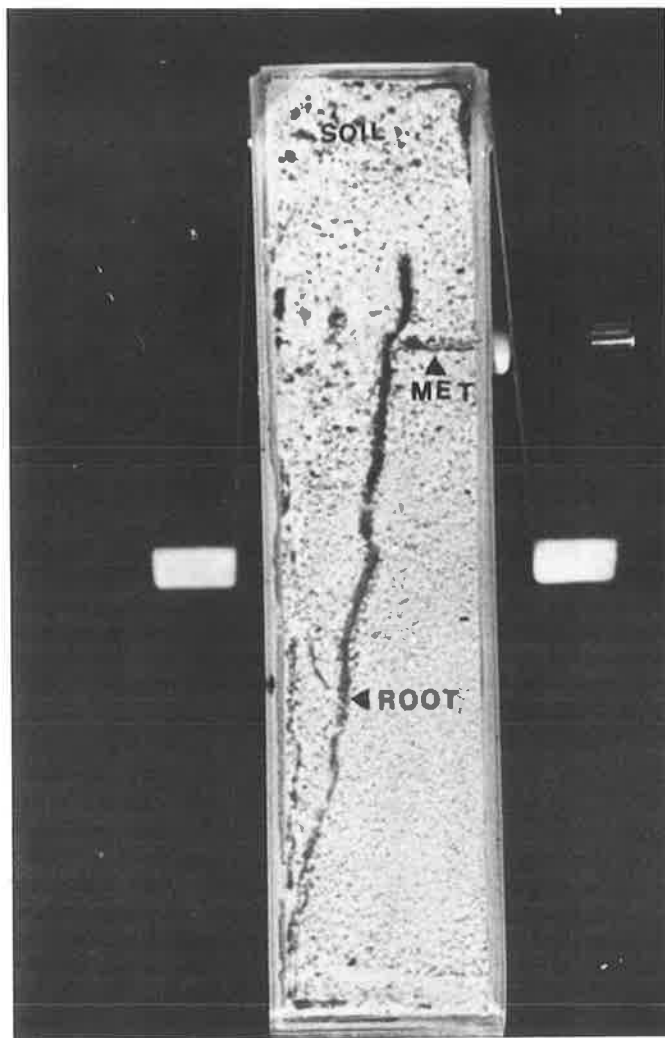


Fig. 2. Acrylic bottom of the microelectrode pot showing a lupine root intercepted by the microelectrode tube (MET). Note how the root has bent at the point of contact.

entering the tube and breaking the delicate microelectrode tip. The microelectrode shaft had a diameter slightly less than that of the plastic tube and could be inserted inside the tube with relative ease until its tip touched the filter paper, then pushed very gently to just penetrate it. Since the plastic tube, the contact point, and the root were visible through the perspex plate, this process was not difficult. Special attention had to be paid to prevent the microelectrode tip from penetrating the root surface, where it would have read the cortex or xylem concentration instead of that at the root surface.

The microelectrode pots were amenable to CAT scanning so that the water drawdown in any layer, and in particular that associated with the microelectrode, could be monitored continuously. Leaf water potentials were monitored using a leaf hygrometer (Model L-51A, Wescor, Logan UT).

Calibration of the Microelectrode

A series of NaCl solutions 5, 10, 20, 40, 60, 80, and 100 mol/m³ were used to construct a calibration curve for the Na⁺-LIX microelectrodes in aqueous solution. The same NaCl solutions were used to irrigate microelectrode pots, uniformly packed with an artificial soil to be used in plant experiments, to a water content of 0.3 m³/m³. The artificial soil consisted of a homogeneous mix of 85% sand from the

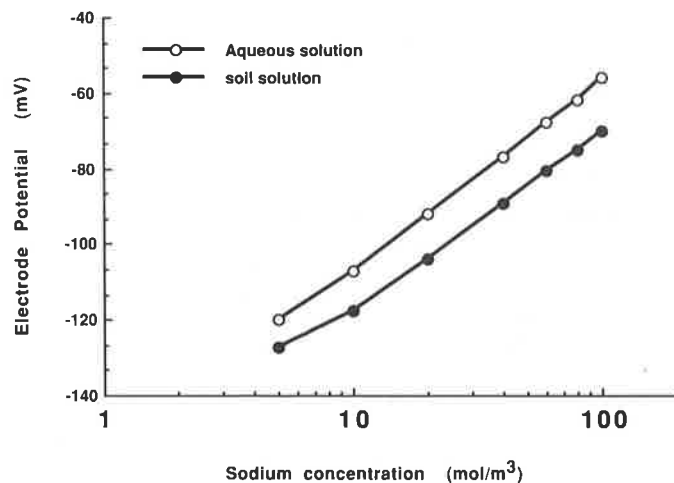


Fig. 3. Calibration curves for Na⁺-liquid ion exchanger microelectrode in aqueous NaCl solutions and NaCl solutions in soil.

Bassendean Association of the Swan Coastal Plain, Western Australia (McArthur and Bettenay, 1960) and 15% Clackline kaolinite from the pallid zone of the Kauring Laterite, Western Australia (Mulcahy and Hingston, 1961). This mix was used to provide a soil medium with the most suitable water-retention and diffusivity characteristics for these studies (Hainsworth and Aylmore, 1986). The irrigated pots were then left for 24 h, allowing the water and solute content in the soil to equilibrate. The Na⁺ concentrations of the soil solutions in the pots were measured, using microelectrodes and the above procedure. Calibrations in the aqueous solution and in the soil were both carried out in a high background Cl⁻ concentration, which was adjusted to maintain a constant total Cl⁻ as the Na⁺ concentration was altered. The relationships between the microelectrode potential readings on the electrometer and the Na⁺ concentrations in the NaCl aqueous solutions and in the solutions applied to the soil are shown in Fig. 3.

The electrode potentials obtained for a solution of a given Na⁺ concentration were invariably lower for the solutions incorporated into the soil than for the original aqueous solutions, presumably as a result of small but constant extraneous potentials at the reference electrode in the soil, or perhaps of Na⁺ exchange on the exchange sites and into the diffuse double layer associated with the clay component of the soil. The extent of these effects will undoubtedly vary, depending on the texture and composition of the soil. It is evident, however, that the slope of the calibration curve is essentially unchanged between the aqueous and soil solutions, giving confidence in the function of the microelectrode system.

Solute Accumulation at Root Surfaces during Transpiration

Lupine (cv. Yandee) and radish (cv. white icicle) seeds were allowed to germinate in the dark on petri dishes containing a thick pad of moist tissue, then transplanted into microelectrode pots so that their emerged radicle was pointed towards the previously made 0.1-mm-diam. hole, 1.5 cm away from the side of the pot, containing the microelectrode hole. The plants were located 1 cm away, but as close as possible on the same line, from the end of the plastic tube. As they grew, the lupine or radish roots intercepted the acrylic bottom of the pots and passed by the inside end of the plastic tube inserts (see Fig. 2).

The single-root lupine and radish plants were grown under laboratory conditions for 18 d under light from eight 20-W fluorescent tubes for 14 h followed by 10 h of darkness each

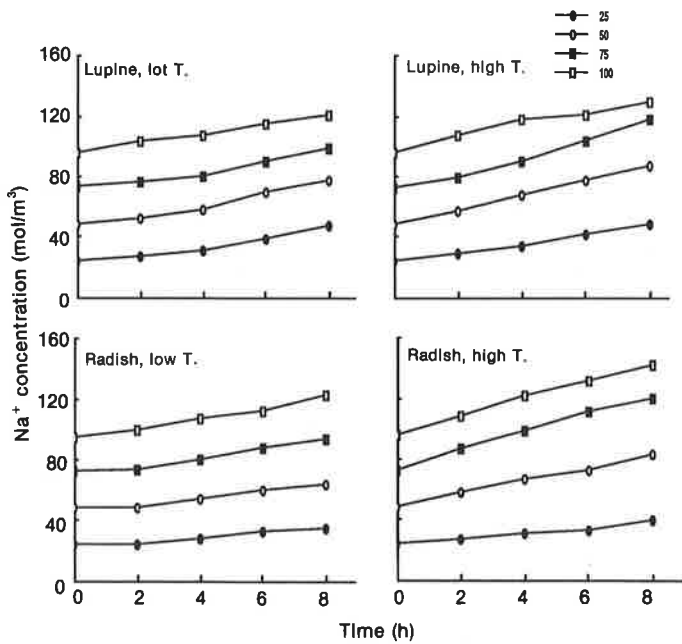


Fig. 4. Sodium concentrations at lupine and radish root surfaces for 25, 50, 75, and 100 mol m⁻³ Na⁺ treatments after 0, 2, 4, 6, and 8 h of low/high transpirational demand (T.).

day. Day and night temperatures were maintained between 23 to 21 °C and the relative humidity at 60 to 70%. Irrigation with saline solutions of the pots containing the plants commenced 11 d after planting. To avoid salt injury, the saline solutions were added gradually (mixed with distilled water) up to Day 14 from planting, where the full-strength solution was added. Four levels of saline solutions containing 25, 50, 75, and 100 mol/m³ Na⁺, as well as the no-solute treatment (distilled water) were used. After 17 d, the pots were rewatered with the saline solutions to a water content of 0.3 cm³/cm³ and the open end of each pot, except for the stem hole, was sealed with cellophane to prevent water evaporation from the soil surface. The plants were kept in darkness for 24 h, allowing the water content in the pots to equilibrate. The plants were subsequently exposed to light and to two levels of transpiration demand imposed by differing air flows from a 390-W fan placed 1 m away. The Na⁺ concentration at the root surface was measured by the microelectrode technique after periods of 2, 4, 6, and 8 h of transpiration.

RESULTS AND DISCUSSION

Figure 4 shows the concentrations of Na⁺ at the root surfaces of the two plant species, measured using the Na⁺-LIX microelectrodes, after the various transpiration periods for the different solute treatments. In all cases the Na⁺ concentrations at the root surfaces increased gradually with time of transpiration in a near-linear fashion and increased slightly more rapidly with increasing Na⁺ concentration in the treatment. At the end of the transpiration period (8 h), the lupine roots had accumulated more Na⁺ at their surfaces than had the radishes except at the two highest concentrations under high transpiration demand. This was to be expected, because the lupine roots generally extracted more water than did the radish roots. For the same reasons, the accumulations of Na⁺ at the root surfaces for both plants were slightly higher under the high transpiration demand.

The cumulative water uptake by the lupine and rad-

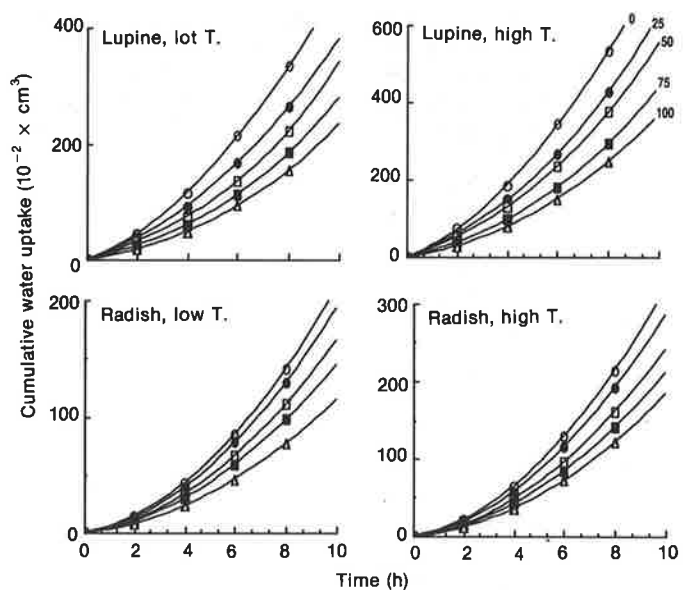


Fig. 5. Cumulative water uptake (cm³) by lupine and radish roots after 2, 4, 6, and 8 h of low/high transpirational demand (T.) for 0, 25, 50, 75, and 100 mol m⁻³ Na⁺ treatments.

ish plants was obtained by weighing the pots after each transpiration interval; these are shown in Fig. 5. Although the cumulative water uptake is clearly progressively reduced by increasing solute concentrations in the treatments, in each case the total amount of water (and hence total solute) transported to the root surface increased in a roughly exponential fashion with time. The decrease in soil-water content in proximity to the plant roots with time of transpiration would, of course, act to increase the concentration of solute accumulation in this region.

The extent of the accumulation of solute at the root surface during transpiration will clearly depend on the soil solute concentration, the rate of water uptake, the reflection coefficient of solute at the root membrane, and the extent of back diffusion of solute to the bulk soil. Other data (Aylmore and Hamza, 1990) demonstrated that the relationships between water uptake and the gradients of hydrostatic pressure potential between leaves and soil in these measurements remained essentially linear and that the increases in hydrostatic potential necessary to initiate flow in the soil-plant systems with decreasing osmotic potential in the treatment were effectively identical with the decrease in osmotic potential at the root surface. These results indicated that the root membranes of both plants acted as near-perfect osmometers. Thus, the reflection coefficient for NaCl is probably close to one and only trivial amounts are expected to cross the root membrane. Passioura (1984) and Munns and Passioura (1984) have suggested that, under these conditions and in the absence of significant back diffusion, the osmotic potential at the root surface should be an exponential function of the rate of water uptake, which is clearly not the case here. Our results are thus consistent with the theoretical argument that any build-up at the epidermis of the root would be trivial (Passioura and Frere, 1967). We concluded that the relatively low values for Na⁺ accumulation at the root surface observed with time of transpiration are due to effective back

diffusion at the high water contents and potentials involved. In fact, the minimum water potential reached in these experiments, determined by CAT scanning, was -140 kPa. Further application of these techniques should make it possible to clarify the combinations of transpiration rates, soil water contents, and solute concentrations at which the potential for solute build-up exceeds back diffusion and the extent to which solute absorption occurs as these factors change.

The accuracy of the microelectrode measurement has been firmly established in the literature (Talibudeen and Page, 1983) and the reproducibility of measurements of solute concentration at a given point on a particular plant root was excellent, not varying by more than 0.1%. It should be noted, however, that measurements of Na^+ concentration and accumulation made using the microelectrode are essentially unique to specific points on the root surface of a given plant. Both water uptake and solute accumulation at any given point are influenced by the structure (i.e., length and thickness) and response of the rest of the root system to adjacent soil water content, potential, and solute-concentration distributions. Previous measurements (Hainsworth and Aylmore, 1989) have demonstrated clearly that water uptake varies markedly along plant roots and so also would the amount of salt accumulation. Since no two plants grow their roots in an identical fashion (i.e., distribution and structure) and the variability within one root system may significantly exceed that between plants, it is essentially impossible to replicate the conditions determining the solute accumulation at any given point on a plant root. Our studies are being extended to examine the variability in solute accumulation along plant roots and between different plants, plant species, etc.

These experiments illustrate the usefulness of the microelectrode technique for studying point concentrations of specific ions and solute potentials within the soil matrix. In conjunction with CAT-scanning measurements of soil water content (and hence, water potentials) they provide a powerful new methodology for studies of soil-plant-water relations.

REFERENCES

Aylmore, L.A.G., and M. Hamza. 1990. Water and solute movement to plant roots. p. 124-129. *In* Trans. Int. Cong. Soil Sci. 14th,

- Kyoto, Japan, 12-18 Aug. 1990. Vol. 7. ISSS, Wageningen, the Netherlands.
- Caldwell, P.C. 1954. An investigation of the intercellular pH of crab muscle fibers by means of micro-glass and micro-tungsten electrodes. *J. Physiol.* (London) 126:169-180.
- Dick, D.A.T., and S.G.A. McLaughlin. 1969. The activities and concentration of sodium and potassium in toad oocytes. *J. Physiol.* (London) 205:61-78.
- Hainsworth, J.M., and L.A.G. Aylmore. 1983. The use of computer assisted tomography to determine spatial distribution of soil water content. *Aust. J. Soil Res.* 21:435-443.
- Hainsworth, J.M., and L.A.G. Aylmore. 1986. Water extraction by single plant roots. *Soil Sci. Soc. Am. J.* 50:841-848.
- Hainsworth, J.M., and L.A.G. Aylmore. 1988. Application of computer assisted tomography (CAT) to gamma attenuation measurement of soil water content. *Aust. J. Soil Res.* 26:105-110.
- Hainsworth, J.M., and L.A.G. Aylmore. 1989. Non-uniform water extraction by a single plant root. *Plant Soil* 113:121-124.
- Hinke, J.A.M. 1969. Glass microelectrodes in the study of binding and compartmentalization of intracellular ions. p. 349-379. *In* M. Lavalley et al. (ed.) *Glass microelectrodes*. John Wiley & Sons, New York.
- Kraig, R.P., and C. Nicholson. 1976. Sodium liquid ion exchanger microelectrode used to measure large extracellular sodium transient. *Science* (Washington, DC) 194:725-726.
- McArthur, W.M., and E. Bettenay. 1960. Development and distribution of soils of the Swan coastal plain, W.A. *CSIRO Aust. Soil Publ.* no. 16.
- Mulcahy, M.J., and F.J. Hingston. 1961. The development and distribution of the soils of the York-Quairading area, Western Australia, in relation to landscape evolution. *CSIRO Aust. Soil Publ.* no. 17.
- Munns, R., and J.B. Passioura. 1984. Hydraulic resistance of plants. III. Effect of NaCl in barley and lupins. *Aust. J. Plant Physiol.* 11:351-359.
- Oster, J.D., and R.D. Ingvalson. 1976. In situ measurement of soil salinity with sensor. *Soil Sci. Soc. Am. Proc.* 31:572-574.
- Passioura, J.B., and M.H. Frere. 1967. Numerical analysis of the convection and diffusion of solutes to roots. *Aust. J. Soil Res.* 5:149-159.
- Passioura, J.B. 1984. Hydraulic resistance of plants. I. Constant or variable? *Aust. J. Plant Physiol.* 11:333-339.
- Rhoades, J.D., and J. van Schifgaarde. 1976. An electrical conductivity probe for determining soil salinity. *Soil Sci. Soc. Am. J.* 40:647-651.
- Richards, L.G. 1966. A soil salinity sensor of improved design. *Soil Sci. Soc. Am. J.* 30:333-337.
- Ross, J.W. 1969. Solid-state and liquid membrane ion-sensitive electrodes. p. 57-88. *In* R.A. Durst (ed.) *Ion-selective Electrodes*. Natl. Bur. Standards, U.S. Gov. Print. Office, Washington, DC.
- Steiner, R.A., M. Oehme, E. Pretsch, and W. Simon. 1979. Neutral carrier sodium ion-selective microelectrodes for intercellular studies. *Anal. Chem.* 51:351-353.
- Talibudeen, O., and B. Page. 1983. Ion-selective electrodes. p. 55-113. *In* K.A. Smith (ed.) *Soil Analysis*. Marcel Dekker, New York.
- Thomas, R.C. 1978. *Ions-sensitive intracellular microelectrodes. How to make and use them*. Academic Press, London.
- Walker, J.L. 1971. Ion specific liquid ion exchanger microelectrodes. *Anal. Chem.* 43:89-92.
- Xuan, J.X. 1982. Mathematical model for the movement of potassium ions to rice roots. *Acta Pedol. Sin.* 19:296-304.

Simultaneous Measurement of the Spatial Distribution of Soil Water Content and Bulk Density

V. K. Phogat, L. A. G. Aylmore,* and R. D. Schuller

ABSTRACT

Continuous nondestructive measurements of the spatial distributions of soil water content and bulk density are essential prerequisites to the resolution of many problems in the study of soil-plant-water systems. Computerized axial tomography (CAT) was applied to dual-source (^{137}Cs and ^{169}Yb) gamma-ray attenuation in soil columns to determine nondestructively the spatial distributions of volumetric water content (θ_v) and bulk density (ρ_s) for two soils that exhibit swelling to different degrees. Beam slice thickness was 2 mm and pixel dimensions 2 by 2 mm. The CAT scanning technique for average ρ_s and θ_v provided excellent agreement with the corresponding values obtained gravimetrically. Average standard deviations (σ) for ρ_s of pixels for the dry soils, although large, were highly reproducible and provide a measure of the structural status of the soils. Changes in the mean and σ of pixel ρ_s following wetting were related to the texture, structure, mineralogy, and Ca or Na exchange status of the soil. Systematic errors arising from the random nature of radioactive emissions, for count times of 2 s, resulted in large σ in estimated θ_v of pixels even for dry soils. Very large counting times (some 169 s for an individual ray-sum and, hence, 112 h to complete a dual-source scan) were required to achieve σ values of pixel θ_v on the order of $0.025 \text{ cm}^3/\text{cm}^3$ for a uniform field of water. Such large count times limit this approach to steady-state or only slowly changing systems. Thus, while the application of CAT to dual-energy-level scanning has the potential to become a major tool for nondestructive studies of soil water content, structural status, and stability, realization of this potential awaits substantial improvements in scanning geometry and counting electronics.

SINGLE- AND DUAL-SOURCE gamma attenuation measurements have been extensively used by soil scientists to obtain nondestructive measurements of ρ_s and θ_v in soil columns. Various isotopes have been used as sources of the gamma radiation including ^{60}Co (Berman and Harris, 1954; Gardner and Calissendorff, 1967); ^{137}Cs (Ferguson and Gardner, 1962; Gurr, 1962); ^{241}Am (King, 1967; Groenevelt et al., 1969) and ^{144}Ce (Gardner and Calissendorff, 1967). Any two gamma radiation sources of sufficiently different energies can be employed for simultaneous and nondestructive measurement of ρ_s and θ_v (Soane, 1967).

More recently, application of CAT (Hounsfield, 1972) to x- and gamma-ray attenuation has provided an exciting new method for nondestructive three-dimensional imaging within a solid matrix. Hopkins et al. (1981) and Davis et al. (1986) demonstrated the application of an x-ray CAT scanning technique to industrial problems, particularly for nondestructive testing of timber poles, concrete pillars, and steel-belted automobile tires. Onoe et al. (1983) illustrated the use of a portable x-ray CAT scanner for measuring annual growth rings of live trees.

The first reported attempts of its use to measure

spatial changes in soil bulk density was by Petrovic et al. (1982). Subsequently, CAT scanning has been applied using single-energy x- or gamma-ray attenuation to measure the spatial variation in θ_v in proximity to plant roots (Hainsworth and Aylmore, 1983, 1986, 1988, 1989; Aylmore and Hainsworth, 1988). Several other investigators (Crestana et al., 1985, 1986; Brown et al., 1987; Anderson et al., 1988; Tollner and Verma, 1989) have also illustrated the use of x-ray CAT for nondestructive measurement of ρ_s and/or θ_v of porous media. Phogat and Aylmore (1989) used single-source (^{137}Cs) gamma CAT scanning to examine the spatial distribution of soil macroporosity and for monitoring the changes that occur during wetting and drying processes in a nondestructive manner. Similarly, x-ray CAT scanning has also been used for characterizing the macropores in soil (Grevers et al., 1989; Warner et al., 1989; Anderson et al., 1990). In addition, roots, seeds, and insects (Tollner et al., 1987) and pesticide granules (Cheshire et al., 1989) within soils have been successfully detected using an x-ray CAT scanner.

One of the limitations of the use of single-energy x- or gamma-ray CAT scanning systems in studies involving measurements of the spatial distribution of θ_v in soils is the assumption of uniform ρ_s . Because the attenuation is a function of both ρ_s and θ_v of the soil, an accurate determination of θ_v in soils is not possible when changes in ρ_s occur during experiments (Petrovic et al., 1982; Hainsworth and Aylmore, 1983; Anderson et al., 1988; Phogat and Aylmore, 1989).

To monitor changes in the spatial distribution of ρ_s and θ_v in situations where the ρ_s of the soil changes due to swelling or shrinking on addition or removal of water requires independent estimates of attenuation associated with both ρ_s and θ_v . This can only be obtained by the simultaneous use of two sources of different energies. Gamma-ray-sourced systems are generally preferred because monochromatic photon beams are readily obtained. However, gamma-ray sources emit a much smaller photon flux than x-ray sources and, unless a very active source is used, scan times are consequently longer. The objective of our study was to evaluate the feasibility of applying the CAT scanning procedure to dual-source gamma attenuation to enable simultaneous measurements of the spatial distributions of ρ_s and θ_v in swelling soils.

THEORY

The theory and use of the CAT technique for medical purposes have been reviewed in some detail by Brooks and Di Chiro (1975, 1976), Budinger and Gullberg (1974), and Panton (1981), and a complete review of various aspects of CAT scanning has been presented by Newton and Potts (1981, p. 3853-3917). A review of CAT-scan theory as it relates to the determination of θ_v was presented in detail by Hainsworth and Aylmore (1983), Crestana et al. (1985), and Anderson et

Soil Science and Plant Nutrition, Univ. of Western Australia, Nedlands, Western Australia 6009. Received 16 July 1990. *Corresponding author.

al. (1988). The following provides a brief outline of the theory as required for dual-gamma-source CAT scanning.

Following Hainsworth and Aylmore (1983), the linear attenuation coefficient (μ) for each pixel for dry soil can be described as

$$\mu_{\text{dry}} = \mu_s \rho_s \quad [1]$$

where μ_s is the mass attenuation coefficient in cm^2/g for soil solids and ρ_s is in g/cm^3 .

Equation [1] can be extended to wet soil as

$$\mu_{\text{wet}} = \mu_s \rho_s + \mu_w \theta_v \quad [2]$$

where μ_w is the mass attenuation coefficient of water.

In situations where the ρ_s of the soil does not change with the addition or removal of water, θ_v can be calculated from a combination of Eq. [1] and [2] to give

$$\theta_v = (\mu_{\text{wet}} - \mu_{\text{dry}})/\mu_w \quad [3]$$

For two gamma-ray energies, the attenuation equations for Eq. [2] may be written as

$$\mu_{\text{wet } a} = \mu_{sa} \rho_s + \mu_{wa} \theta_v \quad [4]$$

$$\mu_{\text{wet } b} = \mu_{sb} \rho_s + \mu_{wb} \theta_v \quad [5]$$

where the subscript *a* refers to the low-energy radiation and subscript *b* refers to the high-energy radiation. Thus, μ_{wa} , μ_{wb} , μ_{sa} , and μ_{sb} are the mass attenuation coefficients for water and soil solid, respectively.

Equations [4] and [5] can be solved simultaneously to give

$$\rho_s = [(\mu_{wb} \mu_{\text{wet } a}) - (\mu_{wa} \mu_{\text{wet } b})] / [(\mu_{wb} \mu_{sa}) - (\mu_{sb} \mu_{wa})] \quad [6]$$

$$\theta_v = [(\mu_{sb} \mu_{\text{wet } a}) - (\mu_{sa} \mu_{\text{wet } b})] / [(\mu_{sb} \mu_{wa}) - (\mu_{wb} \mu_{sa})] \quad [7]$$

Thus, ρ_s and θ_v for an individual pixel can be calculated by scanning the wet soil column with both the radiation sources at a fixed position.

In general, we are interested in the precision of both ρ_s and θ_v measurements. Therefore, the standard deviations in the determination of the dry ρ_s [$\sigma(\rho_s)$] and the θ_v [$\sigma(\theta_v)$] using dual sources can be written, similar to Gardner et al. (1972), as

$$\sigma(\rho_s) = (\mu_{wb}^2 \sigma_{\text{wet } a}^2 + \mu_{wa}^2 \sigma_{\text{wet } b}^2)^{1/2} / A \quad [8]$$

$$\sigma(\theta_v) = (\mu_{sa}^2 \sigma_{\text{wet } b}^2 + \mu_{sb}^2 \sigma_{\text{wet } a}^2)^{1/2} / A \quad [9]$$

where $\sigma_{\text{wet } a}$ and $\sigma_{\text{wet } b}$ are the standard deviations of the attenuations of the wet soil determined by the low- and high-energy sources, respectively, and *A* is equal to $(\mu_{wb} \mu_{sa}) - (\mu_{sb} \mu_{wa})$.

The standard deviations in Eq. [8] and [9] refer to the variation in the wet soil attenuation measurements $\mu_{\text{wet } a}$ and $\mu_{\text{wet } b}$. These are considered to be random variables subject to statistical fluctuation and are the only source of random errors in ρ_s and θ_v , while the attenuation coefficients μ_{wa} , μ_{wb} , μ_{sa} , and μ_{sb} are assumed to be fixed, known constants that do not contribute to the random errors of ρ_s and θ_v . As these are not random variables, we cannot refer to means. In practice, experimental measurements of μ_{wa} , μ_{wb} , μ_{sa} , and μ_{sb} are subject to statistical variation, but it is assumed that these uncertainties can be made negli-

gibly small by taking the mean of repeated measurements, which, in practice, requires making them more than an order of magnitude smaller than the errors in $\mu_{\text{wet } a}$ and $\mu_{\text{wet } b}$. It should also be noted that, although any errors in μ_{wa} , μ_{wb} , μ_{sa} , and μ_{sb} would show themselves as systematic errors in ρ_s , θ_v , $\sigma(\rho_s)$ and $\sigma(\theta_v)$, they do not play any part in the randomness of ρ_s and θ_v , as they are still treated as constants in Eq. [6] to [9].

MATERIALS AND METHODS

Computer-Assisted Tomography Scanning System

A prototype CAT scanning system constructed in the Soil Science and Plant Nutrition Laboratories of the University of Western Australia (Hainsworth and Aylmore, 1988) was used for these studies. Commercially available ^{137}Cs (1.85×10^{10} Bq) and ^{169}Yb (7.4×10^{10} Bq) gamma sources were mounted in a Pb castle opposite to a NaI(Tl) scintillation detector attached to a photomultiplier tube. The signal from the photomultiplier tube passed through a tube base-preamplifier (Model 2007P, Canberra-Packard Instrument Pty Ltd., Mt. Waverly, Victoria, Australia¹) before being fed to an amplifier (Model 2012, Canberra-Packard). Other components of the detection system included a high-voltage power supply (Model NE 4646, Nuclear Enterprises, Reading, England), a single-channel analyzer (SCA) (Model 2030, Canberra-Packard) and a dual counter (Model 2072 A, Canberra-Packard) with an RS-232 interface for communication with an IBM PC. The counts in the desired energy ranges were discriminated by the SCA and subsequently counted separately by the dual counter. The beam was collimated to give a slice thickness of 2 mm and pixel size of 2 by 2 mm. The Pb castle contained a mechanism by which the two sources could be alternately brought into line with the collimator and detector. The data acquisition system as well as the movements of translation and rotation of the sample were controlled by the PC.

As the source and detector were fixed, the object was moved across the beam and scanned at 2-mm intervals. In each linear scan, two air counts were required on both sides of the object to allow the calculation of linear attenuation coefficients for the object. Successive linear scans were made after rotating the object progressively in 5° increments through 180° . Once this process was completed, the linear scans were back-projected by using filtered back-projection (Hermon, 1980) for a given number of rotations to reconstruct an image of the scanned cross-sectional slice. Once the back-projections were completed, the gamma attenuation values for each pixel in the slice were determined. The whole process was repeated for both sources. The values of ρ_s and θ_v for individual pixels were then calculated using Eq. [6] and [7], where $\mu_{\text{wet } a}$ and $\mu_{\text{wet } b}$ correspond to the individual pixel attenuations due to ^{169}Yb and ^{137}Cs , respectively, in each of the scans. This gave separate maps of ρ_s and θ_v in the scanned slice.

Choice of Sources

A combination of ^{137}Cs and ^{241}Am sources has most commonly been used in conventional dual-source scanning because of the tenfold difference in gamma-ray energy (662 and 60 keV, respectively) and their long half-lives. However, both the time required to successfully complete a CAT scan and the precision obtained depend on the transmission intensity and, hence, count rate. Gamma-ray sources generally emit much smaller photon fluxes than x-ray sources. While

¹ System identification is provided solely for the benefit of the reader and does not imply the endorsement of the University of Western Australia.

high-strength ^{137}Cs sources are readily available, the beam strength obtainable from ^{241}Am has a practical limit because of self-absorption (Miller, 1955). Scan times required with this source are not sufficiently rapid to follow the rapid changes in soil θ_v , that may be associated with, for example, water extraction by plant roots or water infiltration into the soil surface. Clearly in dual-source CAT scanning, the minimum scanning time commensurate with adequate precision will generally be desirable. Hainsworth and Aylmore (1988) suggested the use of ^{169}Yb as an alternative source to ^{241}Am , since this provides a similar energy level (63.1 keV) and attenuation coefficient for water, but emits much higher photon outputs (more than 20 times) at high activities (e.g., $3.7\text{--}7.4 \times 10^{10}$ Bq). The major disadvantage of the ^{169}Yb source is its relatively short half-life of 31 d, resulting in a working life of approximately 2 mo. In our study, the combination of a 7.4×10^{10} Bq source of ^{169}Yb and 1.85×10^{10} Bq source of ^{137}Cs was used in an attempt to reduce scan times and increase precision and accuracy.

Experimental Procedure

Physical and chemical properties of two surface (0–7 cm) soils collected from Kulin and York, Western Australia are given in Table 1. The principal differences between the two soils are the higher silt and clay contents in the York soil and a dominant clay mineral of smectite in the York and kaolinite in the Kulin soil. Mass attenuation coefficients for these soils were determined as follows. Soil samples were oven dried, passed through a 2-mm sieve, and packed to a known ρ_s in acrylic columns of 5.4-cm i.d. and 3.0-cm height. An additional column was filled with deionized water. Each column was scanned with each source at four successive layers of 2-mm thickness using a counting time of 2 s for each ray-sum. Average μ over the entire sample cross-sections were obtained for each column and for each source and substituted into Eq. [1] with the known ρ_s values to obtain μ_{sa} and μ_{sb} for the two soils. The values of μ_{wa} and μ_{wb} were taken to be equal to the average values of μ for the water column scanned with ^{169}Yb and with ^{137}Cs , respectively. The density of water was taken as 1.0 g/cm^3 .

To obtain soil samples with different θ_v , segmentable acrylic columns of 5.4-cm i.d. consisting of four 1.0-cm-long segments were used. Whatman no. 50 filter paper was fitted to the bottom of each column. Using oven-dry soil, nine columns of each soil were packed at a ρ_s of $1.41 \pm 0.020 \text{ g/cm}^3$ for Kulin soil and $1.36 \pm 0.023 \text{ g/cm}^3$ for York soil, to a height of 3.0 cm. One centimeter was left empty to allow for any swelling. All columns were saturated from the bottom and then equilibrated at appropriate suctions for a period of 5 d. Three successive slices of 2 mm each were scanned in each column through the second segment from the bottom when dry and rescanned at equilibrium moisture content with each source. Mean μ values over the entire sample cross-sections of all the scanned slices were determined. The average ρ_s and θ_v for each slice were calculated using Eq. [6] and [7], and results were averaged for each column. After scanning, each column was carefully dismantled and average ρ_s and θ_v in the scanned segments were determined.

Table 1. Selected physical and chemical properties of the soils used in this study.

Location	Textural class	Coarse sand	Fine sand	Silt		Clay	Minerals in clay fraction†	Cation-exchange capacity
				(%)	(%)			
Kulin	Sandy loam	47.72	24.52	10.5	17.31		Kaolinite, illite	8.20
York	Sandy clay loam	17.15	32.75	26.5	23.58		Smectite, kaolinite	18.93

† Minerals in clay fraction are by decreasing dominance.

To study the mean and spatial distribution of ρ_s and θ_v , and to monitor the spatial changes in their distribution on wetting or application of salt solutions, three columns (Y1, Y2, and Y3) of 5.4-cm i.d. and 35-cm length were packed with York soil aggregates (2.8–4.0 mm). In addition, one column (K1) was packed with Kulin soil (<2.0 mm). Initially, the four columns were scanned dry at depths of 0.5, 1.5, 4.5, and 9.5 cm from the soil surface with both radiation sources. Deionized water was applied at the soil surface of Columns K1 and Y1, through a coarse porous glass disk (5.1-cm o.d.). A positive head of 0.5 cm of water was maintained at the surface by appropriate positioning of a Mariotte bubbling tube. Water supply to both the columns was stopped after the wetting front had travelled to a depth of 18 to 20 cm. Columns Y2 and Y3 were treated in a similar manner using 0.1 M CaCl_2 and 0.1 M NaCl solutions, respectively. The four columns were again scanned at the same depths. The following day, deionized water was applied to the surface of the columns previously treated with CaCl_2 and NaCl solutions, i.e., Y2 and Y3, and these were scanned at the same positions to observe the relative effects of the divalent and monovalent cations on structural status. The mean and standard deviations of ρ_s and θ_v in each soil slice scanned were determined from the calculated pixel ρ_s and θ_v across the entire cross-section of the slice, using Eq. [6] and [7].

The precision of the dual-gamma-ray CAT scanning technique for obtaining the spatial distributions of ρ_s and θ_v was studied by scanning columns filled with deionized water and York soil (<2.0 mm) with both the sources using a range of counting times. Means and standard deviations of pixel ρ_s and θ_v were calculated for the sample cross-sections for each counting time.

RESULTS AND DISCUSSION

Mean and standard deviations of the mass attenuation coefficients obtained from four slices for the two soils and three for water, using each radioactive source, are given in Table 2. These values of mass attenuation coefficients were used in Eq. [6] and [7] to calculate the unknown ρ_s and θ_v of these columns. The maximum errors associated with the dual-gamma-source CAT scanning technique in the determination of average ρ_s and θ_v were calculated from the values of standard deviation of mass attenuation coefficients for the two soils and deionized water. Using the latter values, Eq. [8] and [9] were solved for the scan of the uniform field of water to yield a value of 0.009 g/cm^3 for $\sigma(\rho_s)$ and $0.011 \text{ cm}^3/\text{cm}^3$ for $\sigma(\theta_v)$. The values of $\sigma(\rho_s)$ calculated in a similar way for Kulin and York soils were 0.039 and 0.038 g/cm^3 , respectively. The value of $\sigma(\theta_v)$ for both the soils was $0.042 \text{ cm}^3/\text{cm}^3$. The larger values of $\sigma(\rho_s)$ and $\sigma(\theta_v)$ for the soils arise from the much greater variation in ρ_s and θ_v in the soil columns compared with those for the water column.

The values of mean θ_v for slices of the two soils

Table 2. Means and standard deviations of mass attenuation coefficients obtained by computerized axial tomography (CAT) scanning for various experimental materials.

Material	Mass attenuation coefficient			
	^{169}Yb		^{137}Cs	
	Mean	SD of mean	Mean	SD of mean
Water	0.175650	0.000276	0.081440	0.000198
Kulin soil	0.207304	0.001256	0.074199	0.000617
York soil	0.222639	0.001483	0.077526	0.000714

determined by the dual-source gamma CAT scanning technique (Fig. 1) showed good agreement ($R^2 = 0.991$) with the values obtained gravimetrically (but expressed volumetrically). The differences in θ_v determined by the two methods fall within the range of $\pm 0.024 \text{ g/cm}^3$. Also shown in Fig. 1 are the relationships between θ_v and the water content that would have been obtained if the calculation had been made on the basis of Cs attenuation alone for both the soils (rather than the dual-source CAT scanning technique), which neglects ρ_s changes. For both soils, the single-source (^{137}Cs) CAT scanning technique markedly underestimated θ_v at or near saturation, undoubtedly as a result of a decrease in ρ_s due to swelling, and slightly overestimated θ_v at or below values of $0.27 \text{ cm}^3/\text{cm}^3$ in the Kulin and $0.05 \text{ cm}^3/\text{cm}^3$ in the York soil. The latter effect is undoubtedly due to an increase in ρ_s because of shrinking of the initially saturated soil matrix with decrease in θ_v . The differences in behavior of the two soils during the desorption cycle with respect to θ_v , compared with the θ_v calculated using ^{137}Cs alone, can be attributed to the differences in the clay mineralogy.

The results for the mean ρ_s in slices of the two soils obtained using dual-gamma-ray CAT scanning and calculated from Eq. [6] are compared with the gravimetrically obtained values in Fig. 2. The agreement is again good, with an R^2 value of 0.995. The variation in the two determinations was approximately $\pm 0.015 \text{ g/cm}^3$.

It is apparent from Fig. 1 and 2 that the intercepts for ρ_s and θ_v do not extrapolate to the origin, as would be anticipated. This may be largely attributed to errors in soil volume measurements arising during dismantling and segmenting of the columns.

It is clear from these results that the dual-gamma-ray CAT scanning technique is capable of successfully measuring, simultaneously and nondestructively, the mean ρ_s and θ_v in both swelling and nonswelling soils with excellent accuracy. However, the primary objective of the CAT technique is not to measure average

ρ_s and θ_v , but to reveal the spatial distributions of ρ_s and θ_v in soils.

Spatial Distribution of Water Content and Bulk Density

The means and standard deviations of ρ_s and θ_v for the pixels in each scan of the Kulin and York soil samples under various treatments and at various depths are shown in Table 3. The average $\sigma(\rho_s)$ for pixels in the initial dry scans for the Kulin and York soil samples were 0.33 and 0.78 g/cm^3 , respectively. The larger value of $\sigma(\rho_s)$ for pixels for the York soil samples reflects the greater heterogeneity arising from the spatial distribution of soil and pore spaces in these columns packed with 2.8- to 4.0-mm size aggregates, compared with the Kulin soil samples, which were packed with < 2.0 -mm size aggregates. Thus, the different values of $\sigma(\rho_s)$ for pixels illustrate the different structural status of the two soils.

When water was applied to the surface of these soil samples, $\sigma(\rho_s)$ for pixels in scans for the York (Y1) soil samples was reduced from 0.796 to 0.560 g/cm^3 , indicating a decrease in heterogeneity of the scanned slices. Presumably, this was because of slaking or swelling of the soil aggregates. In the case of the Kulin soil, the value of $\sigma(\rho_s)$ for pixels remained essentially the same, presumably because of the smaller size (< 2.0 -mm) aggregates used and the lower inherent swelling associated with kaolinite clay. However, the average ρ_s of both the soils decreased on wetting and this is undoubtedly due to the swelling that occurs. In both soils, the magnitude of the reduction in ρ_s was greater in the surface layers compared with the layers at other depths.

A comparison of the values of $\sigma(\rho_s)$ for pixels for scans of the York soil (Y1 and Y2) demonstrates that the soil retained its structure to a greater extent when treated with 0.1 M CaCl_2 (Y2) than when treated with water (Y1). The value of $\sigma(\rho_s)$ for pixels of the surface layer treated with 0.1 M CaCl_2 (Y2) decreased from 0.783 to 0.718 g/cm^3 whereas, in the case where water

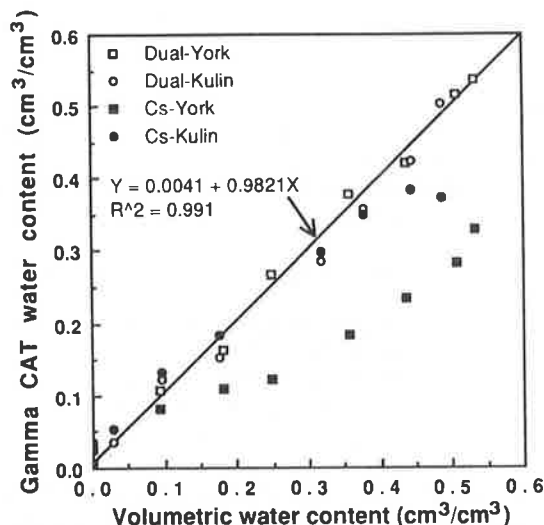


Fig. 1. Relationship between volumetric water content and water content determined by dual- and single-energy gamma computerized axial tomography (CAT) scanning for soils from Kulin and York, Western Australia.

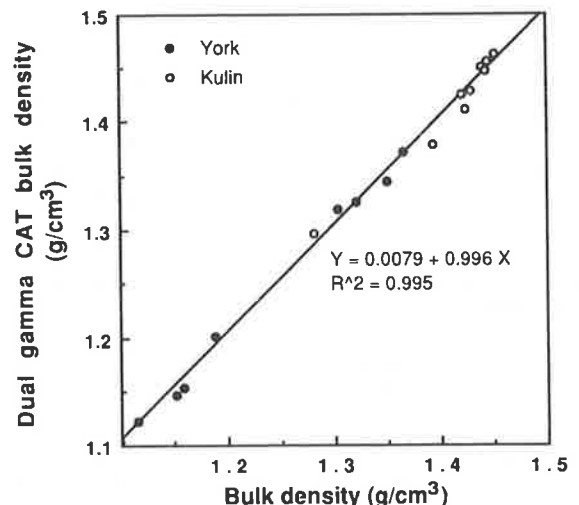


Fig. 2. Relationship between gravimetric bulk density and bulk density determined by dual-energy gamma computerized axial tomography (CAT) scanning for soils from Kulin and York, Western Australia.

Table 3. Means and standard deviations of pixel bulk density and pixel water content in scans for soils from Kulin and York, Western Australia, under various treatments at different depths.

Soil	Depth cm	Initial dry				After solution				After water			
		Bulk density		Water content		Bulk density		Water content		Bulk density		Water content	
		Mean	SD	Mean	SD	Mean	SD	Mean	SD	Mean	SD	Mean	SD
		g/cm ³		cm ³ /cm ³		g/cm ³		cm ³ /cm ³		g/cm ³		cm ³ /cm ³	
Kulin (K1)	0.5	1.424	0.344	-0.003	0.362					1.221	0.336	0.518	0.345
	1.5	1.430	0.342	0.005	0.362					1.242	0.361	0.456	0.368
	4.5	1.403	0.325	-0.001	0.340					1.256	0.362	0.378	0.382
	9.5	1.393	0.320	0.001	0.341					1.393	0.323	0.006	0.344
	Average	1.412	0.333	0.000	0.351					1.278	0.346	0.340	0.360
York (Y1)	0.5	1.060	0.836	0.003	0.708					0.868	0.506	0.491	0.477
	1.5	1.081	0.757	-0.001	0.633					0.880	0.565	0.470	0.480
	4.5	1.066	0.774	0.001	0.633					0.931	0.523	0.429	0.518
	9.5	1.031	0.815	0.001	0.729					1.001	0.647	0.370	0.540
	Average	1.060	0.796	0.001	0.676					0.920	0.560	0.440	0.504
York (Y2)	0.5	1.072	0.783	0.006	0.763	1.051	0.718	0.346	0.534	0.924	0.647	0.436	0.423
	1.5	1.068	0.776	-0.002	0.676	1.035	0.758	0.318	0.523	0.922	0.701	0.403	0.487
	4.5	1.063	0.774	0.014	0.612	1.067	0.572	0.297	0.644	0.987	0.587	0.345	0.558
	9.5	1.012	0.744	0.001	0.741	1.011	0.645	0.275	0.683	1.008	0.685	0.311	0.582
	Average	1.054	0.769	0.005	0.698	1.041	0.673	0.309	0.596	0.960	0.655	0.374	0.513
York (Y3)	0.5	1.109	0.764	0.005	0.638	0.954	0.510	0.414	0.437	0.889	0.444	0.496	0.397
	1.5	1.081	0.721	0.001	0.672	0.922	0.647	0.391	0.422	0.874	0.546	0.429	0.438
	4.5	1.075	0.779	-0.003	0.690	0.959	0.679	0.362	0.545	0.953	0.584	0.334	0.480
	9.5	1.001	0.806	0.002	0.619	0.900	0.705	0.315	0.515	0.997	0.564	0.312	0.492
	Average	1.067	0.767	0.001	0.655	0.935	0.635	0.371	0.480	0.928	0.534	0.393	0.452

was applied (Y1), the decrease was from 0.836 to 0.506 g/cm³. As could be expected, the data illustrate that the presence of Ca²⁺ reduces the swelling or slaking of the York soil aggregates. Under the application of 0.1 M NaCl (Y3), there was a greater reduction in pixel $\sigma(\rho_s)$ in the surface layer (0.764 to 0.510), compared with the CaCl₂ treatment, indicating that aggregates of York soil were more susceptible to slaking or swelling under the NaCl treatment. When water was applied to the columns previously treated with CaCl₂ and NaCl solutions (Y2 and Y3, respectively), $\sigma(\rho_s)$ for pixels for the surface layer in the NaCl-treated soil decreased to 0.444, compared with a value of 0.647 for the CaCl₂ treatment. Thus, as expected, $\sigma(\rho_s)$ for the surface layer demonstrates that the susceptibility of aggregates of York soil to disruption is increased when prewetting with NaCl is followed by water application, because of the dispersive effects of the Na⁺ ion.

Perusal of the values of $\sigma(\theta_v)$ for pixels in scans of the dry soil samples (Table 3) indicates that the average θ_v in scans for the dry Kulin soil approximated to zero, but with a $\sigma(\theta_v)$ for pixels of ± 0.351 cm³/cm³. In the case of scans for the dry York soil samples, the $\sigma(\theta_v)$ for pixels was as high as 0.676 cm³/cm³, with an average θ_v of 0.003 cm³/cm³. The magnitude of $\sigma(\theta_v)$ for pixels in scans for both the dry soils are surprisingly high. These systematic errors can undoubtedly be attributed to propagation of errors associated with the inherent randomness of gamma emissions from the radiation sources. Dual-source scanning is subject to the multiplicative variation applicable to measurements of gamma emission and attenuation for both sources. Clearly, individual pixel values are subject to substantial variation and there are errors in the estimation of both individual pixel ρ_s and θ_v in all scans. As demonstrated above, however, the mean values of ρ_s and θ_v provide accurate estimates of these quantities

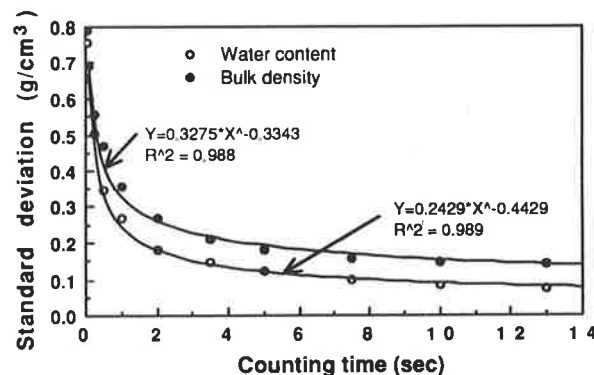


Fig. 3. The standard deviations in dual-gamma computerized axial tomography (CAT) scan determinations of pixel bulk density for a soil from York, Western Australia, and pixel water content in a uniform field of water at different counting times.

and $\sigma(\rho_s)$ and $\sigma(\theta_v)$ for pixels are highly reproducible between slices.

The errors introduced by the random nature of the emission from the radioactive sources can, however, be reduced by increasing the counting time. The values of $\sigma(\rho_s)$ or $\sigma(\theta_v)$ for pixels in scans of a uniform field of water and dry York soil (<2.0 mm) at different counting times are given in Fig. 3. This clearly indicates that the maximum $\sigma(\theta_v)$ for pixels associated with the dual-gamma-ray CAT scanning system (at the counting time of 2 s used in the determinations) is around 0.18 g/cm³, as this value was obtained for a uniform field of water. Furthermore, Fig. 3 shows that further improvement in the determination of the spatial distributions of ρ_s and θ_v can be achieved by using longer counting times, as $\sigma(\theta_v)$ and $\sigma(\rho_s)$ for pixels decrease with increasing counting time. The $\sigma(\rho_s)$ for pixels for York soil scans remained above the values obtained for water scans at each counting time because

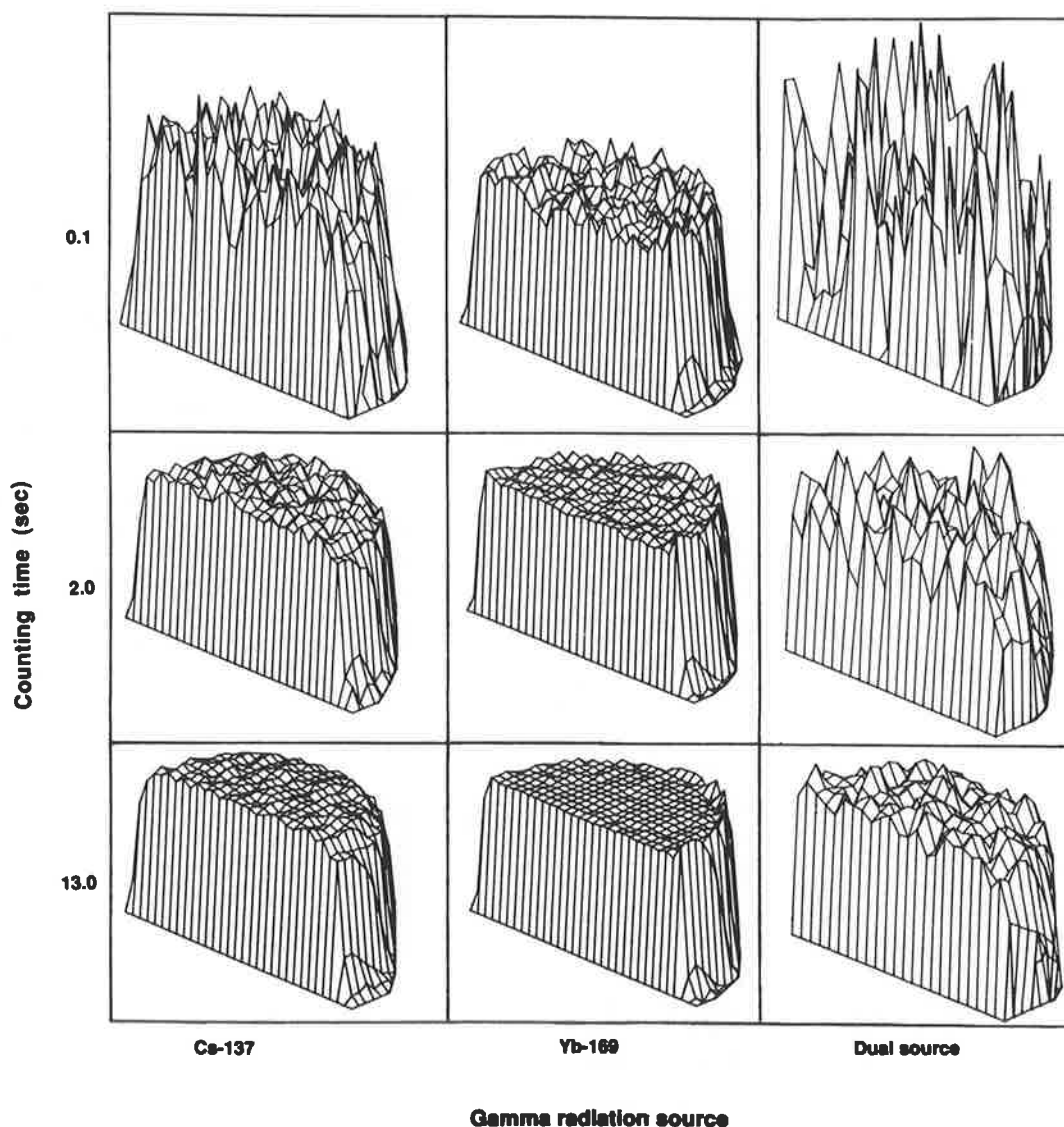


Fig. 4. Reconstructed half-slice three-dimensional computerized axial tomography (CAT) scanning images showing the spatial distribution of water content in slices of a uniform field of water scanned with ^{137}Cs and ^{169}Yb at different counting times and calculated for both single ^{137}Cs - and ^{169}Yb -sources as well as for the dual-gamma-source CAT scanning procedure.

of the inherent variations in the soil samples. A counting time of 13 s gave a $\sigma(\theta_v)$ of $0.073 \text{ cm}^3/\text{cm}^3$ for a uniform field of water, which could be considered as the highest precision using this system and counting time. In contrast, the value of $\sigma(\rho_s)$ for pixels for the York soil at a counting time of 13 s was 0.141 g/cm^3 , showing an increase of 0.068 g/cm^3 due to inherent variations in ρ_s across the entire cross-section of the scanned slice.

To illustrate the effect of counting time on $\sigma(\theta_v)$ and $\sigma(\rho_s)$ for pixels associated with dual-source gamma CAT scanning, three-dimensional representations of the distribution of pixel attenuation and estimated θ_v in a uniform field of water, scanned with ^{137}Cs and ^{169}Yb and calculated using Eq. [7] with counting times of 0.1, 2.0, and 13.0 s are shown in Fig. 4. The height of the surface represents θ_v for each pixel in the slice. These images illustrate that, as the counting time is increased, the variation in pixel θ_v decreases and, as

a result, the surface of the images becomes more uniform for all three methods. The higher photon output of the ^{169}Yb and the fact that the average attenuation due to Yb is greater than that due to Cs reduces the relative error (the absolute error in attenuation being roughly the same) and explains the greater uniformity of the Yb scans compared with the Cs scans. At a counting time of 13 s, ^{137}Cs gave a $\sigma(\theta_v)$ for pixels of $0.016 \text{ cm}^3/\text{cm}^3$, whereas the corresponding value for the ^{169}Yb scan was $\pm 0.007 \text{ cm}^3/\text{cm}^3$. When the scan data of both the sources were used in Eq. [7], it yielded a $\sigma(\theta_v)$ for pixels of $0.073 \text{ cm}^3/\text{cm}^3$. This variation in pixel θ_v using both the sources is high in spite of the very low values for scans of the individual sources (^{137}Cs and ^{169}Yb). This multiplicative propagation of errors is most evident when due to random emissions, a particular pixel estimated to have a low attenuation using ^{137}Cs is estimated to have a high attenuation using ^{169}Yb or vice versa. As a result, small variations

in the Cs and Yb scans can give rise to large and unacceptable variations when Eq. [6] and [7] are applied. The observed errors are confirmed by Eq. [8] and [9], showing that errors are solely attributable to the random variation in the single-source scans resulting from the inherently random nature of gamma emission.

Large variation in pixel ρ_s calculated from Eq. [6] for scans of York soil (Fig. 5) at the three counting times (0.1, 2.0, and 13.0 s), when compared with water scans (Fig. 4), reflects the inherent variation in pixel ρ_s of the soil scans. The distribution of ρ_s in a slice of York soil before and after wetting, as determined by the dual-gamma-ray CAT scanning technique using a counting time of 13.0 s is shown in Fig. 6. The CAT

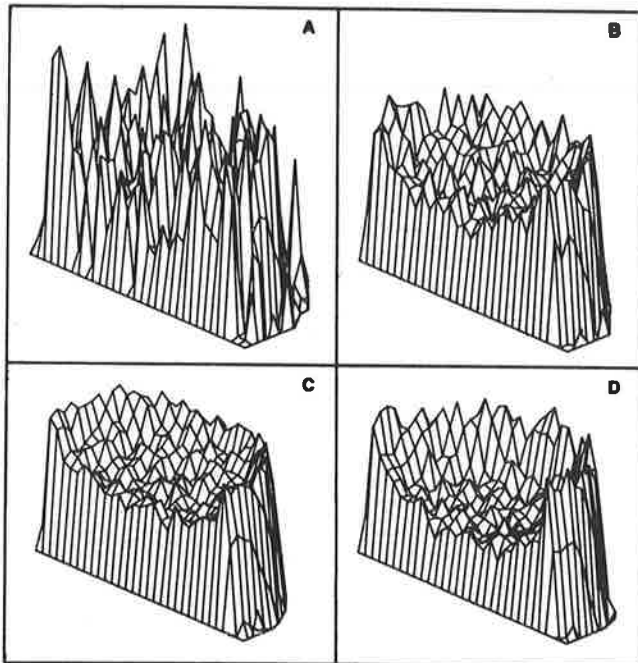


Fig. 5. Reconstructed half-slice three-dimensional computerized axial tomography (CAT) scanning images showing the spatial distribution of pixel bulk density obtained by dual-gamma CAT scanning for counting times of (a) 0.1 s; (b) 2.0 s, (c) 13.0 s for an initially dry soil, and (d) 13.0 s for the soil after wetting.

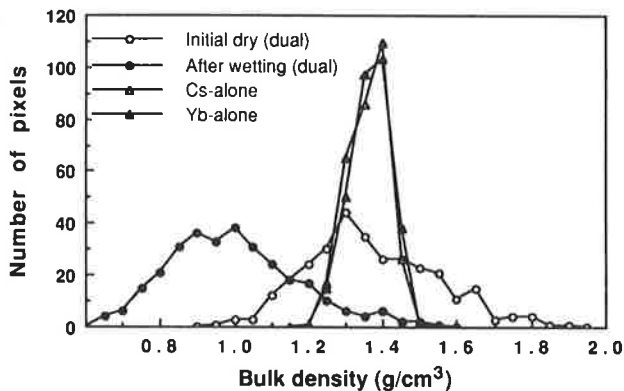


Fig. 6. The distribution of pixel bulk density in a slice of soil obtained by dual-energy gamma computerized axial tomography (CAT) scanning before and after wetting, using a counting time of 13.0 s, and the distribution of bulk density in the slice that would have been calculated if single-energy ^{137}Cs or ^{169}Yb scanning had been used.

images of these scans, showing the spatial distribution of pixel ρ_s before and after wetting are shown in Fig. 5c and d, respectively. The shift in the distribution curve for ρ_s towards the left in Fig. 6 shows the decrease in ρ_s of the York soil on wetting. The distributions of pixel ρ_s using single radioactive sources (^{137}Cs and ^{169}Yb) at the same counting time represents the actual variation in pixel ρ_s within the scanned slice. The excessive spread of the distribution of ρ_s calculated from the dual-gamma-ray CAT scanning, both before and after wetting of York soil, is the result of propagation of the single-source errors described above. The systematically higher ρ_s of York soil near the column walls before and after wetting in Fig. 5c and 5d illustrates the fact that the packing of the soil columns on the vibrator resulted in an uneven ρ_s , since this effect was not visible in scans of the column filled with water (Fig. 4).

Even at the counting time of 13 s used here, the values of $\sigma(\theta_v)$ and $\sigma(\rho_s)$ for pixels remain unacceptably large for most purposes. Estimates of the counting time required to provide values in a more acceptable range can be made using the relationship between $\sigma(\theta_v)$ for pixels in a scan of a uniform field of water and counting time (Fig. 3). Use of this relationship indicates that, to obtain a $\sigma(\theta_v)$ on the order of $0.05 \text{ cm}^3/\text{cm}^3$, an individual ray-sum counting time of 35 s would be required, resulting in a total scan time of 23 h for a 5.8-cm o.d. column. This includes the time taken to obtain air counts on either side for calibration purposes. Assuming a normal distribution of counts, a counting time of 169 s would be required to ensure that 95% of the pixels in the scan for θ_v were $\pm 0.05 \text{ cm}^3/\text{cm}^3$ (i.e., $\sigma(\theta_v) = 0.025 \text{ cm}^3/\text{cm}^3$). This would require a total of 112 h to complete one dual-source scan.

These calculations clearly illustrate that, using dual-source gamma CAT scanning, it is possible to measure the spatial distributions of ρ_s and θ_v in soils simultaneously and nondestructively with a satisfactory level of precision. The total scanning time required to obtain this level of precision, however, severely limits the speed and flexibility of the system and, hence, its usefulness in studying these properties in situations where they change with time, for example, during infiltration and redistribution processes.

CONCLUSIONS

Application of CAT to dual-energy-level scanning clearly has the potential to become a major tool for nondestructive studies of the structural status and stability of soils and for soil-plant-water relationships. However, the use of existing gamma source-detector systems is likely to be limited to steady-state or only slowly changing systems by the scanning times required to obtain satisfactory precision in such measurements. Realization of the full potential of this exciting new technique awaits substantial improvements in scanning geometry and counting electronics.

ACKNOWLEDGMENTS

V.K. Phogat is grateful to the Australian International Development Assistance Bureau for the award of an Australian

Commonwealth Fellowship and to Haryana Agricultural University, Hisar, India, for granting study leave.

REFERENCES

- Anderson, S.H., C.J. Gantzer, J.M. Boone, and R.J. Tully. 1988. Rapid non-destructive bulk density and soil water content determination by computed tomography. *Soil Sci. Soc. Am. J.* 52:35-40.
- Anderson, S.H., R.L. Peyton, and C.J. Gantzer. 1990. Evaluation of constructed and natural soil macropores using x-ray computed tomography. *Geoderma* 46:13-29.
- Aylmore, L.A.G., and J.M. Hainsworth. 1988. Studies of soil plant water systems using CAT scanning. *Search (Sydney)* 19:189-190.
- Berman, A.I., and J.N. Harris. 1954. Precision measurement of uniformity of materials by gamma ray transmission. *The Rev. Sci. Instrum.* 25:21-29.
- Brooks, R.A., and G. De Chiro. 1975. Theory of image reconstruction in computed tomography. *Radiology (Easton, PA)* 117:561-572.
- Brooks, R.A., and G. De Chiro. 1976. Principles of computer assisted tomography (CAT) in radiographic and radioisotopic imaging. *Phys. Med. Biol.* 21:689-732.
- Brown, J.M., W.C. Fonteno, D.K. Cassel, and G.A. Johnson. 1987. Computed tomographic analysis of water distribution in three porous foam media. *Soil Sci. Soc. Am. J.* 51:1121-1125.
- Budinger, T.F., and G.T. Gullberg. 1974. Three dimensional reconstruction in nuclear medicine emission imaging. *IEEE Trans. Nucl. Sci.* 21:2-20.
- Cheshire, J.M., Jr., E.W. Tollner, B.D. Verma, and W.M. Blum. 1989. Radiographic detection of soil-incorporated granular pesticides and impacts of application methods on wireworm management. *Trans. ASAE* 32:415-423.
- Crestana, S., R. Cesareo, and S. Mascarenhas. 1986. Using a computer assisted tomography miniscanner in soil science. *Soil Sci.* 142:56-61.
- Crestana, S., S. Mascarenhas, and R.S. Pozzi-Mucelli. 1985. Static and dynamic three-dimensional studies of water in soil using computed tomographic scanning. *Soil Sci.* 140:326-332.
- Davis, J.R., M.J. Morgan, P. Wells, P. Shadbolt, and B. Suendermann. 1986. X-ray computed tomography. I: A non-medical perspective. *Aust. Phys.* 23:245-247.
- Ferguson, A.H., and W.H. Gardner. 1962. Water content measurements in soil columns by gamma-ray absorption. *Soil Sci. Soc. Am. Proc.* 5:390-398.
- Gardner, W.H., and C. Calissendorff. 1967. Gamma-ray and neutron attenuation in measurement of soil bulk density and water content. p. 101-113. *In* Isotope and radiation techniques in soil physics and irrigation studies. IAEA, Vienna.
- Gardner, W.H., G.S. Campbell, and C. Calissendorff. 1972. Systematic and random errors in dual gamma energy soil bulk density and water content measurements. *Soil Sci. Soc. Am. Proc.* 36:393-398.
- Grevers, M.C.J., E. De Jong, and R.J. St. Arnaud. 1989. The characterization of soil macroporosity with CT scanning. *Can. J. Soil Sci.* 69:629-637.
- Groenevelt, P.H., J.G. De Swart, and J. Cisler. 1969. Water content measurement with 60 KeV gamma-ray attenuation. *Bull. Int. Am. Sci. Hydrol.* 14:67-78.
- Gurr, C.G. 1962. Use of gamma rays in measuring water content and permeability in unsaturated columns of soils. *Soil Sci.* 94:224-229.
- Hainsworth, J.M., and L.A.G. Aylmore. 1983. The use of computer-assisted tomography to determine spatial distribution of soil water content. *Aust. J. Soil Res.* 21:435-443.
- Hainsworth, J.M., and L.A.G. Aylmore. 1986. Water extraction by single plant roots. *Soil Sci. Soc. Am. J.* 50:841-848.
- Hainsworth, J.M., and L.A.G. Aylmore. 1988. Application of computer assisted tomography (CAT) to gamma attenuation measurement of soil water content. *Aust. J. Soil Res.* 26:105-110.
- Hainsworth, J.M., and L.A.G. Aylmore. 1989. Non-uniform water extraction by single plant roots. *Plant Soil* 113:121-124.
- Hermon, G.T. 1980. Image reconstruction from projections. Academic Press, New York.
- Hopkins, F.F., I.L. Morgan, H.D. Ellinger, R.V. Klinksiek, G.A. Meyer, and J.N. Thompson. 1981. Industrial tomography applications. *IEEE Trans. Nucl. Sci.* 28:1717-1720.
- Hounfield, G.N. 1972. A method of and apparatus for examination of a body by radiation such as x- or gamma-radiation. *Brit. Patent* 1 283 915. Date issued: Aug. 1968.
- King, L.G. 1967. Gamma-ray attenuation for soil-water-content measurements using Am-241. p. 17-29. *In* Isotope and radiation techniques in soil physics and irrigation studies. IAEA, Vienna.
- Miller, D.G. 1955. Americium-241 as a photon source for gamma absorptometric technique. p. 17. *In* U.S. Atomic Energy Comm. Rep. HW-39971. Hanford Atomic Products Operation, Richland, WA.
- Newton, T.H., and D.G. Potts. 1981. Radiology of the skull and brain. Vol. 5: Technical aspects of computed tomography. Mosby, St. Louis.
- Onoe, M., J.M. Tsao, H. Nakamura, J. Kogure, H. Kawamura, and M. Yoshimatsu. 1983. Computed tomography for measuring annual rings of a live tree. *Proc. IEEE* 71:907-908.
- Panton, D.M. 1981. Mathematical reconstruction techniques in computed axial tomography. *Math. Scientist* 6:87-102.
- Petrovic, A.M., J.E. Siebert, and P.E. Rieke. 1982. Soil bulk density analysis in three dimensions by computed tomographic scanning. *Soil Sci. Soc. Am. J.* 46:445-450.
- Phogat, V.K., and L.A.G. Aylmore. 1989. Evaluation of soil structure by using computer assisted tomography. *Aust. J. Soil Res.* 27:313-323.
- Soane, B.D. 1967. Dual energy gamma-ray transmission for coincident measurement of water content and dry bulk density of soil. *Nature (London)* 214:1273-1274.
- Tollner, E.W., and B.D. Verma. 1989. X-ray CT for quantifying water content at points within a soil body. *Trans. ASAE* 32:901-905.
- Tollner, E.W., B.D. Verma, and J.M. Cheshire, Jr. 1987. Observing soil-tool interactions and soil organisms using x-ray computer tomography. *Trans. ASAE* 30:1605-1610.
- Warner, G.S., J.L. Nieber, I.D. Moore, and R.A. Geise. 1989. Characterizing macropores in soil by computed tomography. *Soil Sci. Soc. Am. J.* 53:653-660.

The physics of water repellent soils

L.A.G. Aylmore

**Invited Ch. in "Water Repellency in Soils", (J.M. Oades and P.S.
Blackwell eds.)
Proc. Natl. Workshop, Adelaide, 1991, 13-25.**

THE PHYSICS OF WATER REPELLENT SOILS

L.A.G. Aylmore

The increasingly apparent incidence of so called water repellent soils has, to some extent, meant that soil scientists have in the last couple of decades, had to modify their concepts of the physics and in particular, the energy conditions governing the entry, retention and movement of water in soils.

The physical laws governing the situation haven't of course changed, but we are being forced to view the whole picture rather than just part of it. Take for instance the concept of soil water potential:

Concept of Matric Potential

Undoubtedly one of the most important and in fact essential concept in soil science, is that of soil water potential and in particular that component which we describe as the "matric potential" arising from surface tension forces. This is usually based on the development of the role of **cohesive** and **adhesive forces** between similar and dissimilar molecules respectively and of surface tension forces, in capillarity (Figure 1).

The **angle of contact** at the interface between a solid and any liquid in contact with it, is essentially determined by the relative magnitude of the cohesive forces between the molecules in a fluid and the adhesive forces between the molecules of the fluid and a solid in contact with it. When the adhesive forces are greater the angle tends to be less than 90°. When they are less the angle is greater than 90°. Whether liquid in the capillary rises or falls is dependant on this angle of contact (Figure 2). For a liquid which wets the surface there is a tendency for the liquid to be drawn into the capillary by the net component of the surface tension force in that direction. The meniscus will move up or down as required until the hydrostatic head counterbalances the surface tension forces.

Equating the surface tension force with the head of liquid leads to:

$$P = \rho gh = 2(\gamma/r) \cos (\text{angle of contact}) \quad (1)$$

For most purposes the angle of contact between water and soil particles has generally been assumed to be zero (i.e. complete wetting) or at least substantially less than 90° so that the matric potential is always negative and constitutes a positive gradient for the movement of free water into dry soil. Despite the mass of evidence to the contrary most textbooks today still limit their discussion on matric potential to the zero contact angle assumption, paying only small if any attention to the very significant departures which may occur.

A recognition of the extent and progressive increase in the areas of water repellent soils, where water in contact with the soil surface behaves more like mercury, requiring a positive energy input to force it into the soil, means that we must ensure that we recognise the whole picture and not just the simplified one side of the picture.

The major reason for this workshop is that water in contact with soil for which the particles are coated with a hydrophobic material, does not as we commonly observe, spontaneously enter the soil matrix under the influence of a positive gradient of water potential. Rather the soil matrix is effectively at a higher potential than the water and a positive pressure has to be applied or work done, to force water entry. This is of course the whole basis of the mercury injection technique for determining pore size distributions in porous materials using equation (1).

Assessment of Soil Water Repellency

Most procedures for the assessment of soil water repellency and in particular the effectiveness of ameliorative procedures such as wetting agents, have generally focussed on measurements of soil-water contact angles, rates of drop penetration or water infiltration into the soil surface and the like.

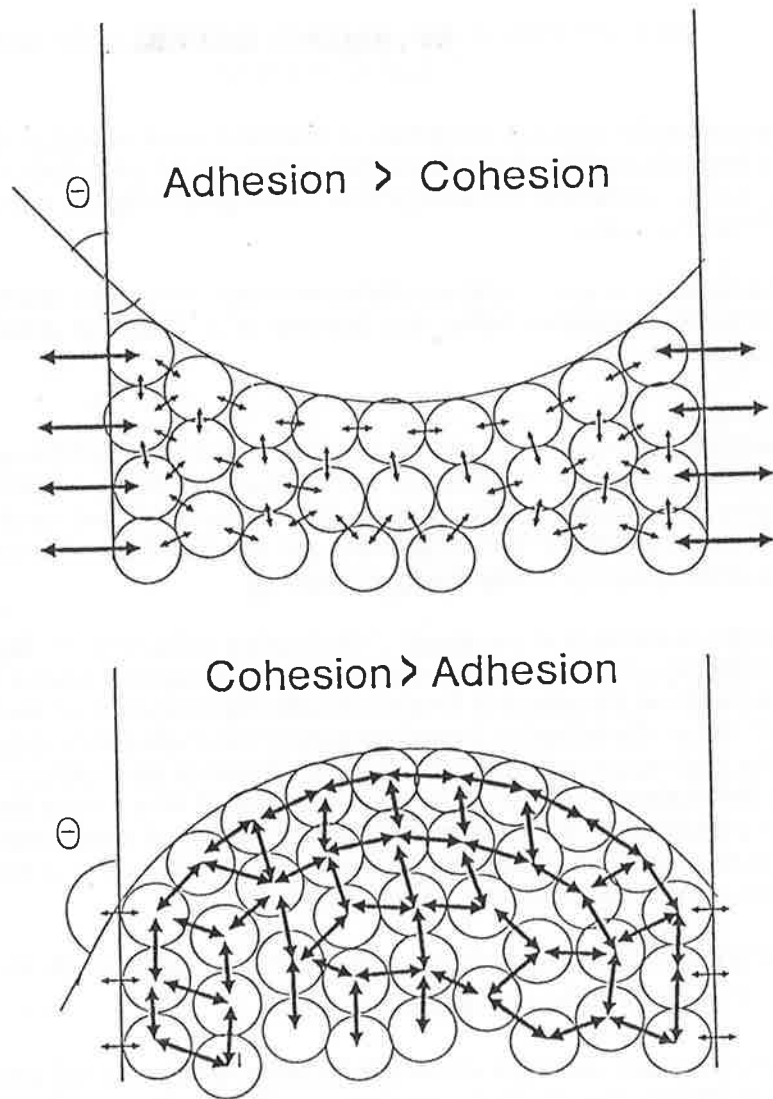


Figure 1. Meniscus dependence on relative magnitude of cohesive and adhesive forces

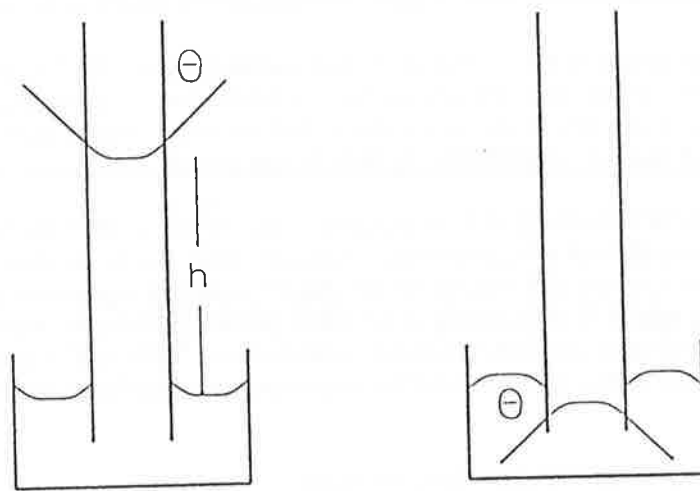


Figure 2. Capillary rise or fall in relation to contact angle

Contact Angle Methods

Measurement of the contact angle between the liquid and solid surface should provide a good indication of the degree of water repellency. In principle this can be measured directly or indirectly (Figure 3). However while the liquid-solid contact angle can readily be geometrically measured for a plane solid surface, in the case of a soil surface the measurement is generally complicated by the effects of surface roughness, pore size distribution and the fact that a water drop will penetrate the surface making direct geometric measurement difficult if not impossible.

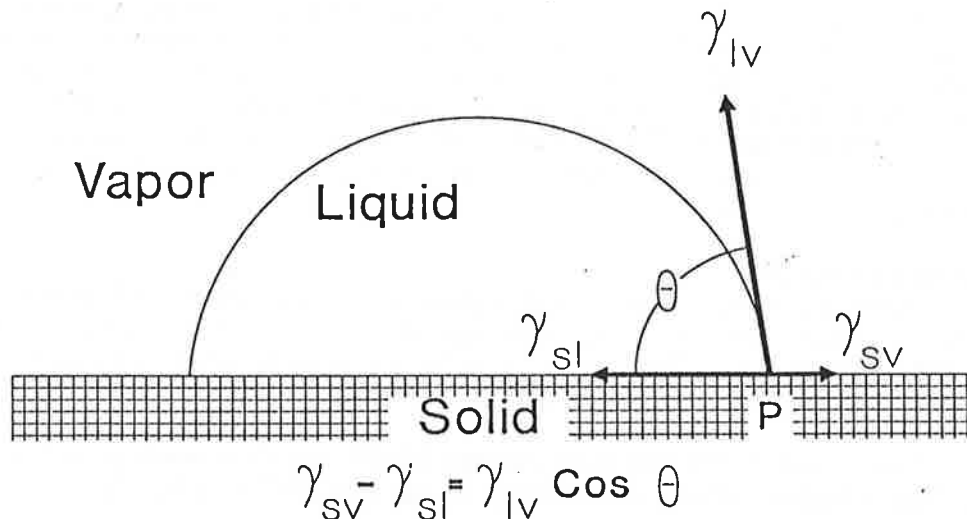


Figure 3. Contact angle for liquid drop

Capillary Rise or Downward Infiltration Rates

Indirect determination of the contact angle can be based upon water flow by capillary rise or downward water infiltration rates. It has been suggested that the infiltration rate approach is less satisfactory, because air may be trapped below a downward advancing front. On the other hand measuring the height of capillary rise has provided reasonably consistent results.

Letey et al (1962) used wetting with ethanol, assumed to have a contact angle of zero, as a benchmark to determine the contact angle for other liquids by comparison on the basis of capillary rise.

Emerson and Bond (1963) used a similar capillary rise approach but used ignited samples as a benchmark on the assumption that this destroyed the water repellency resulting in a contact angle for water of zero. Fink and Meyers (1969) and Nakays et al (1977) have used variations on this approach, the latter immersing tubes packed with soil into water and examining whether the capillary rise was above or below the free surface.

The major disadvantage of these "contact angle" techniques is that they are very time consuming. Also the height of capillary rise does not indicate the initial contact angle since water is in contact with the soil for some time (24 hours). Hysteresis effects arising from the difference between an advancing or receding contact angle may also come into consideration (Hammond and Yuan, 1969).

Water Drop Penetration Time (WDPT)

The method of placing a water drop on the soil surface and recording the time taken for the water to penetrate the sample provides a rapid way of placing the water repellence of the soil into different categories of:

- Wettable (less than a few seconds),
- slightly water repellent (up to 10 seconds),

moderately water repellent (10 seconds to a minute), or severely water repellent (minutes).

These criteria vary between different workers. The fact that the water drop gradually penetrates the soil surface indicates that the contact angle has decreased with time and provides a measure of the stability of the water repellency which can also be of significance.

In general as the surface tension of a liquid decreases, the liquid-solid contact angle decreases. Thus a "critical surface tension" for the solid can be defined as the highest surface tension of a liquid which will wet the solid at zero contact angle (i.e. a property of the solid). Watson and Letey (1970) used this concept to develop an index which they called the "Ninety degree surface tension (NDST) test". This method consists of preparing a series of aqueous ethanol solutions of varying surface tension, and determining the surface tension at which a drop will remain on the soil for 5 seconds.

Molarity Ethanol Drop

A modification of Watson and Letey's (1971) aqueous ethanol drop test involves using droplets of ethanol solution at concentrations of 0.2 m intervals in the range 0-5 m and recording the entry time. The repellence of the soil is represented by the molarity of ethanol which penetrates the soil surface in 10 seconds (MED).

Letey et al (1975) later combined the WDPT and NDST indices to derive a **Water Repellency Index (WRI)**, obtained by dividing WDPT and NDST.

Soils with WRI's less than 0.1 were categorised as wettable
0.1 < WRI < 1.0 slightly repellent
0.1 < WRI < 10 moderately
WRI > 10 severely

In practice the NDST and WRI indices haven't been widely used because of their greater complexity of measurement and the fact that they add little further information than the straight forward WDPT or MED method.

One or other version of the water drop penetration time method has generally been accepted by most workers as the most useful because of its simplicity and rapidity. Although it does not give a quantitative measure of contact angle it can be used in the field as well as in the laboratory, it provides qualitative information on the stability of the water repellence and by and large it correlates reasonably well with the more complex and time consuming contact angle methods.

Bearing in mind the way in which the degree of water repellence for any given soil varies spatially and tends to change in the short term with factors such as time of contact, relative humidity, temperature etc. and in the longer term with various seasonal factors, as has been clearly shown by the work of Peter King, Rob Summers and others, one doubts the virtue of any more accurate measurement of contact angle.

The presence of a substantial angle of contact rather than zero, has a number of important consequences.

Infiltration

Water infiltration and movement through the soil profile has been the subject of a massive amount of experimental and theoretical work over the years to provide an understanding of and the ability to describe and predict, water movement in the unsaturated state.

Bodman and Coleman's (1944) simplistic picture of the characteristic saturation, transmission and wetting front zones during the infiltration of water into a uniform soil under the influence of gravitational plus matric potentials (Figure 4), has generally dominated our

approach. An analysis of the energy conditions governing this process of infiltration on this basis can readily be made.

If the total potential difference influencing water movement into the soil H is given by the sum of the matric potential h_c and the gravitational head $-z$, then the flux of water in the wetted region is given by Darcy's law such that:

$$\text{Flux} = \Theta v = -k (dH/dz) = -k (dh/dz) + k \quad (2)$$

where Θ is the soil water content, k is the hydraulic conductivity, z is the vertical co-ordinate and v is the velocity of the water.

If the soil is uniform down the profile such that the original soil matric potential across the wetting front remains constant at some value h_L the gradient dh/dz becomes progressively smaller as infiltration proceeds. Thus it is evident that these energy conditions will predict a decrease in infiltration rate with time (Figure 5), irrespective of any other decreases resulting from dispersion, structural breakdown, and so on. This is of course a common observation in many circumstances and John Philip, Yves Parlange and many others have developed theoretical treatments based on considerations of these energy conditions, to describe the relationship between infiltration rates and time for different situations.

(e.g. Philip's $i = St^{1/2} + At$)

In contrast, what we commonly see with the presence of water repellent coatings is the reverse of this trend as the degree of interaction between water and the soil surfaces increases with time (Figure 5). That is, the rate of water entry increases with time of wetting.

This may be due to the substances responsible for water repellence being slightly soluble and hence dissolving progressively with time or simply being displaced by water. Water vapour movement by diffusion may make the soil more wettable at less repellent sites (De Bano, 71, 81). Letey (1975) also suggested that the dissolution of materials in the soil may also reduce its surface tension and hence gradually increase wettability.

There is a further consequence of the increased angle of contact for non-wetting soils of some interest. If we consider the energetics of the situation for a uniform non-wetting profile and follow Peter Raats simple (1973) analysis, integration of equation (2) over the region $0 < z < L$, produces:

$$\Theta_s v_s = k_s ((h_0 - h_L)L + 1) \quad (3)$$

The velocity at the wetting front is given by:

$$u = (\Theta_s v_s - \Theta_i v_i) / (\Theta_s - \Theta_i) \quad (4)$$

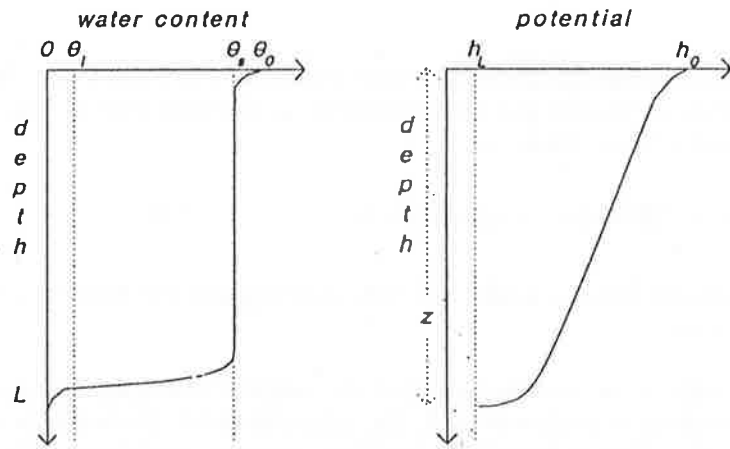
$$(k_s (h_0 - h_L)/L + (k_s - k_i)) / (\Theta_s - \Theta_i) \quad (5)$$

A small perturbation in an initially plane wetting front will tend to disappear if u decreases with L because any element that gets ahead of the rest is slowed up. On the other hand such perturbations will tend to grow if u increases with L . From (5) it follows that:

$$du/dL = -K_s (h_0 - h_L)/L^2 (\Theta_s - \Theta_i) \quad (6)$$

The factor $k_s/L^2(\Theta_s - \Theta_i)$ is inherently positive. Hence it follows that the front is unstable if:

$$h_0 - h_L < 0 \quad (7)$$



h = matric potential
 $-z$ = gravitational head
 v = velocity of water
 k = hydraulic conductivity

Figure 4. Water content and energy relations during infiltration

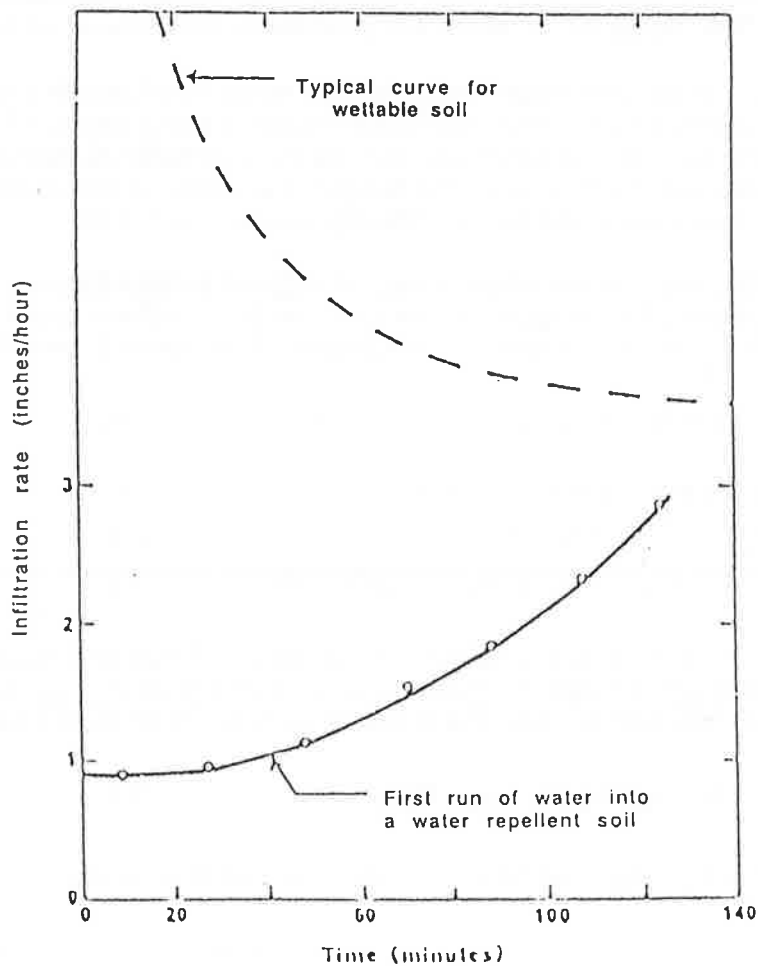


Figure 5. Infiltration rates in a water repellent soil as compared with a typical infiltration curve for a wettable soil (De Bano, 1969).

Since in wetting soils the matric potential at the wetting front (h_L) is inherently negative it follows from the criteria derived in equation (7) that the wetting front will be stable (Figure 6). Consequently in almost all studies of this type it has been tacitly assumed that the advance of the wetting front is stable and that small perturbations in flow patterns will tend to disappear.

On the other hand when h_L , the matric potential in the soil ahead of the wetting front, is effectively positive as for water repellent soils, equation (7) yields a negative value and du/dL in equation (6) is positive, indicating that u increases with depth. In this circumstance any small perturbation in the wetting front will tend to grow and result in the fingering so commonly observed during water entry into water repellent soils.

Of course uneven wetting in a soil profile can and will also result commonly from uneven distribution of hydrophobic materials in the profile as well but it is interesting to note that as for the decrease in infiltration rate with time in wetting soils, the appearance of fingering in the wetting front for a water repellent soil is a natural consequence of the energy conditions prevailing.

There are a number of other physical consequences of water repellence which are of considerable importance including:

Run-off

Reduced infiltration will obviously mean increased run-off. Virtually all workers in the field have noted that the threshold for run-off from water repellent soils is much lower than for wettable as one would expect. In Dough McGhie's report it was less than a third as I recollect. This is obviously a very important consideration in catchment hydrology from the point of view of both water and soil conservation. The implications with respect to erosion are obvious.

Evaporation

A number of workers (Hillel and Berliner, 1974; Fairborn and Gardiner, 1974; Lemon, 1956; Kimball, 1973) have demonstrated that the addition of hydrophobic mulchs to the soil surface is effective in conserving water. Essentially because of the hindrance which they provide to capillary rise. Similarly one could expect that once water had entered a soil through a water repellent layer, this could in turn act to restrict subsequent loss of water through capillarity. The weaker attraction between water and hydrophobic surfaces enables the surface pores to be emptied more easily. Once this happens transport is then largely dependent on vapour transport.

Aggregate Stability

The presence of hydrophobic coatings can also significantly influence aggregate stability by reducing the explosive effects of wetting and hence dispersion. Furthermore it is interesting to note that Hillel and Berliner in 1974 demonstrated that large sized water repellent aggregates can actually greatly increase water infiltration into a soil. However if the aggregate size falls below a critical size (in their case > 2.5 mm) infiltration was decreased).

Factors On Which Water Repellence Depends And Potential Amelioration

Clearly our success in ameliorating water repellence will depend on a full understanding of the physical, chemical and biological factors involved and the roles they play. From the purely physical point of view we have to consider:

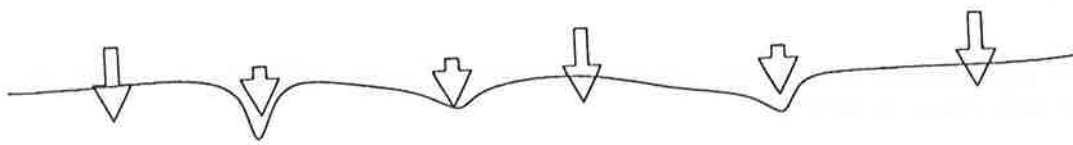
Properties of liquid

Surface tension - Use of wetting agents

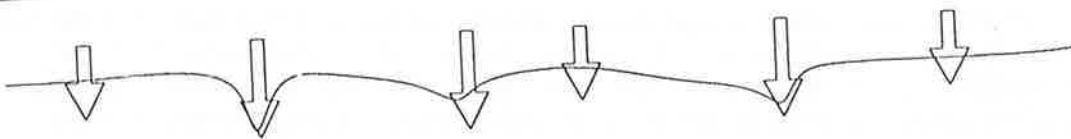
1. Lower contact angle
 - (a) coat surfaces
 - (b) Lower surface tension of water

Front is unstable if $h_o - h_L < 0$

Wetting Soils - h is inherently negative
hence stable front



Non-wetting Soils - h is positive
hence unstable front



leads to fingering

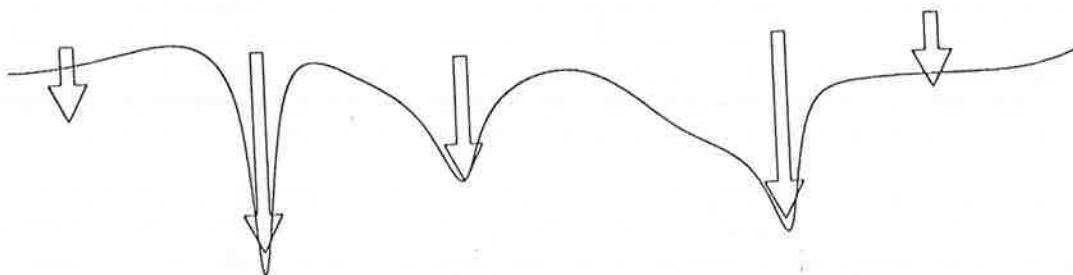


Figure 6. Stability of wetting front

The addition of wetting agents which act to lower the surface tension either by adsorption of appropriate materials at the solid/water interface or by reducing the surface tension at the water/air interface can produce dramatic improvements in infiltration times and quantities. Yoshi Sawada's comparison of infiltration times with and without a number of such wetting agents illustrates how significant this can be and these improvements can mean equally dramatic increases in germination and growth (Figure 7).

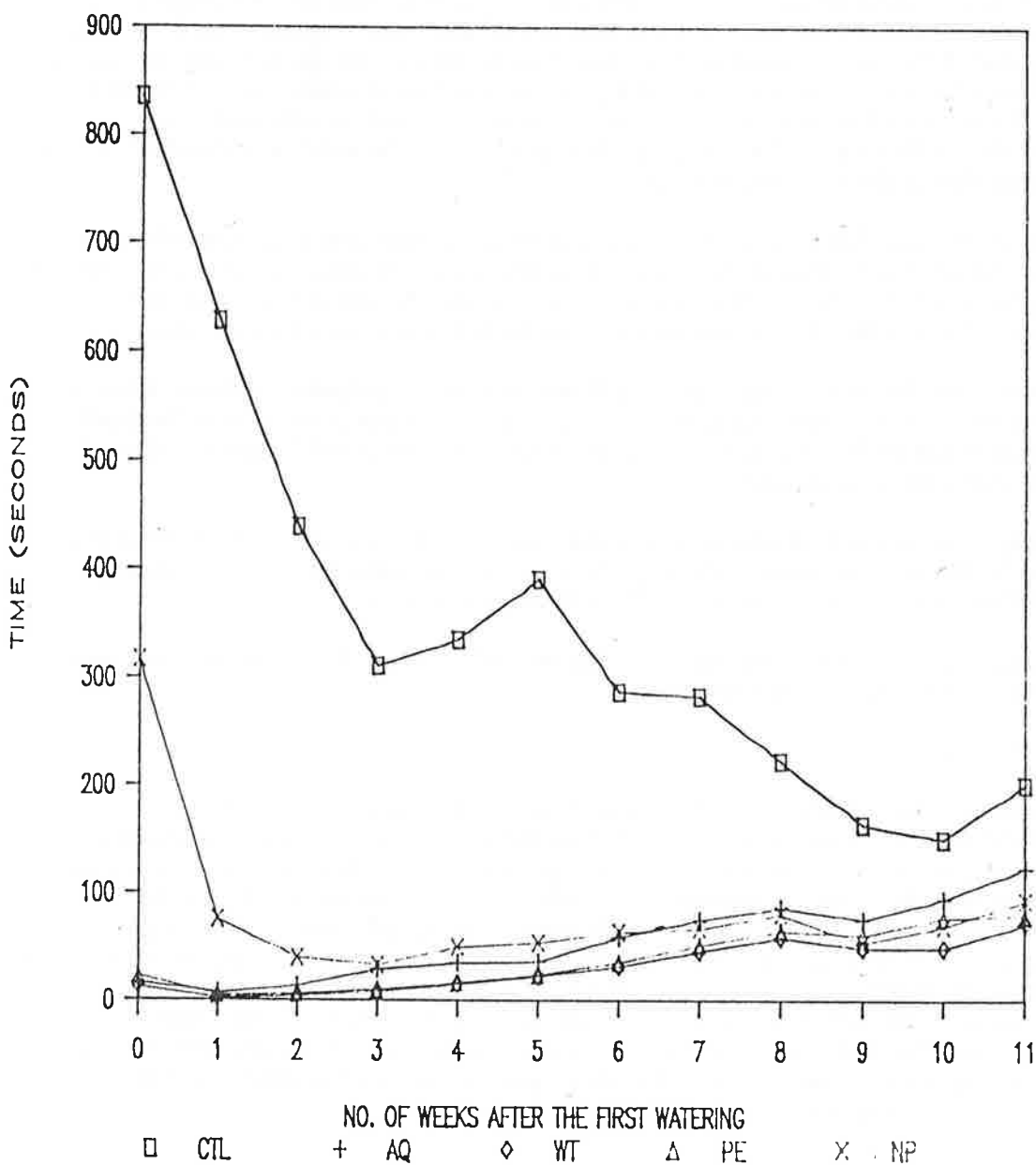


Figure 7. Infiltration time of water (19.2 ml) applied to the Boyanup soil treated with various wetting agents applied at half the recommended rate (i.e. 2.5 ml/l water/m²). AQ - Aqua Soil Wetter; WT - Wetta Soil; PE - PE61; NP - NPEL; CTL - Control

However the cost of applying wetting agents has so far effectively limited their usefulness to specialised applications in horticulture, turf greens and the like and we need to devise more efficient ways of applying these in broad acre usage such as the application in bands used by Dough McGhie and others.

Rob Summers explored the rather novel idea that it might be possible to improve the efficiency of the activity of some of these agents by preventing their adsorption on the soil constituents.

From measurements of liquid surface tension using a Wilhelmy plate surface tension meter, Rob Summers found that neither of the two commonly used 'Aquasoil' and 'Wettasoil' significantly reduced the surface tension of the liquid/air interface. He showed that the surface tension reduction of a solution in water due to a given concentration added, was very little changed after the solution had been in contact with a sand as a result of adsorption and concluded that their activity as soil wetting agents is probably at the soil/water interface i.e. by adsorption rather than at the air/water interface.

On the other hand 'Supa Soak', a commercial wetting agent and a number of others acted to reduce the surface tension at the air/water interface and consequently any adsorption of the wetting agent would reduce its effectiveness. The surface tension of this solution was significantly reduced as a result of adsorption when it had been in contact with a sand.

Rob very logically considered that the addition of suitable polymers to competitively bind to the sites adsorbing the wetting agent, thus maintaining its concentration in the liquid and the lowering of the surface tension, would be an advantage and could significantly reduce the costs of applying the wetting agent.

Unfortunately Rob effectively drew a blank with the polymers which he evaluated in this regard but further investigation of this approach seems warranted since it may greatly improve the economics of broad scale application of wetting agents.

The extent to which a wetting agent is adsorbed will also be significant in determining the depth to which it is effective in a soil profile.

Properties of Solid

Particle size distribution, specific surface area, pore size distribution

These characteristics are closely related. Generally speaking the larger the particle size the larger the pores in the matrix and the lower the specific surface area. Repellency is caused by organic materials which form a hydrophobic coating on soil particles so clearly the effect of the soils constitution on its susceptibility to the deposition of organic molecules and the coverage achieved, will be important. Because of their small surface area per unit volume sandy soils are more likely to be more extensively coated and with thicker hydrophobic films. Consequently sandy soils have been found to be the most susceptible to severe water repellency problems (De Bano et al. 1975 Robs thesis). On the other hand the clay minerals have much higher specific surface areas, are hydrophilic and have little affinity for the amphiphilic molecules responsible for water repellency.

Nature of Surface

The characteristics of the surface available for deposition of layers of organic matter clearly also seems to play a significant role in determining their susceptibility to this effect.

Several workers have demonstrated good inverse correlations between specific surface area and degree of water repellency (Roberts and Carbon, 1971; Letey et al, 1975). However as Dough McGhie has demonstrated for the Mallet hill soils, heavier soils can in appropriate circumstances succumb to water repellency.

Addition of Fine Particulate Matter

Since a low clay content and coarse texture (i.e. low specific surface area) is probably the most susceptible condition for the natural occurrence of water repellence, the application of fine particles to enhance the specific surface area, the water holding capacity and the nature of the soil surfaces, is a very obvious approach to overcoming the problem. Various workers have investigated the feasibility of the addition of clay minerals, fly ash, silica and other fines and their effects on soil properties and plant growth with varying results. One has of course to monitor the possibility of a number of other potential hazards both physical (e.g. structural crusting) or chemical (toxicity) which might be associated with the addition of such materials.

Some preliminary data which Paul Blackwell has obtained illustrates the effect that small additions of clay or fine limestone can have in reducing the infiltration time for water into a water repellent sand. The lime may be effective both from the surface area increase and by increasing the pH since research by some workers has suggested that non-wetting may increase as acidity increases (Figure 8).

Similarly ponding or increasing the water head at the soil surface, will obviously enhance water entry and any surface treatment such as presswheel furrows which achieves this is worth investigation.

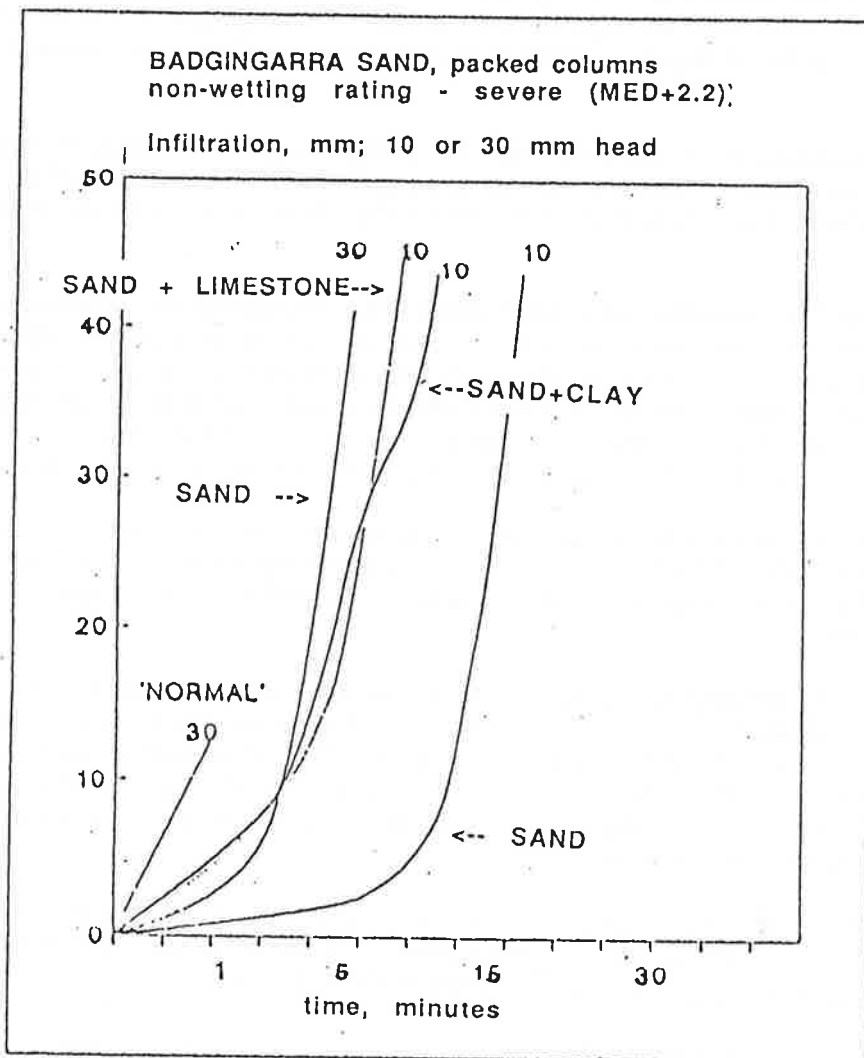


Figure 8. Effect of clay and fine limestone in reducing infiltration time (Paul Blackwell)

Cultivation

Other cultivation techniques may also be useful both in mixing water repellent surface soil with subsoil to increase its wettability. There are some doubts about the value of this approach since it incurs the risk of losses in fertility, increased erosion, soil structural problems etc. and may not last very long. On the other hand I believe some workers in New Zealand have recently espoused the idea of alternate turnover of topsoil followed by burning, as a progressive method of removing the water repellent organic material.

Cationic Effect

There is clear evidence that the nature of the cations associated with the organic coating materials, plays an important role in determining their water repellence and methods of changing this by replacing hydrogen, calcium and magnesium by sodium and potassium either by chemical means or plant rotation seem worthwhile.

Application Of Cat Scanning

It is important to realise that the true test of the effectiveness of the wetting of a soil involves not only the amount of water to enter the soil but also the uniformity of distribution of the water in the soil. As discussed earlier water repellence naturally encourages fingering in the water entry profile and many workers (e.g. Bond, 1964; Gilmour, 1968) have noted that water tends to drain downward through narrow channels in water-repellent soils. Poor water dispersion would thus be an important factor limiting the establishment and growth of plants on such soils.

Over the last decade I have, with a number of my postgraduate students, been using the technique known as computer assisted tomography applied to the attenuation of X - and gamma radiation (CAT scanning) to study soil water content distributions in proximity to plant roots on a microscale.

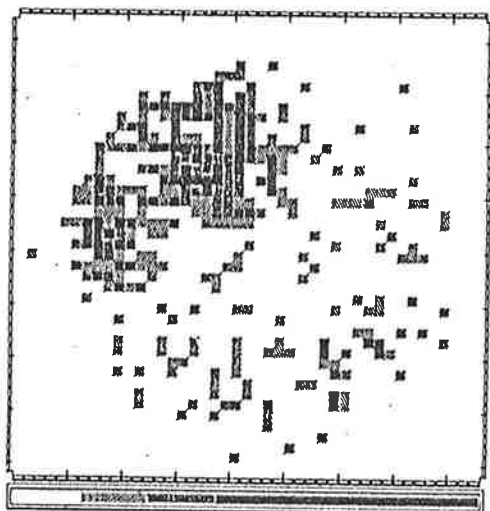
In brief the CAT scanning procedures gives one a measure of the attenuation of the radiation beam and hence the density or water content, in each element of a matrix of small squares known as pixels, in a cross-sectional area of a scanned soil core or column. Thus in a slice through a typical water repellent soil to which a given amount of water has been applied (Figure 9) we see one small area which has wet significantly while the remainder is effectively bone dry. The intensity of shading indicates the degree of wetting or water content.

Sawada et al (1987) in particular used this to devise what we have called a **Soil Water Dispersion Index (SOWADIN for short)** to characterise the proportion of the **surface area wet (SAW)** and the **degree of water dispersion (WD)** in the scanned layer of a soil core or column.

By arbitrarily defining any pixel with a measured water content above the standard deviation of the measuring system as "WET" and those below as "DRY", we obtain a SAW value which is a very accurate description of the "wettability" of the soil in that layer. Similarly the water distribution (WD) can be characterised by the degree of "dispersion" of the water around the slice as opposed to being in discrete areas. This is done on the basis of each pixels proximity to another dry or wet pixel.

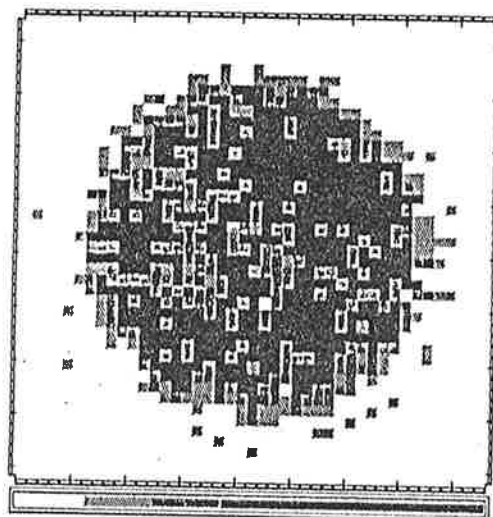
In contrast a scan through a similar core which has previously been treated with a wetting agent (Figure 10) illustrates the more uniform wetting achieved. A more effective agent produces significantly greater water content in the test slice.

Thus the higher the SAW value the more of the slice that has been wet. A low WD means that the water is clustered in discrete regions while a higher value means that it has been distributed more evenly throughout the slice.



cat filename	C6WT12.WAT
maximum	0.370023
third level	0.300000
second level	0.200000
first level	0.100000
minimum	0.000000
image dimensions	43x43 pixels
column radius	18 pixels
n pixels	1009
column mean	0.057330
column stdev	0.094534

Figure 9. Moderately water repellent soil - water only treatment. Scan depth 20 mm. Sowadin WD/SAW = 54/36



cat filename	C6WT13.WAT
maximum	0.588890
third level	0.300000
second level	0.200000
first level	0.100000
minimum	0.000000
image dimensions	43x43 pixels
column radius	18 pixels
n pixels	1009
column mean	0.225309
column stdev	0.133722

Figure 10. Moderately water repellent soil - Wetta Soil treatment. Scan depth 20 mm. Sowadin WD/SAW = 100/98

This technique can be used to characterise the water repellency of cores taken from the field including bowling greens, parks etc. as well as to evaluate the efficiency and longevity of different techniques or wetting agents in overcoming repellency.

The combination of CAT scanning and conventional longitudinal scanning of columns provides a clear overall picture of the distribution and movement of water in a soil column.

In summary it seems reasonable to conclude that the physics of water repellence at the surface of soil particles is well understood. However, the consequences of that repellence with respect to water movement in soil profiles and soil water availability, and the most effective measures for alleviating the problems arising will require substantial laboratory and field investigation.

Numerical Simulation of Pesticide Transport Measured in a Sandy Soil

R.S. KOOKANA, R.D. SCHULLER AND L.A.G. AYLMORE

Soil Science and Plant Nutrition, The University of Western Australia, Nedlands, WA

Pesticide transport models based on the convective-dispersive equation have been developed incorporating both equilibrium and non-equilibrium sorption. The one-dimensional form of the equation was solved numerically by the implicit finite-difference method. These models were tested using transport data for simazine pesticide.

Breakthrough curves (BTCs) of simazine were obtained at various pore water velocities in laboratory columns packed with a sandy soil from the Swan Coastal Plain, Western Australia. The soil is under intensive horticulture and is therefore subjected to repeated applications of pesticides each year. Sorption time-dependency of simazine was studied in separate experiments relevant to the transport situation. The rate parameters were obtained independently rather than by curve fitting to the BTCs.

The experimentally determined time-dependency of the simazine sorption during flow did not conform to first-order kinetics nor did the transport simulations based on a first-order equation accurately describe the BTC. The sorption kinetics of simazine were found to be more accurately represented by a two-site kinetic equation, i.e. with a fraction of total sites (Type-1) showing instantaneous sorption and the remaining sites (Type-2) exhibiting diffusion dependent sorption. The transport model based on this two-site equation satisfactorily described the simazine BTCs observed at four different pore water velocities. The position of the BTC of simazine was found to be mainly dependent on the fraction of Type-1 sites present and the subsequent approach to equilibration on the rate parameter for Type-2 sites. The proportion of Type-1 and Type-2 sites and the rate parameter for type-2 sites varied with pore water velocity.

The study shows that sorption of pesticides during transport depends directly on the accessibility of sorption sites to the pesticide rather than the sorption reaction, that is essentially instantaneous. As the pore water velocity decreases, the residence time of the pesticide in a unit volume of soil increases and thus increases not only the proportion of sites involved in essentially instantaneous reaction (e.g. inter-aggregate or external surface of organic matter) but also the time to diffuse into less accessible regions.

INTRODUCTION

Numerous mathematical models for describing and predicting the transport of non-reactive and reactive solutes (including pesticides) under saturated as well as unsaturated conditions have been developed in recent years. These models are of particular value in that they not only allow more accurate prediction of solute distributions with time but also facilitate the interpretation of measured solute distributions in terms of the specific mechanisms involved in the transport process.

A variety of solute transport models have been applied with varying degrees of success, to simulate the leaching of pesticides through the soil profile (*Brusseau and Rao, 1989*). An essential requirement for the validation of solute transport models is the independent measurement of the input parameters in the model. Under most circumstances this requirement is not or cannot be fulfilled. However, the present paper reports simulations carried out using independently measured parameters.

A brief review of existing solute transport models is provided. The suitability of the sorption rate parameters of pesticide in soils, obtained under flow conditions, is then evaluated for simazine with the equilibrium and nonequilibrium solute transport models incorporating various kinetic equations.

THEORY

Transport Models Based on the Convective-Dispersive Equation

According to the miscible displacement theory, the total mass flux of solute as a result of the combined effects of dispersion and convection (J_s), can be represented as

$$J_s = J_d + J_c \quad (1)$$

where J_d and J_c represent mass of solute transported through a cross-sectional area in a unit time ($\text{kg m}^2\text{d}^{-1}$) by diffusion and convection, respectively.

According to Fick's law, solute mass flux transported by diffusion through bulk soil can be stated as

$$J_d = -\theta D_p(\theta) \frac{dC}{dx} \quad (2)$$

where D_p is the effective diffusion coefficient (m^2d^{-1}), θ is volume fraction of soil water (m^3m^{-3}), C is the solute concentration in liquid phase (kg m^{-3}) and x is distance (m).

For one-dimensional steady flow in a homogeneous soil of uniform water content, the solute mass flux transported by convection and mechanical dispersion is given by

$$J_C = -\theta D_m(v) \frac{dC}{dx} + v \theta C \quad (3)$$

where v is the average interstitial flow velocity ($m d^{-1}$); θ is the water filled porosity and D_m is the mechanical dispersion coefficient as a function of v ($m^2 d^{-1}$). D_m is considered proportional to the first power of average flow velocity

$$D_m = L_{disp} |v| \quad (4)$$

where L_{disp} is the dispersion length (m) and $|v|$ is the absolute value of v .

The total solute flux by diffusion and convection can be represented as

$$J_S = -\theta [D_m(v) + D_p(\theta)] \frac{dC}{dx} + v \theta C \quad (5)$$

or

$$J_S = -\theta D(v, \theta) \frac{dC}{dx} + q C \quad (6)$$

where D is the apparent dispersion coefficient ($m^2 d^{-1}$) and q is the volumetric water flux ($m d^{-1}$).

According to the continuity equation (Kirkham and Powers, 1972) one-dimensional solute mass conservation for the substance in the soil system can be represented as

$$\frac{dC_t}{dt} = -\frac{dJ_S}{dz} - R_t \quad (7)$$

where C_t is the total solute mass in the soil system ($Kg m^{-3}$), J_S is the total mass flux of the solute ($kg m^{-2} d^{-1}$), z is the depth in soil (m) and R_t is the rate of transformation or degradation of the solute in soil ($kg m^{-3} d^{-1}$).

By combining [6] and [7] and considering the various soil interactions for a reactive solute such as sorption, degradation, etc. [7] takes the form

$$\frac{d(\theta C + \beta S)}{dt} = \frac{d(\theta D(v, \theta) dC/dz)}{dz} - \frac{d(qC)}{dz} - R_t \quad (8)$$

where the total amount of the substance in the soil system (C_t) is the sum of the amounts present in liquid (θC) and solid phase of the system (βS), i.e.

$$C_t = \theta C + \beta S \quad (9)$$

where β is the dry bulk density of the soil ($kg m^{-3}$) and S is the solute concentration sorbed ($kg kg^{-1}$). In [8] z has replaced x to specifically designate a positive downward space coordinate.

In short term experiments that result in residence times of a solute in soil of the order of hours, and for persistent solutes, the term representing transformation can be neglected. Equation [8] now becomes

$$\frac{d(\theta C + \beta S)}{dt} = \frac{d(\theta D(v, \theta) dC/dz)}{dz} - \frac{d(qC)}{dz} \quad (10)$$

For a non-reactive solute under laboratory conditions with constant flow velocities (temporally and spatially) and water contents, [10] reduces to

$$\frac{dC}{dt} = D \frac{d^2C}{dz^2} - v \frac{dC}{dz} \quad (11)$$

To solve [10] under given initial and boundary conditions, a specification of the functional relationships between concentrations of solute in soil solution phase, C , and solid phase, S , is required.

When the sorption reaction is instantaneous, equilibrium exists between solution and solid phase concentrations and the relationship between the two concentrations is given by the sorption isotherm. Under such conditions an equilibrium transport model can be used. When the sorption reaction is time dependent then a suitable function describing the time dependency of sorption reaction needs to be incorporated into the solute transport model and thus such models are designated as non-equilibrium models.

Equilibrium Models

The basic assumptions of equilibrium models are that at a given depth (z) and time (t):

- (1) the pesticide in the liquid phase is in equilibrium with that sorbed on the solid phase of the soil, and
- (2) there is a uniform concentration of pesticide in the liquid phase.

For a linear sorption isotherm $S = K C$ and [10] can be restated as

$$R \frac{dC}{dt} = D \frac{d^2C}{dz^2} - v \frac{dC}{dz} \quad (12)$$

where

$$R = \left(1 + \beta \frac{K}{\theta} \right) \quad (13)$$

In [13] R is referred as the retardation factor (Hashimoto et al., 1964).

Defining $D^* = D/R$ and $v^* = v/R$, [12] becomes

$$\frac{dC}{dt} = D^* \frac{d^2C}{dz^2} - v^* \frac{dC}{dz} \quad (14)$$

For a nonlinear sorption isotherm ($S = KC^n$) the retardation function $R(C)$ is concentration dependent and is given by

$$R(C) = (1 + \beta \theta K C^{n-1}) \quad (15)$$

The models described in [12] and [15] assume that the sorption and desorption isotherms are reversible and single-valued. However, the sorption isotherms are not always single-valued and commonly exhibit hysteresis. Thus the parameters representing sorption and desorption isotherms may be different and should be incorporated into [14].

Non-Equilibrium Models

The non-equilibrium models available in the literature can be divided into one-site kinetics models and two-site kinetics models. These are briefly described below.

One-site kinetic models

These models assume that the sorption reaction on all the reaction sites in soil is controlled by a single kinetic rate law (*Hornsby and Davidson, 1973*). A first order reversible kinetic reaction has generally been used by different workers (e.g. *Hornsby and Davidson, 1973*).

A first-order reversible kinetic equation based on linear sorption isotherm can be stated as

$$\frac{dS}{dt} = k (K C - S) \quad (16)$$

where, k is kinetic rate coefficient. For equilibrium sorption the equation reduces to

$$S = K C \quad (17)$$

Equation [16] can be stated in the form

$$\frac{dS}{dt} = k_a C - k_d S \quad (18)$$

where $K = k_a/k_d$ and k_a and k_d are the forward and backward rate coefficients (T^{-1}).

The transport equation [10] with the first-order kinetic equation [16] can be stated as

$$\frac{dC}{dt} + \frac{\beta}{\theta} [k(K C - S)] = D \frac{d^2C}{dz^2} - v \frac{dC}{dz} \quad (19)$$

Generally, these models have been found unsatisfactory in describing pesticide movement in soils (*Rao and Jessup, 1983*), and this has led to the concept of two-site kinetics models.

Two-site kinetic models

The various two-site non-equilibrium models available in the literature can be grouped into two classes, (1) chemical process models and (2) physical process models. While the chemical process models consider non-equilibrium to arise from the actual sorption reaction at the soil surfaces being time dependent, the latter models consider the sorption reaction to be instantaneous with the sorp-

tion being governed by the rate of physical transport of pesticide to and from the reaction sites.

Chemical process models

The two-site non-equilibrium models proposed by *Cameron and Klute (1977)* assume the presence of two types of sites for sorption reaction in soils. While the Type-1 sites are assumed to achieve an instantaneous equilibrium, the sorption on Type-2 sites is described by a first order reversible kinetic reaction. The sites can be different in terms of their constitution (organic and inorganic surfaces) and/or in their accessibility to the solutes. The sites where the sorption is diffusion controlled are also included in Type-2 sites (*Cameron and Klute, 1977*).

At equilibrium, sorption on both sites is described by linear sorption isotherms; i.e.

$$S_1 = f K C \quad (20)$$

$$S_2 = (1 - f) K C \quad (21)$$

$$S = S_1 + S_2 \quad (22)$$

where subscripts 1 and 2 refer to Type 1 and 2 sites, respectively, and f is the total fraction of Type-1 sites.

The Type -1 sites are always in equilibrium and hence,

$$\frac{dS}{dt} = f K \frac{dC}{dt} \quad (23)$$

The sorption on Type-2 sites is governed by the following, linear and reversible first-order kinetic reaction.

$$\frac{dS_2}{dt} = k [(1 - f) K C - S_2] \quad (24)$$

The transport equation [10] takes the form

$$\left(1 + f K \frac{\beta}{\theta}\right) \frac{dC}{dt} + \frac{\beta}{\theta} \frac{dS_2}{dt} = D \frac{d^2C}{dz^2} - v \frac{dC}{dz} \quad (25)$$

$$\frac{dS_2}{dt} = k [(1 - f) K C - S_2] \quad (26)$$

A transport equation for a two-site kinetic model using a non-linear sorption isotherm, can similarly be developed.

Physical process model

This model was applied by *van Genuchten and Wierenga (1976)* for sorbed solutes. The model assumes that the liquid phase in the soil is divided into "mobile" (macroporosity) and "immobile" (microporosity) regions. The transport of the solute in the mobile region is assumed to take place through convection-dispersion but the transport in the immobile region is taken as diffusion controlled. The rate of diffusion depends on the concentration gradient between the two regions. Solute sorption-desorption on both the regions are considered to be instantaneous in nature. According to the physical process model, non-equilibrium phenomena are exhibited

by both sorbing and non-sorbing solutes.

According to this model, the transport equation for linear sorption isotherms can be stated as:

$$f_1 R_1 \frac{dC_1}{dt} + R_2 (1 - f) \frac{dC_2}{dt} = f_1 D \frac{d^2C}{dz^2} - f_1 v_1 \frac{dC_1}{dz} \quad (27)$$

$$\theta_2 R_2 \frac{dC_2}{dt} = a (C_1 - C_2) \quad (28)$$

$$R_1 = \left(1 + \frac{\beta}{\theta} \right) f_1 K \quad (29)$$

$$R_2 = \left(1 + K (1 - f_1) \frac{\beta}{\theta_2} \right) \quad (30)$$

$$f_1 = \frac{\theta_1}{\theta} \quad \text{and} \quad \theta = \theta_1 + \theta_2 \quad (31)$$

$$v_1 = \frac{V}{f_1} = \frac{v \theta}{\theta_1} \quad (32)$$

where subscripts 1 and 2 denote mobile and immobile regions, respectively, a is a mass transfer coefficient (T^{-1}) for solute transfer between mobile and immobile regions and f_1 is the fraction of soil water in the mobile region.

The transport equation for the non-linear sorption isotherm can be obtained and is similar to [26] (*van Genuchten and Wierenga, 1976*).

Nkedi-Kizza et al. (1984) showed that both models (based on chemical and physical processes, [25] and [27]) can be put into exactly the same mathematical form by introducing dimensionless variables. The two models can not be differentiated on the basis of BTC only.

There are a number of other physical diffusion models wherein the aggregate geometry is taken into consideration (*Rao et al., 1980a; van Genuchten, 1985*). However, to extend these models to actual field situations, aggregate size distributions, as well as variations in the shapes of aggregates need to be taken into account. While *Rao et al.* (1982) developed a method to reduce the range of aggregate sizes to a single equivalent aggregate, a model by *Rasmuson* (1985) included the distribution directly in the model. To achieve accurate results a minimum of ten classes of aggregates-size is required according to *Cooney et al.* (1983). Considering the uncertainty with respect to pore geometry analysis, the description of diffusion in the form of first order mass transfer coefficient, as in [28], is more attractive.

Numerical Solution of the Models

The numerical solutions for the various models were obtained by applying finite-difference approximations to [10]. To illustrate the procedure used in obtaining the finite difference solutions, a grid mesh laid over the rectangular $x-t$ plane is shown in Figure 1. The mesh size is determined by x and t that are increments of the variables x and t , respectively. The set of points in the $x-t$ plane are given by $x_i = i x$, $t_j = t$, when $i = 0, 1, \dots, I$ and $j = 0, 1, \dots, J$.

Initial and boundary conditions

A finite-difference scheme was used to solve the transport equations numerically with the following initial and boundary conditions.

$$C = 0, S = 0 \quad 0 \leq z \leq L, t = 0 \quad (33)$$

$$v C - D \frac{dC}{dz} = v C_0 \quad z = 0, t \leq t_1 \quad (34)$$

$$v C D \frac{dC}{dz} = 0 \quad z = 0, t > t_1 \quad (35)$$

$$\frac{dC}{dz} = 0 \quad z = L, t > 0 \quad (36)$$

These conditions represent a soil column of length L cm, that is initially void of the pesticide and to which a pesticide concentration of C_0 is applied at an average pore water velocity, v , for a period of time t_1 .

Stability and Convergence Considerations

Application of the finite-difference technique to transport models has demonstrated that when the dispersion term is small, the solution may develop oscillations and/or be smeared by numerical dispersion. However, the degree of such effects varies with different techniques.

Of the two commonly used finite difference systems, i.e. explicit and implicit, the implicit systems have the advantage of being unconditionally stable (*Richtmeyer and Morton, 1967*). In other words, the value of t can be chosen independently of x , thus providing a method that is computationally efficient. A central difference scheme that reduces the truncation error and thus leads to faster convergence of finite-difference equation was accomplished with the Crank-Nicholson approximation. Thus a system with the advantages of being both convergent and unconditionally stable, was employed.

The finite-difference form of [10] was obtained with second-order finite-difference approximations in time and space obtained from Taylor series expansion using the Crank-Nicholson approximation.

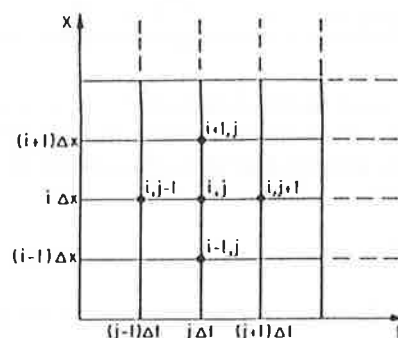


Figure 1. An illustration of a grid mesh used in the numerical solution of the convective-dispersion equation.

MATERIALS AND METHODS

Soil and Pesticide

A sandy soil from the Swan Coastal Plain was used in the study. The soil belongs to the Bassendean association and contains very little silt plus clay (3 %) and organic matter (1.2 %). The physico-chemical properties of the soil have been published elsewhere (*Singh et al.*, 1990). The soil is used for horticultural crop-production and therefore receives repeated applications of pesticides and other agrochemicals.

Simazine [2-chloro-4,6-bis(ethylamino)-1,3,5-triazine] is a commonly used pesticide belonging to the s-triazine family of herbicides. It is a soil applied herbicide and is generally used at a rate of 1-4 kg ha⁻¹ per application. Simazine is a weakly basic herbicide and has a low water solubility.

Soil Column Studies

Chloride and simazine breakthrough curves (BTCs) corresponding to different flow velocities were obtained in stainless steel columns (300 mm long, 25 mm inner diameter) packed with Bassendean sand. To obtain uniform packing, the columns were filled under constant vibration. Several pore volumes of dilute salt solution (0.005 M CaCl₂) were passed through the columns before their use for experimental BTCs. A HPLC pump was used to supply the solution at a constant flow rate. Samples of the soil solution eluting out of the soil column were collected using an automatic fraction collector and were analysed for solute concentrations (chloride or simazine pesticide). Dual peaks for chloride BTCs were taken as an index of unsatisfactory and nonuniform packing of soil in a column. Some details of the experimental conditions for the BTCs are given in Table 1.

Estimation of Parameters

Dispersion coefficients

The dispersion coefficients were obtained through the longitudinal hydrodynamic dispersivity parameter (L_{disp}) in [4]. In soil columns the variance of a BTC resulting from a pulse of chloride was calculated from the zero-, first- and second-order moments of the BTC (*Grubner*, 1968). The value of L_{disp} calculated from the BTCs of chloride was about 4 mm. A similar value has been reported by *Wagenet* (1983). The velocity dependence of L_{disp} has been recently examined by *Gerritse and Singh* (1988). The pore water velocities used in the study were such that L_{disp} was little affected.

Sorption isotherm parameters

The sorption data from the batch equilibrium studies of simazine (*Singh et al.*, 1990) were used in an equilibrium model. The sorption isotherm of simazine, corresponding to low solution concentrations up to 3 5g ml⁻¹, fitted very well ($r^2 = 0.99$) to a linear sorption isotherm. Since the concentration of simazine never exceeded 15 g ml⁻¹

during the experiments to obtain the BTCs, it was appropriate to use the linear sorption isotherm in simulations for simazine. The Freundlich sorption coefficient used in these simulations is given in Table 1.

For non-equilibrium models, additional rate parameters were required. For the one-site kinetic model, the first-order rate coefficient, and for the two-site kinetic models, two additional parameters; (1) the rate coefficient, and (2) the fraction of Type-1 sorption sites, were needed. Both kinetic parameters (i.e. rate coefficient and fraction of Type-1 sites) were obtained by a flow technique applying the peak maxima method to breakthrough curves obtained at various pore water velocities and with various input concentrations. The method has been described in detail by *Singh* (1989). The rate parameters obtained by applying a two-site kinetic equation are given in Table 1. The kinetic data obtained by the flow technique for simazine also fitted a parabolic diffusion law (*Crank*, 1983) very well ($r^2 = 0.96$). The validity/utility of the parabolic diffusion law is discussed below.

RESULTS AND DISCUSSION

Simulations with Equilibrium Model

The linear equilibrium model [12] was tested for the BTCs of simazine in Bassendean sand. A comparison of the experimental and simulated BTCs for the pesticide is shown in Figure 2. The equilibrium model predicted much higher retardation of pesticides (by a factor of 7) than that observed for the experimental BTCs. This is not surprising as many workers have observed that under flow conditions (even at low pore water velocities) the equilibrium conditions for sorption reactions do not exist (reviewed by *Rao and Jessup*, 1983; *Brusseau and Rao*, 1989).

The earlier appearance of the experimental BTCs than that expected from the equilibrium model, can not be attributed to hysteresis, since the hysteresis during sorption-desorption has been shown to only affect the

Table 1. Experimental conditions during the column studies.

Column length	0.300	m
Inner diameter of column	0.025	m
Weight of soil added	0.196	kg
Bulk density	1.34	kg m ⁻³
Pore volume	0.48x10 ⁻⁴	m ³
Porosity	0.31	m ³ m ⁻³
Range of pore water velocities	45-893	m d ⁻¹
Input concentration of Simazine	1.0x10 ⁻⁶	kg m ⁻³
L_{disp}	0.4x10 ⁻²	m
Sorption coefficient (K)	1.85x10 ⁻⁶	kg m ⁻³
Fraction Type-1 site	0.1	m ³ m ⁻³
Rate coefficient for Type-2 sites	0.15	d ⁻¹

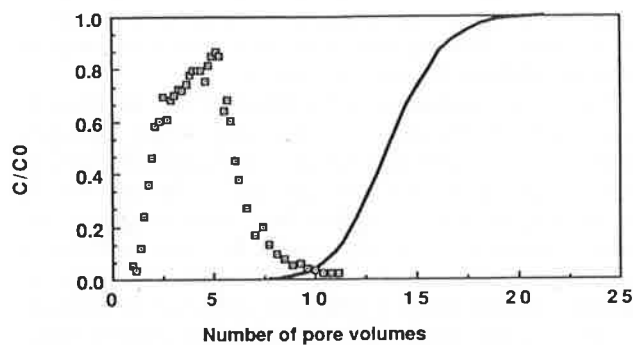


Figure 2. Simulation with equilibrium model (solid line) as compared to observed BTC of simazine. parameters in addition to those in Table 1 were: $v = 6.2 \text{ mm min}^{-1}$, $D = 24.8 \text{ mm}^2 \text{ min}^{-1}$.

shape of BTCs on the flank with progressively decreasing concentration known as the "elution front" (*van Genuchten et al.*, 1977).

The failure of the equilibrium model to describe the experimental BTCs clearly shows that the kinetics of sorption are affecting the retardation of the BTCs of simazine at the flow rates used in this study.

Simulations with Non-Equilibrium Models

First-order kinetic model

Simulations were also carried out using a non-equilibrium model, with a first-order rate equation for sorption. The simulated BTCs for simazine obtained with different values of first-order kinetic parameters (as the experimental rate parameters were not available) are shown in Figure 3. Simulations with the first-order kinetic model could not describe the experimental BTCs satisfactorily.

Two-site kinetic model

The BTC of simazine in Bassendean sand were also simulated with a non-equilibrium model using a two-site Freundlich kinetic equation (*Boesten and van der Pas*, 1988). Using this equation, the fraction of sites showing instantaneous sorption (Type-1 sites) of simazine in Bassendean sand obtained by the flow technique were found to be very low, i.e. only 1.3 % of the total (*Singh*, 1989). With this value of Type-1 sites the two-site non equilibrium model essentially reduces to a one-site model. It has already been shown in the previous figure (Figure 3) that the one-site non-equilibrium model failed to describe the observed BTC.

Batch experiments showed that the chemical reaction of sorption was essentially instantaneous (*Singh*, 1989), yet the retardations of the BTCs were affected by pore water velocities. This is possible only when all the reaction sites are not accessible at a given flow rate and more and

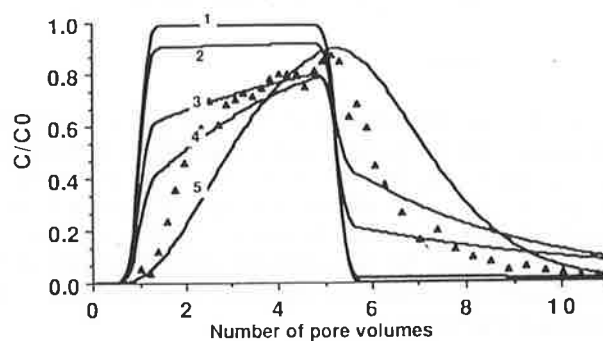


Figure 3. Simulation with non-equilibrium model using first-order kinetic equation. The values of first-order rate coefficient for sorption, corresponding to numbers on curves were: 1 = 0.0001, 2 = 0.001, 3 = 0.005, 4 = 0.01 and 5 = 0.05 min^{-1} . other parameters were: $v = 6.2 \text{ mm min}^{-1}$, $D = 24.8 \text{ mm}^2 \text{ min}^{-1}$ and those given in Table 1.

more sites become accessible with a decrease in pore water velocity. Since the flow technique to study the time dependency of sorption is based on the loci of peaks of BTCs (*Singh*, 1989), it seems to represent the Type-1 sites only.

Since the sorption data for simazine also conformed to a parabolic diffusion law (as mentioned earlier), the fraction of adsorption completed at a given residence time can be obtained directly using this relation. The fractions of Type-1 sites were calculated corresponding to different retention times [ratio of L/V ; where L is length of column (mm) and V is the pore water velocity (mm min^{-1})] at different flow velocities and are given in Table 2. The rate parameter for Type-2 sites could not be measured independently and hence was varied in the simulation.

The simulations carried out with the fractions of Type-1 sites (Table 2) and experimental BTCs corresponding to different flow velocities are shown in Figure 4 (a and b). BTCs at four different pore water velocities were observed. The simulations with various rate parameters for Type-2 sites showed that the retardation of the BTCs were only affected by the fraction of sites in equilibrium and not by the fitted values of the rate parameters for Type-2 sites. The latter affected the tail of the BTCs only. This establishes that the independently measured values of fractions for Type-1 sites by the flow technique (*Singh*, 1989) are valid. At lower pore water velocities the model predicted slightly more retardation than observed. The fraction of Type-1 sites had to be extrapolated for the lower flow velocities studied and, possibly, the relation slightly overestimated the fraction of Type-1 sites.

It should be noted that the rate parameter for Type-2 sites, obtained by the best fit simulation of the observed BTCs, also varied with the flow rates. Considering the instantaneous nature of the sorption reaction, a rate

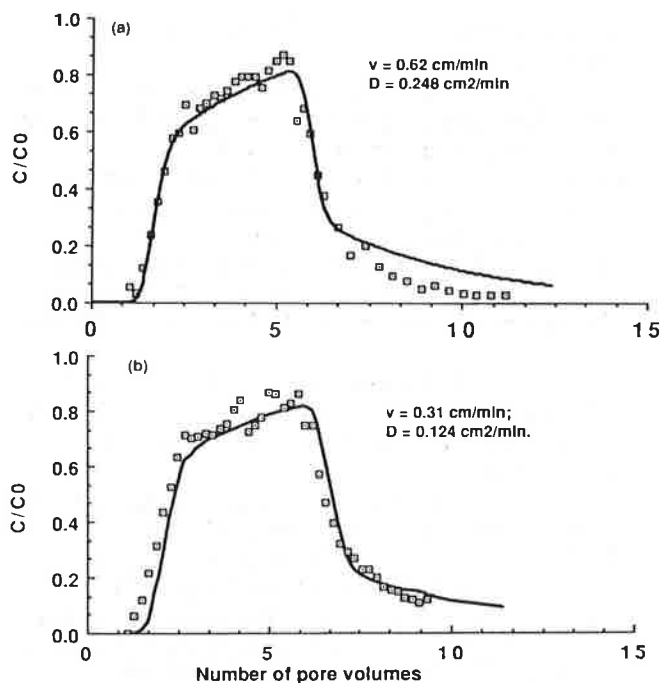


Figure 4a. Simulated and experimental BTCs of simazine at (a) 6.2 and (b) 3.1 mm min⁻¹ pore velocities. Simulation was performed using the fraction of Type-1 site given in Table 2 with values for k for Type-2 sites of (a) 0.005 and (b) 0.001. Other parameters are given in Table 1.

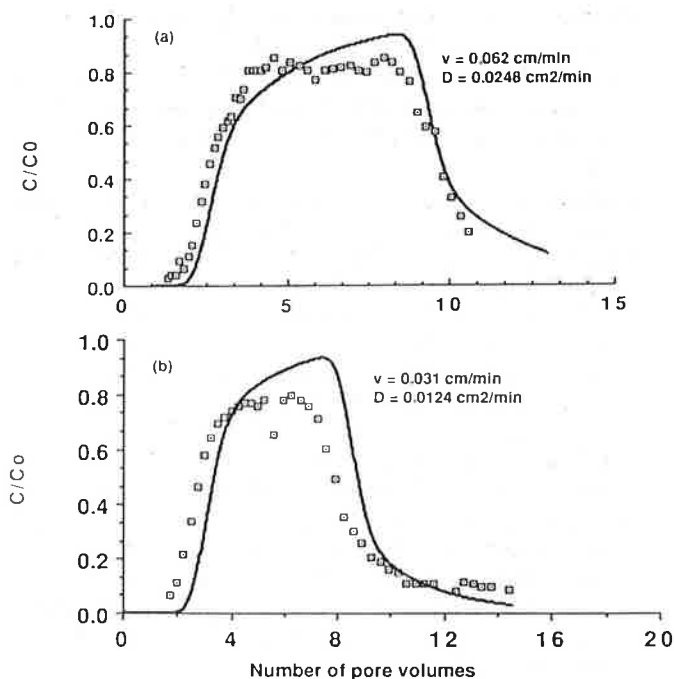


Figure 4b. Simulated and experimental BTCs of simazine at (a) 0.62 and (b) 0.31 mm min⁻¹ pore water velocities. Simulation was performed using the fraction of Type-1 site given in Table 2 with values of k for Type-2 sites, (a) 0.0001 and (b) 0.0005. Other parameters given in table 1.

parameter representing a chemical kinetic reaction is not expected to vary with pore water velocity. Thus, the rate parameter for Type-2 sites represents some physical process such as diffusion into the soil matrix. These observations are consistent with the kinetic studies discussed by Singh (1989). The kinetic data obtained by the batch method suggest an essentially instantaneous sorption and hence the non-equilibrium conditions observed during flow are of a physical nature.

On the basis of the previous kinetic studies (Singh, 1989) and the transport studies described in this paper, it is concluded that during transport of pesticides in soils sorption processes are not in equilibrium. Sorption reaction of pesticides on soil particles occurs instantaneously but access to the sorption sites varies with pore water velocities. The sorption sites vary in terms of their

accessibility to pesticides in moving solution such that some are easily accessible (external) whereas others are less easily accessible (e.g. possibly within organic matter matrix). Thus sorption may be limited by physical processes such as the transport of pesticides to the sites of sorption. With decreasing pore water velocity, not only does the fraction of easily accessible sites increase, but the time available for the pesticides to diffuse to sites that are less accessible, also increases. The fraction of the former type of sites can be measured independently by a flow technique described by Singh (1989).

REFERENCES

Boesten, J.J.T.I. & van der Pas, L.J.T., 1988. Modeling adsorption/desorption kinetics of pesticides in a soil suspension. *Soil Sci.* 146: 221-231.
 Brusseau, M.L. & P.S.C. Rao, 1989. Sorption nonideality during organic contaminant transport in porous media. *CRC Critical Reviews in Environmental Control.* Vol. 19: 33-99.
 Cameron, D.R. & A. Klute, 1977. Convective-dispersive solute transport with a combined equilibrium and kinetic adsorption model. *Water Resour. Res.* 13: 183-188.
 Cooney, D.O., B.A. Adesanya & A.L. Hines, 1983. Effects of particle size distribution on adsorption kinetics in stirred batch systems. *Chem. Eng. Sci.* 38: 1535-1541.

Table 2. Fraction of Type-1 sites calculated from relation based on flow technique.

v (mm min ⁻¹)	L/v (min)	Fraction of Total Sorption	Volume Fraction of Soil Solids
6.2	48.4	0.087	0.126
3.1	96.8	0.109	0.158
0.62	483.9	0.206	0.298
0.31	967.7	0.279	0.404

- Crank, J., 1983. *The Mathematics of Diffusion*. 2nd Ed. Oxford University Press, London.
- Gerritse, R.G. & Rai Singh, 1988. The relationship between pore water velocity and longitudinal dispersivity of Cl^- , Br^- and D_2O in soils. *J. Hydrol.* 104: 173-180.
- Grubner, O., 1968. Statistical moments theory of gas-solid chromatography. *Adv. Chromatogr.* 6: 173-209.
- Hashimoto, I., K.B. Deshpande & H.C. Thomas, 1964. Peclet numbers and retardation factors for ion exchange columns. *Ind. Eng. Chem. Fund.* 3: 213-218.
- Hornsby, A.G. & J.M. Davidson, 1973. Dolution and adsorbed fluometuron concentration distribution in water saturated soil: Experimental and predicted evaluation. *Soil Sci. Soc. Amer. Proc.* 37: 823-828.
- Kirkham, D. & W.L. Powers, 1972. *Advance Soil Physics*. Wiley-Interscience, John Wiley & Sons.
- Nkedi-Kizza, P., J.W. Biggar, H.M. Selim, M.Th. van Genuchten, P.J. Wierenga, J.M. Davidson, & D.R. Nielsen, 1984. On the equivalence of two conceptual models for describing ion exchange during transport through an aggregated oxisol. *Water Resour. Res.* 20: 1123-1130.
- Rao, P.S.C., R.E. Jessup, D.E. Rolston, J.M. Davidson & D.P. Kilcrease, 1980. Experimental and mathematical description of nonadsorbed solute transfer by diffusion in spherical aggregates. *Soil Sci. Soc. Am. J.* 44: 684-688.
- Rao, P.S.C., R.E. Jessup & T.M. Addiscot, 1982. Experimental and theoretical aspects of solute diffusion in spherical and nonspherical aggregates. *Soil Sci.* 133: 342-349.
- Rao, P.S.C. & R.E. Jessup, 1983. Sorption and movement of pesticides and other toxic organic substances in soils. In: *Chemical Mobility and Reactivity in Soil Systems*, D.W. Nelson, K.K. Tanji & D.E. Elrick (eds). Soil Sci. Soc. Am., Madison, Wisc., pp. 183-201.
- Rasmuson, A., 1985. The effects of particles of variable size, shape and properties on the dynamics of fixed beds. *Chem. Eng. Sci.* 40: 621-629.
- Richtmeyer, L.F. & K.W. Morton, 1967. *Difference methods for initial value problems*. Wiley-Interscience, John Wiley & Sons. New York.
- Singh, Rai, 1989. Equilibrium and kinetic aspect of sorption desorption and mobility of pesticides in soils. Doctoral thesis submitted to the University of Western Australia.
- Singh, Rai, R.G. Gerritse & L.A.G. Aylmore, 1990. Adsorption-desorption behaviour of selected pesticides in some Western Australian soils. *Aust. J. Soil Res.* 28: 227-243.
- van Genuchten, M. Th., 1985. A general approach for modeling solute transport in structured soils. In: *Proc. Hydrogeology Rocks Low Hydraulic Conductivity Memoirs of the IAH*, Vol. 17 (part1), pp. 513.
- van Genuchten, M.Th. & P.J. Wierenga, 1976. Mass transfer studies in sorbing porous media: I. Analytical solutions. *Soil Sci. Soc. Am. J.* 40: 473-480.
- van Genuchten, M.Th. & P.J. Wierenga, 1977. Mass transfer studies in sorbing porous media: II. Experimental evaluation with 2,4,5-T. *Soil Sci. Soc. Am. J.* 41: 278-285.
- Wagenet, R.J., 1983. Principles of salt movement in soils. In: *Chemical Mobility and Reactivity in Soil Systems*, D.W. Nelson, K.K. Tanji & D.E. Elrick (eds). Soil Sci. Soc. Am., Madison, Wisc., pp. 123-140.
- R.S. Kookana, R.D. Schuller & L.A.G. Aylmore, Dept. Soil Science & Plant Nutrition, The University of Western Australia, Nedlands, Western Australia 6009.

Soil solute concentration and water uptake by single lupin and radish plant roots

I. Water extraction and solute accumulation

M.A. HAMZA and L.A.G. AYLMORE¹

Soil Science and Plant Nutrition, The University of Western Australia, Nedlands, Western Australia, 6009. ¹Corresponding author

Received 23 September 1991. Revised July 1992

Key words: CAT scanning, ion specific microelectrodes, leaf water potential, lupin, matric potential, osmotic potential, radish, roots, solute accumulation, water uptake

Abstract

Application of computer assisted tomography to gamma and X-ray attenuation measurements and Na⁺-LIX microelectrodes were used to determine the spatial distributions of soil water content and Na⁺ concentrations respectively near single roots of eighteen day old lupin and radish plants. These quantities were monitored at root depths of 3, 6 and 9 cm and at zero, 2, 4, 6, and 8 hour intervals from the diurnal commencement of transpiration. The plants were subjected to two levels of transpirational demand and five Na⁺ soil solution concentration levels. Water extraction rates for the lupin and radish roots increased continuously with time but were substantially reduced with increasing Na⁺ concentration in the treatment. Water uptake was uniform along the length of the essentially constant diameter lupin roots but decreased along the tapering radish roots as the diameter and hence the surface area per unit length of the roots decreased. The accumulation of Na⁺ at the root surfaces of both plants increased gradually with time in a near linear fashion and was slightly higher under the higher transpiration demand. These increases were not exponential as would be expected with non-absorption by the roots and this is considered to be due to back diffusion at the relatively high water contents used. At these water contents matric potentials had a much smaller influence on transpiration than osmotic potentials. The relationships between leaf water potentials (Ψ_1) and osmotic potentials at the root surfaces were linear with the decreases in Ψ_1 almost exactly reflecting the decreases in Ψ_π indicating rapid plant adjustment. Leaf water potentials decreased progressively with time and the relationships between leaf water potential and the transpiration rate were also linear supporting the suggestion of constant plant resistances at any given concentration.

Introduction

The uptake of water and ions by a plant root creates a concentration gradient in response to which water and ions flow from the surrounding soil to the root (Sinha and Singh, 1976). In particular, mass flow associated with high transpiration rates can cause a large flux of ions towards the root and the rapid accumulation of

ions at the soil-root interface may lead to very high concentrations of ions in that zone. Water flow through the root membrane is assumed to be proportional to the difference in the water potential across the membrane (Baveye and Sposito, 1984; Campbell, 1985; Herkelrath et al., 1977). The presence of soluble salts in the soil creates an osmotic potential which lowers the total water potential in the soil (Mengel and

Kirkby, 1982; Nulsen and Thurtell, 1978; Slatyer, 1961). If these salts are excluded by the root the osmotic potential at the root surface should be an exponential function of water uptake (Munns and Passioura, 1984; Passioura, 1984) and will reduce or even prevent further water uptake if the salt concentration in the soil solution is high enough to lower the soil water potential to that of the root. These effects of salt on soil water availability for plant growth have long been recognized (Long, 1943; Wadleigh and Ayers, 1945), but a major problem encountered in any attempt at an exact physical description of soil-water uptake by plant roots, is the inherently complicated space-time relationship involved (Hillel et al. 1975).

Soil water potential at the soil-root interface appears to be the main soil characteristic controlling the availability of soil water for plant growth (Slatyer, 1967) and nutrient concentration at the root surface directly controls nutrient uptake (Claassen and Barber, 1976). However the simultaneous and interactive processes of salt and water transport, as well as the constantly changing status of the plant, makes any attempt to quantitatively describe the drawdown processes of water and solute rather difficult. Consequently, questions as to the extent to which the accumulation of soil solute concentrations (osmotic potentials) influence water availability (Passioura, 1963), the relative magnitudes of soil and plant resistances to water movement under different conditions of soil water potential and transpirational demand (Newman, 1969), and the nature of the water driving forces (Noble, 1974) have remained largely unresolved. Furthermore conflicting results obtained predominantly by the indirect measuring procedures previously only available (Dunham and Nye, 1973; So et al., 1976), raise questions as to the validity of the physical concepts on which previous theoretical treatments (Molz, 1981) have been based. Attempts to resolve these questions have until recently been hindered by the lack of suitable and sufficiently sensitive experimental techniques to measure water and solute potentials in the soil immediately around the root repetitively and in a non-destructive fashion (Dalton and Van Genuchten, 1986). In the present work, an innovative combination of computer assisted to-

mography applied to X- and gamma-ray attenuation (CAT scanning) and sodium-liquid Ion exchanger (Na^+ -LIX) microelectrode techniques has been used to examine, repetitively and in a non-destructive fashion, the dynamics of the simultaneous processes of water uptake and solute (NaCl) accumulation in proximity to single lupin and radish roots.

Materials and methods

Computer assisted tomography

Computer assisted tomography (CAT) applied to X- and gamma-ray attenuation measurement was used to monitor the spatial distribution of water contents in the soil in proximity to single lupin and radish roots subjected to a range of soil solute concentrations and two transpirational demands. A prototype gamma CAT scanner (Hainsworth and Aylmore, 1988) was used in the trial experiments while a medical X-ray Somatom DR/H scanner was used in the major experiments. The Somatom DR/H scanner has a high resolution measuring system SCINTIL-LARC 700 for the highest requirements with respect to image quality and sharpness. The image is displayed immediately following the scan on a video screen in a 512×512 matrix of 2×2 mm pixels. The scan times takes upwards of 1.4 seconds. The software provided with the scanner is able to magnify any area in the scanned slice and pinpoint any pixel (from the root center to the bulk soil) to determine its water content automatically through determining its attenuation coefficient (μ). This can be done in very small distance intervals (i.e. 0.1 mm). Attenuation is expressed in the internationally standardized number scale known as Hounsfield Units (H) given by the relation (Newton and Potts, 1981):

$$H = 1000 \left\{ \frac{(\mu - \mu_w)}{\mu_w} \right\} \quad (1)$$

where μ_w is the linear attenuation coefficient of water (cm^{-1}).

The software is also able to perform some statistical functions to calculate the total water

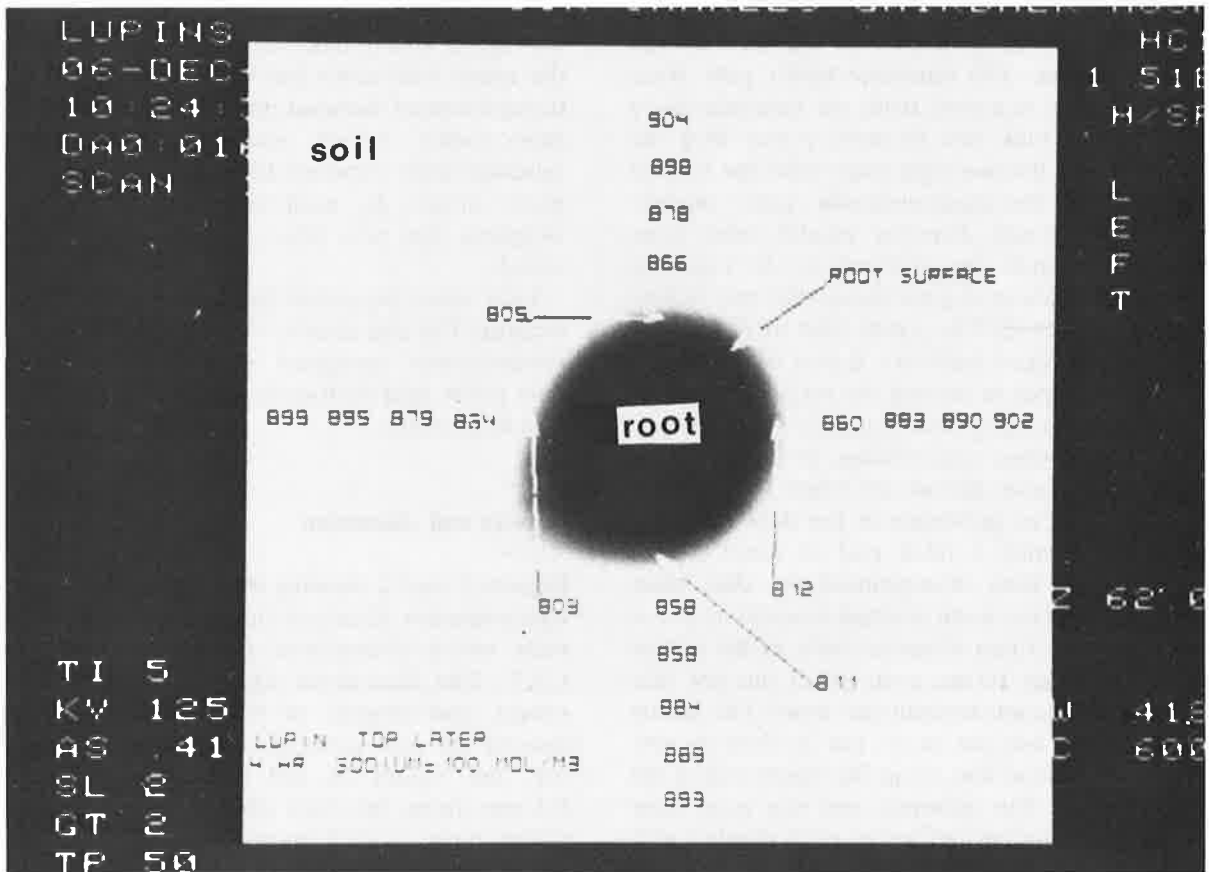


Plate 1. Magnified cross-section through a lupin root showing Hounsfield unit values at root surface and 1.0 mm intervals away from the root surface.

content (through Hounsfield units) of the whole or part of the scanned slice, thus making it easy to calculate water uptake by the plant root for any given section and time. Plate 1 showing a magnified cross-section through a lupin plant root and surrounding soil, illustrates the ease and detail with which measurements near the root can be obtained. Measurable differences in water content of 0.006 g cm^{-3} can be readily detected by both X- or gamma-ray CAT scanning (Hainsworth and Aylmore, 1983, 1988).

Ion sensitive microelectrode technique

Na^+ -LIX microelectrodes as described by Hamza and Aylmore (1991) were used to measure accurately, repetitively, and non-destructively the Na^+ concentrations at appropriate positions adjacent to the plant roots.

Experimental procedure

Experiments were carried out both in cylindrical columns of 4.5 cm diameter and 12 cm tall and in the special microelectrode pots. Twenty containers were uniformly packed to a bulk density of approximately 1.6 g cm^{-3} with an oven dry soil mix consisting of 85% Bassendean sand and 15% Clackline kaolinite from Western Australia. This mix was used to provide a soil medium with negligible swelling and shrinkage and with the most suitable water retention and diffusivity characteristics for these studies (Hainsworth and Aylmore, 1986). All columns and pots were watered with distilled water to a water content of $0.30 \text{ cm}^3 \text{ cm}^{-3}$ and then oven dried again to allow the soil to settle down. The columns were CAT scanned at 3, 6 and 9 cm respectively from the top of the columns. These distances were

chosen to correspond to the top, middle and bottom layers of the roots at the time of the measurements. The microelectrode pots were CAT scanned in a slice from the microelectrode hole to the bulk soil in such a way that the scanning line forms a right angle with the base of the pots at the microelectrode hole. Slightly larger than 2 mm diameter plastic tubes were inserted through the microelectrode holes of each pot to about 1.5 cm inside the pot before packing with soil. The inside end of the plastic tube was covered with two layers of Whatman No 1 filter paper to protect the fragile microelectrode tip from being intercepted by soil particles.

Lupin (*Lupinus angustifolius*, cv Yandee) and radish (*Raphanus sativus*, cv white icicle) seeds were allowed to germinate in the dark on petri-dishes containing a thick pad of moist tissue. These were then transplanted so that their emerged radicles were pointed towards a previously made 0.1 mm diameter hole in the center of the columns 1.5 cm away from the pot side which had the microelectrode hole. The plants were located one cm away, but as close as possible on the same line, from the inside end of the plastic tube. Ten columns and ten pots were planted with lupins and ten of each planted with radishes. As they grew the lupin/radish roots intercepted the perspex bottom of the microelectrode pots, and passed by the inside end of the plastic tube.

Irrigation of the columns and pots containing the plants with saline solutions commenced 11 days after planting. To avoid salt injury the salinity of the solution was increased gradually up to day 14 of planting when the full strength solution was added. Four levels of saline solutions containing 25, 50, 75 and 100 mol m⁻³ Na⁺ respectively, as well as the distilled water treatment were used to irrigate ten individual pots of each plant. After day 17 the soils were rewatered with the saline solution to a water content of 0.3 cm³ cm⁻³. The open end of each container, except for the stem hole, was then sealed with cellophane to prevent water evaporation from the soil surface. The plants were kept in darkness for 24 hours, allowing the water content in the pots to equilibrate. The pots containing the lupins and radishes were then rescanned at the same position after 2,4,6 and 8 hours of exposure

to light and a high transpirational demand (air flow from a fan). The remaining plants received the same treatments but were subjected to low transpirational demand, before being rescanned. Immediately before scanning microelectrode readings were obtained for all pots. Cumulative water uptake by each plant was obtained by weighing the pots after each transpiration interval.

Leaf water potentials for each treatment were measured in situ directly before scanning using a psychrometer equipped with a Wescor HR33 dew point microvoltmeter and a Wescor L-51A leaf hygrometer.

Results and discussion

Figures 1 and 2 showing the effect of electrolyte concentration illustrate the detail and accuracy with which drawdowns can be measured by CAT. The drawdown figures demonstrate the extent and degree of the water drawdowns around the root surfaces and of particular interest, the values of soil water content about 0.1 mm from the root surface. The lupin and radish roots showed markedly different patterns of water extraction along their length. The almost equal diameters and consequently equal root surface areas for all lupin root layers resulted in an essentially uniform absorption along their length. In contrast, the tapering radish roots extracted generally about 50 and 70% more water from their top layers as compared with the middle and bottom layers respectively. Since all layers of the lupin roots absorbed almost the same amount of water, the drawdowns for only the top layers are shown. For the radish plants, a comparison between the top, middle and bottom layer drawdowns is shown for the no-solute treatments (Fig. 2). The drawdown curves for the remainder of the solute treatments and the lower transpirational demand were of similar shape.

The water extraction rates (Q) from individual layers obtained from the CAT scan data, increased with time of transpiration for both plants and for all layers, with the most rapid increases occurring during the first two hours of the transpiration followed by a more gradual increase in

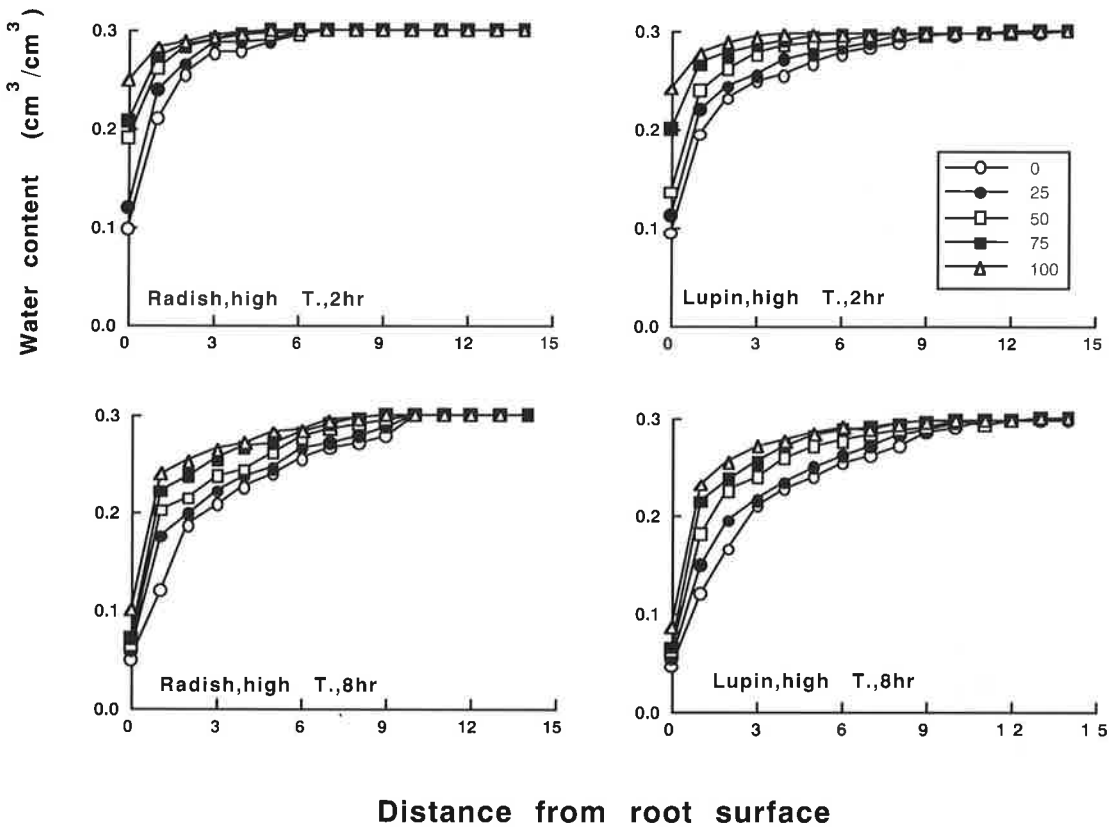


Fig. 1. Water drawdowns from the top layers of single lupin and radish roots subjected to Na⁺ concentrations of 0, 25, 50, 75 and 100 mol m⁻³ Na⁺ after 2 and 8 hours of high transpiration.

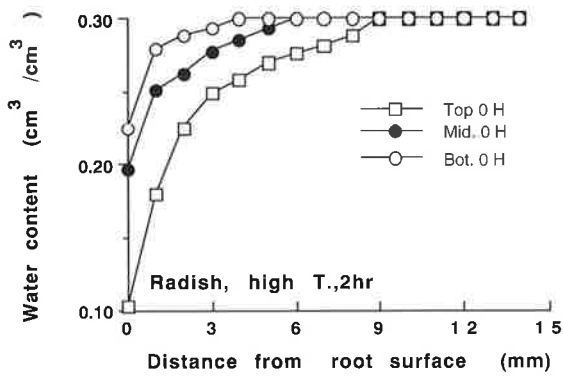


Fig. 2. Water drawdowns from the top, middle and bottom layers of single radish roots after 2 hours of high transpiration demand for the no-solute treatment.

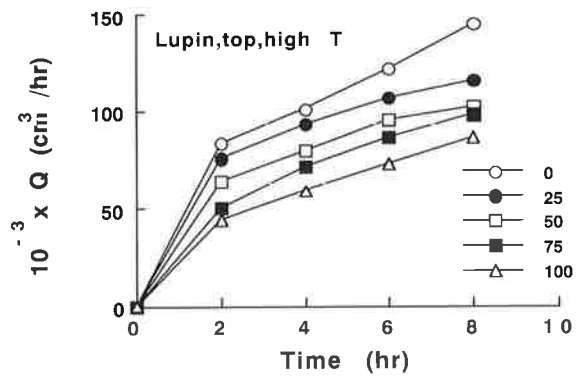


Fig. 3. a Water extraction rates from the top layers of the single lupin roots subjected to high transpiration demand and to solute treatments of 0, 25, 50, 75 and 100 mol m⁻³ Na⁺.

Q in an essentially linear fashion over the remaining 6 hours (Fig. 3). The divergence of the graphs illustrates that the transpiration rate was progressively decreased with increasing solute

concentration in the treatments and this decrease became relatively larger with time of transpiration. The differences in uptake along the radish roots are evident but as uptake along the lupin

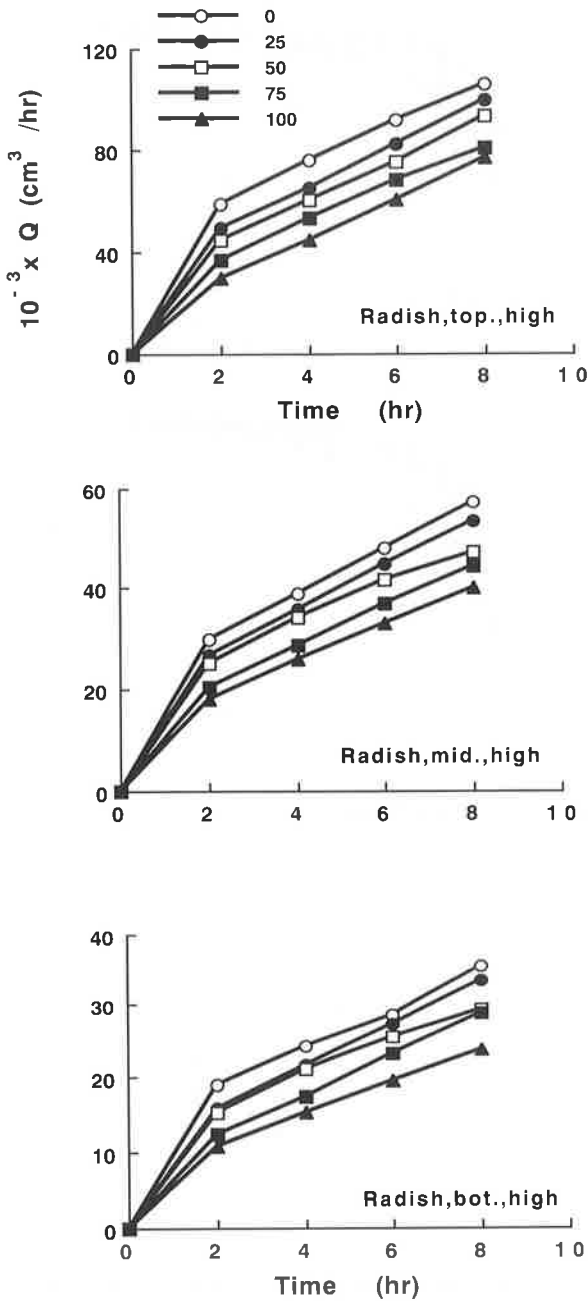


Fig. 3. **b** Water extraction rates from the top, middle and bottom layers of the single lupin roots subjected to high transpiration demand and to solute treatments of 0, 25, 50, 75 and 100 mol m⁻³ Na⁺.

roots was essentially constant, only data from the top layer are shown.

Figure 4 shows the concentrations of Na⁺ at

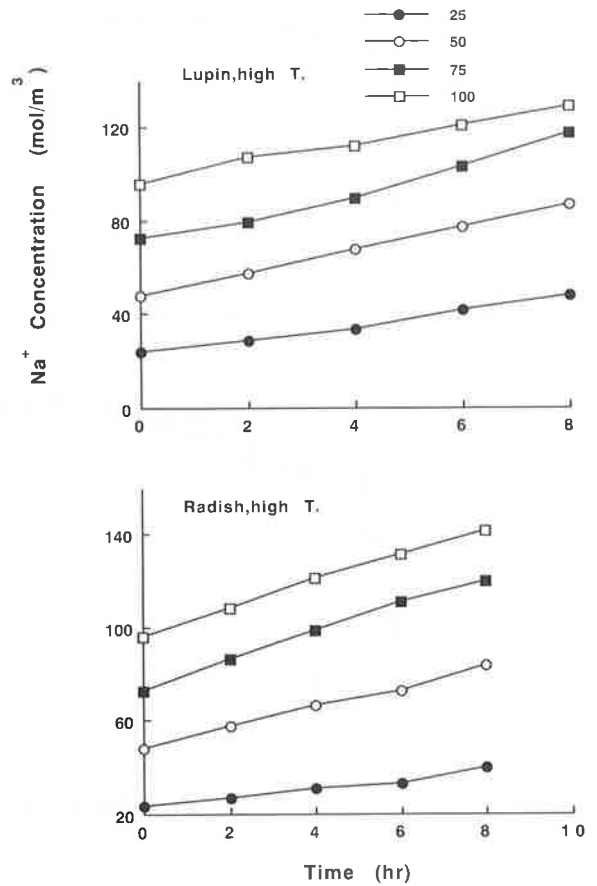


Fig. 4. The relationship between Na⁺ accumulation at the root surface and transpiration interval for the lupin and radish plants subjected to high transpiration demand and solute treatments of 0, 25, 50, 75 and 100 mol m⁻³ Na⁺.

the root surfaces measured using the Na⁺-LIX microelectrode, after various transpiration intervals for the different solute treatments. The Na⁺ concentrations at the root surface increased gradually with time of transpiration in a near-linear fashion. At both lupin and radish root surfaces the concentration of Na⁺ increased more rapidly with increasing Na⁺ concentration in the treatments. At the end of the transpiration period, the lupin roots had accumulated more Na⁺ at their root surface than had the radish. This is to be expected because the lupin roots generally extracted more water per unit length of root than did the radish roots. For the same reason the accumulations of Na⁺ at the root surfaces for both plants were slightly higher under the high transpiration demand.

It is significant that these increases were linear rather than exponential as would be expected with non-adsorption by the roots (Munns and Passioura, 1984; Passioura, 1980). The explanation for this could lie either in absorption of salt by the root or back diffusion from the epidermis or the hypodermis to the bulk soil. Since the reflection coefficient for NaCl at the root surfaces is likely to be close to one, only trivial amounts of solute are expected to cross the root membrane. In addition the linearity of the relationships between the driving forces and Q discussed elsewhere (Hamza and Aylmore, 1992), suggests that the roots act as near perfect osmometers. In this case most or all NaCl should be excluded at the root surface leading to an exponential build-up of NaCl there. However in the present data the increases in NaCl concentrations at the root surfaces were only of roughly the same extent as the increases in the water extraction rates, i.e. about 1.5 to 1.8 times higher under the high transpiration demand compared with the low transpiration demand. Thus it seems likely that, at the relatively high water contents and potentials used, back diffusion from the epidermis or hypodermis to the bulk soil limits accumulation of NaCl (Munns and Passioura, 1984). The minimum matric water potential at the root surfaces reached after 8 hours was -140 kPa.

The values of the instantaneous transpiration rate, Q , after 2, 4, 6 and 8 hours of low and high transpiration demands were calculated as the first derivatives of the third degree polynomial curves fitted to the values of the cumulative water uptakes vs. time. The corresponding values of the matric potentials at the root surface, Ψ_m , were obtained from the CAT scanning data, and the values of the leaf water potentials, Ψ_l , obtained using the psychrometer.

The relationships between Ψ_l and Q were linear for both plants and under both transpiration demands (Fig. 5). Similar linearity was observed for soybean and sunflower by Neumann et al. (1974) who suggested that this indicates a constant plant resistance. As the total root-soil interface potential decreased with time of transpiration, due to the reduction in soil water content and the accumulation of solute at the root surface, the leaf water potentials for both plants

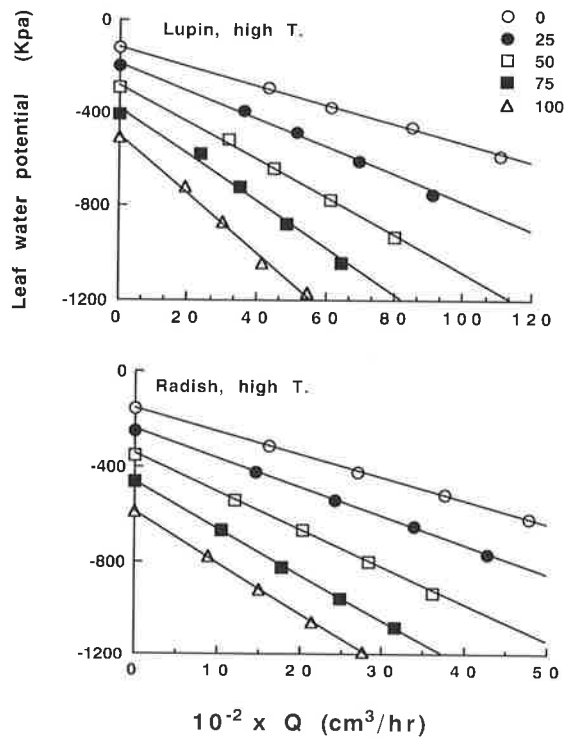


Fig. 5. The relationship between the leaf water potential (Ψ_l) and the transpiration rate (Q) for the lupin and radish plants subjected to high transpiration demand and solute treatments of 0, 25, 50, 75 and $100 \text{ mol m}^{-3} \text{ Na}^+$.

decreased continuously and decreased more rapidly with increasing soil solute concentration. Despite these substantial decreases in the leaf water potentials with increasing solute concentration, the water extraction rates from the individual layers were reduced progressively as the Na^+ concentration in the treatments increased, i.e. the decreases in Ψ_l were inadequate to maintain the same potential gradients and transpiration rates as for the no solute case.

As shown in Figure 6 the values of Ψ_m at the root surface were much higher (i.e. less negative) than the values of Ψ_π for both plants by 3.5 to 10 times. Furthermore, while Ψ_π decreased rapidly with time of transpiration as well as with increasing solute concentration in the treatments, Ψ_m decreased much less rapidly with time and with increasing solute concentration in the treatments. Assuming that the effects of Ψ_m and Ψ_π are additive, it would be expected, because of the relatively high initial water content in the soil ($0.30 \text{ cm}^3 \text{ cm}^{-3}$), that Ψ_m would have

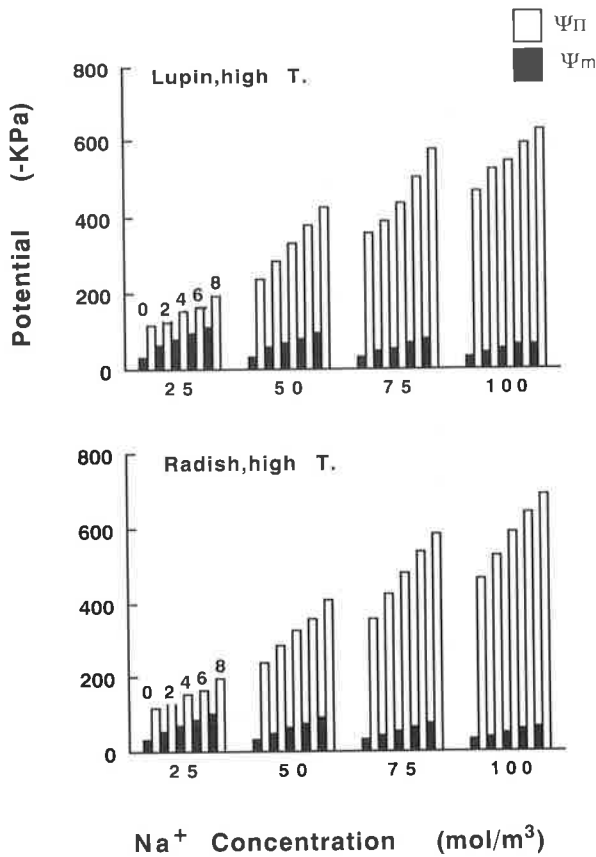


Fig. 6. The relative magnitude of the osmotic and matric potentials at the lupin and radish root surfaces for plants subjected to high transpiration demand and solute treatments of 0, 25, 50, 75 and 100 mol m⁻³ Na⁺. Numbers on the columns refer to the transpiration intervals (hr).

a smaller influence on transpiration, Q , than Ψ_{π} . The increase in Q with time of transpiration indicates that soil water content was not a limiting factor in these experiments.

Figure 7 shows that at any given transpiration interval, the relationship between Ψ_1 and Ψ_{π} at the root surface was essentially linear with the decrease in Ψ_1 approximately matching the decrease in Ψ_{π} associated with increasing solute concentration in the irrigation solutions. Osmotic potentials generally decreased more rapidly with time with increase in solute concentration in the treatment. However despite these differences in concentration between treatments, leaf water potentials decreased with time at much the same rate for all treatments indicating that the main decrease in Ψ_1 with time is undoubtedly associ-

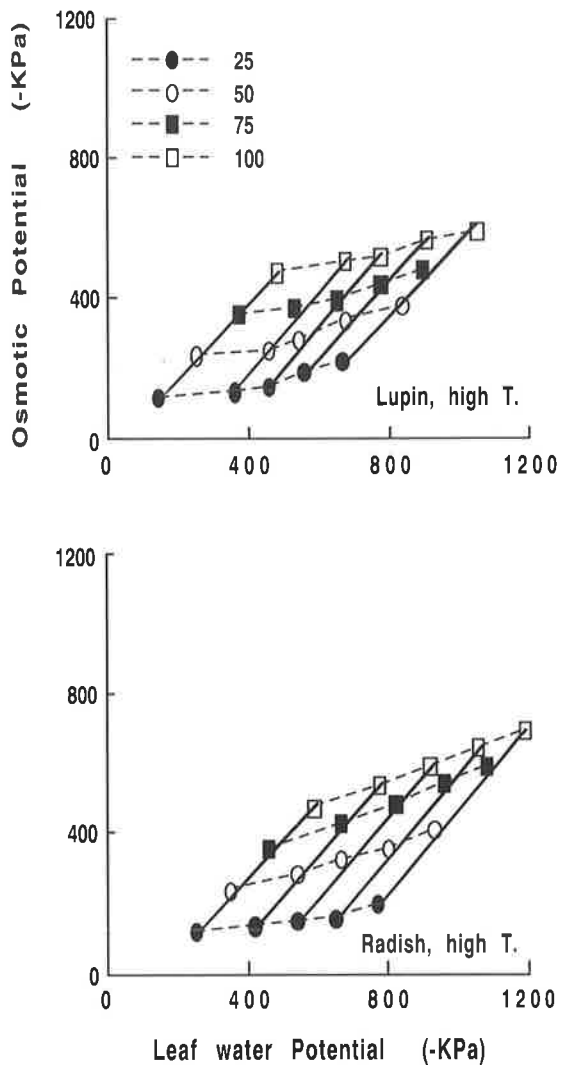


Fig. 7. The relationship between the osmotic potential at the root surface and the leaf water potential for the lupin and radish plants subjected to high transpiration demand and solute treatments of 0, 25, 50, 75 and 100 mol m⁻³ Na⁺.

ated with the plants requirement to increase the water flux, Q (Fig. 3).

The interaction and inter-relation between water and solute at the root surface is clearly complex. A higher initial solute concentration at the root surface (i.e. lower osmotic potential) will tend to reduce water uptake compared with that for the lower solute concentrations. Thus the matric potential at the root surface will remain higher for the higher solute concentration. Solute accumulation at the root surface will

occur because of the inability of the root membrane to absorb the accumulated solute. For any given quantity of water transported to the root surface this accumulation of solute will of course be greater for the higher solute concentration. However more water will be taken up by the root at a lower soil concentration because the accumulation of solute (and hence the decrease in osmotic potential) will be less. Thus the dynamics of water absorption by the root can be expected to involve opposing trends in the contributions of matric and osmotic potentials to the total potential at the root-soil interface dependent on the initial concentration of solute in the soil solution. The occurrence of back diffusion in the soil even at high transpiration rates (Munns and Passioura, 1984) may further complicate the process.

Conclusions

The development of these innovative experimental techniques using computer assisted tomography and ion specific microelectrodes, provides a major advance for soil-plant-water studies and undoubtedly has the potential to elucidate the major controversies surrounding the physics of water and solute uptake by plants. Water extraction rates for the lupin and radish roots were shown to increase continuously with time but to be substantially reduced with increasing Na^+ concentration in the treatment. Water uptake was a function of the surface area per unit length of the roots. The fact that accumulation of Na^+ at the root surfaces of both plants increased gradually with time in a near linear fashion, rather than exponentially as would be expected with non-absorption by the roots, is considered to be due to back diffusion at the relatively high water contents used. At these water contents matric potentials had a much smaller influence on transpiration than osmotic potentials. The relationships between leaf water potentials and osmotic potentials at the root surfaces were linear with the decreases in Ψ_1 almost exactly reflecting the decreases in Ψ_π indicating rapid plant adjustment. Leaf water potentials decreased progressively with time and the relationships between leaf water potential and the trans-

piration rate were also linear supporting the suggestion of constant plant resistances at any given concentration.

The present studies carried out at relatively high initial water contents (i.e. high soil water potential) have demonstrated clearly the interrelations between the important parameters within the soil-plant system. However major questions remain to be answered as to how the relations between the parameters measured here such as leaf water, soil matric and osmotic potentials, change as the soil water diffusivity becomes a more limiting factor in the transpiration process. In drier conditions back diffusion would be reduced and the effect of solute accumulation at the root surface would be enhanced.

Acknowledgement

This work was supported by funding provided by the Australian Research Council.

References

- Baveye P and Sposito G 1984 The operational significance of the continuum hypothesis in the theory of water movement through soils and aquifers. *Water Resource Res.* 20, 521–530.
- Campbell G S 1985 *Soil Physics with Basic Transport Models for Soil-Plant System*. Elsevier Science Publisher, Amsterdam. 150 p.
- Claassen N and Barber S A 1976 Simulation model for nutrient uptake from soil by growing plant root system. *Agron. J.* 68, 961–964.
- Dalton F N and Van Genuchten M Th 1986 The time-domain reflectometry method for measuring soil water content and salinity. *Geoderma* 38, 237–250.
- Dunham R J and Nye P H 1973 The influence of soil water content on the uptake of ions by roots. I. Soil water content gradients near a plane of onion roots. *J. Appl. Ecol.* 10, 585–598.
- Hainsworth J M and Aylmore L A G 1983 The use of computer assisted tomography to determine spatial distribution of soil water content. *Aust. J. Soil Res.* 21, 435–443.
- Hainsworth J M and Aylmore L A G 1986 Water extraction by single plant roots. *Soil Sci. Soc. Am. J.* 50, 841–848.
- Hainsworth J M and Aylmore L A G 1988 Application of computer assisted tomography (CAT) to gamma attenuation measurement of soil water content. *Aust. J. Soil. Res.* 26, 105–110.
- Hamza M and Aylmore L A G 1991 Liquid ion exchanger microelectrodes used to study soil solute concentrations near plant roots. *Soil Sci. Soc. Am. J.* 55, 954–958.

- Hamza M and Aylmore L A G 1992. Soil solute concentration and water uptake by single lupin and radish plant roots. II. Driving forces and resistances. *Plant and Soil* 145, 197–206.
- Herkelrath W N, Miller E E and Gardner W R 1977 Water uptake by plant. II. The root contact model. *Soil Sci. Soc. Am. J.* 41, 1039–1043.
- Hillel D, Van Beck C G E M and Talpaz H 1975 A microscopic-scale model of soil water uptake and salt movement to plant roots. *Soil Science* 120, 385–399.
- Long E M 1943 The effect of salt addition to the substrate on uptake of water and nutrient by root of approach-grafted tomato plants. *Am. J. Bot.* 30, 594–601.
- Mengel K and Kirkby E A 1982 *Principles of Plant Nutrition*, 3rd Edition. International Polish Institute. Bern, Switzerland.
- Molz F J 1981 Models of water transport in the soil-plant system: A review. *Water Resour. Res.* 17, 1245–1260.
- Munns R and Passioura J B 1984 Hydraulic resistance of plants. III. Effect of NaCl in barley and lupins. *Aust. J. Plant. Physiol.* 11, 351–359.
- Neumann H H, Thurtell G W and Stevenson K R 1974 In situ measurement of leaf water potential and resistance to water flow in corn, soybean, and sunflower at several transpiration rate. *Can. J. Plant Sci.* 54, 175–184.
- Newman E I 1969a Resistance to water flow in soil and plant. I. Soil resistance in relation to amount of root: Theoretical estimates. *J. Appl. Ecol.* 6, 261–272.
- Newman E I 1969b Resistance to water flow in soil and plant. II. A review of experimental evidence on the rhizosphere resistance. *J. Appl. Ecol.* 6, 261–272.
- Newton T H and Potts D G 1981 Radiography of the skull and brain: Technical aspects of computed tomography. Mosby, St. Louis, Vol. 5, 3853–3917.
- Nobel P S 1974 *Introduction to Biophysical Plant Physiology*. W.H. Freeman, San Francisco.
- Nulsen R A and Thurtell G W 1978a Recovery of corn leaf water potential after severe water stress. *Agron. J.* 70, 903–907.
- Nulsen R A and Thurtell G W 1978b Osmotically induced changes in the pressure-flow relationship of maize root systems. *Aust. J. Plant Physiol.* 5, 469–576.
- Passioura J B 1963 A mathematical model for the uptake of ions from the soil solution. *Plant and Soil* 18, 225–238.
- Passioura J B 1980 The transport of water from soil to shoot in wheat seedlings. *J. Exp. Bot.* 31, 333–345.
- Passioura J B 1984 Hydraulic resistance of plants. I. Constant or variable? *Aust. J. Plant Physiol.* 11, 333–339.
- Sinha B K and Singh N T 1976 Chloride accumulation near corn root under different transpiration, soil moisture, and soil salinity regimes. *Agron. J.* 68, 346–348.
- Slatyer R O 1961 Effect of several osmotic substrates on the water relationships of tomato. *Aust. J. Biol. Sci.* 14, 519–540.
- So H B, Aylmore L A G and Quirk J P 1976 Measurement of water flux in a single root system. I. The tensiometer-potometer system. *Plant and Soil* 45, 577–594.
- So H B, Aylmore L A G and Quirk J P 1976 Measurement of water flux in a single root system. II. Applications of the tensiometer-potometer system. *Plant and Soil* 49, 461–475.
- Wadleigh C H and Ayers A D 1945 Growth and biochemical composition of bean plant as conditioned by soil moisture tension and salt concentration. *Plant Physiol.* 20, 106–132.

Soil solute concentration and water uptake by single lupin and radish plant roots

II. Driving forces and resistances

M.A. HAMZA and L.A.G. AYLMOORE¹

Soil Science and Plant Nutrition, The University of Western Australia, Nedlands, Western Australia, 6009. ¹Corresponding author

Received 23 September 1991. Revised July 1992

Key words: CAT scanning, driving forces, ion specific microelectrodes, leaf water potential, lupin, matric potential, osmotic potential, radish, roots, soil and plant resistances, water uptake

Abstract

Soil water extraction (Q) and the corresponding values of matric (Ψ_m) and osmotic (Ψ_π) potentials near single roots of eighteen day old lupin and radish plants, subjected to two levels of transpirational demand and five Na^+ soil solution concentration levels, were determined using a combination of computer assisted tomography applied to gamma and X-ray attenuation measurements and Na^+ -LIX microelectrodes. This data together with leaf water potential (Ψ_l) measured by psychrometer, were used to calculate the differences in total water potentials ($\Delta\Psi$) and the differences in hydrostatic pressure (ΔP) between the leaves and the total potentials at the root surfaces, and to estimate soil and plant resistances to water movement. The linear relations for $\Delta\Psi(Q)$ and $\Delta P(Q)$ observed, imply that both plant roots acted as near perfect osmometers under the conditions of the experiments. This is further supported by the close agreement between the increases in ΔP and the decreases in Ψ_π at the root surface with increasing solute concentration in the treatments. Plant resistances were constant with time of transpiration and increased with increasing Na^+ in the treatments. Soil resistances between the root surface and bulk soil increased as the water content decreased remaining lower at the higher solute concentrations due to the lower extraction rates. At the high water potentials used plant resistances were always substantially higher than corresponding soil resistances.

Introduction

The rate of water flow from the soil to the plant is controlled by the total water potential difference along the pathway as expressed in Equation 1:

$$Q = \frac{\Psi_s - \Psi_m}{R_s} = \frac{\Psi_l - \Psi_t}{R_p} \quad (1)$$

where Q is the transpiration rate, Ψ_s is the matric potential in the bulk soil, Ψ_m is the matric potential at the root surface, Ψ_l is the total water

potential at the root surface, Ψ_t is the leaf water potential and R_s and R_p are the soil and plant resistances respectively.

Equation 1, which is based on an analogy with Ohm's law (Van den Honert, 1948) expects a linear relationship between Q and the driving force whether the driving force arises from the difference in hydrostatic pressure, ΔP , or in the total water potential, $\Delta\Psi$, between the root surface and the leaves assuming the plant resistance to be constant. This is not always the case (Janes, 1970; Millar et al., 1971). In theory all components of equation 1 (i.e. Q , $\Delta\Psi$, and R_p)

should vary depending on their location of measurement in a branched system such as a plant (Richter, 1973). Cowan (1965) and Noble (1974) have discussed the mechanistic connection between $\Delta\Psi$ and Q and agree that to satisfy the linearity between the driving force and Q , the flow of water should be liquid not vapor, the system should be isothermal, the plant resistance should be independent of any component of the water potential and there should be no solute flow in the system.

When a plant root is exposed to a saline solution in the soil, the water potential at the root surface is lowered. This decrease is transmitted throughout the plant and the extent of the transmission can be described in terms of the overall apparent hydraulic resistance of the plant and the rate of water flow through the plant (Equation 1). Changing its root resistance enables the plant to satisfy the transpirational demand without developing undue stress by steeply lowering its leaf water potential (Shalhevet et al. 1976). Such changes usually occur either when the soil moisture is depleted or when a substantial amount of salt is present in the soil. However both Dalton et al. (1975) and Fiscus (1975) showed that non-linearity in the relationship between Q and the driving force does not necessarily imply that R_p varies, but it may imply that solutes are involved in driving the flow of water.

Passioura (1984) questioned whether the non-linearity was real at the fundamental level, whether it arose merely because of inadequate measurements of flow rates or driving force or whether it was caused by the involvement of solutes in driving the flow of water as claimed by Dalton et al. (1975) and Fiscus (1975). Fiscus et al. (1983) had argued that the time had come to abandon the analogy with Ohm's law and use instead other equations derived from irreversible thermodynamics. The relative magnitudes of soil and plant resistances to water movement under different conditions of soil water potential and transpirational demand, have also been the subject of some debate (Newman, 1969; So et al., 1976a,b).

The controversy surrounding these considerations arises from the fact that the driving force which moves the water from the root surface to the leaves involves some components which have

been difficult to measure by conventional techniques. In the present paper, data for water uptake and solute accumulation obtained using an innovative combination of computer assisted tomography applied to X- and gamma-ray attenuation (CAT scanning) and sodium-liquid Ion exchanger (Na^+ -LIX) microelectrode techniques (Hamza and Aylmore, 1992), has been used to examine the relationships between the driving forces, rates of water uptake and soil and plant resistances for single lupin and radish plant roots.

Materials and methods

Application of Computer Assisted Tomography CAT to gamma and X-ray attenuation measurements (Hainsworth and Aylmore, 1983, 1986, 1988) was used to determine the spatial distribution of soil water content and hence water uptake by individual root layers of eighteen day old plants subjected to two levels of transpirational demand (with and without a fan) and five Na^+ concentration levels (zero, 25, 50, 75, and 100 mol/m^3) at initial soil water contents of $0.3 \text{ cm}^3/\text{cm}^3$. These were monitored at three root depths of 3, 6 and 9 cm and at zero, 2, 4, 6 and 8 hour intervals from the commencement of transpiration. Na^+ -LIX microelectrodes were used, in situ, to determine Na^+ concentrations at the root surface with time of transpiration. For this purpose soil pots were specifically designed and constructed to allow accurate positioning of the microelectrode tips at the root surface (Hamza and Aylmore, 1991). Full details of the experimental methods used have been presented in the preceding paper in this series (Hamza and Aylmore, 1992).

Results and discussion

Graphs illustrating the experimental data for the changes in the spatial distribution of soil water content (i.e. drawdowns) and Na^+ ion concentrations in proximity to the lupin and radish plant roots for the five Na^+ concentration levels and two rates of transpirational demand with time of transpiration, were presented in Part I

(Hamza and Aylmore, 1992). The values of the instantaneous transpiration rate, Q , after 2, 4, 6 and 8 hours of low and high transpiration demands were calculated as the first derivatives of the third degree polynomial curves fitted to the values of the cumulative water uptakes vs. time. The corresponding values of Ψ_m and Ψ_r at the root surfaces and leaf water potentials Ψ_l , were obtained from CAT scanning, Na^+ -LIX micro-electrode and leaf psychrometer data respectively. The total water potentials at the root surface, Ψ_t were calculated as the sum of the matric and osmotic components.

Driving forces

The relationships between the values of $\Delta\Psi$, the differences in water potentials between the leaves and the total potentials at the root surfaces, which constitute the driving forces for transpiration, and rates of water uptake (Q) were essentially linear (Fig. 1). In all cases as transpiration progressed, leaf water potentials and total water potentials at the root surfaces decreased but both the differences in water potentials between the leaves and root surfaces and the transpiration rate increased.

The relationships between the transpiration rate, Q , and the difference in hydrostatic pressure between the root surface and the leaves, ΔP , were also linear for both the lupins and the radishes subjected to both low and high transpiration demands (Fig. 2). ΔP in this experiment was calculated as the difference between Ψ_m at the root surface and the water potential at the leaves, Ψ_l , for the transpiring plants. Strictly speaking ΔP calculated in this fashion includes changes in osmotic component of the leaf cell walls. However further consideration demonstrated that this component is essentially constant (Munns and Passioura, 1984). This is true if the root membranes act as near perfect osmometer.

Steudle and Jeschke (1983) have suggested that the active uptake of ions into the root xylem provides some of the gradient of water potential for the absorption of water from the soil and the interaction between solute and water flow plays an important role in the water relations of the root. Based on the theory of coupled flow of

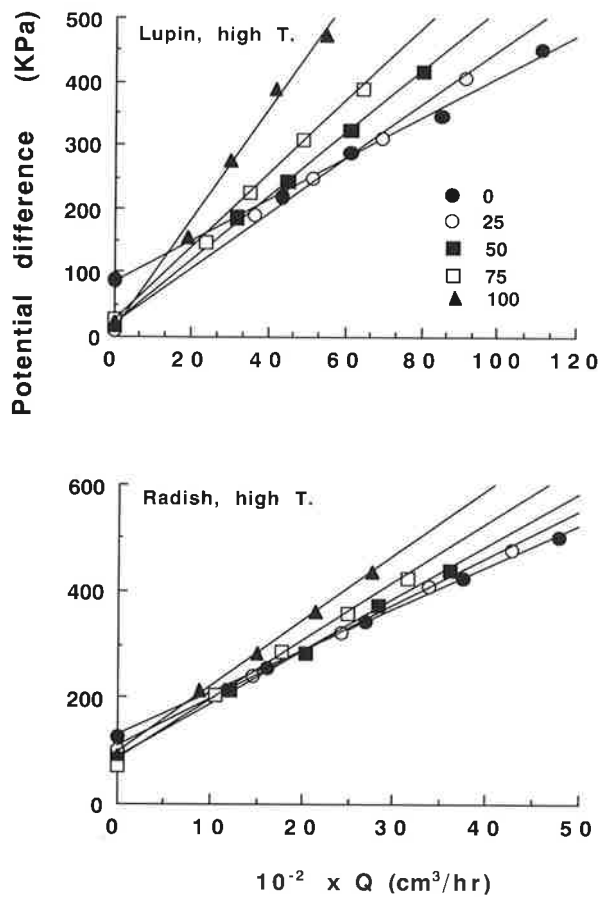


Fig. 1. The relationship between $\Delta\Psi$ and Q for the lupin and radish plants subjected to high transpiration demand and solute treatments of 0, 25, 50, 75 and 100 $\text{mol m}^{-3} \text{Na}^+$. The osmotic component at the root surface was measured using Na^+ -LIX.

solute and water across a semipermeable membrane (Katchalsky and Curran, 1965) ion uptake should be related to water uptake. Both Dalton et al. (1975) and Fiscus (1975) using an equation derived from irreversible thermodynamics, have suggested that non-linearities do not necessarily imply that the plant resistance varies, but rather that solutes are involved to varying extents in driving the flow of water. Conversely it has been argued (Cowan, 1965; Nobel, 1974) that for linearity between Q and the driving force to be satisfied, no solute flow into the plant should occur.

The numerical values of ΔP (Fig. 2) were invariably much higher than the numerical values of the osmotic potential at the root surface (see

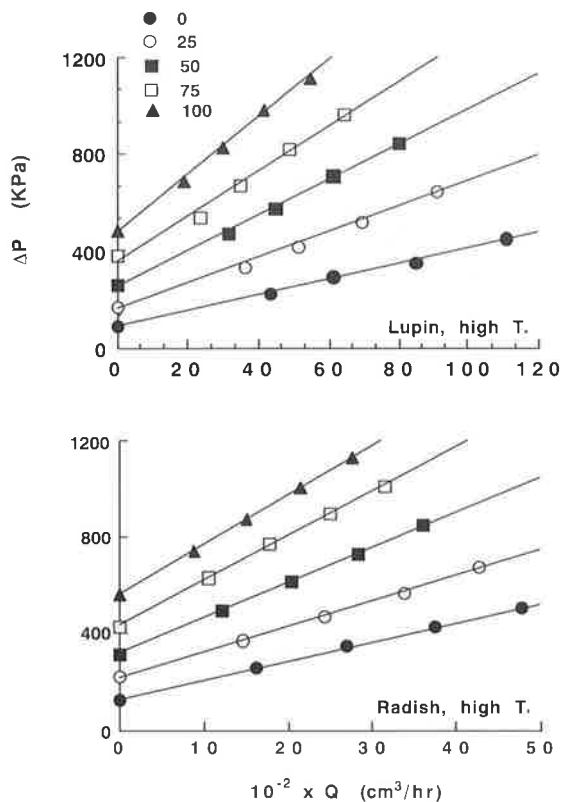


Fig. 2. The relationship between the hydrostatic pressure difference between the lupin and radish root surfaces and leaves (ΔP) and the high transpiration rates (Q) for solute treatments of 0, 25, 50, 75 and 100 mol m^{-3} Na^+ .

Hamza and Aylmore, 1992). Thus the restriction on the flow of water imposed by the osmotic potential at the root surface, is far exceeded by the hydrostatic pressure difference between the root surface and the leaves. Although appreciable amounts of solute are present at the root surface this clearly fails to produce any noticeable curvature in the $\Delta P(Q)$ or $\Delta \Psi(Q)$ curves presumably due to the high values of ΔP . Similar near-linear increases in sap flow rates with applied pressure have been reported by Nulsen and Thurtell (1978) for well watered detopped maize root systems exposed to as low as -380 kPa osmotic potential when their values for ΔP were higher than the numerical values of the solution osmotic potential. However when the applied pressure was less than the numerical value of the solution osmotic potential the exudation rate was a curvilinear function of the applied pressure.

Similarly Passioura (1980) observed that when the soil was wet, the relationship between Q and the driving force was linear, but as the soil dried, non-linearities appeared. ΔP in both these experiments was imposed on the plants using a pressure chamber technique. Although the principle is theoretically the same, an artificial driving force may not necessarily act in exactly the same fashion as one produced by the transpiring plant. In wet soil, especially in sandy soil such as that used here, soil resistance to flow is essentially negligible and almost no restrictions are imposed on water flow towards the plant. In such conditions a linear relationship would be expected to occur between the flow of water and the driving force provided that most osmotica are excluded at the root epidermis. In this experiment the initial water content was high ($0.30 \text{ cm}^3 \text{ cm}^{-3} \equiv -33 \text{ kPa}$) and the lowest Ψ_m value at the root surface at the end of the transpiration period was -140 kPa. This value is not low enough to restrict water availability to the plant. Thus the linearities observed in the present data indicate that either no $NaCl$ was taken up by the plants or that any $NaCl$ taken up had no significant influence on the water driving force. If absorption of salts occurs the amount is small and this has presumably been largely swept away from the root xylem by the transpiration stream.

The intercepts of $\Delta P(Q)$ on the ΔP axis, ΔP_0 (Fig. 2) correspond to the threshold values of the driving force necessary to begin flow through the system and reflect the differences in the osmotic pressure across the root, $\Delta \Psi_r$. ΔP_0 values differ only slightly from the ΔP values obtained from CAT and psychrometer data for the no flow situation (Table 1) in accord with the linear relations observed. The values of ΔP_0 obtained for the "no solute" condition undoubtedly reflect the presence of salts naturally occurring in the soil matrix prior to the saline irrigation treatments and agree very closely with the values of osmotic potential obtained by LIX at zero time. The close values between the decreases in Ψ_r and the increases in ΔP_0 with increasing solute concentration in the treatments (except for the lowest solute treatment) indicates a near-perfect osmotic behaviour by the lupin and radish roots over this range.

Table 1. Values of Ψ_{π} at the root surface at zero time of transpiration, ΔP_0 , the decrease in Ψ_{π} and the increase in ΔP_0 with increasing solute treatments for the different solute treatments and transpiration (low/high) demand, for the lupin and radish plants

Treatments Na ⁺ mol m ⁻³	Ψ_{π} -kPa	ΔP_0 kPa	Decrease in Ψ_{π} (kPa)	Increase in ΔP_0 (kPa)
Lupin, Low transpiration				
0	—	81	—	—
25	117	149	117	68
50	236	245	119	96
75	356	364	120	119
100	467	472	111	108
Lupin, High transpiration				
0	—	84	—	—
25	117	155	117	71
50	234	248	117	93
75	355	351	121	103
100	467	469	112	118
Radish, Low transpiration				
0	—	128	—	—
25	118	216	118	88
50	234	308	116	92
75	355	430	121	122
100	464	546	109	116
Radish, High transpiration				
0	—	128	—	—
25	116	215	116	87
50	236	316	120	101
75	355	431	119	115
100	467	557	112	126

The correct interpretation of Ψ_l is of vital importance in determining the true water potential gradient through the plant because the plant hydraulic system itself acts as a continuum (Nulsen et al., 1977) and any fall in water potential at the root surface, such as occurs when the root system is exposed to osmotic stress, is transmitted through the plant. To describe such transmission, i.e. by applying Ohm's law analogue, the water potential of the leaf cytoplasm should be used rather than the water potential of the cell walls as is usually measured by using a psychrometer. However it can be assumed that if zero or only small amounts of solute are flowing with the water to the leaves, the psychrometer values can be regarded as representing, to a large extent, the true values of the leaf water potential. Even though, both driving forces, ΔP and $\Delta \Psi$, showed linear relationships with Q , it is suggested that $\Delta \Psi$ is the better measure of the

driving force between the root surface and leaves than ΔP , because it takes Ψ_{π} at the root surface into account.

Soil and plant resistances

Plant hydraulic resistances R_p for the lupin and radish plants, obtained from the slopes of the $\Delta \Psi(Q)$ plots, and the corresponding soil resistances, calculated from Q and the differences between potentials at the root surface and bulk soil, for the different solute treatments and transpiration intervals are compared in Fig. 3. In the present experiments both Ψ_{π} and Ψ_m values at the lupin and radish root surfaces were measured simultaneously at about 4 cm below the soil surface and were assumed, for the purpose of calculating R_s and R_p , to be constant along the root length.

Lupin plant resistances, R_p , ranged from 3 to

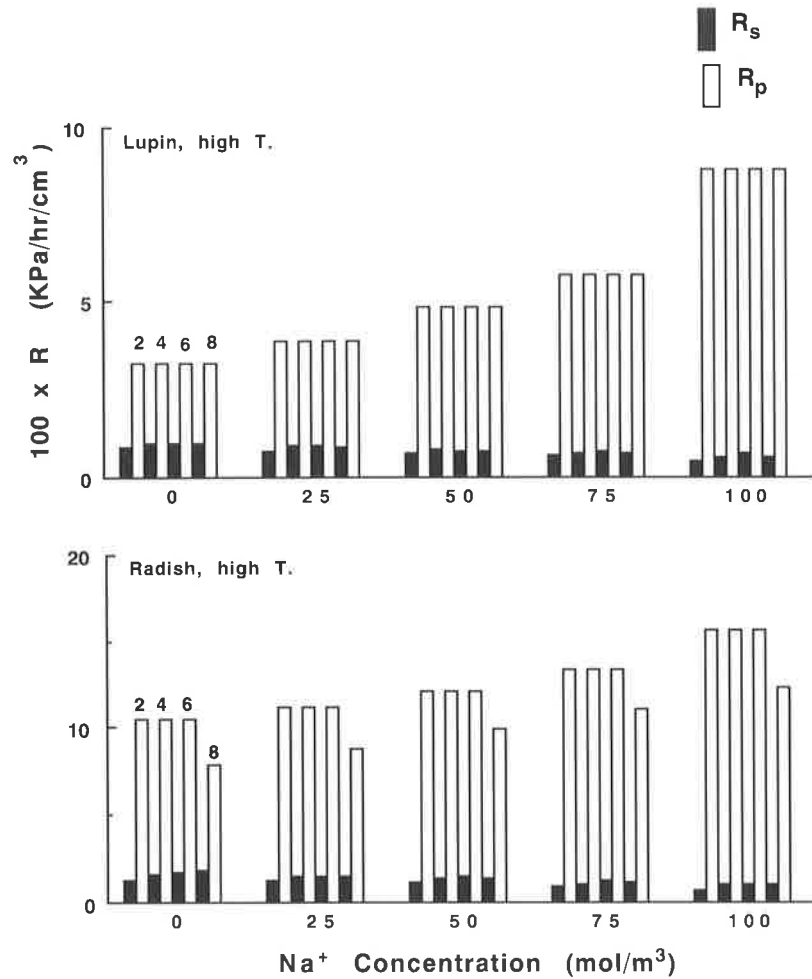


Fig. 3. Soil and plant resistances for the lupin and radish plants for solute treatments of 0, 25, 50, 75 and 100 mol m⁻³ Na⁺ after 2, 4, 6, and 8 hours of high transpiration demand.

15 times higher than the corresponding soil resistances, R_s , and from 4 to 12 times higher in the case of the radish plants depending on the solute concentration and transpiration period. As transpiration progressed and the soil around the root surface dried, R_s increased slightly while R_p remained constant (Fig. 3). Thus the differences between the plant and soil resistances decreased with time of transpiration. While plant resistances increased with increasing solute concentration in the treatments, soil resistances decreased mainly because less water was taken up by the plant and thus the soil remained wetter. Consequently the difference between R_p and R_s increased with increasing solute concentration in the treatments.

The results showed clearly that soil resistances were much less significant than plant resistances under the soil moisture conditions occurring in these experiments. This is consistent with Newman's (1969a,b) suggestion that at high water contents soil resistance is less significant than plant resistance and that only as the soil dries out (e.g. at Ψ_m around -1500 kPa), does soil resistance increase and become the predominant component of the total resistance. In the present experiments the values of Ψ_m at the root surface or at any point throughout the soil never fell below -140 kPa which is clearly far from the wilting point. Burch (1979) for example, found that a large and almost constant plant resistance influenced the pattern of water absorption until

the soil resistance reached about $1.5 \times 10^3 \text{ MPa s cm}^{-3}$ which corresponded to an extraction of almost 80% of the available soil water. Reiscosky and Ritchie (1976) found that the plant resistance was much larger than the soil resistance until the potential was reduced below -100 kPa . The previous workers dealt mainly with whole root systems rather than with single roots and hence Gardner's approach would be less relevant. Other workers have similarly reported that soil resistance is seldom large enough to contribute significantly to the overall resistance (Campbell, 1985) and that the major resistances are within the plant (Ehrlers et al., 1981; Samui and Kar, 1981). In contrast to the above, Gardner (1960) and Carbon (1973) have suggested that the conductivity of soil to water can often be so small that the transport of water to

the plant root may limit uptake even when much available water remains in the soil. Similarly Hulugalle and Willatt (1983) using data for soybean concluded that the soil resistance may be more significant than that of the plant at relatively high water contents.

The nature of the data presented here does not make it possible to differentiate between radial and axial resistances in the plant root. However the values of Hounsfield units (H) (Hamza and Aylmore, 1992) across the lupin root (Plate 1) are clearly much higher (i.e. more dense) across the cortex region of the root than in the stele region. For example the value of H units for the stele of 109 increases progressively over 0.5 mm intervals away from the stele toward the root surface, to 203, 300, 410, 500, 611 then to 725 almost at the root surface. Increasing

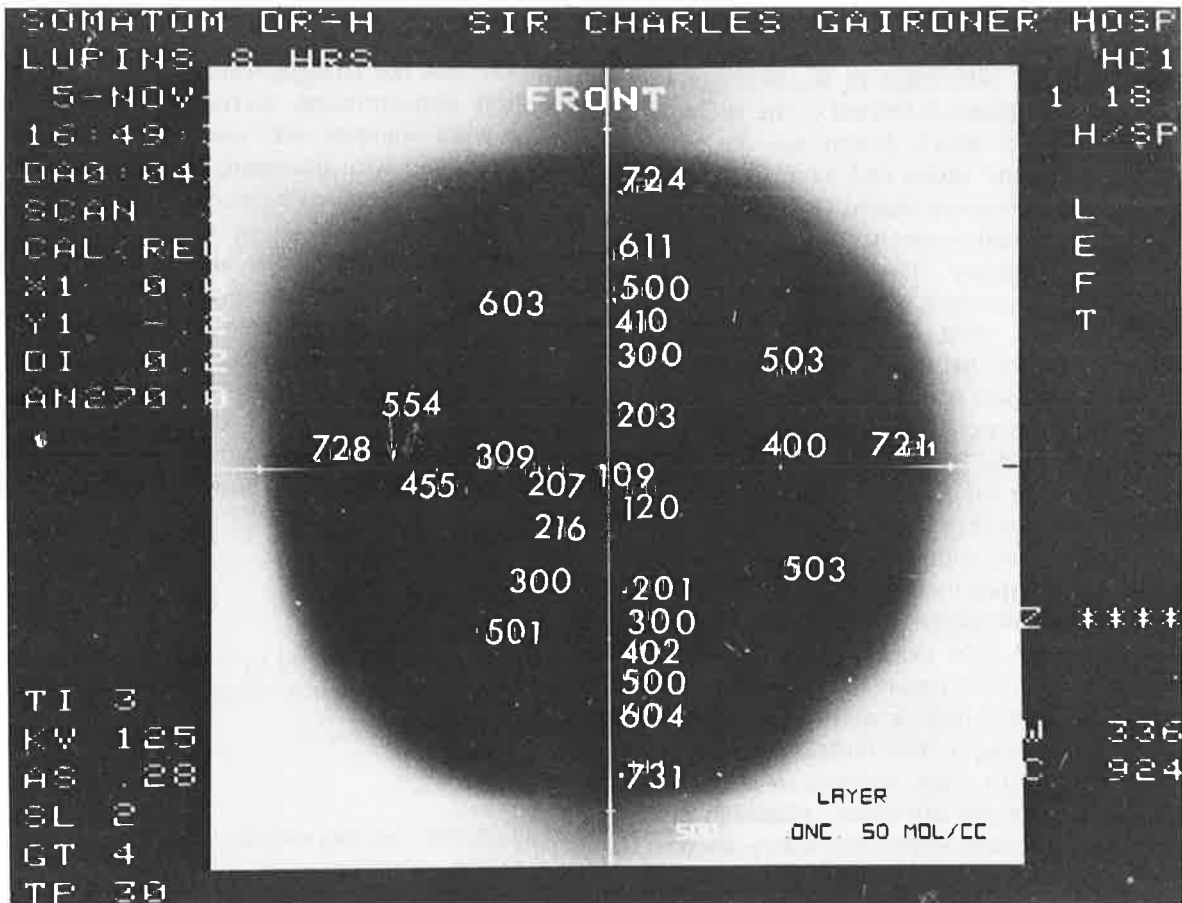


Plate 1. Hounsfield unit values through a cross-section of a lupin root. The root diameter is approximately 4 mm.

values of H units correspond to increasing density of the media (H unit for water is zero or slightly lower). Increasing values of H units toward the root surface may thus indicate higher radial resistance to water flow than that for the stele. If so the radial root resistance would be more important than the axial root resistance in controlling the water flow along the plant root. This suggestion agrees with the published results on the importance of radial root resistance over the axial resistance (Burch, 1979; Oosterhuis, 1981; Rowse and Goodman, 1981).

Plant resistances under the low transpiration demand were higher than those obtained under the high transpiration demand by about 150 to 200 kPa hr cm⁻³ for the lupins but the reverse occurred in the case of the radish plants where R_p values under the high transpiration demand were about 60 kPa hr cm⁻³ higher than those observed under the low transpiration demand. However these differences were small and the radish R_p can be regarded as near constant. It may be that the difference in R_p between the lupin and radish plants is related to the geometry of the plant root which determines the water absorbing area and radial and axial resistances. It is commonly observed that as the transpiration rate increases plant resistance decreases (MacKlon and Weatherley, 1965, for castor bean; Stoker and Weatherley, 1971, for cotton and sunflower; Barrs, 1970, for tomato and maize).

Values of R_p for the radishes were higher than those for the lupins by about 1.5 to 2.5 times. This is to be expected because the total root surface area of the radish single root is much smaller than that for the lupin. This means less radish root surface area is in contact with the soil water as compared with the lupin root. Also, in contrast to the lupin root, the radish root radius and presumably the xylem is much smaller which gives it a much higher axial resistance. Furthermore the radish root radius decreases along its length (i.e. from 0.035 cm at the top layer to 0.230 and 0.090 cm at the middle and bottom layers respectively). This possibly increases the axial resistance along the roots. Although both lupin and radish roots were never water-stressed, if, within the range of soil moisture encountered in this experiment, any root shrinkage occurs, then the effect of losing root hydraulic contact

with the soil (Herkelrath et al., 1977; Huck et al., 1970) will be much greater for the radishes. Such effects may cause a large increase in radish root resistance. However the magnitude of the plant resistance varies considerably from plant to plant even within a single cultivar of one species.

Conclusions

The linear relations for $\Delta\Psi(Q)$ and $\Delta P(Q)$ observed here imply that both plant roots acted as near perfect osmometers under the conditions of the experiments. This is further supported by the close agreement between the increases in ΔP and the decreases in Ψ_π at the root surface. A particularly interesting and important extension of the present studies would be the use of the microelectrode technique developed here to study simultaneous (and preferably in conjunction with the CAT technique) the ionic concentrations both within the root xylem and outside the root and the changes which occur as the soil solution concentration increases. Plant resistances were constant with time of transpiration and increased with increasing Na⁺ in the treatments. Soil resistances between the root surface and bulk soil increased as the water content decreased remaining lower at the higher solute concentrations due to the lower extraction rates. At the high water potentials used plant resistances were always substantially higher than corresponding soil resistances. More information is needed on the role which water potential gradient along the roots plays in the redistribution of water and solutes and how this changes with overall soil water potential.

Acknowledgements

This work was supported by funding provided by the Australian Research Council.

References

- Barrs H D 1970 Controlled environment studies of the effects of variable atmospheric water stress on photosynthesis, transpiration and water status of *Zea mays* L. and other species. In Plant Response to Climatic Factors. Proc. Uppsala Symp. UNESCO.

- Burch G J 1979 Soil and plant resistance to water absorption by plant root systems. *Aust. J. Agric. Res.* 30, 279–297.
- Campbell G S 1985 *Soil Physics with Basic Transport Models for Soil-Plant System*. Elsevier Science Publisher, Amsterdam. 150 p.
- Carbon B A 1973 Water stress in plants in a coarse soil. *Aust. J. Soil. Res.* 11, 33–42.
- Cowan I R 1965 Transport of water in the soil-plant atmosphere system. *J. Appl. Ecol.* 2, 221–239.
- Dalton F N, Raats P A C and Gardner W R 1975 Simultaneous uptake of water and solute by plant roots. *Agron. J.* 67, 334–339.
- Ehlers W, Grimme K, Baeumer R, Stulpnagel R, Kopke U and Bohm W 1981 Flow resistance in soil and plant during field growth of oats. *Geoderma*. 25, 1–12.
- Fiscus E L 1975 The interaction between osmotic and pressure-induced water flow in plant root. *Plant Physiol.* 55, 917–922.
- Fiscus E L, Klute A and Kaufmann M R 1983 An interpretation of some whole plant water transport phenomena. *Plant Physiol.* 71, 810–817.
- Gardner W R 1960 Dynamic aspects of water availability to plants. *Soil Science* 89, 63–73.
- Hainsworth J M and Aylmore L A G 1983 The use of computer assisted tomography to determine spatial distribution of soil water content. *Aust. J. Soil Res.* 21, 435–443.
- Hainsworth J M and Aylmore L A G 1986 Water extraction by single plant roots. *Soil Sci. Soc. Am. J.* 50, 841–848.
- Hainsworth J M and Aylmore L A G 1988 Application of computer assisted tomography (CAT) to gamma attenuation measurement of soil water content. *Aust. J. Soil Res.* 26, 105–110.
- Hamza M and Aylmore L A G 1991 Liquid ion exchanger microelectrodes used to study soil solute concentrations near plant roots. *Soil Sci. Soc. Am. J.* 55, 954–958.
- Hamza M and Aylmore L A G 1992 Soil solute concentration and water uptake by single lupin and radish plant roots. I. Water extraction and solute accumulation. *Plant and Soil* 145, 187–196.
- Herkelrath W N, Miller F F and Gardner W R 1977 Water uptake by plant. II. The root contact model. *Soil Sci. Soc. Am. J.* 41, 1039–1043.
- Huck M G, Klepper B and Taylor H M 1970 Diurnal variation in root diameter. *Pl. Physiol. Lancaster*. 45, 529–530.
- Hulugall N R and Willatt S T 1983 The role of soil resistance in determining water uptake by plant root system. *Aust. J. Soil Res.* 21, 571–574.
- Janes B E 1970 Effect of carbon dioxide, osmotic potential of nutrient solution and light intensity on transpiration and resistance to flowing of water in pepper plant. *Plant Physiol.* 45, 95–103.
- Katchalsky A and Curran P F 1965 *Nonequilibrium thermodynamics in biophysics*. Harvard University Press, Cambridge, MA. 215 p.
- Macklon A E S and Weatherley P E 1965 Controlled environment studies of the nature and origin of water deficits in a plant. *New Phytol.* 64, 414–427.
- Millar A A, Gardner W R and Golz S M 1971 Internal water studies and water transport in seed onion plants. *Agron. J.* 63, 779–784.
- Munns R and Passioura J B 1984 Hydraulic resistance of plants. III. Effect of NaCl in barley and lupins. *Aust. J. Plant. Physiol.* 11, 351–359.
- Newman E I 1969a Resistance to water flow in soil and plant. I. Soil resistance in relation to amount of root: theoretical estimates. *J. Appl. Ecol.* 6, 261–272.
- Newman E I 1969b Resistance to water flow in soil and plant. II. A review of experimental evidence on the rhizosphere resistance. *J. Appl. Ecol.* 6, 261–272.
- Nobel P S 1974 *Introduction to biophysical plant physiology*. W H Freeman, San Francisco.
- Nulsen R A, Thurtell G W and Stevenson K R 1977 Response of leaf water potential to pressure changes at the root surface of corn plant (*Zea mays* L.). *Agron. J.* 69, 951–954.
- Nulsen R N and Thurtell G W 1980 Effect of osmotica around the roots on water uptake by maize plant. *Aust. J. Plant Physiol.* 7, 27–34.
- Nulsen R N and Thurtell G W 1978 Osmotically induced changes in the pressure-flow relationship of maize root systems. *Aust. J. Plant Physiol.* 5, 469–576.
- Oosterhuis D M 1981 Hydraulic conductivity and drought acclimation of cotton root systems. Ph.D. thesis, Utah State University, Logan.
- Passioura J B 1980 The transport of water from soil to shoot in wheat seedlings. *J. Exp. Bot.* 31, 333–345.
- Passioura J B 1984. Hydraulic resistance of plants. I. Constant or variable? *Aust. J. Plant. Physiol.* 11, 333–339.
- Reiscoosky D C and Ritchie J T 1976 Relative importance of soil resistance and plant resistance in root water absorption. *Soil Sci. Soc. Am. J.* 40, 293–297.
- Richter H 1973 Frictional potential losses and total water potential in plants: A re-evaluation. *J. Exp. Bot.* 24, 983–994.
- Rowse H R and Goodman D 1981 Soil and plant resistance effect on transpirational and leaf water responses to soil water potential. *Aust. J. Soil Res.* 19, 51–60.
- Samui R P and Kar S 1981 Soil and plant resistance effect on transpiration and leaf water responses to soil water potential. *Aust. J. Soil Res.* 19, 51–60.
- Shalhevet J, Maas E V, Hoffman G J and Ogata G 1976 Salinity and the hydraulic conductance of root. *Physiol. Plant.* 38, 224–232.
- So H B, Aylmore L A G and Quirk J P 1976 Measurement of water flux in a single root system. I. The tensiometer-potometer system. *Plant and Soil* 45, 577–594.
- So H B, Aylmore L A G and Quirk J P 1976 Measurement of water flux in a single root system. II. Applications of the tensiometer-potometer system. *Plant and Soil* 49, 461–475.
- Stedle E and Jeschke W D 1983 Water transport in barley roots. *Planta* 158, 237–248.
- Stoker R and Weatherley P E 1971 The influence of the root system on the relationship between rate of transpiration and depression of leaf water potential. *New Phytol.* 70, 574–584.
- Van den Honert T H 1948 Water transport in plants as a catenary process. *Discuss. Faraday Soc.* 3, 146–153.

A METHOD FOR STUDYING NONEQUILIBRIUM SORPTION DURING TRANSPORT OF PESTICIDES IN SOIL¹

RAI S. KOOKANA,¹ R. G. GERRITSE² AND L. A. G. AYLMOORE¹

Rate coefficients describing sorption of pesticides in soils are commonly obtained under well stirred conditions from batch equilibration studies. Batch techniques involve high solution-to-soil ratios and mechanical agitation, both of which can influence the sorption characteristics of a soil. In addition, rapid equilibration cannot be studied accurately in batch experiments. These disadvantages can, however, be overcome by studying the sorption of pesticides during leaching in saturated columns of soil. Results in this paper show how time-dependent sorption of pesticides in soil can be calculated by applying the peak maxima method from the gas-chromatographic literature to pesticide breakthrough curves of short pulse injections in soil columns.

In solute transport models, the sorption process in soils is often assumed to be fast enough to achieve instantaneous equilibrium. This assumption is primarily based on mathematical convenience and also on sorption studies using batch techniques that involve shaking. As has been previously illustrated (Murali and Aylmore 1980), this assumption may not be valid under flow conditions. In fact, many laboratory and field investigations have demonstrated that in most cases sorption reactions are not fast enough to reach equilibrium, and consequently nonequilibrium conditions prevail during solute transport (Ardakani and McLaren 1977; Murali and Aylmore 1980; Brusseau and Rao 1989). While a clear understanding of the nature of the sorption nonequilibrium is vital for modeling pesticide transport in soil, such aspects of pesticide sorption are relatively less well understood compared with equilibrium aspects (Yaron et al. 1985). Although well stirred batch systems and

miscible displacement techniques have both been used in studying the kinetics of pesticide sorption in soil (Biggar et al. 1978; Wauchope and Myers 1985), it is the former that has been most commonly employed.

The kinetic parameters obtained by batch techniques are generally inadequate for the accurate description of pesticide transport in soil profiles because they do not accurately represent the processes occurring under field conditions. Batch methods commonly involve unrealistically high solution-to-soil ratios and, in addition, shaking and centrifugation. Furthermore, vigorous shaking of soil suspension may cause changes in surface characteristics of soil particles (Barrow and Shaw 1979; Sparks 1985). Although in recent years batch techniques that avoid vigorous shaking have been devised, flow or miscible displacement techniques remain preferable to batch techniques because they provide better representation of solute transport under field conditions and are more appropriate for obtaining sorption rate coefficients used in solute transport models (Murali and Aylmore 1980). However, it must be emphasized that flow techniques are not suitable for studying the 'chemical kinetics,' which has been specifically defined as the study of the rate of reactions where transport is not limiting (Skopp 1986). In fact, the conditions needed to study chemical kinetics are difficult to achieve in heterogeneous systems such as soils, and hence most kinetic studies in the literature report apparent rate laws (Skopp 1986). The apparent rate parameters obtained by a flow technique should prove more valuable in modeling pesticide transport in soil simply because they are obtained under transport conditions. Furthermore, a comparison of sorption kinetics studied under both batch and flow conditions can also provide valuable information on the nature of sorption time-dependency in soil. This paper describes a new method, hereafter referred to as the flow technique, for studying the kinetics of sorption during pesticide transport in soil. Sorption of pesticides is characterized from breakthrough curves (BTCs), resulting from leaching pulse

¹ Soil Science and Plant Nutrition, The University of Western Australia, Nedlands, 6009.

² Division of Water Resources CSIRO, Private Bag P.O. Wembley, 6014.

Received Sept. 20, 1991; accepted March 6, 1992.

injections of pesticides through saturated columns of soil.

EXPERIMENTAL

Pesticides and Soils

Sorption of two herbicides, linuron (3-(3,4-dichloro phenyl-1-methoxy)-1-methylurea) and simazine (2-chloro-4,6-bis(ethylamino)-1,3,5, triazine), were studied. Analytical grade samples (+99% purity) of herbicides were obtained from Ciba-Geigy Australia Ltd. (simazine) and Hoechst Australia Ltd. (linuron). Both herbicides were analyzed by High Performance Liquid Chromatography (HPLC) following the method given by Vickery et al. (1980). The herbicides were separated on a Spherisorb 10 μ m ODS column, (30 cm \times 1.6 mm ID (Phase Separation Ltd.) in a mobile phase of methanol and water (65:35 v/v) and were monitored with a variable wavelength UV detector. Experiments were carried out on two soils: a Bassendean sand (OM 1.2%; clay 1.3%; pH 5.0 in 0.01 M CaCl₂) and a Cobiac loamy sand (OM 0.6%; clay 13.6%; pH 5.1 in 0.01 M CaCl₂). Other physico-chemical properties of these soils have been published elsewhere (Singh et al. 1990).

Soil Column Study

Cylindrical columns were packed under vibration with air-dried soil and were saturated with a dilute salt solution (0.005 M CaCl₂). The salt solution was passed through the soil columns at a constant rate of flow ranging from 0.01 mL min⁻¹ to 1.0 mL min⁻¹ with an HPLC pump (K 35; ETP Kortec, Sydney, Australia). Samples of herbicide (300 μ L) were injected with a six-port stainless steel valve (Rheodyne No. 7125). BTCs were monitored either in the effluent with a UV detector or, alternatively, off-line in automatically collected fractions. Further details of ex-

perimental conditions for soil columns are given in Table 1.

THEORY AND APPLICATION OF METHOD

Calculation of Sorption from Breakthrough Curves

Sorption isotherms of pesticides were measured by applying the peak maxima method to BTCs, as described by Huber and Gerritse (1971). The required BTCs were obtained at various rates of flow in small columns of saturated soil.

Peak maxima method

The method is commonly used in the chromatography literature for the determination of a distribution isotherm (Huber and Gerritse 1971). It is based on the transport equation for the nonlinear distribution of a solute:

$$(\partial\langle C \rangle / \partial t) + ((1 - \theta) / \theta) (\partial\langle S \rangle / \partial t) = -(\partial\langle VC \rangle / \partial z) + D(\partial^2\langle C \rangle / \partial z^2) \quad (1)$$

where

where z = length co-ordinate

S = concentration of a pesticide on solid phase

C = concentration of a pesticide in liquid phase

V = pore water velocity

$\langle \rangle$ = average over corresponding cross-sectional area

θ = fraction of cross-sectional area occupied by liquid phase

$1 - \theta$ = fraction of cross-sectional area occupied by solid phase

D = dispersion coefficient of the solute in liquid phase.

Assuming a negligible effect of dispersion coefficient on the position of peak maximum

TABLE 1
Soil column parameters

	Column A	Column B	Column C
Length (mm)	50	150	300
Diameter (mm)	4.5	10	25
Soil wt. (g)	1.2	19	198
Bulk density (kg m ⁻³)	1.5	1.6	1.3
Pore volume (cm ³)	0.4	5.4	48.0
Porosity (m ³ m ⁻³)	0.46	0.44	0.31
Pore water velocity (m d ⁻¹)	2-20	1-40	0.4-10

($D = 0$) and a constant pore water velocity, Eq. (1) can be rewritten as

$$(\partial\langle C \rangle / \partial t)(1 + (1 - \theta) / \theta)(d\langle S \rangle / d\langle C \rangle) = -\langle V \rangle(\partial\langle C \rangle / \partial z) \quad (2)$$

where, $d\langle S \rangle / d\langle C \rangle$ is the first derivative of the sorption isotherm.

For a small pulse of solute in a soil column, the migration velocity V_c of the solute concentration $\langle C \rangle$ can be expressed as

$$V_c = \langle V \rangle / [(1 + (1 - \theta) / \theta)d\langle S \rangle / d\langle C \rangle] \quad (3)$$

The denominator on the right hand side of Eq. (3) is essentially the retardation factor, often used in transport studies (Rao and Jessup 1983). From Eq. (3), an expression describing the residence time (t_c) of the maximum solution concentration in the BTC can be derived.

$$(t_c - t_o) / t_o = ((1 - \theta) / \theta)(d\langle S \rangle / d\langle C \rangle) \quad (4)$$

or

$$t_c = t_o[1 + ((1 - \theta) / \theta)(d\langle S \rangle / d\langle C \rangle)] \quad (5)$$

where t_o = retention time of nonretarded solute (Cl^-), ignoring anion exclusion.

Measurement of Rate Parameters

An effective sorption isotherm can be calculated by applying Eq. (4) to the locus of the peak maxima of BTCs obtained by injecting pulses of different amounts of a pesticide and of a nonretarded solute into a soil column. A series of BTCs, obtained by leaching different amounts of simazine at a constant rate of flow, is shown in Fig. 1. The locus of peak maxima of the BTCs is shown by the dotted line. The solid vertical line represents the locus of chloride peaks, and because chloride is a nonretarded solute, the line occurs at one pore volume. The area between these two loci of peak maxima integrated along the y axis from zero concentration to the selected solution concentration represents the sorption of pesticide at the selected concentration. Thus, it is possible to obtain a series of sorption values corresponding to different solution concentrations at a given rate of flow or residence time. Such sorption values will represent an equilibrium sorption isotherm when the flow rates employed are slow enough to allow sufficient time for a solute to react completely with the soil. At higher flow rates, however, the sorption values will represent dynamic distri-

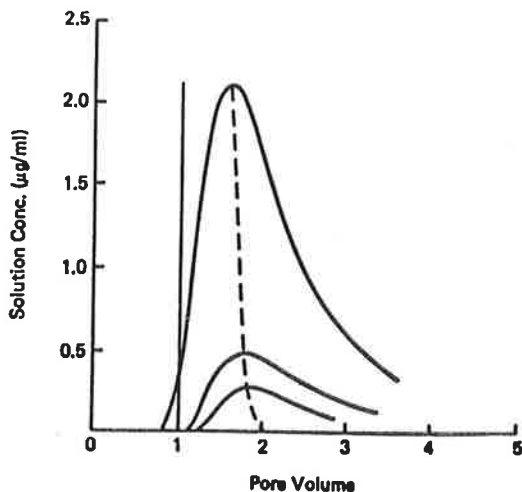


FIG. 1. Breakthrough curves of simazine obtained by pulse injections of different amounts in soil column. The solid line at one pore volume represent the loci of chloride BTCs.

bution isotherms. It is interesting to note that at low input concentrations, the position of the breakthrough peaks for simazine in Fig. 1 shifts to higher pore volumes, thereby indicating a higher retardation at lower solution concentration of the pesticide. Thus, integration of the curve joining the peak maxima of simazine to different concentrations provides a nonlinear sorption isotherm. Similar nonlinearity was observed under batch conditions for this soil (Singh et al. 1990).

The residence time of a pesticide (t_c) in the soil column can be varied by changing the flow rate of the solution entering the soil columns and is calculated by Eq. (5). Each set of BTCs for different amounts injected provides one point on the sorption vs. residence time curve at any given solution concentration (e.g., Fig. 5). In practice, the sorption values vs. residence times obtained from the sets of BTCs at different rates of flow are equivalent to the set of sorption vs. equilibration time data obtained by the batch method. This sorption vs. time data then can simply be subjected to various rate laws, such as first-order kinetic equation, and the rate parameters can be calculated. Sorption rate parameters for selected pesticides in four soils have been obtained by the flow technique and are presented in another paper (Kookana et al. 1992).

Effect of Dispersion Coefficient on the Locus of Peaks

It was assumed while deriving Eq. (2) that the dispersion coefficients have negligible effect on the position of peak maxima of the BTCs. The validity of this assumption was tested by generating BTCs at different values of dispersion coefficient by a numerical simulation (Kookana 1990). The simulated BTCs (Fig. 2) revealed that the loci of peaks were displaced only at large values of the dispersion coefficients and were not significantly affected in the range of dispersion coefficients which corresponded to the flow velocities employed in the study. Therefore the assumption $D(\partial^2c/\partial z^2) = 0$ does not invalidate the method.

Effect of Soil Column Size on Sorption Kinetics

Experimental difficulties can be experienced with flow techniques because the time of contact between a pesticide and soil is determined by a combination of the length of the soil column and the rate of leaching. In practice, with long soil columns, solute breakthrough takes a longer time to occur and consequently the initial sorption reactions generally cannot be studied even at high flow rates. On the other hand, if the column size is too small, wall effects may introduce errors. This concern was evaluated by obtaining sorption data for simazine in Bassendean sand using three different sizes of soil column (Table 1). The amount of soil used in these columns ranged from approximately 1 to 200 g. It is clear from the results shown in Fig. 3 that the sorption was unaffected by the different sizes of soil columns used. Hence, unlike other techniques (Sparks et al. 1980), it is not

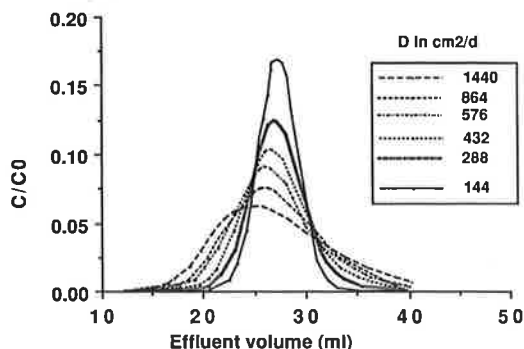


FIG. 2. Simulations showing the effect of dispersion coefficient on position of the peaks of the BTCs.

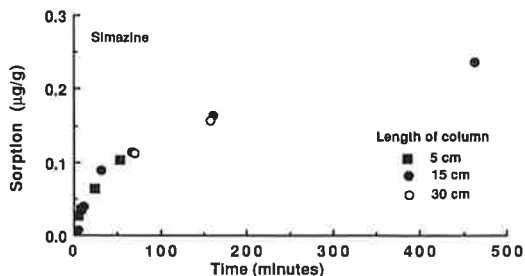


FIG. 3. Sorption of simazine in Bassendean sand calculated from BTCs obtained with soil columns of different sizes.

necessary to use small amounts of soil in the present flow technique. This could be of particular benefit for pesticides showing very low affinity for soils.

Sorption Kinetics of Linuron and Simazine

To obtain the amounts sorbed after different periods of time, BTCs at different flow rates are required. Figure 4 for BTCs of linuron at different flow rates shows that with decreasing rate of flow, the time of contact between soil and pesticide increased, and, as a result, the sorption and consequent retardation of the BTC increased. Sorption of linuron and simazine, at residence times ranging from 5 to 800 min, were obtained by varying the pore water velocity in the soil columns between 3.0 cm min^{-1} and 0.06 cm min^{-1} . Sorption data of linuron in the loamy sand and simazine in the sand are presented in Fig. 5. Sorption of the pesticides is presented as the ratio of sorption at a given time (S) to that at equilibrium (Se). The values reached after shaking for 24 h were taken as equilibrium values (Se). There are reports in the literature that sorption can, in fact, continue for several days;

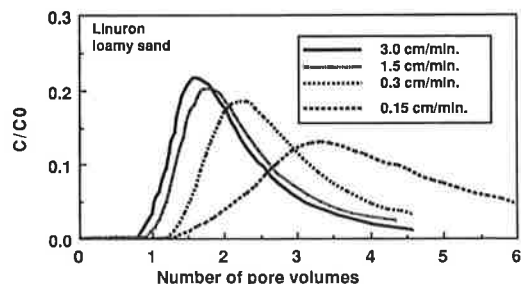


FIG. 4. BTCs of linuron in loamy sand at different rates of flow.

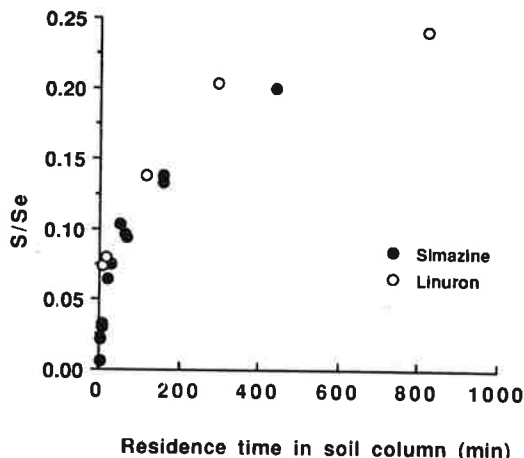


FIG. 5. Sorption data of linuron in loamy sand and of simazine in sand obtained by the flow method.

hence, the 24-h value could be an underestimation of equilibrium sorption. However, from the standpoint of comparing the two methods, it seems reasonable to use 24 h as an equilibrium sorption value. A rapid initial rate followed by a relatively slower rate of sorption is evident from the figure. For comparison, sorption data for simazine in the sandy soil obtained by a batch method are presented in Fig. 6. This figure also shows both rapid and slower components of sorption similar to those observed under flow conditions. However, it must be noted that the magnitude of the rapid component of sorption was much higher for the batch method in comparison with the flow method. After some 300 minutes of shaking, the sorption obtained by the batch method approached the equilibrium value (S_e), whereas it reached to only 20% of S_e at comparable residence times for simazine and linuron in soil columns. The shaking of the soil suspension apparently resulted in faster sorption using the batch method. The presence of rapid and slow components of pesticide sorption by soil, under batch conditions, has also been noted by other workers (Wauchope and Myers 1985; Boesten 1987). However, in all these reports the rapid components were substantially larger than that observed by the flow technique.

Advantages and Disadvantages of the Technique

Existing miscible displacement techniques for determining sorption rate parameters described in the literature (Biggar et al. 1978; review by Sparks 1985) have a number of limitations. It is

essential in these techniques that first, a small amount of soil (e.g., 1 g; Sparks et al. 1980) be used, and second, the soil must be in a dispersed state. This is necessary because it is assumed, while solving the equation for conservation of mass, that dispersion effects are absent in the soil column. This assumption is likely to be true only in a thin column of dispersed soil, which of course rarely represents the conditions during pesticide transport in the field. Another reason for not using a larger soil column is the difficulty in accurately estimating the concentration distribution of a solute in the column (needed for the calculations of sorption), and this may lead to erroneous results (Skopp and McCallister 1986).

The flow technique described here overcomes the previous difficulties associated with the miscible displacement techniques. An additional advantage of the technique is that sorption values corresponding to a number of solution concentrations can be calculated from one set of BTCs obtained at a given flow rate or residence time. Nevertheless, there are some disadvantages to the technique. First, the time involved in generating a complete sorption vs. time curve can be long, primarily because a series of BTCs are required to obtain a sorption value at one particular residence time. However, if the sorption isotherm is assumed to be linear, a single BTC at a given flow rate will be sufficient for one point on the curve. Second, desorption kinetics of pesticides can not be studied by this technique unless the frontal BTCs are used (Huber and Gerritse 1971). Third, as with any flow tech-

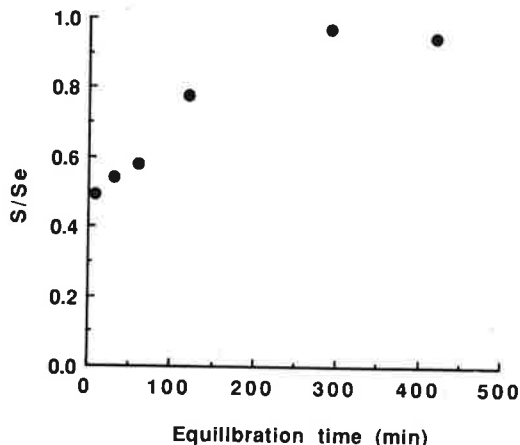


FIG. 6. Sorption data of simazine in Bassendean sand obtained by the batch method.

nique, the present procedure is unsuitable for studying chemical kinetics and can provide only apparent rate laws and kinetic parameters.

DISCUSSION

It is well established that organic matter in soils is the principal sorbent, particularly for nonionic pesticides (Chiou et al. 1983). If the soil organic matter is visualized as a three-dimensional network of randomly oriented polymer chains, and of porous structure (Schnitzer 1978; Kookana et al. 1990), a pesticide molecule will have to diffuse to the reaction site before it can be sorbed. Thus the effective time dependency of a sorption reaction during pesticide transport in a soil will almost invariably be determined by the combined effects of both chemical and physical kinetic processes. Consequently kinetic data obtained from batch experiments are generally unsatisfactory in solute transport models (Rao and Jessup 1983) because the physical effects (diffusion) are eliminated in such experiments, albeit partially in most cases. In contrast, the flow technique quantifies the net kinetics of the sorption process during solute transport, regardless of the nature of the processes. Comparisons of sorption kinetics obtained by the two methods should, however, provide valuable insights into the mechanisms involved in determining the non-equilibrium sorption behavior of pesticides in soil.

For nonequilibrium transport models, the sorption kinetic parameters must be measured independently and under conditions closely representing transport. In contrast to other approaches, the determination of rate constants by the present method does not involve the incorporation of rate laws in the transport equation and the obtaining of the parameters by curve-fitting of the model to the BTC.

REFERENCES

- Ardakani, M. S., and A. D. McLaren. 1977. Absence of local equilibrium during ammonium transport in soil column. *Soil Sci. Soc. Am. J.* 41:877-879.
- Barrow, N. J., and T. C. Shaw. 1979. Effects of solution: Soil ratio and vigour of shaking on the rate of phosphate adsorption by soil. *Soil Sci.* 119:167-177.
- Biggar, J. W., U. Mingelgrin, and M. W. Cheung. 1978. Equilibrium and kinetics of adsorption of picloram and parathion with soils. *J. Agric. Food Chem.* 26:1306-1312.
- Boesten, J. J. T. I. 1987. Modelling pesticide transport with a three site sorption submodel: A field test. *Netherlands J. Agric. Sci.* 35:315-324.
- Brusseau, M. L., and P. S. C. Rao. 1989. Sorption nonideality during organic contaminant transport in porous media. *Crit. Rev. Environ. Control* 19:33-99.
- Chiou, C. T., P. E. Porter, and D. W. Schmedding. 1983. Partition equilibria of nonionic organic compounds between soil organic matter and water. *Environ. Sci. Technol.* 17:227-237.
- Huber, J. F. K., and R. G. Gerritse. 1971. Evaluation of dynamic gas chromatographic methods for the determination of adsorption and solution isotherms. *J. Chromatogr.* 58:137-158.
- Kookana, R. S. 1990. Equilibrium and kinetic aspects of sorption, desorption and mobility of pesticides in soils. Doctoral thesis (unpublished). The Univ. of Western Australia.
- Kookana, R. S., R. G. Gerritse, and L. A. G. Aylmore. 1990. Effect of organic cosolvent on sorption and desorption of simazine and linuron in soil. *Aust. J. Soil Res.* 28:717-725.
- Kookana, R. S., L. A. G. Aylmore, and R. G. Gerritse. 1992. Time-dependent sorption of pesticides during their transport in soil. *Soil Sci.* (*In press*).
- Murali, V., and L. A. G. Aylmore. 1980. No-flow equilibration and adsorption dynamics during ionic transport in soils. *Nature* 283:467-469.
- Rao, P. S. C., and R. E. Jessup. 1983. Sorption and movement of pesticides and other toxic organic substances in soils. In: *Chemical mobility and reactivity in soil systems*. D. W. Nelson, K. K. Tanji, and D. E. Elrick (eds.). *Am. Soc. Agron. and Soil Sci. Soc. Special Publication No. 11*. American Society of Agronomy, Madison, WI, pp. 183-201.
- Schnitzer, M. 1980. Humic substances, chemistry and reactions. In: *Soil organic matter*. M. Schnitzer, and S. U. Khan (eds.). Elsevier Science Publishing Co., New York, 1978.
- Singh, Rai, R. G. Gerritse, and L. A. G. Aylmore. 1990. Adsorption desorption of selected pesticides in some Western Australian soils. *Aust. J. Soil Res.* 28:227-243.
- Skopp, J. 1986. Analysis of time-dependent chemical processes in soils. *J. Environ. Qual.* 15:205-213.
- Skopp, J. and D. McCallister. 1986. Chemical kinetics from a thin disk flow system: Theory. *Soil Sci. Soc. Am. J.* 50:617-623.
- Sparks, D. L. 1985. Kinetics of ionic reactions in clay minerals and soils. *Adv. Agron.* 38:231-266.
- Sparks, D. L., L. W. Zelazny, and D. C. Martens. 1980. Kinetics of potassium desorption in soil using miscible displacement. *Soil Sci. Soc. Am. J.* 44:1205-1208.
- Vickery, T. M., D. L. Karleskey, and G. L. Blackmer. 1980. Colorimetry and high performance liquid chromatography of atrazine residues in soil: Comparison of methods. *J. Assoc. Off. Anal. Chem.* 63:507-510.
- Wauchope, R. D., and R. S. Myers. 1985. Adsorption-desorption kinetics of atrazine and linuron in freshwater-sediment aqueous slurries. *J. Environ. Qual.* 14:132-136.
- Yaron, B., Z. Gerstl, and W. F. Spencer. 1985. Behavior of herbicides in irrigated soils. *Adv. Soil Sci.* 3:121-211.

TIME-DEPENDENT SORPTION OF PESTICIDES DURING TRANSPORT IN SOILS¹

RAI S. KOOKANA, L. A. G. AYLMOORE AND R. G. GERRITSE²

Sorption nonequilibrium of pesticides in soil is relatively less understood compared with equilibrium sorption. Furthermore, batch techniques generally used in kinetic studies do not represent field conditions. Flow techniques, on the other hand, closely represent pesticide transport and have many advantages over batch techniques. A flow technique was used to study the sorption kinetics of three pesticides in four Western Australian soils. Sorption data of all pesticides showed an initial rapid rate followed by a slower rate of sorption. While a first-order equation failed to satisfactorily describe the sorption data, both the Freundlich two-site kinetic equation and the parabolic diffusion law fitted well to the data. The rapid component of sorption varied from 0 to 25% of total sorption (24 h sorption value) for various pesticides. A comparison of sorption data obtained by a batch technique and a flow technique revealed that sorption occurs at a much faster rate under batch conditions, presumably because of shaking and high solution to soil ratio. Under batch conditions, the instantaneous component of sorption was very high (up to 90% of 24-h sorption value). The characteristics of the soil also affected the rate of sorption of the pesticides. A well structured soil with high organic matter content showed slower rate of sorption compared with a dispersed soil with low organic matter content.

The kinetics of pesticides sorption in soil has received little attention since most sorption studies on pesticides in soil deal with the equilibrium aspects (Rao and Jessup 1983; Yaron et al. 1985). Furthermore, the batch technique which is unrepresentative of pesticide transport under field situations (Murali and Aylmore

1980, 1983; Sparks 1985) has commonly been employed for studying the kinetics of pesticide sorption on clay minerals and soils. While batch experiments have generally shown that the sorption reaction of pesticides in soils is essentially instantaneous or very rapid (Rao and Jessup 1983), the results from several transport studies (reviewed by Brusseau and Rao 1989) have shown that local equilibrium of sorption does not usually exist during pesticide transport in soil. Therefore, flow techniques such as that developed by Kookana et al. (1991) are preferable over batch techniques (Murali and Aylmore 1980, 1983; Sparks 1985) because these are realistic and suitable for modelling transport of pesticides in soil profiles.

In solute transport studies, a number of different rate laws describing the time dependency of the sorption reaction in soils have been used with varying degree of success. These include simple one-site linear or nonlinear kinetic models, two-site sorption models and several others (reviewed by Nielsen et al. 1986). More recently, Boesten (1987) used a three-site kinetic model, and Selim and Amacher (1988) used a second-order two-site kinetic model in their solute transport studies. Experimental evidence of such kinetic reactions have been obtained in a few studies only and then only by the batch technique. Since substantial differences in sorption between flow and batch systems have frequently been noted (e.g., Ardakani and McLaren 1977; Wagenet et al. 1977), it is essential that sorption rate coefficients be obtained under flow conditions for such transport studies.

In this paper, kinetic data of sorption for three pesticides in four different Western Australian soils have been obtained by the flow technique described by Kookana et al. (1991). Various rate laws available in literature were used to describe the data. Sorption by batch and flow techniques has also been compared.

MATERIALS AND METHODS

Soils and Pesticides

The four soils used in this study were Bassendean sand, Cobiac loamy sand, Gascoyne sandy

¹ Contribution from Soil Science and Plant Nutrition, The University of Western Australia, Nedlands, 6009 Australia.

² CSIRO Division of Water Resources, PO bag Wembley, 6014 Australia.

Received Sept. 20, 1991; accepted Jan. 16, 1992.

loam, and Wellesley clay. Some of the physico-chemical properties are given in Table 1. Other properties of these soils have been published earlier (Singh et al. 1990). These soils represented a range of soil texture, organic matter contents, pH, and other properties.

Sorption of three pesticides, namely fenamiphos (ethyl 4-methylthio-m-tolyl isopropyl phosphoramidate), an organophosphate nematocidal-insecticide, linuron (3-(3,4-dichlorophenyl)-1-methoxy-1-methylurea), a urea herbicide, and simazine (2-chloro-4,6bis(ethylamino)-1,3,5-triazine), a triazine herbicide was studied. The aqueous solubilities of these pesticides (at 20°C) reported in the literature are 700 mg L⁻¹ for fenamiphos, 81 mg L⁻¹ for linuron, and 3.5 mg L⁻¹ for simazine. These pesticides have low vapor pressures (<5.0 mPa at 30°C) and are commonly used for soil applications in Australia. Hartley and Kidd (1987) have described other properties of the pesticides. Technical grade samples (>99% purity) of the pesticides were obtained from Bayer Australia Ltd. (fenamiphos), Hoechst Australia Ltd. (linuron), and Ciba-Geigy Australia Ltd. (simazine). The pesticides in soil solution were analyzed by High Performance Liquid Chromatography (HPLC) as described in an earlier paper (Singh et al. 1990).

Sorption Kinetics

Flow method

Sorption values of the pesticides were calculated from pulse breakthrough curves (BTCs) using a flow technique described in another paper (Kookana et al. 1991). A column of 150 mm length and 10 mm diameter was packed with air dry soil, and then a dilute CaCl₂ solution was

passed through to condition the column. In chloride BTCs, dual peaks were taken as a sign of unsatisfactory packing, and in such cases columns were repacked. Since dual peaks in chloride BTCs were absent, it was assumed that no preferential flow was taking place along the walls of the soil column. The soils were packed into the columns to bulk densities ranging from 1.2 to 1.6 Mg m⁻³. A 300- μ g pulse of pesticide concentrations ranging from 5 μ g ml⁻¹ to 45 μ g ml⁻¹ was injected into the soil columns, and the concentrations were monitored by HPLC in automatically collected fractions of the effluent. Sorption corresponding to 1 μ g ml⁻¹ solution concentration was measured by the peak maxima method (Kookana et al. 1991). According to the method, a number of BTCs are obtained by injecting pulses of varying concentrations of the pesticides, as well as of a nonreactive solute (chloride) in the soil column, at a given flow rate or pore water velocity. The area between the loci of peak maxima of chloride BTCs and pesticide BTCs is integrated to calculate sorption corresponding to a given solution concentration. This sorption corresponds to a given residence time of the pesticide in the soil, calculated from the flow rate employed to generate BTCs. Thus, by generating BTCs corresponding to various flow rates as well as input concentrations, sorption versus time curves are obtained. The BTCs were obtained at flow rates ranging from 1 to 40 m d⁻¹ for various pesticides and soils.

Batch method

Five-gram samples of soil were equilibrated with 5 ml of 0.005 M CaCl₂ solution containing 1 μ g ml⁻¹ of different pesticides in polypropylene centrifuge tubes. The suspension was shaken on an end-to-end shaker for various lengths of time

TABLE 1
Some Physico-chemical properties of the soils

Property	Bassendean sand	Gascoyne sandy loam	Cobiac loamy sand	Wellesley clay
OM ^a (%)	1.2	1.7	0.6	4.6
Silt (%)	1.5	8.3	2.5	14.2
Clay (%)	1.3	15.3	13.6	63.7
pH (1:5 0.01 M CaCl ₂)	5.0	6.9	5.1	5.9
CEC ^b (cmol (+) kg ⁻¹)	2.4	24.8	3.5	43.0
Surface area ^c (m ² g ⁻¹)	0.4	22.5	13.4	73.1

^a Organic Matter

^b By Sr⁺⁺ saturation at pH 7

^c By applying BET theory to N₂ adsorption

and then centrifuged for 5 min at 12,000 rpm. The supernatant was withdrawn immediately and analysed for pesticide concentration remaining in soil solution. The differences between initial and final solution concentrations of pesticides were attributed to sorption. Pesticide sorption onto the walls of the centrifuge tubes was checked by taking blanks and was found to be negligible. The time elapsed for the sorption reaction was noted from the moment of introduction of pesticide solution in soil until the withdrawal of supernatant. The sorption values obtained after 24 h of shaking were assumed to represent an apparent equilibrium value.

THEORETICAL

Kinetic Equations for Sorption

The kinetic data for pesticide sorption in the soils were fitted to some of the rate laws commonly used in the literature. These rate equations are briefly discussed, below.

First-order kinetic equation

The first-order equation can be expressed as

$$dS/dt = k_d(KC - S) \quad (1)$$

where S is the amount of pesticide sorbed at time t , K is the equilibrium sorption coefficient, C is solution concentration and k_d is the rate coefficient.

The equation for the miscible displacement technique as derived by Sparks (1985) is as follows

$$\ln(l - S/S_e) = -k_a t \quad (2)$$

where $S_e = KC$ and k_a is the apparent rate coefficient.

Freundlich two-site kinetic equation

An equation analogous to Eq. (1) has been commonly used to describe the sorption kinetics of pesticides (Rao and Jessup 1983), i.e.,

$$dS/dt = k_d(KC^n - S) \quad (3)$$

If two different types of sorption sites are considered with the following equations describing sorption on the sites

$$S_1 = K_1 C^n \quad (4)$$

$$S_2 = K_2 C^n \quad (5)$$

(where, $K_1 = Kf$; $K_2 = K(1 - f)$, S_1 and S_2 are amounts sorbed at type-1 and -2 sites, respectively, f is the fraction of type-1 sites, and n is the exponent in Freundlich sorption isotherm) then Eq. (3) combined with Eq. (4) and (5) becomes

$$dS_1/dt = k_{d1}(K_1 C^n - S_1) \quad (6)$$

$$dS_2/dt = k_{d2}(K_2 C^n - S_2) \quad (7)$$

for the two types of sites.

Numerical and analytical solutions of Eq. (6) and (7) have been reported by Boesten and van der Pas (1988).

Parabolic diffusion law

According to Crank (1975, p. 244), a diffusion law with constant diffusion coefficient for early stages of sorption (often as far as $S/S_e = 0.5$) in a sheet of thickness l can be expressed as

$$S/S_e = (4/\pi^{0.5})(Dt/l^2)^{0.5} \quad (8)$$

where S is the sorption at time t , S_e is the sorption at time = infinity. This relation is based on constant surface concentration and uniform initial concentration throughout a plain sheet. However, for these initial and boundary conditions, similar relations can be obtained for a cylinder or a sphere or semi-infinite medium, according to which amount sorbed would be proportional to the square root of time.

A characteristic feature of Fickian diffusion is that in the early stages of sorption when diffusion takes place essentially in a semi-infinite medium, the amount of sorbed or desorbed is directly proportional to the square root of time, irrespective of the relation between diffusion coefficient and concentration (Crank 1975, p. 179). The linear behavior may extend well beyond 50% of equilibrium sorption when D increases with concentration increasing.

Conformation to the $t^{0.5}$ relationship is often observed in the initial stages of sorption-desorption reactions and is generally considered to provide evidence that the rate-limiting step is some diffusion process (Weber and Gould 1966; Sparks et al. 1980; Pavlatou and Polyzopoulos 1988).

RESULTS AND DISCUSSION

Sorption of the pesticides was studied by both batch and flow methods. Amounts sorbed at equilibrium were needed for the calculation of

the rate coefficients from the sorption data obtained by the flow method. Equilibrium values were obtained using a batch method involving a shaking of the soil suspension in the presence of pesticides for 24 h. This is a common practice to obtain equilibrium sorption coefficients of pesticides in soils. The batch data is discussed first.

Sorption Data Obtained by Batch Method

The sorption data for the pesticides followed the Freundlich equation $S = KC^n$, where K is the equilibrium sorption coefficient, and n is the exponent. The values of the Freundlich coefficients are presented in Table 2. The sorption of pesticides in the four soils occurred in the decreasing order linuron > fenamiphos > simazine. The highest sorption of the pesticides was observed in the clay soil with the highest organic matter content and the lowest in the loamy sand with very low organic matter content. The value of the exponent varied from 0.7 to 1.0 for the various pesticide/soil combinations.

The sorption-time relationship was also studied using the batch method. Sorption versus time plots for simazine and linuron are presented in Fig. 1. It is evident from this figure

TABLE 2
Freundlich sorption parameters for the pesticides in soils

Soil	K ($\mu\text{mol}^{1-n} \text{kg}^{-1} \text{L}^{1-n}$)	n ($\text{L} \mu\text{mol kg}^{-1}$)
<i>Simazine</i>		
Sand	1.23	0.90
Sandy loam	0.93	0.97
Loamy sand	0.53	1.00
Clay	13.87	0.70
<i>Linuron</i>		
Sand	7.06	0.85
Sandy loam	5.77	0.76
Loamy sand	4.68	0.70
Clay	38.17	0.81
<i>Fenamiphos</i>		
Sand	6.86	0.71
Sandy loam	2.58	0.80
Loamy sand	0.56	1.00
Clay	19.66	1.00

that, of the total sorption possible in 24 h, some 90% was achieved almost instantaneously. More than half of the total sorption comparatively slow, but within 2 h 80% of sorption occurred.

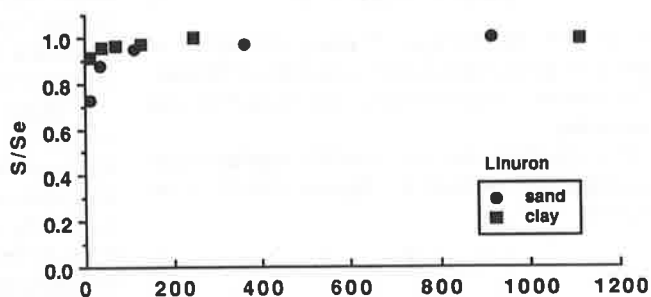
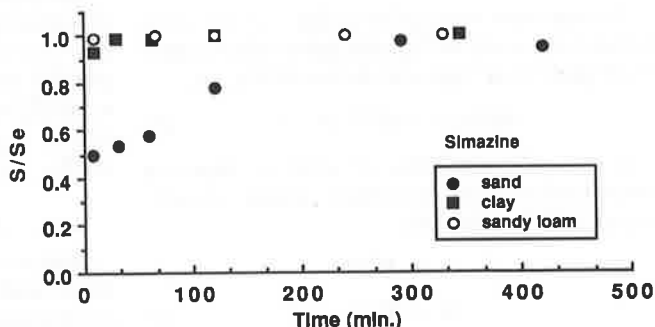


FIG. 1. Sorption kinetic data of simazine and linuron in soils as obtained by the batch method.



Sorption Data Obtained by Flow Method

The rate law describing sorption

To examine the mechanism and to establish the limiting factor for the sorption reaction, sorption data for the pesticides obtained by the flow method were fitted to the various kinetic equations described earlier.

First-order equation

First-order plots for the three pesticides are presented in Fig. 2. In contrast to a linear plot

expected from the first-order equation, a curvilinear relation was obtained for all the pesticides in soils. Therefore first-order rate coefficients cannot be obtained by applying Eq. (1). The observed sorption versus time relationship indicated an initial rapid rate followed by a slower rate of sorption (Fig. 2). Batch experiments by Hamaker et al. (1966), Letey and Oddson (1972), Wauchope and Meyers (1985), and more recently by Boesten and Van der Pas (1988) have shown similar sorption behavior of pesticides in soils. A combination of rapid and slow rates of sorption could possibly be due to the presence

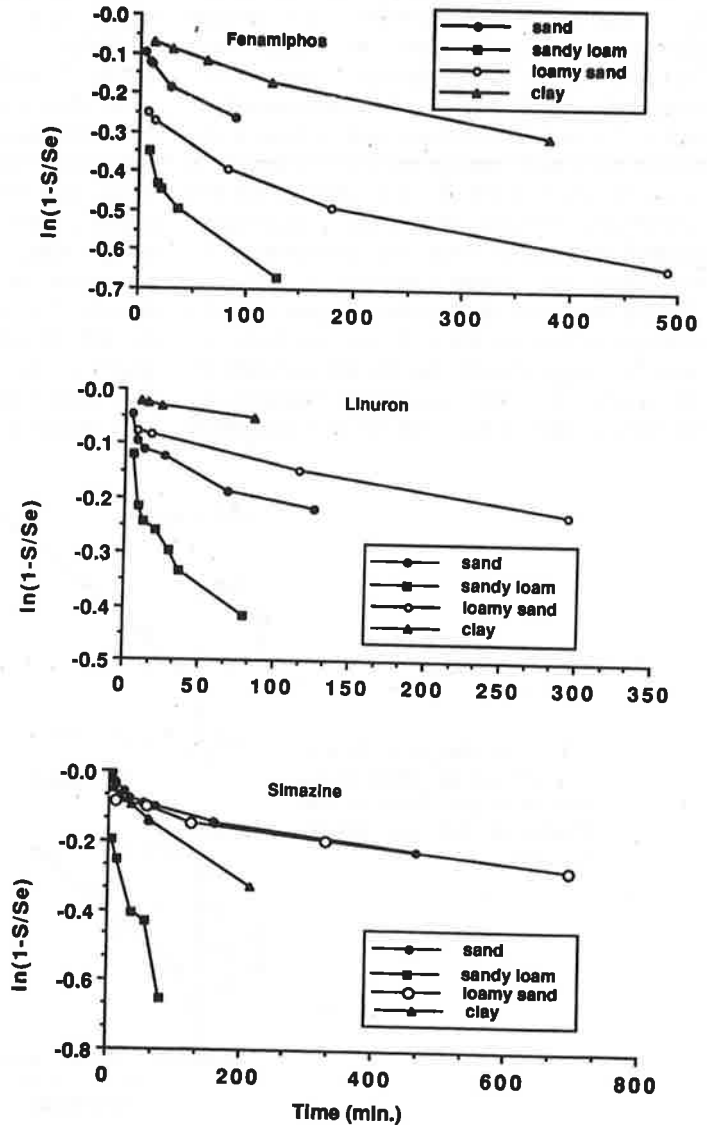


FIG. 2. First order plots of the sorption kinetic data (obtained by the flow technique) for the pesticides in different soils.

of different types of reaction sites in soils, that is, in terms of their nature (e.g., organic matter, minerals etc.) and/or their accessibility to the pesticides.

Freundlich two-site kinetic equation

The sorption data were fitted to the Freundlich two-site kinetic equations (Eq. (6) and (7)) by a numerical program written in PASCAL, essentially similar to that described by Boesten and van der Pas (1988). The integrations were performed using fourth-order Runge-Kutta formulas (Burden and Faires 1985). The program employed routines available in Turbo Pascal Numerical Toolbox (Borland 1985) for the solution of a system of coupled first-order ordinary differential equations using the Runge-Kutta method. The model had five adjustable parameters, kd_1 , kd_2 , K , f and n . Two parameters, K and n , for various pesticides and soils were obtained from the batch experiments (Table 2). A value of $kd_1 = 1000 \text{ d}^{-1}$ was chosen for the simulations because preliminary simulations showed that the sorption rate coefficients for the type-1 sites varied from 800 to 1300 d^{-1} . Despite the range, these values suggest that the reaction is over in the first few minutes, i.e., sorption occurs essentially instantaneously on type-1 sites. The remaining two parameters, i.e., fraction of type-1 sites f and the rate parameter

for type-2 sites kd_2 were varied in the simulations.

The simulated and the observed data for simazine in different soils are presented in Fig. 3, as an example. The sorption data for the other pesticides were similarly well described by the equations. The fractions of both types of sites and their rate coefficients according to the equations are given in Table 3. The fractions of these sites ranged from zero to 0.11 for various pesticides and soils. The coefficients from Table 3 show that the rates of sorption on the type-2 sites were far slower, requiring from hours to weeks to achieve equilibrium. These sites may be located within the aggregates and/or organic matter matrix. In clay soil with a relatively higher organic matter content, the sorption rate coefficients for the type-2 sites were so low (particularly for linuron and fenamiphos) that under flow conditions, sorption on these sites will continue for a number of weeks. It is worth noting also that the sorption on almost all sites in the clay soil was time-dependent since the values of fraction of type-1 sites were found to be very small. Such a low rate of sorption does not appear to be due to slow chemical kinetics on sites of a particular nature but is more likely due to diffusion of pesticide molecules to the sorption sites not readily accessible. Therefore, the sorption data were also fitted to the diffusion law described in an earlier section of this paper.

FIG. 3. Sorption kinetic data of simazine (obtained by flow technique) fitted to the Freundlich two-site kinetic equation.

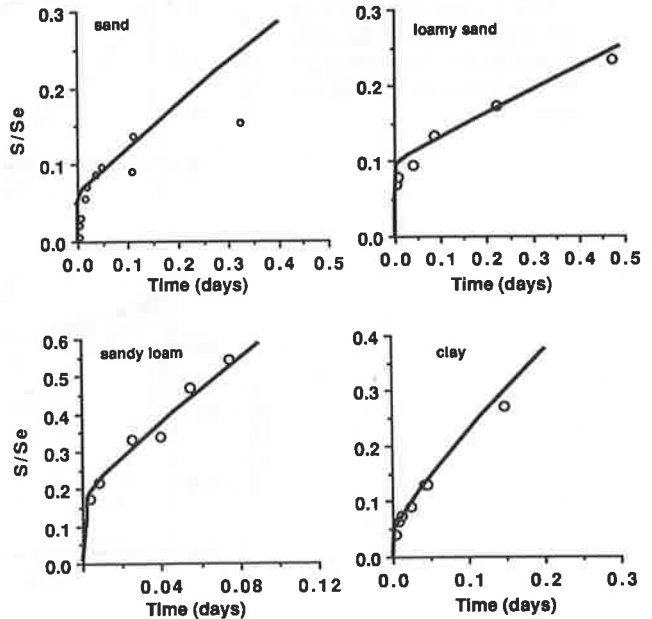


TABLE 3

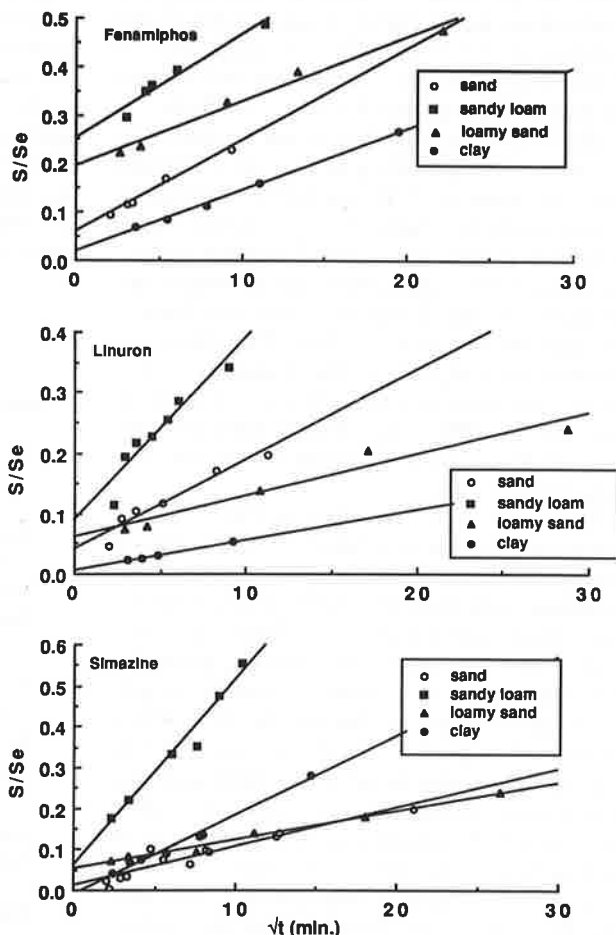
Parameters for two site Freundlich equation ($kd_1 = 1000 d^{-1}$)

Soil	kd_2 (d^{-1})	Fraction of type-1 sites
<i>Simazine</i>		
Sand	0.15	0.013
Sandy loam	4.60	0.110
Loamy sand	0.15	0.038
Clay	0.15	0.004
<i>Linuron</i>		
Sand	0.15	0.005
Sandy loam	2.80	0.060
Loamy sand	0.25	0.017
Clay	0.01	0.001
<i>Fenamiphos</i>		
Sand	0.40	0.010
Sandy loam	1.00	0.100
Loamy sand	0.50	0.110
Clay	0.05	0.002

Parabolic diffusion law

The sorption data plotted according to Eq. (8) is presented in Fig. 4. As mentioned earlier, the equation is valid for the initial stages of sorption. Although the time involved in the present sorption study was as high as 900 min, yet most of the sorption data represent a condition far from equilibrium. During this time, sorption under most pesticide/soil combinations was below 40% of the equilibrium sorption value. Furthermore, the amount sorbed at equilibrium is calculated after 24 h shaking under batch conditions, and this may in fact be an underestimation of the actual value. A number of recent studies show that sorption under field conditions continues for weeks and months (e.g., Pignatello and Huang 1991). Therefore, the application of Eq. (8) to the sorption data is justified. Figure 4 shows a good fit of the data to the parabolic diffusion law. However, as evident from Fig. 4,

FIG. 4. Sorption kinetic data of the pesticides (obtained by flow technique) as fitted to the parabolic diffusion law.



the diffusion plots showed an intercept in most cases of pesticides and soils. Such an intercept from a sorption vs $t^{0.5}$ graph has been taken as a component representing the initial sorption or external sites by a number of workers (Palmer and Bauer 1961; Leenheer and Ahlrichs 1971; Khan 1973). Palmer and Bauer (1961) reported that the sorption of amines on montmorillonite in a batch experiment followed the square root of time relation, but 5 to 20% of sorption was instantaneous suggesting initial sorption on external sites. Leenheer and Ahlrichs (1971) studied sorption rate curves of carbaryl and parathion insecticides on organic matter and found that linearity in square root plots was obtained for times greater than 10 min for both insecticides and all the adsorbents. In their experiments the initial sorption rate appeared to be on external surfaces of the adsorbents, and as the sorption proceeded, rates slowed down since sorption was governed by solute diffusing within adsorbent particles. A similar phenomenon was observed by Khan (1973) in his studies of the sorption of 2,4-D and 2,4,5-T herbicides on humic acid. In this case, the square root of time relation was linear after 4 h and up to 50 h.

Ideally, if Fickian diffusion was occurring in the soils, then according to Eq. (8) a straight line of sorption vs $t^{0.5}$ plot would be expected to pass through the origin. However, as previously discussed, at least two types of sorption sites in soils have been suggested by the successful application of the Freundlich two-site kinetic equation to the sorption data. Therefore, the linear portion of plots in Fig. 4 appears to represent the type-2 sites that show a time-dependent sorption. The slopes of such plots can provide sorption rate parameters which are governed by diffusion.

It is clear from the plots in Fig. 4 that a constant diffusion coefficient is not operative during the whole of the sorption process. The presence of an intercept in the sorption vs. $t^{0.5}$ plots suggests that it is a case of moving boundaries, e.g., where some of the diffusing molecules are immobilized by a chemical reaction or prevented from taking further part in the diffusion process (Crank 1975, p. 287). Crank (1975, p. 288-289) has also noted that when diffusion coefficients change discontinuously, i.e., drop from an infinite initial value to a constant value at a certain concentration, a sheet of sorption sites attains a uniform concentration 'infinitely rapidly,' and the remainder of sorption behavior

is as for constant diffusion coefficient. In the present case, it can be seen that the sorption behavior is of a similar nature. Since the sorption sites of type-1 are external sites, the distance involved from bulk soil to these sites is very small, and the sites are, therefore, rapidly approached by pesticide molecules, resulting in instantaneous sorption.

Thus, assuming that intercepts represent the instantaneous component and slopes the rate parameters for sorption on type-2 sites, linear regression was applied to the sorption data. The parameters obtained by linear regression of fractional sorption (S/Se) vs $t^{0.5}$ are given in Table 4. The values of intercept for the various pesticides in soils ranged from zero to 0.25.

Several other workers have also found the sorption of pesticides in soils to be diffusion controlled (e.g., Weber and Gould 1966; Li and Felbeck 1972; Moreale and Van Bladel 1979). However, it is noteworthy that all the above studies involved batch method, and the initial sorption in these studies was higher than observed here. The conformity of the present sorption data to the diffusion law demonstrates that in the less accessible regions (such as intra-aggregate pores or into the organic matter matrix), the pesticide molecules have to diffuse to the sorption sites before they are sorbed, and, as a result, the sorption reaction is limited by diffusion. Considering the porous nature of or-

TABLE 4
Parameters for parabolic diffusion law for sorption

Soil	Intercept	Slope (d ⁻¹)	r ²
<i>Simazine</i>			
Sand	0.007	0.37	0.960
Sandy loam	0.059	1.73	0.964
Loamy sand	0.053	0.27	0.990
Clay	-0.012	0.73	0.99
<i>Linuron</i>			
Sand	0.040	0.56	0.930
Sandy loam	0.088	1.14	0.893
Loamy sand	0.060	0.26	0.951
Clay	0.006	0.19	0.999
<i>Fenamiphos</i>			
Sand	0.058	0.72	0.989
Sandy loam	0.252	0.82	0.979
Loamy sand	0.195	0.50	0.982
Clay	0.018	0.48	0.998

ganic materials in soil and visualizing it as membrane-like aggregates (Wershaw 1986), intra-organic matter diffusion can indeed be expected to be a significant factor in pesticide sorption.

Effect of Soil Type on Sorption Kinetics

The effect of soil type on sorption is clearly reflected in the kinetic parameters obtained by both two-site kinetic equations as well as parabolic diffusion law. Significant differences in the sorption parameters were found between different soils (Table 3). Not only the fraction of type-1 sites but also the rate coefficient for type-2 sites were found to be significantly higher in Gascoyne sandy loam soil than in other soils. In contrast, the lowest values of these parameters were observed in the clay soil. A comparison of overall diffusion rate coefficients (slope of sorption- $t^{0.5}$ curve) of the pesticides among different soils also shows that the rate of sorption varies with soil type (Table 4). Among the four soils, the values of intercept were maximum, once again, in Gascoyne sandy loam and minimum (almost negligible) in Wellesly clay. The rate parameters from Tables 3 and 4 show clearly that in Gascoyne soil a higher proportion of sites were readily accessible, reacting almost instantaneously with pesticide. Considering the reports of slower sorption of pesticides on humic substances (Khan 1973), the higher organic matter content of Wellesly clay (4.6%) than Gascoyne sandy loam (1.7%) may explain the difference. The two soils differed not only in organic matter contents but also structurally. While the Gascoyne soil was in a dispersed state, to such an extent that the flow of water in soil columns was restricted during experiments, the Wellesly clay had a well developed structure. Furthermore, the latter contained a significant proportion of smectite clay mineral, which caused considerable swelling on wetting. Hence sorption in the intrameller spaces in clay minerals may have occurred in the clay soil. Higher organic matter content, the aggregated nature of soil particles, and the presence of swelling type of clay minerals in Wellesly clay soil appear to have caused a slower rate of diffusion and lower values of sorption rate coefficients for type-2 sites (Table 3). On the basis of the kinetic parameters given in Tables 3 and 4, Cobiac loamy sand and Bassendean sand ranked second and third, respectively. Once again, the second highest value of fraction of type-1 sites and

intercept (Table 3) observed in Cobiac loamy sand can be explained on the basis of organic matter content. Since Cobiac soil is a sub-surface soil, it had the lowest organic matter content (0.6%). Several other workers have found that sorption reaches equilibrium slowly in soils containing high organic matter (Hamaker et al. 1966; Moreale and Van Bladel 1979; Karickhoff and Morris 1985; Brusseau et al. 1989). In sieved soil, the size of the aggregates is such (aggregate radius 1 mm) that diffusion into the aggregates is expected to be rapid (Rao and Jessup 1983). Therefore, the diffusion into the matrix of organic matter is principally the rate-limiting factor in the sorption reaction. This is particularly so when the organic matter is the major soil constituent responsible for sorption of the pesticides.

A Comparison of Sorption by Batch and Flow Techniques

The sorption data obtained by batch technique (Fig. 1) show that a major part (up to 90%) of the sorption took place in the first 5 to 10 minutes. In fact, within the first 2 to 3 h, the sorption approached the apparent equilibrium value (99% of 24 h value). Several studies reported in the literature have also concluded that a major part of the sorption reaction is completed in first few minutes (Wauchope and Myers 1985; Boesten and Van der Pas 1988). Thus, under well stirred conditions, the major portion of the sorption reaction for pesticides is practically instantaneous. In contrast, however, less than 20% of the equilibrium (24 h) sorption value was completed in first 2 to 3 h under flow conditions (Tables 3 and 4). This comparison clearly demonstrates that under flow conditions, a large fraction of the sorption sites is not readily available to the pesticides.

Few comparisons of pesticide sorption by the two methods (batch and flow techniques) have appeared in the literature. However, for inorganic ion exchange reactions, the rate coefficients obtained by flow technique have generally been found to be significantly lower than those from batch data (Sparks and Rehcigl 1982; Hodges and Johnson 1987). Shaking, which is present in the batch but not in the flow technique, appears to be responsible for this discrepancy. In fact, Ogwada and Sparks (1986) reported that the degree of shaking affected the rate of inorganic ion exchange reaction on clay

mineral and soil. They compared the sorption data obtained by five different methods involving different degrees of shaking. The sorption rate coefficients from a miscible displacement technique were found to be similar to those from a static technique. On the other hand, much higher values of these coefficients were obtained under batch, stirred, and vortex batch methods—all involving shaking to different degrees. Similarly, Boesten and Van der Pas (1988) found much slower rates of sorption of two herbicides in unshaken moist soil than in shaken soil suspension.

Apparent versus Mechanistic Rate Laws

In addition to the present study, many reports dealing with inorganic ion exchange reactions have demonstrated that under flow conditions, the kinetics of sorption follow the Parabolic diffusion law (Sparks 1985; Hodges and Johnson 1987). Therefore, it can be concluded that the diffusion of a sorbate to the sorption sites is the rate-controlling step for a major part of sorption reaction during the transport of a pesticide in the soil profile. However, as Skopp (1986) pointed out, this inference relates to the apparent time dependency of sorption and not the chemical kinetics. To study the latter, it is essential to remove all physical barriers between the sorbate and sorbent (Skopp 1986). In fact, in heterogeneous systems such as in soils, it is very difficult to achieve conditions suitable for studying chemical kinetics. Therefore, most kinetic studies in the literature report apparent rate laws. Nevertheless, a batch method involving dilute, dispersed soil suspension appears most suitable for studying the chemical kinetics. In the present study, the results obtained by batch method have clearly shown that the sorption reaction is essentially instantaneous, which is consistent with other reports (e.g., Rao and Jessup 1983). However, it must be noted these inferences are based on short term (24 h) shaking experiments. It has recently been shown that under field conditions, long term sorption occurs at time scales of weeks and months (Boesten 1987; Pignatello 1989; Pignatello and Huang 1991). Pignatello and Huang (1991) compared the sorption coefficients obtained by equilibration for 24 h of herbicide freshly added to soil with those obtained from sorbed and solution concentrations resulting from the suspension of contaminated samples collected from the field

for similar times (24 h). They found that the sorption coefficients of atrazine and metalochlor in contaminated soil samples collected 2–15 months after their last application were higher by a factor ranging from 2.3 to 42 times, depending on the time since their last application. They concluded that age-dependent reversibility may have been due to continued diffusion of labile chemical into more remote or stronger sorption sites. Thus, it is possible that batch sorption values after 24-h shaking may underestimate the true equilibrium sorption.

In batch experiments, the shaking largely eliminates the physical process of diffusion and consequently provides rate parameters representing chemical kinetics of sorption. In contrast, the diffusion-controlled sorption observed under flow conditions signifies the physical transport of sorbate to the sorption sites or, in other words, an apparent rate law. A question arises as to how valuable apparent laws are in pesticide transport studies. The answer is that the sorption rate laws obtained by the flow technique are the only realistic laws (whether apparent or mechanistic), not those obtained by batch methods, even if they are mechanistic. This is because the conditions operative under batch experiments are not realistic; i.e., the soil is generally not in the form of a dilute suspension, nor does shaking occur during solute transport in the soil profile. Batch sorption data alone is not suitable for studies such as transport modelling. However, as demonstrated here, batch data in conjunction with those obtained by flow technique are certainly valuable in providing an accurate understanding of the sorption phenomenon.

In recent years, the use of two-site kinetic models for sorption (those assuming an instantaneous and a kinetic component) have considerably improved the predictive capability of solute transport models (Nielsen et al. 1986). An independent measurement of at least two parameters needed for such models, i.e., the fraction of instantaneous sites and the rate parameters for the remaining sites, is extremely important for the accurate description of the mobility of pesticides in soil. In most studies, such parameters are obtained by curve fitting of the very breakthrough curves for the description of which the parameters are needed. In the present study, these parameters have been obtained independently under flow conditions.

The validity of these parameters for the pesticide transport models is currently being examined.

ACKNOWLEDGMENTS

R.S.K. is grateful to the Australian International Development Assistance Bureau for the Commonwealth Fellowship. The project was funded by the Australian Water Research Advisory Council.

REFERENCES

- Ardakani M. S., and A. D. McLaren. 1977. Absence of local equilibrium during ammonium transport in a soil column. *Soil Sci. Soc. Am. J.* 41:677-679.
- Boesten, J. J. T. I. 1987. Modelling pesticide transport with a three site sorption sub-model: A field test. *Netherlands J. Agric. Sci.* 35:315-324.
- Boesten, J. J. T. I., and L. J. T. van der Pas. 1988. Modeling sorption/desorption kinetics of pesticides in a soil suspension. *Soil Sci.* 146:221-231.
- Borland. 1985. Turbo Pascal Toolbox, Numerical Methods. Borland International Inc. California.
- Brusseau, M. L., and P. S. C. Rao. 1989. Sorption nonideality during organic contaminant transport in porous media. *CRC Crit. Rev. Environ. Control.* 19:33-99.
- Brusseau, M. L., P. S. C. Rao, R. E. Jessup, and J. M. Davidson. 1989. Flow interruption: A method for investigating sorption non-equilibrium. *J. Contam. Hydrol.* 4:223-240.
- Burden, R. L., and J. D. Faires. 1985. Numerical analysis, 3rd Ed. Prindle, Weber & Schmidt, Boston.
- Crank, J. 1975. The mathematics of diffusion, 2nd Ed. Oxford Univ. Press, London.
- Hamaker, J. W., C. A. I. Goring, and C. R. Youngson. 1966. Sorption and leaching of 4 amino-3,5,6-trichloropicolinic acid in soil. *Adv. Chem. Ser.* 60:23-37.
- Hartley, D., and H. Kidd, eds. 1987. The agrochemicals handbook. The Royal Society of Chemistry, Nottingham, England.
- Hodges, S. C., and G. C. Johnson. 1987. Kinetics of sulfate sorption and desorption by Cecil soil using miscible displacement. *Soil Sci. Soc. Am. J.* 51:323-331.
- Karickhoff, S. W., and K. R. Morris. 1985. Sorption dynamics of hydrophobic pollutants on sediment suspensions. *Environ. Toxicol. Chem.* 4:469-479.
- Khan, S. U. 1973. Equilibrium and kinetic studies of the adsorption of 2,4-D and picloram on humic acid. *Can. J. Soil Sci.* 53:429-433.
- Kookana, R. S., R. G. Gerritse, and L. A. G. Aylmore. 1991. A method for studying nonequilibrium sorption during transport of pesticides in soil. *Soil Sci.* (in review).
- Leenheer, J. A., and J. L. Ahlrichs. 1971. A kinetic and equilibrium study of the adsorption of carbaryl and parathion upon soil organic matter surfaces. *Soil Sci. Soc. Am. Proc.* 35:700-704.
- Letey, J., and J. K. Oddson. 1972. Mass transfer. In *Organic chemicals in the soil environment*. C. A. I. Goring and J. W. Hamaker (eds.). Marcel Dekker, New York, pp. 399-442.
- Li, G. C., and G. T. Felbeck. 1972. A study of the mechanism of atrazine sorption by humic acid from muck soils. *Soil Sci.* 113:140-148.
- Moreale, A., and R. van Bladel. 1979. Soil interactions of herbicide derived aniline residues: A thermodynamic approach. *Soil Sci.* 127:1-9.
- Murali, V., and L. A. G. Aylmore. 1980. No-flow equilibration and adsorption dynamics during ionic transport in soils. *Nature* 283:467-469.
- Murali, V., and L. A. G. Aylmore. 1983. Competitive sorption during solute transport in soils: 3. A review of experimental evidence of competitive sorption and an evaluation of simple competition models. *Soil Sci.* 136:279-290.
- Nielsen, D. R., M. Th. van Genuchten, and J. W. Biggar. 1986. Water flow and solute transport processes in the unsaturated zone. *Water Resour. Res.* 22:89s-108s.
- Ogwada, R. A., and D. L. Sparks. 1986. Kinetics of ion exchange on clay minerals and soil: I. Evaluation of methods. *Soil Sci. Soc. Am. J.* 50:1158-1162.
- Palmer, I., and N. Bauer. 1961. Sorption of amines by montmorillonite. *J. Phys. Chem.* 65:894-895.
- Pavlatou, A. and N. A. Kyzopoulou. 1988. The role of diffusion in the kinetics of phosphate desorption: The relevance of the Elovich equation. *J. Soil Sci.* 39:425-436.
- Pignatello, J. J. 1989. Sorption dynamics of organic compounds in soils and sediments. In *Reactions and movement of organic chemicals in soils*. B. L. Sawhney and K. Brown (eds.). SSSA Spec. Publ. 22. ASA and SSSA, Madison, WI, pp. 48-50.
- Pignatello, J. J., and L. Q. Huang. 1991. Sorptive reversibility of atrazine and metolachlor residues in field soil samples. *J. Environ. Qual.* 20:222-228.
- Rao, P. S. C., and R. E. Jessup. 1983. Sorption and movement of pesticides and other toxic organic substances in soils. In: *Chemical mobility and reactivity in soil systems*. D. W. Nelson, K. K. Tanji and D. E. Elrick (eds.). Am. Society of Agronomy and Soil Science. Soc. Spec. Pub. No. 11, Madison, WI, pp. 183-201.
- Selim, H. M., and M. C. Amacher. 1988. A second-order kinetic approach for modeling solute retention and transport in soils. *Water Resour. Res.* 24:2061-2075.
- Singh, R., R. G. Gerritse, and L. A. G. Aylmore. 1990. Adsorption desorption of selected pesticides in some Western Australian soils. *Aust. J. Soil Res.* 28:227-243.
- Skopp, J. 1986. Analysis of time-dependent chemical processes in soils. *J. Environ. Qual.* 15:205-213.
- Sparks, D. L. 1985. Kinetics of ionic reactions in clay minerals and soils. *Adv. Agron.* 38:231-266.
- Sparks, D. L., and J. E. Rechcigl. 1982. Comparison of batch and miscible displacement techniques to describe potassium sorption kinetics in Delaware soils. *Soil Sci. Soc. Am. J.* 46:875-877.
- Sparks, D. L., L. W. Zelazny, and D. C. Martens. 1980. Kinetics of potassium desorption in soil using

- miscible displacement. *Soil Sci. Soc. Am. J.* 44:1205-1208.
- Wagenet, R. J., J. W. Biggar, and D. R. Nielsen. 1977. Tracing of transformations of urea fertilizer during leaching. *Soil Sci. Soc. Am. J.* 41:896-902.
- Wauchope, R. D., and R. S. Meyers. 1985. Sorption-desorption kinetics of atrazine and linuron in freshwater-sediment aqueous slurries. *J. Environ. Qual.* 14:132-136.
- Weber, W. J. Jr., and J. P. Gould. 1966. Sorption of organic pesticides from aqueous solution. *Adv. Chem. Ser.* 60:280-305.
- Wershaw, R. L. 1986. A new model for humic materials and their interactions with hydrophobic organic chemicals in soil-water systems. *J. Contam. Hydrol.* 1:29-35.
- Yaron, B., Z. Gerstl, and W. F. Spencer. 1985. Behaviour of herbicides in irrigated soils. *Adv. Soil Sci.* 3:121-211.

Simulation of simazine transport through soil columns using time-dependent sorption data measured under flow conditions

Rai S. Kookana¹, R.D. Schuller and L.A.G. Aylmore*

*Soil Science and Plant Nutrition, The University of Western Australia, Nedlands,
W.A. 6009, Australia*

(Received July 7, 1992; revised and accepted April 2, 1993)

ABSTRACT

Kookana, R.S., Schuller, R.D. and Aylmore, L.A.G., 1993. Simulation of simazine transport through soil columns using time-dependent sorption data measured under flow conditions. *J. Contam. Hydrol.*, 14: 93–115.

In a single-grained and extremely sandy (98% sand) soil asymmetrical breakthrough curves (BTC's) of simazine, with earlier breakthrough and a delayed approach to equilibrium relative concentration (generally referred as tailing) were obtained at varying pore-water velocities using laboratory columns. These BTC's were successfully described only when the bicontinuum approach of two sites/two regions was used with the convective-dispersive equation. The models using this approach need two additional parameters (namely fraction of type-1 sites or mobile phase f , and the rate parameter for type-2 sites or immobile phase α) and these are generally obtained by curve-fitting procedures. However, considering the importance of independent measurement of input parameters for the numerical simulation of these BTC's, the rate parameters describing the time-dependent behaviour of simazine sorption were sought from a separate experiment performed under realistic (flow instead of batch) conditions. In this experiment sorption values were calculated from retardation factors of pulse BTC's as affected by pore-water velocities. The sorption of simazine under flow conditions was found to be much slower than occurs under the shaking employed in the batch method. Furthermore it followed a linear relation with square root of time. The sorption vs. square root time relation provided one of the two parameters (the fraction of type-1 sites) needed for simulation. Consistent with numerous reports in the literature, the rate parameter for type-2 sites (or mass-transfer coefficient for immobile region α) was found to be dependent on pore-water velocity. Furthermore, the fraction of type-1 sites (or fraction of mobile phase) was also found to vary with pore-water velocity, which has not commonly been observed. Since the organic matter in the soil used here was the predominant source of sorption sites, intra-organic matter diffusion may have been the

¹ Present address: Cooperative Research Centre for Soil and Land Management, Private bag 2, Glen Osmond, S.A. 5064, Australia.

* Corresponding author.

most likely cause of nonequilibrium conditions during simazine transport. The independent measurement of the rate parameter α could not be accomplished. However, the α value from this study as well as those from a number of published studies were found to have essentially similar relationship with pore-water velocity.

INTRODUCTION

A number of simulation models to predict solute leaching in soils have been reported in the literature and these are generally classified into categories such as research, management or screening models on the basis of their intended applications (Addiscot and Wagenet, 1985). Amongst these, the research models are of particular value in that they not only allow more accurate prediction of solute distributions with time but also facilitate the interpretation of measured solute distributions in terms of the specific mechanisms involved in the transport process.

Description of the sorption phenomena between solute and sorbent is a critical component of all transport models. Sorption has often been simplified, particularly in earlier solute transport models, by assuming that local equilibrium is established instantaneously during solute transport in soil. Such an assumption leads to much simpler models requiring fewer parameters. However, in recent years the validity of this assumption has been challenged since numerous studies have shown non-ideal transport of solutes in soils, characterised by asymmetrical breakthrough curves (BTC's) exhibiting delayed approach to the column input concentration in both laboratory and field experiments (Valocchi, 1985; Goltz and Roberts, 1986; Winters and Lee, 1987; Brusseau and Rao, 1989; Brusseau et al., 1989; Gaber et al., 1992).

Models which include sorption nonequilibrium conceptualised in the form of a bicontinuum model of some type, and represented by either a chemical process (i.e. sorption on two different types of sorption sites in soil) or a physical process (the soil matrix consisting of mobile and immobile zones), have been successfully used to simulate solute transport (Cameron and Klute, 1977; van Genuchten et al., 1977; Brusseau et al., 1989; Gamedainger et al., 1991). Both of these chemical process- and physical process- based models can be described in exactly the same mathematical form (Nkedi-Kizza et al., 1984). Consequently, the establishment of the physical or chemical nature of the sorption nonequilibrium in the absence of independently measured parameters is virtually impossible (Nkedi-Kizza et al., 1984). Thus, an independent measurement of the input parameters is crucial for a proper understanding of mechanisms operative during solute transport. This has increasingly being recognised in recent years and some workers have used independently measured parameters for simulation (Brusseau et al., 1989).

The occurrence of sorption nonequilibrium during solute transport in structured soils has been well documented in both laboratory (van Genuchten et al., 1977; Rao et al., 1980b; Nkedi-Kizza et al., 1982; Selim et al., 1987; Seyfried and Rao, 1987) and field studies (Rao et al., 1974; Jury et al., 1986). There are also reports in the literature which show similar behaviour in soils which are not particularly well structured (Bouchard et al., 1988; Brusseau and Rao, 1989). It has becoming increasingly clear that under transport conditions the occurrence of nonequilibrium sorption for many pesticides and organic compounds in soil may result from a variety of processes related to single or multiple sources or be caused by a combinations of transport- and sorption-related processes (Brusseau et al., 1989). Recent laboratory research has revealed very slow rates of sorption and desorption of organic compounds in soils (e.g., Ball and Roberts, 1991). This research has been extensively reviewed (Pignatello, 1989; Brusseau and Rao, 1991). Some recent experiments suggest that sorption nonequilibrium for a large number of organic compounds can be due to time-dependent interactions between sorbate and sorbent organic matter (Brusseau and Rao, 1991).

In the present study we used a very sandy soil with low organic matter and clay contents to obtain simazine BTC's at four different pore-water velocities since relatively few experiments have investigated the effect of varying pore-water velocity on the transport of herbicides (Brusseau, 1992). These BTC's were then numerically simulated with a convective-dispersive equation coupled with suitable forms of sorption nonequilibrium models, using the finite-difference technique. The input parameters were sought from independent experiments. In order to independently measure the sorption rate parameters, the sorption time dependency of simazine pesticide was studied by both flow (Kookana et al., 1992b) and batch experiments. This is in contrast to the common practice of obtaining the parameters by either curve-fitting procedures or by batch methods. The aim of the present studies was to assess the utility of sorption kinetic data obtained from independent flow experiments in describing the transport behaviour of simazine at different pore-water velocities in a sandy soil with low organic matter.

THEORETICAL

Transport models based on advective-dispersive equation

For one-dimensional steady flow in a homogeneous soil of uniform water content, the total amount of a non-reactive solute transported by advection and dispersion across unit area in the direction of flow is given by:

$$\partial C / \partial t = D \cdot \partial^2 C / \partial z^2 - v \cdot \partial C / \partial z \quad (1)$$

where C is solution concentration [$M L^{-3}$]; v is average pore-water velocity [$L T^{-1}$]; t is time [T]; D is the apparent dispersion coefficient [$L^2 T^{-1}$]; and z is the distance [L].

For a reactive solute undergoing sorption in soil, a term accounting for the concentration on the solid phase is added to Eq. 1, i.e.:

$$\partial C/\partial t + \rho/\theta \cdot \partial S/\partial T = D \cdot \partial^2 C/\partial z^2 - v \cdot \partial C/\partial z \quad (2)$$

where θ is the volumetric soil water content [$L L^{-3}$]; ρ is the dry bulk density of soil system [$M L^{-3}$]; and S represents sorbed concentration [$M M^{-1}$].

To solve Eq. 2 under given initial and boundary conditions, the functional relationships between concentrations of solute in the soil solution (C) and solid phase (S) are needed.

Equilibrium models

For a linear sorption isotherm ($S = KC$, where K is sorption coefficient) Eq. 2 can be restated as:

$$R \cdot \partial C/\partial t = D \cdot \partial^2 C/\partial z^2 - v \cdot \partial C/\partial z \quad (3)$$

where the retardation factor R is given by:

$$R = 1 + \rho(K/\theta) \quad (3a)$$

The models described in Eq. 3 assume that the sorption-desorption isotherms are reversible and single-valued. However, the sorption isotherms are not always single-valued but may exhibit hysteresis.

Nonequilibrium models

The conventional transport equation (Eq. 3) is based on local equilibrium assumption (LEA). This assumption is true only when the sorption process is faster than the processes affecting the solute concentration (e.g., advection, hydrodynamic dispersion). The asymmetrical (skewed) and nonsigmoidal BTC's reported for a number of inorganic ions such as Ca, Mg, K, Al, as well as for organic compounds such as pesticides, in soil columns has challenged the validity of this assumption. The characteristics of such BTC's are an early initial breakthrough and tailing or slow approach to input concentration of solute in the soil column. This behaviour has been attributed to sorption nonequilibrium which could arise from several physical or chemical factors (Brusseau et al., 1989).

Sorption kinetics in earlier studies have involved simple one-site first-order models (Hornsby and Davidson, 1973; van Genuchten et al., 1974) wherein the sorption rate was represented by a first-order linear kinetics which can be

written as follows:

$$\partial S/\partial t = k_d(KC - S) \quad (4)$$

where k_d is the desorption rate coefficient [T^{-1}]. This model has generally been successful at low pore-water velocities (Nielsen et al., 1986) but has frequently failed to predict experimental data well (Brusseau and Rao, 1989). However, improved transport descriptions have been achieved through the use of two-site kinetic models.

Two-site kinetic models

A bicontinuum or two-site/two-region approach based on physical or chemical mechanisms limiting the rate of sorption has been used to better describe many experimental BTC's. These models can be placed in at least two groups based on the hypothesised mechanism of sorption nonequilibrium. The "chemical-process" models assume that sorption nonequilibrium is due to a time-dependent sorption reaction at the sorbent surface. Sorbent surfaces are assumed to have two types of sorption sites, one where sorption is instantaneous and one where it is rate limited (Cameron and Klute, 1977). Rate-limited sorption on the sites is represented by a first-order equation and instantaneous sorption by the sorption isotherm equation. Jardine et al. (1985) provided a good illustration of chemical nonequilibrium of this type for aluminium. In the other group of models ("physical-process" models), the asymmetry of the BTC is explained on the basis of physical processes such as the presence of two soil pore-water domains, i.e. a mobile region and a stagnant or immobile region. Advective-dispersive transport is assumed to occur only in the mobile region, while sorption in the stagnant region of the soil is diffusion controlled. Time-dependent solute transfer between these regions results in sorption nonequilibrium. The phenomena attributed to physical nonequilibrium are exhibited by both sorbing and non-sorbing solutes because the mechanism responsible for physical nonequilibrium is a transport component and the sorption reaction itself is not involved (Brusseau and Rao, 1989).

Rate-limiting processes of various kinds have been discussed by Brusseau et al. (1991) identifying transport-related nonequilibrium, chemical nonequilibrium and intrasorbent diffusion as three primary classes of processes which may be responsible for nonequilibrium sorption. The bicontinuum approach can be used to represent all three classes of processes.

In the chemical process model, sorption on the two types of sites is described by following equations:

$$S_1 = fKC \quad (5a)$$

$$dS_2/dt = k_1S_1 - k_2S_2 \quad (5b)$$

where S_1 and S_2 are the sorbed concentrations [$M M^{-1}$] on type-1 and type-2 sites, respectively; f is the total fraction of type-1 sites; and k_1 and k_2 are the forward and backward sorption rate constants [T^{-1}], respectively.

In the physical process model, sorption in both dynamic and stagnant regions is assumed to be an instantaneous, linear and reversible process. Therefore:

$$S_m = KC_m \quad (6a)$$

and

$$S_{im} = KC_{im} \quad (6b)$$

where subscripts m and im represent dynamic (mobile) and stagnant (immobile) phases, respectively.

Nkedi-Kizza et al. (1984) showed that both models (based on chemical and physical processes) can be put into exactly the same mathematical form by introducing dimensionless variables. The following two non-dimensional equations are employed to simulate solute transport:

$$\beta R \cdot \partial C^* / \partial t + (1 - \beta) R \cdot \partial S^* / \partial t = 1/P \cdot \partial^2 C^* / \partial X^2 - \partial C^* / \partial X \quad (7a)$$

$$(1 - \beta) R \cdot \partial S^* / \partial t = \omega(C^* - S^*) \quad (7b)$$

For the physical and the chemical process models, the variables are dimensionalized as follows:

Physical process

$$P = v_m L / D_m,$$

$$T = v_m \phi_m t / L,$$

$$\phi_m = \theta_m / \theta,$$

$$X = z / L,$$

$$C^* = C_m / C_0,$$

$$S^* = C_{im} / C_0,$$

$$R = 1 + (\rho / \theta) K,$$

$$\beta = (\theta_m + f \rho K) / (\theta + \rho K),$$

$$\omega = \alpha L / (\theta_m v_m),$$

Chemical process

$$P = vL/D \quad (8a), (9a)$$

$$T = vt/L \quad (8b), (9b)$$

$$\quad (8c)$$

$$X = z/L \quad (8d), (9d)$$

$$C^* = C/C_0 \quad (8e), (9e)$$

$$S^* = S_2/(1-f)KC_0 \quad (8f), (9f)$$

$$R = 1 + (\rho/\theta)K \quad (8g), (9g)$$

$$\beta = (1 + f(\rho/\theta)K)/R \quad (8h), (9h)$$

$$\omega = k_2(1-\beta)RL/v \quad (8i), (9i)$$

where the symbols not defined earlier are: L = length of column [L]; C_0 = input concentration [$M L^{-3}$]; α = coefficient of mass transfer from

dynamic to stagnant domain [T^{-1}]; β = fraction of instantaneous retardation; and ω = Damköhler number (ratio of hydrodynamic residence time to characteristic time for sorption)

The initial and boundary conditions associated with Eqs. 7 are:

$$C^* = S^* = 0 \quad X > 0, \quad T = 0 \quad (10a)$$

$$-1/P(dC^*/dX) + C^* = 1 \quad X = 0, \quad 0 < T \leq T_0 \quad (10b)$$

$$-1/P(dC^*/dX) + C^* = 0 \quad X = 0, \quad T > T_0 \quad (10c)$$

$$dC^*/dX = dS^*/dX = 0 \quad X = \infty, \quad T > 0 \quad (10d)$$

The finite-difference form of Eqs. 10 was obtained with second-order finite-difference approximations in time and space obtained from Taylor series expansion using the Crank–Nicholson approximation.

MATERIALS AND METHODS

Soil and pesticide

A sandy soil representing nearly 50% of the area under the Swan Coastal Plain (SCP) in Western Australia was used in the study. The aquifers underneath the SCP are being exploited for drinking water and nearly 60% of domestic water in Perth comes from groundwater. Horticultural activities including market gardens, orchards and nurseries are carried out on the SCP and the soil therefore receives repeated applications of pesticides and other agrochemicals. The soil contains very little clay (1.2%) dominated by kaolinite, has low organic carbon content (0.6%), an acidic pH (5.0 in 0.01 M CaCl₂, 1:5 soil/water ratio) and a cation-exchange capacity (CEC) of 2.4 cmol(+) kg⁻¹. The surface area of the soil obtained by low-temperature N₂ adsorption was found to be 0.36 m² g⁻¹. Other physico-chemical properties of the soil have been published elsewhere (Singh et al., 1990).

Simazine (2-chloro-4,6-bis(ethylamino)-1,3,5-triazine) is a commonly used pesticide belonging to the s-triazine family of herbicides. It is a soil applied herbicide and generally used at a rate of 1–4 kg ha⁻¹ per application. Simazine has an aqueous solubility of 5 µg L⁻¹, vapour pressure of 4.8 mPa at 30°C (Hartley and Kidd, 1987) and is a weakly basic compound with a pK_a-value of 1.65 (Weber, 1970).

Simazine analysis

Simazine concentrations in solution were determined using reversed-phase high-performance liquid chromatography (HPLC; ETP-Kortec[®], Sydney,

Australia). Separations were carried out on a HPLC with a reversed-phase column *C18* (Spherisorb[®] ODS, 250 × 4.6 mm, Phase Separation[®], Clwyd, U.K.) using a mobile phase of methanol–water (65:35) at a flow rate of 1 mL min⁻¹. A retention time of 7 min was noted for simazine under these conditions. Detection of peaks was carried out with a UV detector at 220-nm wavelength. All samples were filtered through a 0.45- μ m Nylon[®] membrane filter prior to injection into the column. Chloride BTC were obtained with an on-line conductivity detector, calibrated through Cl⁻ analysis on HPLC (Gerritse and Singh, 1988).

Soil column studies

Chloride and simazine BTC's were obtained at different flow velocities in stainless-steel columns (300 mm long, 25 mm ID) generally used for HPLC separations (Alltech Associates, Australia). The columns had low dead volume and were fitted with stainless-steel filters (0.45 μ m) on both ends. The column was packed with Bassendean sand [from the Swan coastal plain, Western Australia (Singh et al., 1990)] at a uniform bulk density. To obtain uniform packing, the columns were filled under constant vibration. Several pore volumes of dilute salt solution (0.005 M CaCl₂) were passed through the bottom of the columns before obtaining BTC's. A dual-piston HPLC pump (ETP-Kortec[®], Sydney, Australia) was used to supply the solution to the column at a constant rate of flow. Samples of the soil solution eluting out of the soil column were collected using an automatic fraction collector and were immediately capped and removed for storage at 4°C. The samples were analysed for simazine within a day of collection. Packing of the soil in the columns was assessed through chloride BTC's. Dual peaks for chloride BTC's were taken as an index of unsatisfactory and non-uniform packing of the soil in a column. In such cases the column was repacked. Due to the wide ratio between column length and internal diameter of column,

TABLE 1

Experimental conditions during the column studies for simazine BTC's

Column length	0.300 m
Inner diameter of column	0.025 m
Weight of soil in column	0.196 kg
Bulk density	1.34 kg m ⁻³
Pore volume	0.48 · 10 ⁻⁴ m ⁻³
Porosity	0.31 m ³ m ⁻³
Range of pore-water velocities	44.6–892.8 m day ⁻¹
Input concentration of simazine	1.0 · 10 ⁻⁶ kg m ⁻³

some wall effect may occur. However, the retardation factor close to 1 for the BTC of chloride obtained with the columns suggested that wall effects were negligible. The high permeability of the soil may have eliminated such effects. Some details of the experimental conditions for the BTC's are given in Table 1. Chloride ion was used as a non-reactive tracer to characterise the flow of water through the column. The BTC of chloride was obtained by pulse injections of 300 μL of 0.05 M CaCl_2 solution at a pore-water velocity of 0.06 cm min^{-1} .

Estimation of input parameters

Dispersion coefficients. The apparent dispersion coefficients were obtained through the longitudinal hydrodynamic dispersivity parameter (λ) using the relation:

$$D = D_0\tau + \lambda v \quad (11)$$

where D_0 is the diffusion coefficient in water; and τ is the soil tortuosity factor. At the flow velocities used the contribution due to D_0 was negligible. The dispersivity was calculated from the zero-, first- and second-order moments of the BTC resulting from a pulse of chloride into the soil columns. The value of λ calculated from three BTC's of chloride was found to be 4.3 mm for the soil columns used in the study. For small laboratory columns, similar values has been reported by other workers (Wagenet, 1983; Gerritse and Singh, 1988). Gerritse and Singh (1988) indicated that in this soil at the pore-water velocities used in the study, λ would be little affected by changes in flow velocity. The first moment of chloride BTC representing the retardation factor was found to be 1.079.

Sorption parameters

Flow method. Sorption values for the pesticides were calculated from pulse breakthrough curves (BTC's) using a flow technique described elsewhere (Kookana et al., 1992b). In summary, the method commonly employed in chromatographic literature and known as the "peak maxima" method (Huber and Gerritse, 1971) was used. According to the method, a number of BTC's are obtained by injecting pulses of varying concentrations of the reactive as well as of a non-reactive (chloride in this study) solute in the soil column at a given flow rate or pore-water velocity. The peak positions of BTC's obtained at a given pore-water velocity but with varying input concentrations are used for calculating sorption values. Sorption corresponding to a given solution concentration is calculated by integrating the area between the loci of peak maxima of chloride BTC's and the pesticide BTC's. Such sorption values correspond to a given residence time of the pesticide in the soil, determined

by the flow rate employed to generate BTC's. Thus by obtaining BTC's corresponding to various flow rates as well as input concentrations, sorption vs. time curves are obtained.

Three different sizes of columns (lengths 300, 150 and 50 mm and respective internal diameters of 25, 10 and 4.5 mm) were used to cover a range of pore-water velocities (0.4–40 m day⁻¹) and reaction times. Soil was packed in high-quality stainless-steel HPLC columns (Alltech®), fitted with 0.45- μ m filters at both ends. The columns were packed with air-dry soil and then a dilute CaCl₂ (0.005 M) solution was passed through to condition the column. In chloride BTC's, dual peaks were taken as a sign of unsatisfactory packing and in such cases columns were repacked. Since dual peaks in chloride BTC's were absent it was assumed that no preferential flow is taking place along the walls of the soil column. The soils were packed into the columns to bulk densities ranging from 1.4 to 1.6 Mg m⁻³. Other details of these columns have been given in a previous paper (Kookana et al., 1992b). A 300-mg pulse of simazine for concentrations ranging from 5 to 10 mg mL⁻¹, was injected into the soil columns and the outgoing concentrations were monitored either by HPLC in automatically collected fractions of the effluent or by an on-line UV detector at 220 nm connected to a chart recorder. Except for the largest size column, an on-line UV detector was used to monitor the pulse BTC's. Sorption corresponding to 1 mg mL⁻¹ solution concentration was measured by the peak maxima method.

Batch method. Five-gram samples of soil were equilibrated with 5 mL of 0.005 M CaCl₂ solution containing 1 mg mL⁻¹ of different pesticides in polypropylene centrifuge tubes at 20°C. The suspension was shaken on an end-to-end shaker for various lengths of time and then centrifuged for 15 min at 12,000 rpm. The supernatant was withdrawn and immediately analysed for pesticide concentration remaining in the soil solution or stored in a refrigerator at 4°C (analysis was done within 1–2 days). The differences between the initial and final solution concentrations of pesticides were attributed to sorption. Pesticide sorption onto the walls of the centrifuge tubes was checked by taking blanks and was found to be negligible. The time elapsed for the sorption reaction was noted from the moment of introduction of the pesticide solution into the soil until the withdrawal of supernatant. The sorption value obtained after 24 h of shaking was assumed to represent an apparent equilibrium. All samples were run at least in duplicate.

To obtain the equilibrium sorption isotherm, 5-g samples of soil were equilibrated with 10-ml aliquots of a series of simazine concentrations ranging from 1 to 3 μ g mL⁻¹ prepared in 0.005 M CaCl₂ solution. The suspension contained in polypropylene centrifuge tubes was shaken for 24 h at 20°C. The rest of the procedure was the same as described above.

RESULTS AND DISCUSSION

Simazine sorption kinetics under batch and flow conditions

The equilibrium sorption data for simazine obtained by the batch method, corresponding to solution concentrations up to 3 mg mL^{-1} , fitted very well to a linear sorption isotherm (Fig. 1). The concentration of simazine never exceeded 1 mg mL^{-1} during the transport experiments, hence it was appropriate to use the linear sorption isotherm during simulations. The value of the equilibrium sorption coefficient was found to be 0.61 L kg^{-1} ($r^2 = 0.98$).

The sorption kinetic data for simazine obtained by the flow technique and by a batch method are presented in Fig. 2a. The sorption values have been presented as a fraction of the apparent equilibrium value (i.e. the value obtained after 24-h shaking by the batch method). Sorption was found to occur at a much faster rate under the batch conditions involving shaking, than under the flow conditions. For example, after shaking the soil suspension for a period of 0.2 days, the sorption almost reached the apparent equilibrium value under batch conditions, whereas under flow conditions during this period sorption equal to only 20% of the equilibrium value was achieved. This difference may be attributed to the elimination (albeit partially) of transport-related processes, such as diffusion, due to the shaking of the soil suspension under the batch conditions. Conversely, a much slower approach to equilibrium obtained with the flow technique is presumably due to the absence of accelerated mixing which occurs due to shaking under the batch method. Such effects of shaking on sorption kinetics have previously been noted. For example, Ogwada and Sparks (1986) compared five methods of

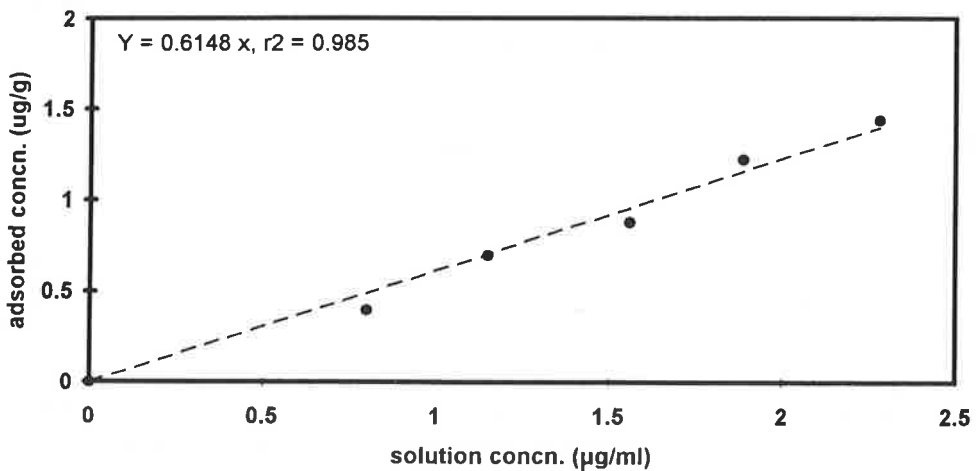
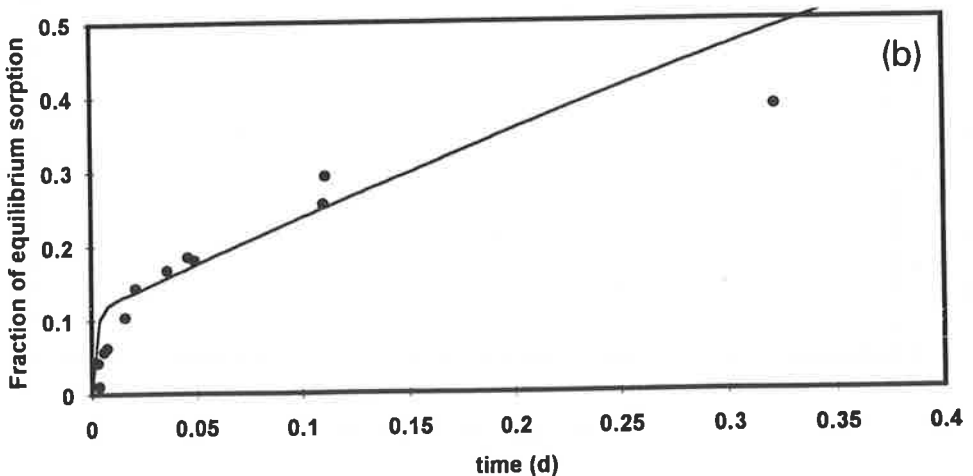
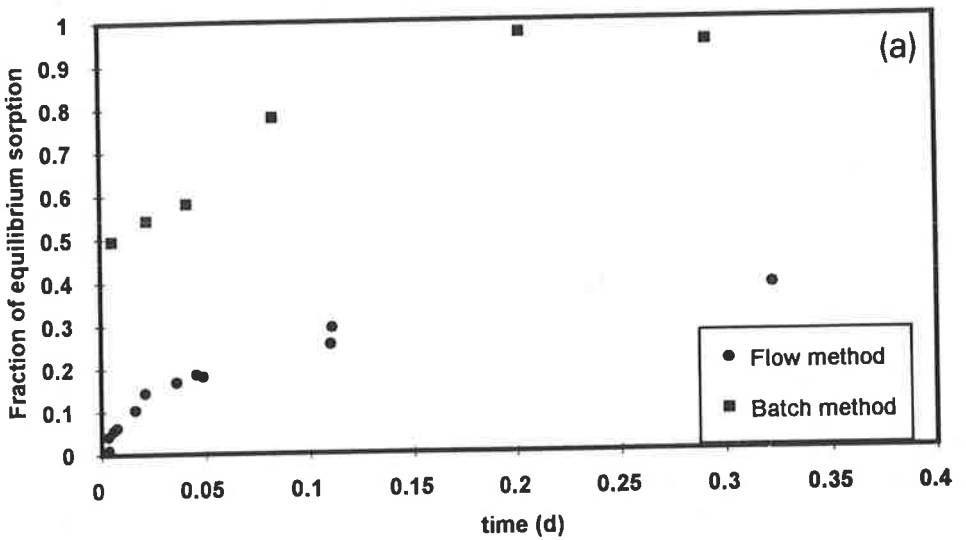


Fig. 1. Sorption isotherm of simazine in Bassendean sand.

studying sorption kinetics which differed with respect to the degree of shaking and found that the rate parameters of potassium sorption were affected by the vigour of shaking. Significantly slow rates of sorption and desorption of organic compounds have also been observed in recent laboratory research (Pignatello, 1989; Ball and Roberts, 1991).

The kinetic data were fitted to various rate equations (Sparks, 1989). That obtained by the flow technique did not conform to a first-order equation. However, the data could be fitted to either a two-site kinetic equation (Fig. 2b), or a parabolic diffusion law (Fig. 2c). The following relation for a parabolic



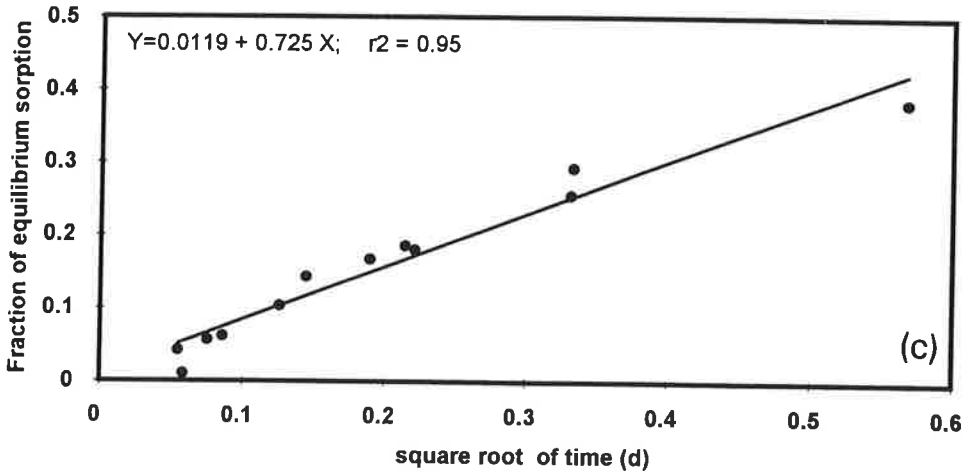


Fig. 2. Time-dependent sorption data for simazine: (a) obtained by batch and flow methods; (b) data obtained by the flow technique and fitted to a two-site kinetic equation; and (c) data obtained by flow technique fitted to a parabolic diffusion law.

diffusion law was used:

$$S/S_{\infty} = (4/\pi^{0.5})(Dt/l^2)^{0.5} \quad (12)$$

where S_{∞} is sorption at time = infinity. Similar square root time relations can be obtained for a cylinder or sphere of semi-infinite medium. The relation is valid for the early stages of diffusion (often up to 50% fractional uptake) into a plain sheet having constant surface and uniform initial concentration and of thickness l (Crank, 1975).

A good fit of the sorption data to the square root time relationship indicates (but not necessarily unequivocally) that the sorption of simazine during transport was controlled by some diffusion processes. It has previously been reported by Kookana et al. (1992a) that the sorption data obtained by the flow technique for three different pesticides in four soils followed the diffusion law.

Simulations with equilibrium model

Although, as described above, the sorption of simazine during transport was found to be time dependent, simulation with an equilibrium model (3) was carried out for the BTC's of simazine in Bassendean sand to assess the extent of early appearance of the BTC compared to that expected from the equilibrium sorption coefficient. A comparison of the experimental and simulated BTC's for the pesticide is shown in Fig. 3. The equilibrium model predicted much higher retardation of pesticide than that observed through the experi-

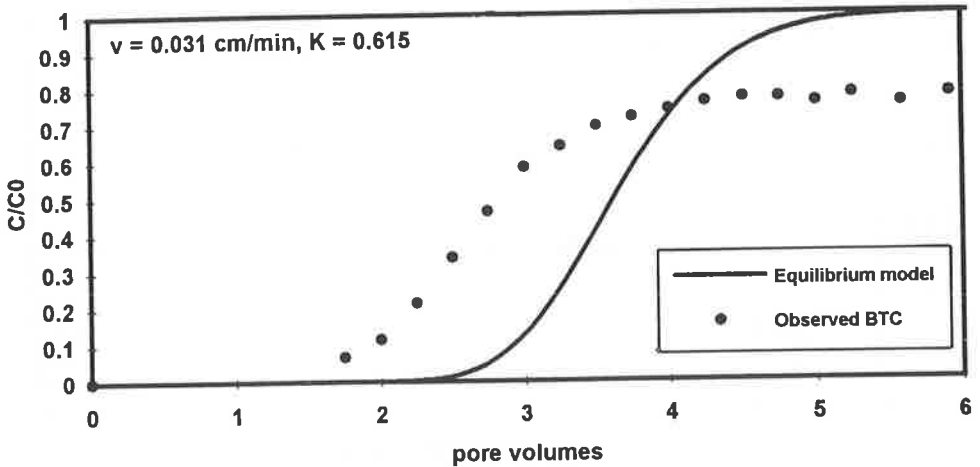


Fig. 3. Simazine BTC obtained at $v = 8.93 \text{ m day}^{-1}$ (data points) compared with that simulated with the equilibrium model (solid line). $D = 3.57 \text{ m}^2 \text{ day}^{-1}$; $K = 0.615 \text{ L kg}^{-1}$; other parameters as given in Table 1.

mental BTC. Many workers have similarly observed that under flow conditions (even at low pore-water velocities) the equilibrium conditions for sorption reactions do not always exist (reviewed by Brusseau and Rao, 1989). The failure of the equilibrium model to describe the observed BTC's clearly shows that the batch sorption data are not appropriate for transport studies. The observed BTC's also show that, at the flow rates used in this study, the kinetics of sorption have not only resulted in extensive tailing but also have affected the retardation of the BTC's of simazine.

Simulations with sorption–nonequilibrium models

First-order kinetic model. Although the sorption data did not conform to a first-order rate law the simulations were carried out using the first-order kinetic model in order to test whether it is at all possible to describe the observed BTC's with any value of a single sorption rate parameter. The simulated BTC's for simazine obtained with different values of first-order kinetic parameters (k_d) are shown in Fig. 4. As expected, the simulations with this model also failed to describe the experimental BTC's satisfactorily. At very low values of the rate parameter, the model essentially reduced to a model for non-reactive solute whereas at very high values, it behaved as an equilibrium sorption model. Similar results have been reported by other workers (e.g., Schwarzenbach and Westall, 1981; Wu and Gschwend, 1986).

These results with equilibrium and first-order kinetic models are consistent with the sorption kinetic data described earlier.

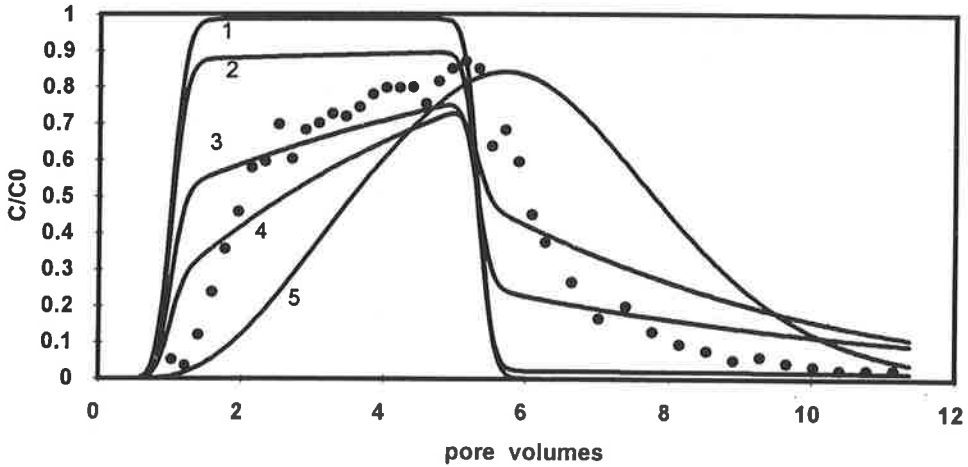


Fig. 4. BTC's simulated with nonequilibrium model using first-order kinetic equation (4). The parameters k_d used for BTC's numbered from 1 to 5 were 0.144, 1.44, 7.20, 14.40 and 72.00 day^{-1} , respectively. Other parameters in addition to those in Table 1 were $v = 8.93 \text{ m day}^{-1}$, $D = 3.57 \text{ m}^2 \text{ day}^{-1}$. The *data points* represent the experimental BTC's.

Two-site kinetic model. For simulations with a two-site/two-region models (Eq. 7) two sorption-related parameters are needed — the fraction of type-1 sites (mobile fraction) and the rate parameter for type-2 sites (mass-transfer coefficient). Preliminary simulations with the sorption kinetic data obtained by the flow technique (Fig. 2) revealed that only one of the two parameters, i.e. fraction of sites showing instantaneous sorption (type-1 sites), can be obtained by the technique.

It must be noted here that the flow technique used in the study to examine the time dependency of sorption (Kookana et al., 1992b) utilises only the loci of peaks of BTC's to calculate the retardation factors or sorption values and not the concentration profile as a result of dispersion or kinetic sorption (such as tailing). The tailing phenomenon in BTC's is generally a consequence of the kinetic component of sorption. Hence, the flow technique used in this study provides values of sorption which takes place on type-1 sites only.

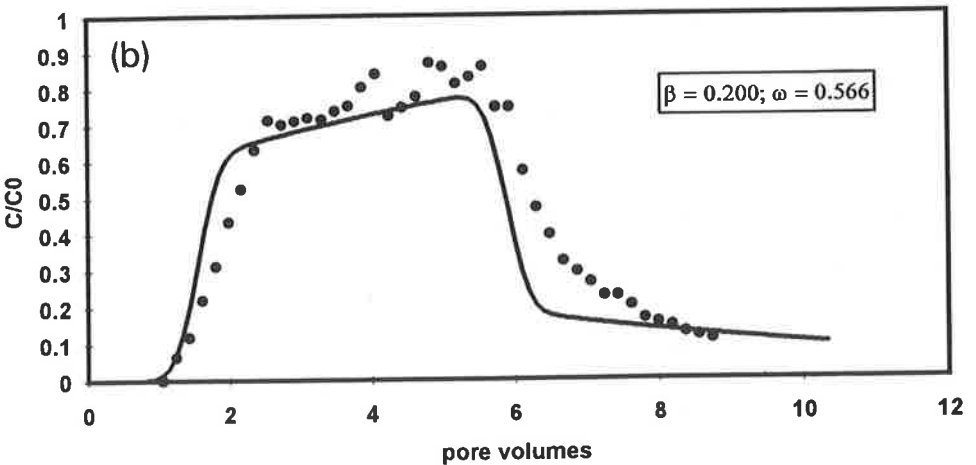
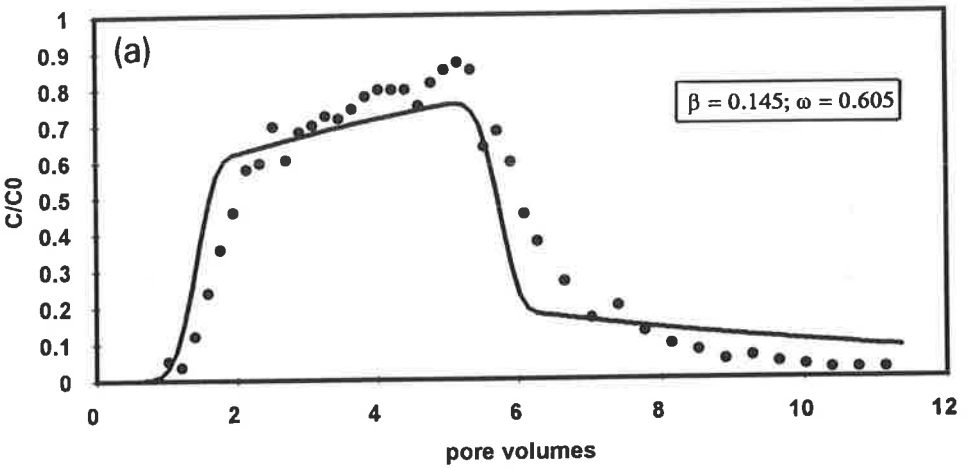
TABLE 2

Parameters used in the simulation of simazine BTC's with two-site model

Experiment No.	v (m day^{-1})	P	R	β	ω
1	8.93	70	3.66	0.145	0.605
2	4.46	70	3.66	0.200	0.566
3	0.893	13	3.66	0.432	0.503
4	0.446	13	3.66	0.606	0.418

However, in this study, the sorption on these sites was found to vary with pore-water velocity which shows that not all reaction sites are effectively accessible at a given flow rate and more and more sites are reached with a decrease in pore-water velocity. This is consistent with the observed BTC's of simazine at four different pore-water velocities. Other workers have also noted a shift to the left on a pore volume basis with increasing pore-water velocities (Lee et al., 1988; Brusseau et al., 1991; Gamedainger et al., 1991; Gaber et al., 1992).

For simulations, the fraction of sorption completed at a given residence time was obtained directly from the sorption-time relationship (Fig. 2c). The fractions of type-1 sites were calculated corresponding to different retention



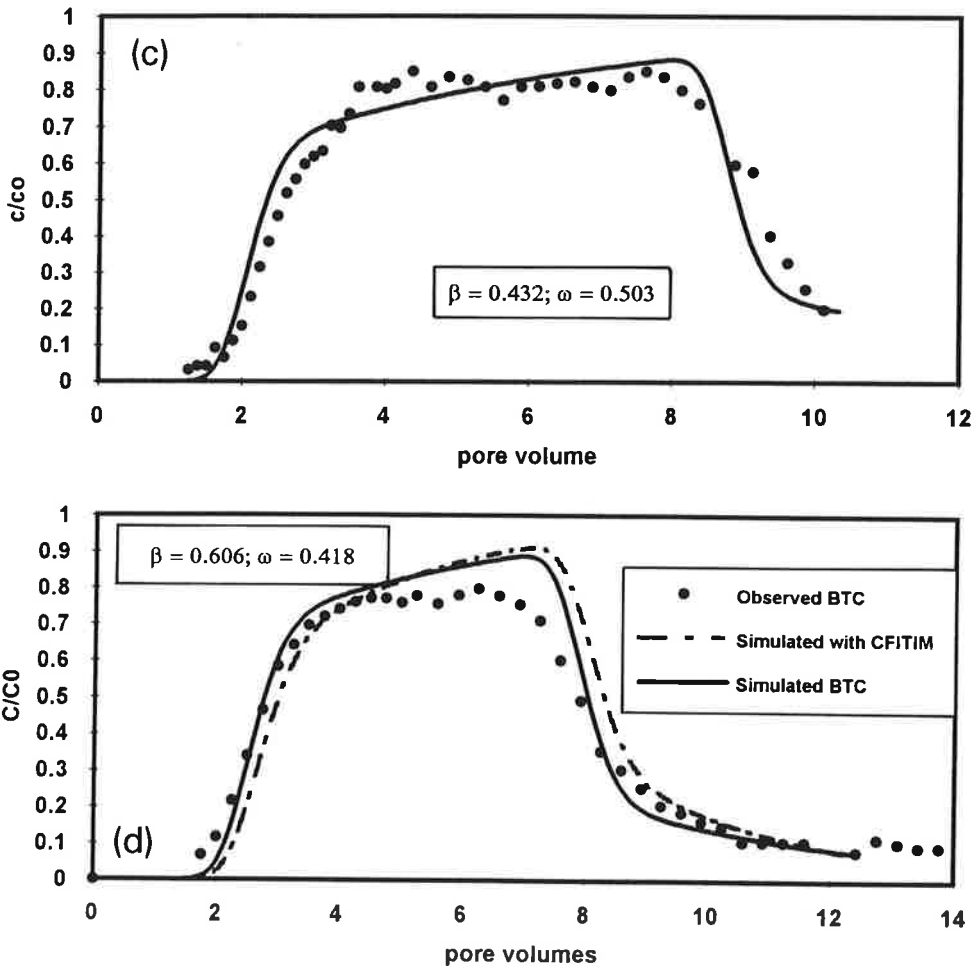


Fig. 5. Experimental BTC's (data points) and simulated BTC's with a two-site nonequilibrium model (solid lines) at four different v (as labelled). The values of parameters used in simulation are given in Table 2. (a) to (d) correspond to experiments 1 to 4 in Table 2. Dotted line in (d) was simulated using β - and ω -values obtained by CFITIM.

times (L/v ratio, where L is length of column in cm and v is the pore-water velocity in cm min^{-1}) at different flow velocities and are given in Table 2. Since the rate parameter for type-2 sites could not be measured independently it was varied in the simulation. The non-linear least-squares optimization programme CFITIM (van Genuchten, 1981) was used to estimate the value of the second parameter ω . Model B of CFITIM was used for obtaining the two parameters β and ω under first-type, constant-concentration boundary conditions. However, for simulations only ω from CFITIM with the measured β was used.

The simulations carried out with the parameters given in Table 2 are shown

in Fig. 5a–d together with the experimental BTC's corresponding to different flow velocities. Close agreements, particularly between the breakthrough portion of the simulated and experimental BTC's at four different pore-water velocities were observed. Preliminary simulations with various rate parameters for type-2 sites k_2 or α showed that the parameter affected the tail of the BTC's only and not the retardation except at very high values of k (as shown in Fig. 4). The good agreement of the simulated breakthrough fronts (before it starts tailing) with the observed ones at various pore-water velocities establishes the validity of independently measured values of fractions for type-1 sites by the flow technique. The values of measured β agreed well with that obtained by CFITIM particularly for experiment 4 (lowest pore-water velocity). This is shown by the dotted line of Fig. 5d. For other experiments β obtained by least-squares fit of CFITIM were found to be higher than measured in the study.

The relatively better description of simazine BTC's by the bicontinuum approach in the soil studied here suggests that the early breakthrough and tailing effects in the present study are due to rate-limited interactions such as intra-organic matter diffusion of simazine. Sorption at the external surfaces of the organic matter showing instantaneous sorption correspond to the type-1 domain and the rate-controlled diffusion of simazine into the organic matter correspond to the type-2 domain. This is a strong possibility because of the negligible contribution expected from mineral surfaces to the sorption of simazine in this study since the soil contains very little clay and that being of the kaolinitic type. Contribution of mineral surfaces to sorption of organic compounds has been shown to be negligible when organic matter content of soil is $>0.1\%$ (cf. Brusseau and Rao, 1989).

It should be noted that not only the fraction of type-1 sites but also the rate parameter for type-2 sites varied with the flow rates. As discussed in the theory section of the paper, the chemical-process model assumes the presence of materials of different nature in soil, such as mineral and organic matter, which give rise to the two types of sorption sites. Given such a basis for the chemical-process model, the fraction of type-1 sites and the rate coefficient for type-2 sites are not expected to vary with pore-water velocity. The velocity dependence of both of these parameters is further indication of a physical process such as diffusion into the soil matrix being the limiting factor for sorption. Nevertheless, the chemical-process model can successfully describe the observed BTC's, because the "physical-process" and "chemical-process" two-site/two-region models are mathematically equivalent (Nkedi-Kizza et al., 1984).

The velocity dependence of these parameters makes their independent measurement very difficult. In this study only one of the two parameters could be obtained from independent experiments. The following section examines

the velocity dependence of the mass-transfer coefficient from a number of published studies with a view to its independent measurement.

Velocity dependence of mass-transfer coefficient. It should be noted here that if α represents a true first-order process as assumed in Eqs. 7 it should be independent of input concentration and pore-water velocity. However, its velocity dependence has been reported by a number of workers (van Genuchten et al., 1977; Rao et al., 1980a; Nkedi-Kizza et al., 1984; De Smedt et al., 1986). In order to examine the nature of the velocity dependence of α , the values of the coefficient from the present study as well as those from a number of other studies have been plotted against pore-water velocity in Fig. 6. The decrease in α with decreasing pore-water velocity is a common feature of the data from different studies. Although, there is a very large scatter in the α -values corresponding to a given value of pore-water velocity between the various studies, yet a similar dependence of mass-transfer coefficient with v is evident in all the studies. A large variation between different studies is to be expected because of the complex nature of the parameter, for it is known to depend on sorption and input concentration of the solutes. These studies involved not only a variety of solutes such as Ca^{2+} , Mg^{2+} , Al^{3+} , tritium, lindane, simazine, etc., but also different soils and aggregate sizes. Nevertheless, the similarity of the velocity dependence of α between different studies involving non-reactive to highly reactive solutes gives some hope for expressing it in terms of measurable physical parameters. For example, Selim et al.

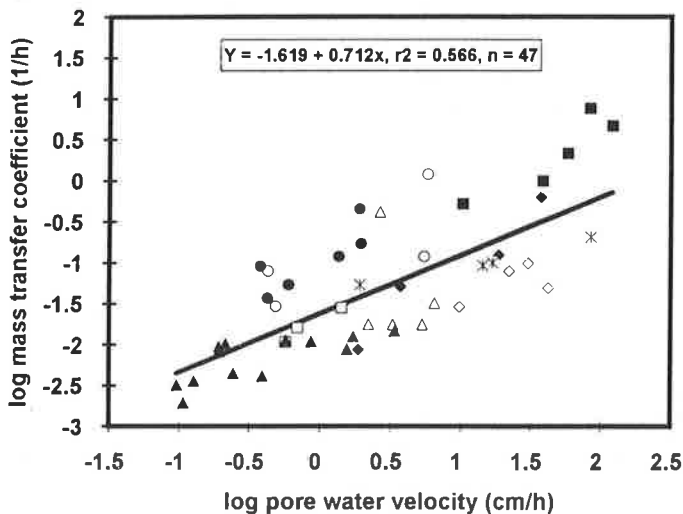


Fig. 6. The velocity dependence of the rate parameter for type-2 sites, α in physical process model (8i), from a number of different studies (\diamond = Gaudet et al. (1977); \blacktriangle = van Genuchten et al. (1977); $*$ = Rao et al. (1980b); \circ = Nkedi-Kizza et al. (1984); \square = De Smedt et al. (1986); \bullet = Selim et al. (1987); \blacksquare = Seyfried and Rao (1987); \triangle = Miller and Weber (1988); \blacklozenge = present study; — = fitted line).

(1987) estimated α using a relation based on the time-moment analysis of BTC given by Valocchi (1985). The relation used by these workers shows essentially similar velocity dependence of α . Nevertheless, considering the complex and empirical nature of the mass-transfer coefficient its independent estimation is indeed a challenge to solute transport modellers. The coefficient α (Eq. 8i) is a lumped and empirical parameter which depends in some ways upon aggregate geometry and dispersion coefficient (Valocchi, 1985) and is interpreted as a diffusion coefficient divided by some average diffusional path length (Nielsen et al., 1986). In addition to its velocity dependence, it has also been observed that the magnitude of α is inversely correlated with the equilibrium sorption coefficient (Karickhoff and Morris, 1985; Brusseau and Rao, 1989) and is affected by the input concentration of solute.

CONCLUSIONS

On the basis of the transport studies described in this paper and the previous kinetic studies (Kookana et al., 1992a, b), it is evident that during transport of pesticides such as simazine in soils the sorption processes are not in equilibrium. The nonequilibrium sorption conditions may be due to intrasorbent diffusion in either organic matter or mineral particles in the soil. Since, the sorption sites for simazine in this soil are mainly provided by the organic matter fraction of the soil, the rate of sorption of pesticides is likely to be determined by intra-organic matter diffusion. Organic matter has been shown to be the predominant sorbent for organic compounds with contributions of mineral surfaces to sorption being relatively negligible when the fraction of organic carbon exceeds 0.001 (Brusseau and Rao, 1989). Sorption of pesticides on inorganic surfaces has been found to be independent of time (LaFleur, 1979a, b), whereas the sorption on organic matter-rich sorbents has been reported to take a long time (Moyer et al., 1972; Saltzman et al., 1972; Grover, 1974; Bouchard et al., 1988). A number of recent studies further support this conclusion (Pignatello, 1990; Brusseau and Rao, 1991; Brusseau et al., 1991).

In this study such intra-organic matter diffusion appears to have resulted in the dependence of both the parameters (f and α representing the two regions or two types of site) on pore-water velocity. The study shows that the fraction of type-1 sites or mobile fraction can be independently obtained from separate experiments under transport conditions. However, independent estimation of the mass-transfer coefficient as a function of pore-water velocity is difficult to obtain. The velocity dependence of α from a number of studies has been shown to be of similar nature, which suggests that there is scope for a physi-

cally meaningful expression of mass-transfer coefficient as a function of pore-water velocity.

ACKNOWLEDGEMENT

This work was funded by grants from the Land and Water Resources Research and Development Corporation of Australia.

REFERENCES

- Addiscot, T.M. and Wagenet, R.J., 1985. Concepts of solute leaching in soils: a review of modelling approaches. *J. Soil Sci.*, 36: 411–424.
- Ball, W.P. and Roberts, P.V., 1991. Long-term sorption of halogenated organic chemicals by aquifer material, 2. Intraparticle diffusion. *Environ. Sci. Technol.*, 25: 1237–1249.
- Bouchard, D.C., Wood, A.L., Campbell, M.L., Nkedi-Kizza, P. and Rao, P.S.C., 1988. Sorption nonequilibrium during solute transport. *J. Contam. Hydrol.*, 2: 209–223.
- Brusseau, M.L., 1992. Nonequilibrium transport of organic chemicals: The impact of pore-water velocity. *J. Contam. Hydrol.*, 9: 353–368.
- Brusseau, M.L. and Rao, P.S.C., 1989. Sorption nonideality during organic contaminant transport in porous media. *CRC (Chem. Rubber Co.) Crit. Rev. Environ. Control*, 19: 33–99.
- Brusseau, M.L. and Rao, P.S.C., 1991. Influence of sorbate structure on nonequilibrium sorption of organic compounds. *Environ. Sci. Technol.*, 25: 1501–1506.
- Brusseau, M.L., Jessup, R.E. and Rao, P.S.C., 1989. Modeling the transport of solutes influenced by multiprocess nonequilibrium. *Water Resour. Res.*, 25: 1971–1988.
- Brusseau, M.L., Jessup, R.E. and Rao, P.S.C., 1991. Nonequilibrium sorption of organic chemicals: Elucidation of rate-limiting processes. *Environ. Sci. Technol.*, 25: 134–142.
- Cameron, D.R. and Klute, A., 1977. Convective–dispersive solute transport with a combined equilibrium and kinetic adsorption model. *Water Resour. Res.*, 13: 183–188.
- Crank, J., 1975. *The Mathematics of Diffusion*. Oxford University Press, London, 244 pp.
- De Smedt, F., Wauters, F. and Sevilla, J., 1986. Study of tracer movement through unsaturated sand. *J. Hydrol.*, 85: 169–181.
- Gaber, H.M., Comfort, S.D., Inskeep, W.P. and El-Attar, H.A., 1992. A test of local equilibrium assumption for adsorption and transport of picloram. *Soil Sci. Soc. Am. J.*, 56: 1392–1400.
- Gamerding, A.P., Lemley, A.T. and Wagenet, R.J., 1991. Nonequilibrium sorption and degradation of three 2-chloro-s-triazine herbicides in soil–water systems. *J. Environ. Qual.*, 20: 815–822.
- Gaudet, J.P., Jegat, H., Vachaud, G. and Wierenga, P.J., 1977. Solute transfer, with exchange between mobile and stagnant water, through unsaturated sand. *Soil Sci. Soc. Am. J.*, 41: 665–671.
- Gerritse, R.G. and Singh, R., 1988. The relationship between pore water velocity and longitudinal dispersivity of Cl^- , Br^- and D_2O in soils. *J. Hydrol.*, 104: 173–180.
- Goltz, M.N. and Roberts, P.V., 1986. Interpreting organic solute data from a field experiment using physical non-equilibrium models. In: D.L. Macalady (Editor), *Transport and Transformations of Organic Contaminants*. *J. Contam. Hydrol.*, 1: 77–93 (special issue).

- Grover, R., 1974. Adsorption and desorption of trifluralin, triallate, and diallate by various adsorbents. *Weed Sci.*, 22: 405–408.
- Hartley, D. and Kidd, H. (Editors), 1987. *The Agrochemicals Handbook*. R. Soc. Chem., London.
- Hornsby, A.G. and Davidson, J.M., 1973. Solution and adsorbed fluometuron concentration distribution in water saturated soil: experimental and predicted evaluation. *Soil Sci. Soc. Am. Proc.*, 37: 823–828.
- Huber, J.F.K. and Gerritse, R.G., 1971. Evaluation of dynamic gas chromatographic methods for the determination of adsorption and solution isotherms. *J. Chromatogr.*, 58: 137–158.
- Jardine, P.M., Parker, J.C. and Zelazny, L.W., 1985. Kinetics and mechanisms of aluminium adsorption on kaolinite using a two-site nonequilibrium transport model. *Soil Sci. Soc. Am. J.*, 49: 867–873.
- Jury, W.A., Ebad, H. and Resketo, M., 1986. Field study of napropamide movement through unsaturated soil. *Water Resour. Res.*, 22: 749–755.
- Karickhoff, S.W. and Morris, K.R., 1985. Sorption dynamics of hydrophobic pollutants in sediment suspensions. *Environ. Toxicol. Chem.*, 4: 469–479.
- Kookana, R.S., Aylmore, L.A.G. and Gerritse, R.G., 1992a. Time-dependent sorption of pesticides during transport in soils. *Soil Sci.*, 154: 214–225.
- Kookana, R.S., Gerritse, R.G. and Aylmore, L.A.G., 1992b. A method for studying nonequilibrium sorption during transport of pesticides in soil. *Soil Sci.*, 154: 344–349.
- LaFleur, K.S., 1979a. Sorption of metribuzin by model soils and agronomic soils: rates and equilibria. *Soil Sci.*, 127: 51–55.
- LaFleur, K.S., 1979b. Sorption of pesticides by model soils and agronomic soils: rates and equilibria. *Soil Sci.*, 127: 94–101.
- Lee, L.S., Rao, P.S.C., Brusseau, M.L. and Ogwada, R.A., 1988. Nonequilibrium sorption of organic contaminants during flow through columns of aquifer materials. *Environ. Toxicol. Chem.*, 7: 779–793.
- Miller, C.T. and Weber, J.W., 1988. Modeling the sorption of hydrophobic contaminants in aquifer materials, II. Column reactor systems. *Water Res.*, 22: 465–474.
- Moyer, J.R., Mckercher, R.B. and Hance, R.J., 1972. Desorption of some herbicides from montmorillonite and peat. *Can. J. Soil Sci.*, 52: 439–447.
- Nielsen, D.R., van Genuchten, M.Th. and Biggar, J.W., 1986. Water flow and solute transport processes in the unsaturated zone. *Water Resour. Res.*, 22: 89s–108s.
- Nkedi-Kizza, P., Rao, P.S.C., Jessup, R.E. and Davidson, J.M., 1982. Ion exchange and diffusive mass transfer during miscible displacement through an aggregated oxisol. *Soil Sci. Soc. Am. J.*, 46: 471–476.
- Nkedi-Kizza, P., Biggar, J.W., Selim, H.M., van Genuchten, M.Th., Wierenga, P.J., Davidson, J.M. and Nielsen, D.R., 1984. On the equivalence of two conceptual models for describing ion exchange during transport through an aggregated oxisol. *Water Resour. Res.*, 20: 1123–1130.
- Ogwada, R.A. and Sparks, D.L., 1986. Kinetics of ion exchange on clay minerals and soil, I. Evaluation of methods. *Soil Sci. Soc. Am. J.*, 50: 1158–1162.
- Pignatello, J.J., 1989. Sorption dynamics of organic compounds in soils and sediments. In: B.L. Shawhney and K. Brown (Editors), *Reactions and Movement of Organic Chemicals in Soils*, Ch. 3. Am. Soc. Agron./Soil Sci. Soc. Am., Madison, WI, SSSA Spec. Publ. 22.
- Pignatello, J.J., 1990. Slowly reversible sorption of aliphatic halocarbons in soils, II. Mechanistic aspects. *Environ. Toxicol. Chem.*, 9: 1117–1126.

- Rao, P.S.C., Green, R.E., Balasubramaniam, V. and Kanehiro, Y., 1974. Field study of solute movement in a highly aggregated oxisol with intermittent flooding, II. Picloram. *J. Environ. Qual.*, 3: 197–202.
- Rao, P.S.C., Jessup, R.E., Rolston, D.E., Davidson, J.M. and Kilcrease, D.P., 1980a. Experimental and mathematical description of nonadsorbed solute transfer by diffusion in spherical aggregates. *Soil Sci. Soc. Am. J.*, 44: 684–688.
- Rao, P.S.C., Rolston, D.E., Jessup, R.E. and Davidson, J.M., 1980b. Solute transport in aggregated porous media: theoretical and experimental evaluation. *Soil Sci. Soc. Am. J.*, 44: 1139–1146.
- Saltzman, S., Kliger, L. and Yaron, B., 1972. Adsorption desorption of Parathion as affected by soil organic matter. *J. Agri. Food Chem.*, 20: 1224 – 1229
- Schwarzenbach, R.P. and Westall, J., 1981. Transport of non-polar organic compounds from surface water to groundwater — Laboratory sorption studies. *Environ. Sci. Technol.*, 15: 1360–1367.
- Selim, H.M., Schulin, R. and Fluhler, H., 1987. Transport and ion exchange of calcium and magnesium in an aggregated soil. *Soil Sci. Soc. Am. J.*, 51: 876–884.
- Seyfried, M.S. and Rao, P.S.C., 1987. Solute transport in undisturbed columns of an aggregated tropical soil: Preferential flow effects. *Soil Sci. Soc. Am. J.*, 51: 1434–1444.
- Singh, R., Gerritse, R.G. and Aylmore, L.A.G., 1990. Adsorption–desorption behaviour of selected pesticides in some Western Australian soils. *Aust. J. Soil Res.*, 28: 227–243.
- Sparks, D.L., 1989. *Kinetics of Soil Chemical Processes*. Academic Press, New York, NY, 210 pp.
- Valocchi, A., 1985. Validity of the local equilibrium assumption for modeling sorbing solute transport through homogeneous soils. *Water Resour. Res.*, 21: 808–820.
- van Genuchten, M.Th., 1981. Non-equilibrium transport parameters from miscible displacement experiments. U.S. Dep. Agric., U.S. Salin. Lab., Riverside, CA, Res. Rep. No. 119, 88 pp.
- van Genuchten, M.Th., Davidson, J.M. and Wierenga, P.J., 1974. An evaluation of kinetic and equilibrium equations for the prediction of pesticide movement in porous media. *Soil Sci. Soc. Am. Proc.*, 38: 29–35.
- van Genuchten, M.Th., Wierenga, P.J. and O'Connor, G.A., 1977. Mass transfer studies in sorbing porous media, III. Experimental evaluation with 2,4,5-T. *Soil Sci. Soc. Am. J.*, 41: 278–285.
- Wagenet, R.J., 1983. Principles of salt movement in soils. In: D.W. Nelson, K.K. Tanji and D.E. Elrick (Editors), *Chemical Mobility and Reactivity in Soil Systems*. Soil Sci. Soc. Am., Madison, WI, pp. 123–140.
- Weber, J.B., 1970. Mechanisms of adsorption of s-triazines by clay colloids and factors affecting plant availability. *Residue Rev.*, 32: 93–130.
- Winters, S.L. and Lee, D.R., 1987. In situ retardation of trace organics in groundwater discharge to a sandy stream bed. *Environ. Sci. Technol.*, 21: 1182–1186.
- Wu, S. and Gschwend, P.M., 1986. Sorption kinetics of hydrophobic organic compounds to natural sediments and soils. *Environ. Sci. Technol.*, 20: 717–725.

USE OF COMPUTER-ASSISTED TOMOGRAPHY IN STUDYING WATER MOVEMENT AROUND PLANT ROOTS

L. A. G. Aylmore

Department of Soil Science and Plant Nutrition,
The University of Western Australia,
Nedlands, Western Australia 6009, Australia

- I. Introduction
- II. Computer-Assisted Tomography
 - A. Theory of Attenuation
 - B. Principles of Computer-Assisted Tomography
- III. X-Ray CAT Scanners
 - A. Construction
 - B. Detection
 - C. Collimation
 - D. Reconstruction
 - E. Hounsfield Units
 - F. Difficulties with X-Ray Scanners
- IV. γ -Ray CAT Scanners
 - γ -Ray Scanning System
- V. Application of Computer-Assisted Tomography to Soil-Water Studies
 - A. Linearity
 - B. Structural Definition
 - C. Water Movement to Plant Roots
- VI. Nuclear Magnetic Resonance Imaging
- VII. Dual-Energy Scanning
 - A. Theory of Dual-Energy Scanning
 - B. Choice of Sources
 - C. Application of CAT to Dual-Energy Scanning
- VIII. Recent and Future Developments
- IX. Summary and Conclusions
- References

I. INTRODUCTION

An appreciation of the physical, chemical, and biological factors determining the supply, availability, and movement of water in soil/plant ecosystems, together with suitable techniques for the measurement of the forces involved, is essential to the development of an understanding of the mechanisms and dynamics of water movement in soils and their biological implications. The importance of this field of study cannot be overemphasized, particularly in semiarid and saline environments, where the availability of scarce water resources for agriculture makes it imperative that the most efficient water utilization by plants is achieved, and where limits to growth and production are most commonly set by limitations on our knowledge of such factors.

A serious difficulty encountered in attempts to relate soil water to plant response is the fact that the water content in a plant root zone varies markedly in both time and space. Slatyer (1967) emphasized the importance of the soil water potential at the root/soil interface as the main soil characteristic controlling the availability of soil water for plant growth, with its value depending on both the soil water potential of the bulk soil and the potential gradient from the bulk soil to the root surface, which develops as a result of water removal by the root. Philip (1966) also suggested that the value of the water potential at the root surfaces was critical to the distribution of water potential (and to the possibility of wilting) throughout much of the plant domain. Furthermore, although the soil water tension, or matric suction, at a given depth in the root zone may correlate well with plant response in some circumstances and provide a useful basis for irrigation, a clearer understanding of water availability to plants requires some means of resolving changes in soil suction or water content over the entire root zone.

Unfortunately, progress in this area has been severely limited because of the difficulties associated with direct experimental measurement of soil water content or potential at the root/soil interface and in the soil immediately around the root. Until recently, techniques for the direct measurement of soil water content or potential have either been destructive (and hence lacked continuity), have perturbed the sensitive balance being examined, were too slow in their response time, or simply lacked the dimensional resolution necessary for meaningful definition of water content distributions. Although Dunham and Nye (1973) were able to measure one-off drawdowns in proximity to curtains of roots by destructive sectioning and So *et al.* (1976, 1978) were able to determine water potentials at the root surface by extrapolation using a collar tensiometer-potometer system, these techniques provided only very limited insights into the dy-

namics of the availability of soil water for plant growth. Consequently, questions concerning the relative magnitudes of soil and plant resistances to water movement under different conditions of soil water potential and transpirational demand (Newman, 1969a,b), concerning the nature of the water driving forces (Nobel, 1974), and concerning the extent to which root/soil contact resistance (Herkelrath *et al.*, 1977), accumulation of soil solute concentrations (osmotic potentials) (Passioura and Frere, 1967), etc., influence water availability have remained largely unresolved. Furthermore, conflicting results obtained predominantly by the indirect measuring procedures that previously were the only available techniques (Dunham and Nye, 1973; So *et al.*, 1976, 1978) raise questions as to the validity of the physical concepts on which theoretical treatments (Molz, 1981) have been based.

Similar problems had long existed in medical diagnostic radiology in seeking a method by which the interior of a section of the human body could be viewed in a nondestructive manner without interference from other regions. With advances in X-ray physics, detector technology, and mathematical reconstruction theory, a solution to the problem was essentially achieved in the early 1970s by Hounsfield (1972), who developed the technique known as computer-assisted tomography (CAT), or more simply, computed tomography (CT). (The word tomography is derived from two Greek words: *tomo*, meaning slice or section, and *graphy*, meaning to write or display.) CAT enables the three-dimensional, nondestructive imaging of the internal structure of the object under examination using measurements of the attenuation of a beam of radiation. The application of the technique to the attenuation of X-rays (colloquially referred to as CAT scanning) allowed dramatic advances in medical diagnostic capability and benefited the medical profession greatly by reducing the need for exploratory surgery to examine the internal structures of the human body. For this work Godfrey Hounsfield shared the 1979 Nobel Prize for Medicine with A. M. Cormack, who had earlier, in 1963, developed and applied a mathematical model that allowed the determination of absorption coefficients at specific points in scanned sections from the measured attenuation of collimated beams of ^{60}Co γ -radiation.

Tomographic imaging in various forms is applicable to a number of different types of energy beams, including electrons, protons, α particles, lasers, radar, ultrasound, and nuclear magnetic resonance. However, because of its convenience and versatility in medical, industrial, and scientific applications, most attention has been directed to X-ray CT. In recent years, the opportunity to use CAT scanning for nonmedical applications has blossomed, particularly in the United States, Canada, Europe, Australia, and Japan. Hopkins *et al.* (1981) and Davis *et al.* (1986) demonstrated

its application to industrial problems, particularly for nondestructive testing of timber poles, plastics, concrete pillars, steel-belted automobile tires, and electronic components. Onoe *et al.* (1983) described the use of a portable X-ray CAT scanner for measuring annual growth rings of live trees.

The potential applications of CAT scanning in the soil and plant sciences have also attracted increasing interest over the past decade. Numerous workers (Petrovic *et al.*, 1982; Hainsworth and Aylmore, 1983, 1986; Crestana *et al.*, 1985; Anderson *et al.*, 1988, 1990; Tollner *et al.*, 1987; Tollner and Verma, 1989) have demonstrated that commercially available X-ray medical scanners can provide excellent resolution for some studies of the spatial distributions of bulk density and water content in soil columns, including in particular those near plant roots (Hainsworth and Aylmore, 1983, 1986; Aylmore and Hamza, 1990; Hamza and Aylmore, 1991, 1992a,b). The quantitative usefulness of such systems in soil studies has, however, been limited by the polychromatic nature of the X-ray beam and its inability to distinguish between changes in water content and bulk density in swelling soils. Furthermore, these instruments are prohibitively expensive (about \$2 million) and hence have not been generally accessible to soil and plant scientists. Consequently, work in several laboratories has sought to provide experimentally more suitable systems and to reduce vastly the cost of the equipment, by the modification of "conventional" γ scanning systems (Gurr, 1962; Groenevelt *et al.*, 1969; Ryhiner and Pankow, 1969) to utilize the CAT approach (Hainsworth and Aylmore, 1983, 1988; Crestana *et al.*, 1986). γ -Rays are essentially monochromatic, and the ready availability of sources providing large differentials in energy level offers the potential to distinguish quantitatively between simultaneous changes in water content and bulk density. However, the relatively low photon emission from γ -ray sources compared with X-ray tubes requires much longer scanning times and has as yet limited measurements by this means to slow or steady-state processes.

Despite these current limitations there is no doubt that the application of this exciting new technique will, with further developments, provide a major tool for soil and plant scientists and has the potential to resolve the major controversies with respect to the physics of water uptake by plant roots.

II. COMPUTER-ASSISTED TOMOGRAPHY

The theory and use of the CAT technique for medical purposes has been reviewed in some detail by Budinger and Gullberg (1974), Brooks and Di Chiro (1975, 1976), and Panton (1981), and complete reviews of various

aspects of CAT scanning have been presented by Newton and Potts (1981) and Kak and Slaney (1988). Brief reviews of CAT scanning theory as it relates to the determination of soil water content have been presented by Hainsworth and Aylmore (1983), Crestana *et al.* (1985), and Anderson *et al.* (1988). However, as the technique has only recently been introduced in soil science, an outline of the theory of CAT is given here to familiarize readers with the technique.

A. THEORY OF ATTENUATION

In conventional radiography the transmission of radiation through a three-dimensional object is used to produce a two-dimensional image of the internal features of the object on a radiation-sensitive film. Attenuation occurs because the photons in the incident beam may be absorbed by the material and disappear, or may be deflected out of the path of the beam, leading to a decrease in the detected radiation intensity (Fig. 1). The image formation relies on the spatial variation of radiation attenuation in the object, which gives rise to a contrast in the transmitted radiation recorded on the film. The physical quantity that characterizes the attenuation of radiation by matter is called the linear attenuation coefficient (μ).

The three principal mechanisms of radiation attenuation in matter are photoelectric absorption, Compton scattering, and electron-positron pair production (Cullity, 1978). In photoelectric absorption, the photon collides directly with an atom of the absorber and transfers all of the energy to one of the orbital electrons, which is ejected from the atom. This is the most important process for low-energy photons (<500 keV). Because photons with energy in excess of that required to eject an electron are unlikely to be absorbed, the photoelectric absorption coefficient decreases rapidly with

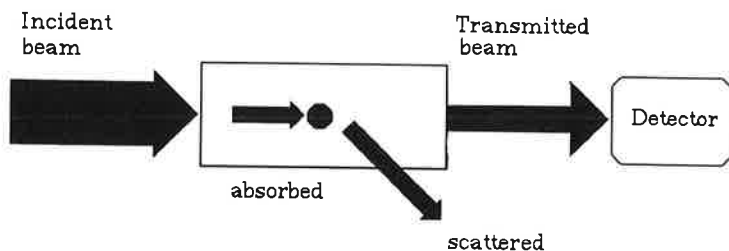


Figure 1. Attenuation of a narrow beam of radiation by absorption and scattering.

increasing photon energy. Compton scattering is the predominant scattering process in which a photon collides with an atom and is deflected from its original direction with the loss of only a portion of its energy. This energy is transferred to an atomic electron, which recoils out of the atom. The absorption of photons by Compton scattering is most probable for intermediate-energy photons (500–1000 keV). The photon continues on at a reduced energy to undergo additional Compton scattering or to be absorbed by photoelectric interaction with a second electron. Of secondary importance may be Rayleigh scattering, in which a photon may be deflected with no loss of energy and the whole atom recoils under the impact. This can occur for photons of low energy, i.e., in the region where the photoelectric effect is dominant. At very high photon energy, > 1000 keV, a photon may be absorbed in the neighborhood of an atomic nucleus or atomic electron and produce an electron–positron pair. In soil water studies, the highest photon energy used is 662 keV from a γ -radiation source of ^{137}Cs , thus electron–positron production is not important in the attenuation process.

The attenuation of a collimated beam of monoenergetic photons of intensity I_0 , as a result of passing through a sample of material of thickness D , yields a transmitted intensity I behind the sample, as illustrated in Fig. 2a (Anderson *et al.*, 1988); this can be described by Beer's Law,

$$I = I_0 \exp(-\mu D) \quad (1)$$

where μ , the linear attenuation coefficient (often referred to as attenuation coefficient), represents the fractional attenuation per unit length of the material traversed by the radiation. The value of μ depends primarily on the energy of the radiation, the electron density, and the packing density of the material. Equation (1) assumes that the material is homogeneous in composition and density over the distance D . For heterogeneous materials, one can subdivide the length D into n subdivisions (of length d), each having a different linear attenuation coefficient, and can describe the attenuation over the length D as the sum of the attenuation of these small subdivisions (Fig. 2b). The transmitted radiation intensity is then

$$I = I_0 \exp\left(-d \sum_{i=1}^n \mu_i\right) \quad (2)$$

For real objects, such as soil, the attenuating material is continuously rather than discretely distributed, so Eq. (2) takes the form of an integral

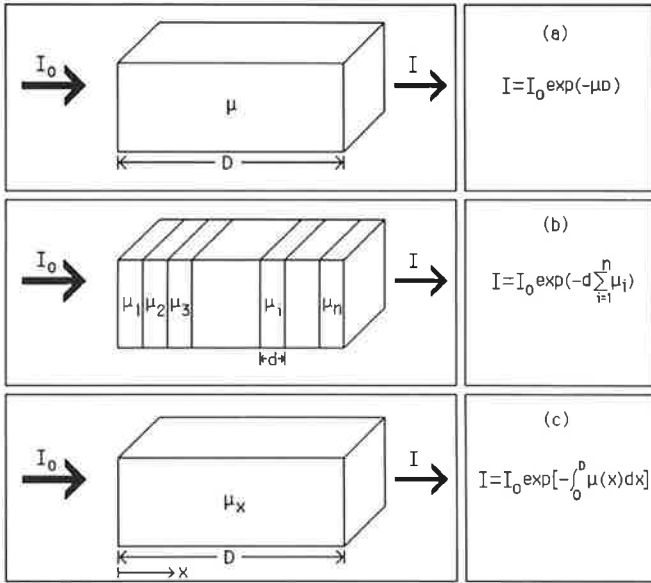


Figure 2. Schematic representation of the attenuation of monochromatic radiation of initial intensity I_0 by (a) homogeneous material, (b) nonhomogeneous material consisting of discrete units with different attenuation coefficients, and (c) nonhomogeneous material consisting of a variable attenuation coefficient, μ_x , over the distance x from the source. (After Anderson *et al.*, 1988.)

(Fig. 2c),

$$I = I_0 \exp \left[- \int_0^D \mu(x) dx \right] \tag{3}$$

where x is the distance from the radiation source and varies between 0 and D , the thickness of the sample.

Equation (3) can be rearranged to yield

$$\ln(I_0/I) = \int_0^D \mu(x) dx \tag{4}$$

The logarithm of I_0/I is effectively a sum of the attenuation coefficients along the ray path and is called a ray sum or ray projection. Obviously, a single ray sum cannot give any information about the distribution of attenuation coefficients at discrete points within the material along the ray path. Thus interpretative difficulties can arise because the image obtained is really a two-dimensional projection of a three-dimensional object. The

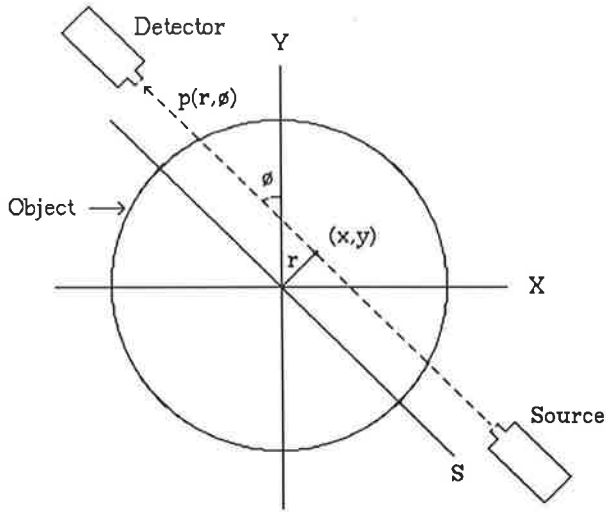


Figure 3. Coordinate system for calculation of the photon attenuation coefficient at a given point. Points within the object are described by fixed (x, y) coordinates. Rays (dashed lines) are specified by their angle (ϕ) with the y axis and their distance (r) from the origin. The S coordinate denotes distance along the way.

aim of the CAT technique is to overcome this difficulty and to reveal the spatial distribution of attenuation coefficients unambiguously.

B. PRINCIPLES OF COMPUTER-ASSISTED TOMOGRAPHY

In CAT, multiple scans from different angles in a given plane provide a large number of ray sums or projections. Using these projections, a two-dimensional image of the slice is reconstructed numerically to give the distribution of attenuation coefficients at discrete points within the slice.

For image reconstruction, an (x, y) coordinate system (Fig. 3) is used to describe points in the slice. As the slice is scanned, ray paths through the slice can be defined by ϕ , the angle of the ray with respect to the y axis, and r , its distance from the origin. The distance of a point from the source on any ray path is given by the coordinate S , which varies from 0 to S .

The contribution of each point to the attenuation of a ray (r, ϕ) with initial intensity I_0 and transmitted intensity I is denoted by

$$I_{r\phi} = I_0 \exp \left[- \int_0^S \mu(x, y) ds \right] \quad (5)$$

Equation (5) can be rearranged to obtain the projection value, p , of the

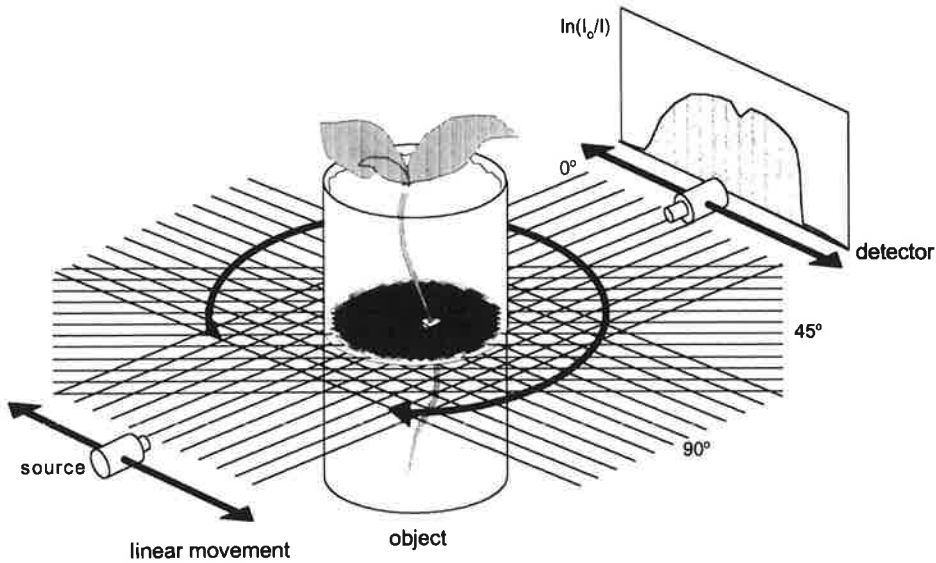


Figure 4. Schematic illustration of a parallel-beam CAT scanning procedure showing a single projection consisting of a set of parallel ray sums and the linear and rotational movements involved in the collection of data prior to image reconstruction for a cross-section of the object.

ray (r, ϕ)

$$p(r, \phi) = \ln(I_0/I_{r\phi}) = \int_{r\phi} \mu(x, y) ds \quad (6)$$

In Eq. (6), $\mu(x, y)$ is determined using many independent views or projections through the object. In the simplest scanning systems these are obtained using a scanning procedure involving both linear and rotational movements of the source detector system (Fig. 4). A complete set of parallel ray sums represents a single projection for that view of the cross-sectional layer of the object.

Ideally, $\mu(x, y)$ is a continuous two-dimensional function and an infinite number of projections are required for reconstruction. Because in practice it is physically impossible to obtain an infinite number of projections, $\mu(x, y)$ is calculated at a finite number of points from a finite number of projections. If the object is confined to a circular domain of diameter d , and the image is reconstructed at points arranged rectangularly with spacing w , then there are $n = d/w$ points along a principal diameter. Each square cell of width w is called a pixel (an acronym for picture element). It is also assumed that there are m projections spaced equally from 0 to 180°, each consisting of n ray sums at intervals w . The minimum number of

rotations required for accurate image reconstruction is given by $\pi n/4$ (Panton, 1981).

1. Numerical Reconstruction

In theory, if $p(r, \phi)$ is known for every line of width w passing through a pixel of dimension w , then $\mu(x, y)$ can be determined if Eq. (6) can be inverted (Panton, 1981). Bracewell (1956) was the first to devise a numerical reconstruction technique for determining $\mu(x, y)$ from Eq. (6), and with subsequent advances there are now more than a dozen different approaches available for reconstructing $\mu(x, y)$ (Budinger and Gullberg, 1974). However, these approaches can be classified broadly into three methods: (1) back-projection, (2) iterative reconstruction, and (3) filtered back-projection (Brooks and Di Chiro, 1975, 1976).

a. Back-Projection Reconstruction

In the back-projection method, reconstruction is performed by applying the magnitude of each projection to all points that make up the ray, or, in other words, the back-projected $\mu(x, y)$ value is obtained by superimposing projections together. The process can be described by Eq. (7),

$$\mu(x, y) = \sum_{j=1}^m p(r_j, \phi_j) \Delta\phi \quad (7)$$

where $r_j = x \cos \phi_j + y \sin \phi_j$, the distance of the ray from the origin; ϕ_j is the j th projection angle and $\Delta\phi$ is the angular distance between projections (i.e., $\Delta\phi = \pi/m$) and the summation extends over all m projections.

Back-projection, however, does not produce a good reconstruction because each ray sum or projection is applied not only to points of high density but to all points along the ray. This defect shows up most strikingly with discrete areas of high density, producing a star artifact. The star artifact causes the density function to vary from the true density function by an intolerable margin, hence this method is rarely used these days.

b. Iterative Reconstruction

In the iterative methods of reconstruction, the basic strategy is to apply corrections to arbitrary initial $\mu(x, y)$ values in an attempt to match the measured ray projections. Because former matchings are lost as new corrections are made, the procedure is repeated until the calculated projections agree with the measured ones within the desired accuracy. Iterative methods are primarily classified according to the sequence in which corrections are made and incorporated during an iteration, as this choice

has a significant effect on the performance of the method. Three such variations have been proposed:

1. Simultaneous correction: all projections are calculated at the beginning of the iteration and corrections are applied simultaneously to all points (x, y) . This method has sometimes been referred to as the *iterative least-squares technique* (ILST) (Goitein, 1972).

2. Point-by-point correction: each point is corrected simultaneously for all rays passing through it and corrections are incorporated before moving to other points. This technique was introduced in electron microscopy by Gilbert (1972), who named it the *simultaneous iterative reconstruction technique* (SIRT).

3. Ray-by-ray correction: a given set of ray projections is calculated and corresponding corrections are applied to all points. The updated $\mu(x, y)$ values are then used for calculating the next projection. Ray-by-ray correction was used in the original version of the EMI scanner (Hounsfield, 1972) and was independently discovered in electron microscopy by Gordon *et al.* (1970), who named it the *algebraic reconstruction technique* (ART). The iterative reconstruction methods are slow and hence are not very popular.

c. Filtered Back-Projection

Filtered back-projection methods are the most commonly used and are considered to be the most accurate. The basis of the analytical methods involves a fundamental relationship between the Fourier transform of the linear attenuation function $\mu(x, y)$ and the projection function $p(r, \phi)$. Such a relationship filters the projection, accounting for the portions of the projection that may pass outside a given pixel, thereby eliminating the star artifact mentioned earlier in the back-projection reconstruction method. The filtered projections are then back-projected, i.e., the reconstructed $\mu(x, y)$ is analogous to Eq. (7) except that the p is replaced by the filtered version p^* :

$$\mu(x, y) = \sum_{j=1}^m p^*(r_j \phi_j) \Delta \phi \quad (8)$$

A number of filtering techniques (Fourier, Radon, convolution filtering, etc.) have been developed, but the performance of filtered back-projection is not greatly affected by the choice of filtering technique. Derivation of the formula for the different filters can be found in works by Brooks and Di Chiro (1976), Herman (1980), and Kak and Slaney (1988).

A schematic illustration of a reconstructed image with direct back-projection and back-projection after filtration of projections (profiles) measured for a homogeneous cylinder is shown in Fig. 5. After direct back-

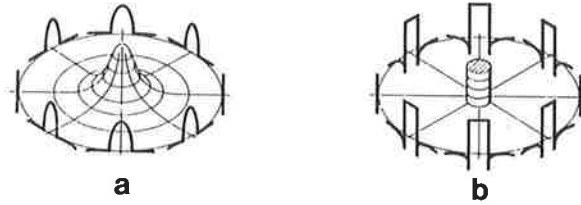


Figure 5. Schematic illustration of a reconstructed image with (a) direct back-projection and (b) back-projection after filtration of profiles measured for a homogeneous cylinder.

projection of the profiles measured, image details would be smeared if no further corrections were carried out. For this reason, back-projection is preceded by a filtration or convolution process.

Filtered back-projection has the advantage that the data can be processed as they are collected and the image can be built up and displayed projection by projection, thus allowing a useful saving in measurement time, particularly when data rates are low. An added advantage is that the final image is ready virtually immediately after the scans are completed and image quality can be progressively assessed. Iterative techniques need a larger data set before image reconstruction can commence, but are capable of giving better results from fewer projections than is normally required for the convolution method (Gilboy, 1984).

2. Aliasing Artifacts

Reconstruction procedures are only as good as the data on which they are based and a number of errors or artifacts can arise through the availability of insufficient data or by the presence of random noise in the measurements. An insufficiency of data may occur either through under-sampling of projection data or because not enough projections are recorded. The distortions that arise as a result of inadequate data are called aliasing artifacts and generally appear as streaks, blurring, rings, or interference patterns in the reconstructed image. Aliasing distortions may also be caused by using an undersampled grid for displaying the reconstructed image (Brooks and Di Chiro, 1976; Kak and Slaney, 1988). Regions of overestimated or underestimated attenuation associated with sharp changes in attenuation and appearing as rings or oscillations are called the Gibbs effect. Moiré patterns are interference patterns that can dominate the entire image. The occurrence of these effects depends largely on the relative number of projections and rays in each projection, and it has been shown (Kak and Slaney, 1988) that a balanced image reconstruction re-

quires that the number of projections should be roughly equal to the number of rays in each projection.

III. X-RAY CAT SCANNERS

A. CONSTRUCTION

X-Ray sources were chosen for medical scanners because of their absorption characteristics in bone and body tissues and because of the high photon output from intense tube sources, providing rapid measurements within a few seconds. Any scanning pattern that provides a suitable number of ray sums to reconstruct a satisfactory two-dimensional image can be used. Whereas the reconstruction algorithms for a parallel beam system, as used in first- and second-generation commercial X-ray systems, are simpler, the time to scan across an object and then rotate the entire source/detector arrangement is usually too long for many (including medical) purposes. This time can be reduced by using an array of sources, but only at greatly increased cost. Consequently, most third-generation scanners use a fan-shaped beam with multiple detectors to minimize scanning time. Both the source and the detector array are mounted on a yoke that rotates continuously around the object over 360° . This principle enables the scanner to obtain high-resolution scan images in typical scan times of 3 to 7 sec. More recently, fourth-generation fixed-detector and rotating source scanners have been developed in which a large number of detectors are mounted on a fixed ring and an X-ray tube inside this ring continually rotates around the object.

In a typical third-generation scanner, the beam is collimated to form an emerging beam angle of 42° with a variable thickness of 1 to 8 mm. The detector system consists of a scintillation detector array containing 704 individual NaI detectors lined up, without a gap, over an arch of 42° . The X-ray source (an oil-cooled rotating anode tube) and detector system are connected mechanically and face each other; they are located inside the gantry. A general view of the gantry and object table is shown in Fig. 6. The gantry aperture for object positioning is 70 cm in diameter. The scanning beam penetrates the object in a scan field of 51 cm, thus an object up to 51 cm in diameter can be imaged.

To produce a tomogram, the tube-detector system is rotated continuously around the object. During this scan process, the object is projected 1440 times in increments of 0.25° over a rotation of 360° . The intensity distribution of each projection is recorded with the detector system. The

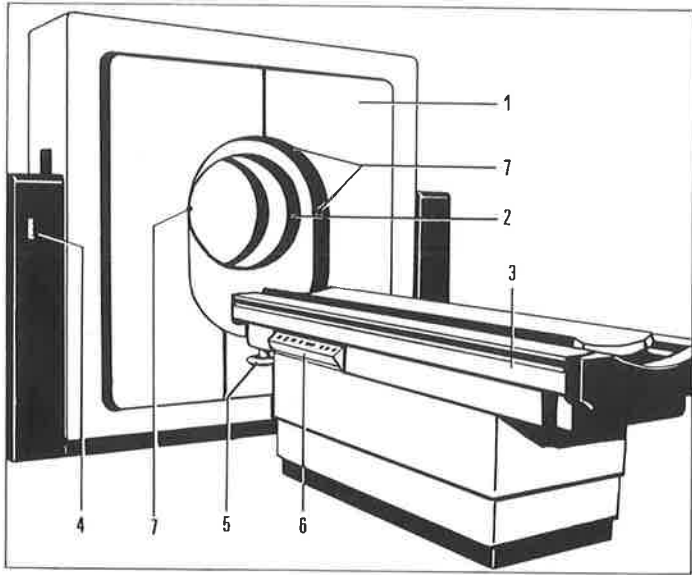


Figure 6. General view of the gantry and object table of a typical medical X-ray CAT scanner: (1) gantry, (2) gantry aperture, (3) object table with motor-driven height adjustment, (4) gantry angular indication, (5) hand wheel for manual horizontal movement, (6) control panel for the object table, and (7) positioning lights for exact object positioning. (From operating manual, Siemens SOMATOM DR-H.)

geometry and measuring principle of the scanner are illustrated in Fig. 7. The operation characteristics of the X-ray tube are 96 kV/125–1350 mA · sec or 125 kV/100–1240 mA · sec; the milliamperage depends on the scanning time. The scan time may change from 1.4 to 14 sec. The slice thickness may be 1, 2, 4, or 8 mm. Details of the CAT scanner operation are given in the review articles previously cited.

B. DETECTION

The two most commonly used X-ray detectors in medical CAT scanners are xenon gas ionization detectors and solid-state scintillation detectors, including sodium iodide, bismuth germanate, or cesium iodide (Kak and Slaney, 1988). The primary advantage of xenon gas detectors is that they are inexpensive and can be closely spaced, providing resolution down to 1 mm. Their overall efficiency is, however, lower (around 60%) compared

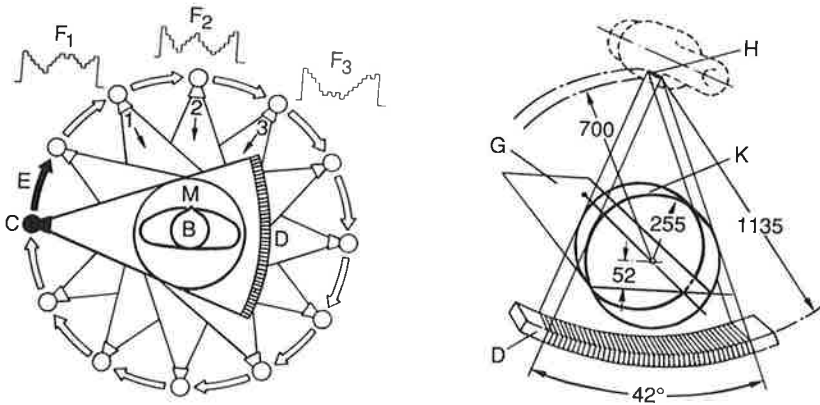


Figure 7. Illustration of the geometry and measuring principle of a third-generation fan beam X-ray scanner. B, Object; C, X-ray tube assembly; D, detector system; E, sense of rotation, F, single absorption profile; G, object positioning plane; H, focus; M, scan field; K, slice under examination. (From operating manual, Siemens SOMATOM DR-H.)

with scintillation crystals coupled to a photomultiplier tube or solid-state photodiode (close to 100%).

C. COLLIMATION

Compton and Rayleigh scattering can lead to errors in measurement of attenuation and subsequent image reconstruction if not excluded. Although the angle of scatter is random, generally more photons are scattered in the forward direction. Although the intensity of the scattered radiation impinging on the detector is approximately constant for different rotations, its significance will vary with the degree of attenuation of the incident beam. This directional dependence leads to streaks in the reconstructed image. However, by collimating the entrance to the detector so that photons that are not traveling in a straight line between the source and the detector are excluded, this effect can be substantially reduced. Collimation largely determines the thickness of the slice scanned and spatial resolution of attenuation.

D. RECONSTRUCTION

Typically a two-dimensional mapping of attenuation coefficient values into a 512×512 element array $[\mu(x, y)]$ is constructed from the projection data acquired during a scan. The array is graphically displayed as an image

on a high-resolution monitor. As in most current commercial CAT scanners, a reconstruction algorithm, called the convolution method or filtered back-projection, generates $\mu(x, y)$ (Herman, 1980; Chase and Stein, 1978). Image reconstruction utilizes a specialized extensive computer system to produce the resultant array in about 6 sec.

Depending on the selected mathematical scaling (zoom factor), the effective area of the 512×512 matrix of picture elements (pixels) comprising the image ranges from 0.1 to 1 mm² in the actual measured field or scanning plane. Hence, an individual pixel value can represent the attenuation value of a volume element (sometimes referred to as voxel) from $0.1 \times 0.1 \times 1$ mm³ up to $1 \times 1 \times 8$ mm³.

E. HOUNSFIELD UNITS

The attenuation coefficient values (μ) of the material within the volume of the object, which are represented by the pixel in the image matrix, are not displayed in the conventional μ units of cm⁻¹. Before the image is viewed, these coefficients are converted into an internationally standardized number scale known as Hounsfield units (H), usually expressed as follows (Newton and Potts, 1981):

$$H = 1000(\mu - \mu_w) / \mu_w \quad (9)$$

where μ_w is the linear attenuation coefficient of water (cm⁻¹). The scale is linear, and H units for air and water are defined as -1000 and 0 , respectively. Each H unit represents about 0.1% change in the attenuation coefficient of the material. The scale runs between $-1000H$ and $+3000H$, where, for medical purposes, soft tissues are mainly in the range of $-200H$ to $+200H$ and values for bones range up to $+1000H$. The value of $+3000H$ corresponds to materials of high density.

In practice this range is more than adequate to handle the values commonly experienced with soil constituents. Petrovic *et al.* (1982) listed values ranging from 450 to 800 for a fine sandy loam soil. Grevers *et al.* (1989) reported Hounsfield values for various materials in a polyvinyl chloride (PVC) cylinder that had been filled with uniform sand. The Hounsfield values obtained for air, water, styrene resin, glass, aluminum, sand, and the PVC cylinder were -835 , 80 , 197 , 2010 , 1972 , 783 , and 821 , respectively. The Hounsfield values for the soil matrix in the two sets of soil samples used in their study ranged from $945H$ to $1236H$. A similar range of values have been reported by other workers.

The whole range of values, i.e., from $-1000H$ to $+3000H$, can be displayed in corresponding depth-of-gray values on the system monitor. As

a rule, the values in the "+" direction are recorded bright and those in the "-" direction are recorded dark. To portray the array effectively, the operator interactively selects the mean value (window center) and the range (window width) of attenuation values.

Several software features assist the operator in printing out or plotting the numerical pixel values within the interactively selected region of interest (ROI). ROI can be circular, rectangular, elliptical, or irregular in shape. The size and location of the ROI can be controlled. Increasingly magnified cross-sections through a lupine plant root and surrounding soil, illustrated in Fig. 8, show the ease with which measurements near the root can be obtained and viewed. Total number of pixels, mean, standard deviation, and root mean square deviation of pixel values in the selected region, its area and volume, and the distance between two points are available instantly by manipulation of the selected region. The images can be stored on magnetic tape for subsequent analysis.

F. DIFFICULTIES WITH X-RAY SCANNERS

Although conventional X-ray scanners provide excellent outputs in the form of pictorial displays and arrays of Hounsfield units associated with pixel densities, there are major limitations on their current usefulness for the quantitative determination of parameters of interest to soil and plant scientists. These arise from several sources.

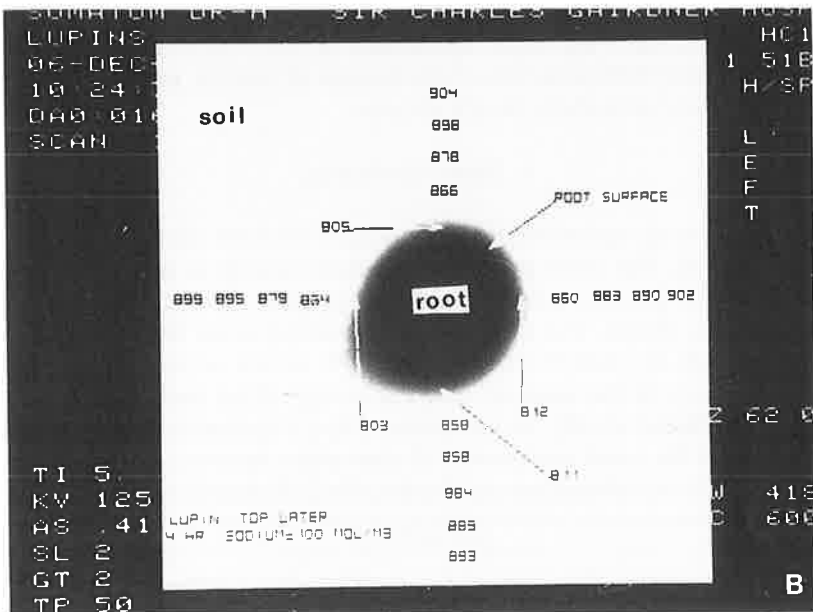
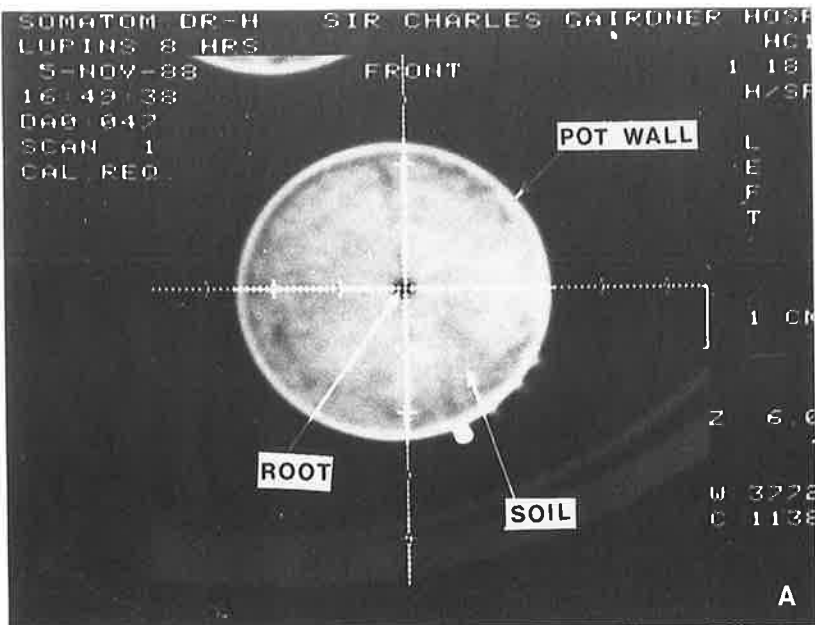
1. Beam Hardening

X-ray beams are generated by impinging an electron beam on a suitable target material. The beam generated is polychromatic in nature, with the distribution of photon wavelengths being typically normal and related to the excitation energy. The subsequent attenuation of an X-ray beam as it passes through any sample depends primarily on the electron density, the packing density of the material, and the energy of the radiation. Because X-ray CT systems usually do not exceed 140 kV excitation, photoelectric absorption is the main mechanism of absorption involved. For any given wavelength, X-ray absorption can be described (Richards *et al.*, 1960) as

$$\mu = k\lambda^3 Z^3 \rho \quad (10)$$

where k is an empirical constant of proportionality, λ is the wavelength, Z is the effective atomic number (electron density), and ρ is the specific gravity of the soil particles.

The applicability of Beer's Law [Eq. (1)] requires a monochromatic



Figures 8A and 8B.

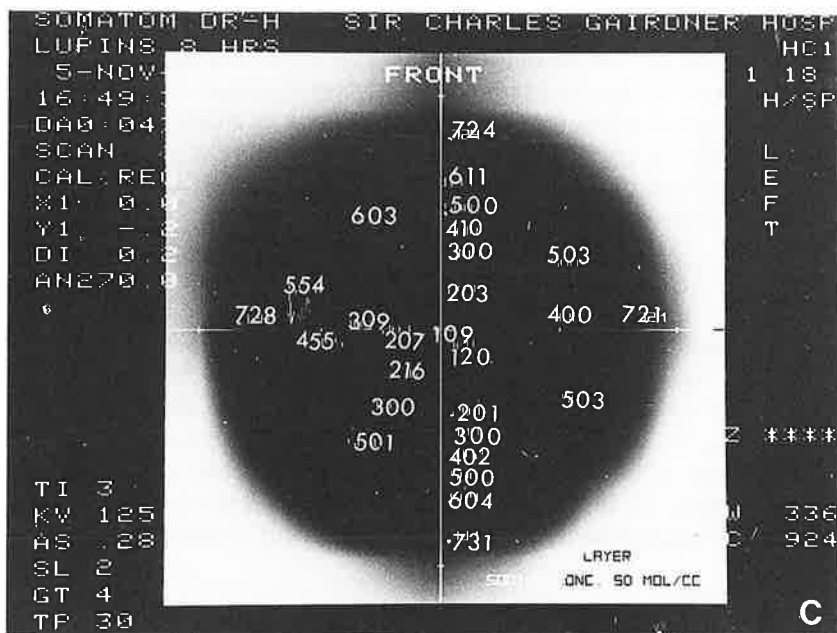


Figure 8. CAT scan image showing three increasingly magnified cross-sections through a lupine plant root and surrounding soil. (A) Scale imposed on the center of the lupine root for location of pixels. (B) Magnified image showing Hounsfield unit values at the root surface and at 1.0-mm intervals away from the root surface. (C) Hounsfield unit values throughout a section of lupine root. The root diameter is about 4 mm. (After Hamza and Aylmore, 1992a,b.)

X-ray source and one predominant mechanism of X-ray absorption. However, from Eq. (10), the shorter the wavelength, the higher the energy, and the more penetrating the radiation. Thus because dense materials will selectively absorb lower energy X-rays from polychromatic sources, there will be a progressive filtering of the beam to higher energies (i.e., lower average wavelength) as the distance traversed by the beam increases. The process is referred to as “beam hardening” (Herman, 1980). Tollner and Murphy (1991) quoted evidence showing that a 40-cm water body caused an effective shift in wavelength from 0.21×10^{10} m to 0.125×10^{10} m with a Siemens system having a copper-tungsten target. The distribution would be even more skewed toward the minimum possible wavelength after passing through soil.

The CT scanner reconstructs an image of a soil sample from multiple scans in a given plane, producing essentially a map of attenuation coefficients. However, depending on the total length and composition of material in each transect, the effective wavelength and hence absorption at any

given location or pixel may vary, resulting in a decrease in quantitative definition. That is, the relationship between measured attenuation and density is not in fact linear, because the location of a pixel in the object can influence the attenuation measured. Attempts can be made physically and mathematically to correct for beam hardening (Brooks and Di Chiro, 1976), but such artifacts will undoubtedly occur under the conditions that exist in soils (Petrovic *et al.*, 1982).

2. Absorption Edge Phenomena

The attenuation of the X-ray beam passing through the sample is further complicated by the nature of the absorption process. In photoelectric absorption, X-rays are absorbed by the electron cloud of an element, with each shell (e.g., K, L, M, and N) of the cloud contributing to the absorption process. A plot of the linear absorption coefficient versus wavelength exhibits a number of sharp discontinuities (Fig. 9) known as absorption edges. These absorption edges are associated with crossing energy level

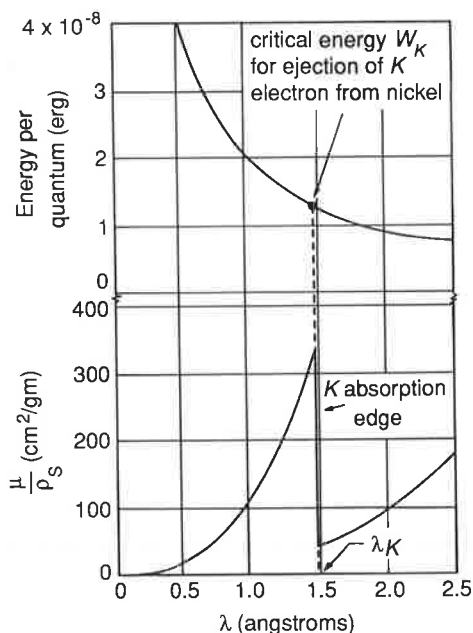


Figure 9. Variation with wavelength of the energy per X-ray quantum and of the mass absorption coefficient of nickel. (From Cullity, *Elements of X-ray Diffraction*, © 1978 by Addison-Wesley Publishing Co. Reprinted by permission of Addison-Wesley Publishing Co., Inc., Reading MA.)

thresholds associated with each shell and mark the points on the frequency scale where the X-ray possesses sufficient energy to eject an electron from one of the shells. In practice, all wavelengths shorter than that corresponding to a given absorption edge will possess sufficient energy to eject electrons from that particular shell, and those immediately shorter will be strongly absorbed. As the wavelength decreases and the energy of the photon increases above the critical excitation value, there is less likelihood of ionization and more chance that the photon will simply pass through unabsorbed. The absorption thus decreases rather rapidly on the short-wavelength side of the absorption edge. Coupled with the polychromatic nature of the X-ray beam and consequent beam hardening, absorption edges may cause a given zone to absorb differently, depending on the total length of a particular X-ray transect. Because multiple transects with different lengths traverse each location in the scanned area, the effective wavelength may vary at a location during scanning, causing the effective absorption to vary instead of being constant.

Although the beam from an X-ray tube contains a continuous spectrum ranging over a wide band of wavelengths, the $K\alpha$ doublet of the target material is of most use because of its great intensity. The existence of absorption edges is commonly used to reduce the polychromaticity of the X-ray beam by passing the beam through an appropriate filter. The distribution of wavelengths in the polychromatic X-ray beam is typically normal, with most photons having wavelengths near the minimum absorption edges for the target material in the X-ray tube. By choosing for the filter an element whose K absorption edge is just to the short-wavelength side of the $K\alpha$ line of the target material (i.e., with an atomic number one less than that of the target metal), the intensity of undesirable $K\beta$ wavelengths can be decreased. The presence of such a filter also decreases the content of softer radiation and helps to reduce subsequent beam hardening. However, filtration is never perfect, and because of the range of materials in soils both beam hardening and absorption edge effects are to be expected. X-Rays in general must possess short wavelengths in order to penetrate materials with a high atomic number, and absorption edge problems are especially acute in dense materials. Beam hardening is of greatest concern because the soil is an absorber at least equal to the filtering element on first- and second-generation CT systems (Tollner and Murphy, 1991).

3. Other Limitations

In addition to such quantitative limitations, their expense, and problems of accessibility, commercially available medical X-ray scanners, being generally designed to monitor horizontal patients, are not conveniently constructed for soil/plant/water studies involving plants growing vertically in

soil columns. Although they provide excellent resolution for some studies, detecting attenuation as low as 0.1% (Brooks and Di Chiro, 1976), their usefulness in studying soil systems has invariably been restricted by their inability to distinguish between changes in water content and bulk density in swelling soils. Furthermore, the proprietary nature of these commercial systems generally makes software modification or extensions impossible.

IV. γ -RAY CAT SCANNERS

Most medical CT scanners employ intense X-ray tube sources in order to complete the measurements within run times of a few seconds. The X-ray tube in a medical scanner typically can have an equivalent source strength of 15,000 Ci distributed over a few square millimeters. However, for precise quantitative imaging, γ -ray sources are superior to X-ray tubes in almost all respects apart from the question of source brightness, which is several orders of magnitude less than X-ray tubes (MacCuaig *et al.*, 1986). Despite this drawback, γ -ray sources ranging from a few millicuries to 200 Ci have been used to achieve useful tomographic images in acceptable run times. Use of γ -ray sources eliminates the beam hardening and absorption edge problems if single-photon counting is employed with energy-dispersive detectors. (Note that γ -ray photons are indistinguishable from X-ray photons, with the different terms being used simply to indicate their origin.) γ -Ray sources also offer additional advantages compared with X-ray tubes, including lower cost, compactness, portability, and ready access to a very wide range of photon energies. The constancy of γ -ray photon energy over space and time also renders γ -ray tomography a more objective method of imaging (Gilboy, 1984).

With these advantages in mind, work in several laboratories has been directed to the modification of "conventional" γ -ray scanning systems to utilize the CAT approach, to provide experimentally more suitable systems, and to vastly reduce the cost of the equipment (Hainsworth and Aylmore, 1983, 1988; Crestana *et al.*, 1986). Single- and dual-energy γ -ray attenuation measurements have been used for many years to monitor changes in average bulk density and water content in soil columns (Gurr, 1962; Groenevelt *et al.*, 1969; Ryhiner and Pankow, 1969). The mass attenuation coefficients for soil and water both vary with the energy of the radiation. Consequently, solution of the two attenuation equations for measurements made at two different γ -ray energies allows the simultaneous determination of water content and bulk density. Because bulk density often changes significantly with wetting and drying, use of the

dual-energy technique greatly improves the accuracy of water content measurements over that possible when bulk density must be assumed to remain constant (Corey *et al.*, 1971; Gardner *et al.*, 1972).

γ -RAY SCANNING SYSTEM

1. Logistic System

A general view of the γ -ray CAT scanning system constructed in the soil science and plant nutrition laboratories of the University of Western Australia (Hainsworth and Aylmore, 1983, 1988) is shown in Fig. 10. The main body of the system consists essentially of two platforms, the γ platform, which provides vertical up and down motions for conventional γ scanning, and the CAT scan platform, which provides linear translation and rotational motions required in a CAT scan procedure.

The γ platform supports the lead shielding for the source and scintillation detector mounted directly opposite to each other. The CAT scan platform is placed at a fixed level in the middle of the γ platform such that the γ platform can move independently of the CAT scan platform. Three stepper motors were used with worm drive shafts to provide the scanning motion required. A close-up photo of the CAT scan platform, where the soil column being scanned is placed, is shown in Fig. 10B. The system is capable of scanning columns up to 10 cm in diameter and 150 cm in length. A block diagram illustrating the operation of the system is shown in Fig. 11. The system consists of three subsystems: motion control system, data acquisition system, and computer system. The motion control system is linked with the computer using an interface card, which drives the platform's stepper motors.

As shown in Figs. 10 and 11, an XT-compatible personal computer (PC-XT) is used for performing the task of controlling the scanning motions and acquiring data from the radiation measurement system. Processing the data and final presentation of the results in graphic form or producing hard copies of the results are carried out by a 386-based IBM-compatible computer.

The lead source housing can accommodate two sources, which may be selected by means of a rotating axle that swings the desired source in line with the collimator. Commercially available ^{137}Cs (0.5 Ci), ^{241}Am (0.2 Ci), and ^{169}Yb (up to 2.6 Ci) sources have been used with this system. The beam is collimated by a 2×5 -mm rotatable collimator mounted on the front of the source housing and a 2×2 -mm collimator mounted on the detector to

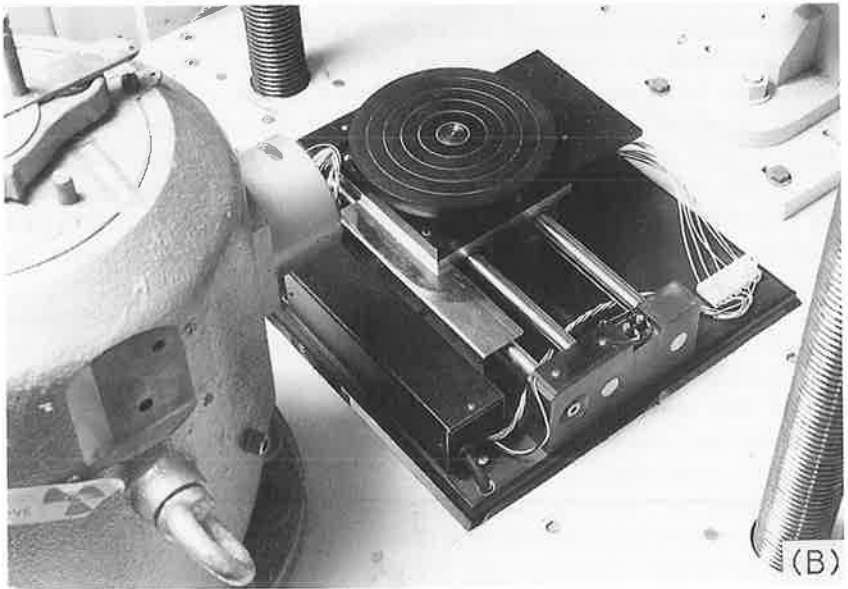


Figure 10. The γ scanning system constructed at the University of Western Australia. (A) Scanning system with associated scalar and microcomputer control unit. (B) Close-up of CAT scan platform. (After Hainsworth and Aylmore, 1988.)

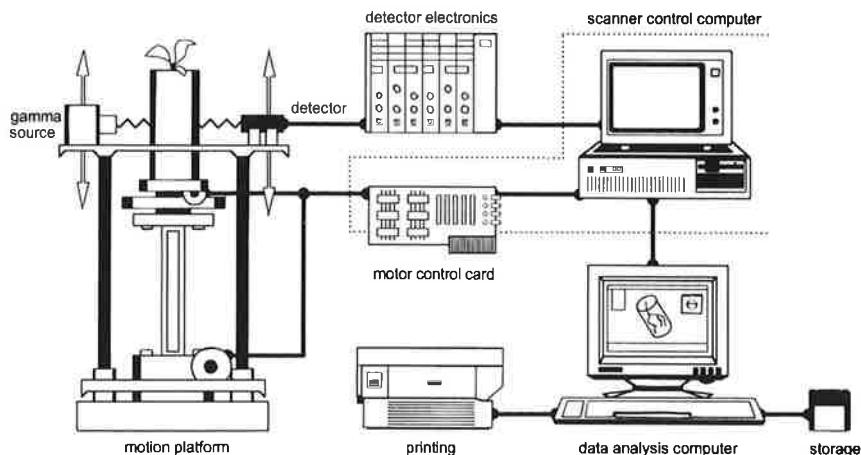


Figure 11. Block diagram of γ -ray CAT scanning system constructed at the University of Western Australia. The system consists of three subsystems: the computer system, the data acquisition system, and the motion control system.

ensure maximum beam “sharpness” and to allow use of voxel dimensions of $2 \times 2 \times 2$ mm or $2 \times 2 \times 5$ mm.

2. Radiation Detection

The radiation detection and measurement system consists of a scintillation detector (Model 802-3)—a monoline crystal assembly that includes a high-resolution NaI(Tl) crystal (50×50 mm), photomultiplier tube, and preamplifier (Model 2007P). The scintillation detector is directly connected to the spectrometer, which incorporates a long-term, stable, high-voltage (HV) supply (NE 4646), an amplifier (Model 2012), single-channel analyzer (Model 2030), and dual counter (2072A) with a 207X-03 Electronics Industries Association (EIA) interface for communication with a PC. All these modules of the spectrometer are installed in an NE 4626 nuclear instrument modules bin. All components except the high-voltage power supply were supplied by Canberra-Packard Pty. Ltd.

Crestana *et al.* (1986) also developed an inexpensive CT miniscanner platform for laboratory soil research of construction similar to the above-mentioned system, but allowing a range of photon energies to be obtained by using a combination of X-ray and ^{241}Am sources. Being custom systems, these scanners are open to modification and adaption suited to current research interests.

V. APPLICATION OF COMPUTER-ASSISTED TOMOGRAPHY TO SOIL-WATER STUDIES

A. LINEARITY

Knowledge of the spatial distribution of the linear attenuation coefficient in the material may be of interest but not the desired end product in the CAT process. Generally, information about the density distribution or composition of the material is desired. Thus it is necessary to obtain theoretical or empirical relationships between the linear attenuation coefficients and the parameter of interest.

If a linear relationship holds, then μ is the product of the mass attenuation coefficient of the material and its physical density, and the value of μ for dry soil can be described (Hainsworth and Aylmore, 1983) by

$$\mu_{\text{dry}} = \mu_s \rho_s \quad (11)$$

where μ_s is the mass attenuation coefficient (cm^2/g) of soil solids and ρ_s is the bulk density of soil (g/cm^3). In order to obtain experimentally the relationship between μ_{dry} and ρ_s , the soil must be oven dry.

Equation (11) can be extended to wet soil as

$$\mu_{\text{wet}} = \mu_s \rho_s + \mu_w \theta_v \quad (12)$$

where μ_w is the mass attenuation coefficient of water and θ_v is the volumetric water content of the soil. Application of Eq. (12) requires that the bulk density of soil remain constant, i.e., no swelling or shrinking on addition or removal of water.

In situations in which the bulk density of the soil does not change with the addition or removal of water, θ_v can be calculated from a combination of Eqs. (11) and (12) to give

$$\theta_v = (\mu_{\text{wet}} - \mu_{\text{dry}}) / \mu_w \quad (13)$$

Thus, in principle, the water content distribution in the soil can then be determined by first scanning the soil column when the soil is dry and rescanning it in exactly the same position when the soil is wet.

The performance characteristics of medical CT scanners have naturally been optimized for X-ray absorption relevant to body tissues, which have absorptivities close to that of water [$\mu = 0.191 \text{ cm}^{-1}$ at X-ray tube voltages around 120 peak kV (McCullough, 1975)]. However, a number of workers (Petrovic *et al.*, 1982; Hainsworth and Aylmore, 1983; Crestana *et al.*, 1985; Brown *et al.*, 1987; Anderson *et al.*, 1988; Tollner and Murphy, 1991) have demonstrated that these systems still provide essentially linear

relationships between attenuation and bulk density/water content at the higher values associated with soil and similar porous materials. As might be expected, bearing in mind the dependence of the mass attenuation coefficient on the energy of the radiation, the chemical composition of the soil matrix, and the packing or bulk density, as well as differences in effects such as beam hardening, source detector geometry, and degree of electronic discrimination, substantial variations in the slope of the linear regressions have been noted with different soils and scanners. Furthermore, plots of these relationships do not always extrapolate to the origin as required by Eqs. (11) and (12).

The mass attenuation coefficient of a chemical compound, or a mixture, is more sensitive to variations in the chemical composition the lower the photon energy and the heavier the elements that are subject to abundance variations. In examining the influence of chemical composition on photon attenuation by soils, Coppola and Reiniger (1974) had earlier demonstrated that variation of the mass attenuation coefficient with soil composition becomes significant at energies below about 200 keV and is at a maximum below 50 keV (Fig. 12). Above 300 keV any difference in the value of the attenuation coefficient was negligible. Thus in the case of an ^{241}Am source (59.6 keV), the γ -ray attenuation by soil was influenced rather strongly by the particular soil composition (differences as large as 200% were calculated). In contrast, the influence was essentially negligible at the energy of ^{137}Cs (662 keV). They also concluded that although variations in the abundance of heavier elements such as Fe can cause significant variations in μ , rather large changes in the abundance of other elements, e.g., of Si, have no comparable effect on the μ coefficient. Because most commercially available medical X-ray CT scanners operate at around 120 keV excitation, significant differences in attenuation resulting from variations in chemical composition could be expected to occur.

The first reported attempt to use commercial medical X-ray CAT scanners to measure spatial changes in soil bulk density was by Petrovic *et al.* (1982), who showed that attenuation for an American Science and Engineering CT scanner was linearly related to the bulk density of soil from the surface horizon of Metea fine sandy loam over the range of 1.2 to 1.6 Mg/m^3 . The sensitivity to density changes for the Metea soil was about 0.02 Mg/m^3 , with a maximum observed deviation from predicted of 0.07 Mg/m^3 . Only a slightly different regression slope was observed for a mixture of glass beads and spheres and this was attributed to the differences in atomic number of the absorbing materials. Hainsworth and Aylmore (1983), using an EMI 1007 X-ray CT scanner, demonstrated that spatial changes in soil water content with time of the order of 0.006 g/cm^3 could be readily resolved by the CAT technique in nonswelling soils (Fig. 13) and

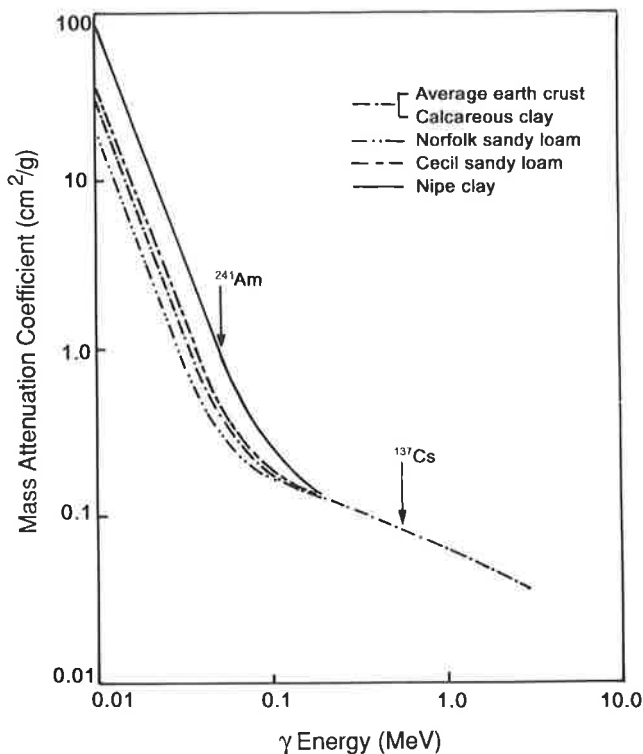


Figure 12. Mass attenuation coefficients for soils of various chemical compositions versus γ -ray energy. [After Coppola and Reiniger, 1974. © by Williams & Wilkins (1974).]

illustrated the scanner's potential for studies of soil/plant/water relations. Crestana *et al.* (1985) also obtained essentially linear calibration curves between the output from a General Electric T 8800 scanner and soil bulk density and soil water content for a sandy soil from the Ap horizon from Trieste, Italy, and a fine sandy loam from Barretos, Brazil. However, the linear calibration curves for bulk density for the two soils diverged markedly. Changing the bulk density caused a roughly parallel displacement of the calibration curves for attenuation as a function of water content. Crestana *et al.* (1985) used their CT scanner to observe the change in the X-ray attenuation coefficient with time at a single point in space within a homogeneous soil core as a wetting front passed. They showed that CT scanners could be used to measure the movement of water in soils at rates of 1.6 mm/sec.

Similar more detailed linear relationships between attenuation coeffi-

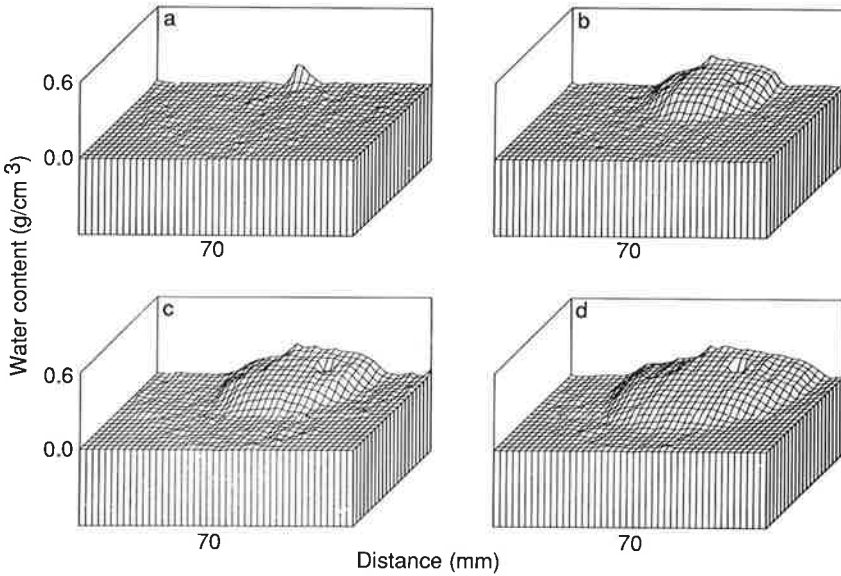


Figure 13. Half-slice three-dimensional plots showing changes in soil water content with time due to the infiltration of water into a soil column from an artificial root (alundum tube). Representations at (a) 1 min, (b) 10 min, (c) 15 min, and (d) 20 min of infiltration are illustrated. (After Hainsworth and Aylmore, 1983.)

cients (using a Philips Tomoscan 310) and volume fractions of soil solids were obtained by Anderson *et al.* (1988) for two silt loams from Missouri. Over 99% of the variation in CT attenuation coefficients for 40 dry soil cores for each of the two soils could be accounted for by linear regression relationships with the volume fraction of soil solids (f_s). Approximately 98% of the variation in CT attenuation coefficients for the 40 wet cores for each of the two soils was accounted for by regression relationships with the volume fraction of soil water (f_w), after correcting for swelling effects and differences in bulk density. Differences in attenuation coefficients for the two soils were shown to be largely due to differences in Fe content. Parameter values for the Mexico silt loam compared favorably with those determined for Metea fine sandy loam used by Petrovic *et al.* (1982) but differed markedly from values given in the earlier work by Crestana *et al.* (1985), where larger sampling volumes had been used. They suggested the possibility of developing a universal relationship between X-ray CT data versus bulk density and water content if differences in the electron densities of the soils are known and the effect of soil core size on computed tomography results could be characterized.

Tollner and Murphy (1991) also reported linear relationships among the absorption coefficients for solids and liquid portions in five soils ranging in texture from sand to loam and concluded that, for many applications and providing that zero swelling and shrinkage could be assumed, one calibration relationship could be applicable to a wide range of soils. For all soils tested, except for the Wilcox clay, which contained 66% clay of 2:1 clay mineralogy and exhibited significant shrinkage and swelling, the predicted soil density term was constant within 5% when the water term was fixed. The assumption of zero shrinkage during drying was largely met for all soils except the Wilcox clay.

Equally good linearity of response between the γ attenuation coefficient and the average bulk density/water content was observed by Phogat and Aylmore (1989) using a ^{137}Cs source (Fig. 14), but again significant variation in slope between materials is evident. Furthermore, although the relationships between γ attenuation and water content for both a sand from Bassendean, Western Australia, and a kaolinite-dominated sandy loam from Kulin, Western Australia, were also essentially linear, a degree of swelling resulted in the slope of the linear regression for the Kulin soil being substantially less than that for Cs radiation as measured for the nonswelling sand (Fig. 14B). Phogat and Aylmore (1989) suggested that variations in the mean and standard deviations of pixel attenuation coefficients for a scanned layer could be used to assess the structural status of the soil, because these changes reflect changes in the uniformity of the layer arising from changes in the spatial distribution of pore volume and soil matrix (soil aggregate). However, although some correction for bulk density changes on swelling can be made on the basis of appropriate calibrations, the difficulty in accounting for swelling and bulk density changes, in general, particularly when using polychromatic X-rays, remains a major impediment in studies of soil/plant/water relations. Taking into account the number of variables that may influence the regression for bulk density, it seems unlikely that a truly universally applicable relationship for attenuation at the energy levels used in medical CT scanners can be derived, and independent calibration for specific soils will remain an essential prerequisite to their use. More generally applicable relationships may, however, be possible using higher energy monochromatic γ -rays (e.g., from ^{137}Cs).

Differences in soil water salinity or chemical composition of practical interest in soil science have no appreciable effect on the γ -ray attenuation (Coppola and Reiniger, 1974). In most of the previous studies using X-rays, values close to the standard measured absorption value for water of 0.0191 mm^{-1} at energies around 120 keV (McCullough, 1975) have been observed, implying that one need not determine this coefficient for each soil. However, this value will of course change with the energy of the

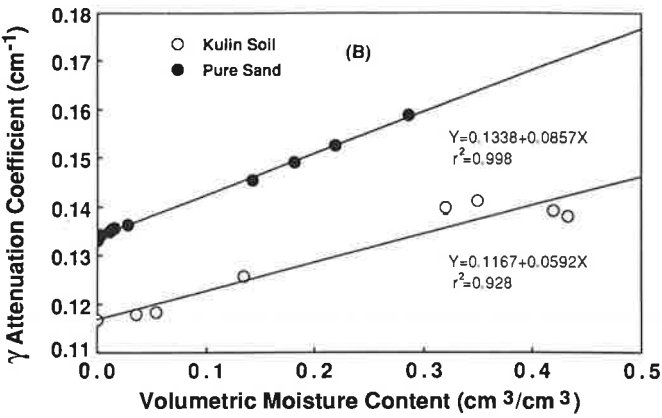
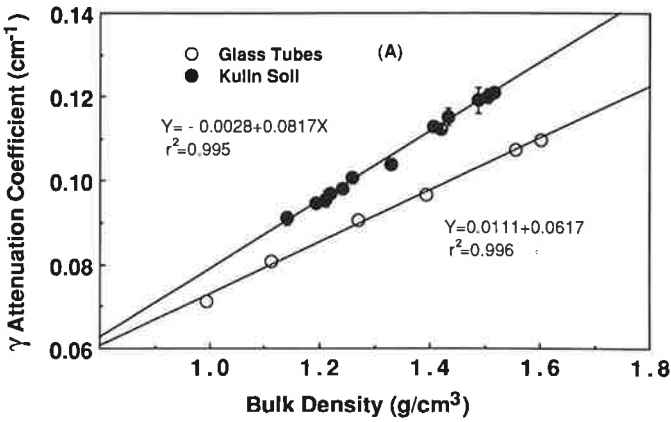


Figure 14. Linear relations between attenuation coefficient and (A) bulk density for Kulin soil and glass tubes and (B) volumetric moisture content for Kulin soil and pure sand. Vertical lines represent standard deviations. (After Phogat and Aylmore, 1989.)

radiation, and for γ -rays from ^{241}Am , ^{169}Yb , and ^{137}Cs the coefficients are around 0.201, 0.176, and 0.083 cm^{-1} , respectively.

B. STRUCTURAL DEFINITION

Of considerable interest is the ability of CAT scanners to characterize the internal structure and the nature of components present in the soil. A knowledge of the size and distribution of pores is, for example, relevant to

an understanding of many important processes that take place in soils, including water entry and redistribution, aeration, and root penetration. In particular, the ability to monitor root proliferation and distribution by a noninvasive technique is an essential prerequisite to detailed studies of water uptake by plant roots.

The ability of the scanner to resolve voids and objects of different sizes and spacing is obviously a function of the pixel dimensions, which for most commercial scanners is of the order of 1×1 mm. Spatial resolution of objects is based on the difference in attenuation of the transmitted X-rays by the object and the adjoining soil mass. Good spatial resolution can best be achieved when there is a large difference in H values between the subject (e.g., a void) and the background (e.g., the soil mass). Most workers (e.g., Petrovic *et al.*, 1982; Anderson *et al.*, 1990) have found that under such conditions CT scanners are able to detect holes of the order of 1 mm in diameter but are not necessarily able to separate adjoining holes of similar diameter. Although the spatial resolution as determined by the scanner and image reconstruction algorithm used by Warner *et al.* (1989) was approximately 0.5 mm, the practical resolution was about twice this value due to boundary effects. If the boundary of an air-filled pore 0.5 mm in diameter exactly coincides with the pixel edges, a scan image can theoretically show that pore. However, if the pore boundary falls in the middle of the pixel, the scanner will produce an attenuation value that is an average value for the materials within the pixel (e.g., soil and air). In practice, the scanner actually monitors a volume of soil (in this case voxel dimensions were $0.5 \times 0.5 \times 8$ mm). Hence if any part of the voxel is filled with air and the rest is filled with solid, the attenuation value for the voxel will be an average between that for the solid and that for the air. Consequently, studies of porous structure have been largely limited to macropores of dimensions similar to pixel size.

The CAT image of an acrylic cylinder containing various sizes of holes is shown in Fig. 15. The CAT scanner accurately depicted the location and size (in millimeters) of the air-filled holes. Holes of 2.0 mm and larger in diameter could easily be distinguished when the image was enlarged to actual size or larger. Smaller pores, down to approximately 1.0 mm, were distinguishable from the images but were often greyish in tone. Holes 0.5 mm diameter could not be distinguished with the pixel dimensions used. The scanner used in this study had a scan field of 510 mm with 512 pixels, i.e., one pixel corresponds to an object size of approximately 1 mm (0.996 mm actual). Any part of the measured field can be reconstructed with a pixel size between 1 and 0.1 mm by selecting the zoom factor between 1 and 10. For example, a zoom factor of 10 corresponds to a measured field 510 mm in diameter with an object size of 0.1 mm per pixel. Thus, the use

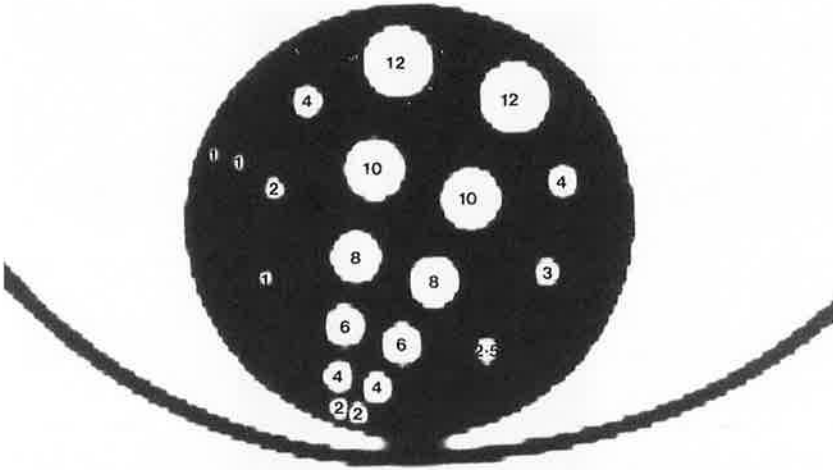


Figure 15. X-Ray CAT scanning image of an acrylic cylinder containing various sizes of holes (in millimeters).

of an object size of 51 mm in diameter would result in a higher resolution (0.1 mm). However, large objects may have the advantage of greater statistical significance.

Difficulties may also arise in high-contrast resolution because a zone of drastically changing density, such as an air-filled hole or a stone in the soil, can cause the destruction or blurring of information elsewhere in the scan due to beam hardening and other mathematical anomalies. These include lines and streaks (Fig. 16) developed in the plane of symmetry at a density gradient interface and the Gibbs phenomena (Bracewell, 1956; Brooks and Di Chiro, 1976), where large changes in attenuation from high-density to low-density areas cause the calculated values in the adjacent low-density area to be less than the actual attenuation coefficient in that region, i.e., an overshoot. The size of object required to cause this type of artifact or the extent of the perturbation will depend mainly on the attenuation differential and the characteristics of the CT scanner used. Many scanners are better able than others to compensate for this artifact (Petrovic *et al.*, 1982).

When only small differences in attenuation exist between an object and the surrounding soil, the ability to resolve the object accurately is reduced. Thus Petrovic *et al.* (1982) found that objects within the scanning plane that differed in attenuation by 1%, or about 10 Hounsfield units, had to be at least 6.4 mm in diameter to be detectable using a pixel size of 1×1 mm. Grevers *et al.* (1989) observed that spatial resolution in CT scans between



Figure 16. Streaking artifact in a CAT image of a vertical slice through a soil column.

soil pores and the soil matrix decreased as a result of impregnation with resin because of the lower contrast in attenuation coefficient between pores and the soil matrix than in the nonimpregnated samples. The difference in Hounsfield values between the soil matrix and air-filled pores was around $1900H$, whereas that between resin-filled pores and soil matrix was around $900H$. Consequently, classification of the image into pore and soil matrix was more difficult and led to an underestimation of macroporosity. These CT images were, however, analyzed by applying an image-analyzing computer to grey-scale images from the scanner, which would have contributed to the difficulty in spatial resolution. The use of actual Hounsfield values for pixels from the CT scanner would undoubtedly have reduced this discrepancy. Grevers *et al.* (1989) concluded that the images of a soil macropore system obtained from CT scanning compared favorably with those obtained from thin sections and had the advantage of being nondestructive and less time consuming. Similarly, Anderson *et al.* (1990) examined the influence on effective resolution of blurring at the boundary of constructed macropores by comparing measured hole diameters on the basis of 50 and 75% differences in mean bulk density (MBD) as determined by the CT scanner. Although good agreement ($r = 0.97$) was found between the CT-measured hole diameters and the wire diameters used in constructing the holes for both the 50 and 75% MBD methods, fewer holes

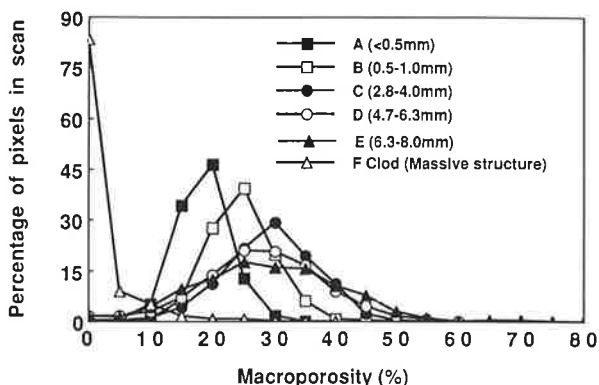


Figure 17. Macroporosity distribution for scans of different sizes of aggregates of Kulin soil. (After Phogat and Aylmore, 1989.)

were detected using the more restrictive 50% MBD criteria as compared to the 75% MBD method.

Several attempts have been made to develop quantitative characterizations of porosity and water content in soils on the basis of the distribution of pixel attenuation. Phogat and Aylmore (1989) determined average macroporosity and the spatial and frequency distribution of macroporosity for soil samples by assigning the value of zero macroporosity to pixels having γ attenuation coefficients corresponding to the bulk density of a soil aggregate, 100% macroporosity to pixels with zero attenuation coefficients, and proportional values to pixels with intermediate coefficients (Fig. 17). CAT scanning of soil samples before and after a wetting and drying cycle provided a quantitative illustration of the greater reduction in macroporosity for soil wetted under flooding compared with that wetted under capillary action (Fig. 18). A similar analysis of the distribution of pixel attenuation values was used by Sawada *et al.* (1989) to characterize the degree and extent of dispersion of soil water content and hence to evaluate the efficiency of soil wetting agents in overcoming water repellence. The possibility of relating the hydraulic conductivity of a porous glass bead system directly to the spatial distribution and continuity of pore space as measured by the CAT scanning procedure was examined by Phogat and Aylmore (1993). A useful preliminary relationship for glass bead systems was obtained, indicating considerable potential usefulness in this approach.

Because of their inherent limitations, commercially available medical X-ray scanners have thus far proved of most use in visual studies of soil structure (Anderson *et al.*, 1988; Jenssen and Heyerdahl, 1988; Tollner and Murphy, 1991; Grevers *et al.*, 1989), the advancement and stability of

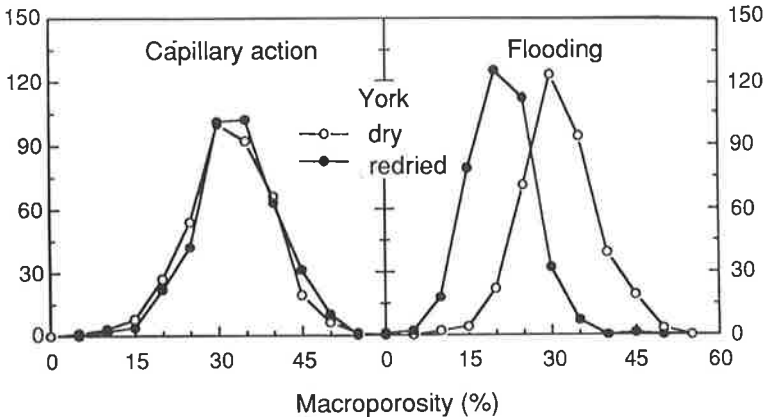


Figure 18. Changes in frequency distributions of macroporosity for York soil after wetting under flooding or capillary action, followed by drying.

wetting fronts, and the structural changes following wetting and drying (Phogat, 1991). In addition, roots, seeds, insects (Tollner *et al.*, 1987), and pesticide granules (Cheshire *et al.*, 1989) within soils have been successfully detected using an X-ray CAT scanner. In the author's laboratory CAT scanning has also been used successfully in continuous monitoring of the activity of worms and dung beetles under different soil conditions as well as in studying the intensity of root nodule development. The quantitative applications of CAT to soil water studies have, however, been largely limited to statistical assessments of macroporosity distributions before and after complete wetting and drying cycles and to the measurement of water drawdowns in proximity to plant roots in nonswelling soils (Hainsworth and Aylmore, 1986; Aylmore and Hamza, 1990; Hamza and Aylmore, 1992a,b).

C. WATER MOVEMENT TO PLANT ROOTS

The flow of water to plant roots is part of an overall catenary process of water transport from the soil through the plant and into the atmosphere. It is a predominantly passive process whereby water moves in response to gradients in its total water potential. Van der Honert (1948) applied an analog of Ohm's Law to the steady-state transpirational flux, and although he did not examine water movement through the soil to the root surface, this can be easily incorporated because the whole pathway from soil to atmosphere forms a thermodynamic continuum (Slatyer, 1967).

Consequently, the pathway of water flow can be conveniently represented by a series of resistances: the flux of water (F) from the soil to the plant and out into the atmosphere under steady-state conditions is given by the gradient in water potential through the soil/plant/atmosphere continuum divided by the total resistance. Thus

$$F = (\Psi_s - \Psi_1)/R_t \quad (14)$$

where Ψ_s is the average soil water potential, Ψ_1 is the average leaf water potential, and R_t is the total resistance to water flow. Thus as a first approximation, R_t can be assumed to be the sum of the soil and plant resistances in series,

$$R_t = R_p + R_s \quad (15)$$

with the soil resistance R_s and the plant resistance R_p being defined by

$$R_s = \Psi_s - \Psi_o/F \quad (16)$$

and

$$R_p = \Psi_o - \Psi_1/F \quad (17)$$

respectively, in which Ψ_o is the average water potential at the outside surface of the root.

In recent years numerous models aimed at a quantitative formulation and prediction of the processes involved in the movement of soil water and its extraction by plant roots have been developed (Hillel, 1982). Not only do these models differ in aim and level of detail, but also in approach. Two alternative approaches have generally been taken in modeling water uptake by plant roots. The first can be described as the microscale or single-root approach based on the radial flow of water to a cylindrical sink. Solutions to this approach have been attempted both by analytical means (Gardner, 1960; Cowan, 1965), usually requiring restrictive assumptions (Hillel, 1982), and by numerical means (Molz and Remson, 1970; Hillel *et al.*, 1975). However, such models have differed widely in their quantitative prediction of water extraction. Thus, as pointed out by Hillel (1982), there are numerous theoretical models, lacking in consensus, which remain largely untested and hence unproved. It has become easier to formulate than to validate models of water extraction by plant roots (Belmans *et al.*, 1979).

There has, in particular, been considerable controversy as to the relative magnitudes of the soil and plant resistances (Newman, 1969a,b; So *et al.*, 1976, 1978; Reicosky and Ritchie, 1976). When soil moisture is at field capacity, the influence of soil resistance on water uptake by the plant is likely to be small. As soil moisture approaches the wilting point, the

influence of soil resistance increases and undoubtedly becomes limiting (Passioura, 1980). However, the extent of its influence between these two points remains a matter of considerable controversy. Some workers (e.g., Carbon, 1973) have argued that the conductivity of soil to water is frequently so small that the transport of water to the plant root may be limited, even though there may be considerable available water left in the soil. Others (e.g., Newman, 1969a,b; Lawlor, 1972) have argued that the properties of the plant and its aerial environment dominate water uptake unless the soil is so dry that there is virtually no water left. Still others (Herkekrath *et al.*, 1977) have suggested that, under some conditions, neither soil nor plant resistance controls uptake, but that the resistance to water flow from soil to plant at the root/soil interface is the controlling factor.

Because of the difficulties encountered with bulk density changes associated with swelling soils, direct studies of soil water extraction by plant roots using CAT have so far been limited to measurements of drawdowns in essentially nonswelling soils. Hainsworth and Aylmore (1983, 1986, 1989) measured the drawdowns in soil water content associated with single radish roots in a nonswelling 15% kaolinite clay and 85% sand mixture, providing the first detailed and repetitive observations of this type. Uptake of water along the radish roots was clearly shown to be nonuniform, with the plant sequentially removing water from the top to the bottom of the root as soil hydraulic resistance became a major limiting factor in the upper layers, even at the high soil water potential used (Hainsworth and Aylmore, 1989). Comparisons between the experimentally determined drawdowns and those predicted by Cowan's (1965) analytical model indicated that such an approach was unlikely to provide a satisfactory description of drawdowns due to the restrictive assumptions required for their solution. Although the numerical model of Hillel *et al.* (1975) provided a reasonable approximation to the position and shape of the measured drawdowns, significant improvements in the physical concepts on which these are based are still clearly required.

Subsequently, Aylmore and Hamza (1990) and Hamza and Aylmore (1991, 1992a,b) used a combination of CAT scanning and ion-specific microelectrode techniques to measure concomitantly the spatial distribution of soil water content and Na^+ ion concentrations in close proximity to lupine and radish plant roots. Figures 19 and 20 illustrate the detail and accuracy with which the CAT technique was able to resolve the changes in drawdown at different depths along the roots resulting from differences in evaporative demand and electrolyte concentration, over periods up to 8 hr from commencement of transpiration. These studies demonstrated clearly the interrelations between the important parameters within the soil/plant

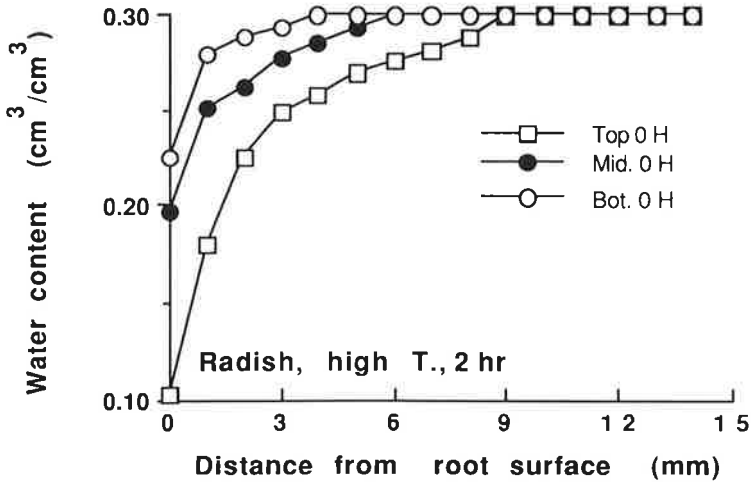


Figure 19. Water drawdowns near top, middle, and bottom sections of single radish roots after 2 hr of transpiration (T) measured by CAT scanning. (After Hamza and Aylmore, 1992a.)

system, such as matric, osmotic, and leaf water potentials. Water uptake was uniform along the length of the essentially constant-diameter lupine roots but decreased along the tapering radish roots as the diameter and hence the surface area per unit length of the roots decreased. The accumulation of Na^+ at the root surfaces of both plants increased gradually with time in a near linear fashion and was slightly higher under the higher transpiration demand. These increases were not exponential, as would be expected with nonabsorption by the roots (Passioura, 1963), and this was considered to be due to back-diffusion at the relatively high water contents used. Both the potential difference and the hydrostatic pressure difference between the roots and the leaves were observed to be linear functions of the transpiration rate, implying that both plant roots acted as near-perfect osmometers under the conditions of the experiments. Plant resistances were constant with time of transpiration and increased with increasing Na^+ in the treatments. Soil resistances between the root surface and bulk soil increased as the water content decreased, remaining lower at the higher solute concentrations due to the lower extraction rates. At the high water potentials used, plant resistances were always substantially higher than corresponding soil resistances. However, in these studies the minimum soil water potential reached was -140 kPa and major questions remain to be answered as to how the relations between the parameters measure change

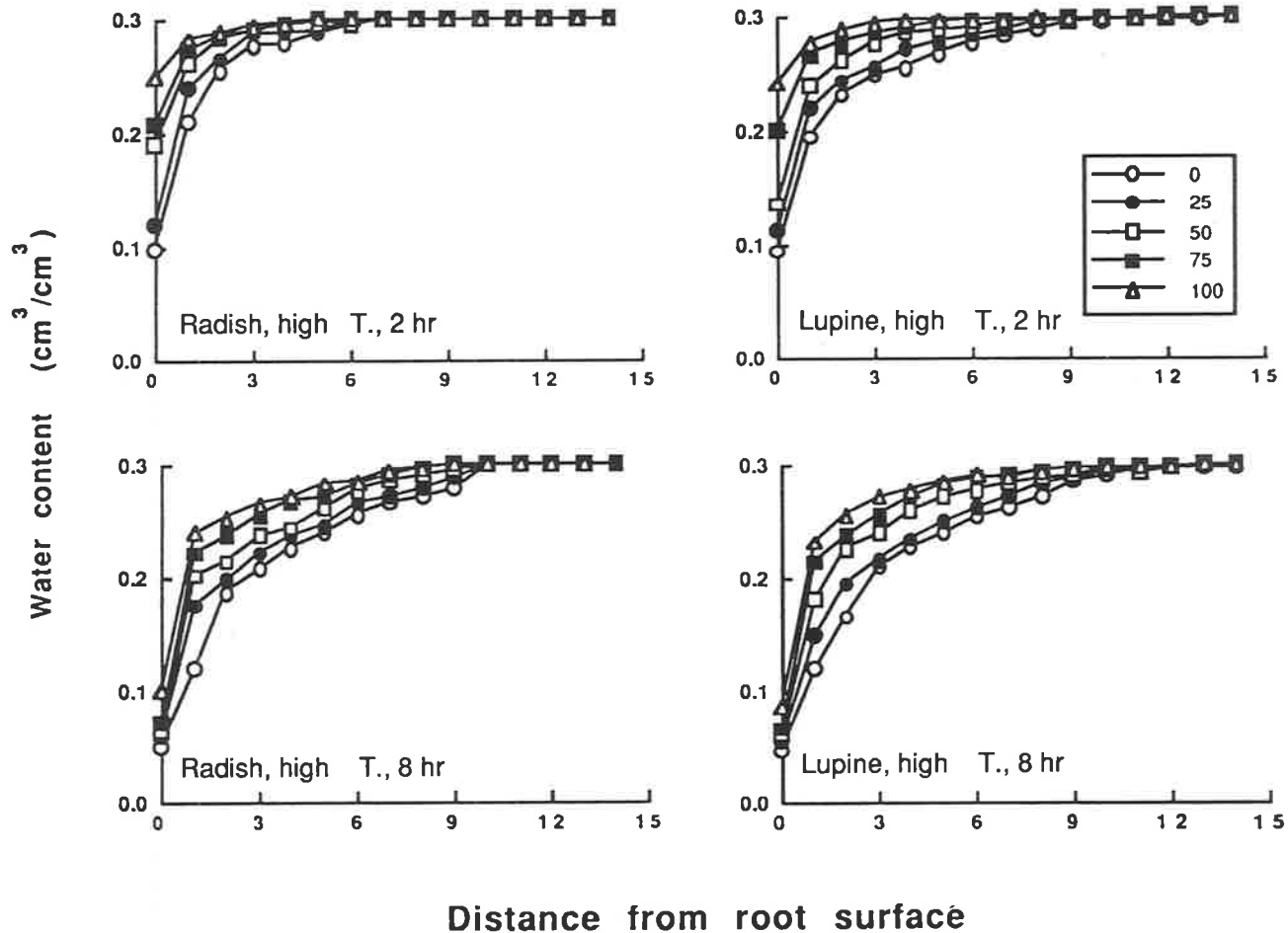


Figure 20. Effect of Na⁺ concentration on water drawdowns near single radish and lupine roots after 2 hr of transpiration measured by CAT scanning. (After Hamza and Aylmore, 1992a.)

as the soil water diffusivity becomes a more limiting factor in the transpiration process. In drier conditions, back-diffusion would be reduced and the effect of solute accumulation at the root surface would be enhanced.

The alternative approach to modeling water uptake is the macroscale or whole-root system approach in which the soil/root system is assumed to be a continuum and water movement is assumed to be essentially a one-dimensional flow (e.g., Ogata *et al.*, 1960; Molz and Remson, 1970, 1971; Nimah and Hanks, 1973; Hillel *et al.*, 1975). Absorption of water by the root is treated as a sink term that is distributed in a certain pattern throughout the soil. The major disadvantage of the macroscopic approach in understanding mechanisms is that it is based on spatial averaging of soil water content or potential and thus does not allow quantitative description of the magnitude of the gradients from bulk soil to individual plant roots. CAT scanning has the power to overcome these limitations by providing detailed volume distributions of water content and potential throughout a complete plant root system and by allowing the efficiency of different parts of the root system in extracting water and interaction between adjacent roots to be examined. Unfortunately, attempts in this direction (L. A. G. Aylmore and P. J. Gregory, unpublished observations; J. B. Reid, R. D. Schuller, and L. A. G. Aylmore, unpublished observations) have, as yet, been largely confounded by difficulties in obtaining uniform packing, in compensating for variations in soil bulk density, and in the accuracy of repositioning of the column in the scanner.

VI. NUCLEAR MAGNETIC RESONANCE IMAGING

An alternative approach to studying soil water extraction by plant roots has involved the use of proton (^1H) nuclear magnetic resonance (NMR) computerized microimaging (Woods *et al.*, 1989). As with X-ray CAT scanning, this technique stems from recent rapid advances in medical uses of NMR imaging for clinical diagnosis and research (Wehrli *et al.*, 1988). NMR microimaging utilizes the interactions of the magnetic moments of some nuclei (e.g., protons) with a strong magnetic field. These interactions can be perturbed by radio waves. In a uniform magnetic field all similar protons resonate at the same frequency. If, however, a field gradient is applied, spatially different protons resonate at different frequencies. When three orthogonal gradients are applied, analysis of the different frequencies can be used to generate a proton density map or image. By changing the three gradients it is possible to control variables such as slice position, slice

thickness, and resolution. If the principal source of hydrogen protons is from water, then the hydrogen proton concentration can be correlated with water content. By using different methods of generating the image, differences in the nature of the protons can be accentuated, e.g., the mobile proton density, relaxation time, or magnetic susceptibility. The images are produced by protons with motional correlation times faster than about 10^{-8} sec. Computed tomography can be used to reconstruct a slice of the spatial distribution of water content with resolution as low as $50 \times 50 \mu\text{m}$ with a slice thickness of 1.25 mm (Johnson *et al.*, 1986; Woods *et al.*, 1989; Wehrli *et al.*, 1988).

NMR imaging has been successfully used in the nondestructive measurement of water content in plants (Bottomley *et al.*, 1986; Brown *et al.*, 1986; Omasa *et al.*, 1985; Williamson *et al.*, 1992). Bottomley *et al.* (1986) used a spatial resolution of 0.6 mm with an unidentified slice definition to observe the movement of a dilute solution of CuSO_4 into and through roots of *Vicia faba*. Brown *et al.* (1986) were able to differentiate anatomical regions of the *Pelargonium hortorum* roots with a spatial resolution of $0.1 \times 0.1 \times 1.2$ mm. Omasa *et al.* (1985) used NMR imaging with a spatial resolution of 2 mm to image root seedlings and show changes in water content in the seedlings, and Williamson *et al.* (1992) used NMR for noninvasive histological studies of ripening red raspberry fruits.

However, Anderson and Gantzer (1989), in comparing results obtained by X-ray CT with those obtained by NMR imaging, were unable to obtain images of the soil cores with NMR. They attributed their failure to the limited range in settings of the pulse repetition time and the spin-echo time on the commercial magnetic resonance imaging (MRI) unit used in the study. Paetzold *et al.* (1985, 1987; Paetzold, 1986) used NMR spectroscopy to measure the water content of bulk soil, but not in specific regions. More recently, McFall *et al.* (1991), by using a series of reference tubes (sand phantoms) filled with acid-washed sand at various water contents to provide a rapid reference calibration curve, were able to monitor water uptake by loblolly pine seedlings from a fine sand and to compare qualitatively the relative efficiencies of fine, lateral, and taproots in water uptake.

Naturally occurring soil materials, both organic and inorganic, are generally poor specimens for direct NMR study because line broadening due to chemical heterogeneity severely reduces resolution and cannot be removed by magic-angle spinning (MAS) or technologically accessible field strengths (Bleam, 1991). In addition, major difficulties arise in quantitatively measuring water which is physically bound within the soil matrix. Hence the value of this technique is likely to be limited in its usefulness for studying soil/plant/water relations.

VII. DUAL-ENERGY SCANNING

A major limitation of the use of single-energy X- or γ -ray CAT scanning systems in studies involving measurements of the spatial distribution of water content in soils has been the necessary assumption of uniform or constant bulk density. Because the attenuation is a function of both the bulk density and the water content of the soil, an accurate determination of water content in soils is not possible when changes in bulk density occur during experiments (Petrovic *et al.*, 1982; Hainsworth and Aylmore, 1983; Anderson *et al.*, 1988; Phogat and Aylmore, 1989). Even in effectively nonswelling soils the difficulties in obtaining uniformly packed soil columns pose problems in applying Eq. (12) to monitor water contents near plant roots, because this requires the exact superposition of wet and dry scans. Any redistribution of soil as a result of wetting will also degrade the accuracy of water content determination.

To monitor changes in the spatial distribution of bulk density and water content in situations in which the bulk density of the soil changes due to swelling, shrinking, or redistribution on addition or removal of water, independent estimates of attenuation associated with both bulk density and water content are required. This can only be obtained by the simultaneous use of two sources of different energies.

A. THEORY OF DUAL-ENERGY SCANNING

For two γ -ray energies the attenuation equations for Eq. (12) may be written as

$$\mu_{\text{wet a}} = \mu_{\text{sa}}\rho_s + \mu_{\text{wa}}\theta_v \quad (18)$$

$$\mu_{\text{wet b}} = \mu_{\text{sb}}\rho_s + \mu_{\text{wb}}\theta_v \quad (19)$$

where subscript "a" refers to the low-energy radiation and subscript "b" refers to the high-energy radiation. Thus μ_{wa} , μ_{wb} , μ_{sa} , and μ_{sb} are the mass attenuation coefficients for water and soil solids, respectively.

Equations (18) and (19) can be solved simultaneously to give

$$\rho_s = [(\mu_{\text{wb}}\mu_{\text{wet a}}) - (\mu_{\text{wa}}\mu_{\text{wet b}})] / [(\mu_{\text{wb}}\mu_{\text{sa}}) - (\mu_{\text{sb}}\mu_{\text{wa}})] \quad (20)$$

$$\theta_v = [(\mu_{\text{sb}}\mu_{\text{wet a}}) - (\mu_{\text{sa}}\mu_{\text{wet b}})] / [(\mu_{\text{sb}}\mu_{\text{wa}}) - (\mu_{\text{wb}}\mu_{\text{sa}})] \quad (21)$$

Thus, ρ_s and θ_v for an individual pixel can be calculated by scanning the wet soil column with both radiation sources at a fixed position.

B. CHOICE OF SOURCES

Although the average energy of X-radiation can be adjusted in some commercially available medical systems, the range is usually relatively narrow and the polychromatic nature of the beams would greatly complicate the application of Eqs. (20) and (21). A combination of ^{137}Cs and ^{241}Am sources has most commonly been used in conventional dual-source γ scanning because of the 10-fold difference in γ -ray energy (662 and 59.6 keV, respectively) and the long half-lives involved (Corey *et al.*, 1971; Gardner *et al.*, 1972; Nofziger and Swartzendruber, 1974). However, both the time required to complete successfully a CAT scan and the precision obtained depend on the transmission intensity and hence count rate. γ -Ray sources generally emit much smaller photon fluxes than do X-ray sources. Whereas high-strength ^{137}Cs sources are readily available, the beam strength obtainable from ^{241}Am has a practical limit because of self-absorption (Miller, 1955). Scan times required with this source are not sufficiently rapid to follow the rapid changes in soil θ_v , which may be associated with, for example, water extraction by plant roots or water infiltration and redistribution in the soil profile. Clearly the minimum scanning time, commensurate with adequate precision, will be generally desirable and will be particularly necessary in dual-source CAT scanning.

Hainsworth and Aylmore (1988) suggested the use of ^{169}Yb as an alternative source to ^{241}Am because this provides a similar energy level (63.1 keV) and attenuation coefficient for water (0.176 cm^{-1}), but emits much higher photon outputs (more than 20 times) at high activities (e.g., 1.0 to 2.0 Ci). The major disadvantage of the ^{169}Yb source is its relatively short half-life of 31 days, resulting in a working life of approximately 2 months.

C. APPLICATION OF CAT TO DUAL-ENERGY SCANNING

The feasibility of applying the CAT scanning procedure to dual-source γ attenuation to enable simultaneous measurements of the spatial distributions of bulk density (ρ_s) and water content (θ_v) in swelling soils was examined by Phogat *et al.* (1991). The values of mean water content for slices of both swelling and nonswelling soils determined by the dual-source (^{137}Cs and ^{169}Yb) γ CAT scanning technique showed excellent agreement ($R^2 = 0.991$) with the values obtained gravimetrically (but expressed volumetrically) for water contents from 0 to $0.55\text{ cm}^3/\text{cm}^3$ (Fig. 21). The differences in water content fell within the range $\pm 0.024\text{ cm}^3/\text{cm}^3$. Similar agreement ($R^2 = 0.995$) was obtained between mean bulk density values obtained by the two methods, with a variation in the two determinations of

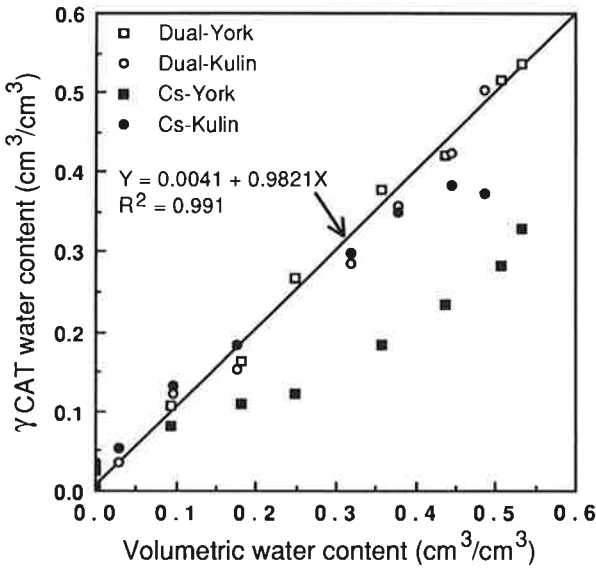


Figure 21. Relationships between volumetric water content and water content determined by dual- and single-energy γ computerized axial tomography scanning for soils from Kulin and York, Western Australia. (After Phogat *et al.*, 1991.)

approximately $\pm 0.015 \text{ cm}^3/\text{cm}^3$. Use of a single source (^{137}Cs) markedly underestimated soil water content particularly in a structurally unstable soil (Fig. 21). The results for the single ^{137}Cs source scanning of Kulin and York soils in Figs. 14B and 21 illustrate the effects of bulk density changes during wetting on the attenuation coefficient measurement. The kaolinite-dominated Kulin soil exhibits some swelling, leading to a lower estimate of the mass attenuation coefficient for water (Fig. 14B). The smectite-dominated York soil swells substantially on wetting, reducing the effective bulk density and leading to a marked underestimation of water content by the single γ technique.

However, the primary objective of the CAT technique is not to measure average bulk density and water content but to reveal the spatial distributions of these quantities. The results of Phogat *et al.* (1991) demonstrated that, using dual-source γ CAT scanning, it is possible to measure the spatial distributions of θ_v and ρ_s in soils simultaneously and nondestructively with a satisfactory level of precision. Unfortunately, despite the enhanced output from the ^{169}Yb source, the accumulation of statistical errors arising from the random nature of radioactive emissions still necessitated excessively large counting times to provide acceptable accuracy. The height of

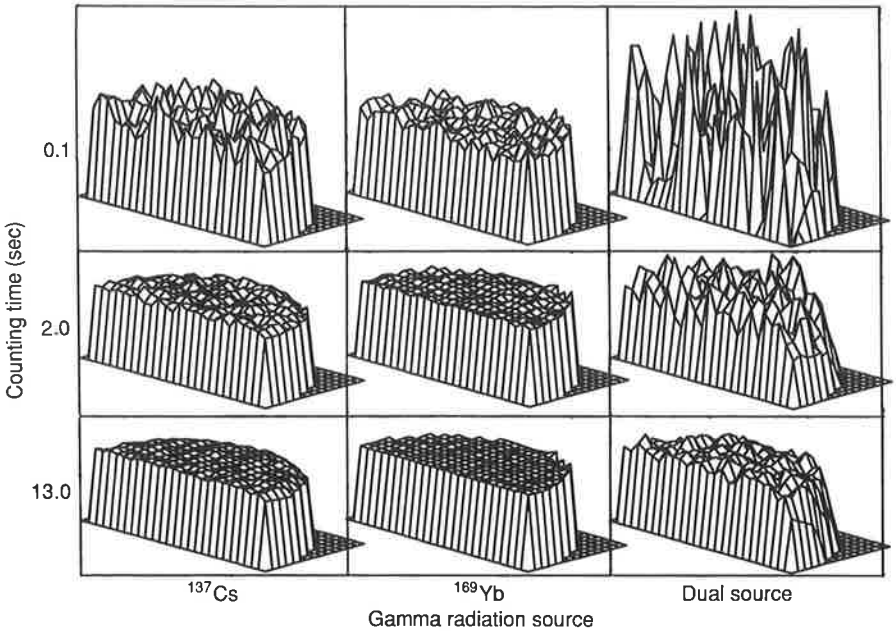


Figure 22. Reconstructed half-slice three-dimensional computerized axial tomography scanning images showing the spatial distribution of water content in slices of a uniform field of water scanned with ^{137}Cs and ^{169}Yb at different counting times and calculated for both single ^{137}Cs and ^{169}Yb sources as well as for the dual- γ -source CAT scanning procedure. (After Phogat *et al.*, 1991.)

the surface in Fig. 22 represents θ_v for each pixel in a slice through a uniform field of water, scanned with ^{137}Cs and ^{169}Yb and calculated using Eq. (20) with counting times of 0.1, 2.0, and 13 sec. These images illustrate that as the counting time is increased, the variation in pixel θ_v decreases and, as a result, the surface of the images becomes more uniform for all three methods. The higher photon output of the ^{169}Yb and the fact that the average attenuation from ^{169}Yb is greater than that from ^{137}Cs reduces the relative error (the absolute error in attenuation being roughly the same) and explains the greater uniformity of the Yb scans compared to the Cs scans. At a counting time of 13 sec, ^{137}Cs gave a standard deviation for θ_v for pixels of $0.016 \text{ cm}^3/\text{cm}^3$ whereas the corresponding value for the ^{169}Yb scan was $\pm 0.007 \text{ cm}^3/\text{cm}^3$. When the scan data of both the sources were used in Eq. (21), it yielded a standard deviation for θ_v for pixels of $0.073 \text{ cm}^3/\text{cm}^3$. This variation in pixel θ_v using both sources is high in spite of the very low values for scans of the individual sources (^{137}Cs and ^{169}Yb). This multiplicative propagation of errors is most evident when, due to

random emissions, a particular pixel, estimated to have a low attenuation using ^{137}Cs , is estimated to have a high attenuation using ^{169}Yb , or vice versa. As a result, small variations in the Cs and Yb scans can give rise to large and unacceptable variations when Eqs. (20) and (21) are applied. Some 169 sec for an individual ray sum and, hence 112 hr to complete a dual-source scan were required to achieve average standard deviation values of pixel water content of the order of $0.025 \text{ cm}^3/\text{cm}^3$ for a uniform field of water. Such large count times limit the equipment used to the study of steady-state or only slowly changing systems.

VIII. RECENT AND FUTURE DEVELOPMENTS

Current medical X-ray CT systems are designed for low-radiation dosage and are high speed to freeze the motion, resulting in only moderate spatial and contrast resolution. In contrast, industrial CT systems designed for object size/weight/density flexibility and high sensitivity, and not restricted by object motion or radiation dose level, have recently been developed [e.g., at Advanced Research and Applications Corporation (ARACOR), Sunnyvale, California, and Surrey Medical Imaging Systems (SMIS), Surrey, England]. These include systems capable of inspecting objects up to 2.4 m in diameter by 5 m long and weighing up to 49,500 kg. In contrast, inspection requirements in the advanced materials, electronics, and printed circuit-board industries have also resulted in the development of X-ray CT systems that provide $25\text{-}\mu\text{m}$ spatial resolution for such objects (ARACOR). Similar work is in progress at EMBRAPA (Brazil) to improve resolution capabilities to $1 \mu\text{m}$ (S. Crestana, personal communication, 1991). Future developments may also include CT systems using backscatter radiation from the object or emission computed tomography (where the decay of *in situ* radioactive isotopes produces γ -rays) to form the image, thus facilitating the measurements in inaccessible regions.

Improved image and data analysis software for the γ CAT scanning system at the University of Western Australia (Schuller and Aylmore, 1993) allows two- and three-dimensional visualization and quantitative analysis of scan data not offered on typical medical scanners. This software permits a three-dimensional image to be constructed from multiple contiguous scans, which can then be viewed from any angle and distance, sectioned and sliced, or stripped away by subtractive imaging using 32 colors or shades to represent variable attenuation ranges. Figure 23 illustrates the way in which both higher attenuating compacted soil layers or less atten-

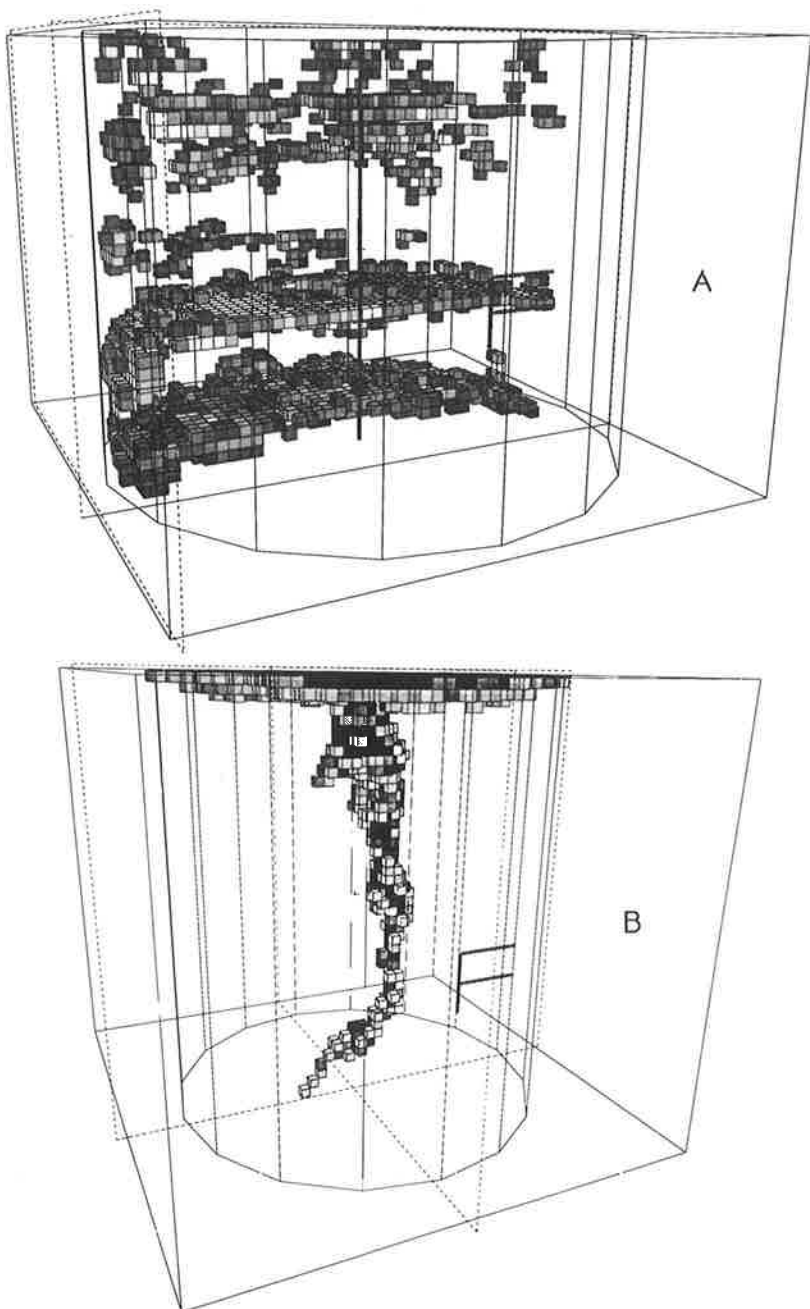


Figure 23. Three-dimensional image reconstructions obtained by subtractive imaging. (A) Three high-density layers in soil core. Note curvature at edges caused by entry of coring tube into profile. (B) Lupine root in soil column.

uating root material can be clearly defined in a soil column. The distortion of the soil layers by the passage of the corer is clearly shown in Fig. 23A.

IX. SUMMARY AND CONCLUSIONS

Application of computer-assisted tomography to X- and γ -ray attenuation measurements has provided an exciting new method for nondestructive imaging within a solid matrix, with considerable potential for studying soil behavior and soil/plant/water relations in space and time. However, the information provided is currently limited by the capabilities of the instrumentation available.

Commercially available medical CT scanners have proved useful for visual studies of soil structure, the advancement and stability of wetting fronts, and the structural changes following wetting and drying. However, the usefulness of these systems and of single-source γ CAT scanning systems in studying soil systems is invariably restricted by their inability to distinguish between changes in water content and bulk density in swelling and shrinking soils and by the associated physical relocation of soil elements that can occur. Thus their quantitative applications have been limited to the measurement of water drawdowns in proximity to plant roots in nonswelling soils and statistical assessments of macroporosity distributions before and after complete wetting and drying cycles. Though fast in operation, the quantitative usefulness of X-ray scanners is limited by the polychromatic nature of the beam and the process known as "beam hardening." Furthermore, the proprietary nature of these commercial systems usually makes software modification or extensions impossible.

In view of their substantially lower cost and superior quantitative characteristics, γ -ray tomographic systems are likely to prove ultimately the most useful for soil and plant studies. Simultaneous measurement of the spatial distributions of water content and bulk density in soils that exhibit swelling and dispersion has been shown to be feasible using CAT applied to dual-source (^{137}Cs and ^{169}Yb) γ -ray attenuation. However, the relatively low photon emission from γ sources and the propagation of statistical errors necessitate large counting times to provide acceptable accuracy and restrict the use of present γ systems to the study of steady-state or only slowly changing systems. Realization of the full potential of this technique will require substantial improvements in scanning geometry and counting electronics to improve the speed and precision of measurements. Incorporation of fan beam geometry together with improved multiple-beam detection systems (MacCuaig *et al.*, 1986) will reduce scanning times by an

order of magnitude, but will inevitably increase overall instrument costs. Improved dimensional resolution will enhance structural definition in soil systems. However, current pixel dimensions of the order of 0.5 to 1 mm are quite adequate to allow meaningful resolution of many of the controversies associated with water extraction by plant roots. Reduction in scanning times to allow more rapid monitoring of changes in soil water content would seem a priority for soil and plant studies. Improved image and data analysis software allowing two- and three-dimensional visualization and quantitative analysis of scan data will also greatly enhance these activities.

ACKNOWLEDGMENTS

Much of my work in this area was funded by the Australian Research Grants Committee whose support is gratefully acknowledged. I am grateful to my colleagues in the Soil Physics Section of the Department of Soil Science and Plant Nutrition, The University of Western Australia, in particular Mr. R. D. Schuller, Dr. M. A. Hamza, and Dr. V. K. Phogat, for their helpful comments on the manuscript.

REFERENCES

- Anderson, S. H., and Gantzer, C. J. 1989. Determination of soil water content by X-ray computed tomography and magnetic resonance imaging. *Irrig. Sci.* **10**, 63-71.
- Anderson, S. H., Gantzer, C. J., Boone, J. M., and Tully, R. J. 1988. Rapid nondestructive bulk density and soil water content determination by computed tomography. *Soil Sci. Soc. Am. J.* **52**, 35-40.
- Anderson, S. H., Peyton, R. L., and Gantzer, C. J. 1990. Evaluation of constructed and natural soil macropores using X-ray computed tomography. *Geoderma* **46**, 13-29.
- Aylmore, L. A. G., and Hamza, M. 1990. Water and solute movement to plant roots. *Trans. Int. Congr. Soil Sci.*, 14th II, 124-129.
- Belmans, C. J., Feyen, J., and Hillel, D. 1979. An attempt at experimental validation of macroscopic-scale models of soil moisture extraction by roots. *Soil Sci.* **127**, 174-186.
- Bleam, W. F. 1991. Soil science applications of nuclear magnetic resonance spectroscopy. *Adv. Agron.* **46**, 91-155.
- Bottomley, P. A., Rogers, H. H., and Foster, T. H. 1986. NMR imaging shows water distribution and transport in plant root systems *in situ*. *Proc. Natl. Acad. Sci. U.S.A.* **83**, 87-89.
- Bracewell, R. M. 1956. Strip integration in radio astronomy. *Aust. J. Phys.* **9**, 198-217.
- Brooks, R. A., and Di Chiro, G. 1975. Theory of image reconstruction in computed tomography. *Radiology (Easton, Pa.)* **117**, 561-572.
- Brooks, R. A., and Di Chiro, G. 1976. Principles of computer assisted tomography (CAT) in radiographic and radioisotopic imaging. *Phys. Med. Biol.* **21**, 689-732.
- Brown, J. M., Johnson, G. A., and Kramer, P. J. 1986. *In vitro* magnetic resonance micros-

- copy of changing water content in *Pelargonium hortorum* roots. *Plant Physiol.* **82**, 1158–1160.
- Brown, J. M., Fonteno, W. C., Cassel, D. K., and Johnson, G. A. 1987. Computed tomographic analyses of water distribution in three porous foam media. *Soil Sci. Soc. Am. J.* **51**, 1121–1125.
- Budinger, T. F., and Gullberg, G. T. 1974. Three dimensional reconstruction in nuclear medicine emission imaging. *IEEE Trans. Nucl. Sci.* **NS-21**, 2–20.
- Carbon, B. A. 1973. Water stress in plants on a coarse soil. *Aust. J. Soil Res.* **11**, 33–42.
- Chase, R. C., and Stein, J. A. 1978. An improved imaged algorithm for CT scanners. *Med. Phys.* **5**, 497–499.
- Cheshire, J. M., Jr., Tollner, E. W., Verma, B. D., and Blum, W. M. 1989. Radiographic detection of soil-incorporated granular pesticides and impacts of application methods on wireworm management. *Trans. ASAE* **32**, 415–423.
- Coppola, M., and Reiniger, P. 1974. Influence of the chemical composition on the gamma-ray attenuation by soils. *Soil Sci.* **117**, 331–335.
- Corey, J. C., Peterson, S. F., and Wakat, M. A. 1971. Measurement of attenuation of Cs-137 and Am-241 gamma rays for soil density and water content determinations. *Soil Sci. Soc. Am. Proc.* **35**, 215–219.
- Cormack, A. M. 1963. Representation of a function by its line integrals, with some radiological applications. *J. Appl. Phys.* **34**, 2722–2727.
- Cowan, I. R. 1965. Transport of water in the soil–plant atmosphere system. *J. Appl. Ecol.* **2**, 221–239.
- Crestana, S., Mascarenhas, S., and Pozzi-Mucelli, R. S. 1985. Static and dynamic three-dimensional studies of water in soil using computed tomographic scanning. *Soil Sci.* **140**, 326–332.
- Crestana, S., Cesareo, R., and Mascarenhas, S. 1986. Using a computer assisted tomography miniscanner in soil science. *Soil Sci.* **142**, 56–61.
- Cullity, B. D. 1978. "Elements of X-Ray Diffraction." Addison-Wesley, Reading, Massachusetts.
- Davis, J. R., Morgan, M. J., Wells, P., Shadbolt, P., and Suendermann, B. 1986. X-Ray computed tomography. 1: A non-medical perspective. *Aust. Phys.* **23**, 245–247.
- Dunham, R. J., and Nye, P. H. 1973. The influence of soil water content on the uptake of ions by roots. I. Soil water content gradients near a plane of onion roots. *J. Appl. Ecol.* **10**, 585–598.
- Gardner, W. R. 1960. Dynamic aspects of water availability to plants. *Soil Sci.* **89**, 63–73.
- Gardner, W. H., Campbell, G. S., and Calissendorff, C. 1972. Systematic and random errors in dual gamma energy soil bulk density and water content measurements. *Soil Sci. Soc. Am. Proc.* **36**, 393–398.
- Gilbert, P. F. C. 1972. Iterative methods for the three-dimensional reconstruction of an object from projections. *J. Theor. Biol.* **36**, 105–117.
- Gilboy, W. B. 1984. X- and gamma-ray tomography in NDE applications. *Nucl. Instr. Methods* **221**, 193–200.
- Goitein, M. 1972. Three dimensional density reconstruction from a series of two dimensional projections. *Nucl. Instr. Methods* **101**, 509–518.
- Gordon, R., Bender, R., and Herman, G. T. 1970. Algebraic reconstruction techniques (ART) for three-dimensional electron microscopy and X-ray photography. *J. Theor. Biol.* **29**, 471–481.
- Grevers, M. C. J., De Jong, E., and St. Arnaud, R. J. 1989. The characterization of soil macroporosity with CT scanning. *Can. J. Soil Sci.* **69**, 629–637.

- Groenevelt, P. H., De Swart, J. G., and Cisler, J. 1969. Water content measurement with 60 keV gamma-ray attenuation. *Bull. Int. Am. Sci. Hydrol.* **14**, 67–78.
- Gurr, C. G. 1962. Use of gamma rays in measuring water content and permeability in unsaturated columns of soils. *Soil Sci.* **94**, 224–229.
- Hainsworth, J. M., and Aylmore, L. A. G. 1983. The use of computer assisted tomography to determine spatial distribution of soil water content. *Aust. J. Soil Res.* **21**, 435–443.
- Hainsworth, J. M., and Aylmore, L. A. G. 1986. Water extraction by single plant roots. *Soil Sci. Soc. Am. J.* **50**, 841–848.
- Hainsworth, J. M., and Aylmore, L. A. G. 1988. Application of computer assisted tomography (CAT) to gamma attenuation measurement of soil water content. *Aust. J. Soil Res.* **26**, 105–110.
- Hainsworth, J. M., and Aylmore, L. A. G. 1989. Non-uniform soil water extraction by plant roots. *Plant Soil* **113**, 121–124.
- Hamza, M., and Aylmore, L. A. G. 1991. Liquid ion exchanger microelectrodes used to study soil solute concentrations near plant roots. *Soil Sci. Soc. Am. J.* **55**, 954–958.
- Hamza, M., and Aylmore, L. A. G. 1992a. Soil solute concentration and water uptake by single lupin and radish plant roots. I. Water extraction and solute accumulation. *Plant Soil* **145**, 187–196.
- Hamza, M., and Aylmore, L. A. G. 1992b. Soil solute concentration and water uptake by single lupin and radish plant roots. II. Driving forces and resistances. *Plant Soil* **145**, 197–205.
- Herkelrath, W. N., Miller, E. E., and Gardner, W. R. 1977. Water uptake by plants: II. The root contact model. *Soil Sci. Soc. Am. J.* **41**, 1039–1043.
- Herman, G. T. 1980. "Image Reconstruction from Projections: The Fundamentals of Computed Tomography." Academic Press, New York.
- Hillel, D. 1982. "Applications of Soil Physics." Academic Press, New York.
- Hillel, D., Van Beck, C. G. E. M., and Talpaz, H. 1975. A microscopic-scale model of soil water uptake and salt movement to plant roots. *Soil Sci.* **120**, 385–399.
- Hopkins, F. F., Morgan, I. L., Ellinger, H. D., Klinksiek, R. V., Meyer, G. A., and Thompson, J. N. 1981. Industrial tomography applications. *IEEE Trans. Nucl. Sci.* **NS-28**, 1717–1720.
- Hounsfield, G. N. 1972. "A Method of and Apparatus for Examination of a Body by Radiation Such as X- or Gamma-Radiation," British Patent No. 1283915. British Patent Office, London.
- Jenssen, P. D., and Heyerdahl, P. H. 1988. Soil column descriptions from X-ray computed tomography density images. *Soil Sci.* **146**, 102–107.
- Johnson, G. A., Thompson, M. B., Gewart, S. L., and Hayes, C. E. 1986. Nuclear magnetic resonance imaging at microscopic resolution. *J. Magn. Reson.* **68**, 129–137.
- Kak, A. C., and Slaney, M. 1988. "Principles of Computerized Tomographic Imaging." IEEE Press, New York.
- Lawlor, D. W. 1972. Growth and water use of *Lolium perenne*. I. Water transport. *J. Appl. Ecol.* **9**, 79–98.
- MacCuaig, N., Tajuddin, A. A., and Gilboy, W. B. 1986. Industrial tomography using a position sensitive carbon fibre anode proportional counter. *Nucl. Instr. Methods* **A242**, 620–625.
- McCullough, E. C. 1975. Photon attenuation in computed tomography. *Med. Phys.* **2**, 307–320.
- McFall, J. S., Johnson, G. A., and Kramer, P. J. 1991. Comparative water uptake by roots of different ages in seedlings of loblolly pine (*Pinus taeda* L.). *New Phytol.* **119**, 551–560.

- Miller, D. G. 1955. "Americium-241 as a Photon Source for Gamma Absorptometric Technique," U.S. At. Energy Comm. Rep. HW-39971. Hanford Atomic Products Operation, Richland.
- Molz, F. J. 1981. Models of water transport in the soil-plant system: A review. *Water Resour. Res.* 17, 1245-1260.
- Molz, F. J., and Remson, I. 1970. Extraction-term model of soil moisture use by transpiring plants. *Water Resour. Res.* 6, 1346-1356.
- Molz, F. J., and Remson, I. 1971. Application of an extraction-term model to the study of moisture flow to plant roots. *Agron. J.* 63, 72-77.
- Newman, E. I. 1969a. Resistance to water flow in soil and plant. I. Soil resistance in relation to amount of root: Theoretical estimates. *J. Appl. Ecol.* 6, 1-12.
- Newman, E. I. 1969b. Resistance of water flow in soil and plant. II. A review of experimental evidence on the rhizosphere resistance. *J. Appl. Ecol.* 6, 261-272.
- Newton, T. H., and Potts, D. G. 1981. "Radiology of the Skull and Brain: Technical Aspects of Computed Tomography," Vol. 5, pp. 3853-3917. Mosby, St. Louis, Missouri.
- Nimah, M. N., and Hanks, R. J. 1973. Model for estimating soil water, plant, and atmospheric interrelations: I. Description and sensitivity. *Soil Sci. Soc. Am. J.* 37, 522-527.
- Nobel, P. S. 1974. "Introduction to Biophysical Plant Physiology." Freeman, San Francisco.
- Nofziger, D. L., and Swartzendruber, D. 1974. Material content of binary physical mixtures as measured with a dual-energy beam of gamma rays. *J. Appl. Phys.* 45, 5443-5449.
- Ogata, G., Richards, L. A., and Gardner, W. R. 1960. Transpiration of alfalfa determined from soil water content changes. *Soil Sci.* 89, 179-182.
- Omasa, K., Onoe, M., and Yamada, H. 1985. NMR imaging for measuring root systems and soil water content. *Seibutsu Kankyo Chosetsu* 23, 99-102.
- Onoe, M., Tsao, J. M., Nakamura, H., Kogure, J., Kawamura, H., and Yoshimatsu, M. 1983. Computed tomography for measuring annual rings of a live tree. *Proc. IEEE* 71, 907-908.
- Paetzold, R. F. 1986. NMR instrument for soil moisture ground-truth data collection. *ITC J.* 1, 9-13.
- Paetzold, R. F., Matzkanin, G. A., and De Los Santos, A. 1985. Surface soil water content measurement using pulsed nuclear magnetic resonance techniques. *Soil Sci. Soc. Am. J.* 49, 537-540.
- Paetzold, R. F., De Los Santos, A., and Matzkanin, G. A. 1987. Pulsed nuclear magnetic resonance instrument for soil-water content measurement: Sensor configurations. *Soil Sci. Soc. Am. J.* 51, 287-290.
- Panton, D. M. 1981. Mathematical reconstruction techniques in computed axial tomography. *Math. Sci.* 6, 87-102.
- Passioura, J. B. 1963. A mathematical model for the uptake of ions from the soil solution. *Plant Soil* 18, 225-238.
- Passioura, J. B. 1980. The transport of water from soil to shoot in wheat seedlings. *J. Exp. Bot.* 31, 333-345.
- Passioura, J. B., and Frere, M. H. 1967. Numerical analysis of the convection and diffusion of solutes to roots. *Aust. J. Soil Res.* 5, 149-159.
- Petrovic, A. H., Siebert, J. E., and Lieke, P. E. 1982. Soil bulk density analysis in three dimension by computed tomographic scanning. *Soil Sci. Soc. Am. J.* 46, 445-450.
- Philip, J. R. 1966. Plant water relation—Some physical aspects. *Annu. Rev. Plant Physiol.* 17, 245-268.
- Phogat, V. K., and Aylmore, L. A. G. 1989. Evaluation of soil structure by using computer assisted tomography. *Aust. J. Soil Res.* 27, 313-323.

- Phogat, V. K., and Aylmore, L. A. G. 1993. Computation of hydraulic conductivity of porous media using computer assisted tomography. *Aust. J. Soil Res.* (submitted).
- Phogat, V. K., Aylmore, L. A. G., and Schuller, R. D. 1991. Simultaneous measurement of the spatial distribution of soil water content and bulk density. *Soil Sci. Soc. Am. J.* **55**, 908–915.
- Reicosky, D. C., and Ritchie, J. T. 1976. Relative importance of soil resistance and plant resistance in root water absorption. *Soil Sci. Soc. Am. J.* **40**, 293–297.
- Richards, J. A., Sears, F. W., Wehr, M. R., and Zamansky, M. W. 1960. "Modern University Physics." Addison-Wesley, London.
- Ryhiner, A. H., and Pankow, J. 1969. Soil moisture measurement by the gamma transmission method. *J. Hydrol. (Amsterdam)* **9**, 194–205.
- Sawada, Y., Aylmore, L. A. G., and Hainsworth, J. M. 1989. Development of a soil-water dispersion index (SOWADIN) for testing the effectiveness of soil-wetting agents. *Aust. J. Soil Res.* **27**, 17–26.
- Schuller, R. D., and Aylmore, L. A. G. 1993. Three dimensional image reconstruction from computer assisted tomography applied to gamma attenuation in soil columns. Manuscript in preparation.
- Slatyer, R. O. 1967, "Plant–Water Relationships." Academic Press, New York.
- So, H. B., Aylmore, L. A. G., and Quirk, J. P. 1976. Measurement of water flux in single root system. I. The tensiometer–potometer system. *Plant Soil* **45**, 577–594.
- So, H. B., Aylmore, L. A. G., and Quirk, J. P. 1978. Measurement of water flux in single root system. II. Applications of tensiometer–potometer system. *Plant Soil* **49**, 461–475.
- Tollner, E. W., and Murphy, C. 1991. Factors affecting soil X-ray absorption coefficients with computed tomography. *Trans. ASAE* **34**, 1047–1053.
- Tollner, E. W., and Verma, B. D. 1989. X-Ray CT for quantifying water content at points within a soil body. *Trans. ASAE* **32**, 901–905.
- Tollner, E. W., Verma, B. D., and Cheshire, J. M., Jr. 1987. Observing soil–tool interactions and soil organisms using X-ray computer tomography. *Trans. ASAE* **30**, 1605–1610.
- Van den Honert, T. H. 1948. Water transport in plants as a catenary process. *Discuss. Faraday Soc.* **3**, 146–153.
- Warner, G. S., Nieber, J. L., Moore, I. D., and Geise, R. A. 1989. Characterizing macropores in soil by computed tomography. *Soil Sci. Soc. Am. J.* **53**, 653–660.
- Wehrli, F. W., Shaw, D., and Kneeland, J. B. (eds.). 1988. "Biomedical Magnetic Resonance Imaging, Principles, Methodology and Applications." VCH Publ., New York.
- Williamson, B., Goodman, B. A., and Chudek, J. A. 1992. Nuclear magnetic resonance (NMR) micro-imaging of ripening red raspberry fruits. *New Phytol.* **120**, 21–28.
- Woods, R. T., Hennessy, J. J., Kwok, E., and Hammer, B. E. 1989. NMR microscopy—A new biological tool. *BioTechniques* **7**, 616–622.

Soil and Water Management and Conservation

Retention and Release of Diquat and Paraquat Herbicides in Soils*Rai S. Kookana*^{A,B} and *L. A. G. Aylmore*^A^A Soil Science and Plant Nutrition, The University of Western Australia, W.A. Nedlands, 6009.^B Present address: CRC for Soil and Land Management, PMB No. 2, Glen Osmond, S.A. 5064.*Abstract*

The sorption and desorption behaviour of diquat and paraquat, in the presence of different salt concentrations, has been studied in some Western Australian soils varying in physical and chemical properties. Sorption isotherms were found to be of the 'L' type according to the Giles classification with the data fitting well to the Langmuir equation. The sorption capacities of soils for diquat ranged from very high in clay soil ($146\,400\ \mu\text{mol kg}^{-1}$) to very low in sand ($1765\ \mu\text{mol kg}^{-1}$) and followed the order of clay content in the soils. The clay soil also showed the highest value for the Langmuir coefficient representing bonding energy. The sorption capacities for the herbicides were less than the CEC of the soils. Both the type and content of clay minerals present in soil were important for sorption and subsequent desorption of the dipyrindylum herbicides. An increase in the salt concentration of the soil solution (from 0.005 to 0.05 M CaCl_2) resulted in decreases in sorption capacities for the herbicides ranging from some 17% to 40% in the different soils. Both Ca^{2+} and Na^+ cations competed for the sorption sites with the herbicides, but Na^+ was not as effective as Ca^{2+} . Desorption of the herbicides was also significantly affected by the salt concentrations of the extractant. After five successive extractions with 0.005 M CaCl_2 , the total amounts of equilibrium sorption desorbed from the Bassendean surface soil were 13% and 7% for diquat and paraquat, respectively. The percentages of diquat removed by extractions decreased with increasing clay contents in the soils studied. Desorption of diquat was higher than that of paraquat at all salt concentrations. Hysteresis was evident between sorption and desorption isotherms. As sorption increased, the desorption became easier, indicating that the herbicides were less strongly held. Sorption which occurred in the presence of higher ionic strength solutions of inorganic cations was relatively less susceptible to desorption.

Keywords: diquat, paraquat, sorption, desorption, hysteresis, salt concentration.

Introduction

Pesticides have become an essential part of modern agricultural production systems and their importance is now well recognized. Conservation production systems rely heavily on the use of agro-chemicals as many tillage and cultural practices adopted for pest control have been replaced by the use of pesticides. Consequently, the use of pesticides has increased throughout the world in recent years. In Australia, for example, during the last decade the sale of herbicides jumped from \$50 million to \$367 million between 1978 and 1988. Pesticides, being toxic by design, evoke natural public concern about their possible harmful impact on non-target organisms. If applied according to the recommended procedures

and in appropriate amounts, they are likely to result in little adverse effect on the environment. However, their residues have now been detected in soil, water and air (Cheng 1990). A sound understanding of the behaviour of pesticides in the soil environment is thus imperative to avoid the potential hazard they may pose to the environment. The fate of pesticides in soil is governed largely by their sorption-desorption, degradation, transformation and transport processes. Of these factors, sorption-desorption is the most important as it can influence other processes.

Diquat (1,1'-ethylene-2,2'-dipyridylum dibromide) and paraquat (1,1'-dimethyl-4,4'-dipyridylum dichloride) are extensively used as knockdown herbicides. The area sprayed with Sprayseed[®] (a mixture of paraquat and diquat) in Western Australia alone has increased 25-fold to more than 1 million hectares, since 1978 (Poole 1987). Key reasons for the popularity of these herbicides are their rapid deactivation and non-residual properties in soil (Calderbank and Slade 1976). The divalent cations of these herbicides are readily sorbed from aqueous solutions onto the negatively charged sites at mineral and organic surfaces in soil. Once sorbed, they are strongly retained by soil clays in biologically inactive/unavailable forms which protect them from microbial degradation (Weber and Coble 1968; Riley *et al.* 1976).

These herbicides are toxic to man (oral LD₅₀ for rat, 150–231 mg kg⁻¹) and degrade very slowly in soils. The half-life of paraquat in soil has been reported to be as high as 26 years when applied at a rate five times the sorption capacity of soil (ICI 1984). Furthermore, at lower application rates, degradation could be even slower. Riley *et al.* (1976) noted no loss of paraquat after 4.5 years at low application rates (4–50 mg kg⁻¹) in a number of soils. Osborne and Donohoe (1977) reported that after seven years of repeated applications to a red earth soil from New South Wales, some 50–78% of applied paraquat was recovered. Repeated applications are thus likely to result in a build-up of the herbicide levels in soils.

Desorption of these herbicides from soil is generally difficult; for some soils harsh treatment such as boiling in 18 M sulfuric acid is needed for complete extraction of these compounds (Tucker *et al.* 1967). However, this varies with the type of clay mineral sorbing the herbicides. Weber and Weed (1968) reported that extractions with 1 M BaCl₂ removed 80% of sorbed diquat from kaolinite in contrast to only 5% from montmorillonite clay mineral because of a relatively weaker sorption by the kaolinite. Similarly Weed and Weber (1969) extracted some 70–80% of adsorbed diquat and paraquat from vermiculite clay minerals using dilute (0.005 M) salt solutions. Sorption of these herbicides by organic matter in soils is also considered to be weak. In addition, the nature and concentration of inorganic ions competing with these herbicides for sorption sites affect their release (Best *et al.* 1972). Nevertheless, the release of even small amounts in soil solution can be harmful to crops as these herbicides are non-selective and can be phytotoxic at very low levels (0.01 µg mL⁻¹; Riley *et al.* 1976). There is evidence that agronomic practices such as liming, gypsum application and heavy fertilization can result in significant increases in localized salt concentrations (Isensee and Walsh 1971). Thus it is important to examine the retention and release of these herbicides in the presence of salts in soil solution, particularly in soils showing weaker affinity for the herbicides.

Information on sorption-desorption of these herbicides by Australian soils is not available in the published literature. Weaker sorption and relatively easier desorption is to be expected in many Australian soils, not only because of their low clay and organic matter contents, but also because frequently kaolinite is the dominant clay mineral in highly weathered Australian soils. In this paper we report the sorption and desorption of paraquat and diquat in some Western Australian soils. In particular, both sorption and desorption processes have been examined in the presence of different levels of salt concentrations in the equilibrating solution.

Table 1. Selected properties of the soils

Soil	Class ^A	OM (%)	Clay (%)	Silt (%)	pH ^B	CEC ^C	Surface area (m ² g ⁻¹)	Clay minerals ^D
Bassendean sand								
Surface	Uc1	1.2	1.2	1.5	5.0	2.42	0.36	K
Subsoil	Uc1	0.3	3.0	2.0	6.1	1.23	1.51	K, Go
Cobiac loamy sand	Uc1.2	0.2	13.6	2.5	5.1	3.50	22.48	K, Go, Gi
Gascoyne sandy loam	Um5.2	1.7	15.3	8.3	6.9	24.79	13.39	K, I
Wellesley clay	Ug5.1	4.6	63.7	14.2	5.9	42.96	73.05	K, S

^A Northcote classification.

^B pH in (1:5) 0.01 M CaCl₂.

^C CEC units cmol(+) kg⁻¹.

^D Clay minerals: K, kaolinite; Go, goethite; Gi, gibbsite; I, illite; S, smectite.

Materials and Methods

Soils and Pesticides

Four soils (a sand, a loamy sand, a sandy loam and a clay) differing widely in their physical and chemical properties were used. With the exception of the loamy sand, these soils are under horticulture where repeated applications of pesticides are made every year. The sand, the loamy sand and the clay were collected from the Swan Coastal Plain (McArthur and Bettenay 1960), whereas the sandy loam was collected from the Ord River Irrigation area. The soils were air-dried and passed through a 2 mm sieve. Particle size distributions were measured by the pipette method; organic carbon, by the Walkley-Black method (Nelson and Sommers 1982); cation exchange capacities (CECs) of the soils, by Sr²⁺ saturation at pH 7; and specific surface areas, by applying the BET theory to N₂ sorption at 78 K (Aylmore *et al.* 1970). The physico-chemical properties of the soils are given in Table 1.

Analytically pure paraquat and diquat compounds (>99%) were supplied by ICI Ltd., Australia. These herbicides are non-volatile, highly soluble in water, and are typically used at rates ranging from 0.1 to 1.0 kg ha⁻¹ (active ingredient). Other properties of these compounds have been discussed by Hartley and Kidd (1987).

Sorption-Desorption Experiments

The sorption and desorption isotherms were obtained using a batch method. A series of herbicide concentrations in CaCl₂ solutions (0.005–0.05 M) were prepared. A 10 mL aliquot of each herbicide concentration was equilibrated with 5 g air-dry soil in polypropylene centrifuge tubes by end-to-end shaking for 24 h. Preliminary experiments showed no change in the solution concentrations of the herbicides beyond a 3 h period. The tubes were then centrifuged

at approx. 20 000 *g* for 15 min; the supernatants were carefully removed with the help of a glass syringe and immediately analysed. Desorption was carried out in herbicide-free CaCl_2 solutions. The contents of the centrifuge tubes were weighed to account for the amount of herbicide present in the solution before desorption occurred. After addition of herbicide-free solutions, the tubes were shaken for 24 h, centrifuged, and the herbicide concentrations in the equilibrium solutions were measured.

Herbicide Analysis

A high performance liquid chromatographic (HPLC) method for the analysis of paraquat and diquat (Gill *et al.* 1983) was used. The method is based on reversed phase chromatography, involving an ion-pair mechanism. A reversed phase column (C_{18} , Phase Separation Ltd. U.K.) was preconditioned with heptane sulfonate anions to impart cation exchanger properties to the column. A mobile phase was prepared by mixing orthophosphoric acid (0.2 mol), diethylamine (0.1 mol), sodium heptane sulfonate (0.01 mol), and then diluting to 1 L with methanol (25% V/V) in water.

Flow rate was set at 1 mL min^{-1} on an HPLC pump (ETP-Kortec, Australia). Wavelengths of 309 nm for diquat and 258 nm for paraquat were chosen on a u.v. detector (ETP-Kortec) on the basis of the spectrophotometric scans of the compounds.

Results and Discussion

Sorption

Initially, sorption of only diquat was studied in four soils differing in clay and organic matter contents and other properties (Table 1). It is generally known that diquat and paraquat exhibit very similar sorption behaviour in soils

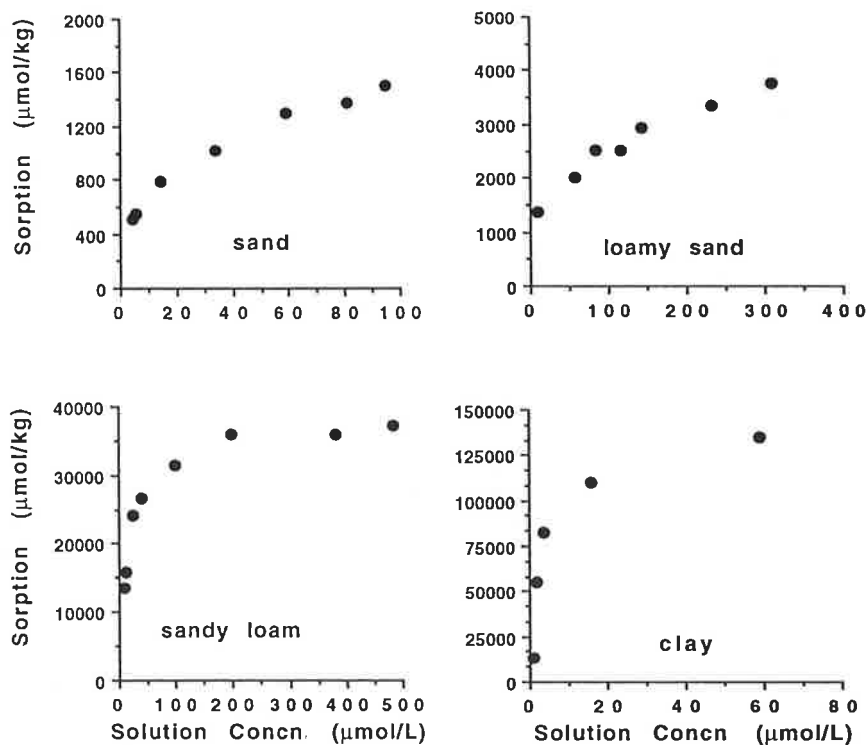


Fig. 1. Sorption isotherms of diquat in soils of different texture.

(Gamar and Mustafa 1975). Therefore the sorption of diquat alone was used to identify the soil with the minimum of sorption capacity for use in more detailed investigations on both the herbicides.

Sorption of diquat in four soils

The sorption isotherms of diquat in the four soils are presented in Fig. 1. Sorption increased sharply with increasing herbicide concentration in solution, so that at low solution concentrations almost all of the herbicide present in solution was sorbed by the soils. The soils could sorb amounts ranging from some $400 \mu\text{mol kg}^{-1}$ in the sand to $10\,000 \mu\text{mol kg}^{-1}$ in clay, while leaving very low concentrations in soil solution. However, with further increases in solution concentration, the sorption increased gradually and finally levelled off. Such sorption isotherms can be classified as 'L' type according to Giles *et al.* (1974).

The sorption data fitted well to the linear form of the Langmuir equation:

$$C/S = 1/Kb + C/K, \quad (1)$$

where C is the equilibrium solution concentration ($\mu\text{mol L}^{-1}$), S is the amount sorbed per unit weight of the sorbent ($\mu\text{mol kg}^{-1}$), K is the sorption maxima ($\mu\text{mol kg}^{-1}$) and b is a constant related to the bonding energy of sorbent for sorbate. Several other workers have also reported that sorption of these herbicides follows the Langmuir equation. For example, sorption of paraquat and diquat in eight arid zone soils (Gamar and Mustafa 1975) and of paraquat in acid tropical soils of Nigeria (Juo and Oginni 1978) obeyed the Langmuir isotherm. The values of the Langmuir constants (K and b) and the ratios of K to CEC are presented in Table 2. The sorption capacities of the soils ranged from very high in clay soil (about $146\,400 \mu\text{mol kg}^{-1}$) to very low in sand (about $1765 \mu\text{mol kg}^{-1}$). The clay soil also showed the highest value for the coefficient b representing binding strength. The sorption capacities of soils followed the order of clay contents of the soils rather than organic matter contents. In contrast, organic matter was found more important than clay content for the sorption of non-ionic pesticides on the same soils (Singh *et al.* 1990).

Table 2. Langmuir coefficients for diquat in four soils

Soil	0.005 M CaCl ₂				0.05 M CaCl ₂			Reduction in K (%)
	K^A	b	r^2	$K/$ CEC	K	b	r^2	
Sand	1765	0.05	0.97	0.15	1410	0.01	0.95	20.1
Loamy sand	4905	0.01	0.99	0.28	3400	0.01	0.99	31.0
Sandy loam	39067	0.03	0.99	0.31	32437	0.02	0.94	17.0
Clay	146430	0.19	0.98	0.68	118210	0.09	0.98	19.3

^A K units: $\mu\text{mol kg}^{-1}$.

The initial portions of sorption isotherms, exhibiting almost complete removal of the herbicides from the soil solution, represent the strongly sorbed components. The term 'strong sorption capacity' was defined for paraquat by Riley *et al.* (1976) as 'the concentration of soil sorbed paraquat when the concentration of paraquat in equilibrium solution is sufficient to reduce the length of 14-day old wheat roots

by 50%'. This concentration was found to be around $0.01 \mu\text{g mL}^{-1}$ by Riley *et al.* (1976). The determination of amounts of diquat sorbed corresponding to this solution concentration requires preconcentration which was not carried out. Calculation of sorption by extrapolation of the Langmuir isotherms may not be accurate for such low concentrations. However, at a relatively higher concentration ($0.05 \mu\text{g mL}^{-1}$), sorption of diquat in Bassendean soil was measured by the batch technique and was found to be $20 \mu\text{g g}^{-1}$ at equilibrium. This value is very low compared with those reported in the literature. Approximately 40 applications of diquat at 1.0 kg ha^{-1} (active ingredient) would be required to reach this sorption concentration in a 15 cm layer of this soil (assuming a bulk density of 1330 kg m^{-3}). Furthermore, to reach the sorption corresponding to a solution concentration of $0.01 \mu\text{g mL}^{-1}$, the number of applications required would be much less than 40. This would be particularly true in the no-till situation where the pesticide is likely to be retained in only the top few mm of soil.

Since Bassendean sand has the lowest sorption capacity amongst the four soils, this soil was used in the following more detailed investigation of sorption-desorption for both diquat and paraquat herbicides.

Table 3. Langmuir parameters for the sorption of diquat and paraquat in surface and subsoil of Bassendean sand at different levels of background salt concentrations

CaCl ₂ concn (M)	Surface soil					Subsoil				
	<i>K</i> ^A	<i>b</i>	<i>r</i> ²	<i>K</i> / CEC	Reduction in <i>K</i> (%)	<i>K</i>	<i>b</i>	<i>r</i> ²	<i>K</i> / CEC	Reduction in <i>K</i> (%)
<i>Diquat</i>										
0.005	1765	0.05	0.97	0.15	—	1714	0.06	0.99	0.28	—
0.025	1587	0.02	0.96	0.13	10.1	1385	0.06	0.99	0.23	19.1
0.05	1410	0.01	0.95	0.12	20.1	1318	0.03	0.98	0.21	23.1
<i>Paraquat</i>										
0.005	2303	0.06	0.99	0.19	—	2061	0.11	0.97	0.34	—
0.025	1893	0.16	0.97	0.16	17.8	1791	0.04	0.94	0.29	13.0
0.05	1400	0.02	0.99	0.12	39.2	1363	0.04	0.99	0.22	33.9

^A *K* units: $\mu\text{mol kg}^{-1}$.

Sorption of diquat and paraquat in Bassendean sand

Generally in soils, organic matter contents decrease with depth in the profile, but for clay content the reverse is generally true. Thus, subsurface soils may have even higher sorption capacities for these cationic herbicides, compared with those for non-ionic pesticides.

Sorption and desorption of the herbicides were studied in both surface and subsurface horizons of Bassendean sand and in the presence of different concentrations of CaCl₂ in soil solution. The sorption isotherms for diquat and paraquat once again followed the Langmuir equation. The sorption coefficients for the herbicides derived from equation (1) are given in Table 3. These demonstrate that the sorption capacities of the two horizons were essentially similar for both diquat and paraquat. However, paraquat showed a slightly higher affinity (*b*) than diquat for the soils. The binding strength (*b*) was higher for both herbicides in the subsurface horizon of the Bassendean sand. The subsurface soil contained

significantly lower organic matter but had a slightly higher clay content and cation exchange capacity than the surface soil. While the overall capacity of the soil remained unchanged with depth, the binding strength (b) for the herbicide was higher in the subsurface soil because clay binds these herbicides more strongly. The ratios of sorption capacity (K) to the CEC of soil (Table 3) show that the sorption did not reach the cation exchange capacities of soil and only a maximum of 20% of cation exchange sites were satisfied by the herbicides. In comparison, the ratios for the other three soils (Table 2) were relatively higher and were found to be 0.28, 0.31 and 0.68 for diquat in the loamy sand, sandy loam and clay soils, respectively. The highest ratio was observed in the clay soil because of the presence of smectitic clay minerals in the soil. It has been noted that on pure clay minerals, particularly on smectite, sorption of these herbicides can even exceed their CEC (Weber and Weed 1968). On the other hand, on kaolinite and organic matter the sorption capacity does not reach the CEC (Best *et al.* 1972; Khan 1973). The low ratios observed in these soil samples result from the presence of kaolinite clay minerals and the organic matter being substantially responsible for the sorption. In Bassendean sand, in particular, the contribution of organic matter towards sorption is expected to be some 10–15 times more than that of clay because the contents of clay and organic matter are similar and a unit weight of organic matter has 10–15 times higher CEC than kaolinite. The discrepancies between sorption capacities and CEC may reflect differences

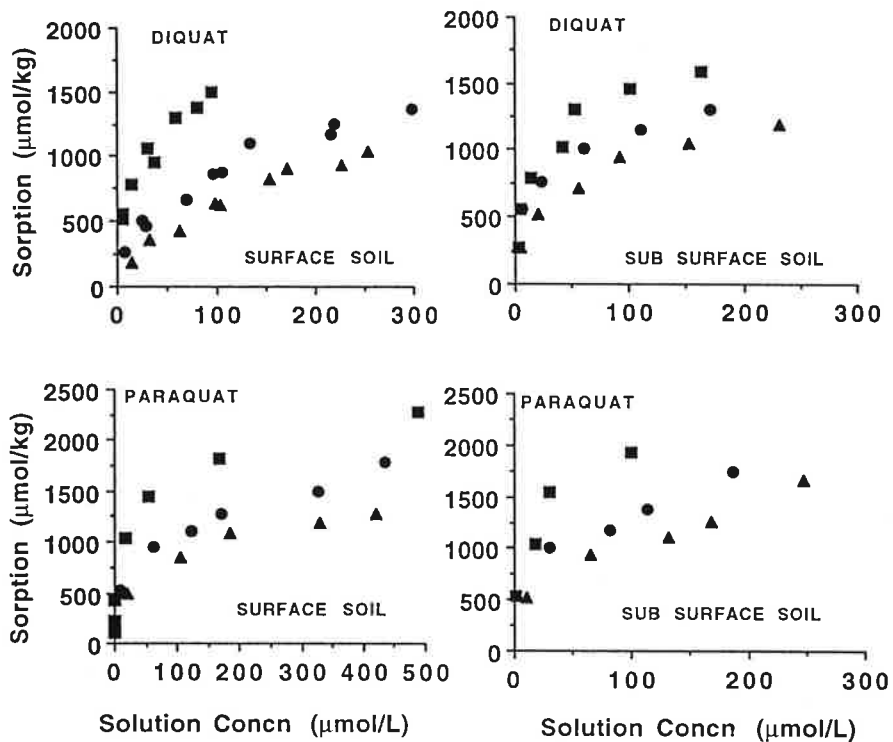


Fig. 2. Sorption isotherms of diquat and paraquat herbicides in the two horizons of Bassendean sand obtained in the presence of various concentrations of CaCl_2 in the soil solution (■, 0.005 M; ●, 0.025 M; ▲, 0.05 M).

in accessibility to sorption sites, with the larger pesticide cations being sterically hindered from sites accessible to the Sr^{2+} ion used to measure CEC (Khan 1973).

Effect of salt concentration on sorption of diquat and paraquat

Sorption of the two herbicides on Bassendean sand decreased significantly with increasing concentration of CaCl_2 in the equilibrating solution (Fig. 2). The effect is clearly reflected in the values of the Langmuir coefficients of the two herbicides given in Table 3. Both K and b decreased with increase in the salt concentration in the soil solution. The decrease in K due to the increase in salt concentration from 0.005 to 0.05 M ranged from 20 to 23% for diquat and from 34 to 39% for paraquat. In the presence of high background CaCl_2 concentration, the sorption capacities of the soil for both herbicides were roughly the same, whereas these were significantly higher for paraquat than diquat at the lower salt concentrations. The reductions in sorption capacities of the other three soils for diquat, due to a similar increase in CaCl_2 concentration, were found to be 31% in the loamy sand, 17% in the sandy loam and 19% in the clay soil. Clearly a competition between the inorganic and organic cations for sorption sites was occurring, as has been noted by other workers (Best *et al.* 1972; Burns *et al.* 1973). Burns *et al.* (1973) reported that the sorption maximum of paraquat on Ca^{2+} humate was lowered by a factor of 2.7 due to the addition of Ca^{2+} ions (0.33 M).

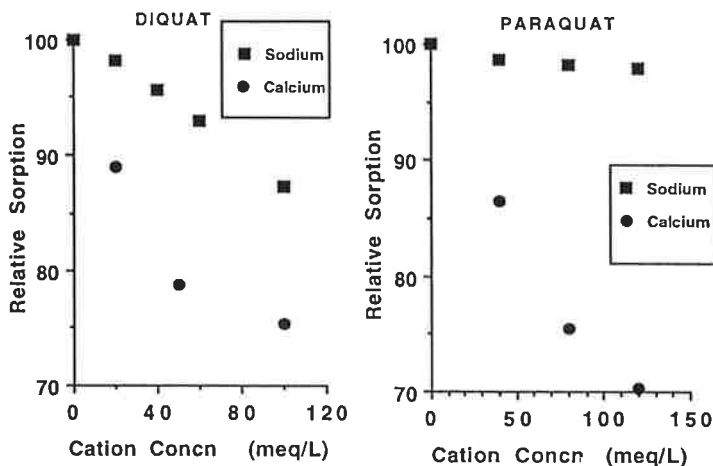


Fig. 3. Relative sorption of diquat and paraquat in the presence of different concentrations of Ca^{2+} and Na^+ cations in soil solution compared with that at zero salt concentration.

Fig. 3 compares the sorption of diquat and paraquat corresponding to various concentrations of Ca^{2+} and Na^+ in soil solution. Both inorganic cations competed for the sorption sites with the herbicides, but Na^+ was not as effective as Ca^{2+} , even when present at double the concentration of the latter. This effect was more pronounced in the case of paraquat. As shown earlier (Table 3), paraquat is bound relatively more strongly than diquat, possibly because of differences in the charge distribution on the herbicide molecules. Thus both the inorganic

cations compete more effectively with diquat than paraquat and this effect is more evident in the case of Na^+ .

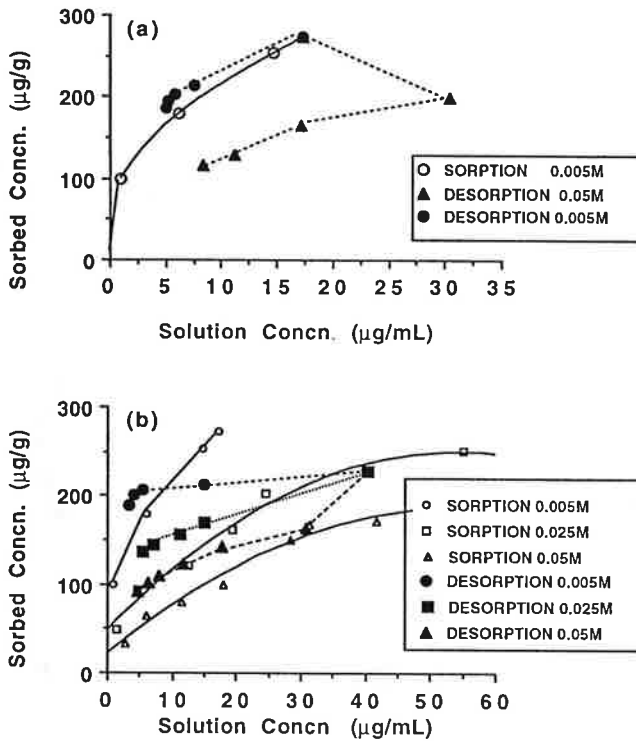


Fig. 4. Sorption isotherms in comparison with desorption isotherms obtained in the presence of various salt solutions for diquat in Bassendean sand. Open symbols represent sorption values and closed symbols represent desorption values in both (a) and (b).

Desorption

Desorption isotherms of diquat in the presence of different salt concentrations

Following the sorption of diquat on Bassendean sand at a given salt concentration, desorption isotherms were obtained by shaking the soil in various herbicide-free CaCl_2 solution concentrations. Fig. 4a depicts the sorption isotherm of diquat in the presence of 0.005 M CaCl_2 compared with the desorption isotherms obtained using 0.005 and 0.05 M CaCl_2 solutions. The shapes of the desorption isotherms are strongly influenced by the salt concentrations of the desorbing solution. Hysteresis was evident at any given salt concentration (Fig. 4b). When a solution of higher salt concentration was used for desorption, the isotherm followed a completely different path showing greater release and consequently much lower sorption at any solution concentration. Apparently, the introduction of herbicide-free solution of higher ionic strength (0.05 M CaCl_2) compared with that present during sorption (0.005 M) forced the establishment of a new equilibrium and as a result the soil lost significant amounts of sorbed herbicide, causing a dramatic increase in herbicide concentration in solution. In Fig. 4b the sorption isotherms

obtained using three CaCl_2 concentrations are compared with the desorption isotherms obtained from a point on the 0.025 M CaCl_2 sorption isotherm using three different salt concentrations. Both lower and higher salt concentrations than that involved in sorption forced the establishment of a new equilibrium and, as a result, the desorption isotherms were closer to the corresponding sorption isotherms obtained using solutions of the same salt concentration. The shape of the desorption curve is determined not only by the salt concentration in the desorbing solution but also by the previous history of sorption, including the concentration of salt solution previously present. Addition of 0.05 M CaCl_2 to the sorbed value in 0.025 M CaCl_2 will clearly reach a different equilibrium (Fig. 4b) to that reached following addition of 0.05 M CaCl_2 to the sorbed value in 0.005 M CaCl_2 (Fig. 4a).

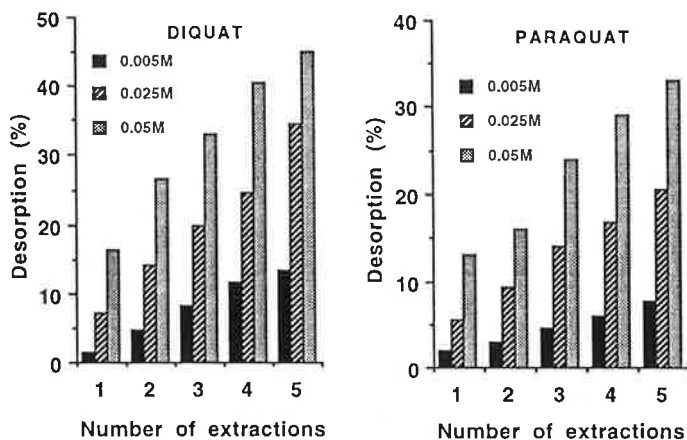


Fig. 5. Desorption of diquat and paraquat from the sand following sequential extractions with the solutions of various salt concentrations.

Effect of salt concentration on total desorbed amount of diquat and paraquat

The salt concentrations of the extractant significantly affected the amounts of the herbicides desorbed. Fig. 5 shows increasing diquat and paraquat desorption with increasing ionic strength of the desorbing solutions in Bassendean sand. Diquat was more readily desorbed than paraquat at all salt concentrations. After five successive extractions with 0.005 M CaCl_2 , the total amounts desorbed were 13% and 7% of presorbed diquat and paraquat, respectively, in the surface soil. However, with 0.05 M CaCl_2 solution, these values increased to 45% and 35% of equilibrium sorption, respectively. Similar observations have been made by other workers. Juo and Oginni (1978) reported that desorption of paraquat from kaolinitic soils after 12 extractions with 0.01 M CaCl_2 ranged from 20% to 60%. Gamar and Mustafa (1975) reported that after three extractions with distilled water, only less than 1% of the sorbed dipyrldylum herbicides was desorbed from two clay soils (containing >40% clay) as compared with 50% with 1 M BaCl_2 . The types of clay minerals present in these soils were not reported.

In the other three soils used here, the quantities of diquat recovered following five successive extractions with 0.005 and 0.05 M CaCl_2 solutions were 34% and

62% in the loamy sand, 11% and 18% in the sandy loam, and 3% and 7% in the clay soil, respectively. It is noteworthy that in the clay soil not only was the sorption substantially higher (Table 2) but only very little of the sorbed herbicide was released. The higher bonding energy (b in Table 2) shown by the smectite clay minerals in the soil is responsible for this. The other soils were dominated by kaolinite clay and hence a greater desorption occurred from these soils. Thus, substantial proportions of sorbed dipyriddylium herbicides are likely to be desorbed from soils which are dominated by kaolinite, on the addition of a solution of high ionic strength.

Table 4. Desorption of diquat after five successive extractions from Bassendean sand (surface soil) as influenced by initial sorbed concentrations and the salt (CaCl_2) concentrations of the extractant

Salt concn during sorption (M)	Sorbed concn ($\mu\text{mol kg}^{-1}$)	Desorption %		
		0.005 M	0.025 M	0.05 M
0.005	510	13.0	30.4	45.2
0.005	950	17.8	46.4	60.8
0.005	1360	23.1	52.7	68.4
0.025	460	7.0	21.0	39.9
0.025	870	9.2	29.8	48.0
0.025	1170	13.1	36.5	51.9

Effect of initial sorbed concentration on desorption

Results of the desorption experiments on diquat from three levels of initial sorbed concentrations using three extractants of different salt concentration are presented in Table 4. The desorption was not only affected by the concentration of CaCl_2 in the desorbing solution but also by the amount sorbed before the desorption started. The higher the presorbed concentration, the greater were the amounts of diquat desorbed, which indicates that as sorption increases, desorption becomes easier. For example, when the initial sorbed concentration was $250 \mu\text{g g}^{-1}$, some 13% of presorbed herbicide was desorbed after five successive extractions with 0.005 M CaCl_2 solution as compared with 23% when the presorbed concentration was only $95 \mu\text{g g}^{-1}$. When the herbicide sorbed in the presence of a relatively higher CaCl_2 concentration (0.025 M) was extracted from the soil with the solutions of three different salt concentrations, the percentage recoveries were lower (Table 4). This means that sorption which occurred in the presence of higher ionic strength solutions of inorganic cations was on relatively stronger sorption sites and therefore was less prone to desorption.

Agronomic practices such as liming, gypsum application, fertilization, and irrigation with salty water (Cole 1982) can significantly increase the salt concentrations of the soil solution, even if only temporarily. For example, Isensee and Walsh (1972) reported changes in Ca^{2+} concentrations up to 1200 ppm around KCl or ammonium nitrate fertilizer bands. Gypsum application can result in high electrolyte concentration in the soil solution, particularly in the presence of NaCl (Williams 1988). The behaviour of these herbicides, particularly with accumulation following their prolonged use, should be seriously considered prior to the introduction of a change in management practices or land-use.

The present study shows that both the type and the content of clay minerals present in soil are important for both sorption and subsequent desorption of the dipyrindylum herbicides. Desorption in particular is dependent upon the concentration of inorganic cations present in the background solution and the total sorbed concentration. Soils containing significant clay contents (e.g. >5%) have very high sorption capacities for these herbicides. However, in soils with lower clay contents (particularly if kaolinitic) such as Bassendean sand, the sorption capacities could be low and a substantial proportion of sorbed herbicides could be released in salt solutions. Considering the effectiveness of these herbicides at very low levels ($0.01 \mu\text{g g}^{-1}$), such desorption can result in phytotoxicity to crops after their repetitive use.

Acknowledgment

This work was funded by a grant from the Australian Water Research Advisory Council whose support is gratefully acknowledged.

References

- Aylmore, L. A. G., Sills, I. D., and Quirk, J. P. (1970). Surface area of homoionic illite and montmorillonite clay minerals as measured by the sorption of nitrogen and carbon dioxide. *Clays Clay Miner.* **18**, 91–6.
- Best, J. A., Weber, J. B., and Weed, S. B. (1972). Competitive adsorption of Diquat²⁺, Paraquat²⁺, and Ca²⁺ on organic matter and exchange resins. *Soil Sci.* **114**, 444–50.
- Burns, I. G., Hayes, M. H. B., and Stacey, M. (1973). Some physico-chemical interactions of paraquat with soil organic materials and model compounds. *Weed Res.* **13**, 79–90.
- Calderbank, A., and Slade, P. (1976). Diquat and paraquat. In 'Herbicides: Chemistry, Degradation and Mode of Action'. Vol. 2. (Eds P. C. Kearney and D. D. Kaufman.) pp. 501–40. (Marcel Dekker: NY.)
- Cheng, H. H. (1990). Pesticides in the soil environment—An overview. In 'Pesticides in the Soil Environment Processes, Impacts & Modelling'. (Ed. H. H. Cheng.) SSSA Book Series No. 2.
- Cole, K. (1982). Irrigation of vegetables with salty water. W.A. Dept Agriculture, Agdex 250/563. Farm Note No. 93/82.
- Gamar, Y., and Mustafa, M. A. (1975). Adsorption and desorption of Diquat²⁺ and Paraquat²⁺ on arid-zone soils. *Soil Sci.* **119**, 290–5.
- Giles, C. H., Smith, D., and Huitson, A. (1974). A general treatment and classification of the solution adsorption isotherms. I. Theoretical. *J. Colloid Interface Sci.* **47**, 755–65.
- Gill, R., Qua, S. C., and Moffat, A. C. (1983). High-performance liquid chromatography of Paraquat and Diquat in urine with rapid sample preparation involving ion-pair extraction on disposable cartridges of octa-decyl silica. *J. Chromatogr.* **255**, 483–90.
- Hance, R. J., Byast, T. H., and Smith, P. D. (1980). Apparent decomposition of paraquat in soil. *Soil Biol. Biochem.* **12**, 447–8.
- Hartley, D., and Kidd, H. (1987). (Eds) 'The Agrochemicals Handbook.' (The Royal Soc. Chem.: The University of Nottingham.)
- ICI (1984). Paraquat: its fate and effects in the soil. ICI Agrochemical Monograph Sept. 1984.
- Isensee, A. R., and Walsh, L. M. (1972). Influence of banded fertilizer on the chemical environment surrounding the band. II. Effect on soil solution cations, cation-anion balance and solution phosphorus. *J. Sci. Food Agric.* **23**, 509–16.
- Juo, A. S. R., and Oginni, O. O. (1978). Adsorption and desorption of paraquat in acid tropical soils. *J. Environ. Qual.* **7**, 9–12.
- Khan, S. U. (1973). Interaction of humic substances with bipyridylum herbicides. *Can. J. Soil Sci.* **53**, 199–204.
- McArthur, W. M., and Bettenay, E. (1960). Development and Distribution of Soils of the Swan Coastal Plain, W.A. CSIRO Soil Publ. No. 16.

- Nelson, D. W., and Sommers, L. E. (1982). In 'Methods of Soil Analysis Part II'. (Ed. A. L. Page.) Agron. Monogr. No. 9, pp. 539-77. (Am. Soc. Agron.: Madison, Wis.)
- Osborne, G. J., and Donohoe, T. M. (1977). Residual levels of paraquat in a red earth soil after 7 years of minimum and reduced cultivation. *J. Aust. Inst. Agric. Sci.* **43**, 169-70.
- Poole, M. L. (1987). Tillage practices for crop production in winter rainfall areas. In 'Tillage—New Directions in Australian Agriculture'. (Eds P. S. Cornish and J. E. Pratley.) pp. 24-47 (Inkata Press: Melbourne.)
- Riley, D., Wilkinson, W., and Tucker, B. V. (1976). Biological unavailability of bound paraquat residues in soils. In 'Bound and Conjugated Pesticide Residues'. (Ed. D. D. Kaufman *et al.*) pp. 301-53. ACS Symp. Series 29, ACS Washington, DC.
- Singh, R., Gerritse, R. G., and Aylmore, L. A. G. (1990). Adsorption-desorption behaviour of selected pesticides in some Western Australian soils. *Aust. J. Soil Res.* **28**, 227-43.
- Tucker, B. V., Pack, D. E., and Ospenson, J. N. (1967). Adsorption of bipyridylum herbicides in soil. *J. Agric. Food Chem.* **15**, 1005-8.
- Weber, J. B., and Coble, H. D. (1968). Microbial decomposition of diquat adsorbed on montmorillonite and kaolinite clays. *J. Agric. Food Chem.* **16**, 475-8.
- Weber, J. B., and Weed, S. B. (1968). Adsorption and desorption of diquat, paraquat and prometon by montmorillonitic and kaolinitic clay minerals. *Soil Sci. Soc. Am. Proc.* **32**, 485-7.
- Weed, S. B., and Weber, J. B. (1969). The effect of cation exchange capacity on the retention of diquat and paraquat by three layer type clay minerals: I. Adsorption and release. *Soil Sci. Soc. Am. Proc.* **33**, 379-82.
- Williams, B. G. (1988). Management of saline and alkaline soils in Australia. CSIRO Aust. Division of Water Resources, Tech Memo. No. 88/4.

Australian Society of Soil Science Incorporated Publication Medal

Nomination of candidates for the Australian Society of Soil Science Publication Medal, awarded annually, close with the committee on 30 April.

The following guidelines are provided to help nominators. By-law 29 of the ASSSI states

- (a) The award will be made on the basis of scientific merit, relevance to soil science, and effectiveness in communicating the paper's contents to the reader. The award will normally be for work carried out in Australia.
- (b) The award may be given annually for publications on any subject of soil research as currently defined in the Australian Journal of Soil Research. A submitted paper not receiving an award in one year may be resubmitted in a subsequent year. If in the opinion of the awarding committee no entry for a particular year is of sufficiently high standard, the committee may decline to make an award for that year.
- (c) Publications on which the award is based, should carry a date of receipt not later than the candidate's 34th birthday and applicants should be under 35 on the first day of January on the year of the award.
- (d) Publications may include those under joint authorship. A written assurance must be given by the other author(s) that the candidate for the Medal has made the major contribution to the research and writing of the paper.
- (e) Application for the award may be made by either the candidate or on the candidate's behalf by a member of the Society.
- (f) The candidate need not be a member of the Society.
- (g) Applicants may suggest the names of up to two referees on whom the Society may call.
- (h) Applications will be judged by a committee consisting of the President, plus three members appointed by Council. The committee members will serve initially for three years and then their appointment will be terminated on a rotational basis. The committee will have the power to call for opinions from any competent scientist to help in their judgement of the applications.
- (i) The award will be a medal of substantial value.
- (j) The medal will be presented by the local branch President if the Federal President is unable to attend.
- (k) The award will be called the Australian Society of Soil Science Publication Medal for 1993.

Dr Mark Conyers
Honorary Federal Secretary
Australian Society of Soil Science Inc.
Agricultural Research Institute
Wagga Wagga, 2650.

Description and prediction of pesticide leaching

L.A.G. Aylmore¹ & R.S. Kookana²

A sound understanding of the factors affecting the mobility of pesticides in soil is an essential prerequisite to the development of functions which can accurately represent the array of processes which pesticides may undergo in soils. This requires detailed investigations on equilibrium and kinetic aspects of the sorption and desorption involved, the nature, extent and rate of any chemical transformation or biological degradation, and the roles of convection, diffusion and dispersion in the mobility of the pesticides in relevant soil structures. While a substantial amount of data is available on the interactions of pesticide chemicals with soil constituents, much of this has been obtained overseas. Also, the effects on these processes of soil properties, such as texture, clay mineral species, organic matter content, pH, salts and solvents present, need to be measured in detail for a much wider range of

local soil-pesticide combinations in Australia. In particular, the significance of sorption time-dependency and long-term reversibility of sorption on the mobility of pesticides and the effects of soil environment on the rates of degradation under natural leaching conditions in the field remain poorly understood. The literature contains a multiplicity of predictive models varying greatly in terms of their complexity and claimed applicability. There is an urgent need to define the degree of complexity with which fundamental processes are treated in such models and the extent of characterisation of the range of physical, chemical and biological mechanisms required to avoid problems of site specificity and to provide a satisfactory database for predictive modelling. The development of practical methodologies, both for simulation modelling and compatible data collection, is essential.

Introduction

Pesticides play a vital role in maintaining adequate food quality and quantity. Total sales of pesticides in Australia increased nearly six fold to some \$A 530 million during the last ten years, and it is estimated that the benefit of pesticide use to the Australian economy is as high as \$A 4.5 billion. However, as a result of the massive use of pesticides in horticulture, and to a lesser extent in agriculture, there is increasing concern at the extent to which these chemicals may contaminate surface and groundwaters.

In the near future, both Federal and State Governments will be required to legislate or to act on existing legislation (such as the Soil and Water Conservation or Health Acts,) to restrict landholders and industry from discharging pollutants. A sound basis for understanding the potential hazards to water quality posed by the various chemicals concerned is essential in implementing such legislation.

As the expanding water catchment areas frequently involve areas of past, present or future horticultural use, the environmental challenge per unit area of land from pesticide use in horticulture is exceptionally high, particularly when such waters are also exploited for domestic uses (e.g. the Riverland areas of South Australia, the Sunraysia area of Victoria, the Murrumbidgee Irrigation area and Richmond River Valley of NSW, and the Pemberton–Manjimup and Ord River irrigation areas of Western Australia). In addition, there are numerous small catchment areas around several capital cities in close proximity to horticultural activities.

Systemic monitoring studies of pesticides in groundwaters are lacking. However, a recent report (EPA, 1989) indicated that an increasing number of samples, with levels of organochlorine pesticides exceeding EPA criteria, have been obtained from groundwaters in Western Australia. Similarly, increasing levels of the pesticides have also been found in river and estuarine waters of Western Australia. It is significant that under horticultural areas in Australia,

very high levels of nitrates (up to 8 times the permissible limit) have been found in some groundwaters (Pionke & others, 1990). In a horticultural catchment in South Australia (Piccadilly Valley), some 83% of surface water and 100% of sediment samples tested were found to contain pesticide residues (Thoma, 1990). Stadter & others (1992) have similarly reported the presence of atrazine and simazine in groundwaters in South Australia. The detection by 1988 of some 73 pesticides in groundwaters of various states in the USA has induced a massive research effort on pesticide–soil interactions in that country. A recently conducted preliminary survey of groundwater contamination from various sources in Australia (Jacobson & Lau, 1988) recommended that evaluation of non-point source pollution from herbicides and pesticides is urgently required.

While it is relatively easy to enunciate the objectives of a comprehensive research program to understand the factors determining pesticide leaching, the development of practical methodologies for simulation and predictive modelling and compatible data collection pose many problems requiring integration and rationalisation of input from soil scientists, industrial chemists and hydrologists. This paper provides a brief review of the major aspects of concern and the work recently undertaken at the University of Western Australia under funding provided by the AWRAC and LWRRDC.

Pesticide mobility

The large number of pesticides currently in use include a wide variety of compounds differing markedly in both their physical and chemical properties, i.e. whether ionic or non-ionic, weakly acidic or basic, hydrophobic or hydrophilic. The ionic pesticides include both cationic (e.g. paraquat, diquat) as well as anionic (2,4-D). They differ greatly in their aqueous solubility and volatility, i.e. from highly soluble and non-volatile (e.g. paraquat) to sparingly soluble and highly volatile (e.g. trifluralin). When pesticides enter the soil, they are subjected to a variety of physical, chemical and biological processes including sorption–desorption, chemical transformation and biological degradation. Previous studies here and elsewhere have shown that the retention and release processes for pesticides are not only directly related to their chemical nature, but also to the nature and properties of the soil and its

¹ Soil Science and Plant Nutrition, University of Western Australia, Nedlands, WA 6009.

² CRC for Soil and Land Management, Glen Osmond, South Australia 5064.

constituents (Singh & others, 1988a,b; Kookana & Aylmore, 1993a)). Soils vary tremendously in their composition, physical structure and chemical environment. While substantial data on pesticide/soil interactions are available, much of this has been obtained overseas and work here (Singh & others, 1988a) has demonstrated that the effects on these processes of soil properties (such as texture, clay mineral species, organic matter content, pH, salts and solvents present, etc.) need to be measured in detail for a much wider range of local soil-pesticide combinations.

Sorption-desorption processes

Sorption of pesticides by soil is undoubtedly one of the major processes influencing their accessibility to target organisms and their potential to reach non-target organisms by leaching to groundwater. Sorption may result in decreasing biological activity with respect to the target organism, in enhanced degradation of the pesticide before leaching and in retardation in movement with leaching solutions (Weed & Weber, 1974). Organic matter and clay minerals are undoubtedly the major constituents in determining the extent of sorption in soils and numerous studies on pesticide sorption have been reported including both inorganic and organic surface interactions (reviewed by Bailey & White, 1970; Weber, 1972; Weed & Weber, 1974; Calvet, 1980; Koskinen & Harper, 1990). Interactions of pesticides with model materials, such as homoionic clays and ion exchange resins, have been widely studied as these well-defined systems allow clearer elucidation of mechanisms and specific interactions (Mortland, 1970). However, in natural soils the interactions can be expected to be much more complex than in pure materials (Hamaker & Thompson, 1972). Kookana & Aylmore (1993a) found that the sorption of cationic diquat and paraquat in some Western Australian soils followed the order of clay content in the soils and that both the type and contents of clay minerals present in the soil were important for sorption and subsequent desorption of the dipyridylum herbicides. For some other pesticides, in particular non-ionic compounds, the amounts sorbed were more directly related to organic matter contents than to clay contents (Singh & others, 1989; Aylmore & others, 1989). However, comparisons between data obtained on Australian soils with those for other world soils (Singh & others, 1990b) have demonstrated that substantial variation occurs, for example, in the adsorption of linuron and fenamiphos per unit weight of organic matter (K_{OM}), not only between soils from different regions but also between soils from the same region, clearly indicating that organic matter in Australian soils can behave quite differently in terms of the retention of pesticides.

In recent decades, various approaches have been used to describe solute-soil interactions. Considerable attention has been given to adsorption models based on gas-solid interactions that lead to Langmuir and Freundlich-type equations. These have sometimes been criticized for neglecting the generally electrostatic nature of the ion-soil interactions and for ignoring the heterogeneity of the surface adsorption energy. Preference has often been given to models based on the diffuse double layer (DDL) theories (Bowden & others 1974). In its complete form, the DDL adsorption model of Bowden & others (1974) requires five simultaneous equations that have to be solved by iterative procedures to estimate the equilibrium distribution of ions between solution and solid (adsorbed) phases. However, such complexity, while requiring large computational time, brings little useful refinement in the simulation of break-

through curves (Murali & Aylmore, 1981). Singh & others (1988b) found that sorption data for fenamiphos, linuron and simazine could readily be fitted to a Freundlich-type equation, while that for Diquat more closely fitted the Langmuir equation. As discussed later it has become increasingly clear that the kinetic aspects of the sorption processes need to be considered when dealing with solute transport.

While the organic matter and clay contents of a soil are undoubtedly the main substrates for pesticide sorption (Hamaker & Thompson, 1972; Weed & Weber, 1974; Green, 1974; Koskinen & Harper, 1990) the extent and reversibility of these interactions can be greatly influenced by other factors such as pH, soil solute concentration or the presence of organic cosolvents and competitive ions (Kookana & others, 1989; Singh & others 1988b).

Effect of pH

Both organic matter and clays have pH-dependent charges and hence their ion exchange capacities change with pH. The relative quantities of basic and acidic pesticide in ionic form are also dependent on the pH of the system. Organobasic compounds (s-triazines) become cations at low pH and this results in increased sorption (Weber & others, 1969), whereas the acidic compounds are proton donors (2,4-D, dinoseb sulfonyl ureas) which at high pH (one or more pH units above the pKa of acid) become anions due to dissociation. The adsorption of simazine and to a lesser extent of linuron and fenamiphos, were shown to decrease with increasing pH in Western Australian soils varying in texture from sand to clay (Aylmore & others, 1989). Simazine is a weakly basic herbicide and has a pKa of 1.4. As the pH increases, the proportion of simazine cations in solution decreases and hence the adsorption decreases. In contrast to the weakly basic Simazine, the adsorptions of paraquat and diquat (both strongly cationic) were unaffected by change in pH (Singh & others, 1988a). Soil acidification, as a result of fertilization and cropping, is a major problem in many areas of Australia as elsewhere, and management practices (such as liming) can also play a significant role in determining the pH of a soil and hence pesticide sorption (Singh & others, 1988a). It has also been suggested that the pH at the surface of soil colloids can be up to two units lower than that measured in the soil solution (Hayes, 1970) and that the pH of rhizosphere soil may differ from that of bulk soil by up to 1 pH unit (Nye, 1986). Such effects clearly need to be considered in assessing pesticide-leaching potential.

Reversibility of sorption — hysteresis

The reversibility of sorption reactions plays a significant role in determining the behaviour of any pesticide in the soil profile. That is, whether the solid phase provides a permanent sink or merely a temporary reservoir, releasing the chemical back into solution in response to a decrease in solution concentration. Numerous workers (Swanson & Dutt, 1973; van Genuchten & Wierenga, 1974; Bowman & Sans, 1977; Rao & others, 1978; Koskinen & Cheng, 1979; Di Toro & Horzempa, 1982; Brusseau & Rao, 1989; among others) have reported that the sorption-desorption reaction was non-singular. Hysteresis has frequently been observed in the sorption-desorption isotherms for pesticides [(e.g. atrazine; Swanson & Dutt, 1973); picloram (van Genuchten & others, 1974); diuron (Peck & others, 1980); 2,4,5-T (van Genuchten & others, 1977); parathion (Bowman & Sans, 1985); linuron, simazine (Singh & others, 1990)]. The

mechanisms underlying measurements of apparent hysteresis appear many and varied, sometimes being attributed to experimental artifacts, such as changes in sorption capacity arising from shaking and centrifugation, incomplete equilibration, the presence of 'implicit sorbate' altering competitive sorption, as well as degradation or transformation of the pesticide during longer term experiments. However, true hysteresis as a result of the entrapment of pesticides in the organic matter matrix (Ogner & Schnitzer, 1971; Johnson & Starr, 1972; Khan, 1978; Burchill & others, 1981; Kookana & others, 1990) or within mineral particles (McCloskey & Bayer, 1987) seems likely to occur (Singh & others, 1990b). This is an important consideration since the effects of various factors, such as soil solution concentration and organic cosolvents on the extent of hysteresis and ease of desorption, have been shown to have serious implications for the mobility of pesticides in soil profiles (Singh & others, 1990b, Kookana & Aylmore, 1993b).

Effect of competitive species

Competition for sorption sites by other inorganic and organic compounds present in the solution can modify the behaviour of pesticides in the soil. Inorganic cations compete directly with cationic and cationizable pesticides and reduce their sorption (Weber & Weed, 1968; Hance, 1969; Best & others, 1972; Hayes & others, 1975). Increases in the salt concentration of the soil solution (from 0.005 to 0.05 M CaCl₂) were observed to result in decreases in sorption capacities for diquat and paraquat herbicides ranging from some 17% for a sandy soil to 40% for a clay soil (Kookana & Aylmore, 1993a). Desorption of the herbicides was also significantly enhanced by increase in the salt concentration, indicating that the herbicides were less strongly held. Both Ca²⁺ and Na⁺ competed with the herbicides for the sorption sites but Na⁺ was not as effective as Ca²⁺. While pesticides, such as diquat and paraquat, are generally considered to be essentially irreversibly retained by soil, it is significant that some 60% of adsorbed diquat could be released to solution from a loamy sand soil by extraction with 0.05 M CaCl₂. In contrast, the adsorption of linuron, simazine and fenamiphos were only slightly decreased by increasing soil solution concentration (Singh & others, 1988a,b).

Effect of organic cosolvent

Interest in the behaviour of pesticides in soils in the presence of organic cosolvents arises from possible implications with respect to the transport of pesticides and other organic solutes in any situation where organic solvents may be involved, e.g. at waste disposal sites, at land treatment sites for concentrated wastes containing solvents, and in cases of accidental spills. In addition, it is common practice among workers to use pesticide stock solutions prepared in organic solvents for sorption studies (Calvet, 1980), particularly for pesticides having low aqueous solubility (Dunigan & McIntosh, 1971). Recent studies (Singh & others, 1990) have shown that the adsorption and desorption behaviour of the pesticides linuron and simazine are both significantly affected by the presence of methanol. Adsorption of the herbicides decreased with increasing methanol content of the water/methanol mixture and followed the solvophobic theory, which describes the adsorption of hydrophobic organic compounds in soils. Hysteresis, observed after

desorption in CaCl₂ solution, decreased with increasing methanol content for both herbicides. The decrease in hysteresis was attributed to the swelling of the organic matter and the accompanying increased accessibility to solutes. In addition to their direct effect on adsorption, increased reversibility of the adsorption process (i.e. less hysteresis) in the presence of organic solvents, will obviously increase the mobility of a pesticide in the soil profile. At 10% methanol content, the retardation factor (R) for these herbicides decreased to almost half the value in aqueous solution. The presence of methanol at levels of 50% and 60% of solvent mixture, decreased R for simazine and linuron by factors of 10 and 12 respectively (Singh & others, 1990).

Degradation

Whether a pesticide persists for a long time or is rapidly degraded in soil is also a major determinant of the extent to which it can pose a pollution hazard. Those that degrade rapidly are less exposed to leaching effects, since the rate of degradation to their metabolites will determine the residence times of the parent compounds in the soil profile. However, for certain pesticides the degradation process leads to the formation of metabolites which are themselves equally, or more toxic than the parent compound, thus maintaining or even increasing the potential hazard to groundwater (e.g. fenamiphos nematicide which transforms to its sulfoxide and sulfone). The significance of these processes in soils under Australian climatic conditions is poorly understood (Ferris & Haigh, 1992). The role of other factors, such as organic matter, moisture content and temperature in the degradation process, also need to be investigated. In the field, temperature is a function of depth in a soil profile, and hence may be of considerable importance in controlling pesticide degradation and susceptibility to leaching.

Sorption time-dependency

The kinetics of pesticide sorption in soil has until recently received relatively little experimental attention, and most sorption studies on pesticides in soil have dealt with equilibrium aspects (Rao & Jessup, 1983; Yaron & others 1985). Much previous work has been limited to the measurement of sorption equilibrium by batch methods involving shaking or stirring of soil suspensions. Consequently, studies of pesticide sorption by batch methods have frequently indicated that the major fraction of pesticide sorption in soil is essentially instantaneous. However, there is substantial evidence from breakthrough curves involving flow in soil columns, that the sorption process is almost invariably time dependent under the flow conditions (Murali & Aylmore, 1980; Kookana & others, 1991). Recent studies have confirmed the time-dependency of sorption in the field (Pignatello, 1990; Brusseau & others, 1991). The effects of such sorption dynamics may arise both from structural limitations on diffusion into micropores as well as from the kinetics of the sorption process itself. Acceptance of an invalid instantaneous reaction could clearly lead to serious underestimation of potential leaching and transport of a pesticide to groundwater (Kookana & others, 1991). Flow techniques, such as that developed by Kookana & others (1991), are preferable over batch techniques (Sparks, 1985) for estimating relevant parameters because these are realistic and suitable for modelling transport of pesticides in soil profiles.

Modelling of pesticide sorption and transport

Numerous mathematical models for describing and predicting the transport of non-reactive and reactive solutes, such as pesticides under saturated as well as unsaturated flow conditions, have been developed in recent decades. Common models of organic chemical transport and their strengths and weaknesses have recently been reviewed by Gallant & Moore (1991) and by Parthapar & Bowmer (1991). Such models can be broadly divided into two classes on the basis of the degree of complexity with which fundamental processes are incorporated and the extent of characterisation of the range of physical, chemical and biological factors required. Recent reviews of mechanistic or process-based models employing the classical convection-diffusion-dispersion equations have been provided by different workers (van Genuchten, 1991; Jury & Ghodrati, 1989; Brusseau & Rao, 1989). The development of mechanistic models and their evaluation under controlled laboratory conditions provides important insights into the significance of the various physical and chemical processes involved in determining pesticide movement in soils (research oriented). However, the complexity attendant on the multiplicity of factors frequently operating in the field, is likely to make such models extremely cumbersome and of restricted applicability. In contrast, models based on stochastic representation of the transport properties (Jury & others, 1987; Rao & Jessup, 1983) provide little understanding of the underlying physical and chemical processes and seek a more functional description in terms of readily accessible parameters (i.e. management oriented). Despite this simplification, functional models often give simulations that are at least as good as those of mechanistic models (e.g. Nicholls & others, 1982; De Willigen, 1991) while using far less computer time. They seem likely to be increasingly advantageous as the physical scale of the modelling exercise increases (Addiscott, 1992).

Independent measurement of parameters under realistic conditions

In solute transport studies, a number of different rate laws describing the time dependency of the sorption reaction in soils have been used with varying degrees of success. These include simple one-site linear or non-linear kinetic models, two-site sorption models and several others (reviewed by Nielsen & others, 1986; Brusseau & Rao, 1989). More recently, Boesten (1987) used a three-site kinetic model, and Selim & Amacher (1988) a second-order two-site kinetic model in their solute transport studies. Experimental evidence of such kinetic reactions have been obtained in a few studies only and even then by the batch technique. Since substantial differences in sorption between flow and batch systems have frequently been noted (e.g. Ardakani & McLaren, 1977; Wagenet & others, 1977; Gaber & others, 1992), it is essential that sorption rate coefficients be obtained under flow conditions for such transport studies. The peak maxima method applied to breakthrough curves (BTCs) is commonly used in the chromatography literature for the determination of a distribution isotherm (Huber & Gerritse, 1971). By comparing the BTCs for a pesticide for different amounts of pesticide injected into a soil column with those for a non-retarded solute, it is possible (Kookana & others 1992b) to obtain a series of sorption values corresponding to different solution concentrations at a given rate of flow

or residence time. When the flow rates employed are slow enough to allow solute to react completely with the soil, such sorption values will represent an equilibrium sorption isotherm comparable with those obtained by batch methods, at least in principle. However, at higher rates the sorption values will represent dynamic distribution isotherms. The residence time of a pesticide in the soil column can be varied by changing the flow rate of the solution entering the soil columns. In practice, the sorption values versus residence times obtained from the sets of BTCs at different rates of flow, are equivalent to the set of sorption versus equilibration-time data obtained by the batch method. This sorption versus time data can then simply be subjected to various rate laws, such as the first-order kinetic equation, and the rate parameters can be calculated.

Kookana & others (1992a) used this flow technique to study the sorption kinetics of three pesticides in laboratory studies on four Western Australian soils. Sorption data of all pesticides showed an initial rapid rate followed by a slower rate of sorption. While a first-order equation failed to satisfactorily describe the sorption data, both the Freundlich two-site kinetic equation and the parabolic diffusion law fitted well to the data. The rapid component of sorption varied from 0 to 25% of total sorption (24 h sorption value) for the various pesticides. A comparison of sorption data obtained by a batch technique and a flow technique revealed that sorption occurs at a much faster rate under batch conditions, presumably because of shaking and the high solution to soil ratio. Under the batch conditions, the instantaneous component of sorption was very high (up to 90% of 24 h sorption value). The characteristics of the soil also affected the rate of sorption of the pesticides. A well-structured soil with high organic matter content showed a slower rate of sorption compared with a dispersed soil with low organic matter. Although time-dependency of sorption is demonstrably a fact in practical situations, the extent to which it plays a significant role and needs to be accounted for in determining the overall leaching of pesticides in the field where water infiltration and redistribution generally follow a stop/go scenario remains to be established.

For the most effective pesticide usage and rapid assessment of their likely pollution potential at any given location, management models need to be designed requiring the minimum number of parameters while effective and with structures that can be readily modified for site specific purposes. Kookana & Aylmore (1993b) examined the groundwater pollution potentials predicted for a number of pesticides and the influence of organic matter distribution by calculating the mass of pesticides leaching past the zone of maximum sorption and biological activity in a sandy soil profile of the Swan Coastal Plain, W.A., using a simple screening model (Jury & others, 1987). Hydrological parameters were estimated from local soil and climatic data, and in the absence of local data sorption (Koc) and degradation (half-life) parameters were obtained from the literature. Assuming a uniform OM content, the model predicted that of 40 pesticides evaluated, 20 have the potential to reach groundwater in significant amounts (>0.1% of applied mass). However, when an exponentially decreasing OM content with depth in the soil profile was incorporated in the model, the number of pesticides reaching groundwater increased to 30 and the residual concentrations were dramatically increased. The use of local Koc and half-life values for seven pesticides, yielded substantially different residual concentrations to those obtained on the basis of literature values, emphasising the

need for site specific data. A clearer understanding of the extent to which the neglect of factors (such as dispersion and diffusion, sorption non-equilibrium, water repellancy and preferential flow paths, hysteresis and the use of average recharge rates), will lead to significant over- or under-estimation of pollution potentials is vital to the development of effective and practical management models.

Although the individual mechanisms involved in transport have been extensively studied and modelled in isolation, it is of particular importance to develop predictive capabilities of their integrated consequences. While the different aspects are most readily characterized under controlled laboratory conditions, extrapolation to field conditions is invariably complicated by climatic and other variables. In particular, the structure of the soil plays an important part in the leaching process. Although some progress has been made in characterising soil structure (Dexter, 1988), little success has been achieved in relating water movement, and hence solute transport, to pore size distribution and continuity. While predictive models provide important tools in both research and management, comprehensive field data sets on pesticide transport and volatilization remain needed to accurately assess and improve the performance of these models. There is an urgent need to define the degree of complexity with which fundamental processes need to be treated in such models as well as the extent of characterisation of the variety of physical, chemical and biological parameters required in order to avoid problems of site specificity and to provide an effective approach to defining the potential hazard posed by particular pesticide/soil combinations. Improved technologies for measuring pesticide transport and degradation processes in heterogeneous field soils are also needed.

References

- Addiscott, T.M., 1992 — Simulation modelling and soil behaviour. *Proceedings International Society Soil Science Symposium on "Operational Methods to Characterise Soil Behaviour in Space and Time."*, Cornell University, Ithaca, July.
- Ardakani, M.S. & McLaren, A.D., 1977 — Absence of local equilibrium during ammonia transport in a soil column. *Soil Science Society of America Journal*, 41, 677–679.
- Aylmore, L.A.G., Singh, Rai & Gerritse, R.G., 1989 — Adsorption-desorption behaviour of pesticides and implications for groundwater pollution. *Water 89 Inter. Conf., Bangkok, Thailand*. EQM, 4–9.
- Bailey, G.W. & White, J.L., 1970 — Factors influencing the adsorption, desorption and movement of pesticides in soils. *Residue Reviews*, 32, 29–92.
- Best, J.A., Weber, J.B. & Weed, S.B., 1972 — Competitive adsorption of Diquat²⁺, Paraquat²⁺, and Ca²⁺ on organic matter and exchange resins. *Soil Science* 114, 444–450.
- Bowden, J.W., Posner, A.M. & Quirk, J.P., 1974 — A model for ion adsorption on variable charge surfaces. *Transactions 10th International Congress Soil Science, Moscow*, 2, 29–36.
- Boesten, J.J.T.I., 1987 — Modelling pesticide transport with a three site sorption sub-model: a field test. *Netherlands Journal of Agricultural Science*, 35, 315–324.
- Bowman, B.T. & Sans, W.W., 1985 — Partitioning behaviour of insecticides in soil-water systems. II. Desorption hysteresis effects. *Journal of Environmental Quality*, 14, 270–273.
- Burchill, S., Hayes, M.H.B. & Greenland, D.J., 1981 — Adsorption. In Greenland, D.J. & Hayes, M.H.B. (editors), *The Chemistry of Soil Processes*. John Wiley & Sons Ltd, 221–400.
- Brusseau, M.L. & Rao, P.S.C., 1989 — Sorption nonideality during organic contaminant transport in porous media. *CRC Critical Reviews in Environmental Control*, 19, 33–99.
- Brusseau, M.L., Jessup, R.E. & Rao, P.S.C., 1991 — Nonequilibrium sorption of organic chemicals. *Environmental Science and Technology*, 25, 134–142.
- Calvet, R., 1980 — Adsorption-desorption phenomena. In Hance, R.J. (editor), *Interactions between herbicides and the soil*. Academic Press, London, 1–30.
- De Willigen, P., 1991 — Nitrogen turn-over in the soil-crop system: comparison of fourteen models. *Fertilizer Research*, 27, 141–149.
- Dexter, A.R., 1988 — Advances in characterisation of soil structure. *Soil and Tillage Research*, 11, 199–238.
- Di Toro, D.M. & Horzempa, L.M., 1982 — Reversible and resistant components of PCB adsorption-desorption: Isotherms. *Environmental Science and Technology*, 16, 594–602.
- Dunigan, E.P. & MacIntosh, Th., 1971 — Atrazine — soil organic matter interaction. *Weed Science*, 19, 279–282.
- EPA, 1989 — Monitoring Pesticides — A review. *The Environment Protection Authority, Perth, Western Australia, Bulletin No. 407*, pp 67.
- Ferris, I.G. & Haigh, B.M., 1992 — Herbicide persistence and movement in Australian soils: Implications for agriculture. In Altman, J. (editor), *Pesticide Interaction in Crop Production*. CRC Press (in press).
- Gaber, H.M., Comfort, S.D., Inskip, W.P. & El-Attar, H.A., 1992 — A test of local equilibrium assumption for adsorption and transport of picloram. *Soil Science Society of America Journal*, 56, 1392–1400.
- Gallant, J.C. & Moore, I.D., 1991 — Models of organic contaminant transport and degradation: A review. In Moore, I.D. (editor), *Modelling the Fate of Chemicals in the Environment*. CRES, ANU, Canberra. 22–39.
- Green, R.E., 1974 — Pesticide-clay-water interactions. In Guenzi, W.D. (editor), *Pesticides in soil and water*. Soil Science Society of America Inc. Publ., Madison, 33–37.
- Hayes, M.H.B., 1970 — Adsorption of triazine herbicides on soil organic matter, including a short review on soil organic chemistry. *Residue Reviews*, 32, 131–168.
- Hayes, M.H.B., Pick, M.E. & Toms, B.A., 1975 — Interaction between clay minerals and bipyridylum herbicides. *Residue Reviews*, 57, 1–25.
- Hamaker, J.W. & Thompson, J.M., 1972 — Adsorption. In Goring, C.A.I. & Hamaker, J.W. (editors), *Organic Chemicals in the Soil Environment*, Vol. 1. Marcel Dekker Inc., N.Y. 49–143.
- Hance, R.J., 1969 — The influence of pH, exchangeable cation and the presence of organic matter on the adsorption of some herbicides by montmorillonite. *Canadian Journal of Soil Science*, 49, 357–364.
- Huber, J.F.K. & Gerritse, R.G., 1971 — Evaluation of dynamic gas chromatographic methods for the determination of adsorption and solution isotherms. *Journal of Chromatography*, 58, 137–158.
- Jacobson, G. & Lau, J.E., 1988 — Groundwater contamination incidents in Australia: An initial survey, *Bureau of Mineral Resources, Australia, Report 287*.
- Johnson, R.E. & Starr, R.I., 1972 — Ultrarapid extraction of insecticides from soil using a new ultrasonic technique. *Journal of Agriculture and Food Chemistry*, 20, 48–51.
- Jury, W.A. & Ghodrati, M., 1989 — Overview of organic chemical environmental fate and transfer modelling

- approaches. *In Reactions and Movement of Organic Chemicals in Soil. Soil Science Society of America Journal Special Publication*, 22, 271–304.
- Jury, W.A., Foch, D.D. & Farmer, W.J., 1987 — Evaluation of pesticide groundwater pollution potential from standard indices of soil-chemical adsorption and biodegradation. *Journal of Environmental Quality*, 16, 422–428.
- Khan, S.U., 1973 — Interaction of humic substances with bipyridylum herbicides. *Canadian Journal of Soil Science*, 53, 199–204.
- Kookana, R.S. & Aylmore, L.A.G., 1993a — Retention and release of Diquat and Paraquat herbicides in soils. *Australian Journal of Soil Research*, 31, 97–109.
- Kookana, R.S. & Aylmore, L.A.G., 1993b — Estimating groundwater pollution potential of pesticides. *Australian Journal of Soil Research* (in prep).
- Kookana, R.S., Aylmore, L.A.G. & Gerritse, R.G., 1992a — Time dependent sorption of pesticides during transport in soils. *Soil Science*, 154, 214–225.
- Kookana, R.S., Gerritse, R.G. & Aylmore, L.A.G., 1992b — A method for studying nonequilibrium sorption during transport of pesticides in soil. *Soil Science*, 154, 344–349.
- Kookana, R.S., Schuller, R.D. & Aylmore, L.A.G., 1991 — Numerical simulation of pesticide transport measured in a sandy soil. *In Moore, I.D. (editor), Proceedings of Workshop on Modelling the fate of chemicals in the environment. Centre for Resource and Environmental Studies, Canberra*, 75–82.
- Kookana, R.S., Schuller, R.D. & Aylmore, L.A.G., 1992c — Simulation of simazine transport through soil columns using time-dependent sorption data measured under flow conditions. *Journal of Contaminant Hydrology*, (in press).
- Koskinen, W.C. & Cheng, H.H., 1979 — Effects of experimental variables on 2,4,5-T adsorption-desorption in soil. *Journal of Environmental Quality*, 12, 325–330.
- Koskinen, W.C. & Harper, S.S., 1990 — The retention process: mechanisms. *In Cheng, H.H. (editor), Pesticides in the Soil Environment: Processes, Impacts and Modelling. Soil Science Society of America Book Series No. 2* 51–78.
- McCloskey, W.B. & Bayer, D.E., 1987 — Thermodynamics of fluridone adsorption and desorption on three Californian soils. *Soil Science Society of America Journal*, 51, 37–44.
- Mortland, M.M., 1970 — Clay organic complexes and interactions. *Advances in Agronomy*, 22, 75–114.
- Murali, V. & Aylmore, L.A.G., 1980 — No-flow equilibration and adsorption dynamics during ionic transport in soils. *Nature*, 283, 467–469.
- Murali, V. & Aylmore, L.A.G., 1981 — Modelling adsorption in solute flow simulations: diffuse double layer versus gas-solid interaction approaches. *Soil Science*, 131, 76–81.
- Nicholls, P.H., Bromilow, R.H. & Addiscott, T.M., 1982 — Measured and simulated behaviour of fluometuron, aldoxycarb and chloride ions in a structured soil. *Pesticide Science*, 13, 475–483.
- Nielsen, D.R. van Gebuchten, M. Th. & Biggar, J.W., 1986 — Water flow and solute transport processes in the unsaturated zone. *Water Resources Research*, 22, 89–108.
- Nye, P.H., 1986 — Acid-base changes in the rhizosphere. *In Advances In Plant Nutrition. Praeger Scientific, N.Y.*, 129–154.
- Ogner, G. & Schnitzer, M., 1971 — Chemistry of fulvic acid, a soil humic fraction, and its relation to lignin. *Canadian Journal of Chemistry*, 49, 1053–1063.
- Parthapar, S.A. & Bowmer, K.H., 1991 — Pesticide issues in irrigation agriculture — Can modelling help. *In Moore, I.D. (editor), Modelling the Fate of Chemicals in the Environment. CRES, ANU, Canberra*, 9–12.
- Peck, D.E., Corwin, D.L. & Farmer, W.J., 1980 — Adsorption desorption of diuron by freshwater sediments. *Journal of Environmental Quality*, 9, 101–106.
- Pignatello, J.J., 1990 — Slowly reversible sorption of aliphatic hydrocarbons in soils II. Mechanistic aspects. *Environmental Toxicology and Chemistry*, 9, 1117–1126.
- Pionke, H.B., Sharma, M.L. & Hosking, J.A., 1990 — Horticulturally cropping effects on groundwater quality in the Swan Coastal Plain. *CSIRO Division of Water Resources Series*, No. 2.
- Rao, P.S.C. & Jessup, R.E., 1983 — Sorption and movement of pesticides and other toxic organic substances in soils. *In Nelson, D.W., Tanji, K.J. & Elrick, D.E. (editors), Chemical Mobility and Reactivity in Soil Systems. Soil Science Society of America Madison, Wisc.*, 183–201.
- Rao, P.S.C., Davidson, J.M. & Kilcrease, D.P., 1978 — Examination of nonsingularity of adsorption-desorption isotherms for soil-pesticide systems. *Agronomy Abstracts* 34.
- Selim, H.M. & Amacher, M.C., 1988 — A second-order kinetic approach for modelling solute retention and transport in soils. *Water Resources Research*, 24, 2061–2075.
- Singh, Rai, Aylmore, L.A.G. & Gerritse, R.G., 1990 — Evaluation of potential for groundwater pollution by some pesticides in a deep sand of Western Australia. *Proceedings of National Workshop on Herbicide Persistence, Melbourne, Nov., 1989*.
- Singh, R., Gerritse, R.G. & Aylmore, L.A.G., 1988 — Effect of soil conditions associated with management practices on the retention and release of pesticide. *Australian Society of Soil Science Conference, Merredin, W.A., August*, 119–123.
- Singh, Rai, Gerritse, R.G. & Aylmore, L.A.G., 1988 — Physico-chemical interaction and mobility of pesticides in soils. *National Workshop on Persistence of Herbicide Residues in Wheat Cropping Systems in Australia, Melbourne, Oct.*, 32–47.
- Singh, R., Gerritse, R.G. & Aylmore, L.A.G., 1990 — Adsorption-desorption behaviour of selected pesticides in some Western Australian soils. *Australian Journal of Soil Research*, 28, 227–243.
- Singh, R., Gerritse, R.G. & Aylmore, L.A.G., 1990 — Effect of organic co-solvent on adsorption and desorption of Linuron and Simazine in soil. *Australian Journal of Soil Research*, 28, 717–725.
- Sparks, D.L., 1985 — Kinetics of ionic reactions in clay minerals and soils. *Advances in Agronomy*, 38, 231–266.
- Stadter, F.A., Emmett, A. & Dillon, P., 1992 — Occurrence of Atrazine in groundwater in the southeast of South Australia. Report of Stage 2 of Investigation, *CSIRO, Centre for Groundwater Studies Report*, No. 45.
- Swanson, R.A. & Dutt, G.R., 1973 — Chemical and physical processes that affect atrazine and distribution in soils. *Soil Science Society of America Journal*, 37, 872–876.
- Thoma, K., 1990 — Pilot survey of pesticides residues in streams draining horticultural catchment, Piccadilly Valley, South Australia. *South Australian Department of Agriculture, Adelaide*.
- van Genuchten, M.Th., 1991 — Recent progress in

- modelling water flow and chemical transport in the unsaturated zone. In Kienitz, G. & others (editors), *Hydrological Interaction Between Atmosphere, Soil and Vegetation. IAHS Publ. No. 204, Institute of Hydrology, Wallingford, Oxfordshire, U.K.* 169–183.
- van Genuchten, M.Th., Wierenga, P.J. & O'Connor, G.A., 1977 — Mass transfer studies in sorbing porous media: III. Experimental evaluation with 2,4,5-T. *Soil Science Society of America Journal*, 41, 278–285.
- van Genuchten, M.Th. & Wierenga, P.J., 1974 — Simulations of one-dimensional solute transport in porous media. *New Mexico Agricultural Experimental Station Bulletin* 628.
- van Genuchten, M.Th., Davidson, J.M. & Wierenga, P.J., 1974 — An evaluation of kinetic and equilibrium equation for the prediction of pesticide movement through porous media. *Soil Science Society of America Proceedings*, 38, 29–36.
- Wagenet, R.J., Biggar, J.W. & Nielsen, D.R., 1977 — Tracing of transformations of urea fertilizer during leaching. *Soil Science Society of America Journal*, 41, 896–902.
- Weber, J.B., Weed, S.B. & Ward, T.M., 1969 — Adsorption of s-triazines by soil organic matter. *Weed Science*, 17, 417–421.
- Weber, J.B., 1972 — Interactions of organic pesticides with particulate matter in aquatic and soil systems. In Gould, R.F. (editor), *Fate of Organic Pesticides in Aquatic Environment. American Chemical Society*, 111, 55–120.
- Weber, J.B. & Weed, S.B., 1968 — Adsorption-desorption of diquat, paraquat and prometon in montmorillonitic and kaolinitic clay minerals. *Soil Science Society of America Proceedings*, 32, 485–487.
- Weed, S.B. & Weber, J.B., 1974 — Pesticide — Organic matter interactions. In Guenzi, W.D. (editor), *Pesticides in Soil and Water. Soil Science Society of America Inc. Publisher, Madison, Wisc. USA*, 39–66.
- Yaron, B., Gerstl, Z. & Spencer, W.F., 1985 — Behaviour of herbicides in irrigated soils. *Advances in Soil Science*, 3, 121–211.
- physical, chemical and biological processes involved in the leaching of different pesticides in Australian soil profiles; and (3) to identify appropriate parameters and develop a comprehensive model to enable the realistic description and prediction of potential pesticide movement to groundwater under different soil and climatic conditions.

The objectives of the workshop were to disseminate information on current progress in understanding the nature of the processes determining the mobility of pesticides and methodologies available for modelling their transport within soil profiles. Feedback was sought from workers in relevant organisations on the problems likely to be encountered in acquiring relevant data and in developing management models of practical use.

Workshop presentations

The workshop was chaired by Richard Lakey (Department of Conservation, Victoria).

Graham Aylmore (see paper above) outlined the current progress made in understanding the interactions of pesticide chemicals with soil constituents and the influence on these processes of soil properties, such as texture, clay mineral species, organic matter content, pH, salts and solvents present, with particular reference to Australian soils and conditions. While biological or chemical degradation and transformation of pesticides to their metabolites will determine the residence times of the parent compounds in the soil and will undoubtedly affect the extent to which they pose a pollution hazard, the significance of these processes in soils under Australian conditions is poorly understood. Similarly, the significance of other factors, such as sorption-time dependency arising both from structural limitations on diffusion into micropores as well as from the kinetics of the sorption process itself, and the effects of competition between differing chemicals for sorption sites in any particular situation, need to be assessed.

Rai Kookana (see paper above) summarized the multiplicity of predictive models ranging from process-based models employing the classical convection–diffusion–dispersion equations to stochastic models, the latter incorporating a random component and producing results in terms of probability distributions. While comprehensive process-based research models provide quantitative estimation of pesticide behaviour in soils, these are invariably “data-hungry” and likely to be too cumbersome for use in field situations. Management models put relatively less input data demand on the system and are capable of predicting pesticide behaviour in the field. However, few of these have actually been tested in the field. On the other hand, simple screening models designed to compare the relative mobility of pesticide chemicals, require few input parameters and hence are very attractive. However, these are not suitable for accurately predicting the environmental fate of a given pesticide.

Ian Ferris (this issue) dealt with the practical implications of these considerations in relation to the new generation of relatively water-soluble sulfonyleurea herbicides. He illustrated and emphasised the enormous benefit of pesticide use to Australian farmers in sustaining the viability of our farming system in difficult economic times. He cited risk assessment case studies which illustrated the dependency of leaching potential on the chemistry of the soil environment. While in one particular case, in a typical Western

Appendix 1

Workshop report

This workshop, on the evaluation of the groundwater pollution potential of pesticides was one of three conducted at the *Aquifers at Risk Conference*. These workshops were based on a research project entitled *Groundwater Quality: A systematic basis for aquifer protection in rural areas* funded by the Land and Water Resources Research and Development Corporation of Australia. The presently considered workshop examined the factors controlling and methods for modelling the mobility and persistence of pesticides within the soil profile with respect to their potential for groundwater pollution. The other two workshops, dealing with spatial modelling for aquifer vulnerability and design methods for sustainable land-treatment of rural industry and sewage effluent, are reported elsewhere in this volume.

The objectives of this component of the project are: (1) to quantitatively define the extent to which commonly used pesticides present a hazard in terms of groundwater pollution as a result of their mobility through soil profiles; (2) in practice to provide a detailed understanding of the

Australian sandy soil, there was not a great deal of leaching, the results were qualified by the sodicity and alkalinity of the soil and exhibited substantial variation. In other cases, in Victoria and South Australia there was evidence that long-term applications can result in accumulation and in some circumstances substantial leaching occurred. Coupled with overseas data the conclusion is that sulfonylureas are very vulnerable to leaching and clearly do leach. A major factor influencing leaching was rainfall infiltration and recharge.

Overview

Graham Aylmore briefly summarized the major points of concern arising from the previous presentations. He stressed the importance of recognizing the rooting and unsaturated zone as having a major influence in filtering out contaminants and in determining the extent to which pesticides will move from the surface down to the groundwater. The data presented clearly illustrated the dependence of pesticide mobility on the nature and chemistry of the pesticides and the way they are influenced by the chemical environment of the soil. The different modelling approaches serve different purposes with simple screening models giving useful comparisons of the likely impact of the hazards posed by these materials and research models being essentially of use to demonstrate mechanisms; for example time dependency of sorption processes. Particular emphasis was placed on the need to define the degree of complexity with which fundamental processes need to be treated in effective management models and the extent of characterisation of the variety of physical, chemical and biological parameters required to avoid problems of site specificity.

Main points of discussion

Greg Davis (CSIRO Division of Water Resources, W.A.):

You have outlined a lot of things, which could take 50 years of study. What are your immediate aims in terms of the LWRRDC project? What is your strategy and what areas do you hope to target?

Graham Aylmore:

Essentially we have two objectives. The first is to try to characterise the significance of the various factors involved and we have restricted ourselves to different representative classes of pesticide to try to get a handle on this. Initially we were working with laboratory-based experiments using soil columns and research-type models to evaluate the significance of the various mechanisms. We have also undertaken some field experiments at the Western Australian Horticultural Research Station at Medina, where we have applied representative pesticides in the field and monitored them over time by soil sampling and also by taking groundwater samples. The purpose of these studies is to determine how effectively existing screening and management models describe the processes that we are looking at and at the same time to refine these by investigating the processes in the laboratory. The overhead illustrates what I have been saying about the main points of concern and we are seeking feedback on these points. This emphasises firstly the importance of the unsaturated plant rooting zone. Secondly, there is the characterisation of sites: the sorptive properties, pH, and physical factors such as the soil structure, water repellency, and preferential flow paths. Thirdly, there is

the spatial variability, and finally the number of pesticide classes.

Chairman:

The reality is that in many instances the number of residual pesticides, fungicides, and the like, are added simultaneously. It is not just a case of adding one continually to a particular paddock — you might apply two or three in the course of a normal agricultural cycle, and often these are applied together. What complexity does that pose for the research models in understanding the sorption process? Are the pesticides compatible and do they mix? I might add that working out what pesticides can be used together is a major headache for the farmer. The real question is what happens sub-surface. This is a very big issue.

Rai Kookana:

One area in which the mixing of a number of herbicides and pesticides together makes the situation complex is in the degradation process. It is not just the mixing of a number of herbicides; it is in fact that this induces a certain type of bacterial population which is capable of degrading one type rather than another. With repeated applications of the pesticide, if you apply 24D in a soil this year, next year, the year after, the degradation will be faster. It is in terms of degradation that the influence will be greatest.

Chairman:

So we could be looking at a collectively longer half-life?

Rai Kookana:

That could be so.

Graham Aylmore:

Competitive adsorption is a major complexing factor which needs to be understood and anticipated.

Libbie Lau (Lau and Associates, ACT):

With pesticides you can regard the fraction that is leached into groundwater as virtually a waste. But it is not as simple as that with pesticides. I gather you can not just cut back the amount of pesticide you apply. Can you change the application rate of the pesticide? Is that immutable, or can it be changed to stop the amount of leaching into the groundwater so that you apply only as much as you need.

Ian Ferris:

There are guidelines for the concentration of pesticides in groundwater. We have a standard. Normally, I have grave reservations about standards, but in this case I believe that the 100 parts per trillion standard for sulfonylureas is about the toxicological level where we see an effect on plants. I hasten to add that this does not apply to people. This does not pose a problem for human beings. The LD50s for all these compounds are greater than 5000 mg per kilogram, so they are not a toxicological threat to people, but they can be for plants and trees in particular. We have a toxicological level that has been formulated, and that is the one we should try to work to. We are now undertaking a fairly intensive program to try to look at the management package, and that includes reducing the rate and the frequency. In the case of

sulfonylureas in alkaline soils, a reduction in both the rate and the frequency will have to be achieved. By and large, the regulation of these compounds is fairly strict and we need to ensure that the existing regulations regarding these compounds are adhered to.

There is a problem. When these materials were first introduced, the companies established very long recropping periods for these compounds — about two to three years — and in most cases growers found that they could recrop the following year. Thus, the guidelines were ignored because farmers felt that they were not relevant. Quite clearly in some cases they are relevant. So perhaps we should reinforce the existing guidelines on these compounds, in particular in the high-risk areas. In the northern areas where the risk is not so great, maybe we should cut it down. We could probably increase the frequency in many instances. Long-term simulations have shown that there is no need to have such a low frequency of application.

I might add that these chemistries are applying very low use rates, and that is very important in terms of how we perceive this type of exercise. Many people argue that these chemicals are the bridge between our non-sustainable systems of agriculture, which utilise large quantities of fossil fuel and sustainable systems and substitute very low use rates of these materials for mechanical cultivation.

John Bauld (AGSO, ACT):

I am interested in the way that these models may or may not deal with degradation products. As I understand it, they approach the disappearance of the present compound that is applied to the system. In some cases, degradation products may behave differently in soils or in the water table, and they may have greater or lesser degrees of toxicity. I am not suggesting that this is true in all cases, but some of those may be just as important as the parent compounds.

Rai Kookana:

This is a very important point. We know that certain compounds have given a lot of problems to citrus growers in Florida because they oxidise, first to sulfoxide and then to sulfones, which are equally toxic. One of our models, ERZM, has the capacity to deal with such problems. It has the capacity to include those daughter compounds which, as you said, are in some cases even more toxic.

One example of this is fenamiphos, a nematicide used in horticulture. This is incorporated in the soil as sulfoxide and sulfone. Because of the polarity of these daughter compounds, they are more mobile but more toxic. Therefore, it is very important to consider those daughter compounds.

Graham Aylmore:

We have done some work on materials that degrade into metabolites and we are trying to incorporate that into the management models.

Chairman:

What happens when sulfonylureas leach through to the water tables? What work has been done on that?

Ian Ferris:

Sulfonylureas derive in part from sulfonamide, which has been widely used since the 1930s as a bacterial static agent. Another part is triazine — most of us are familiar with atrazine and simazine, for example — and there is a bridge component as well. The unique feature is that when you put these chemistries together the result is an extremely active compound, and this is a novel feature of sulfonylureas.

The high activity is great for sustainability because it requires less energy. We do not have to put as much out and it is environmentally friendly for a lot of non-target organisms. Those are the good features.

The bad feature for analytical chemists is that we cannot measure them because at toxicological concentrations for highly susceptible plants, we do not have any adequate analytical procedures. The closest we have at the moment are the Eliza techniques, which although available, can be very unreliable. I would not recommend them. To get down to that 100 parts per trillion level — and I think you will all appreciate that it is a low level — is really a tough job which will require a lot more work.

Peter McDowall (Commonwealth Environmental Protection Agency, ACT):

There are indicated plant techniques using a root involving the use of lentil bioassays and things like that, using a specific known variety of lentil grown in soils. By measuring the root growth of that lentil you can quickly estimate the amount of chemistry left in the soil.

Ian Ferris:

We use lentil bioassays for nearly all our analytical work and our validation. There are two problems. The technique is very time-consuming, and its reliability is very questionable unless you have a lot of experience with it. In general, the technique works, but it is subject to a lot of interactions. For example, in these highly sodic soils (up to pH 10) the lentils will not grow, or they are severely affected. There are big interactions and it is a bit of a problem.

Graham Aylmore:

I would like to ask some of the hydrologists to comment on our emphasis on the rooting zone and unsaturated zone as the major filtration region for pesticides. My observation is that very often hydrologists tend to think of soils as a black box: "some goes in, some comes out, some stays in" and that the system can be readily characterised in a simple way. Am I right or am I wrong in thinking that?

Chris Barber (CSIRO Division of Water Resources, WA):

I particularly like the risk approach that you use to assess the leaching potential. But it struck me at the time that it only told half the story; the rest of it was, where did it go once it got through the rooting zone? That highlights the link with the vulnerability assessment project which really focuses on the groundwater resources. It is important to link the two and not just keep them separate. You will need to have a broader regional idea of what happens in the groundwater resource, as well as the localised information.

George Gates (Department of Water Resources, NSW):

We have recently been looking at pesticides and herbicides in groundwater in the cotton-growing areas of New South Wales. I guess we have sampled fewer than 100 bores, but we have found atrazine in about six out of 100 at depths in the water table of perhaps 25 m from the surface. The level has been between one and four parts per billion. Does it surprise you to find atrazine at that depth? Does it cause you concern?

Ian Ferris:

Chris Barber raised a good point. I did not mean to imply that there is no problem from sulfonyleureas. Obviously they impinge on farmers whose recropping is affected. If that involves a contained, perched water table, we do have a potential problem. Obviously we are working very hard to try to address that specific question. I try to refer to my risk analysis in terms of the whole of Australia. It is a national picture, but local people can be very badly affected, so we need to work on some of those site-specific issues.

On the question of atrazine, I must say that I am not really surprised about the problem that George raised in the cotton-growing areas. Although our models suggest that movement through the soil structure will not cause a large leaching problem, we certainly can have preferential flow in some of these areas. We have the possibility of preferential flow and we also have the possibility of movement of soils down the profile.

In case people are not familiar with this area of discussion, I point out that these soils are sodic, very often they can disperse under the influence of rainfall, and some of that soil can actually move down the profile, taking some of these materials, such as atrazine, which normally would not leach. They can get down to more than a metre below the rooting zone, so some of these hydrological processes can be important. In some cases, we have shallow water tables, and in other cases we have what I regard as unsafe disposal practices for atrazine. Perhaps I should broaden that out a little. Although it is registered for such use, I would not really recommend using atrazine in irrigation water situations. You can imagine what it is used for: weed control on river banks and aquatic weed control, where the risk is greater.

We must also couple that with point source pollution, i.e. the way people handled disposal of containers in the past. These were not little containers, like those used for sulfonyleureas, but huge drums. In the past, those drums were not recycled, but dumped in the local municipal tips. We have a number of potential sources which I would not regard as non-point source pollution. I have a feeling that if we look hard enough we will find a point source, or with aquatic weed control almost a point source application.

Pere Wyles (Sydney Water Board):

I am curious as to how your models might handle a situation such as that described earlier: the one at Yass, where there is highly volatile chemistry as a result of clearing the surface. Would your models not give unpredictable results, or are they all right?

Rai Kookana:

I thought we had already demonstrated so much more complexity in that instance. I think we are already too far away from the real situation because there are so many aspects which we do not understand too well. I do not quite know what to say about this one.

Graham Aylmore:

I think the answer is that you cannot be all things to all men. You can just try to solve the problems one at a time as best you can. There is just such complexity in the whole system. We have to learn to crawl before we can walk. We do not pretend that we can rapidly handle every situation.

Ray Evans (AGSO, ACT):

Are there any strategies in train to identify on a rigorous basis the areas in which we might expect to find potential problems? That might be of some use in helping to target research results towards problems in the community.

Graham Aylmore:

We are certainly seeking input from people nationally on the identification of problems. However, we have not yet reached the point where we want to go out and be troubleshooters, tackling specific field problems that people might come up with. I do not see us as having that state-of-the art expertise. Anyone who is doing any pesticide work anywhere gets inundated by investigative journalists, who know of a particular problem and want to involve you in solving it. As I said, I do not see us as troubleshooting, but we are interested in receiving information or input from people.

Ray Evans:

My impression is that much of the investigation is occurring on an opportunistic basis, where problems are being identified in the environment. Is there any plan to collect pesticide-use data on a national scale?

Graham Aylmore:

We would certainly like to, and intend to do that. We only started this program in the last six months. But certainly we would have that approach in mind further down the track.

How do Sodic Soils Behave? The Effects of Sodicity on Soil Physical Behaviour

H. B. So^A and L. A. G. Aylmore^B

^A Department of Agriculture, University of Queensland,
St Lucia, Qld 4072.

^B Department of Soil Science and Plant Nutrition,
University of Western Australia, Nedlands, W.A.6009.

Abstract

A model has been presented to illustrate the way in which the influence of exchangeable Na on the fundamental processes of dispersion and flocculation on Na-Ca systems affects the various soil physical properties in the field. Most cultivated soils slake (breakdown into microaggregates) when subjected to rapid wetting, giving rise to a surface seal and a reduction in infiltration rate. However, slaking alone may not necessarily reduce the soil's productivity, e.g. surface aggregates of the highly productive self-mulching black earths slake even when in the virgin state. If dispersion follows slaking, in most cases it will lead to poor physical properties which may manifest as poor drainage, surface crusting, hardsetting and poor trafficability or workability of the soil and eventually lead to reduced crop yields.

It is the dispersion phase that is affected by the presence of excessive sodium on the exchange complex of the soil, and this may have a profound effect on the soil's physical properties and behaviour. This paper reviews the possible mechanisms by which excessive sodicity may manifest in undesirable soil physical behaviour. It also attempts to relate observations made in the laboratory on pure Na-Ca-clay systems to the behaviour of the soil in the field.

The effect of sodium on the dispersive behaviour of a soil is discussed in relation to its hydraulic conductivity and the processes of infiltration, redistribution and evaporation of water which in turn affects the subsoil water storage in a soil profile. The presence of sodium is also discussed in relation to changes in soil strength characteristics, the soils workability and ease of tillage and ultimately the soil's productivity. Data are presented which show that the validity of a threshold ESP and the exclusive use of ESP as a measure of sodicity are open to question.

Keywords: sodicity, sodic soil, physical behaviour, dispersion, structural stability, exchangeable sodium percentage.

Introduction

Most cultivated soils slake, i.e. break down into smaller aggregates or microaggregates, when subjected to rapid wetting, giving rise to a surface seal and a reduction in infiltration rate. This is a result of the differential swelling of the soil aggregates and/or the entrapment of air (Quirk and Panabokke 1962). However, slaking alone may not necessarily reduce the soil's productivity; for example, surface aggregates of the highly productive self-mulching black earths slake even when in the virgin state. If slaking is followed by dispersion, observations shows that this leads in most cases to undesirable physical properties such as poor drainage, surface crusting, hardsetting and poor trafficability or workability of the soil and eventually leads to reduced crop yield. The mechanisms by which dispersion give rise to these field problems is not well understood.

It is difficult to discuss soil sodicity problems without reference to soil solution electrolyte concentrations (or salinity in its extreme), as they are very strongly related, and this interaction is an important factor in the management of sodic soils (Quirk and Schofield 1955). Although sodic soils are defined as soils with exchangeable sodium percentage (ESP) greater than 15 (USA; Richards 1954) or 6 (Australia; Northcote and Skene 1972), the basis for these critical values is not well defined. Differences between the two critical levels are partly related to the electrolyte levels of the water used in the investigations (Shainberg and Letey 1984), as well as differences in the mineralogy of the dominant colloidal clay present in the soils of the two continent. While in pure clay water systems the existence of a critical ESP can be clearly shown, in real soils a multitude of factors may influence the relationship between ESP and other soil physical parameters, and mask the critical ESP values.

A review of the effect of sodicity on water flow through soils and the response of soils to rainfall was presented by Shainberg and Letey (1984) and will not be repeated here. This paper will provide a framework that should enhance the understanding of the likely mechanisms by which sodicity may give rise to a variety of soil physical problems in the field. The framework will also provide a means of relating laboratory observations on the processes and behaviour of Na-Ca-clay systems to the behaviour of soils in the field. This paper will also review available data pertaining to some of the processes within that framework.

Much of the early work with sodicity attempted to generalize the results across a range of soils, and one way of achieving this is to eliminate or minimize the effect of soil texture by expressing the amount of sodium as a percentage of the exchange capacity, which represents the active fraction of the soil, i.e. clay and colloidal materials. This leads to the use of ESP as a measure of the sodicity of the soil. However, when one is concerned with bulk soil properties, the use of ESP is open to question and will be discussed.

The Effect of Structural Instability on the Soils Field Behaviour

Fig. 1 is a proposed framework showing the possible mechanisms by which sodicity may affect soil physical behaviour. When a soil slakes under rapid wetting followed by dispersion, it will result in the formation of a surface seal with a reduced hydraulic conductivity. This in turn will give rise to reduced rates of infiltration, redistribution and evaporation from the soil (So and McKenzie 1984). These are three fundamental processes determining the rate of water recharge in the subsoil, which is a major determinant of the growth and yield of crops grown on this soil (i.e. soil's productivity).

A consequence of the reduced rate of redistribution or drainage of the surface soil is temporary surface waterlogging, which is not conducive to seed germination and generally delays farm operations. Waterlogging is associated with a lack of oxygen needed for seed respiration. Hence an extended period of waterlogging may result in excessive imbibition of water without adequate embryo development resulting in a failure to germinate, known as 'seed bursting'.

The high water contents during periods of waterlogging at the surface are followed by high initial rates of evaporation (stage 1 evaporation), similar to evaporation from a free water surface. However, if the hydraulic conductivity of the soil is very low and unable to match the rate of water loss, the surface will

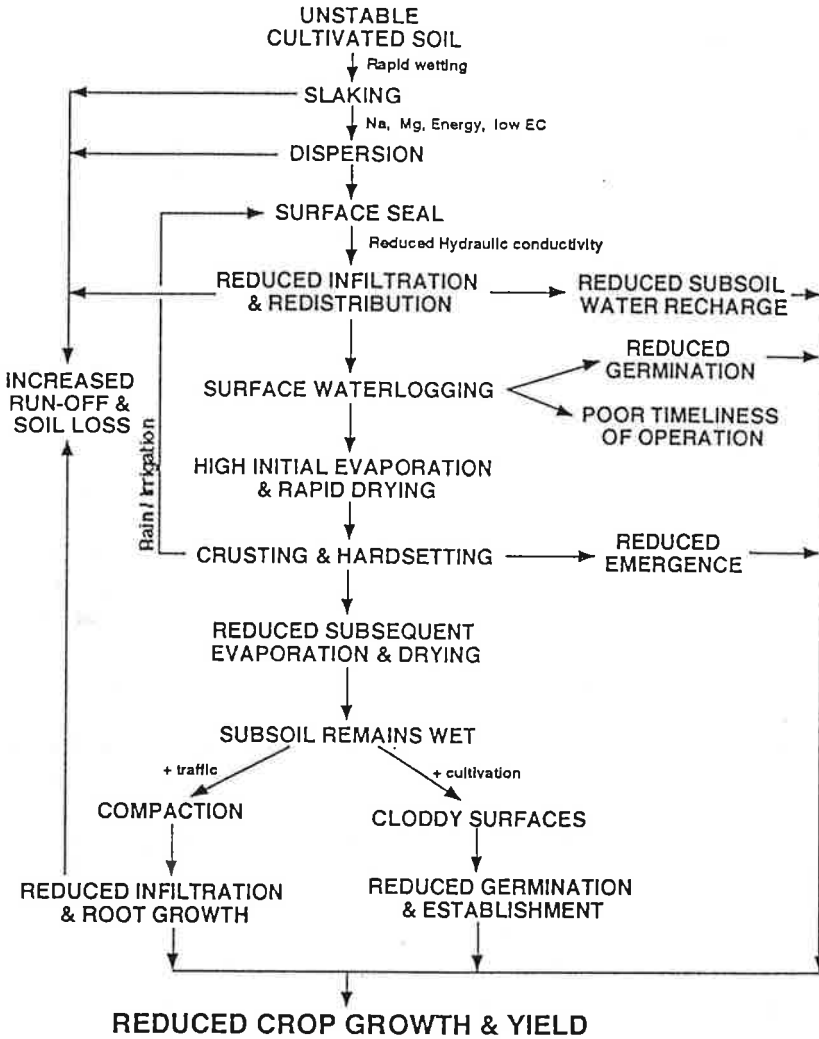


Fig. 1. Model showing the mechanism of how slaking and dispersion may affect soil physical properties and eventually crop yield. (adapted from So 1987).

dry rapidly followed by shrinkage and a breaking away of the dry surface into crusts. This is generally limited to a few centimetres in thickness. In contrast, if the soil hydraulic conductivity is sufficiently high and soil shrinkage capacity is limited, such as in loamy soils with high contents of sand and silt, drying may extend to a considerable depth resulting in a hardsetting soil. Both crusting and hardsetting reduce emergence of seedlings. However, hardsetting may also impede the germination and development of the seedling.

A surface crust or hardsetting surface represents a dry surface mulch where water movement is slow and predominantly in the vapour phase (advanced stage 2 evaporation). Therefore the rate of evaporation is reduced considerably, resulting in a slower rate of drying. Consequently the subsoil tends to remain wet and become susceptible to compaction or shearing. Traffic and cultivation at this time

will result in subsoil compaction and excessively cloddy surface tilth which is not conducive to seed germination. Alternatively, more cultivation is required to produce a suitably fine seedbed. Wet subsoils are also susceptible to compaction from swelling pressures from expanding clays and/or overburden pressures of wet soil. They are likely to give rise to the formation of subsoils with massive or coarse blocky structure.

Reduced germination or establishment coupled with reduced subsoil water is certain to cause significant reductions in crop yield. Furthermore, reduced infiltration and increased run-off coupled with slaking and dispersion will increase soil loss and erosion.

Sodicity, Dispersion and Hydraulic Conductivity of Clay Water Systems

It is important to understand the fundamental interaction between the negatively charged colloidal clay particles in the soil and the distribution of the counterbalancing exchangeable cations which control the processes of flocculation and dispersion.

In homoionic clay systems, the development of the diffuse double layer and the associated swelling or dispersive forces depend both on the valency of the exchangeable cation and the concentration of the external bulk solution. Aylmore and Quirk (1962) showed that Na-clay swells considerably more than Ca-clay, and that swelling in Na-clay increases rapidly as the electrolyte concentrations decreases. Furthermore, in distilled water or low electrolyte concentrations, it swells to the extent that the clay particles become detached from each other, producing spontaneous dispersion. On the other hand, Ca-clay exhibits limited swelling, associated with a much reduced zeta potential (Horikawa *et al.* 1988; Quirk and Murray 1991). Therefore, Ca-clay tends to remain clustered into domains (Aylmore and Quirk 1960), sometimes referred to as tactoids (Shainberg *et al.* 1971), even in deionized water (Rengasamy 1982). These effects are in turn modified by the mineralogy of the colloidal clay, in particular by its specific surface area. Thus, although the degree of swelling differs between clays of different mineralogy, the swelling pattern remains similar between illites and montmorillonites (Aylmore and Quirk 1960; Quirk and Murray 1991), but are reduced with kaolinitic materials. The concept of domains are now generally accepted as the correct model of how clay particles are found in the soil, associated with the dominance of Ca ions (Aylmore and Quirk 1962).

Fig. 2 shows that in a mixed cation system, the limited swelling of Ca-dominated clay systems are essentially unaffected until Na reaches a threshold of about 7–20% of the total cation suite (Shainberg *et al.* 1971), depending on the prevailing overburden pressure. When the exchangeable sodium percentage (ESP) exceeds the threshold value, swelling increases significantly with an increase in ESP. In contrast, small increases in ESP tend to have a large effect on the hydraulic conductivity of the clay paste and the decrease starts from a value of zero ESP (Shainberg and Caiserman 1971). This contradiction was explained in terms of the domain theory. At low values of ESP, Na ions were adsorbed on the outer surfaces of the domains, and it is only when the threshold ESP is exceeded that Na starts to enter the space within the domains, resulting in macroscopic swelling. The destruction of the domains was complete at ESP of around 50%. Therefore it can be concluded that initially, increasing sodium results in the dispersion of

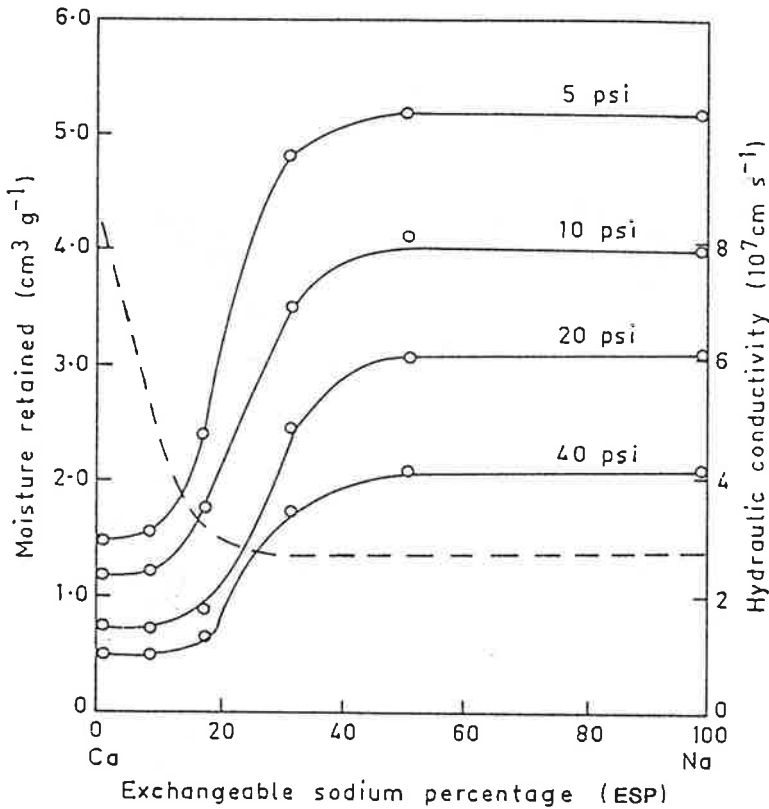


Fig. 2. The moisture content (swelling) in solid lines and the hydraulic conductivity (broken line) of montmorillonite as affected by exchangeable sodium percentage (adapted from Shainberg *et al.* 1971 and Shainberg and Caiserman 1971).

the aggregates into domains, which are small enough to be transported with the water and block the larger pores resulting in a reduced hydraulic conductivity (K). At higher values of ESP, macroscopic swelling may contribute to a further reduction in K .

Sodicity, Dispersion and Hydraulic Conductivity of Soils

The effect of increasing sodium on the amount of dispersed clay in Vertisols from the Darling Downs in Queensland is shown in Fig. 3 (Cook 1988; So and Cook 1992). Data represent soils with clay contents from 39 to 75%. Dispersion is expressed as either Dispersion Ratio (DRC, dispersed clay as a proportion of clay content) or the amount of Dispersed Clay (DC, as a proportion of the bulk soil). Exchangeable sodium is expressed as either ESP or ES (as a proportion of the bulk soil). All samples have low concentration of soluble salts with a range of EC (1:5) between 0.11 and 0.17 dS/m. Fig 5 shows that the relationships are better when sodium is expressed as ES, with the best relationship obtained between the bulk soil parameters ES and DC:

$$DC = 0.029 + 0.023*ES, \quad R^2 = 0.77***. \quad (1)$$

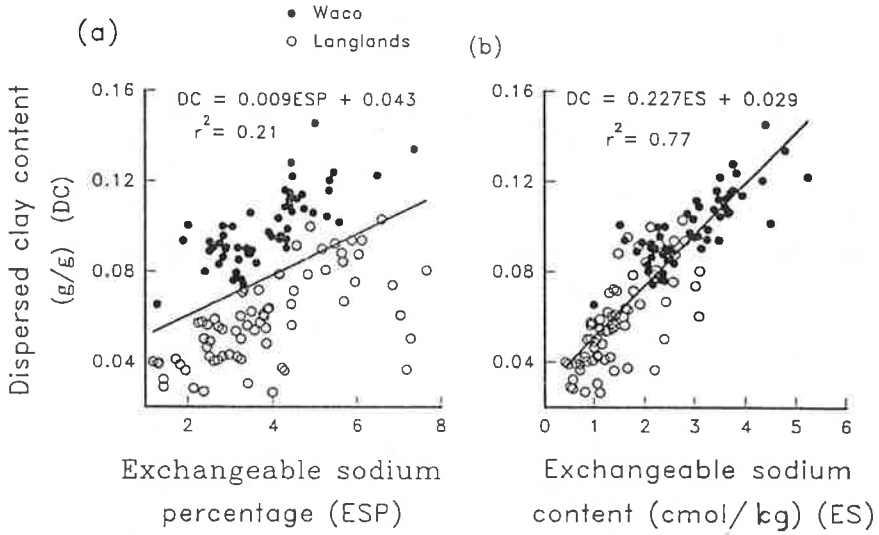


Fig. 3. Dispersed clay content of two Vertisols from the Darling Downs, Queensland, as a function of (a) the exchangeable sodium percentage (ESP) and (b) exchangeable sodium content (ES) (after So and Cook 1992).

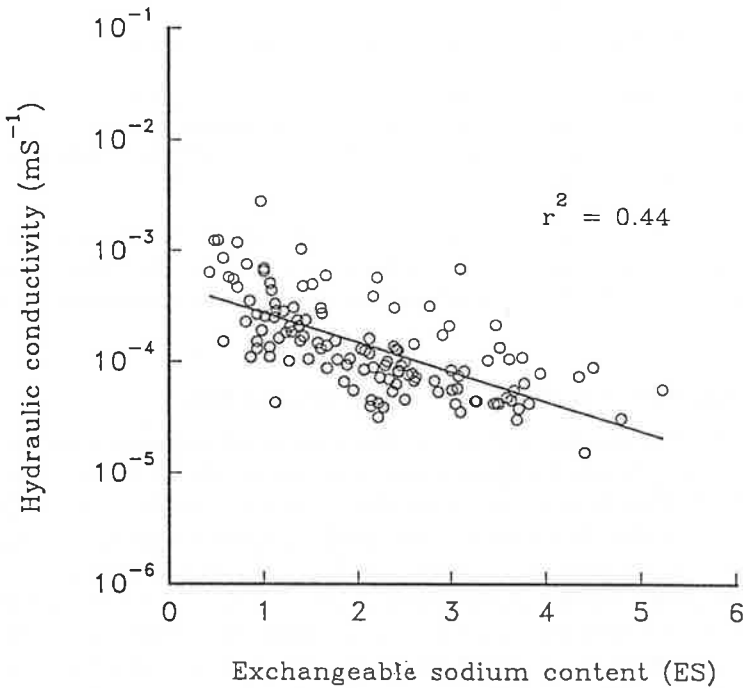


Fig. 4. The relationship between hydraulic conductivity and exchangeable sodium content (ES) for the same Vertisols from the Darling Downs, Queensland as in Fig. 5a.

The relationship between ESP and DRC is poor with an R^2 of 0.38, but is significant at $P < 0.001$. One possible reason for the poor relationship is the failure to include other colloidal fractions (organic matter) which contribute to the cation exchange capacity in the parameter DRC. Dispersion is also affected by clay content and the relationship in equation 1 can be further improved by the inclusion of this parameter:

$$DC = -0.021 + 0.013*ES + 0.0012*Clay, \quad R^2 = 0.88***. \quad (2)$$

If particles of $<20 \mu\text{m}$ equivalent diameter are taken as dispersed material, similar equations can be shown for the parameter (Dispersed Silt+Clay contents -DS), which requires a much shorter sampling time:

$$DS = 0.170 + 0.066*ES, \quad R^2 = 0.66*** \quad (3)$$

$$DS = -0.019 + 0.028*ES + 0.0044*Clay, \quad R^2 = 0.82***. \quad (4)$$

It is important to note that in equations 1 to 4, ES starts from zero with no threshold value in its effect on dispersion of clay or silt+clay.

Similarly Rengasamy and Olsson (1991) showed significant relationships between the dispersive potential, partly a function of sodicity, and the amount of spontaneously dispersed clay for illite dominated soils.

Fig. 5 shows the effect of ESP on the hydraulic conductivity of the same range of Darling Downs Vertisols measured after 6 h of flow under constant head (Cook 1988; So and Cook 1992) and Fig. 5 a similar relationship for kaolinitic dominated soils from the Western Australian wheatbelt (Aylmore and Sills 1982). The relationship between ESP and K can be improved if ESP is replaced with the bulk soil parameter ES (Fig. 6) where the latter parameter accounts for 44% of the variability of the data. A better relationship is obtained if K is regressed against dispersed clay DC ($R^2 = 0.56***$), which is consistent with the findings of Shainberg and Caiserman (1971), that the effect of exchangeable sodium on hydraulic conductivity is mediated through the effect of sodium on dispersion.

For some Darling Downs Vertisols subjected to continuous wheat cropping, the ES of the surface soils tends to increase with the period of cultivation. This is thought to be associated with the loss of topsoil through water erosion, since many Vertisols have increasing sodicity with depth, and soil loss will expose increasingly sodic soil (Cook *et al.* 1991). Vertisols under 15 years of continuous irrigated cotton also showed an increase in ESP of the surface soils, associated with mixing of the subsoil and surface soil from deep tillage practices (McKenzie *et al.* 1991)

The data in Fig. 6 were derived from surface soils where the electrolyte concentrations of the soil solutions were relatively low. If the electrolyte concentration is increased, it may suppress the effect of sodium on dispersion.

Effect of Exchangeable Magnesium

The effect of Na on dispersion and the soils hydraulic conductivity can be exacerbated by the presence of excessive exchangeable Mg as shown by Bakker *et al.* (1973) on the subsoils of the red brown earth (RBE) from Shepparton, Victoria

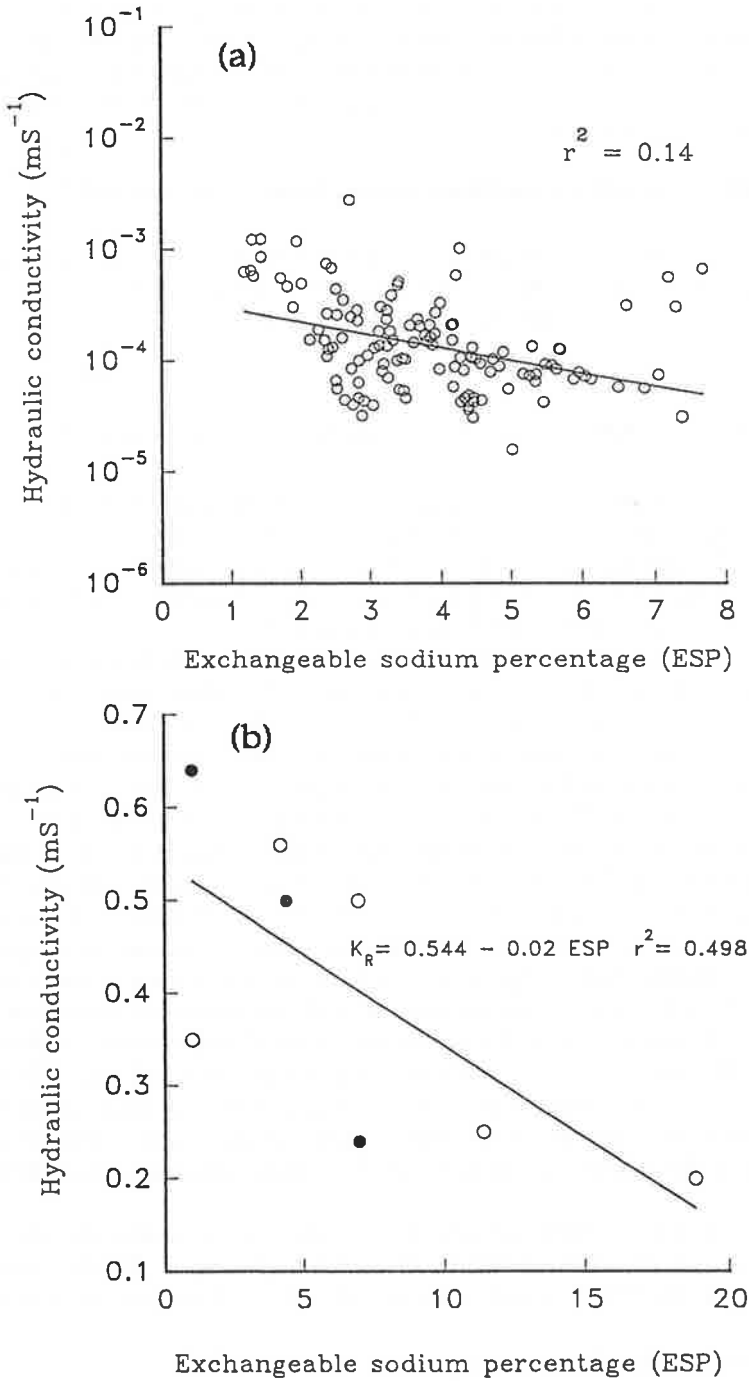


Fig. 5. The effect of exchangeable sodium percentage on the hydraulic conductivity of (a) Vertisols from the Darling Downs, Queensland and (b) kaolinitic-dominated soils from Merridin, W.A.

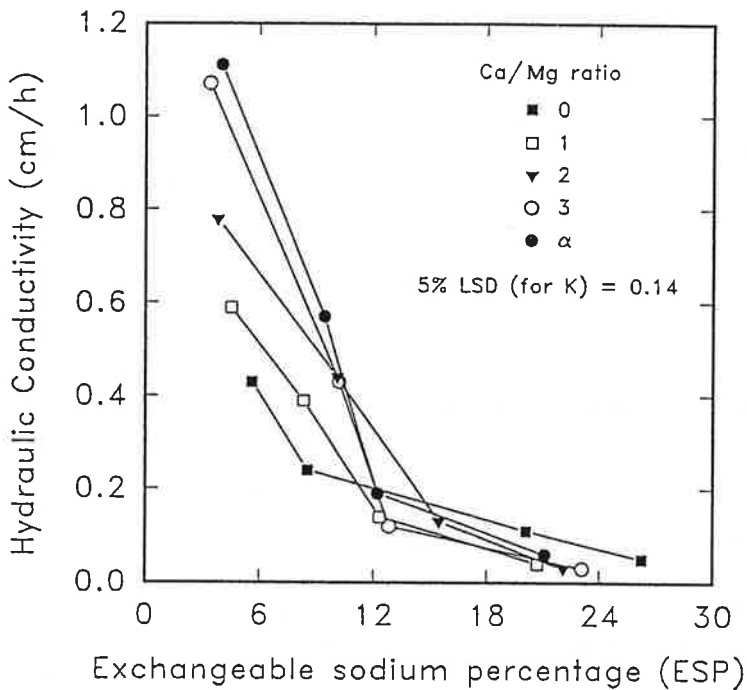


Fig. 6. The effect of ESP and Ca/Mg ratios on the hydraulic conductivity of a Vertisol (72% clay) from northern N.S.W. (after Horn 1983).

and in Fig. 6 for a Vertisol (Horn 1983). Although Bakker *et al.* concluded that Ca/Mg ratios of less than 2 indicates potential physical problems on the RBE, no similar threshold value was found for the Vertisols. The action of magnesium is obvious until the ESP reaches a value of 12, beyond which the effect of Na becomes dominant.

Despite these effects of Mg on soil materials in the laboratory, detrimental effects of exchangeable Mg is often not observed in field soils. However, as Emerson (1977) pointed out, Na-Mg-clay disperses at a considerably lower water contents than Na-Ca-clay when remoulded. Therefore, soils high in exchangeable Mg are potentially dispersive when cultivation is carried out at high water contents.

Sodicity and Soil pH

In mixed cation systems where both Na and Ca are present on the clay, the ratio of Na and Ca concentrations in the soil solution affects the ratio of the exchangeable Na and Ca according to the Gapon equation (Quirk and Murray 1991):

$$E_{Na}/E_{Ca} = K_G * [Na]/[Ca]^{0.5}$$

or

$$ESR = K_G * (SAR),$$

where E_{Na} and E_{Ca} are the fractions of the exchange complex occupied by those ions, K_G is the Gapon constant and the square brackets indicate concentrations (in mmol dm^{-3}) of the ions in solution. ESR and SAR are the exchangeable sodium ratio and sodium adsorption ratio respectively. The reported values of K_G range from 0.0072 to 0.020 (Richards 1954; Bakker *et al.* 1973, Shainberg and Letey 1984), depending on the mineralogy of the clay. The Gapon equation shows that a small change in ESR will result in a large change in SAR. Therefore, a small increase in ESR or ESP (the two are similar at low values) will result in a large increase in the proportion of Na ions in the equilibrium soil solution. This will give rise to an increase in the soil pH, and values of 8.5–9.5 are common and generally indicative of sodic soils.

Sodicity and Available Soil Water

The detrimental effect of sodium on the processes of soil water redistribution and evaporation are seen in Fig. 7 where gypsum application was used to suppress the dispersion from a sodic Vertisol (McKenzie 1982; So and McKenzie, 1984). Furthermore, the same experiments show that the rate of infiltration on undisturbed columns of this Vertisol (72% clay, ESP 7%) was increased 12-fold by the application of 7.5 t/ha gypsum. On another lighter-textured Vertisol (34% clay, ESP 11%) the same application of gypsum resulted in infiltration rates 2.5 times that of the untreated soil. Similarly, Loveday (1976, 1984) observed a 14-fold increase in the hydraulic conductivity (48-hour value) of a transitional red-brown earth (clay loam) typical of the Riverina, N.S.W., following the application of 12.5 tons/ha of gypsum.

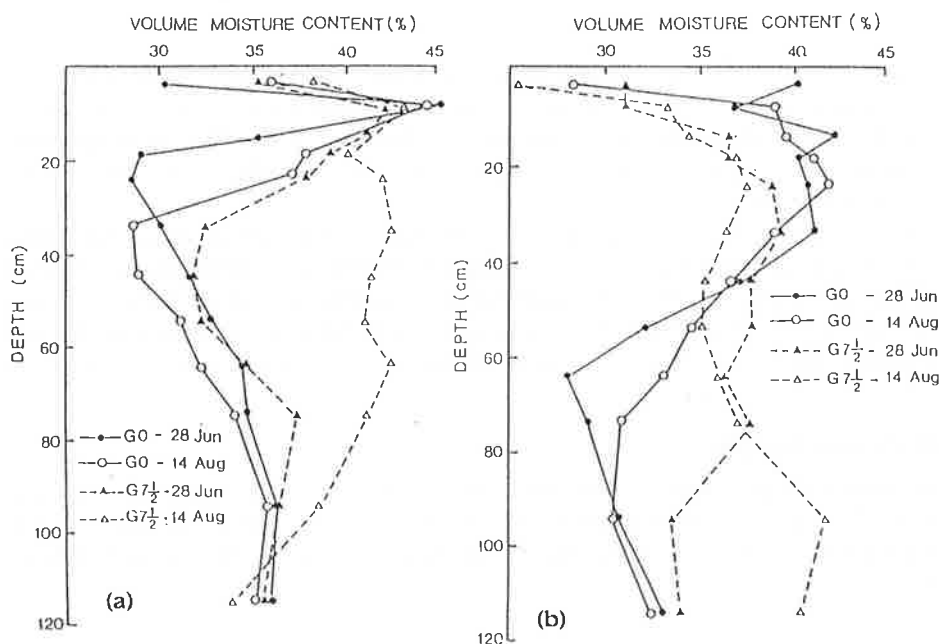


Fig. 7. Volumetric water contents as a function of depth for two Vertisols at (a) Delvin (72% clay) and (b) Wyndella (34% clay), N.S.W., in the winter of 1978 (after So and McKenzie 1984).

It is not surprising then that a reduced rate of water redistribution into the soil profile, associated with excessive Na, may result in transient waterlogging of the surface soil, which in turn may prevent seed germination due to a lack of oxygen. It will also result in longer periods of excessive wetness and hence poor timeliness for tillage operations.

Sodicity and Soil Strength

Surface waterlogging gives rise to high initial rates of evaporation and rapid drying of the surface soil and can result in the development of hardsetting or surface crusting to an extent depending on the soil texture. Fig. 8a shows the linear relationship between ESP and the strength of two hardsetting soils from Meridin, W.A. The slopes of these relationship indicates the sodium sensitivity of the soil, which increases with the net negative charge of the clay fraction (Rengasamy and Olsson 1991). An important point of this relationship is that for a given soil, ESP is a good indicator of its hard-setting behaviour. The effect of increasing ESP on MOR is mediated through the effect of ESP on the

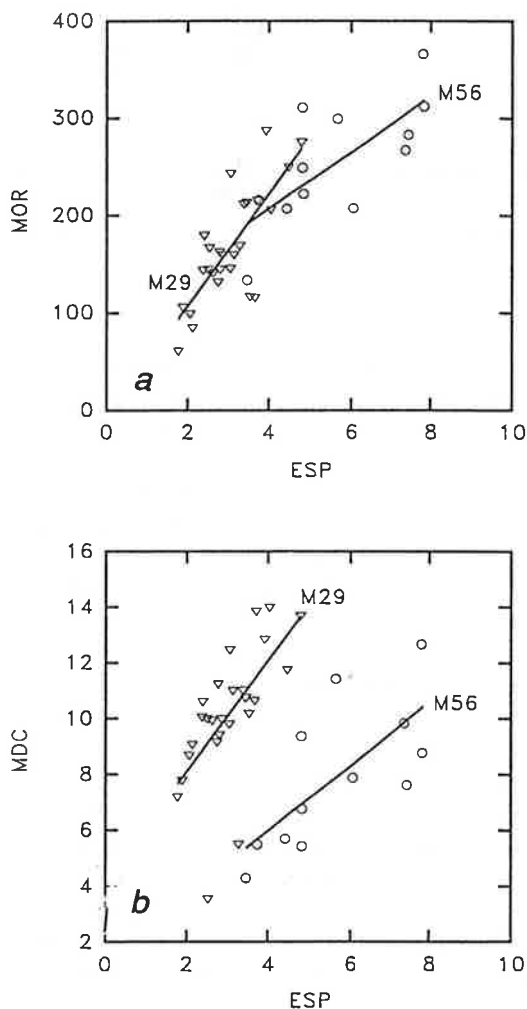


Fig. 8. The Modulus of Rupture, MOR (a) and Mechanically Dispersed Clay, MDC (b) as a function of ESP for three soils from the Meridin region of W.A. The relationships for soil M56: $MOR = 28.6ESP + 94.4$ ($R^2 = 0.50$) and $MDC = 1.16ESP + 1.32$ ($R^2 = 0.50$) and for soil M29: $MOR = 56.02ESP - 1.7$ ($R^2 = 0.59$) and $MDC = 1.96ESP + 4.2$ ($R^2 = 0.40$).

dispersed clay (Fig. 8b) and is similar to the effects observed on illite dominated soils (Rengasamy and Olsson 1991). However, ESP by itself is not a particularly good indicator of physical behaviour across a group of soils (Fig. 9a), as there are large differences between the sodium sensitivities of these hardsetting soils. Hardsetting of the surface soil invariably results in reduced seedling emergence and Fig. 9b demonstrated that increasing values of MOR are associated with decreasing seedling emergence across the soils.

Rapid drying of the immediate surface layer may give rise to surface crusting on the Vertisols which will also reduce seedling emergence (Doyle *et al.* 1979). Suppressing dispersion on these soils results in a reduction of crust strength and increased emergence (Davidson and Quirk 1961; Doyle *et al.* 1979).

Sodicity and the Soils Workability

Dry surface layers can constitute a surface mulch where water transport is predominantly in the vapour form, with the result that the rate of subsequent drying is reduced and the subsoil remains wet and susceptible to compaction and shearing. The use of gypsum to suppress dispersion results in greater soil hydraulic conductivity and a faster rate of water redistribution from the surface to the subsoil. Waterlogging is prevented and timeliness of operation is improved. However, it will also result in an increased ability of the subsoil to supply and maintain the surface soil in a moist and friable condition. This results in an increased ease of tillage, which can be manifested in one or more of the following parameters: reduced fuel consumption, increased velocity of tractor, reduced wheelslip and greater depth of working (McKenzie 1982; McKenzie and So 1989).

Sodicity and Soil Productivity

Assuming adequate nutrition, a soils productivity is largely determined by the probability of successful seedling establishment, the depth of root development and the amount of water stored in the subsoil. The effect of sodium on seedling establishment has already been discussed. However, for small grain crops which exhibit strong tillering characteristics, reduced establishment is generally not a problem unless it results in very low plant densities. Poor establishment is a major limitation to productivity with single tiller crops (summer crops).

Sodicity may affect root development when the subsoil pH is high. Experience with solution cultures showed that root growth ceased at pH values of around 9; however, it is not clear if soil pH values of 9–9.5 will actually stop root growth. Sodicity, however, may affect root development indirectly through high soil strength associated with soil compaction and reduced soil water contents.

The ability of a sodic soil to replenish its subsoil water storage is generally poor as shown in Fig. 9. In the Gwydir Valley Vertisols increased dispersion is most strongly associated with increasing sodicity (Yates 1972; Yates and McGarity 1984), and the survey by So and Onus (1984) showed that increasing dispersion is largely responsible for the reduced productivity of these soils (Fig. 10). Abrol *et al.* (1973) reported that the use of gypsum on the highly sodic soils from India resulted in greatly increased yields of a variety of crops, associated with increased water infiltration rates. On the kaolinite dominated soils of the W.A.

Influence of ESP on MOR

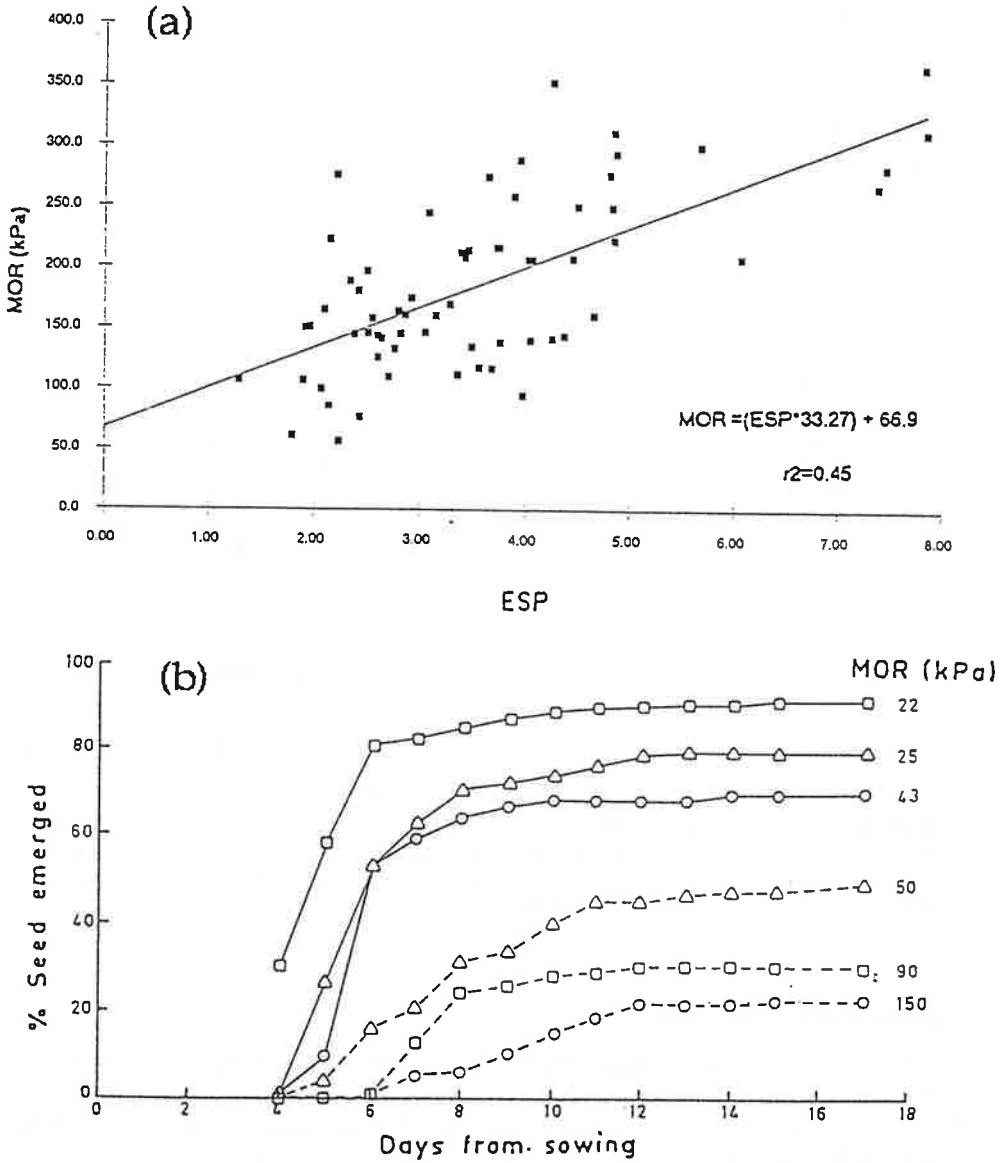


Fig. 9. (a) The Modulus of Rupture (MOR) for soils from the Meridin region, W.A. as a function of ESP. (b) The effect of MOR on the percentage emergence of seeds sown into hardsetting soils from W.A.

wheat-belt, the application of 5 tons/ha of gypsum significantly increased wheat yields (Cochrane and Aylmore 1991). The relative increase in wheat yields were associated with the dispersive failure, which is the reduction in the modulus of rupture resulting from the application of gypsum and presumably associated to a considerable extent with the suppression of dispersion.

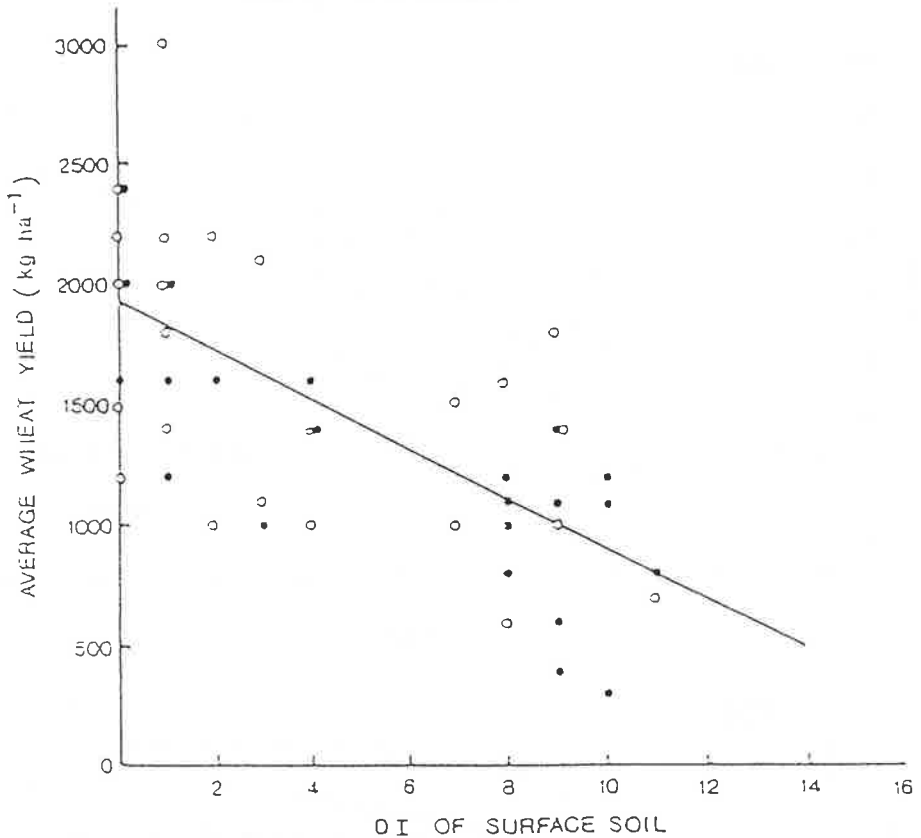


Fig. 10. Average wheat yield (Y) (estimate given by farmers) plotted against the Dispersion Index (DI) of the soil from the Gwydir Valley, N.S.W. Open circles are samples collected south of Moree and closed circles from north of Moree. $Y = -97.8DI + 1921.8$, $r = -0.67$ ($P = 0.01$) (after So and Onus 1984).

Summary and Conclusion

The model presented here illustrates the way in which the influence of exchangeable Na on the fundamental processes of dispersion and flocculation in Na-Ca systems affects the various soil physical processes in the field. While quantitative data are not available to validate every step within that model, circumstantial evidence derived from the use of gypsum on sodic soils as well as field observations are consistent with the model where dispersion plays a central role in determining the behaviour of sodic soils. The role of dispersion in kaolinite dominated soils is less dominant than in the 2:1 clay systems.

Data have been presented to show that in pure clay systems macroscopic swelling is not significant until ESP reaches threshold values between 7 and 20%. This threshold value is not translated into processes directly observable in the field. None of the measured soil physical parameters to date have shown that a threshold value of 6% or 15% for ESP is valid. In fact the survey by Yates (1972) of 18 properties in the Gwydir Valley, N.S.W., showed that of the paired

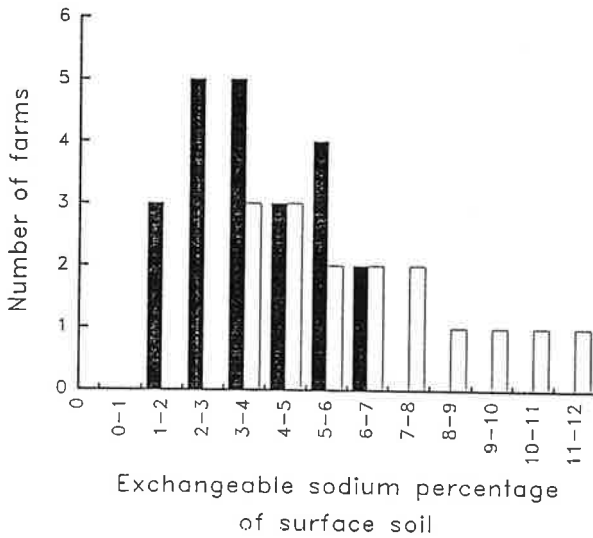


Fig. 11. Frequency distribution of ESP on paired sites from 18 farms in the Gwydir Valley, N.S.W. Solid bars refers to sites with good establishment and yields for wheat, and open bars refers to sites with poor establishment and yields (adapted from Yates 1972).

sites on each property, associated with poor and good establishment and yield of wheat on the Grey Clay soils, the poor sites showed a range of ESP between 3 to 12%, whereas the good sites had a range of 1 to 7% (Fig. 11).

The data presented indicate that the exclusive use of ESP as a measure of soil sodicity may not always be appropriate. It is suggested that the use of the term Exchangeable Sodium Content (ES) be retained where bulk soil properties are being considered, at least until the conditions for which ES or ESP is the most appropriate parameter to use have been defined.

Future Work

Some of the relevant agronomic work reported here has been derived from a narrow range of soils and some was inferred from the use of gypsum which suppressed the dispersion caused by Na. To develop improved management practices for sodic soils, a coordinated approach is needed to develop functional relationships between sodicity and the relevant parameters of structural stability, soil strength, soil water etc.

References

- Abrol, I. P. Dargan, K. S., and Bhumbla, D. R. (1973). Reclaiming alkali soils. Central Soil Salinity Res. Inst. Bull. No. 2, Karnal, India.
- Aylmore, L. A. G., and Quirk, J. P. (1960). Domain or turbostratic structure of clays. *Nature*, **187**, 1046-8.
- Aylmore, L. A. G., and Quirk, J. P. (1962). The structural status of clay systems. *Clays & Clay Miner.* **9**, 104-30.
- Aylmore, L. A. G., and Sills, I. D. (1982). Characterization of soil structure and stability using modulus of rupture-exchangeable sodium percentage relationships. *Aust. J. Soil Res.* **20**, 213-24.

- Bakker, A. C., and Emerson, W. W. (1973). The comparative effect of exchangeable calcium, magnesium, and sodium on some physical properties of red-brown subsoils. III. The permeability of Shepparton soil and comparison of methods. *Aust. J. Soil Res.* **11**, 159-65.
- Bakker, A. C., Emerson, W. W., and Oades, J. M. (1973). The comparative effects of exchangeable calcium, magnesium and sodium on some physical properties of red brown earth subsoils. 1. Exchange reactions and water contents for dispersion of Shepparton soil. *Aust. J. Soil Res.* **11**, 143-50.
- Cochrane, H. R., and Aylmore, L. A. G. (1991). Assessing management-induced changes in the structural stability of hardsetting soils. *Soil & Tillage Res.* **20**, 123-32.
- Cook, G. D. (1988). Degradation of soil structure under continuous cultivation on the Darling Downs, Queensland. Ph.D. Thesis, University of Queensland.
- Cook, G.D., So, H. B., and Dalal, R. C. (1992). Structural degradation of two Vertisols under continuous cultivation. *Soil & Tillage Res.* **24**, 47-64.
- Davidson, J. L., and Quirk, J. P. (1961). The influence of dissolved gypsum on pasture establishment on irrigated sodic clays. *Aust. J. Agric. Res.* **12**, 100-12.
- Doyle, A. D., Tayler, D. W., Yates, W. J., So, H. B., and McGarity, J.W. (1979). Amelioration of structurally unstable grey clay soils in the north-western wheatbelt of NSW. *Aust. J. Exp. Agric. Anim. Husb.* **19**, 590-8.
- Emerson, W. W. (1977). Physical properties and structure in soil factors. (Eds J. S. Russell and E. L. Greacen.) pp. 78-105. (University of Queensland Press: Brisbane.)
- Horikawa, Y., Murray, R. S., and Quirk, J. P. (1988). The effect of electrolyte concentrations on the Zeta-potentials of homoionic montmorillonite and illite. *Colloids and Surfaces* **32**, 181-95.
- Horn, C. P. (1983). The effect of cations on soil structure. Dip.Ag.Sc. Thesis, University of New England, Armidale, N.S.W.
- Loveday, J. (1976). Relative significance of electrolyte and cation exchange effects when gypsum is applied to a clay soil. *Aust. J. Soil Res.* **14**, 361-72.
- Loveday, J. (1984). Amendments for reclaiming sodic soils. In 'Soil Salinity under Irrigation'. (Eds I. Shainberg and J. Shalhevet.) Ecol. Ser. No. 51. pp. 220-37. (Springer Verlag: Berlin.)
- McKenzie, D. C. (1982). Amelioration of structurally unstable grey clays. M.Ag.Sc. Thesis, University of New England, Armidale, N.S.W.
- McKenzie, D. C., and So, H. B. (1989). Effect of gypsum on Vertisols of the Gwydir Valley, New South Wales. 2. Ease of Tillage. *Aust. J. Exp. Agric.* **29**, 63-7.
- McKenzie, D. C., Abbott, T. S., and Higginson, F. R. (1991). The effect of irrigated crop production on the properties of a sodic Vertisol. *Aust. J. Soil Res.* **29**, 443-53.
- Northcote, K. H., and Skene, J. K. M. (1972). Australian soils with saline and sodic properties. CSIRO Aust. Soils Publ. No. 27.
- Quirk, J. P., and Panabokke, C. R. (1962). Incipient failure of soil aggregates. *J. Soil Sci.* **13**, 60-70.
- Quirk, J. P., and Murray, R. S. (1991). Towards a model for soil structural behaviour. *Aust. J. Soil Res.* **29**, 829-68.
- Quirk, J. P., and Schofield, R. K. (1955). The effect of electrolyte concentration on soil permeability. *J. Soil Sci.* **6**, 163-78.
- Rengasamy, P. (1982). Dispersion of calcium clay. *Aust. J. Soil Res.* **20**, 153-8.
- Rengasamy, P., and Olsson, K. A. (1991). Sodicity and soil structure. *Aust. J. Soil Res.* **29**, 935-52.
- Richards, L. A. (1954). (Ed) Diagnosis and improvement of saline and alkali soils. U.S.D.A. Agricultural Handb. 60. (Government Printer; Washington D.C.)
- Shainberg, I., Bresler, E., and Klausner, Y. (1971). Studies on Na/Ca montmorillonite systems. 1. The swelling pressure. *Soil Sci.* **111**, 214-19.
- Shainberg, I., and Caiserman, A. (1971). Studies on Na/Ca montmorillonite systems. 2. The hydraulic conductivity. *Soil Sci.* **111**, 277-81.
- Shainberg, I., and Letey, J. (1984). Response of soils to saline and sodic conditions. *Hilgardia* **52**, 1-57.
- So, H. B. (1987). Soil physical factors limiting crop establishment. In 'Crop Establishment in Queensland: Recognition, Research and Resolution'. (Eds I. M. Wood, W. H. Hazard and F. R. From). AIAS Occasional Publication No. 34. pp. 154-65.

- So, H. B., and Cook, G. D. (1992) The effect of slaking and dispersion on the hydraulic conductivity of clay soils. *Catena* (in press).
- So, H. B., and McKenzie, D. C. (1984). Use of gypsum in the management of the grey and brown clays of the Lower Gwydir Valley, N.S.W. In 'The Properties and Utilization of Cracking Clay Soils'. (Eds J. W. McGarity, E. H. Hoult and H. B. So.) *Reviews Rural Sci., University of New England*, pp. 329-34.
- So, H. B., and Onus, G. C. (1984). The extent of unstable grey and brown clays in the Lower Gwydir Valley, New South Wales, and its relationship to wheat yields. In 'The Properties and Utilization of Cracking Clay Soils'. (Eds J. W. McGarity, E. H. Hoult and H. B. So.) *Reviews in Rural Sci., University of New England*, pp. 132-5.
- Yates, W. J. (1972). Factors affecting the structural instability of clay soils in the Moree area, NSW. M.Rur.Sc. Thesis, University of New England, Armidale, N.S.W.
- Yates, W. J., and McGarity, J. W. (1984). Structural instability in grey clay soils. In 'The Properties and Utilization of Cracking Clay Soils'. (Eds J. W. McGarity, E. H. Hoult and H. B. So.) *Reviews Rural Sci., University of New England*, pp. 123-31.

Manuscript received 31 May 1993, accepted 13 September 1993

MECHANISMS AND MODELLING OF HERBICIDE MOBILITY AND POTENTIAL FOR GROUNDWATER POLLUTION : AN OVERVIEW

R.S. Kookana¹ and L.A.G. Aylmore

Soil Science and Plant Nutrition, University of Western Australia, Nedlands, WA 6009, Australia

¹ Present address : Cooperative Research Centre for Soil and Land Management
Private Bag No. 2, Glen Osmond, SA 5064, Australia

Abstract

The use of herbicides and the processes determining their behaviour and fate in the soil environment together with the mathematical models available to predict their mobility and potential for groundwater pollution, are briefly reviewed. Herbicides are of tremendous benefit to agriculture and modern agricultural systems rely heavily on chemical means of weed control. Their increasing use has, however, resulted in contamination of ground and surface waters under certain conditions with consequent growing concern in the international community regarding their potential effects on non-target organisms. A sound understanding of the factors affecting the mobility of pesticides in soil is an essential prerequisite to the development of functions/models which can accurately represent and describe the array of processes which pesticides may undergo in soils. This requires detailed investigations on equilibrium and kinetic aspects of the sorption and desorption processes involved, the nature, extent and rate of any chemical transformation or biological degradation which occurs and the roles of volatilization, convection, diffusion and dispersion in the mobility of the pesticides in relevant soil structures. While a substantial amount of data is available on the interactions of pesticide chemicals with soil constituents, much of this has been obtained on European and North American soils. In addition to the differences in nature and properties of soils and climatic conditions between various regions of the world, there are a number of factors which modify the behaviour of pesticides at a specific site. The effects of soil properties such as texture, clay mineral species, organic matter content, pH, salts and competitive species present, previous use of herbicides, product formulations and combinations of herbicides applied, need to be measured in detail for a range of local soil-pesticide combinations relevant to any given region. In particular the significance of sorption/desorption time-dependency and long-term reversibility of sorption on the mobility of pesticides, mechanisms of volatilization and its contribution towards herbicide dissipation and the effects of soil environment on the rates of degradation under natural leaching conditions in the field, remain poorly understood. The literature contains a multiplicity of predictive models varying tremendously in terms of their complexity and proposed applicability. On the one hand simple screening models are easy to use and less data intensive but for that reason are less credible. Research models or detailed management models on the other hand lose credibility because of their complexity, difficulty in use and their data demand which cannot be satisfied with accurate information. While models based on the current state of knowledge in this area are unlikely to be particularly accurate or globally applicable, they nevertheless provide very useful tools for predicting the potential fate of herbicides in the soil environment. There is, however, an urgent need to define the degree of complexity with which fundamental processes are treated in such models and the extent of characterisation of the range of physical, chemical and biological mechanisms required to avoid problems of site specificity and to provide a satisfactory data base for predictive modelling.

Keywords : Herbicides, sorption, degradation, volatilization, transport, modelling approaches, groundwater pollution, models

Introduction

Since the discovery of the potential of organic chemicals in controlling weeds and other pests, there has been a rapid rise in their use as herbicides. Agricultural productivity has increased tremendously during this period and the use of herbicides has contributed significantly towards this increase. Weed control through herbicides is preferred over mechanical methods not only for economic reasons but also to avoid soil degradation through continuous cultivation. With the adoption of reduced tillage practices, the use of herbicides has increased considerably in many countries. In Australia, for example, herbicides have generally constituted some two thirds of the total sale of pesticides and during the last fifteen years (1978 to 1992), the sale of pesticides at the factory gate has increased from \$90 millions to \$703 millions (4). Notwithstanding inflation, this is a rapid increase indeed. Pesticides, if used as recommended, generally lead to little adverse impact on the environment. However, in recent years it has become evident that pesticides residues are present in soil, water and air which may result in harmful effect on human and environmental health. Consequently community concerns regarding the potential effects of pesticides on non-target organisms have also grown immensely in recent years.

Many herbicides are applied directly to soil while others reach it in substantial proportions by means of foliar wash-off with rain, spray drift, plant residues etc. Hence the processes which herbicides undergo in the soil need to be properly understood in order to evaluate their relative importance in governing the transport of herbicides from the intended zone of their activity to non-target zones. The processes which largely determine the fate of herbicides in the soil environment are retention/release, transformation and transport and of course, the interactions between these processes. Modern computers have made it possible to integrate these processes through simulation models using numerical methods and to predict the behaviour of herbicides under a given set of conditions and their likely impact on the environment.

In this paper, we provide an overview of the various processes together with a short review of mathematical models available to predict the behaviour and fate of herbicides in the soil environment. Although the processes governing the mobility of herbicides and the

modelling aspects are discussed separately, the implications of processes/concepts on modelling have been discussed throughout the paper.

Benefits of Herbicides to Agriculture

The benefits of herbicides to agriculture are immense and modern agricultural systems rely heavily on chemical means of weed control. It has long been recognised that weed control through the use of herbicides is a cost effective measure. However, in recent years agricultural systems have undergone substantial changes which have led to even greater dependence on chemical methods of weed control. The sustainability of the present level of agricultural activity has been questioned in the wake of global problems such as soil erosion, land degradation and eutrophication. In Australia, land degradation in its various forms has been recognised as one of the most serious problems facing the community (7) and large areas are affected by soil erosion. According to an estimate (113) some 68% of the area under cropping and 37% of the non-arid grazing area are at risk. Consequently there has been a marked change to the use of reduced tillage practices in Australian agriculture over the past decade since these reduce erosion of soil particles and in turn minimise nutrient runoff and eutrophication of surface waters. The use of herbicides facilitates the practice of minimum-tillage or no-till and together with crop rotations has a very important role under these circumstances. In Australian irrigated agriculture, herbicides facilitate the operation of thousands of kilometre long irrigation and drainage channels (77). While it is difficult to accurately quantify the benefits of pesticides to Australian agriculture, it is likely to range between \$4 to \$5 billion. For example, financial losses due to weeds alone have been estimated at some \$3.3 billion dollars (20). Recently, LeBaron (60) estimated that the direct benefit to US farmers from the use of pesticides, would range between \$3 - \$5 for every dollar invested.

Pollution of Waterways

As a result of the increasing use of herbicides in agriculture, there is a growing concern at the extent to which these chemicals may contaminate surface and groundwaters. Horticulture is generally the most intensive user of herbicides and other pesticides because of the number of high value crops grown per year coupled with

higher and repeated application rates. As the expanding water catchment areas frequently involve areas of past, present or future horticultural use, the environmental challenge per unit area of land from herbicide use in horticulture is exceptionally high, particularly when such waters are also exploited for domestic uses. In Australia, and in many other countries, there are numerous small catchment areas around capital cities in close proximity to horticultural activities. These are clearly at considerable risk in terms of potential pollution.

Monitoring of Water Pollution

Australia

Although systemic monitoring studies of pesticides in groundwaters of Australia are lacking, there are clear indications that herbicides have contaminated surface and groundwaters in certain areas. Stadler *et al.* (93) have recently reported the presence of atrazine and simazine in groundwaters in South Australia. In a horticultural catchment in South Australia (Piccadilly Valley) some 83% of surface water and 100% of sediment samples tested were found to contain pesticide residues including herbicides (97). Indicators such as nitrate in groundwaters generally demonstrate the vulnerability of an aquifer for pollution. Therefore, it is significant that under horticultural areas in Western Australia, very high levels of nitrates (up to 8 times the permissible limit) have been found (80). A review by the Environmental Protection Authority (EPA) of Western Australia (27) shows that the number of samples showing one or more pesticides in groundwaters at levels exceeding EPA criteria, have increased over recent years. According to this report pesticides have also been found in river and estuarine waters of Western Australia. On the national level, a preliminary survey of groundwater contamination from various sources in Australia (44), recommended that evaluation of non-point source pollution from herbicides and pesticides was urgently required.

Overseas

By far the most extensive and comprehensive monitoring survey for residue of pesticides in waterways has been carried out in the USA in recent years. A five year National Survey of Pesticides in Drinking Water Wells by the US Environment Protection Agency (EPA)

has revealed that 10.4% of 94,600 community water wells and 4.2% of 10.5 million rural domestic wells contained one or more pesticides (99). Pesticide levels in about 1% of all drinking water wells in US exceeded the health based limit. The two most commonly detected pesticides were both herbicides: namely, DCPA acid metabolites and atrazine. Four other herbicides detected were bentazone, dinoseb, simazine, and prometon.

Diffuse source pollution by pesticides, particularly herbicides, in waterways has been recognised as a major problem in Europe for several years. The current EEC directives allow 0.1 mg/L as the maximum acceptable concentration (MAC) of a single pesticide (almost the detection limit for many herbicides) and 0.5 mg/L for total pesticide residue. Commonly used herbicides such as ureas, s-triazines, acid herbicides and organophosphorus pesticides have been detected (sometimes at levels greater than MAC) in surface and groundwaters of the United Kingdom (81, 21). In the Netherlands by 1988, 35 pesticides were banned and another 15 were restricted (64). The list included several commonly used herbicides. Similarly, pesticides have been reported in groundwater of the FRG (66). Decisions to reduce pesticide use by 35-50% during this decade have been taken in Denmark, Sweden and the Netherlands (98).

PROCESSES GOVERNING HERBICIDE MOVEMENT IN SOIL

The large number of herbicides currently in use include a wide variety of compounds differing markedly in both their physical and chemical properties, i.e. whether ionic or non-ionic, weakly acidic or basic, hydrophobic or hydrophilic. The ionic herbicides include both cationic (e.g. paraquat, diquat) as well as anionic (2, 4-D, sulfonylureas). They differ greatly in their aqueous solubility and volatility, i.e. from highly soluble and non-volatile (e.g. paraquat) to sparingly soluble and highly volatile (e.g. trifluralin). When pesticides enter the soil they are subjected to a variety of physical, chemical and biological processes including sorption-desorption, chemical transformation and biological degradation. Previous studies in Australia and elsewhere have shown that the retention and release processes for pesticides are not only directly related to their chemical nature but also to the nature and properties of the soil and its constituents (e.g.

87, 52). Soils vary tremendously in their composition, physical structure and chemical environment. While substantial data on pesticide/soil interactions are available, much of this has been obtained in North America and Europe. Work in recent years (e.g. 87, 88, 55) has demonstrated that the effects on these processes of soil properties such as texture, clay mineral species, organic matter content, pH, salts and solvents present etc. need to be measured in detail for a much wider range of local soil-pesticide combinations.

Sorption-Desorption Processes

Sorption of herbicides by soil is undoubtedly one of the major processes influencing their accessibility to target organisms and their potential to reach non-target organisms by leaching to groundwater. Sorption may result in decreasing biological activity, in enhanced rates of non-biological degradation, e.g. through catalysing hydrolysis (94), and in retardation of the movement with leaching solutions (112). Organic matter and clay minerals are undoubtedly the major constituents in determining the extent of sorption in soils and numerous studies on herbicide sorption have been reported including both inorganic and organic surface interactions (6, 109, 112, 17, 59).

Interactions of pesticides with model materials such as homoionic clays and ion exchange resins, have been widely studied as these well defined systems allow clearer elucidation of mechanisms and specific interactions (69). However, in natural soils the interactions can be expected to be much more complex than in pure materials (37). Kookana and Aylmore (52) found that the sorption of cationic diquat and paraquat in some Western Australian soils followed the order of clay content in the soils and that both the type and contents of clay minerals present in the soil were important for sorption and subsequent desorption of the dipyridylum herbicides (52). For some other pesticides, in particular non-ionic compounds, the amounts sorbed were more directly related to organic matter contents than to clay contents (5, 87). The retention mechanism of non-ionic organic compounds in soils has been suggested to be a partitioning of the chemical between the aqueous phase and the hydrophobic organic matter (19), akin to partitioning of the compound in octanol from octanol/water systems. Consequently,

the sorption coefficient (K) of a pesticide in soil is generally expressed on the basis of the organic matter content in the soil i.e. $K_{oc} = K f_{oc}$, where f_{oc} is the fraction of organic carbon. This is a very attractive approach to modellers, since it facilitates the estimation of K_{oc} values for non-ionic organic compounds from their octanol/water partition coefficient (13, 34). Despite some reservations about the concept (68), many pesticide fate models make use of this approach as the organic matter content of the soil is all that is needed to calculate the value of the sorption coefficient of a given pesticide. Indirect ways of obtaining sorption coefficients for modelling purposes have been recently discussed (34).

On the other hand, attempts to develop a comprehensive description of solute-soil interactions have produced various approaches in recent decades. Considerable attention has been given to adsorption models based on gas-solid interactions that lead to Langmuir and Freundlich type equations. The assuming that sorption is in equilibrium i.e. independent of time, simplifies the modelling process considerably. A further simplification is possible through representation of sorption in the form of a Freundlich equation: $S = KC^n$, where S is sorbed concentration, C is the solution concentration, K and n are empirical coefficients. The value of n is usually less than 1 for many herbicides (37) but for the sake of simplicity n is often assumed equal to 1, thus $S = KC$. The error introduced will depend upon the extent of the non-linearity in the isotherm and the concentration of herbicide in solution. However, for many situations it may be quite adequate and acceptable.

The use of relations such as the Freundlich equation has sometimes been criticised for neglecting the generally electrostatic nature of the ion-soil interactions and for ignoring the heterogeneity of the surface adsorption energy. Preference has often been given to models based on the diffuse double layer (DDL) theories (10). In its complete form the DDL adsorption model of Bowden *et al.* (10) requires five simultaneous equations that have to be solved by iterative procedures to estimate the equilibrium distribution of ions between solution and solid (adsorbed) phases. However, such complexity, while requiring large computational time, brings little useful refinement in the simulation of breakthrough curves (71). It was found that sorption data for fenamiphos,

linuron and simazine could readily be fitted to a Freundlich-type equation, while that for diquat more closely fitted the Langmuir equation (87). A greater degree of refinement of equilibrium sorption isotherm is perhaps unwarranted as it has become increasingly clear that other considerations such as the kinetic aspects of the sorption processes and long-term desorption/release behaviour of herbicides in soils, play a greater role and need to be examined when dealing with solute transport.

Sorption Kinetics

The kinetics of pesticide sorption in soil has until recently received relatively little experimental attention, and most sorption studies on pesticides in soil have dealt with equilibrium aspects (84, 115). Much previous work has been limited to the measurement of sorption equilibrium by batch methods involving vigorous shaking or stirring of soil suspensions. Consequently studies of pesticide sorption by batch methods have frequently indicated that the major fraction of pesticide sorption in soil is essentially instantaneous. However, there is substantial evidence from laboratory and field experiments that the sorption process is almost invariably time-dependent under flow conditions (70, 14, 15, 79, 54). The effects of such sorption dynamics may arise both from structural limitations on diffusion of organic compounds into micropores as well as from the kinetics of the sorption process itself. Acceptance of an invalid instantaneous reaction could clearly lead to serious underestimation of potential leaching and transport of a pesticide to groundwater (53). Flow techniques such as that developed by Kookana *et al.* (56) are preferable over batch techniques (91) for estimating relevant parameters because these are realistic and suitable for modelling transport of pesticides in soil profiles. Kookana *et al.* (54) used this flow technique to study the sorption kinetics of three pesticides in laboratory studies on four Western Australian soils. Sorption data of all pesticides showed an initial rapid rate followed by a slower rate of sorption. While a first-order equation failed to satisfactorily describe the sorption data, both the Freundlich two-site kinetic equation and the parabolic diffusion law fitted well to the data. The rapid component of sorption varied from 0 to 25% of total sorption (24 h sorption value) for the various pesticides. A comparison of sorption data obtained by a batch technique and a flow technique revealed that sorption

occurred at a much faster rate under batch conditions, presumably because of shaking and the high solution to soil ratio. Furthermore, under the batch conditions, the instantaneous component of sorption was very high (up to 90% of 24 h sorption value). The characteristics of the soil also affected the rate of sorption of the pesticides. A well structured soil with high organic matter content showed a slower rate of sorption compared with a dispersed soil with low organic matter. Although time dependency of sorption is demonstrably a fact in practical situations, the extent to which it plays a significant role and needs to be accounted for in determining the overall leaching of pesticides in the field where water infiltration and redistribution generally follow a stop/go scenario, remains to be established.

Reversibility of Sorption - Hysteresis

The reversibility of sorption reactions plays a significant role in determining the behaviour of any pesticide in the soil profile. That is, whether the solid phase provides a permanent sink or merely a temporary reservoir, releasing the chemical back into solution in response to a decrease in solution concentration. Numerous workers (95, 11, 85, 58, 24, 14) have reported a non-singular sorption-desorption reaction. Hysteresis has frequently been observed in the sorption-desorption isotherms for pesticides (e.g. atrazine (95); picloram (102); diuron (78); 2, 4, 5-T (101); parathion (11); linuron, simazine (87)). The mechanisms underlying measurements of apparent hysteresis appear many and varied: sometimes being attributed to experimental artefacts such as changes in sorption capacity arising from shaking and centrifugation, incomplete equilibration, the presence of 'implicit sorbate' altering competitive sorption, as well as degradation or transformation of the pesticide during longer term experiments. However, true hysteresis as a result of the entrapment of pesticides in the organic matter matrix (76, 45, 50, 16, 55) or within mineral particles (65) seems likely to occur (55). This is an important consideration since the effects of various factors, such as soil solution concentration and organic cosolvents on the extent of hysteresis and ease of desorption, may have serious implications for the mobility of pesticides in soil profiles (55).

Factors Affecting Sorption-Desorption

While the organic matter and clay contents of a soil are undoubtedly the main substrates for pesticide sorption (37, 112, 34, 59) the extent and reversibility of these interactions can be greatly influenced by other factors such as pH, soil solute concentration or the presence of organic cosolvents and competitive ions (55, 90).

Both organic matter and clays can have pH dependent charges and hence their ion exchange capacities will change with pH. The relative quantities of basic and acidic pesticide in ionic form are also dependent on the pH of the system. Organo-basic compounds (s-triazines) become cations at low pH and this results in increased sorption (111); whereas the acidic compounds are proton donors (2, 4-D, dinoseb, sulfonylureas) which at high pH (one or more pH units above the pKa of acid) become anions due to dissociation. The sorption of simazine and to a lesser extent of linuron and fenamiphos were shown to decrease with increasing pH in Western Australian soil varying in texture from sand to clay (5). Soil acidification as a result of fertilization and cropping is a major problem in many areas of Australia as elsewhere, and management practices such as liming can result in soil pH and hence pesticide sorption (88). It has also been suggested that the pH at the surface of soil colloids can be up to two units lower than that measured in the soil solution (39) and that the pH of rhizosphere soil may differ from that of bulk soil by up to 1 pH unit (75). Such effects clearly need to be considered in assessing pesticide leaching potential.

Competition for sorption sites by other inorganic and organic compounds present in the solution can modify the behaviour of pesticides in the soil. Inorganic cations compete directly with cationic and cationizable pesticides and reduce their sorption (110, 8, 40). Increases in the salt concentration of the soil solution (from 0.005 to 0.05 M CaCl_2) were observed to result in decreases in sorption capacities for diquat and paraquat herbicides ranging from some 17% for a sandy soil to 40% for a clay soil (52). Desorption of the herbicides was also significantly enhanced by increase in the salt concentration, indicating that the herbicides were less strongly held. Both Ca_2^+ and Na^+ competed with the herbicides for the sorption sites but Na^+ was not as effective as Ca_2^+ . While pesticides such as diquat and paraquat are gener-

ally considered to be essentially irreversibly retained by soil, it is significant that some 60% of adsorbed diquat could be released to solution from a loamy sand soil by extraction with 0.05 M CaCl_2 . In contrast the adsorption of linuron, simazine and fenamiphos were only slightly decreased by increasing soil solution concentration (89).

Degradation

The term degradation generally includes the processes producing losses of herbicides in soil through microbiological and chemical pathways of transformation. Depending on the nature of a herbicide and its location in the soil profile, either the microbiological or chemical aspects may dominate. For example, in the root zone microbiological pathways are generally assumed to be the predominant mechanisms of loss, whereas once the herbicide leaches beyond the root zone, the microbial activity is likely to be small (e.g. in the saturated zone) and hence chemical pathways may dominate the degradation processes. Whether a pesticide persists for a long time or is rapidly degraded or transformed in soil is also a major determinant of the extent to which it can pose a pollution hazard. A herbicide which quickly degrades or transforms to harmless daughter compounds has a much lower potential to pollute groundwater than a persistent one despite a possibly greater mobility of the former arising due to a negligible sorption on soil. For example, 2,4, D being an anion is little sorbed by soil at the normal pH encountered in soils but because it degrades rapidly has a very low pollution potential. On the other hand, atrazine which is substantially retained in soil and therefore has low mobility has, due to its relatively slower rate of degradation, caused groundwater pollution problems in many countries. Furthermore, for certain pesticides the transformation process leads to the formation of metabolites which are themselves equally active or toxic as the parent compound thus maintaining or even increasing the potential hazard to groundwater (e.g. fenamiphos nematocid which transforms to its sulfoxide and sulfone). The significance of these processes in soils under Australian climatic conditions is poorly understood (29). The role of other factors such as organic matter, moisture content, temperature etc. in the degradation process also need to be investigated. In the field, temperature is a function of depth in a soil profile and hence may be of considerable importance in controlling pesticide degrada-

tion and susceptibility to leaching.

In transport modelling degradation processes are often, for the sake of simplicity, represented by a first-order kinetic rate law leading to the concept of a half-life. It has been shown that this approximation is often an adequate representation of the degradation process in soil. Values of first-order rate coefficients or half-lives for a number of pesticides have been collected (82, 49). In addition to the properties of the chemical, the rate coefficient will depend upon soil and environmental factors such as soil moisture content, pH, temperature, organic matter content, concentration and history (106, 72). This multiplicity of factors makes it difficult to have confidence in half-life values of herbicides obtained from the literature for use in the prediction of their fate in a soil. Furthermore, most of the values of degradation rate coefficients tabulated in the literature are based on laboratory experiments, and could be substantially different from the values relevant in the field. Under these circumstances, it is advisable, in simulations of the fate of herbicides, to cite a range of half-life values to cover the variation in environmental conditions over time. Some attempts have been made to estimate degradation rate coefficients from the chemical structure of herbicides, however the inadequacy of this approach has been highlighted by a recent review (41).

While the use of pesticides subject to substantial sorption and a relatively faster rate of degradation may be attractive from the groundwater pollution point of view, the desired duration of weed control may not be achievable with such a herbicide. In fact, the sulfonyl-urea herbicides which exhibit longer persistence and lower retention in soil are currently very popular among farmers in Australia. The sorption, degradation and leaching behaviour of these herbicides deserves particular attention and is discussed in the following sections.

Sorption, Persistence and Mobility of Sulfonyl-Urea Herbicides

Since their introduction in Australia in 1983, the sulfonylurea group of herbicides have been rapidly adopted by farmers due to their long-term weed control and very low application rates (in g/ha as opposed to in kg/ha for other common herbicides). The most important members of this group are chlorsulfuron, triasulfuron, metsulfuron-

methyl. The degradation rate and pathways for these herbicides are pH dependent as also is their sorption by soil. Because these are weakly acidic herbicides and with increasing pH become anionic upon dissociation of the molecule (108), their persistence in soil increases, whereas their sorption decreases with increasing pH. In acidic soils chemical hydrolysis dominates the degradation pathways of the herbicides, whereas in alkaline soils microbial degradation is more important than hydrolysis. Considering their higher solubility, lower sorption and longer persistence in alkaline soils, irrigated alkaline soils would fall in the high risk category for both their leaching and persistence. Legumes are highly sensitive to residues of sulfonyl-ureas and therefore recropping of legumes after application of these herbicides in alkaline soils could be affected. Pasture/legumes have an important role in Australian agriculture as these not only counter the problem of cereal monoculture but are also highly beneficial through nitrogen fixation and in reducing pest pressure. In soils with alkaline subsoil, these herbicides have the potential to leach down quickly to sub-surface layers and remain active in the subsoil for longer periods.

Need for Site Specific Data

While it is widely recognised that soils differ greatly in their organic matter contents, differences in the nature of the organic matter in soils is not generally appreciated. These differences arise in terms of the degree of humification and in composition with respect to the proportions of fats, waxes, resins, proteins and carbohydrates present in organic matter (94). Humic material of grassland soils are rich in humic acids, whereas in forest soils fulvic acids dominate. The sorption capacities of humic and fulvic acids have been found to be different (38). It has long been reported that both the type of organic material and its decomposition stage were important in determining the adsorption of some herbicides (107). Comparisons between organic matter based sorption partition coefficients (K_{oc}) obtained on Australian soils with those for other world soils (90) have demonstrated that substantial variation occurs, for example, in the sorption of linuron and fenamiphos, not only between soils from different regions but also between soils from the same region. For a given herbicide, a wide range of K_{oc} has been noted in different studies (68). Thus, it is apparent that organic matter in different soils can behave quite differently in terms of the retention of pesticides and

hence the reliance on overseas data could lead to erroneous results.

Recently Ferris *et al* (29) carried out predictions of the fate and behaviour of sulfonyl-ureas in different soils and climatic conditions in Australia using the CALculates Flow (CALF) model developed by Nicholls *et al.* (73). They concluded that paucity of sorption and degradation parameters in local high pH soils prevented them from drawing any definitive conclusions about the fate of the herbicides in alkaline subsoils. It is noteworthy that the functional relations used in the model were developed on the basis of research in the UK and Europe and these were not adequate mainly because many Australian soils have much higher pH than commonly found in Europe.

Volatalization

Volatalization can be an important pathway for dissipation of herbicides, particularly for those exhibiting significant volatility such as, EPTC, Dicamba, Triallate, Trifluralin etc. Compared to surface runoff and leaching components of pesticide removal from soil profiles (usually < 10%), volatalization has been estimated to be as high as 80-90% (96). However, some herbicides are essentially non-volatile and a very wide range of vapour pressure has been noted among various herbicides. For example the vapour pressure of EPTC (2800 mPa) is higher by about six orders of magnitude than that of picloram (0.00074 mPa). The vapour density of a given herbicide in the air is governed by its solution concentration through Henry's Law, $p = HC$, which simply states that vapour density of a pesticide (p) is proportional to solution conc (C); H being the Henry's Law coefficient. In addition to the chemical nature of a herbicide and its formulation, several soil and climatic factors also affect its potential volatalization losses. For example, factors such as soil moisture content, temperature, soil organic matter content, herbicide concentration, method of application and weather conditions such as wind velocity, have significant effect on the volatalization loss. Drying of soil and subsequent increase in sorption have been observed by many workers (32) to result in a reduction in volatalization losses. Similarly, partitioning of herbicides on organic matter surfaces causes a reduction in volatalization (92).

The process of herbicide loss through volatalization has not received the same degree of attention from research workers as have the sorption and degradation aspects. Consequently, this aspect has generally been either neglected or incorporated in a very simplistic way in herbicide fate models (2). Jury *et al.* (48) incorporated volatalization in their screening model assuming a stagnant boundary layer at the soil-air interface through which vapour must diffuse to reach the atmosphere. The predictions of the model highlighted the importance of the Henry's law coefficient in governing the volatalization behaviour of pesticides.

MODELLING OF PESTICIDE TRANSPORT

Types of Models and Modelling Approaches

Numerous mathematical models for describing and predicting the transport of non-reactive and reactive solutes such as pesticides under saturated as well as unsaturated flow conditions have been developed in recent decades. Common models of organic chemical transport and their strengths and weaknesses have recently been reviewed (31, 77). On the basis of the degree of complexity with which fundamental processes are incorporated and the extent of characterisation of the range of physical, chemical and biological factors required in the model, these can be broadly divided into two classes i.e. mechanistic and stochastic. Mechanistic models are process-based models employing the classical convection-diffusion-dispersion equations and have been the most widely used approaches for transport modelling in soil science. Reviews of these have been provided by Jury and Ghodrati (46) and Brusseau and Rao (14). Stochastic models incorporate a random component and produce results in terms of probability distributions (47). These models recognise that the processes in soil-water systems are uncertain and vary both spatially and temporally. While conceptually attractive, these models have not yet been applicable for routine use.

Transport models have also been classified in categories such as research, management and screening models on the basis of their intended use (2). Research models are comprehensive and hence provide quantitative estimations of pesticide behaviour in soils but are often data-hungry. Management models put relatively less input data demand on the system and are capable of

predicting pesticide behaviour in the field. However, few of these have actually been tested in the field. Screening models on the other hand require few input parameters and hence are very attractive. However, these are not suitable for accurately predicting the environmental fate of a given pesticide. Nevertheless, these have proved very useful in categorising a large number of chemicals into different behavioural classes (48). Given the large number of models available in the literature, their detailed review is beyond the scope of this paper. However, a brief overview of some screening, research and management models is presented in Table 1. The table describes how various processes such as sorption, degradation, volatilization and water flow are handled by each model.

Screening Models

The objective of screening models is to evaluate the behaviour of herbicides relative to each other under a standard set of soil and environmental conditions and to classify herbicides into groups containing those of similar behaviour (48). Such classifications provide an assessment of the relative risk of potential pollution of groundwater by the pesticides. These models include the following: PESTicide ANalytical Solution (PESTAN, 26), Behaviour Assessment Model (BAM, 48), Pesticide Mobility Index (PMI, 83) and Groundwater Ubiquity Score (GUS, 35). They are based on one-dimensional steady state water-flow (i.e. a constant flow of water

which does not change with time) and use analytical solutions of the transport equation. While BAM takes sorption, degradation and volatilization of pesticides into account for assessing their leaching potential, PESTAN incorporates sorption and degradation only and neglects volatilization. BAM was modified by Jury *et al.* (49) to include a depth dependent rate of degradation. Similarly, the PMI model estimates pesticide mobility through an attenuation factor based on sorption (retardation factor) and degradation (half-life) of the pesticide in soil. The value of the factor ranges from 0 to 1; a higher value suggesting higher pollution potential. Loaugé *et al.* (62) used PMI interfaced with a Geographical Information System to generate pesticide rating maps showing qualitative potential of pesticide leaching to groundwaters of Hawaii. However, their results showed considerable degrees of uncertainties in estimates of pesticide hazard due to the need to extrapolate soil properties between different taxonomic categories and the unreliability of the data used (63).

Research Models

Research models tend to simulate the physical processes to the highest degree of accuracy amongst the various types of models available. Consequently, such models are invariably more complex, data intensive, may require long computer run-times and hence are generally of limited value for field application. Obtaining large

Table 1. Some available pesticide leaching models

Name	Year	Sorption	Degradation	Volatilization	Water flow	Purpose
PESTAN	1982	LINEAR	HALF-LIFE	NO	STEADY STATE	SCREENING (ANALYTICAL)
BAM 8-9 Parameters	1987	LINEAR	HALF-LIFE*	YES	STEADY STATE	SCREENING (ANALYTICAL)
PISTON	1981	LINEAR	HALF-LIFE	NO	TRANSIENT	?
CALF	1984	FREUNDLICH	HALF-LIFE@	NO	TRANSIENT	MANAGEMENT
PRZM = > 21 Parameters	1984/1987	LINEAR	HALF-LIFE*	NO	TRANSIENT	MANAGEMENT
SESOIL	1984/1989	LINEAR	HALF-LIFE	YES	TRANSIENT	MANAGEMENT
LEACHMP = > 22 Parameters	1986/1989	LINEAR	HALF-LIFE*#@	YES	TRANSIENT	RESEARCH
PESTLA	1991	FREUNDLICH*	HALF-LIFE*#@	NO	TRANSIENT	RESEARCH

* Depth dependence considered; # Plant uptake considered; @ Temperature dependence considered

amounts of input data is costly and time consuming and sometimes not all parameters can be obtained independently or under realistic conditions. However, these models are of great value in the interpretation of measured solute distributions in terms of the specific mechanism involved in the transport process and lead to a better understanding of fundamental processes. Research models such as Pesticide Root Zone Model (PRZM) (18) and the Leaching Estimation and CHEmistry Model (LEACHM) (43), which are comprehensive and yet not excessively demanding in terms of field measured data, can however, prove very useful for management purposes.

Research models are very useful in providing insight into the fundamental mechanisms to which pesticides in soils are subjected. It has, for example, been shown by many workers (14) that asymmetrical breakthrough curves of herbicides in laboratory soil columns and in the field are caused by sorption nonequilibrium during their transport in soil. It has been noted that the rate parameters vary with the flow conditions thus suggesting a physical basis to sorption nonequilibrium (53). Research models have also been instrumental in demonstrating that nonequilibrium conditions can originate from multiple sources, including both transport and sorption related processes (14). Nonequilibrium processes can be of significant consequences not only in the leaching behaviour of pesticides but also in the process of remediation of a contaminated aquifer.

Importance of Independent Measurements of Model Parameters

In many solute transport studies, a number of different rate laws describing the time dependency of the sorption reaction in soils have been used with varying degrees of success. These include simple one-site linear or non-linear kinetic models, two-site sorption models and several others (74, 14). More recently, Boesten (9) used a three-site kinetic model, and Selim and Amacher (86) a second-order two-site kinetic model in their solute transport studies. Experimental evidence of such kinetic reactions have been obtained in only a few studies and even then only by the batch technique. Since substantial differences in sorption between flow and batch systems have frequently been noted (e.g. 3, 104, 30, 54), it is

essential that sorption rate coefficients be obtained under flow conditions for such transport studies.

Australian Experience with Models

A number of the models available in the literature (including CALF (73), PRZM (18), PREFECT (61) CREAMS (51); BAM (49), Walker and Barnes model (105) have been used under Australian conditions with varying degree of success. Haigh and Ferris (36) and Ferris *et al.* (29) used the CALF model to predict the behaviour of atrazine and sulfonyl urea herbicides in soils. For atrazine, CALF predicted longer persistence and lesser movement than was observed, possibly through their ignoring bypass flow. This illustrates that the lack of local data has proven to be a major constraint in prediction of sulfonylureas' behaviour in Australian soils. The CALF model has also been used to predict the persistence of trifluralin, diclofop-methyl and chlorsulfuron in Victoria (28). Bowmer (12) used the Walker and Barnes model to predict atrazine persistence in two irrigated soils of Australia and reported that the model overestimated the atrazine residue, possibly due to volatilization and anaerobic degradation not being accounted for in the model. Deficiencies have been identified with the CREAMS model (a surface runoff model) for its use in Australia (61). On the other hand, a similar model PERFECT was successfully used in Queensland by these workers.

The PRZM model was used (67) for a regional risk assessment of groundwater pollution by pesticides in New South Wales. Once again, due to the lack of local data, the information based on overseas soil was used assuming that the generalized assessment would still be valid. This study identified the Richmond River area on the north coast of NSW to be the most vulnerable to groundwater pollution. The main characteristics of the area are: shallow unconfined aquifers, rainfall in excess of evaporation from summer through to winter and intensive horticulture and sugarcane production. The model predicted that up to some 11% of applied 2,4, D would leach to groundwater every year through a 1.8 m thick alluvial soil profile. In the worst case up to 70% of the herbicide could migrate to groundwater with a probability of once in forty years.

For the most effective pesticide usage and rapid

assessment of their likely pollution potential at any given location, models need to be designed requiring the minimum number of parameters while effective and with structures that can be readily modified for site specific purposes. Kookana and Aylmore (53) examined the groundwater pollution potential predicted for a number of pesticides and the influence of organic matter distribution, by calculating the mass of pesticides leaching past the zone of maximum sorption and biological activity in a sandy soil profile of the Swan Coastal Plain, Western Australia, using the simple BAM screening model (49). Hydrological parameters were estimated from local soil and climatic data, and in the absence of local data, sorption (K_{oc}) and degradation (half-life) parameters were obtained from the literature. Assuming a uniform OM content, the model predicted that, of 40 pesticides evaluated, 20 have the potential to reach groundwater in amounts $> 0.1\%$ of applied mass under the conditions considered in the model. However, when an exponentially decreasing OM content with depth in the soil profile was incorporated in the model, the number of pesticides reaching groundwater increased to 30 and the residual concentrations were dramatically increased. The use of local K_{oc} and half-life values for seven pesticides, yielded substantially different residual concentrations to those obtained on the basis of literature values, emphasising the need for site specific data. A clearer understanding of the extent to which the neglect of factors such as dispersion and diffusion, sorption nonequilibrium, water repellency and preferential flow paths, hysteresis and the use of average recharge rates, will lead to significant over- or under-estimation of pollution potential is vital to the development of effective and practical management models.

Some Limitations of the Models

The development of mechanistic models and their evaluation under controlled laboratory conditions provides important insights into the significance of the various physical and chemical processes involved in determining pesticide movement in soils (i.e. research oriented studies). However, the complexity attendant on the multiplicity of factors frequently operating in the field, is likely to make such models extremely cumbersome and of restricted practical applicability. In contrast models based on stochastic representation of the transport prop-

erties (47) provide little understanding of the underlying physical and chemical processes and seek a more functional description in terms of readily accessible parameters (i.e. management oriented). Despite this simplification, functional models often give simulations that are at least good as those of mechanistic models (73, 22) while using far less computer time. They seem likely to be increasingly advantageous as the physical scale of the modelling exercise increases (1).

As described earlier in this paper, leaching of herbicides through soil is the result of interaction of numerous complex processes. The runoff of herbicides from an agricultural system is an even more complex process. Mathematic representation of the various processes in an integrated manner requires complex models. Unfortunately, as attempts are made to improve the accuracy of the models by using detailed fundamental processes, the complexity of the model increases. For example, although sorption of herbicides in soil is frequently represented in models by a linear equilibrium isotherm, it is in practice, usually a time dependent, non-linearly dependent on concentration and partially reversible process. The complete incorporation of this process will tremendously increase the amount of input data required. Furthermore it is not always possible to obtain some of the data required from independent experiments. It is paradoxical, that on one hand screening models are simplistic, easy to use and less data intensive and for that reason are less credible. Research models or detailed management models on the other hand, lose their credibility because of their complexity, difficulty in use and their high data demand which cannot be satisfied with accurate information. Clearly the predictions of a model are only as good as the parameters on which it is based and user confidence may only be satisfied by the development of new models or the refinement of those currently available. In this respect Wauchope (114) has recently discussed procedures by which realistic but complex models can be made credible. Finally, there are certain processes such as plant uptake, foliar washoff and degradation, volatilization, etc., which are not yet fully understood and hence have not been incorporated into existing models.

Apart from the processes of pesticide soil interactions, some aspects of the flow of water in soil require.

further attention and improvement in modelling. Although the individual mechanisms involved in transport have been extensively studied and modelled in isolation, it is of particular importance to develop predictive capabilities of their integrated consequences. While the different aspects are most readily characterised under controlled laboratory conditions, extrapolation to field conditions is invariably complicated by climatic and other variables. In particular, the structure of the soil plays an important part in the leaching process. Although some progress has been made in characterising soil structure (23), little success has been achieved in relating water movement and hence solute transport, to pore size distribution and continuity. Preferential flow paths and the movement of dissolved organic matter and clay colloids as carriers of pesticides sorbed on them, present particular challenges for modellers.

Concluding Remarks

While predictive models provide important tools in both research and management, comprehensive field data sets on pesticide transport and volatilization are required to accurately assess and improve the performance of these models. There is an urgent need to define the degree of complexity with which fundamental processes need to be treated in such models and the extent of characterisation of the variety of physical, chemical and biological parameters required to avoid problems of site specificity and to provide an effective approach to defining the potential hazard posed by particular pesticide/soil combinations. Improved technologies for measuring pesticide transport and degradation processes in heterogeneous field soils are also needed.

While it is relatively easy to enunciate the importance of various processes and the factors determining pesticide leaching, the development of practical methodologies for simulation and predictive modelling and compatible data collection, pose many problems requiring integration and rationalisation of input from soil scientists, industrial chemists and hydrologists.

References

- Addiscott, T.M. 1992. Proc. Inter. Soc. Soil Sci. Symp. on "Operational Methods to Characterise Soil Behaviour in Space and Time", Cornell University, Ithaca, July.
- Addiscott, T.M. and Wagenet, R.J. 1985. *J. Soil Sci.* 36 : 411-424.
- Ardakani, M.S. and McLaren, A.D. 1977. *Soil Sci. Soc. Am. J.* 41 : 677-679.
- AVCA 1992. The Agricultural & Veterinary Chemicals Association of Australia Ltd. Sydney, Australia. (personal communication).
- Aylmore, L.A.G., Singh, R. and Gerritse, R.G. 1989. *Water 89 Intern. Conf.*, Bangkok, Thailand, EQM, 4-9.
- Bailey, G.W. and White, J.L. 1970. *Residue Rev.* 32 : 29-92.
- Balderstone, J.S. 1982. Agricultural Policy Issues and Options for the 1980s. Working group Report to the Minister for Primary Industry (AGPS : Canberra).
- Best, J.A., Weber, J.B and Weed, S.B. 1972. *Soil Sci.* 114 : 444-450.
- Boesten, J.J.T.I. 1987. *Netherlands J. Agric. Sci.* 35 : 315-324.
- Bowden, J.W., Posner, A.M. and Quirk, J.P. 1974. *Trans. 10th Intern. Congr. Soil Sci.*, Moscow 2 : 29-36.
- Bowman, B.T. and Sans, W.W. 1985. *J. Environ. Qual.* 14 : 270-273.
- Bowmer, K.H. 1991. *Aust. J. Soil Res.* 29 : 339-350.
- Briggs, G.G. 1981. *Aust. J. Soil Res.* 19 : 61-68.
- Brusseau, M.L. and Rao, P.S.C. 1989. *CRC Critical Reviews in Environmental Control* 19 : 33-99.
- Brusseau, M.L., Jessup, R.E. and Rao, P.S.C. 1991. *Environ. Sci. Technol.* 25 : 134-142.
- Burchill, S., Hayes, M.H.B. and Greenland, D.J. 1981. Adsorption in 'The Chemistry of Soil Processes' (Eds. Greenland, D.J. and Hayes, M.H.B.). pp. 221-400 (John Wiley & Sons Ltd.).
- Calvet, R. 1980. Adsorption-desorption phenomena. In: (R.J. Hance (ed.), *Interactions between herbicides and the soil.* pp. 1-30, Academic Press, London.
- Carsel, R. F., Mulkey, L.A., Smith, C.N., Dean, J.D. and Jowise, P. 1984. User's manual for the pesticide root zone model (PRZM). EPA/600/3-84/109, USEPA, Athens, Georgia.
- Chiou, C.T., Peters, L.J. and Freed, V.H. 1979. *Science* 206: 831-832.
- Combella, J.H. 1989. *Plant Protection Quarterly* 4 : 14-32.
- Croll, B.T. 1991. *J. IWEM (UK)* 5 : 389-395.
- De Willigen, P. (1991). *Fert. Res.* 27 : 141-149.
- Dexter, A.R. 1988. *Soil Tillage Res.* 11 : 199-238.

24. Di Toro, D.M. and Horzempa, L.M. 1982. Environ. Sci. Technol. 16 : 594-602.
25. Dunigan, E.P. and MacIntosh, Th. 1971. Weed Sci. 19 : 279-282.
26. Enfield, C.G., Carsel, R.F., Cohen, S.Z., Phan, T. and Walters, D.M. 1982. Ground Water 20 : 711-722.
27. EPA 1989. The Environment Protection Authority, Western Australia, Bulletin No. 407. pp. 67. Dec. 1989.
28. Ferris, I.G. and Haigh, B.M. 1993. Herbicide persistence and movement in Australian soils : Implications for agriculture. In : J. Altman (ed.) "Pesticide Interaction in Crop Production" CRC Press. pp. 133-160.
29. Ferris, I.G., Fawcett, R., Flynn, A., Haigh, B.M., Pederson, N. and Rovira, A. 1993. Aust. J. Soil Res. (in press).
30. Gaber, H.M., Comfort, S.D., Inskip, W.P. and El-Attar, H.A. 1992. Soil Sci. Soc. Am. J. 56 : 1392-1400.
31. Gallant, J.C. and Moore, I.D. 1991. Models of organic contaminant transport and degradation: A review. In : Moore, I.D. (ed.) Modelling the Fate of Chemicals in the Environment. CRES, ANU, Canberra. pp. 22-39.
32. Glotfelty, D.E., Leech, M.M., Jersey, J. and Taylor, A.W. 1989. J. Agric. Food Chem. 37 : 546-555.
33. Green, R.E. 1974. Pesticide-clay-water interactions. In : "Pesticides in soil and water". (W.D. Guenzi, ed.). Soil Sci. Soc. Amer. Inc. Publ., Madison, pp. 3-37.
34. Green, R.E. and Karickhoff, S.W. 1990. Sorption Estimates for Modelling. In : Cheng, H.H. (ed.) "Pesticides in the Soil Environment : Processes, Impacts and Modelling". Soil Sci. Soc. Am. Book Series No. 2. pp. 79-101.
35. Gustafson, D.I. 1989. Environ. Toxicol. Chem. 8 : 339-357.
36. Haigh, B.M. and Ferris, I.G. 1991. Predicting herbicide persistence using the CALF model. In : Moore, I.D. (ed.) "Modelling the Fate of Chemicals in the Environment". CRES, ANU, Canberra. pp. 50-60.
37. Hamaker, J.W. and Thompson, J.M. 1972. Adsorption. In : Goring, C.A.I. and Hamaker, J.W. (eds.) "Organic Chemicals in the Soil Environment". Vol. 1. pp. 49-143. Marcel Dekker Inc., N.Y.
38. Hayes, M.H.B., Stacy, M. and Thompson, J.M. 1968. In : "Isotopes and Radiation in Soil Organic Matter Studies". Int. Atomic Energy Agency, Vienna. pp. 75-90.
39. Hayes, M.H.B. 1970. Residue Rev. 32 : 131-168.
40. Hayes, M.H.B., Pick, M.E. and Toms, B.A. 1975. Residue Rev. 57 : 1-25.
41. Howard, P.H., Hueber, A.E. and Boething, R.S. 1987. Environ. Toxicol. Chem. 6 : 1-10.
42. Huber, J.F.K. and Gerritse, R.G. 1971. J. Chromatogr. 58 : 137-158.
43. Hutson, J.L. and Wagenet, R.J. 1992. LEACHM : Version 3, New York State College of Agriculture and Life Sciences, Cornell Univ. Ithaca, NY.
44. Jacobson, G. and Lau, J.E. 1988. Groundwater contamination incidents in Australia : An initial survey, Bureau of Mineral Resources, Geology and Geophysics, Report 287.
45. Johnson, R.E. and Starr, R.I. 1972. J. Agric. Food Chem. 20 : 48-51.
46. Jury, W.A. and Ghodrati, M. 1989. Overview of organic chemical environmental fate and transfer modelling approaches. In : Reactions and Movement of Organic Chemicals in Soil. Soil Sci. Soc. Amer. J. Spec. Publ. 22 : 271-304.
47. Jury, W.A. and Roth, K. 1990. Transfer functions and solute movement through soil. Theory and Applications. Birkhauser Verlag, Berlin.
48. Jury, W.A., Spencer, W.F. and Farmer, W.J. 1983. J. Environ. Qual. 12 : 558-564.
49. Jury, W.A., Focht, D.D. and Farmer, W.J. 1987. J. Environ. Qual. 16 : 422-428.
50. Khan, S.U. 1973. Can. J. Soil Sci. 53 : 199-204.
51. Kinsel, W.G. 1980. (Ed.). CREAMS : Conservation Res. Report, 26, USDA, p. 640.
52. Kookana, R.S. and Aylmore, L.A.G. 1993a. Aust. J. Soil Res. 31 : 1-13.
53. Kookana, R.S. and Aylmore, L.A.G. 1993b. Aust. J. Soil Res. (under review).
54. Kookana, R.S., Aylmore, L.A.G. and Gerritse, R.G. 1992a. Soil Sci. 154 : 214-225.
55. Kookana, R.S., Gerritse, R.G. and Aylmore, L.A.G. 1990. Aust. J. Soil Res. 28 : 717-725.
56. Kookana, R.S., Gerritse, R.G. and Aylmore, L.A.G. 1992b. Soil Sci. 154 : 344-349.
57. Kookana, R.S., Schuller, R.D. and Aylmore, L.A.G. 1993. J. Contam. Hydrol. (submitted).
58. Koskinen, W.C. and Cheng, H.H. 1979. J. Environ. Qual. 12 : 325-330.
59. Koskinen, W.C. and Harper, S.S. 1990. The retention process : mechanisms. In : Cheng, H.H. (ed.) "Pesticides in the Soil Environment : Processes, Impacts and Modelling". Soil Sci. Soc. Am. Book Series No. 2. pp. 51-78.
60. LeBaron, H.M. 1990. Weed Technol. 4 : 671-689.

61. Littleboy, M., Silburn, D.M., Freebairn, D.M., Woodruff, D.R. and Hammer, G.L. 1989. PERFECT - Qld. Dept. Primary Ind. Bull. QB 890005.
62. Loague, K.M., Green, R.E., Giambelluca, T.W., Liang, T.C. and Yost, R.S. 1990. *J. Contamin. Hydrol.* 5 : 171-194.
63. Loague, K.M., Yost, R.S., Green, R.E. and Liang, T.C. 1989. *J. Contamin. Hydrol.* 4 : 139-161.
64. Loch, J.P.G., van Dijk-Looyaard, A. and Zoetman, B.C. 1989. Organics in groundwater. In: Watershed 89. (Eds.) D. Wheeler, M.L. Richardson and J. Bridges. Proc. IAWPRC Conf. Guildford, UK Vol 1. pp. 39-54.
65. McCloskey, W.B. and Bayer, D.E. 1987. *Soil Sci. Soc. Am. J.* 51 : 37-44.
66. Milde, G. and Friesel, P. 1986. (Eds.) Pflanzenbehandlungsmittel und Gewässer. V. Schr. R. Ver. WaBoLu, Band 68, G. Fischer Verlag, Stuttgart 1986.
67. Milne-Holme, W.A., Finlayson, D. and Yu, X. 1991. Generalised risk assessment of ground water contamination by pesticides: An expert system approach to PRZM. In: Moore, I.D. (ed.) Modelling the Fate of Chemicals in the Environment. CRES, ANU, Canberra. pp. 40-49.
68. Minglegrin, U. and Gerstl, Z. 1983. *J. Environ. Qual.* 12 : 1-11.
69. Mortland, M.M. 1970. *Adv. Agron.* 22 : 75-114.
70. Murali, V. and Aylmore, L.A.G. 1980. *Nature* 283 : 467-469.
71. Murali, V. and Aylmore, L.A.G. 1981. *Soil Sci.* 131 : 76-81.
72. Nash, R.G. 1988. Dissipation in soil. In: R. Grover (ed.) Environmental chemistry of herbicides. Vol. 1. CRC Press, Boca Raton. FL. pp. 131-170.
73. Nicholls, P.H., Bromilow, R.H. and Addiscott, T.M. 1982. *Pesticide Sci.* 13 : 475-483.
74. Nielsen, D.R., van Genuchte, M.Th. and Biggar, J.W. 1986. *Water Resour. Res.* 22 : 89s-108s.
75. Nye, P.H. 1986. Acid-base changes in the rhizosphere. In: 'Advances in Plant Nutrition'. Praeger Scientific, NY. pp. 129-154.
76. Ogner, G. and Schnitzer, M. 1971. *Can. J. Chem.* 49 : 1053-1063.
77. Parthapar, S.A. and Bowmer, K.H. 1991. Pesticide issues in irrigated agriculture - can modelling help? In: Moore, I.D. (ed.) Modelling the Fate of Chemicals in the Environment. CRES, ANU, Canberra. pp. 9-12.
78. Peck, D.E., Corwin, D.L. and Farmer, W.J. 1980. *J. Environ. Qual.* 9 : 101-106.
79. Pignatello, J.J. 1990. *Environ. Toxicol. Chem.* 9 : 1117-1126.
80. Pionke, H.B., Sharma, M.L. and Hosking, J.A. 1990. Horticulturally cropping effects on groundwater quality in the Swan Coastal Plain. CSIRO Division of Water Resources Series No. 2.
81. Price, D.R.H. 1991. Proc. Brighton Crop Protection Conf. - Weeds - 1991. pp. 1279-1284.
82. Rao, P.S.C. and Davidson, J.M. 1980. Estimation of pesticide retention and transformation parameters required in non-point source pollution models. In: M.R. Overcash and J.M. Davidson, (eds) Environmental impact of non-point source pollution. Ann. Arbor Sci. Publ. Ann. Arbor, MI. pp. 23-67.
83. Rao, P.S.C., Hornsby, A.G. and Jessup, R.E. 1985. *Soil Crop Sci. Soc. Florida Proc.* 44: 1-8.
84. Rao, P.S.C. and Jessup, R.E. 1983. Sorption and movement of pesticides and other toxic organic substances in soils. In: (D.W. Nelson, K.J. Tanji and D.E. Elrick (eds.) "Chemical Mobility and Reactivity in Soil Systems". Soil Sci. Soc. Amer., Madison, Wisc. pp. 183-201.
85. Rao, P.S.C., Davidson, J.M. and Kilcrease, D.P. 1978. *Agron. Abstr.* pp. 34.
86. Selim, H.M. and Amacher, M.C. 1988. *Water Resour. Res.* 24: 2061-2075.
87. Singh, R., Aylmore, L.A.G. and Gerritse, R.G. 1990. Proc. National Workshop on Herbicide Persistence, Melbourne, Nov., 1989.
88. Singh, R., Gerritse, R.G. and Aylmore, L.A.G. 1988a. Proc. Aust. Soc. Soil Sci. Conf., Merredin, W.A., August. pp. 119-123.
89. Singh, R., Gerritse, R.G. and Aylmore, L.A.G. 1988b. Proc. National Workshop on Persistence of Herbicide Residues in Wheat Cropping Systems in Australia, Melbourne, Oct., pp. 32-47.
90. Singh, R., Gerritse, R.G. and Aylmore, L.A.G. 1990. *Aust. J. Soil Res.* 28: 227-243.
91. Sparks, D.L. 1985. *Adv. Agron.* 38: 231-266.
92. Spencer, W.F. 1970. Distribution of pesticides between soil, water, and air. In: Pesticides in the soil: Ecology, Degradation, and Movement. Michigan State Univ., East Lansing. pp. 120-128.
93. Stadler, F.A., Emmett, A. and Dillon, P. 1992. CSIRO, Centre for Groundwater Studies Report No. 45.
94. Stevenson, F.J. 1982. Organic matter reactions involving pesticides in soil. In: Humus Chemistry, Genesis, Composition, Reactions. Wiley- Interscience Pub. NY. pp. 403-419.
95. Swanson, R.A. and Dutt, G.R. 1973. *Soil Sci. Soc. Am. Proc.* 37: 872-876.

96. Taylor, A.W. and Spencer, W.F. 1990. Volatilization & vapour transport processes. In : Cheng, H.H. (ed.) "Pesticides in the Soil Environment: Processes, Impacts and Modelling". Soil Sci. Soc. Am. Book Series No. 2. pp. 213-269.
97. Thoma, K. 1988. South Australian. Dept. of Agric., Tech. paper no. 131, June 1988.
98. Thonke, K.E. 1991. Proc. Brighton Crop Protection Conf. - Weeds - 1991. pp. 1183-1190.
99. USEPA 1992. National Survey on Pesticides, Phase II report. EPA 570/9-01-021.
100. van Genuchten, M.Th. 1991. Recent progress in modelling water flow and chemical transport in the unsaturated zone. In : G. Kienitz *et al.* (eds.) Hydrological Interaction Between Atmosphere, Soil and Vegetation. IAHS Publ. No. 204, pp. 169-183, Institute of Hydrology, Wallingford, Oxfordshire, U.K.
101. van Genuchten, M.Th., Wierenga, P.J. and O'Connor, G.A. 1977. Soil Sci. Soc. Am. J. 41 : 278-285.
102. van Genuchten, M.Th. and Wierenga, P.J. 1974. New Mexico Agric. Exp. Stn. Bull. 628.
103. van Genuchten, M.Th., Davidson, J.M. and Wierenga, P.J. 1974. Soil Sci. Soc. Am. Proc. 38 : 29-36.
104. Wagenet, R.J., Biggar, J.W. and Nielsen, D.R. 1977. Soil Sci. Soc. Am. J. 41 : 896-902.
105. Walker, A. 1987. Weed Res. 27 : 143-152.
106. Walker, A. 1976. Pest. Sci. 7 : 41-49.
107. Walker, A. and Crawford, D.V. 1968. The role of organic matter in adsorption of the triazine herbicides by soil. In : Isotopes and Radiation in Soil Organic Matter Studies. Int. Atomic Energy Agency, Vienna. pp. 91-108.
108. Walker, A. and Welch, S.J. 1989. Weed Res. 29 : 375-383.
109. Weber, J.B. 1972. Interactions of organic pesticides with particulate matter in aquatic and soil systems. In : Gould, R.F. (ed) Fate of Organic Pesticides in Aquatic Environment. Amer. Chem. Soc. 111 : 55-120.
110. Weber, J.B. and Weed, S.B. 1968. Soil Sci. Soc. Am. Proc.:32 : 485-487.
111. Weber, J.B., Weed, S.B. and Ward, T.M. 1969. Weed Sci. 17 : 417-421.
112. Weed, S.B. and Weber, J.B. 1974. Pesticide - Organic matter interactions. In : 'Pesticides in Soil and Water'. (Ed. Guenzi, W.D.). pp. 39-66. Soil Sci. Soc. Am. Inc. Publisher Madison, Wisc. USA.
113. Woods, L.E. 1984. Land Degradation in Australia. AGPS, Dept. Home Affairs and Environ. Australian Environment Statistics Project. p. 105.
114. Wauchope, R.D. 1991. Weed Technol. 6 : 753-759.
115. Yaron, B., Gerstl, Z. and Spencer, W.F. 1985. Adv. Soil Sci. 3 : 121-211.

1 Application of Computer Assisted Tomography to Soil-Plant-Water Studies: An Overview

L. A. G. Aylmore

*University of Western Australia
Nedlands, Western Australia*

ABSTRACT

Application of the technique known as computer assisted tomography (CAT) to x- and gamma-ray attenuation measurements has provided an exciting new method for nondestructive imaging within a solid matrix with considerable potential for studying soil behaviour in space and time. The information provided, however, is currently limited by the capabilities of the instrumentation available. Commercially available medical CAT scanners have proven useful for visual studies of soil structure, the advancement and stability of wetting fronts and the structural changes following wetting and drying. The usefulness of these systems and of single source gamma CAT scanning systems in studying soil-plant-water systems, however, is invariably restricted by their inability to distinguish between changes in water content and bulk density in swelling and shrinking soils, and by the associated physical relocation of soil elements that can occur. Thus their quantitative applications have been limited to the measurement of water drawdowns in proximity to plant roots in nonswelling soils or statistical assessments of macroporosity distributions before and after complete wetting and drying cycles. Though fast in operation, the quantitative usefulness of x-ray scanners is limited by the polychromatic nature of the beam and the process known as *beam hardening*. Furthermore the proprietary nature of these commercial systems also makes software modification or extensions impossible. Simultaneous measurement of the spatial distributions of water content and bulk density in soils that exhibit swelling and dispersion, has been shown to be feasible using CAT applied to dual source (Cs-137 and Yb-169) gamma-ray attenuation. The relatively low photon emission from gamma sources and the propagation of statistical errors, however, necessitates large counting times to provide acceptable accuracy and restricts the use of present gamma systems to the study of steady state or only slowly changing systems. Realization of the full potential of this technique will require substantial improvements in scanning geometry and counting electronics to improve the speed and precision of measurements. With further development, however, dual source gamma-ray systems should ultimately prove most effective for quantitative soil studies.

It is now more than a decade that CAT (Hounsfield, 1972) (also termed computed tomography [CT]) in various forms has been applied to a number of different energy beams including: electrons, protons, positrons, alpha particles, lasers, radar, ultra-sound, and nuclear magnetic resonance (NMR), to provide three dimensional imaging of the internal structure of solid objects. Detailed reviews of various aspects of CAT scanning have been presented by Newton and Potts (1981) and by Kak and Slaney (1988) and of its use in studying water movement around plant roots by Aylmore (1993). From the point of view of soil and plant scientists interested in understanding the processes of soil structure development, water movement in soils and its availability for plant growth, application of CAT to measurements of the attenuation of energy beams undoubtedly provides one of the most exciting new techniques ever developed. Its promise of the ability to see inside soil columns and monitor the processes occurring in a continuous, nondestructive manner, clearly has the potential to resolve the major controversies in soil physics and soil-plant-water relations. This special publication provides the opportunity to review and evaluate the progress that has and has not been made in the application of CAT to soil-plant-water studies and to define the steps necessary to obtain the maximum benefit from this technique.

X-RAY SYSTEMS

Because of the development of sophisticated x-ray CAT scanning systems for medical diagnostic purposes, most attention has naturally been directed to the potential use of these systems. The effectiveness of commercially available x-ray CT scanners has been examined by a number of workers and the last decade has seen quite a number of publications extolling the potential of CAT in soil studies and evaluating the relationships between measured attenuation and soil characteristics (Petrovic et al., 1982; Hainsworth & Aylmore, 1983, 1986; Crestana et al., 1985; Anderson et al., 1988, 1990; Tollner et al., 1987; Tollner & Murphy, 1991; Grevers et al., 1989). Very few workers, however, have actually used the technique to investigate the problems to which it seems admirably suited. The reasons for this lie partly in the limited access of interested workers to suitable instruments, but also substantially in the limited capabilities of the instrumentation available.

Commercially available medical x-ray scanners provide excellent outputs in the form of pictorial displays and arrays of Hounsfield units associated with picture element (pixel) densities. Although their performance characteristics were naturally optimized for x-ray absorption relevant to that of body tissues (i.e., close to that of water), these systems still provide essentially linear relationships between attenuation and bulk density and water content at the higher values associated with soil and similar porous materials (Anderson et al., 1988). As might be expected, bearing in mind the dependence of the mass attenuation coefficient on the energy of the radiation, the chemical composition (Coppola & Reiniger, 1974) and packing or bulk density of the soil

matrix, as well as, differences in effects such as beam hardening as a result of the polychromatic nature of x-ray beams, source-detector geometry and degree of electronic discrimination, substantial variations in the slope of the linear regressions have been noted with different soils and scanners. By and large these effects do not constitute a major impediment to their use for many purposes. They are thus extremely valuable not only for medical diagnostic purposes, but in many other applications such as industrial testing for faults in plastic, concrete, metal and other constructions (Hopkins et al., 1981; Davis et al., 1986).

The CAT scans through soil columns or cores provide very nice visual illustrations of the structural configuration (Petrovic et al., 1982; Jenssen & Heyerdahl, 1988; Grevers et al., 1989; Warner et al., 1989; Anderson et al., 1990) that can be quantified in various ways (e.g., Anderson et al., 1990; Phogat & Aylmore, 1989). When dealing with essentially rigid porous media including those soils that for all intents and purposes do not shrink or swell, the linear relationships not only enable one to readily characterize porous structure, but also changes in the spatial distribution of the soil water content. The water content distribution in the soil can be determined by first scanning the soil column when dry and rescanning it in exactly the same position when the soil is wet (Hainsworth & Aylmore, 1983). Measurements of the drawdowns in soil water content associated with single radish roots in a nonswelling 15% kaolinite clay-85% sand mixture by Hainsworth and Aylmore (1983, 1986, 1989) provided the first detailed and repetitive observations of this type. Subsequently Aylmore and Hamza (1990) and Hamza and Aylmore (1991, 1992a, b) used a combination of CAT scanning and ion specific microelectrode techniques to measure concomitantly, the spatial distribution of soil water content and Na^+ ion concentrations in close proximity to lupine (*Lupinus augustifolius* L.) and radish (*Raphanus sativus* L.) plant roots. When structural changes occur on wetting and drying, however, the quantitative usefulness of CAT has been essentially limited to statistical assessments of macroporosity distributions before and after complete wetting and drying cycles (Phogat & Aylmore, 1989).

SPATIAL RESOLUTION

The ability of the scanner to resolve voids and objects of different size is obviously a function of beam collimation and consequent pixel dimensions, which for most commercial scanners is the order of 1 by 1 mm. In general the boundaries of the object can only be accurately defined when it is at least twice the pixel dimensions. Only if the boundary of an object of one pixel size coincides exactly with pixel edges can it be correctly identified. If the boundary falls in the middle of the pixel, however, the scanner will produce an attenuation value that is an average for the materials within the pixel (Warner et al., 1989). Despite these limitations the current spatial resolution of these instruments, providing pixel dimensions of the order of 0.5 to 1 mm,

is quite adequate to allow meaningful resolution of many of the controversies associated with water extraction by plant roots. The achievement of finer resolution is inevitably accompanied by longer counting times and slower scanning.

PROBLEMS WITH X-RAY SYSTEMS

Though generally very fast in operation the quantitative usefulness of commercially available medical x-ray systems for many studies, is limited by the polychromatic nature of the x-ray beams leading to problems of beam hardening and absorption edge phenomena. These can produce lines and streaks at a density gradient interface and the Gibbs phenomena (Bracewell, 1965; Brooks & Di Chiro, 1976; Kak & Slaney, 1988) where large changes in attenuation from high density to low density areas cause the calculated values in the low density area to be less than the actual attenuation coefficient in that region, i.e., an overshoot. A major deterrent limiting the extensive use of these systems has also been their cost, even as second hand instruments, or the limits on accessibility to even cooperative hospital facilities. For most soil-plant experimentation we need to have continuous measurement over a substantial period of time. The alternative involves repositioning the soil column or whatever is being studied, extremely accurately or losing spatial coincidence of measurement. Furthermore the proprietary nature of these commercial systems also makes software modification or extensions near impossible.

GAMMA-RAY SYSTEMS

Because of the quantitative limitations and restricted accessibility of x-ray systems, work in several laboratories has sought to provide experimentally more suitable and vastly less expensive CAT systems by the use of gamma ray sources. Radioactive gamma emitters provide a far cheaper source of photons and for precise quantitative imaging, gamma-ray sources are, in fact, superior in almost all respects to x-ray sources apart from source brightness. Firstly the constancy of gamma photon energy over space and time renders gamma tomography a more objective method of imaging. Apart from much lower cost gamma-ray sources also offer additional advantages compared with x-ray tubes including compactness, portability and in particular ready access to a very wide range of photon energies (Gilboy, 1984). Hainsworth and Aylmore (1983, 1988) modified a conventional gamma scanning system to utilize the CAT approach and demonstrated that equally good resolution to x-ray scanners could be obtained. Similar systems have been independently constructed by Crestana et al. (1986) and Brown et al. (1993). The major disadvantage of gamma scanners is the question of source brightness. The x-ray tube in a medical scanner can have typically an equivalent source

strength of 15 000 Ci distributed across a few square millimeters compared with the one or two Ci generally available in gamma sources.

SWELLING AND SHRINKING SOILS

Undoubtedly the greatest disadvantage of any single energy source system in studying soil systems, particularly pertinent to most commercial x-ray systems, is that their usefulness is invariably restricted by their inability to distinguish between changes in water content and bulk density in swelling and shrinking soils and the associated physical relocation of soil elements that can occur. Several workers have suggested the possibility of deriving a universal relationship between x-ray CT data vs. bulk density and water content if differences in the electron densities of the soils are known (Anderson et al., 1988; Tollner & Murphy, 1991). However, if one takes into account the number of variables that may influence the regression for bulk density, including texture, mineralogy, and cation status, it seems unlikely that a truly universally applicable relationship for attenuation at the energy levels used in medical scanners, can be derived. Independent calibration for specific soils will remain an essential prerequisite to their use. More generally applicable relationships may, however, be possible using higher energy monochromatic gamma rays (e.g., from Cs-137) (Coppola & Reiniger, 1974).

DUAL ENERGY APPROACH

Any realistic approach to studying soil-plant-water relations demands the ability to monitor simultaneously and continuously, the spatial distributions of both water content and soil structure (i.e., bulk density). Soil scientists and others have for decades used the differential attenuation of different gamma energy beams to discriminate between the two effects in bulk measurements on soil columns and it is here that the particular advantage of gamma attenuation comes to the fore. By solving the simultaneous equations relating attenuation to the combination of soil and water contents for two discrete and sufficiently distinct energy beams, independent estimates of attenuation associated with bulk density and water content can be obtained (Gurr, 1962; Ryhiner & Pankow, 1969; Corey et al., 1971). Although the average energy of x-radiation can be adjusted in some commercially available medical systems, the range is usually relatively narrow and the polychromatic nature of the beams would greatly complicate the practical solution of the simultaneous equations.

CHOICE OF SOURCES

A combination of Cs-137 and Am-241 sources has most commonly been used in conventional dual source gamma scanning because of the 10-fold

difference in gamma ray energy (662 and 59.6 KeV, respectively) and their long half-lives. Both the time required to successfully complete a CAT scan and the precision obtained, however, depend upon the transmission intensity and hence count rate. While high strength Cs-137 sources are readily available, the beam strength obtained from Am-241 has a practical limit because of self-absorption. A useful alternative source is Yb-169 (Phogat et al., 1991), which has a similar energy level (63.1 KeV) and attenuation coefficient for water (0.176 cm^{-1}) to Am-241, but emits much higher photon outputs (>20 times) at the higher activities that can be obtained (2–3 Curies). The major disadvantages of the Yb-169 source is its relatively short half-life of 31 d, resulting in a working life of ≈ 2 mo.

The effectiveness of the dual source approach in differentiating the changes in attenuation arising from changes in water content and bulk density was illustrated by Phogat et al. (1991). The values of mean water content for slices of both swelling and nonswelling soils determined by the dual source technique, showed excellent agreement with gravimetric values ($R^2 = 0.991$) for water contents from zero to $0.55 \text{ cm}^3 \text{ cm}^{-3}$. The differences in water content fell within the range $\pm 0.024 \text{ cm}^3 \text{ cm}^{-3}$. In contrast use of a single source (Cs-137) markedly underestimated soil water content particularly in a structurally unstable smectite dominated soil.

The primary object of the CAT technique is not to measure average bulk density and water content but to reveal the spatial distributions of these quantities. Using a combination of Cs and Yb sources, Phogat et al. (1991) demonstrated that using dual-source gamma CAT scanning, it is possible to measure the spatial distribution of both water content and bulk density in soils simultaneously and nondestructively with a satisfactory level of precision. Unfortunately, despite the enhanced output from the Yb-169 source used, the accumulation of statistical errors, arising from the random nature of radioactive emissions, still necessitated excessively large counting times to provide acceptable accuracy. At a counting time of 13 s, Cs-137 gave a standard deviation (SD) for pixel water content of $0.016 \text{ cm}^3 \text{ cm}^{-3}$, whereas the corresponding value for the Yb-169 scan was $0.007 \text{ cm}^3 \text{ cm}^{-3}$. The higher photon output of the Yb-169 and the fact that the average attenuation of the Yb gamma is greater than that for Cs-137, reduces the relative error and explains the greater uniformity of the Yb scans compared with the Cs scans. When the scan data of both sources were used in the combined simultaneous equations, it yielded a SD for pixels of $0.073 \text{ cm}^3 \text{ cm}^{-3}$. This multiplicative propagation of errors is most evident when, due to random emissions, a particular pixel estimated to have a low attenuation using Cs is estimated to have a high attenuation using Yb or vice versa. Unfortunately this means that to obtain satisfactory resolution with dual source scanning (say a SD of $0.05 \text{ cm}^3 \text{ cm}^{-3}$) an individual ray-sum counting time of 35 s would be required resulting in a total scan time of some 23 h for a 6 cm in diam. column. Assuming a normal distribution of counts, a counting time of 169 s would be required to ensure that 95% of the pixels in the scan for water content

are $\pm 0.05 \text{ cm}^3 \text{ cm}^{-3}$ (i.e., $SD = 0.025 \text{ cm}^3 \text{ cm}^{-3}$). Thus it would require a total of 112 h to complete one dual source scan.

NUCLEAR MAGNETIC RESONANCE IMAGING

The use of proton (^1H) NMR computerized microimaging (Johnson et al., 1986; Woods et al., 1989) has similarly excited interest because of its ability to provide detailed nondestructive imaging of water contents in biological materials (Bottomley et al., 1986; Brown et al., 1986; Omasa et al., 1985). As with x-ray CAT scanning this technique stems from recent rapid advances in medical uses of NMR imaging for clinical diagnostic purposes. However, while qualitative evaluations of soil water content distributions have been achieved using this approach (McFall et al., 1991), major difficulties arise in quantitatively measuring water that is physically bound within a soil matrix. Naturally occurring soil materials, both organic and inorganic, are generally poor specimens for direct NMR study. Hence the value of this technique using existing equipment appears limited.

CONCLUSIONS

In conclusion there seems little doubt that CAT scanning will become a major, if not the major tool in studies of soil-plant-water systems. To make optimum use of the technique, however, substantial improvements in the equipment readily available are needed. The speed and resolution possible with commercial x-ray systems makes them ideal for rapid monitoring of the movement of water fronts in soil columns and enables detailed studies of water content distributions in essentially rigid porous media. The usefulness of single energy scanning systems (both x-ray and gamma-ray) will, however, always be severely limited by their inability to distinguish between changes in water content and bulk density in swelling and shrinking soils. Though fast in operation, the quantitative usefulness of x-ray scanners is restricted by the polychromatic nature of the beam and beam hardening. In addition the proprietary nature of commercial medical systems makes software modification or extension impossible. In view of their substantially lower cost and superior quantitative characteristics, gamma systems may ultimately prove of most use for soil and plant studies. Substantial improvements in scanning geometry and counting electronics, however, are required for full realization of their potential. The incorporation of fan beam geometry together with improved multiple beam detection systems will undoubtedly reduce scanning times by an order of magnitude, but will inevitably increase overall instrument costs. The availability of improved image and data analysis software allowing two and three dimensional visualization and quantitative analysis of scan data, will also greatly enhance these activities.

REFERENCES

- Anderson, S.H., C.J. Gantzer, J.M. Boone, and R.J. Tully. 1988. Rapid non-destructive bulk density and soil water content determination by computed tomography. *Soil Sci. Soc. Am. J.* 52:35-40.
- Anderson, S.H., R.L. Peyton, and C.J. Gantzer. 1990. Evaluation of constructed and natural soil macropores using X-ray computed tomography. *Geoderma* 46:13-29.
- Aylmore, L.A.G. 1993. The use of computer assisted tomography in studying water movement around plant roots. *Adv. Agron.* 49:1-54.
- Aylmore, L.A.G., and M. Hamza. 1990. Water and solute movement to plant roots. p. 124-129. *In Trans. 14th Congr. Soil Science. Kyoto, Japan. 12-18 Aug. ISSS, Wageningen, The Netherlands.*
- Bottomley, P.A., H.H. Rogers, and T.H. Foster. 1986. NMR imaging shows water distribution transport in plant root systems in situ. *Proc. Natl. Acad. Sci. U.S.A.* 83:87-89.
- Bracewell, R.M. 1965. The fourier transform and its applications. McGraw-Hill, New York.
- Brooks, R.A., and G. Di Chiro. 1976. Principles of computer assisted tomography (CAT) in radiographic and radioisotopic imaging. *Phys. Med. Biol.* 21:689-732.
- Brown, J.M., G.A. Johnson, and P.J. Kramer. 1986. In vitro magnetic resonance microscopy of changing water content in *Pelargonium hortorum* roots. *Plant Physiol.* 83:1158-1160.
- Brown, G.O., M.L. Stone, and J.E. Gazin. 1993. Accuracy of gamma ray computerized tomography in porous media. *Water Resour. Res.* 29:479-486.
- Coppola, M., and P. Reiniger. 1974. Influence of the chemical composition on the gamma-ray attenuation by soils. *Soil Sci.* 117:331-335.
- Corey, J.C., S.F. Peterson, and M.A. Wakat. 1971. Measurement of attenuation of Cs-137 and Am-241 gamma rays for soil density and water content determinations. *Soil Sci. Soc. Am. Proc.* 35:215-219.
- Crestana, S., R. Cesareo, and S. Mascarenhas. 1986. Using a computer assisted tomography miniscanner in soil science. *Soil Sic.* 142:56-61.
- Crestana, S., S. Mascarenhas, and R.S. Pozzi-Mucelli. 1985. Static and dynamic three-dimensional studies of water in soil using computer tomographic scanning. *Soil Sci.* 140:326-332.
- Davis, J.R., M.J. Morgan, P. Wells, P. Shadbolt, and B. Suendermann. 1986. X-ray computed tomography: 1. A non-medical perspective. *Aust. Phys.* 23:245-247.
- Gilboy, W.B. 1984. X- and gamma-ray tomography in NDE applications. *Nucl. Instrum. Methods* 221:193-200.
- Grevers, M.C.J., E. De Jong, and R.J. St. Arnaud. 1989. The characterization of soil macroporosity with CT scanning. *Can. J. Soil Sci.* 69:629-637.
- Gurr, C.G. 1962. Use of gamma rays in measuring water content and permeability in unsaturated columns of soils. *Soil Sci.* 94:224-229.
- Hainsworth, J.M., and L.A.G. Aylmore. 1983. The use of computer assisted tomography to determine spatial distribution of soil water content. *Aust. J. Soil Res.* 21:435-443.
- Hainsworth, J.M., and L.A.G. Aylmore. 1986. Water extraction by single plant roots. *Soil Sci. Soc. Am. J.* 50:841-848.
- Hainsworth, J.M., and L.A.G. Aylmore. 1988. Application of computer assisted tomography (CAT) to gamma attenuation measurement of soil water content. *Aust. J. Soil Res.* 26:105.
- Hainsworth, J.M., and L.A.G. Aylmore. 1989. Non-uniform water extraction by a single plant root. *Plant Soil* 113:121-124.
- Hamza, M., and L.A.G. Aylmore. 1991. Liquid ion exchanger microelectrodes used to study soil solute concentrations near plant roots. *Soil Sci. Soc. Am. J.* 55:954-958.
- Hamza, M., and L.A.G. Aylmore. 1992a. Soil solute concentration and water uptake by single lupin and radish plant roots: I. Water extraction and solute accumulation. *Plant Soil* 145:187-196.
- Hamza, M., and L.A.G. Aylmore. 1992b. Soil solute concentration and water uptake by single lupin and radish plant roots: II. Driving forces and resistances. *Plant Soil* 145:197-205.
- Hopkins, F.F., I.L. Morgan, H.D. Ellinger, R.V. Klinksiek, G.A. Meyer, and J.N. Thompson. 1981. Industrial tomography applications. *IEEE Trans. Nucl. Sci.* 28:1717-1720.
- Hounsfield, G.N. 1972. A method of and apparatus for examination of a body by radiation such as X- or gamma radiation. *Britian Patent* 1283915.
- Jensen, P.D., and P.H. Heyerdahl. 1988. Soil column descriptions from X-ray computed tomography density images. *Soil Sci.* 146:102-107.

- Johnson, G.A., M.B. Thompson, S.L. Gewart, and C.E. Hayes. 1986. Nuclear magnetic resonance imaging at microscopic resolution. *J. Magn. Reson.* 68:129-134.
- Kak, A.C., and M. Slaney. 1988. Principles of computerized tomographic imaging. IEEE Press, New York.
- McFall, J.S., G.A. Johnston, and P.J. Kramer. 1991. Comparative water uptake by roots of different ages in seedlings of loblolly pine (*Pinus taeda* L.). *New Phytol.* 119:551-560.
- Newton, T.H., and D.G. Potts. 1981. Technical aspects of computed tomography. p. 3853-3917. *In* T.H. Newton and D.G. Potts (ed.) Radiography of the skull and brain. Mosby Publ., St. Louis, MO.
- Omasa, K., M. Onoe, and H. Yamada. 1985. NMR imaging for measuring root systems and soil water content. *Environ. Control Biol.* 23:99-102.
- Petrovic, A.H., J.E. Siebert, and P.E. Lieke. 1982. Soil bulk density analysis in three dimension by computed tomographic scanning. *Soil Sci. Soc. Am. J.* 46:445-450.
- Phogat, V.K., and L.A.G. Aylmore. 1989. Evaluation of soil structure by using computer assisted tomography. *Aust. J. Soil Res.* 27:313-323.
- Phogat, V.K., L.A.G. Aylmore, and R.D. Schuller. 1991. Simultaneous measurement of the spatial distribution of soil water content and bulk density. *Soil Sci. Soc. Am. J.* 55:908-915.
- Ryhiner, A.H., J. Pankow. 1969. Soil moisture measurement by the gamma transmission method. *J. Hydrol. (Amsterdam)* 9:194-205.
- Tollner, E.W., and C. Murphy. 1991. Factors affecting soil X-ray absorption coefficients with computed tomography. *Trans. ASAE* 34:1047-1053.
- Tollner, E.W., B.D. Verma, and J.M. Cheshire, Jr. 1987. Observing soil-tool interactions and soil organisms using X-ray computer tomography. *Trans. ASAE* 30:1605-1610.
- Warner, G.S., J.L. Nieber, I.D. Moore, and R.A. Geise. 1989. Characterizing macropores in soil by computed tomography. *Soil Sci. Soc. Am. J.* 53:653-660.
- Woods, R.T., J.J. Hennessy, E. Kwok, and B.E. Hammer. 1989. NMR microscopy—a new biological tool. *Biol. Techniques* 7:616-622.

Soil Pollution and Waste Disposal

Estimating the Pollution Potential of Pesticides to Ground Water

Rai S. Kookana^A and L. A. G. Aylmore^B

^A Cooperative Research Centre for Soil and Land Management,
Private Bag No. 2, Glen Osmond, S.A. 5064.

^B Soil Science and Plant Nutrition, University of Western Australia,
Nedlands, W.A. 6009.

Abstract

A screening model available in the literature has been used to evaluate the ground water pollution potential of a number of commonly used pesticides under irrigated horticulture in Bassendean sand of the Swan Coastal Plain of Western Australia. The original model assumed a decreasing rate of pesticide degradation but a constant organic matter content with depth in the soil profile. A modified version of the model was developed to take into account the generally decreasing organic matter contents with depth in the soil profile. Residual masses and travel times of 40 pesticides were calculated by the model using sorption and degradation data available from the literature. The calculations based on the constant OM mode predicted that for a recharge rate of 0.5 m/yr, some 14 of the pesticides were likely to reach ground water at appreciable levels of the residue (>0.1% of applied mass). The number increased to 21 and was accompanied by a decrease in the travel times required for the pesticides to reach ground water when the decreasing organic matter contents of the profile with depth were taken into consideration.

To assess the validity of using sorption and degradation data from the literature for the local soil, comparisons of model calculations were made for five pesticides whose sorption coefficients and degradation half-lives were measured on the local soil. For some pesticides, the predictions based on literature values were significantly different from those based on measured parameters indicating, as expected, that overseas data may not always represent local conditions. However, they may still provide valuable first approximations of the likely relative pollution potentials of different pesticides.

Keywords: pesticides, ground water pollution, sorption, degradation, screening model, Swan Coastal Plain.

Introduction

There are numerous reports of pesticides having been detected in ground waters throughout the world. In California (U.S.A.) alone, about 50 different pesticides have been found in various ground waters, while 84 pesticides have been thought to pose a hazard to ground waters when used as a potable source (Holden 1986). Similar reports are also available from other parts of the world, pesticides having been found in surface as well as ground waters of the U.K. (Croll 1991), and in ground waters of the FRG (Friesel *et al.* 1986) and the Netherlands (Loch *et al.* 1989). In the Netherlands, some 35 pesticides are now banned and admission of a further 15 pesticides has been restricted in ground water protection areas (Loch *et al.* 1989).

In Australia, reports of ground water contamination from pesticides are meagre, presumably because of the general lack of systematic ground water monitoring programs. However, pesticides have been detected in Australian ground waters (EPA 1989; Stadter *et al.* 1992). A recently conducted preliminary survey of ground water contamination from various sources reported 106 incidents of pollution, mostly from industrial effluent (Jacobson and Lau 1988). The report concluded that an evaluation of non-point source pollution from herbicides and pesticides was urgently required. This is particularly important because of the increasing dependence in recent years of agriculture and horticulture practices in Australia on pesticide usage. The total sale of pesticides increased nearly sixfold from \$90 million in 1978 to \$703 million during 1992 (AVCA, pers. comm.).

The aquifer beneath the Swan Coastal Plain of Western Australia is currently being exploited for drinking water purposes (Whelan and Barrow 1984; EPA 1989). The soils of the coastal plain, in general, are highly leached, coarse textured and contain very low organic matter and clay contents. Nearly 50% of the area of the plain is comprised of the soils of Bassendean association (Bettenay *et al.* 1960). A large area of these soils is used for irrigated horticulture where relatively high amounts of pesticides and fertilizers are used. The high permeability of the soil provides conditions which favour leaching. Consequently, very high levels of nitrates (up to 8 times acceptable drinking water levels) have been found in the ground waters under market gardens (Pionke *et al.* 1990). Similarly, leaching of phosphorus through the sand has contributed to the eutrophication of the Peel-Harvey Estuary (Birch 1982). Systematic monitoring of pesticides in these ground waters has not been undertaken. However, the scale of pesticide use in irrigated horticulture, together with the existing favourable conditions for leaching, are a cause for considerable concern from the point of view of the potential for pesticide pollution (Pionke *et al.* 1990; Sharma 1990).

An evaluation of the potential of any given pesticide to reach ground water needs to take into account both the extent of its retention and the rate of degradation. Jury *et al.* (1987) developed a screening model based on the mobility and the persistence of pesticides in soils and used it for estimating the pollution potential of a number of pesticides. A similar approach was used by Rao *et al.* (1985) who developed an index for this purpose based on the residence time and half-life of the pesticides in the vadose zone. However, other relatively more complex models such as PRZM, LEACHM and GLEAMS have also been developed in recent years. These models require a large number of input parameters which are generally not available. Wagenet and Rao (1990) have discussed the pros and cons of the various models available in the literature. In the present paper we have used the Jury *et al.* (1987) model to evaluate the pollution potential of a number of commonly used pesticides under irrigated horticulture in Bassendean sand of the Swan Coastal Plain. The model developed by Jury *et al.* (1987) assumes a constant organic matter content throughout the soil profile. This is clearly not consistent with the fact that levels of organic matter almost invariably decrease sharply with depth in the soil profile. Consequently, to examine the significance of this assumption, results were obtained with a modified version of the model derived to take the changing organic matter distribution with depth in the soil profile into consideration.

Theory

The model developed by Jury *et al.* (1987) assumes a steady water flow, equilibrium sorption and a depth-dependent rate of biodegradation. It takes into account the decrease in microbial population with depth in a soil profile, but assumes a uniform organic carbon content throughout the soil profile.

While being leached at a uniform average drainage rate J_w (m day^{-1}), a chemical is assumed to undergo linear, reversible, equilibrium sorption and first-order biochemical decay. The soil profile is divided into three zones:

- (1) surface zone from the surface $z = 0$ to a depth $z = L$ with a constant microbial population density and therefore a constant rate of degradation of the chemical;
- (2) a lower vadose zone from $z = L$ to $z = H$ with an exponentially declining microbial population density and wherein the degradation constant is proportional to microbial population; and
- (3) a deep zone below depth H with a residual value of both microbial population density and the degradation constant.

The sorption of a chemical by a soil is given by its organic carbon distribution coefficient K_{oc} ($\text{m}^3 \text{kg}^{-1}$) and the degradation by the biochemical half-life $t^{1/2}$ (days). A constant value of volumetric water content θ , soil bulk density B_d (kg m^{-3}) and fraction of organic carbon (f_{oc}) is assumed. The assumption in the model of constant OC with depth means that the K_{oc} value will be constant throughout the profile.

The chemical is assumed to be applied at the soil surface ($z = 0$) in a single application of mass M_0 per unit area at time $t = 0$.

For simplicity, piston flow is assumed and diffusion and dispersion are neglected. Under these assumptions, the resultant mass balance equation can be written as (Jury *et al.* 1987)

$$\partial C_t / \partial t + J_w \partial C / \partial z + \mu(z) C_t = 0, \quad (1)$$

where J_w is the water flux, C (g m^{-3}) is the solution concentration, and $\mu(z)$ (days^{-1}) is the biochemical rate constant. Total solute concentration (C_t in g m^{-3}) is given by

$$C_t = B_d S + \theta C, \quad (2)$$

where S (g kg^{-1}) is the sorbed concentration.

By assuming a linear sorption isotherm, i.e.

$$S = K_d C = f_{oc} K_{oc} C, \quad (3)$$

where K_d ($\text{m}^3 \text{kg}^{-1}$) is the distribution coefficient and f_{oc} is the fraction of organic carbon, then

$$C_t = (B_d f_{oc} K_{oc} + \theta) C = R_L C \quad (4)$$

where R_L is the ratio of total to solution concentration; in other words, the retardation factor.

Combining equations (1) and (4) we have

$$\partial C_t / \partial t + V_E \partial C_t / \partial z + \mu(z) C_t = 0, \quad (5)$$

where the effective solute velocity $V_E = J_w / R_L$.

By assuming the soil to be initially free of solute, i.e. $C_t(0, z) = 0$, and considering an amount of solute M_0 applied to the soil at $t = 0$, the amount of solute reaching a depth z is given (Jury *et al.* 1987) by

$$M(z) = M_0 \exp[-1/V_E \int_0^z \mu(z) dz]. \quad (6)$$

The degradation rate coefficient μ is assumed proportional to the microbial population density of the different zones. In the surface zone

$$(0 < z < L) \mu = \mu_0 = 0.693/t^{1/2},$$

where $t^{1/2}$ is the half-life of the pesticide; in the transition zone

$$(L < z < H) \mu = \mu_0 \exp[-\Omega(z - L)]$$

and, in the residual zone ($z > H$)

$$\mu = \mu_r = \mu_0 \exp[-\Omega(H - L)],$$

where Ω (m^{-1}) is the depth coefficient representing the steepness of decrease in microbial population with depth.

With the depth dependence of degradation constant described above, Jury *et al.* (1987) derived the following relations from equation (6) for the fraction of solute applied at the surface that has not degraded:

1. In the surface zone

$$M(z)/M_0 = \exp(-\mu_0 z/V_E). \quad (7)$$

2. In the transition zone

$$M(z)/M_0 = \exp[-\mu_0/(\Omega V_E) (1 - \exp\{-\Omega(z - L)\})]. \quad (8)$$

For $\Omega(z - L) \gg 1$, $M(z)/M_0$ approaches the constant value M_r in the transition zone given by

$$M(z)/M_0 = M_r = \exp[-\mu_0/V_E (L + \Omega^{-1})]. \quad (9)$$

3. In the residual zone, the mass will continue to degrade at a rate described by μ_r given above. Thus, for time greater than the residence time ($t_H = H/V_E$) required to reach $z = H$, the mass fraction $M(t)/M_0$ will follow the equation

$$M(t)/M_0 = M_r \exp(-\mu_r t). \quad (10)$$

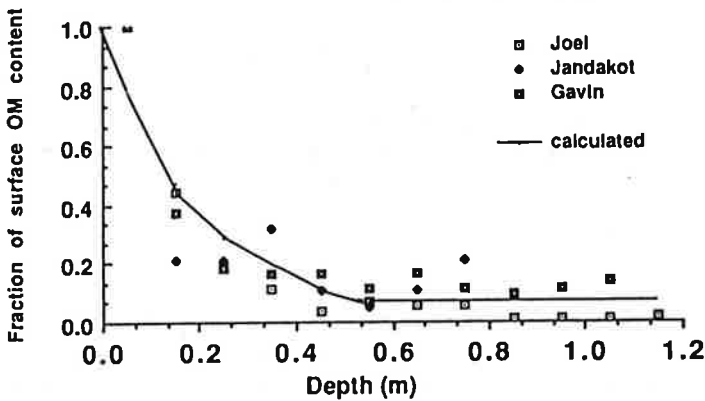


Fig. 1. Organic matter distributions in three soil profiles.

Modification of the Model

In practice, the subsurface layers of soil profiles almost invariably have significantly lower organic carbon contents than the surface layers. Consequently, the screening model was modified to take into account the decreasing organic carbon content with depth in the soil profile. As an example, organic carbon data from three soil profiles of the Bassendean Association of the Swan Coastal Plain, plotted as ratio of organic carbon content at a given depth to that in the surface layer against depth, are presented in Fig. 1. An exponential decrease in organic carbon contents was observed up to 0.5 m depth of soil. A best fit line for three soil profiles was obtained with

$$f_{oc_z}/f_{oc_0} = \exp(-5.0z), \quad (11)$$

where z is the depth in the soil profile (m).

At soil depths greater than 0.5 m, organic carbon contents were taken as a residual value constant with depth. Hence, based on organic carbon contents, the soil profile was divided into two zones:

a surface zone ($0 < z < L$), where

$$f_{oc} = f_{oc_0} \exp(-5.0z) \quad (12)$$

and a subsurface zone ($z > L$), where

$$f_{oc_z} = f_{oc_0} \exp(-5.0L). \quad (13)$$

The organic carbon contents of the soil profiles given by equations (12) and (13) determine the solute flow velocity V_E , which is given for the surface zone ($0 < z < L$) by

$$V_E = J_w / [\exp(-5.0z) f_{oc} K_{oc} B_d + \theta], \quad (14)$$

and for transition and deep zones ($z > L$) by

$$V_E = J_w / [\exp(-5.0L) f_{oc} K_{oc} B_d + \theta]. \quad (15)$$

The fraction of mass applied at the surface that has not degraded is given by equations (7)–(10) combined with equations (14)–(15) for the respective zones.

Model Parameters

Pesticide Sorption and Degradation Parameters

A compilation of sorption parameters (K_{oc}) and the half-lives ($t^{1/2}$) for a large number of pesticides is available in the literature (e.g. Rao *et al.* 1985; Jury *et al.* 1987). However, due to the differences in the soil and climatic conditions, these values may not truly represent the behaviour of pesticides in Bassendean sand, particularly because of the extremely sandy nature (approx. 1% clay). To assess this, a comparison was made between results obtained from the literature and measured values.

Sorption and degradation were measured for the different pesticides in the Bassendean sand to obtain K_{oc} and $t^{1/2}$ values. The general characteristics of soils of the Swan Coastal Plain have been reported by Bettenay *et al.* (1960). The soil used in the present study was collected from the vegetable research station of the Western Australian Department of Agriculture at Medina, W.A. The soil from 0–25 cm was composited and passed through a 2 mm sieve. Important physio-chemical properties were: organic carbon, 0.6%; pH (1:5 water), 5.3; silt+clay, 1.0%; CEC, 2.4 cmol(+) kg^{-1} with kaolinite the dominant clay mineral. The K_{oc} values were calculated from K_d values obtained from batch experiments (Singh *et al.* 1990) and organic carbon (OC) contents of the soil. The half-lives for the pesticides were calculated from laboratory incubation experiments. Soil (1 kg), freshly collected from the field, was incubated at 25°C in the dark and at a moisture content representing 100 cm matric potential. The concentrations of the pesticides (mg kg^{-1} a.i.) for the experiments were chosen as those recommended for horticulture crops and were: fenamiphos, 4 mg kg^{-1} ; linuron, 1.25 mg kg^{-1} ; metalaxyl, 0.08 mg kg^{-1} ; metribuzin, 0.5 mg kg^{-1} ; and prometryne, 1.0 mg kg^{-1} . Application rates were estimated on the assumption that the pesticides were retained in the top 10 cm of soil with a bulk density of 1.5 g cm^{-3} . At 0, 1, 4, 8, 18, 39, 74 and 139 days from the start of the experiment, a 50 g subsample was withdrawn in duplicate and analysed on the HPLC. The microbial population density was assumed to decrease with a depth coefficient, 3 m^{-1} , as reported by Focht and Joseph (1973) and used by Jury *et al.* (1987).

Recharge Rate and other Hydrological Parameters

The ground water recharge rate is the most difficult parameter to estimate accurately. However, with the help of previous studies by other workers, the parameter was calculated as follows. Precipitation, which on the Swan Coastal Plain mostly occurs in winter, is about 775 mm per year (Sharma and Hughes 1985). Irrigation adds about 500–1000 mm per year, depending upon the intensity of cropping. Luke (1988) estimated some 85–90 m^3 water for 8300 ha of irrigated horticultural lands. Thus, the average total input of water (precipitation plus

irrigation) is approximately 1800 mm per year. Pionke *et al.* (1990) estimated an actual evapotranspiration to be 1000 mm yr⁻¹, and therefore at least the excess 800 mm can contribute to ground water recharge. Under irrigated horticulture, an intensive cropping system requires 120–150% of class A pan evaporation. A lysimetric study conducted under these conditions (Sharma 1990) showed that 40% of irrigation water applied in such market gardens reaches ground water. Although under irrigated horticulture the recharge may occur throughout the year, the winter rains result in most of the precipitation-induced recharge. On the basis of these studies, the recharge rate was estimated to be between 0.5 and 1 m yr⁻¹.

Other required soil and environmental parameters were measured in the laboratory. Moisture content at saturation (θ_s) of the sand was 0.3 m³ m⁻³, which decreased rapidly to 0.05 m³ m⁻³ at a water potential of 10 kpa. An average of 0.1 m³ m⁻³ was chosen for the calculations. Values of parameters used in the calculations are summarized in Table 1.

Table 1. Parameters used in the calculations

Parameter	Value
Bulk density, B_d	1450 kg/m ³
Moisture content, θ	0.1 m ³ /m ³
Organic carbon fraction, f_{oc}	0.006 kg/kg
Depth of surface zone, L	0.25 m
Depth of lower vadose zone, H	3.0 m
Annual recharge rate, J_w	0.5 and 1.0 m/yr
Microbial depth factor Ω	3 m ⁻¹

Results and Discussion

Concentration Distribution in the Soil Profile

Examples of the distribution of simazine concentration in the soil profile, as predicted using the parameters given in Table 1 and two values of biochemical half-life reported in the literature, are shown in Fig. 2. Simazine concentrations initially decreased exponentially with depth in the zone of constant degradation and approached residual values in the transition zone. In this zone, the residual concentrations are little affected by the depth in the soil profile. The distance a pesticide needs to travel in the transition zone would only affect the time it requires to reach ground water and not so much the concentration.

Effect of Half-life

Values of the half-lives of particular pesticides reported in the literature vary considerably, with consequent effects on the pollution hazard predicted. For example, the marked effect of biochemical half-life on the concentration distribution of simazine is evident from Fig. 2. A decrease in half-life from 75 to 32 days resulted in a decrease of residual concentration from 10⁻³ to 10⁻⁹ of applied mass. In other words, of a surface application of 1 kg of simazine, 1 g will reach ground water under the longer $t^{1/2}$ and only 1 μ g with the shorter half-life.

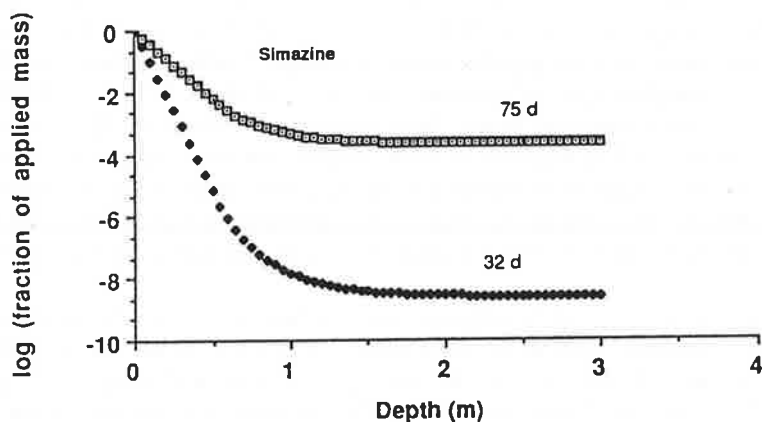


Fig. 2. Distribution of Simazine residual mass under two rates of degradation (calculated assuming constant K_{oc} throughout the soil profile and $L = 0.5$ m).

It should be noted that, in calculating the pollution potential of certain pesticides, the rate of degradation or transformation of the parent compound alone can be misleading, particularly when metabolites or daughter compounds retain the pesticidal properties of the parent compound. For example, fenamiphos is oxidized very quickly (half-life 10 days; Jury *et al.* 1987) to its sulfoxide and sulfone. However, the nematicidal/pesticidal properties of the chemicals remain unaffected. For degradation of fenamiphos and its two metabolites as total residue, a half life of some 70 days has been found (Bilkert and Rao 1986). In addition, the sorption properties of the metabolites have been reported to be different from those of the parent compound, and the two metabolites are considered to be more mobile than fenamiphos.

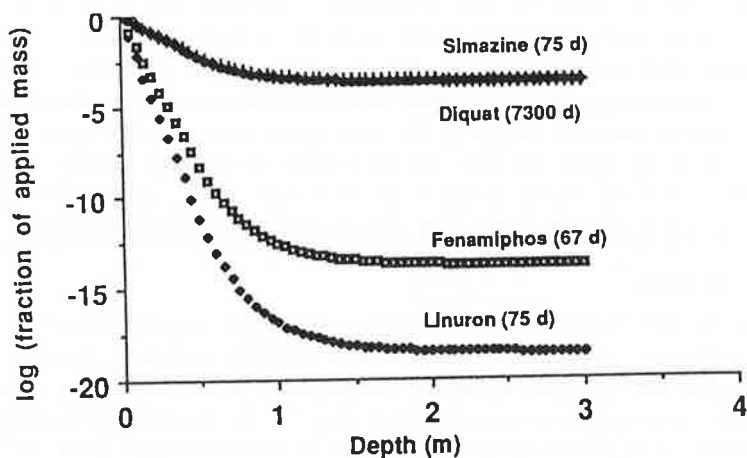


Fig. 3. Residual mass reaching various depths for four pesticides. Values in parentheses are half-lives (calculated assuming constant K_{oc} throughout the soil profile and $L = 0.5$ m).

Effect of Sorption

The effect of sorption on the residue reaching a given depth becomes evident from a comparison of predicted concentration profiles of simazine and linuron in Fig. 3. Both herbicides have been reported to have similar rates of degradation (Jury *et al.* 1987) but different sorption coefficients. Because of the higher sorption of linuron compared with simazine, and consequent larger residence time (several days under the conditions given in Table 1) in the surface zone of constant degradation, the linuron mass decreased to a value equivalent to 10^{-17} of the applied mass by the time it reached the transition zone (1 m depth). A comparison of the residual mass profiles of diquat and simazine shows that these are similar despite the 100 fold difference in their half-lives. [In the absence of reports on degradation for diquat (Corwin and Farmer 1985), a half-life of 20 years, as reported for paraquat (ICI 1984), was used in the calculations.] The effect of the much larger half-life of diquat is counteracted by its equally larger sorption in comparison with simazine and results in similar distribution profiles for these herbicides. Nevertheless, because of its higher sorption, the prediction is that it would take many hundreds of years for diquat to reach a 3 m depth. As discussed later, and elsewhere (Kookana and Aylmore 1993), the validity of this prediction is subject to a number of qualifications.

Effect of Surface Zone Thickness

The role of the surface zone, in which the degradation rate is assumed to be constant, in determining the residual mass of a pesticide is crucial because of the higher microbial activity in this zone and correspondingly higher rate of degradation. There are reports in the literature that the microbial biomass decreases very rapidly with depth in a soil profile. For example, Van Gestel *et al.* (1992) found that, in a topsoil of an Australian Alfisol, the microbial biomass decreased to half every 2.5 cm depth. Jury *et al.* (1987) assumed the top 0.5 m of the soil profile as the surface zone. The residual masses of pesticides reaching a 3 m depth in the soil profile, calculated using surface zones of 0.25 and 0.5 m thickness respectively, demonstrate that by doubling the thickness of the surface zone the residual masses would be reduced to at least one third of that for the lower thickness. For example, the residual masses of simazine and metalaxyl decreased from 6.69 and 7.60% to 2.10 and 2.52% respectively when the thickness of the surface zone was increased from 0.25 to 0.5 m. The effect of profile moisture content on the mass leaching to deeper depths was found to be relatively smaller.

Table 2. Comparison of residues (% of applied mass reaching 3 m depth) calculated with measured and literature values (Jury *et al.* 1987) of parameters (K_{oc} and $t^{1/2}$)
Recharge rate of 1.0 m/yr; constant OC contents; other parameters in Table 1

Pesticide	K_{oc}		Half-life (days)		Residual mass	
	Meas.	Lit.	Meas.	Lit.	Meas.	Lit.
Fenamiphos	0.55	0.17	30	10	6.2×10^{-9}	1.3×10^{-8}
Linuron	0.84	0.86	143	75	0.05	4.6×10^{-5}
Metalaxyl	0.09	—	48	—	7.6	—
Metribuzin	0.25	0.024	46	37	0.08	29.97
Prometryne	1.22	0.61	64	60	3.2×10^{-9}	2.2×10^{-4}
Simazine	0.15	0.14	75	75	6.69	7.91

Use of Literature Parameters

For five pesticides, whose K_{oc} and $t^{1/2}$ values were measured for Bassendean sand, a comparison between the residues calculated from the measured values, and from values obtained from the literature was made (Table 2). The residual masses calculated from measured parameters were found to be similar in the cases of fenamiphos and simazine, but lower in the cases of metribuzin and prometryne. In contrast, the values for linuron were found to be much higher than those calculated using literature values. Differences in soil properties, such as pH and ionic strength, can significantly affect sorption (Singh *et al.* 1990) and the degradation behaviour of pesticides. Hence, it is not possible to predict whether the literature values of sorption and degradation parameters apply to the local soil type.

Table 3. Residual mass (%) and travel times (yrs) for six pesticides, based on measured sorption and degradation parameters (at 1.0 m/yr recharge rate)

Pesticide	Residual mass		Travel time	
	Const. OM	Var. OM	Const. OM	Var. OM
Fenamiphos	6.2×10^{-9}	7.2×10^{-3}	14.3	4.69
Linuron	0.06	4.96	21.7	7.01
Metribuzin	0.08	4.98	6.67	2.29
Metalaxyl	7.6	29.30	2.51	1.01
Prometryne	3.2×10^{-9}	6.5×10^{-3}	31.4	10.05
Simazine	6.69	30.70	4.12	1.49

Effect of Decreasing OC (K_{oc}) with Depth

The residual masses of six pesticides, calculated by assuming constant and decreasing OC contents respectively in the soil profile, are presented in Table 3. An exponentially decreasing OC content with depth (equation 11) dramatically affected not only the residual masses but also the travel times required for the pesticides to reach a 3 m depth. For example, under constant OC content, fenamiphos and prometryne showed negligible residue (some $10^{-9}\%$ of applied), whereas, when decreasing OC contents with depths were considered, the residual masses increased to 0.007% of the applied pesticide. Similarly, the residual masses of linuron and metribuzin increased between 60- and 80-fold, and that of simazine and metalaxyl between 3- and 5-fold. The greatest effect was noticed for pesticides showing little residue under constant OC content.

Pollution Potential of 40 Pesticides in the Swan Coastal Plain

To further investigate the pollution potential of pesticides, similar calculations were made for 40 pesticides, whose sorption and degradation parameters are readily available in the literature, using the parameters given in Table 1. The masses reaching 3 m depths and travel times needed to reach the depth under constant and variable OC scenarios are presented in Table 4. A survey of 15 farmers in the Peel-Harvey catchment area revealed that most of these pesticides have been used on the Swan Coastal Plain in recent years. Pesticides such as dieldrin, DDT and heptachlor are no longer in use but their possible legacy is of some interest. Details of the actual amounts being used in this area are

Table 4. Residual mass of different pesticides reaching 3 m depth in Bassendean sand with a recharge rate of 0.5 and 1.0 m/yr (parameters from Table 1)

Travel time under $J_w = 1.0$ m/yr will be half of the values calculated for $J_w = 0.5$ m/yr.
 K_{oc} and $t^{1/2}$ taken from Jury *et al.* (1987)

Pesticide	Residual mass (%)				Travel time (yr)	
	Constant OM		Variable OM		Constant OM	Variable OM
	0.5 m/yr	1.0 m/yr	0.5 m/yr	1.0 m/yr	0.5 m/yr	0.5 m/yr
EDB	96.25	98.10	98.04	99.0	2.83	1.29
Bromacil	54.92	74.11	86.68	75.14	4.26	1.74
DBCP	40.26	63.45	64.67	80.42	4.16	1.71
Picloram	22.44	47.40	46.62	68.28	3.04	1.35
Aldicarb	18.19	42.60	39.82	63.10	2.42	1.16
Dicamba	8.56	29.30	10.88	33.00	0.70	0.62
Metribuzin	8.98	29.97	24.13	49.12	1.81	0.97
Carbofuran	8.37	28.93	24.32	49.32	2.02	1.04
Terbacil	7.16	26.75	24.96	49.96	2.68	1.24
Monuron	5.51	23.50	28.78	53.64	9.78	3.47
Diuron	4.98	22.37	29.14	53.98	20.01	6.66
Simazine	0.62	7.91	10.75	32.79	7.74	2.83
Ethrophosphos	0.13	3.68	5.24	22.88	6.72	2.51
Atrazine	0.12	3.40	5.38	23.20	8.76	3.15
2,4,5-T	0.09	3.07	3.80	19.49	4.67	1.87
Oxamyl	0.06	2.57	0.30	5.50	0.89	0.68
Diazinon	0.05	2.26	2.94	17.14	4.93	1.95
2,4-D	0.00	0.38	0.11	3.25	1.61	0.91
Metalochlor	0.00	0.33	0.73	8.53	9.78	3.47
Lindane	0.00	0.20	0.72	8.46	66.98	21.38
Dichloro- propene	0.00	0.19	0.25	4.97	4.06	1.67
Alachlor	0.00	0.01	0.03	1.66	6.70	2.51
Phorate	0.00	0.00	0.02	1.57	34.30	11.15
Prometryne	0.00	0.00	0.00	0.52	31.70	10.35
Chlordane	0.00	0.00	0.00	0.46	1942.0	608.5
Linuron	0.00	0.00	0.00	0.28	44.70	14.40
Carbaryl	0.00	0.00	0.00	0.30	12.28	4.25
Dieldrin	0.00	0.00	0.00	0.00	614.0	192.0
Cyanazine	0.00	0.00	0.00	0.00	9.2	3.32
Chlorthalonil	0.00	0.00	0.00	0.00	71.0	22.66
Fenamiphos	0.00	0.00	0.00	0.00	9.4	3.06
Captan	0.00	0.00	0.00	0.00	2.27	1.11
Napropamide	0.00	0.00	0.00	0.00	15.90	5.39
Propachlor	0.00	0.00	0.00	0.00	22.04	7.30
Chlorthal- dimethyl	0.00	0.00	0.00	0.00	204.9	64.58
Methyl parathion	0.00	0.00	0.00	0.00	262.0	82.20
Chlorpyrifos	0.00	0.00	0.00	0.00	310.6	97.7
Trifluralin	0.00	0.00	0.00	0.00	374.0	117.4
Heptachlor	0.00	0.00	0.00	0.00	1226.0	384.5
DDT	0.00	0.00	0.00	0.00	12259.0	3840.0

difficult to obtain. However, a number of the pesticides, including fenamiphos, metalaxyl, chlorthalonil, chlorpyrifos, linuron, propachlor, metribuzin, trifluralin, prometryne, carbaryl, simazine, chlorthal-dimethyl and phorate, are in common use. Some pesticides such as EDB, dicamba and cyanazine are registered for

use in horticulture in other parts of Australia but not in Western Australia. Fenamiphos, diazinon, dicamba and chlorthalonil are used on turf on the Swan Coastal Plain.

Once again, the calculated masses for those pesticides which showed little residues left under a constant OC content situation were markedly affected by the decreasing OC contents of the profile. Out of 40 pesticides considered, the number of those showing a residue $>0.1\%$ of that applied was found to be 14 under constant OC as compared with 21 under variable OC for a recharge rate of 0.5 m/yr (Table 5). Three pesticides showed residues of more than 60% of the applied mass, whereas only one pesticide of fourteen fell into this category under constant OC. The travel times for these pesticides were also greatly reduced (to approx. one third) by taking decreasing OC contents into account. Few data are available on the concentrations of these pesticides in ground water with which to compare these predictions. However, the present data are valuable in providing a guide for any monitoring exercise and selection of potential pesticide penetration to ground waters. Some of the organochlorines, which have been used in the past but not currently in use, have in fact been detected by the Water Authority of Western Australia, at times at levels exceeding health limits (EPA 1989). However, the source of these pesticides is not clear and may not be horticulture.

Most of the pesticides showing significant residues ($>1\%$) in the soil profile were predicted to have very short travel times in the profile, i.e. <5 years, even under a recharge rate of 0.5 m/yr. Out of 21 such pesticides, only two showed travel times more than 5 years under decreasing OC contents in the soil profile. Doubling the recharge rate to 1.0 m/yr would halve the values for travel times calculated.

Other Factors Influencing the Mobility of Pesticides

According to the model predictions, a very large number of pesticides have the potential to reach to ground water under the conditions considered here. The validity of these predictions will, however, depend on the significance of a number of other factors which have not been taken into account in the model. Some of these factors will increase the potential mobilities of the pesticides in the soil profile while others will decrease them.

Assumption of Negligible Dispersion

The dispersion effect neglected in the model can be significant in terms of both the time taken by a pesticide to reach ground water and the concentration distribution with depth in the soil profile. By ignoring dispersion, the predictions are likely to underestimate the travel times and overestimate maximum concentrations appearing in ground water (Singh 1989).

Seasonal Variability of Recharge Rate

This parameter is particularly crucial since the mobility is governed primarily by the water percolating down the profile. In the present calculations, an average recharge rate, uniform throughout the year, has been assumed. However, under irrigated conditions, the winter-dominant rainfall is likely to result in greater recharge in winter, while there will be relatively little percolation in summer.

Hence, pesticides with high pollution potential (Table 4), when applied to winter crops, are likely to leach down the profile more rapidly than predicted.

Table 5. Frequency distribution of pesticides based on their residue levels

Residue level	Constant OM		Variable OM	
	0.5 m/yr	1.0 m/yr	0.5 m/yr	1.0 m/yr
total number	40	40	40	40
>0.1%	14	21	21	27
>5%	10	12	14	20
>20%	4	11	10	14
>60%	1	3	3	5

Preferential flow

Another important factor which can significantly affect the amount of a pesticide reaching ground water, as well as the time required, is the occurrence of preferential flow paths in the soil profile. A recent study (Kung 1990) and several others have clearly demonstrated that under certain conditions the flow of soil water can concentrate in individual columns in a soil profile and can lead to what is termed the 'funnel effect'. The study also showed that such a phenomenon can significantly affect the monitoring of pesticides in ground water, as a pesticide can be concentrated in certain pockets at the time of sampling. Preferential or bypass flow can be particularly important for pesticides because these have to bypass only the top 10–15 cm of the profile to avoid significant biochemical degradation. Water repellency, in particular, is a common characteristic which can result in bypass flow in Bassendean sand and other soils of the Swan Coastal Plain.

Sorption non-equilibrium, competition and hysteresis

The present calculations were based on the equilibrium sorption values obtained in the laboratory using a batch method, which involves shaking and centrifugation with high solution to soil ratios. Recent studies (Kookana *et al.* 1992) have shown that sorption under flow conditions, as generally experienced in the field, can be significantly different from that under batch sorption and, in particular, is generally time-dependent. During flow, the time of contact between soil and pesticides may not be long enough to reach sorption values obtained under batch conditions. Hence, the calculations based on equilibrium sorption are likely to underestimate the mobility of pesticides. Furthermore, numerous studies (Best *et al.* 1972; Murali and Aylmore 1983; Kookana and Aylmore 1993) have demonstrated that significant decreases in sorption occur for many chemicals in the presence of other species which compete for adsorption sites. Conversely, it has been observed by many workers (e.g. Singh *et al.* 1990) that certain portions of sorbed pesticides resist desorption and therefore such hysteresis may result in decreased concentrations leaching down the profile.

Conclusions

The simple screening model proposed by Jury *et al.* (1987) provides a useful preliminary procedure for comparing the relative ground water pollution potentials

of pesticides. However, the neglect of a number of other factors of potential significance in determining pesticide mobility in a soil profile means that the predictions of residue concentrations and travel times obtained are unlikely in many cases to be, and should not be regarded as, accurate for realistic field conditions. In particular, the comparisons obtained here demonstrate clearly that the assumption of the distribution of organic matter in the surface horizon, i.e. whether uniform or decreasing exponentially with depth, can appreciably alter the predictions of both parameters. Furthermore, the use of local K_{oc} and half-life values for five pesticides yielded substantially different residual concentrations to those obtained on the basis of literature values, emphasizing the need for site-specific data. In fact, there are very large variations in both K_{oc} and $t^{1/2}$ in the literature and, in the absence of local information the predictions should be treated merely as rough approximations. Despite these reservations, it is of concern that a substantial number of the commonly used pesticides considered are estimated to pose a significant hazard to ground water quality.

Acknowledgment

These studies form part of a comprehensive program of research on ground water quality funded by the Land and Water Resources Research and Development Corporation of Australia whose financial support is gratefully acknowledged.

References

- Best, J. A., Weber, J. B., and Weed, S. B. (1972). Competitive adsorption of Diquat²⁺, Paraquat²⁺ and Ca²⁺ on organic matter and exchange resins. *Soil Sci.* **114**, 444–50.
- Bettenay, E., McArthur, W. M., and Hingston, F. J. (1960). Soil associations of the Swan Coastal Plain, W.A. CSIRO Aust. Soils and Land Use Series No. 35.
- Bilkert, J. N., and Rao, P. S. C. (1985). Sorption and leaching of three non fumigant nematicides in soils. *J. Environ. Sci. Health B20* 1–26.
- Birch, P. B. (1982). Phosphorus export from coastal plain drainage to the Peel–Harvey Estuarine system, Western Australia. CSIRO Aust. Soils and Land Use Ser. No. 35.
- Corwin, D. L., and Farmer, W. J. (1985). A mathematical model of diffusion under saturated conditions to assess the pollution potential of herbicides to aquatic systems. *Hilgardia* **53**, 1–35.
- Croll, B. T. (1991). Pesticides in surface waters and ground waters. *J. Inst. Wat. Envir. Mangt.* **5**, 389–95.
- EPA (1989). Monitoring pesticides, a review. The Environment Protection Authority, Perth, Western Australia, Bull. No. 407.
- Focht, D. D., and Joseph, H. (1973). An improved method for the enumeration of denitrifying bacteria. *Soil Sci. Soc. Am. Proc.* **37**, 698–9.
- Friesel, P., Milde, G., Stock, R., and Ahlsdorf, B. (1986). Impact of agricultural pesticide application on ground water in Western Germany—Latest results and an attempt of assessment. Proc. 13th Congr. International Soil Sci. Soc. Hamburg. pp. 856–71.
- Holden, P. W. (1986). 'Pesticides and ground water quality. Issues and Problems in Four States.' Board of Agriculture. National Res. Council. (National Academy Press: Washington, DC.)
- ICI (1984). Paraquat: its fate and effects in the soil. ICI Agrochemical Monograph.
- Jacobson, G., and Lau, J. E. (1988). Ground water contamination incidents in Australia: An initial survey. Bureau of Mineral Resources, Geology & Geophysics, Report 287.
- Jury, W. A., Focht, D. D., and W. J. Farmer (1987). Evaluation of pesticide ground water pollution potential from standard indices of soil-chemical adsorption and biodegradation. *J. Environ. Qual.* **16**, 422–8.
- Kookana, Rai S., and Aylmore, L. A. G. (1993). Retention and release of Diquat and Paraquat herbicides in soils. *Aust. J. Soil Res* **31**, 97–109.

- Kookana, Rai S., Aylmore, L. A. G., and Gerritse, R. G. (1992). Time-dependent sorption of pesticides during transport in soils. *Soil Sci.* **154**, 214–25.
- Kung, K-J. S. (1990). Preferential flow in a sandy vadose zone. *Geoderma* **46**, 51–9.
- Loch, J. P. G., van Dijk-Looygaard, A., and Zoetman, B.C. (1989). Organics in ground water. In 'Watershed 89'. (Eds D. Wheeler, M. L. Richardson and J. Bridges.) Proc. IAWPRC Conf. Guildford, U.K. Vol 1. pp 39–54.
- Luke, G. J. (1988). Water and nutrient use in horticultural crops. In 'The Swan Coastal Plain in Crisis'. W.A. Inst. Agric. Sci. Occas Publ. No. 10, 53–8.
- Murali, V., and Aylmore, L. A. G. (1983). Competitive adsorption during solute transport in soils: 3. A review of experimental evidence of competitive adsorption and an evaluation of simple competition models. *Soil Sci.* **136**, 279–90.
- Pionke, H. B., Sharma, M. L., and Hosking, J. K. (1990). Effect of irrigated horticultural cropping on ground water quality; Swan Coastal Plain, Western Australia. CSIRO Aust. Water Resources Series No. 2, p. 19.
- Rao, P. S. C., Hornsby, A. G., and Jessup, R. E. (1985). Indices for ranking the potential for pesticide contamination of ground water. *Proc. Soil Crop Sci. Soc. Fla.* **44**, 1–8.
- Sharma, M. L. (1990). Leaching of nutrients under horticultural systems on the Swan Coastal Plain, Western Australia. In 'Horticulture and the Environment'. W.A. Dept. Agric. Miscellaneous Publ. No. 20/90.
- Sharma, M. L., and Hughes, M. W. (1985). Ground water recharge estimation using chloride, deuterium and oxygen-18 profiles in the deep coastal sands of Western Australia. *J. Hydrol.* **81**, 93–109.
- Singh, Rai (1989). Equilibrium and kinetic aspects of sorption-desorption and mobility of pesticides in soils. Ph. D. Thesis, School of Agriculture, University of W.A.
- Singh, Rai, Gerritse, R. G., and Aylmore, L. A. G. (1990). Adsorption-desorption behaviour of selected pesticides in some Western Australian soils. *Aust. J. Soil Res.* **20**, 227–43.
- Stadter, F. A., Emmett, A., and Dillon, P. (1992). Occurrence of Atrazine in ground water in the southeast of South Australia. CSIRO Aust. Centre for Ground water Studies, Report No. 45.
- Van Gestal, M., Ladd, J. N., and Amato, M. (1992). Microbial biomass response to seasonal changes and imposed drying regimes at increasing depths of undisturbed topsoil profiles. *Soil Biol. Biochem.* **24**, 103–11.
- Wagenet, R. J., and Rao, P. S. C. (1990). Modelling pesticide fate in soils. In 'Pesticides in the Soil Environment: Processes, Impacts and Modelling'. (Ed. H. H. Cheng.) pp. 351–400. (Soil Sci. Soc. Am. Inc.: Madison.)
- Whelan, B., and Barrow, J. W. (1984). The movement of septic tank effluent through sandy soils near Perth. 1. Movement of nitrogen. *Aust. J. Soil Res.* **22**, 283–92.

The effects of plant roots on soil structure

Proc. 3rd Trienn. Conf, Aust. Soc. Soil Sci., Sept 1994, 207-212.

Cochrane, H.R. and Aylmore, L.A.G.

The effects of plant roots on soil structure

H.R. Cochrane and L.A.G. Aylmore.

*Soil Science and Plant Nutrition, Faculty of Agriculture,
The University of Western Australia, Nedlands, 6009, W.A..*

Abstract

The effects of root growth on soil aggregate stability and dispersion characteristics were measured for 12 common crop and pasture species grown for 3 to 4 weeks on six wheatbelt soils. Plants were grown under controlled conditions at close to optimum soil moisture contents and structural analyses were carried out on air dry soils.

Averaged over all soils, root growth increased macroaggregate stability and reduced the proportion of soil disaggregated into particles smaller than 50 micron. There were large differences between species, with legumes more effective in stabilising structure than non-legumes and lupins the most structurally efficient species. Variations between cultivars of the same species were generally small relative to differences between species. The plant species used did not have the same ranking for structural efficacy in all soils, the effects of root growth being dependant on initial structural status. For particular plant/soil combinations roots were found to stabilise some soil fractions while destabilising others

Plants grown to maturity in field structured soil produced effects on structural stability comparable in magnitude to those effected by tillage, plant residue and gypsum application. However as plant roots occupy much larger volumes of soil than these treatments can influence, roots may have a more dominant role in determining soil physical fertility than has previously been appreciated.

Introduction

Poor structural conditions limit the productivity of a significant area of W.A. wheatbelt soil. For most of these soils, structure improves and becomes more resistant to degradation as organic matter content increases. Plant roots constitute a major source of soil organic matter and while growing are capable of both creating and stabilising useful soil structural features. Roots can alter the physical, chemical and biological properties of the soil with which they interact, changing both structural form and stability by a number of mechanisms, for example:-

- By altering the arrangement of soil particles; penetrating existing cracks and pores, enlarging them by compressing or fracturing surrounding soil.
- By physically enmeshing soil particles.
- By water uptake and ion absorption and by producing exudates which are capable of acting as binding agents and can enhance either flocculation or dispersion of soil colloids.

The effect of roots on soil structure depends on the species grown, soil constitution, and environmental factors (Monroe and Kladviko 1987). Soil microflora associated with plant

roots may also have a significant effect on soil structure (Tisdall 1991). The overall effect that a crop has on soil structure is determined by plant growth characteristics and the management requirements of the crop. As technology changes so does the effect of the management component, for example the change from conventional to reduced tillage results in less direct soil disturbance but may also influence root growth and distribution (Kirkegaard et al 1994). In the work reported here we are aiming to quantify the effects of root growth on structure independent of these management effects and at two stages in the life of the plant, during early growth, when, under wheatbelt conditions soil is most vulnerable to structural disruption and structural stability is of most importance to crop performance; and at maturity when the structural changes wrought by plant roots will have their effect for the succeeding crop.

Materials and methods

Effects of young growing plants

Surface soils (approx 0-7 cm) varying in texture from sandy loam to clay loam and in structural stability from severely hardsetting to stable (by wheatbelt standards) were collected from six sites in the wheatbelt, gently crushed and sieved to pass a 2mm aperture. A range of 12 common crop and pasture species were grown in these soils for a period of 3 to 4 weeks in a continuously illuminated growth chamber using high plant densities and day/night temperatures of 15/20°C. Close to optimal soil moisture conditions were maintained for a period of three weeks after sowing.

The "pots" were polycarbonate vials 67mm internal diameter (I.D.) at the top, 76 mm deep and were designed to enable plants to be grown without the need for frequent handling or watering. A 5.5mm hole, used for watering, was drilled in the wall each pot, 27mm from the base. The pot was filled to a depth of 35mm with washed "Hydrokorn" expanded clay beads (2-8mm diameter, smallest beads concentrated at the top of the layer). The bed of clay beads was compressed using a plunger and capped with a 70 mm diameter Whatman no. 3 filter paper to provide a rigid, porous base, penetrable by plant roots and capable of acting as a water reservoir to supply overlaying soil by capillary action. A disk of cotton mosquito netting (hole size 2-3mm) was placed on top of the filter paper, a 28 mm depth of test soil was added and another disk of mosquito netting placed on top of the soil bed. The base of the pot was filled with deionised water to a depth of 25mm. Water was drawn from this reservoir slowly, by capillary action, into the overlaying soil. Pots were left to equilibrate for 2 to 3 days, then dry seed was placed on the soil surface and covered immediately with a 5-10 mm layer of soil (thickness depending on seed size). No nutrients were added to the soil or water.

For the next three weeks the pot reservoirs were refilled with deionised water when all free water had been drawn from the reservoir - thus watering was required infrequently, minimising the risk of causing soil structural damage when handling the pots. Twenty one days after sowing, water levels in the reservoir of each pot were adjusted, according to the estimated rate of water loss, so that water remaining in each pot would be used up in approximately the same time. Plants continued to grow until soil had been dried to permanent wilting point. Pots were harvested when all had plants which were permanently wilted. Soil was removed from the pot by applying compressed air through the watering hole, plant material and soil either side of the mosquito net sandwich was severed and discarded. The remaining disk of soil with roots was dried at 35°C for 24 hours before being broken gently into fragments less than 4mm across, visible root material was removed.

Effects of plants grown to maturity.

Plots (0.5 m square) of field structured hardsetting soil within the University grounds were subjected to selected combinations of the treatments listed in table 1 and soil (5-50 mm depth) collected for structural analysis one year later in late autumn.

Table 1. Treatments applied to field structured plots

Category	Treatment	Application rate
Plant grown	Sub clover	2000 seed/m ²
	Wheat	300 seed/m ²
	Ryegrass	5000 seed/m ²
Crop residue	Fresh harvested wheat straw	500g/m ²
	Weathered wheat straw	500g/m ²
Gypsum		500g/m ²

The 'tillage' treatment involved complete soil disturbance by spade and rake, incorporating amendments uniformly to 50 mm depth where applied. No till plots were scratched with a rake to a depth of 5mm to break the existing surface crust but were otherwise undisturbed except for narrow seeding slots 30mm deep, cut with a broad knife. Slots were seeded then pressed closed by hand. Amendments were placed uniformly on the soil surface and mixed by hand with the loosened crust material to reduce movement by wind. Plots were untrafficked and were maintained weed free by hand weeding for the growing season.

Measurement of structural stability.

Air dry soil was gently crushed to pass a 4 mm aperture then sieved to remove the majority of particles <0.25mm. This 0.25-4 mm fraction was retained for analyses. Approximately 3.5g of soil was placed in the base of a 0.25mm sieve I.D. 47.5mm (an average soil depth of about 1.5mm over the area of the sieve). Sieves were placed in holders on a specially constructed sieving machine similar in concept to the one described by Kemper and Rosenau (1986) and lowered into individual vessels 67mm I.D. containing 100ml deionised water. Soil was soaked for 10 minutes then oscillated at frequency of 35 strokes per minute for a further 10 minutes with soil remaining immersed throughout the 11mm stroke length. Sieves were then raised and allowed to drain into the sieving vessels for 1 minute. Soil remaining on the sieve was washed onto a Petrie dish and dried at 105°C for 24 hours. For each sample sieved, material retained in the sieving vessel was resuspended by 20 gentle strokes of a broad flat paddle, then poured immediately into a vial 41mm I.D., 70 mm deep. This suspension was retained for determination of particles less than 2, 20 and 50 micron equivalent diameter respectively.

Oven dried soil retained on the sieve was weighed, then dispersed in alkaline sodium hexametaphosphate and washed over a 0.25mm mesh. Primary particles > 0.25mm retained on the mesh were dried to constant weight at 105°C and reweighed. Water stable aggregation (WSA) calculated by the following formula.

$$\%WSA(> 0.25mm) = \frac{(wt. \text{ water stable material } > 0.25mm - wt. \text{ primary particles } > 0.25mm) * 100}{(wt. \text{ total soil } - wt. \text{ primary particles } > 0.25mm)}$$

Calculations are based on the oven dry weight of all fractions

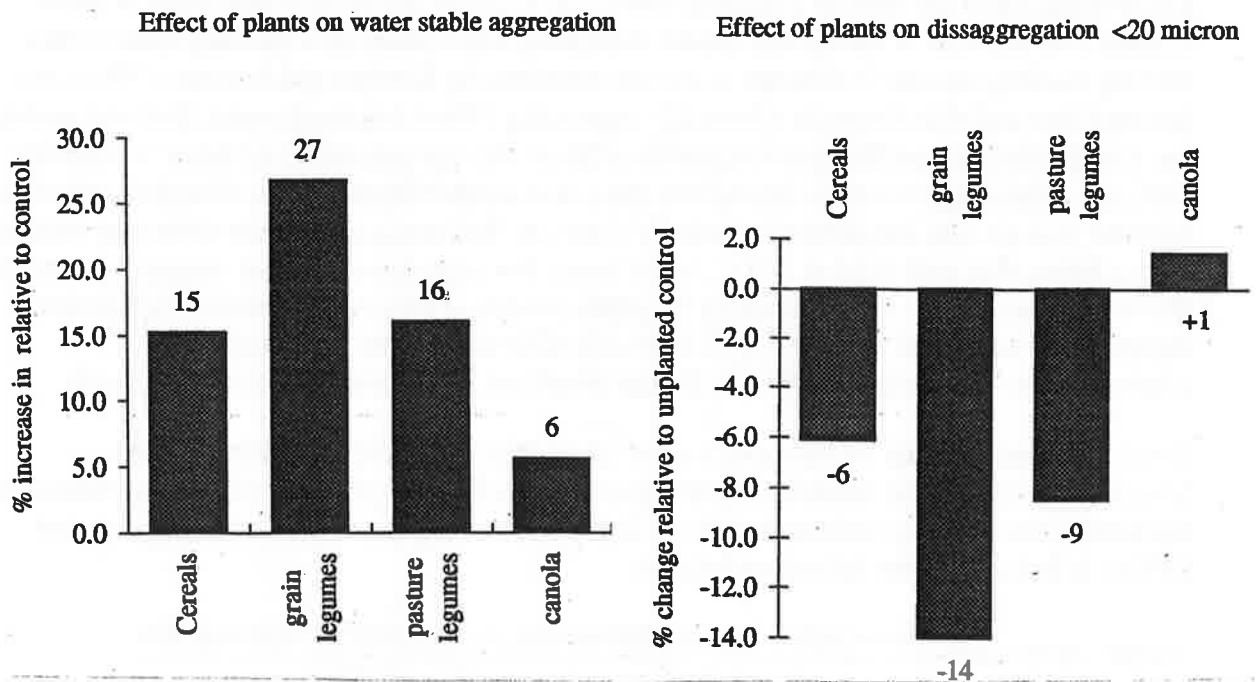
Water stable aggregation calculated by this method measures the percentage of soil material finer than 0.25mm which has been aggregated into compound particles larger than 0.25mm. To determine the percentage of soil disaggregated into particle fractions less than 50, 20 and 2 micron equivalent diameter, suspensions were rehomogenised by gently inverting vials 15 times and, after the appropriate settling time for each fraction (determined for particles with a density of 2.65 using Stoke's Law) reading suspension turbidity with a nephelometer. Suspensions made from the 'no plants' treatment of each soil were used to derive a calibration relationship between nephelometer readings and suspension concentration (w/v). These relationships were used to calculate the percentage of soil disaggregated into each size fraction for each treatment.

Results

Effects of early growth

Averaged over all soils, root growth increased macroaggregate stability and reduced the proportion of soil disaggregated into particles smaller than 50 micron, the effect being greatest in the least stable soils. The effects of growing cereals (average of two cultivars each of wheat, barley and oats, one of triticale), grain legumes (three cultivars of lupin, two of peas), pasture legumes (two cultivars each of sub-clover and medic) and canola (two cultivars) on water stable aggregation > 0.25mm and on soil disaggregation into particles smaller than 20 micron are shown in figures 1a and 1b respectively; The values presented in these figures are an average for the six soils of the percentage change in each parameter for each soil relative to its control value (soil wet but with no plants through the growth period). A positive change in WSA and a negative change in disaggregation to particles less than 50 micron indicate improved structural stability associated with the growth of plants

Figure 1 Effects of growing plants averaged for six soils

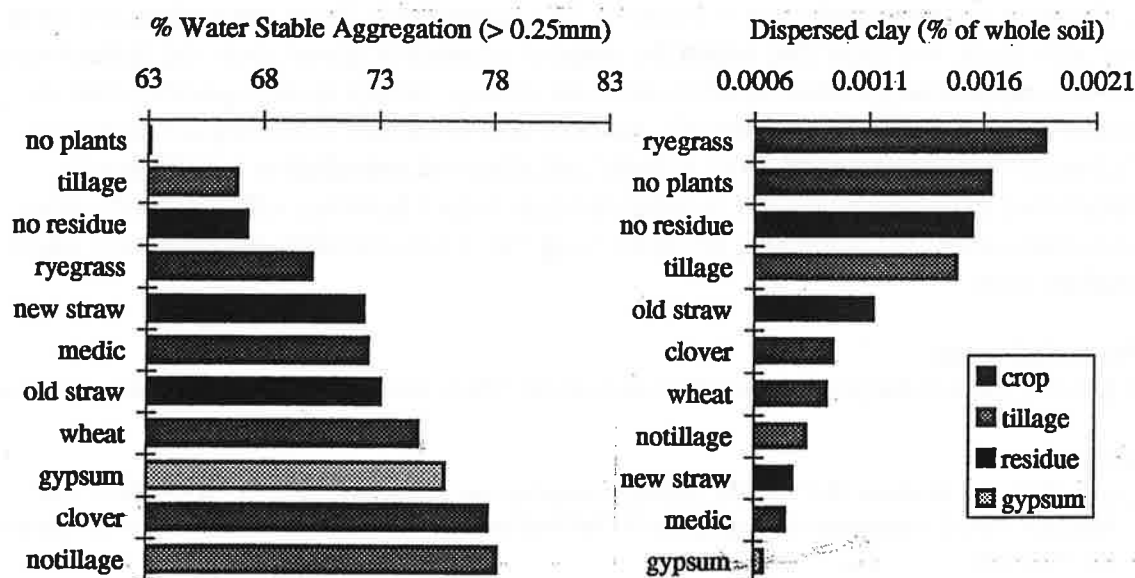


Legumes were more effective stabilisers of soil structure than non legumes, grain legumes were more consistent structure improvers over the six soils than pasture legumes, with lupins the most effective species used. Ryegrass, perhaps the most widely acknowledged of plants recommended for stabilising soil structure (Tisdall & Oades 1979) did not rate well as a structure enhancer for the soils and conditions used in these experiments. Despite these trends, there is no simple quantitative relationship between plant effect and pretreatment physical properties; at least within the structurally diverse group of soils used. Thus while root growth improves structural stability for the majority of plant/soil combinations tested, it does not invariably do so; plants may even simultaneously stabilise one soil fraction while destabilising another. The mechanisms of effect are complex, requiring more extensive experimentation than has been possible to date, For individual soil/plant combinations however the effect of plant growth is positive, highly significant and consistently observed and deserves further investigation.

Effects of plants grown to maturity.

The effects on structural stability of plants grown to maturity, relative to the effects of simulated tillage, wheat residue and gypsum addition are presented in figure 2a (WSA) and 2b (aggregate disaggregation). The figures show absolute values for each parameter (not percentage change relative to a control as in figure 1). Treatments are listed in order of increasing structural stability.

Figure 2 The effect of growing plants, simulated tillage and amendment on soil structural stability



Growing plants increased structural stability for all species - with the exception that ryegrass caused an increase in dispersible clay, (a measurement which corroborates the farmer's observation that structure improved on the paddock that this soil came from after he had achieved effective ryegrass control). Differences between wheat and pasture legumes were small but plant growth had a greater effect on structural stability than wheat residue addition, suggesting that in the management of unstable soils, root growth effects may be a more important factor than residue retention. Although the soil used for these experiments was not

highly dispersive it is interesting to note that the growth of medic was almost as effective as gypsum in suppressing clay dispersion.

Discussion

The effects of plant roots measured in the work reported here are only one component of the overall effect that a growing crop has on soil structure. The management requirements of the crop in terms of tillage and traffic for example, climatic conditions and the effect of canopy cover in protecting the soil surface from environmental stresses all contribute to the overall effect. In addition, the physical properties of roots: their mechanical strength, distribution and density (per unit soil volume) have been partially excluded in applying the techniques used in this study. The results of this work cannot therefore be used in isolation to assess the effect of a particular crop on soil structure. The effects we have measured are attributable to a combination of the compression and shearing of soil particles by growing roots, the effects of root exudates, rhizosphere microorganisms and the presence of fine roots and root hairs. The analysis of root effect we have used also averages that effect for soil at varying distances from the growing root, analysis at finer spatial resolutions reveals a marked decrease in effect with distance from the root surface. Thus for those soil/plant combinations where stability is increased by the growth of the plant, the overall contribution of roots to soil structure - in stabilising the continuous pores they create, will be greater than that estimated by the techniques employed here.

Plant roots are responsible for creating many of the structural features observed in wheatbelt soils - this is particularly apparent in the case of native perennial vegetation, but annual crop and pasture species may also make a significant contribution, creating, stabilising or even destabilising soil structural units throughout the rooting depth. From the exploratory work we have carried out, it is clear that within the range of commonly grown crop and pasture species there is considerable potential to effect structural change simply by incorporating into the rotation, species that have a structurally restorative effect suited to healing the structural deficiencies of particular soils. Root induced soil structural remediation is undoubtedly underutilised in current wheatbelt farming systems. It does however, offer an inexpensive, sustainable option for maintaining and improving the physical fertility of structurally fragile wheatbelt soils.

Acknowledgment

We gratefully acknowledge the financial support of the Grains Research & Development Corporation

References

- Kemper, W.D. and Rosenau, R.C. (1986) Aggregate stability and size distribution. In "Methods of Soil Analysis, Part 1. Agronomy Monograph no.9 (2nd Edition). pp.425-442. American Society of Agronomy, Inc. Madison.
- Kirkegaard, J.A., Angus, J.F., Gardner, P.A. and Muller, W. (1994) Reduced growth and yield of wheat with conservation cropping. I. Field studies in the first year of the cropping phase. *Australian Journal of Soil Research* 45:511-528.
- Monroe, C.D. and Kladviko, E.J. (1987) Aggregate stability of a silt loam as affected by roots of maize, soybeans and wheat. *Communications in Soil Science and Plant Analysis*. 18: 1077-1087.
- Tisdall, J.M. (1991) Fungal hyphae and structural stability of soil. *Australian Journal of Soil Research* 29: 729-743
- Tisdall, J.M. and Oades, J.M. (1979) Stabilisation of soil aggregates by the root systems of rye-grass. *Australian Journal of Soil Research* 17: 429-441.

CHARACTERISTICS OF FINE PORES IN SOME HALLOYSITES

G. J. CHURCHMAN, T. J. DAVY*, L. A. G. AYLMOORE*, R. J. GILKES*
AND P. G. SELF

CSIRO Division of Soils, Glen Osmond, South Australia and *Soil Science and Plant Nutrition, Faculty of Agriculture,
The University of Western Australia, Nedlands, Western Australia

(Received 22 July 1993; revised 8 September 1994)

ABSTRACT: Isotherms were obtained for nitrogen adsorption and desorption on seven halloysite-rich samples from New Zealand and Western Australia. Calculations from these isotherms indicate that halloysites with mainly small particles ($< c. 0.08 \mu\text{m}$ in width) had abundant cylindrical pores with narrow size distributions in the 5–15 nm range. They also indicate that halloysites with mainly large particles ($> c. 0.1 \mu\text{m}$ in width) had few if any pores in the mesopore range (2–50 nm). Transmission electron microscopy (TEM) shows that cylindrical pores originate from the central holes in tubular particles. The TEM also suggests that slit-shaped pores can originate from the shrinkage of blocks of layers upon dehydration of halloysite.

Halloysites include a significant concentration of fine pores (Diamond, 1970; Jackson *et al.*, 1971; Churchman & Payne, 1983; McCrea & Gilkes, 1987; McCrea *et al.*, 1990). Diameters recorded for the largest concentration of pores have depended upon the resolution of the techniques used for the measurement. Diamond (1970), Churchman & Payne (1983), McCrea & Gilkes (1987) and McCrea *et al.* (1990), all using mercury intrusion porosimetry, found that pores in the < 50 nm range provided most of the pore volume. Jackson *et al.* (1971), using isotherms for nitrogen and also for water sorption, found a sharp peak at 2.3 nm in the pore-size distribution.

The high concentration of very small pores in halloysites contrasts with the situation in kaolinites. These tend to show larger pores without a marked concentration in any particular size range (Aylmore & Quirk, 1967; Diamond, 1970; Sills *et al.*, 1973a; 1974; Aylmore & Sills, 1978). Generally, kaolinites comprise platy particles and pores in clay samples with platy particles are likely to form from the interleaving of the plates and should be similar in size to the thickness of the particles in the samples (Aylmore & Quirk, 1960; 1967; Sills *et al.*, 1973a)

A review of the literature (Churchman & Carr,

1975) revealed that halloysites can be distinguished from kaolinites most reliably by the presence of interlayer water or by evidence for its prior occurrence in the structure. Halloysite particles often occur as non-platy shapes, and a tubular shape is common. The concentration of fine pores observed for halloysites has often been attributed to the tubular shape of many halloysite particles. The tubes have been considered to provide the characteristic small pores, both directly, from their hollow interiors, and also indirectly, from the voids created when they pack together with other tubes (Churchman & Payne, 1983; McCrea & Gilkes, 1987). Halloysite particles, however, can occur in shapes other than tubes, e.g. spheroidal and blocky shapes (Churchman & Carr, 1975; Churchman & Theng, 1984; Dixon, 1989).

Until now, each study of pore-size distribution in halloysite has been carried out on only one sample of the mineral (Diamond, 1970; Jackson *et al.*, 1971), on a single halloysite-containing soil (Churchman & Payne, 1983), or, at most, on a small number of halloysite-containing soils, but all from the same locality (McCrea & Gilkes, 1987; McCrea *et al.*, 1990). Particle shapes provided the explanations both for the apparently characteristic pore-size distribu-

tions of halloysite and also for the differences between pore-size distributions of halloysites and kaolinites. Consequently, we considered it worthwhile to examine the relationships between pore-size distributions and particle shapes (and sizes) for halloysites with different shapes.

Gas sorption was used because comparisons of gas sorption measurements with those made using mercury intrusion porosimetry (e.g. Sills *et al.*, 1973b) indicate that only gas sorption, which measures smaller pore sizes than mercury intrusion porosimetry, would enable determination of the sizes of the dominant fine pores in at least some of the halloysites.

By obtaining information on the shapes of the pores from the gas sorption measurements and also from transmission electron microscopy (TEM), we were able to examine the origins of the fine pores in halloysites.

MATERIALS

Table 1 gives the characteristics of the seven samples used. Four of the samples studied (Dunedin, Te Akatea, Hamilton and Te Puke) were from the same sites as the halloysites studied as clay fraction samples by Churchman & Theng (1984). Two samples (Opotiki fine and Opotiki coarse) were from the Opotiki area of New Zealand. Churchman & Theng (1984) studied the clay fraction of just one sample from the same area. The remaining sample, from Jarrahdale, Western Australia, is sample D9 in Churchman & Gilkes (1989).

Kaolin mineral contents given in Table 1 were determined by differential thermal analyses (Whitton & Churchman, 1987) of samples that had previously been dried at 105°C for several hours. Previous work (Churchman & Theng, 1984; Churchman & Gilkes, 1989) had shown virtually all of the kaolin present in these samples, or in samples from the same areas, to be halloysite. Transmission electron microscopy confirmed that halloysite was the predominant kaolin mineral in the samples. Contents of allophane and ferrihydrite were determined from acid oxalate analyses (Blakemore *et al.*, 1987), leading to estimates of allophane by Parfitt & Wilson's (1985) method and ferrihydrite following Parfitt & Childs (1988). Organic matter contents were invariably low. Only the brownish-yellow Hamilton soil sample was not white in

colour. Nevertheless, the organic carbon content of the Hamilton soil IIC horizon, from which this sample was taken, is only 0.1% (New Zealand Soil Bureau, 1968).

METHODS

Approximately 1 g of each sample, except the Hamilton soil sample, was sealed into a sample bulb as an intact block, as taken from the field. Since a mismatch between the isotherms for adsorption and desorption at low relative pressures implied the possible perturbation of blocks of the Hamilton soil sample by the analytical procedure, this sample was examined as a powder formed by light hand-grinding and 0.2 g was used. Each sample was then heated at 105–110°C to degas in a vacuum of better than 10^{-4} torr until the pressure remained below 10^{-3} torr for 15 min after the vacuum pumps were isolated. Complete adsorption-desorption isotherms to saturation were obtained at 78°K, using a liquid nitrogen bath. The apparatus used for all except the Hamilton soil sample is described in Sills *et al.* (1973a,b). An automated volumetric instrument, Omnisorp 100, was used for the Hamilton soil sample.

The specific surface areas of the heated samples were derived from the low pressure range of the isotherms by the BET method (Brunauer *et al.*, 1938) and differential pore-size distributions for both branches calculated using the Kelvin equation modified to account for physical sorption on exposed surfaces (Aylmore, 1974a). Cumulative specific surface areas (S_{ads} and S_{des}) were calculated from pore filling and emptying on the adsorption and desorption branches respectively. The extent of the agreement between the BET area and S_{des} or S_{ads} is indicative of the extent to which the assumption of a predominance of slit-shaped or cylindrical shaped pores respectively is valid (Aylmore, 1974b).

Plots of V vs. n (Lippens & de Boer, 1965; Aylmore, 1974a) were obtained, where the volume adsorbed, V , is plotted against n , a statistical average of the number of layers which would be adsorbed onto a similar but non-porous material at the same relative vapour pressure. The usefulness of V - n plots derives from observations that nitrogen adsorption on different non-porous materials gives essentially the same isotherm when plotted in the 'reduced' form of $n(=V/V_m)$ against p/p_0 , where V_m is the volume adsorbed in a monolayer and p/p_0 is

TABLE 1. Characteristics of halloysite samples studied.

Name	Parent material	Kaolin content (%)	Other minerals (by XRD)	Oxalate-extractable values (%)			Allophane content (%)	Ferrihydrite content (%)
				Al	Fe	Si		
Dunedin ^a	Phonolite	55	Quartz, ferromagnesians	0.17	0.02	0.04	<1 ^c	<0.2
Te Akatea ^a	Andesite	69	Quartz	0.29	0.10	0.09	1.3	<0.2
Hamilton ^a	Andesite	46	Cristobalite, quartz, goethite	0.33	0.41	0.07	1 ^c	0.7
Te Puke ^a	Rhyolite/andesite	60	Cristobalite, quartz	0.17	0.07	0.06	0.7	<0.2
Opotiki fine ^a	Rhyolite	30	Feldspar, quartz, cristobalite	0.28	0.13	0.09	1.2	0.2
Opotiki coarse ^a	Rhyolite	23	Feldspar, quartz, ferromagnesians, cristobalite	0.11	0.10	0.04	0.4	<0.2
Jarrahdale ^b	Dolerite	30	Quartz, gibbsite	0.17	0.03	0.04	<1 ^c	<0.2

^a From New Zealand

^b From Western Australia

^c Estimate only; ratio of Al:Si (oxalate-extractable values) exceeds 3.5 (Parfitt, 1990).

Characteristics of pores in halloysites

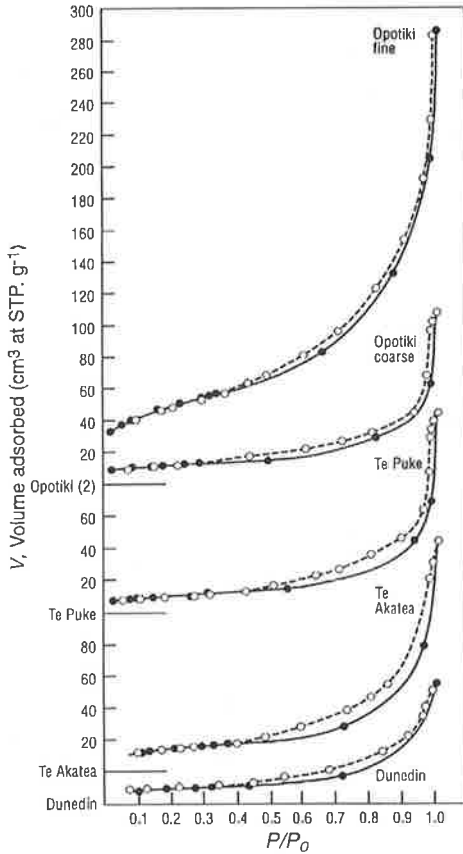


FIG. 1. Nitrogen adsorption-desorption isotherms on Dunedin, Te Akatea, Te Puke, Opotiki coarse and Opotiki fine halloysite samples. The closed circles indicate adsorption and the open circles, desorption. Volume adsorbed is plotted to the same scale but from different origins for each sample. The origins for each are indicated on the ordinates.

the relative pressure (Shull, 1948; Lippens & de Boer, 1965; Pierce, 1968). Deviations from linear $V-n$ plots, which indicate simple monolayer-multilayer adsorption, enable the occurrence of pore filling to be detected and the nature of such deviations indicate the general shape of the relevant pores (Aylmore, 1974a 1974b, 1977).

X-ray diffraction analyses of all of the samples had been obtained in previous studies. Transmission electron microscopy was carried out using a Philips 400 electron microscope. Samples for TEM were prepared by either dispersing in water and allowing

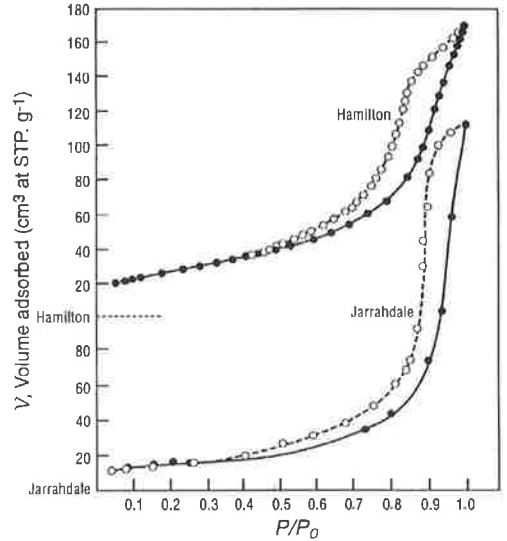


FIG. 2. Nitrogen adsorption-desorption isotherms on Hamilton soil sample and Jarrahdale sample. The closed circles indicate adsorption and the open circles, desorption.

the suspension to dry on a carbon support film or by embedding in Spurr's resin (Spurr, 1969) and sectioning using a Riechert Ultramicrotome. In addition, intact blocks of air-dried samples of each of the clays and soils were examined by scanning electron microscopy, using a Cambridge Stereoscan instrument.

RESULTS AND DISCUSSION

Isotherms

The nitrogen-sorption isotherms for most of the samples from New Zealand are shown in Fig. 1 and those for the New Zealand soil sample (Hamilton) and the Jarrahdale sample in Fig. 2. The isotherms in Fig. 1 show either very little or no hysteresis whereas those in Fig. 2 show substantial hysteresis.

Differential pore-size distributions

Figure 3 shows differential pore-size distributions corresponding to the isotherms which showed substantial hysteresis, i.e. those in Fig. 2. The

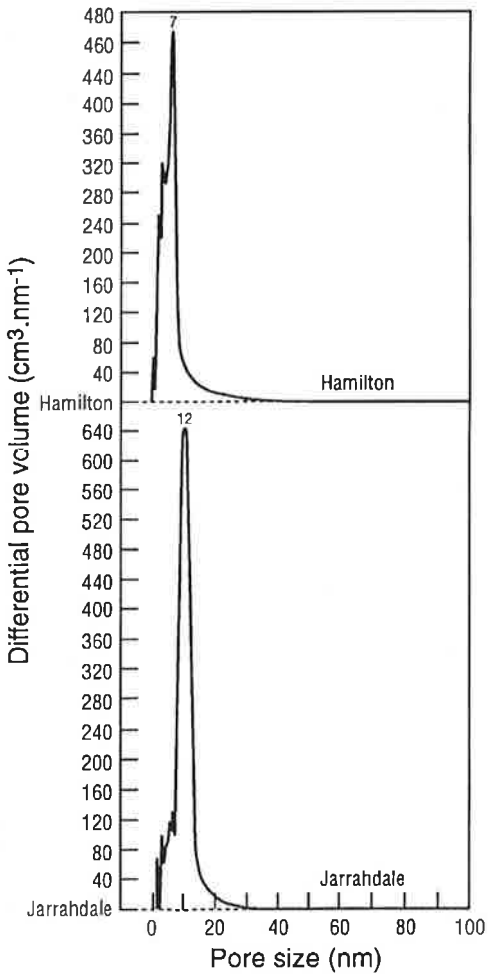


FIG. 3. Differential pore-size distributions from the desorption isotherms (Fig. 2) for Hamilton soil sample and Jarrahdale sample.

distributions in Fig. 3 each show a single sharp peak; these are at 7 nm for Hamilton and at 12 nm for Jarrahdale.

Although the isotherms in Fig. 1 show little or no hysteresis, differential pore-size distributions derived from them suggested that the five halloysites represented could have pores that have narrow size distributions, with sharp peaks in the 2.4–2.8 nm size range. The calculated distributions were very similar to that shown by Jackson *et al.* (1971) for a sample of one of the halloysites we

also studied (Te Puke). However, the reported closure of many isotherms at relative pressures of 0.42–0.50 (work cited by Gregg & Sing, 1967), means that the Kelvin equation may not apply at the small pore sizes i.e. $< c. 2$ nm which are equivalent to these relative pressures.

Specific surface areas

Values for specific surface areas of the various samples, as determined by the BET equation (S_{BET}), are compared in Table 2 with the cumulative specific surfaces obtained from the isotherms for both adsorption (S_{ads}) and desorption (S_{des}) of nitrogen on each sample.

Among the samples giving isotherms with considerable hysteresis (Fig. 2), the S_{des} value is substantially higher than the corresponding BET area for the Jarrahdale sample, indicating that retention of capillary condensate by narrow-necked pores controls desorption from larger volumes (Aylmore, 1974a). There is close agreement between S_{ads} and the BET area. Following de Boer *et al.* (1964) and Aylmore & Quirk (1967), this sample is likely to contain mainly 'bottle-shaped', tubular or cylindrical pores (hereafter referred to as 'cylindrical pores') of varying radius.

In the case of the Hamilton soil sample, while $S_{\text{des}} > S_{\text{BET}}$, there is a similar discrepancy between S_{des} and S_{BET} , on the one hand, and S_{ads} and S_{BET} , on the other. This suggests that there are both cylindrical and slit-shaped pores in this sample. Slit-shaped pores give rise to S_{ads} values in deficit of S_{BET} and equal values for S_{des} and S_{BET} (de Boer *et al.*, 1964; Aylmore & Quirk, 1967).

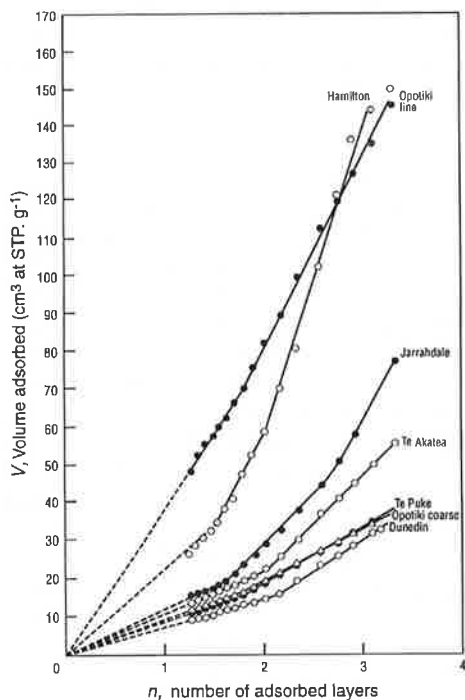
For the samples represented in Fig. 1, the criteria for surface areas (Table 2) indicate that pores in only the Te Akatea halloysite could be largely cylindrical.

The Opotiki fine sample has a very high specific surface (Table 2). It has significant allophane (Table 1), and also iron oxides (Churchman & Theng, 1984).

The Hamilton sample also has a relatively large specific surface (Table 2). It contains considerable Fe (Churchman & Theng, 1984), including significant ferrihydrite (Table 1). These amounts are insufficient to explain completely its high surface area (Churchman & Burke, 1991). The high concentration of very small halloysite particles could explain much of the high specific surface of this sample.

TABLE 2. Comparison of various measures of specific surface areas of samples.

Sample	Specific surface (m^2g^{-1})				
	From BET equation (S_{BET})	Cumulative, from adsorption isotherm (S_{ads})	Cumulative, from desorption isotherm (S_{des})	$S_{\text{ads}} - S_{\text{BET}}$	$S_{\text{des}} - S_{\text{BET}}$
Dunedin	30.3	26.2	29.0	-4.1	-1.3
Te Akatea	46.1	51.3	55.2	+5.2	+9.1
Hamilton	93.8	87.9	98.7	-5.9	+4.9
Te Puke	35.4	27.5	38.4	-7.9	+3.0
Opotiki fine	169.2	127.5	153.1	-41.7	-16.1
Opotiki coarse	42.4	25.4	37.2	-17.0	-5.2
Jarrahdale	56.2	53.7	81.3	-2.5	+25.1

FIG. 4. Plots of V vs. n from the adsorption isotherms (Figs. 1 and 2) for all samples.

V - n plots

Plots of V vs. n for the different samples (Fig. 4) all show an increase in slope with increasing values of n . This indicates the occurrence of some cylindrical pores in all samples (Aylmore, 1974a,b; 1977).

The samples differ in the extent of change of slope at their inflection points. The V - n plots for the Jarrahdale, Hamilton and Te Akatea samples exhibit the greatest changes of slope. These materials apparently contain the greatest proportion of cylindrically-shaped pores.

Electron microscopy

Transmission electron microscopy confirmed the general shapes of the halloysite particles that have been recorded in the relevant publications, i.e. Churchman & Theng (1984) for Dunedin, Te Akatea, Hamilton, Te Puke and Opotiki fine halloysite samples and Churchman & Gilkes (1989) for the sample from Jarrahdale. The Opotiki coarse sample also contained spheroidal particles. Particles in all halloysite samples were of four main types. These are represented in the micrographs of particles shown in Fig. 5. The main types are: thick tubular (Fig. 5a, Dunedin); spheroidal (Fig. 5b, Opotiki); blocky (Fig. 5c, Te Puke); thin tubular (Fig. 5d, Jarrahdale). 'Tubular' particles may also include laths and many tubes have a polyhedral rather than a circular cross-sectional shape.

Particles of these different types were often found together in the same sample, suggesting a range of particle shapes for halloysites.

Effect of particle shapes and sizes on shapes and sizes of pores in halloysites

Table 3 details the particle shapes and sizes in the samples which give rise to dominantly cylindrical

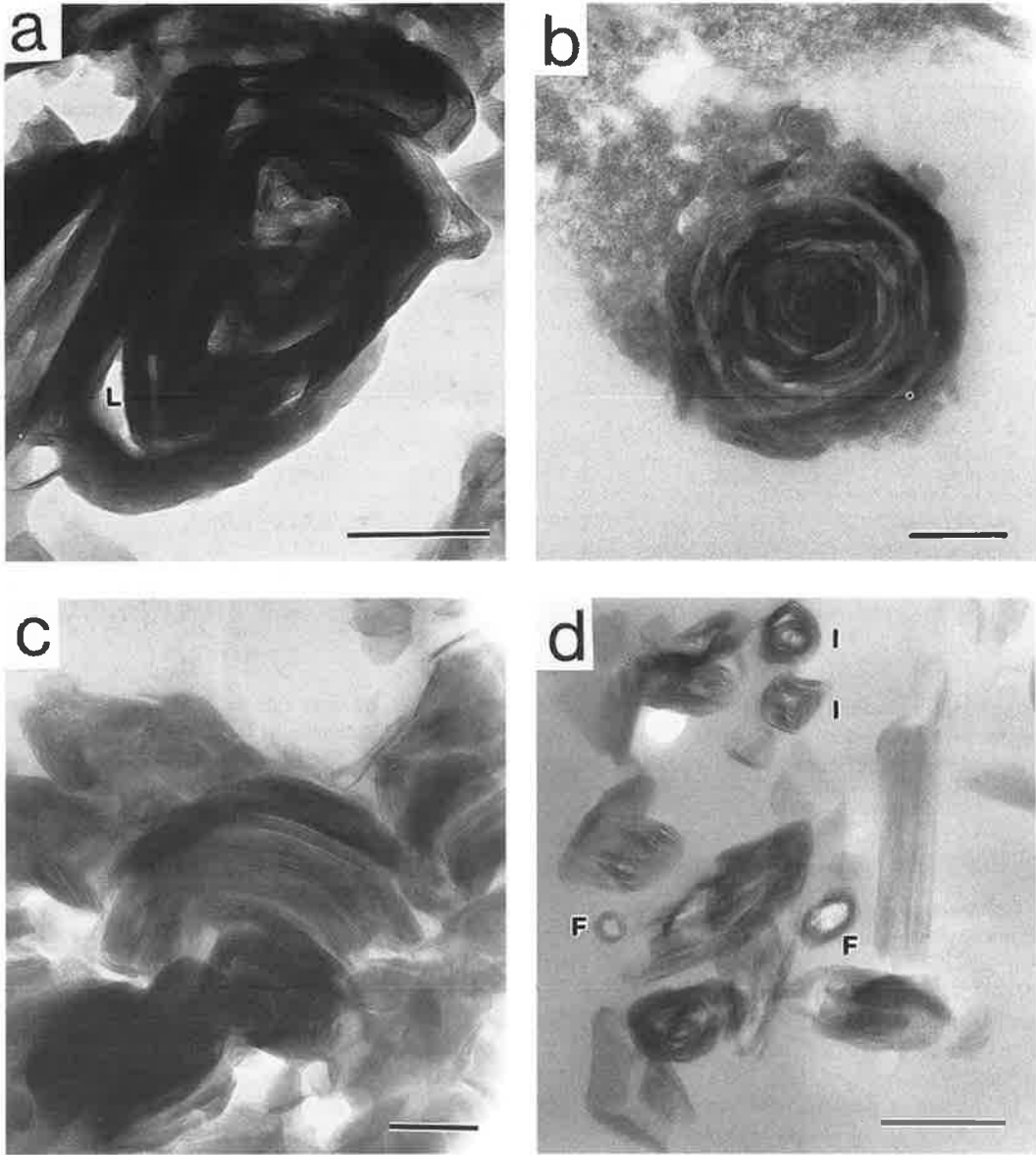


FIG. 5. Transmission electron micrographs of cross-sections of halloysites with (a) thick tubular (Dunedin); (b) spheroidal (Opotiki fine); (c) blocky (Te Puke); and (d) thin tubular (Jarrahdale) particles. Note the gel (allophane) also present in the Opotiki sample. Particles in a and c were embedded in resin while those in b and d were dispersed in water before examination by TEM. Bars indicate 0.1 μm . See text for description and labelling of pores.

pores according to the comparisons of different measurements of surface area (Table 2) and $V-n$ plots (Fig. 4). These are compared with the same characteristics of particles in the other samples.

Table 3 shows that, when there was a substantial volume of fine pores (or 'mesopores' — Gregg & Sing, 1967) present in the halloysites (Hamilton and Jarrahdale), a high proportion of these pores were

TABLE 3. Shapes and mean sizes of dominant types of particles in relation to occurrence of cylindrical pores in halloysites.

Sample	Dominant shape	Average length (μm)	Average width (μm)	Number counted
A. Abundant pores				
1. Cylindrical pores dominant				
Jarrahdale	Tubular	0.29 (± 0.19)	0.05 (± 0.01)	54
2. Abundant cylindrical pores				
Hamilton	Tubular	0.15 (± 0.09)	0.07 (± 0.07)	23*
B. Few, if any, pores				
1. Cylindrical pores dominant				
Te Akatea	Tubular	0.51 (± 0.27)	0.08 (± 0.05)	32*
2. Cylindrical pores not dominant				
Dunedin	Tubular	0.52 (± 0.30)	0.12 (± 0.06)	26*
Te Puke	Tubular	0.27 (± 0.12)	0.08 (± 0.05)	25*
	+ blocky			
Opotiki fine	Spheroidal	0.30 (± 0.10)	0.30 (± 0.10)	52
Opotiki coarse	Spheroidal	0.24 (± 0.06)	0.24 (± 0.06)	45

* Data from Churchman & Theng (1984)

cylindrical in shape. The dominant tubular particles in these halloysites were either the shortest (Hamilton) or the narrowest (Jarrahdale) among those studied.

Location of pores in halloysites

Representative transmission electron micrographs of the cross-sections of the halloysites (Fig. 5) show that particles of all shapes generally are made up of blocks of layers bent around one another. Only the smaller, tubular particles shown in Fig. 5d, contain a cylindrical or near-cylindrical pore in the centres of their tubes.

In the larger particles, i.e. the particles in Fig. 5a–c, there are gaps between successive blocks which constitute virtually all of the visible pores. The intra-crystal pores in these larger particles tend to be both narrow and slit-shaped. The small tubular particles (F) show few visible slit-shaped pores from gaps between blocks of layers, but slightly larger tubes, such as those labelled I, can show both slit-shaped and cylindrical pores.

While the presence of central holes may explain the occurrence of cylindrical pores in samples containing small tubular particles, the large pore L shown in Fig. 5a of a large tube in Dunedin halloysite may also exhibit some cylindrical character.

Using an electron microscope with an environmental cell, Kohyama *et al.* (1978) showed that a hydrated halloysite did not contain pores within the tubes. Pores within the tubes were created by dehydration of the 10 Å form of the mineral to give the 7 Å form. Groups of layers apparently shrink as a block, creating pores between each group. Such pores may arise from dehydration occurring in the field or during preparation of samples for analyses in the laboratory, including gas sorption and electron microscopy.

Singh & Gilkes (1992) have also shown that wedge-shaped voids can form by the folding of layers of kaolinites to form tubular halloysite. However, there is no evidence that the halloysite samples in this study had originated from kaolinite.

Primary minerals (quartz, ferromagnesian, cristobalite, feldspars, mica), and also vermiculite (altered from, but pseudomorphous with, mica) should not contribute to the pores <c. 15 nm which are of interest in this study. Gibbsite is only ever present in trace amounts in the Jarrahdale samples (Churchman & Gilkes, 1989). Allophane tends to give rise to cylindrical pores with radii near 1 nm (Rousseaux & Warkentin, 1976).

In general, pore sizes and shapes derived from the sorption of nitrogen on a number of halloysites can be explained as intra-crystalline phenomena.

Pores resulting from the packing together of different particles have also been suggested as explanations of the characteristic pore-size distributions for halloysites (Churchman & Payne, 1983; McCrea & Gilkes, 1987). Scanning electron micrographs of the samples used in this study suggest that this explanation is unlikely as pores from packing would be neither small enough nor concentrated enough in narrow ranges to provide the types of pore size distributions shown in Fig. 3.

CONCLUSIONS

(1) Halloysites with mainly small particles ($< c.$ 0.08 μm in width) had many cylindrical pores.

(2) These cylindrical pores showed a narrow distribution of sizes (from $c.$ 5–15 nm).

(3) Halloysites with mainly large particles ($> c.$ 0.1 μm in width) had few, if any, pores in the mesopore size range (2–50 nm).

(4) Cylindrical pores probably derive mainly from the central holes in tubular particles.

(5) Slit-shaped pores in halloysites may arise from the shrinkage on dehydration of blocks of layers.

ACKNOWLEDGMENTS

GJC is grateful to the University of Western Australia for the award of a Gladden Senior Visiting Fellowship which provided financial support for this work and his former employers, New Zealand Soil Bureau, DSIR, for study leave in order to carry it out. We thank Dr Rob Hayes, of the University of South Australia for the determination of the isotherms for the powdered Hamilton halloysite sample, Kay Card, formerly of the Physics and Engineering Laboratories, DSIR, New Zealand for scanning electron microscopy and Adrian Beech, Trevor Cock and Jim Thompson, of CSIRO Division of Soils, for oxalate-extractable cation determinations, TEM plate preparation and differential thermal analyses, respectively. We also thank Dr Chris Pope of the University of Otago, New Zealand for helpful comments on the manuscript.

REFERENCES

- AYLMORE L.A.G. (1974a) Gas sorption in clay mineral systems. *Clays Clay Miner.* **22**, 175–183.
- AYLMORE L.A.G. (1974b) Hysteresis in gas sorption. *J. Colloid Interf. Sci.* **46**, 410–416.
- AYLMORE L.A.G. (1977) Microporosity in montmorillonite from nitrogen and carbon dioxide sorption. *Clays Clay Miner.* **25**, 148–154.
- AYLMORE L.A.G. & QUIRK J.P. (1960) Domain or turbostratic structure of clays. *Nature*, **187**, 1046–1048.
- AYLMORE L.A.G. & QUIRK J.P. (1967) The micropore size distribution of clay mineral systems. *J. Soil Sci.* **18**, 1–17.
- AYLMORE L.A.G. & SILLS I.D. (1978) Pore structure and mechanical strength of soils in relation to their constitution. Pp. 69–78 in: *Modification of Soil Structure* (W.W. Emerson, R.D. Bond & A.R. Dexter, editors). John Wiley and Sons, New York.
- BLAKEMORE L.C., SEARLE P.L. & DALY B.K. (1987) Methods for chemical analysis of soils. *N.Z. Soil Bureau Scientific Report*, **80**.
- BRUNAUER S., EMMETT P.H. & TELLER E. (1938) Adsorption of gases in multimolecular layers. *J. Am. Chem. Soc.* **60**, 309–310.
- CHURCHMAN G.J. & BURKE C.M. (1991) Properties of subsoils in relation to various measures of surface area and water content. *J. Soil Sci.* **42**, 463–478.
- CHURCHMAN G.J. & CARR R.M. (1975) The definition and nomenclature of halloysites. *Clays Clay Miner.* **23**, 382–388.
- CHURCHMAN G.J. & GILKES R.J. (1989) Recognition of intermediates in the possible transformation of halloysite to kaolinite in weathering profiles. *Clay Miner.* **24**, 579–590.
- CHURCHMAN G.J. & PAYNE D. (1983) Mercury intrusion porosimetry of some New Zealand soils in relation to clay mineralogy and texture. *J. Soil Sci.* **34**, 437–451.
- CHURCHMAN G.J. & THENG B.K.G. (1984) Interactions of halloysites with amides: mineralogical factors affecting complex formation. *Clay Miner.* **19**, 161–175.
- DE BOER J.H., VAN DEN HEUVAL A. & LINSEN B.G. (1964) Studies of pore systems in catalysis. IV. The two causes of reversible hysteresis. *J. Catalysis*, **3**, 268–273.
- DIAMOND S. (1970) Pore size distribution in clays. *Clays Clay Miner.* **18**, 7–23.
- DIXON J.B. (1989) Kaolin and serpentine group minerals. Pp. 467–525 in: *Minerals in Soil Environments* (J. B. Dixon & S. B. Weed, editors). Soil Science Society America, Madison, Wisconsin.
- GREGG S.J. & SING K.S.W. (1967) *Adsorption, Surface Area and Porosity*. Academic Press, London.
- JACKSON B.L.J., METCALFE A. & WILCOCK R.J. (1971) Adsorption hysteresis on disordered kaolinite. *Trans. Farad. Soc.* **67**, 2137–2144.
- KOHYAMA N., FUKUSHIMA K. & FUKAMI A. (1978) Observation of the hydrated form of tubular halloysite by an electron microscope equipped with an environmental cell. *Clays Clay Miner.* **26**, 25–40.
- LIPPENS B.C. & DE BOER J.H. (1965) Studies on pore systems in catalysis. V. The t method. *J. Catalysis* **4**, 319–323.

- MCCREA A.F. & GILKES R.J. (1987) The microstructure of lateritic pallid zone. Pp. 501–506 in: *Micromorphologie des Sols — Soil Micromorphology*. Proc. VIIth Int. Working Meeting on Soil Micromorphology, Paris, July 1985. Association Francaise pour l'Etude du Sol.
- MCCREA A.F., ANAND R.R. & GILKES R.J. (1990) Mineralogical and physical properties of lateritic pallid zone materials developed from granite and dolerite. *Geoderma*, **47**, 33–47.
- NEW ZEALAND SOIL BUREAU (1968) Soils of New Zealand, Part 3. *N.Z. Soil Bureau Bulletin* **26**, (3).
- PARFITT R.L. (1990) Allophane in New Zealand — a review. *Aust. J. Soil Res.* **28**, 343–360.
- PARFITT R.L. & CHILDS C.W. (1988) Estimation of forms of Fe and Al: a review, and analysis of contrasting soils by dissolution and Mössbauer methods. *Aust. J. Soil Res.* **26**, 121–144.
- PARFITT R.L. & WILSON A.D. (1985) Estimation of allophane and halloysite in three sequences of volcanic soils, New Zealand. *Catena Supplement* **7**, 1–8.
- PIERCE C. (1968) The universal nitrogen isotherm. *J. Phys. Chem.* **72**, 3673–3676.
- ROUSSEAUX J.M. & WARKENTIN B.P. (1976) Surface properties and forces holding water in allophane soils. *Soil Sci. Soc. Am. J.* **40**, 446–451.
- SHULL C.G. (1948) The determination of pore size distribution from gas adsorption data. *J. Am. Chem. Soc.* **70**, 1405–1414.
- SILLS I.D., AYLMOORE L.A.G. & QUIRK J.P. (1973a) An analysis of pore size in illite-kaolinite mixtures. *J. Soil Sci.* **24**, 480–490.
- SILLS I.D., AYLMOORE L.A.G. & QUIRK J.P. (1973b) A comparison between mercury injection and nitrogen sorption as methods of determining pore size distributions. *Soil Sci. Soc. Am. Proc.* **37**, 535–537.
- SILLS I.D., AYLMOORE L.A.G. & QUIRK J.P. (1974) Relationship between pore size distributions and physical properties of clay soils. *Aust. J. Soil Res.* **12**, 107–117.
- SINGH B. & GILKES R.J. (1992) An electron optical investigation of the alteration of kaolinite to halloysite. *Clays Clay Miner.* **40**, 212–229.
- SPURR A.R. (1969) A low-viscosity epoxy resin embedding medium for electron microscopy. *J. Ultrastructure Res.* **26**, 31–43.
- WHITTON J.S. & CHURCHMAN G.J. (1987) Standard methods for mineral analysis of soil survey samples for characterisation and classification. *N.Z. Soil Bureau Scientific Report*, **79**.

A field study of leaching and degradation of nine pesticides in a sandy soil

R. S. Kookana,^{A,B} H. J. Di^A and L. A. G. Aylmore^A

^A Department of Soil Science and Plant Nutrition, University of Western Australia, Nedlands, WA 6009.

^B Present address: C.R.C. for Soil and Land Management, Glen Osmond, SA 5064.

Abstract

A field study was conducted on a coastal sandy soil (Karrakata sand) of Western Australia from July to December 1990, to measure the leaching and degradation rates of chlorpyrifos, chlorthal dimethyl, fenamiphos, linuron, metalaxyl, metribuzin, prometryne, propyzamide and simazine. Commercial grade products were sprayed in dilute solution form at recommended rates to the surface of field plots. Irrigation was applied daily which together with rainfall gave effective rainfall equivalent to at least 120% of potential evaporation. Pesticide residue concentrations in soil samples taken at 5 cm increments down to 50 cm, at different days after application, were determined by high performance liquid chromatography (HPLC). Mean leaching depths (MLDs) were calculated by weighting the percentage residues remaining at different depths in the soil profile. The MLDs for the 5 month period followed the order: chlorpyrifos and chlorthal dimethyl (<5 cm) < linuron and simazine (6) < propyzamide (8) and prometryne (9) < metribuzin (12) < metalaxyl (18) < fenamiphos and metabolites (28). This generally corresponded inversely with the sorption coefficients (K_{oc}). The degradation rates (i.e. decreases with time of total residue concentration in the sampled profile) could mostly be described by first-order regressions ($R^2 = 0.59-0.95$). Calculated half-lives showed the order: metribuzin (27 days), simazine (28) < fenamiphos (43), chlorthal dimethyl (45) < prometryne (58), propyzamide (59) < metalaxyl (70) < chlorpyrifos (81) < fenamiphos plus metabolites (98) < linuron (219). The potential for causing ground water contamination, as indicated by the ratio of half-life to K_{oc} followed the order: chlorthal dimethyl, chlorpyrifos < metribuzin, prometryne < simazine, propyzamide < linuron < metalaxyl < fenamiphos and metabolites.

Keywords: pesticides, leaching, degradation, half-life, ground water contamination, field study.

Introduction

Pesticides used for agricultural and horticultural productions have the potential to contaminate the ground water (USEPA 1977, 1978; Cohen *et al.* 1986; Kookana and Aylmore 1994). Governments have been urged to introduce legislative measures to regulate the use of pesticides in order to limit the contamination of ground water by pesticides from non-point sources. Pesticide movement and degradation in soil are, however, influenced by a number of factors, including pesticide properties, soil properties and environmental conditions (Cheng 1990). The development of an effective management scheme, with regard to pesticide use to minimize the negative impact on the environment, relies on a sound understanding of the mobility and persistence of pesticides as affected by the

Table 1. Pesticides used, their water solubility and application rates

Common name	Chemical name	Trade name of commercial product	Uses	Water solubility (mgL ⁻¹)	Application rate (kg a.i. ^A ha ⁻¹)
Chlorpyrifos	<i>O,O</i> -diethyl <i>O</i> -3,5,6-trichloro-2-pyridyl phosphorothioate	Lorsban 50EC	Insecticide	2	3
Chlorthal dimethyl	Dimethyl tetrachloroterephthalate	Prothal	Herbicide	<0.5	9.1
Fenamiphos	Ethyl 4-methylthio- <i>m</i> -tolyl isopropylphosphoramidate	Nemacur	Nematicide	700	9.6
Linuron	3-(3,4-dichlorophenyl)-1-methoxy-1-methylurea	Linuron	Herbicide	81	1.25
Metalaxyl	Methyl <i>N</i> -(2-methoxyacetyl)- <i>N</i> -(2,6-xylyl)-DL-alaninate	Ridomil MZ	Fungicide	7100	0.14
Metribuzin	4-amino-6- <i>tert</i> -butyl 4,5-dihydro-3-methylthio-1,2,4-triazine-5(4 <i>H</i>)-one	Sencor 70WP	Herbicide	1200	0.525
Prometryne	<i>N,N'</i> -di-isopropyl-6-methylthio-1,3,5-triazine-2,4-diyldiamine	Gesagard	Herbicide	33	1.1
Propyzamide	3,5-dichloro- <i>N</i> -(1,1-dimethyl-2-propynyl)benzamide	Kerb 50WP	Herbicide	15	2.25
Simazine	6-chloro- <i>N,N'</i> -diethyl-1,3,5-triazine-2,4-diyldiamine	Simazine	Herbicide	5	2

^A Active ingredient.

various factors. While laboratory studies (e.g. Singh *et al.* 1989; Kookana *et al.* 1992a, 1992b) and simulation modelling (e.g. Nicholls *et al.* 1982; Hutson and Wagenet 1992; Mullins *et al.* 1993) are important approaches for elucidating the processes which affect pesticide mobility in soil, field studies are essential for monitoring pesticide mobility and persistence under more realistic conditions, and for providing data with which to assess simulation models (Nicholls *et al.* 1982; Pennell *et al.* 1990). Little field research has, however, been conducted in Australia.

In Western Australia, an area particularly vulnerable to ground water contamination by pesticides is the Swan Coastal Plain, where the soils have a generally low capacity to retain pesticide residues and where the pesticides are extensively used for horticultural productions. The aim of the experiments reported in this paper was to determine, in the field, the leaching and degradation rates of nine pesticides representing a wide range in chemical properties (e.g. water solubility and soil sorption coefficient) in a coastal sandy soil of Western Australia.

Materials and methods

Soil and pesticides

The experiment was conducted on a sandy soil (Karrakata sand) at a vegetable research station (Western Australian Department of Agriculture) located about 20 km south of Perth on the Swan Coastal Plain of Western Australia. The experimental area was newly cleared and had not received pesticides previously. Both surface (0–25 cm) and subsurface (25–50 cm) soil had 98% sand. The surface soil had a pH (H₂O) of 5.3 and organic carbon of 0.53%; the subsurface soil had a pH of 5.5 and organic carbon of 0.15%. The area was divided into 3×1.5 m plots with 1 m buffer zones along each side of the plot. Some other properties of the soil have been reported by Kookana and Aylmore (1994).

Nine pesticides were used in the study (Table 1). Each pesticide was applied separately at the recommended rates by spraying dilute aqueous solutions on the surface of the appropriate plots. The required weight/volume of the pesticide product for each plot was dissolved in 5 L of water just before spraying for all pesticides, except fenamiphos, prometryne and chlorthal, for which 10 L of water was used. To minimize drift across the plots, a Knap sac sprayer with shrouded nozzle was used. Irrigation was applied daily with a plot irrigator fitted with an automatic volume controller and designed to spray a calibrated volume of water over an area of 6.6×4.0 m² uniformly. A beam fitted with 12 spray nozzles moved forward and backward until the preselected volume of water was delivered. Irrigation together with rainfall provided effective rainfall equivalent to at least 120% of daily pan evaporation (Figs 1 and 2). The experiment was started in July and terminated in December 1990. The mean minimum and maximum temperatures during the period were 10 and 22°C respectively.

Sampling, extraction and analysis

At different intervals following the application of the pesticides, soil samples were taken with a split core auger at 5 cm increments to 50 cm depth of the profile. Three cores were taken from each plot on each sampling day. The core holes were refilled with soil from the buffer zones. For each layer, the three soil core samples taken from each plot at each sampling day were bulked together and mixed thoroughly for analysis. All pesticides, except chlorpyrifos, were extracted in 90% acetonitrile in water by overnight shaking 5 g of moist soil with 10 mL of extractant. For chlorpyrifos, acetone : phosphoric acid (99 : 1) was used as extractant. After shaking, the solution was centrifuged and filtered through a 0.22 µm membrane (Swinnex-GS filter). Pesticide concentration in the solution was determined on a Waters® high performance liquid chromatograph (HPLC) equipped with a multiple wavelength u.v./visible detector (Waters 490), an autosampler (Waters WISP 710) and an automated gradient controller (Waters 680). The analytical methods published in the literature were

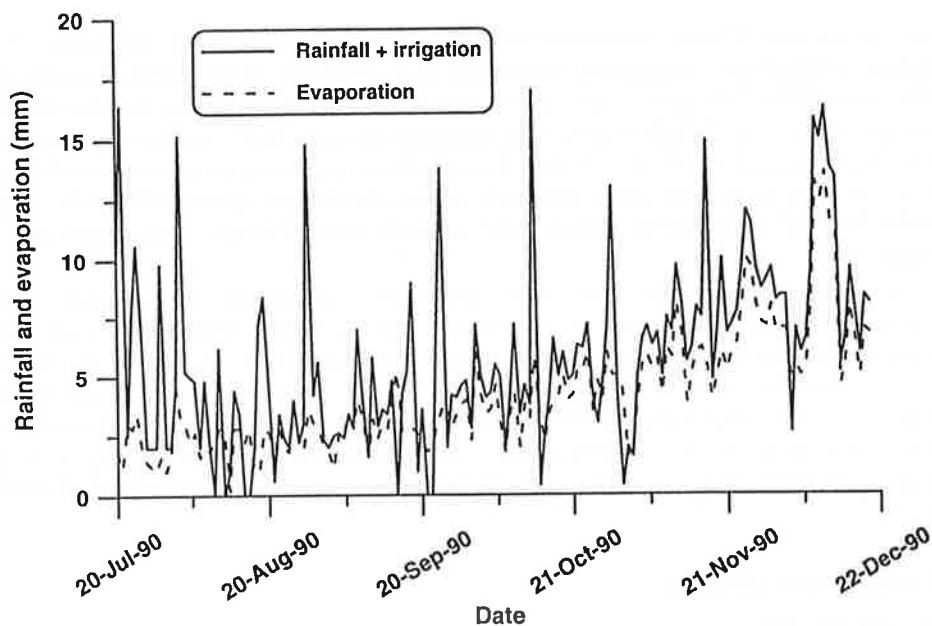


Fig. 1. Daily effective rainfall and evaporation.

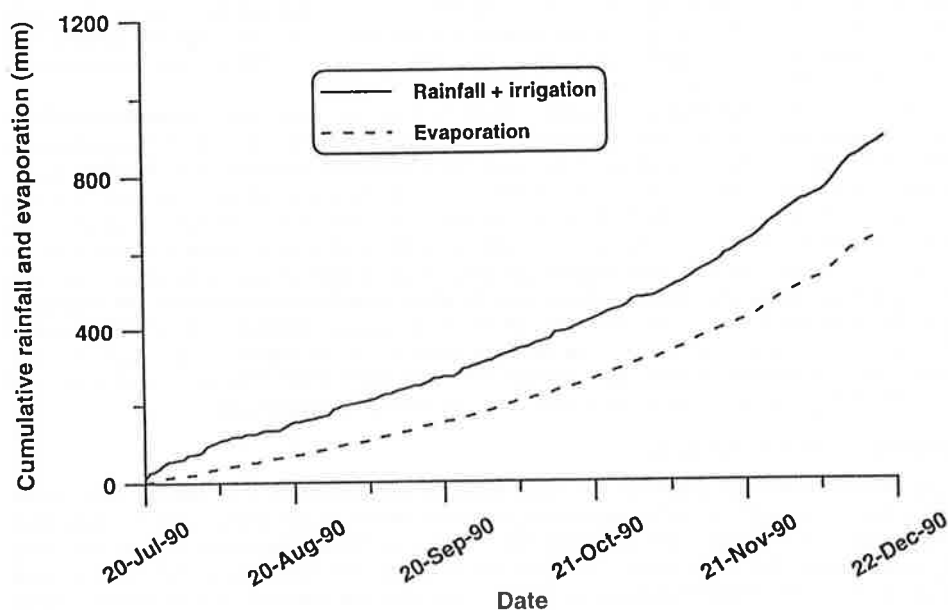


Fig. 2. Cumulative effective rainfall and evaporation.

used. The methods for simazine, metribuzin, linuron, prometryne and chlorpyrifos have been compiled by Lawrence (1982). Briefly, reversed phase chromatography was employed for all these pesticides; column: μ Bondpak, C_{18} , $10\ \mu m$, $3.9 \times 300\ mm$, mobile phase: acetonitrile or methanol in water (the concentration of which ranged from 80% in the case of chlorpyrifos to

50% in the case of metalaxyl). Analyses were carried out at 30°C with 50 μ L injections and by employing flow rates between 1.5 and 2.0 mL min⁻¹. The wavelengths for various compounds, considering their peak maxima, were 210 nm for metalaxyl and chlorthal dimethyl, 220 nm for simazine, metribuzin, prometryne, propyzamide and linuron, 226 nm for fenamiphos and its two metabolites and 230 nm for chlorpyrifos. Data acquisition and processing were done on a computer with DAPA, a commercially available software designed for HPLC and GC.

In addition to the nine pesticides, the two toxic metabolites of fenamiphos, fenamiphos sulfoxide and fenamiphos sulfone, were also analysed. Separation of F. sulfoxide and F. sulfone peaks was obtained by decreasing the acetonitrile concentration in the mobile phase as compared to that used in the case of fenamiphos (Singh 1989). Five- to ten-fold preconcentrations were needed for fenamiphos and chlorpyrifos, which were achieved through the rotary evaporator. The recoveries varied with the nature of pesticides. For simazine, linuron, metalaxyl, metribuzin, propyzamide and fenamiphos, reproducible recoveries better than 80% were obtained. In the case of chlorpyrifos and chlorthal dimethyl, the recoveries were lower but reproducible. Considering good reproducibility, the amounts of pesticides recovered at day zero were assumed as 100% in various experiments.

Results and discussion

Leaching depth

Distribution of the pesticides in the soil profile, measured at three different intervals after application, are shown in Fig. 3. The concentration of pesticide in any soil layer at any particular sampling time was controlled by two processes: leaching (involving adsorption-desorption and transport) and degradation, both of which may vary between different depths of soil profile because of changes in soil properties, such as organic matter content. Obviously, not only the soil properties but also the chemical properties of a pesticide play a major role in determining its leaching behaviour. Figs 3a and b show that chlorpyrifos and chlorthal dimethyl did not leach below 5 cm depth within 148 and 142 days, respectively. The apparent resistance of the two pesticides to leaching agrees with their high sorption coefficients normalized by soil organic carbon (K_{oc}) (6070 and 5000 for chlorpyrifos and chlorthal dimethyl respectively; Wauchope *et al.* 1992). Strong sorption of the two pesticides by surface soil therefore prevented

Table 2. Mean leaching depth

Pesticide	Days after application	MLD ^A (cm)	D _L ^C (cm)
Chlorpyrifos	148	<5	0
Chlorthal dimethyl	142	<5	0
Fenamiphos+ metabolites	152	28 ^B	6.8
Linuron	142	6	0.2
Metalaxyl	142	18	1.6
Metribuzin	146	12	0.9
Prometryne	152	9	0.7
Propyzamide	144	8	0.2
Simazine	142	6	0.1

^A Calculated from equation (1).

^B Fenamiphos and metabolites might have leached below the maximum sampling depth (50 cm). The mean leaching depth is therefore likely to be deeper than 28 cm calculated on the basis of concentrations within 50 cm.

^C Calculated from equations (2) and (3).

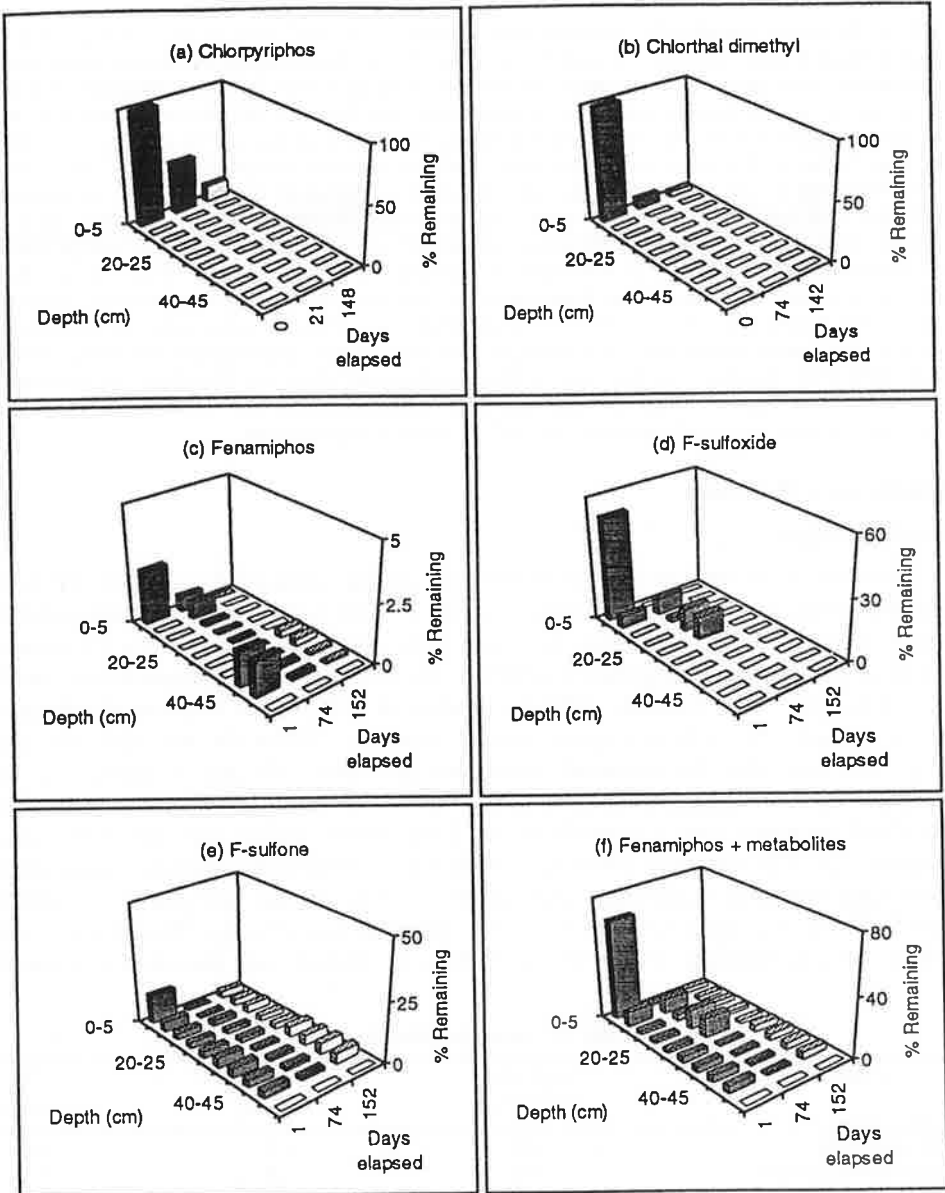


Fig. 3. Distribution of the nine pesticides studied in the soil profile, measured at three different intervals after application.

any significant downward movement. The fraction of both pesticides remaining in the soil profile, however, decreased steadily due to degradation losses.

In contrast, fenamiphos and its metabolites leached rapidly (Figs 3c-f). Fenamiphos was rapidly oxidized producing fenamiphos sulfoxide and fenamiphos sulfone, both of which are toxic and have nematicidal properties. Metalaxyl also showed considerable mobility, reaching 30 cm depth (Fig. 3g). The greater

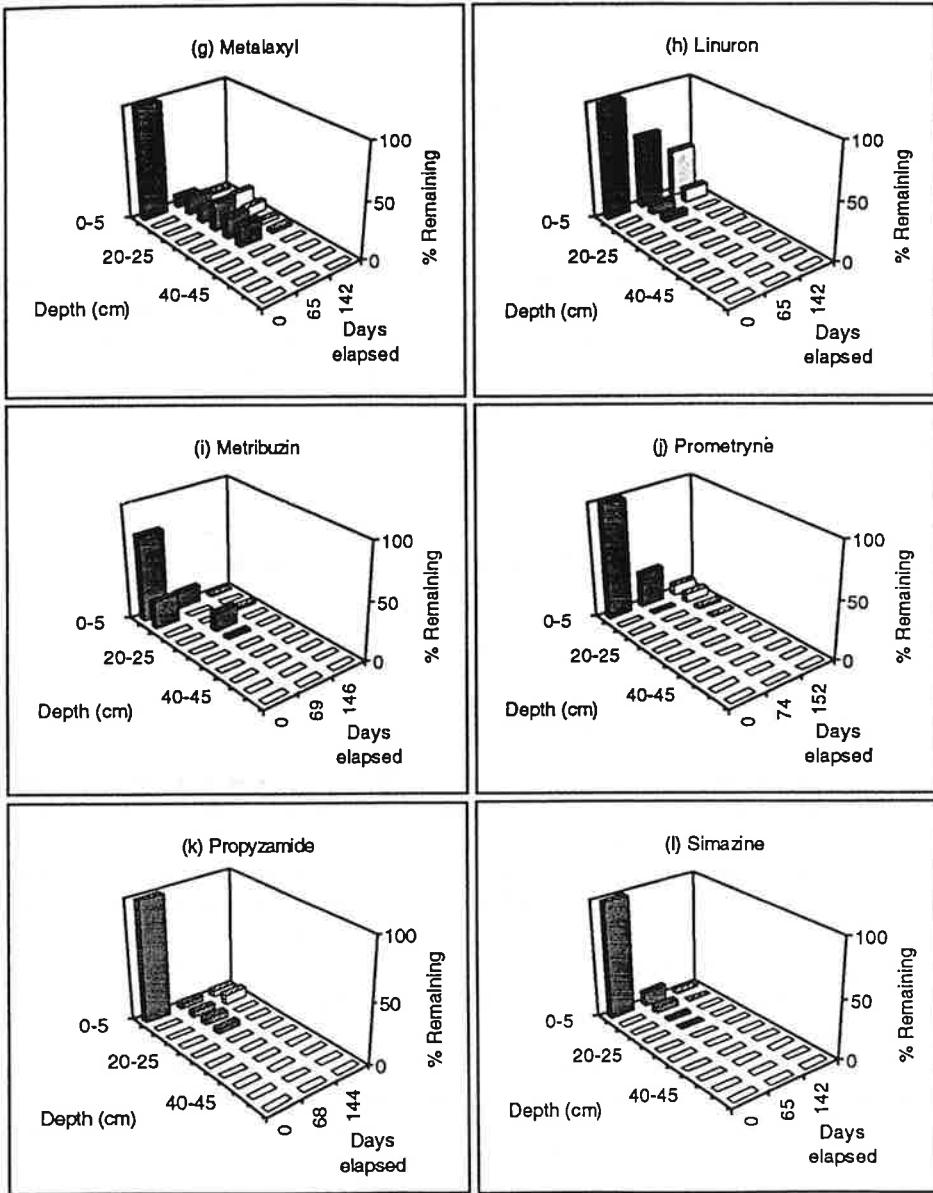


Fig. 3 (Continued)

penetration depths of these compounds correspond to their lower soil sorption coefficients, with K_{oc} values below 100 (Wauchope *et al.* 1992). The depth of the pesticide front for the rest of the pesticides studied, including linuron (Fig. 3h), metribuzin (Fig. 3i), prometryne (Fig. 3j), propyzamide (Fig. 3k) and simazine (Fig. 3l), varied between about 10 and 25 cm within the periods of study.

To compare the leaching depth between pesticides, mean leaching depths (MLDs) were calculated using moments theory (Grubner 1968), where the leaching depths

were weighted by the percentages of pesticide remaining at the different depths (Table 2):

$$\text{MLD} = \frac{\sum_{i=1}^n Q_i D_i}{\sum_{i=1}^n Q_i}, \quad (1)$$

where Q_i is the quantity of pesticide in layer i and D_i is the depth of layer i . In this equation, MLD is a ratio of the first moment (M_1) and the zero moment (M_0), where the moments represent mean position and total amount of solute within the soil, respectively. The first moment is a measure of central tendency and may not identify the peak or modal position. Similarly, from the second moment (M_2) of pesticide distribution through the soil profile, one can estimate the variance (σ^2) or width of the distribution by the equation (Gerritse and Singh 1988)

$$\sigma^2 = M_2/M_0 - (M_1/M_0)^2. \quad (2)$$

Dispersion length or dispersivity (D_L) can be calculated from σ^2 through the relation

$$D_L = 2\sigma^2/L, \quad (3)$$

where L is the length of the profile sampled.

The values of D_L calculated from this equation are presented in Table 2 along with the MLDs. The mean leaching depth at the last sampling followed the order: chlorpyrifos, chlorthal dimethyl < linuron, simazine < propyzamide, prometryne < metribuzin < metalaxyl < fenamiphos and metabolites. The dispersivity of the pesticides also followed the same order as for MLDs. The results in Table 2 show that not only the MLDs but also the dispersion associated with MLDs were higher for fenamiphos, metalaxyl and metribuzin. This means that for relatively mobile pesticides, substantial dispersion can occur during leaching and consequently small concentrations of pesticides can move much deeper than indicated by their MLDs.

The MLD would be expected to be related to the sorption affinities of the soil for the pesticides, since depth of pesticide movement is governed by the sorption coefficient (K_{oc}). However, the actual residual concentration at any given depth is also determined by the rate of degradation. Obviously, for pesticides which show rapid degradation, the residue is totally degraded after sufficient time and hence no further leaching is possible. The MLD for a pesticide is related to K_{oc} according to the relation

$$\text{MLD} = \text{MLD}_0(1 + f_{oc} K_{oc} \rho/\theta), \quad (4)$$

where MLD_0 (cm) is the mean leaching depth for a non-sorbed solute or water, f_{oc} is the fraction of organic carbon in soil, K_{oc} ($\text{cm}^3 \text{g}^{-1}$) is the sorption coefficient based on organic carbon of soil, ρ is bulk density (g cm^{-3}) and θ is the moisture content ($\text{cm}^3 \text{cm}^{-3}$) at field capacity of the soil. The MLDs for the nine pesticides studied showed some correlation with K_{oc} (R^2 0.86).

Degradation half lives

One of the most important parameters that control the ground water contamination potential of a pesticide is its resistance to degradation (or persistence). In models designed to predict the fate of the pesticides in the soil environment (e.g. Jury *et al.* 1983), this parameter is usually represented by a simple degradation rate constant or half-life by assuming first-order degradation.

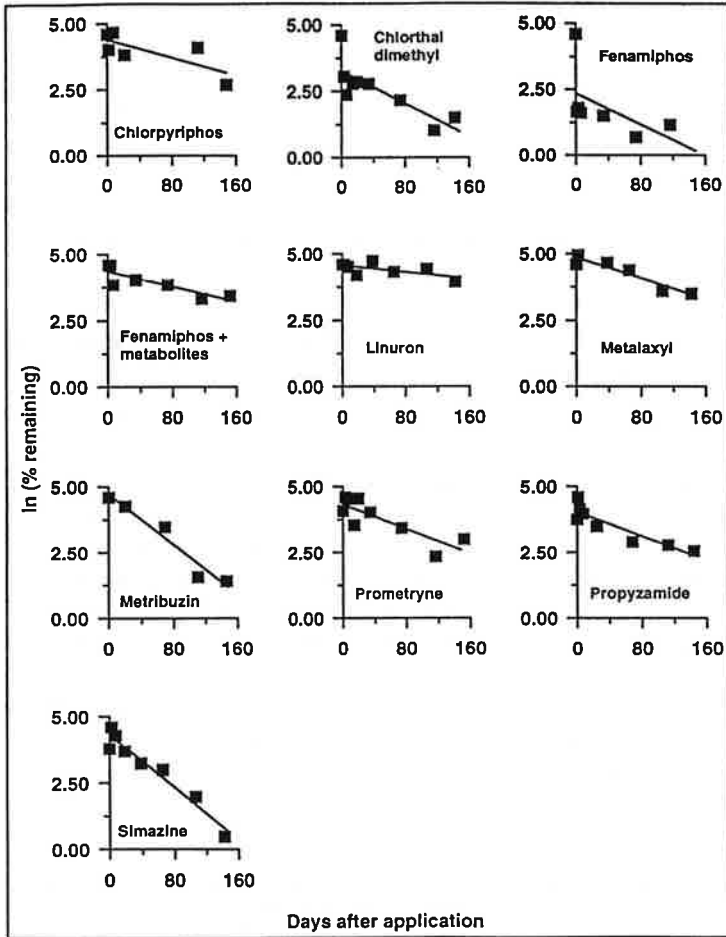


Fig. 4. Plots of the first-order regressions of percentage pesticide remaining in the soil profile with time elapsed.

First-order regressions were made between the percentage of pesticide remaining in the profile and the time elapsed (Fig. 4 and Table 3). A majority of the regressions were satisfactory, judging by the shape of the plots (Fig. 4) and by the amount of variation accounted for by the regression (Table 3). However, the degradation of fenamiphos and chlorthal dimethyl were very rapid immediately after application, and slowed down thereafter (Fig. 4). In addition, the regressions were not statistically significant at the 0.05 level for chlorpyrifos and linuron, probably due to field variability (Table 3).

Table 3. Degradation rate constants and half-lives derived by first-order regression of percentage pesticide remaining in the soil profile with time elapsed

Pesticide	Degradation rate constant (day ⁻¹)	Half-life (day)	R ²	F significance
Chlorpyrifos	0.0085	81	0.59	0.07
Chlorthal dimethyl	0.0154	45	0.64	0.009
Fenamiphos	0.0163	43	0.48	0.05
Fenamiphos+ metabolites	0.0070	98	0.73	0.01
Linuron	0.0032	219	0.44	0.07
Metalaxyl	0.0099	70	0.90	0.004
Metribuzin	0.0253	27	0.95	0.001
Prometryne	0.0119	58	0.71	0.005
Propyzamide	0.0117	59	0.82	0.002
Simazine	0.0247	28	0.94	0.00005

The nine pesticides varied widely in their degradation rates, with half-lives ranging from 27 to 219 days (Table 3). The pesticides may be ranked in the following order based on their degradation half-lives:

metribuzin, simazine < fenamiphos, chlorthal dimethyl < prometryne,
propyzamide < metalaxyl < chlorpyrifos < fenamiphos+metabolites < linuron.

Many of these half-lives differ significantly from those reported in the literature (Wauchope *et al.* 1992), which is of no surprise as the degradation rate is affected by environmental conditions, such as soil moisture, temperature and organic matter content (Hamaker 1972). The order of ranking in degradation rate may also change given a different set of soil and environmental conditions, as each pesticide may respond differently in degradation to the new environment. Walker (1978), for instance, studied the degradation rates of eight pesticides in soil and found that the degradation rates for the various pesticides did not change uniformly with changes in soil moisture content and temperature. Linuron degradation was found to be the least dependent on temperature whereas chlorthal dimethyl degradation was the most dependent on temperature.

Table 4. Half-life to K_{oc} ratios showing the relative ground water contamination potential of the pesticides

Pesticide	Half-life : K_{oc} ratio	Relative ratio ^A
Chlorpyrifos	0.013	1
Chlorthal dimethyl	0.009	0.7
Fenamiphos+ metabolites	2.2	169
Linuron	0.55	42
Metalaxyl	1.1	85
Metribuzin	0.1	8
Prometryne	0.15	12
Propyzamide	0.24	18
Simazine	0.22	17

^A Half-life to K_{oc} ratios were normalized assuming that of chlorpyrifos as 1.

The half-life for fenamiphos, when metabolites were included, was more than double that for fenamiphos alone; this illustrates the importance of the analysis of metabolites which may be just as toxic as the parent compound for some pesticides. In addition, because fenamiphos and its metabolites probably leached beyond the maximum sampling depth of 50 cm, the half-life calculated on the basis of the rate of disappearance of the compounds in the sampled profile is likely to be shorter than the actual rate of breakdown.

Ground water contamination potential

The potential of pesticides to contaminate ground water increases with half-life and decreases with increasing sorption. Ratios of half-life to K_{oc} were calculated from the half-life values obtained in this study and K_{oc} values reported by Wauchope *et al.* (1992) (Table 4). The higher the ratio, the greater the contamination potential of a pesticide. The potential for causing ground water contamination by the pesticides (discounting metabolites that were not analysed) thus follows the order:

chlorthal dimethyl, chlorpyrifos < metribuzin, prometryne < simazine,
propryzamide < linuron < metalaxyl < fenamiphos and metabolites.

Chlorpyrifos and chlorthal dimethyl are degraded to insignificant concentrations before reaching ground water (cf. Fig. 2). In contrast, fenamiphos and its metabolites, metalaxyl and linuron have much greater leaching potentials, and thus deserve attention in further studies.

The half-life to K_{oc} ratio is an index for comparing and ranking organic pesticides in terms of their potential for ground water contamination and cannot be used to quantify pesticide concentration distributions in the soil profile. The significance of these ratios can only be shown by ground water monitoring studies.

Conclusions

The nine pesticides studied differed widely in their mobility which varied by an order of magnitude. Chlorpyrifos and chlorthal dimethyl showed significant degradation but essentially no movement during the study period. In contrast, fenamiphos, its metabolites and metalaxyl showed substantial leaching during this period. The variations in leaching depth corresponded inversely with the soil sorption coefficients. Similarly, some 8-fold difference was observed in the degradation rates of the pesticides. Metribuzin had the shortest half-life (27 days) and linuron the longest (219 days). From the leaching and persistence studies presented here it is concluded that, while chlorpyrifos and chlorthal dimethyl are highly unlikely to reach ground water, fenamiphos and metalaxyl have the potential to rapidly leach to the subsurface layers of the soil profile studied here. Due to a much lower microbial population in the lower vadose zone, these pesticides may persist longer than expected and may present contamination hazard to ground water underneath the sandy soil profile considered in this study.

Acknowledgments

Funding of the project by the Land and Water Resources Research and Development Corporation of Australia is gratefully acknowledged. We would also like to thank Cajé Tan Phang and Anthony Aylmore (both from the University of W.A.) for technical support. Robert Gerritse (Division of Water Resources, CSIRO)

for advice in the experiment, and staff at the Merdina Vegetable Research Station of W.A. for their cooperation.

References

- Cheng, H. H. (1990). 'Pesticides in the Soil Environment: Processes, Impacts, and Modelling.' (Soil Science Society of America: Madison, Wisconsin.)
- Cohen, S. Z., Eiden, C., and Lorber, M. N. (1986). Monitoring ground water for pesticides. In 'Evaluation of Pesticides in Ground Water.' (Eds W. Y. Garner, R. C. Honeycutt and H. N. Nigg) pp. 170-96. ACS Symposium Series, Vo. 315. (American Chemical Society: Washington, D.C.)
- Gerritse, R. G., and Singh, R. (1988). The relationship between pore water velocity and longitudinal dispersivity of Cl^- , Br^- and D_2O in soils *J. Hydrol.* **104**, 173-80.
- Grubner, O. (1968). Statistical moments theory of gas-solid chromatography. *Adv. Chromatogr.* **6**, 173-209.
- Hamaker, J. W. (1972). Decomposition: quantitative aspects. In 'Organic Chemicals in the Soil Environment'. Vol. 1. (Eds C. A. I. Goring and J. W. Hamaker.) pp. 253-340. (Marcel Dekker: New York.)
- Hutson, J. L., and Wagenet, R. J. (1992). 'Leaching Estimation and Chemistry Model, a Process-based Model of Water and Solute Movement, Transformation, Plant Uptake and Chemical Reactions in the Unsaturated Zone.' Version 3. Department of Soil, Crop and Atmospheric Sciences Research Series No. 92-3. (Cornell University: Ithaca, New York.)
- Jury, W. A., Spencer, W. F., and Farmer, W. J. (1983). Behaviour assessment model for trace organics in soil: I. Model description. *Journal of Environmental Quality* **12**, 558-64.
- Kookana, R. S., and Aylmore, L. A. G. (1994). Estimating pollution potential of pesticides to ground water. *Aust. J. Soil Res.* **32**, 1141-55.
- Kookana, R. S., Aylmore, L. A. G., and Gerritse, R. G. (1992a). Time dependent sorption of pesticides during transport in soils. *Soil Science* **154**, 214-25.
- Kookana, R. S., Gerritse, R. G., and Aylmore, L. A. G. (1992b). A method for studying nonequilibrium sorption during transport of pesticides in soil. *Soil Science* **154**, 344-9.
- Lawrence, J. F. (1982). High performance liquid chromatography of pesticides. In 'Analytical Methods for Pesticides and Growth Regulators'. Vol. XIII. (Eds G. Zweek and J. Sherma.) (Academic Press: New York.)
- Mullins, J. A., Carsel, R. F., Scarbrough, J. E., and Ivery, A. M. (1993). 'PRZM-2, A Model for Predicting Pesticides Fate in the Crop Root and Unsaturated Soil Zones: Users Manual for Release 2.0.' (USE PA: Athens, GA.)
- Nicholls, P. H., Walker, A., and Baker, R. J. (1982). Measurement and simulation of the movement and degradation of atrazine and metribuzin in a fallow soil. *Pesticide Science* **12**, 484-94.
- Pennell, K. D., Hornsby, A. G., Jessup, R. E., and Rao, P. S. C. (1990). Evaluation of five simulation models for predicting aldicarb and bromide behaviour under field conditions. *Water Resources Research* **26**, 2679-93.
- Singh, R. (1989). Simultaneous determination of fenamiphos, its sulfoxide and sulfone in water by high performance liquid chromatography. *Analyst* **114**, 425-7.
- Singh, R., Gerritse, R. G., and Aylmore, L. A. G. (1989). Adsorption-desorption behaviour of selected pesticides in some Western Australian soils. *Australian Journal of Soil Research* **28**, 227-43.
- USEPA (1977). 'Waste Disposal Practices and Their Effects on Groundwater.' Report to Congress, Washington, DC. (USEPA: Washington, DC.)
- USEPA (1978). 'Surface Impoundments and Their Effects on Groundwater Quality in the U.S.—A Preliminary Survey.' EPA/9-78-004. (USEPA: Washington, DC.)
- Walker, A. (1978). Simulation of the persistence of eight soil-applied herbicides. *Weed Research* **18**, 305-13.
- Wauchope, R. D., Buttler, T. M., Hornsby, A. G., Augustijn-Beckers, P. M. W., and Burt, J. P. (1992). The SCS/ARS/CES pesticide properties database for environmental decision-making. *Reviews of Environmental Contamination and Toxicology* **123**, 1-164.

Application of a simple model to assess the ground water contamination potential of pesticides

H. J. Di,^A R. S. Kookana^{A,B} and L. A. G. Aylmore^A

^A Soil Science and Plant Nutrition, University of Western Australia, Nedlands, W.A. 6009.

^B Present address: CRC for Soil and Land Management, Glen Osmond, S.A. 5064.

Abstract

A simple model is described for assessing the ground water contamination potential of pesticides. This model, based on simple processes of linear, equilibrium and singular partition between solution and soil organic matter, steady convective flow, and first-order degradation, calculates fractions of pesticides remaining in the soil as they leach to greater depth. Possible effects by preferential flow that may be present in structured soils are ignored. The soil profile is divided into a number of layers which may differ in bulk density, moisture content at field capacity, organic C content, and degradation half-life. The leaching depths predicted by this model generally agreed with the mean leaching depths measured in a field study, and with those predicted by the CALF model. The leaching depths by the simple model were also statistically related to those simulated by the LEACHM model, although the values by LEACHM were found to be much higher than those by the simple model and by CALF. Under the soil and environmental conditions given, the simple model predicted that chlorpyrifos and chlorthal dimethyl would not leach to any noticeable depth before being completely degraded, that metribuzin, prometryne, propyzamide and simazine would mostly degrade to insignificant concentrations before reaching 500 cm, and that traces of fenamiphos, metalaxyl and linuron might reach beyond 1000 cm.

Keywords: pesticide, ground water, contamination, leaching, modelling.

Introduction

The mobility and persistence of pesticides in the soil which essentially determine their ground water contamination potentials vary widely depending on pesticide properties, soil properties and environmental conditions (Cheng 1990). Numerous laboratory and field investigations have been conducted in attempting to characterize the behaviour and fate of pesticides in the soil (e.g. Walker 1978; Singh *et al.* 1989; Pennell *et al.* 1990; Kookana *et al.* 1992*a*, 1992*b*). Experimental investigations, however, are expensive and the large number of pesticides that are increasingly being used in agriculture and horticulture makes it impractical to study every pesticide under different combinations of soil and environmental conditions. Simulation models have been developed to predict the environmental fate of pesticides (Nicholls *et al.* 1982; Jury *et al.* 1983; Hutson and Wagenet 1992; Mullins *et al.* 1993). These models vary in their complexity and in the representation of leaching and degradation processes. Models with more detailed representation of pesticide processes usually demand more data input which may

or may not be readily available. A balanced modelling approach is particularly desirable for providing management guidance, where the model is based on solute transport processes, but has a minimum data requirement. The objective of this paper is to describe a simple model and to evaluate its usefulness in assessing the ground water contamination potential of nine pesticides whose leaching and degradation behaviour were studied in a field experiment. The results from this simple model will be compared with those from the increasingly more complex models of CALF (Nicholls *et al.* 1982) and of LEACHM (Hutson and Wagenet 1992).

Materials and Methods

Description of the simple model

The ground water contamination potential of a pesticide is largely determined by two key variables, namely the velocity at which the pesticide leaches downward and the rate at which the pesticide degrades. When a dose of organic pesticide is applied to the surface of the soil, the pesticide is assumed to undergo linear, instantaneous and reversible partition between soil solution and soil solid (organic matter in particular) phases, i.e.

$$S = k_d C = f_{oc} k_{oc} C, \quad (1)$$

where S is the sorbed concentration, k_d is the sorption coefficient, C is the solution concentration, f_{oc} is the organic C fraction of soil, and k_{oc} is the sorption coefficient normalized to the organic C fraction, where

$$k_{oc} = k_d / f_{oc}. \quad (2)$$

The values of k_{oc} have been reported to be generally stable for organic pesticides across a range of soils (Hamaker and Thompson 1972; Rao and Davidson 1980; Green and Karickhoff 1990). The assumption is made that sorption of a pesticide is entirely by soil organic matter, and that organic matter in different soils possesses the same sorption capacity. These assumptions may not always be valid and errors may be introduced when using k_{oc} values measured from one soil to another. However, compared with the significant variability of soil properties in the field, these errors may be limited and thus tolerable for management purposes.

Assuming pesticide leaching by steady piston flow, the effective pesticide velocity (V) is

$$V = q / (\rho_b f_{oc} k_{oc} + \theta) \quad (3)$$

and time (t) required to travel through increment depth (ΔD) is

$$t = \Delta D (\rho_b f_{oc} k_{oc} + \theta) / q, \quad (4)$$

where q is the steady drainage rate, ρ_b is the bulk density, and θ is the water content at field capacity.

While leaching down the profile, the pesticide undergoes degradation. Assuming first-order degradation, the fraction (f) of pesticide remaining in the soil profile is

$$f = \exp(-0.693t/t_{1/2}), \quad (5)$$

where t is the time elapsed and $t_{1/2}$ is the half-life of the pesticide in the soil layer where the pesticide concentration peak exists. Substitution of equation (4) into equation (5) gives

$$f = \exp[-\Delta D (\rho_b f_{oc} k_{oc} + \theta) 0.693 / (qt_{1/2})]. \quad (6)$$

Equation (6) gives the fraction of pesticide remaining in the soil profile as it travels a depth ΔD , or as it reaches the total depth D .

The soil profile may be divided into a number of layers of varying thickness (ΔD). Each layer may have different values in bulk density (ρ_b), organic C fraction (f_{oc}), water content (θ) at field capacity (-0.01 MPa potential), and degradation half-life ($t_{1/2}$). These properties are assumed to be uniform within each layer. The fraction of pesticide remaining (f_n) when reaching the bottom layer n is

$$f_n = \prod_{i=1}^n \exp[-\Delta D(\rho_b f_{oc} k_{oc} + \theta)0.693/(qt_{1/2})]_i. \quad (7)$$

Equation (7) was used to estimate whether or not a pesticide will reach ground water in significant amounts.

The leaching depth (D_n) after a given time is calculated with equation (4) written as

$$D_n = \sum_{i=1}^n [t_i q / (\rho_b f_{oc} k_{oc} + \theta)]_i, \quad (8)$$

where t_i is the time to travel through each i th layer.

Application of the simple model

A field experiment was carried out on a sandy soil to study the leaching and degradation behaviour of nine pesticides. Details of the experiment and results obtained will be reported elsewhere (Kookana *et al.* 1995). In brief, dilute aqueous pesticide solutions of commercial products were sprayed to the surface of field plots. Irrigation was applied daily which together with rainfall provided an average net daily recharge rate of 1.59 mm during the experimental period which was between July and December. The mean minimum and maximum temperatures during this period were 10 and 22°C respectively. Soil samples were taken at different intervals after pesticide application at 5 cm increments down to 50 cm of the profile and were analysed for pesticide concentration by using high performance liquid chromatography. The relevant soil and pesticide properties are presented in Tables 1 and 2 respectively. The soil has three layers which differ in bulk density, moisture content at field capacity (-0.01 MPa) and, in particular, organic C content.

Table 1. Soil properties

Soil layer	Texture		pH (H ₂ O)	Organic C (%)	Bulk density (g cm ⁻³)	Water content ^A (% v/v)
	Sand (%)	Silt+clay (%)				
0-25	98	1	5.3	0.53	1.58	5.1
25-50	98	1	5.5	0.15	1.62	2.4
50-1000	98	1	5.5	0.06	1.62	2.4

^A At -0.01 MPa.

To compare predicted with measured results, leaching depths were calculated with equation (8) and the parameters presented in Tables 1 and 2. A single half-life as measured in the experiment (Table 2) was assumed for each pesticide. The average drainage rate (q) used was 1.59 mm per day estimated on the basis of effective rainfall and evaporation records.

Fractions of pesticide remaining in the soil profile (to a maximum of 1000 cm) were calculated using equation (7). Computations were made for the following three scenarios.

- (1) Single half-life: Parameters used for the computations in this case were exactly the same as those measured in the field study (Tables 1 and 2). The degradation half-lives were assumed to be constant in the entire soil profile.

- (2) Incremental half-life: Half-lives for the surface layer (0–25 cm) were the same as those measured at the site (Table 2), but were assumed arbitrarily to increase by a factor of 2 and 3 for the depth 25–50 and 50–1000 cm respectively. This was on the consideration that the pesticides were mostly limited to the surface layer when the half-lives were determined in the field study, and that the half-life might increase at greater depth due to decreased microbial activities.
- (3) Higher rainfall: Soil and pesticide parameters were the same as those in scenario (1), but the steady net recharge was increased from 1.59 to 2.5 mm per day, to accommodate situations with greater irrigation.

Table 2. Pesticide properties

Common name	Chemical name	k_{oc}^A	Solubility ^B (mg L ⁻¹)	Half-life ^C (days)
Chlorpyrifos	<i>O,O</i> -diethyl <i>O</i> -3,5,6-trichloro-2-pyridyl phosphorothioate	6070	0.4	81
Chlorthal dimethyl	Dimethyl tetrachloroterephthalate	5000	0.5	45
Fenamiphos	Ethyl 4-methyl- <i>m</i> -tolyl isopropylphosphoramidate	100	400	43
Linuron	3-(3,4-dichlorophenyl)-1-methoxy-1-methylurea	400	75	219
Metalaxyl	Methyl <i>N</i> -(2-methoxyacetyl)- <i>N</i> -(2,6-xylyl)-DL-alaninate	61	8400	70
Metribuzin	4-amino-6- <i>tert</i> -butyl-3-methylthio-1,2,4-triazine-5(4 <i>H</i>)-one	268	1220	27
Prometryne	<i>N,N'</i> -diisopropyl-6-methylthio-1,3,5-triazine-2,4-diyldiamine	400	33	58
Propyzamide	3,5-dichloro- <i>N</i> -(1,1-dimethyl propynyl)benzamide	243	15	59
Simazine	6-chloro- <i>N,N'</i> -diethyl-1,3,5-triazine-2,4-diyldiamine	130	6.2	28

^A From Wauchope *et al.* (1992). ^B From Worthing (1983). ^C From Kookana *et al.* (1995).

These variations were made to illustrate, as examples, how these parameters could affect pesticide environmental fate. Other soil parameters in equation (7) could similarly be varied to show their impact on pesticide leaching in the soil.

Comparison of the simple model (SM) with CALF and LEACHM

CALF and LEACHM (the LEACHP version) are two of the more complex models that have been developed. The simple model was compared with these two models to examine whether there were significant departures in the predictions of leaching depths between the simple model and the more complex ones. Details of CALF and LEACHM may be found in Nicholls *et al.* (1982) and Hutson and Wagenet (1992) respectively. Major features of the CALF model include: (1) pesticide sorption is assumed to be linear but increases with time; (2) transport of pesticides is by non-steady water convection; and (3) soil water is divided into mobile and immobile phases (separated at -200 kPa). The time-dependent sorption/desorption parameters were estimated on the basis of findings by Walker (1987). First-order degradation rates were used.

A major feature of the LEACHM model, as used in this study, is that pesticide transport is by non-steady convection-dispersion in water and in air. The diffusion coefficients of 0.43 m² day⁻¹ in air and 4.3 × 10⁻⁵ m² day⁻¹ in water as suggested by Jury *et al.* (1983) were used as representative values for all the pesticides. The Campbell (1974) water retention and conductivity function parameters as required by the LEACHM model were estimated on the basis of measured water retention curves. The estimated *A* and *B* values are -1.08

and 0.785 respectively for the surface soil (0–25 cm), and are –1.32 and 0.583 respectively for the subsurface soil (below 25 cm). Constant linear sorption coefficients and first-order degradation rates were used for the simulation.

Results and Discussion

Comparison of predicted with measured leaching depths

Table 3 shows that the leaching depths predicted by the simple model were similar to the measured mean leaching depths for a majority of the pesticides. Differences, however, were noticeable in the cases of metalaxyl and simazine. A regression made between the predicted and measured depths showed that there was a significant relationship between the two leaching depths (Fig. 1, Table 4). It should be noted that the measured mean leaching depths were mostly less than 40 cm. The significant relationship between the predicted and the measured values may or may not be extrapolated to greater depth.

Table 3. Comparison of leaching depths predicted by the simple model (SM), CALF and LEACHM, with those measured in the field

Pesticide	Elapsed time (days)	Mean leaching depth ^A (cm)			
		Measured	SM	CALF	LEACHM
Chlorpyrifos	148	<5	0.5	5	5
Chlorthal dimethyl	142	<5	0.5	5	20
Fenamiphos	152	34	32	26	97
Linuron	142	6	7	7	13
Metalaxyl	142	18	40	29	149
Metribuzin	147	12	10	9	17
Prometryne	152	9	7	5	14
Propyzamide	148	8	11	5	23
Simazine	142	6	20	5	42

$$^A \text{ Mean leaching depth} = \frac{\sum_{i=1}^n Q_i D_i}{\sum_{i=1}^n Q_i},$$

where Q_i is the quantity of pesticide in layer i , D_i is the depth of layer i and n is the number of layers.

Table 4. Regressions of predicted and observed leaching depths

The regression equation is $y = ax$

y variable	x variable		
	SM	CALF	LEACHM
Observed	a	0.96	0.20
	r^2	0.71**	0.37
SM	a	1.31	0.30
	r^2	0.81**	0.89**
CALF	a	—	0.22
	r^2	—	0.84**

The leaching depths simulated by CALF also showed a good agreement with those observed (Tables 3 and 4). The values derived from the LEACHM model, however, were in many cases significantly higher than those observed, and the

regression coefficients were low (Tables 3 and 4). This lesser agreement was probably due to errors associated with the determination and estimation of some parameters required by the LEACHM model.

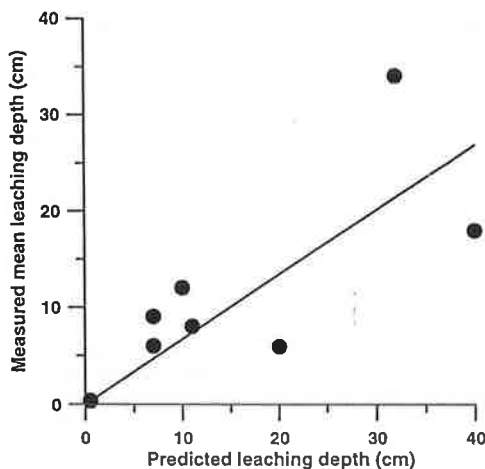


Fig. 1. Regression plot showing the relationship between the predicted (by the simple model) and measured leaching depths.

The predicted leaching depths by the simple model showed good agreement with those obtained by the CALF model (Tables 3 and 4). Several values from the simple model, however, were slightly higher than those found by CALF. The predictions by the simple model were also statistically related to those by LEACHM, although the values by LEACHM were much higher. These results suggest that similar conclusions may be arrived at by all three models with regard to the *relative* ground water contamination potential of the pesticides. They also indicate that models which assume simpler solute transport processes in the soil media can be valuable tools for management purposes to identify pesticides with higher contamination potentials. Complex models (such as LEACHM) are valuable tools for research purposes to study the various processes that affect solute transport in the soil; their successful application depends on our accessibility to the large volume of data required by the models.

Ground water contamination potential as assessed by the simple model

Fig. 2 shows the predicted percentage of pesticide remaining as it travels to greater depths (up to 1000 cm). In Table 5, the time required for the pesticides to reach a depth of 1000 cm ($t_{1000\text{ cm}}$) is compared with the time required for degradation to 0.01% of the amount initially applied ($t_{0.01\%}$). The value of 0.01% was used as a lower limit below which the fraction of pesticides remaining in the soil was assumed to be insignificant. If the value of $t_{0.01\%}$ is equal to or greater than that of $t_{1000\text{ cm}}$, then the pesticide is likely to reach 1000 cm in significant amounts, and vice versa.

Chlorpyrifos and chlorthal dimethyl will remain close to the surface of the soil profile until they are completely degraded (Figs 2a, b). They are unlikely to

cause contamination to ground water by leaching (Table 5). This is mainly due to their very low mobility caused by the high sorption coefficient (Table 2). The scenarios of incremental half-life, or higher rainfall, did not make any significant impact on the movement of these two pesticides.

Significant fractions of fenamiphos, linuron and metalaxyl, however, could reach as deep as 1000 cm, particularly if the half-life increases at greater depth as assumed, or under higher irrigation conditions (Figs 2*c-e*). The time required for these pesticides to reach 1000 cm, under the soil and environmental conditions at the field experimental site, ranges from about 1.5 to 8.5 years (Table 5). The

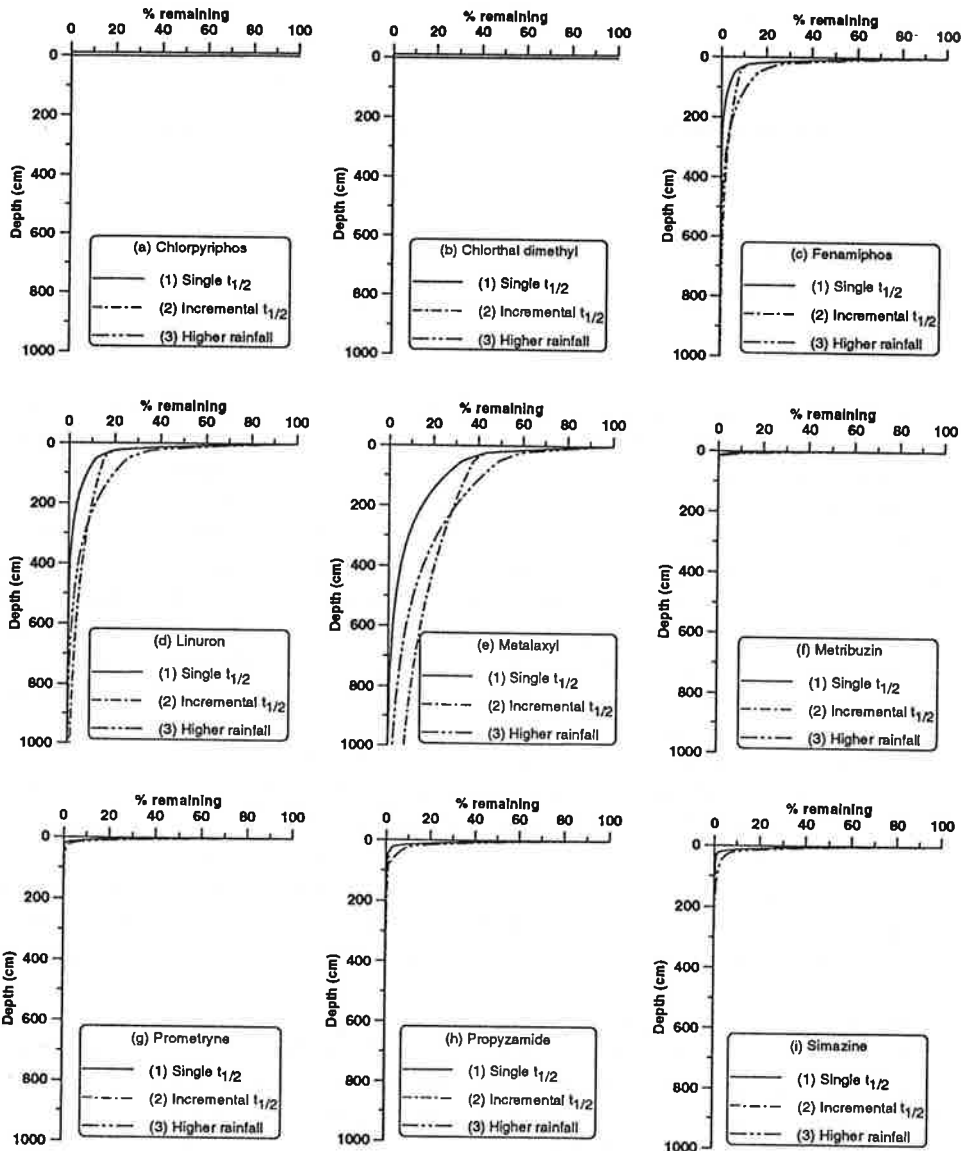


Fig. 2. Predicted percentages of pesticides remaining as they leach to greater depths. The conditions in scenarios (2) and (3) are the same as in (1) except those specified in the legend.

higher contamination potential of fenamiphos and metalaxyl is related to their higher mobility due to the significantly lower sorption coefficients (Table 2); but that of linuron is related to its longer half-life in combination with a medium sorption (Table 2). These pesticides therefore deserve closer attention in further studies and in ground water monitoring programs.

Table 5. Time required for the pesticides to degrade to 0.01% of the amounts initially applied ($t_{0.01\%}$), and time required for the pesticides to leach 1000 cm in the soil ($t_{1000\text{ cm}}$), based on the first scenario

Pesticide	$t_{0.01\%}$ (year)	$t_{1000\text{ cm}}$ (year)
Chlorpyrifos	2.95	124.63
Chlorthal dimethyl	1.64	102.73
Fenamiphos	1.56	2.47
Linuron	7.97	8.61
Metalaxyl	2.55	1.67
Metribuzin	0.98	5.91
Prometryne	2.11	8.61
Pripyzamide	2.15	5.40
Simazine	1.02	3.09

The remaining pesticides assessed, including metribuzin, prometryne, propyzamide and simazine (Figs 2*f-i*), will mostly remain above 500 cm before degrading to insignificant fractions. The contamination potential of these pesticides will depend on the ground water level.

The predicted leaching curves (Fig. 2), such as those of fenamiphos, linuron and metalaxyl, show that, mainly because of the higher organic C content in the surface soil (0-25 cm), pesticides move much more slowly, i.e. it takes a longer time to travel through a given distance; greater proportions of the pesticides are thus degraded at the surface layer than lower down for the same travelling distance. The surface layer with high organic C content therefore plays a particularly important role in retaining and degrading pesticides. Once the chemicals have passed this filtering layer, their mobility is greatly increased.

The curves also show the important impact of incremental half-life at deeper layers compared with single half-life on contamination potential. The incremental factors of 2 and 3 for the second (25-50 cm) and third (50-1000 cm) layers over the first layer were arbitrarily assumed. There is an urgent need to understand the nature of the depth function of degradation rate. This depth function is rather complex and is likely to be affected by changes with depth in soil conditions, such as organic matter content which may affect both microbial activity and pesticide sorption, temperature and aeration.

The changes in degradation half-life down the profile or in effective rainfall only made significant differences in the amount of pesticide leaching to greater depth in cases where the contamination potential of the pesticides was high (e.g. fenamiphos linuron and metalaxyl in Fig. 2); they did not make a significant impact where the pesticides were highly immobile (e.g. chlorpyrifos and chlorthal dimethyl), or had a very short half-life (e.g. metribuzin).

It should be noted that intermediate degradation products of some pesticides are also toxic. The simple model described in this paper cannot be used directly to assess the contamination potential of these intermediate degradation products which are gradually produced as the parent compound moves to greater depth. For instance, the contamination potential for fenamiphos would be greater if the two toxic metabolites, sulfoxide and sulfone, are taken into consideration, because of increased half-lives and smaller sorption coefficients. An estimate of contamination potential for individual metabolites could be made by assuming that they are applied at the surface or produced at certain depth. In addition, possible effects on pesticide movement by preferential flow which may be significant in structured soils are ignored in the simple model.

Conclusions

The simple model described in this paper, based on simple processes of linear, instantaneous and singular partition, steady convective flow, and first-order degradation, provides an effective approach for management purposes in identifying priority pesticides for further studies and for environmental monitoring. The leaching depths predicted by this simple model generally agreed with those measured in a field study, and with those predicted by the CALF model. The leaching depths predicted by the simple model were also statistically related to those simulated by the LEACHM model, although the values by LEACHM were much higher than those found by the simple model and by the CALF. The simple model predicts that under the environmental and soil conditions specified, chlorpyrifos and chlorthal dimethyl will be retained near the surface before disappearing by degradation; that metribuzin, prometryne, propyzamide and simazine will not leach below 500 cm in their entire life-times; and that traces of fenamiphos, metalaxyl and linuron will reach 1000 cm or deeper.

Acknowledgments

Funding of the project by the Land and Water Resources Research and Development Corporation of Australia is gratefully acknowledged. We would also like to thank Cajé Tan and Anthony Aylmore (both at the University of W.A.) for their technical support and Robert Gerritse (Division of Water Resources, CSIRO) for advice in the field experiment.

References

- Campbell, G. (1974). A simple method for determining unsaturated conductivity from moisture retention data. *Soil Science* **117**, 311–14.
- Cheng, H. H. (1990). 'Pesticides in the Soil Environment: Processes, Impacts, and Modelling.' (Soil Science Society of America: Madison, Wisconsin.)
- Green, R. E., and Karickhoff, S. W. (1990). Sorption estimates for modelling. In 'Pesticides in the Soil Environment: Processes, Impacts, and Modelling'. (Ed. H. H. Cheng) pp. 79–101. (Soil Science Society of America: Madison, Wisconsin.)
- Hamaker, J. W., and Thompson, J. M. (1972). Adsorption. In 'Organic Chemicals in the Soil Environment'. Vol. 1. (Eds C. A. I. Goring and J. W. Hamaker.) pp. 49–143. (Marcel Dekker: New York.)
- Hutson, J. L., and Wagenet, R. J. (1992). 'Leaching Estimation and Chemistry Model, a Process-based model of Water and Solute Movement, Transformation, Plant Uptake and Chemical Reactions in the Unsaturated Zone.' Version 3. Department of Soil, Crop and Atmospheric Sciences Research Series No. 92-3. (Cornell University: Ithaca, New York.)

- Jury, W. A., Spencer, W. F., and Farmer, W. J. (1983). Behaviour assessment model for trace organics in soil: I. Model description. *Journal of Environmental Quality* **12**, 558-64.
- Kookana, R. S., Aylmore, L. A. G., and Gerritse, R. G. (1992a). Time dependent sorption of pesticide during transport in soils. *Soil Science* **154**, 214-25.
- Kookana, R. S., Gerritse, R. G., and Aylmore, L. A. G. (1992b). A method for studying nonequilibrium sorption during transport of pesticides in soil. *Soil Science* **154**, 344-9.
- Kookana, R. S., Di, H. J., and Aylmore, L. A. G. (1995). A field study of leaching and degradation of nine pesticides in a sandy soil. *Australian Journal of Soil Research*. **33**, 1019-30.
- Mullins, J. A., Carsel, R. F., Scarbrough, J. E., and Ivery, A. M. (1993). 'PRSM-2, A Model for Predicting Pesticides Fate in the Crop Root and Unsaturated Soil Zones: Users Manual for Release 2.0.' (USEPA: Athens, GA.)
- Nicholls, P. H., Walker, A., and Baker, R. J. (1982). Measurement and simulation of the movement and degradation of atrazine and metribuzin in a fallow soil. *Pesticide Science* **12**, 484-94.
- Pennell, K. D., Hornsby, A. G., Jessup, R. E., and Rao, P. S. C. (1990). Evaluation of five simulation models for predicting aldicarb and bromide behaviour under field conditions. *Water Resources Research* **26**, 2679-93.
- Rao, P. S. C., and Davidson, J. M. (1980). Estimation of pesticide retention and transformation parameters required in nonpoint source pollution models. In 'Environment Impact of Nonpoint Source Pollution'. (Eds M. R. Overcash and J. M. Davidson.) pp. 23-67. (Ann Arbor Publishers: Michigan.)
- Singh, R., Gerritse, R. G., and Aylmore, L. A. G. (1989). Adsorption-desorption behaviour of selected pesticides in some Western Australian Soils. *Australian Journal of Soil Research* **28**, 227-43.
- Walker, A. (1978). Simulation of the persistence of eight soil-applied herbicides. *Weed Research* **18**, 305-13.
- Walker, A. (1987). Evaluation of a simulation model for prediction of herbicide movement and persistence in soil. *Weed Research* **27**, 143-52.
- Wauchope, R. D., Buttler, T. M., Hornsby, A. G., Augustijn-Beckers, P. M. W., and Burt, J. P. (1992). The SCS/RS/CES pesticide properties database for environmental decision-making. *Reviews of Environmental Contamination and Toxicology* **123**, 1-164.
- Worthing, C. R. (1983). 'The Pesticide Manule.' 7th Edn. (British Crop Protection Council: Suffolk.)

Computation of hydraulic conductivity of porous materials using computer-assisted tomography

V. K. Phogat and L. A. G. Aylmore

Soil Science and Plant Nutrition, School of Agriculture,
The University of Western Australia, Nedlands, WA 6009.

Abstract

The spatial distribution of porosity and continuity of pore space in glass bead and soil aggregate systems has been characterised by application of computer-assisted tomography to gamma-ray attenuation measurements. It has been demonstrated that a useful empirical relationship between hydraulic conductivity and pore size and continuity for the glass bead system as measured by CAT scanning can be derived.

Additional keywords: permeability, pore continuity, computed tomography.

Introduction

Information on *in situ* and non-destructive measurements of the spatial, horizontal, and vertical distribution of soil pore systems is essential to an improved understanding of hydraulic processes, particularly hydraulic conductivity (K). Hydraulic conductivity is recognised as an important soil parameter for modelling the movement of both water (Philip 1969) and solutes (Bresler 1973) in soils and, in particular, for evaluating runoff and erosion as well as the soil water regime in relation to the potential for crop production (Bouma 1981; King and Franzmeier 1981; Topp and Davis 1981; McKeague *et al.* 1982). While there are several methods for determining hydraulic conductivity either in the laboratory (Gardner 1956; Nielsen and Biggar 1961) or in the field (Rose *et al.* 1965), considerable interest has also centred on the possibility of relating K in some functional way to other readily measurable properties of the soil, for example particle size and pore geometry involving total porosity, pore-size distribution, pore continuity, tortuosity, shape, and internal surface area (Carman 1939; Jacob 1946; Childs and Collis-George 1950; Franzini 1951; Marshall 1958; Scheidegger 1960; Millington and Quirk 1959, 1961, 1964).

One of the earliest and most widely used theories on the relation of permeability to the geometric properties of porous media was the Kozeny theory, and particularly its modification by Carman (1939). This theory is based on the concept that an average size of conducting tube can be obtained from the hydraulic radius (the ratio of the porosity, ϵ , in m^3/m^3 of soil to the surface area, S , of the particles in m^2/m^3 of the soil).

However, there are serious difficulties in applying the Kozeny-Carman equation to materials containing widely different pore sizes, especially when numerous small particles, which contribute largely to both the surface area and porosity, may act towards fluid flow as a single aggregate of much smaller external area. A

more profitable approach to the prediction of permeability from the basic physical properties of the porous medium is to seek a connection between permeability and pore-size distribution. With the development of suction and associated methods for measuring size distribution of pores (Richards 1949), Childs and Collis-George (1950) explored the possibility of using pore size instead of particle properties as the basis for a permeability expression. They proposed an approach wherein the flow through a porous medium is determined by the pore radii and by the probability of the continuity of pores of different radii in adjacent planes within the porous medium. Subsequently, Marshall (1958) developed an equation which is essentially similar to that of Childs and Collis-George (1950), where total pore space is divided into n equal volume fractions or pore classes, each containing pores of 1 mean radius, r_1, r_2, \dots and r_n , respectively, where $r_1 > r_2 > \dots > r_n$. The permeability is then given by

$$k = \left(\frac{1}{8}\epsilon^2/n^2\right)[r_1^2 + 3r_2^2 + 5r_3^2 + \dots + (2n-1)r_n^2] \quad (1)$$

where $\frac{1}{8}$ is the Poiseuille coefficient.

Thus, in theory permeability can be calculated from the curve relating water content to suction. Equation 1 is regarded as describing both the saturated and unsaturated permeability of porous materials. For calculation of unsaturated permeability, the value of ϵ adopted is that of the water-filled pore space and n remains constant. The r^2 series is commenced at the largest water-filled class. Generally a 'matching factor' (usually the ratio of measured to calculated hydraulic conductivity at saturation) is required in the Childs and Collis-George approach to compute values for unsaturated hydraulic conductivity. If instead of the matching factor, pore radii and the Poiseuille coefficient are used, the computation yields the same results as the method of Marshall (1958).

Millington and Quirk (1961) further developed and improved the theory proposed by Childs and Collis-George by considering both pore radius and effective area available for flow, and replacing ϵ^2 with $\epsilon^{4/3}$. Millington and Quirk were able to describe both saturated and unsaturated permeability of a variety of porous media with improved accuracy compared with the methods of Childs and Collis-George (1950) and Marshall (1958).

However, the equations used by these workers assume that (a) the porous medium is a symmetrical and isotropic material, and (b) the conducting pores are circular in cross section and are randomly dispersed throughout the material. The permeability is then calculated from the probability of continuity of pores of different radii in adjacent planes within the porous material. The criticisms of these assumptions are that the majority of soils never exhibit such properties, and if there is an equal probability of continuity of pores of different radii in adjacent planes, the field capacity in soils would never be reached. In addition, the pore size distribution required in the calculation of the permeability of porous media is generally determined from a water content-suction curve, which is not only time-consuming but also subject to significant sources of errors. For example, the clay within the rigid matrix of a sandy loam soil will change volume on wetting, altering the pore-size distribution and resulting in a defective prediction of permeability. However, the use of a 'formation factor' (Millington and Quirk 1964), which is related to the effective area and porosity, circumvents some of

these criticisms. Nevertheless, with existing knowledge and techniques, it is very difficult to compute the permeability of a soil from the characteristics of its pore system.

The recent development of CAT scanning (Aylmore 1993) and image analysis procedures, which enable the internal structure of solid objects to be characterised quantitatively in a continuous non-destructive manner, opens up exciting prospects for overcoming many of these difficulties and the possibility of studying the interrelation of structure and conductivity. The present research was carried out to investigate the relation between K and the spatial distribution of porosity within porous materials, and the possibility of computing K of porous materials from the spatial distribution and continuity of porosity within the material as obtained non-destructively by computer-assisted tomography (CAT) scanning of the columns containing the material.

Materials and methods

Computer-assisted tomography scanner

A prototype CAT scanning system constructed in the Soil Science and Plant Nutrition Laboratories of the University of Western Australia (Hainsworth and Aylmore 1988) was used for these studies. This scanner utilises a gamma source (1.85×10^{10} Bq of ^{137}Cs) which is monitored by a NaI (Tl) scintillation detector. The beam is collimated to give a slice thickness of 2 mm and pixel (picture element) size of 2 by 2 mm. As the source and detector are fixed, the object is moved across the beam and scanned at 2-mm intervals. Successive linear scans are made after rotating the object progressively in 5° increments through 180° . Once this process is completed, the linear scans are back-projected by using filtered back-projection (Herman 1980) for a given number of rotations to reconstruct an image of the scanned cross-sectional slice. Once the back projections have been completed, the gamma attenuation values for each pixel in the slice are determined.

The columns used

Columns (perspex) used in these studies were specially designed in order to allow the measurements of both K and the CAT scan data on the same column containing the porous material. The columns were 66 mm in height and of 54 mm internal diameter (i.d.), and had fine wire mesh on their perforated bases to hold the material. A perspex tube (10 mm i.d.) was attached horizontally between the perforated base and a solid 10-mm height bottom of each column to provide an outlet for water. The solid bases of the columns were designed to assist accurate positioning of the columns in the centre of the CAT scanner platform.

The porous materials used

The porous materials used in the study were glass beads and aggregates of surface (0–7 cm) soil collected from Kulin, Western Australia. Different-sized glass beads (0.176–0.249, 0.895–1.225, 1.225–1.390, 2.0, 3.0, 4.0, 5.0, and 6.0 mm) and the soil aggregates (0.5–1.0, 1.0–2.0, 2.0–2.8, 2.8–4.0, 4.0–4.75, and 4.75–6.30 mm) were packed into the specially designed perspex columns to a constant height. To determine the K value of the glass bead and soil aggregate samples, a constant head of water was maintained at the surface of each column by use of a Mariotte bottle. The volume of water flowing out of the columns with time was measured and a steady outflow of water was obtained. The K value was then calculated using the Darcy equation

$$q = V/At = K(\Delta H/L) \quad (2)$$

where q is the volume V of water flowing through a cross-sectional area A of the column per time t ; L is the length of the column, and ΔH is the hydraulic head difference between inflow and outflow boundaries of the column.

Special precautions were taken in the determination of the K value of the soil aggregates to ensure that there was no collapse of the aggregate structure. The soil aggregates in the columns were very slowly and carefully wetted under suction. When the aggregates were completely saturated, only a small constant head of water was maintained on the surface of the soil aggregates.

Prior to the determination of K for the bead and the aggregate samples, each column was scanned at 3 successive layers of 2 mm thickness each. Mean and standard deviation values of the gamma attenuation coefficient of pixels over the entire cross-sections of the scanned slices were determined. After calibrating the attenuation coefficients for glass bead samples with their known bulk densities, the porosity of individual pixels in the entire cross-sectional area of the scanned slices for glass bead samples was determined from the gamma attenuation coefficient of each pixel. The bulk density of a particular soil has been demonstrated to be essentially linearly related to attenuation. While the coefficient of this relationship is, in principle, different for different soils (different soils having different atomic compositions), in practice most soils tend to have the same coefficient. A comprehensive study of many soils packed to various bulk densities using different packing techniques and column sizes has shown a good, and potentially universal, linear relationship between bulk density and attenuation. In the present studies, the bulk densities of the columns containing soil aggregates ranged from 1110 kg/m^3 (0.5–1.0 mm aggregates) to 896 kg/m^3 (4.75–6.30 mm aggregates).

Results and discussion

The plots of the measured K values of the glass bead and soil aggregate samples against their size (Fig. 1) clearly illustrate that the K values of both materials are functionally related to the sizes of beads or aggregates in the samples. As expected, the K values of both materials increased with increase in the size of bead or soil aggregate. The functional relationships between K and the sizes of beads or aggregates are, however, different for each system. The porous structure of the soil aggregates, their irregular shapes, and the variation in aggregate size within each range used in the experiment, compared with the glass bead samples, are undoubtedly responsible for the differences between the two materials.

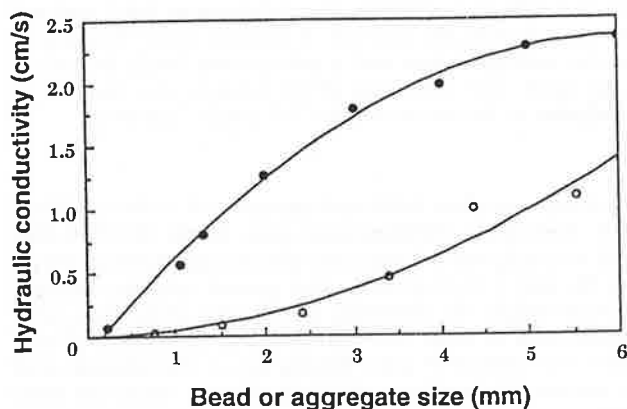


Fig. 1. Hydraulic conductivities of glass bead (●) and soil aggregate (○) samples *v.* size.

The K values of the materials plotted against the standard deviations of gamma attenuation coefficient of pixels within the scanned slices of the materials are shown in Fig. 2. Although the standard deviations of the attenuation coefficients of pixels for the glass bead samples were very small compared with those for the soil aggregate samples, the K values of the glass bead samples

varied markedly within this small range of standard deviation compared with those for the soil samples. The lower values of the standard deviations of pixel attenuation coefficients in the glass bead samples compared with the soil samples are due to the more even distribution of glass and pore space over the entire cross sections in the glass bead samples.

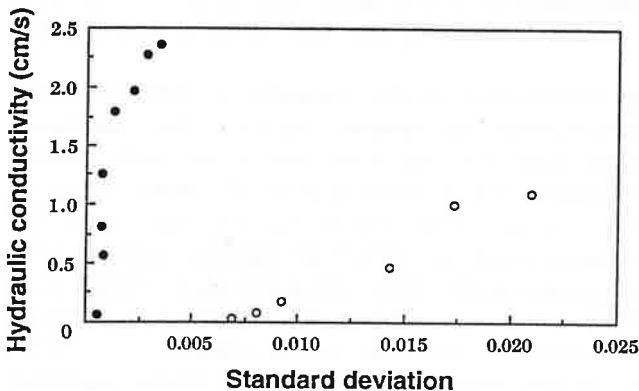


Fig. 2. Hydraulic conductivities *v.* standard deviations of pixel attenuation coefficients within scanned slices for glass bead (●) and soil aggregate (○) samples.

The standard deviation of pixel attenuation coefficients within the material is a measure of the extent of the spatial variability in the distribution of bulk density or porosity within the material (Phogat and Aylmore 1989). The K value of the porous material is, on the other hand, controlled by the spatial distribution of the various sizes of pores and their continuity within the material. According to Poiseuille's law, the volume flow rate through a cylindrical pore is proportional to the 4th power of the radius of the pore, and hence a slight increase in pore size can cause a large increase in the conductivity of the pore. Thus, there is unlikely to be any unique relationship between K and standard deviation. The CAT scanning procedure provides the spatial distribution of attenuation coefficient values and hence the spatial distribution of bulk density or porosity within the material. By using this technique, it is not, at present, possible to state that a particular porosity of a given pixel is due to the presence of a single large pore or a joint contribution of various pores of small sizes. However, this uncertainty may be improved by increasing the resolution of CAT scanning systems.

Although the pixel size of the system used in the study was relatively large (2 by 2 mm) for the purpose, an attempt was made to estimate the continuity of pixel porosity throughout the material. The contributions of the continuity of porosity between sequential pixels to the total flow of water per unit cross-sectional area of glass bead samples were established through an empirically developed relationship between the measured K value and the proportion of pixel area providing continuous porosity from one slice to the next over the entire cross-sectional area of flow for the glass bead samples. The soil aggregate samples were excluded for developing such relationships, as it was not possible to determine the exact porosity of pixels for soil aggregate samples in their wet or swollen state by using single source CAT scanning.

To determine the continuity of sequential pixel porosity, each pixel in the top slice scanned for the glass bead samples was matched with the adjacent pixel in

the next, lower slice. When the porosity of a pixel in the surface slice matched exactly with the porosity of the adjacent pixel in the next, lower slice of the material, the sequential pixel porosity was taken as 100% continuous. When the porosity of a pixel in the surface slice did not match exactly with the porosity of the adjacent pixel in the next, lower slice, the smaller porosity in either of the 2 pixels in sequence was taken as the proportion of continuous porosity. The spatial distribution of continuous pixel porosities thus obtained was used to represent the porosities of pixels controlling the flow of water through the material.

In order to determine the contribution of the porosities of different pixels towards the total flow of water through the samples, curves of the cumulative pore volume against continuous pixel porosity were plotted for each sample. Examples of such curves for the selected glass bead samples are shown in Fig. 3. Although based on a different concept, these curves resemble the curves for cumulative pore space plotted against pore size which are used in equation 1 for computing the permeability of porous media. The cumulative pore volume-pixel porosity curves were then divided into n equal porosity classes. The porosity class interval was 1%. This 1% porosity class interval was taken to account for the errors in the determination of the porosity of pixels due to random emission of the gamma radiation.

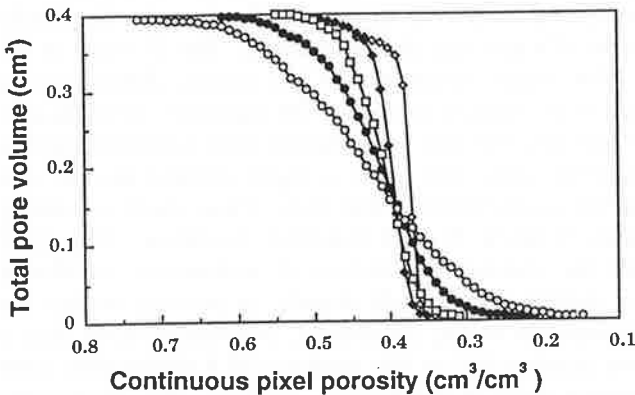


Fig. 3. Cumulative pore volume $v.$ pixel porosity curves for samples of different-sized glass beads: \diamond , 0.21 mm; \blacklozenge , 2.00 mm; \square , 3.00 mm; \bullet , 4.00 mm; \circ , 6.00 mm.

In an attempt to match the total contribution of the porosities of each class with the measured saturated K value of the sample, the following empirical relationship was obtained by iteration:

$$K_{\text{sat}} = N^{-1} \sum_{i=1}^n 2.685 \epsilon_i^{1.2} x_i \quad (3)$$

where K_{sat} is the saturated hydraulic conductivity (cm/s), ϵ_i is the porosity of the i th porosity class; x_i is the number of pixels in the i th porosity class, and N is the total number of pixels in the slice cross-section. The value 2.685 is a correlation factor (cm/s).

The measured K_{sat} and the K_{sat} values calculated using equation 3 for different-sized glass bead samples are shown in Fig. 4. These results suggest that

K_{sat} values of glass bead samples could be estimated with considerable accuracy if the continuity and the distribution of pixels having different porosities are known.

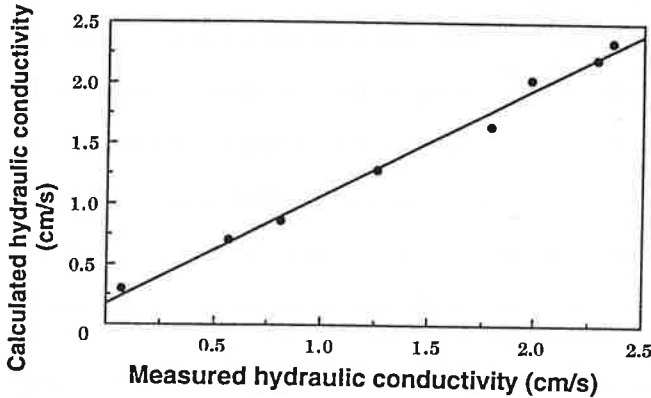


Fig. 4. Measured hydraulic conductivities *v.* hydraulic conductivities calculated using equation 3 for glass bead samples.

While this is only the first step towards obtaining relationships between CAT scanning data and hydraulic conductivity, and only data for the readily measured saturated hydraulic conductivity of materials of different aggregate size have been used here, the methodology should be equally applicable to measurements of the spatial distribution of cross-section for flow under unsaturated conditions. This is much more difficult to measure with the current limitations of CAT scanning to measure 3 phases in porous media (solid, liquid, air). The potential of improved dual energy gamma CAT scanning to handle swelling soils (Phogat *et al.* 1991), and 3-phase data, presents the exciting possibility of at last effectively undertaking studies of the relation between soil structural status and stability and changing hydraulic conductivity in unstable soils. Extensions of this approach using fractal dimensional and other image analysis techniques applied to CAT scanning data are being investigated.

Conclusions

While the present approach to estimating the continuity of pixel porosities and to computing the K values of porous materials using CAT scanning is clearly of limited value, the study indicates that by using CAT scanning it is possible to develop empirical relationships between K and the spatial distribution and continuity of porosity within porous materials. The validity of such relationships would, however, rely on extensive scanning of a wide range of porous materials using a high resolution CAT scanner and the development of more sophisticated approaches to estimate the continuity of porosities of pixels within the porous material.

Acknowledgments

V. K. Phogat is grateful to the Australian International Development Assistance Bureau for the award of a Commonwealth Scholarship and to Haryana Agricultural University, Hisar, India, for granting study leave. This work is supported by funding from the Australian Research Council.

References

- Aylmore, L. A. G. (1993). Use of computer-assisted tomography in studying water movement around plant roots. *Adv. Agron.* **49**, 1–54.
- Bouma, J. (1981). Soil survey interpretation: estimating use-potentials of a clay soil under various moisture regimes. *Geoderma* **26**, 165–77.
- Bresler, E. (1973). Simultaneous transport of solutes and water under transient unsaturated flow conditions. *Water Resour. Res.* **9**, 975–86.
- Carman, P. C. (1939). Permeability of saturated sands, soils and clays. *J. Agric. Sci.* **29**, 262–73.
- Childs, E. C., and Collis-George, N. (1950). The permeability of porous materials. *Proc. R. Soc. London A* **201**, 392–405.
- Franzini, J. B. (1951). Porosity factor for case of laminar flow through granular media. *Trans. Am. Geophys. Union* **32**, 443–6.
- Gardner, W. R. (1956). Calculation of capillary conductivity from pressure plate outflow data. *Soil Sci. Soc. Am. Proc.* **20**, 317–20.
- Hainsworth, J. M., and Aylmore, L. A. G. (1988). Application of computer assisted tomography (CAT) to gamma attenuation measurement of soil water content. *Aust. J. Soil Res.* **26**, 105–10.
- Herman, G. T. (1980). 'Image Reconstruction from Projections.' (Academic Press: New York.)
- Jacob, C. E. (1946). Radial flow in a leaky artesian aquifer. *Trans. Am. Geophys. Union* **27**, 198–208.
- King, J. J., and Franzmeier, D. P. (1981). Estimation of saturated hydraulic conductivity from soil morphology and genetic information. *Soil Sci. Soc. Am. J.* **45**, 1153–6.
- McKeague, J. A., Wang, C., and Topp, G. C. (1982). Estimating saturated hydraulic conductivity from soil morphology. *Soil Sci. Soc. Am. J.* **46**, 1239–44.
- Marshall, T. J. (1958). A relation between permeability and size distribution of pores. *J. Soil Sci.* **9**, 1–8.
- Millington, R. J., and Quirk, J. P. (1959). Permeability of porous media. *Nature* **183**, 387–8.
- Millington, R. J., and Quirk, J. P. (1961). Permeability of porous solids. *Trans. Faraday Soc.* **57**, 1200–7.
- Millington, R. J., and Quirk, J. P. (1964). Formation factor and permeability equations. *Nature* **202**, 143–5.
- Nielsen, D. R., and Biggar, J. W. (1961). Measuring capillary conductivity. *Soil Sci.* **92**, 192–3.
- Philip, J. R. (1969). Theory of infiltration. *Adv. Hydrosci.* **5**, 215–96.
- Phogat, V. K., and Aylmore, L. A. G. (1989) Evaluation of soil structural conditions by application of computer assisted tomography to gamma ray attenuation. *Aust. J. Soil Res.* **27**, 313–23.
- Phogat, V., Aylmore, L. A. G., and Schuller, R. (1991) Simultaneous measurement of the spatial distribution of soil water content and bulk density. *Soil Sci. Soc. Am. J.* **55**, 908–15.
- Richards, L. A. (1949). Methods of measuring soil moisture tension. *Soil Sci.* **68**, 95–112.
- Rose, C. W., Stern, W. R., and Drummond, J. E. (1965). Determination of hydraulic conductivity as a function of depth and water content for soil *in situ*. *Aust. J. Soil Res.* **3**, 1–9.
- Scheidegger, A. E. (1960). 'Physics of Flow through Porous Media.' (MacMillan: New York.)
- Topp, G. C., and Davis, J. L. (1981). Detecting infiltration of water through soil cracks by time-domain reflectometry. *Geoderma* **26**, 13–23.

The Importance of Soil Structure in the Management of Semi arid Lands of Western Australia.

L.A.G. AYLMORE* and H.R. COCHRANE

Abstract - Soils throughout much of the semi arid cropping and rangeland areas of Western Australia are poorly structured and highly susceptible to further structural degradation. Under inappropriate management, soil physical properties may deteriorate rapidly to the point where soils become incapable of supporting plant life under prevailing environmental conditions. Sustainable agricultural and pastoral land use in this area requires that maintenance of soil structure should be a major consideration. This paper examines some aspects of the physical properties of the region's soils that need to be taken into account in designing sustainable land management practices.

Key Words: Soil structure, Western Australia, Hardsetting, Compaction, Crusting.

1. Introduction

Western Australia covers just over 2.5 million km²; almost one third of the Australian continent. The majority of this area has an arid or semi-arid climate (Fig.1). The desert region (zone 6, fig.1) has a low, sporadic and unreliable rainfall and does not support agricultural production. The semi-arid rangelands (zone 3, fig.1) support a pastoral industry along with isolated, very small areas of horticultural production. Cleared land to the south and west of the rangelands, where mean annual rainfall exceeds approximately 275mm, is used for arable farming, predominantly cereal cropping combined with sheep production (zone 4, fig 1). In the semi arid agricultural and pastoral areas climate, particularly rainfall, is the major determinant of biological productivity but soil physical conditions also have a substantial influence on both native vegetation and the productivity of agricultural land. Poor soil structure constitutes the major limitation to plant growth on a significant proportion of this land and is thus also a major determinant of desertification processes in the region.

2. Soils

Soils throughout the area are predominantly highly weathered, have low nutrient status and poor physical properties, Sandy surfaced soils dominate but there is a great diversity of soil types; including deep sands, duplex soils which are dominant in the agricultural regions, and fine textured soils common in lower parts of the landscape. In the context of the region, soils are classed as being either coarse (sand to loamy sand) or fine textured (sandy loam to clay). Kaolinite and illite are the dominant clay minerals and their susceptibility to slaking, ready dispersivity and relatively small swell-shrink characteristics contribute to poor aggregate formation. The distribution of soils is poorly defined and for a large proportion of the area very little data is available on soil chemical or physical status, thus it is not possible to give accurate estimates of the areal extent of particular soil physical problems encountered in the region. Figure 1 indicates the distribution of dominant soil types along with their associated major degradation hazards.

3. Effects of land management practice on soil physical conditions.

The effect of agricultural and pastoral activities on soil physical fertility has generally been deleterious and in some cases catastrophic. Causes of soil structural degradation vary from loss of vegetative cover following overgrazing in pastoral areas, to excessive cultivation and traffic on agricultural land. Effects of inappropriate management range from complete removal of topsoil by wind or water erosion to the ubiquitous but less visually striking soil compaction and structural deterioration. Given the unreliability of rainfall and fragility of soils in the region, land use should be limited to activities that will maintain or improve soil physical, chemical and biological fertility. The impact of land management practices on soil physical properties is determined both by the disruptive forces imposed and by soil susceptibility to structural change. In turn susceptibility to structural change depends on inherent soil characteristics such as particle size distribution and the position of soil in the profile. The following is a brief account of some common soil physical problems known to affect land productivity in the region.

* Soil Science, The University of Western Australia, Nedlands 6907, W. Australia. (Fax +61-9-3801050).

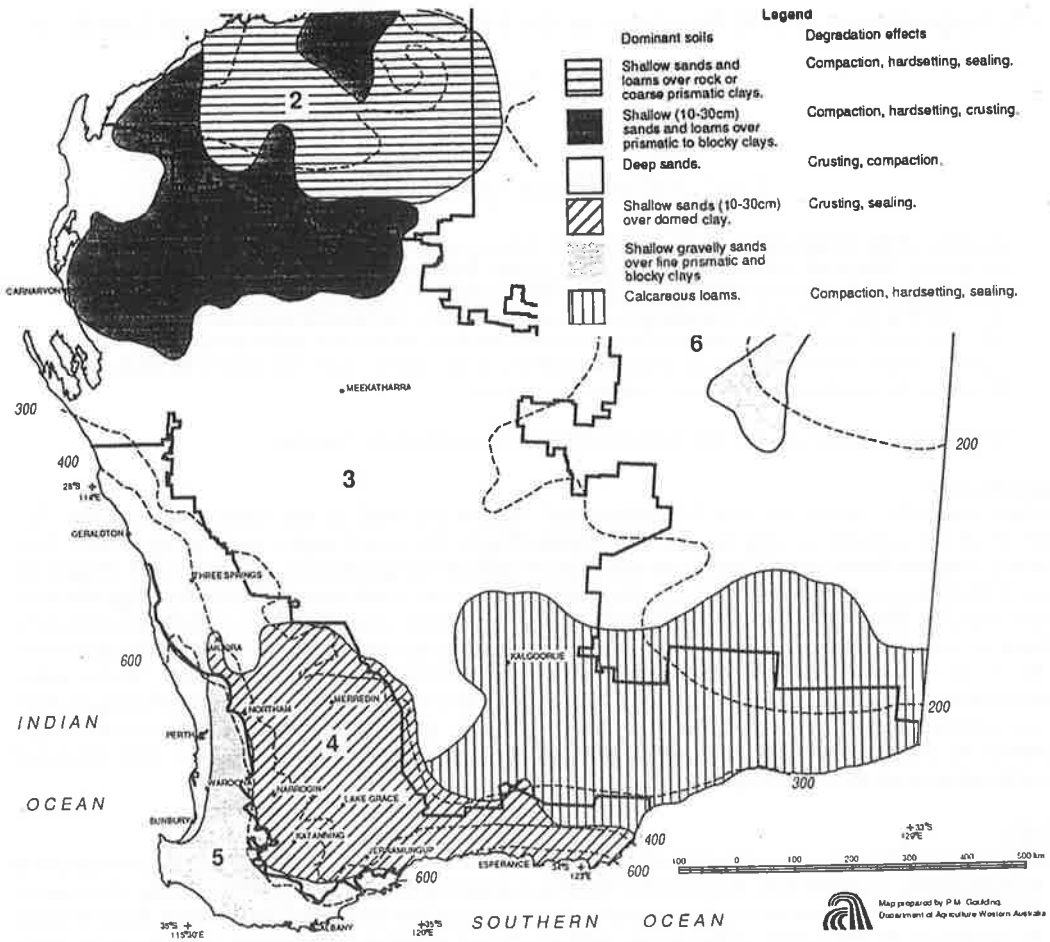


Figure 1. Soils and climatic zones in the south of Western Australia

4. Common Soil Physical Problems

4.1 Soil structural instability. The fine textured soils are most severely affected by structural instability. They were originally the most productive soils in the region, providing preferred grazing under pastoral management and being the first brought into cultivation following European settlement. Almost invariably soil structural quality has deteriorated since grazing or clearing and has been accompanied by a significant drop in soil organic matter content, especially in the surface soil. Fine textured surface soils of the region tend to become hardsetting as structure deteriorates under poor management. Characteristically hardsetting soils are apedal, have low permeability and bearing capacity when wet, and on drying develop sufficient strength to inhibit plant emergence and root growth. Soils of the region vary greatly in their potential to set hard depending on factors such as particle size composition, exchangeable and soluble cation composition and organic carbon (Aylmore and Sills 1982). The extent to which the potential for hardsetting is expressed depends on soil susceptibility to slaking and clay dispersion, factors which are influenced by the management regime imposed. Cochrane and Aylmore (1991) measured the impact of a range of management practices on the severity of hardsetting in agricultural soils. A sample of results obtained is illustrated in fig. 2. Figure 2a shows the effects of three levels of tillage intensity (3, 1 and 0 cultivations annually) and gypsum application on the structural stability of soil collected from a trial in its tenth season of continuous wheat production (gypsum was applied in the seventh season at 5 T ha⁻¹). Structural instability was assessed by modulus of rupture (MOR) measurements performed under conditions which allowed separate assessment of the contributions made by dispersion and slaking to

structural instability. The third component of structural instability shown (residual) is associated with inherent soil characteristics not dependant on soil management. Increasing MOR indicates decreasing structural stability.

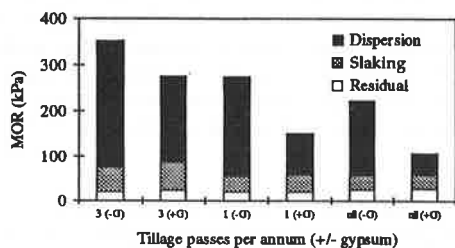


Fig 2a Stacking permitted

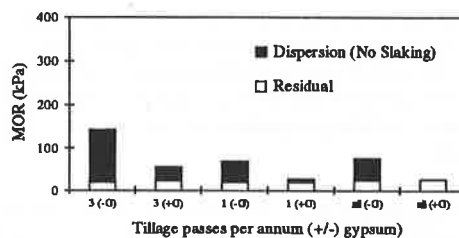


Fig 2b Stacking inhibited

Figure 2 Effects of tillage intensity and gypsum application on soil structural stability

As with most severely hardsetting soils, dispersive failure was the dominant mechanism contributing to structural instability. Increasing tillage intensity significantly increased dispersive failure and to a lesser extent slaking failure. Gypsum application reduced dispersive failure but had no significant impact on slaking. Although the slaking component of structural instability is small relative to dispersion the expression of dispersive failure is highly dependant on the severity of slaking, this is demonstrated in figure 2b which shows the level of dispersive failure when slaking is minimised in the same set of soils. Dispersive failure is reduced by a factor varying from 55% to 100% of the level found in soil tested under conditions which allow full expression of slaking. This analysis indicates that for these soils adoption of management practices that improve soil resistance to slaking (ie. reducing soil disturbance and improving soil organic matter content), have the potential to be as effective in ameliorating hardsetting as direct manipulation of dispersive failure through gypsum application.

Although hardsetting is probably more widespread in agricultural than in pastoral regions, farmers have a wide range of management options available (altering tillage and traffic intensity, rotation, amendment application, stubble and grazing management to suit soil conditions) to effect soil structural stabilisation.

The most severely hardsetting soils in the region have been found in the pastoral areas, on scalds created by overgrazing. Some soils attain tensile strengths twice as high as any encountered in the most degraded agricultural soils and are extremely sensitive to small changes in soil solution electrolyte concentration. Management options for structural amelioration on rangeland soils are limited to grazing control and a variety of soil preparation techniques suitable for initiating revegetation on small areas of degraded land.

4.2. Soil crusting Crusting occurs on arable clayey and loamy sands but neither the significance of the problem nor specific ameliorative practices have yet been investigated. Such crusting reduces rainfall acceptance and inhibits seedling emergence but is of minor significance in comparison with hardsetting. Much uncleared land throughout both agricultural and pastoral areas has a thin crusted surface layer. Surface sealing can occur quickly following rainfall or run-on, particularly on finer textured soils but the significance of these layers is unclear: Nulsen et.al. (1986) noted no runoff from an uncleared catchment within the agricultural area, although crusted soil within the catchment produced runoff at low rainfall intensities; water was redistributed and infiltrated elsewhere within the catchment.. Graetz and Tongway (1986) found cryptogam-soil surface crusts from semi arid rangeland sites in South Australia to be much less permeable than uncrusted soil at the same site but considered that the impermeability of these crusts was a desirable feature for the rangeland ecosystem as it facilitated concentration of water and nutrients at the soil surface where they would be most accessible to plant seedlings. If this is the case more generally throughout the region, management should aim to avoid destruction of these crusts.

4.3. Subsoil structural deterioration. There is virtually no information on the structural condition of subsoils in the rangelands. Fine textured subsoils in the agricultural areas however can exhibit very undesirable structural characteristics. Bulk densities in excess of 1.7 are common, the majority are sodic and have impermeable layers which cause temporary waterlogging, low water entry and storage and poor root penetration. Relative to topsoils, structural degradation in subsoils is an insidious process which is not only more difficult to detect but is much more difficult and expensive to remedy. The physical fertility of

many fine textured subsoils is dependant on structural features developed under native vegetation. These features include networks of cracks and channels created by numerous wet/dry cycles, plant root and soil faunal activity. Although there is evidence that subsoil structure was generally poor prior to grazing and clearing, agricultural and pastoral land management practices have undoubtedly caused further structural deterioration; resulting from loss of the perennial vegetation and soil faunal populations capable of creating and maintaining a continuous pore system. Under arable farming, and to a lesser extent under grazing, the rate at which continuous biopores and cracks are infilled by detached soil material probably exceeds the rate at which new structural pores are created. The interdependence of vegetation quality and soil physical fertility properties has not been fully appreciated in management systems imposed on these fragile soils.

4.4. Soil compaction. Compaction is an inevitable consequence of many agricultural and pastoral management practices. Sheep hooves exert considerable pressure capable of compressing surface soils and significantly reducing permeability and aggregate stability while increasing the mechanical impedance of fine textured soils of then region (Proffitt et al 1993).. Agricultural traffic causes compaction to a greater depth in the profile and many coarse textured soils are very susceptible to development of traffic induced hardpans with a maximum mechanical impedance at depths in the profile from 10 to 30 cm depending on particle size distribution and stresses imposed. For soils with little stable aggregation and low organic matter contents susceptibility to compaction can be predicted on the basis of primary particle size distribution. (Daniel et. al. 1992). Sandy soils with a well graded range of particle sizes, pack naturally to high densities and are easily further compressed by traffic. Mechanical ripping to disrupt hardpans has been used successfully on sand to loamy sands throughout the agricultural areas but on susceptible soils pans reform quickly if heavy vehicle traffic is not kept to a minimum

4.5. Soil erosion. Every conceivable form of soil erosion is represented in the region and significant land areas are affected. Wind erosion has removed the entire A horizon of some overgrazed rangeland soils, exposing massive, sodic B horizons incapable of supporting plant life. Revegetation of such areas is slow, expensive and uncertain of success, requiring extensive earthworks to improve water detention, and possibly chemical and/or physical amendments to overcome specific soil deficiencies. Water erosion can be equally devastating and land use planning on a catchment scale is required to minimise this hazard. Many soil, management and environmental factors combine to create an erosion risk. One particularly widespread condition which can predispose soil to both wind and water erosion is water repellence. This is caused by hydrophobic organic coatings on soil particles and the presence of fungal hyphae. Water repellent sands may shed a very high proportion of incident rainfall, creating a water erosion hazard and once cleared lack the cohesion and vegetative cover required to provide resistance to wind erosion.

5. Conclusion

Resistance to desertification processes in the semi arid regions of south western Australia is highly dependant on maintenance of adequate soil physical fertility. Soils of the region are structurally fragile and susceptible to a wide range of degradation hazards. Development of land management practices aimed at minimising the impact of these hazards requires improved knowledge of soil distribution, physical behaviour and improved techniques for assessing soil structural status and it's susceptibility to change.

Acknowledgment

We gratefully acknowledge the assistance of Dr. G. Scholz and Mr. Phil Goulding in preparing the map (figure 1)

References

- Aylmore, L.A.G. and Sills, I.D. (1982): *Aust. J. Soil Res.*, **20**: 213-224.
 Cochrane, H.R. and Aylmore, L.A.G. (1991): *Soil and Tillage Research*, **20**: 123-132.
 Daniel, H., Sawada, Y. and Aylmore, L.A.G. (1992): *Aust. J. Exp. Agric.*, **32**, 996.
 Graetz, R.D. and Tongway, D.J. (1986) *Australian Journal of Ecology* **11** 347-360
 Nulsen, R.A., Bligh, K.J., Baxter, I.N., Solin, E.J. and Imrie, D.H. (1986) *Aust. J. Ecol.* **11** 361-371.
 Proffitt, A.P. B., Bendotti, S. Howell, M.R. and Eastham, J. (1993) *Aust. J. Agric. Res.*, **44** 317-331.

Transformation and degradation of fenamiphos nematicide and its metabolites in soils

Rai S. Kookana^A, C. Phang^B, and L. A. G. Aylmore^B

^A Cooperative Research Centre for Soil and Land Management,
CSIRO Land and Water, PMB No. 2, Glen Osmond, SA 5064, Australia.

^B Soil Science and Plant Nutrition, University of WA, Nedlands, WA 6009, Australia.

Abstract

Fenamiphos is an important nematicide-insecticide and commonly used in horticultural crops and turfs in Australia. We studied the transformation/degradation of fenamiphos under controlled conditions, in surface and subsurface soils from the Swan Coastal Plain of Western Australia. In the sandy surface soil, fenamiphos (F_{en}) was rapidly oxidised to its sulfoxide ($F_{en}SO$) analogue. Further oxidation of $F_{en}SO$ to sulfone ($F_{en}SO_2$), however, was found to be very slow, resulting in an accumulation of $F_{en}SO$. Little accumulation of $F_{en}SO_2$ occurred during the study period (139 days). The time taken for 50% loss of the total residue of fenamiphos ($F_{en} + F_{en}SO + F_{en}SO_2$) was found to be approximately 50 days in the surface soil and about 140 days in the subsurface soil. Simulations using the LEACHM model showed that the rate of transformation of F_{en} to $F_{en}SO$ in the surface soil ($k_1 = 0.5/\text{day}$) was 100 times faster than that of $F_{en}SO$ to $F_{en}SO_2$ ($k_2 = 0.005/\text{day}$). In the subsurface soil, the difference between the 2 oxidation steps was much smaller (4-fold). The conversion of F_{en} to $F_{en}SO$ was much faster in the surface soil ($k_1 = 0.5/\text{day}$) than the subsurface soil ($k_1 = 0.02/\text{day}$). The observed differences in transformation behaviour of F_{en} between the surface and subsurface layers of soil appear to be associated with the differences in the microbial biomass and the organic matter contents of the soils. The slower transformation of F_{en} in the subsurface soils can have major implications on its potential for groundwater contamination in vulnerable areas, such as the Swan Coastal Plain of Western Australia.

Additional keywords: organophosphates, pesticide, oxidation, hydrolysis, LEACHM.

Introduction

Fenamiphos (ethyl 3-methyl-4-(methylthio)phenyl isopropyl phosphoramidate) is an important soil-applied nematicide-insecticide which is commonly used in horticultural soils, turfs, and bowling greens across Australia. To achieve effective pest control under horticultural crops, fenamiphos is often incorporated into the entire root-zone through irrigation or cultivation. Organophosphate pesticides such as fenamiphos are relatively short-lived, but they are more toxic to mammals than organochlorine pesticides (now mostly restricted). Since 1979, several studies in the USA have detected a number of pesticides in groundwaters (Ritter 1990; USEPA 1992). In recent years, pesticides have also been detected in Australian groundwaters (Bauld 1996). Consequently, the fate and behaviour of commonly used pesticides such as fenamiphos in Australian soils warrant urgent attention.

Several studies have been carried out overseas on fenamiphos degradation in soils and turfs (e.g. Ou and Rao 1986; Simon *et al.* 1992; Ou *et al.* 1994), and these show that fenamiphos (F_{en}), like some other pesticides such as aldicarb [2-Methyl-2-(methylthio) propionaldehyde *O*(methylcarbonyl)oxime] and phorate

[*O,O*-diethyl-*S*-([ethylthio]methyl)phosphorodithioate], possesses a thioether group and can undergo oxidation to produce sulfoxide ($F_{en}SO$) and then sulfone ($F_{en}SO_2$) metabolites. These daughter compounds are, in fact, more active than the parent compound in terms of their inhibition of acetylcholinesterase activity (Waggoner 1972). Therefore, during transformation the parent compound does not lose its nematicidal properties. The 2 metabolites $F_{en}SO$ and $F_{en}SO_2$ are, however, more polar, have lower sorption affinity to soil, and are therefore more mobile in the soil profile (Lee *et al.* 1986; Ou and Rao 1986). Data on F_{en} behaviour in Australian soils are very limited. Singh *et al.* (1990) studied the sorption of fenamiphos in 4 Western Australian soils. Recently, Kookana *et al.* (1995) studied the leaching and degradation behaviour of F_{en} in a sandy soil of the Swan Coastal Plain of Western Australia and found that fenamiphos was more mobile than several other pesticides under field conditions.

Due to the transformation and degradation pathways of pesticides such as aldicarb and fenamiphos, pesticide metabolites are receiving increasing attention for the assessment of the fate of pesticides in the environment. For example, the pesticide leaching model LEACHM (Hutson and Wagenet 1992) has a source/sink module which is based on the transformation/degradation pathways applicable to aldicarb and F_{en} in soils. While most studies on pesticide behaviour in the literature deal with the surface layer of the soil, for models such as LEACHM, the sorption and degradation parameters with depth are needed. Since the organic matter content and the microbial activity in soil generally vary markedly with depth, the pesticide behaviour in the subsurface soil is likely to be significantly different from that in the surface soil. This is particularly important for relatively mobile pesticides, such as F_{en} , which are also incorporated into the soil (Kookana and Aylmore 1994). We undertook this study to examine the transformation and degradation behaviour of F_{en} , $F_{en}SO$, and $F_{en}SO_2$ in a surface and subsurface soil, and to quantify the rate coefficients of the various transformation/degradation pathways of these compounds.

Materials and methods

Soils

Studies of fenamiphos degradation in the laboratory were carried out on a sandy soil (with no history of fenamiphos) collected from the Research Station at Medina, Western Australia. The soil collected from the site belongs to the Bassendean association (Bettenay *et al.* 1960), which covers nearly 50% of the area of the Swan Coastal Plain of Western Australia. A large area under Bassendean soils is used for irrigated horticulture (market gardens) where pesticides and fertilisers are frequently applied. These soils are highly permeable and are prone to leaching of contaminants to groundwater (Pionke *et al.* 1990). The soil at the Research Station is typically a Spodosol and consists of a uniform deep sandy profile; however, 2 visibly different soil layers are evident in the top 50 cm of the soil profile. A bleached surface layer of grey colour (0–25 cm), relatively richer in organic matter, and a yellowish subsurface soil (25–50 cm), relatively richer in iron oxides, were identified and used for these studies. The soil layers from 10 different profiles were composited to obtain a representative sample from an area of about 1 ha. Some soil characteristics are given in Table 1.

Pesticides

Fenamiphos (Nemacur) is a broad spectrum organophosphorus nematicide. Its molecular formula is $C_{13}H_{22}NO_3PS$ and molecular weight 303.40 g. The technical grade fenamiphos has a solubility of 700 mg/L at 20°C and is non-volatile with a vapour pressure of 0.133 Pa. It is sufficiently soluble to allow incorporation into the soil root-zone with irrigation water.

Table 1. Physio-chemical properties of soils used in the study

Soil layer	pH 1:5 (H ₂ O)	OC, organic carbon					
		OC (%)	Silt+ clay ² (%)	Surface area ^A (m ² /g)	Microbial biomass ^B (μg/g)	Mean respiration ^C (μg/g soil·h)	Moisture content ^D (cm ³ /cm ³)
Surface	5.3	0.53	1.0	0.36	196.0	0.058	0.051
Subsurface	5.5	0.02	1.0	1.51	60.9	0.089	0.024

^A Measured by N₂ adsorption using the BET isotherm.

^B At -10 kPa; measured by an assay based on ninhydrin-reactive nitrogen in fumigated soils (Amato and Ladd 1988).

^C Measured by trapping CO₂ produced in KOH and subsequent titration following the standard method.

^D At -10 kPa.

It is a cholinesterase inhibitor, with EPA Toxicity Class 1, ADI(man) 0.005 mg/kg (Hartley and Kidd 1991).

Laboratory incubation study

A solution of fenamiphos (Nemacur) was added to 1 kg of the freshly collected soil to produce a concentration of 10 mg a.i./kg at the moisture level corresponding to -10 kPa matric potential. The concentration of F_{en} was chosen on the basis of the recommended rate of application of 24 L/ha of Nemacur (a.i. 400 g/L) for some crops such as carrot and celery, in Western Australia. Although the concentration of F_{en} is likely to be lower than 10 mg/kg in the subsurface soil, the same concentration was used for comparison. Uniform mixing of the pesticide in the soil was achieved by spreading the soil on a plastic sheet and spraying it with fine droplets of the pesticide, followed by a thorough mixing. The treated soil was placed in loosely sealed polythene bags and incubated in the dark at 25°C, at field capacity (-10 kPa). A 50-g sample was removed in duplicate from each bag at 0, 4, 18, 39, 74, and 139 days for the surface soil, and 0, 3, 10, 31, 66, and 131 days for the subsurface soil. The soil moisture content was maintained during the experiment by weighing the bags regularly and replenishing the amount of water lost. The soils in the bags were frequently mixed thoroughly to ensure uniform conditions.

Extraction of compounds (F_{en}, F_{en}SO, and F_{en}SO₂) and their analysis

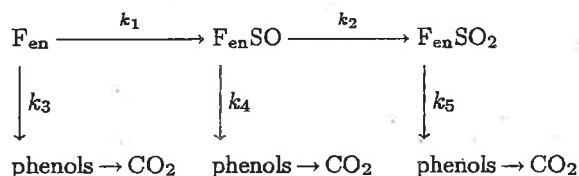
Technical grade samples of F_{en}, F_{en}SO, and F_{en}SO₂ were obtained from Bayer Australia Ltd (Botany, NSW) for the preparation of standards. HPLC grade acetonitrile and double-deionised water were used to prepare the extractant and the mobile phases. The soil samples were mixed thoroughly before the extraction of pesticide residues in organic solvent. Subsamples (5 g) of soils, were weighed (in duplicate) in centrifuge tubes and 10 mL of acetonitrile-water (90+10, v/v) extractant was added to the tubes. Recovery tests with the extractant showed >89% reproducible recovery for the 3 compounds in these soils. The soil and the extractant were shaken for 1 h (end-over-end) and the tubes were centrifuged (approximately 2000 G for 15 min) to obtain the supernatant. An aliquot of the supernatant solution was withdrawn and filtered through 0.22 μm GV Millipore filter paper using a syringe filled with a Swinnex-GS 25, 0.22 μm filter adaptor. The soils were subjected to a second extraction, by adding a further 10 mL of the extractant to the soil. This time the tubes were shaken continuously for 24 h followed by centrifugation and the withdrawal of the supernatant, as described above. The aliquots from the 2 extraction steps were mixed and a known volume was preconcentrated down to dryness, if needed, on a rotary evaporator before the residue was redissolved in 1 mL of the mobile phase for analysis.

The concentrations of pesticides in the solution were determined using HPLC by following the analytical method previously developed in our laboratory (Singh 1989). Briefly, the extract was analysed using a HPLC-UV detector and a reversed-phase C₁₈ column (μBondapak C₁₈ 10 μm 3.9 mm by 300 mm). Simultaneous determination of F_{en}SO and F_{en}SO₂ was

carried out using acetonitrile–water (54+46, v/v) as the mobile phase, wavelength 226 nm, injection volume 50 μ L, flow rate 1 mL/min, and ambient temperature $30 \pm 2.0^\circ\text{C}$. Retention times observed were 4.1 and 5.2 min for $F_{\text{en}}\text{SO}$ and $F_{\text{en}}\text{SO}_2$, respectively. Fenamiphos was eluted by using a mobile phase of acetonitrile–water (60+40, v/v), wavelength 248 nm, and other conditions were the same as for $F_{\text{en}}\text{SO}$ and $F_{\text{en}}\text{SO}_2$. The retention time under the above conditions was found to be 7.2 min. The calibration curves showed a linear response in the range of interest, as published by Singh (1989). Minimum detection limits of technical grade samples were 0.5 mg/L for F_{en} , and 0.2 mg/L for $F_{\text{en}}\text{SO}$ and $F_{\text{en}}\text{SO}_2$. The chromatographic conditions were chosen to give a good peak separation of the metabolites at a short elution time, as well as to avoid interfering peaks arising from the soil.

Simulations with LEACHM for quantisation of rate coefficients

As discussed above, F_{en} and other similar pesticides undergo oxidation to produce the sulfoxide and sulfone analogues. These oxidation products can simultaneously undergo hydrolysis and other degradation pathways. Lee *et al.* (1986) measured the F_{en} transformation/degradation in soils under field conditions and fitted the observed data to a model, in which degradation was assumed to occur by hydrolysis or ring cleavage of sulfone only. However, Ou and Rao (1986) found the presence of $F_{\text{en}}\text{SO}$ phenol in their study, which demonstrated that, besides undergoing oxidation, $F_{\text{en}}\text{SO}$ also undergoes hydrolysis. Recent work by Ou *et al.* (1994) further supports this. Consequently, the pathways of transformation/degradation of F_{en} are as follows:



where k_1 and k_2 represent oxidation rate coefficients, and k_3 , k_4 , and k_5 represent hydrolysis rate coefficients. This model is the basis of the source/sink module of LEACHP (Hutson and Wagenet 1992), which can handle up to 3 steps each of transformation (4 rate coefficients of transformation) and degradation of pesticides in soils. However, in the present study only 2 steps of oxidation and simultaneous degradation, as shown above, were used. The simulation of the F_{en} transformation/degradation was carried out under constant temperature and moisture conditions used in the study, and in the absence of flow. The calculations were made using 0.05 day as the largest computational time interval.

Results and discussion

Sulfoxidation of fenamiphos in surface and subsurface soils

Surface soil

The transformation and degradation of F_{en} and its 2 metabolites in the surface and subsurface soils are shown in Fig. 1a and b. In the surface soil, the parent compound F_{en} was rapidly converted to $F_{\text{en}}\text{SO}$. Indeed, the oxidation process was so fast that during the short time from sampling to analysis (<48 h) F_{en} had transformed into $F_{\text{en}}\text{SO}$, as indicated by the data for time zero in Fig. 1a. Within 3 days, approximately 85% of the applied F_{en} had undergone oxidation in the surface soil, producing mainly $F_{\text{en}}\text{SO}$. Oxidation of the remaining F_{en} appeared to be rather slow, as residual F_{en} was detectable even after 74 days. The oxidation of $F_{\text{en}}\text{SO}$ to $F_{\text{en}}\text{SO}_2$ was also slow, as indicated by the slower transformation of F_{en} and $F_{\text{en}}\text{SO}$. There was little accumulation of $F_{\text{en}}\text{SO}_2$ during the study period. The highest concentration of $F_{\text{en}}\text{SO}_2$ was in soil sampled at 139 days of incubation.

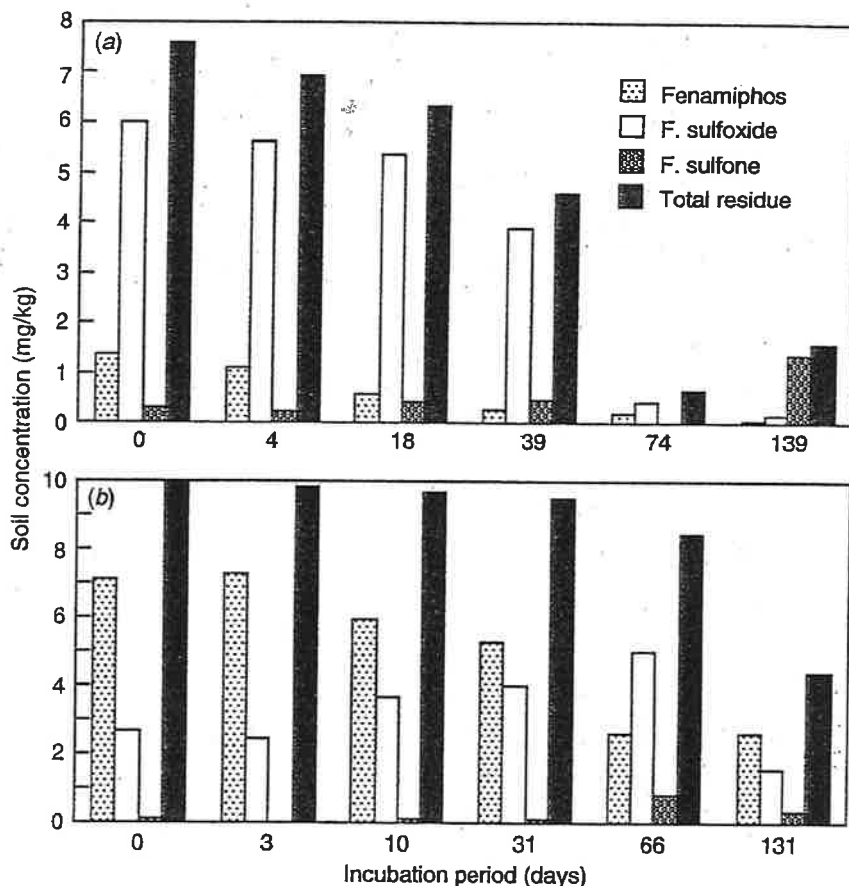


Fig. 1. Distribution of fenamiphos and its 2 metabolites in (a) the surface soil and (b) the subsurface soil. The total residue is the sum of the 3 products ($F_{en} + F_{en}SO + F_{en}SO_2$) present at any given time.

Subsurface soil

In the subsurface soil (Fig. 1b), the rate of F_{en} oxidation to $F_{en}SO$ was much slower than in the surface soil. After 3 days, only 25% of the parent compound had oxidised in the subsurface soil, which is only about one third of that observed in the surface layer. The concentration of $F_{en}SO$ increased gradually, and after 66 days of incubation, it exceeded that of F_{en} . Little $F_{en}SO_2$ was noted until 66 days. The loss of total residue ($F_{en} + F_{en}SO + F_{en}SO_2$) was minimal in subsurface soil, even after 31 days. At the end of experiment (131 days), about 50% of the total residue was still present in the subsurface soil.

The results obtained in this study are consistent with those observed by Ou and Rao (1986) in 3 surface soils from southeastern USA, and more recently by Ou *et al.* (1994) in turf soils. Ou and Rao (1986) observed that the half-life for F_{en} was <3 days, and in some cases, within 3 days >80% of F_{en} was oxidised to $F_{en}SO$. Similarly, Ou *et al.* (1994) noted that in a surface soil collected from the rough in a golf course, more than 90% of F_{en} was oxidised to $F_{en}SO$ within 3 days (first sampling).

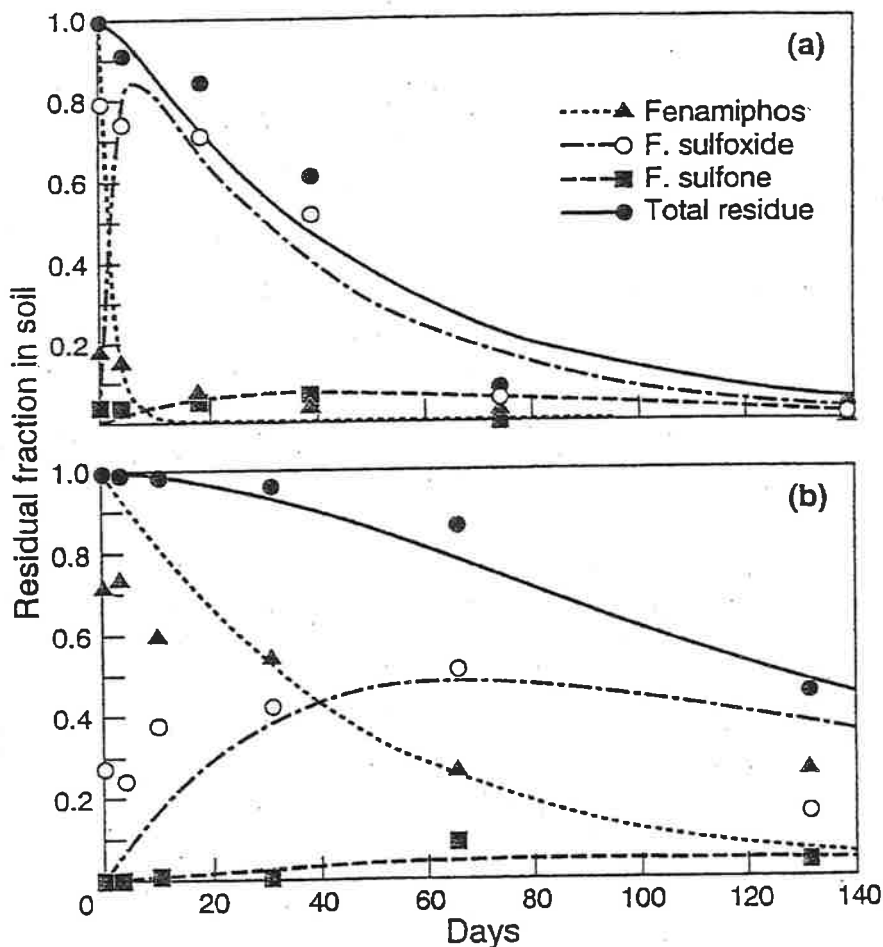


Fig. 2. Observed (data points) and simulated (lines) distributions of fenamiphos and its 2 oxidation products in (a) the surface soil and (b) the subsurface soil. The simulations were based on the pesticide degradation module of the LEACHM model, assuming constant moisture and temperature conditions. The fitted rate coefficients are given in Table 2. The total residue is the sum of the 3 products ($F_{en} + F_{enSO} + F_{enSO_2}$) present at any given time.

Quantification of transformation/degradation rates with LEACHM

The simulations carried out for F_{en} and the oxidation products for the surface and subsurface soils are presented in Fig. 2a and b. The model described the observed behaviour of the 3 compounds reasonably well for the surface soil. In the subsurface soil, however, there was considerable deviation between the observed and simulated values. This indicates that the assumption of first-order transformation and degradation is not valid for all pathways considered here, especially in the subsurface soil.

The rate coefficients fitted to the observed data are presented in Table 2. The results demonstrate that the sulfoxidation of F_{en} to F_{enSO} (k_1) is up to 2 orders

Table 2. Rate coefficients (per day) for sulfoxidation and degradation of fenamiphos, and its sulfoxide and sulfone

Soil	k_1	k_2	k_3	k_4	k_5
Surface	0.50	0.005	0.001	0.02	0.025
Subsurface	0.02	0.005	0.001	0.005	0.050

of magnitude faster than that of $F_{en}SO$ to $F_{en}SO_2$ (k_2) in the soils studied. Similarly, there was a 25-fold difference in the k_1 values between the surface and subsurface soils. While a major difference in the oxidation rate coefficients (k_1 and k_2) was noted, the variation among the degradation (hydrolysis) rate coefficients (k_3 , k_4 , k_5) was relatively smaller. The fitted values of the hydrolysis rate coefficients of the 3 compounds followed the order $F_{en} < F_{en}SO \leq F_{en}SO_2$.

From these data, it was not possible to calculate half-lives of fenamiphos, when represented as total residue ($F_{en} + F_{en}SO + F_{en}SO_2$), because the transformation/degradation did not follow a first-order reaction, especially in the subsurface soil. However, the time taken for a 50% loss of total residue of F_{en} in the surface soil was about 50 days, compared with about 140 days in the subsurface soil (Fig. 2a and b). A half-life of 50 days is listed in the database developed by Wauchope *et al.* (1992), which is a weighted value considering $F_{en}SO$ as a major metabolite of F_{en} , and most likely from surface soils of USA.

In a study by Pennell *et al.* (1990), the LEACHM model was found satisfactory to describe degradation data of aldicarb and its 2 oxidative metabolites (sulfoxide and sulfone) under field conditions. They used the oxidation and hydrolysis rate coefficients obtained from laboratory incubation data (Ou *et al.* 1988), which were generally well described by the first-order reactions. The differences between the rate coefficients k_1 and k_2 obtained by Ou *et al.* (1988) for aldicarb were of the same order as those observed in the present study for F_{en} . They also noted that oxidation and hydrolysis constants in the surface soils (0–30 cm) were higher than those in the subsurface soil (30–300 cm).

Possible role of microbial activity in F_{en} transformations/degradation

In the present study, the soil and environmental conditions during incubation, such as texture, pH, temperature, and moisture contents, were essentially the same for the 2 soils. However, the significant difference was in the organic matter content, microbial biomass, and microbial activity, indicated by the respiration rates (Table 1) in the soils. The microbial biomass in the surface soil was nearly 3 times greater than that in the subsurface soil. The association of the large difference in the rate of oxidation between the 2 soils with the differences in microbial activity in the 2 soil horizons indicates a possible role of microbial activity in the transformation reaction. This is also supported by Ou *et al.* (1988), who noted that the rapid oxidation and hydrolysis of aldicarb in surface soils were associated with high aerobic microbial activity. In their study, the microbial oxidation appeared to be the major route for aldicarb degradation up to a depth of 150 cm in the soil, below which chemical hydrolysis dominated. They also attributed the differences in aldicarb oxidation rates among different soils to the differences in microbial activity. Simon *et al.* (1992) observed a relationship

between the mineralisation rate of $F_{en}+F_{en}SO$ and microbial biomass expressed per unit organic carbon in soils. The highest rate of mineralisation was found in soils where conditions were favourable for microbial activity. However, there is no direct evidence of the role of microbial activity in the oxidation of either F_{en} or aldicarb in the above studies. According to Bollag and Liu (1990) 'oxidation of pesticides that occur frequently in microorganisms is one of the most important and basic metabolic reactions', and the sulfoxidation is one of the major reactions. However, it is often difficult to distinguish between biological and chemical oxidation of thioethers. For example, it has been observed for the fungicide carboxin (5,6-dihydro-2-methyl-*N*-phenyl-1,4-oxathiin-3-carboxamide) that while a fungus can cause its oxidation, the same reaction can also occur in a sterile, i.e. biologically inactive, soil (Bollag and Liu 1990). Further studies should be carried out to directly establish whether the oxidation reactions of these pesticides are microbially mediated.

The results presented above show that the degradation/transformation behaviour of F_{en} in subsurface soil can be markedly different to that observed in the surface soil. Therefore, the degradation half-lives of pesticides based on surface soils (available in current databases) are unlikely to yield an adequate assessment of their environmental fate, especially the movement through the soil profile to groundwater. Given that the metabolites of fenamiphos are toxic, provide the pest control, and have different persistence and mobility than the parent compound, their monitoring and appropriate management is crucial to minimise their non-target impacts. A further complicating factor in the case of fenamiphos, as well as for several other compounds, is the enhanced degradation following their repeated use (e.g. Ou *et al.* 1994). Evidence from Australia also shows that F_{en} , the only registered nematicide for turfgrass in Australia, is giving erratic efficacy because of the enhanced degradation in intensively managed turfs (Beehag 1995). Clearly, in the process of the development of best management practices for pesticides such as F_{en} , the factors such as the history of their use, their mobility in the soil profile, and interactions with soil and environmental conditions deserve an adequate consideration.

Acknowledgments

These studies were partly funded by the Land and Water Resources Research and Development Corporation of Australia. We wish to thank Dr Robert Gerritse, CSIRO Land and Water, for the contribution in the early phase of this study, and Mr Kelvin Webb for carrying out biomass and respiration tests on the soils.

References

- Amato, M., and Ladd, J. N. (1988). Assay for microbial biomass based on ninhydrin reactive nitrogen in extracts of fumigated soils. *Soil Biology and Biochemistry* 20, 107-14.
- Bauld, J. (1996). Groundwater quality: Human impact on a hidden resource. Proc. Hydrology and Water Resources Symp. on 'Water and the Environment'. Hobart, 1996. pp. 143-7.
- Beehag, G. (1995). Nematicur—could the turfgrass industry manage without it? *Turf Craft* July 1995, 74-7.
- Bettenay, E., McArthur, W. M., and Hingston, F. J. (1960). Soil associations of the Swan Coastal Plain, WA. CSIRO Aust., Soils and Land Use Series No 35.
- Bollag, J. M., and Liu, S. Y. (1990). Biological transformation processes of pesticides. In 'Pesticides in the Soil Environment: Processes, Impacts and Modelling'. (Ed. H. H. Cheng.) pp. 169-211. (Soil Science Society of America; Madison, WI.)

- Hartley, D., and Kidd, H. (1991). 'The Agrochemicals Handbook.' (The Royal Society of Chemistry, The University of Nottingham: Nottingham, UK.)
- Hutson, J. L., and Wagenet, R. J. (1992). 'LEACHM, Leaching Estimation and Chemistry Model: A Process-based Model of Water and Solute Movement, Transformations, Plant Uptake and Chemical Reactions in the Unsaturated Zone.' Version 3. Department of Soil, Crop and Atmospheric Sciences Research Series No. 92-3. (Cornell University: Ithaca, NY.)
- Kookana, R. S., and Aylmore, L. A. G. (1994). Estimating the pollution potential of pesticides to ground water. *Australian Journal of Soil Research* **32**, 1141-55.
- Kookana, R. S., Di, H. J., and Aylmore, L. A. G. (1995). A field study of leaching and degradation of nine pesticides in a sandy soil. *Australian Journal of Soil Research* **33**, 1019-30.
- Lee, C. C., Green, R., and Apt, W. J. (1986). Transformation and adsorption of Fenamiphos, F. sulfoxide and F. sulfone in Molokai soil and simulated movement with irrigation. *Journal of Contaminant Hydrology* **1**, 211-25.
- Ou, L-T., and Rao, P. S. C. (1986). Degradation and metabolism of oxamyl and phenamiphos in soils. *Journal of Environmental Science and Health B* **21**, 25-40.
- Ou, L-T., Rao, P. S. C., Edvardsson, K. S. V., Jessup, R. E., Hornsby, A. G., and Jones, R. L. (1988). Aldicarb degradation in sandy soils from different depths. *Pesticide Science* **23**, 1-12.
- Ou, L-T., Thomas, J. E., and Dickson, D. W. (1994). Degradation of fenamiphos in soil with a history of continuous fenamiphos application. *Soil Science Society America Journal* **58**, 1139-47.
- Pennell, K. D., Hornsby, A. G., Jessup, R. E., and Rao, P. S. C. (1990). Evaluation of five simulation models for predicting aldicarb and bromide behaviour under field conditions. *Water Resources Research* **26**, 2679-93.
- Pionke, H. B., Sharma, M. L., and Hosking, J. A. (1990). Horticultural cropping effects on groundwater quality in the Swan Coastal Plain. CSIRO Aust. Division of Water Resources Series No. 2.
- Ritter, W. F. (1990). Pesticide contamination of ground water in the United States—A review. *Journal of Environmental Science and Health B* **25**, 1-29.
- Simon, L., Spittler, M., Haisch, A., and Wallnofer, P. R. (1992). Influence of soil properties on the degradation of the nematocide fenamiphos. *Soil Biology and Biochemistry* **24**, 769-73.
- Singh, R. (1989). Simultaneous determination of fenamiphos, its sulfoxide and sulfone in water by high-performance liquid chromatography. *Analyst* **114**, 425-7.
- Singh, R., Gerritse, R. G., and Aylmore, L. A. G. (1990). Adsorption-desorption of selected pesticides in some Western Australian soils. *Australian Journal of Soil Research* **28**, 227-43.
- USEPA (1992). Another look: National survey of pesticides in drinking water wells. Phase II report. US Environmental Protection Agency EPA 579/09-91-020, Washington DC.
- Waggoner, T. B. (1972). Metabolism of nemacur (ethyl 4-(methylthio)-m tolyl isopropylphosphoramidate) and identification of two metabolites in plants. *Journal of Agricultural and Food Chemistry* **20**, 157-60.
- Wauchope, R. D., Buttler, T. M., Hornsby, A. G., Augustijn-Beckers, P. M. W., and Burt, J. P. (1992). The SCS/ARS/CES pesticide properties database for environmental decision-making. *Reviews of Environmental Contamination and Toxicology* **123**, 1-164.

Modeling the Probabilities of Groundwater Contamination by Pesticides

H. J. Di and L. A. G. Aylmore*

ABSTRACT

Field soils show significant spatial variations in properties, such as organic matter content, bulk density, and moisture content, that can affect the mobility and persistence and thus fate of organic pesticides in the soil environment. A simple model incorporating the variations in soil and pesticide parameters has been developed to assess the groundwater contamination potential of pesticides. The model is based on linear, equilibrium, and reversible sorption, first-order degradation, and steady piston flow, and allows the unsaturated soil zone to be divided into a number of layers of different thickness and properties. For each input parameter, 500 random data were generated from normal distributions that characterize the variability of the parameters. The fate of 29 pesticides were assessed using soil and environmental conditions of the Swan Coastal Plains of Western Australia and pesticide properties reported in the literature. The predicted pesticide residue fractions remaining at 150-, 300-, and 500-cm depths were described by beta distributions, and the corresponding travel times by normal distributions. Fourteen out of the 29 pesticides are predicted to reach 150 and 300 cm and 13 are predicted to reach the 500-cm depth with mean residue fractions $\geq 0.01\%$. The predicted mean travel times for pesticides that may reach 300 cm vary from about 2 mo to about 18 yr. Significant standard deviations are associated with these mean residue fractions and travel times. Six pesticides, fenamiphos, simazine, metribuzin, linuron, fenarimol, and metalaxyl, have been identified as having high cumulative probabilities of 0.82 to 1.00 for residue concentrations to be $>0.01\%$ at the 300-cm depth.

THE USE OF PESTICIDES (including herbicides, fungicides, and insecticides) has become an integral part of modern agriculture and horticulture for the efficient production of quality food and fiber. There is increasing evidence, however, that pesticide residues from these non-point sources have the potential to contaminate groundwater (U.S. Environmental Protection Agency, 1977, 1978; Cohen et al., 1986; Beitz et al., 1994). In many parts of the world groundwater is making up increasing proportions of water supplies for human consumption. In Perth, Western Australia, for instance, nearly 50% of the water supply is from groundwater and this figure is increasing. The use of pesticides thus needs to be regulated to protect the aquifer from contamination.

The potential of pesticides to contaminate groundwater depends on a number of soil and pesticide properties that directly or indirectly affect the mobility and persistence of the pesticides in the soil environment. While a number of studies have been carried out in attempts to understand the behavior and fate of pesticides in soils (e.g., Singh

et al., 1989; Pennel et al., 1990; Kookana et al., 1992a,b; Green et al., 1995), the high expenses of these studies combined with the large number of pesticides make it prohibitive to study every pesticide under various soil and environmental conditions. Increasingly scientists and environmental managers use computer models to study the complex pesticide processes in soils and to provide management guidance (e.g., Nicholls et al., 1982; Jury et al., 1987; Hutson and Wagenet, 1992, 1993; Mullins et al., 1993).

The choice of models is determined not only by the objectives, but also by the availability of data that are required by the models. There are significant differences in input data demand between models due to their differences in formulation. For purposes of screening or general management guidance, the use of simpler models with less data demand, such as those of Rao et al. (1985), Nofziger and Hornsby (1986), Jury et al. (1987), and Di et al. (1995) is justified.

One of the limitations with these models, however, is that they do not provide any information on uncertainties of modeling outcomes associated with variations in input soil and pesticide parameters. Regulatory decisions may be required regarding the use of pesticides for a region (e.g., a catchment, a farm, or a particular type of land use area), which may be significantly heterogeneous or variable in soil properties. Spatial variations of soil properties can have a significant impact on the movement and fate of pesticides in the soil environment (Biggar and Nielsen, 1976). Under these circumstances, quantitative information of uncertainties associated with modeling predictions would be particularly useful for the decision-making process regarding pesticide uses. Recent efforts have therefore been made to quantify the uncertainties in regional modeling predictions by using soil data bases collected from national or local soil surveys and Monte Carlo simulations (Oliver and Laskowski, 1986; Carsel et al., 1988; Loague et al., 1989, 1990; Petach et al., 1991; Fousserau et al., 1993; National Research Council, 1993).

In Western Australia, the Swan Coastal Plains are vulnerable to groundwater contamination by pesticides because the soils are sandy, with a low capacity to retain pesticide residues, and pesticides are extensively used in the region for horticultural production. We used a simple model to assess the groundwater contamination potential of 29 pesticides used in the region, taking into account variations in input soil and pesticide data. Random data were generated from distributions characterizing the variations of input parameters; these were fed into the simulation model, and the outputs were statistically analyzed. The soil and environmental condi-

Soil Science and Plant Nutrition, Univ. of Western Australia, Nedlands, WA 6907, Australia. Received 14 Nov. 1995. *Corresponding author (aylmore@uniwa.uwa.edu.au).

tions used were based on those of the local Swan Coastal Plains of Western Australia.

MODELING METHOD

Description of Model

A simple model was formulated to calculate the fraction of pesticide remaining and travel time as the pesticide leaches deeper in the soil profile, based on the following assumptions (Rao et al., 1985; Jury et al., 1987).

1. Pesticide sorption is linear, at equilibrium, and reversible:

$$C_s = K_D C_L = f_{oc} K_{oc} C_L \quad [1]$$

where C_s is sorbed pesticide concentration, K_D is the linear sorption coefficient, C_L is pesticide concentration in the soil solution, f_{oc} is weight fraction of soil organic C, and K_{oc} is the sorption coefficient normalized by soil organic C fraction:

$$K_{oc} = K_D / f_{oc} \quad [2]$$

2. The pesticide undergoes first-order degradation in soil, and the fraction of pesticide remaining undegraded (F) as it leaches in the soil is

$$F = \exp(-kt) = \exp(-0.693t/t_{1/2}) \quad [3]$$

where k is the degradation rate constant, t is time, and $t_{1/2}$ is degradation half-life.

3. The pesticide leaches by steady piston water flow (ignoring diffusion and dispersion), and the effective pesticide leaching velocity is

$$V = q / (\rho_b f_{oc} K_{oc} + \theta) \quad [4]$$

where q is steady recharge rate, ρ_b is soil dry bulk density, and θ is soil moisture content, which was assumed to equal field capacity.

The unsaturated soil zone may be divided into N layers with different thickness (Δz) and with different soil properties. Time (t) required for the pesticide to travel to the bottom of layer N is:

$$t = \sum_{i=1}^N [\Delta z (\rho_b f_{oc} K_{oc} + \theta) / q]_i \quad [5]$$

where i indicates different layers. The fraction of pesticide remaining (F) as the moving pulse reaches the bottom of layer N is

$$F = \prod_{i=1}^N \exp[-\Delta z (\rho_b f_{oc} K_{oc} + \theta) 0.693 / (qt_{1/2})]_i \quad [6]$$

Input Data

To calculate the fractions of pesticide remaining as the pesticide pulse travels down the soil profile and the corresponding travel times using Eq. [6] and [5], respectively, the following parameters are required: soil bulk density, organic C fraction, moisture content at field capacity, pesticide sorption coefficient, and pesticide degradation half-life for each different

Table 1. Soil properties used for modeling. These properties are based on local soil surveys on the Swan Coastal Plains of Western Australia.

Depth	Bulk density†	Field capacity†	Organic C†
cm	g cm ⁻³	%	
0-25	1.4	10.0	1.0
25-50	1.5	6.0	0.5
50-500	1.5	4.0	0.05

† These are mean values. The coefficients of variation are 7-14% for bulk density, 13-50% for field capacity, and 10-50% for organic C content.

soil layer, and average recharge rate. For Monte Carlo simulation, the means and standard deviations of these parameters (except the recharge rate) are required. The soil parameters were obtained from reports of soil surveys conducted on the Swan Coastal Plains of Western Australia, and from more detailed studies on local experimental research stations (Table 1). These properties represent those of major sandy soils that are used for horticultural production. The recharge rate used was equivalent to 800 mm rainfall per year.

Twenty-nine pesticides were assessed (Table 2). These pesticides are the more commonly used ones in the horticultural production systems on the coastal plains of Western Australia. The mean values of sorption coefficients (K_{oc}) and degradation half-lives ($t_{1/2}$) were mainly from the literature (Wauchope et al., 1992) with a few determined under local conditions (Kookana et al., 1995). The sorption coefficient and half-life of each pesticide vary significantly with environmental and soil conditions (Rao and Davidson, 1980; Singh et al., 1989). In this study, arbitrary standard deviations equivalent to a 30% coefficient of variation for K_{oc} and 50% for half-life were used. These variations are somewhat less than those reported by Rao and Davidson (1980) on the consideration that the soils in this region might not be as diverse as those referenced by Rao and Davidson (1980), which were from a wide range of sources and geographical areas. Degradation half-lives were assumed to increase by 125% from the top layer (0-25 cm) to the second layer (25-50 cm), and by 150% in the third layer (50-500 cm) compared with the top layer. This was

Table 2. Pesticide sorption coefficients and degradation half-lives.

Pesticides†	$K_{oc}‡$	Half-life (0-25 cm)‡
		d
	Insecticides	
Chlorpyrifos	6 070	81
Cyfluthrin	100 000	30
Dicofol	180 000	60
Dimethoate	20	7
Endosulfan	12 400	50
Fenamiphos	100	43
Fenvalerate	5 300	35
Malathion	1 800	1
Methamidophos	5	6
Methiocarb	300	3
Methomyl	72	30
Mevinphos	44	3
Permethrin	100 000	30
	Fungicides	
Benomyl	1 900	240
Chlorothalonil	1 380	30
Fenarimol	600	360
Iprodione	700	14
Metalaxyl	50	70
Thiram	670	30
	Herbicides	
Chlorthal-dimethyl	5 000	45
Linuron	400	219
Methazole	3 000	14
Metolachlor	200	90
Metribuzin	60	40
Prometryne	400	60
Propyzamide	243	59
Simazine	130	60
Trifluralin	8 000	60

† Chemical names for the compounds may be found in Tomlin (1994).

‡ The mean values listed here are mostly from Wauchope et al. (1993); some half-life values are from Kookana et al. (1995). The sorption coefficient normalized by the soil organic C fraction (K_{oc}) values are assumed to have standard deviations equivalent to a 30% coefficient of variation; the half-lives are assumed to increase by 125% in the layer 25-50 cm from the surface layer (0-25 cm), and by 150% in the layer 50-500 cm. The standard deviations in the three layers, from top to bottom, give 50, 30, and 20% coefficients of variation, respectively.

based on the assumption that soil conditions (e.g., microbial population, temperature, and aeration status) become less favorable for degradation with increasing depth. Other parameters also changed with depth as shown in Table 1.

Modeling Procedure

Random values of the parameters required by the calculations were generated from probability distributions as specified by the means (μ) and standard deviations (σ), assuming normal distributions with the probability density function being

$$f(x) = \frac{1}{\sigma\sqrt{2\pi}} e^{-(x-\mu)^2/(2\sigma^2)} \quad [7]$$

Although some properties might deviate somewhat from a normal distribution, they were approximated as a normal distribution. This was considered acceptable in view of the objectives of the study, and of the fact that there were in some cases insufficient data for a distribution assessment. All the parameters have specified lower and upper bounds, and values drawn beyond these bounds were rejected.

Computations were carried out for t (travel time) and F (fraction of pesticide remaining) for three different depths, 150, 300, and 500 cm, to accommodate variations of water table in the Swan Coastal Plains region.

Analysis of Output

Probability density functions of computed fractions of pesticides remaining and travel times were analyzed and calculations were made for the means, standard deviations, standard errors of means, cumulative probabilities for pesticides reaching the three depths at fractions $>0.01\%$, and the 95th percentiles of travel times. The value of 0.01% is regarded as a threshold value below which the fraction of pesticide remaining becomes insignificant (Jury et al., 1987). The 95th percentile indicates that 95% of the travel times will be less than this value.

RESULTS AND DISCUSSION

Figures 1 and 2 show the frequency distributions of pesticide fractions remaining and travel times, respectively, using metalaxyl as an example; similar distributions are found with the other pesticides. Most distributions for travel time are near normal (Eq. [7]) with slight positive skewness. They were approximated as normal distributions. The frequency distributions of residue fractions for all the pesticides, however, show significant positive skewness, with the peak frequency toward the lower bound of 0 (Fig. 1). These distributions were described by beta distribution functions (Benjamin and Cornell, 1970). Beta distribution is characterized by two shape parameters, a and b , with values of the variable ranging from 0 to 1, as a fraction of the pesticide remaining in the soil profile:

$$f(x) = \frac{\Gamma(a+b)}{\Gamma(a)\Gamma(b)} x^{a-1} (1-x)^{b-1} \quad 0 \leq x \leq 1 \quad [8]$$

Judged by the mean residue percentage, 14 pesticides out of the 29 studied will leach beyond 300 cm with values $\geq 0.01\%$, and 13 pesticides will reach beyond 500 cm (Tables 3-5). The other pesticides will be degraded to insignificant concentrations before reaching these depths. As expected, the residue fraction values are smaller at

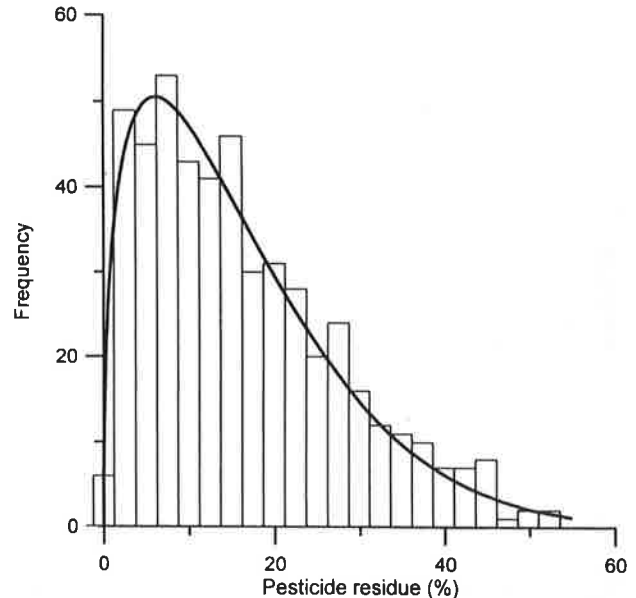


Fig. 1. Frequency distribution of predicted metalaxyl residue fractions at 300 cm. A beta distribution function was used to describe the distribution. Similar patterns of distribution are found with the other pesticides and at 150 and 500 cm.

the greater depths. Although the standard errors of the means are small, due to the large number of random data generated (500), significant amounts of variation are expected for the residue values greater than $>0.01\%$, as shown by the standard deviations.

Because of the variations in pesticide residue fractions, the cumulative probability values (for residue fractions $\geq 0.01\%$) provide a better indication of groundwater contamination potential than the mean values alone. The changes in cumulative probabilities with pesticide residue concentrations at the three soil profile depths are shown

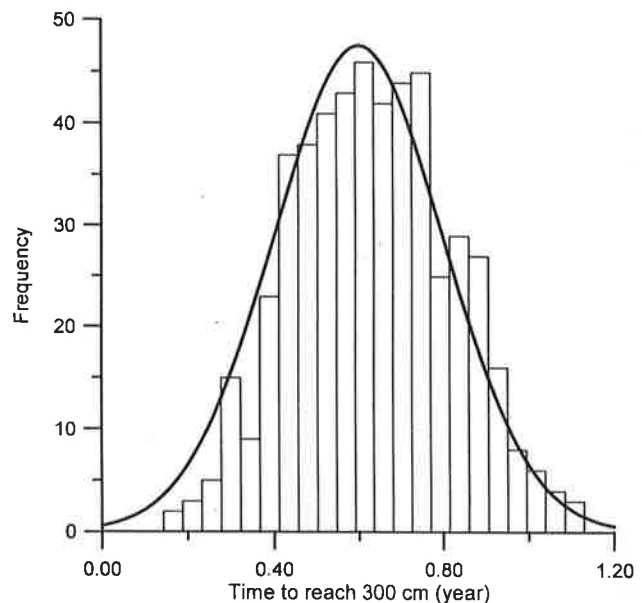


Fig. 2. Frequency distribution of predicted metalaxyl travel times to 300 cm. A normal distribution function was used to describe the distribution. Similar distributions are found with the other pesticides and at 150 and 500 cm.

Table 3. Predicted pesticide residue fractions and travel times at 150-cm depth.

Pesticides	Residue at 150 cm (beta distribution)				Time to reach 150 cm (normal distribution)			
	Mean	STD†	SEM†	P(>0.01%)†	Mean	STD	SEM	95th P.†
	%				yr			
Dicofol	0.00	0.00	0.00	0.00	1443.4	624.9	27.9	2470.0
Cyfluthrin	0.00	0.00	0.00	0.00	787.7	336.7	15.1	1340.0
Permethrin	0.00	0.00	0.00	0.00	773.3	341.1	15.3	1330.0
Endosulfan	0.00	0.00	0.00	0.00	96.4	40.1	1.8	162.4
Trifluralin	0.00	0.00	0.00	0.00	62.9	18.6	0.8	93.5
Chlorpyrifos	0.00	0.00	0.00	0.00	47.7	20.8	0.9	81.9
Fenvalerate	0.00	0.00	0.00	0.00	42.5	18.1	0.8	72.3
Chlorthal-dimethyl	0.00	0.00	0.00	0.00	39.6	17.3	0.8	68.1
Methazole	0.00	0.00	0.00	0.00	24.1	10.2	0.5	40.9
Malathion	0.00	0.00	0.00	0.00	14.5	6.1	0.3	24.5
Chlorothalonil	0.00	0.00	0.00	0.00	10.9	4.9	0.2	19.0
Iprodione	0.00	0.00	0.00	0.00	5.5	2.3	0.1	9.3
Thiram	0.00	0.00	0.00	0.00	5.4	2.2	0.1	9.0
Mevinphos	0.00	0.00	0.00	0.00	0.4	0.1	0.01	0.6
Methiocarb	0.06	0.54	0.02	0.06	2.5	1.0	0.05	4.1
Benomyl	0.15	0.84	0.04	0.16	15.0	6.7	0.3	26.0
Dimethoate	0.28	0.80	0.04	0.45	0.3	0.1	0.0	0.4
Prometryne	0.37	2.81	0.13	0.10	3.3	1.5	0.1	5.8
Propyzamide	1.04	3.13	0.14	0.47	2.0	0.8	0.04	3.3
Methamidophos	1.29	1.74	0.08	0.94	0.1	0.03	0.0	0.2
Methomyl	2.51	5.36	0.24	0.72	0.7	0.2	0.01	1.0
Fenamiphos	3.36	5.41	0.24	0.89	0.9	0.3	0.01	1.4
Simazine	4.09	6.50	0.29	0.90	1.1	0.4	0.02	1.8
Metolachlor	4.37	7.25	0.32	0.88	1.7	0.7	0.03	2.9
Metribuzin	6.60	7.75	0.35	0.99	0.6	0.2	0.01	0.9
Linuron	6.64	9.44	0.42	0.94	3.3	1.4	0.1	5.6
Fenarimol	8.56	10.6	0.47	0.98	4.8	1.9	0.1	7.9
Metalaxyl	22.3	15.2	0.68	1.00	0.5	0.2	0.01	0.8

† STD = standard deviation; SEM = standard error of mean; P(>0.01%) = cumulative probability that pesticide residue fraction is >0.01%; 95th P. = the 95th percentile, indicating 95% of the travel times will be less than this.

in Fig. 3, using metalaxyl as an example. Although methiocarb, benomyl, and prometryne have mean residue values >0.01% at 300 cm (Table 4), their cumulative probabilities for residue fraction $\geq 0.01\%$ are rather

small, indicating an overall low potential of groundwater contamination. The cumulative probabilities for fenamiphos, simazine, metribuzin, linuron, fenarimol, and metalaxyl are >0.80, indicating high potential for

Table 4. Predicted pesticide residue fractions and travel times at 300 cm.

Pesticides	Residue at 300 cm (beta distribution)				Time to reach 300 cm (normal distribution)			
	Mean	STD†	SEM†	P(>0.01%)†	Mean	STD	SEM	95th P.†
	%				yr			
Dicofol	0.00	0.00	0.00	0.00	1700.7	686.4	30.7	2830.0
Cyfluthrin	0.00	0.00	0.00	0.00	928.1	367.1	16.4	1530.0
Permethrin	0.00	0.00	0.00	0.00	912.2	374	16.7	1530.0
Endosulfan	0.00	0.00	0.00	0.00	113.7	43.8	2.0	185.7
Trifluralin	0.00	0.00	0.00	0.00	74.3	18.9	0.8	105
Chlorpyrifos	0.00	0.00	0.00	0.00	56.2	22.7	1.0	93.5
Fenvalerate	0.00	0.00	0.00	0.00	50.2	19.9	0.9	82.9
Chlorthal-dimethyl	0.00	0.00	0.00	0.00	46.6	19.0	0.8	77.9
Methazole	0.00	0.00	0.00	0.00	28.4	11.2	0.5	46.8
Malathion	0.00	0.00	0.00	0.00	17.1	6.7	0.3	28.1
Chlorothalonil	0.00	0.00	0.00	0.00	12.9	5.4	0.2	21.8
Iprodione	0.00	0.00	0.00	0.00	6.6	2.5	0.1	10.7
Thiram	0.00	0.00	0.00	0.00	6.4	2.4	0.1	10.3
Mevinphos	0.00	0.00	0.00	0.00	0.6	0.2	0.01	0.9
Methiocarb	0.02	0.22	0.01	0.04	3.0	1.1	0.05	4.8
Dimethoate	0.04	0.12	0.01	0.29	0.4	0.1	0.0	0.5
Benomyl	0.07	0.52	0.02	0.09	17.7	7.3	0.3	29.7
Methamidophos	0.17	0.32	0.01	0.65	0.2	0.03	0.3	0.3
Prometryne	0.20	1.95	0.09	0.06	3.9	1.6	0.07	6.5
Propyzamide	0.48	1.67	0.07	0.37	2.4	0.9	0.04	3.9
Methomyl	1.16	3.10	0.14	0.56	0.8	0.3	0.01	1.3
Fenamiphos	1.74	3.17	0.14	0.82	1.1	0.4	0.02	1.8
Simazine	2.28	4.09	0.18	0.84	1.4	0.5	0.02	2.2
Metolachlor	2.58	5.01	0.22	0.78	2.0	0.8	0.03	3.3
Metribuzin	3.58	4.71	0.21	0.96	0.7	0.2	0.01	1.0
Linuron	4.47	7.19	0.32	0.90	4.0	1.5	0.1	6.5
Fenarimol	5.96	8.09	0.36	0.96	5.7	2.1	0.1	9.2
Metalaxyl	15.91	11.6	0.52	1.00	0.6	0.2	0.01	0.9

† STD = standard deviation; SEM = standard error of mean; P(>0.01%) = cumulative probability that pesticide residue fraction is >0.01%; 95th P. = the 95th percentile, indicating 95% of the travel times will be less than this.

Table 5. Predicted pesticide residue fractions and travel times at 500 cm.

	Residue at 500 cm (beta distribution)				Time to reach 500 cm (normal distribution)			
	Mean	STD†	SEM†	P(>0.01%)†	Mean	STD	SEM	95th P.†
	%				yr			
Dicofol	0.00	0.00	0.00	0.00	2043.8	775.4	34.7	3320
Cyfluthrin	0.00	0.00	0.00	0.00	1115.3	411.3	18.4	1790
Permethrin	0.00	0.00	0.00	0.00	1097.3	421.8	18.9	1790
Endosulfan	0.00	0.00	0.00	0.00	136.7	49.1	2.2	217.5
Trifluralin	0.00	0.00	0.00	0.00	89.3	19.4	0.9	57.4
Chlorpyrifos	0.00	0.00	0.00	0.00	67.5	25.4	1.1	109.3
Fenvalerate	0.00	0.00	0.00	0.00	60.4	22.5	1.0	97.4
Chlorthal-dimethyl	0.00	0.00	0.00	0.00	56.1	21.3	1.0	91.1
Methazole	0.00	0.00	0.00	0.00	34.2	12.7	0.6	13.3
Malathion	0.00	0.00	0.00	0.00	20.6	7.6	0.3	33.1
Chlorothalbnil	0.00	0.00	0.00	0.00	15.6	6.0	0.3	25.5
Iprodione	0.00	0.00	0.00	0.00	8.0	2.9	0.1	12.8
Thiram	0.00	0.00	0.00	0.00	7.8	2.7	0.1	12.2
Mevinphos	0.00	0.00	0.00	0.00	0.8	0.2	0.01	1.1
Dimethoate	0.00	0.00	0.00	0.00	0.5	0.1	0.004	0.6
Methiocarb	0.01	0.08	0.00	0.00	3.6	1.3	0.06	5.7
Methamidoptus	0.02	0.05	0.00	0.29	0.3	0.04	0.002	0.4
Benomyl	0.03	0.32	0.01	0.04	21.4	8.2	0.4	34.9
Prometryne	0.10	1.23	0.06	0.04	4.8	1.8	0.1	7.8
Propyzamide	0.19	0.78	0.03	0.26	2.9	1.0	0.05	4.5
Methomyl	0.46	1.63	0.07	0.46	1.1	0.3	0.01	1.6
Fenamiphos	0.77	1.68	0.08	0.67	1.36	0.41	0.02	2.0
Simazine	1.11	2.40	0.11	0.69	1.7	0.5	0.02	2.5
Metolachlor	1.34	3.38	0.15	0.60	2.5	0.9	0.04	4.0
Metribuzin	1.66	2.60	0.12	0.89	0.9	0.3	0.01	1.4
Linuron	2.74	5.22	0.23	0.80	4.9	1.7	0.1	7.7
Fenarimol	3.81	5.89	0.26	0.91	6.9	2.4	0.1	10.8
Metalaxyl	10.3	8.24	0.37	1.00	0.8	0.2	0.01	1.1

† STD = standard deviation; SEM = standard error of mean; P(>0.01%) = cumulative probability that pesticide residue fraction is >0.01%; 95th P. = the 95th percentile, indicating 95% of the travel times will be less than this.

groundwater contamination beyond 300 cm. The probabilities of metalaxyl being <0.01% at all three depths are clearly minimal (Fig. 3). Therefore, there is a very high probability that metalaxyl will leach beyond the specified depths at significantly higher concentrations. As expected, the cumulative probabilities for pesticide residues to exceed 0.01% (Tables 3-5) or to exceed other percentages (Fig. 3) decrease with increasing depth.

There is little data available in Western Australia on the presence and concentrations of pesticides in local groundwaters, as monitoring programs are only just starting. Those pesticides that have been identified in this study as having high probabilities of groundwater contamination certainly deserve particular attention in these

monitoring programs. Some of these pesticides have, however, already been detected in groundwater and drinking water surveys in the USA and Europe (Beitz et al., 1994).

The mean travel times to the depth of 150 cm range from just over a month to more than 1400 yr (Table 3). The mean travel times and cumulative probabilities for exceeding certain travel times increase with increasing depth (Tables 3-5, Fig. 4). Many of the pesticides, however, will not reach the specified depths before they are degraded to insignificant concentrations, as shown by the 0 mean residue concentrations and low probabilities of exceeding 0.01% (Tables 3-5). While many of the

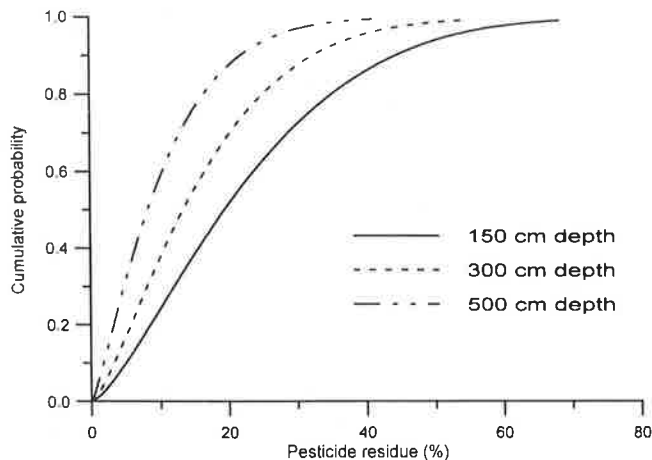


Fig. 3. Cumulative probability distributions of residue fractions at 150, 300, and 500 cm, using metalaxyl as an example.

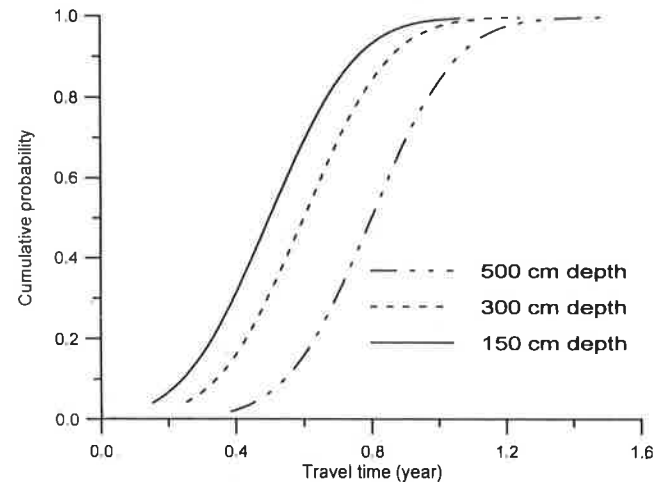


Fig. 4. Cumulative probability distributions of travel times to 150, 300, and 500 cm, using metalaxyl as an example.

pesticides with higher potential for groundwater contamination have shorter travel times, pesticides such as linuron and fenarimol are noticeable for their fairly long mean travel times of about 5 and 7 yr to reach 500 cm (Table 5). Because of the variations in the input modeling parameters, the travel times also show significant variation as shown by the standard deviations (Tables 3-5), and the 95th percentiles are significantly greater than the respective mean travel times.

This study shows that because of field variations in soil properties and related pesticide properties, the residue fractions of pesticides at specified depths and the corresponding travel times will also vary significantly (as indicated by the significant standard deviations). The groundwater contamination potential of pesticides for a region can be assessed by examining the probability distributions of predicted pesticide residue fractions, and the uncertainties associated with the predictions can be quantitatively analyzed. This approach is advantageous over the method of using a single value for each model parameter, which does not provide any information about prediction uncertainties. The magnitudes of variations associated with predictions will depend on the variabilities in input parameters. Detailed knowledge of soil properties in the region of interest will improve the representation of probability distributions of relevant soil properties, as will locally measured pesticide sorption and degradation properties.

For management purposes, the model can be coupled with a geographic information system to present the results in a map form (Loague et al., 1990; Petach et al., 1991; Fousseureau et al., 1993). For each region on the map (e.g., a soil mapping unit, a farm, a type of land use area, a catchment), means and standard deviations of the relevant soil and pesticide parameters are needed for the simulation. It must be noted that some parameters may not be normally distributed, and the right distribution, if known, should naturally be used. However, the use of normal distributions may be justified for management purposes when there are insufficient data available.

It must be noted that the model used in this study is based on simplified processes of pesticide transport, degradation, and sorption, some of which may not be valid under realistic field conditions. The advantage of this simple model over more complex ones, e.g., LEACHM (Hutson and Wagenet, 1992), is that it requires less input data and computing time, and can still provide useful information for management decision purposes. The model is also flexible in that it allows the soil profile to be divided into soil layers of any thickness instead of fixed equal increments (cf. Nofziger and Hornsby, 1986; Fousseureau et al., 1993), and it allows all the soil and pesticide parameters, rather than just some of the parameters, to vary spatially (cf. Jury et al., 1987; Petach et al., 1991; Fousseureau et al., 1993). This flexibility is important as many of the soil data from soil surveys are for soil layers with contrasting pedological features, with both the thickness and properties varying widely. Although Monte Carlo simulation requires probability distribution parameters of soil and pesticide properties, which may be estimated from soil

survey data and pesticide studies reported in the literature, it does not require a predefined probability density function of solute travel time or distance, which is required by stochastic transfer function models (Jury, 1982).

ACKNOWLEDGMENTS

Funding of the project by the Australian Land and Water Resources Research and Development Corporation is gratefully acknowledged.

REFERENCES

- Beitz, H., H. Schmidt, and F. Herzel. 1994. Occurrence, toxicological and ecotoxicological significance of pesticides in groundwater and surface water. p. 1-56. *In* H. Börner (ed.) Pesticides in groundwater and surface water. Chemistry of plant protection 9. Springer-Verlag, Berlin.
- Benjamin, J.R., and C.A. Cornell. 1970. Probability, statistics and decision for civil engineers. McGraw-Hill, New York.
- Biggar, J.W., and D.R. Nielsen. 1976. Spatial variability of the leaching characteristics of a field soil. *Water Resour. Res.* 12:78-84.
- Carsel, R.F., R.S. Parrish, R.L. Jones, J.L. Hansen, and R.L. Lamb. 1988. Characterizing the uncertainty of pesticide leaching in agricultural soils. *J. Contam. Hydrol.* 2:111-124.
- Cohen, S.Z., C. Eiden, and M.N. Lorber. 1986. Monitoring ground water for pesticides. *ACS Symp. Ser.* 315:170-196.
- Di, H.J., R.S. Kookana, and L.A.G. Aylmore. 1995. Application of a simple model to assess the groundwater contamination potential of pesticides. *Aust. J. Soil Res.* 33:1031-1040.
- Fousseureau, X., A.G. Hornsby, and R.B. Brown. 1993. Accounting for variability within map units when linking a pesticide fate model to soil survey. *Geoderma* 60:257-276.
- Green, J.D., R. Horton, and J.L. Baker. 1995. Crop residue effects on the leaching of surface-applied chemicals. *J. Environ. Qual.* 24:343-351.
- Hutson, J.L., and R.J. Wagenet. 1992. Leaching estimation and chemistry model, a process-based model of water and solute movement, transformation, plant uptake and chemical reactions in the unsaturated zone, Version 3. Dep. of Soil, Crop and Atmospheric Sci. Res. Ser. 92-3. Cornell Univ., Ithaca, NY.
- Hutson, J.L., and R.J. Wagenet. 1993. A pragmatic field-scale approach for modeling pesticides. *J. Environ. Qual.* 22:494-499.
- Jury, W.A. 1982. Simulation of solute transport using a transfer function model. *Water Resour. Res.* 18:363-368.
- Jury, W.A., D.D. Focht, and W.J. Farmer. 1987. Evaluation of pesticide groundwater pollution potential from standard indices of soil-chemical adsorption and biodegradation. *J. Environ. Qual.* 16: 422-428.
- Kookana, R.S., L.A.G. Aylmore, and R.G. Gerritse. 1992a. Time dependent sorption of pesticide during transport in soils. *Soil Sci.* 154:214-225.
- Kookana, R.S., H.J. Di, and L.A.G. Aylmore. 1995. A field study of leaching and degradation of nine pesticides in a sandy soil. *Aust. J. Soil Res.* 33:1019-1030.
- Kookana, R.S., R.G. Gerritse, and L.A.G. Aylmore. 1992b. A method for studying nonequilibrium sorption during transport of pesticides in soil. *Soil Sci.* 154:344-349.
- Loague, K.M., R.E. Green, T.W. Giambelluca, T.C. Liang, and R.S. Yost. 1990. Impact of uncertainty in soil, climate, and chemical information in a pesticide leaching assessment. *J. Contam. Hydrol.* 5:171-194.
- Loague, K.M., R.S. Yost, R.E. Green, and T.C. Liang. 1989. Uncertainty in a pesticide leaching assessment for Hawaii. *J. Contam. Hydrol.* 4:139-161.
- Mullins, J.A., R.F. Carsel, J.E. Scarbrough, and A.M. Ivery. 1993. PRZM-2, a model for predicting pesticides fate in the crop root and unsaturated soil zones: Users manual for release 2.0. USEPA, Athens, GA.
- National Research Council. 1993. Ground water vulnerability assessment: predicting relative contamination potential under conditions of uncertainty. *Natl. Acad. Press*, Washington, DC.

- Nicholls, P.H., A. Walker, and R.J. Baker. 1982. Measurement and simulation of the movement and degradation of atrazine and metribuzin in a fallow soil. *Pestic. Sci.* 12:484-494.
- Nofziger, D.L., and A.G. Hornsby. 1986. A microcomputer-based management tool for chemical movement in soil. *Appl. Agric. Res.* 1:50-56.
- Oliver, G.R., and D.A. Laskowski. 1986. Development of environmental scenarios for modeling the fate of agricultural chemicals in soil. *Environ. Toxicol. Chem.* 5:225-231.
- Pennell, K.D., A.G. Hornsby, R.E. Jessup, and P.S.C. Rao. 1990. Evaluation of five simulation models for predicting aldicarb and bromide behavior under field conditions. *Water Resour. Res.* 26:2679-2693.
- Petach, M.C., R.J. Wagenet, and S.D. DeGloria. 1991. Regional water flow and pesticide leaching using simulations with spatially distributed data. *Geoderma* 48:245-269.
- Rao, P.S.C., and J.M. Davidson. 1980. Estimation of pesticide retention and transformation parameters required in nonpoint source pollution models. p. 23-67. *In* M.R. Overcash and J.M. Davidson (ed.) *Environmental impact of nonpoint source pollution*. Ann Arbor Sci. Publ., Ann Arbor, MI.
- Rao, P.S.C., A.G. Hornsby, and R.E. Jessup. 1985. Indices for ranking the potential for pesticides contamination of groundwater. *Proc. Soil Crop Sci. Soc. Fla.* 44:1-8.
- Singh, R., R.G. Gerritse, and L.A.G. Aylmore. 1989. Adsorption-desorption behaviour of selected pesticides in some Western Australian soils. *Aust. J. Soil Res.* 28:227-243.
- Tomlin, C. 1994. *The pesticide manual, incorporating the agrochemicals handbook*. 10th ed. British Crop Protection Council, Surrey, UK.
- U.S. Environmental Protection Agency. 1977. *Waste disposal practices and their effects on groundwater*. Report to Congress. USEPA, Washington, DC.
- U.S. Environmental Protection Agency. 1978. *Surface impoundments and their effects on groundwater quality in the US—A preliminary survey*. EPA/9-78-004. USEPA, Washington, DC.
- Wauchope, R.D., T.M. Buttler, A.G. Hornsby, P.M.W. Augustijn-Beckers, and J.P. Burt. 1992. The SCS/ARS/CES pesticide properties database for environmental decision-making. *Rev. Environ. Contam. Toxicol.* 123:1-164.

CHARACTERIZING THE CHANGES IN SOIL POROSITY BY COMPUTED TOMOGRAPHY AND FRACTAL DIMENSION

V. Rasiah and L. A. G. Aylmore

Information in regard to nondestructive and repetitive measurements of changes in soil porosity (ϵ) that may occur during wetting and drying is limited, particularly information regarding changes on a very small scale. The objectives of this study were (i) to determine whether the changes in ϵ that may occur during wetting and drying at scales as small as 2×2 mm can be discriminated by computer-assisted tomography and (ii) to use a published theoretical equation to estimate surface fractal dimension (D) from ϵ and to determine whether D is sensitive to wetting and drying. Computer-assisted tomography was applied to gamma-ray attenuation to measure dry bulk density (ρ), before and after wetting, at 2×2 -mm resolution of water-stable soil aggregates (WSA) 2 to 4, 0.71 to 1.40, and 0.25 to 0.71 mm in size and packed separately in acrylic cylinders. Columns with similar particle size were also prepared for unstable soil aggregates (USA). Before wetting, ϵ computed from ρ in WSA, ranged from 0.621 to 0.740; after wetting the range was 0.604 to 0.709. In USA, ϵ ranged from 0.489 to 0.562 before wetting and from 0.457 to 0.516 after wetting. The lack of a 1:1 relationship between the before and after wetting data for ϵ indicated there were significant differences between the two. Initial aggregate size (x), wetting, (w), and the interaction $w \times x$ accounted for 74% of the variability in ϵ of USA compared with only 47% of the variability for WSA. The estimates of D , obtained using the theoretical equation and ϵ , ranged from 2.154 to 2.236 for WSA and from 2.055 to 2.12 for USA. Wetting, x , and $w \times x$ accounted for 47% of the variability in D of USA compared with 69% for WSA. Pore continuity (PC), estimated using a theoretical relation involving PC, ϵ , and D , decreased from 0.45 to 0.30 after wetting in USA and from 0.60 to 0.55 in WSA.

Key words: Hydraulic conductivity, porosity, computed tomography, fractal dimension.

THE changes in porosity (ϵ) that may occur on a very small scale during wetting and drying of unstable soils or during compaction can have a significant impact on transport and biological processes in soil (Cornish and Lymbery 1987; Jakobsen and Dexter 1987; Masle and Farquhar 1988; McFarlane and Davies 1985, unpublished information). Using the existing conventional experimental techniques, it is difficult, if not impossible, to measure the changes in ϵ in a nondestructive

and repetitive manner, particularly at very small scale.

The application of computer-assisted tomography (CAT) to X- and gamma-ray attenuations has been shown to be very useful for nondestructive, three-dimensional imaging of solid matrices (Hounsfield 1972). The X-ray CAT scanning technique has been used successfully to characterize bulk density (ρ) in soil columns at resolutions as small as 2×2 mm (Petrovic et al. 1982; Grevers et al. 1989; Warner et al. 1989; Anderson et al. 1990). However, the equipment and operational costs involved with X-ray scanning are generally too high for soil scientists. Consequently, attempts have been made to develop less expensive and more readily accessible alternatives.

Soil Science and Plant Nutrition, The University of Western Australia

Nedlands, Western Australia 6907. Dr. Aylmore is corresponding author. E-mail: aylmore@cylle.uwa.edu.au

Received Feb. 3, 1997; accepted Nov. 3, 1997.

For example, a prototype dual-source (^{137}Cs and Yb^{169}) gamma CAT scanning unit has been developed in the Soil Science Laboratories of the University of Western Australia (Aylmore and Hainsworth 1988; Hainsworth and Aylmore 1988). The results from this unit indicate that reliable measurements of spatial distribution of ρ are possible in a nondestructive and repetitive manner (Hainsworth and Aylmore 1988; Phogat and Aylmore 1989; Phogat et al. 1991). A comprehensive review of the use and limitations of X-ray and single- and dual-source gamma CAT scanning for spatial distribution of ρ in soil columns at resolutions as small as 2×2 mm has been provided by Aylmore (1993).

Usually ϵ is computed from ρ , which is also used widely as an index of the state of compaction in cultivated soils. There is limited information, however, on whether and how management-induced changes in ρ , obtained using CAT, can be utilized to characterize the dynamics of ϵ , particularly in structurally unstable soils.

Management-induced changes in ϵ , e.g., wetting and drying, are caused largely by changes in pore-number-size distribution (PNSD), particularly the larger size pores. Experimental determination of PNSD, particularly nondestructive and repetitive measures at very small scales, is laborious and expensive. Recently, Fuentes et al. (1996) proposed a theoretical equation to compute surface fractal dimension (D) from ϵ for a fractal soil. This relationship offers a simple approach for the estimation of D that may be used as an index to characterize the changes in ϵ (Rieu and Sposito 1991 a and b; Logsdon 1995; Rasiah 1995). It has also been suggested that D can be incorporated into transport models to account for the influence of the changes in ϵ on soil water flow (Rieu and Sposito 1991 a and b). The objectives of this study were (i) to determine whether changes in ϵ at scales as small as 2×2 mm that may occur during wetting and drying can be discriminated by CAT and (ii) to use the Fuentes theoretical equation to estimate D from ϵ and determine whether D is sensitive to wetting.

MATERIALS AND METHODS

The Scanning System

A prototype CAT scanning system constructed in the Soil Science and Plant Nutrition Laboratories of the University of Western Australia was used in this study for radiation count (Hainsworth and Aylmore 1988; Aylmore 1993). In these studies, a gamma source (500 mCi of Caesium-137) monitored by a NaI (TI) scintillation detector (Model 202-3) attached to photomultiplier tube was used. The signal from the pho-

tomultiplier tube was passed through a base-amplifier (Model 2007P) before it was put into another amplifier (Model 2012). Other components include a high-voltage power supply (Model NE 4646) and a single source channel analyzer (Model 2030) with an RS-232 interface to communicate with an IBM-compatible personal computer (PC). The counts at desired energy were discriminated by the single source analyzer and subsequently counted by a dual counter (Model 2072). All the components in the system, exclusive of the high-voltage power supply, were supplied by Canberra-Packard Pty. Ltd. The system is automated and controlled by two IBM-compatible PCs, one for data acquisition and platform control and the other for image reconstruction and data analysis.

The beam was collimated to produce a slice thickness of 2 mm and a pixel (picture element) size of 2×2 mm. As the source and the detector were fixed, the object, i.e., the soil column, was moved across the beam and scanned at 2-mm intervals. Successive linear scans were taken after rotating the object progressively in 5° increments through 180° . When this process was completed, the linear scans were back-projected, using filtered back-projection (Hermon 1980), for a given number of rotations to reconstruct an image of the scanned slice. When the back-projections were completed, the gamma attenuation for each pixel in the slice was determined. The system is capable of scanning columns up to 100 mm in diameter and 1.5 m in height.

The Porous Materials

The porous materials used in this study were water-stable artificial soil (Hydrokorn, an expanded and stabilized clay) and a water-unstable soil collected from the surface (0–7 cm) on a farm in Calingri, Western Australia. This water-unstable soil is a sandy loam that is 19.3% clay, 12.6% silt, and 68.1% sand. The air-dried soil and the water-stable material were crushed separately to obtain 2 to 4-, 0.71 to 1.4-, and 0.25 to 0.71-mm size aggregates. Aggregates of a given size range from each material were packed to a height of 10 cm in a 7.2-cm-i.d., 15-cm-high acrylic cylinder with a closed end base. The base of each column had 24 1.5-mm-diameter holes drilled in two concentric rings. These holes enabled the columns to be wetted slowly from the base. Care was taken while packing to produce uniformity in density along the length of the column. The dry bulk density, ρ_c , for each column is provided in Table 1. The column with water stable aggregate is abbreviated WSA and those with unstable aggregates as USA.

TABLE 1

The measured bulk density (ρ_b) values, the average linear attenuation coefficient (μ_m), and the mass attenuation (μ_m) for each column

Aggregate size mm	Dry bulk density Mg m ⁻³	Linear attenuation. m ² Mg ⁻¹	Mass	Dry bulk density Mg m ⁻³	Linear attenuation. m ² Mg ⁻¹	Mass
	Before wetting			After wetting		
<u>For the water stable aggregates</u>						
(. . . x 10 ⁻³)						
2.0 to 4.0	0.507	3.710	7.316	0.551	5.999	10.88
0.71 to 1.4	0.536	4.324	8.074	0.558	6.410	11.48
0.25 to 0.71	0.656	4.833	7.367	0.676	7.197	10.65
<u>For the unstable aggregates</u>						
2.0 to 4.0	1.196	9.504	7.947	1.224	9.367	7.652
0.71 to 1.4	1.246	9.701	7.786	1.295	9.819	7.582
0.25 to 0.71	1.387	9.944	7.544	1.318	10.55	7.604

The column with 2 to 4-mm water-stable aggregate is abbreviated 2-4WSA, and similar abbreviations were followed for the other aggregate sizes of WSA and USA.

After packing, each column was scanned at 10-mm-depth increments using a counting time of 3 s. The columns were then wetted slowly from the base with deionized water contained in a large beaker and allowed to saturate. After saturation, the columns were air-dried in an oven at 35°C to constant moisture content equal to that which existed before wetting. The decrease or increase in column height, if any, was recorded and used in the computation of wetting- and drying-induced changes in ρ_c (Table 1). The redried columns were rescanned as described previously.

THEORY

Computation of Bulk Density and Porosity

Recently, a comprehensive review of CAT scanning theory as it relates to ρ and water content determination in soil has been provided by Aylmore (1993). According to Aylmore (1993) and Hainsworth and Aylmore (1983), the linear attenuation coefficient (μ_d) is,

$$\mu_d = \mu_m \rho_d \quad (1)$$

where the subscript d refers to dry, μ_m is mass attenuation (m² mg⁻¹) for soil solids, and ρ_d is dry bulk soil density of pixel in Mg m⁻³. To solve Eq. (1) for ρ_d , we need data on μ_m , which is computed as follows:

$$\mu_m = \mu_w / \rho_c \quad (2)$$

where μ_w is the average linear attenuation coefficient for the entire column and ρ_c is the measured dry bulk density of the column.

The Multi-CAT computer program, written in Pascal, uses the radiation count data for the computation of μ_d for each pixel, an average μ_d , and the corresponding standard deviation (σ) for each depth increment. An average μ for the entire column (μ_{av}) was then computed using the average μ_d for each depth increment. The measured ρ_c and μ_{av} for the columns were then used in Eq. (2) to solve for μ_m , which is used in Eq. (1) to solve for ρ_d .

The values of ρ_d obtained using Eq. (1) were used for the computation of ϵ using the following equation,

$$\epsilon = 1 - \rho_d / \rho_p \quad (3)$$

where ρ_p is the solid particle density. The ρ_p assumed for the unstable soil is 2.65 Mg m⁻³, and that measured (Blake and Hartage 1986) for the artificial stable aggregates was 1.85 Mg m⁻³.

Computation of Fractal Dimension

Values of fractal dimension are usually computed from number-size distributions. This approach is laborious and expensive. Recently, Fuentes et al. (1996) proposed a theoretical equation to estimate D from ϵ ,

$$D = 2 + 3 \frac{\epsilon^{4/3} + (1 - \epsilon)^{2/3} - 1}{\epsilon^{4/3} \ln \epsilon^{-1} + (1 - \epsilon)^{2/3} \ln(1 - \epsilon)^{-1}} \quad (4)$$

where $2 \leq D \leq 3$ and D is defined as the surface fractal dimension for the incompletely fragmented porous medium (Rieu and Sposito 1991a). Equation (4) contains two terms, ϵ and surface grain coverage $(1 - \epsilon)$. Thus, the estimates of D obtained using Eq. (4) cannot be compared strictly with those obtained using the conventional estimates based on PNSD. Equation (4) is

essentially based on a reinterpretation of the Millington and Quirk (1961) approach for soil-water conductivity in porous medium. Because the data derived from CAT in our study is only for ϵ , Eq. (4) is the most appropriate for our purpose. Further, repetitive measurements on PNSD from the sample after wetting and drying are not feasible if the conventional procedures are used for D estimation. The $\epsilon^{2D/3}$ and $(1-\epsilon)^{D/3}$ are subsequently computed using ϵ and D . According to Fuentes et al. (1996) $\epsilon^{2D/3}$ is the intersection of pore area between two section of pathways, the entrance and exit, i.e., it is a measure of PC, and $(1-\epsilon)^{D/3}$ is grain surface coverage. The values of D computed using Eq. (4) have practical implications in the estimation of unsaturated hydraulic conductivity (Fuentes et al. 1996), and we are dealing with this issue in a follow-up paper.

Statistical Analysis

Simple correlations were performed to determine the existence or nonexistence of 1:1 relationships between the before and after wetting data obtained for a given parameter, e.g., ϵ . Preliminary analysis indicated nonexistence of 1:1 relationships between the ϵ data obtained before and that obtained after wetting from a given column packed with a given aggregate type. In order to report the results in a comprehensive form, we pooled the data across columns for a given aggregate type and repeated the analysis, and these results are reported in the text. The stepwise multiple regression procedure was used for multivariable best fit analysis using the SAS software package (1985).

RESULTS AND DISCUSSION

Bulk Density

Because the primary data from CAT is dry ρ , we provide a brief discussion of this first. Before wetting, the dry ρ in the 2-4 WSA column ranged from 0.481 to 0.582 Mg m^{-3} , and the standard deviation, σ , for ρ ranged from 0.00203 to 0.00216 (Fig. 1a and b). The dry ρ increased after wetting (Fig. 1a). For example, the minimum ρ increased from 0.489 to 0.539 Mg m^{-3} (Table 2). After wetting, the σ at each depth increment was about one-half of that observed before wetting (Fig. 1b). Similar trends were observed for ρ distributions in the 0.71-1.4 WSA and 0.25-0.71 WSA (Table 2) and in the USA columns (Fig. 2a and b, and Table 2).

The nonexistence of 1:1 relationships between the before and after wetting ρ data, of a given aggregate type indicated they are significantly different from each other (Table 3). In gen-

eral, the ρ increased with wetting (w) and decreased with increasing initial aggregate size, x , ($R^2 = 0.47$ to 0.74). The positive interaction involving w and x indicated the impact of w on ρ was large when x was high in USA. This interaction was not significant in WSA.

The increase in ρ in WSA after wetting was probably attributable to reorientation and consolidation of aggregates during wetting and drying. Consolidation that occurred during wetting and drying resulted in a decrease in the length of the WSA columns from 100 mm to 92 mm. The decrease in column height in USA was small compared with WSA, and the increase in ρ after wetting in USA was probably attributable to aggregate slaking in water followed by reorientation and consolidation.

The magnitude of σ reflects the heterogeneity of ρ in the horizontal plane. The larger its value, the greater is the heterogeneity. In the USA columns, σ increased with increasing ρ , x , d , and w (Table 3). The influence of ρ and x was not significant on the σ of WSA, and w had negative impact on σ . The latter was probably caused by wetting in WSA producing more uniformity in ρ than in USA through consolidation and reorientation. On the other hand wetting in USA produced slaking, which lead to increased heterogeneity in ρ .

The accuracy and reliability of ρ values obtained using the same gamma-ray equipment, and the associated CAT technique, have already been verified (Phogat and Aylmore 1989; Phogat et al. 1991). We therefore conclude that the CAT technique is a very useful approach to successfully discriminate the influence of aggregate size and type and wetting and drying on the spatial distribution of ρ on a very small scale in two planes.

Porosity

The values of ϵ in the columns are mirror reflections of ρ (Figs. 1a and c and 2a and c). This is not surprising but, rather, anticipated because ϵ values were computed from ρ . The nonexistence of a 1:1 relationship between the before and after wetting ϵ data for a given aggregate type across columns indicated the former is significantly different from the latter (Table 3). The ϵ increased initial x and decreased with w . The negative interaction involving w and x for USA indicated that wetting-induced loss in ϵ was high in larger aggregates. The loss in ϵ during wetting depended not only on w and x but also on aggregate type. For example, the loss in ϵ in the 2-4 USA was 0.101 compared with 0.033 for 2-4 WSA.

The loss in ϵ in USA was probably caused by losses in both inter- and intra-aggregate pore

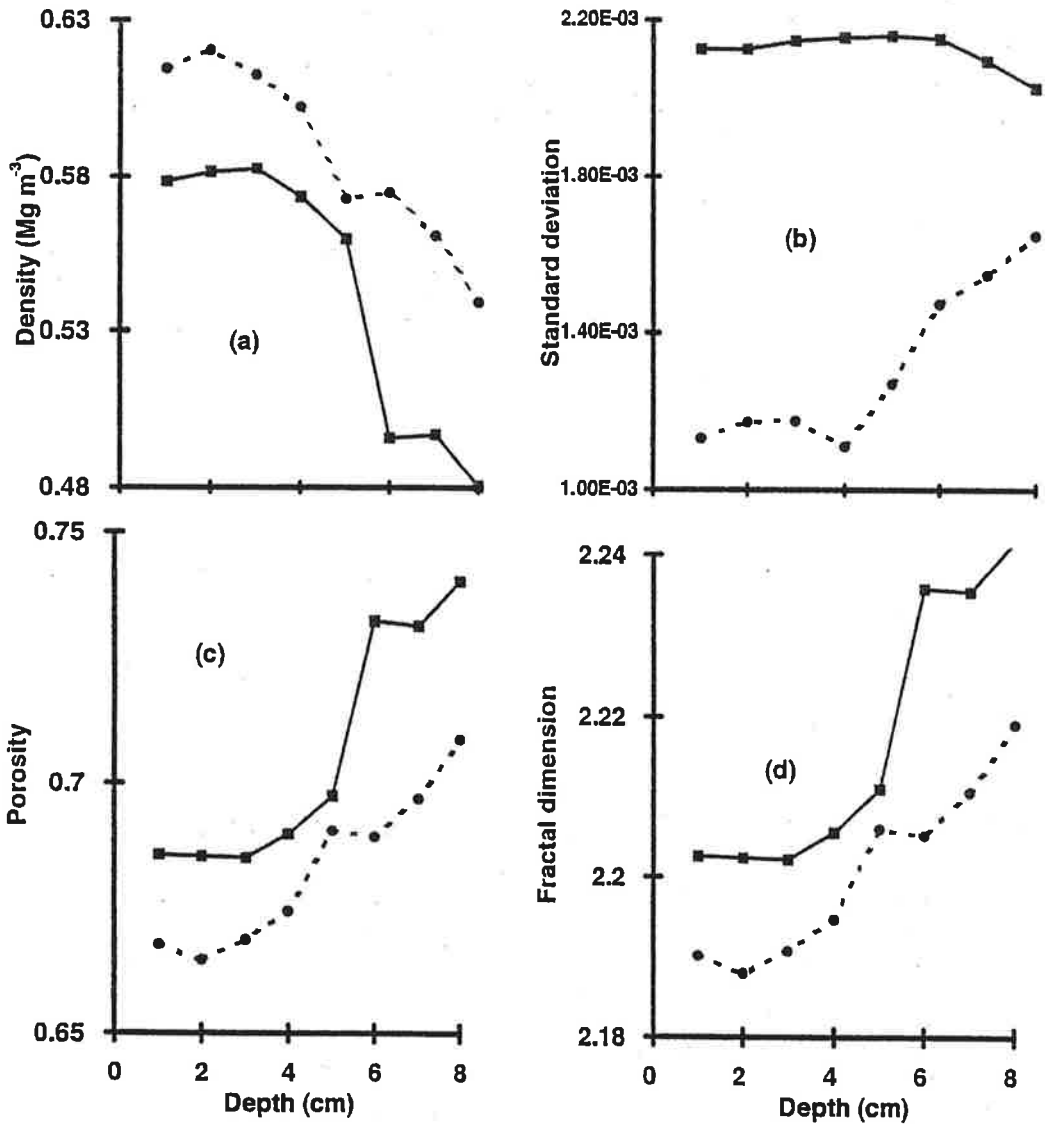


Fig. 1. Spatial distribution of bulk density (a), standard deviation (b), porosity (c), and fractal dimension (d) in the 2 to 4-mm stable aggregate column. The solid lines are for before wetting and the broken lines for after wetting. Please note the differences in y-axis.

spaces compared with only the interaggregate spaces in WSA. Visually, aggregate slaking was evident in USA, and this, in general, led to increased losses in ϵ . Further, a rapid increase in ϵ with increasing x in USA lends support to the hypothesis that slaking in unstable soils increased with increasing x (Rasiah and Kay 1995). The results show that we were able to monitor the *in-situ* changes in ϵ at a scale as small as 2×2 mm using CAT and were able to discriminate and quantify these changes accurately. Such information ob-

tained in a nondestructive and repetitive manner may be useful to account for the influence of the changes in ϵ on transport processes.

Fractal Dimension

Subject to the conditions and assumptions invoked in the formulation of Eq. (4), the estimates of D obtained using this equation from ϵ followed trends similar to ϵ (Figs. 1c and d and 2c and d). This was anticipated because D depended only on ϵ . For WSA, the estimates of D ranged from 2.147 to

TABLE 2

Ranges in values of dry bulk density (ρ), before and after wetting and the corresponding standard deviations (σ) computed using the scanning data.

Aggregate size mm	Range in bulk density Mg m^{-3}		Range in standard deviation	
	Before wetting	After wetting	Before wetting	After wetting
<u>In the water stable aggregate columns</u>				
			(..... $\times 10^{-3}$	
2.0 to 4.0	0.481–0.582	0.539–0.620	2.03–2.16	1.11–1.65
0.71 to 1.4	0.479–0.555	0.482–0.629	1.98–2.21	0.868–1.21
0.25 to 0.71	0.627–0.687	0.581–0.732	2.31–2.54	0.826–1.28
<u>In the unstable aggregate columns</u>				
2.0 to 4.0	1.161–1.265	1.284–1.377	2.64–3.00	3.20–3.55
0.71 to 1.4	1.211–1.300	1.295–1.427	2.61–3.00	2.90–3.48
0.25 to 0.71	1.282–1.354	1.381–1.439	2.74–3.10	3.09–3.27

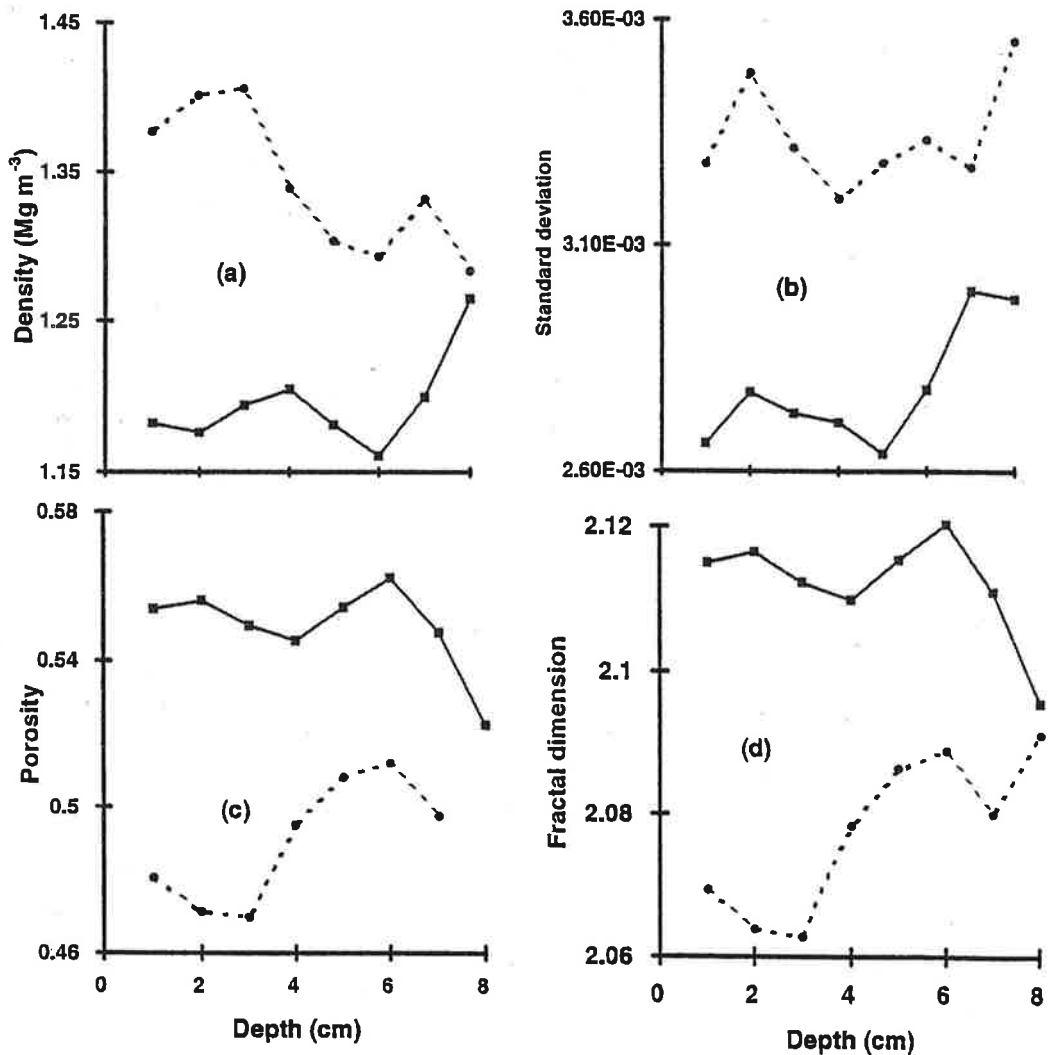


Fig. 2. Spatial distribution of bulk density (a), standard deviation (b), porosity (c), and fractal dimension (d) for the 2 to 4-mm unstable aggregate column. The solid lines are for before wetting and the broken lines for after wetting. Please note the differences in y-axis.

TABLE 3

A summary of the simple correlation and stepwise multiple regression analyses

Simple correlations		<i>r</i>	<i>P</i>
For the stable aggregates			
$\rho_{aw} = 0.097(0.061) + 0.84(0.04) \rho_{bw}$		0.88	< 0.01
$\epsilon_{aw} = 0.048(0.072) + 0.84(0.04) \epsilon_{bw}$		0.88	< 0.01
$D_{aw} = 0.25(0.23) + 0.82(0.04) D_{bw}$		0.88	< 0.01
$PC_{aw} = 0.081(0.044) + 0.78(0.06) PC_{bw}$		0.92	< 0.01
For the unstable aggregates			
$\rho_{aw} = 0.84(0.17) + 0.42(0.14) \rho_{bw}$		0.55	< 0.05
$\epsilon_{aw} = 0.26(0.072) + 0.42(0.14) \epsilon_{bw}$		0.55	< 0.05
$D_{aw} = 2.21(0.21) - 0.065(0.10) D_{bw}$		0.32	< 0.09
$PC_{aw} = 0.22(0.06) + 0.34(0.14) PC_{bw}$		0.47	< 0.05
Multiple regression equations			
For the stable aggregates		<i>R</i> ²	<i>P</i>
$\rho = 0.67 - 0.011 d - 0.032 x + 0.039 w$		0.47	< 0.01
$\epsilon = 0.64 + 0.0060 d + 0.017 x - 0.021 w$		0.47	< 0.01
$\sigma = 0.002 - 0.0012 w + 0.000023 d$		0.90	< 0.01
$D = 2.20 + 0.0406 d + 0.0122 w x - 0.0495 w$		0.69	< 0.01
For the unstable aggregates			
$\rho = 1.33 + 0.065 w - 0.046 x + 0.027 w x$		0.74	< 0.01
$\epsilon = 0.50 + 0.018 x - 0.024 w - 0.010 w x$		0.74	< 0.01
$\sigma = -0.00069 + 0.00097 x + 0.00012 w + 0.00024 d + 0.0026 \rho$		0.76	< 0.01
$D = 2.072 + 0.0131 x - 0.0115 w x$		0.45	< 0.01

ρ refers to bulk density, ϵ to porosity, σ to standard deviation, D to fractal dimension, x to initial aggregate diameter (mm), d to depth (mm), w to wetting ($w = 1$ for wetted and zero for unwetted aggregates), r to correlation coefficient, R^2 to coefficient of determination, P to significance, and the subscripts bw and aw to before and after wetting. All the coefficients in the above equations are significant at $P < 0.05$.

2.243 compared with a range from 2.055 to 2.096 for USA (Table 4). Values of D are within the theoretical limit set by Feuntes et al. (1996), i.e., $2 \leq D \leq 3$. The D increased with increasing x and decreased after wetting ($R^2 = 0.45-0.69$), indicating that wetting-induced changes in surface ϵ and grain surface coverage, $(1-\epsilon)$, can be characterized by values of D (Table 3).

Because D was computed from ϵ only, we make qualitative comparisons with results obtained using PNSD (Brakensiek et al. 1992; Logsdon 1995; Rasiah 1995). These workers reported that stable soils were characterized by larger values of D , which

is consistent with our findings. Even though these workers used PNSD data, they first computed areal porosity from PNSD and then used the data in a relation similar to Eq. (4) to compute values for D , i.e., similar to the approach used in our study. Thus, we conclude the values of D obtained using Eq. (4) are sensitive enough to discriminate structural differences among soils, wetting-induced changes in ϵ , and are comparable to those obtained using conventional equations based on PNSD.

The estimates of PC , i.e., $\epsilon^{2D/3}$, and grain surface coverage, $(1-\epsilon)^{D/3}$, show the latter increased (Figs. 3b and d) at the expense of the former (Figs.

TABLE 4

Ranges in values of porosity (ϵ), before and after wetting, and surface fractal dimension (D)

Aggregate size (mm)	Range in porosity		Range in fractal dimension	
	Before wetting	After wetting	Before wetting	After wetting
<u>In the water stable aggregate columns</u>				
2.0 to 4.0	0.685-0.740	0.665-0.709	2.202-2.242	2.188-2.218
0.71 to 1.4	0.703-0.741	0.660-0.739	2.213-2.243	2.184-2.241
0.25 to 0.71	0.629-0.661	0.604-0.686	2.163-2.185	2.147-2.202
<u>In the unstable aggregate columns</u>				
2.0 to 4.0	0.523-0.562	0.470-0.516	2.096-2.120	2.064-2.091
0.71 to 1.4	0.503-0.550	0.462-0.506	2.086-2.094	2.056-2.085
0.25 to 0.71	0.489-0.516	0.457-0.479	2.075-2.092	2.055-2.069

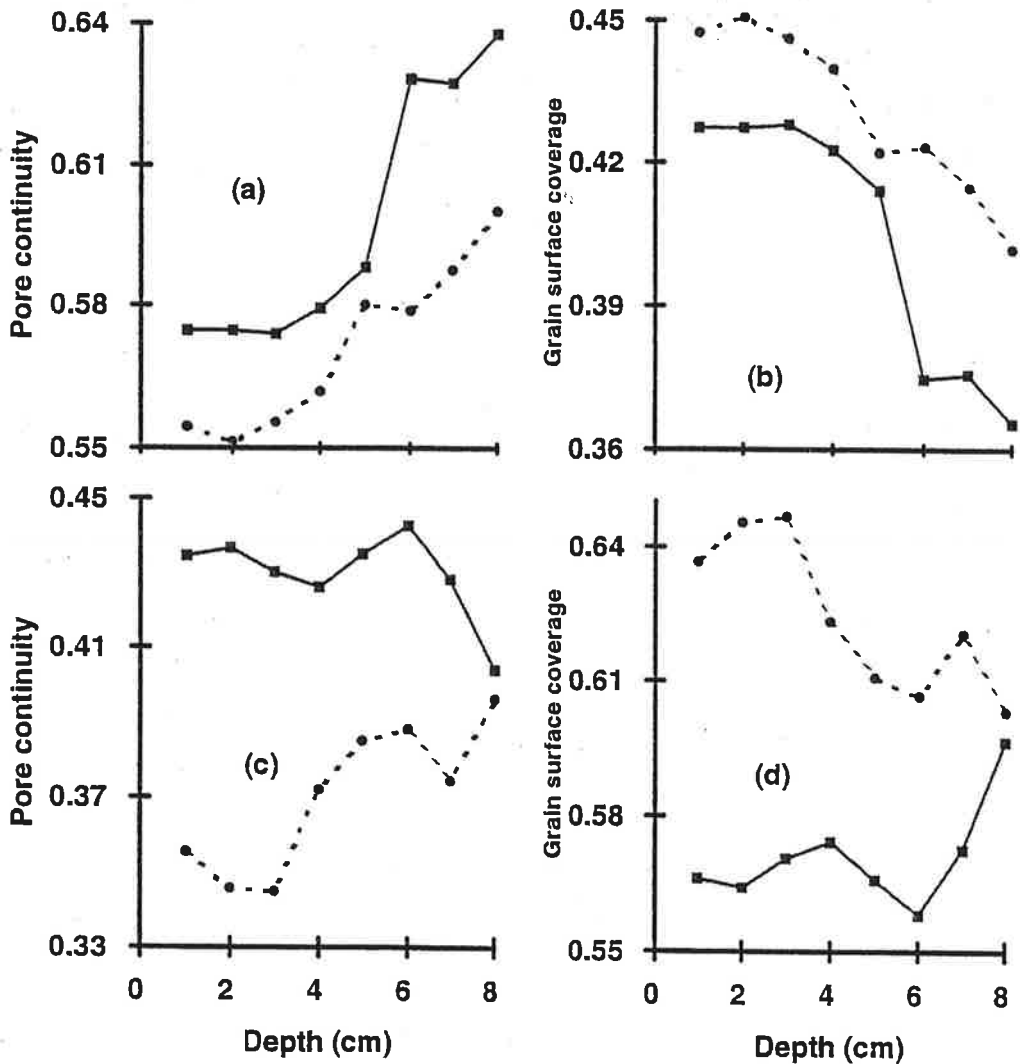


Fig. 3. Pore continuity (a) and the corresponding grain surface coverage (b) in the 2 to 4-mm stable aggregate column and in the unstable column (c and d). The solid lines are for before wetting and the broken lines for after wetting.

3a and c) after wetting. The decrease in PC was much larger in USA than in WSA columns. Even though PC in USA columns was higher at 6 cm depth than at depths less than 6 cm, transport would probably be limited by the minimum continuity, which was estimated to be at 3 cm depth (Fig. 3c). This illustrates the importance of the information about PC, particularly when there are the transport-limiting layers in the upper sections of profiles.

CONCLUSIONS

The CAT technique was applied to gamma-ray attenuation to measure the changes in spatial dis-

tribution of porosity in water stable and unstable soil aggregate columns during wetting and drying at a scale as small as 2×2 mm. The results indicated the technique successfully discriminated the influence of wetting and aggregate size and type on the changes in ϵ at a very small scale in both the horizontal and vertical planes. Thus, we recommend the use of the CAT technique to discriminate the changes in ϵ in a nondestructive and repetitive manner at scales as small as 2×2 mm. Such information at these scales may be useful for improved elucidation of the physicochemical mechanisms involved in aggregate destabilization.

Using a theoretical equation, we show that estimates for surface fractal dimension, D , that are sensitive to structural differences and wetting and drying can be computed from CAT-derived ϵ data. Our approach eliminates the need for the difficult to obtain data on number-size distributions to estimate D using conventional equations. Sensitive estimates of D have potential use in transport simulation models to account for the influence of the changes in ϵ on transport processes in unstable soils.

Estimates of PC, obtained using ϵ and D , appear promising to discriminate transport limiting layers at scales as small as 1-cm depth increments.

REFERENCES

- Anderson, S. H., R. L. Peyton, and C. J. Gantzer. 1990. Evaluation of constructed and natural soil macropores using x-ray computed tomography. *Geoderma* 46:13-29.
- Aylmore, L. A. G. 1993. Use of computer-assisted tomography in studying water movement around plant roots. *Adv. Agron.* 49:1-54.
- Aylmore, L. A. G., and J. M. Hainsworth. 1988. Studies of soil plant water systems using CAT scanning. *Search (Sydney)*. 19:198-190.
- Blake, G. R., and K. H. Hartage. 1986. Bulk density. In *Methods of soil analysis, Part 1*. A. K. Klute (ed.). Agron. Monograph No. 9. ASA, Madison, WI.
- Brakensiek, D. L., W. J. Rawls, S. D. Logsdon, and W. M. Edwards. 1992. Fractal description of macroporosity. *Soil Sci. Soc. Am. J.* 56:1721-1723.
- Cornish, P. S., and J. R. Lymbery. 1987. Reduced early growth of direct drilled wheat in southern New South Wales: Causes and consequences. *Aust. J. Exp. Agric.* 27:869-880.
- Fuentes, C., M. Vauclin, J. Parlange, and R. Haverkamp. 1996. A note on the soil-water conductivity of a fractal soil. *Transport in Porous Media*. 23:31-36.
- Grevers, M. C. J., E. De Jong, and R. J. St. Arnaud. 1989. The characterization of soil macroporosity with CT scanning. *Can. J. Soil Sci.* 69:629-637.
- Hainsworth, J. M., and L. A. G. Aylmore. 1988. Application of computer assisted tomography (CAT) to gamma attenuation measurement of soil water content. *Aust. J. Soil Res.* 26:105-110.
- Hainsworth, J. M., and L. A. G. Aylmore. 1983. The use of computer-assisted tomography to determine spatial distribution of soil water content. *Aust. J. Soil Res.* 21:435-443.
- Hermon, G. T. 1980. *Image reconstruction from projections*. Academic Press, New York.
- Hounsfield, G. N. 1972. A method of and apparatus for examination of a body by radiation such as x- or gamma-radiation. Brit. Patent 1 283 915. Issued: Aug. 1968.
- Jakobsen, B. F., and A. R. Dexter. 1987. Effect of soil structure on wheat root growth, water uptake and grain yield. A computer simulation model. *Soil Tillage Res.* 10:331-345.
- Logsdon, S. D. 1995. Analysis of aggregate fractal dimensions and aggregate densities back-calculated from hydraulic conductivity. *Soil Sci. Soc. Am. J.* 59:1216-1221.
- Masle, J. and G. D. Farquhar. 1988. Effects of soil strength on the relation of water-use efficiency and growth carbon isotope discrimination in wheat seedlings. *Plant Physiol.* 86:32-38.
- Millington, R. J., and J. P. Quirk. 1961. Permeability of porous solids. *Trans. Faraday Soc.* 57:1200-1206.
- Petrovic, A. M., J. E. Siebert, and P. E. Rieke. 1982. Soil bulk density analysis in three dimensions by computed tomographic scanning. *Soil Sci. Soc. Am. J.* 46:445-450.
- Phogat, V. K., L. A. G. Aylmore, and R. D. Schuller. 1991. Simultaneous measurement of the spatial distribution of soil water content and bulk density. *Soil Sci. Soc. Am. J.* 55:908-915.
- Phogat, V. K., and L. A. G. Aylmore. 1989. Evaluation of soil structure by using computer-assisted tomography. *Aust. J. Soil Res.* 27:313-323.
- Rasiah, V. 1995. Fractal dimension of surface-connected macropore count-size distributions. *Soil Sci.* 159:105-108.
- Rasiah, V. and B. D. Kay. 1995. Characterizing rate of wetting: Impact on structural destabilization. *Soil Sci.* 160:176-182.
- Rieu, M., and G. Sposito. 1991a. Fractal fragmentation, soil porosity, and soil water properties: I. Theory. *Soil Sci. Soc. Am. J.* 55:1231-1238.
- Rieu, M., and G. Sposito. 1991b. Fractal fragmentation, soil porosity, and soil water properties: II. Application. *Soil Sci. Soc. Am. J.* 55:1239-1244.
- SAS Institute. 1985. *SAS/STAT procedures guide for personal computers*, Version. 6 Ed. SAS Institute, Inc., Cary, NC.
- Warner, G. S., J. L. Nieber, I. D. Moore, and R. A. Geise. 1989. Characterizing macropores in soil by computed tomography. *Soil Sci. Soc. Am. J.* 53:653-660.

Estimating Microscale Spatial Distribution of Conductivity and Pore Continuity Using Computed Tomography

V. Rasiah and L. A. G. Aylmore*

ABSTRACT

Despite the importance of information on the spatial distribution of unsaturated hydraulic conductivity (K_{us}) at microscale in soil, experimental determination of this property is difficult. The objectives of this study were to: (i) seek a simple, but reliable, procedure for the estimation of K_{us} at microscale and (ii) determine the sensitivity of the estimates to wetting-induced changes in selected structural parameters (porosity, ϵ , surface fractal dimension, D , and pore continuity, PC). Using computer-assisted tomography (CAT), spatial distributions of soil water content (θ) and changes in ϵ that occurred during wetting were monitored at 2 by 2 mm resolution at 1-cm depth increments in water-stable (WSA) and unstable aggregate (USA) columns. The Fuentes theoretical equation, which requires data on saturated hydraulic conductivity (K_s), θ , ϵ , and D , was used for the estimation of the spatial distribution of K_{us} . The spatial distribution of θ in WSA columns ranged from 0.113 to 0.327 $\text{cm}^3 \text{cm}^{-3}$ and from 0.175 to 0.567 $\text{cm}^3 \text{cm}^{-3}$ in the USA columns. The spatial distribution of ϵ_{us} ranged from 0.46 to 0.74 and was used in the computation of D and PC. Values of K_s ranged from 0.006 to 0.745 cm h^{-1} . The spatial distribution of K_{us} ranged from 6.87×10^{-4} to $1.49 \times 10^{-2} \text{ cm h}^{-1}$ in WSA compared with 7.3×10^{-4} to $4.11 \times 10^{-2} \text{ cm h}^{-1}$ in USA. Pore continuity, θ , D , and initial aggregate diameter (x) accounted for 94 to 95% of the variability in K_{us} distributions. The results indicate that reliable estimates of K_{us} distributions at microscale can be computed from single-source CAT-derived data on θ and ϵ .

RELIABLE ESTIMATES on the spatial distribution of K_{us} at the microscale is essential for a better understanding of the mechanisms and processes involved and to identify the factors controlling water flow, root water uptake, and solute transport in soil. Experimental determination of the spatial distribution of K_{us} at the microscale is time consuming and laborious, and at times the data may be not reliable, particularly when structural changes occur during wetting. The estimation procedure for K_{us} should incorporate the influence of structural changes that may occur during wetting. Data on in situ, nondestructive, and repetitive measurements in structural changes are thus essential.

Soil porosity is a sensitive structural parameter, particularly for water-unstable soils. In situ, nondestructive, and repetitive measurements of ϵ and θ at the microscale have been successfully carried out using a dual-source (^{137}Cs and ^{109}Yb) gamma CAT scan unit (Aylmore, 1993; Phogat et al., 1991; Phogat and Aylmore, 1989). Rasiah and Aylmore (1998) showed that in situ changes in ϵ , derived from CAT, that occurred at the microscale during wetting of stable and unstable soil can be characterized by values of D computed using the Fuentes et al. (1996) model. Phogat and Aylmore (1996) showed that

an empirical relation could be derived between K_s and ϵ measured using CAT data. Furthermore, PC at the microscale, particularly in water-unstable soils, would have an influence on K_{us} estimates.

Using indirect approaches, several empirical functions, primarily based on water content-suction data, have been proposed for the estimation of K_{us} . The advantages, disadvantages, and limitations on the use of these functions have been discussed in several reports (e.g., Alexander and Skaggs, 1986). In general, most of these functions do not account for structural changes, particularly ϵ and PC, that may occur in water-unstable soils during wetting. Recently, there have been limited attempts to account for the influence of structural changes on soil water transport using the concept of D (Fuentes et al., 1996; Logsdon, 1995; Crawford, 1994; Rieu and Sposito, 1991; Tyler and Wheatcraft, 1990). The values of D required for soil water transport were usually computed from number-size distributions, except in the Fuentes et al. (1996) procedure where D is computed from ϵ . Computation of D from number-size distributions is laborious, time consuming, and involves destructive procedures, i.e., repetitive measurements on the same samples are not possible. The other input required for K_{us} estimation is either θ or water potential. The former is relatively easier to measure at the microscale than the latter and θ was used in the Fuentes et al. (1996) model. On this basis, the Fuentes et al. (1996) model appears the most appropriate for K_{us} estimates at the microscale.

The objectives of this study were to: (i) seek a simple, but reliable, procedure for the estimation of K_{us} at the microscale and (ii) determine the sensitivity of the estimates to wetting-induced changes in ρ , ϵ , D , and PC.

THEORY

Computation of Porosity and Water Content

We use the CAT technique for in situ, nondestructive, and repetitive measurements of ϵ and θ at scales as small as 2 by 2 mm resolution and at 1-cm depth increments (Aylmore, 1993). The theory involved in the simultaneous determination of ϵ and θ using the CAT technique has already been reported (e.g., Aylmore, 1993). Briefly, the linear attenuation coefficient, μ , for each voxel in soil is

$$\mu_d = \mu_m \rho_d \quad [1]$$

where the subscript d refers to dry, μ_m is mass attenuation ($\text{m}^2 \text{Mg}^{-1}$) for soil solids, and ρ_d is dry bulk soil density (Mg m^{-3}). To solve Eq. [1] for ρ_d , we need data on μ_m , which is computed as follows:

Soil Science and Plant Nutrition, Faculty of Agriculture, The Univ. of Western Australia, Nedlands, WA 6009, Australia. Received 25 March 1997. *Corresponding author (aylmore@cyllene.uwa.edu.au).

$$\mu_m = \mu_c/\rho \quad [2]$$

where μ_c is the average linear attenuation coefficient for the entire column and ρ is column bulk density.

A computer program, Multi-Cat, written in Pascal coding specifically for this purpose, uses the radiation count data from the scanner and computes μ_d for each voxel, an average linear attenuation (μ_{av}) for each depth increment, and the corresponding standard deviation (s). The μ_{av} is then used to compute μ_c for each column. The ρ and μ_c for a given column are used in Eq. [2] to solve for μ_m , which is then used in Eq. [1] to solve for ρ_d .

The ρ_d from Eq. [1] is used for the computation of ϵ as follows:

$$\epsilon = 1 - \rho_d/\rho_p \quad [3]$$

where ρ_p is particle density of soil. Equation [1] is extended for wet soils as

$$\mu_w = \mu_d + \mu_{wat} \theta \rho_{wat} \quad [4]$$

where μ_w is the linear attenuation coefficient of wet soil, μ_{wat} is the mass attenuation coefficient for water, and ρ_{wat} is the density of water. Equations [1] and [4] are combined to solve for θ :

$$\theta = (\mu_w - \mu_d)/(\mu_{wat} \rho_{wat}) \quad [5]$$

Estimation of Conductivity and Pore Continuity

For the reasons mentioned above, we choose the Fuentes et al. (1996) model:

$$K_{us} = K_e (\theta/\epsilon)^{[2D/3+2(3-D)]} \quad [6]$$

for K_{us} estimation. In Eq. [6], K_e is saturated hydraulic conductivity and D is surface fractal dimension. A detailed description and discussion on ϵ and D distributions, used in this study, from CAT has been already reported (Rasiah and Aylmore, 1998). Briefly, they used the CAT data in ρ_d to compute ϵ , using Eq. [3], which was then used in the Fuentes fractal model,

$$D = 2 + 3 \frac{\epsilon^{4/3} + (1 - \epsilon)^{2/3} - 1}{2\epsilon^{4/3} \ln \epsilon^{-1} + (1 - \epsilon)^{2/3} \ln(1 - \epsilon)^{-1}} \quad [7]$$

for the computation of D . In Eq. [7] $1.5 \leq D \leq 3$ (Millington and Quirk, 1961). According to Fuentes et al. (1996), $\epsilon^{2D/3}$ is the intersection of pore area between two consecutive layers, i.e., the entrance and exit, and we define this as pore continuity (PC), i.e.

$$PC = \epsilon^{2D/3} \quad [8]$$

and $(1 - \epsilon)^{D/3}$ is the surface coverage for grains.

MATERIALS AND METHODS

The Porous Materials

The details on the type of porous materials used, column packing, etc., have already been reported (Rasiah and Aylmore, 1998). Briefly, water-stable artificial and unstable soil aggregates (2–4, 0.71–1.4, and 0.25–0.71 mm) were separately packed in 7.2-cm i.d. and 15-cm height acrylic cylinders to 10-cm height. The columns were then CAT scanned (Aylmore, 1993; Hainsworth and Aylmore, 1988) using a single gamma source (1.85×10^{10} Bq of ^{137}Ce). The radiation count data and column bulk density (Rasiah and Aylmore, 1998) were used in Eq. [1] and [2] to solve for ρ_d , which along with particle

density (2.65 Mg m^{-3} for unstable and 1.85 Mg m^{-3} for stable aggregates) were used in Eq. [3] to solve for ϵ .

After scanning air dry, the columns were slowly wetted from the base with deionized water, contained in a large beaker, and allowed to saturate slowly. Using a Mariotte bottle, the K_e for each saturated column was determined by maintaining a constant 20-mm head of water. The K_e was computed using Darcy's equation:

$$q = V/At = K_e (\Delta H/L) \quad [9]$$

where q is the volume of water flowing through column cross-sectional area A in time t , L is the height of column, and ΔH is hydraulic head difference between inflow and outflow in the column. The K_e determination was repeated four times for each column by varying t (in Eq. [9]), 1.0, 1.5, 2.0, and 2.5 min for WSA and 3.0, 6.0, 9.0, and 15 min for USA, and maintaining the constant head for each t .

After K_e determination, the columns were drained for 15 min to 1 h, depending on soil type, and rescanned to obtain μ_w , in Eq. [4], and hence θ . After rescanning, the wet columns were forced-air dried in an oven at 35°C to constant moisture content equal to the air-dried moisture that existed before wetting. The decrease or increase in column height, if any occurred, was recorded. These changes were used in the computation of the changes in column ρ that occurred during wetting and drying. The redried columns were then rescanned as described above to compute the changes in ϵ that occurred during wetting.

Statistical Analysis

The SAS/STAT computer software package (SAS Institute, 1991) was used for the statistical analysis of data. The influence of aggregate size (x), depth increment (d), aggregate type (w), and the interactions involving d and x , as well as w and x on θ were determined using the simple and stepwise multiple regression procedures. We considered w to be a qualitative variable and assigned $w = 1$ for stable aggregates and zero for unstable aggregates. Using the same procedures, K_e was explored as a function of x , w , and wx . The paired t -test was used to test significant differences between the before- and after-wetting data on ϵ , D , and PC for each column. The stepwise multivariable selection procedure was used to explore K_{us} as a function of x , ϵ , θ , ρ , PC, and D . In the multivariable best-fit analysis, both the before- and after-wetting data for each variable were included initially. Preliminary analysis, however, indicated that the influence of before-wetting data was not significant; therefore, we used only the after-wetting data in the final analyses.

RESULTS AND DISCUSSION

Water Content

The spatial distribution of θ in the WSA varied with aggregate size (Fig. 1a). The range in θ for the 0.25- to 0.71-mm aggregate column was narrower than for the columns with larger aggregates (Table 1). The regression equations (Table 2) indicate that θ in the WSA columns increased with decreasing aggregate size, x . The standard deviation, s , across the WSA columns ranged from 0.0101 to 0.0149 and the average s across the WSA columns was 0.011. Even though the θ distribution in the USA columns varied with aggregate size (Fig. 2a) and increased with decreasing x (Table 2), the θ at any given depth increment was higher than the corre-

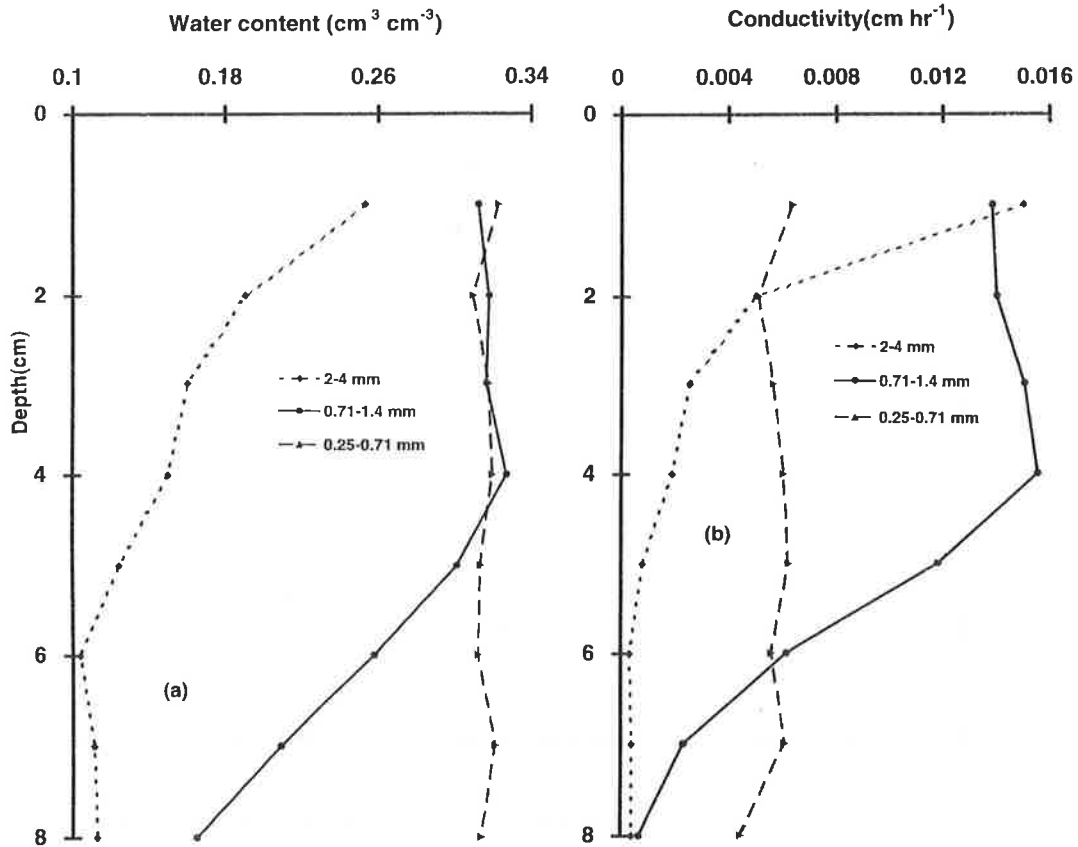


Fig. 1. Spatial distributions of (a) water content and (b) unsaturated hydraulic conductivity in the water-stable aggregate columns.

sponding θ in WSA, i.e., the multiple regression in Table 2. Since the θ in the USA columns was higher than WSA, the s was large and it ranged from 0.010 to 0.029 across USA columns. The average s across USA columns was 0.02.

Even though the linear relation between θ and d in columns was not significant (not shown) the interaction involving d and x was significant and it indicated that θ decreased with increasing d (Table 2).

Phogat et al. (1991) reported, using the same instrumentation as used in this study, that single-source (^{137}Cs) scanning markedly underestimated θ at or near saturation

tion for unstable soils and they attributed this to swelling. Overestimation was observed when the soils underwent shrinkage (Phogat et al., 1991). In our study, the column heights in USA decreased after wetting and redrying, providing evidence for shrinkage and increases in bulk density (Rasiah and Aylmore, 1998). Thus, it is possible that θ might have been overestimated, particularly in the 0.71- to 1.4-mm USA column (Fig. 2a). Nevertheless, the primary purpose of the CAT technique in our study was not to measure average θ accurately but to reveal the spatial distribution of K_{us} at the microscale. In this regard, the results presented in Fig. 1a and 2a indicate that the single-source CAT technique

Table 1. Saturated hydraulic conductivity (K_s), the ranges in soil water content, and the estimates of unsaturated conductivity, K_{us} .

Aggregate size mm	Saturated conductivity† cm h ⁻¹	Ranges in‡	
		Unsaturated conductivity cm h ⁻¹	Unsaturated water content cm ³ cm ⁻³
Water-stable aggregates			
2.00-4.00	0.754	3.14×10^{-4} - 1.49×10^{-2}	0.113-0.253
0.71-1.40	0.335	6.87×10^{-4} - 1.55×10^{-2}	0.166-0.327
0.25-0.71	0.086	4.7×10^{-4} - 6.22×10^{-3}	0.313-0.323
Unstable aggregates			
2.00-4.00	0.147	2.81×10^{-3} - 4.11×10^{-2}	0.175-0.391
0.71-1.40	0.045	2.32×10^{-2} - 5.88×10^{-2}	0.441-0.567
0.25-0.71	0.006	7.3×10^{-4} - 1.26×10^{-3}	0.267-0.331

† The saturated conductivity is the mean of four repeated measurements in each column.

‡ The ranges in water content refer to the minimum and maximum values in the drained columns as measured by computed tomography.

Table 2. The regression equations for water content (θ), saturated hydraulic conductivity (K_s), and pore continuity (PC).

Equation†	R ²
For the stable aggregates	
$\theta = 0.35 - 0.35x - 0.0076dx$	0.89
$K_s = 0.011 + 0.25x$	0.88
$PC = 0.51 + 0.25x$	0.42
For the unstable aggregates	
$\theta = 0.42 - 0.0088dx$	0.34
$K_s = -0.011 + 0.055x$	0.98
$PC = 0.51 + 0.0018dx$	0.32
For the combined data	
$\theta = 0.43 - 0.010dx - 0.12w$	0.57
$K_s = -0.0049 + 0.049x + 0.21wx$	0.98

† x = initial aggregate diameter (mm); d = depth in column (cm) and w = stability in water, which was assumed to be one for stable aggregates and zero for unstable aggregates. All equations and the coefficients in them are significant at $P < 0.05$.

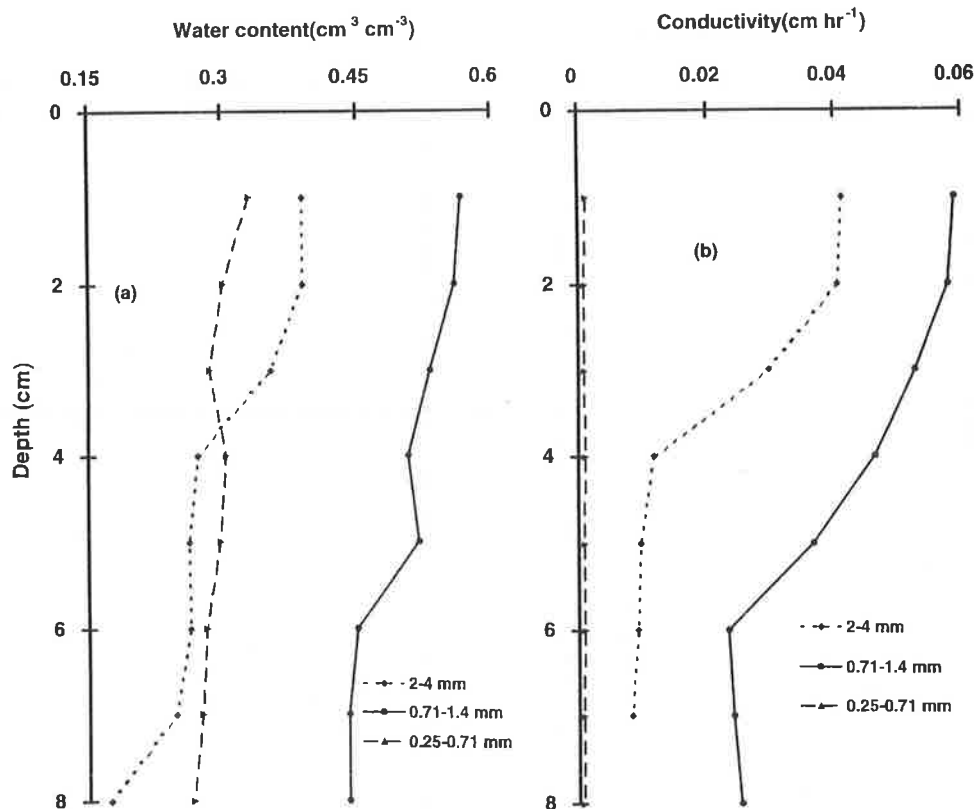


Fig. 2. Spatial distributions of (a) water content and (b) unsaturated hydraulic conductivity in the water-unstable aggregate columns.

can satisfactorily describe both the vertical and horizontal spatial distributions of θ .

Conductivity

The simple regression equations in Table 2 indicate that K_e increased with increasing x and was higher in WSA than in USA, i.e., the multiple regression equation in Table 2. The K_e of the smallest WSA was approximately an order of magnitude higher than the corresponding K_e of USA (Table 1). A similar trend existed for the medium-size aggregates. Even though the K_e of the largest USA was about one-fifth of WSA, we anticipated this to be much smaller because larger size USA could be expected to slake more extensively than smaller USA during wetting (Rasiah and Kay, 1995).

The paired t -test between the before- and after-wetting data for ϵ indicated that the before-wetting ϵ is different from the after-wetting ϵ (Tables 3 and 4). Similar results were obtained for PC and D , except the D for the 0.71- to 1.40-mm USA. Regardless of the aggregate size and type, the after-wetting ϵ , D , and PC were less than the corresponding before-wetting values. The after-wetting ϵ and D (see statistical analysis above) along with θ , used in Eq. [6], produced K_{us} spatial distributions that followed, as expected from Eq. [6], that of θ (Fig. 1 and 2). When the ranges in θ were wide, e.g., in the 2- to 4- and 0.71- to 1.4-mm WSA columns (Fig. 1a), the K_{us} distributions ranged by two orders of magnitude (Table 1). On the other hand, little variation was observed in the distribution of θ in the 0.25- to 0.71-mm WSA column (Fig. 1a), consequently the variation

in K_{us} distribution was small, except at 1-cm depth (Fig. 1b). In the USA columns, the widest range in θ distribution was observed in the 2- to 4-mm column where the K_{us} distribution ranged by an order of magnitude (Table 1). Even though an order of magnitude variation in K_{us} was observed in the 0.25- to 0.71-mm column, the variation in θ distribution was small (Fig. 2).

Pore Continuity

The data shown in Fig. 3 illustrates the changes in PC that occurred during wetting. The paired t -test, while confirming that the before-wetting PC is different from the after-wetting PC, also indicated that PC decreased

Table 3. A summary of the paired t -test results for wetting and drying influence on total porosity, fractal dimension, and pore continuity for the stable aggregates.

Variable	Mean before wetting	Mean after wetting	SE† of difference	P
For the 2- to 4-mm aggregates				
Total porosity	0.701	0.679	0.022	0.038
Fractal dimension	2.214	2.198	0.016	0.038
Pore continuity	0.586	0.564	0.022	0.003
For the 0.71- to 1.40-mm aggregates				
Total porosity	0.706	0.679	0.027	0.010
Fractal dimension	2.217	2.198	0.019	0.011
Pore continuity	0.601	0.559	0.042	0.000
For the 0.25- to 0.71-mm aggregates				
Total porosity	0.640	0.619	0.021	0.000
Fractal dimension	2.171	2.157	0.014	0.000
Pore continuity	0.525	0.499	0.026	0.000

† SE refers to standard error of difference between means.

Table 4. A summary of the paired *t*-test results for wetting and drying influence on total porosity, fractal dimension, and pore continuity for the unstable aggregates.

Variable	Mean before wetting	Mean after wetting	SE† of difference	<i>P</i>
For the 2- to 4-mm aggregates				
Total porosity	0.548	0.496	0.053	0.000
Fractal dimension	2.112	2.079	0.033	0.000
Pore continuity	0.429	0.378	0.051	0.000
For the 0.71- to 1.40-mm aggregates				
Total porosity	0.525	0.489	0.035	0.003
Fractal dimension	2.088	2.073	0.002	0.228
Pore continuity	0.401	0.347	0.055	0.000
For the 0.25- to 0.71-mm aggregates				
Total porosity	0.498	0.472	0.026	0.000
Fractal dimension	2.080	2.064	0.016	0.000
Pore continuity	0.380	0.356	0.024	0.000

† SE refers to standard error of difference between means.

after wetting (Tables 3 and 4). The loss in PC in the WSA columns was probably due to reorientation and consolidation, which occurred during wetting and drying. On the other hand, the loss in PC in the USA columns was most probably due to sealing or clogging of pores by slaked particles and reorientation and consolidation. The greatest loss in PC in USA occurred near the surface of the columns (e.g., at 1-cm depth) (Fig. 3), whereas the trends are reversed in the WSA columns.

The PC increased with increasing *x*, regardless of the aggregate type (Table 2). The nonexistence of signifi-

cant correlations (not shown) between PC and depth increment in the columns indicated random spatial distribution of PC, which may have an influence on K_{us} .

Variables Controlling Conductivity

The stepwise variable selection produced the following equation for K_e :

$$K_e = 0.127x + 1.836 PC - 0.079$$

$$R^2 = 0.86, P < 0.05 \quad [10]$$

In Eq. [10], all the coefficients are significant at $P < 0.05$ and Eq. [10] indicates the influence of PC and *x*, particularly the wetting-induced changes in the structural parameter PC, on K_e .

Equation [6] indicates that the estimates of K_{us} depend on θ , ϵ , and *D*. We did not measure K_{us} . Thus, to assess the accuracy of the estimates of K_{us} , we explored it as a function of ρ , PC, and *x* along with the variables in Eq. [6], i.e., ϵ , θ , *D*, and K_e . The analysis produced the following equations for WSA and USA, respectively:

$$K_{us} = 0.099PC + 0.12\theta + 0.0041x - 0.082$$

$$R^2 = 0.94, P < 0.01 \quad [11]$$

$$K_{us} = 0.902 - 0.51D + 0.25PC + 0.19\theta + 0.0074x$$

$$R^2 = 0.95, P < 0.01 \quad [12]$$

High R^2 values obtained for Eq. [11] and [12] indicate that the microscale K_{us} estimate distributions obtained

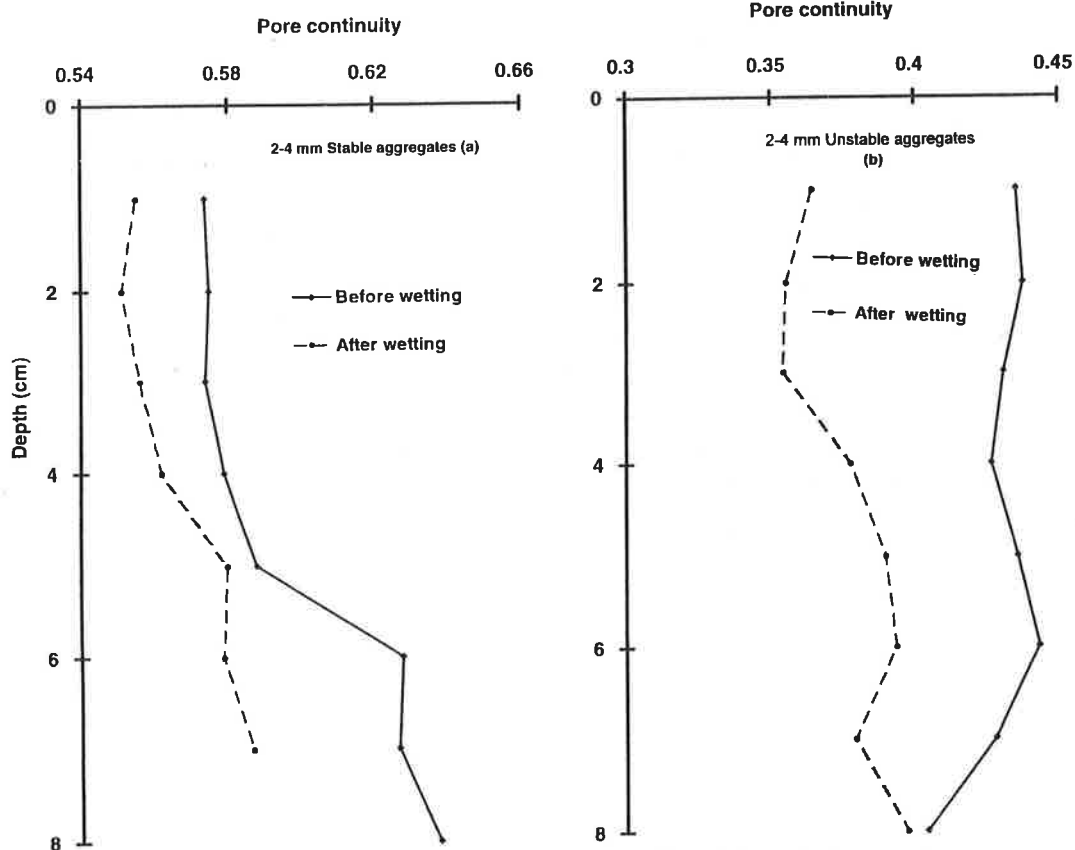


Fig. 3. Spatial distributions of pore continuity, PC, in the 2- to 4-mm (a) water-stable and (b) unstable aggregate columns.

using Eq. [6] are accurate. It could, however, be argued that the same variables (ϵ , θ , and D used in Eq. [6]) were also used in the regression analysis (Eq. [11] and [12]), thus the R^2 were high. There are at least two differences. First, Eq. [6] is a nonlinear power form, whereas Eq. [11] and [12] are linear. Second, the regression analysis included seven variables, compared with four in Eq. [6]. Equations [11] and [12] indicate that in addition to θ , the PC and x had significant influences on K_{us} of both WSA and USA. The D had significant influence on the K_{us} of USA but not WSA. The ϵ is not a variable controlling K_{us} of either USA or WSA aggregates. The variables PC, D , and θ in Eq. [12] are ones that often change at the microscale during wetting of unstable soils. Both PC and D are structural indices. Thus, Eq. [12] indicates that the structural parameters D and PC play important roles in determining the spatial distribution of K_{us} at the microscale, particularly in unstable soils.

Even though K_{us} was computed using D , i.e., Eq. [6], Eq. [11] indicates that the accuracy of K_{us} of WSA is independent of D . On the other hand the accuracy of K_{us} of USA is strongly influenced by D (Eq. [12]). The results indicate that D should be determined more accurately using Eq. [6] for K_{us} estimation of unstable soil than stable soil. The increased sensitivity of K_{us} to D in USA may be due to slaking, which might have brought about significant changes in both inter- and intraaggregate ϵ and $1 - \epsilon$, i.e., variables used in the computation of D and thereby of K_{us} .

Equation [12] indicates that the larger the value of D , the smaller was K_{us} . This is similar to that reported by Rasiah (1995) for the influence of D , computed from number-size distribution of aerial ϵ , on K_e . The D used for K_{us} distribution estimations at the microscale in this study was from CAT and was obtained in a nondestructive and repetitive manner, which is not feasible in the conventional procedure (the number-size distributions) used for routine D computation.

CONCLUSIONS

Based on theoretical considerations, simplicity, and the type of data (moisture content vs. suction) required for K_{us} distribution estimation at the microscale, we chose the Fuentes equation. Water content and ϵ data from CAT along with D computed using ϵ , were used in the Fuentes equation for K_{us} distribution estimation. Stepwise regression analysis indicated that K_{us} estimates were sensitive to structural parameters, D and PC, which

changed during wetting of unstable soils. This indicates the importance and the need for the incorporation of data on structural parameters in equations used for K_{us} estimations of unstable soils. Because θ , ϵ , PC, and D are computed from CAT data, the ability of the CAT system to discriminate the attenuation between θ and soil particles of wet soil would largely determine the accuracy of K_{us} estimates. The s associated with θ is large, indicating inaccuracies in attenuation discrimination of wet soil. Currently, we are working on improvements in instrumentation including a gamma attenuation amplifier and the use of dual-source gamma attenuation (Phogat et al., 1991) to remedy the situation. Because ϵ , PC, and D computations do not involve wet soil data, their estimates from CAT are accurate.

REFERENCES

- Alexander, L., and R.W. Skaggs. 1986. Predicting unsaturated hydraulic conductivity from soil water characteristics. *Trans. ASAE* 29: 176-184.
- Aylmore, L.A.G. 1993. Use of computer-assisted tomography in studying water movement around plant roots. *Adv. Agron.* 49:1-54.
- Crawford, J.W. 1994. The relationship between structure and the hydraulic conductivity of soil. *Eur. J. Soil Sci.* 45:493-501.
- Fuentes, C., M. Vauclin, J. Parlange, and R. Haverkamp. 1996. A note on the soil-water conductivity of a fractal soil. *Transp. Porous Media* 23:31-36.
- Hainsworth, J.M., and L.A.G. Aylmore. 1988. Application of computer assisted tomography (CAT) to gamma attenuation measurement of soil water content. *Aust. J. Soil Res.* 26:105-110.
- Logsdon, S.D. 1995. Analysis of aggregate fractal dimensions and aggregate densities back-calculated from hydraulic conductivity. *Soil Sci. Soc. Am. J.* 59:1216-1221.
- Millington, R.J., and J.P. Quirk. 1961. Permeability of porous solids. *Trans. Faraday Soc.* 57:1200-1206.
- Phogat, V.K., and L.A.G. Aylmore. 1989. Evaluation of soil structure by using computer assisted tomography. *Aust. J. Soil Res.* 27: 313-323.
- Phogat, V.K., and L.A.G. Aylmore. 1996. Computation of hydraulic conductivity of porous material using computer assisted tomography. *Aust. J. Soil Res.* 34:671-678.
- Phogat, V.K., L.A.G. Aylmore, and R.D. Schuller. 1991. Simultaneous measurement of the spatial distribution of soil water content and bulk density. *Soil Sci. Soc. Am. J.* 55:908-915.
- Rasiah, V. 1995. Fractal dimension of surface-connected macropore count-size distributions. *Soil Sci.* 159:105-108.
- Rasiah, V., and L.A.G. Aylmore. 1998. Characterizing the changes in soil porosity by computed tomography and fractal dimension. *Soil Sci.* 163:203-211.
- Rasiah, V., and B.D. Kay. 1995. Characterizing rate of wetting: Impact on structural destabilization. *Soil Sci.* 160:176-182.
- Rieu, M., and G. Sposito. 1991. Fractal fragmentation, soil porosity, and soil water properties: I. Theory. *Soil Sci. Soc. Am. J.* 55: 1231-1238.
- SAS Institute. 1991. SAS/STAT procedures guide for personal computers. Version 6 ed. SAS Inst., Cary, NC.
- Tyler, S.W., and S.W. Wheatcraft. 1990. Fractal processes in water retention. *Water Resour. Res.* 26:1047-1054.

Sensitivity of selected water retention functions to compaction and inherent soil properties

V. Rasiyah^A and L. A. G. Aylmore^{AB}

^A Soil Science and Plant Nutrition, The University of Western Australia, Nedlands, WA 6907.

^B Corresponding author; e-mail: aylmore@cyllene.uwa.edu.au

Abstract

It is known that field-scale variations in subsurface hydraulic characteristics are influenced, to a large extent, by soil properties. Limited information, however, exists on the sensitivity of hydraulic functions to field-scale variations in soil properties. The sensitivity of 4 soil water retention functions, $\theta(h)$, to variations in soil properties and changes in bulk density (ρ) across and within soils along a 500-m transect has been assessed in this study. The $\theta(h)$ functions compared are those of van Genuchten, Brooks and Corey, Campbell, and Gardner. Water retention characteristics for 7 soils, each packed to 2 relative ρ , were established for each function. The coefficient of determination, R^2 , for the best fit of water retention ranged from 0.79 to 0.98 for the Gardner and Campbell functions, from 0.92 to 0.99 for the Brooks and Corey function, and from 0.83 to 0.99 for the van Genuchten function. Simple linear regression analysis indicated the nonlinear slope parameters of the 4 functions were more strongly correlated with soil properties. However, only the van Genuchten slope parameters were sensitive to changes in ρ . No consistency existed between the sensitivity of the linear parameters of the 4 functions and soil properties, and none were sensitive to changes in ρ . Except for the α parameter in the van Genuchten function, all the parameters in this function can be predicted with satisfactory confidence from soil properties and ρ . The results indicate that, of the 4 functions assessed, the van Genuchten $\theta(h)$ function is the most sensitive to field-scale variations in soil properties along a transect in a landscape unit and to changes in ρ .

Additional keywords: soil water, bulk density, texture.

Introduction

Information on field-scale variations in subsurface soil hydraulic characteristics is required for the modelling of water and solute transport and for efficient allocation of resources in precision farming in a landscape unit. Experimental determination of field-scale variations in hydraulic characteristics is time-consuming and costly. Recently, large emphasis has been placed on the estimation of water retention, i.e. the relation between volumetric water content (θ) and pressure head (h), the $\theta(h)$ function, from inherent soil properties (e.g. Puckett *et al.* 1985; Rajkai *et al.* 1996). Because all of the existing $\theta(h)$ functions are empirical, the selection of an appropriate function for a specific purpose is laborious and time-consuming.

McCuen *et al.* (1981) related the parameters in the Brooks and Corey (1964) $\theta(h)$ function to soils belonging to different textural classes. Madankumar (1985) correlated the parameters in the Campbell (1974) function to bulk density (ρ), sand, silt, and clay contents of different soils. Different forms of the van Genuchten (1980) $\theta(h)$ function have been tested for Belgian soils by Vereecken

et al. (1989). Recently, Rajkai *et al.* (1996) assessed the use of several forms of the van Genuchten (1980) $\theta(h)$ function to predict water retention of Swedish soils from soil properties and ρ . Their results indicate that $\theta(h)$ can be predicted for a wide range of soil textures even though the parameters of the van Genuchten $\theta(h)$ function, which have been shown to be sensitive to ρ across soils, were not sensitive to the changes in ρ of a given soil. Further, the soils used in the above studies were collected from different unrelated locations, i.e. not representing the influence of the gradual changes in soil properties in a landscape unit or along a transect, on water retention.

The influence of the changes in ρ on the $\theta(h)$ function is important, particularly when the tillage systems change or when compaction occurs. No-till and reduced-till systems are receiving attention among farmers as sustainable systems for arable cropping. It is well known that a switch from conventional to a no-till or reduced-till system usually results in increases in ρ , at least in the top 0–5 cm. Thus, it seems clear the procedures used to predict the $\theta(h)$ function from soil properties should take into consideration the influence of the changes in ρ induced by management practices on $\theta(h)$. However, Carter (1990) indicated that soil texture has an impact on ρ , implying that ρ should be standardised for textural differences. To this end, he proposed the concept of relative ρ . The objectives of this study were to investigate whether the parameters of the Brooks and Corey (1964), Gardner *et al.* (1970), Campbell (1974), and van Genuchten (1980) $\theta(h)$ functions are sensitive to variations in soil properties along a transect in a landscape unit and changes in ρ across and within soil along the transect, and whether changes in the $\theta(h)$ function can be predicted from soil properties and ρ .

Materials and methods

Water retention functions

Of the several $\theta(h)$ functions that exist, the van Genuchten (1980) function is now most commonly used, although the Brooks and Corey (1964) function was, until recently, frequently used. The simplest form of the $\theta(h)$ functions is that proposed by Gardner *et al.* (1970). Because the λ parameter in the Brooks and Corey (1964) equation is related to the b parameter of the Campbell (1974) equation, it seems logical that any comparison involving the Brooks and Corey (1964) function should include the Campbell (1974) form.

The Brooks and Corey (1964) equation is

$$\theta(h) = \theta_r + (\theta_s - \theta_r)\beta h^{-\lambda} \quad (1)$$

where θ_s is saturation water content, θ_r is residual water content, and β and λ are fitting parameters. The β parameter is equal to $h_e^{-\lambda}$ where h_e is the air-entry value. The λ parameter is considered as an index of pore size distribution.

The van Genuchten (1980) equation is

$$\theta(h) = \theta_r + (\theta_s - \theta_r)/[(1 + (\alpha h)^n)^m] \quad (2)$$

where α , m , and n are fitting parameters with $0 < m < 1$ and $m = 1 - 1/n$.

The Campbell (1974) equation is

$$\theta(h) = \theta_s(h/h_e)^{-1/b} \quad (3)$$

where b is a fitting parameter and $1/b$ is assumed equal to λ in Eqn 1.

The Gardner *et al.* (1970) equation is

$$\theta(h) = ph^{-q} \quad (4)$$

where p and q are fitting parameters.

A comparison of Eqns 1-4 indicates that the slope parameters of these functions are nonlinear. The best fit of these functions, except Eqn 2, has usually been carried out using a linear best fit procedure, after log transformation. For consistency, we used the Marquardt (1963) nonlinear optimisation procedure to fit the 4 functions.

Soil samples

The soils used in this study were collected from a farm in Ontario, Canada. In the general classification system, the soil at the site is classified as a Brookston clay to clay loam (Typic Haplaquept). Soil samples were collected from 7 locations along a 500-m transect, 9 m wide, in a landscape unit under a conventional tillage system (ploughing in autumn followed by secondary tillage in spring). The transect traversed a range of soil mapping units. With a spade, about 10 kg of soil was collected from the 0-15 cm depth from each location. These samples were separately air-dried to constant moisture content and the large clods in the samples were manually broken to aggregates (<2 cm). The samples were then passed through a sieve with mesh openings of 4 mm and the material <4 mm was transferred to labelled bags for use in water retention determination and soil characterisation.

Soil characterisation

Determinations of texture (Gee and Bauder 1986), organic matter content (Nelson and Sommers 1986), and pH (McLean 1986) were carried out using the <4 mm material. All determinations were repeated 4 times and the results of these analyses are summarised in Table 1.

Table 1. Selected properties of the soils
OM, organic matter; values are averages of 4 measurements

Soil no.	Clay	Silt (%)	OM	pH	Soil no.	Clay	Silt (%)	OM	pH
1	8.5	18.4	2.3	7.33	5	27.6	52.5	2.7	7.40
2	24.1	50.8	3.3	7.20	6	35.3	47.3	4.3	7.50
3	25.7	49.7	3.7	7.30	7	36.7	50.4	3.7	7.40
4	25.8	54.5	3.2	7.30					

Bulk density adjustments

Bulk density can be used as an index to characterise the state of compaction of a given soil under different management practices. It has, however, limited value when different soils are compared, because density can vary with texture and organic matter. In order to remove this limitation, the concept of relative bulk density has been introduced (Carter 1990). Briefly, the relative bulk density is equal to the measured bulk density divided by the maximum bulk density of the soil obtained under a standard compaction treatment (-200 kPa). The bulk densities for these soils under the standard compaction were calculated using the regression equations developed by Kay *et al.* (1993). These equations were developed using the same inherent soil properties listed in Table 1. The relative bulk densities along the zero and conventional till transects were 0.87 (s.e. 0.02) and 0.79 (s.e. 0.02), respectively (Kay *et al.* 1993). The maximum bulk density under standard compaction for a given soil multiplied by 0.79 is referred to as low ρ for that soil. Similarly the value obtained after multiplication by 0.87 is referred to as high ρ . The values of low ρ computed for the soils from locations 1-7 are 1.288, 1.288, 1.327, 1.311, 1.327, 1.264, and 1.288 g/cm³, respectively, and the corresponding high ρ are 1.451, 1.433, 1.433, 1.415, 1.433, 1.362, and 1.362 g/cm³, respectively.

Water retention

Water retention for the 7 soils, separately packed in columns to low and high ρ for each soil, was determined using a pressure plate apparatus. The soil (i.e. <4 mm in size) was packed in aluminum columns 4.8 cm internal diameter and 2.5 cm in height. Subsequent to adjustment for air-dry moisture content, the amount of soil required to pack a column at a given density for a given soil was weighed and the packing was carried out using the procedure described by Klute (1986). A cheesecloth was tied to one of the circular faces of the columns to hold the soil in the columns while packing and wetting. There were 6 replicates for a soil packed to given ρ . The packed columns were set on a tray, containing 1 cm depth of distilled water, for 48 h to reach saturation. After saturation, the columns were transferred to a pressure plate apparatus and the water content was determined after equilibration at tensions of -5, -10, -30, -60, -100, and -200 kPa.

The saturation water content, θ_s , used in Eqns 1-3, was computed as

$$\theta_s = 1 - \rho/\rho_p$$

where ρ_p is particle density which was taken as 2.65 g/cm³ and ρ is the density of soil in the packed column.

Statistical analysis

The statistical analysis of the data was conducted using the SAS/STAT computer software packages (SAS Institute 1991). The simple linear best fit procedure was used for correlation analysis and the multiple regression procedure was used for multivariable best fit analysis. The water content-tension data were fitted to the 4 $\theta(h)$ functions using the Marquardt (1963) nonlinear fitting procedure.

Table 2. R^2 values obtained for the different water retention functions during optimisation using the Marquardt (1963) technique

Soil no.	van Genuchten		Brooks and Corey		Campbell and Gardner	
	Low ρ	High ρ	Low ρ	High ρ	Low ρ	High ρ
1	0.98	0.90	0.98	0.99	0.98	0.98
2	0.97	0.90	0.99	0.95	0.84	0.96
3	0.93	0.90	0.96	0.94	0.96	0.95
4	0.95	0.83	0.99	0.92	0.81	0.92
5	0.96	0.99	0.98	0.99	0.98	0.97
6	0.94	0.91	0.99	0.97	0.79	0.98
7	0.95	0.91	0.99	0.95	0.84	0.96

Results and discussion

Comparison of best fits

The water retention data fitted to the 4 $\theta(h)$ functions, for each soil packed to both low and high ρ , produced significant fits at $P = 0.05$ (Table 2). Fig. 1 shows that the retention curves varied with the $\theta(h)$ function and soil type. Similar trends were observed for the other 5 soils (not shown). The functions seem to fit the range in suction for the 7 soils without leaving any outlier, implying no limitation of fitting the functions to the ranges in suction used in this study. The R^2 values for the best fits were >0.90, except for 5 of the 56 best fits (Table 2). The R^2 for each of the 4 functions fitted to the low ρ condition in soil

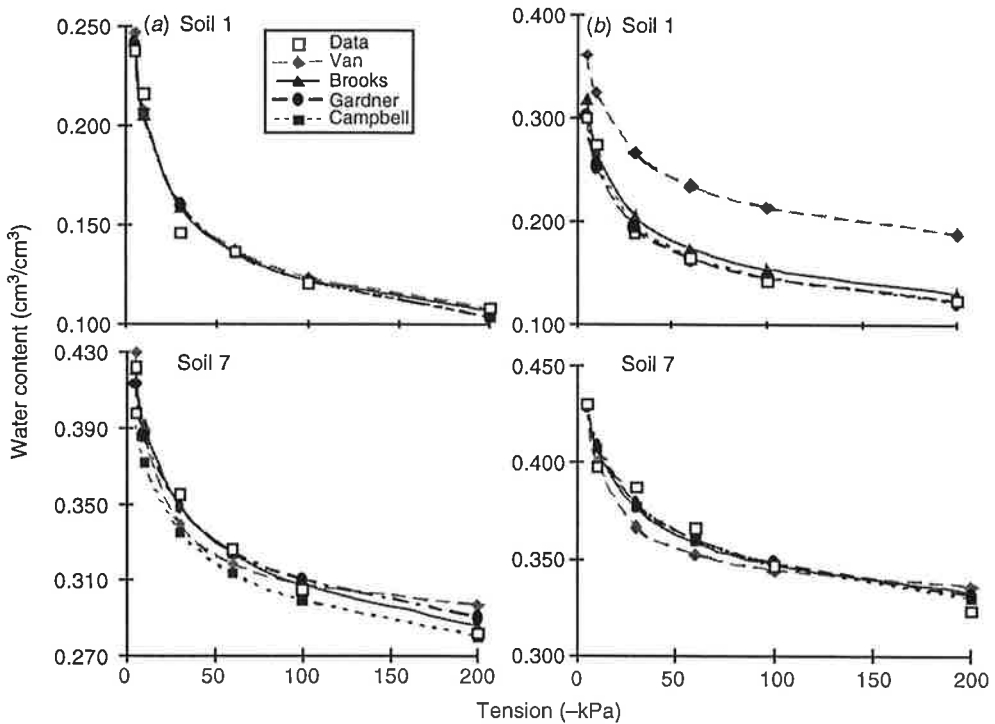


Fig. 1. Relation between water content and soil water pressure head for the soils at locations 1 and 7, at (a) low and (b) high densities.

Table 3. Estimates of the parameters in Eqns 1-4 obtained using the Marquardt (1963) nonlinear optimisation technique

Soil	p	q	h_e	b	$\theta_r(1)$	β	λ	$\theta_r(2)$	α	n	m
<i>At low ρ</i>											
1	0.349	0.229	0.401	4.358	0.035	0.840	0.290	0.043	1.437	1.316	0.240
2	0.382	0.212	0.519	4.706	0.010	0.874	0.224	0.112	0.561	1.562	0.360
3	0.391	0.159	0.318	6.272	0.010	0.833	0.166	0.137	0.784	1.425	0.298
4	0.411	0.121	0.371	7.595	0.003	0.870	0.117	0.223	0.629	1.500	0.333
5	0.424	0.104	0.322	8.311	0.010	0.910	0.138	0.192	0.530	1.484	0.326
6	0.476	0.098	0.279	10.159	0.045	0.964	0.119	0.263	0.468	1.528	0.346
7	0.482	0.096	0.305	10.453	0.016	0.922	0.110	0.271	0.470	1.518	0.341
<i>At high ρ</i>											
1	0.446	0.243	1.124	4.105	0.010	1.090	0.268	0.042	0.339	1.233	0.189
2	0.441	0.202	1.071	4.937	0.010	1.078	0.225	0.060	0.195	1.191	0.160
3	0.443	0.102	0.366	9.796	0.066	0.898	0.131	0.193	0.726	1.350	0.259
4	0.436	0.081	0.205	11.399	0.053	0.968	0.125	0.299	0.741	1.510	0.338
5	0.450	0.077	0.191	12.957	0.125	0.858	0.120	0.287	0.662	1.490	0.329
6	0.460	0.066	0.143	15.106	0.223	0.836	0.166	0.318	0.633	1.542	0.352
7	0.479	0.070	0.143	14.259	0.184	0.836	0.135	0.316	0.861	1.445	0.308

1 was 0.98. On the other hand, the R^2 obtained using Eqn 2 for the same soil under high ρ was the lowest and there were few or no differences among the R^2 values obtained for Eqns 1, 3, and 4. Similar difficulties were encountered

in identifying the most suitable function, for a given soil, based on R^2 values alone. The results suggest that other criteria, in addition to R^2 , have to be used to select the most appropriate function for a given soil and the test condition imposed.

Table 4. Simple linear correlations between soil properties and the parameters in Eqns 1-4

Parameter	Clay+silt	pH	Organic matter	Bulk density
p	+0.47n.s.	+0.52*	+0.31n.s.	+0.43n.s.
q	-0.77**	-0.85**	-0.56*	-0.10n.s.
h_e	-0.52n.s.	-0.69*	-0.43n.s.	+0.39n.s.
b	+0.61*	+0.83**	+0.54*	+0.12n.s.
β	-0.25n.s.	-0.34n.s.	-0.22n.s.	-0.45n.s.
$\theta_r(1)$	+0.27n.s.	+0.59*	+0.40n.s.	+0.22n.s.
λ	-0.83**	-0.72**	-0.54*	+0.08n.s.
α	-0.35n.s.	-0.10n.s.	-0.22n.s.	-0.28n.s.
$\theta_r(2)$	+0.73*	+0.84**	+0.57*	-0.06n.s.
n	+0.61*	+0.63*	+0.46n.s.	-0.53*
m	+0.59*	+0.64*	+0.45n.s.	-0.54*

* $P < 0.05$; ** $P < 0.01$; n.s., not significant.

Estimates of parameters, their dependency on soil properties, and the interrelations

The parameter values in Table 3 suggest that they varied with soil type and ρ . The discussions in this report will concentrate mostly on the nonlinear slope parameters, because the shape of the water retention curves depended largely on the values of these parameters (De Jong *et al.* 1983). The values of λ , in Eqn 1, ranged from 0.11 to 0.29 and decreased with increasing clay+silt and organic matter (OM) contents, and pH (Table 4). The influence of ρ on λ was not significant. Values of n ranged from 1.191 to 1.562 and those of m from 0.16 to 0.36 (Table 3). The n or m values increased with increasing clay+silt content and pH, and decreased with increasing ρ (Table 4). Values of b ranged from 4.105 to 15.106 and q from 0.066 to 0.243 (Table 3). The b parameter increased with increasing clay+silt and OM contents, and pH, whereas the opposite trend was observed for q (Table 4). Neither b nor q was sensitive to changes in ρ .

Recently, Rajkai *et al.* (1996) indicated that, for Swedish soils, larger values of n were characteristic of coarse-textured soils, whereas the opposite was the case for fine-textured soils. Our results are just the opposite to those reported by the above workers. Rajkai *et al.* (1996) reported that larger values of n and m for coarse-textured soils are consistent with the hypothesis that water retention decreased rapidly with increasing n and m . Even though water retention decreased rapidly in the coarse-textured soil in the present study (Fig. 1), we suggest the shape of the retention curves depends not only on the values of n and m but on a combination of n , m , θ_s , θ_r , and α . This is supported by the fact that the correlation between soil properties and θ_r is much stronger than that between n and soil properties (Table 4). Further, according to van Genuchten and Nielsen (1985), values of n should be greater than unity. In our study, all of the values of n are >1 , whereas the majority of the values of n reported by Rajkai *et al.* (1996) are <1 . Thus, the values of n obtained in this study and the trend shown with soil properties seem to be satisfactory.

The trend for the values of λ to decrease with increasing clay+silt and OM contents and pH is consistent with the findings of Blumb *et al.* (1992). Values of b showed a trend similar to that observed for λ which is consistent with the findings of Cosby *et al.* (1984). Even though q showed a trend similar to b and λ , comparable information with regard to the sensitivity of q to variations in soil properties is scarce. The results indicate, in general, the nonlinear slope parameters of water retention functions are sensitive to variations in clay+silt and OM contents and pH along the transect. However, only n and m of Eqn 2 are sensitive to changes in ρ , in addition to variations in soil properties.

The linear parameters in the $\theta(h)$ functions seem to be less strongly influenced by soil properties or ρ than the nonlinear slope parameters (Table 4). For example, α in Eqn 2 or β in Eqn 1 are not significantly influenced by soil properties or ρ . The θ_r in Eqn 2 was influenced by soil properties but not that in Eqn 1. The linear parameters θ_e , in Eqn 3, and p , in Eqn 4, are sensitive to variations in soil properties. The results suggest that, unlike the nonlinear parameters, the linear parameters did not show consistent trends to variations in soil properties.

Table 5. Linear correlation matrix for the parameters in Eqns 1-4

	q	h_e	b	β	$\theta_r(1)$	λ	$\theta_r(2)$	α	n	m
p	-0.63*	n.s.	n.a.	n.s.	n.a.	n.a.	n.a.	-0.54*	n.a.	n.a.
q		n.a.	0.99**	n.a.	n.a.	0.81**	n.a.	n.a.	-0.63*	-0.65*
h_e			0.73**	0.81**	n.a.	n.a.	n.a.	n.s.	n.a.	n.a.
b				n.a.	n.a.	-0.71*	n.a.	n.a.	0.55*	0.56*
β					n.s.	n.s.	n.a.	-0.68*	n.a.	n.s.
$\theta_r(1)$						n.s.	0.64*	n.a.	n.a.	n.a.
λ							n.a.	n.a.	-0.64*	-0.65*
$\theta_r(2)$								n.s.	0.73*	0.73*
α									n.s.	n.s.
n										0.99*

* $P < 0.05$; ** $P < 0.01$; n.s., not significant; n.a., not applicable.

The nonlinear slope parameters n , m , λ , b , and q are correlated with each other (Table 5). The parameters n and m were negatively correlated with λ , whereas the opposite trend was observed between b and n or m , and between b and q . The linear parameters of the 4 functions were not correlated to each other, except for p and α . It seems the nonlinear slope parameters in a given function can be predicted from the values of the corresponding parameters in the other functions, i.e. using relations similar to those in Table 5. However, similar predictions of linear parameters seem difficult. The linear parameter p and the nonlinear parameter q of Eqn 4 were correlated to each other. A similar trend existed between h_e and λ of Eqn 3, suggesting that if one of the parameters is known the other could be predicted. No similar correlations existed between the linear and nonlinear parameters of Eqns 1 and 2, suggesting the linear and nonlinear parameters of these two functions are independent and difficult to predict one from the other.

Predictive equations

Soil properties and ρ values that had significant influence on the parameters of the $\theta(h)$ functions (Table 4) were used as predictor variables in multiple regression analysis to develop predictive equations for nonlinear slope parameters. The predictive equations are

$$n = -0.29 + 0.0021(\text{clay} + \text{silt}) + 0.35(\text{pH}) - 0.73\rho \quad (6)$$

$$(R^2 = 0.64, P < 0.01)$$

$$m = -0.71 + 0.0011(\text{clay} + \text{silt}) + 0.20(\text{pH}) - 0.39\rho \quad (7)$$

$$(R^2 = 0.64, P < 0.01)$$

$$\lambda = 1.77 - 0.0019(\text{clay} + \text{silt}) - 0.19(\text{pH}) \quad (8)$$

$$(R^2 = 0.76, P < 0.01)$$

$$b = -177.15 + 0.034(\text{clay} + \text{silt}) - 25.04(\text{pH}) \quad (9)$$

$$(R^2 = 0.71, P < 0.01)$$

$$q = 2.87 - 0.0013(\text{clay} + \text{silt}) - 0.36(\text{pH}) \quad (10)$$

$$(R^2 = 0.81, P < 0.01)$$

In the above equations, all the coefficients are significant at $P = 0.05$. Simple linear correlations (Table 4) showed that OM content had a significant influence on λ , b , and q . However, when the multivariable fit was carried out, the coefficient for OM was found not to be significant. Consequently, we excluded OM as a predictor variable for λ , b , and q and repeated the analysis, obtaining Eqns 8–10. Only 64% of the variability in n or m was accounted for by soil properties and ρ , compared to more than 70% by soil properties alone for λ , b , and q . The magnitude of the R^2 values obtained for the above equations suggests the predictions obtained using Eqns 8–10 should be better than those obtained using Eqns 6 or 7. However, the sensitivity analysis indicated this was not so. For example, the predicted value of n , obtained using Eqn 6, for soil 7 at low ρ is 1.54, whereas the experimental value is 1.52. On the other hand, the predicted value of λ , obtained using Eqn 8, for soil 7 is 0.20, whereas the experimental value is 0.11. Similar trends were observed for b and q . Further, the predicted values of λ , b , and q are independent of ρ and this led to unrealistic predictions for changes in ρ . The analysis indicated the slope parameters of the van Genuchten $\theta(h)$ function are more sensitive to variations in soil properties and to changes in ρ than those in the other 3 functions.

In the context of Australian soils, we foresee that in addition to clay, silt, and OM contents and pH, aluminium content, soil acidity, shrink–swell characteristics, and the duplex nature may have an influence on the hydraulic parameters of water retention functions. The shrink–swell characteristics and the duplex nature may have a direct impact on bulk density. Thus, further research

should be directed to elucidate the influence of these factors on water retention parameters.

Conclusions

The 4 water retention functions, $\theta(h)$, of van Genuchten, Brooks and Corey, Campbell, and Gardner were assessed for their sensitivity to variations in soil properties and to changes in bulk density (ρ) within and across soils along a transect. The results indicate that variations in soil properties along the transect had significant influence on the water retention parameters of the 4 functions. However, out of the 4 $\theta(h)$ functions assessed, the van Genuchten equation was the most sensitive to spatially variable soil properties, the only function sensitive to changes in ρ , across and within soil, and was predicted with the highest confidence. The results from this study indicate that unsaturated flow and water balance simulations in spatially variable landscape units require information on $\theta(h)$ which is sensitive to inherent soil properties and to changes in ρ . The results also indicate a potential for these $\theta(h)$ functions to be predicted from easily available soil survey data, provided a large data set is initially used to establish the predictive equations.

Acknowledgments

The authors gratefully acknowledge the resources provided by the Australian Research Council (Project No. A39231995) during the preparation of this manuscript.

References

- Blumb, A. C., Murphy, C. L., and Everett, L. G. (1992). A comparison of three functional forms for representing soil moisture characteristics. *Ground Water* **30**, 177–85.
- Brooks, R. H., and Corey, A. T. (1964). Hydraulic properties of porous media, Hydrology paper no. 3. Colorado State University, Fort Collins, Colorado, USA.
- Campbell, G. S. (1974). A simple method for determining unsaturated conductivity from moisture retention data. *Soil Science* **117**, 311–14.
- Carter, M. R. (1990). Relative measures of soil bulk density to characterize compaction in tillage studies on fine loamy sands. *Canadian Journal of Soil Science* **70**, 425–33.
- Cosby, B. J., Hornberger, G. M., Clapp, R. B., and Ginn, T. R. (1984). A statistical extrapolation of the relationships of moisture characteristics to the physical properties of soils. *Water Resources Research* **14**, 682–90.
- De Jong, R., Campbell, C. A., and Nicholaichuk, W. (1983). Water retention equations and their relationship to soil organic matter and particle size distribution for disturbed samples. *Canadian Journal of Soil Science* **63**, 291–302.
- Gardner, W. R., Hillel, D., and Benyamini, Y. (1970). Post-irrigation movement of soil water. 1. Redistribution. *Water Resources Research* **6**, 851–61.
- Gee, G. W., and Bauder, J. W. (1986). Particle-size analysis. In 'Methods of Soil Analysis, Part 2'. (Ed. A. Klute.) pp. 383–411. (ASA and SSSA: Madison, WI.)
- van Genuchten, M. Th., and Nielsen, D. R. (1985). On describing and predicting the hydraulic properties of unsaturated soils. *Annals Geophysics* **3**, 615–28.
- van Genuchten, M. Th. (1980). A closed form equation for predicting hydraulic conductivity of unsaturated soils. *Soil Science Society of America Proceedings* **35**, 3–8.
- Kay, B. D., da Silva, A., Denholm, K., Eshraghi, N., Perfect, E., and Rasiah, V. (1993). Methodologies for assessing soil structure and for predicting crop response to changes in soil quality. Final Report on National Soil Conservation Project. Project, XSE90-00403-302, University of Guelph.
- Klute, A. (1986). 'Water Retention: Laboratory Methods, Methods of Soil Analysis, Part 1.' (Ed. A. Klute.) pp. 635–60. (ASA and SSSA: Madison, WI.)

- McCuen, R. H., Rawls, W. H., and Brakensiek, D. L. (1981). Statistical analysis of Brooks-Corey and Green-Ampt parameters across soil textures. *Water Resources Research* **17**, 1005-13.
- McLean, E. O. (1986). Soil pH and lime requirement. In 'Methods of Soil Analysis, Part 2'. (Ed. L. A. Page.) pp. 539-79. (ASA and SSSA: Madison, WI.)
- Madankumar, N. (1985). Prediction of soil moisture characteristics from mechanical analysis and bulk density data. *Agricultural Water Management* **10**, 305-12.
- Marquardt, W. D. (1963). An algorithm for least squares sum of nonlinear parameters. *Journal Society of Industrial Applied Mathematics* **11**, 431-41.
- Nelson, D. W., and Sommers, L. E. (1986). Total carbon, organic carbon, and organic matter content. In 'Methods of Soil Analysis, Part 2'. (Ed. L. A. Page.) pp. 539-79. (ASA and SSSA: Madison, WI.)
- Puckett, W. E., Dane, J. H., and Hajek, B. F. (1985). Physical and mineralogical data to determine soil hydraulic properties. *Soil Science Society of America Journal* **49**, 831-6.
- Rajkai, K., Kabos, S., van Genuchten, M. Th., and Jansson, P. (1996). Estimation of water-retention characteristics from bulk density and particle-size distribution of Swedish soil. *Soil Science* **161**, 832-44.
- Statistical Analysis System Institute (1991). 'SAS/STAT Procedure Guide for Personal Computers.' Version 5. (SAS Institute, Inc.: Cary, NC.)
- Vereecken, H., Maes, H., Feyen, J. and Darius, P. (1989). Estimating the soil moisture retention characteristic from texture, bulk density, and carbon content. *Soil Science* **148**, 389-403.

DEGRADATION RATES OF EIGHT PESTICIDES IN SURFACE AND SUBSURFACE SOILS UNDER LABORATORY AND FIELD CONDITIONS

H. J. Di, L. A. G. Aylmore, and R. S. Kookana¹

The rate at which a pesticide is degraded in both the surface and subsurface soils is an important factor in determining the groundwater contamination potential of the pesticide. Degradation rates of eight pesticides used commonly in Western Australia—chlorpyrifos, chlorothal dimethyl, fenamiphos, linuron, metalaxyl, metribuzin, prometryne and propyzamide—in the surface (0–25 cm) and subsurface (25–50 cm) layers of a sandy soil, were studied under controlled incubation conditions and were compared with those under field conditions. Field degradation rates were also simulated on the basis of degradation rates measured in the laboratory, taking into account the effects of temporal variations in field moisture and temperature.

The incubation study showed that the eight pesticides had widely different degradation rates in both the surface and subsurface soils, with half-lives ranging from 23 to 142 days. Four of the pesticides had lower degradation rates in the subsoil than in the surface soil, but the reverse was observed for the other four pesticides. It is postulated that the nonuniform changes in degradation rates with soil depth were probably caused by interactive effects of changes in soil microbial activities and in organic matter content (and thus pesticide sorption) in the different soil layers. No consistent relationship was found between field degradation rates and those measured in the laboratory. The simulated field half-lives were all longer than those measured in the laboratory and did not match all the field-measured degradation rates. (Soil Science 1998;163:404–411)

Key words: Pesticide, degradation, half-life, surface soil, subsurface soil, incubation, field study, simulation.

THE rate at which an organic pesticide is degraded in the soil, mainly by micro-organisms, is one of the key factors that affects the pesticide's groundwater contamination potential. A given pesticide's likelihood of reaching the groundwater is affected by degradation rates in subsurface as well as surface layers of the unsaturated soil zone (Bromilow et al. 1986; Pothuluri et al. 1990; Bergstrom 1996). Degradation rates in subsurface layers may differ significantly from

those in the surface layer because of changes in soil conditions such as organic matter content, microbial activity, moisture content, and temperature (Hamaker 1972; Bollag and Liu 1990; Fomsgaard and Albaiges 1995; Smelt et al. 1995). Inasmuch as *in situ* degradation rates in the field are difficult to measure, they are often assumed to decrease with soil depth in modeling studies (Jury et al. 1987; Di et al. 1995; Di and Aylmore 1997) because soil conditions are less favorable for pesticide degradation in subsoil than in the surface soil. However, at this time there is insufficient understanding of how pesticide degradation rates change with soil depth in the unsaturated soil zone.

It is easier to measure pesticide degradation rates under controlled laboratory conditions than under field conditions. However, laboratory

Soil Science and Plant Nutrition, University of Western Australia, Nedlands, W.A. 6009. Dr. Aylmore is corresponding author. E-mail: aylmore@cyllene.uwa.edu.au

¹Present address: CRC for Soil and Land Management, Glen Osmond, South Australia.

Received July 24, 1997; accepted Jan. 5, 1998.

degradation rates may be significantly different from those measured under field conditions as a result of differences in factors, such as moisture and temperature, that affect bio-degradation greatly. Walker and associates (Walker 1974; Walker and Barnes 1981) attempted to simulate field degradation rates based on those measured under controlled laboratory conditions, taking into account the moisture and temperature effects. This method of simulation, however, has not been widely tested.

The objectives of this study were: (i) to compare the degradation rates of eight pesticides in the surface and subsurface layers of a sandy soil in Western Australia; (ii) to compare degradation rates measured in controlled laboratory conditions with those from field conditions; and (iii) to compare simulated field degradation-rates with those measured in the field. Pesticide degradation rate in this study was measured by the rate of decline of pesticide concentration in the soil, presumably attributable mainly to microbial breakdown although other dissipation processes cannot be ruled out (Torstensson 1987; Scheu-ner 1992).

MATERIALS AND METHODS

Laboratory Incubation

Surface (0–25 cm) and subsurface (25–50 cm) samples were taken from a sandy soil located in a vegetable research station about 20 km south of Perth in Western Australia. The area had not previously been treated with pesticides. The samples were sieved (2 mm) while moist. Relevant properties of the soil are summarized in Table 1.

Eight pesticides used widely in horticulture and agriculture in the region were studied (Table 2). These pesticides represent a wide range of water solubility and sorption coefficient (Green and Karickhoff 1990).

An amount of moist soil equivalent to 1 kg of oven-dry soil was used for each pesticide. The moisture content of the soil was adjusted to that equivalent to a 100-cm water-head suction. An appropriate amount of pesticide (ranging from 1 to 10 mg active ingredient per kg soil, depending

on recommended rates) was mixed thoroughly with the soil and incubated at a constant 25°C under aerobic conditions. Three replicate pots were set up for each pesticide. Subsamples of 50 g of soil were taken at different intervals up to about 130 days after application. The three samples for each treatment were bulked together for each sampling time and were mixed thoroughly for subsequent extraction and analysis.

Detailed extraction and analytical procedures can be found in Kookana et al. (1995), and a summary is provided here. The pesticides were extracted by shaking 5 g moist soil overnight with 10 mL of 90% acetonitrile in water. The solution was then centrifuged and filtered through a 0.22 µm membrane. Pesticide concentration in the solution was then determined on a high performance liquid chromatograph (HPLC, Waters) equipped with a multiple wavelength UV/visible detector, an autosampler, and an automated gradient controller. Reversed-phase chromatography was employed using a µBondapak-C18 column (Lawrence 1982), with acetonitrile or methanol in water as the mobile phase. Analyses were carried out at 30°C with 50-µL injections and flow rates between 1.5 and 2.0 mL min⁻¹. In addition to the eight pesticides, the two toxic metabolites of fenamiphos—fenamiphos sulfoxide and fenamiphos sulfone—were also analyzed. Separation of F. sulfoxide and F. sulfone peaks was obtained by decreasing the acetonitrile concentration in the mobile phase compared with that used for fenamiphos (Singh 1989). The recoveries varied with the pesticides. Reproducible recoveries greater than 80% were obtained for most of the pesticides studied, except for chlorthal dimethyl, where the reproducible recovery was 60%. Pesticide concentrations in the soil were calculated on the basis of the recoveries at day zero.

Field Experiment

A field experiment to study the leaching and degradation behavior of the pesticides was carried out on the same sandy soil as that used for the incubation. Details of the experiment have been given elsewhere (Kookana et al. 1995). In

TABLE 1
Soil properties

Soil layer (cm)	Texture		pH (H ₂ O)	Organic C (%)	Microbial C (µg C/g soil)	Bulk density (g/cm ³)
	Sand (%)	Silt+clay (%)				
0–25	98	1	5.3	0.53	21	1.58
25–50	98	1	5.5	0.15	15	1.62

TABLE 2
Pesticides studied and their properties

Common name	Chemical name	Uses	Water solubility† (mg/L)	k_{oc} †
Chlorpyrifos	O,O-diethyl O-3,5,6-trichloro-2-pyridyl phosphorothioate	Insecticide	0.4	6070
Chlorthal dimethyl	Dimethyl tetrachloroterephthalate	Herbicide	0.5	5000
Fenamiphos	Ethyl 4-methylthio- <i>m</i> -tolyl isopropylphosphoramidate	Nematicide	400	100
Linuron	3-(3,4-dichlorophenyl)-1-methoxy-1-methylurea	Herbicide	75	400
Metalaxyl	Methyl <i>N</i> -(2-methoxyacetyl)- <i>N</i> -(2,6,xylyl)-DL-alaninate	Fungicide	8400	61
Metribuzin	4-amino-6- <i>tert</i> -butyl-3-methylthio-1,2,4-triazine-5(4H)-one	Herbicide	1220	268
Prometryne	<i>N,N'</i> -di-isopropyl-6-methylthio-1,3,5-triazine-2,4-diyldiamine	Herbicide	33	400
Propyzamide	3,5-dichloro- <i>N</i> -(1,1-dimethyl propynyl)benzamide	Herbicide	15	775

†From Worthing (1983) and Wauchope et al. (1992).

brief, aqueous pesticide solutions of commercial products were sprayed to the surface of field plots. Irrigation was applied daily and, together with rainfall, provided an average net daily recharge rate of 1.59 mm during the experimental period from July to December. The mean minimum and maximum temperatures during this period were 10 and 22°C, respectively. Soil samples were taken at different intervals after pesticide application at 5-cm increments down to 50 cm of the profile. Three cores were taken from each of three replicate plots on each sampling day. The core holes were refilled with soil from the buffer zones. For each layer, the soil core samples for each treatment at each sampling day were bulked together and mixed thoroughly for extraction and analysis as outlined above.

Simulation of Field Degradation Rate

A summary of the simulation model is included below and more details can be found in Walker (1974) and Nicholls et al. (1982). The model simulates pesticide degradation rates in the surface layer of field soils, using degradation rates measured in the laboratory for the same layer of soil, taking into account moisture and temperature effects. Pesticide degradation is assumed to follow a first-order reaction. An empirical relationship between degradation half-life and moisture content is used:

$$t_{1/2} = a(MC)^{-b} \quad (1)$$

where $t_{1/2}$ is degradation half-life, MC is moisture content, and a and b are constants.

The relationship between degradation half-life and temperature is assumed to follow the Arrhenius equation:

$$\log[(t_{1/2})_1/(t_{1/2})_2] = [\Delta E/2.303R](1/T_1 - 1/T_2) \quad (2)$$

where $(t_{1/2})_1$ and $(t_{1/2})_2$ are the half-lives at temperature T_1 and T_2 respectively, ΔE is the activation energy and R is the gas content. A combined form of Eqs. (1) and (2) was given by Graham-Bryce et al. (1982).

Field soil-moisture content in the surface layer is simulated by assuming that incoming rain occurs at an even rate during the first half of the day and evaporation occurs at an even rate during the second half of the day. The moisture content increases with incoming rain up to the field capacity.

Field soil temperature is simulated on the basis of mean air temperature and daily amplitude about the mean empirical equations that have been shown to be applicable to a number of different soils in different parts of the world (Walker and Barnes 1981).

RESULTS AND DISCUSSION

Comparison of Degradation Rates in Surface and Subsurface Soils

Changes of residual pesticide concentration in the soil as a function of time, measured under laboratory incubation conditions, can generally be described by first-order reaction equations (Figs. 1 and 2 and Table 3). Deviations from the first-order reaction, however, were obvious for

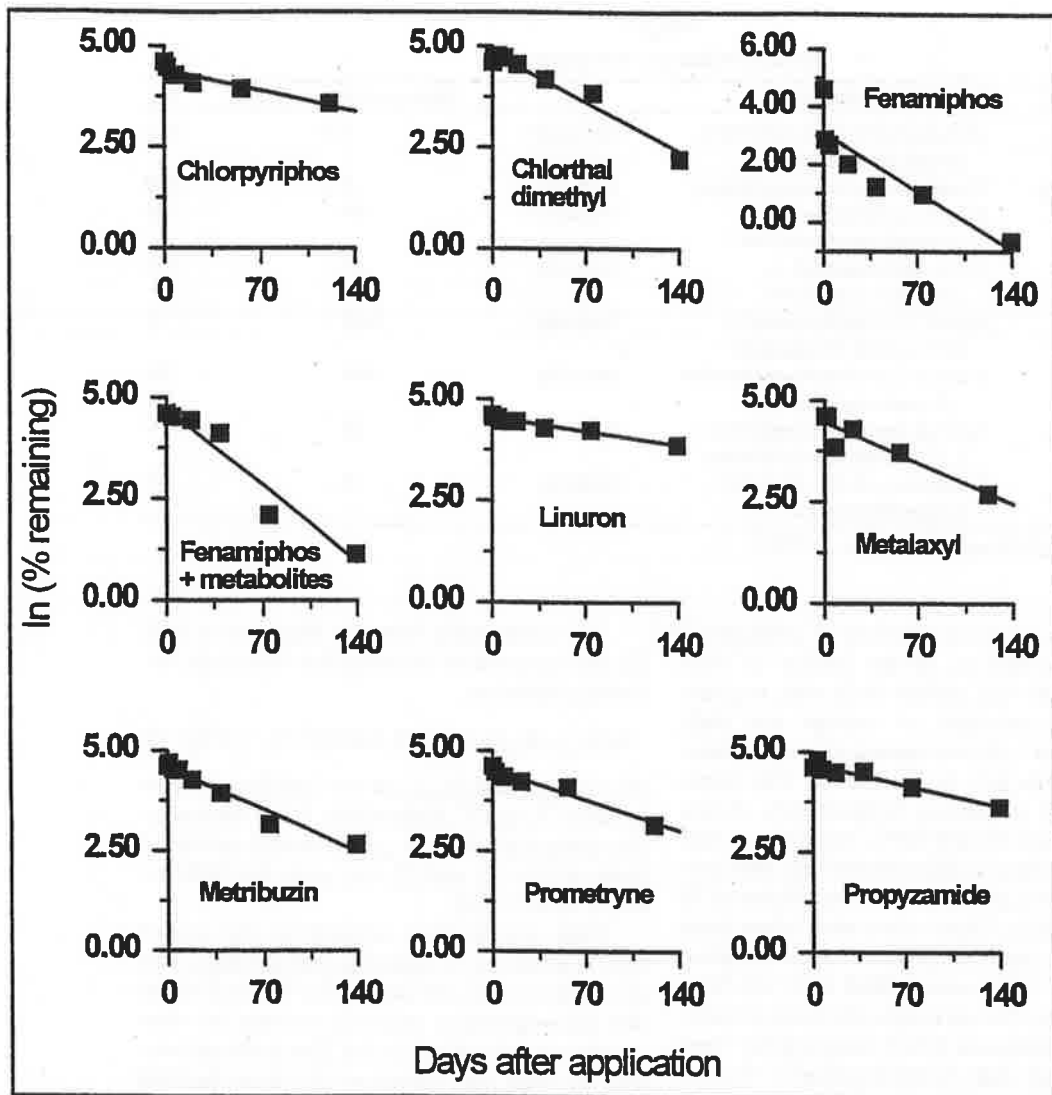


Fig. 1. Plots of first-order regressions between percentage pesticide remaining and days after application in the surface soil.

fenamiphos in the surface soil and for chlorthal-dimethyl in the subsurface soil.

The eight pesticides showed widely different degradation rates in both the surface and subsurface soils, as illustrated by the different degradation rate constants or half-lives (Table 3). Many of these half-lives differ significantly from those reported in the literature (Wauchope et al. 1992) because of differences in soil and environmental conditions.

Four of the pesticides—fenamiphos, metalaxyl, metribuzin, and prometryne—had half-lives in the subsurface soil from two to more than

four times those in the surface soil, probably because of lower microbial activities in the subsoil (Tables 1 and 3). However, the other four pesticides—chlorpyrifos, chlorthal dimethyl, linuron, and propyzamide—had shorter half-lives in the subsoil. The higher degradation rates in the subsoil than in the surface soil contradicted the usual assumption in modeling studies that degradation rates decrease with soil depth (Jury et al. 1987; Di and Aylmore 1997).

This nonuniform trend in degradation rates with soil depth may be partly attributable to a dual role that soil organic matter plays in affecting

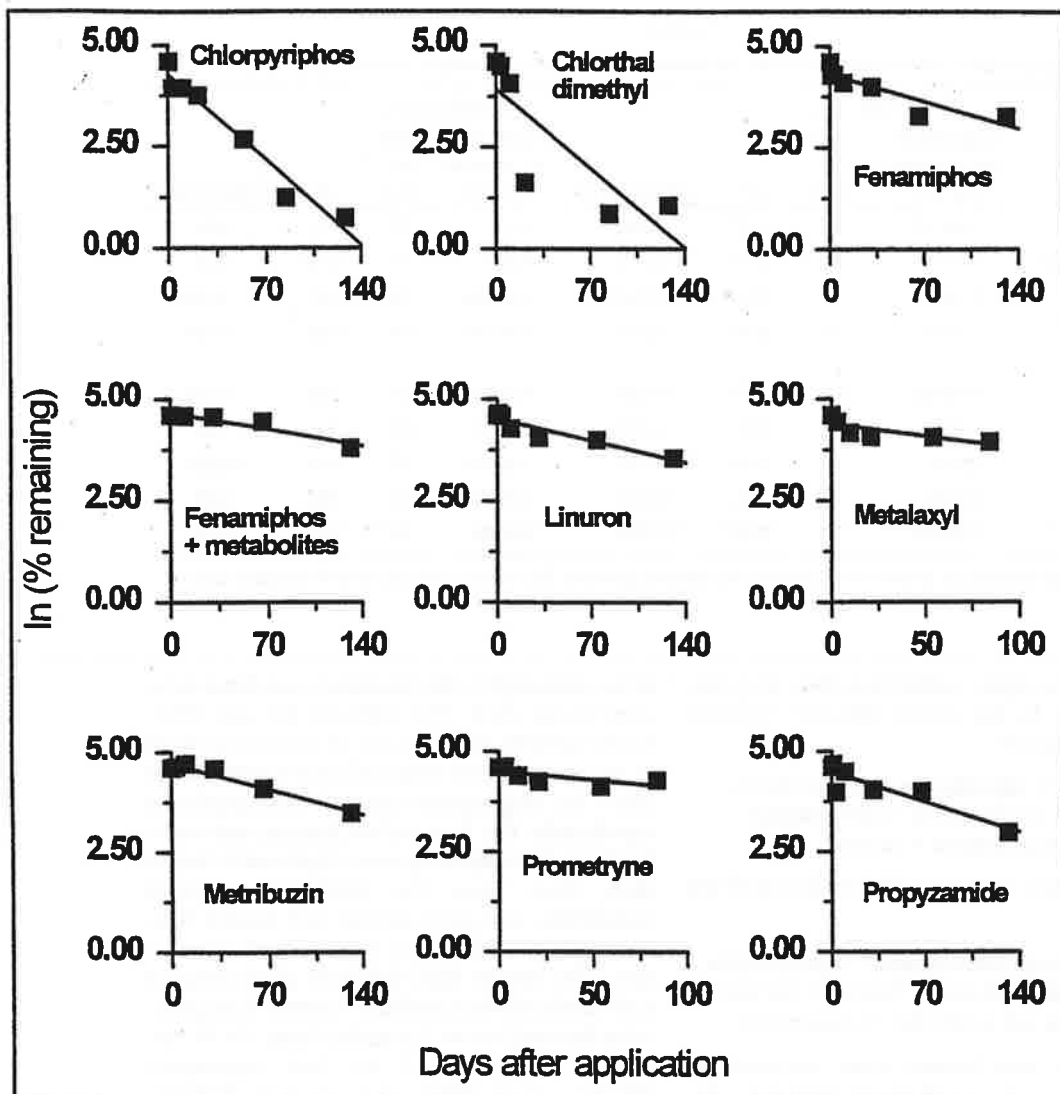


Fig. 2. Plots of first-order regressions between percentage pesticide remaining and days after application in the subsurface soil.

microbial activity on the one hand and pesticide sorption on the other (Rao et al. 1993). A decrease in soil organic matter content with soil depth may reduce soil microbial activity and thus pesticide degradation rate; however, a decrease in soil organic matter content also reduces pesticide sorption, and this may increase the degradation rate (Hamaker 1972). The pesticides that showed higher degradation rates in the subsoil in this study were generally less water soluble and had higher sorption coefficients (Table 2). Therefore, as organic matter decreases in the subsoil, a positive effect on degradation rate due to decreased

sorption, might outweigh a negative effect on degradation rate due to increased microbial activity, particularly for those pesticides with lower water solubility and higher sorption coefficients (Tables 2 and 3). This interactive effect on sorption on degradation rate may depend on soil organic matter content, the capacity of the organic material to stimulate microbial activity, and on the sorption coefficient of the pesticide. However, it is also possible that the different soil layers contain different microbial populations, which are preferential degraders of different compounds. This could be one reason for the different rank-

TABLE 3
Degradation rates in the surface and subsurface soils from the laboratory incubation study

Pesticide	Surface soil				Subsurface soil			
	Degradation rate constant (per day)	Half life (day)	R ²	F Significance	Degradation rate constant (per day)	Half life (day)	R ²	F Significance
Chlorpyrifos	0.00747	93	0.88	0.006	0.03	23	0.91	0.01
Chlorthal dimethyl	0.0173	40	0.96	<0.001	0.029	24	0.63	0.03
Fenamiphos	0.0289	24	0.8	0.006	0.00956	72	0.81	0.005
Fenamiphos + metabolites†	0.0270	26	0.94	0.001	0.00580	119	0.90	0.004
Linuron	0.00487	142	0.97	<0.001	0.00786	88	0.88	0.005
Metalaxyl	0.0144	48	0.87	0.006	0.0059	117	0.62	0.06
Metribuzin	0.0151	46	0.96	<0.001	0.00905	77	0.96	<0.001
Prometryne	0.0108	64	0.96	<0.001	0.0049	141	0.56	0.08
Propyzamide	0.00755	92	0.95	<0.001	0.0108	64	0.82	0.005

†Analyses included fenamiphos and two intermediate degradation products, fenamiphos sulfoxide and fenamiphos sulfone.

ing order of the eight pesticides in their degradation half-lives. In the surface soil, the half-lives followed the order:

fenamiphos < chlorthal dimethyl, metribuzin,
metalaxyl < prometryne < propyzamide,
chlorpyrifos < linuron;

In the subsurface soil, the half-lives followed the order:

chlorpyrifos, chlorthal dimethyl < propyzamide
< fenamiphos, metribuzin < linuron < metalaxyl,
fenamiphos and metabolites < prometryne.

There are two known toxic intermediate degradation products from fenamiphos: fenamiphos sulfoxide and fenamiphos sulfone. In the surface soil, the two intermediate products did not register a significant effect on the degradation half-life; in the subsoil, a significantly longer half-life was observed when the two intermediate degradation products were taken into account than when these products were ignored (Table 3). This indicates that the two intermediate degradation products were more resistant in the subsoil.

Comparison of Degradation Rates from Incubation, Field Study, and Simulation

Table 4 shows there was no consistent relationship between the half-lives measured in the laboratory and those measured in the field. For chlorpyrifos, chlorthal dimethyl, and prometryne, the half-lives were rather similar between

those measured in the laboratory and those measured in the field. This indicates that the differences between the two sets of conditions (field vs. incubation) were of insufficient magnitudes to affect the degradation rates of these pesticides significantly. For fenamiphos, linuron, and metalaxyl, the field half-lives were significantly longer than those from the incubation, whereas metribuzin and propyzamide had shorter half-lives from the field study than from the incubation. The longer field half-lives of fenamiphos and metalaxyl were probably because both pesticides leached below the surface layer (0–25 cm) during the period of the field experiment (Kookana et al. 1995) and because the half-lives of these pesticides were in the subsoil longer than in the surface soil (Table 3). The other pesticides remained mostly within the surface soil during the field experiments. It is clear that for some pesticides, significant errors may occur if the laboratory degradation rates are used directly to represent those for the field conditions.

The simulation (Walker 1974) was aimed at relating the degradation rates measured under controlled laboratory conditions to those of variable field conditions. Table 4 shows that the simulated field half-lives were all longer than the laboratory half-lives on which the simulations were based. This indicates that the field conditions (temperature and moisture) were less favorable for degradation than were the laboratory conditions. For fenamiphos, linuron, and metalaxyl, the simulated half-lives were better estimates of the

TABLE 4

Comparison of degradation half-lives from laboratory incubation (surface soil, 0–25 cm), field study, and from simulation

Pesticide	Half-life		
	By incubation	Field-measured	Simulated†
Chlorpyrifos	93	81	115
Chlorthal dimethyl	40	45	50
Fenamiphos	24	43	32
Fenamiphos + metabolites	26	98	30
Linuron	142	219	172
Metalaxyl	48	70	60
Metribuzin	46	27	56
Prometryne	64	58	80
Propyzamide	92	59	114

†Simulated field half-lives using those from the laboratory incubation.

Regression results:

Field-measured (y) vs. incubation (x): $y=1.19x$; $R^2=0.54$;Field-measured (y) vs. incubation (x): $y=0.96x$; $R^2=0.52$.

field half-lives than the laboratory measured half-lives; for chlorpyrifos, metribuzin, prometryne, and propyzamide, the laboratory-measured half-lives were better estimates of the field half-lives than the simulated ones. Overall, no clear improvement was provided by the simulation to estimate field degradation rates on the basis of those measured in the laboratory.

Handling of the soil samples used in the laboratory incubation could have had a significant impact on the composition and activity of micro-organisms, thus differentiating the degradation rates measured in the laboratory from those measured in the field. The possibility of changes in microbial properties as a result of sample handling deserves close attention when translating laboratory-measured degradation rates to field degradation rates. Errors could also have been introduced to the simulated degradation rates by inaccurate predictions of field soil moisture and temperature conditions.

CONCLUSIONS

Degradation rates of the eight pesticides differed widely in both the surface and subsurface soils, with degradation half-lives ranging from 23 to 142 days. Although the microbial biomass was lower in the subsurface than in the surface soil, all of the degradation rates did not decrease in the subsoil: four of the eight pesticides showed higher degradation rates in the subsoil than in the surface soil. No consistent relationship was found between laboratory-determined and field-determined degradation rates, and, overall, no clear improvement was provided by the simulation to

estimate field degradation rates on the basis of those measured in the laboratory.

ACKNOWLEDGMENTS

Funding of the project by the Land and Water Resources Research and Development Corporation of Australia is gratefully acknowledged.

REFERENCES

- Bergstrom, L. 1996. Model predictions and field measurements of chlorsulfuron leaching under non-steady-state flow conditions. *Pest. Sci.* 48:37–45.
- Bollag, J. M., and S. Y. Liu. 1990. Biological transformation processes of pesticides. In *Pesticides in the soil environment: Processes, impacts, and modelling*. H. H. Cheng (ed.). SSSA, Madison, WI, pp. 169–211.
- Bromilow, R. H., G. G. Briggs, M. R. Williams, J. H. Smelt, L. G. M. T. Tuinstra, and W. A. Traag. 1986. The role of ferrous ions in the rapid degradation of oxamyl, methomyl and aldicarb in anaerobic soils. *Pest. Sci.* 17:535–547.
- Di, H. J., R. S. Kookana, and L. A. G. Aylmore. 1995. Application of a simple model to assess the ground water contamination potential of pesticides. *Aust. J. Soil Res.* 33:1031–1040.
- Di, H. J., and L. A. G. Aylmore. 1997. Modeling the probabilities of groundwater contamination by pesticides. *Soil Sci. Soc. Am. J.* 61:17–23.
- Fomsgaard, I., and J. Albaiges. 1995. Degradation of pesticides in subsurface soils, unsaturated zone—A review of methods and results. *Int. J. Environ. Anal. Chem.* 58:231–245.
- Green, R. E., and S. W. Karickhoff. 1990. Sorption estimates for modeling. In *Pesticides in the soil environment: Processes, impacts, and modelling*. H. H. Cheng (ed.). SSSA, Madison, WI, pp. 79–101.

- Graham-Bryce, I. J., P. H. Nicholls, R. J. Baker, R. J. Hance, S. J. Embling, and D. Hill. 1982. Movement of fluometuron and ^{14}C in soil under field conditions: Computer simulations. *Weed Res.* 22: 271-283.
- Hamaker, J. W. 1972. Decomposition: Quantitative aspects. In *Organic chemicals in the soil environment*, vol. 1. C. A. I. Goring and J. W. Hamaker (eds.). Marcel Dekker, New York, pp. 253-340.
- Jury, W. A., D. D. Focht, and W. J. Farmer. 1987. Evaluation of pesticide groundwater pollution potential from standard indices of soil-chemical adsorption and biodegradation. *J. Environ. Qual.* 16: 422-428.
- Kookana, R. S., H. J. Di, and L. A. G. Aylmore. 1995. A field study of leaching and degradation of nine pesticides in a sandy soil. *Aust. J. Soil Res.* 33: 1019-1030.
- Lawrence, J. F. 1982. High performance liquid chromatography of pesticides. In *Analytical methods for pesticides and growth regulators*, vol. XIII. G. Zweeig and J. Sherma (eds.). Academic Press, New York.
- Nicholls, P. H., R. H. Bromilow, and T. M. Addiscott. 1982. Measured and simulated behavior of fluometuron, aldoxycarb and chloride ion in a fallow structured soil. *Pest. Sci.* 13:475-483.
- Pothuluri, J. V., T. B. Moorman, D. C. Obenhuber, and R. D. Wauchope. 1990. Aerobic and anaerobic degradation of alachlor in samples from a surface-to-groundwater profile. *J. Environ. Qual.* 19:525-530.
- Rao, P. S. C., C. A. Bellin, M. L. Brusseau, and D. L. Linn. 1993. Coupling biodegradation of organic chemicals to sorption and transport in soils and aquifers: Paradigms and paradoxes. In *Sorption and degradation of pesticides and organic chemicals in soil*. Proceedings of a symposium, Denver, CO, 30 Oct 1991. SSSA, Madison, WI, pp. 1-26.
- Scheunert, I. 1992. Transformation and degradation of pesticides in soil. In *Chemistry of plant protection*. 8. Terrestrial behavior of pesticides. W. Ebing (ed.). Springer-Verlag, Berlin, pp. 23-75.
- Singh, R. 1989. Simultaneous determination of Fenamiphos, its sulfoxide and sulfone in water by high performance liquid chromatography. *Analyst* 114:425-427.
- Smelt, J. H., A. E. van de Peppel-Groen, M. Leistra, and A. E. Van de Peppel-Groen. 1995. Transformation of aldicarb sulfoxide and aldicarb sulfone in four water-saturated sandy subsoils. *Pest. Sci.* 44: 323-334.
- Torstensson, N. T. L. 1987. Microbial decomposition of herbicides in soil. In *Herbicides*. D. H. Hutson and T. R. Roberts (eds.). John Wiley & Sons, Ltd, New York, pp. 249-270.
- Walker, A. 1974. A simulation model for prediction of herbicide persistence. *J. Environ. Qual.* 3:396-401.
- Walker, A. 1987. Evaluation of a simulation model for prediction of herbicide movement and persistence in soil. *Weed Res.* 27:143-152.
- Walker, A., and A. Barnes. 1981. Simulation of herbicide persistence in soil: a revised computer model. *Pest. Sci.* 12:123-132.
- Wauchope, R. D., T. M. Buttler, A. G. Hornsby, P. M. W. Augustijn-Beckers, and J. P. Burt. 1992. The SCS/ARS/CES pesticide properties database for environmental decision-making. *Rev. Environ. Contamin. Toxicol.* 123:1-164.
- Worthing, C. R. 1983. *The pesticide manual*, 7th Ed. The British Crop Protection Council, Suffolk, UK.

Computed tomography data on soil structural and hydraulic parameters assessed for spatial continuity by semivariance geostatistics

V. Rasiah^A and L. A. G. Aylmore^{AB}

^A Soil Science and Plant Nutrition, The University of Western Australia, Nedlands, WA 6907, Australia.

^B Author to whom correspondence should be addressed.

Abstract

Visual observations on the spatial distribution, at 1-cm intervals, of bulk density (ρ), porosity (ϵ), fractal dimension (D), water content (θ), and unsaturated hydraulic conductivity (K_{us}) in uniformly packed soil columns showed randomness. We explore the use of semivariance geostatistics to clarify the issue of randomness and continuity on the spatial distribution of ρ , ϵ , D , θ , and K_{us} data obtained using a custom-built gamma scanner and computed tomography technique. Semivariance increased with increasing lag distance and plots of semivariance *v.* lag distance produced spherical semivariograms for most of the soil parameters investigated. This indicated that even though randomness existed in the spatial distribution of the soil parameters, there existed specific trends in their spatial continuity. Higher spatial continuity, in water stable aggregates, was characterised by smaller values of semi-, sill-, and nugget-variances and larger values of span. Opposite trends were observed for unstable aggregates. Wetting in unstable aggregates produced further reductions in span increases for other geostatistical parameters, indicating that wetting decreased spatial continuity. The results indicate that geostatistical analysis is useful to clarify the issue of randomness at very small scales and to quantify and discriminate the influence of differences in structural stability and wetting-induced changes in the spatial continuity of soil parameters, particularly ϵ .

Additional keywords: spatial continuity, porosity, water content, conductivity, CAT scanning.

Introduction

The spatial distribution, particularly the vertical distribution, in soil pore systems can have a significant impact on water transport. In unstable soils the distribution may change during wetting and drying or compaction. These changes are usually characterised by dry bulk density (ρ) (Carter 1990), porosity (ϵ) (Phogat and Aylmore 1989; Phogat *et al.* 1991; Rasiah and Aylmore 1998a), and/or fractal dimension, (D), (Rasiah 1995; Rasiah and Aylmore 1998a). Fuentes *et al.* (1996) proposed a theoretical relation between unsaturated hydraulic conductivity (K_{us}), and ϵ and D and this has been experimentally verified by Rasiah and Aylmore (1998b). Although the latter workers indicated that ϵ varied randomly in space, they did not provide statistical evidence to support their claim.

Geostatistics is a powerful tool to quantify spatial variability and continuity of soil properties (Burgess and Webster 1980; Knighton and James 1984; Grevers and de Jong 1994). Geostatistics is based on the observation that the variabilities of all regionalised variables, i.e. variables distributed in space, have a particular structure (Journel and Huijbregts 1978) where they vary randomly in space but also have some degree of spatial continuity (Davis 1986). Geostatistical analyses

have often been applied to macro- or field-scale variations (e.g. Knighton and James 1985), but very seldom to variations at the micro-scale, i.e. at scales <1 cm (e.g. Grevers and de Jong 1994). For example, Grevers and de Jong (1994) used 50 X-ray scan sections, each of 1 mm, and showed that geostatistical analysis was useful to discriminate the spatial variability and continuity of soil macropores in subsoils. Even though the macropore system plays a major role in water and solute transport under saturated conditions, it is ϵ that has a large impact under unsaturated conditions, a condition that is common in the field. Further, Grevers and de Jong (1994) obtained their data in a destructive manner and used an impregnation technique which may alter pore sizes during impregnation, thereby rendering the data less reliable. On the other hand, the data on ϵ from the laboratories of the Soil Science and Plant Nutrition Department, University of Western Australia (Phogat *et al.* 1991; Rasiah and Aylmore 1998a) were obtained *in situ*, in a non-destructive and repetitive manner, and are free from any impregnations. These workers have successfully used a custom-built scanner and computed tomography techniques to gather data on ϵ at scales as small as 2 mm. In this study we explore the use of semivariance geostatistics to clarify the issue of randomness and continuity on the spatial distribution of ρ , ϵ , D , θ , and K_{us} , at scales as small as 1-cm intervals, obtained using a custom-built scanner and computed tomography techniques.

Materials and methods

Porous materials

The porous materials used in this study were water-stable artificial soil aggregates and an unstable soil. The unstable soil material was collected from the surface (0–7 cm) at a farm in Calingri, Western Australia. It is a sandy loam with 19.3% clay, 12.6% silt, and 68.1% sand. The air-dried soil and the water-stable material were separately crushed to obtain 2 aggregates of 4 and 0.25–0.71 mm. Aggregates of a given size from each material were packed in acrylic cylinders (i.d. 7.2 cm, height 15 cm) to a height of 10 cm. The base of each column had 24 holes (diam. 1.5 mm) drilled in 2 concentric rings. This enabled the columns to be wetted slowly from the base. During packing care was taken to produce uniformity in ρ along the length of the column. The ρ values for each column are given in Table 1.

Table 1. Measured bulk density (ρ) before and after wetting, and saturated hydraulic conductivity (K_ϵ) in the columns

Aggregate size (mm)	ρ		K_ϵ (cm/h)
	Before	After	
	(Mg/m ³)		
	<i>Stable aggregates</i>		
2–4	0.507	0.551	0.745a
0.25–0.71	0.656	0.676	0.086b
	<i>Unstable aggregates</i>		
2–4	1.196	1.224	0.147a
0.25–0.71	1.387	1.318	0.006b

^A Values followed by the same letter are not significantly different at $P = 0.05$.

After packing, each column was scanned at 10-mm depth increments using a counting time of 3 s. The linear attenuation (μ) obtained from scanning was the input to a 'Multi-CAT' program which computed an average μ and σ for each depth increment. The columns were

then slowly wetted from the base in deionised water, contained in a large beaker, and allowed to saturate. After saturation, the saturated hydraulic conductivity (K_e) was determined using a constant head of water and a Mariotte bottle (Table 1). The columns were then drained for 15 min to 1 h depending on soil type and rescanned for the determination of θ (Table 2). Subsequent to the determination of θ , the columns were force air-dried in an oven at 35°C to constant moisture content equal to that which existed before wetting. The decrease or increase in column height, if any, was recorded and these changes were used for the computation of measured ρ that occurred during wetting and drying. The columns were then rescanned as previously described.

Scanning system

A prototype CAT scanning system constructed in the Soil Science and Plant Nutrition Laboratories of the University of Western Australia was used in this study (Hainsworth and Aylmore 1988; Aylmore 1993). The scanner utilises a gamma source (500 mCi of caesium-137; 1 Ci = 3.7×10^{10} Bq) which is monitored by a NaI (TI) scintillation detector (Model 202-3). A detailed description and the use of the system for ρ and θ are given in Phogat *et al.* (1991) and Aylmore (1993). In this study, the beam from the scanner is collimated to produce a slice thickness of 2 mm and a pixel (picture element) size of 2 by 2 mm. As the source and the detector are fixed, the object is moved across the beam and scanned at 2-mm intervals. Successive linear scans were taken after rotating the object progressively in 5° increments through 180°. When this process was completed, the linear scans were back-projected, using filtered back-projection (Hermon 1980), for a given number of rotations to reconstruct an image of the scanned slice. When the back-projections were completed, the gamma attenuation for each pixel in the slice was determined. The system is capable of scanning columns up to 100 mm diameter and 1.5 m in height.

Computations

Bulk density and porosity

A comprehensive review of CAT scan theory, as it is applied for ρ and θ determination in porous media, is provided by Aylmore (1993). A detailed discussion on the data for ρ , and consequently ϵ , and θ used in this study is available in Rasiah and Aylmore (1998a, 1998b). In brief, the CAT scan data obtained before wetting were used for the computation of ρ , and consequently ϵ , for every 10-mm depth increment. The scan data obtained after draining the saturated columns were used for θ computation. The data obtained after redrying the wetted columns were used for computation of changes in ρ and ϵ that occurred during wetting. The ranges in ρ and ϵ for the 100 mm depth are given in Table 2.

Table 2. Ranges in unsaturated conductivity (K_{us}), water content (θ), fractal dimension (D), porosity (ϵ), and bulk density (ρ) obtained from computed tomography after wetting of columns

Aggregate size	K_{us} (cm/h)	σ (cm ³ /cm ³)	D	ϵ	ρ (Mg/m ³)
<i>Stable aggregates</i>					
2-4	3.14×10^{-4} - 1.49×10^{-2}	0.11-0.25	2.19-2.24	0.67-0.71	0.54-0.62
0.25-0.71	4.47×10^{-3} - 6.22×10^{-3}	0.31-0.32	2.15-2.20	0.60-0.69	0.58-0.73
<i>Unstable aggregates</i>					
2-4	2.81×10^{-3} - 4.11×10^{-2}	0.17-0.39	2.06-2.09	0.47-0.52	1.28-1.38
0.25-0.71	7.3×10^{-4} - 1.26×10^{-3}	0.27-0.33	2.05-2.06	0.46-0.48	1.38-1.44

Fractal dimension and unsaturated hydraulic conductivity

We used the theoretical relation provided by Fuentes *et al.* (1996) for the computation of surface D for incompletely fragmented porous media and their equation extended to predict K_{us} (Rasiah and Aylmore 1998b). Computation of D requires data on ϵ , whereas the estimation of K_{us} requires data on K_ϵ , θ , ϵ , and D . The data on ϵ , D , and θ were from the CAT scan. The K_ϵ was experimentally determined for each column, as described earlier in the text. The computed ranges in D , θ , and K_{us} for the 100-mm depth are given in Table 2.

Semivariance and semivariogram

The semivariogram is used in the theory of regionalised variables to describe spatial variations (Journel and Huijbregts 1978; Burgess and Webster 1980; Davis 1986). For example, if the values of ρ determined at points x_i , where $i = 1, 2, \dots, n$, are in a straight line in the column, then they are used to generate the values $\rho(x_i)$. The difference between $\rho(x_i)$ and $\rho(x_{i+h})$, separated by distance h (called lag distance) is characterised by the semivariance $\gamma(h)$. According to Burgess and Webster (1980), the semivariance is

$$\gamma(h) = \sum [\rho(x_i) - \rho(x_{i+h})]^2 \quad (1)$$

The plot of $\gamma(h)$ *v.* h is a semivariogram. The estimator $\gamma^*(h)$ of the semivariance $\gamma(h)$ is

$$\gamma^*(h) = [2n(h)]^{-1} \sum_{i=1}^{n(h)} [\rho(x_i) - \rho(x_{i+h})]^2 \quad (2)$$

The semivariance $\gamma(h)$ in Eqn 1 is a measure of the similarity between points separated by the lag distance h . The smaller the value of $\gamma(h)$, the more alike are the points and vice versa. The shape of the semivariogram provides a qualitative description of spatial continuity (Burgess and Webster 1980).

The values of ρ , ϵ , D , θ , and K_{us} in Table 2 were used for the computation of semivariance and the other geostatistical parameters.

Results and discussion

Shape of semivariograms

The semivariograms for the different soil parameters of the 2–4 mm water-stable aggregates (2–4WSA) and unstable aggregates (2–4USA) are shown in Figs 1 and 2, respectively. In general, the semivariograms for the water-stable aggregates are non-linear (Fig. 1); Burgess and Webster (1980) defined the non-linear forms as spherical variograms (Fig. 1). Spherical variograms indicate excellent spatial dependence or continuity of the investigated parameters (Journel and Huijbregts 1978; Davis 1986). Even though spherical variograms were obtained for the unstable aggregates, they were mostly associated with the data obtained after wetting and drying. For example, the semivariograms for ρ , ϵ , and D are spherical only for the data obtained after wetting and drying, whereas those obtained before wetting tended to be linear for ϵ and D (not shown). Compared with the spherical model, a linear model indicates only a moderate spatial dependence (Journel and Huijbregts 1978; Davis 1986).

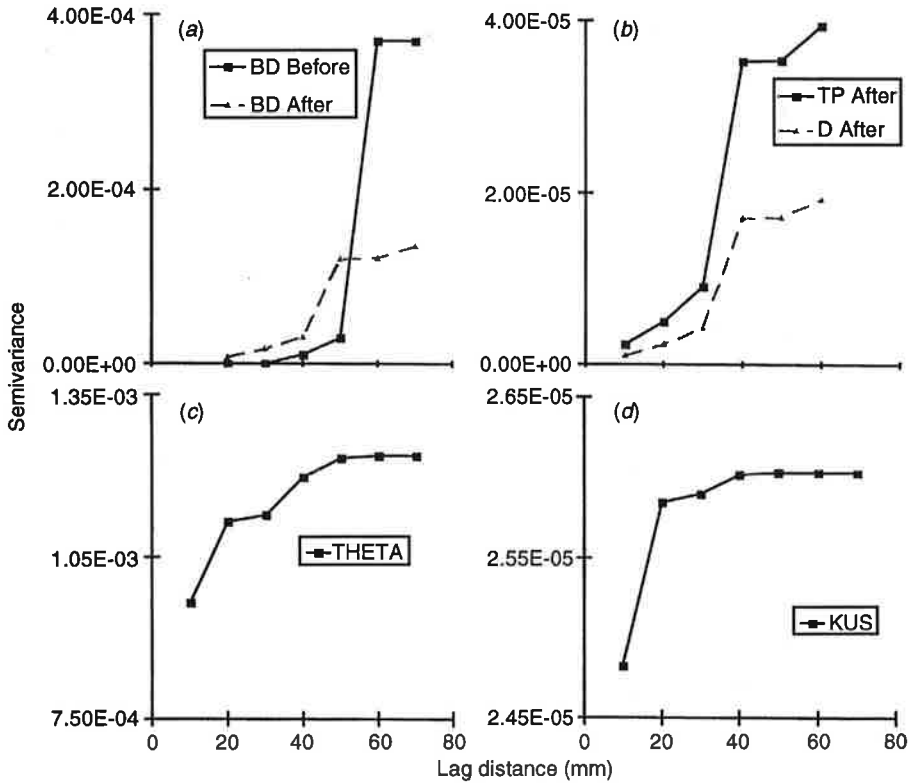


Fig. 1. Spatial distribution of (a) bulk density, (b) porosity and fractal dimension, (c) water content, and (d) unsaturated hydraulic conductivity in the 2–4 mm stable aggregate column.

For the water-stable aggregates, wetting and drying, in general, decreased the semivariance (for ρ , ϵ , and D), indicating wetting induced increases in spatial continuity (Fig. 1). On the other hand, wetting increased the semivariance in the unstable aggregates (Fig. 2), indicating that wetting induced a reduction in spatial continuity. The decreased spatial continuity in the unstable aggregates was probably due to slaking in water. In the absence of slaking, i.e. in the water-stable aggregates, wetting and drying might have enhanced favourable reorientation when wet, thereby increasing spatial continuity. In general, the semivariances for ρ , ϵ , D , and K_{us} of the water-stable aggregates were less compared with the unstable aggregates, suggesting reduced continuity in the unstable aggregates (Figs 1 and 2). The results indicate that the variations in spatial continuity induced by structural differences, at intervals as small as 1 cm, or by wetting can be quantitatively discriminated by values of semivariance.

The semivariograms for different sizes of unstable aggregates, particularly those obtained after wetting, showed spherical trends (Fig 3). In general, the semivariance was highest for ρ and least for D (Fig. 3a,c) and greater for larger aggregates than smaller aggregates (Fig. 3). The results show that semivariance varied with soil parameters and the size of aggregates.

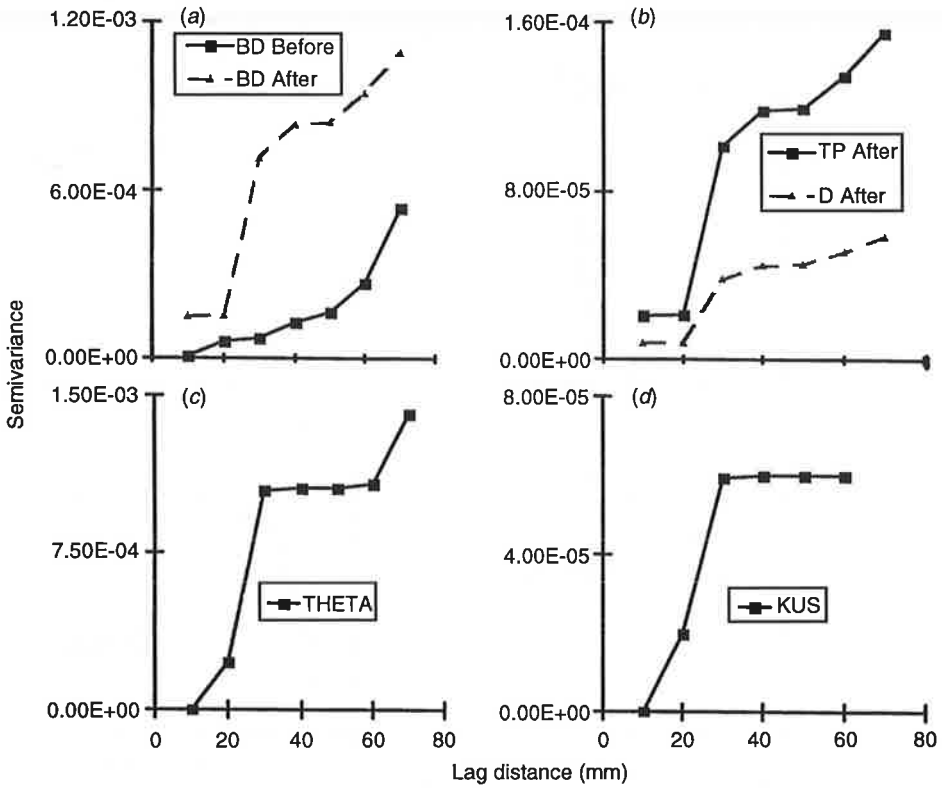


Fig. 2. Spatial distribution of (a) bulk density, (b) porosity and fractal dimension, (c) water content, and (d) unsaturated hydraulic conductivity in the 2-4 mm unstable aggregate column.

Span and sill-variance

In most instances the semivariance (Figs 1-3) asymptotically approached a maximum at a finite lag distance known as the span; the corresponding semivariance is known as the sill-variance (Burgess and Webster 1980). Most of the soil parameters of the unstable aggregates are characterised by smaller values for the span and larger values for the sill-variance, compared with the water-stable aggregates. According to Burgess and Webster (1980), the span is defined as the neighbourhood within which all the locations are related to another, i.e. indicating the region of spatial continuity. Thus, the region of spatial continuity for the unstable aggregates is smaller than that for the water-stable aggregates. An inverse relation between span and sill-variance also indicates that spatial continuity in the unstable aggregates is smaller than in the water-stable aggregates. The results indicate that span and sill-variance varied with aggregate type and size, and the soil parameters. We therefore propose the use of span and sill-variance as indices to characterise spatial continuity, at intervals as small as 1 cm, as influenced by changes in structural stability. The span values for the primary variables ρ and θ of the water-stable aggregates tended to increase with aggregate size (Table 3). No difference existed between the span of the larger and smaller unstable aggregates, suggesting that in unstable soil, aggregate slaking

during wetting produced similar spatial continuity regardless of the initial size of the unstable aggregates. The results suggest that soils with size distributions dominated by larger aggregates would probably be characterised by larger values of span and smaller values of sill-variance.

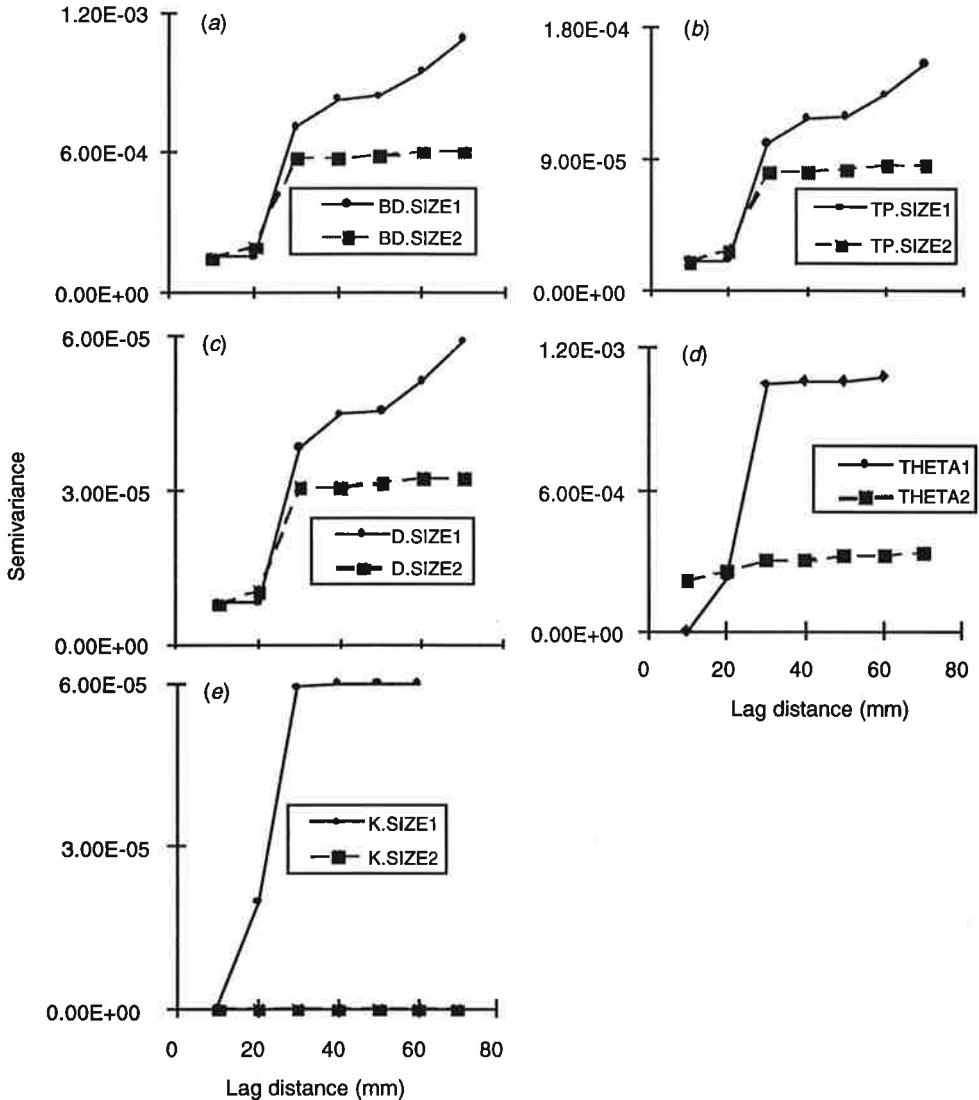


Fig. 3. Spatial distribution of (a) bulk density, (b) porosity, (c) fractal dimension, (d) water content, and (e) unsaturated hydraulic conductivity in the 2–4 mm (size 1) and 0.25–0.71 mm (size 2) unstable aggregate columns.

The span for the various parameters of different size unstable aggregates was the same (30 mm), whereas differences existed among parameters ρ , θ , and K_{us} of the water-stable aggregates. It seems that span could be used as an index to discriminate spatial continuity between structural and soil water parameters.

Table 3. Span and the corresponding semivariance for soil properties of different size aggregates obtained after wetting and drying

Parameter	Span		Semivariance	
	Size 1	Size 2	Size 1	Size 2
<i>Stable aggregates</i>				
Density	60	40	1.35×10^{-4}	1.26×10^{-4}
Porosity	40	40	3.53×10^{-5}	3.69×10^{-5}
Fractal dimension	40	40	1.71×10^{-5}	1.61×10^{-5}
Water content	40	30	1.20×10^{-3}	6.17×10^{-5}
Conductivity	20	30	2.58×10^{-5}	4.82×10^{-7}
<i>Unstable aggregates</i>				
Density	30	30	7.13×10^{-4}	5.76×10^{-4}
Porosity	30	30	1.01×10^{-4}	8.21×10^{-5}
Fractal dimension	30	30	3.83×10^{-5}	3.08×10^{-5}
Water content	30	30	1.05×10^{-3}	2.99×10^{-4}
Conductivity	30	30	5.94×10^{-5}	2.15×10^{-8}

Nugget variance

Theoretically when h (Eqn 2) approaches zero, the semivariance $\gamma(h)$ will become zero. However, the data shown in Figs 1–3 indicate this seldom occurred. The value of the intercept, i.e. that of $\gamma(h)$, when h approaches zero, is known as the nugget variance. Most of the soil parameters were characterised by finite nugget variance (Figs 1–3). Nuggets were higher for soil water parameters of the water-stable aggregates than structural parameters (Fig. 1). Wetting in general induced nuggets in the unstable aggregates and it was a less common occurrence before wetting (Figs 2 and 3). Nuggets indicate fluctuations in soil parameters that occur over distances much shorter than the sampling distance (Burgess and Webster 1980). In our study the nuggets represent fluctuations that occurred at <1 cm intervals. The existence of nuggets for soil parameters observed in our study is consistent with other reports (Webster and Cuanalo 1975; Burgess and Webster 1980).

The nuggets for ρ , ϵ , and D were similar in magnitude for the different sizes of the unstable aggregates (Fig 3). This suggests the fluctuations of the above parameters in the top 10 mm were less dependent on aggregate size. This was probably due to the fact that slaking produced similar physical conditions regardless of the initial aggregate size. Soil water parameters of the smaller unstable aggregates were characterised by distinct nuggets, but this was not so for the larger unstable aggregates. We are unable to provide any reason for this behaviour, because we anticipated the nuggets to be independent of initial aggregate size.

Conclusions

We used semivariance geostatistics to clarify the issue of randomness observed in the spatial distributions of ρ , ϵ , D , θ , and K_{us} at 1-cm intervals. Parabolic semivariograms and finite values for the geostatistical parameters semi-, sill-, and nugget-variances, and span, indicated that the distribution of the soil parameters was random but followed specific spatial continuity. The parameters quantitatively discriminated the influence of wetting and differences in structural stability on the spatial continuity of soil parameters at 1-cm intervals. Soils with high stability

were characterised by large span and semi-, sill-, and nugget variances. Therefore, we conclude that the randomness observed in the spatial distribution at 1-cm intervals was real. The spatial continuity analysis for the unstable soil indicated that the continuity broke down at depths as low as 3 cm from the surface. We therefore recommend the use of semivariance geostatistical parameters to clarify the issue of randomness, at very small scales, and spatial continuity of soil parameters such as ϵ , which has significant impact on the transport process in soil.

Acknowledgments

The authors gratefully acknowledge the financial support provided by the Australian Research Council (Project No. A39231995) during the preparation of this manuscript.

References

- Aylmore, L. A. G. (1993). Use of computer-assisted tomography in studying water movement around plant roots. *Advances in Agronomy* **49**, 1–54.
- Burgess, T. M., and Webster, R. (1980). Optimal interpolation and isarithmic mapping of soil properties. I. The semivariogram and punctual kriging. *Journal of Soil Science* **31**, 315–31.
- Carter, M. R. (1990). Relative measures of soil bulk density to characterize compaction in tillage studies of fine loamy sands. *Canadian Journal of Soil Science* **70**, 425–33.
- Davis, J. C. (1986). 'Statistics and Data Analysis in Geology.' 2nd Edn. (John Wiley: New York.)
- Fuentes, C., Vauclin, M., Parlange, J., and Haverkamp, R. (1996). A note on the soil–water conductivity of a fractal soil. *Transport in Porous Media* **23**, 31–6.
- Grevers, M. C. J., and de Jong, E. (1994). 'Evaluation of Soil-pore Continuity using Geostatistical Analysis on Macroporosity in Serial Sections Obtained by Computed Tomography Scanning.' SSSA Special Publication No. 36. pp. 73–86. (SSSA: Madison, WI.)
- Grevers, M. C. J., de Jong, E., and Arnaud, R. J. (1989). The characterization of soil macroporosity with CT scanning. *Canadian Journal of Soil Science* **69**, 629–37.
- Hainsworth, J. M., and Aylmore, L. A. G. (1988). Application of computer assisted tomography (CAT) to gamma attenuation measurement of soil water content. *Australian Journal of Soil Research* **26**, 105–10.
- Hermon, G. T. (1980). 'Image Reconstruction from Projections.' (Academic Press: New York.)
- Journel, A. G., and Huijbregts, Ch. J. (1978). 'Mining Geostatistics.' (Academic Press: London.)
- Knighton, R. E., and James, D. W. (1985). Soil test phosphorus as a regionalized variable in levelled land. *Soil Science Society of America Journal* **49**, 675–9.
- Phogat, V. K., and Aylmore, L. A. G. (1989). Evaluation of soil structure by using computer assisted tomography. *Australian Journal of Soil Research* **27**, 313–23.
- Phogat, V. K., Aylmore, L. A. G., and Schuller, R. D. (1991). Simultaneous measurement of the spatial distribution of soil water content and bulk density. *Soil Science Society of America Journal* **55**, 908–15.
- Rasiah, V. (1995). Fractal dimension of surface-connected macropore count-size distributions. *Soil Science* **159**, 105–8.
- Rasiah, V., and Aylmore, L. A. G. (1998a). Characterizing the changes in soil porosity by computer tomography and fractal dimension. *Soil Science* (in press).
- Rasiah, V., and Aylmore, L. A. G. (1998b). Estimating spatial distribution of hydraulic conductivity and pore continuity using computed tomography. *Soil Science Society of America Journal* (in press).
- Webster, R., and Cuanalo de la, H. E. (1975). Soil transect correlograms of north Oxfordshire and their interpretation. *Journal of Soil Science* **26**, 176–94.

11. Soil factors in the transport of pesticides from cotton farms: overview paper

L.A.G. Aylmore

Department of Soil Science and Plant Nutrition,
The University of Western Australia

Introduction

Basic understanding of the processes involved is the key to the development of sound management practices for controlling the various mechanisms by which pesticides used in cotton production may be transported off-site from cotton farms and thus pose a hazard to the health of the surrounding ecosystem.

While off-farm movement of pesticides such as endosulfan through spray drift during application (Woods, 1998) and subsequent volatilization from plant leaves, water reservoirs etc. is generally amenable to rigorous control and attention to conditions at the time of application (Edge, 1998), the pesticide residues which find their way into the soil profile are subject to a wide range of varying physical, chemical and biological processes which can significantly complicate the management procedures necessary.

By sorption onto soil components, principally clay minerals and organic matter, and in some cases the production of toxic daughter compounds (eg. endosulfan sulphate), the persistence (half-lives) of the pesticides can be greatly enhanced and increase the potential for off-site movement.

Such movement can include wind erosion in the form of dust or run-off, either in solution or through water erosion of mobile sediments. More strongly adsorbed pesticides such as endosulfan and trifluralin generally pose little hazard in terms of their potential for leaching to groundwater but the mobility in the soil profile of the numerous other herbicides used in cotton production should not be overlooked. Because of the different physical and chemical properties of each pesticide and variable soil properties, the dominant mechanism for off-site transport can be expected to vary significantly.

Dust erosion appears to be a minor concern, largely limited to that from unsealed roads and should be relatively easily countered (Edge, 1998; Leys, 1998). However it is clear from other presentations at this conference (Silburn et al., 1998; Simpson et al., 1998 and Kennedy et al., 1998) that run-off and consequent soil loss can be substantial and will require careful ongoing research and remedial attention to reduce this source of off-farm contamination. Two critical factors in controlling water run-off and the extent of associated sediment transport, are the infiltration capacity of the soil profile relative to precipitation or irrigation rates, and the inherent erodibility of the soil surface.

Infiltration

Run-off will occur when the ability of the soil profile to absorb incident water (ie. the soil water storage capacity), is exceeded and this can occur under conditions described by hydrologists as either:

1. *Infiltration excess* - the rate of infiltration generally asymptotes to the saturated hydraulic conductivity of the soil with time due largely to the decreasing matric water potential gradient between the surface and the wetting front moving downwards. If the surface horizon has the lowest hydraulic conductivity, this will determine the maximum infiltration rate and when run-off occurs.
2. *Saturation excess* - if the sub-surface soil has a lower hydraulic conductivity the maximum infiltration will be determined by the storage capacity of the surface horizon.

Infiltration rate is not an intrinsic property for any given soil and can change significantly depending on surface condition (roughness, sealing etc.), plant coverage and soil management practices. It is subject to considerable spatial and temporal variability and seasonal conditions. Understanding the site specific hydrological characteristics of the whole soil profile is thus an essential prerequisite to the planning of irrigation strategies and successful water management on the farm.

Erodibility

Erodibility has been defined in terms of what is known as the *Universal Soil Loss Equation* (Wischmeier and Smith, 1978) written in the form:

$$A = R.K.LS.PC$$

where R is a *Rainfall Erosion Index* related to the intensity and length of precipitation events; K is the *Soil Erodibility Factor* depending primarily on the texture, organic matter content, structural stability and hydraulic conductivity of the soil; L and S are respectively the *Slope Length* and *Gradient Factors*; C is the *Crop Management Factor* identifying the effects of specific cropping practices on the susceptibility of the soil to erode and P the *Erosion Control Practice Factor*, indicates the fractional amount of erosion that occurs with special conservation practices (eg. contour tillage) as compared to what it would be without them (ie. worst case). See also the Revised Universal Soil Loss Equation (RUSLE) (Renard et al., 1983) incorporating recent improvements.

Soil losses reported for some farms are clearly substantial and unacceptable (Silburn et al., 1998) leading to unwanted consequences such as pesticide export and the need for frequent de-silting of drains. Addressing the above variables can substantially reduce the susceptibility of the surface soil to removal by the action of wind and water. For example, reducing the slope of irrigation furrows from 1.2 % to 0.8 % was observed to reduce the export of the pesticides triflurin by up to 90 % (Simpson et al., 1998) and soil protection under cover of plant residues and improved soil structural stability under minimum tillage or by artificial means, could be expected to significantly reduce sediment loads (Silburn et al., 1998).

Soil structure

Of fundamental importance to both infiltration and erodibility are the structural status and stability of the surface soil. This in turn will be determined by a range of factors including its composition and management history. Good soil structure is most generally provided by soils containing appreciable amounts of fine particles (ie. high surface area clays) combined into small crumbs or aggregates which are stable to wetting and drying processes. Stability is usually derived from a combination of favourable surface properties (exchangeable cations) and binding by organic matter or cementing materials such as iron and aluminium oxides. Soil degradation and susceptibility to erosion occurs as a result of mechanical trauma (tillage and traffic) and the disruptive forces associated with wetting. Structural breakdown almost inevitably leads to problems of poor permeability and hard-setting behaviour.

The disruption of structure which occurs on wetting arises from two mechanisms: (1) dispersion - caused by double layer swelling forces (Quirk, 1994) and characterized by the detachment of clay-sized particles; and (2) slaking or non-dispersive failure where larger compound particles are broken down by rapid wetting but clay dispersion does not necessarily occur (Cochrane and Aylmore, 1991).

Numerous methods have been proposed for assessing the dispersive and slaking behaviour of soils. The most widely adopted quantitative tests measure clay dispersion in soil/water suspension and water-stable aggregation by wet sieving with many variants being suggested for each method (Williams et al., 1966; Rengasamy et al., 1984). Where such behaviour is evident remedial practices aimed at modifying the surface physicochemical characteristics of the soil clay particles are required.

Non-dispersive failure on the other hand results from a combination of differential swelling forces and explosive compression of entrapped air (surface tension forces) associated with rapid wetting. Since this can occur in the absence of dispersion alternative

methods are required for quantitative assessment of its significance and control particularly in hard-setting and apedal soils (Aylmore and Sills, 1982; Cochrane and Aylmore, 1991). The relative roles played by these mechanisms influence the choice of management strategy best suited to reducing soil structural instability.

The susceptibility of the soil to the previous forces can vary dramatically between different soil types depending on the surface physicochemical characteristics of the soil components and their interdependence. Consequently management practices need to be tailored to the particular structure forming characteristics of individual soils. It is equally important to recognise the contribution of the structural properties of the total soil profile since these can greatly influence soil water infiltration, redistribution and storage.

Mineralogy

Identification of the mineralogical composition of the soil provides an immediate clue to its likely physical behaviour. The presence of smectite, a high specific surface area, finely divided layer-lattice aluminosilicate clay mineral common to Vertisol soils, may indicate a potentially high swelling soil particularly prone to dispersion under specific conditions. Depending on the prevailing surface physicochemical characteristics such clays can exhibit either desirable attributes such as self-mulching or undesirable features such as poor permeability.

Red brown earths on the other hand, dominated by illitic and kaolinitic clay minerals are less strongly hydrated and generally more stable than the grey and black cracking clays common on many cotton farms. All clay soils are however potentially dispersive under favourable conditions associated with their surface physico-chemical characteristics (evidenced by hard-setting of some red-brown soils) and it is important for farmers to recognize the specific features of their soil.

Exchangeable cations and total dissolved salts

Basic determinants of the physicochemical behaviour of a soil are the magnitude of the cation exchange capacity balancing the negative charge on the crystalline clay minerals (derived from isomorphous substitution of ions within the clay lattice), the nature of the exchangeable cations themselves (whether monovalent or polyvalent) and the electrolyte (solute) concentration in the soil solution. If the exchange complex contains a significant proportion of monovalent cations such as sodium and the soil solution is relatively dilute (ie. high quality water with low total dissolved salts) strong osmotic imbibition of water can occur leading to swelling, the disruption of any aggregate structure and ultimately dispersion. Sodic soils are variously defined as soils with exchangeable sodium percentage (ESP) greater than 15 (USA; Richards, 1954) or 6 (Australia; Northcote and Skene, 1972) depending largely on the quality of the irrigation water. Susceptibility to structural failure on wetting can occur even at lower ESPs and may require ameliorative procedures.

While the use of artificial soil stabilizers such as polyacrylamide (PAM) or PVA can effectively prevent these consequences, application can be expensive and these chemicals may themselves pose health hazards. The traditional agricultural use of gypsum (hydrated calcium sulphate) added to the soil or irrigation water (Davidson and Quirk, 1961) to improve the physical structure and hence productivity, warrants attention in relation to potential sediment and associated pesticide transport even on non-sodic soils. Gypsum is only sparingly soluble (<2 g/L) but the electrolyte effect is sufficient to compress the ionic distribution associated with the clay surfaces (diffuse double layer) thus reducing swelling and dispersion. The long-term stabilisation of the surface soil is best achieved by combining gypsum treatment with management practices designed to enhance the soil organic matter content (ie. reduced or zero tillage).

Crop residues

The susceptibility of farm soils to soil loss is demonstrably greatest early in the season with bare soils exposed to erosive forces. The benefits of stubble retention to protect the soil surface from wind erosion, raindrop impact and water erosion are self evident. One or two tonnes per hectare of crop residue can usually reduce the erosion of even highly erosive soils to a negligible or at least acceptable factor.

While cotton cropping generally results in insufficient residue to provide adequate cover for erosion control (Simpson et al., 1998) rotation with wheat crops appears a profitable and effective approach. To be most effective plant residue cover should remain anchored to the soil since root systems can both help to bind the soil and to enhance infiltration.

Leaching to groundwater

The pesticide of major interest in the recent program has been the insecticide endosulfan which because of its strong retention by the soil can generally be considered essentially immobile in the soil profile. However the possibility, in vulnerable circumstances, of leaching to groundwater of other potentially more mobile pesticides used such as the herbicides fluometuron, diuron, prometryn and trifluralin should not be overlooked. Whether a pesticide persists for a long time or is rapidly degraded or transformed in soil is a major determinant of the extent to which it can pose a pollution hazard.

Organic matter provides not only a major substrate for pesticide retention but determines the degree of microbial activity and hence the degradation rate. Literature values for the sorption coefficients (k_{oc}) and half-lives ($t_{1/2}$) for most pesticides commonly vary substantially between various authors indicating that not only the content but also the nature of the organic matter present is important (Singh et al., 1989). In addition other factors such as the presence of

competition for sorption sites by other chemicals present, preferred flow paths derived from plant root channels, clay cracking or soil water repellency, and passenger transport of pesticides on soluble organic and other colloidal materials may require evaluation in terms of their influence on mobility.

Modelling

The literature contains a multiplicity of predictive models for chemical and particulate transport varying greatly in terms of their complexity and claimed applicability. Such models are best used in combination with experimental data to identify the relative contributions of the different pathways for off-farm transport (eg. Raupach, 1998). However the complexity attendant on the multiplicity of factors operating in the field is likely to make the more comprehensive mechanistic models somewhat cumbersome and restrictive in user-friendly terms.

As such their use is principally of value to researchers in providing insights into the relative effectiveness of individual management procedures eg. GLEAMS (Connolly, 1998). Farmers themselves are likely to be more comfortable with, and in daily practice, make use of simpler assessment models such as PIRI (Kookana, 1998) or scaling models directed to individual aspects of the potential transport processes and requiring only limited data input eg. PESTCSRN (Aylmore and Di, 1998).

There is a need to define the degree of complexity with which fundamental processes need to be treated in such models and the extent of characterization of the range of physical, chemical and biological mechanisms required to avoid problems of site specificity and to provide a satisfactory data base for predictive modelling.

Conclusions

The outcomes from the present extensive program of policy and research, presented at this meeting, has provided a sound basis for defining Best Management Practice for cotton farming. However ongoing research is necessary for continued development and refinement of the template provided.

The basic principles of successful soil and water conservation are now very well defined (see for example the recent *Soil Guide - A handbook for understanding and managing agricultural soils* Ed. Geoff Moore, Agriculture Western Australia) but evaluation of site specific parameters remains an essential prerequisite to their successful implementation.

Continued collaboration between scientists, policy makers, regulators, extension workers and individual farmers, as demonstrated at this workshop, in the evaluation of soil characteristics and their management requirements, will help to ensure the continued sustainability of the cotton industry and community confidence in its environmental safety.

References

- Aylmore, L.A.G. and Di, H.J. 1998. Variable recharge and the probabilities of groundwater contamination by pesticides. Proc. National Conference, Aust. Soc. Soil Sci., Brisbane, pp. 422-428.
- Aylmore, L.A.G. and Sills, I.D. 1982. Characterization of soil structure and stability using modulus of rupture-exchangeable sodium percentage relationships. *Aust. J. Soil Res.*, **20**: pp. 213-224.
- Cochrane, H.R. and Aylmore, L.A.G. 1991. Assessing management-induced changes in the structural stability of hardsetting soils. *Soil and Tillage Research*, **20**: pp. 123-132.
- Connolly, R. 1998. Exploring farm design and management options with modelling, in *Minimising the Impact of Pesticides on the Riverine Environment: Key Findings from Research with the Cotton Industry*, LWRRDC Occasional Paper 23/98, Land and Water Resources Research and Development Corporation, Canberra.
- Davidson, J.L. and Quirk, J.P. 1961. The influence of dissolved gypsum on pasture establishment on irrigated sodic soils. *Aust. J. Agric. Res.*, **12**: pp. 100-110.
- Edge, V. 1998. Aerial transport of endosulfan: vapour and dust movement, in *Minimising the Impact of Pesticides on the Riverine Environment: Key Findings from Research with the Cotton Industry*, LWRRDC Occasional Paper 23/98, Land and Water Resources Research and Development Corporation, Canberra.
- Kennedy, I.R., Sanches-Bayo, F., Kimber, S.W.L., Beasley, H. and Ahmad, N. 1998. Movement and fate of endosulfan on-farm, in *Minimising the Impact of Pesticides on the Riverine Environment: Key Findings from Research with the Cotton Industry*, LWRRDC Occasional Paper 23/98, Land and Water Resources Research and Development Corporation, Canberra.
- Kookana, R. 1998. Assessing risk at the catchment or regional level through a pesticide impact ranking index, in *Minimising the Impact of Pesticides on the Riverine Environment: Key Findings from Research with the Cotton Industry*, LWRRDC Occasional Paper 23/98, Land and Water Resources Research and Development Corporation, Canberra.
- Leys, J. 1998. Aerial transport: dust and associated endosulfan, in *Minimising the Impact of Pesticides on the Riverine Environment: Key Findings from Research with the Cotton Industry*, LWRRDC Occasional Paper 23/98, Land and Water Resources Research and Development Corporation, Canberra.
- Northcote, K.H. and Skene, J.K.M. 1972. Australian soils with saline and sodic properties. CSIRO Aust. Soils Publ. No. 27.
- Quirk, J.P. 1994. Interparticle forces: A basis for the interpretation of soil physical behaviour. *Advances in Agronomy*, **53**: pp. 121-183.
- Raupach, M. 1998. Integrative assessment of off-site transport pathways, in *Minimising the Impact of Pesticides on the Riverine Environment: Key Findings from Research with the Cotton Industry*, LWRRDC Occasional Paper 23/98, Land and Water Resources Research and Development Corporation, Canberra.
- Renard, K.G., Foster, G.R., Weesies, G.A. and Porter, J.P. 1983. RUSLE, Revised universal soil loss equation. *Journal of Soil and Water Conservation*. **46**: pp. 30-33.
- Rengasamy, P., Greene, R.S.B., Ford, G.W. and Mehanni, A.H., 1984. Identification of dispersive behaviour and the management of red-brown earths, *Aust. J. Soil Res.*, **22**: pp. 413-431.
- Richards, L.A. 1954. (Ed.) Diagnosis and improvement of saline and alkali soils. U.S.D.A. Agricultural Handb. 60. (Government Printer, Washington D.C.)
- Silburn, D.M., Waters, D.K., Connolly, R.F, Simpson, B.W. and Kennedy, I.K. 1998. Techniques for stabilising soil erosion on cotton farms, in *Minimising the Impact of Pesticides on the Riverine Environment: Key Findings from Research with the Cotton Industry*, LWRRDC Occasional Paper 23/98, Land and Water Resources Research and Development Corporation, Canberra.
- Simpson, B.W., Hargreaves, R.M., Noble, E. Thomas, Kuskopi, B. and Carroll, C., 1998. Pesticide behaviour on farm: persistence and off-site transport (Queensland), in *Minimising the Impact of Pesticides on the Riverine Environment: Key Findings from Research with the Cotton Industry*, LWRRDC Occasional Paper 23/98, Land and Water Resources Research and Development Corporation, Canberra.
- Singh, R., Gerritse, R.G. and Aylmore, L.A.G. 1989. Adsorption-desorption behaviour of selected pesticides in some Western Australian soils. *Australian Journal of Soil Science* **28**: pp. 227-243.
- Williams, B.G., Greenland, D.J., Lindstrom, G.R. and Quirk, J.P., 1966. Techniques for the determination of the stability of soil aggregates. *Soil Science*, **101**: pp. 101-163.
- Wischmeier, W.H. and Smith, D.D. 1978. Predicting rainfall erosion losses - A guide to conservation and planning. USDA, Agriculture Handbook 537. US Government Printing Office, Washington D.C.
- Woods, N. 1998. Aerial transport of endosulfan: droplet movement, in *Minimising the Impact of Pesticides on the Riverine Environment: Key Findings from Research with the Cotton Industry*, LWRRDC Occasional Paper 23/98, Land and Water Resources Research and Development Corporation, Canberra.

**Dynamics of organic carbon in the Ellen Brook Catchment, Perth, Western
Australia**

Proc. 9th Inter. Conf. on Humic Substances, Adelaide, Sept. 1998.

Samson, N., Gerritse, R. and Aylmore, L.

Dynamics of organic carbon in the Ellen Brook Catchment, Perth, Western Australia.

Nicole Sampson¹, Robert G. Gerritse² and L.A.G. Aylmore¹.

¹Soil Science and Plant Nutrition, University of Western Australia, Nedlands, WA 6907, Australia.

²CSIRO Land and Water, Private Bag, Wembley, WA 6014, Australia.

Key words : aquatic humus, spectral absorbance, fractionation, turnover time.

Abstract

Algal blooms are becoming increasingly common in the Swan River, Perth, Western Australia and aquatic humus is recognised as important in restricting the growth of algae by shading sunlight needed for photosynthesis.

High levels of organic carbon (OC) exist in Ellen Brook, a tributary of the Swan River. Ellen Brook is the main contributor to the total input of OC to the Swan River (Gerritse 1994). This OC originates from native vegetation within the catchment, of which over 60% has been cleared over the last 50 to 60 years. With fewer inputs, levels of OC in soils and consequently in Ellen Brook and the Swan River, are slowly being depleted.

This paper reports on the characteristics of organic carbon in Ellen Brook and an agricultural drain within the catchment, and compares it with samples from the Avon River. Samples were fractionated according to molecular weight into 5 dissolved and suspended particulate fractions and characterised, along with unfractionated samples, in terms of spectral quality and total OC. Preliminary ¹³C and ¹⁴C results give an estimation of the origins, age and turnover time of OC. Soil column experiments describe C absorption of Ellen Brook soil.

Introduction

The Swan River, in Perth, Western Australia, has experienced an increase in the occurrence of algal blooms in recent years, particularly in the upper reaches of the river. This appears to be due largely to a high input of nutrients from Ellen Brook, especially biologically available phosphate (Gerritse 1994).

Inputs of OC to the Swan play an important role in the ecology of the river in restricting the growth of algae by shading sunlight needed for photosynthesis. Aquatic humus gives water a yellow to brown colour and is one of the most important sunlight absorbers in natural waters (Zepp and Schlotzhauer 1981).

Ellen Brook, a tributary of the Swan River (Fig 1), contains high levels of dissolved and particulate organic carbon (OC) and, as the major source of the total input of OC from humic material to the Swan River, contributes about 1500 tonnes of OC per year. The grey sandy Bassendean soils which make up 30% of the catchment contribute most of the OC (and phosphorus) leached into Ellen Brook. This OC is derived from tannins and oils in the leaves and bark of native vegetation in the catchment (Gerritse 1994). However, the vegetation in the catchment has been largely cleared for farming and residential development.

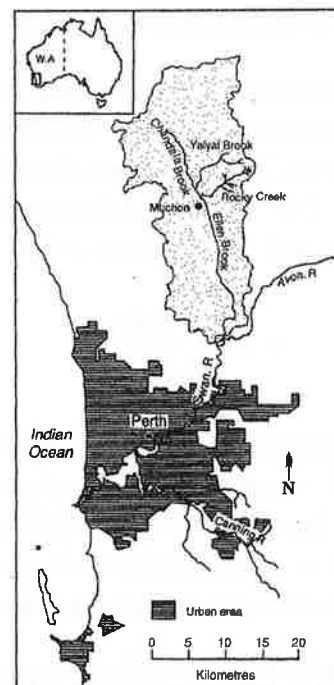


Fig. 1 : Location of Ellen Brook in relation to its catchment (dotted area) and confluence with the Swan/Avon River (Gerritse 1996).

Over 80% of sandy soils and over 60% of the total catchment has been cleared in the last 50 to 60 years (Hammond and Mauger 1984).

With fewer inputs and leaching of OC from the sandy catchment soils, the levels of OC in these soils are slowly being depleted. It is expected that eventually the OC levels in Ellen Brook and therefore the Swan River will progressively decrease and this will significantly alter the ecology of the two rivers. In particular it will enable light to penetrate further into the water column and this might subsequently encourage the growth of algal blooms in the Swan.

The study aims to characterise OC in Ellen Brook stream water. It also seeks to quantify the sources and rates of decline of soil OC following the changes in land use which have occurred in the Ellen Brook catchment. Little is known about the time scales involved in leaching and decomposition of OC from the Ellen Brook catchment and this information is vital to the effective long term management of water quality in the Swan River.

Materials and Methods

Sampling

Surface water sampling occurred weekly from June to October in 1996 and 1997. The sites included "Ellen Brook" (EBR) at Rose Street, Upper Swan and an agricultural drain within the catchment "Ellen Brook Drain" (EBD), situated at Railway Parade/Stock Road Bullsbrook. The Avon River (AR), which continues as the Swan River at its confluence with Ellen (Fig 1), was sampled at the Great Northern Highway Bridge in Belhus, for comparison with Ellen Brook. 250 mL samples were filtered to 0.45 µm.

TOC and spectral absorbance

Samples were analysed for total OC (TOC) by combustion/non-dispersive infra-red gas analysis using a Shimadzu TOC-5000A.

Spectral absorbance of samples was determined using a Philips Pye Unicam PU 8650 visible spectrophotometer at wavelengths 400 nm and 440 nm and a 4cm cuvette. The relationship between TOC and light absorbance and the ratios of absorbances were calculated from measured TOCs and absorbances. Specific absorption coefficients were also evaluated according to Zepp and Schlotzhauer (1981) using the formula

$$k_{\lambda} = \frac{\ln(10)A_{\lambda}}{C_0 d}$$

where A_{λ} = absorbance at wavelength λ (m^{-1})
 C_0 = TOC (mg/L)
 d = cell length (m)

Fractionation of OC and analysis of fractions

100 L samples were collected from EBD, EBR, AR and a site on the Swan River (SR) in August/September 1995; at EBD, EBR and AR in June/July, August and October of 1996; and at EBD in June and September of 1997. Stream water was pumped through a 1000 µm mesh filter to eliminate large particles and debris.

Samples were then fractionated according to the size of suspended particles using a continuous flow centrifuge and tangential flow filter (Douglas et. al. 1993). Five fractions were separated; fine particulate (>1000 nm), coarse colloidal (200-1000 nm), fine colloidal (6-200 nm \approx >100 000 MW), ultrafine colloidal (3-6 nm \approx 10 000–100 000 MW) and dissolved (<3 nm \approx <10 000 MW). This method of fractionation is unique in that it gives gram quantities of sample and small colloidal sample fractions of reasonable size.

Subsamples were analysed for TOC and spectral absorbance. In each fraction a proportion of the TOC measured is background unfractionated TOC; this has been subtracted from TOC values. Ratios of absorbances 400:440 nm and specific absorption coefficients were calculated as above.

Subsamples were oven dried at 80°C and analysed for 13C by mass spectrometry. Some EBD samples were analysed for 14C by Linear Accelerator Mass Spectrometry.

C adsorption

A glass column (0.01 m diameter x 0.13 m) was gravity packed with 13.5 g of soil sampled from the A1 horizon of a railway reserve/native bush area within the catchment (Gerritse 1996). The column was assembled and connected to a dual-piston pump according to Gerritse (1996). The soil was saturated with 0.0005 M CaCl₂ and leached under pressure to eliminate air bubbles. The soil column was then leached with 0.0005 M CaCl₂ at 10 mL/h. The pore volume of the packed soil was determined by monitoring the breakthrough curve of 0.001 M CaCl₂ injected into the stream. Cl⁻ is not absorbed by soil, so the breakthrough of CaCl₂ is equivalent to one pore volume. C adsorption was determined by injecting varying concentrations of 3-6 nm and 200-1000 nm fractionated C solutions (6-120 mgC/L) into the streamflow at 10 mL/h and monitoring the leachate C emergence time. A delay in C emergence compared to Cl⁻ indicates absorption of C by the soil.

Results and Discussion

TOC and spectral absorbance

High levels of TOC are found in the drains of the catchment. TOC averaged 88.6 ± 4.3 mg/L in 1996 and 63.2 ± 2.0 mg/L in 1997. This water is dark in colour due to the high humic content being flushed from OC rich paddock soils, and the low volumes of water in the drains. TOC is readily leached from the sandy catchment soils rich in OM.

Ellen brook also has a high TOC content (average 55.2 ± 3.7 mg/L in 1996 and 32.9 ± 2.5 mg/L in 1997). The main source is dark coloured water from agricultural drains on sandy soils.

Average TOC levels in the Avon River were 32.0 ± 3.4 mg/L in 1996 and 10.8 ± 0.4 mg/L in 1997 which is still high compared to waterbodies world wide (Briggs et.al. 1993). The Avon River is not as coloured as Ellen Brook; the water is clear and light in colour.

TOC concentrations in 1996 were higher than in 1997. This could be due to the higher total rainfall received in 1996 (663.0 mm) than in 1997 (413.2 mm). Rainfall does not however appear to influence TOC

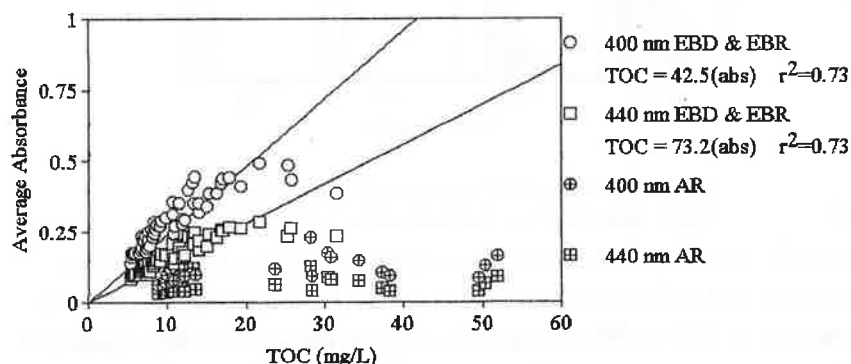


Fig. 2 : Relationship between TOC and absorbance at 400 and 440 nm for EBD, EBR and AR samples, 1996-1997.

appear to influence TOC winter fluctuation patterns in the Ellen or Avon.

A strong positive linear relationship exists between TOC and light absorbance at 400 and 440 nm for water sampled from EBR and EBD (Fig 2). This relationship ap-

appears to be specific to the Ellen Brook catchment as the Avon shows a different pattern (Fig. 2), as do other river catchments reported in literature (Banoub 1973; Lewis and Tyburczy 1974; Zepp and Schlotzhauer 1981; Grieve 1985; Moore 1985). AR samples show a constant low absorbance with increasing TOC levels. Ratios of absorbances are widely used to characterise humic compounds (Visser 1984) and vary due to different origins (Schnitzer 1978). Values are related to the degree of aromatic content (Kononova 1966). EBD averaged 1.76 ± 0.01 for the sampling period and EBR 1.72 ± 0.02 . This indicates that EBR and EBD organic matter are similar in molecular structure. AR ratios averaged 2.02 ± 0.03 indicating that OC from AR is different in origin. Aromatics absorb light more strongly at lower wavelengths, a higher ratio indicates a higher degree of aromaticity in the Avon.

Specific absorption coefficients define the spectral quality of stream samples and allow direct comparison of samples analysed at different wavelengths. Data for Ellen, Avon and other river systems calculated for 400 and 440 nm (Table 1), show that EBD and EBR are similar in spectral quality and are also similar to other blackwater systems whose values reflect soil humic substances (Zepp & Schlotzhauer 1981). AR values are much lower than that of Ellen Brook and the other river systems listed in Table 1.

Table 1: Specific absorption coefficients (K_h) showing spectral quality for humics of aquatic systems in Perth (Western Australia) and in the United States.

Source of humic material	Average K_h at 400 nm ($LmgC^{-1}m^{-1}$)	SE	Average K_h at 440 nm ($LmgC^{-1}m^{-1}$)	SE
*Ellen Brook Drain, Perth WA	1.67	0.05	0.95	0.03
*Ellen Brook, Perth WA	1.55	0.06	0.91	0.04
Avon River, Perth WA	0.44	0.05	0.22	0.03
*Aucilla River, Lamont FL USA	1.42		0.79	
*Okefenokee Swamp, Waycross GA	1.31		0.73	
*Fenholloway River, Foley FL	2.13		1.25	
St. Marks River, St. Marks FL	1.39		0.88	
Williamson River, Klamath Agency OR	0.82		0.44	
*Econfina River, Perry FL	1.50		0.82	

* Blackwater systems

Source : Zepp & Schlotzhauer (1981)

Fractionated streamwater

Figure 3, illustrating TOC content in size fractions of EBD, EBR, AR and SR, shows that TOC levels decrease as the size of the colloid particles increase. The smallest size fraction (< 3 nm) contains the highest TOC levels and TOC content of the coarse particulate fractions of each site is almost negligible.

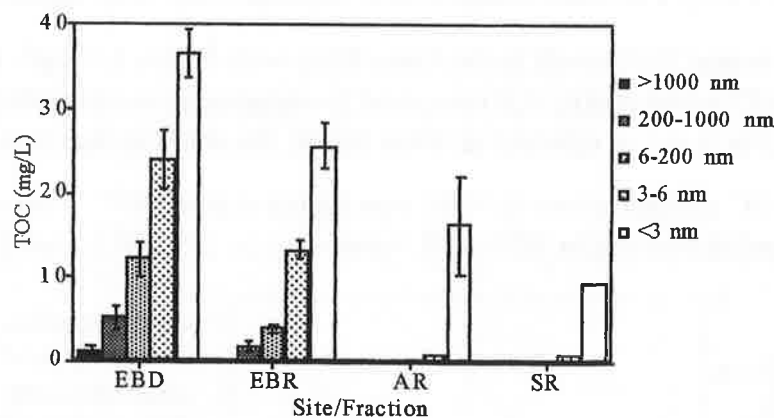


Fig. 3 : Average TOC content in 5 fractions of water sampled from 4 stream sites, 1995-1997

Absorbance ratios for EBD and

EBR fractions appear to be inversely correlated with the molecular size of the material (Fig. 4). As the molecular weight increases, the ratio, and aromatic content decreases (absorbance at 400 nm begins to decrease). However at 200-1000 nm there is a slight increase in absorbance at 400 nm. Scattering of light by these larger particles will increase absorbance for both wavelengths (Tyndall scattering), but will be higher at lower wavelengths (Owen 1996), thus

the higher ratio for this fraction.

The average ^{13}C shift for fraction samples was $26.28 \pm 0.28 \text{ ‰}$ for EBD and $26.60 \pm 0.60 \text{ ‰}$ for EBR. This indicates that the origin of OC in Ellen Brook is C-3 type plants. This finding is to be expected, as the original melaleuca/leptospermum vegetation and current pasture and vineyard vegetation are C-3 type. ^{13}C data for soil and leaf matter will consolidate this finding.

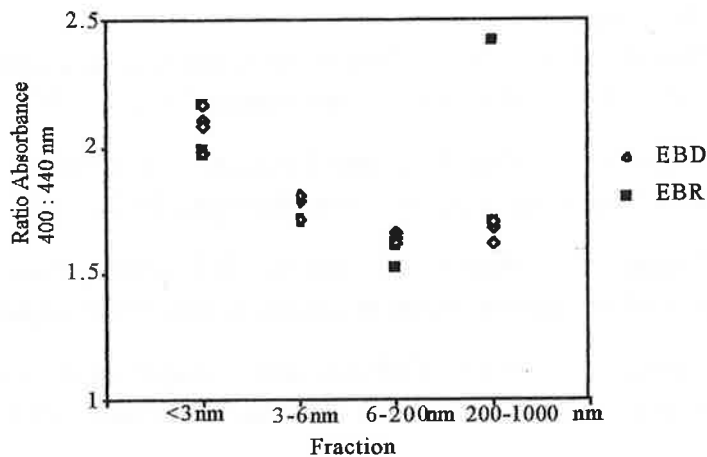


Fig. 4. : Ratio of absorbance 400 : 440 nm for fractionated EBD and EBR samples, 1996

Preliminary ^{14}C data for OC fractions in water from the agricultural drain have allowed the estimation of an approximate turnover time for OC in each fraction (Table 2). Turnover times were estimated using a model described by Hsieh (1993). The largest size OC particles (>1000 nm) are from the most recent source, as would be expected.

Table 2 : Estimation of approximate turnover time for OC in each EBD fraction

Particle Size of OC (nm)	^{14}C (Per cent modern)	Estimated turnover time (half life) (y)
>1000	136.3 ± 1.0	10 - 50
200-1000	103.6 ± 0.7	100
6-200	106.6 ± 0.7	100
3-6	104.6 ± 0.7	100

C absorption

Comparisons of C breakthrough times with Cl⁻ breakthrough indicate that there is no significant absorption of dissolved OC by soil in the column, regardless of C concentration or particle size. Breakthrough times were shorter for higher C concentrations.

Conclusion

- EBD, EBR, and even AR contain high levels of TOC compared to waterbodies worldwide.
- OC from the Ellen Brook catchment is less aromatic than OC from AR.
- There is a strong positive linear trend between TOC and light absorbance which is specific to Ellen Brook.
- Highest TOC levels exist in the dissolved fraction (< 3 nm) for Ellen Brook and the Avon and Swan Rivers. TOC concentrations of colloid particles decrease as the size increases.
- Smallest fractions have a higher aromatic content.
- The largest particles of fractionated OC are ~ 10-50 years in age whilst the smaller particles are >100 years in age.
- Ellen Brook soil does not absorb dissolved OC.

Acknowledgments

This research is funded by the West Australian Estuarine Research Foundation. Many thanks to CSIRO Land and Water, Murdoch University Marine and Freshwater Laboratory, CSIRO Plant Industries, and the Nuclear Sciences Group at the Institute of Geological and Nuclear Sciences, New Zealand for their assistance with sample analysis.

References

- Banoub, M.W. (1973). Ultra violet absorption as a measure of organic matter in natural waters in Bodensee. *Archiv Für Hydrobiologie* 71(2):159-165.
- Briggs, S.V., Maher, M.T. and Tongway, D.J. (1993). Dissolved and particulate organic carbon in two wetlands in NSW. *Hydrobiologia* 264(1):13-19.
- Douglas, G.B., Beckett, R. and Hart, B.T. (1993). Fractionation and concentration of suspended particulate matter in natural waters. *Hydrological Processes* 7:177-191.
- Gerritse, R.G. (1996). Column- and catchment-scale transport of cadmium: effect of dissolved organic matter. *Journal of Contaminant Hydrology* 22:145-163.
- Gerritse, R.G. (1994). Impact of nutrients from Ellen Brook on the Swan River. In 'Land use effects on the quality of water discharged to Ellen Brook'. (Eds M.L. Sharma, P.G. Kin and D.E. Herne.) Annual Report No.94/33, July 1993-1994, Division of Water Resources, CSIRO, Perth, Western Australia.
- Grieve, I.G. (1985). Determination of dissolved organic matter in streamwater using visible spectrophotometry. *Earth Surface Processes and Landforms* 10:75-78.
- Hammond, R. and Mauger, G. (1984). Salinity study of Ellen Catchment. Water Authority of Western Australia. Water Resources Directorate.
- Hsieh, Y. (1993). Radiocarbon signatures of turnover rates in active soil organic carbon pools. *Soil Science Society of America Journal* 57:1020-1022.
- Kononova, M.M. (1966). Soil organic matter: Its nature, its role in soil formation and in soil fertility. 2nd Edn. Pergamon Press, Oxford.
- Lewis, W.M. and Tyburczy, J.A. (1974). Amounts and spectral properties of dissolved organic compounds from some freshwaters of the southeastern U.S. *Archiv Für Hydrobiologie* 74(1):8-17.
- Moore, T.R. (1985). The spectrophotometric determination of dissolved organic carbon in peat waters. *Soil Science Society of America Journal* 49:1590-1592.
- Owen, T. (1996). Fundamentals of modern UV-visible spectroscopy. Hewlett-Packard Company, Germany.
- Schnitzer, M. (1978). Binding of humic substances by soil mineral colloids. In 'Interactions of soil minerals with natural organics and microbes'. (Eds P.M. Huang and M. Schnitzer.) SSSA Spec. Publ. 17, SSSA Madison, W.I.
- Visser, S.A. (1984). Seasonal changes in the concentration and colour of humic substances in some aquatic environments. *Freshwater Biology* 14:79-87.
- Zepp, R.G and Schlotzhauer, P.F. (1981). Comparison of photochemical behaviour of various humic substances in water : III. Spectroscopic properties of humic substances. *Chemosphere* 10(5):479-486.

Predicting the probabilities of groundwater contamination by pesticides under variable recharge

L. A. G. Aylmore^A and H. J. Di^{AB}

^A Department of Soil Science and Plant Nutrition, The University of Western Australia, Nedlands, WA 6907, Australia.

^B Present Address: Department of Soil Science, Lincoln University, Canterbury, New Zealand.

Abstract

A major deficiency in many models used to assess the groundwater contamination potential of organic pesticides used in agricultural and horticultural systems has been the assumption of a constant average groundwater recharge rate. This paper describes an enhanced version of a simple model designed to screen out or identify those pesticides that have a high probability for causing groundwater contamination in a region (e.g. a catchment, farm, or cropping area), which enables the temporal variability of recharge to be taken into account and illustrates the influence of a seasonal pattern of leaching and variations in predicted mobilities and persistence from those associated with averaging the recharge rate. The model is available as a user-friendly software package (PESTSCRN 3).

The model was formulated based on the following assumptions: (1) linear, equilibrium, and reversible sorption; (2) first-order breakdown or degradation; (3) pesticide leaching by steady convective flow; and (4) recharge rate varying with time. Random values of the input parameters required by the calculations are generated from probability distributions as specified by the means (μ) and standard deviations (σ), assuming normal distributions. Outputs provide a statistical analysis of travel time and fraction of pesticide remaining at different soil depths. Most distributions for travel time are near normal with slight positive skewness and can be approximated as normal distributions. The frequency distributions of residue fractions for all the pesticides examined to date show significant positive skewness (Beta distributions), with the peak frequency towards the lower bound of 0. Simulations using metalaxyl as an example demonstrate that, depending on recharge conditions, the use of daily data instead of mean recharge data can result in important differences in the predicted values of both travel times and residue percentages.

Additional keywords: pollution, degradation, leaching, modelling.

Introduction

The use of pesticides (including herbicides, fungicides, and insecticides) in agricultural and horticultural practices has increased dramatically in recent decades throughout the world, with a corresponding increase in concern with respect to the potential of residues from these non-point sources to leach to and contaminate groundwaters (USEPA 1977, 1978; Cohen *et al.* 1986; Beitz *et al.* 1994). In these circumstances, the ability to predict the fate of such chemicals released into the environment is an essential prerequisite to their efficient and safe management as well as to the establishment of realistic regulatory controls.

Experimental evaluation of the multiplicity of pesticide, soil, and environmental combinations experienced is prohibitively expensive and essentially impractical. Consequently, attention has focused on the use of mathematical simulation models designed to describe and predict the transport of solutes in soil profiles. While the

numerous detailed mechanistic models developed have proven valuable in investigating the various physical and chemical processes involved, the complexity attendant on the multiplicity of factors operating generally makes such models cumbersome and of restricted practical use in the field. On the other hand, simple functional models, based on stochastic representation of the transport processes and requiring relatively few and readily accessible input parameters, are generally more user-friendly and often give simulations that are at least as good as those obtained from more complex mechanistic models (Jury *et al.* 1987; Rao *et al.* 1985; Di *et al.* 1995).

Di *et al.* (1995) and Di and Aylmore (1997) developed a simple model designed to screen out or identify those pesticides which have a high probability for causing groundwater contamination in a region (e.g. a catchment, farm, or particular cropping area). A particular feature of the model is the ability to take into account the often significant spatial variability in soil and pesticide properties, such as organic matter content, bulk density, moisture content, sorption characteristics, and degradation half-lives, which can affect the mobility and persistence and thus the fate of organic pesticides in the soil profile (Biggar and Nielsen 1976; Rao and Davidson 1980; Singh *et al.* 1989). On the other hand, in common with most such models, a major deficiency in the model was the assumption of a constant average groundwater recharge rate with time. This paper describes an enhanced version of the model, which is available as a user-friendly software package (PESTSCRN 3), and which enables the temporal variability of recharge to be taken into account and illustrates the influence of seasonal patterns of leaching and variations in predicted mobilities and persistence from those associated with averaging the recharge rate.

Modelling procedure

The simple model formulated by Di and Aylmore (1997) calculates the fraction of pesticide remaining and travel time as the pesticide leaches deeper in the soil profile. It is based on the following assumptions.

- (i) Pesticide sorption is linear, at equilibrium, and reversible:

$$C_S = K_D C_L = f_{OC} K_{OC} C_L \quad (1)$$

where C_S is sorbed pesticide concentration, K_D is the linear sorption coefficient, C_L is pesticide concentration in the soil solution, f_{OC} is the weight fraction of soil organic carbon, and K_{OC} is the sorption coefficient normalised by the soil organic carbon fraction where:

$$K_{OC} = K_D / f_{OC} \quad (2)$$

- (ii) The pesticide undergoes first-order degradation in the soil, and the fraction of pesticide remaining undegraded (F) as it leaches in the soil is:

$$F = \exp(-kt) = \exp(-0.693t/t_{1/2}) \quad (3)$$

where k is the degradation rate constant, t is time, and $t_{1/2}$ is degradation half-life.

- (iii) The pesticide is assumed to leach by steady piston water flow (ignoring diffusion and dispersion), and the effective pesticide leaching velocity is (Jury *et al.* 1987):

$$V = q / (\rho_b f_{OC} K_{OC} + \theta) \quad (4)$$

where q is daily recharge rate, ρ_b is soil dry bulk density, and θ is soil moisture content, which is assumed to equal field capacity. The unsaturated soil zone may be divided into N layers with different thickness and with different soil properties. The differences in soil properties, and the half-life of the pesticide being simulated, change according to the values and depths specified for each layer.

The time (t_i) required to travel through incremental depth Δz_i is:

$$t_i = \Delta z (\rho_b f_{OC} K_{OC} + \theta) / q_i \quad (5)$$

The fraction of pesticide remaining (F) as the moving pulse reaches the bottom of layer N is given by:

$$F = \prod_{i=1}^N \exp[-\Delta z (\rho_b f_{oc} K_{oc} + \theta) 0.693 / (q t_{1/2})_i] \quad (6)$$

Input data

The following parameters are required as input data, and sample values, which can be modified, and are automatically read in from default files:

- (1) soil organic carbon fraction (f_{OC});
 - (2) soil bulk density (ρ_b);
 - (3) soil moisture content at field capacity (θ);
 - (4) pesticide sorption coefficient (K_{OC});
 - (5) degradation half-life ($t_{1/2}$);
- (The default files contain K_{OC} and $t_{1/2}$ values for some 32 pesticides which can be modified and added to as required.)
- (6) thickness of each soil layer (Δz);
- (Properties 1–5 may be different in each layer, and the individual thickness and number of layers (N) may be varied.)
- (7) daily rainfall plus irrigation and evaporation data for any given period may be entered and the recharge rate is automatically calculated as the difference. (Recharge is equated to zero when evaporation exceeds rainfall plus irrigation. The option is available to use the mean recharge rate if required).

Table 1. Soil properties used for modelling

Depth (cm)	Bulk density (g /cm ³)	Field capacity (%)	Organic C (%)
0–25	1.4	10.0	1.0
25–50	1.5	6.0	0.5
50–500	1.5	4.0	0.05

The soil parameters used in the default files provided were obtained from reports of soil surveys conducted on the Swan Coastal Plain of Western Australia, and from more detailed studies on experimental research stations (Table 1). These properties are representative of those for major sandy soils which are used for horticultural productions. Total daily rainfall plus irrigation and evaporation data were measured at the Medina Research Station of the Western Australian Department of Agriculture during experimental studies of pesticide leaching (Kookana *et al.* 1995).

The mean values of sorption coefficients (K_{OC}) and degradation half-lives ($t_{1/2}$) are taken mainly from the literature (Wauchope *et al.* 1992), with a few determined under local conditions (Kookana *et al.* 1995) (see Table 2). Since sorption coefficients and half-lives of pesticides vary significantly with environmental and soil conditions (Rao and Davidson 1980; Singh *et al.* 1989), for the purpose of the present exercise, arbitrary standard deviations equivalent to 30% coefficient of variation for K_{OC} and 50% for half-life are used. These variations are somewhat less than those reported by Rao and Davidson (1980) on the consideration that the soils in this region might not be as diverse as those referenced by Rao and Davidson (1980), which were from a wide range of sources and geographical areas. For the purpose of this exercise, degradation half-lives were assumed to progressively increase to double the surface value at a depth of 50 cm in inverse proportion to an exponential decrease in organic carbon with depth (Kookana and Aylmore 1994). This was on the assumption that soil conditions (e.g. microbial population, temperature, aeration status) become less favourable for degradation with increasing depth. These values may be varied as desired.

Random values of the parameters required by the calculations are generated from probability distributions as specified by the means (μ) and standard deviations (σ), assuming normal distributions with the probability density function being:

$$f(x) = \frac{1}{\sigma(2\pi)^{1/2}} \exp[-(x - \mu)^2 / (2\sigma^2)] \quad (7)$$

Although some properties might deviate somewhat from a normal distribution, they are approximated as a normal distribution. This was considered acceptable in view of the objectives of the model, and the fact that in some cases insufficient data for a distribution assessment will be available. All the parameters have specified lower and upper bounds, and values drawn beyond these bounds are rejected.

Computations can be carried out for t (travel time) and F (fraction of pesticide remaining) for depths appropriate to the watertable in the region.

Analysis of output

Outputs from the model, using mean or daily recharge rates and single value soil and pesticide parameters, provide tables and graphical illustrations of travel time and fraction of the pesticide remaining at different soil depths.

Outputs from the model, using mean or daily recharge rates and random values of soil and pesticide input, provide a statistical analysis of travel time and fraction of pesticide remaining at any given soil depth. The statistical parameters in the output for both travel time and fraction of residue remaining include mean, standard deviation, standard error of the mean, percentiles, and probability of the pesticide to exceed a specified fraction at a specified depth (e.g. the depth to groundwater).

Probability density functions of computed fractions of pesticides remaining and travel times are analysed and calculations are provided for the means, standard deviations, standard errors of means, cumulative probabilities for pesticides reaching a given depth at fractions greater than 0.01%, and the 95th percentiles of travel times. The value of 0.01% is regarded as a threshold value below which the fraction of pesticide remaining becomes insignificant (Jury *et al.* 1987). The 95th percentile is a value to indicate that 95% of the travel times will be less than this value.

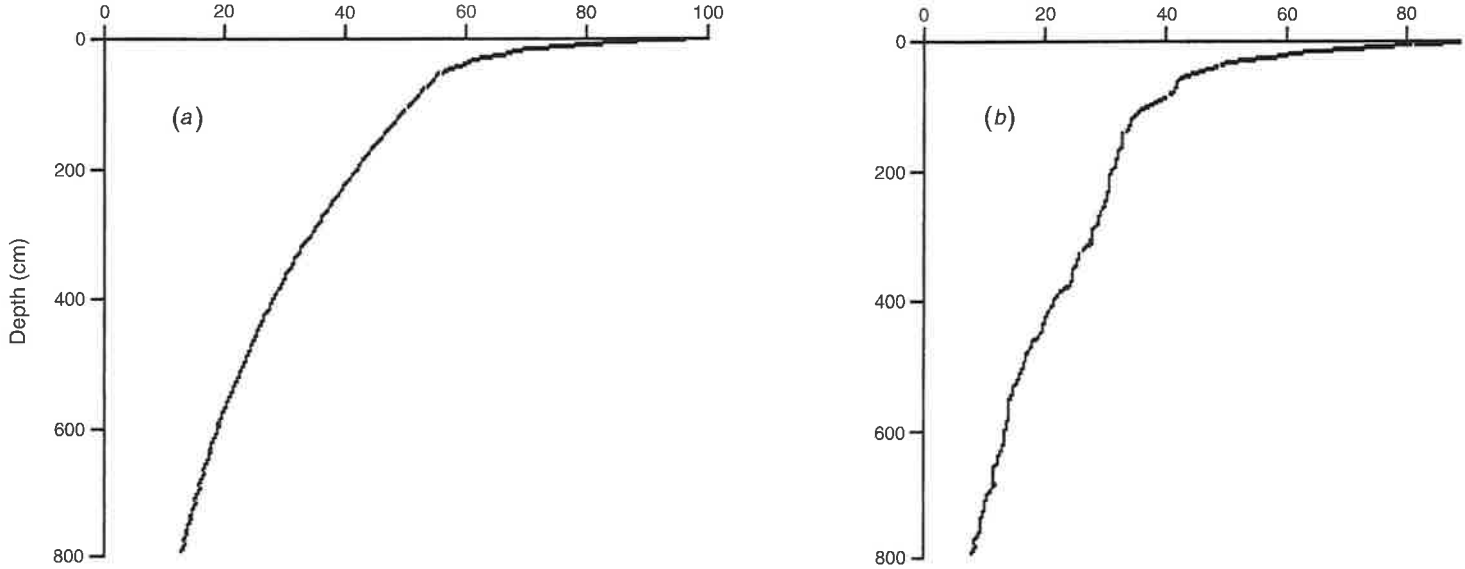


Fig. 1. Percentages remaining v. depth estimated using (a) average recharge rate and (b) daily recharge rates over the period of study and on the basis of single input parameters.

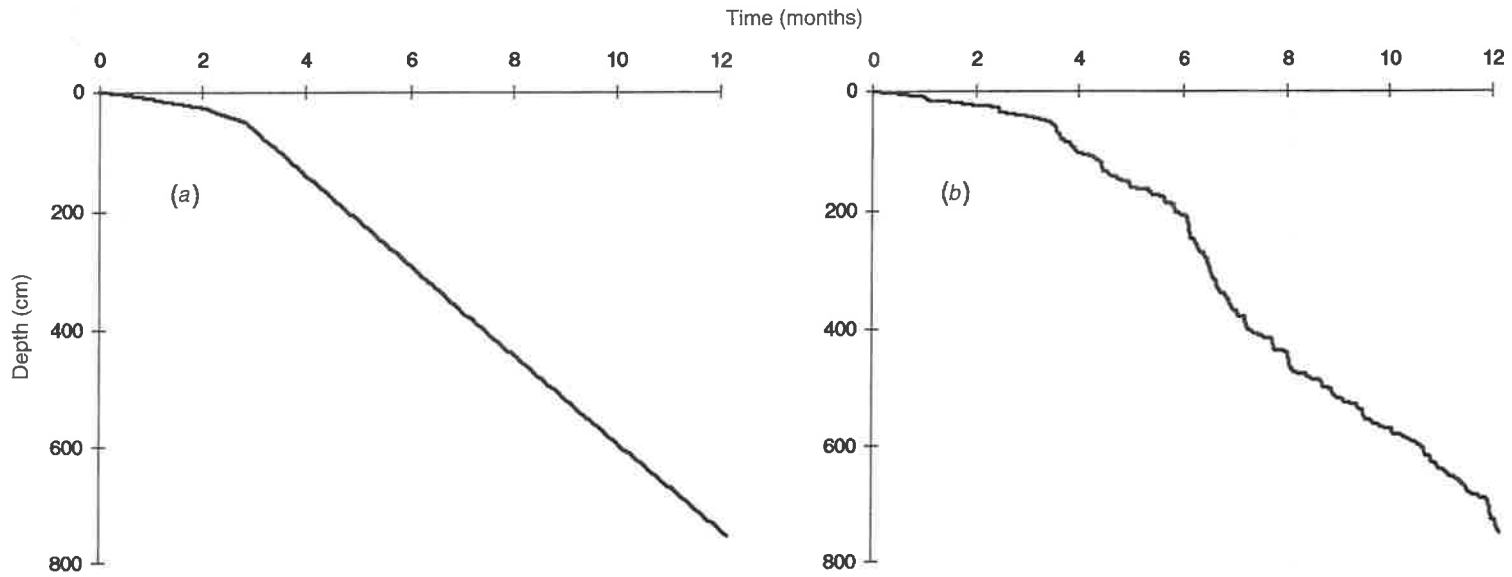


Fig. 2. Time to reach a given depth estimated using (a) average recharge rate and (b) variable daily recharge rates over the period of study and on the basis of single input parameters.

Results and discussion

The distributions of percentages remaining versus depth (Fig. 1) and time to reach a given depth (Fig. 2), predicted by the PESTSCRN 3 model, are presented for metalaxyl using both the average recharge rate and the daily recharge rates over the period of the study and on the basis of single value input parameters. Table 2 presents the predicted time to reach 100 cm and the percentage remaining at that depth for 30 pesticides commonly used in the region either previously or currently. Even at such a relatively shallow depth, it is evident that significant differences can arise on the basis of the two approaches and these would certainly be magnified over successive seasons for the more persistent chemicals. The basic causes for the variations are undoubtedly the effects of the different times estimated to be spent by the pesticide in the more active, with respect to microbial degradation, of the horizons in the soil profile. This is illustrated by the contrasting conclusion previously reached by Jury and Gruber (1989) that the distribution of precipitation within the season does not significantly affect the amount leached, and the stochastic description of the climate may be replaced by the annual average water application without too serious an error. The assumption of 50–100 cm zones of uniform

Table 2. Predicted time (days) to reach 100 cm and percentage remaining

Pesticide	K_{oc}	$t_{1/2}$	Mean recharge		Daily recharge	
			Time	(%)	Time	(%)
Atrazine	100	60	235	12.51	263	10.17
Benomyl	1900	240	3135	0.23	3286	0.18
Chlorothalonil	1380	30	2284	0.00	2400	0.00
Chlorpyrifos	6070	81	9967	0.00	10014	0.00
Chlorthal-dimethyl	5000	45	8214	0.00	8288	0.00
Cyfluthrin	100 000	30	163 842	0.00	16 2043	0.00
DDT	25 000	10 000	40 978	14.93	40 606	15.20
Dicofol	189 000	60	29 4897	0.00	29 1542	0.00
Dimethoate	20	7	56.08	2.83	68.00	0.00
Endosulfan	12 400	50	20 337	0.00	20 209	0.00
Fenamiphos	100	43	187.14	13.60	239.00	8.31
Fenarimol	600	360	1006	27.41	1111	24.20
Fenvalerate	5300	35	8705	0.00	8759	0.00
Iprodione	700	14	1170	0.00	1264	0.00
Linuron	400	219	678.5	23.85	764.0	19.95
Malathion	1800	1	2972	0.00	3083	0.00
Metalaxyl	50	70	105.23	50.54	146.00	39.53
Methamidophos	5	6	31.51	10.44	32.00	10.00
Methazole	3000	14	4938	0.00	5093	0.00
Methiocarb	300	3	515.0	0.00	626.0	0.00
Methomyl	72	30	179.14	4.30	206.00	2.67
Metolachlor	200	90	350.95	16.56	419.0	11.89
Metribuzin	60	40	121.61	25.05	159.00	16.77
Mevinphos	44	3	95.40	0.00	129.0	0.00
Permethrin	100 000	30	16 3842	0.00	16 2043	0.00
Prometryn	400	60	678.6	0.53	764.0	0.28
Propyzamide	243	59	421.4	3.70	528.0	1.67
Simazine	130	60	236.20	16.37	301.0	10.36
Thiram	670	30	1120.9	0.00	1237.0	0.00
Trifluralin	8,000	60	13 128	0.00	13 254	0.00

degradation by those authors contrasts strongly with the present use of an essentially exponential decline in organic matter with depths, which is consistent with experimental data on the soil described and a common observation in other soils (Kookana and Aylmore 1994). One would expect periodic recharge to have a greater influence on the pesticide fraction remaining than on the travel time, since the former decreases more or less exponentially with depth and the latter is essentially directly related to recharge rate.

The differences in the frequency distributions of pesticide fractions remaining (Fig. 3) and travel times (Fig. 4) are presented using metalaxyl as an example, predicted on the basis of average recharge rates and variable daily recharge rates. These figures also illustrate the way in which statistical information such as the mean, standard deviation, beta parameters, and 95th percentile data are presented in the software output. Most distributions for travel time (Fig. 4) are near normal (Eqn 7) with slight positive skewness and are approximated as normal distributions. The frequency distributions of residue fractions (Fig. 3) for the pesticides, however, generally show significant positive skewness with the peak frequency toward the lower bound of zero. These distributions are more readily described by Beta distribution functions (Benjamin and Cornell 1970) which are characterised by two shape parameters, a and b , with values of the variable ranging from 0 to 1, as is the fraction of pesticide remaining in the soil profile:

$$f(x) = \frac{\Gamma(a+b)}{\Gamma(a)\Gamma(b)} x^{a-1} (1-x)^{b-1} \quad 0 \leq x \leq 1 \quad (8)$$

These probability distributions illustrate that as a result of field variations in soil properties, related pesticide properties, and variability in daily recharge, the residue fractions of pesticides at specified depths and the corresponding travel times will also vary significantly. The present approach allows the uncertainties associated with the predictions to be quantitatively analysed. It is interesting to note, for example, that the travel times predicted, which differ significantly from the mean value, are significantly less uniformly distributed when variable recharge input is used and this can no doubt be attributed to the occurrence of individual significant recharge events (both high or low), which are essentially smoothed out by the use of mean values.

The leaching depths predicted by the simple model using average recharge rate for a number of commonly used pesticides have been shown to give reasonable agreement with the mean leaching depths measured in a field study (Di *et al.* 1995). The recharge rates operating during that field experiment were probably not varied to a great extent due to the reasonably uniform water input obtained by adjusting irrigation requirements to reach 120% evaporation losses. In circumstances where the recharge rate may vary widely on a daily basis, the use of mean recharge rate is likely to lead to inadequate prediction of the potential hazard posed by the pesticides to groundwater contamination. However, Table 2 shows that the ranking of the pesticides in terms of their potential for groundwater contamination (i.e. the percentage remaining at 100 cm) is basically the same whether mean recharge rate or daily recharge rate is used. Therefore, if the purpose of the simulation is to assess the relative groundwater contamination potential of a range of pesticides, then either average rate or daily recharge rate may be acceptable.

Conclusions

The use of average recharge data may lead to inadequate prediction of the potential hazard posed by pesticides to groundwater contamination, depending on the weather and

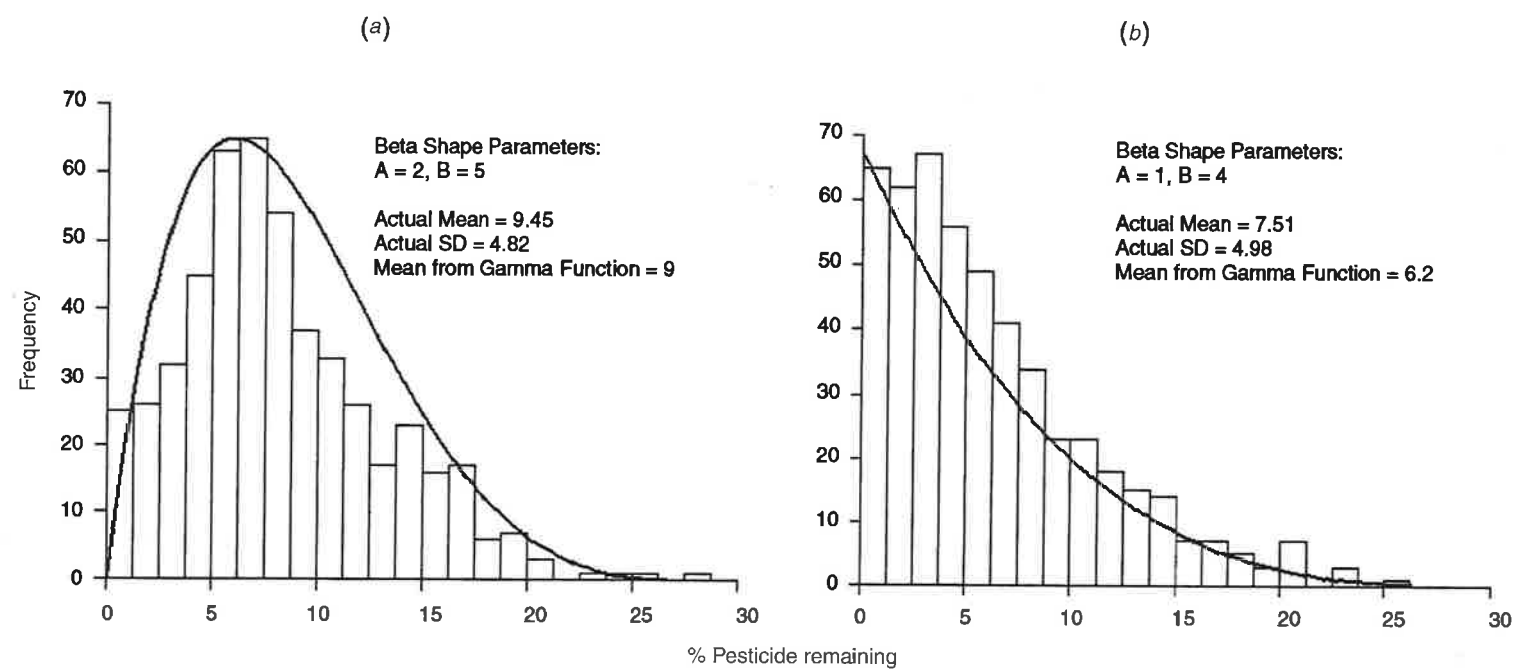


Fig. 3. Frequency distributions of pesticide remaining predicted on the basis of (a) average recharge rate and (b) variable daily recharge rates over the period of study.

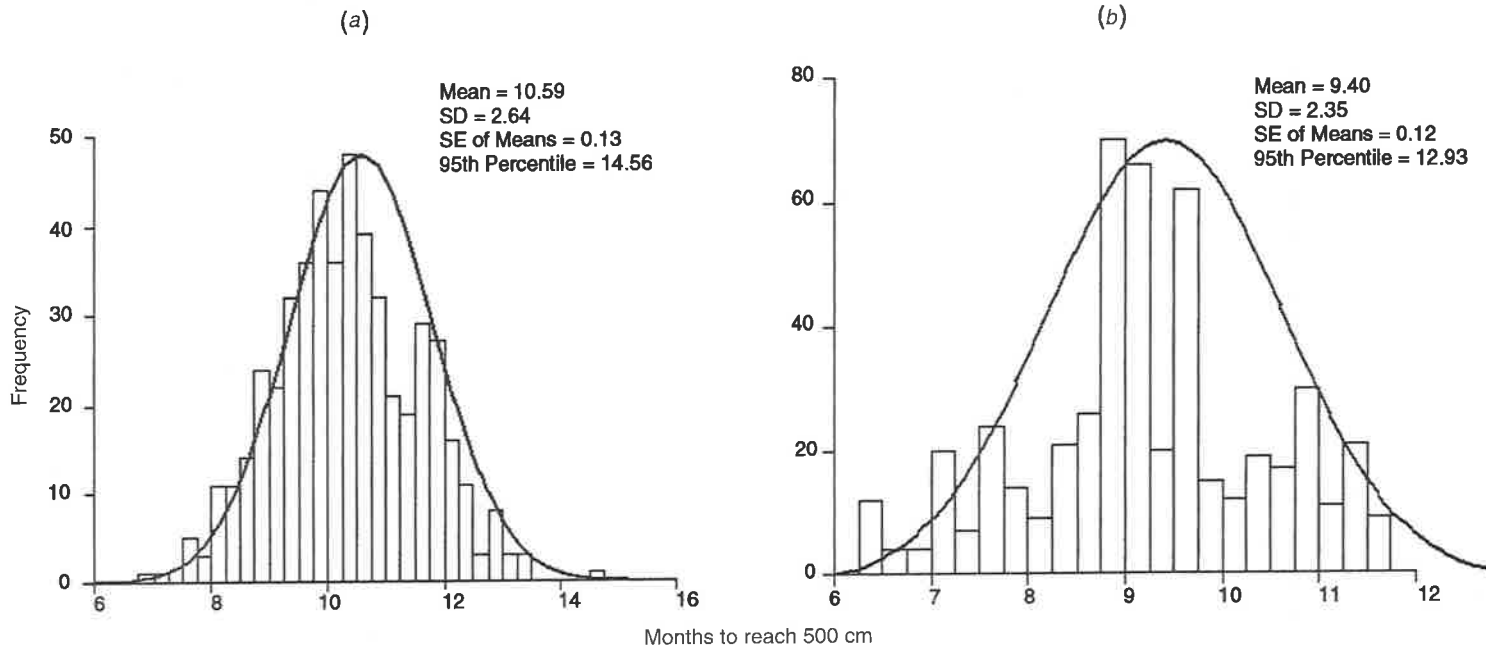


Fig. 4. Frequency distributions of travel times predicted on the basis of (a) average recharge rate and (b) variable daily recharge rates over the period of study.

irrigation conditions at the site concerned. Even over a relatively short period, it is evident that under the soil and environmental conditions of the present study, significant differences can arise on the basis of the two approaches and these would certainly be magnified over successive seasons or in the absence of controlled irrigation rates, particularly for the more persistent chemicals. Monte Carlo simulation of pesticide transport in soil profiles allows the uncertainties associated with the predictions to be quantitatively analysed and provides a more realistic assessment of the groundwater pollution hazards posed by pesticide leaching. The choice of using average or daily recharge rates will depend on the availability of the recharge data and the purpose of a particular modelling exercise.

Acknowledgments

The authors are grateful to Dr Marion Cottingham of the Computer Science Department, The University of Western Australia, for assistance in developing the PESTSCRN software and Dr K. Webb of this Department for assistance with figure presentation. Funding of this research by the Australian Research Council is gratefully acknowledged.

References

- Beitz H, Schmidt H, Herzel F (1994) Occurrence, toxicological and ecotoxicological significance of pesticides in groundwater and surface water. In 'Pesticides in groundwater and surface water. Chemistry of plant protection 9'. (Ed H. Börner) pp. 1–56. (Springer-Verlag: Berlin)
- Benjamin JR, Cornell CA (1970) 'Probability, statistics and decision for civil engineers.' (McGraw-Hill: New York)
- Biggar JW, Nielsen DR (1976) Spatial variability of the leaching characteristics of a field soil. *Water Resources Research* **12**, 78–84.
- Cohen Z, Eiden C, Lorbe MN (1986) Monitoring ground water for pesticides. In 'Evaluation of pesticides in ground water'. (Eds WY Garner, RC Honeycutt, HN Nigg) pp. 170–196. ACS Symposium Series, Vol. 315. American Chemical Society, Washington, DC.
- Di HJ, Aylmore LAG (1997) Modeling the probabilities of groundwater contamination by pesticides. *Soil Science Society of America Journal* **61**, 17–23.
- Di HJ, Kookana R, Aylmore LAG (1995) Application of a simple model to assess the groundwater contamination potential of pesticides. *Australian Journal of Soil Research* **33**, 1031–1040.
- Jury WA, Focht DD, Farmer WJ (1987) Evaluation of pesticide groundwater pollution potential from standard indices of soil-chemical adsorption and biodegradation. *Journal of Environmental Quality* **16**, 422–428.
- Jury WA, Gruber J (1989) A stochastic analysis of the influence of soil and climate variability on the estimate of pesticide groundwater pollution potential. *Water Resources Research* **25**, 2465–2474.
- Kookana RS, Aylmore LAG (1994) Estimating the pollution potential of pesticides to ground water. *Australian Journal of Soil Research* **32**, 1141–1155.
- Kookana, RS, Di HJ, Aylmore LAG (1995) A field study of leaching and degradation of nine pesticides in a sandy soil. *Australian Journal of Soil Research* **33**, 1019–1030.
- Rao PSC, Davidson JM (1980) Estimation of pesticide retention and transformation parameters required in nonpoint source pollution models. In 'Environmental impact of nonpoint source pollution'. (Eds MR Overcash, JM Davidson) pp. 23–67. (Ann Arbor Science Publishers: Ann Arbor, MI)
- Rao PSC, Hornsby AG, Jessu RE. (1985) Indices for ranking the potential for pesticides contamination of groundwater. *Soil Crop Science Society Florida Proceedings* **44**, 1–8.
- Singh R, Gerritse RG, Aylmore LAG (1989) Adsorption–desorption behaviour of selected pesticides in some Western Australian Soils. *Australian Journal of Soil Research* **28**, 227–243.
- USEPA (1977) Waste disposal practices and their effects on groundwater. Report to Congress, Washington, DC, USEPA, Washington, DC.

- USEPA (1978) Surface impoundments and their effects on groundwater quality in the US—A preliminary survey. EPA/9-78-004. USEPA, Washington, DC.
- Wauchope RD, Buttler TM, Hornsby AG, Augustijn-Beckers PMW, Burt JP (1992) The SCS/ARS/CES pesticide properties database for environmental decision-making. *Review of Environmental Contamination and Toxicology* **123**, 1–164.

Manuscript received 31 May 1999, accepted 15 November 1999

Computer-Assisted Tomography and Magnetic Resonance Imaging

S. Asseng¹, L.A.G. Aylmore², J.S. MacFall³, J.W. Hopmans⁴ and P.J. Gregory⁵

¹ CSIRO, Division of Plant Industry, Private Bag, PO, Wembley, Western Australia 6014, Australia

² The University of Western Australia, Soil Science and Plant Nutrition, Nedlands, Western Australia 6907, Australia

³ School of the Environment, Duke University, Durham, North Carolina 27706, USA

⁴ University of California, Dept. Land, Air and Water Resources, Hydrology Program, 123 Veihmeyer Hall, Davis, California 95616, USA

⁵ Department of Soil Science, The University of Reading, Whiteknights, PO Box 233, Reading, RG6 6DW, UK

CONTENTS

11.1	Introduction	343
11.2	X-ray Computed Tomography	345
11.2.1	Applications	345
11.2.2	Limitations	348
11.3	Gamma-Ray Computer-Assisted Tomography	351
11.3.1	Applications	352
11.3.2	Limitations	352
11.4	Dual-Energy Scanning	353
11.4.1	Applications	353
11.4.2	Limitations	353
11.5	Magnetic Resonance Imaging	354
11.5.1	Applications	355
11.5.2	Limitations	358
11.6	Future Prospects	358
11.6.1	Conclusions	359
	References	360

11.1 Introduction

Until recently, techniques for direct measurements on roots and soil water in the rooting zone have been largely destructive, or simply lacked the spatial resolution necessary for meaningful definition of root and water content distrib-

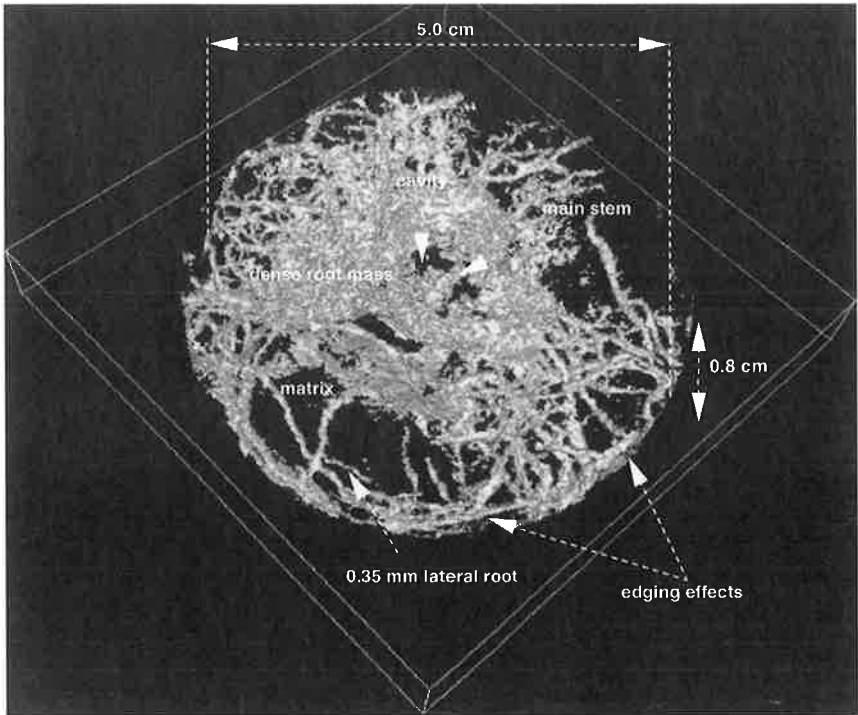


Fig. 11.2. An image of 14-day-old bush bean (*Phaseolus vulgaris* L.) roots in situ, derived from a high-energy industrial X-ray CT. (After Heeraman et al. 1997; with kind permission from Kluwer Academic Publisher)

1989; Vaz et al. 1989; Hopmans et al. 1992) have demonstrated that conventional X-ray medical scanners can provide information otherwise not obtainable on the spatial distributions of bulk density and water content in soil columns and in particular that associated with plant roots (Hainsworth and Aylmore 1983, 1986; Aylmore and Hamza 1990; Hamza and Aylmore 1991, 1992a, b).

Total root length has been estimated from an image of a plant root system in situ (Fig. 11.2) with a resolution of 0.16 mm by Heeraman et al. (1997; Box 11.1). The image was derived with a high-energy industrial X-ray CT system. Although alternative CT techniques using, for example, cone beam geometry in combination with an areal detector array, could potentially improve the spatial resolution to 5–20 μm , it would not necessarily make possible the imaging of very fine roots of this size. First, it would greatly reduce the maximum sample size to 1 cm diameter or smaller. Secondly, when reducing the voxel size further, it would become much more difficult to separate roots from the soil matrix, as roots and water-filled pores have similar attenuation values.

BOX 11.1. Root Length Estimate with a High-energy Industrial X-ray CT System

In an experiment by Heeraman et al. (1997), bush bean plants were transplanted to 5-cm-diameter PVC columns containing a fine sandy soil maintained at field capacity, after pre-germinating the seeds on paper towel. Plants were allowed to grow for 14 days in a controlled growth chamber. Three plants were destructively sampled and analyzed for root growth parameters, including root length, root dry weight, specific root length and root volume. One plant was used for the CT measurements. The stem of the plant was excised at its base, and the root system was imaged with a high-energy (420 keV) third generation industrial X-ray CT scanner (Steude et al. 1994). The scanner was equipped with a linear detector array of 125 detectors with each detector being 0.2109×0.2109 mm in size. Final spatial resolution after reconstruction was 0.16 mm. Horizontal slices (tomograms) were obtained by rotating the object; the time to scan a single slice was 6.2 min. Forty slices were obtained for a total rooting depth of 8 mm (1.2–2 cm depth below the soil surface). Three-dimensional images were obtained by combining a series of 40 individual tomograms into a three-dimensional data set of 8 mm height. The three-dimensional data set was visualized using a modified version of VIS-5D version 4.0 (Fig. 11.2). The volumetric rendering image of roots at the 1.2–2 cm depth uses this imaging software to construct a three-dimensional isosurface of attenuation coefficients. Total root length was estimated from root volume, assuming that the roots are cylindrical. Total root volume as estimated from CT was 2.97 cm^3 , whereas destructive root measurements yielded a total root volume of 2.2 cm^3 for the same depth interval. Total root length as estimated from destructive and CT measurements were 8.65 and 11.7 m for the 1.2–2.0 cm depth. The overestimation of root volume using CT can be caused by signal noise and volume averaging assumptions.

An alternative means of improving the spatial resolution while still retaining the ability to scan large samples is to use a microfocal X-ray beam and to employ “area of interest” scanning techniques. Columns can be scanned rapidly at several angles to identify areas where roots are likely to be present and then those areas can be scanned in more detail. This procedure has the advantages of reducing scanning time and data storage while improving resolution.

Another example of the application of X-ray CT in root research is presented in Fig. 11.3 from Hamza and Aylmore (1992b) which shows a cross section through a lupin plant root and surrounding soil. The total number of pixels, mean, standard deviation and root mean square deviation of pixel values

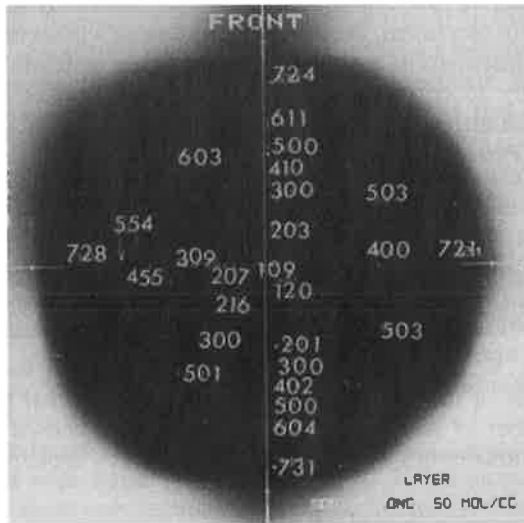


Fig. 11.3. X-ray CT scan showing a cross-section through a lupin plant root and surrounding soil. Hounsfield unit values vary throughout the section of the root. The root diameter is about 4 mm. (After Hamza and Aylmore 1992b)

in the selected region, its area and volume, and the distance between two points are instantly available.

In root water uptake studies by Hainsworth and Aylmore (1983, 1986, 1989), changes in volumetric water associated with single radish roots in a non-swelling 15% kaolinite clay and 85% sand mixture provided the first detailed observations of this type. Uptake of water along the radish roots was clearly shown to be non-uniform with depth, with the roots first removing water from the top, and later drawing water at greater depths, as soil hydraulic resistance became a major limiting factor in the upper soil layer (Hainsworth and Aylmore 1989). Subsequently, Aylmore and Hamza (1990) and Hamza and Aylmore (1991, 1992a, b) used a combination of CT scanning and a Na-ion specific microelectrode technique to measure concomitantly the spatial distribution of soil water content and Na⁺ ion concentration in close proximity to lupin and radish plant roots (Box 11.2). Figure 11.4 illustrates the detail and accuracy with which the CT technique was able to resolve the changes in water content by root water uptake at different positions along the root resulting from differences in water content and electrolyte. Recently, Hamza et al. (1996) have used CT to study the spatial distribution of water content in the vicinity of interacting multiple radish roots and the effects of water stress on root shrinkage and recovery.

11.2.2 Limitations

A number of factors impose limitations on the applicability of X-ray CT which are related to spatial resolution, energy absorption, and changing soil bulk density. For example, the true spatial resolution value in the study by Warner

BOX 11.2. Monitoring Soil Water Content and Na⁺ Concentrations Near Plant Roots

A combination of computer-assisted tomography applied to X- and γ -ray attenuation and Na⁺ liquid ion-exchanger microelectrodes was used by Hamza and Aylmore (1992a,b) to monitor soil water contents and Na⁺ ion concentrations at root depths of 3, 6 and 9 cm and at zero, 2, 4, 6, and 8 h intervals from the diurnal commencement of transpiration. The plants were subjected to two levels of transpirational demand and five Na⁺ soil solution concentration levels.

The scan times took upwards of 1.4 s. The image was displayed immediately following the scan on a video screen in a 512×512 matrix of 2×2 mm pixels (Fig. 11.3). The software provided with the scanner (Somatom DR/H scanner with SCINTILLARC 700) was able to magnify any area in the scanned slice and pinpoint any pixel (from the root center to the bulk soil) to determine its water content automatically through determining its attenuation coefficient. This could be done in very small distance intervals (i.e. 0.1 mm).

The software was also able to perform some statistical functions to calculate the total water content (through Hounsfield units) of the whole or part of the scanned slice, thus making it easy to calculate water uptake by the plant root for any given section and time. Measurable differences in water content of 0.006 g/cm^3 can be readily detected by both X- or γ -ray CAT scanning (Hainsworth and Aylmore 1983, 1988).

In combination with the monitoring of soil water content, Na⁺-LIX microelectrodes were used, in situ, to determine Na⁺ concentrations at the root surface. For this purpose soil pots were specifically designed and constructed to allow accurate positioning of the microelectrode tips at the root surface (Hamza and Aylmore 1991). To ensure root/electrode contact, a 0.1 mm-diameter hole was made from the surface of the soil to the bottom to encourage the root subsequently planted, to follow. The microelectrode shaft was manoeuvred inside a slightly larger plastic tube. Special attention had to be paid to prevent the microelectrode tip from penetrating the root surface where it would read the cortex or xylem concentration instead of that at the root surface. The microelectrode pots were amenable to CAT scanning so that the water drawdown in any layer, and in particular that associated with the microelectrode, could be monitored continuously.

et al. (1989) was about twice the spatial resolution determined by the scanner. This results from the volume averaging that occurs if the interface of two or more materials with different attenuation values are present within a voxel. For

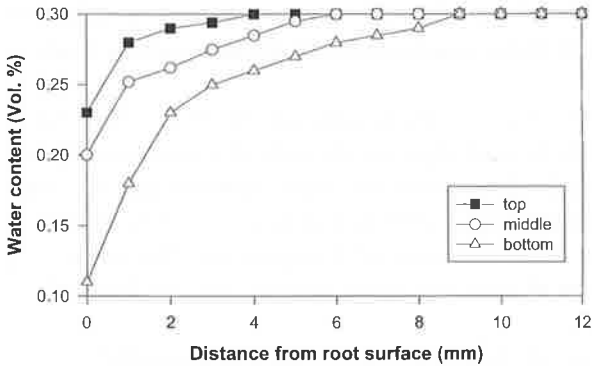


Fig. 11.4. Water drawdowns near top, middle, and bottom sections of a single radish root after 2 h of transpiration measured by CT scanning. (After Hamza and Aylmore 1992a)

example, if two materials each occupy half of the volume of a voxel (e.g., a root surrounded by a soil matrix), then the attenuation of the voxel will be the arithmetic average of the two. Consequently, studies have been largely limited to soils having macropores of a dimension equal to or larger than the voxel size.

Another limitation of X-ray CT in soils arises from the selective absorption of low-energy X-rays. The energy spectrum of X-ray scanners is polychromatic, and preferential absorption of the lower energy X-rays occurs as the beam traverses the soil. This process is referred to as “beam hardening” (Herman 1980). Physical or mathematical filters can partially correct for beam hardening (Brooks and Di Chiro 1976), but such artefacts will undoubtedly occur in soils when using relatively low-energy X-rays.

When only very small differences in attenuation exist between an object and the surrounding soil, the ability to accurately resolve the object (imaging contrast) is also reduced. While X-ray CT provides excellent resolution for some studies, its usefulness in soil systems has invariably been restricted by its inability to distinguish between changes in water content and bulk density in swelling soils. Consequently, the applications of X-ray CT to quantitative soil-water studies in swelling soils have been largely limited to statistical assessments of macroporosity distributions before and after complete wetting and drying cycles (Phogat and Aylmore 1989), and the measurement of water uptake in proximity to plant roots in non-swelling soils (Hainsworth and Aylmore 1986; Aylmore and Hamza 1990; Hamza and Aylmore 1992a, b). Even in non-swelling soils, however, localised changes in bulk density may occur close to roots caused by the root displacing particles when elongating. These changes are not detected by current X-ray systems and may lead to errors in estimates of water uptake.

Their quantitative limitations, great expense and low accessibility have seriously limited the use of medical X-ray scanners for soil-water-plant studies. Moreover, these scanners are designed to monitor patients in a horizontal posi-

tion, and their construction is not generally suitable for studies involving plants growing in vertically-positioned soil columns. Finally, the proprietary nature of these commercial systems makes software modifications difficult.

11.3 Gamma-Ray Computer-Assisted Tomography

Because of the quantitative limitations and restricted accessibility of X-ray systems, work in several laboratories has concentrated on potentially more suitable and less expensive CT systems using γ -ray sources (Hainsworth and Aylmore 1983, 1988; Crestana et al. 1986; Brown et al. 1993). Gamma-ray sources range in strength from a few millicuries to 500 Ci and have been used to obtain useful tomographic images in acceptable scanning times, even with a source brightness which is several orders of magnitude less than that produced by X-ray sources (MacCuaig et al. 1986). The use of γ -sources where the energy spectrum is monochromatic, eliminates the beam hardening and absorption edge problem. Gamma-ray sources also offer additional advantages compared with X-ray tubes, including lower cost, compactness, portability and easy access to a very wide range of photon energies.

A block diagram illustrating the operation of a γ -CT system (Aylmore 1993) is shown in Fig. 11.5. The main body consists essentially of two platforms, with one allowing for vertical motion of the source/detector system, and the other providing linear translation and rotational motions of the object to be scanned.

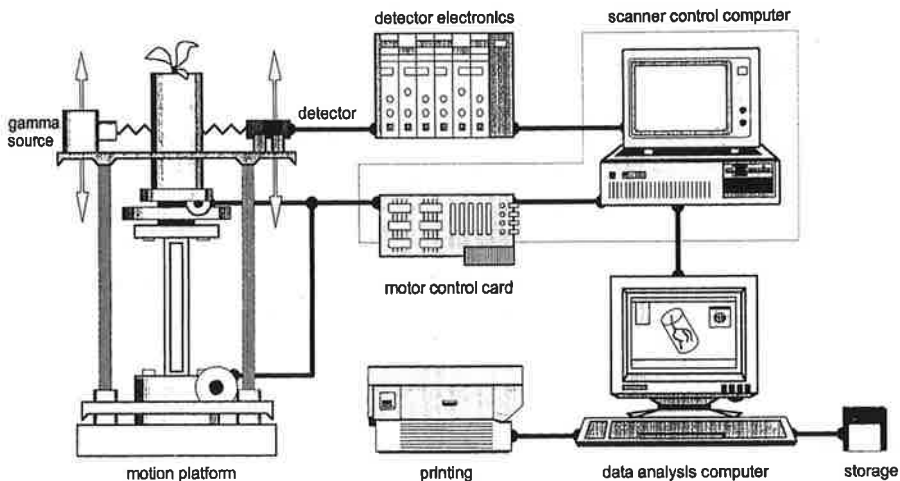


Fig. 11.5. Block diagram of γ -ray CT scanning system constructed at the University of Western Australia, consisting of three subsystems: computer, data acquisition, and motion control systems. (After Aylmore 1993)

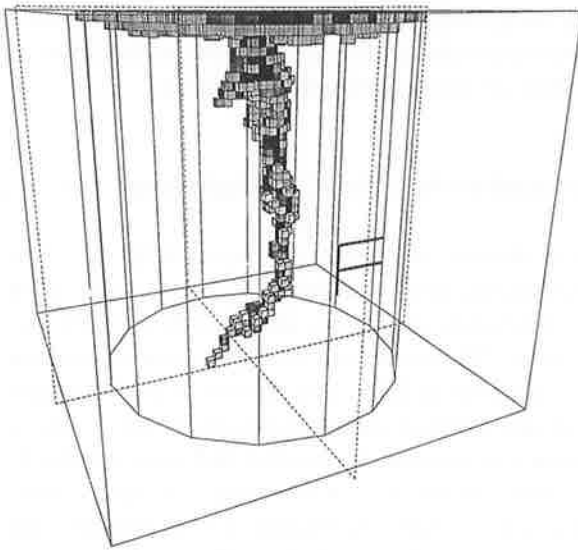


Fig. 11.6. Lupin root in a soil column. Three-dimensional image reconstruction obtained by subtractive imaging using a γ -ray CT. (After Aylmore 1993)

The main platform supports the lead shielding for the source and scintillation detector. The CT scan platform is placed at a fixed level in an opening in the middle of the γ -platform, so that the γ -platform can move independently of the CT scan platform. This system is capable of scanning columns up to 10 cm in diameter and 150 cm in length. The systems developed by Crestana et al. (1986) and Brown et al. (1993) use a similar parallel beam approach.

11.3.1 Applications

Gamma attenuation measurements have been used for many years to monitor changes in average bulk density and water content in sections through soil columns (Gurr 1962; Groenveld et al. 1969; Ryhiner and Pankow 1969). The application of CT to γ -attenuation is illustrated in Fig. 11.6, showing how the development of a lupin tap root in a soil column can be accurately defined by subtractive imaging, thereby eliminating the soil's contribution to the image.

11.3.2 Limitations

The major disadvantage of γ -scanners is their low source brightness (Aylmore 1994). The relatively low photon emission from γ -sources as compared with X-ray sources requires much longer scanning times and larger voxel sizes (5 mm^3 ,

Brown et al. 1993), and measurements are largely restricted to slowly changing or steady state processes. As with X-ray CT, measurements of the spatial distribution of water content in soils by a single γ -source is limited to uniform and non-swelling soils.

11.4 Dual-Energy Scanning

A major limitation of the use of single energy X- or γ -ray CT scanning has been the necessary assumption of uniform or constant bulk density. As soil attenuation is a function of both bulk density and volumetric water content, an accurate determination of water content in soils by these methods is impossible if the bulk density changes during the experiment (Petrovic et al. 1982; Hainsworth and Aylmore 1983; Anderson et al. 1988; Phogat and Aylmore 1989). Even in non-swelling soils, the general non-uniformity of packed soil columns makes accurate measurement of water content distribution near plant roots difficult, since the technique requires exact positioning of the soil column in a sequence of scans.

To monitor changes in the spatial distribution of both bulk density and water content in swelling and shrinking soils, independent estimates of attenuation associated with both bulk density and water content with different energies can be combined. In dual energy γ -CT scanning, a low-energy and a high-energy γ -source have been used (e.g., Cs-137 and Am-235 or Yb-169; Aylmore 1993).

11.4.1 Applications

Effective studies of plant root development and water uptake demand the ability to accurately and simultaneously monitor changes in water content and bulk density in close proximity to the roots. Phogat et al. (1991) demonstrated that, using dual-source γ -CT scanning, it is possible to measure the spatial distributions of bulk density and water content in swelling soils simultaneously and non-destructively with a satisfactory level of precision.

11.4.2 Limitations

Unfortunately, the relatively long scanning time required has limited the efficient application of γ -CT to plant root studies. For example, the study of Phogat et al. (1991) showed that about 169 s was needed for an individual ray-sum. In their study, 112 h were needed to complete a dual-source scan, which resulted

in an average standard deviation in pixel water content values of 0.025 cm^3 . Such large counting times limit its applicability to steady-state systems only.

11.5 Magnetic Resonance Imaging

An alternative approach to studying soil water extraction by plants uses proton (^1H) nuclear magnetic resonance imaging (MRI), as presented in Woods et al. (1989). Nuclei suitable for MRI are characterised by a non-zero spin quantum number I and include ^1H , ^2H , ^{13}C , ^{31}P , ^{17}O , ^{19}F , ^{23}Na , ^{27}Al , and ^{31}P . Of the NMR detectable nuclei, ^1H is intrinsically the most sensitive to detection. It is for this reason that most imaging experiments focus on ^1H , with biological and/or soil water being the most abundant detectable pool of nuclei. In practice, the sample is surrounded with a radiofrequency (rf) coil, and placed into the bore of a superconducting magnet. In a uniform magnetic field all protons resonate at the same specific frequency (Larmor frequency), which is determined by magnetic field strength. Following placement in the static magnetic field, the rf transmitter is used to apply a pulse of radio waves at the Larmor frequency. This generates a magnetic field, designated B_1 , which can be sensed by the nuclei, causing them to “tip sideways”. The degree of tipping is dependent on the strength and duration of the applied rf pulse (Fig. 11.7). When the rf radiation is turned off, the spins realign with the static magnetic field. As they re-align, energy from the transverse magnetisation is detected as an AC current by a receiver coil placed near the specimen. Detected signals are then amplified, filtered and sent to a computer for digitisation and recording of the signal frequency, amplitude and decay. If a magnetic field gradient is applied, protons at different locations will resonate at different frequencies. If three orthogonal

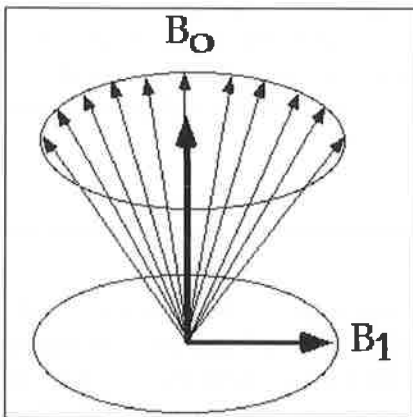


Fig. 11.7. Vector diagram showing the orientation of the primary magnetic field (B_0) which is created by the superconducting magnet, and the perpendicular field created by the radio frequency pulse (B_1). Following placement in the magnet bore, nuclei align themselves so that they process in alignment with B_0

gradients are applied, analysis of the different frequencies can be used to generate a proton density map or image. By changing the three gradients it is possible to control such variables as slice position, slice thickness and resolution, thus producing a magnetic resonance image. These differences in detected signals provide "contrast" to the image, or the ability to distinguish different physiological, biochemical or anatomical properties within a specimen, including the water distribution in soil surrounding roots as well as roots themselves.

There are basically five fundamental parameters in nuclear magnetic resonance (NMR) studies which will determine signals detected from a localised region of tissue, the voxel. The fundamental parameters are spin density (how many detectable nuclei are present within a voxel, representing volumetric water content), spin-lattice relaxation (T_1), spin-spin relaxation (T_2), experimental spin-spin relaxation (T_2^*), and movement (e.g. diffusion and flow). Spin-lattice relaxation and spin-spin relaxation are functions of the degree of interaction of the water with its external molecular environment. For example, soil type affects the binding energy of the water at the liquid-solid interface which may depend on the chemical composition of the soil and soil solution as well. The wide range of properties which determine detection ability and image contrast makes MRI an extremely flexible and powerful technique, but they also greatly complicate the image interpretation. Choice of image acquisition protocol will greatly change the appearance of an image and provides a much wider range of applications than X-ray CT scans, γ -detection or dual-energy scanning.

11.5.1 Applications

It has been demonstrated that large roots (Omasa et al. 1985) and seedlings (Rogers et al. 1985) can be detected in soil by MRI. In an extensive examination of the MRI properties of soil, plant roots were imaged when grown in 30 different agricultural and 8 artificial soils. Image quality and the ability to detect roots suffered significantly when the ferromagnetic particle content was larger than 4%. Below 4%, there was still significant variation in the suitability of a soil as a root imaging substrate. Seven native soils, however, presented excellent delineation of the root systems, suggesting that MRI holds great promise for the non-destructive study of roots within a soil matrix (Bottomley et al. 1986; Rogers and Bottomley 1987). Magnetic resonance imaging has also been demonstrated to give information on the pore structure and wettability of natural sandstone, providing visualisation of wetting heterogeneities (Guillot et al. 1994). The T_1 relaxation time of natural sandstone was shown to increase significantly with salinization, changing the wettability of the surface from

moderately hydrophilic to hydrophobic. Similarly, the binding properties of water, as reflected by the relationship between relaxation time and water content, have been studied for samples of fine sand. When moistened with distilled water, the T1 values increased from 472 ms at 5% (w/w) to 1265 ms at 25% (w/w) water. The increase was linear between 5 and 20%, with a slight reduction in slope between 20 and 25%. The water potential measured by the pressure plate method showed the water potential ranged from 0.01 to 0.0 MPa (J.S. MacFall 1990, unpubl. data), indicating water was not tightly held by the sand grains. Further studies with a variety of sand samples of the same approximate particle size showed a range of T1 relaxation times, ranging from 565 to 1474 ms when the sample contained 25% water (MacFall and Johnson 1994a). In an early study, MacFall et al. (1991) used a series of reference tubes (sand phantoms) filled with acid-washed sand at various water contents to provide a rapid reference calibration curve. This was used to monitor water uptake by Loblolly pine seedlings from a fine sand and to quantitatively compare the relative efficiencies of fine, lateral and taproots in water uptake.

Similar experiments can be conducted for other plants, examining effects of stress, cultivar comparisons, competition, etc. Image acquisition protocols have also been developed to enhance signals detected from functional roots, suppressing signals from water in the surrounding soil/sand. This approach allows enhanced visualisation of the root system, potentially providing new tools to study root water content, conductance, growth, distribution, architecture and turnover. In an early work, Bottomley et al. (1986) used a spatial resolution of 0.6 mm with an unidentified slice definition to observe the movement of a dilute solution of CuSO_4 (a contrast agent which enhanced the detected signal) into and through roots of *Vicia faba*. Brown et al. (1986) were able to differentiate anatomical regions of the *Pelargonium hortorum* roots with a spatial resolution of $0.1 \text{ mm} \times 0.1 \text{ mm} \times 1.2 \text{ mm}$ without the use of contrast agents. In other work, a synthetic soil mix was developed which gave a small magnetic resonance detectable signal while supporting plant root growth (Brown et al. 1991).

These image acquisition protocols have been extended from only two-dimensional image sets to three-dimensional acquisition, reconstruction and views of intact roots in a soil container (MacFall and Johnson 1994a). Images acquired with specially tailored pulse sequences provide sufficient contrast between roots and surrounding soil or sand to allow digital extraction of the root system or segments from the data set. Roots can be extracted either through use of a seeding algorithm or simply by adjusting the viewing opacity and window/level during rendering of the three-dimensional volume (MacFall and Johnson 1994b; Fig. 11.8). This approach has allowed not only visualisation but quantitative measurement of changes in root volume, surface area, and total

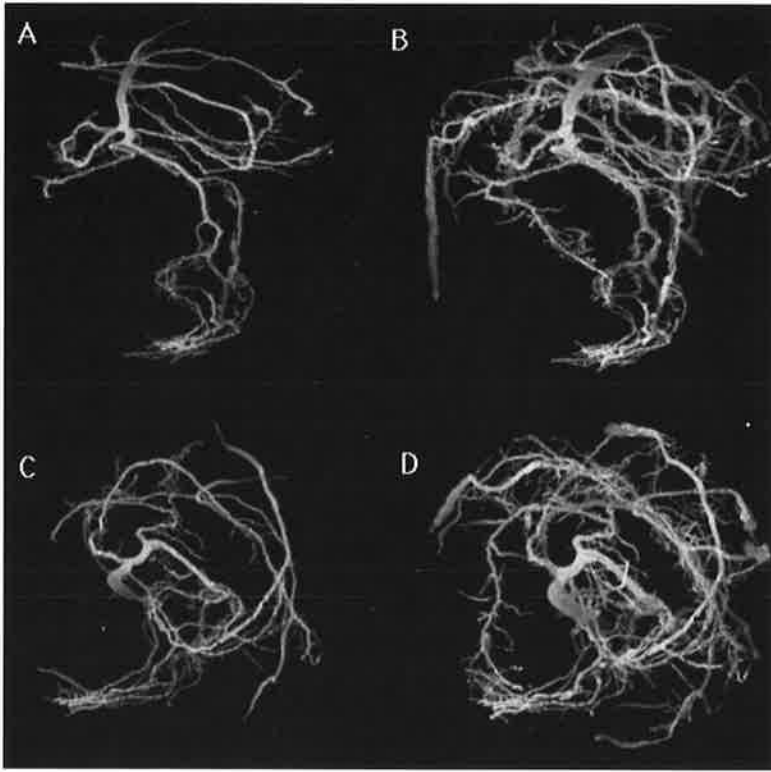


Fig. 11.8. Magnetic resonance images acquired of a pine seedling root system at two points in time. Views A (side view) and C (top view) were acquired soon after plants were transplanted into fine sand. Views B (side view) and D (top view) were acquired 6 weeks after the initial imaging experiments and clearly show the extent of root growth over this period. (J.S. MacFall, unpubl. data)

root length of the root systems of potted Loblolly pine seedlings over a period of several months. Similar studies can be done with other plants, allowing study of many topics such as pathogen effects, root turnover, comparative growth rates, etc. More recent work with pulse sequence parameter optimisation has demonstrated that three-dimensional root images can be acquired, both of intact, entire root systems within a container and of roots within intact field soil cores, further enhancing the potential utility of the technique. Roots can also be studied in a solid, synthetic matrix. Root decay was observed by three-dimensional imaging techniques of detopped root systems embedded in plaster of paris. As roots decayed, preferential patterns of water flow could be observed following the root channels (Liu et al. 1994).

11.5.2 Limitations

The presence of paramagnetic elements such as Fe^{2+} , Fe^{3+} , Mn^{2+} and Cu^{2+} at levels commonly found in soils may cause interference, thus requiring plants to be grown in porous media other than soil or in synthetic soil mixes (Cassel and Nielsen 1994).

One major difficulty is in the adsorption of water to soil particles such as clays. The signal becomes non-detectable when water becomes tightly bound to a solid substrate and less mobile, creating difficulties in quantitatively measuring water which is physically bound within the soil matrix (MacFall et al. 1991). In many cases, however, when the water content becomes low enough that detection becomes limiting, the water potential is also so low that the remaining water would be unavailable for plant uptake. Preliminary work has shown a correlation between water content (and relaxation time) with soil water potential (J.S. MacFall, unpubl.), therefore, from the perspective of water flux, the inability to detect bound water may simply reflect a limiting soil water potential.

Another constraint to the application of MRI is the available scanner time. For the acquisition of a three-dimensional data set, the imaging time required is the product of the time for each slice and the number of slices in the three-dimensional image set. For measurement of water depletion zones, the acquisition time may be up to 8 h, and if the plant is rapidly transpiring, there may be substantial changes in the shape of the depletion zone in this period. Nevertheless, as rapid pulse sequences (e.g. fast spin echo) are developed for plant imaging applications, much shorter acquisition periods will be required.

Similar to X- and γ -ray CT, most existing measuring systems are non-portable and plants have to be grown in soil cores or taken as core samples from the field. The size of MRI systems limits the size of the sample, with sample sizes ranging from <1 cm to 80 cm diameter depending on the opening size of the magnet and field strength. Generally, the larger the sample which can be accommodated, the larger the voxel sizes comprising the image. A limitation of MRI is also the high cost of the system.

11.6 Future Prospects

Industrial CT systems designed for object size/weight/density flexibility and high sensitivity, and not restricted by object motion or radiation dose level, have recently been developed [e.g., at Advanced Research and Applications Corporation (ARACOR), Sunnyvale, California, USA, and Surrey Medical Imaging Systems (SMIS), Surrey, UK]. These include systems capable of inspecting objects up to 2.4 m in diameter by 5 m long and weighing up to 49 500 kg.

Reduction in scanning times to allow more rapid monitoring of changes in soil water content would seem a priority for soil and plant studies. Recently, to reduce scanning time, fourth generation fixed-detector and rotating source scanners have been developed, in which a large number of detectors are mounted on a fixed ring and an X-ray tube inside this ring continually rotates around the object. Furthermore, improved dimensional resolution will enhance structural definition in soil systems. X-ray CT systems have been developed recently to provide $1\ \mu\text{m}$ spatial resolution [e.g., synchrotron X-ray computed macrotomography (CMT), Brookhaven National Synchrotron Light Source X26 beam line, Spanne et al. 1994]. However, current pixel dimensions of the order of 0.5 to 1 mm are quite adequate to allow meaningful resolution of many of the controversies associated with water extraction by plant roots. CT scanning has the potential to provide detailed volume distributions of water content and potential throughout a complete plant root system and to allow the efficiency of different parts of the root system in extracting water and interaction between adjacent roots to be examined. Unfortunately, attempts in this direction (L.A.G. Aylmore and P.J. Gregory, unpubl.; A. Reid, R.D. Schuller and L.A.G. Aylmore, unpubl.) have, as yet, been largely confounded by difficulties in obtaining uniform packing, compensating for variations in soil bulk density and accuracy of repositioning of the column in the scanner. Future portable CT systems will allow scans under field conditions. For example, Onoe et al. (1983) described the use of a portable X-ray CT scanner for measuring annual growth rings of live trees.

In view of their substantially lower cost and some superior quantitative characteristics, such as the absence of beam hardening and absorption edge problems, γ -ray tomographic systems are likely to become a useful tool for soil and plant studies.

Although MRI has its limitations as well, particularly in the study of high Fe-containing soils, it clearly has enormous potential in the study of plant physiological processes and water uptake by plant roots. The flexibility of the imaging protocols provides the tools to study not only root distributions and anatomy, but to probe physiological function. Low cost, portable units for veterinary applications are currently in development, and these may open the doors for greater utility in field applications and to a wider range of users. The development of broad-line MRI techniques may also allow sub-millimetre spatial resolution of water distribution in soils and plants.

11.6.1 Conclusions

Possible applications, advantages and present constraints of X-ray, γ -ray, dual energy systems and MRI for root related studies are summarised in Table 11.1.

Table 11.1. Summarised applications, advantages and present constrains of X-ray, γ -ray, dual energy systems and MRI for root related studies. Note that all applications refer to studies with soil columns

System	Applications	Advantages	Limitations
X-ray CT	Dynamics of roots, soil water or bulk density	High resolution Fast scanning	Beam hardening and edge absorption Requires uniform soil density Requires non-swelling soils
Gamma-ray CT	Steady state roots, soil water or soil density	No beam hardening and edge absorption problems Relative low costs	Requires uniform soil density Requires non-swelling soils Low resolution Slow scanning
Dual energy scanning	Soil water content and bulk density	Can simultaneously quantify changes in soil water content and bulk density (swelling soils)	Very slow scanning
MRI	Dynamics of root structure and soil water	High resolution No soil density effects	Requires absence of paramagnetic elements and high clay contents Slow scanning

Despite some of the current limitations there is no doubt that the application of these innovative techniques will, with further developments, provide major tools for soil and plant scientists and have the potential to resolve major controversies with respect to the dynamics of plant root systems and water uptake by plant roots.

Acknowledgements. We thank Drs D. Rolin and A. Perry for helpful discussions, Drs K. Shackel and A. McNeill for comments on the manuscript and the Grains Research and Development Corporation for financial support.

References

- Anderson SH, Hopmans JW (eds) (1994) Tomography of soil-water-root processes. Proc Symp sponsored by Division S-1 and S-6 of the Soil Science Society of America in Minneapolis,

- Minnesota, 4 November 1992. SSSA Special Publication No 36. American Society of Agronomy, Soil Science Society of America, Madison, Wisconsin
- Anderson SH, Gantzer CJ, Boone JM, Tully RJ (1988) Rapid non-destructive bulk density and soil water content determination by computed tomography. *Soil Sci Soc Am J* 52: 35–40
- Aylmore LAG (1993) Use of computer-assisted tomography in studying water movement around plant roots. *Adv Agron* 49: 1–54
- Aylmore LAG (1994) Application of computer-assisted tomography to soil-plant-water studies – an overview. In: Anderson SH, Hopmans JW (eds) *Tomography of soil-water-root processes*. Proc Symp sponsored by Division S-1 and S-6 of the Soil Science Society of America in Minneapolis, Minnesota, 4 November 1992. SSSA Special Publication No 36. American Society of Agronomy, Soil Science Society of America, Madison, Wisconsin, pp 7–16
- Aylmore LAG, Hamza M (1990) Water and solute movement to plant roots. In: *Transactions 14th Congr of Soil Science*. Kyoto, Japan, 12–18 Aug. ISSS, Wageningen, pp 124–129
- Bottomley PA, Rogers HH, Foster TH (1986) NMR imaging shows water distribution and transport in plant root systems in situ. *Proc Natl Acad Sci* 83: 87–89
- Brooks RA, Di Chiro G (1976) Principles of computer-assisted tomography (CAT) in radiographic and radioisotopic imaging. *Phys Med Biol* 21: 689–732
- Brown DP, Pratum TK, Bledsoe C, Ford ED, Cothorn JS, Perry D (1991) Noninvasive studies of conifer roots: nuclear magnetic resonance (NMR) imaging of Douglas-fir seedlings. *Can J For Res* 21: 1559–1566
- Brown GO, Stone ML, Gazin JE (1993) Accuracy of gamma ray computerised tomography in porous media. *Water Resour Res* 29: 479–486
- Brown JM, Johnson GA, Kramer PJ (1986) In vitro magnetic resonance microscopy of changing water content in *Pelargonium hortorum* roots. *Plant Physiol* 82: 1158–1160
- Cassel DK, Nielsen DR (1994) The realization of a dream. In: Anderson SH, Hopmans JW (eds) *Tomography of soil-water-root processes*. Proc Symp sponsored by Division S-1 and S-6 of the Soil Science Society of America in Minneapolis, Minnesota, 4 November 1992. SSSA Special Publication No 36. American Society of Agronomy, Soil Science Society of America, Madison, Wisconsin, pp 1–6
- Crestana S, Mascarenhas S, Pozzi-Mucelli RS (1985) Static and dynamic three-dimensional studies of water in soil using computed tomographic scanning. *Soil Sci* 140: 326–332
- Crestana S, Cesareo R, Mascarenhas S (1986) Using a computer-assisted tomography miniscanner in soil science. *Soil Sci* 142: 56–61
- Groenvelt PH, De Swart JG, Cislser J (1969) Water content measurement with 60 keV gamma ray attenuation. *Bull Int Assoc Sci Hydrol* 14: 67–78
- Guillot G, Chardaire-Riviere C, Bobroff S, Le Roux A, Roussel JC, Cuiec L (1994) Characterisation of wetting heterogeneities in sandstone rocks by MRI. *Magn Reson Imaging* 12: 365–368
- Gurr CG (1962) Use of gamma rays in measuring water content and permeability in unsaturated columns of soils. *Soil Sci* 94: 224–229
- Hainsworth JM, Aylmore LAG (1983) The use of computer-assisted tomography to determine spatial distribution of soil water content. *Aust J Soil Res* 21: 435–443
- Hainsworth JM, Aylmore LAG (1986) Water extraction by single plant roots. *Soil Sci Soc Am J* 50: 841–848
- Hainsworth JM, Aylmore LAG (1988) Application of computer-assisted tomography (CAT) to gamma attenuation measurement of soil water content. *Aust J Soil Res* 26: 105–110

- Hainsworth JM, Aylmore LAG (1989) Non uniform soil water extraction by plant roots. *Plant Soil* 113: 121–124
- Hamza M, Aylmore LAG (1991) Liquid ion exchanger microelectrodes used to study soil solute concentrations near roots. *Soil Sci Soc Am J* 55: 954–958
- Hamza M, Aylmore LAG (1992a) Soil solute concentration and water uptake by single lupin and radish plant roots. I. Water extraction and solute accumulation. *Plant Soil* 145: 187–196
- Hamza M, Aylmore LAG (1992b) Soil solute concentration and water uptake by single lupin and radish plant roots. II. Driving forces and resistances. *Plant Soil* 145: 197–206
- Hamza MA, Anderson SH, Aylmore LAG (1996) Studies of root function using computer-assisted tomography. *Proc ASSSI and NZSSS National Soils Conf, Melbourne*, pp 97–98
- Heeraman DA, Hopmans JW, Clausnitzer V (1997) Three-dimensional imaging of plant roots in situ with X-ray computed tomography. *Plant Soil* 189: 167–179
- Herman GT (1980) Image reconstruction from projections: the fundamentals of computed tomography. Academic Press, New York
- Hopmans JW, Vogel T, Koblik PD (1992) X-ray tomography of soil water distribution in one-step outflow experiments. *Soil Sci Soc Am J* 56: 355–362
- Hounsfield GN (1972) A method of an apparatus for examination of a body by radiation such as X- or gamma-radiation. British Patent No. 1283915. British Patent Office, London
- Liu IY, Waldron LJ, Wong STS (1994) The application of nuclear magnetic resonance imaging to study preferential water flow through root channels. In: Anderson SH, Hopmans JW (eds) *Tomography of soil-water-root processes*. Proc Symp sponsored by Division S-1 and S-6 of the Soil Science Society of America in Minneapolis, Minnesota, 4 November 1992. SSSA Special Publication No 36. American Society of Agronomy, Soil Science Society of America, Madison, Wisconsin, pp 135–148
- MacCuaig N, Tajuddin AA, Gilboy WB (1986) Industrial tomography using a position-sensitive carbon-fibre anode proportional counter. *Nucl Instrum Methods* 242: 620–625
- MacFall JS, Johnson GA (1994a) Use of magnetic resonance imaging in the study of plants and soils. In: Anderson SH, Hopmans JW (eds) *Tomography of soil-water-root processes*. Proc Symp sponsored by Division S-1 and S-6 of the Soil Science Society of America in Minneapolis, Minnesota, 4 November 1992. SSSA Special Publication No 36. American Society of Agronomy, Soil Science Society of America, Madison, Wisconsin, pp 99–114
- MacFall JS, Johnson GA (1994b) The architecture of plant vasculature and transport as seen with magnetic resonance microscopy. *Can J Bot* 72: 1561–1573
- MacFall JS, Johnson GA, Kramer PJ (1991) Comparative water uptake by roots of different ages in seedlings of Loblolly pine (*Pinus taeda* L.) *New Phytol* 119: 551–560
- Omasa K, Onoe M, Yamada H (1985) NMR imaging for measuring root system and soil water content. *Environ Control Biol* 23: 99–102
- Onoe M, Tsao JM, Nakamura H, Kogure J, Kawamura H, Yoshimatsu M (1983) Computed tomography for measuring annual rings of live trees. *Proc IEEE* 71: 907–908
- Petrovic AM, Siebert JE, Rieke PE (1982) Soil bulk density analysis in three dimensions by computed tomographic scanning. *Soil Sci Soc Am J* 46: 445–450
- Phogat VK, Aylmore LAG (1989) Evaluation of soil structure by using computer-assisted tomography. *Aust J Soil Res* 27: 313–323
- Phogat VK, Aylmore LAG, Schuller RD (1991) Simultaneous measurement of the spatial distribution of soil water content and bulk density. *Soil Sci Soc Am J* 55: 908–915
- Rogers HH, Bottomley PA (1987) In situ nuclear magnetic resonance imaging of roots: influence of soil type, ferromagnetic particle content, and soil water. *Agron J* 79: 957–965

- Rogers HH, Bottomley PA, Foster TH (1985) Application of nuclear magnetic resonance imaging to plant root studies. *Proc Int Conf Soil Dynam* 5: 1152–1157
- Ryhiner AH, Pankow J (1969) Soil moisture measurement by the gamma transmission method. *J Hydrol* 9: 194–205
- Spanne P, Jones KW, Prunty L, Anderson SH (1994) Potential applications of synchrotron computed microtomography to soil science. In: Anderson SH, Hopmans JW (eds) *Tomography of soil-water-root processes*. Proc Symp sponsored by Division S-1 and S-6 of the Soil Science Society of America in Minneapolis, Minnesota, 4 November 1992. SSSA Special Publication No 36. American Society of Agronomy, Soil Science Society of America, Madison, Wisconsin, pp 43–58
- Stuede JS, Hopkins F, Anders JE (1994) Industrial X-ray computed tomography applied to soil research. In: Anderson SH, Hopmans JW (eds) *Tomography of soil-water-root processes*. Proc Symp sponsored by Division S-1 and S-6 of the Soil Science Society of America in Minneapolis, Minnesota, 4 November 1992. SSSA Special Publication No 36. American Society of Agronomy, Soil Science Society of America, Madison, Wisconsin, pp 29–42
- Stuede JS, Sullivan CP, Chaney RC, McKee M, O'Shea LE (1989) Tracer experiments in saturated sand by computed tomography and inductively coupled plasma. In: Hoddinott K, Lamb RO (eds) *Proceeding of the Symposium on Physio-Chemical Properties of Soil, Rock, and Related Materials*. St Louis, Missouri 29 June 1989. American Society of Testing and Materials, Philadelphia, pp 171–184
- Tollner EW, Verma BD, Cheshire JM (1987) Observing soil-root-interactions and soil organisms using X-ray computer tomography. *Trans Am Soc Agric Engin* 30: 1605–1610
- Tollner EW, Murphy C, Ramseur EL (1994) Techniques and approaches for documenting plant root development with X-ray computed tomography. In: Anderson SH, Hopmans JW (eds) *Tomography of soil-water-root processes*. Proc Symp sponsored by Division S-1 and S-6 of the Soil Science Society of America in Minneapolis, Minnesota, 4 November 1992. SSSA Special Publication No 36. American Society of Agronomy, Soil Science Society of America, Madison, Wisconsin, pp 115–134
- Vaz CMP, Crestana S, Mascarenhas S, Cruvinel PE, Reichardt K, Stolf R (1989) Using a computed tomography miniscanner for studying tillage-induced soil compaction. *Soil Technol* 2: 313–321
- Warner GS, Nieber JL, Moore ID, Geise RA (1989) Characterizing macropores in soil by computed tomography. *Soil Sci Soc Am J* 53: 653–660
- Woods RT, Hennessy JJ, Kwok E, Hammer BE (1989) NMR microscopy – A new biological tool. *Bio Techniques* 7: 616–622

PESTSCRN 4 – An innovative approach to the prediction of groundwater pollution by pesticides

Melissa J. Bromly, L. A. Graham Aylmore and Kelvin M. Webb

Soil Science and Plant Nutrition Faculty of Agriculture, The University of Western Australia.

Abstract

In this paper we develop an innovative approach to the prediction of pesticide movement in soil profiles based on the use of surrogate variables and graphical representations (Beta distributions) to describe the influence of soil properties and conditions such as texture and structure, on the spatial distribution of pesticide concentration within the profile as leaching occurs. This extension of the PESTSCRN model does not require detailed specification or quantification of transport mechanisms and offers the prospect of a user friendly facility requiring a minimum of readily available input parameters while providing practical estimates of the mobility and concentration distribution with time of pesticides in a soil profile for use by managerial and regulatory agencies.

Introduction

There is increasing community and professional concern at the extent to which field-applied solutes, most commonly pesticides and fertilisers may contaminate groundwaters. The most reliable way of testing groundwater pollution potential remains through field tests. However, the large number of pesticides in use, the wide range of soil types and environmental conditions encountered and the costs involved, essentially preclude experimental evaluation of the hazards posed in each situation. Consequently considerable attention has recently been directed to the use of computer simulation models to provide regulatory and management guidance (e.g. Jury *et al.* 1987; Nicholls *et al.* 1982; Di and Aylmore, 1997).

Pesticide leaching models are invariably based on the observation that the potential of a pesticide to pollute groundwater is determined essentially by: (a) the movement of water, (b) equilibrium and kinetic aspects of sorption/desorption, and (c) chemical and biological degradation (Jury and Ghodrati, 1989; Aylmore and Kookana 1993). Such models vary widely in their complexity and detail in representation of these processes.

The development of mechanistic models based on the classical convective-dispersive-equation and their evaluation under controlled laboratory conditions (Jury and Ghodrati, 1989; Brusseau and Rao, 1989; van Genuchten, 1991) provides important insights into the significance of the various physical and chemical processes involved in determining pesticide movement in soils (i.e. are research oriented). However, given the extreme complexity and spatial variability in texture and structure in soil profiles, in addition to variations in the magnitude and timing of recharge, initial and transient soil water contents, and the many other possible complicating factors, a practical management model for pesticide leaching based on detailed mechanistic representation of all physical processes appears neither feasible nor likely to be user friendly in terms of input parameter requirements.

In contrast models based on stochastic representation of the transport properties (Jury and Ghodarti, 1989; Di et al., 1995) while providing little understanding of the underlying physical and chemical processes, seek a more functional description in terms of readily accessible parameters (i.e. are management oriented). Such models use far less computer time and can be more easily adopted by management agencies because of their simplicity and limited data requirements

Di *et al.* (1995) and Di and Aylmore (1997) developed a simple model to assess the groundwater contamination potential of organic pesticides used in agricultural and horticultural systems. The model was designed to screen out or identify pesticides which have a high probability of causing groundwater contamination in a region (e.g. a catchment, farm or particular cropping area). Subsequently an enhanced version of the model, now available as a user-friendly software package (PESTSCRN 3, Aylmore and Di, 1998, 2000) was developed which enables the temporal variability of recharge to be taken into account and illustrates the influence of seasonal patterns of leaching and variations in predicted mobilities and persistence from those associated with averaging the recharge rate.

While models such as PESTSCRN have in some circumstances been shown to compare favourably to more complex models against field experimental data (e.g. Kookana et al., 1995) they are frequently restricted to a scaling procedure only predicting the relative mobility of the pesticides in a soil profile with no indication of the distribution down the profile at any given time. However, incorporation of transient convection and/or diffusive/dispersive mechanisms into the modelling process to provide a realistic description of the changing distribution within a soil profile, is essentially self defeating because accessibility or acquisition of the parameters relevant to these processes and their temporal and spatial variability within soil profiles, is generally beyond the resources or desire of most managerial and regulatory users.

In the present paper we seek to develop an innovative approach to the prediction of pesticide movement in soil profiles based on the use of readily available surrogate variables and graphical representations to describe the influence of soil properties and conditions such as texture and structure, on the spatial distribution of pesticide concentration within the profile as leaching occurs.

Model Development

The PESTSCRN model was formulated based on the following assumptions:

- (1) Linear, equilibrium and reversible sorption;
- (2) First-order breakdown or degradation;
- (3) Pesticide leaching by steady convective flow and
- (4) Recharge rate varying with time.

The following two computations are carried out for travel time (t) and for fractions (F) of the pesticide remaining as it travels to different depths of the unsaturated soil zone

$$t_i = \sum [\Delta z (\rho_b f_{OC} K_{OC} + \theta) / q] \quad (1)$$

$$F = \prod_{i=1}^N \exp[-\Delta z (\rho_b f_{OC} K_{OC} + \theta) 0.693 / (qt_{1/2})]_i \quad (2)$$

where f_{OC} is weight fraction of soil organic carbon, K_{OC} is the sorption coefficient normalized by soil organic carbon fraction, q is recharge rate, ρ_b is soil dry bulk density, θ is soil moisture content which is assumed to equal field capacity and Δz is layer thickness.

Briefly, PESTSCRN 3 estimates the position of the peak of an applied pesticide slug and the time taken to reach a given depth. Outputs from the model can be obtained using either single

value input parameters or random values of input parameters generated from probability distributions as specified by the means (μ) and standard deviations (σ), assuming normal distributions (Monte Carlo simulations). The outputs provide a statistical analysis of travel time and fraction of applied pesticide remaining at a given depth Figure 1a). The frequency distributions of residue fractions for all pesticides examined to date, show significant positive skewness with the peak frequency towards the lower boundary of 0 (Figure 1b). These distributions can be described by Beta distribution functions (Benjamin and Cornell, 1970) (outlined below).

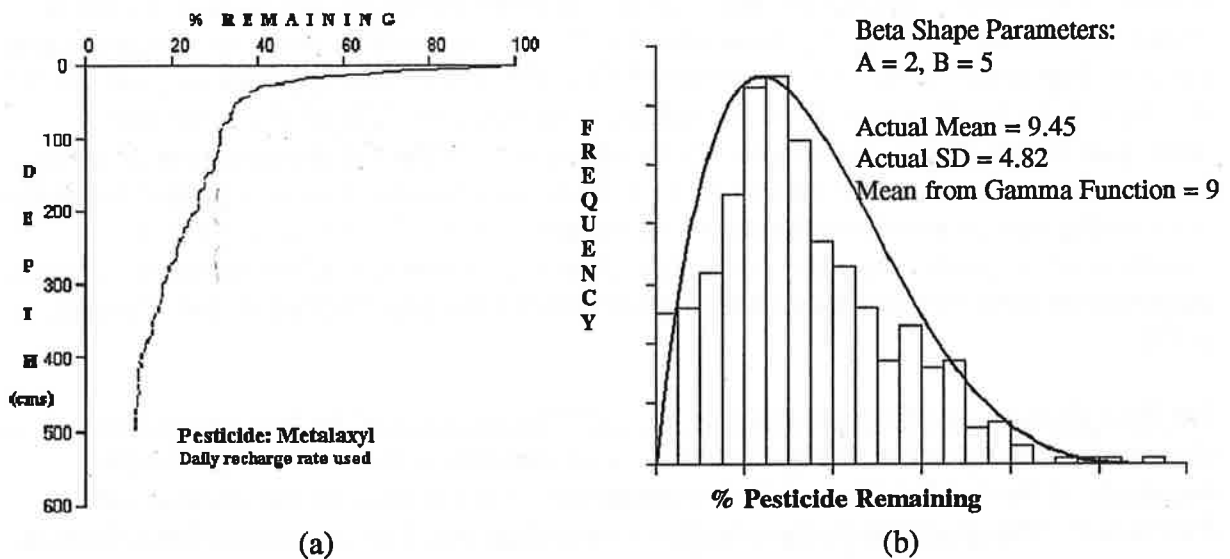


Figure 1

Model extension

In the absence of any significant perturbations, such as occurs in chromatographic flow, the distribution of solute concentration moving through a porous medium follows essentially a normal distribution in which the peak height decreases and standard deviation increases as the distribution progresses down the column. This approach formed the basis for Day's (1956) successful use of Einstein's statistics of complete disorder or theory of "random walk" to describe Wetsell's (1962) data for the distribution of a conservative solute (nitrate) in a homogeneous soil profile.

Perturbations to the transport process can act in several ways to skew the distribution either towards the advancing or receding front. Sorption interactions invariably retard the downward leaching velocity of the overall solute slug in the soil profile and any deviation from ideality such as time dependency or effective hysteresis, will tend to skew the distribution towards the receding front. The nature of the pore size distribution can result in effects on both the advancing and receding fronts. For example intra-aggregate diffusion in structured systems will act to produce a "hold-back" of solute and skew the distribution towards the receding front. Conversely, the presence of macro-porosity and preferred flow channels will accelerate solute movement and skew the distribution towards the advancing front. Thus the spread of the front and tail of a slug is an integrated consequence of the soil texture and/or structure, occurring as a perturbation of the dominant type of spreading being induced by the soil physical characteristics.

A recent detailed survey of literature breakthrough curves and measured solute distributions undertaken in these laboratories (Bromly, 1999), has demonstrated that for many purposes, the influence of both pesticide/soil interactions and hydrodynamic processes on the spread of pesticide around the peak concentration in the longitudinal direction can be effectively described by means of graphical representations based on surrogate parameters. There are a number of potentially suitable equations for this purpose including Beta, Gamma, Lognormal and/or the use of statistical moments.

The approach used here involves defining suitable empirically determined graphical parameters to reflect the effects of soil texture and degree of aggregation on the spreading of solutes in typical soil profiles and coupling these with the effects of convection, sorption retardation and pesticide degradation kinetics in the simple PESTSCRN model. The approach proposed here is thus akin to the highly successful Universal Soil Loss Equation (USLE) where simpler "surrogate variables" are used to quantify the effects of different soil attributes and conditions (e.g. texture, structure, water content etc.) on the erosion process. That is, a bulked description of spreading may be used in conjunction with the assumption of piston flow of the peak concentration to predict the peak depth. Spreading effects may be neglected, and the computed magnitude of these effects subsequently imposed around the peak (Addiscott and Wagenet, 1985).

The Beta distribution (Benjamin and Cornell, 1970) is characterised by four parameters, allowing for either positive or negative skew. Two parameters (L_a and L_b) describe the magnitude of the front and tail, while two parameters (r and t) describe the shape of the distribution. This graphical characterisation of spreading, based upon literature breakthrough curves, takes into account a bulked empirical measure of diffusion, dispersion, preferential flow and holdback effects.

For r and $t - r$ positive, the beta distribution is given by:

$$f(x) = \frac{1}{B} x^{r-1} (1-x)^{t-r-1} \quad 0 \leq x \leq 1$$

where the normalising constant, B , is given by:

$$B = \frac{(r-1)!(t-r-1)!}{(t-1)!}$$

if r and $t - r$ are integer valued, or

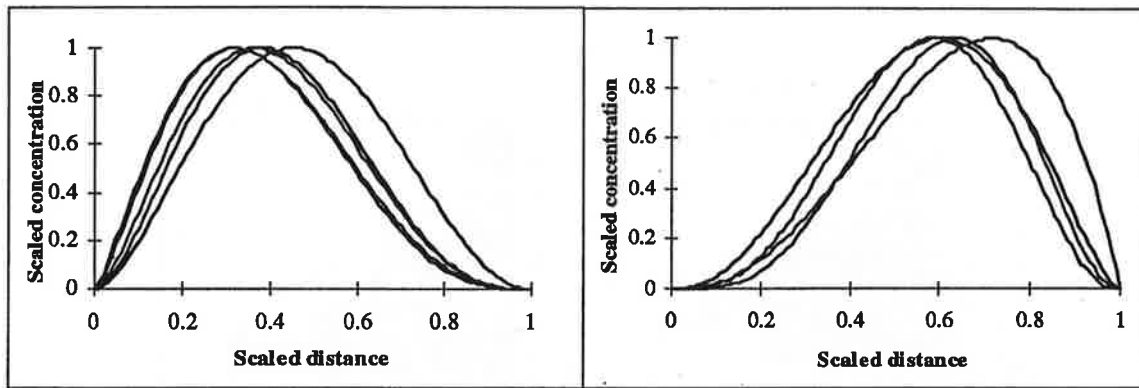
$$B = \frac{\Gamma(r)\Gamma(t-r)}{\Gamma(t)}$$

if r and $t - r$ are non-integer values, where Γ denotes the gamma distribution, given by:

$$\Gamma(k) = \int_0^{\infty} e^{-u} u^{k-1} du$$

Application

The parameters describing the solute distributions were found relatively consistent within a soil textural class for non-aggregated soils (Figures 2a and 2b). However, no clear trend was discernible across the soil textural spectrum. This can be largely attributed to the lack of detailed specification of soil textural and structural characteristics in much of the published literature. Current experimental work here is aimed at providing a better definition of these relationships.



(a) Loam

(b) Loamy sand

Figure 2

For any given textural class PESTSCRN can be programmed to provide a description of the changing distribution with depth as leaching proceeds. Figure 3 illustrates the computer screen display for pesticide distribution

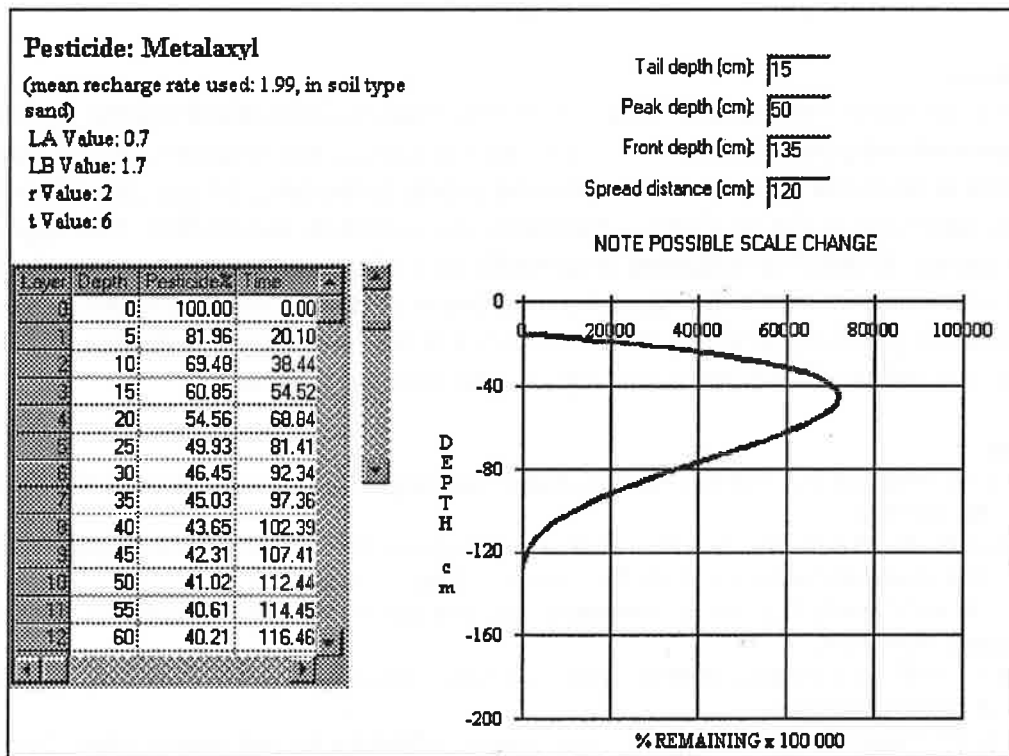


Figure 3

The current accuracy of these predictions, based on limited data from the literature, is problematical and improvements will await definitive experimental evaluation of these parameters as information is accrued.

Figure 4, showing comparisons between measured metribuzin spreading in a sandy loam soil after (a) 56 days and (b) 112 days (Walker et al. , 1996) and Beta distributions, illustrates how the Beta distribution can, using the appropriate empirically determined surrogate parameters, describe the skewed distributions associated with pesticide leaching.

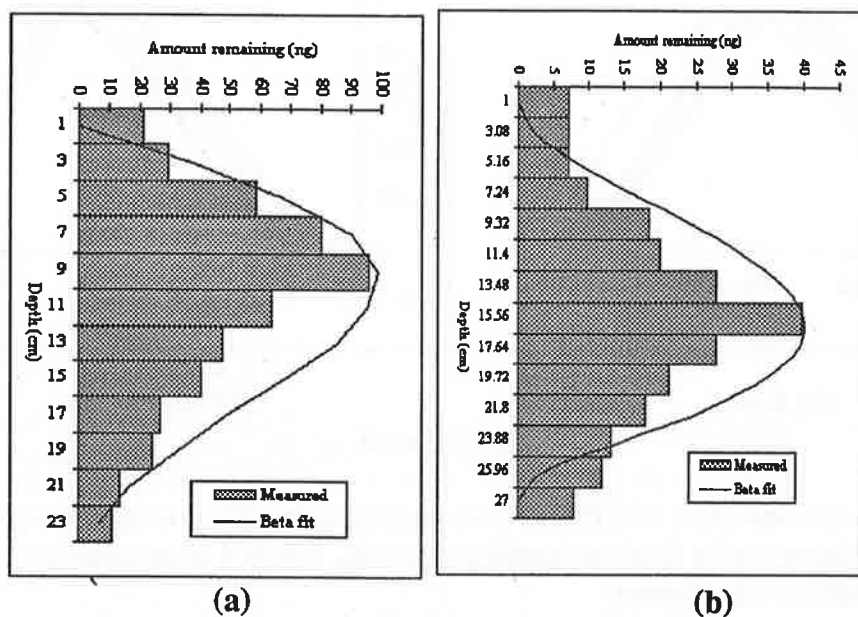


Figure 4

Conclusions

The use of surrogate variables and graphical representations (Beta distributions) to describe the influence of soil properties and conditions such as texture and structure, on the spatial distribution of pesticide concentration within the profile as leaching occurs, provides an innovative approach to the prediction of pesticide movement in soil profiles. This approach does not require detailed specification or quantification of transport mechanisms and offers the prospect of a user friendly facility requiring a minimum of readily available input parameters while providing practical estimates of the mobility and concentration distribution with time of pesticides in a soil profile for use by managerial and regulatory agencies.

References

- Addiscott, T.M, Wagenet, R.J. (1985). Concepts of solute leaching in soils: a review of modelling approaches. *J. Soil Sci.* **36**, 411-424.
- Aylmore, L.A.G., Di, H.J. (1998). Variable recharge and the probabilities of groundwater contamination by pesticides. Proc. National Conference, Aust. Soc. Soil Sci., Brisbane, 422-428.
- Benjamin, J.R. and Cornell, C.A. (1970). Probability, statistics and decision for civil engineers. McGraw-Hill Book Company, New York.
- Bromly, M.J. (1999) An evaluation of the basis for modelling pesticide transport in soils. Honours Thesis, University of Western Australia.
- Day, P.R. (1956) Dispersion of a moving salt water boundary advancing through saturated sand, *Trans. Am. Geophys. Union* **37**, 595-601.
- Di, H.J. and Aylmore, L.A.G. (1997). Modeling the probabilities of groundwater contamination by pesticides. *Soil Sci. Soc. Am. J.* **61**, 17-23.
- Di, H.J., Kookana, R.S. and Aylmore, L.A.G. (1995). Application of a simple model to assess the ground water contamination potential of pesticides. *Aust. J. Soil Res.* **33**, 1031-1040.
- Jury, W. A., Ghodrati, M., (1989) *Overview of Organic Chemical Environmental Fate and Transport Modeling Approaches* in "Reactions and Movement of Organic Chemicals in Soils", SSSA Special Publication No. 22, Wisconsin, U.S.A. p. 271-304.
- Kookana, R.S., Di, H.J. and Aylmore, L.A.G. (1995). A field study of leaching and degradation of nine pesticides in a sandy soil. *Aust. J. Soil Res.* **33**, 1019-1030.
- Van Genuchten, M.Th., (1991) Recent progress in modelling water flow and chemical transport in the unsaturated zone. In G. Keinitz et al (eds) IAHS Publ. No. 204, pp. 169-183 Instit. Hyd. Oxfordshire, U.K.
- Walker, A., Welch, S.J., Melacini A. and Moon, Y.H. (1996). Evaluation of three pesticide leaching models with experimental data for alachlor, atrazine and metribuzin. *Weed Res.*, **36**, 37-47.

Studies of soil water drawdowns by single radish roots at decreasing soil water content using computer-assisted tomography

M. A. Hamza^A, S. H. Anderson^B, and L. A. G. Aylmore^{AC}

^ADepartment of Soil Science and Plant Nutrition, The University of Western Australia, Nedlands, Australia.

^BSoil Science, University of Missouri-Columbia, USA.

^CCorresponding author; email: aylmore@cyllene.uwa.edu.au

Abstract

Application of computer-assisted tomography to the attenuation of X-rays has been used to compare the drawdowns in soil water content associated with radish roots at starting soil water contents (θ_v) of 0.3 cm³/cm³ and 0.1 cm³/cm³, respectively. Decreasing soil water content results in an increase in the appearance of 'beam hardening'. Decreasing soil water content from 0.3 to 0.1 cm³/cm³ caused the transpiration rate to decrease by 6–10 times. This was presumably due to a reduction in the water potential gradient across the root membrane. The transpiration rate decreased less rapidly than did the water content at the soil–root interface, suggesting some osmotic adjustment by the leaves. This osmotic adjustment would allow the plant to maintain transpiration rate even at relatively low soil water content. The drawdown distances associated with roots growing at the lower soil water content were 8 times smaller than those at the high soil water content and the value of θ_v at the soil–root interface at the end of the transpiration period was 2.5 times lower. The radish roots exhibited a temporary slight decrease in diameter after the transpiration commenced followed by a significant temporary increase. However, root diameter stabilised around its original value when the plant attained an almost steady water uptake rate. Despite the complexity arising from 'beam hardening', CAT scanning can provide valuable information on processes at the root–soil interface.

Additional keywords: CAT scanning, water uptake, radish, matric potential, osmotic potential, soil and plant resistance.

Introduction

Water drawdowns by plant roots grown in soil at high water potential (≥ -30 kPa) have been studied in some detail using X- and gamma-ray computed tomography (Hainsworth and Aylmore 1986; Aylmore and Hamza 1990; Hamza and Aylmore 1992a, 1992b). In contrast, water drawdown by plant roots grown at low soil water potential (< -30 kPa) has received much less attention from researchers. This is mainly due to the increasing complexity of the soil water–plant relationship and the changes in water energy status of both soil and plant.

Water movement in the soil–plant–atmosphere continuum is initiated and maintained by differences between the chemical potential (total potential) of water in the leaves and in the soil (McCoy *et al.* 1984). Similarly soil water flow is controlled by the potential gradient between the soil and the plant root (Herkelrath *et al.* 1977; Baveye and Sposito 1984; Campbell 1985). Soil and plant resistances to water flow are strongly related to soil water potential, and as this decreases, the magnitude and the nature of both resistances undergo changes which are not yet fully understood.

In a transpiring plant, the following equation, derived from irreversible thermodynamic considerations, is commonly used to describe the volume flux of water, or more correctly, of solution, J_v , across the plant root (Dainty 1976):

$$J_v = L_p (\Delta p - \sigma \Delta \pi) \quad (1)$$

where L_p is the hydraulic conductivity of the membrane, Δp is the drop in hydraulic pressure, p , across the membrane, σ is the reflection coefficient of the given solute, and $\Delta \pi$ is the osmotic pressure difference across the root membrane. If the gradient of solute concentration is very low and $\sigma \Delta \pi$ can be ignored, then the hydrostatic pressure drop across the root membrane Δp is the main factor controlling root uptake. In a drying soil L_p declines with the decline in soil water potential faster than it regains its original value after rewetting (Nobel 1991).

Gardner (1960) and Cowan (1965) concluded, using numerical examples of constant daily transpiration fluxes and constant root density, that the unsaturated conductivity of the soil is the dominant factor controlling water flux through the soil-plant system as the soil dried and this theoretical prediction was supported experimentally by Macklon and Weatherley (1965). On the other hand Newman (1969), on the basis of available field data, argued that at high water content, soil resistance is insignificant, the major resistance to liquid water flow lies in the plant, and only as the soil dried and the soil resistance increased (e.g. at Ψ_m around -1500 kPa) did the soil resistance become the dominant component of the total resistance. Newman's conclusion has been supported by CAT studies on water drawdown by lupin and radish plants at high water potentials (Hamza and Aylmore 1992a).

The increase in soil resistance to flow as the soil water content decreases (Hamza and Aylmore 1992b) arises largely as a result of the reduction of soil water content in the rhizosphere (Carbon 1973; Hanson 1974). As the soil dries the macropores empty first and in accord with Poiseuille's equation, micropores conduct water much less readily. Water diffusivity is further rapidly reduced because the water flow pathways become more tortuous. It has also been reported that as the soil dries an air gap is likely to develop between the soil and root (Faiz and Weatherley 1977). Nye (1992) reported that main roots (1 mm diam.) will lose full hydraulic contact at a soil matric suction of 20 kPa, while finer roots (0.1 mm diam.) will lose contact at about 70 kPa and root hairs (<0.1 mm diam.) at about 230 kPa. This air gap will cause discontinuity in soil water and thus prevent soil water-root contact.

Elucidation of these uncertainties requires the ability to study soil water drawdowns around plant roots quantitatively *in situ* in a non-destructive, non-invasive, and continuous fashion using a high resolution technique, such as computer-assisted tomography, applied to the attenuation of X- and gamma-radiation (CAT scanning) (Aylmore 1993). However, at low soil water contents the difficulty of such studies is compounded by experimental artifacts arising from the abrupt changes in bulk density within the rhizosphere (Aylmore 1993). The present studies were undertaken to assess the extent of such problems and to evaluate the ability of CAT to elucidate water drawdowns over a wider range of soil water contents.

Materials and methods

Five acrylic columns, 4.5 cm in diameter and 12 cm long, were uniformly packed to a bulk density of approximately 1.6 g/cm^3 with an oven dry soil mix consisting of 85% Bassendean sand and 15% Clackline kaolinite from Western Australia (Hamza and Aylmore 1992a). The columns were especially designed to accommodate single-rooted radish plants and to be suitable for CAT scanning. The bases of the columns were perforated and covered with filter paper to allow drainage. The dry soil was wet to field capacity and then oven dried at 105°C for 24 h to allow the soil to settle down after the initial irrigation. Soil slumping, undoubtedly due to structural rearrangement of the soil matrix, was accompanied by some leaching and

redposition lower down the column of a small amount of fine particles (clay fraction). No further changes in overall bulk density were observed during subsequent experiments. Radish seeds (*Raphanus sativus* cv. White Icicle) were germinated in the dark on Petri dishes containing a thick pad of moist paper tissue and then transplanted into the columns with their emerged radicals pointed toward a 0.2-mm-diameter hole made at the center of each column. The holes extended downward to encourage the single root to grow close to the centre of the column. The radish plants were grown under laboratory conditions for 25 days using eight 20 W fluorescent tubes to simulate 14 h of daylight followed by 10 h of darkness. Day/night temperature and relative humidity were maintained at 23/18°C and 60/70%, respectively.

Surface irrigation of the columns containing the plants with nutrient solution to field capacity continued up to 15 days after planting. The columns were then left to dry to a water content of $0.1 \text{ cm}^3/\text{cm}^3$, which was reached 25 days after planting. The plants were kept in darkness for 24 h to allow the water content in the columns to equilibrate. The columns were then scanned at 3 cm depth from the soil surface after 2, 4, 6, and 8 h of exposure to light and a high transpirational demand from a fan, using a Somatom DR/H X-ray scanner (Image matrix: 512×512 pixels). The thickness of the scanned layer was 2 mm. Finally the columns were oven dried at 60°C to keep the decomposition of root organic matter to a minimum. The dried column then was scanned at the same depth as that of the wet column.

In computer-assisted tomography (Brooks and DiChiro 1976), a slice of the object under examination is divided into a $M \times M$ matrix consisting of small squares called pixels (Hounsfield 1972). The CAT produces an array of numbers representing the values of the linear attenuation coefficient, μ , for each pixel. The value of μ for dry soil is given by $\mu_{\text{dry}} = \mu_s \rho_s$, where μ_s is the mass attenuation of the soil solids and ρ_s is the bulk density of the soil. For wet soil the μ term becomes $\mu_{\text{wet}} = \mu_s \rho_s + \mu_w \theta_v$, where μ_w is the linear attenuation coefficient of water and θ_v is the volumetric water content of the soil. In commercial CAT scanners it has been found more convenient to express the values of μ as Hounsfield units (H) defined by the equation:

$$H = 1000(\mu - \mu_w)/\mu_w$$

where μ_w is the linear attenuation coefficient of water. The scale is linear and H units for air and water are defined as -1000 and 0 respectively. Thus the water content is given by the equation:

$$\theta_v = (H_{\text{wet}} - H_{\text{dry}})/1000$$

The data obtained here were compared with data previously obtained using the same procedure but determined at a soil water content of $0.3 \text{ cm}^3/\text{cm}^3$ (Hamza and Aylmore 1992a).

Results and discussion

Figure 1 shows the water uptake rates, Q , per scanned layer for radish roots growing at high ($0.3 \text{ cm}^3/\text{cm}^3$) and low ($0.1 \text{ cm}^3/\text{cm}^3$) water contents. The root section growing in the high water content layer absorbed 6.4–10.2 times as much water as did that growing in the low

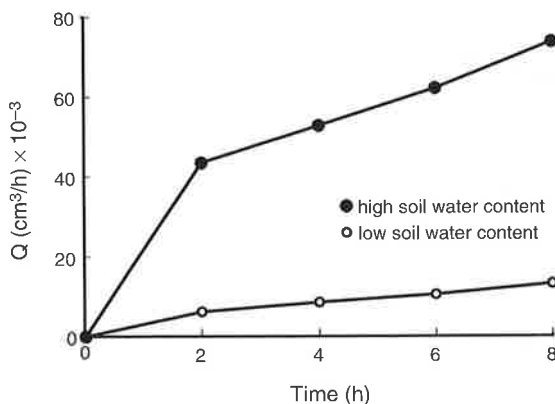


Fig. 1. High and low transpiration rates per layer of radish root after 0, 2, 4, 6, and 8 h.

soil water content layer. Interestingly the extraction rate in both cases increased with time of transpiration, indicating the ability of the plant to maintain sufficient water potential gradient across the root membrane even at the low water content. The matric potential at the soil-root interface in the high θ_v layers just before transpiration began was -30 kPa. This value corresponds to a soil water diffusivity of 0.71 cm^2/h . The corresponding matric potential in the low θ_v layers before transpiration commenced was -70 kPa, which corresponds to a soil water diffusivity value of 0.02 cm^2/h . Thus a decrease in matric potential at the soil-root interface by 2.3 times caused a corresponding decrease of 35 times in the value of soil water diffusivity. This exponential relation between water potential and water diffusivity causes the interfacial resistance to increase rapidly with decreasing water potential at the soil-root interface. However, it seems that the decrease in transpiration, which is proportional to water uptake by the plant root, is less sensitive to decreasing water potential at the soil-root interface. For example, while the soil water diffusivity decreased by a factor of 35, the decrease in transpiration rate was around 6–10 times. This means that the decrease in water potential gradient across the root is not equally proportional to the decrease in water potential at the soil-root interface. Presumably the compensation comes from osmotic adjustment. As indicated earlier, even at low water content, the osmotic adjustment was sufficient to keep the transpiration increasing though at a much lower rate.

Figure 2 shows the drawdowns of water by layers of radish roots at the high (Hamza and Aylmore 1992a) and low water contents. Analysing CAT drawdown data for plant roots

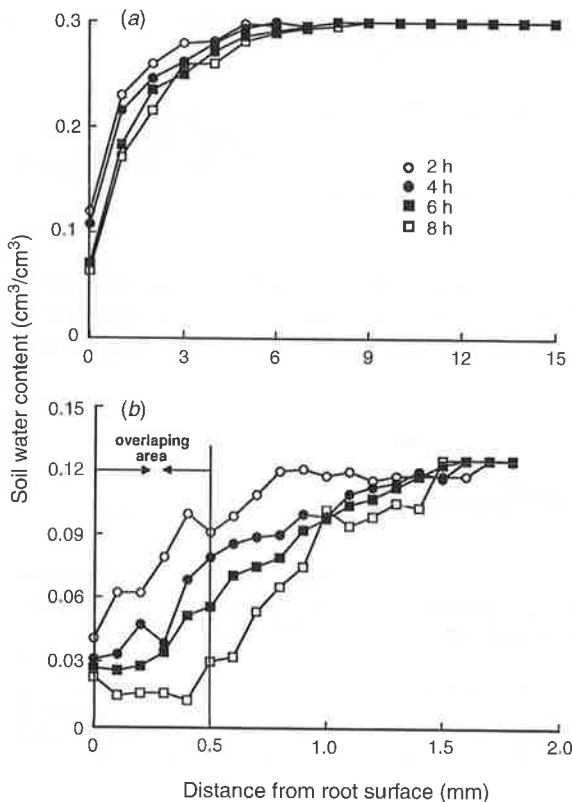


Fig. 2. Water drawdown by radish root growing at (a) high soil water content after 2, 4, 6, and 8 h and (b) low soil water content after 2, 4, 6, and 8 h.

growing in low water content soil is rather more complex than for roots growing at a high soil water content. The nature of this complexity arises from the fact that the size of drawdown areas for the roots growing at low water content is much smaller and extends only a few millimetres from the root surface (see Fig. 2a, b). Moreover, the bulk density of the soil adjacent to the soil-root interface may increase through compaction associated with root growth and this can lead to an overestimation of the attenuation coefficient used to derive water content. In scanning a plant root growing in soil the photons pass from a high density media (soil) through a low density media (root), and then back through a high density media (soil again). Since mineral soils attenuate X-rays more strongly than plant roots (Hamza and Aylmore 1992a), the abrupt change in the bulk density between root and soil causes an effect known as 'beam hardening' (Cupping effect) arising from the preferential attenuation of the lower energy X-rays in the polychromatic beam. The effect is especially noticeable when a low energy level scanner is used (Aylmore 1993) and X-ray tubes used in medical scanners usually produce a low X-ray energy level below 140 kV. Without adequate beam hardening correction, the changes in the attenuation coefficients of the rays as they pass through different densities are not proportional to the abrupt changes in the bulk densities of the media. Understanding the nature and extent of the overlapping between the drawdown areas and the beam hardening-altered bulk density area is thus important in studying water drawdown by plant roots growing at low soil water content. The following section deals with this point in detail.

Overlapping area

Figure 3 shows that the overlapping area around a radish root grown in soil at low θ_v extends to about 0.5 mm from the root surface and Fig. 2b shows that almost one-third of the

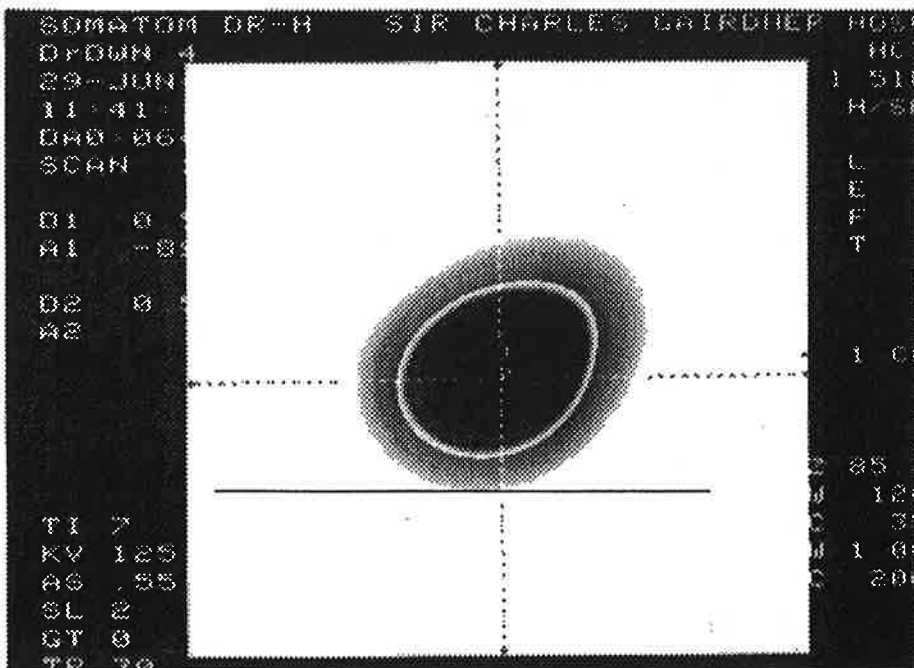


Fig. 3. CAT picture of cross-section through 25-day-old radish root of 1.5 mm diameter.

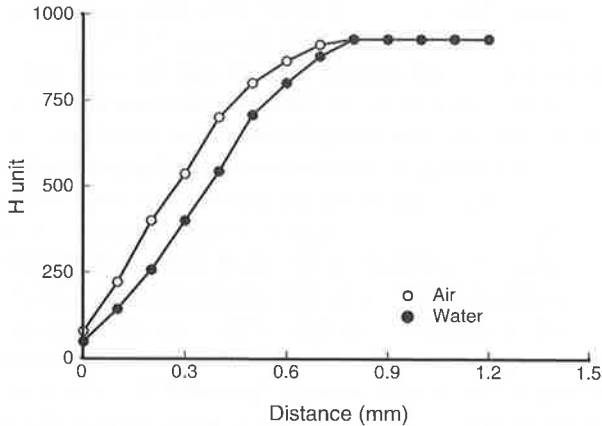


Fig. 4. Hounsfield units (H) for holes filled with air and water.

drawdown area at the lower water content lies within this overlapping area. In contrast, most of the drawdown area around the radish root growing at high θ_v (Fig. 2a) is located outside the overlapping area (the drawdown distance is 8 mm). To study the influence of the overlapping area on water content or bulk density in the vicinity of plant root, 2 plastic tubes of i.d. 4.5 mm and wall thickness 1.0 mm were glued in an upright position to the bottom of a PVC pot. The pot was then filled at similar bulk density with the same soil mix used to grow the radish plants. The soil was then wetted and oven dried to allow it to settle. One of the plastic tubes was filled with deionised water and sealed while the other tube was sealed with air inside. The pot was then scanned at 3 depths and the depth with the most homogeneous Hounsfield unit values (H) of the bulk soil was chosen to examine the beam hardening effect.

Figure 4 shows the H unit values from the tube wall to the bulk soil. H unit values are lower at the tube surface and increase away from it up to 0.8 mm for water and 0.7 mm for air. The values of the H unit as a function of distance from the hole wall are higher for air than for water. Beyond these distances the values of the H unit equal the average values of the bulk soil. This area, between the tube wall and the uniform values of H units, is considered as the overlapping area. Since $\theta_v = (H_{\text{wet}} - H_{\text{dry}}) / 1000$, then it is important to obtain the H_{dry} values for the soil at the end of the experiment with the plant roots in position. In this case the effect of the overlapping area (due to beam hardening, edge effect, and altered bulk density) can to a large extent be taken into account. The root location will be a channel filled partially by air and partially by organic material with a low bulk density for which the H unit values will in fact be negative. Thus scanning the dry soil before growing the plant in it ignores the effect of the overlapping area, and leads to greatly overestimating water content around the roots. However, while the effect of the overlapping area cannot be completely eliminated it can be minimised by scanning the dry soil with the root in position at the end of the experiment, since the increase in bulk density will be evident.

Drawdown distance

Figure 2 shows that the main difference between water drawdowns by roots growing in high and low θ_v is the extent of the drawdown distance from the root surface to the point in the bulk soil where H units are essentially constant. The drawdown distance of the high θ_v is

about 8 mm, whereas it is about 1.25 mm for the low θ_v . This is almost proportional to the difference in Q between the high and low water content layers, which is, as mentioned earlier, about 6–10 times. The lowest θ_v values attained under the low and high θ_v were $0.023 \text{ cm}^3/\text{cm}^3$ and $0.057 \text{ cm}^3/\text{cm}^3$, respectively, after 8 h of transpiration. Soil water diffusivity corresponding to the lowest θ_v of the low water content layer was $0.0038 \text{ cm}^2/\text{h}$. It would be of particular interest to study water drawdowns and transpiration at even lower θ_v values, i.e. down to the threshold of wilting point for example, and further work at this level is planned.

The average θ_v of the scanned layer of soil was determined using a statistical collar with exclusion of the root area. Software features of the Somatom scanner enable the numerical pixel values within such regions of interest to be readily analysed. The average θ_v values per layer were 0.109, 0.108, 0.106, 0.103, and $0.099 \text{ cm}^3/\text{cm}^3$ for 0, 2, 4, 6, and 8 h of transpiration, respectively. The average θ_v value at zero time of transpiration measured by CAT ($0.109 \text{ cm}^3/\text{cm}^3$) can be compared with the initial water content, $0.1 \text{ cm}^3/\text{cm}^3$, calculated gravimetrically ($\theta_v = \theta_g \times \text{bulk density}$). The slightly higher value of θ_v determined by CAT arises because of the slight increase in the soil bulk density upon successive wetting during the growing period.

The average H values of the roots indicate that the water content of the root is decreasing with time of transpiration (Table 1) and air from the soil is progressively entering, presumably, the cortex layers of the roots. The H unit for pure water is around 0–10 (Hamza 1989) but this value becomes more negative when the water is contained in soil because the X-ray beams must pass through the soil and hence have been partially attenuated before being attenuated again by water. The values of the H units for water contained in a plastic tube buried in a soil mix, similar in bulk density to the one used in this experiment, is –140 and for air is –1013 (Fig. 5). The average H units for the radish roots are –190, –196, –203, –210, and –214 for 2, 4, 6, and 8 h of transpiration. The average H unit for the hole left by the root after the soil is oven dried was –221. Unfortunately, we do not have the H unit values for the radish roots growing at high θ_v to compare with these values. However, it seems likely that as soil water content decreases and air replaces water some gas exchange occurs between soil and roots. We would expect such exchange to occur mainly in the Donnan free space of the root cortex through diffusion. Since the diffusion coefficients of gases are roughly 10 000 times that of liquid water (Nye and Tinker 1977) this process might well occur at even higher θ_v than the initial water content value in this experiment. Since all molecules, including air, should pass through the Casprian strip in the endodermis we expect far less concentration of air inside the stele and naturally none in the xylem. If

Table 1. Numbers of pixels (PC) and values of Hounsfield units (HU) for 0, 2, 4, 6, and 8 h after transpiration and for the dry soil

Time	PC	HU
0	39 699	–190
2	38 992	–196
4	43 767	–203
6	46 847	–210
8	40 638	–215
Dry soil	52 708	–221

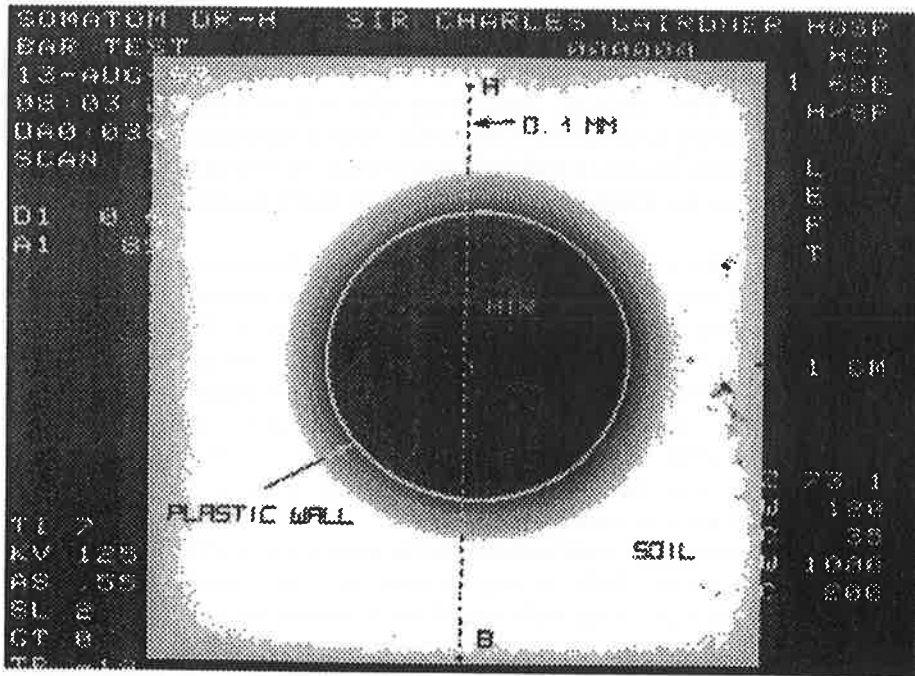


Fig. 5. CAT picture of cross-section through plastic tube filled with water and buried in soil.

this happened the water column would be discontinued by an air bubble and transpiration would cease.

The root diameter at zero time of transpiration was 1.5 mm and occupied a pixel count (PC) of 39 699 pixels. Since the values of H units of the radish root were all negative, then pixels between -1024 and 0 (the 2 limits for air and water, respectively) were regarded as possible root pixels and their numbers were calculated. The numbers of root pixels for 0, 2, 4, 6, and 8 h of transpiration are shown in Table 1. The number of pixels per root layer surface area decreased by 707 pixels after the first 2 h of transpiration. This represents some 1.8% decrease in the cross-sectional area of the root layer which is about 1.75 mm^2 . This area is almost twice the 1 mm^2 calculated using the statistical function and appears in the CT picture because a distance function is used here to impose a graded scale, which is more accurate at very short distances. Roots usually shrink when a negative pressure or suction develops in their conductive tissues. Such a case occurs when a sudden drop in water potential gradient between soil and leaves occurs causing water to lag behind plant demands as a suction is developing. This would explain the 1.8% reduction in the root cross-sectional area after 2 h of transpiration. After the first 2 h of transpiration the number of pixels per layer starts to increase (Table 1) indicating an increase in root diameter. This represents an increase in root diameter of 10, 18, and 2% after 4, 6, and 8 h, respectively. These data confirm the findings by other researchers (Huck *et al.* 1970; Faiz and Weatherley 1982) that plant roots experience diurnal changes in their diameter depending on the ability of the roots to maintain an adequate water uptake, which in turn depends on the soil water status.

In the present experiments the plants were kept in darkness for 24 h to equilibrate before transpiration commenced. Just before exposing the plants to light the water potential difference from soil to leaves is probably between 0 and 100 kPa (Hamza 1989) and the stomata are closed. Once the plant is exposed to light the stomata open and water evaporates from the leaves. This evaporation is often associated with the temporary development of a negative pressure (suction) in the conducting vessels and the roots shrink slightly. If the water content around the roots is low, the plant cannot meet the evaporative demands unless it adjusts by decreasing the leaf water potential. Once the plant adjusts it is able to extract more water and so soil water becomes less of a limiting factor as shown by the ever-increasing Q (Fig. 1) and the increase in root diameter (Table 1). However, as the water content around the root starts to deplete, i.e. after some 6 h of transpiration, the amount of water moving through the root xylem decreases causing the root to shrink again. If the transpiration continued until θ_v of the soil–root interface became critically low, the root may have shrunk beyond its original value at zero time of transpiration.

Conclusions

The transpiration rate of a radish plant decreases less rapidly than the decrease in water content at the soil–root interface presumably due to an osmotic adjustment in the leaves. This allows the plant to maintain transpiration rate even at relatively low soil water content. Decreasing soil water content from 0.3 to 0.1 cm³/cm³ caused the transpiration rate to decrease by 6–10 times. This was due mainly to the development of a lower water potential gradient across the root membrane. The drawdown distances produced by roots growing at the lower soil water content were 8 times smaller than those at the high soil water content and the value of θ_v at the soil–root interface following 8 h of transpiration was 2.5 times lower. The radish roots exhibited a temporary, albeit slight decrease in diameter after the transpiration commenced followed by a substantial temporary increase. However, root diameter stabilised around its original diameter when the plant attained an almost steady water uptake rate. Despite the added complexity of beam hardening, CAT scanning can provide valuable information on processes at the root–soil interface.

Acknowledgment

This work was funded by the Australian Research Council whose support is gratefully acknowledged.

References

- Aylmore LAG (1993) Use of computer-assisted tomography in studying water movement around plant roots. *Advances in Agronomy* **49**, 1–54.
- Aylmore LAG, Hamza M (1990) Water and solute movement to plant roots. In 'Transactions of the 14th International Congress of Soil Science'. Kyoto, Japan, Vol. 7, pp. 124–129. (ISSS: Wageningen, The Netherlands)
- Baveye P, Sposito G (1984) The operational significance of the continuum hypothesis in the theory of water movement through soils and aquifers. *Water Resource Research* **20**, 521–530.
- Brooks RA, DiChiro G (1976) Principles of computer-assisted tomography (CAT) in radiographic and radioisotopic imaging. *Physics in Medicine and Biology* **21**, 689–732.
- Campbell GS (1985) 'Soil physics with basic transport models for soil-plant system.' (Elsevier Science Publisher B.V.: Amsterdam)
- Carbon BA (1973) Water stress in plants in a coarse soil. *Australian Journal of Soil Research* **11**, 33–42.
- Cowan IR (1965) Transport of water in the soil plant atmosphere system. *Journal of Applied Ecology* **2**, 221–239.
- Dainty J (1976) Water relation in plant cells. In 'Encyclopaedia of plant physiology—New series'. (Springer: Berlin, Heidelberg, New York)

- Faiz SMA, Weatherley PE (1977) The location of the resistance to water movement in the soil supplying the roots of transpiring plants. *New Phytologist* **78**, 337–347.
- Faiz SMA, Weatherley PE (1982) Root contraction in transpiring plants. *New Phytologist* **92**, 333–343.
- Gardner WR (1960) Dynamic aspects of water availability to plants. *Soil Science* **89**, 63–73.
- Hainsworth JM, Aylmore LAG (1986) Water extraction by single plant roots. *Soil Science Society of American Journal* **50**, 841–848.
- Hamza MA (1989) Studies of the effect of solute concentration on water uptake by single lupin and radish plant roots using computer assisted tomography and liquid ion exchanger microelectrodes. PhD thesis, University of Western Australia.
- Hamza MA, Aylmore LAG (1992a) Soil solute concentration and water uptake by single lupin and radish plant roots. I. Driving force and resistance. *Plant and Soil* **145**, 197–205.
- Hamza MA, Aylmore LAG (1992b) Soil solute concentration and water uptake by single lupin and radish plant roots. II. Water extraction and solute concentration. *Plant and Soil* **145**, 187–196.
- Hanson GK (1974) Resistance to water transport in soil and young wheat plants. *Acta Agriculturae Scandinavica* **24**, 37–48.
- Herkelrath WN, Miller EE, Gardner WR (1977) Water uptake by plant: II. The root contact model. *Soil Science Society of America Journal* **41**, 1039–1043.
- Hounsfield GN (1972) A method of and apparatus for examination of a body by radiation such as X- or gamma-radiation. British Pat. No. 1283915, London.
- Huck MG, Betty Klepper, Taylor HM (1970) Diurnal variations in root diameter. *Plant Physiology* **45**, 529–530.
- McCoy EL, Boersma MLU, Akrotanakul S (1984) Toward understanding of soil water uptake by plant root. *Soil Science* **173**, 69–77.
- Macklon AES, Weatherley PE (1965) Controlled environment studies of the nature and origin of water deficit in plant. *New Phytologist* **64**, 414–427.
- Newman EI (1969) Resistance to water flow in soil and plant, II. A review of experimental evidence on the rhizosphere resistance. *Journal of Applied Ecology* **6**, 261–272.
- Nobel PS (1991) Ecophysiology of roots desert plants, with special emphasis on Agaves and Cacti. In 'Plant root, the hidden half'. (Eds Y Waisel, A Eshel, and U Kafkafi) pp. 839–866. (Marcel Dekker Inc.: New York)
- Nye PH, Tinker PB (1977) 'Solute movement in the soil-root system.' (Blackwell Scientific Publications: Oxford)
- Nye Peter H (1992) Toward the quantitative control of crop production and quality. III. Some recent developments in research into the root-soil interface. *Journal of Plant Nutrition* **15**, 1175–1192.

Manuscript received 22 June 1998, accepted 23 April 2001

FLY ASH AMENDMENT OF SANDY SOIL TO IMPROVE WATER AND NUTRIENT USE EFFICIENCY IN TURF CULTURE

S.M. Pathan, L. A. G. Aylmore, and T. D. Colmer*

ABSTRACT

Sandy soils pose a particular challenge for water and nutrient management due to the low water retention and low ionic adsorption capacities of these substrates. Fly ash is comprised primarily of fine sand- and silt-sized particles so, if applied at sufficient rates, can permanently change soil texture. Fly ash from Kwinana Power Station (Western Australia) and also Karrakatta sand were evaluated for a range of physical and chemical properties. Field plots of Karrakatta sand were amended to a depth of 12-15 cm with several rates (0 to 20 %, wt/wt) of fly ash and effects on soil water holding capacity, hydraulic conductivity, plant nutrition, and turf growth during establishment were assessed. Plant available water increased progressively with increasing rates of fly ash additions, whereas hydraulic conductivity decreased. Fly ash also provided a source of plant available phosphorus. Possible release of heavy metals was evaluated using the toxicity characteristic leaching procedure. Values obtained for heavy metals were all well below the regulatory guideline levels. Turf (*Cynodon dactylon* cv. "Wintergreen") planted as rhizomes had a 1.3- to 1.6-fold larger root biomass after 9 weeks of growth in plots amended with fly ash when compared to non-amended plots. Thus, fly ash amendment may be a useful management option for turf culture on sandy soils.

Keywords

Cynodon dactylon; heavy metals; soil hydraulic conductivity; plant available water; phosphorus

INTRODUCTION

Efficient use of water and nutrients in managed plant systems, including turf culture, is required to minimize adverse environmental impacts. Sandy soils, however, pose a particular challenge to managers due to the low ionic adsorption capacities and high hydraulic conductivities contributing to the potential for large amounts of water and nutrients to pass beyond the plant-rooting zone. Thus, plant culture on sandy soils has potential to contribute to pollution of ground water and wetlands.

Fly ash is the fine residue captured from flue exhausts when coal is burnt in power stations. Fly ash is comprised primarily of fine sand- and silt-sized particles, therefore if applied at sufficient rates it can be used to change soil texture in order to increase water holding capacity [Chang et al., 1977; Salter et al., 1971; Campbell et al., 1983]. Fly ash has also been reported to improve the nutritional status of soils via increases in cation exchange capacity (CEC), by provision of some essential nutrients [Roberts, 1966; Summers et al., 1998], and in some cases by acting as a liming material to neutralize soil acidity

[Martens, 1971; Taylor and Schuman, 1988]. However, some types of fly ash contain trace elements (e.g. Cd, Se) that, if present at high concentrations, may have adverse effects on crops and the environment; the composition and levels being dependant on the coal source [Adriano et al., 1980; Page et al., 1979]. Nevertheless, fly ash incorporation into sandy soils can improve water and nutrient retention, with potential to increase plant productivity [Rees and Sidrak, 1956; Adriano et al., 1980] and reduce nutrient leaching.

The experiments reported here evaluated the use of fly ash from Kwinana Power Station in Western Australia as a soil amendment to improve water and nutrient management in turf grown on a sandy soil of the Swan Coastal Plain, Western Australia. The impacts of fly ash amendments at several rates on soil physical and chemical properties and subsequently on turf growth and phosphorus (P) nutrition were assessed, in laboratory and field experiments. The potential for release of heavy metals from the fly ash, as well as uptake of these by turfgrass, were also evaluated.

MATERIALS AND METHODS

Characterization of selected physical and chemical properties of soil and fly ash samples

A series of physical and chemical analyses were undertaken to characterize fly ash from Kwinana Power

S.M. Pathan and T. D. Colmer: Department of Plant Sciences;
 L. A. G. Aylmore: Department of Soil Science and Plant
 Nutrition, Faculty of Agriculture, The University of Western
 Australia, 35 Stirling Highway,
 Crawley 6009, Western Australia, Australia.

*Corresponding author: tdcolmer@cyllene.uwa.edu.au.

Station and Karrakatta sand from the Spearwood dune system of the Swan Coastal Plain [McArthur and Bettenay, 1960], both in Western Australia. The fly ash samples were either taken from a ~ 3 yr old stockpile (weathered) or directly from the hopper (unweathered). The stockpiled fly ash was collected from the electrostatic precipitators and pumped as a slurry to an old limestone quarry where the water drains/evaporates, leaving the solid particles. These two samples were taken in order to evaluate the effects of the slurry process and possible weathering in the stockpile on the ash properties.

Particle size distributions for fly ash and soil samples were determined using the Pipette method [Day, 1965; Green, 1981]. Samples were pretreated with dispersing agent prior to the measurements. Specific surface area (surface area per unit mass) was determined following standard protocols using a Gemini Surface Area Analyzer (Gemini III 2375). Hydraulic conductivity of soil, fly ash (weathered), and mixtures of fly ash with soil (0, 5, 10, 20, 50, and 100 % by wt fly ash in Karrakatta sand) were measured in the laboratory by passing solution through fly ash/soil mixtures within Buchner funnels (permeameter) using a constant head method [Klute, 1986]. 'Plant available water' in other samples of these mixtures was measured using pressure-plates [Klute, 1986]. Samples were loosely packed into a core of radius 2.68 cm and height 1.0 cm and then saturated with water at atmospheric pressure. The cores were then placed on a porous ceramic plate in a pressure chamber and equilibrated with matric potential values of -5 or -1500 KPa. Gravimetric moisture content of each fly ash/soil mixture was then measured after equilibration at each matric potential. Volumetric moisture contents were calculated after correcting for the bulk density measured for each sample.

The pH of soil or fly ash extracts in 0.01 M CaCl₂ (1:5, wt/vol) and electrical conductivity (EC) of extracts in de-ionized water (1:5, wt/vol) were measured. Total carbon and total nitrogen were determined using a LECO carbon and nitrogen Analyzer (LECO, CHN 1000). Exchangeable cations and cation exchange capacity (CEC) were measured using the silver thiourea extraction method and atomic absorption spectroscopy (Perkin Elmer, AAnalyst 3000). Samples were pretreated by washing with an aqueous solution of glycol prior to CEC measurements [Rayment and Higginson, 1992]. Subsequently, a single extraction method using silver thiourea was found to be suitable for rapid determination of CEC and exchangeable cations in the samples [Pleysier and Juo, 1980].

Extractable P in 1g samples of soil or fly ash shaken in 100 ml of 0.5 M sodium bicarbonate at room temperature for 16 h [Olsen et al., 1954; modified by Colwell 1965; Rayment and Higginson 1992] was quantified using the colourmetric method of Murphy and Riley [1962] and a spectrophotometer (Shimadzu, UV 1601). The P retention index (PRI), a measure of the ability of a substrate to adsorb P [Allen and Jeffery, 1990], was determined by measuring the P remaining in a solution that originally contained 10

mg kg⁻¹ P and 0.02 M KCl after incubation with soil or fly ash samples (1:20, wt/vol) for 16 h at room temperature. The toxicity characteristic leaching procedure (TCLP) was used to determine the amount of heavy metals that can potentially leach from the soil and fly ash samples. The samples were mixed with 0.57 % glacial acetic acid (1:20, wt/vol) and extracted according to standard procedures [Method-1311, EPA SW-846, 1992; see Testa, 1997]. Heavy metals in the extraction solution were measured using inductively coupled plasma-mass spectrometry (ICP-MS) (Pescien, Elan 6000). Recoveries of spikes of the various metals when added to the extracts ranged from 93 to 112%.

Establishment of plots with four rates of fly ash amendment

Field experiments were conducted at the University of Western Australia Turf Research Facility located in Shenton Park, approximately 8 km west of Perth CBD. The soil is virgin Karrakatta sand, cleared of the native vegetation 2 years prior to the plots being planted. The experimental design consisted of four rates (0, 5, 10 and 20% by wt; equivalent to 0, 75, 150 and 300 t ha⁻¹) of fly ash from the stockpile at Kwinana incorporated into the top 12-15 cm of a series of 12 m² plots arranged in a completely randomised design. Fly ash was incorporated into individual plots using a rotary hoe, and 7 d later shredded, washed rhizomes of couch (*Cynodon dactylon* cv. "Wintergreen") were planted (1:10 planting ratio). Three replicates of each fly ash treatment were established and planted with rhizomes, and two plots of bare soil (non-amended, without turf) were also maintained in a weed-free condition.

Rhizomes were planted on November 24, 1999 so that the majority of the experimental period was during a summer in southwest Australia (December 1999 to March 2000). The average maximum and minimum temperatures were 30.4 and 17.8°C, respectively, average monthly rainfall was 42.0 mm, and average daily net evaporation was 9.2 mm. Mowing, at a height of 15 mm with a cylinder mower, commenced 9 weeks after planting and thereafter every 14 d.

Irrigation and fertilizer applications were as "current Western Australian Industry practice". The fertilizer regime consisted of a pre-plant application of pelletised poultry manure at 2100 kg ha⁻¹ and superphosphate with micronutrients at 200 kg ha⁻¹. Horticultural

Table 1. Particle sizes in Karrakatta sand and Kwinana fly ash, from Western Australia. Values given are means of 3 replicates ± standard errors.

Sample	Size categories			
	Coarse sand (2.0-0.2 mm)	Fine sand (0.2-0.02 mm)	Silt (0.02-0.002mm)	Clay (< 0.002 mm)
Karrakatta sand	92 ± 0.06	2 ± 0.06	2 ± 0.05	4 ± 0.26
Fly ash (weathered)	15 ± 2.53	29 ± 0.59	49 ± 0.28	7 ± 0.29
Fly ash (unweathered)	6 ± 0.46	29 ± 1.30	52 ± 1.98	13 ± 0.79

Table 2. Hydraulic conductivity in Kwinana fly ash, Karrakatta sand, and several fly ash:soil mixtures, as measured using a constant head method in a laboratory. Values given are means of 3 replicates \pm standard errors. ANOVA was conducted on the data set (significance level $p < 0.001$) and means compared using the LSD.

Fly ash: soil mixture	Hydraulic conductivity
% wt/wt	mm hr ⁻¹
0 (soil only)	167.7 \pm 4.75
5	7.33 \pm 0.32
10	5.62 \pm 0.55
20	3.30 \pm 0.14
50	1.67 \pm 0.04
100 (fly ash only)	1.66 \pm 0.08
LSD (0.05)	5.99

Special (12.2 % N, 3.5 % P) was applied at 328 kg ha⁻¹ every 14 d. The irrigation regime for the first 7 d was 3.5 mm applied three times per d, followed by 5.0 mm twice per d for the next 21 d, and then for the remainder of the summer one irrigation was given each morning to replace 100 % of the previous days net evaporation. A variable-speed travelling irrigator with a fixed-boom was used to apply the water, as described previously [Short and Colmer, 1998].

Measurements taken for field plots

Turf growth rates were measured by taking two cores (radius 3.14 cm) from each plot every 14 d. The shoot (leaf plus rhizome) and root dry weights in each sample were determined. Samples of turf leaf and rhizomes were also collected for elemental analyses. Total arsenic (As), barium (Ba), boron (B), cadmium (Cd), cobalt (Co), chromium (Cr), copper (Cu), lead (Pb), mercury (Hg), manganese (Mn), nickel (Ni), selenium (Se), silver (Ag) and zinc (Zn) in nitric/perchloric digests were determined using ICP-MS (Pescien, Elan 6000). Recoveries of spikes added to the digests were 94 to 109 %, and results were also validated against plant tissue standards taken through the same procedures as the samples. Total P was measured using X-ray fluorescence spectrometry (XRFS) (Phillips, PW 1400). Saturated infiltration rates of water were measured in the field using disc permeameters [Perroux and White, 1988], 3 weeks after planting. Soil moisture content in the top 10 cm of each plot was measured at selected times using a hand-held TDR-type probe. After 15 weeks, soil cores were taken from each plot, and extractable P in these soil volumes was determined.

Table 3. pH, electrical conductivity (EC), cation exchange capacity (CEC), extractable phosphorus and phosphorus retention index (PRI) of Karrakatta sand and Kwinana fly ash. Data given are means of 3 replicates \pm standard errors.

Sample	pH	EC	CEC	Extractable P	PRI
	1:5 CaCl ₂	dS m ⁻¹	m.e. 100 g ⁻¹	mg kg ⁻¹	
Karrakatta sand	4.70 \pm 0.02	0.03 \pm 0.00	2.25 \pm 0.33	2.50 \pm 0.6	2.08 \pm 0.38
Fly ash (weathered)	5.55 \pm 0.03	0.51 \pm 0.003	6.07 \pm 0.08	92.5 \pm 3.1	4.11 \pm 0.19
Fly ash (unweathered)	7.93 \pm 0.05	1.35 \pm 0.005	10.3 \pm 0.40	409.9 \pm 3.1	123.91 \pm 3.0

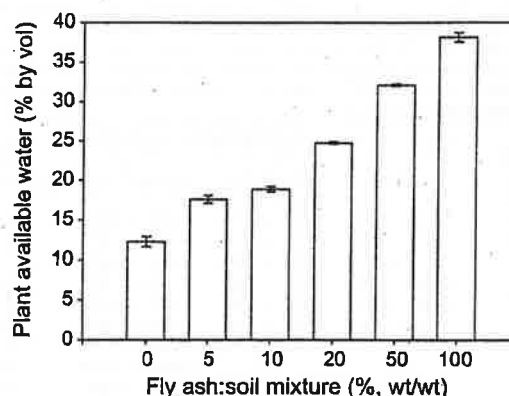


Figure 1. Plant available water (-5 to -1500 KPa) held in fly ash:soil mixtures (% wt/wt, Kwinana fly ash:Karrakatta sand). Measurements were taken using pressure plates in a laboratory. Data given are means of 3 replicates \pm standard errors.

RESULTS AND DISCUSSION

Physical properties of Kwinana fly ash, Karrakatta sand, and mixtures of these two substrates

Particle size influences soil texture, aeration, water movement, and root growth, all of which depend on the size of the pore spaces between the solid particles. Karrakatta sand is comprised primarily of particles of the size classified as "coarse sand", whereas the fly ash is comprised primarily of fine sand- and silt-sized particles (Table 1). The specific surface areas of the Karrakatta sand and the weathered and unweathered fly ash were 0.52, 8.22 and 19.93 m² g⁻¹ dry wt, respectively. Therefore, fly ash amendment of the coarse Karrakatta sand would be expected to have large effects on the physical properties of this substrate.

Plant available water in the soil, when at field capacity, was increased progressively with each larger addition of fly ash (Figure 1). For example, addition of 20 % fly ash to the soil almost doubled the amount of plant available water when the substrate was at field capacity. The large increase in plant available water in the fly ash amended soil, relative to the native soil, undoubtedly resulted from incorporation of the fine-sized particles leading to increased total porosity and specific surface area and perhaps more importantly a shift in pore size distribution from primarily large 'macropores' to many more 'micropores'. [cf. Ghodrati et al., 1994]. Fly ash in-

Table 4. "Leachable" heavy metal concentrations from Karrakatta sand and Kwinana fly ash, as determined using the toxicity characteristic leaching procedure (TCLP). Data given are means of 3 replicates \pm standard errors. Soluble threshold limit concentrations (STLC) are taken from figures published by the US EPA (Table 5-6, Testa, 1997). Note: n.d. = not detected (i.e. below detection limit).

Element	Concentrations in extracts			STLC regulatory level
	Karrakatta sand	Fly ash (weathered)	Fly ash (unweathered)	
	mg L ⁻¹			
As	0.0002 \pm 0.000	0.052 \pm 0.001	0.299 \pm 0.011	5
Ba	3.04 \pm 0.81	0.845 \pm 0.057	0.701 \pm 0.070	100
Cd	n.d.	0.003 \pm 0.000	0.024 \pm 0.000	1
Co	0.0005 \pm 0.000	0.038 \pm 0.002	0.061 \pm 0.001	25
Cr	0.009 \pm 0.0021	0.032 \pm 0.002	0.045 \pm 0.002	5
Cu	0.001 \pm 0.0001	0.072 \pm 0.001	0.130 \pm 0.000	50
Pb	0.0002 \pm 0.000	0.003 \pm 0.000	0.0003 \pm 0.000	5
Hg	n.d.	n.d.	0.0001 \pm 0.000	0.2
Mn	0.149 \pm 0.017	0.156 \pm 0.015	1.228 \pm 0.046	350
Ni	0.002 \pm 0.000	0.099 \pm 0.005	0.148 \pm 0.001	20
Se	n.d.	0.054 \pm 0.002	0.115 \pm 0.000	1
Ag	n.d.	n.d.	n.d.	5
Zn	1.94 \pm 0.39	2.40 \pm 0.26	1.56 \pm 0.17	250

corporation, however, caused a significant reduction in hydraulic conductivity of the Karrakatta sand, even at rates as low as 5% (Table 2). This reflected the hydraulic conductivity in the fly ash being 160-170 times slower than in Karrakatta sand. Nevertheless, fly ash amendments at appropriate rates are likely to aid water management in turf systems grown on sandy soils, particularly during hot and dry periods with high potential evapotranspiration, such as experienced during summer in regions of the world with a Mediterranean-type climate, for example southern Australia. The fly ash amended soil should hold more water initially, and retain more water between irrigations, than the native soil.

Chemical properties of Kwinana fly ash, Karrakatta sand, and mixtures of these two substrates

The analyses of selected chemical properties (Table 3) showed:

(i) pH and EC of the unweathered fly ash were substantially higher than of the weathered fly ash; however, when incorporated into soils these values should not affect plant growth.

(ii) The total CEC of the Karrakatta sand was lower than that of the fly ash. Incorporation of fly ash may therefore improve the retention and availability of some

Table 5. Effect of fly ash amendment at increasing rates on water infiltration in field plots planted with rhizomes of *Cynodon dactylon*. Infiltration measurements were taken when the soil was at field capacity, using disc permeameters, 3 weeks after the rhizomes were planted. Fly ash was incorporated to a depth of 12-15 cm one week prior to planting. Data given are means of 3 replicates \pm standard errors. ANOVA was conducted on the data set (significance level $p < 0.001$) and means compared using the LSD.

Fly ash incorporation rate	Infiltration rate
%, wt/wt	cm hr ⁻¹
0	117 \pm 17
5	60 \pm 8
10	35 \pm 1
20	15 \pm 1
LSD (0.05)	
	30.7

cationic plant nutrients.

(iii) Karrakatta sand contained low levels of total carbon (1.77%), and the carbon:nitrogen ratio was 22:1. Total carbon and carbon:nitrogen ratio in Kwinana fly ash was much higher, being 3.0-9.0% and 60-68:1, respectively.

(iv) The PRI of unweathered fly ash was much higher than that of Karrakatta sand, but this was not also the case for weathered fly ash. The weathering process resulted in substantial losses of soluble P and alkali material and a reduction in PRI.

(v) Extractable P levels in the fly ash were relatively high, which suggests that it will provide a source of P to plants. Reduced use of P fertilizers may therefore be possible when planting turf into sites newly amended with fly ash.

One important environmental concern when any material is added to a soil is the potential solubilization and leaching of heavy metals to groundwater. The amount of heavy metals in coal and therefore fly ash can vary widely, and depends on the chemistry of the coal source [Adriano et al., 1980; Page et al., 1979]. The potential for release of heavy metals from soil and fly ash samples were evaluated using the TCLP; the results are shown in Table 4. The values obtained for Kwinana fly ash for all 13

Table 6. Effect of fly ash amendment at increasing rates on extractable phosphorus in the top 10 cm of soil and on phosphorus levels in *Cynodon dactylon* grown in field plots. Plots were managed as described in the Materials and Methods and soil samples were taken 15 weeks and leaf samples 9 weeks after the rhizomes were planted. Fly ash was incorporated to a depth of 12-15 cm one week prior to planting. Data given are means of 3 replicates \pm standard errors. ANOVA was conducted on the data set (significance level $p < 0.001$) and means compared using the LSD. (n.s. = not statistically significant; $p > 0.05$).

Fly ash incorporation	Extractable P in soil	P in leaf tissue	P in rhizome tissue
%, wt/wt	mg kg ⁻¹	% dry wt	% dry wt
0	18.45 \pm 0.96	0.304 \pm 0.01	0.257 \pm 0.00
5	42.57 \pm 4.02	0.305 \pm 0.02	0.259 \pm 0.01
10	46.11 \pm 4.68	0.312 \pm 0.00	0.263 \pm 0.01
20	51.15 \pm 3.69	0.320 \pm 0.01	0.269 \pm 0.01
LSD (0.05)		n.s.	n.s.

elements tested were well below the regulatory guidelines set by the US Environmental Protection Agency (EPA). For example, the amount of Cd extracted even from the unweathered ash was very small (0.024 mg L^{-1}), when compared to the threshold limit concentration set by the US EPA for this element at 1.0 mg L^{-1} (Table 4). Moreover, the TCLP is a measure of the potential for leaching, so even these low concentrations of metals found in the extracts may not all become available in the field situation, and any leaching from fly ash amended soils may be a slow process. So detrimental impacts of heavy metals on groundwater quality from the use of Kwinana fly ash as a soil amendment are very unlikely.

Effects of fly ash on soil moisture in field plots

Field plots of Karrakatta sand amended with fly ash showed substantial increases in soil moisture content measured *in situ* in the top 10 cm (Figure 2). For example, on one of the days measurements were taken the volumetric water content in control plots 24 h after the last irrigation was 13.9%, whereas in plots amended with 10% fly ash it was 24.0%. These field results extend our findings of progressive improvements in moisture holding capacity in fly ash:soil mixtures as determined in the laboratory (Figure 1). Measurements of water infiltration rates in the plots showed that fly ash amendments reduced infiltration rates (Table 5), even in a field situation where the fly ash:soil mixtures were much less uniform than those used in the laboratory studies. Since higher applications of fly ash progressively reduced infiltration, this characteristic may define the maximum limit of

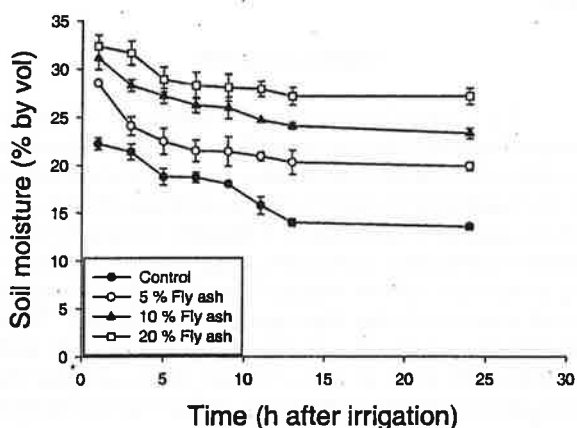


Figure 2. Change in soil moisture content with time after irrigation in field plots of Karrakatta sand amended with four rates of Kwinana fly ash. Plots were watered daily at 100% replacement of net evaporation and measurements were taken in the top 10 cm using a hand-held TDR probe. Plots were managed as described in the Materials and Methods and fly ash was incorporated to a depth of 12-15 cm one week prior to planting. Net evaporation from an A class pan during the 24 h period was 11.5 mm. Data given are means of 3 replicates \pm standard errors.

incorporation for practical use in turf systems, as ponding and/or runoff during major rainfall events should be avoided.

Effect of fly ash on turf growth, plant nutrition and heavy metals in leaf tissues

Turf growth during establishment from shredded rhizomes was slightly enhanced in plots amended with fly ash. Root growth was stimulated in the soil layer amended with fly ash but not in the soil zone below the layer containing fly ash (Figure 3). These small, although significant, improvements in growth were somewhat remarkable since the plots were supplied with adequate water (at least 100% replacement of net daily evaporation) and frequent applications of fertilizer (see Materials and Methods). Larger benefits of fly ash amendments on turf growth may be expected under conditions in which nutrient and water supply are more restricted, as was previously documented for broad acre, rain-fed pastures on sandy soils for which 100 t ha^{-1} fly ash increased above-ground dry matter production by 56% [Summers et al., 1998]. Positive yield responses to other sources of fly ash have also been reported for several other crop species on different soil types [Rees and Sidrak, 1956; Adriano et al., 1980].

An increase in extractable P was observed for the fly ash amended zone of soil in the field plots (Table 6). Tissue P levels also increased slightly for turf grown in fly ash amended plots (Table 6), but levels were all regarded as sufficient for turf growth. Marschner [1995] stated that 0.3 to 0.5% P per unit dry weight (leaf tissue) is optimal for vegetative growth of plants. For couch turf, leaf tissue P between 0.2 to 0.5% is sufficient, whereas below 0.15% is

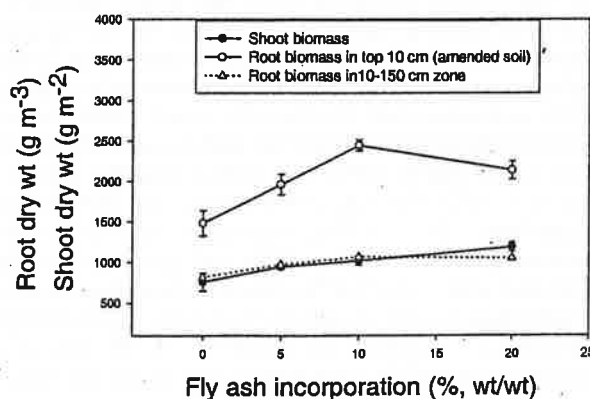


Figure 3. Effect of rate of Kwinana fly ash incorporation in field plots of Karrakatta sand on shoot and root growth during establishment of *Cynodon dactylon*. Cores were taken 9 weeks after rhizomes were planted. Shoot (leaf and rhizomes) and root were washed free of soil, oven dried at 60°C for 3 d, and dry weights were determined. Plots were managed as described in the Materials and Methods and fly ash was incorporated to a depth of 12-15 cm one week prior to planting. Data given are means of 3 replicates \pm standard errors.

Table 7. Effect of fly ash amendment at increasing rates on concentrations of heavy metals in leaf tissue of *Cynodon dactylon*. Samples were taken from field plots 9 weeks after the rhizomes were planted. Plots were managed as described in the Materials and Methods and fly ash was incorporated to a depth of 12-15 cm one week prior to planting. Data given are means of 3 replicates \pm standard errors. ANOVA was conducted on the data set (*significance level $p < 0.05$ **significance level $p < 0.001$) and means compared using the LSD. (n.s = not statistically significant; $p > 0.05$).

Elements	Trace element concentrations				LSD (0.05)
	Fly ash incorporation rate (% wt/wt)				
	0	5	10	20	
	mg kg^{-1}				
As	0.436 \pm 0.09	0.599 \pm 0.04	0.560 \pm 0.00	0.543 \pm 0.02	n.s
Ba	39.99 \pm 3.40	40.92 \pm 4.85	36.50 \pm 3.92	33.07 \pm 0.37	n.s
B	20.47 \pm 2.06	16.11 \pm 2.14	21.71 \pm 0.48	19.84 \pm 1.35	n.s
Cd	0.117 \pm 0.00	0.137 \pm 0.00	0.140 \pm 0.00	0.165 \pm 0.01	**0.015
Co	0.582 \pm 0.05	0.565 \pm 0.03	0.582 \pm 0.03	0.660 \pm 0.01	n.s
Cr	40.99 \pm 2.98	45.70 \pm 6.11	32.49 \pm 1.26	35.51 \pm 1.60	n.s
Cu	11.36 \pm 1.66	11.42 \pm 1.61	9.108 \pm 0.28	10.55 \pm 0.30	n.s
Pb	0.636 \pm 0.07	0.561 \pm 0.11	0.364 \pm 0.10	0.444 \pm 0.04	n.s
Hg	0.030 \pm 0.00	0.024 \pm 0.00	0.024 \pm 0.00	0.021 \pm 0.00	n.s
Mn	97.87 \pm 6.48	100.7 \pm 11.9	101.6 \pm 2.43	136.2 \pm 11.9	*29.79
Ni	53.45 \pm 5.85	46.46 \pm 2.48	36.39 \pm 1.30	39.99 \pm 1.42	n.s
Se	0.102 \pm 0.01	0.404 \pm 0.01	0.760 \pm 0.05	1.352 \pm 0.15	**0.272
Ag	24.97 \pm 4.99	25.87 \pm 4.77	28.70 \pm 2.79	26.67 \pm 3.75	n.s
Zn	52.69 \pm 3.45	54.10 \pm 2.08	55.97 \pm 2.15	68.43 \pm 2.57	*8.56

considered deficient [Johnston, 1996]. The adequate levels of P in the tissues from all treatments reflect the generous supply of fertilizer given during the experimental period (see Materials and Methods).

In order to assess the issue of potential release of heavy metals from the fly ash, and uptake of these by turfgrass, we determined the concentrations of the same elements measured using the TCLP (Table 4), and also B, in leaf tissues sampled from the plots (Table 7). Concentrations of As, Ba, B, Co, Cr, Cu, Pb, Ni, Hg, and Ag were not statistically different, or in some cases lower, in leaf tissue from turf grown in fly ash amended compared with non-amended Karrakatta sand. Leaf tissue concentrations increased for Mn, and Zn (essential plant micronutrients) for turf grown in plots amended with fly ash ($p < 0.05$). For Cd, and Se, small but statistically significant ($p < 0.001$) increases in leaf tissue concentrations were detected for turf grown in fly ash amended plots. The leaf Se concentrations were much smaller than those (4 to 5 mg kg^{-1}) regarded as potentially hazardous (Comm. on MBEEP, 1976) and the concentrations of Cd were at the lower end of the range regarded as normal (0.1-1.0 mg kg^{-1}) and much lower than levels considered to be toxic (5-700 mg kg^{-1}) [Logan and Chaney, 1983]. Furthermore, the levels of Cd in the turf grown in the present study were much lower than those reported for clover grown on a range of soil types (non-amended) in Western Australia [Summers et al., 1998 and references therein]. In earlier studies, other plant species grown on fly ash amended soils also contained higher levels of Se [Gutenmann et al., 1981]; whereas in other

cases the tissue concentrations of some heavy metals, including Cd, Cu, Cr, Fe, Mn and Zn, were decreased in plants grown in fly ash amended soil [Schnappinger, et al., 1975; Elseewi, et al., 1980; Adriano, et al., 1980]. Thus, turf grown in soil amended with Kwinana fly ash had tissue concentrations of heavy metals regarded as "normal", even when fly ash application rates were as high as 20%.

CONCLUSIONS

This study showed that amendment of coarse-textured sand with fine-textured fly ash leads to substantial improvements in plant available water and also reductions in soil hydraulic conductivity. In addition fly ash provided a source of extractable P. Possible release of heavy metals was evaluated using the toxicity characteristic leaching procedure; values obtained for all 13 trace elements tested were well below the regulatory guidelines. Thus, amendment of sandy soils in Western Australia with Kwinana fly ash, in combination with appropriate management systems, has potential to increase turf growth by reducing episodes of moisture deficit and also by aiding in the retention of nutrients in the rooting-zone. The large reductions in hydraulic conductivity with progressively higher applications of fly ash may define the maximum rates for use in practical turf management systems, as ponding and/or run-off during major rainfall events should be avoided. Finally it should be noted, that fly ash from around the world can differ widely in several properties [Adriano et al., 1980], so local trials are required to evaluate the use of a particular ash source in

combination with the target soil(s).

ACKNOWLEDGMENTS

We thank the members of the UWA "Turf Industries Research Steering Committee" for their valuable advice and enthusiastic support during this project. The research was supported by the Western Power Corporation and Ash Development Association of Australia.

REFERENCES

- Adriano, D.D., A.L. Page, A.A. Eseewi, A.C. Chang, and I. Straughan. 1980. Utilization and disposal of fly ash and other coal residues in terrestrial ecosystems: A Review. *J. Environ. Qual.* 9: 333 - 344.
- Allen, D.G., and R.C. Jeffery. 1990. Methods for analysis of phosphorus in Western Australian soils. Chemistry Center, Report of Investigation No. 37.
- Campbell, D.J., W.E. Fos, R.L. Aitken., and L.C. Bell. 1983. Physical characteristics of sand amended with fly ash. *Aust. J. Soil Res.* 21: 147 - 154.
- Chang A.C., L.J. Lund, A.L. Page., and J.E. Warneke. 1977. Physical properties of fly ash amended soils. *J. Environ. Qual.* 6: 267 - 270.
- Colwell, J.D. 1965. An automatic procedure for the determination of phosphorus in sodium hydrogen carbonate extract of soil. *Chem. Ind.* 10: 893-895.
- Committee on Medical and Biological Effects on Environmental Pollution. 1976. Selenium. *Natl. Acad. Sci., Washington D.C.*, p. 203.
- Day, P.R. 1965. Particle fractionation and particle size analysis. In C.A. Black (Ed.), *Method of Soil Analysis, Part 1. Agronomy Monograph Series*, 9: 545 - 567.
- Elseewi, A.A., I.R. Straughan., and A.L. Page. 1980. Sequential cropping of fly ash amended soils: effects on soil chemical properties and yield and elemental composition of plants. *Sci. Total Environ.* 15: 247-259.
- Ghodrati, M., J.T. Sims., and B.L. Vasilas. 1995. Evaluation of fly ash as a soil amendment for the atlantic coastal plain: soil hydraulic properties and elemental leaching. *Water, Air, and Soil Pollut.* 81:349-361.
- Green, A.J. 1981. Particle size analysis. In J.A. McKeague (Ed.) *Manual on soil sampling and methods of analysis.* Canadian Society of Soil Sci. Ottawa, p. 4 - 29.
- Gutenmann, W.H., D.C. Eifving, D.I. Valentino., and D.J. Lisk. 1981. Trace element absorption on soil amended with soft-coal fly ash. *Biocycle* 20: 42-44.
- Johnston, K.J. 1996. Turf irrigation and nutrient study: Turf manual. Royal Australian Institute of Parks and Recreation, WA Region.
- Klute, A. 1986. *Method of soil analysis. Part 1, 2nd Edition,* Soil Science Society of America, Wisconsin, USA.
- Logan, T.J., and R.F. Chaney. 1983. 'Metals'. In A.L. Page (Ed), *Utilization of municipal wastewater and sludge on land.* University of California, Riverside, CA, pp.235-329.
- Martens, D.C. 1971. Availability of plant nutrients in fly ash. *Compost Sci.* 12: 15-19.
- Marschner, H. 1995. *Mineral nutrition of higher plants.* 2nd Edition, Academic Press, Limited, London.
- McArthur, W.M., and E. Bettenay. 1960. The development and distribution of the soils of the Swan Coastal Plain, Western Australia. Soil Publication No. 16, CSIRO, Melbourne, Australia.
- Method 1311: Toxicity characteristic leaching procedure. 1992. Test method for evaluating solid waste: Physical and chemical methods. US EPA Publication, SW-846.
- Murphy, J., and J.P. Riley. 1962. A modified single solution method for the determination of phosphorus in natural waters. *Anal. Chim. Acta.* 27: 31 - 36.
- Olsen, S.R., C.V. Cole, F.S. Watanabe., and L.A. Dean. 1954. Estimation of available phosphorus in soils by extraction with sodium bicarbonate. US Dep. Agric. *Cric. No.* 939.
- Page, A.L., A.A. Elseewi., and I.R. Straughan. 1979. Physical and chemical properties of fly ash from coal-fired power plants with reference to environmental impacts. *Residue Reviews* 71: 83 - 120.
- Perroux, K.M., and White, I. 1988. Design for disc permeameter. *Soil Sci. Soc. Am. J.* 52: 1205-1215.
- Pleysier, J.L., and A.S.R. Juo. 1980. A single-extraction method using silver-thiourea for measuring exchangeable cations and effective CEC in soils with variable charges. *Soil Sci.* 129: 205 - 211.
- Rayment, G.E., and Higginson, F.R. 1992. *Australian soils and land survey handbook: Australian laboratory handbook of soil and water chemical methods.* Inkata Press, North Ryde, Sydney.
- Rees, W.J., and G.H. Sidrak. 1956. Plant nutrition on fly ash. *Plant and Soil* 8: 141-157.
- Roberts, F.J. 1966. The Effects of sand type and fine particle amendments on the emergence and growth of subterranean clover (*Trifolium subterraneum* L.) with particular reference to water relations. *Aust. J. Agric. Res.* 17: 657-672.
- Salter, P.J., D.S. Webb., and J.C. Williams. 1971. Effects of pulverized fuel ash on the moisture characteristics of coarse-textured soils and on crop yields. *J. Agric. Sci.* 77: 53-60.
- Schnappinger, M.F., D.C. Martens, Jr., and C.D. Plank. 1975. Zinc availability as influenced by application of fly ash to soil. *Environ. Sci. Technol.* 9: 258-261.
- Short, D.C., and T.D. Colmer. 1998. Water use and drought tolerance in turfgrasses: New research in Western Australia. *Irrigation Australia* 13: 4-7.
- Summers, R., M. Clarke, T. Pope., and T. O'Dea. 1998. Western Australia fly ash on sandy soils for clover production. *Commun. Soil Sci. Plant Anal.* 29: 2757 - 2767.
- Taylor, E.M., and G.E. Schuman. 1988. Fly ash and lime amendment of acidic coal spoil to aid revegetation. *J. Environ. Qual.* 17: 120-124.
- Testa, S.M. 1997. *The reuse and recycling of contaminated Soil.* CRC Press, New York, USA.

Developments in Soil Science Vol. 28A, "Soil Mineral-Organic Matter – Microorganism Interactions and Ecosystem Health, Dynamics, Mobility and Transformations of Pollutants and Nutrients" (Violante, A, Huang, P.M., Bollag, J.M. and Gianfreda, L., eds) Elsevier Publ. (2002) 117-125.

THE ROLE OF SOIL ORGANIC MATTER AND WATER POTENTIAL IN DETERMINING PESTICIDE DEGRADATION

K.M. Webb and L.A.G. Aylmore

Soil Science and Plant Nutrition, The University of Western Australia, Nedlands, Western Australia 6907

Four pesticides (Simazine, Metribuzin, Fenamiphos and Metalaxyl) chosen for their known or suspected potential to contaminate soil and groundwater, were investigated in terms of their degradation properties in a sandy soil from Medina, Western Australia. Samples were incubated for up to 190 days in a batchwise arrangement with periodic monitoring and sampling. A range of soil physical, chemical and biological properties were simultaneously measured on the samples. Measurements obtained principally allow comparison of residual soil pesticide concentrations with soil water potential and soil respiration rate over time. Results show variation across pesticide type and soil conditions (principally moisture), however trends do not always relate well to a first-order degradation approach and treatment of the data. The surface soil containing the highest organic matter and highest moisture content produced the greatest rates of degradation and generally showed very good agreement with first order degradation behaviour (corroborated with other measures of soil activity). In sub-surface soils conditions apparently conducive to pesticide breakdown were not always realized and the data significantly challenge the view that first order degradation can be used to describe pesticide breakdown in this soil profile.

1. INTRODUCTION

The potential for pesticides to contaminate soil profiles and groundwater has become a major concern throughout the world. Leaching of pesticides is primarily determined by the recharge rate, pesticide sorption and degradation properties in the soil. Knowledge of these factors is essential to the successful development of practical management models [1-3].

The key soil component responsible for sorption of non-ionic organic compounds is soil organic matter. In most agricultural and horticultural soils, sorption is regarded as a hydrophobic partition of the non-ionic organic compounds from the soil aqueous phase to soil organic matter [4]. Sorption retards the downward leaching velocity of pesticides by water in the soil profile.

The rate of degradation essentially determines the rate at which the pesticide compound is eliminated from the soil environment. However, in the case of pesticides, some intermediate

metabolites may be just as toxic as, or more toxic than, the parent compound (e.g. fenamiphos nematicide which transforms to its sulfoxide and sulfone forms). In agricultural and horticultural soils, degradation is primarily due to microbial processes [5]. The rate of microbial degradation for a given pesticide depends on two fundamental variables: (1) availability of the pesticide for degradation; and (2) density and activity of the degrading microbes or extra-cellular enzymes. Other soil and environmental variables, such as soil organic matter content, moisture, temperature, pH and aeration status, affect the degradation rate by modifying these two fundamental variables. In addition, individual pesticides differ significantly in their vulnerability to degradation due to their intrinsic structural differences.

Degradation of pesticides in soil is commonly assumed to obey first order kinetics , without regard to soil biomass, organic matter or moisture content, such that the fraction of pesticide remaining un-degraded as it leaches in the soil is expressed as

$$F = \exp(-kt) = \exp(-0.693t/t_{1/2}) \quad (1)$$

where k is the degradation rate constant, t is time and $t_{1/2}$ is the degradation half-life.

Recent studies have raised questions as to the validity of this assumption [6].

Most of the half-life values that have been studied and reported, whether obtained from field or laboratory investigations, are for surface soils [7]. However, whether or not a pesticide will reach ground water in significant amounts is not only affected by the degradation rate in the surface layer, but by the degradation rate in every soil layer above the ground water (the unsaturated zone). As it is impractical to measure the degradation rate of every pesticide in every soil layer of the profile, it is usually assumed when modelling the pesticide ground water pollution potential, that the half-life increases with depth in response to decreases in microbial density and activity, caused, in particular, by decreases in the concentration of organic substrate [2,8]. This assumption, however, has not been experimentally verified. The product of soil microbial biomass content and soil microbial activity is essentially an index of the metabolic state of the soil biomass. By measuring these quantities in the same soil sub-samples from which residual pesticide is determined, valuable corroborating evidence as to the significance and meaning of measured degradation half-lives (in a specific soil sample) can be obtained. The present investigation sought to clarify the interaction of these factors in determining pesticide degradation with depth in a sandy soil of Western Australia.

2. MATERIALS AND METHODS

2.1. Soil properties

Soil samples were taken from the Agriculture Western Australia Medina Vegetable Research Station, Western Australia. The site contained remnant native vegetation, had no previous history of pesticide application and had been partially disturbed by the itinerant movement of and provision for penned emus. The soil, which is a Karrakatta sand of the Spearwood Association was collected as 2 fractions - above approximately 20cm and below 25cm to approximately 50cm. A distinct change in soil composition is noted at approximately

25cm. A buffer zone from approximately 20-25cm was not collected. The upper and lower fractions were ascribed the labels Karrakatta Topsoil (KT) and Karrakatta Subsoil (KS). After collection, two separate batches of KT and KS were air dried (at 30°C), sieved (4mm) and re-bagged for storage. Organic carbon was determined by analysis by LECO® 1000 CHN analyser, pH by measurement on 0.01M CaCl₂ solution extract and soil moisture-potential characteristics by gravimetric analysis of soil samples equilibrated with tension plate and pressure plate apparatus. Relevant properties of the soil are summarized in Table 1.

Table 1
Measurements made on the soils selected for incubation studies

Soil	Texture	pH (0.01M CaCl ₂)	Organic C (w/w%)	Field Capacity (v/v %)	Bulk Density (g/cm ³)
Topsoil (0-25 cm)	Sand	5.5 ± 0.1	1.1 ± 0.1	4.8 ± 0.1	1.31 ± 0.03
Subsoil (25-50 cm)	Sand	5.4 ± 0.1	0.14 ± 0.02	2.1 ± 0.1	1.47 ± 0.01

2.2. Laboratory incubation

Four pesticides widely used in horticulture and agriculture in the region were studied (Table 2). These pesticides represent a significant range in water solubility and sorption coefficient [4].

Table 2
Pesticides studied and their properties

Common name	Chemical name	Uses	Water solubility [†] (mg/L)	k _{oc} [†]
Simazine	2-chloro-4,6-bis(ethylamino)- 1,3,5-triazine	Herbicide	3.5	130
Fenamiphos	Ethyl 4-methylthio- <i>m</i> -tolyl isopropylphosphoramidate	Nematicide	400	100
Metalaxyl	Methyl <i>N</i> -(2-methoxyacetyl)- <i>N</i> -(2,6-xylyl)-DL-alaninate	Fungicide	8400	61
Metribuzin	4-amino-6- <i>tert</i> -butyl-3- methylthio-1,2,4-triazine- 5(4 <i>H</i>)-one	Herbicide	1220	268

[†] From Worthing [9] and Wauchope et al. [10].

For each pesticide, amounts of moist soil equivalent to 1 kg oven-dry soil were used. The moisture contents of soil samples were initially adjusted to those equivalent to water potentials

(Ψ) of -5 and -100 kPa respectively. Moisture content was then maintained by periodic (weekly to fortnightly) monitoring and amendment with the required amount of water. Some difficulty in maintaining the water potential at -100kPa was experienced, owing to the tight range in soil moisture-potential characteristic for this soil below ψ of -10kPa. 10 mg active pesticide ingredient per kg, simulating usual application rates, was thoroughly mixed with the soil and incubated at constant 18°C under aerobic conditions. Replicate bags were set up for each pesticide and whole bags removed for sampling at different intervals up to 190 days after application. Sub-samples from each removed bag were bulked together for each sampling time, and thoroughly mixed for subsequent extraction and analysis.

Detailed analytical procedures can be found in Kookana et al. [7]. The pesticides were extracted by shaking 5 g moist soil overnight with 10 mL of methanol. The solution was then centrifuged and filtered through a 0.22 μ m membrane filter. Pesticide concentration in the solution was then determined on a high performance liquid chromatograph (HPLC, Waters®) equipped with a multiple wavelength UV/visible detector (model 490), an autosampler (model 717plus) and an automated pump controller (model 600E). Reversed-phase chromatography was employed (isocratically) using a Waters® μ Bondapak-C18 column with acetonitrile (50-70% v/v) in water (50-30% v/v) as mobile phase. Analyses were carried out at 20 °C with 10-20 μ L injections and a flow rate of 1mL min⁻¹. In addition to the five pesticides, the two toxic metabolites of fenamiphos - fenamiphos sulfoxide and fenamiphos sulfone, were also analysed. Separation of F. sulfoxide and F. sulfone peaks was obtained by monitoring multiple wavelengths with the detector [11]. The recoveries varied with pesticides. Reproducible recoveries better than 80% were obtained for all of the pesticides studied. Pesticide concentrations in the soil were calculated on the basis of the recoveries at day zero. Soil microbial biomass was obtained by measurement of Ninhydrin positive compounds following chloroform fumigation and extraction with 0.5M K₂SO₄ [12] and soil respiration rates by back titration (with HCl) of KOH which had been reacted with CO₂ evolved from 7 day incubation in a sealed container.

3. RESULTS AND DISCUSSION

For all the chosen pesticides, the surface soil containing the highest organic matter and highest moisture content produced the greatest rates of degradation. Those shaded in Table 3 were able to be fitted to a first order degradation model (R^2 of 0.67 to 0.96). While residual pesticide breakdown often followed first order degradation behaviour, in some cases conditions conducive to pesticide breakdown were not fully realized, for example for simazine, fenamiphos and metalaxyl in the sub-soils (for these, reliable half-lives could not be estimated, Table 3).

Figures 1 to 5 illustrate the residual pesticide concentrations, soil respiration rates and water potentials measured over the incubation period together with first order degradation fits to the data where relevant. Soil Microbial Biomass (SMB) was unaltered in all soil samples as a consequence of the presence of the pesticides and did not vary significantly between treatments in comparison to controls. Initial SMB carbon was approximately 200 and 50 g kg⁻¹ soil for topsoil and subsoil respectively and decreased to approximately half these values over time.

Biomass respiration rates have an effective detection limit of 50 mg CO₂-C/kg soil and so respiration data presented should be considered in light of this limit.

Table 3

First-order degradation data fits for all experiments

Pesticide	Sample*	(Ψ ,kPa)	R ²	t _{1/2} (d)
Fenamiphos	Topsoil KT	-5	0.96	35
	Topsoil	-100	0.61	27
	Subsoil KS	-5	0.13	
	Subsoil	-100	0.02	
Metribuzin	Topsoil	-5	0.94	145
	Topsoil	-100	0.89	212
	Subsoil	-5	0.93	222
	Subsoil	-100	0.96	193
Metalaxyl	Topsoil	-5	0.96	181
	Topsoil	-100	0.59	428
	Subsoil	-5	0.19	
	Subsoil	-100	0.54	
Simazine	Topsoil	-5	0.67	84
	Topsoil	-100	0.94	107
	Subsoil	-5	0.02	
	Subsoil	-100	0.26	

For fenamiphos, the soil conditions which most clearly demonstrated degradation were those in the higher organic matter topsoil (KT)/higher moisture treatment (-5kPa, Figure 1) with first order fit R² 0.96 giving t_{1/2} of 35 days). Here soil respiration rate and residual pesticide concentrations over the incubation period related well to one another indicating a clear dependence of pesticide degradation on microbial activity. In the sub-soil (KS) respiration rates and corresponding degradation rates were substantially lower and did not conform to first order degradation kinetics (Table 3).

Metribuzin demonstrated the most consistent degradation behaviour with depth, (Table 3 and Figure 2). For this pesticide, good first order degradation fits (R² 0.88-0.96) applied to all treatments giving half-lives between 145 and 222 days (Table 3). Note that the degradation half-life for the soil with the lowest organic matter and moisture contents is lower than for all but the highest organic matter and moisture soil treatment. This suggests the possibility of an abiotic degradation mechanism, since there is little difference in the rates of degradation with different treatments. While residual metribuzin concentration was closely related to respiration rate in the surface soil, this was less evident in the sub-soil.

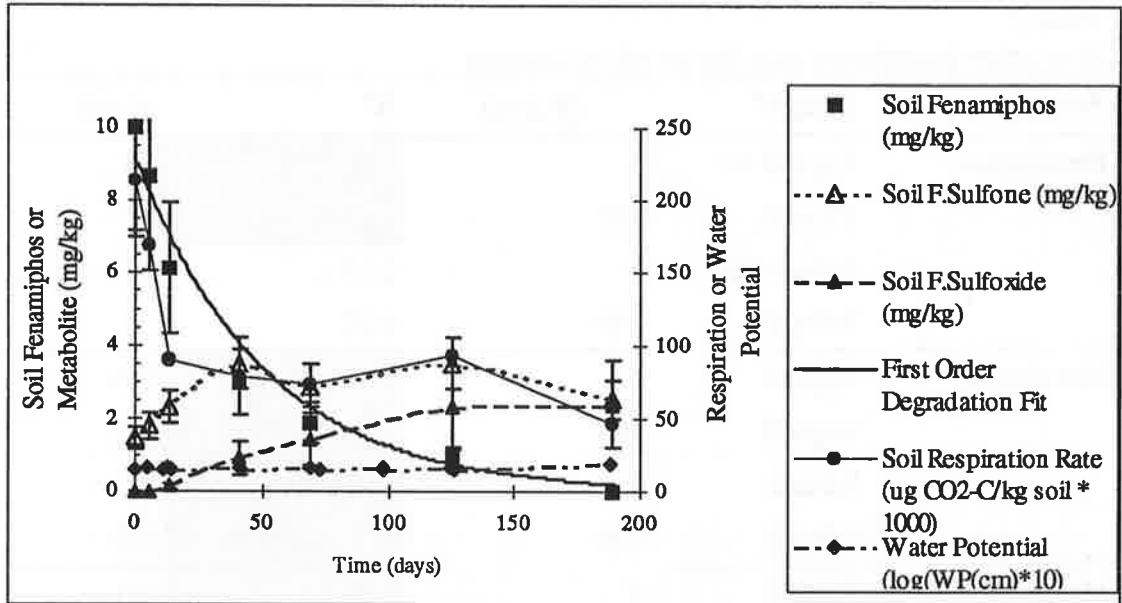


Figure 1. Fenamiphos degradation – Karrakatta surface soil (ψ -5kPa).

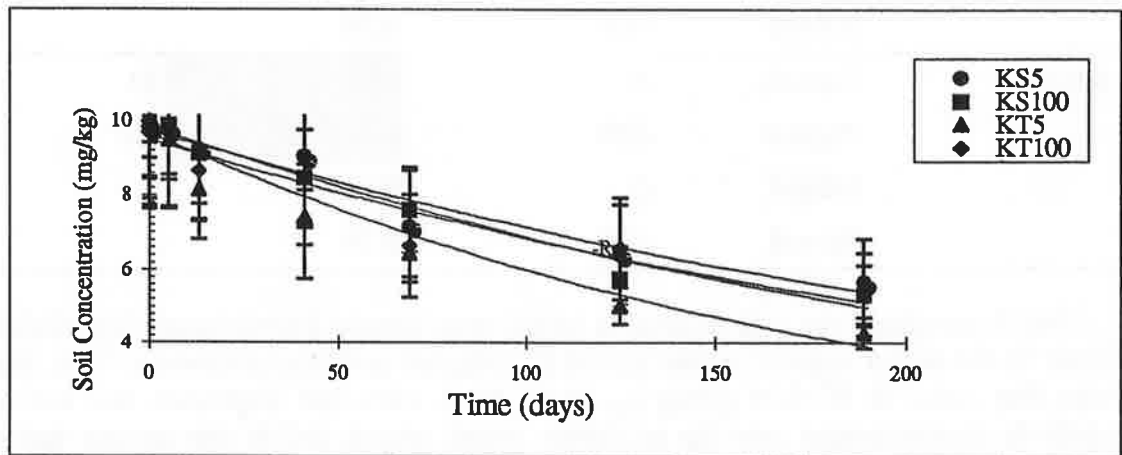


Figure 2. Metribuzin Degradation - Karrakatta Sand.

Metalaxyl demonstrated decreasing degradation with depth (Figure 3) and soil moisture potential but only conformed to first order degradation kinetics at the high moisture potential in the topsoil (Table 3).

Simazine demonstrated the least consistent degradation behaviour compared to metribuzin, fenamiphos and metalaxyl, conforming to first order degradation in the topsoil (Figure 4) but exhibiting essentially no degradation in the subsoil (Figure 5).

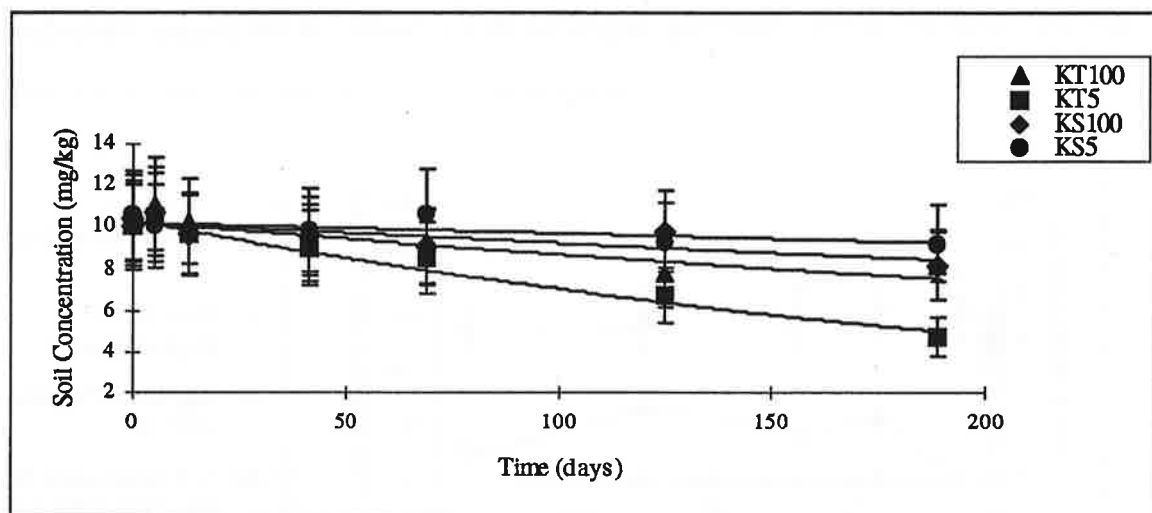


Figure 3. Metalaxyl degradation – Karrakatta sand.

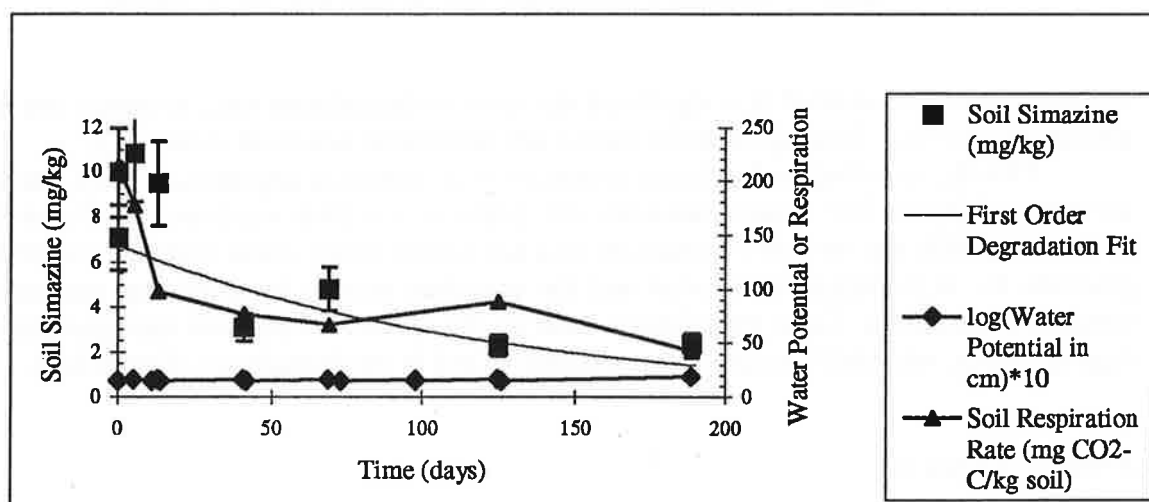


Figure 4. Simazine Degradation - Karrakatta Soil (KT Ψ -5kPa).

Previous studies in these laboratories have shown that degradation half-lives of pesticides in subsoil layers are not always longer than in the surface layer despite significantly lower organic matter content in the subsoil layers [8]. There may be several causes for these unexpected results. Firstly, soil organic matter may affect both fundamental variables that determine the degradation rate. On the one hand, it may increase the microbial density and activity by providing organic substrate; on the other hand, it may reduce the availability of pesticide compound for degradation by sorbing the pesticides [13].

The magnitude of the two opposing effects may vary depending on a number of factors: the sorption capacities of the organic materials; the capacity of the organic material to stimulate microbial activities; and the water solubility and sorption coefficient of the pesticide. Secondly, microbial activities also depend on other environmental conditions, e.g. moisture, temperature,

pH and aeration status which may vary between soil layers. In the present study decreasing soil

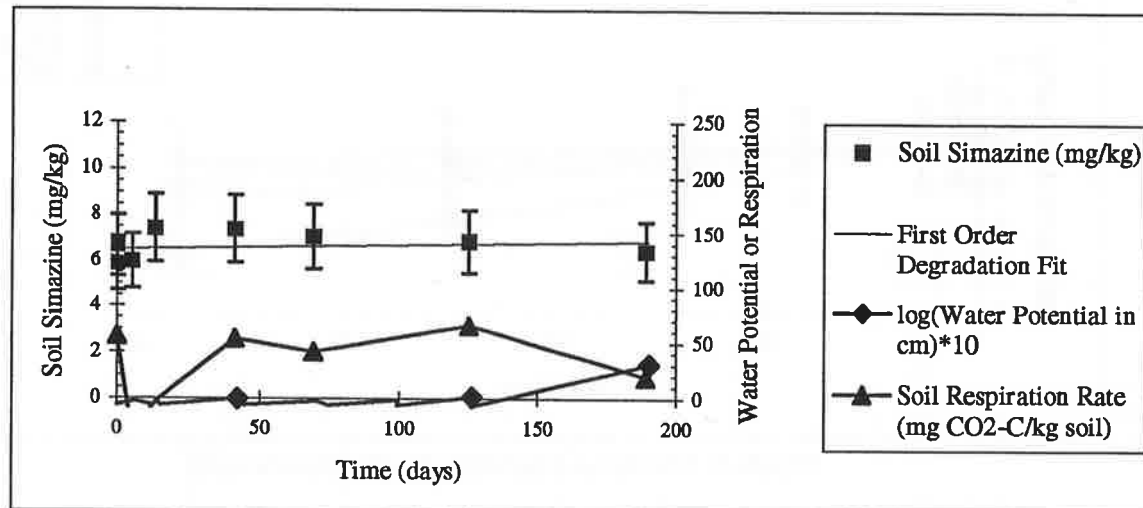


Figure 5. Simazine Degradation - Karrakatta Soil (KS Ψ -5kPa)

moisture generally resulted in a significant decrease in degradation rate, although this is not always the case (e.g. fenamiphos in the topsoil and metribuzin across all treatments).

Thirdly, contribution by abiotic processes (e.g. chemical degradation) may also differ between soil layers. The concentration and composition of organic substrate at different layers of the soil profile and moisture content are thus key factors which affect both the availability of pesticide for degradation by sorption and the microbial activity by providing substrate and conducive conditions. These experiments illustrate the interaction between moisture potential, organic matter, microbial biomass and respiration of soil in the degradation of pesticides.

4. CONCLUSIONS

The surface soil containing the highest organic matter and highest moisture content produced the greatest rates of degradation and were able to be fitted to a first order degradation model (R^2 of 0.67 to 0.96). Pesticide degradation rates were in most cases generally much lower, sometimes negligible, in the sub-surface soil compared to the surface soil, although in many cases respiration rates appeared comparable at both depths. Degradation rates generally decreased with decreasing soil moisture content over the potential range -5kPa to -100kPa. For all pesticides other than metribuzin, there appeared to be good correlation between soil respiration rate and pesticide degradation rate in the topsoil. Thus soil respiration rate appears a valid gauge of the presence of a predominantly biotic pesticide degradation process. The results of these experiments also show that fluctuating soil moisture potentials have a major effect on the degradation rate of pesticides, particularly those thought to undergo biotic degradation. This has implications for the realistic representation of pesticide degradation rates (*viz.* half-lives) in predicting pesticide fate and transport in landscapes which experience major fluctuations in soil water potential over time. The results challenge the view that first

order degradation kinetics can invariably be applied to pesticide breakdown in soil. Recognition of these complexities is essential for the development and successful application of practical management models.

ACKNOWLEDGMENTS

Funding of this research by the Australian Research Council is gratefully acknowledged.

REFERENCES

1. Rao, P.S.C., Davidson, J.M., 1980. Estimation of pesticide retention and transformation parameters required in nonpoint source pollution models. *In: Overcash, M.R., Davidson, L.M (Eds.), Environmental Impact of Nonpoint Source Pollution*. 67 Ann Arbor Science Publishers: Ann Arbor, MI. pp. 23.
2. Jury, W.A., Focht, D.D., Farmer, W.J., 1987. Evaluation of pesticide groundwater pollution potential from standard indices of soil-chemical adsorption and biodegradation. *J. Environ. Qual.* 16, 422-428.
3. Aylmore, L.A.G., Di, H.J., 2000. Predicting the groundwater pollution potential of pesticides under variable recharge, *Aust. J. Soil Res.* 38, 591-602.
4. Green, R.E., Karickhoff, S.W., 1990. Sorption estimates for modeling, *In: Cheng, H.H. (Ed.), Pesticides in the Soil Environment: Processes, Impacts and Modeling*. Soil Sci. Soc. Amer., Madison, WI, pp.79-101.
5. Tortensson, . N.T.L., 1987. Microbial decomposition of herbicides in soil. *In: Hutson, D.H., Roberts, T.R. (Eds.) Herbicides*. John Wiley and Sons, Ltd. New York. pp. 249-270.
6. Di, H.J., Aylmore, L.A.G., Kookana, R.S., 1998. Degradation rates of eight pesticides in a sandy soil from laboratory incubation, field study and simulation. *Soil Sci.* 163, 404-411.
7. Kookana, R.S., Di, H.J., Aylmore, L.A.G., 1995. A field study of leaching and degradation of nine pesticides in a sandy soil. *Aust. J. Soil Res.* 33, 1019-1030.
8. Di, H.J., Kookana, R.S., Aylmore, L.A.G., 1995. Application of a simple model to assess the groundwater contamination potential of pesticides. *Aust. J. Soil Res.* 33, 1031-1040.
9. Worthing C.R., 1983. *The Pesticide Manual*, 7th Ed. The British Crop Protection Council, Suffolk, UK.
10. Wauchope, R.D., Buttler, T.M., Hornsby, A.G., Augustjin-Beckers, P.M.W. Burt, J.P., 1992. The SCS/ARS/CES pesticide properties database for environmental decision-making. *Rev. Environ. Contamin. Toxicol.* 123, 1-164.
11. Singh, R., 1989. Simultaneous determination of Fenamiphos, its sulfoxide and sulphone in water by high performance liquid chromatography. *Analyst* 114, 425-427.
12. Amato, P.L., Ladd, J.N., 1988. Assay for microbial biomass based on ninhydrin-reactive nitrogen in extracts of fumigated soils. *Soil Biol.Biochem.* 20, 107-114.
13. Hamaker, J.W., 1972. Decomposition: quantitative aspects. *In: Goring, C.A.I., Hamaker. J.W. (Eds), Organic Chemicals in the Soil Environment*. Vol. 1. Marcel Dekker, New York, pp. 253-340.